Indian Journal of Natural Sciences www.tnsroindia.org.in ©IJONS

Vol.15 / Issue 88 / Feb / 2025 *International Bimonthly (Print) – Open Access* *ISSN: 0976 – 0997*

RESEARCH ARTICLE

Water Quality Assessment of Sogane Pond in Shivamogga Taluk, Karnataka

S.Thirumala[1]* and B.R.Kiran[2]

[1]Associate Professor, Department of Environmental Science, Government First Grade College, Harihara, (Affiliated to Kuvempu University) Karnataka, India.
[2]Faculty Member Department of Environmental Science, University SMR College of Arts and Commerce, Shankaraghatta, Karnataka, India.

Received: 23 Sep 2024 Revised: 03 Dec 2024 Accepted: 31 Jan 2025

***Address for Correspondence**
S.Thirumala,
Associate Professor,
Department of Environmental Science,
Government First Grade College, Harihara,
(Affiliated to Kuvempu University) Karnataka, India.
E.Mail: drst2008@gmail.com

ABSTRACT

Assessment of physico-chemical characteristics of water in Sogane pond of Shivamogga taluk, Karnataka was carried out during January to December 2019. This water body is situated 10 Km away from Shivamogga town and the total area of is about 9hectares. The climate of the area is almost semi-arid. Water quality parameters were estimated as per standard procedure and compared with WHO and Indian standards. The water temperature was between 25^{O} C and 30.5^{O} C. pH of the water ranged from 6.9 to 7.5, which is in the desired limit values of WHO and BIS standards. The turbidity of water ranged 90 to 130 NTU. The lowest EC value in the winter season with 80 µmhos/cm. CO_2 content deviated from 12 to 16.5 mg/l. The dissolved oxygen content varied between 5.48 mg/l and 8.16 mg/l . The calcium concentration in water varied between 12.9 and 24.5 mg/L. Magnesium concentrations (4.12-10.3 mg/L) was also within acceptable limits. The chloride content ranged from 18.2 mg/l to 38.4mg/l , BOD values varied between 2.2 and 3.45 mg/L. Sulfate content varied between 20.20 and 24 mg/L Phosphate concentrations in water samples varied from 3.1 to 5.50 mg/L. Nitrate content was highest with 4.6 mg/L during summer season and lowest with 0.06 mg/L during the winter season. TDS content varied between 49.5mg/l and 80 mg/l, The total hardness values compared with different standards and ranged from 26.1 to 38 mg/l. Acidity levels varied from a minimum of 14.2 mg/L to a maximum of 15.08 mg/L. Water quality is influenced by environmental factors, which cause variations in nutrients. Seasonal variations in water quality are due to allochthonous and autochthonous factors of the water body. The physico-chemical analysis of water in this pond showed that the water is within the safe limits of

irrigation, fisheries and used for human consumption after proper treatment. Hence, this water body is included under mesotrophic category.

Keywords: Sogane pond, physico-chemical characteristics, Mesotrophic, Shivamogga taluk.

INTRODUCTION

The study of variations in the hydrological conditions of water bodies represents an important aspect of fisheries research, especially considering that the chemical environment has a strong influence on aquatic organisms. Physico-chemical properties are of great importance in the study of any environment, especially aquatic environments. In addition to the general interest in understanding water conditions and their effects on aquatic biota, the observation of short-term changes in physicochemical parameters can also have practical implications for pollution studies (Kulkarni *et al.,* 2009). It is very necessary and important to test water before using it as drinking water, domestic, agricultural or industrial water. Water should be tested for various physicochemical parameters. Water contains suspended, dissolved, airborne, and microbiological contaminants (Bhateria and Jain, 2016). Water bodies are important resources exploited for inland fisheries and the recognition of a range of fish fauna, which offers great prospects for the improvement and sustainable management of water bodies (Krishna and Piska, 2006). Water is a renewable natural resource and the basis of living organisms. Lentic water is used for drinking and household purposes. Physicochemical factors are developed based on scientific data on the impact of pollutants on specific water uses (Rashmi *et.al.,* 2013; Thirumala and Kiran, 2018). The effects of chemicals on the environment can be seen as a deterioration of biological systems, ranging from the expansion of convergence beyond natural levels of ions and organic compounds in plants and animals. (Holdgate, 1983; Rathore *et al.,* 1996). Water is a fundamental need for inland fisheries, and understanding fish fauna diversity is an important consideration for fish fauna improvement and sustainable management. Wetlands in India are home to a wide variety of fish species, which increases the business viability of fishing (Krishna and Piska, 2006). The present study aims to know the seasonal variations in few physico-chemical parameters of Sogane pond, Shivamoggaa district since recently no studies have been carried out on this aspect prevailing in this area.

MATERIALS AND METHODS

Study area

Sogane Pond (Figure 1) is located at Sogane village and situated between latitude of 13°, 55' N and Longitude 75°, 50' E in the Shivamogga city at the distance of about 10 km.

Water sampling and Statistical analysis

Regular sampling of the Sogane pond water was made from the Shivamogga district during January to December 2019. The physico-chemical parameters like pH, air temperature, water temperature and dissolved oxygen were recorded at the sampling site itself. pH was recorded by pH pen. Temperature of the water was recorded with the help of standard centigrade thermometer in degree celsius. For estimating Dissolved Oxygen (DO) water samples were collected in standard 300 ml, BOD bottles and was estimated by the Winkler's method. Turbidity of water were estimated by turbidity meter. Other parameters were estimated in the laboratory using standard methods of Trivedy and Goel (1986) and APHA (2008). One-way ANOVA with post-Hoc Tukey HSD with Bonferroni and Holm multiple tests for physico-chemical characteristics of Sogane pond water is analysed by statistical software of astatsa.com

RESULTS AND DISCUSSION

Table 1 depicts the BIS drinking water standards. While, Table 2 and Figure 3 gives the seasonal physico-chemical properties of the surface water of Sogane pond . Atmospheric temperature varied from a minimum of 28^{O}C during winter season to a maximum of 34^{O}C in Summer. Analysis of surface water samples involves determining the concentration of the analyzed parameters. The desirable limit of pH for drinking water is 6.5 to 8. The pH of the water sample in the Sogane pond was between 6.9 (Rainy season) to 7.5 (Summer). On average, the pH of all the seasons were within the desirable limit prescribed by WHO and BIS standards. The water temperature ranged from 25^{O}C (Winter) to 30.5^{O}C (Summer) respectively. The TDS values of the Sogane water samples ranged from 49.5 (Winter) to 80 mg/l(Summer). Nutrient like phosphate content fluctuated from 3.1 mg/l in Summer to 5.5 mg/l during rainy season. Dissolved oxygen values were comparatively moderate. The DO found in the Sogane pond samples is between 5.48 mg/l in winter and 8.16 mg/l during rainy season. Nevertheless, the highest desirable limit for dissolved oxygen was 4 to 8 mg. Therefore ,the water is moderately safe for domestic usage The total hardness found in lake surface samples ranged from 26.1mg/l (Winter) to 38 mg/l (Summer), showing that the water is soft. The highest hardness value prescribed for drinking water is 300 mg/l.. Based on this, the results show that all samples were soft category. McGowan (2000) reported that total hardness is expressed in milligrams of calcium carbonate equivalent/litre. Water containing $CaCO_3$ at concentrations below 60 mg/l is consider as soft; 60–120 mg/l, moderately hard; 120–180 mg/l, hard; and more than 180 mg/l, very hard. Hence, the present water body is included under soft category.

The Electrical conductivity is the capacity of the solutions to conduct electricity and the values for pond water was ranged from 80 (Winter) to 160 μmhos/cm (Summer). The values of calcium of the Sogane pond water samples ranged from 12.9 mg/l in Summer to 24.5 mg/l during Rainy season. However, in all the sites the values of calcium are below the desirable limit (75 mg/l) of BIS standards for drinking water (BIS, 2008) . The magnesium (mg) content of the water samples are in the ranged 4.12(Winter) to 10.3mg/l (Rainy. In all the months the values are below the permissible limit (100 mg/l) of BIS standards for drinking water (BIS, 2008). Regarding chloride lowest value of chloride was recorded with 18.2 mg/l during winter season and highest value with 38.4mg/l recorded in rainy season. The values of chloride are within the desirable limit (250 mg/l) and within permissible limit (1000 mg/l) of BIS standards for drinking water. Free carbon dioxide (CO_2) is soluble in water, primary wellspring of carbon way route in the nature, is contributed by the respiratory activity of creatures and can exist in water as bicarbonate or carbonates in the broke down or bound structure in earth crust, in limestone and coral reefs areas (Anita Bhatnagar and Pooja Devi, 2013). At the point when broken up in water it structures carbonic acids which decline the pH of any framework, particularly inadequately buffered frameworks, and this pH drop can be hurtful for aquatic living beings (Anita Bhatnagar and Pooja Devi, 2013). CO_2 content in this investigation fluctuated from 12 mg/l (Rainy) to 16.5 mg/l (Winter). Bhatnagar et al. (2004) have reported 5-8 ppm for photosynthetic activity, 12-15 ppm was sublethal to fishes and 50-60 ppm is lethal to fishes. 5 mg/l of free carbon dioxide in water supporting fish population (Santhosh and Singh, 2007; Anita Bhatnagar and Pooja Devi, 2013). Ajai Vyas *et al*.(2007) and Seema Tiwari (2015) reported that the most of the fresh water bodies globally are tends to be polluted due to domestic sewage and industrial effluents, agricultural runoff and idol immersion. Rahashyamani Mishra et al.,(2011) worked on the Rani lake water and they recorded minimum Dissolved oxygen. Their findings has showed that pond was mesotrophic in nature due to the anthropogenic activity by the human beings.

DISCUSSION

Satishagowda *et al.* (2022) have studied the physic-chemical parameters and biological factors of Chikkere water body in Sira in February 2020, including temperature, pH, EC, turbidity, DO, TDS, total hardness, calcium, magnesium, total alkalinity, chloride, Physicochemical parameters such as BOD were studied. Their results showed that most of the physicochemical parameters were within acceptable ranges, except for turbidity.

The total dissolved solids values were within the acceptable limits prescribed by BIS (1991) and WHO (1997). Increased TDS levels due to pollution from domestic sewage, garbage, fertilizer runoff, etc. have been recorded by various researchers (Singh and Mathur, 2005; Swaranlatha and Rao , 1998. Chaurasia and Pandey, 2007). The decrease in conductivity may be a result of absorption of sedimented minerals by submerged macrophytes that are usually abundant in lakes (Iqbal and Kataria, 1995; Kaushik and Saksena, 1999; Radhika *et al.* (2004). The pH values recorded were within the BIS and WHO acceptable limits. The alkalinity values were significantly below the BIS (1991) and WHO (1997) acceptable limits. The total hardness values observed in this pond were well within the acceptable limits of BIS (1991) and WHO (1997). Calcium itself has no dangerous effects on human health. It is known to be non-toxic at low concentrations (Mohan *et al.* 2007). Low magnesium levels reported in the current study. Higher magnesium concentrations were previously reported to be due to the presence of soluble magnesium salts in sedimentary rock layers (Mohan *et al.* 2007). Elevated nitrite levels are due to concentration followed by evaporation and anthropogenic effects, and such high nitrite levels have been reported to cause methemoglobinemia (Kaushik et al. 1991; Khatavkar and Trivedy, 1992, and Radhika et al.,2004) Nitrate levels were observed to be within acceptable limits (BIS 1991; WHO 1997). However, Chloride (Cl) levels were within acceptable limits (BIS, 1991; WHO, 1997). Sulfate content (SO4) was observed to be within acceptable limits (BIS 1991, WHO 1997). Lower phosphate values were recorded in this pond studied. Higher phosphate values may be due to continuous discharge of wastewater into the pond (Sunkad *et al*. 2004). It has been reported that heavy rainfall increases DO values (Radhika *et al.* 2004). The decrease in DO content may be a result of low precipitation and high oxygen consumption due to oxidizing substances associated with wastewater and agricultural runoff (Sharma and Sarang, 2004). The observed low values of Biological Oxygen Demand (BOD) may be due to low temperatures, low amounts of total and dissolved solids in the water, and even microbial counts, as reported by various researchers. (Shardendu and Ambasht 1988; Radhika *et al.* 2004)..

One-way ANOVA, Post-hoc Tukey HSD with Scheffe, Bonferroni and Holm multiple tests

The p-value corresponding to the F-statistic of one-way ANOVA is lower than 0.05, suggesting that the one or more treatments are significantly different.

CONCLUSION

High turbidity in the water body indicate that higher rainfall and surface run off in the study area. Thus in the present study, concludes that the pond is not polluted, as most of the parameters except turbidity are within permissible limit when compared with WHO and BIS standards and the water quality parameters indicate that the pond is in mesotrophic stage. The water from the present pond is useful for irrigation and pisciculture. From the present observed water quality parameters it is concluded that the nutrient load in the pond is moderate. The data certainly justifies the need to take up a detailed study on the impact of water quality parameters on the freshwater lentic Santhekadur pond, should be taken up for the further study in future. A regular monitoring of pond water quality is essential. It is advocated to take urgent steps by governmental and NGO organizations to protect this precious natural resource. Hence, there is an urgent need to undertake appropriate management measures to restore the water quality of this pond.

REFERENCES

1. Ajai Vyas, Seon-Kyeong Kim, Nicholas Giacomini, John C. Boothroyd, and Robert M. Sapolsky 6442–6447 PNAS April 10, 2007 vol. 104 no. 15 .
2. Anita Bhatnagar and Pooja Devi .2013. Water quality guidelines for the management of pond fish culture. International Journal of Environmental Sciences Volume 3 No.6: 1980-2009.
3. APHA (2008) Clescerl, Leonore S., Greenberg, Arnold E., Eaton, Andrew D. (Editors). Standard methods for the Examination of Water and Wastewater, 20th Edition. American Public Health Association, Washington, DC.

4. Bhateria, R., Jain, D. Water quality assessment of lake water: a review. Sustain. Water Resour. Manag. 2, 161–173 (2016). https://doi.org/10.1007/s40899-015-0014-7.
5. Bhatnagar, A., Jana, S.N., Garg, S.K. Patra, B.C., Singh, G. and Barman, U.K., (2004), Water quality management in aquaculture, In: Course Manual of summerschool on development of sustainable aquaculture technology in fresh and saline waters, CCS Haryana Agricultural, Hisar (India), pp 203- 210.
6. BIS 1991. Indian Standard Specification for Drinking Water IS: 10500, Bureau of Indian Standards, New Delhi.
7. Chaurasia and Pandey, G.C. 2007. Study of Physico-chemical characteristics of some water ponds of Ayodhya - Faizabad. IJEP. 27 (11) : 1019-1023.
8. Holdgate, M. 1983. Chemistry in Britain 19:3.
9. Iqbal, S.A. and Katariya, H.C. 1995. Physico-chemical analysis and water quality assessment of Upper Lake of Bhopal. Indian J. Environmental protection. 1(15) : 7.
10. Kaushik, S. and Saksena, D.N. 1999. Physico-chemical Limnology of certain water bodies of Central India In :K.Visayman edited Fresh water Ecosystem of India. Daya Publishing House, Delhi. 336.
11. Kaushik, S., Agarker, M.S. and Saksena, D.N 1991. Water quality and periodicity of phytoplanktonic algae in chambal tank Gwalior, Madhya Pradesh. Bionature. 11 : 87-94.
12. Khatavkar, S.D. and Trivedy, R.K. 1992. Water quality parameters of river Panchganga Kolhapur and Ichalkaranji, Maharashtra. Indian J. Toxicol. Env. Monit. 2 (2) : 113-118/
13. Kowsalya R , A.Uma , S.Meena , K. Saravanabava , C. M Karrunakaran and M. Decca Raman.2010.Assessment of water quality and pollution of Porur double lake (Erettai Eri), Chennai. Journal of Industrial Pollution Control 26 (1) : 61-69.
14. Krishna, M and Piska, R. S. 2006. Ichtyofaunal diversity in secret lake Durgamcheruvu, Ranga Reddy District, Andhra Pradesh, India. J.Aqua. Biol, vol. 21 (1): 77079.
15. Kulkarni A. S., Medha Tendulkar, Sayali Mavalankar and Guhagarkar, A.M., (2009). Study on select water quality parameters from Peth-killa region, Ratnagiri, West coast of India, Maharashtra. *J.Aqua.Biol*., 24 (2) : 82 - 85.
16. McGowan W (2000) Water processing: residential, commercial, light-industrial, 3rd ed. Lisle, IL, Water Quality Association.
17. Mohan, A., Singh, R.K., KirtiPandey, Kumar, V. and Jain V. 2007. Assessment of water quality in industrial zone of Moradabad :Physico-chemical Parameters and Water Quality Index. IJEP. 27(11) : 1031-1035.
18. Radhika, C.G., Mini, I. and Gangadevi, T. 2004. Studies on abiotic parameters of a tropical fresh water lake - Vellayani Lake, Thiruvananthapuram district, Kerala.Poll. Res. 23 (1) : 49-63.
19. Rahashyamani Mishra, Rajesh Kumar Prajapati, Virendra Kumar Dwivedi and Arpana Mishra," Water Quality Assessment of Rani Lake of Rewa (M.P.)," India. GERF Bulletin of Biosciences. 2011, 2(2), 11-17.
20. Rashmi, B.S. and Somashekar Malammanavar, G. 2013. Diversity of Phytoplankton of Lakkinakoppa pond Shivamogga dist, Karnataka. Indian Journal of Plant Sciences 2(3): 87-91.
21. Rathore, O.P., Lavale, A.K. and S.C. Lavale. 1996. Physicochemical data and biological parameters of water samples of Betul region. In: Herbal medicines, Biodiversity and Conservation Strategies (Edited by Rajak R.C. and M.K. Rai). International Book Distributors, Dehradun: 276-282.
22. Santhosh, B. and Singh, N.P. 2007. Guidelines for water quality management for fish culture in Tripura, ICAR Research Complex for NEH Region, Tripura Center, Publication no.29.
23. Sathishagouda S., Shashikanth H. Majagi and K. Vijaykumar.2022.Investigations of Water Quality of Chikkere Water Body, Sira, Tumkur District. Indian J. Applied and Pure Biol. Vol. 37(2), 420-428.
24. Seema Tiwari.2015. Water Quality Parameters –A Review. International Journal of Engineering Science Invention Research & Development; Vol. I Issue IX :319-324.
25. Shardendu and Ambasht, R. 1998. Limnological studies of a rural and urban tropical aquatic ecosystem, oxygen forms and ionic strength. Tropical Ecology. 29 (2) : 98-109.
26. Sharma, L.L. and Sarang, N. 2004. Physico-chemical Limnology and Productivity of Jaisamand Lake, Udaipur (Rajasthan). Poll. Res. 23 (1) : 87-92.

27. Singh, R.P. and Mathur,2005.Investigation of variations in physico-chemical characteristics of a fresh water reservoir of Ajmer city, Rajasthan. Ind. J. Env.Sci. 9: 57-61.
28. Sunkad, B.N. and Patii, H.S. 2004. Water quality assessment of Fort Lake of Belgaum (Karnataka) with special reference to zooplankton. J. of Environ. Biol. 25 (1) : 99-102.
29. Swaranlatha, N., Narsingh A., NarsingRao. 1998. Ecological studies of Banjaralake with reference to water pollution. J. Env. Biol. 19 : 179-186.
30. Thirumala,S and B.R.Kiran.2018. Studies on Physico-Chemical parameters of water samples in Shivamogga area, Karnataka. Research Review International Journal of Multidisciplinary Vol 3(8):85-88.
31. Trivedy, R. K. and Goel, P. K. (1986) Chemical and Biological method for water pollution studies. Environmental publication (Karad, India), 6: 10-12.
32. WHO (1997) Guidelines for drinking-water quality, 2nd ed. Vol. 3. Surveillance and control of community supplies. Geneva, World Health Organization

Table.1: Drinking water quality standards

Parameter	Permissible limit	
	WHO, 1994	(BIS,1991)
Colour, Hazen unit, max	Nil	5.0
Turbidity, NTU	5.0	5.0
Odour	Nil	Unobjectionable
Dissolved solids	500	500
Total hardness	100	300
Calcium hardness	75	75
Magnesium hardness	30	30
Alkalinity	200	200
Dissolved oxygen	4-6	4-6
Chloride	250	250
Nitrate	45	45
Iron	0.3	0.3
pH	6.5-8.5	-
BOD	5	-
Potassium	12	-

Table.2: Descriptive statistics of independent water parameters

Treatment →	A (WT,pH,EC)	B (TDS,Tur,Acidity)	C (CO_2,DO,BOD)	D (SO_4,PO_4,NO_3)	Pooled Total
Sum	445.3000	541.7800	73.9900	85.5000	1,146.5700
Mean	49.4778	60.1978	8.2211	9.5000	31.8492
Sum of squares	44,497.8700	48,048.2964	843.4085	1,569.2900	94,958.8649
Sample variance	2,808.1769	1,929.2930	29.3911	94.6300	1,669.7590
Sample std. Dev.	52.9922	43.9237	5.4214	9.7278	40.8627
Std. Dev. Of mean	17.6641	14.6412	1.8071	3.2426	6.8104

Table.3:One-way ANOVA of independent parameters

Source	Sum of squares	Degrees of freedom	Mean square	F statistic	P-value
Treatment	19,549.6375	3	6,516.5458	**5.3618**	**0.0042**
Error	38,891.9284	32	1,215.3728		
Total	58,441.5659	35			

Table.4: Tukey HSD data

Treatments pair	Tukey HSD q statistic	Tukey HSD p-value	Tukey HSD inference
A vs B	0.9225	0.8999947	insignificant
A vs C	3.5503	0.0774272	insignificant
A vs D	3.4402	0.0910464	insignificant
B vs C	4.4728	0.0170841	* p<0.05
B vs D	4.3627	0.0206899	* p<0.05
C vs D	0.1101	0.8999947	insignificant

Table.5 : Scheffe data

Treatments pair	Scheffe t-statistic	Scheffe p-value	Scheffe inference
A vs B	0.6523	0.9341462	insignificant
A vs C	2.5104	0.1196561	insignificant
A vs D	2.4326	0.1379086	insignificant
B vs C	3.1627	0.0315647	* p<0.05
B vs D	3.0849	0.0374514	* p<0.05
C vs D	0.0778	0.9998720	insignificant

Table.6:Bonferroni and Holm data: all parameters simultaneously compared

Treatments	Bonferroni & holm t-statistic	Bonferroni p-value	Bonferroni inference	Holm p-value	Holm inference
A vs B	0.6523	3.1132035	insignificant	1.0377345	insignificant
A vs C	2.5104	0.1038493	insignificant	0.0692329	insignificant
A vs D	2.4326	0.1245681	insignificant	0.0622840	insignificant
B vs C	3.1627	0.0204808	* p<0.05	0.0204808	* p<0.05
B vs D	3.0849	0.0250637	* p<0.05	0.0208864	* p<0.05
C vs D	0.0778	5.6307407	insignificant	0.9384568	insignificant

Table.7: Bonferroni and Holm datas: only pairs relative to A simultaneously compared

Treatments pair	Bonferroni and holm t-statistic	Bonferroni p-value	Bonferroni inference	Holm p-value	Holm inference
A vs B	0.6523	1.5566018	insignificant	0.5188673	insignificant
A vs C	2.5104	0.0519247	insignificant	0.0519247	insignificant
A vs D	2.4326	0.0622840	insignificant	0.0415227	* p<0.05

Table.8: Seasonal fluctuations in physico-chemical characteristics of Sogane pond water

Parameter	Summer	Rainy	Winter
Air temperature	34	31	28
Water temperature	30.5	28	25
pH	7.5	6.9	7.4
Electrical conductivity	160	100	80
Total Dissolved solids	80	38	49.5
Turbidity	90	130	110
Acidity	14.2	15	15.08
CO_2	16	12	16.5
Dissolved Oxygen	6.8	8.16	5.48
Biochemical oxygen demand	3.4	2.2	3.45

Total hardness	38	34	26.2
Calcium	12.9	24.5	18.69
Magnesium	4.2	10.3	4.12
Chloride	24.8	38.4	18.2
Sulphate	20.2	24	22.5
Phosphate	3.10	5.5	4.1
Nitrate	0.9	4.6	0.6

All the parameters are expressed in mg/L except air and water temperature (°C), pH, turbidity (NTU) and electrical conductivity (µmhos/cm).

Figure.1 : View of Sogane pond

Figure.2: study area map

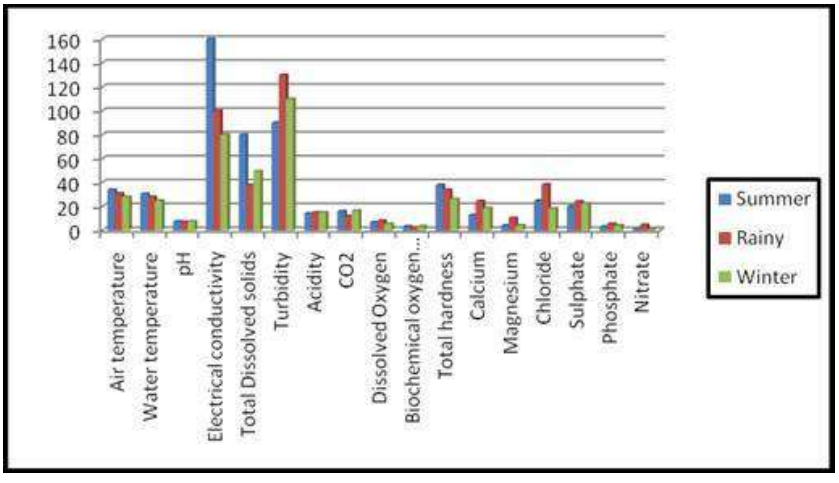

Figure.3 : Seasonal data of physico-chemical characteristics of Sogane pond water

RESEARCH ARTICLE

Optimal Pricing for Substitute Products with Deterioration Constraints

Amarat H. Rathod[1]*, Kunal T. Shukla[2] and Dharmesh K. Katariya[3]

[1]Research Scholar, Gujarat Technological University, Ahmedabad, Gujarat, India and Lecturer, Department of Sciences and Humanities, Government Polytechnic for Girls, (Affiliated to Gujarat Technological University), Ahmedabad, Gujarat, India.
[2]Assistant Professor, Department of Sciences and Humanities, Vishwakarma Government Engineering College, (Affiliated to Gujarat Technological University), Ahmedabad, Gujarat, India.
[3]Assistant Professor, Department of Sciences and Humanities, Shantilal Shah Engineering College, Bhavnagar, (Affiliated to Gujarat Technological University, Ahmedabad), Gujarat, India.

Received: 21 Nov 2024 Revised: 03 Dec 2024 Accepted: 31 Jan 2025

***Address for Correspondence**
Amarat H. Rathod
Research Scholar, Gujarat Technological University,
Ahmedabad, Gujarat, India and Lecturer,
Department of Sciences and Humanities, Government Polytechnic for Girls,
(Affiliated to Gujarat Technological University),
Ahmedabad, Gujarat, India.
E.Mail: amitrathod77@gmail.com

ABSTRACT

In today's market, customers need substitute goods for numerous reasons. There are several factors that influence the decision to choose a substitute product, including price sensitivity, convenience, regional availability, and individualization. Seller can improve consumer satisfaction, sales, and gain by offering substitute items. We highlighted the potential benefits of applying a cross-price selling strategy to maximize sales of high-deteriorating substitute goods. This study aim is to find the optimal selling price, order quantity, and cycle time that maximize the joint profit of two substitutable products subject to deterioration. The global optimality of total average profit is verified through the Hessian matrix method. The result shows that the profit can be increased by providing substitute products and which depend on degree of substitution. This framework is validated through numerical example. Conclusion that discusses potential future paths, constraints, and challenges.

Keywords: Inventory, Deterioration, Substitute Products, Selling Price, Cycle Time.

INTRODUCTION

A substitute product is one that can meet the same objectives or needs of the consumer as the original product, usually providing comparable features, advantages, or functionalities. For example, smartphones from different brands, laptop and desktop computer, LED and LCD TV. For various reasons, such as price sensitivity, convenience, regional availability, and individualization, that influence the decision to choose a substitute product. In today's competitive market, customers often request substitute products from the same store, given the variety and flexibility. This challenge is directly related to customer satisfaction. Customer satisfaction is one of the most important factors in a business (Lee et al. (2016)). Demand for substitute goods has a positive cross-price elasticity, which means that when the price of one product rises, correspondingly increases the demand for the rival. As a result, the seller earns even more by offering different alternatives to the same product. In this paper, we examine the interplay between scale demand, price elasticity, deterioration, degree of substitution, and inventory costs, which shed light on their collective impact on the retailer's business from sales of substitute products in a business environment. For this, we consider two products with different selling prices and different spoilage rates depending on the substitutes. The proposed approach proposes to determine the optimal selling price, order quantity, cycle time and seller's profit, taking into account the effects of positive cross-price elasticity of demand. By understanding customer demands for substitute products, businesses can develop effective competitive strategies, improve product offerings, enhance customer satisfaction, identify market opportunities, and optimize pricing and marketing. In real practice, various industries, including food and beverages, electronics, fashion and apparel, automotive, personal care, and travel and hospitality, provide substitute products, enabling customers to select from similar offerings. The organization of this paper is as follows: Introduction with a brief literature review and research gap; Presenting assumptions and notations; Mathematical formulation; Solution procedure; The numerical example; Sensitivity analysis and finally, article is summarized with concluding remarks and future directions.

LITERATURER RIEVEW

By virtue of its vital role of fostering the connection between producers and end customers, the supply chain has attracted an abundance of attention from researchers. It is an integral component of corporate operations. By providing substitutes at a single location, retailers, who serve as the final link in the supply chain, are essential in establishing a connection between manufacturers and consumers. The following are literature reviews of two significant research areas that form the basis of this article.

The substitution effect in forecasting a business environment

The first relevant literature is research on the cross-price selling strategy approach. Businesses face significant implications from cross-price elasticities, whether positive or negative, across their product offerings. The effect of the presence of positive cross-price elasticity of products in the business environment has attracted the attention of many researchers.McGillivray and Silver (1978) indicated that transferred demand is relatively unimportant for substitutable items with equal unit costs and shortage penalties, particularly when few items are stocked and substitution probabilities are small. Pasternack and Drezner (1991) analyzed optimal inventory levels for single substitution versus no substitution, showing that total optimal order quantities may increase or decrease with substitution revenue. Drezner et al. (1995) also developed an EOQ model for two products with potential substitution, exploring three scenarios: no substitution, full substitution, and partial substitution. Anupindi et al. (1998) created a model for customer behavior, incorporating product substitution and lost sales due to stock outs, specifically tailored to retail vending. Gurnani and Drezner (2000) developed an inventory model that reduces holding costs by determining the optimal runout time, transitioning from high to low inventory holdings. Maity and Maiti (2005) introduced an inventory model for substitute and complementary products with stock-dependent effects on demand and deterioration, and salvage opportunities. Salameh et al. (2014) also integrated research on substitution and joint replenishment, proposing a solution method for the joint replenishment model with substitution (JRMS) for dual-product inventory systems. Rasouli and Kamalabadi (2014) introduced a mathematical

model for coordinated pricing and inventory management of seasonal and substitutable products in a competitive market with finite planning horizon. Krommyda et al. (2015) developed a mathematical model for managing inventory of two mutually substitutable products, where demand for one product can be partially fulfilled by the other during stock outs. Giri et al. (2016) also developed a mathematical model for a two-echelon supply chain, analyzing competition among two substitutable products and one complementary product sold through a common retailer. Taleizadeh et al. (2018) proposed four innovative economic production quantity models, addressing various shortage scenarios for sustainable production. Hadi (2018) formulated an EOQ model to determine optimal joint ordering policies for two products with complementary and substitution effects. Taleizadeh et al. (2019) also examined pricing and inventory strategies for deteriorating complementary and substitutable products, considering demand dependence on selling prices and cross-product price effects.Shah et al. (2019) examined an inventory control problem involving two similar items that can substitute for each other, aiming to improve inventory management decisions. Giri et al. (2022) investigated a single-period joint ordering policy for two deteriorating substitute products with price and inventory dependent demand.

A deterioration constraint factor in supply chain optimization

Another related stream of research explores the concept of inventory deterioration in supply chain management. Deterioration refers to the process of decay, obsolescence, degradation, and decline in quality, condition, and value over time. Ghare and Schrader (1963) were the first to integrate deterioration effects into inventory systems. Goyal (1985) introduced EOQ models incorporating a fixed payment delay offered by suppliers. Benkherouf (1995) also developed an inventory model that accounts for deterioration, time-dependent demand with a downward trend, and shortage constraints. Abad (1996) presented a study on optimal pricing and inventory management for perishable products with partial backordering. Thereafter, Shah and Shah (2000) presented a comprehensive literature survey on inventory models for deteriorating items. Li et al. (2010) conducted an updated literature review on deteriorating inventory models. Bakker et al. (2012) expanded knowledge on inventory management for perishable items, offering new insights. Janssen et al. (2016) conducted a comprehensive review of deteriorating inventory models, covering key developments from 2012-2015.Nath and Sen (2021) also designed an optimization model for managing deteriorating inventory with imperfect quality under advance payment conditions. Kaushik (2023) developed a comparative framework for analyzing EOQ models with preservation and non-preservation approaches, incorporating Weibull deterioration and dynamic demand. Table 1 provides a comparative analysis of the literature, emphasizing the study's unique contributions and research gaps This study examines the interplay between substitute products, deterioration, and demand pattens uncovering gaps in effective inventory management and providing insights for optimizations.

NOTATIONS AND ASSUMPTIONS

The following notations are consistently used through this study.

Symbol	Description (i=1,2)
K_i	Set-up cost ($\$ / order$) for X_i
C_i	Purchase cost ($\$ / unit$) for X_i
h_i	Holding cost ($\$ / unit / time$) for X_i
M_i	Deterioration cost ($\$ / unit / cycle$) for X_i
θ_i	Constant rate ($unit / time$) of deterioration for X_i
T	Cycle time ($year$) (Decision variables)
P	Selling price ($\$ / unit$) for X_i , $P > C$ (Decision variables)
$\Pi(P_1, P_2, T)$	Average total profit (in \$), (Objective function)

$D_i(P_1,P_2)$	Demand rate ($unit/time$) for X_i
$I_i(t)$	Inventory level ($unit$)at time $0 \le t \le T$ for X_i
Q_i	Ordering quantity per cycle ($unit$) for X_i

Assumptions

The following assumptions are considered to develop models:

1. Two products (say) X_1 and X_2 are considered.
2. Lead time is zero and shortages are not allowed.
3. The planning horizon is infinite.
4. Demand rate for X_1 is $D_1(P_1,P_2)=\alpha_1-\beta_1P_1+kP_2$ where $D_1(P_1,P_2)>0$, scale demand $\alpha_1>0$, price elasticity $\beta_1>0$, and degree of substitution $k>0$.
5. Demand rate for X_2 is $D_2(P_1,P_2)=\alpha_2-\beta_2P_2+kP_1$ where $D_2(P_1,P_2)>0$, scale demand $\alpha_2>0$ and $\beta_2>0$ price elasticity.
6. Product X_i deteriorate at a constant rate θ_i ($0<\theta_i<1$). The deteriorated products have no salvage value. $i=1,2$

MATHEMATICAL MODEL

Consider for ($i=1,2$) $I_i(t)$ be the product X_i stock level at any time t with due to deterioration constant rate θ_i per time and customers demand $D_i(P_1,P_2)$ per time starts decline at time over the period $[0,T]$ can be represented by the following differential equation.

$$\frac{dI_i(t)}{dt}+\theta_iI_i(t)=D_i(P_1,P_2),\ 0\le t\le T \tag{1}$$

At $t=T$, $I_i(T)=0$ using this boundary condition solution of Equation (1) gives

The inventory level of product X_1 at time t

$$I_1(t)=\frac{D_1}{\theta_1}\left(e^{\theta_1(T-t)}-1\right) \tag{2}$$

The inventory level of product X_2 at time t

$$I_2(t)=\frac{D_2}{\theta_2}\left(e^{\theta_2(T-t)}-1\right) \tag{3}$$

Also $I_i(0)=Q_i$, Then Equation (2) and (3) gives

Initial inventory level of product X_1

$$Q_1=\frac{D_1}{\theta_1}\left(e^{\theta_1T}-1\right) \tag{4}$$

Initial inventory level of product X_2

$$Q_2 = \frac{D_2}{\theta_2}\left(e^{\theta_2 T} - 1\right) \tag{5}$$

Inventory revenue and cost components define as follows,

The total revenue generated form product X_1 and product X_2

$$SR = \sum_{i=1}^{2} P_i \int_0^T D_i(P_1, P_2)dt \tag{6}$$

The total cost components consist following components

Purchase cost

$$PC = \sum_{i=1}^{2} C_i Q_i \tag{7}$$

Holding cost

$$HC = \sum_{i=1}^{2} h_i \int_0^T I_i(t)dt \tag{8}$$

Ordering cost

$$OC = \sum_{i=1}^{2} K_i \tag{9}$$

Deterioration cost

$$DC = \sum_{i=1}^{2} M_i\left(Q_i - D_i T\right) \tag{10}$$

Therefore, the total average profit per time is given by

$$\prod\left(P_1, P_2, T\right) = \begin{pmatrix} Sales\ revenue - Purchase\ cost - Holding\ cost \\ Ordering\ cost - Deterioration\ cost \end{pmatrix} \tag{11}$$

$$= \frac{1}{T}\sum_{i=1}^{2}\left(P_i \int_0^T D_1(P_1, P_2)dt - C_i Q_i - h_i \int_0^T I_i(t)dt - K_i - M_i\left(Q_i - D_i T\right)\right) \tag{12}$$

SOLUTION PROCEDURE

We use the following process to determine decisions variables optimal levels.

- Step 1: Assign values to all inventory parameters in Equations(12),excluding the decision variable;
- Step 2:Partially differentiate Equations (12) with respect to $P_1, P_2,$ and T to obtain $\frac{\partial \Pi}{\partial P_1}, \frac{\partial \Pi}{\partial P_2},$ and $\frac{\partial \Pi}{\partial T}$.
- Step 3:Solve $\frac{\partial \Pi}{\partial P_1} = 0, \frac{\partial \Pi}{\partial P_2} = 0,$ and $\frac{\partial \Pi}{\partial T} = 0$ simultaneously by mathematical software Maple 18 to obtain value of $P_1, P_2,$ and T respectively.
- Check the concavity of the Equation(10) at solution point through Hessian Matrix method

i.e. $\frac{\partial^2\Pi}{\partial^2 P_1}<0, \frac{\partial^2\Pi}{\partial^2 P_2}<0, \frac{\partial^2\Pi}{\partial^2 T}<0, \det\left(\begin{bmatrix} \frac{\partial^2\Pi}{\partial P_1^2} & \frac{\partial^2\Pi}{\partial P_1 \partial P_2} \\ \frac{\partial^2\Pi}{\partial P_2 \partial P_1} & \frac{\partial^2\Pi}{\partial P_2^2} \end{bmatrix}\right)>0,$

and $\det\left(\begin{bmatrix} \frac{\partial^2\Pi}{\partial P_1^2} & \frac{\partial^2\Pi}{\partial P_1 P_2} & \frac{\partial^2\Pi}{\partial P_1 T} \\ \frac{\partial^2\Pi}{\partial P_2 P_1} & \frac{\partial^2\Pi}{\partial P_2^2} & \frac{\partial^2\Pi}{\partial P_2 T} \\ \frac{\partial^2\Pi}{\partial T P_1} & \frac{\partial^2\Pi}{\partial T P_2} & \frac{\partial^2\Pi}{\partial T^2} \end{bmatrix}\right)<0$

Otherwise, different value in step 1.

- Step 4: Using solutions from Step 2 evaluate optimal ordering quantity of products Q_1^* and Q_2^* from Equation(4) and (5). Obtains total average profit using Equations (12)

NUMERICAL ILLUSTRATION

To illustrate the practical application of proposed model, the following numerical example is considered.

Example 1:The following input key parameters in proper unit are considered.

$\alpha_1 = 10000\, units$, $\alpha_2 = 8000\ units$, $\beta_1 = 2, \beta_2 = 2,\ C_1 = \$800\ per\ unit$, $C_2 = \$800\ per\ unit$, $\theta_1 = 0.2,$ $\theta_2 = 0.2, K_1 = \$200\ per\ order$, $K_1 = \$200\ per\ order$, $k = 0.3,\ h_1 = \$20/unit/time$, $h_2 = \$20/unit/time$, $M_1 = \$50/unit$ / Cycle time, $M_2 = \$50/unit$ / Cycle time.

The optimal solution is derived using the described procedure, facilitated by Maple 18software.

To verify the concavity of the example at the optimal solution using Hessian Matrix method.

$$\frac{\partial^2\Pi}{\partial^2 P_1}=-4<0, \frac{\partial^2\Pi}{\partial^2 P_2}=-4<0, \frac{\partial^2\Pi}{\partial^2 T}=-5.16\times10^7<0, \det\left(\begin{bmatrix} \frac{\partial^2\Pi}{\partial P_1^2} & \frac{\partial^2\Pi}{\partial P_1 \partial P_2} \\ \frac{\partial^2\Pi}{\partial P_2 \partial P_1} & \frac{\partial^2\Pi}{\partial P_2^2} \end{bmatrix}\right)=15.64>0$$

and $\det\left(\begin{bmatrix} \frac{\partial^2\Pi}{\partial P_1^2} & \frac{\partial^2\Pi}{\partial P_1 P_2} & \frac{\partial^2\Pi}{\partial P_1 T} \\ \frac{\partial^2\Pi}{\partial P_2 P_1} & \frac{\partial^2\Pi}{\partial P_2^2} & \frac{\partial^2\Pi}{\partial P_2 T} \\ \frac{\partial^2\Pi}{\partial T P_1} & \frac{\partial^2\Pi}{\partial T P_2} & \frac{\partial^2\Pi}{\partial T^2} \end{bmatrix}\right)=\det\left(\begin{bmatrix} -4 & 0.6 & 171.06 \\ 0.6 & -4 & 101.83 \\ 171.06 & 101.83 & -5.16\times10^7 \end{bmatrix}\right)=-8.08\times10^8<0$

SENSITIVE ANALYSIS

A sensitivity analysis is conducted for Example 1, examining the impact of inventory parameter variations (-20%, -10%, +10%, +20%) on optimal solutions. Observation and managerial insight. From Table 3the following points are observed.

- Increasing scale demand (α_1) yields significant profit growth , boosts selling prices (P_1, P_2), and increases ordering quantity (Q_1),but reduces cycle length (T) and ordering quantity (Q_2). This implies that products experiencing high market demand command premium prices, as customers are willing to pay more for trending items.
- Increasing scale demand (α_2) yields significant profit growth , boosts selling prices (P_1, P_2), and increases ordering quantity (Q_2), but reduces cycle length (T) and ordering quantity (Q_1).
- Price elasticity (β_1) positively impacts cycle time (T) and order volume (Q_2) but negatively affects selling prices (S_1, S_2), order volume (Q_1), and total average profit, reversing when elasticity decreases. This implies that an increase in the price of one substitute product leads to a rise in demand for its alternative product(s).
- Price elasticity (β_2) positively impacts cycle time (T) and order volume (Q_1) but negatively affects selling prices (S_1, S_2), order volume (Q_2), and total average profit, reversing when elasticity decreases.The study provides actionable recommendations for marketers to drive business growth. When designing alternative product offerings, marketers should emphasize key factors like variety, value, tailoring, and sustainability.
- Parameters $h_1, C_1, \theta_1,$ and M_1 positively influence selling price (P_1) but adversely affect cycle time (T), selling price (P_2), initial order volumes (Q_1, Q_2), and total average profit.This shows that effective cost management is vital for maintaining control over product pricing and ensuring long-term profitability.
- Parameters $h_2, C_2, \theta_2,$ and M_2 positively influence selling price (P_2) but adversely affect cycle time (T), selling price (P_1), initial order volumes (Q_1, Q_2), and total average profit.

DISCUSSION AND CONCLUSION

This research examines the interplay between scale demand, price elasticity, deterioration, substitute degree, and inventory costs, shedding light on their collective impact on substitute products in business environments. Nowadays, numerous businesses achieve significant growth through customer satisfaction, brand visibility, and additional revenue by offering substitute products at one location. Major players like Apple (iPhones), Dell (budget-friendly laptops), and Samsung (affordable smartphones) now prioritize selling core products with substitute options. This study shows the impact of the presence of positive cross-price elasticity of products in the business environment, such as substitution pricing techniques and cross-price effects that allow sellers to earn higher profits. The numerical example suggests that retailers can apply the model as a tool that helps in making decisions. Sensitivity analysis, trade credit, and advance cash credit payment under various assumptions may all be taken into consideration in future research on this subject. It can be expanded further to address the actual situation, for as by examining consumer preference patterns that include spending patterns, choices, trends, and environmental concerns. Predicting the customer's decision is just like the limitation of this study. Further research on this topic could consider sensitivity analysis, trade credit, and also advance-cash-credit payment under several assumptions. It can be extended in other directions to catch up with the real case, like analyzing the customer return pattern including shipping, repacking, and resale costs.

ACKNOWLEDGMENTS

We appreciate the valuable time and expertise of the reviewers and the journal editor, whose feedback and acceptance have contributed significantly to the improvement of this manuscript.

REFERENCES

1. Abad PL. Optimal pricing and lot-sizing under conditions of perishability and partial backordering. Management Science 1996; 42(8):1093–1104.
2. Anupindi R, Dada M and Gupta S. Estimation of consumer demand with stock out based substitution: an application to vending machine products. Market Science 1998;17(4):406–423.
3. Bakker M, Riezebos J, and Teunter RH. Review of inventory systems with deterioration since 2001. European Journal of Operational Research 2012;221(2):275–284.
4. Benkherouf L. On an inventory model with deteriorating items and decreasing time-varying demand and shortages. European Journal of Operational Research 1995; 86(2):293–299.
5. Drezner Z, Gurnani H, Pasternack BA. EOQ model with substitution between products. Journal of the Operational Research Society 1995; 46(7):887–891.
6. Ghare PM and Schrader GF. A model for an exponential decaying inventory. Journal of Industrial Engineering 1963; 14:238-243.
7. Giri RN, Mondal SK, and Maiti M. Analysis of pricing decision for substitutable and complementary products with a common retailer. Pacific Science Review A: Natural Science and Engineering 2016;18(3):190-202.
8. Giri RN, Kumar SK, and Maiti M. Joint ordering inventory policy for deteriorating substitute products with price and stock dependent demand. International Journal of Industrial Engineering: Theory, Applications and Practice 2022; 27(1).
9. Goyal SK. Economic order quantity under conditions of permissible delay in payments. Journal of the Operational Research Society 1985; 36:335-338.
10. Gurnani H, Drezner Z. Deterministic hierarchical substitution inventory models. Journal of the Operational Research Society 2000; 51(1):129–133.
11. Hadi M. Economic order quantity for joint complementary and substitutable items, Mathematics and Computers in Simulation 2018; 154:34-47.
12. Janssen L, Claus T, and Sauer J. Literature review of deteriorating inventory models by key topics from 2012 to 2015. In International Journal of Production Economics 2016; 182:86-112.
13. Kaushik J. Inventory model for perishable items for ramp type demand with an assumption of preservative technology and Weibull deterioration, International Journal of Procurement Management 2023; 18(2):238–259.
14. Krommyda IP, Skouri K, and Konstantaras I. Optimal ordering quantities for substitutable products with stock-dependent demand. Applied Mathematical Modeling 2015; 39(1):147–164.
15. Lee, Yu-Cheng & Wang, Yu-Che & Lu, Shu-Chiung & Hsieh, Yi-Fang & Chien, Chih-Hung & Tsai, Sang-Bing & Dong, Weiwei. (2016). An Empirical research on customer satisfaction study: a consideration of different levels of performance. SpringerPlus 2016;5
16. Li R, Lan H, and Mawhinney JR. A review on deteriorating inventory study, Journal of Service Science and Management 2010; 03(01):117–129.
17. Maity K, and Maiti M. Inventory of deteriorating complementary and substitute items with stock dependent demand. American Journal of Mathematical and Management Sciences 2005; 25(1–2):83–96.
18. McGillivray AR, Silver EA. Some concepts for inventory control under substitutable demand. Information Systems and Operation Research 1978; 16(1):47–63.
19. Nath BK, and Sen N. An inventory model for deteriorating items with imperfect quality under advance payment policy. Operations Research and Decisions 2021; 31(3):109–135.
20. Pasternack B, Drezner Z. Optimal inventory policies for substitutable commodities with stochastic demand. Naval Research Logistics 1991; 38:221–240.

21. Rasouli N and Kamalabadi I. Joint pricing and inventory control for seasonal and substitutable goods mentioning the symmetrical and asymmetrical substitution. International Journal of Engineering 2014; 27(9):1385–1394.
22. Salameh MK, Yassine AA, Maddah B. and Ghaddar L. Joint replenishment model with substitution. Applied Mathematical Modelling 2014; 38(14):3662–3671.
23. Shah NH, Chaudhari U, and JaniMY. Inventory Control Policies for Substitutable Deteriorating Items Under Quadratic. Operations and Supply Chain Management 2019; 12(1):42–48.
24. Shah NH and Shah YK. Literature survey on inventory models for deteriorating items, Ekonomski anali 2000; 44(1):221–237.
25. Taleizadeh AA, Babaei MS, Sana SS, & Sarkar B. Pricing decision within an inventory model for complementary and substitutable products. Mathematics 2019; 7(7):568.
26. Taleizadeh AA, Soleymanfar VR, & Govindan K. Sustainable economic production quantity models for inventory systems with shortage. Journal of Cleaner Production 2018; 174: 1011-1020.

Table 1. Comparative analysis of literature and contribution of this study

Author(s) name	Demand	Deterioration	Substitute items
Ghare and Schrader (1963)	Exponentially decreasing	Constant	×
McGillivray and Silver (1978)	Substitutable	×	✓
Pasternack and Drezner (1991)	Stochastic demand	×	✓
Benkherouf (1995)	Time varying	Constant	×
Maity and Maiti (2005)	Stock out based	Stockdependent	✓
Krommyda et al.(2015)	Stock-dependent	×	✓
Giri et al. (2016)	Selling price dependent	×	✓
Shah et al. (2019)	Quadratic	Constant	✓
Giri et al. (2020)	Price and stock dependent	Constant	✓
This study	Selling price dependent	Constant	✓

Table 2. Optimal solutions for Example

$P_1^*(\$)$	$P_2^*(\$)$	$T^*(year)$	$Q_1^*(unit)$	$Q_2^*(unit)$	$\prod(P_1,P_2,T)^*(\$)$
3265.64	2680.48	0.02493	106.82	90.46	18393861.80

Table 3. Sensitivity analysis of key inventory parameters for Example 1.

Parameter	Value	% Changes	T^* *year*	P_1^* \$	P_2^* \$	Q_1^* *unit*	Q_2^* *unit*	$\prod^*(P_1,P_2,T)$ \$
α_1	10000	+20%	0.02327	3777.066	2757.151	123.010	84.420	23831980.44
		+10%	0.02406	3521.349	2718.814	115.124	87.285	20985024.19
		-10%	0.02591	3009.929	2642.148	98.019	94.015	16058498.50
		-20%	0.02702	2754.227	2603.821	98.022	88.651	13978938.59
α_2	8000	+20%	0.02398	3326.972	3089.655	106.235	102.729	22207422.36
		+10%	0.02445	3296.304	2885.067	104.712	98.484	20218794.49
		-10%	0.02546	3234.971	2475.893	109.051	82.148	16732625.55
		-20%	0.02601	3204.307	2271.307	111.433	73.510	15235086.11
β_1	2	+20%	0.02524	2779.120	2607.510	104.049	91.559	15733672.28
		+10%	0.02509	2999.801	2640.608	105.439	91.006	16937336.02
		-10%	0.02479	3592.063	2729.439	108.180	89.930	20189697.80
		-20%	0.02465	4002.459	2790.995	109.532	89.406	22455765.81

β_2	2	+20%	0.02506	3203.740	2267.801	107.363	88.406	16458783.86
		+10%	0.02500	3231.816	2454.990	107.088	89.437	17335360.06
		-10%	0.02487	3307.166	2957.362	106.545	91.485	19696485.44
		-20%	0.02481	3359.380	3305.470	106.276	92.501	21337425.44
k	0.3	+20%	0.02488	3356.951	2782.848	106.942	90.853	19247853.05
		+10%	0.02491	3310.388	2730.829	106.879	90.658	18812993.40
		-10%	0.02497	3222.608	2631.704	106.752	90.268	17989647.61
		-20%	0.02499	3181.222	2584.418	106.689	90.072	17599593.91
h_1	2	+20%	0.02477	3265.654	2680.474	106.109	89.866	18393649.27
		+10%	0.02485	3265.645	2680.477	106.461	90.163	18393755.29
		-10%	0.02502	3265.628	2680.482	107.174	90.766	18393969.02
		-20%	0.02510	3265.619	2680.485	107.536	91.072	18394076.11
h_2	2	+20%	0.02480	3265.630	2680.500	106.218	89.955	18393681.85
		+10%	0.02487	3265.633	2680.489	106.515	90.208	18393771.68
		-10%	0.02501	3265.640	2680.469	107.118	90.720	18393952.50
		-20%	0.02508	3265.643	2680.459	107.424	90.979	18394043.18
C_1	800	+20%	0.02398	3345.783	2680.448	98.864	87.572	17721384.47
		+10%	0.02443	3305.710	2680.463	102.693	88.929	18054401.29
		-10%	0.02550	3225.561	2680.498	111.278	92.199	18739769.21
		-20%	0.02613	3185.484	2680.518	116.136	94.168	19092126.49
C_2	500	+20%	0.02437	3265.610	2730.583	104.759	85.961	18036118.73
		+10%	0.02464	3265.623	2705.531	105.749	88.164	18213731.91
		-10%	0.02525	3265.651	2655.426	107.967	92.868	18576509.14
		-20%	0.02558	3265.667	2630.372	109.210	95.390	18761674.45
θ_1	0.2	+20%	0.02363	3265.776	2680.437	101.252	85.719	18392093
		+10%	0.02426	3265.708	2680.457	103.922	87.996	18392965.54
		-10%	0.02568	3265.562	2680.503	109.965	93.149	18394784.04
		-20%	0.02648	3265.484	2680.530	96.088	96.088	18395734.08
θ_2	0.2	+20%	0.02419	3265.601	2680.589	103.633	87.803	18392880.48
		+10%	0.02456	3265.619	2680.535	105.189	89.103	18393367.55
		-10%	0.02533	3265.655	2680.422	108.519	91.887	18394364.02
		-20%	0.02575	3265.675	2680.364	110.306	93.380	18394873.89
M_1	50	+20%	0.02485	3265.645	2680.477	106.461	90.163	18393755.49
		+10%	0.02489	3265.641	2680.478	106.638	90.313	18393808.78
		-10%	0.02498	3265.632	2680.481	106.994	90.614	18393915.34
		-20%	0.02502	3265.628	2680.482	107.174	90.766	18393969.00
M_2	50	+20%	0.02487	3265.633	2680.489	106.515	90.208	18393771.84
		+10%	0.02490	3265.635	2680.484	106.665	90.335	18393816.78
		-10%	0.02497	3265.638	2680.474	106.967	90.591	18393907.14
		-20%	0.02501	3265.640	2680.469	107.118	90.720	18393952.58

Indian Journal of Natural Sciences *www.tnsroindia.org.in ©IJONS*

Vol.15 / Issue 88 / Feb / 2025 *International Bimonthly (Print) – Open Access* *ISSN: 0976 – 0997*

RESEARCH ARTICLE

Nano - Pesticides: in Enhancing Agricultural Productivity and Managing Associated Risk

Satyalakshmi S, Srinivasa Rao Y and Vandana Rani M*

Department of Pharmaceutics, Vignan Institute of Pharmaceutical Technology, Duvvada, Visakhapatnam, Andhra Pradesh, India

Received: 21 Nov 2024 Revised: 03 Dec 2024 Accepted: 23 Jan 2025

***Address for Correspondence**
Vandana Rani M,
Student,
Department of Pharmaceutics,
Vignan Institute of Pharmaceutical Technology,
Visakhapatnam,
Andhra Pradesh, India.
E.Mail: lakshmisiragam48@gmail.com

ABSTRACT

Nano-pesticides represent a burgeoning field in agriculture, leveraging nanotechnology to revolutionize pest management. Their benefits include enhanced efficacy, reduced environmental impact, and targeted delivery mechanisms. However, challenges persist in their application, including regulatory hurdles, environmental concerns, and scalability issues. Understanding their toxicological impact on human health and the environment is crucial. Nano-pesticides function through various mechanisms, and their formulation continues to evolve. Despite advancements, their widespread adoption remains limited. This review provides a concise overview of nano-pesticides, highlighting their benefits, application challenges, toxicological impacts, mechanism of action, formulation, and current status in agricultural practices.

Keywords: Nanotechnology, Nano-pesticides, Toxicology, Environmental impact, Targeted delivery.

INTRODUCTION

Pesticides are widely used in agriculture to increase crop yields and operational effectiveness. The application of nanotechnology to the development of pesticides presents innovative ways to improve upon conventional farming practices. The incorporation of nanotechnology into pesticide formulation holds significant promise for enhancing pesticide efficacy and mitigating adverse ecological impacts.[1] Between 2020 and 2027, the global nanopesticide market is expected to increase at a notable compound annual growth rate (CAGR) of 14.6 %.[2] The fast-developing

field of nanotechnology holds the potential to revolutionize food systems and tackle the urgent problem of food security. It has the potential to move agriculture away from wasteful resource use and environmental damage and toward more advanced systems with more effective material utilization and targeted applications. This would lessen crop losses brought on by different stresses while simultaneously giving environmental concerns a top priority. Pesticides are frequently used in agriculture to control insect pests and plant diseases. Nevertheless, there are a lot of concerns to the environment and human health as a result of the overuse of these chemicals per hectare. The advent of nanotechnology has made it easier to manufacture nano pesticides, which are more effective despite having less active components, to address these problems with conventional pesticides. With their extraordinarily high surface area-to-volume ratios, carrier molecules or active nanosized components provide nanopesticides unique and marketable advantages.[3] Physical, physicochemical, and chemical methods are used to produce chemicals known as nano pesticides, which are intended to eradicate weeds, insects, and germs at the nanoscale. At the moment, the classification of nanopesticides is based mostly on particle size, and there is no globally accepted definition for this term. Some studies have suggested classifying nanopesticides based on a size threshold of 100 nm; yet, this standard is deemed excessively general and ignores a large number of nanopesticides. According to Kah and Hofmann, nano pesticides are plant protection agents that have particle sizes of less than 1000 nm and are prefixed with "nano," or they are small-particle agents that have unique features. Therefore, in a larger sense, nanopesticides are not limited to a size of 100 nm.[4] Fig. 1 represents the significance of nanopesticides. It is still unknown how pesticide nanoformulations may affect groundwater, soil, and non-target creatures in the environment. Because of their huge surface area, nano-particles can break down quickly in the presence of sunlight, which could lessen the effectiveness of active substances. Small droplet sizes may also cause premature evaporation before the intended aim is reached. It is vital yet mainly unknown to comprehend how nanoformulations interact with different trophic levels, plants, and microbes. Conversely, because of their improved toxicity, extended durability, and greater mobility, these formulations may pose additional pollution concerns to soils and aquatic bodies. Their release into the environment is determined by the characteristics of the nanocarriers and the way the active components are arranged within the nano formulation matrix. According to reports, long-term delayed release of nanoparticles may affect organisms that are not the intended target.[5] Nano-pesticides, with their ability to reduce chemical consumption overall, minimize harmful residues, and improve overall crop protection, provide a wonderful approach to developing an environmentally friendly and sustainable agricultural system

.

Nanopesticides formulations and mechanism

Formulations[6]

Formulation of nano pesticides represented in Fig.2

a) Nanospheres: Aggregates, in which the active ingredient is uniformly dispersed throughout the polymer matrix, are the most common kind of nanomaterials used in biocidal release formulations.

b) Nano capsules: Aggregates, usually found close to the center, concentrate the active component encircled by a matrix polymer.

c) Nano gel: Water-absorbing hydrophilic polymers, usually cross-linked, are prone to absorbing large amounts of water.

d) Nano Micelles: A mixture of hydrophilic and hydrophobic molecules in aqueous solutions that form an aggregation.

e) Nanofibers: Structures that are created by a variety of techniques, such as electrospinning, thermally induced phase separation, drawing, template, and self-assembly, are referred to as nanostructures.[8] Table 1 describes various nanoformulations in controlled release systems.

Mechanism

Ticks are affected by nanopesticides in a variety of ways, including by altering proteins or lipids, causing oxidative stress, or interfering with tick metabolism (Figure 3). Because of their surface property-driven toxicity in biological

models, silver nanoparticles have been thoroughly investigated for their cytotoxicity and genotoxicity cycles. By piercing the cuticle layer and producing cellular dehydration, silicon and aluminum nanopesticides ultimately lead to tick fatality.[27]

Benefits of nanopesticides in agricultural productivity

In contrast to conventional pesticide compositions, nanoformulations are designed to improve the solubility of insoluble or weakly soluble active components, allowing for the biocide to be released in a controlled and targeted manner. Therefore, a lower concentration of the active ingredient per unit area works well for application, providing continuous administration that keeps the product effective for extended periods. Reduced dosages thereby reduce phytotoxicity, non-target effects, and production costs. Furthermore, until the active ingredient is released, controlled-release formulations need to stay inert.[3] Because most nano-pesticide formulations have a high specificity, nanotechnology is a useful technique for creating novel, environmentally acceptable pesticide formulations. Nano-pesticides' targeted distribution and controlled release can increase pesticide efficacy while lowering residual levels and pollution in the environment. For example, by using light-sensitive, thermo-sensitive, humidity-sensitive, enzyme-sensitive, and soil pH-sensitive high-polymer materials for pesticide administration, nano-microcapsule formulations demonstrate gradual release and protective qualities. By increasing droplet adherence to plant surfaces, nano-pesticide formulations improve the dispersion and bioactivity of the active components in the pesticide and decrease drift losses. Because of their small size, improved droplet ductility, wettability, and target adsorption when applied in fields, nano-pesticides outperform conventional formulations (D-Dust, G-Granule, P-Pellet, EC-Emulsifiable Concentrate, WP-Wettable Powder, and WDG-Water Dispersible Granule, for example) in terms of efficacy. The use of nanopesticides is. Nano-pesticides are a great way to create a sustainable and environmentally friendly agricultural system since they use fewer chemicals, leave fewer harmful residues, and improve crop protection in general.[28] Benefits of nano-pesticides over conventional pesticides were shown in Fig. 4.

Challenges in nano-pesticide application

Nanopesticides have several advantages; however they are also known to have ecotoxicological effects. Concerning food security, nutrition, and environmental sustainability, nanopesticides are a revolutionary development in agriculture. Significant progress has been made in tackling issues related to forestry, the environment, and public health, including urbanization, energy scarcity, resource sustainability, and ecotoxicity. The environmental problems caused by traditional pesticides are successfully addressed by nanopesticides. Utilizing functional molecules as agrochemical carriers, these formulations operate at the nanoscale (sizes range from 1 nm to 200 nm). Their greater surface area and reduced size provide. Compared to typical pesticides, their higher surface area and smaller size provide many benefits, such as uniform dispersion on insect surfaces, improved mobility, solubility, biodegradability of active components, and improved formulation stability. As a result, when it comes to controlling target pests, nanopesticides work better than bulk chemicals. To provide a strong and focused effect, several innovative formulations have been created, including metal compound-based nanopesticides, nano emulsions, nanosuspensions, and nanogels. Nanoformulations provide increased soil quality, more leaf coverage, and systemic target efficiency, all of which boost agricultural productivity and nutritional security. Because of their reduced dosage effectiveness, they are being used more frequently as nano-pesticides, nano fertilizers, and nano delivery systems. However, the extensive use of innovative nanopesticides results in the introduction of a fresh environmental contaminant. Thus, before they are widely used in crop production and protection, a thorough understanding of nanopesticide formulations, their interactions, and any potential detrimental effects is crucial.[29] Many factors, such as the characteristics of the nano pesticide, its concentration, how it is applied, how long it is exposed, and the surrounding environment, might harm non-target organisms. The soil microbiota is negatively impacted by commercial nanopesticides that use copper oxide (CuO) and silver oxide (AgO) formulations at the physiological, metabolic, and genetic levels. Due to the resilience and self-recovery mechanisms of soil ecosystems, these impacts are only temporary at concentrations relevant to agriculture over long-term trials.[30] Although research on the long-term effects of nano pesticides on soil health is ongoing, possible detrimental effects are a source of worry. Because of their greater surface area and reactivity, nano pesticides may be more toxic, which could hurt soil microorganisms,

plant growth, and soil fertility as a whole. Furthermore, they might eventually collect in the soil and endanger the ecology, possibly contaminating groundwater.

Toxicity and environmental impact

The possible hazards and ecological consequences linked to formulations based on nanoscale technology are highly concerning and necessitate prompt action. Regarding the existence and impacts of nanoformulations in soil, surface water, and groundwater as well as their effects on creatures that are not targets, precise predictions are still lacking. Several chemical characteristics, including pH, ionic strength, and the presence of dissolved molecules in the surrounding environment, influence the fate of nanoformulations. This emphasizes how crucial it is to address several essential issues that are covered in the sections that follow.[31]

Direct toxicity on humans and environment

Many pesticides have known adverse consequences when applied in nano-scale formulations, according to experts. When formulating at this scale, it is imperative to carefully analyze the potential repercussions linked with nano dimensions as well as the expected unfavorable outcomes. To definitively prove that nano-scale formulations are detrimental and to comprehend the relevant elements, including particle size, charge, shape, and chemistry, more research is required.[31] Nanopesticides seem to have a bright future in agricultural development. But there is serious worry about human exposure to dangerous agrochemicals that can cross biological barriers (blood-brain, blood-placental, and blood-retinal, for example) and cause irreparable harm to important organs. At this time, there is a greater focus on evaluating the dangers related to exposure to hazardous nanopesticides, which can have both toxic and genotoxic effects. This entails looking into the physicochemical aspects of nanopesticides, such as size, electrical charge, and surface features, in addition to the effect on the bulk material's chemical composition.[32]

When nano pesticides are prevalent in the environment surrounding the pathogen of interest, there is a substantial risk to human health. These pesticides include nanoparticles that can get into the respiratory system or nose of a person and end up in the lungs. Smaller than 20 nm nanoparticles have the ability to become lodged in the nasopharyngeal region. Smaller particles are more dangerous if they share the same crystalline composition and structure. Consequently, microscopic nanoparticles possess the capacity to induce fibrosis, inflammation, and tumorigenesis. Certain types of nanoparticles produce an increase in inflammation and macrophage activity by promoting the production of viral receptors. Conversely, SiO_2 and TiO_2 nanoparticles reduce the expression of receptors.[33]

Durability and Persistence

The persistence of nano pesticides in the environment is the main determinant of the dangers associated with their use. Continuous release or suspension over an extended period makes non-target organisms susceptible.

Bioavailability

The persistence of nano pesticides in the environment is the main determinant of the dangers associated with their use. For an extended period, continual release or suspension makes non-target organisms susceptible.

Release profile/degradation

The kind of nanocarrier used and how these components are distributed throughout the matrix are two important variables that affect the release of active ingredients. Research suggests that several parameters, such as surface desorption, dispersion within the polymer matrix, and polymer degradation, affect the effectiveness of active substances and their impact on the environment.

Fate of the carrier

The focus of current research is on carriers made of naturally biodegradable polymers, including lipids or polysaccharides, which break down into byproducts that are not very harmful.[31]

Current research and future direction

Advanced technologies have made it feasible for agrochemicals, a family of fertilizers and inorganic insecticides, to be widely used, but prolonged and acute exposure to them endangers the ecosystem. Green technologies are being used by scientists from all around the world to address these problems and safeguard the food supply and way of life. Notwithstanding some environmental concerns during the synthesis process, nanotechnologies provide promising opportunities for agricultural solutions. Many different types of nanomaterials enable the synthesis of natural insecticides that are both environmentally safe and highly effective. The application of nano-formulations extends the shelf life of products, lowers dosage needs, and enhances efficacy; controlled-release techniques also aid in the administration of pesticides. By altering the kinetics, mechanisms, and routes of conventional pesticides, nanotechnology increases their bioavailability while preventing resistance mechanisms and boosting efficacy. A brand-new, more secure, and ongoing development of nanoparticles is bringing about a new era of safer, more ecologically friendly pesticides that are more effective for all living things, and they also benefit life and the environment.[34] Given their greater efficiency, several research findings suggest that nano pesticides may eventually totally replace conventional pesticides. This is mainly because nanoparticles have different properties from bigger materials because of their higher surface-to-volume ratio.[35] Silicon nanoparticles (SiNPs) present a novel and environmentally acceptable substitute for storage pest control. They solve issues related to chemical pesticides by leaving no residue in the environment or on stored goods. With a focused mode of action and little harm to organisms that are not targeted, SiNPs also aid in preventing the emergence of pest resistance.[36]

CONCLUSION

Compared to conventional pesticides, nano pesticides have better-targeted delivery, greater efficacy, and less environmental impact, making them potential options for raising agricultural productivity. Their characteristics at the nanoscale enable more accurate application and less environmental pollution. Additionally, by lowering exposure levels and providing regulated release mechanisms, they can reduce toxicological risks to human health. Notwithstanding, obstacles still exist for their extensive implementation, such as regulatory apprehensions, possible inadvertent ecological ramifications, and vagueness regarding the ultimate effects on soil well-being and biodiversity. To ensure the safe integration of nano pesticides into agricultural practices, it is imperative to weigh their benefits against thorough risk assessment processes. To make informed decisions and promote sustainable agricultural development, more investigation is needed on their ecological effects, environmental fate, and potential for bioaccumulation. Researchers, legislators, and stakeholders must work together to overcome these obstacles and fully utilize nanopesticides while preserving the environment and public health.

Declaration of competing interest

The authors declare that they have no known competing financial interests or personal relationships that could have appeared to influence the work reported in this paper.

ACKNOWLEDGMENTS

We are grateful to the Chairman of the Vignan Group of Institutions, Dr. L. Rathaiah, for giving facilities for this review.

REFERENCES

1. Tang Y, Zhao W, Zhu G, Tan Z, Huang L, Zhang P, Gao L, Rui Y. Nano-pesticides and fertilizers: solutions for global food security.2024; 14(1): 90.
2. Global Nanopesticide Market Size, Share, Growth, Industry Trends, Competitive Analysis and Forecast to 2030. 2023; Report ID: RC14462.

3. Yadav JJ, Poonam B, Ajay K, Prem K, Sudheer J, Maha SG. Nanopesticides: current status and scope for their application in agriculture.2022; 58: 1-17.
4. Yin J, Su X, Yan S, Shen J. Multifunctional nanoparticles and nanopesticides in agricultural application. 2023; 13(7): 1255.
5. Kah M, Beulke S, Tiede K, Hofmann T. Nanopesticides: state of knowledge, environmental fate, and exposure modeling.2013; 43(16): 1823-1867.
6. Harish V, Tewari D, Gaur M, Yadav AB, Swaroop S, Bechelany M, Barhoum A. Review on nanoparticles and nanostructured materials: bioimaging, biosensing, drug delivery, tissue engineering, antimicrobial, and agro-food applications. 2022; 12: 457.
7. Harish V, Tewari D, Gaur M, Yadav AB, Swaroop S, Bechelany M, Barhoum A. Review on nanoparticles and nanostructured materials: bioimaging, biosensing, drug delivery, tissue engineering, antimicrobial, and agro-food applications.2022; 12: 457.
8. Rathna VN, Gundloori AS, Naresh K. Chapter 19 - Nanobased intravenous and transdermal drug delivery systems, applications of targeted nano drugs and delivery systems.2019; 551-594.
9. Xing K, Chen XG, Liu CS, Cha DS, Park HJ. Oleoyl-chitosan nanoparticles inhibit *Escherichia coli* and *Staphylococcus aureus* by damaging the cell membrane and putative binding to extracellular or intracellular targets.2009; 132: 127-133.
10. Liang W, Yu A, Wang G, Zheng F, Hu P, Jia J, Xu H. A novel water-based chitosan-La pesticide nanocarrier enhancing defense responses in rice (*Oryza sativa L.*) growth. 2018; 199: 437-444.
11. Chen H, Zhi H, Liang J, Yu M, Cui B, Zhao X, Sun S, Wang Y, Cui H, Zeng Z. Development of leaf-adhesive pesticide nanocapsules with pH-responsive release to enhance retention time on crop leaves and improve utilization efficiency. 2021; 9: 783-792.
12. Mustafa IF, Hussein MZ. Synthesis and technology of nanoemulsion-based pesticide formulation. 2020; 10: 1608.
13. de Oliveira JL, Campos EVR, Pereira AES, Pasquoto T, Lima R, Grillo R, de Andrade DJ, *et al*. Zein nanoparticles as eco-friendly carrier systems for botanical repellents aiming sustainable agriculture. 2018; 66: 1330-1340.
14. Tong Y, Wu Y, Zhao C, Xu Y, Lu J, Xiang S, Zong F, Wu X. Polymeric nanoparticles as a metolachlor carrier: Water-based formulation for hydrophobic pesticides and absorption by plants.2017; 65: 7371-7378.
15. Jacques MT, Oliveira JL, Campos EVR, Fraceto LF, Silva AD. Safety assessment of nanopesticides using the roundworm *Caenorhabditis elegans*. 2017; 139: 245-253.
16. de Oliveira JL, Campos EVR, Germano-Costa G, Lima R, Della Vechia JF, Soares ST, *et al*. Association of zein nanoparticles with botanical compounds for effective pest control systems. *2019;* 75: 1855-1865.
17. Zhang J, Zhao C, Liu Y, Cao L, Wu Y, Huang Q. Size-dependent effect of prochloraz-loaded PEG-PLGA micro- and nanoparticles.2016; 16: 6231-6237.
18. da Silva Gundel S, Rodrigues dos Reis T, Marquezan Copetti P, Reis Favarin F, RoratoSagrillo M, Schafer da Silva A. Evaluation of cytotoxicity, genotoxicity and ecotoxicity of nanoemulsions containing Mancozeb and Eugenol. 2019; 169: 207-215.
19. Saini A, Panwar D, Singh Panesar P, Bandhu Bera M. Encapsulation of functional ingredients in lipidic nanocarriers and antimicrobial applications: A review. 2021; 19: 1107-1134.
20. Cui J, Sun C, Wang A, Wang Y, Zhu H, Shen Y, Li N, Zhao X, Cui B, Wang C. Dual-functionalized pesticide nanocapsule delivery system with improved spreading behavior and enhanced bioactivity. 2020; 10: 220-228
21. Heydari M, Amirjani A, Bagheri M, Sharifian I, Sabahi Q. Eco-friendly pesticide based on peppermint oil nanoemulsion: Preparation, physicochemical properties, and its aphicidal activity against cotton aphid. 2020; 27: 6667-6679.
22. Sharma A, Kumar Sharma N, Srivastava A, Kataria A, Dubey S, Sharma S, Kundu B. Clove and lemongrass oil based non-ionic nanoemulsion for suppressing the growth of plant pathogenic Fusarium oxysporum f. sp. lycopersici. 2018; 23: 353-362.
23. de CSP, Silva PLA, de Rezende EM, Valquiria dos Reis M, Teixeira Lago AM, Ribeiro Carvalho G, Paiva R. Production and efficacy of neem nanoemulsion in the control of *Aspergillus flavus* and *Penicillium citrinum* in soybean seeds. 2019; 155: 1105-1116.

24. Keskin D, Zu G, Forson AM, Tromp L, Sjollema J, Van Rijn P. Nanogels: A novel approach in antimicrobial delivery systems and antimicrobial coatings. 2021; 6: 3634-3657.
25. Czarnobai De Jorge B, Bisotto-de-Oliveira R, Nunes Pereira C, Sant'Ana J. Novel nanoscale pheromone dispenser for more accurate evaluation of *Grapholita molesta* (Lepidoptera: Tortricidae) attract-and-kill strategies in the laboratory. 2017; 73: 1921-1926.
26. Kikionis S, Ioannou E, Konstantopoulou M, Roussis V. Electrospun micro/nanofibers as controlled release systems for pheromones of Bactroceraoleae and *Prays oleae*. 2017; 43: 254-262.
27. Tean Z, Muhammad MA, Rao Zahid A, Khazeena A, Iqra A, Anum S, Zain K. Insights into Nanopesticides for Ticks: The Superbugs of Livestock.2022; 1942-0900, 7411481.
28. Rajna S, Paschapur AU, Raghavendra KV. Nanopesticides: Its scope and utility in pest management. 2019; 6(1):17-21.
29. Romica V, Shveta S. Chapter 11 - Impact of nanopesticides in the environment: Solutions, threats, and opportunities, Pesticides in the Environment.2024;11: 251-292.
30. Fraceto LF, DeCastro VLS, Grillo R, Avila D, Oliveira HC, Lima R. Nanopesticides from research and development to mechanisms of action and sustainable use in agriculture. 2020; Springer.
31. Malik Asif, Shayesta Islam, Mushtaq, Malik ZMD, Amjad M, Saima S, Bisma R, Showkat S. Nano pesticides application in agriculture and their impact on environment. 2022; doi: 10.5772/intechopen.100690,
32. Zielinska A, Costa B, Ferreira MV, Migueis D, Louros JMS, Durazzo A. Nanotoxicology and nanosafety: Safety-by-design and testing at a glance. 2020; 17: 4657.
33. Usef HA, Fahmy HM, Arafa FN. Nanotechnology in pest management: advantages, applications, and challenges. 2023; 43:1387-1399.
34. Mubeen I, Fawzi BMM, Razaq Z, Iqbal S, Naqvi SAH, Hakim F. Nanopesticides in comparison with agrochemicals: Outlook and future prospects for sustainable agriculture.2023;198:107670.
35. Krish CP, Sarita K. Nanopesticides: A review on current research and future perspective.2023; 13:125-132.
36. Bhatnagar S, Mahanta DK, Vyas V. Storage pest management with nanopesticides incorporating silicon nanoparticles: a novel approach for sustainable crop preservation and food security. 2024; 16: 471-483.

Table 1: Different types of potential nano pesticides based on the controlled release system

Formulation	Active ingredients	Size (nm)	Targeted organism	References
Nano-capsules				
Chitosan	Pepper tree essential oil	20-100	*Aspergillus parasiticus*	9
Chitosan Functionalized with β-cyclodextrin	Carvacrol linalool	175.2–245.8	*Tetranychus urticae*	10
Chitosan	Avermectin	310	*Magnaporthe grisea*	11
Poly(ε- caprolactone)	Atrazine	240.7	*Brassica juncea*	6
Lignin	Pyraclostrobin	162.4	*Fusarium oxysporum f.sp. radicis-lycopersici*	12
mPpeg-PLGA	Metolachlor	90.49–128.7	*Oryza sativa-Digitaria Saguinalis*	13
mPEG-PLGA	Prochloraz	190.7	*Fusarium graminearum*	14
Poly(εcaprolactone)	Atrazine	260	*Bidens pilosa Amaranthus viridi*	15
Zein	Essential oil of citronella	142.5–172.3	*Tetranychus urticae Koch mite*	16
PCL	Essential oil of Zanthoxylum rhoifolium	500	*Bemisia tabaci*	17

Nano-emulsions				
Neem	Oil *Azadirachta indica*	59	*Aspergillus flavus* *Penicillium citrinum*	18
Polylactide	Validamycin Thifluzamide	260	*Rhizoctonia solani*	19
Span 80	Mancozeb Eugenol	200–300	*Glomerella cingulata*	20
Sunflower oil	R-(+)- pulgone	131–558	*Sitophilus oryzae L.* *Tribolium castaneum*	21
Mentha piperita oil and Tween 80	Mentha piperita essential oil	20–60	*Cotton aphid*	22
Propylene glycol	Clove and lemongrass oil	76.73	*Fusarium oxysporum f.sp. lycopersic*	23
Lipid nanoparticles				
Percirol ATO5 + campritol 888	Essential oil of Ziziphora clinopodioides Lam.	241.1	*Tribolium castaneum*	24
Nanogels				
Polyethylene glycol 4,4-methylenediphenyl diisocyanate	λ-cyhalothrine	120	Athetis dissimilis	25
Nanofibers				
Poly-εcaprolactone Polyethylene glycol	Cypermethrin (Z)-8-Dodecenyl acetate (Z)-8-Dodecanol	-	*Grapholita molesta* (Lepidoptera: Tortricidae)	26

Figure.1: Significance of the nano pesticides

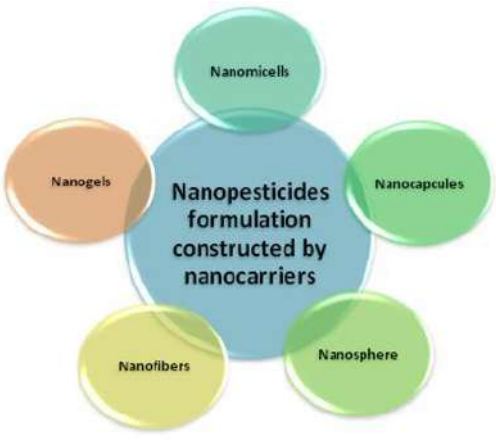

Figure.2: Nano pesticides formulation constructed by nanocarriers

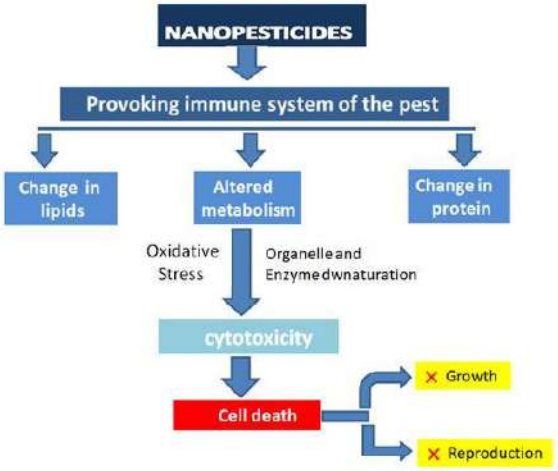

Figure.3: General mechanism of nano-pesticides

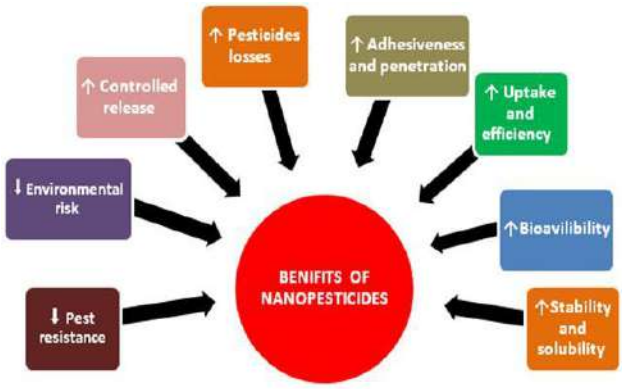

Figure.4: Advantages of nano pesticides in comparison to conventional pesticides

Indian Journal of Natural Sciences www.tnsroindia.org.in ©IJONS

Vol.15 / Issue 88 / Feb / 2025 *International Bimonthly (Print) – Open Access* *ISSN: 0976 – 0997*

RESEARCH ARTICLE

Multi Objective Assignment Problem based on Pythagorean Neutrosophic Normal Interval Valued Set for Paring Organ Donors and Recipients

V. Surya[1]* and R. Sophia Porchelvi[2]

[1]Research Scholar, Department of Mathematics, A.D.M. College for Women (Autonomous), Nagapattinam, (Affiliated to Bharathidasan University, Tiruchirappalli), Tamil Nadu, India.
[2]Associate Professor, Department of Mathematics, A.D.M. College for Women (Autonomous), Nagapattinam, (Affiliated to Bharathidasan University, Tiruchirappalli), Tamil Nadu, India.

Received: 21 Nov 2024 Revised: 03 Dec 2024 Accepted: 30 Jan 2025

***Address for Correspondence**
V. Surya
Research Scholar,
Department of Mathematics,
A.D.M. College for Women (Autonomous),
Nagapattinam, (Affiliated to Bharathidasan University, Tiruchirappalli),
Tamil Nadu, India.
E.Mail: suryavictorraj@gmail.com

ABSTRACT

This paper discusses about a new method for solving a multi-objective assignment problem (MOAP) using Pythagorean neutrosophic normal interval valued fuzzy sets (PNSNIVS). The process of converting all objective values to a single scale is the main component of the work. A novel score function for PNSNIVS is proposed to solve the assignment prolem. In this method a set of donors are paired to a set of recipients. Illustration of numerical examples are provided to test its viability.

Keywords: Multi-objective Assignment Problem (MOAP), Pythagoreanneutrosophic normal interval valued set (PNSNIVS) pythagoreanneutrosophic normal interval - valued weighted averaging (PNSNIVWA).

INTRODUCTION

Zadeh introduced the concept of fuzzy set in the year 1965 [6]. In order to address the uncertainties in real-world problems, a number of unreliable theories have been proposed which includes, the intuitionistic fuzzy set (IFS) theory by Atanassov (1986) [1], the pythagorean fuzzy set (PFS) by Yager (2014), and the neutrosophic set (NSS) theory by Samarandache (1995) [13]. The degree of membership for each element in fuzzy set theory ranges from zero to one.The sum of the membership and non-membership degrees in IFS is either zero or less. PFS is an extension

of IFS when the square sum of membership and non-membership degree is less than or equal to one [9]. Samarandache introduced the idea of a neutrosophic fuzzy set (NS), where the components have varying degrees of veracity, ambiguity, and falsity. The interval value PFS (IVPFS) was first introduced by Zhany (2016) as the PFS's extent. Here, the degree values for membership and non-membership range from 0 to 1. And the squared sum of the upper bounds of the two intervals is either zero or less than one. The concept of the normal fuzzy number (NFN) was developed by Yang &Ko [8]. NFN resembles human decision-making processes more than the other fuzzy numbers. Pythagorean neutrosophic normal interval valued set is a notion that is utilized in this essay. One of the most fundamental concepts is the assignment issue, where the goal is to distribute N jobs to N workers while taking certain restrictions into account. It is a unique instance of a transportation issue. Afaq Ahmad and A. Ahmed talked about how to approach an assignment challenge. A. Khandelwal provided a methodical solution to the assignment challenge. An approach for tackling assignment problems using the fuzzy programming technique was provided by R. Sophia Porchelvi and M. Anitha (2018) [10].For the purpose of solving an assignment problem, R. Sophia Porchelvi and M. Anitha (2018) used the average total opportunity cost technique [11]. A fuzzy fuzzy multi-objective assignment problem was resolved by Jaesh M. Dhodiya and Anita Ravi Tailor (2016) using an exponential membership function [4]. Zaoli yang and Jinping chang (2020) discussed about interval - valued pythagorean normal fuzzy and their aggregation operators [14].M.Palanikumar, K. Arulmozhi and chiranjibejana (2022) done a work by using Pythagorean neurtosophic interval-valued fuzzy aggregation [7]. Harish Garg (2020) gave a paper abut normal intuitionistic sets [3]. This paper is organized as follows: The basic definitions are given in section 2. Notations, Mathematical model, methodology and a numerical example is given in section 3 to check the feasibility of the method.Conclusion is given in section 4.

PRELIMINARIES

Definition 1: Let R denote real number set, the membership function of fuzzy number $A(x) = e^{-\left(\frac{x-\alpha}{\beta}\right)^2}$, $\beta > 0$ is called as normal fuzzy number (NFN) $A(x) = (\alpha, \beta)$ and it is enoted by $\bar{N}$.

Definition 2: Let X be a universe of discourse. A Pythagorean neutrosophic set (PN) N on X is defined as
$PN = \{\langle x, \Phi_{PN}(x), \Psi_{PN}(x), \text{Ĵ}_{PN}(x)\rangle / x \in X\}$,
where $0 \le \Phi_{PN}^2(x) + \text{Ĵ}_{PN}^2(x) + \Psi_{PN}^2(x) \le 2$ and $\Phi_{PN}(x), \Psi_{PN}(x), \text{Ĵ}_{PN}(x) \in [0,1]$
$\Phi_{PN}(x), \Psi_{PN}(x), \text{Ĵ}_{PN}(x)$ denotes degree of membership, degree of non-membership and degree of indeterminacy.

Definition 3: Let $(\alpha, \beta) \in \bar{N}$, $\tilde{A} = \{(\alpha, \beta): [\Phi^-, \Phi^+], [\text{Ĵ}^-, \text{Ĵ}^+], [\Psi^-, \Psi^+]\}$ is a Pythagorean neutrosophic normal interval-valued number (PNSNIVN). Where $[\Phi^-, \Phi^+], [\text{Ĵ}^-, \text{Ĵ}^+][\Psi^-, \Psi^+] \in [0,1]$ and the degree of truth, indeterminacy and falsity are denoted as
$[\Phi^-, \Phi^+] = \Phi^- e^{-\left(\frac{x-\alpha}{\beta}\right)^2}, \Phi^+ e^{-\left(\frac{x-\alpha}{\beta}\right)^2}$ $[\text{Ĵ}^-, \text{Ĵ}^+] = \text{Ĵ}^- e^{-\left(\frac{x-\alpha}{\beta}\right)^2}, \text{Ĵ}^+ e^{-\left(\frac{x-\alpha}{\beta}\right)^2}$
$[\Psi^-, \Psi^+] = \Psi^- e^{-\left(\frac{x-\alpha}{\beta}\right)^2}, \Psi^+ e^{-\left(\frac{x-\alpha}{\beta}\right)^2}$ And $0 \le \Phi^2{}_A(x) + \Psi^2{}_A(x) + \text{Ĵ}^2{}_A(x) \le 2$.

Definition 4: Addition of two PNSNIVN is given as follows. Let
$\tilde{A} = \{(\alpha_1, \beta_1): [\Phi_1{}^-, \Phi_1{}^+], [\text{Ĵ}_1{}^-, \text{Ĵ}_1{}^+], [\Psi_1{}^-, \Psi_1{}^+]\}$
$\tilde{B} = \{(\alpha_2, \beta_2): [\Phi_2{}^-, \Phi_2{}^+], [\text{Ĵ}_2{}^-, \text{Ĵ}_2{}^+], [\Psi_2{}^-, \Psi_2{}^+]\}$ then

$$\tilde{A} + \tilde{B} = \left[\begin{array}{c} (\alpha_1 + \alpha_2, \beta_1 + \beta_2); \\ \left[\sqrt[2\lambda]{((\Phi_1{}^-)^{2\lambda} + (\Phi_2{}^-)^{2\lambda}) - ((\Phi_1{}^-)^{2\lambda}(\Phi_2{}^-)^{2\lambda})}, \sqrt[2\lambda]{\left((\Phi_1{}^+)^{2\lambda} + (\Phi_2{}^+)^{2\lambda}\right) - \left((\Phi_1{}^+)^{2\lambda}(\Phi_2{}^+)^{2\lambda}\right)}; \right] \\ \left[\sqrt[\lambda]{((\text{Ĵ}_1{}^-)^{\lambda} + (\text{Ĵ}_2{}^-)^{\lambda}) - ((\text{Ĵ}_1{}^-)^{\lambda}(\text{Ĵ}_2{}^-)^{\lambda})}, \sqrt[\lambda]{\left((\text{Ĵ}_1{}^+)^{\lambda} + (\text{Ĵ}_2{}^+)^{\lambda}\right) - \left((\text{Ĵ}_1{}^+)^{\lambda}(\text{Ĵ}_2{}^+)^{\lambda}\right)}\right]; \\ [\Psi_1{}^-.\Psi_2{}^-, \Psi_1{}^+.\Psi_2{}^+] \end{array}\right]$$

Definition 5: $\tilde{A} = \{(\alpha, \beta): [\Phi^-, \Phi^+], [\Jmath^-, \Jmath^+], [\Psi^-, \Psi^+]\}$ be a family of PNSNIVN. And w=$\{w_1, w_2, \ldots w_n\}$be weight of $\tilde{A}$, $\sum_{i=1}^{n} w_i$Then generalized Pythagorean neutrosophic normal interval-valued weighted averaging (PNSNIVWA) is defined as

$$\tilde{A}_1, \tilde{A}_2, \ldots\ldots \tilde{A}_n = \begin{bmatrix} \left(\sum_{i=1}^{n} w_i\, {\alpha_i}^{\lambda}, \sum_{i=1}^{n} w_i\, {\beta_i}^{\lambda}\right); \\ \left[\sqrt[2\lambda]{1 - \prod_{i=1}^{n}\left(1 - \left(\Phi^{-2\lambda}\right)\right)^{w_i}}, \sqrt[2\lambda]{1 - \prod_{i=1}^{n}\left(1 - \left(\Phi^{+2\lambda}\right)\right)^{w_i}}; \right] \\ \left[\sqrt[\lambda]{1 - \prod_{i=1}^{n}\left(1 - \left(\Jmath^{-2\lambda}\right)\right)^{w_i}}, \sqrt[\lambda]{1 - \prod_{i=1}^{n}\left(1 - \left(\Jmath^{+2\lambda}\right)\right)^{w_i}}\right]; \\ \left[\prod_{i=1}^{n} (\Psi^-)^{w_i}, \prod_{i=1}^{n} (\Psi^+)^{w_i}\right] \end{bmatrix}$$

Definition 6: Let $\tilde{A} = \{(\alpha, \beta): [\Phi^-, \Phi^+], [\Jmath^-, \Jmath^+], [\Psi^-, \Psi^+]\}$ be an PNSNIVN then the proposed score S($\tilde{A}$) and accuracy A($\tilde{A}$) function is defined as

$$S_1(\tilde{A}) = \frac{\alpha}{3}\left(\frac{(\Phi^-)^2+(\Phi^+)^2}{3} + 2 - \frac{(\Psi^-)^2+(\Psi^+)^2}{3} + \frac{(\Jmath^-)^2+(\Jmath^+)^2}{3}\right) \quad (1)$$

$$S_2(\tilde{A}) = \frac{\beta}{3}\left(\frac{(\Phi^-)^2+(\Phi^+)^2}{3} + 2 - \frac{(\Psi^-)^2+(\Psi^+)^2}{3} + \frac{(\Jmath^-)^2+(\Jmath^+)^2}{3}\right) \quad (2)$$

$$A_1(\tilde{A}) = \frac{\alpha}{3}\left(\frac{(\Phi^-)^2+(\Phi^+)^2}{3} + \frac{(\Psi^-)^2+(\Psi^+)^2}{3} + \frac{(\Jmath^-)^2+(\Jmath^+)^2}{3}\right) \quad (3)$$

$$A_2(\tilde{A}) = \frac{\beta}{3}\left(\frac{(\Phi^-)^2+(\Phi^+)^2}{3} + \frac{(\Psi^-)^2+(\Psi^+)^2}{3} + \frac{(\Jmath^-)^2+(\Jmath^+)^2}{3}\right) \quad (4)$$

NOTATION

i - Donor number
j –recipient number
n- total number of donor/recipients
A – Pre surgical compatibility
B – Post surgical survival rate
T – Time to reach donor and recipients
W_A – Weightage for Pre surgical compatibility
W_B – Weightage for post-surgical survival rate
W_T - Weightage For Time to Reach Donor and Recipients

MATHEMATICAL FORMULATION

The challenge is to assign each worker to just one job in order to maximize the given measure of effectiveness, given n workers, n jobs, and the effectiveness of each worker for each job (in terms of cost, profit, time, etc.). Let C_{ij} denote the cost of assigning worker i to job j and X_{ij} denote the assignment of worker I to job j.

Workers\Jobs	1	2		n	
1					1
2					1
n					1
	1	1		1	

Then the mathematical model of the assignment problem is given as follows $Minimize\ Z = \sum_{i=1}^{n}\sum_{j=1}^{n} X_{ij}\, C_{ij}$

$$X_{ij} = \begin{cases} 1, & if\ i^{th}\ worker\ is\ assigned\ to\ j^{th}\ job \\ 0, & Otherwise \end{cases}$$

$\sum_{i=1}^{n} X_{ij} = 1$, j=1, 2, …, n (only one worker is assigned to j^{th} job)
$\sum_{j=1}^{n} X_{ij} = 1$,i=1, 2, …, n (only one job is assigned to i^{th} worker)

METHODOLOGY

This portion explains about the steps for solving the assignment problem.

Step 1: Consider m donors and n recipients and for Pre surgical compatibility (Table 1), post-surgical survival rate (Table 2), and time to reach donor and recipients (Table 3). Here m=n (i.e.) it is a balanced assignment problem.

Step 2: Normalize the values using the following equation. The matrix is normalized into

$$\overline{A_{ij}} = \left\{(\bar{\alpha}_{ij}, \bar{\beta}_{ij}): \left[\overline{\Phi^{-}}_{ij}, \overline{\Phi^{+}}_{ij}\right], \left[\overline{\Pi^{-}}_{ij}, \overline{\Pi^{+}}_{ij}\right], \left[\overline{\Psi^{-}}_{ij}, \overline{\Psi^{+}}_{ij}\right]\right\}$$

and $\bar{\alpha}_{ij} = \frac{\alpha_{ij}}{\max(\alpha_{ij})}$, $\bar{\beta}_{ij} = \frac{\beta_{ij}}{\max(\beta_{ij})}\frac{\beta_{ij}}{\alpha_{ij}}$,
$\overline{\Phi^{+}_{ij}} = \Phi^{+}_{ij}$, $\overline{\Phi^{-}_{ij}} = \Phi^{-}_{ij}$

Step 3: Using the Pythagorean neutrosophic normal interval valued weighted averaging (PNSNIVWA) assuming λ =1 aggregate the Tables 4, 5, 6 to form Table 7.

Step 4: Now using the proposed score function find score values for Table 4. If tie occurs then use formula (2) to find score values.

Step 5: Find the difference between maximum and minimum value for each row and note that along the side of each row. Similarly find for each column.

Step 6: Select the row with maximum difference and in that row fix the largest value and cross out the corresponding row and column.

Step 7:Repeat steps5,6 until all donors are assigned to exactly onerecipient.

ILLUSTRATIVE EXAMPLE

This MOAP discuss about finding a match between donor and recipients for transplant surgery. Here the objectives are to maximize the Pre surgical compatibility, post-surgical survival rate and minimize the time to reach donor and recipients. Let Pre surgical compatibility be A_{ij}, post-surgical survival rate B_{ij}, Time to reach donor and recipients T_{ij}. Let $w = \{0.4, 0.4, 0.2\}$ be weight for objectives.
The MOAP can be defined as follows,

$$Maximize \sum_{i=1}^{n}\sum_{j=1}^{n} X_{ij}\, A_{ij}$$

$$Maximize \sum_{i=1}^{n}\sum_{j=1}^{n} X_{ij}\, B_{ij}$$

$$Minimize \sum_{i=1}^{n}\sum_{j=1}^{n} X_{ij}\, T_{ij}$$

Here $X_{ij} = \begin{cases} 1, & if\ i^{th}\ donor\ is\ paired\ to\ j^{th} recipient \\ 0, & Otherwise \end{cases}$
$\sum_{i=1}^{n} X_{ij} = 1$, j=1, 2,…, n (only one donor is paired to j^{th} recipient)
$\sum_{j=1}^{n} X_{ij} = 1$,i=1, 2, …, n (only one donor is paired to i^{th} donor)

Step 1:

Table 1

(0.7,0.6):(0.2,0.3) (0.65,0.7)(0.5,0.6)	(0.85,0.8): (0.17,0.2) (0.6,0.7)(0.3,0.35)	(0.2,0.1): (0.3,0.35) (0.6,0.7)(0.45,0.5)	(0.8,0.6): (0.5,0.6) (0.6,0.7)(0.5,0.55)
(0.85,0.65): (0.3,0.35) (0.5,0.58)(0.6,0.65)	(0.8,0.7): (0.6,0.7) (0.5,0.7) (0.17,0.2)	(0.9,0.75): (0.45,0.5) (0.5,0.55) (0.1,0.12)	(0.7,0.65): (0.6,0.65) (0.1,0.15) (0.2,0.3)
(0.75,0.7): (0.6,0.8) (0.6,0.7) (0.5,0.55)	(0.65,0.6): (0.7,0.8) (0.2,0.22) (0.3,0.35)	(0.75,0.65): (0.3,0.35) (0.2,0.3)(0.4,0.45)	(0.8,0.6): (0.35,0.45) (0.23,0.3)(0.45,0.5)
(0.75,0.7): (0.18,0.3) (0.56,0.62) (0.19,0.3)	(0.7,0.6): (0.16,0.2) (0.3,0.36)(0.6,0.71)	(0.8,0.76): (0.12,0.2) (0.55,0.8) (0.6,0.7)	(0.8,0.75): (0.55,0.6) (0.65,0.7)(0.5,0.54)

Table 2

(0.8,0.6): (0.5,0.55) (0.6,0.65)(0.6,0.7)	(0.7,0.65): (0.6,0.69) (0.4,0.5)(0.54,0.55)	(0.9,0.85): (0.5,0.6) (0.55,0.6)(0.6,0.7)	(0.7,0.65): (0.1,0.5) (0.2,0.25) (0.3,0.35)
(0.6,0.55): (0.4,0.45) (0.6,0.65) (0.5,0.55)	(0.9,0.6): (0.2,0.25) (0.4,0.45)(0.7,0.75)	(0.7,0.6): (0.3,0.35) (0.35,0.45) (0.45,0.5)	(0.6,0.3): (0.50.55) (0.6,0.65)(0.7,0.75)
(0.8,0.5): (0.3,0.33) (0.35,0.45) (0.6,0.65)	(0.6,0.4): (0.2,0.3) (0.35,0.4)(0.4,0.45)	(0.6,0.5): (0.2,0.25) (0.3,0.35)(0.35,0.45)	(0.9,0.7): (0.4,0.45) (0.45,0.5)(0.6,0.65)
(0.9,0.8): (0.6,0.7) (0.6,0.63)(0.4,0.55)	(0.7,0.6): (0.3,0.35) (0.35,0.4)(0.4,0.45)	(0.6,0.55): (0.8,0.65) (0.65,0.7)(0.8,0.85)	(0.8,0.7): (0.5,0.55) (0.5,0.6)(0.6,0.7)

Table 3

(0.8,0.5): (0.4,0.5) (0.4,0.45)(0.5,0.55)	(0.9,0.6): (0.6,0.65) (0.5,0.6)(0.5,0.54)	(0.85,0.7): (0.3,0.33) (0.3,0.4)(0.5,0.55)	(0.8,0.7): (0.7,0.75) (0.6,0.63)(0.4,0.55)
(0.7,0.6): (0.5,0.55) (0.4,0.54)(0.3,0.42)	(0.8,0.7): (0.5,0.56) (0.6,0.67)(0.6,0.7)	(0.5,0.2): (0.4,0.45) (0.45,0.5)(0.5,0.6)	(0.6,0.5): (0.66,0.75) (0.7,0.8)(0.75,0.9)
(0.9,0.7): (0.2,0.22) (0.3,0.36)(0.3,0.4)	(0.4,0.3): (0.5,0.54) (0.3,0.35)(0.33,0.4)	(0.6,0.3): (0.47,0.5) (0.5,0.56)(0.6,0.64)	(0.7,0.65): (0.5,0.6) (0.55,0.65)(0.3,0.4)
(0.8,0.7): (0.1,0.15) (0.5,0.6)(0.5,0.55)	(0.5,0.4): (0.6,0.66) (0.6,0.7)(0.7,0.75)	(0.7,0.4): (0.7,0.75) (0.6,0.62)(0.64,0.7)	(0.8,0.7): (0.45,0.5) (0.65,0.7)(0.7,0.75)

Step 2: Normalizing tables 1,2,3 gives the following tables 4,5,6

Table 4

(0.82,0.74) :(0.2,0.3) (0.65,0.7) (0.5,0.6)	(1,0.94): (0.17,0.2) (0.6,0.7) (0.3,0.35)	(0.22,0.06): (0.3,0.35) (0.6,0.7)(0.45,0.5)	(1,0.6): (0.5,0.6) (0.6,0.7)(0.5,0.55)
(1,0.71): (0.3,0.35) (0.5,0.58)(0.6,0.65)	(0.94,0.76): (0.6,0.7) (0.5,0.7) (0.17,0.2)	(1,0.82): (0.45,0.5) (0.5,0.55) (0.1,0.12)	(0.88,0.8): (0.6,0.65) (0.1,0.15) (0.2,0.3)
(0.88,0.93): (0.6,0.8) (0.6,0.7) (0.5,0.55)	(0.76,0.69): (0.7,0.8) (0.2,0.22) (0.3,0.35)	(0.8,0.74): (0.3,0.35) (0.2,0.3)(0.4,0.45)	(1,0.6): (0.35,0.45) (0.23,0.3) (0.45,0.5)
(0.88,0.93): (0.18,0.3) (0.56,0.62) (0.19,0.3)	(1.21,0.64): (0.16,0.2) (0.3,0.36)(0.6,0.71)	(0.88,0.95): (0.12,0.2) (0.55,0.8) (0.6,0.7)	(1,0.94): (0.55,0.6) (0.65,0.7)(0.5,0.54)

Table 5

(0.88,0.56): (0.5,0.55) (0.6,0.65)(0.6,0.7)	(0.77,0.93): (0.6,0.69) (0.4,0.45) (0.5,0.55)	(1,0.94): (0.5,0.6) (0.55,0.6)(0.6,0.7)	(0.77,0.86): (0.1,0.5) (0.2,0.25)(0.3,0.35)
(0.66,0.63): (0.4,0.45) (0.6,0.65) (0.5,0.55)	(1,0.62): (0.2,0.25) (0.4,0.45) (0.7,0.75)	(0.77,0.61): (0.3,0.35) (0.35,0.45) (0.45,0.5)	(0.66,0.21): (0.5,0.55) (0.6,0.65) (0.7,0.75)

(0.88,0.39): (0.3,0.33) (0.35,0.45)(0.6,0.65)	(0.66,0.41): (0.2,0.3) (0.35,0.4)(0.4,0.45)	(0.66,0.49): (0.2,0.25) (0.3,0.35) (0.35,0.45)	(1,0.77):(0.4,0.45)(0.45,0.5)(0.6,0.65)
(1,0.88): (0.6,0.7) (0.6,0.63) (0.4,0.55)	(0.77,0.79): (0.3,0.35) (0.35,0.4) (0.4,0.45)	(0.66,0.59): (0.6,0.65) (0.65,0.7) (0.8,0.85)	(0.88,0.87):(0.5,0.55) (0.5,0.6) (0.6,0.7)

Table 6

(0.8,0.45): (0.4,0.5) (0.4,0.45) (0.5,0.55)	(1,0.57): (0.6,0.65) (0.5,0.6) (0.5,0.54)	(1,0.82): (0.3,0.33) (0.3,0.4) (0.5,0.55)	(1,0.88): (0.7,0.75) (0.6,0.63) (0.4,0.55)
(0.77,0.73): (0.5,0.55) (0.4,0.54) (0.3,0.42)	(0.88,0.88): (0.5,0.56) (0.6,0.67) (0.6,0.7)	(0.59,0.11): (0.4,0.45) (0.45,0.5) (0.5,0.6)	(0.75,0.59): (0.66,0.75) (0.7,0.8) (0.75,0.9)
(0.9,0.7): (0.2,0.22) (0.3,0.36) (0.3,0.4)	(0.44,0.32): (0.5,0.54) (0.3,0.35) (0.33,0.4)	(0.73,0.21): (0.47,0.5) (0.5,0.56) (0.6,0.64)	(0.88,0.86): (0.5,0.6) (0.55,0.65) (0.3,0.4)
(0.8,0.7): (0.1,0.15) (0.5,0.6) (0.5,0.55)	(0.56,0.46): (0.6,0.66) (0.6,0.7) (0.7,0.75)	(0.82,0.28): (0.7,0.75) (0.6,0.62) (0.64,0.7)	(1,0.88): (0.45,0.5) (0.65,0.7) (0.7,0.75)

Step 3: Aggregating tables 4,5,6 gives the following table

Table 7

(0.84,0.61): (0.15,0.21) (0.77,0.8) (0.54,0.63)	(0.91,0.86) :(0.25,0.33) (0.71.0.7) (0.41,0.46)	(0.69,0.56) :(0.16,0.29) (0.62,0.67) (0.53,0.59)	(0.91,0.76):(0.22,0.3)(0.49 ,0.57)(0.39,0.46)
(0.82,0.68):(0.15,0.19)(0.43 ,0.6)(0.49,0.56)	(0.95,0.73):(0.23,0.3)(0.69 ,0.78)(0.39,0.44)	(0.83,0.59):(0.15,0.19)(0.44 ,0.5)(0.25,0.29)	(0.77,0.52):(0.34,0.4)(0.6, 0.59)(0.43,0.54)
(0.88,0.67): (0.2,0.37)(0.68,0.75) (0.49,0.55)	(0.66,0.5): (0.29,0.41)(0.54,0.56)(0.3 4,0.39)	(0.73,0.53) :(0.1,0.13) (0.56,0.62) (0.41,0.48)	(0.98,0.72): (0.16,0.2)(0.41,0.48) (0.47,0.53)
(0.91,0.87): (0.18,0.27) (0.75,0.79) (0.31,0.43)	(0.9,0.66): (0.13,0.17)(0.41,0.48) (0.53,0.59)	(0.78,0.67): (0.28,0.33) (0.77,0.85) (0.68,0.76)	(0.95,0.9): (0.26,0.32)(0.59,0.66)(0.5 8,0.64)

Step 4: Applying score function in table 7 we get following table 8

Table 8

0.52	0.55	0.45	0.59
0.55	0.71	0.54	0.52
0.55	0.43	0.46	0.68
0.6	0.63	0.51	0.66

RESULTS AND DISCUSSION

Performing step 5,6 will end up with the following paring between donors and recipients.

D_1 - R_3

D_2 - R_2

D_3 - R_4

D_4 - R_1

So, the optimum value for Pre surgical compatibility, post-surgical survivalrate, and time to reach donor and recipients is (2.55,2.1) :(0.59,0.89)(1.36,1.5)(0.006,0.015), (1.8,2.95):(0.8,1.11)(1.39,1.45)(0.1,0.19)and (3.15,2.75):(0.59,0.8)(1.37,1.41)(0.045,0.085) The most important step in the organ transplant process is pairing the right donor with the right recipient. Finding the right donor might be challenging because there are many patients waiting for transplants but few willing donors. The National Organ Transplant Programme (NOTP) of the Indian government promotes organ donation and transplantation throughout the nation. In terms of donated organs from deceased people, Tamil Nadu comes in first. This research offers a novel approach to resolving a multi-objective

assignment problem in order to overcome the challenges in donor recipients matching. This solution approach will be a useful resource in fields whenever assignment difficulties arise in a Pythagorean neutrosophic environment.

CONCLUSION

This paper gave a new method for MOAP to pair donors with recipients for transplant surgery under Pythagorean neutrosophic normal interval valued number. It gives the optimal solution for the objectives. In future this problem can be solved by using some other multi-objective optimization method.

REFERENCES

1. Atanassov K, Gargov G (1989), "Interval-valued intuitionistic fuzzy sets". *Fuzzy Sets Syst*. Vol:31, PP: 343–349.
2. Atanassov KT (1986), "Intuitionistic fuzzy sets", *Fuzzy Sets Syst,* vol.20, no.1, pp: 87-96.
3. Harish Garg (2020), "New ranking method for normal intuitionistic sets under crisp, interval environments and its applications to multiple attribute decision making process",*Complex& Intelligent Systems*, Vol:6, PP: 559–571.
4. Jayesh M. Dhodiyaand Anita Ravi Tailor (2016), "Genetic algorithm-based hybrid approach to solve fuzzy multi-objective assignment problem using exponential membership function", s*pringer Plus,*Vol:5, PP:2028.
5. Jun Ye (2017), "Multiple Attribute Decision-Making Method Using Correlation Coefficients of Normal Neutrosophic Sets", *Symmetry*, Vol:9, PP: 80.
6. L. A. Zadeh (1965), ''Fuzzy sets,'' *Inf. Control*, vol: 8, pp. 338–353.
7. M. Palanikumar, K. Arulmozhi and Chiranjibe Jana (2022), "Multiple attribute decision-making approach for Pythagorean neutrosophic normal interval-valued fuzzy aggregation operators",*Computational and Applied Mathematics*.
8. M.-S. Yang and C.-H. Ko (1996), ''On a class of fuzzy c-numbers clustering procedures for fuzzy data,'' *Fuzzy Sets Syst.*, vol. 84, no. 1, pp. 49–60.
9. R. R. Yager (2014), ''Pythagorean membership grades in multicriteria decision-making,'' *IEEE Trans. Fuzzy Syst*, vol. 22, no. 4, pp. 958–965.
10. R. Sophia Porchelvi and M. Anitha (2018), "an algorithm to solve multi objective assignment problem using fuzzy programming technique", *International Journal of Current Research and Modern Education,* vol:3, PP: 2455-5428.
11. R. Sophia Porchelvi and M. Anitha (2018), "Optimal Solution for Assignment Problem by Average Total Opportunity Cost Method", *Journal of Mathematics and Informatics,* vol:13, PP:21-27.
12. Rıdvansahin(2016),"Normal neutrosophic multiple attribute decision making based on generalized prioritized aggregation operators"*NeuralComput&Applic*.
13. Smarandache F (1998), "Neutrosophy. Neutrosophic probability, set, and logic. *American Research Press*, Rehoboth, pp: 1–105
14. zaoliyangandjinpingchang (2020), "Interval-Valued Pythagorean Normal Fuzzy Information Aggregation Operators for Multi-Attribute Decision Making", *IEEE Access.*

Vol.15 / Issue 88 / Feb / 2025 *International Bimonthly (Print) – Open Access* *ISSN: 0976 – 0997*

RESEARCH ARTICLE

Eccentric Domination and Restrained Eccentric Domination in Circulant Graphs $C_p\langle 1, 2, 4\rangle$

M. Bhanumathi[1] and R. Niroja[2]*

[1]Principal (Retd.), Department of Mathematics, Government Arts College for Women, Sivagangai, (Affiliated to Alagappa University, Karaikudi), Tamil Nadu, India.
[2]Research Scholar, Department of Mathematics, Kalaignar Karunanidhi Government Arts College for Women (Autonomous), Pudukkottai (Affiliated to Bharathidasan University, Tiruchirappalli), Tamil Nadu, India.

Received: 21 Dec 2024 Revised: 10 Jan 2024 Accepted: 06 Feb 2025

***Address for Correspondence**
R. Niroja,
Research Scholar,
Department of Mathematics,
Kalaignar Karunanidhi Government Arts College for Women (Autonomous),
Pudukkottai
(Affiliated to Bharathidasan University, Tiruchirappalli),
Tamil Nadu, India.
E.Mail: nironeela@gmail.com

ABSTRACT

A subset D of the vertex set V(G) of a graph G is said to be a dominating set if every vertex not in D is adjacent to at least one vertex in D. A dominating set D is said to be an eccentric dominating set if for every $v \in V-D$, there exists at least one eccentric vertex of v in D. The minimum cardinality of an eccentric dominating set is called the eccentric domination number and is denoted by $\gamma_{ed}(G)$. A subset D of V(G) is a restrained eccentric dominating set if D is a restrained dominating set of G and for every $v \in V - D$, there exists at least one eccentric vertex of v in D. The minimum of the cardinalities of the restrained eccentric dominating set of G is called the restrained eccentric domination number of G and is denoted by $\gamma_{red}(G)$. Let $p \geq 8$ be a positive integer. The circulant graph $C_p\langle 1, 2, 4\rangle$ is the graph with vertex set {v0, v1, v2, …, vp-1} and edge set $\{\{v_i, v_{i+j}\}: i \in \{0, 1, 2, \ldots, p-1\}$ and $j \in \{1, 2, 4\}\}$. In this paper, we initiate the study of domination number, restrained domination number, eccentric domination number and restrained eccentric domination number in the circulant graphs $C_p\langle 1, 2, 4\rangle$.

Keywords: Domination, Restrained Domination, Eccentric Domination, Restrained Eccentric Domination, Circulant Graphs.
Mathematics Subject Classification: 05C12, 05C69.

INTRODUCTION

Let G be a finite, simple, undirected (p, q) graph with vertex set V(G) and edge set E(G). For graph theoretic terminology refer to Harary [8], Buckley and Harary [6]. The concept of domination in graphs is originated from the chess games theory and that paved the way to the development of the study of various domination parameters and its relation to various other graph parameters. For details on domination theory, refer to Haynes, Hedetniemi and Slater [9]. Janakiraman, Bhanumathi and Muthammai [10] introduced Eccentric domination in Graphs. Bhanumathi, John Flavia and Kavitha [1] introduced and studied the concept of Restrained Eccentric domination in Graphs.

Definition 1.1: Let $p \geq 8$ be a positive integer. The circulant graph $Cp\langle 1, 2, 4\rangle$ is the graph with vertex set {v0, v1, v2, …, vp-1} and edge set $\{\{vi, vi+j\}: i \in \{0, 1, 2, \ldots, p-1\}$ and $j \in \{1, 2, 4\}\}$.

Definition 1.2: Let G be a connected graph and v be a vertex of G. The eccentricity e(v) of v is the distance to a vertex farthest from v. Thus, $e(v) = \max\{d(u, v) : u \in V\}$. The radius r(G) is the minimum eccentricity of the vertices, whereas the diameter diam(G) = d(G) is the maximum eccentricity. For any connected graph G, $r(G) \leq diam(G) \leq 2r(G)$. The vertex v is a central vertex if e(v) = r(G). The center C(G) is the set of all central vertices. For a vertex v, each vertex at a distance e(v) from v is an eccentric vertex of v. Eccentric set of a vertex v is defined as $E(v) = \{u \in V(G) / d(u, v) = e(v)\}$.

Definition 1.3: A graph G is called a m-eccentric point graph if each point of G has exactly $m \geq 1$ eccentric points.

Definition 1.4 [7, 9]: A set $D \subseteq V$ is said to be a dominating set in G, if every vertex in V–D is adjacent to some vertex in D. The minimum cardinality of a dominating set is called the domination number and is denoted by $\gamma(G)$.

Definition 1.5 [8]: A set $D \subseteq V(G)$ is a restrained dominating set if every vertex not in D is adjacent to a vertex in D and to a vertex in V–D. The cardinality of minimum restrained dominating set is called the restrained domination number and is denoted by $\gamma r(G)$.

Definition 1.6 [10]: A set $D \subseteq V(G)$ is an eccentric dominating set if D is a dominating set of G and for every $v \in V–D$, there exists at least one eccentric vertex of v in D. The minimum cardinality of an eccentric dominating set is called the eccentric domination number and is denoted by $\gamma ed(G)$.

Definition 1.7 [1]: A subset D of V(G) is a restrained eccentric dominating set if D is a restrained dominating set of G and for every $v \in V–D$, there exists at least one eccentric vertex of v in D. The minimum of the cardinalities of the restrained eccentric dominating set of G is called the restrained eccentric domination number of G and is denoted by $\gamma red(G)$.

Theorem 1.1 [9]: For any graph G, $\lceil p/(1+\Delta(G)) \rceil \leq \gamma(G) \leq p–\Delta(G)$.

Theorem 1.2 [3]: Let G be a connected graph. Let $u \in V(G)$ be eccentric to atmost m vertices, then $\lceil p/(1+m) \rceil \leq \gamma ed(G)$.

Domination, Restrained domination, Eccentric domination and Restrained eccentric domination in Circulant Graph $Cp\langle 1, 2, 4\rangle$

Let $p \geq 8$ be a positive integer. The circulant graph $Cp\langle 1, 2, 4\rangle$ is the graph with vertex set {v0, v1, v2, …, vp – 1} and edge set $\{\{vi, vi + j\}: i \in \{0, 1, 2, \ldots, p – 1\}$ and $j \in \{1, 2, 4\}\}$. In this section, we determine the domination number, the restrained domination number, the eccentric domination number and the restrained eccentric domination number of circulant graph $Cp\langle 1, 2, 4\rangle$, for any integer $p \geq 8$. Cleary, $Cp\langle 1, 2, 4\rangle$ is a 6-regular graph on p vertices.

Example 2.1

In Figure 2.1, S1 = {v0, v7} is a minimum dominating set. It is also a minimum restrained dominating set. Therefore, $\gamma(C11\langle 1, 2, 4\rangle) = \gamma r(C11\langle 1, 2, 4\rangle) = 2$. S2 = {v0, v4, v8} is a minimum eccentric dominating set and is also a minimum restrained eccentric dominating set. Therefore, $\gamma ed(C11\langle 1, 2, 4\rangle) = \gamma red(C11\langle 1, 2, 4\rangle) = 3$.

Theorem 2.1: For any integer $p \geq 8$,

$\lfloor \frac{p}{7} \rfloor + 1 \; if \; p \equiv 6 \; (mod \; 7)$

$\gamma(Cp\langle 1, 2, 4\rangle) = \gamma r(Cp\langle 1, 2, 4\rangle) = \{\lceil \frac{p}{7} \rceil + 1 \; if \; p \equiv 6 \; (mod \; 7)$

Proof: Let $p \geq 8$ and let Cp represent the cycle in $Cp\langle 1, 2, 4\rangle$ with vertices v0, v1, v2, …, vp – 1 and edges v0v1, v1v2, …, vp – 2vp – 1, vp – 1v0. $Cp\langle 1, 2, 4\rangle$ is a six regular graph. Hence, $\gamma(Cp\langle 1, 2, 4\rangle) \geq \lceil p/1 + 6 \rceil = \lceil p/7 \rceil$.

Let $k \geq 1$ be a positive integer.

Now, when p = 7k, consider S = {v0, v7, v14, …, v7(k – 1)}. S is a dominating set of $Cp\langle 1, 2, 4\rangle$ with cardinality $\lceil p/7 \rceil$ and $|S| = \lceil p/7 \rceil$.

When p = 7k + 1, consider S = {v0, v7, v14, …, v7k}. S is a dominating set of $Cp\langle 1, 2, 4\rangle$ with cardinality $\lceil p/7 \rceil$ and $|S| = \lceil p/7 \rceil$.

When p = 7k + 2, consider S = {v0, v7, v14, …, v6k}. S is a dominating set of $Cp\langle 1, 2, 4\rangle$ with cardinality $\lceil p/7 \rceil$ and $|S| = \lceil p/7 \rceil$.

When p = 7k + 3, consider S = {v0, v7, v14, …, v6k}. S is a dominating set of $Cp\langle 1, 2, 4\rangle$ with cardinality $\lceil p/7 \rceil$ and $|S| = \lceil p/7 \rceil$.

When p = 7k + 4, consider S = {v0, v7, v14, …, v7k}. S is a dominating set of $Cp\langle 1, 2, 4\rangle$ with cardinality $\lceil p/7 \rceil$ and $|S| = \lceil p/7 \rceil$.

When p = 7k + 5, consider S = {v0, v7, v14, …, v7k}. S is a dominating set of $Cp\langle 1, 2, 4\rangle$ with cardinality $\lceil p/7 \rceil$ and $|S| = \lceil p/7 \rceil$.

When p = 7k + 6, consider S = {v0, v7, v14, …, v7k, v7k + 5}. S is a dominating set of $Cp\langle 1, 2, 4\rangle$ with cardinality $\lceil p/7 \rceil + 1$ and $|S| = \lceil p/7 \rceil + 1$.

In all cases, $\gamma(C_p\langle 1, 2, 4\rangle) = \{ \lceil \frac{p}{7} \rceil + 1 \; if \; p \equiv 6 \; (mod \; 7) \;\; \lceil \frac{p}{7} \rceil \; if \; p \not\equiv 6 \; (mod \; 7)$

In all the above cases, S is also a restrained dominating set of $Cp\langle 1, 2, 4\rangle$. Therefore, $\gamma r(Cp\langle 1, 2, 4\rangle) = \gamma(Cp\langle 1, 2, 4\rangle)$.

Theorem 2.2: For any integer $p \geq 10$,

(i) $\lceil p/3 \rceil \leq \gamma ed(Cp\langle 1, 2, 4\rangle) \leq p/2$ if p = 24k + 8, k ≥ 1.

(ii) $\lceil p/3 \rceil \leq \gamma ed(Cp\langle 1, 2, 4\rangle) \leq \lceil p/2 \rceil - 2$ if p = 24k + 9, k ≥ 1.

(iii) $\lceil p/4 \rceil \leq \gamma ed(Cp\langle 1, 2, 4\rangle) \leq \lceil p/3 \rceil$ if p = 24k + 10, k ≥ 0.

(iv) $\lceil p/5 \rceil \leq \gamma ed(Cp\langle 1, 2, 4\rangle) \leq \lceil p/4 \rceil$ if p = 24k + 11, k ≥ 0.

(v) $\lceil p/6 \rceil \leq \gamma ed(Cp\langle 1, 2, 4\rangle) \leq p/4$ if p = 24k + 12, k ≥ 0.

(vi) $\lceil p/7 \rceil \leq \gamma ed(Cp\langle 1, 2, 4\rangle) \leq \lceil p/6 \rceil$ if p = 24k + 13, k ≥ 0.

(vii) $\gamma ed(Cp\langle 1, 2, 4\rangle) = p/2$ if p = 24k + 14, k ≥ 0.

(viii) $\lceil p/7 \rceil \leq \gamma ed(Cp\langle 1, 2, 4\rangle) \leq \lceil p/4 \rceil - 1$ if p = 24k + 15, k ≥ 0.

(ix) $\lceil p/3 \rceil \leq \gamma ed(Cp\langle 1, 2, 4\rangle) \leq p/2$ if p = 24k + 16, k ≥ 0.

(x) $\lceil p/3 \rceil \leq \gamma ed(Cp\langle 1, 2, 4\rangle) \leq \lceil p/2 \rceil - 1$ if p = 24k + 17, k ≥ 0.

(xi) $\lceil p/4 \rceil \leq \gamma ed(Cp\langle 1, 2, 4\rangle) \leq p/3$ if p = 24k + 18, k ≥ 0.

(xii) $\lceil p/5 \rceil \leq \gamma ed(Cp\langle 1, 2, 4\rangle) \leq \lceil p/4 \rceil - 1$ if p = 24k + 19, k ≥ 0.

(xiii) $\lceil p/6 \rceil \leq \gamma ed(Cp\langle 1, 2, 4\rangle) \leq p/4$ if p = 24k + 20, k ≥ 0.

(xiv) $\lceil p/7 \rceil \leq \gamma ed(Cp\langle 1, 2, 4\rangle) \leq \lceil p/4 \rceil - 1$ if p = 24k + 21, k ≥ 0.

(xv) $\gamma ed(Cp\langle 1, 2, 4\rangle) = p/2$ if p = 24k + 22, k ≥ 0.

(xvi) $\lceil p/7 \rceil \leq \gamma ed(Cp\langle 1, 2, 4\rangle) \leq \lceil p/4 \rceil - 1$ if p = 24k + 23, k ≥ 0.

(xvii) $\gamma ed(Cp\langle 1, 2, 4\rangle) = p/3$ if $p = 24k + 24$, $k \geq 0$.
(xviii) $\lceil p/3 \rceil \leq \gamma ed(Cp\langle 1, 2, 4\rangle) \leq \lceil p/2 \rceil - 1$ if $p = 24k + 25$, $k \geq 0$.
(xix) $\lceil p/4 \rceil \leq \gamma ed(Cp\langle 1, 2, 4\rangle) \leq \lceil p/3 \rceil$ if $p = 24k + 26$, $k \geq 0$.
(xx) $\lceil p/5 \rceil \leq \gamma ed(Cp\langle 1, 2, 4\rangle) \leq \lceil p/4 \rceil$ if $p = 24k + 27$, $k \geq 0$.
(xxi) $\lceil p/6 \rceil \leq \gamma ed(Cp\langle 1, 2, 4\rangle) \leq p/4$ if $p = 24k + 28$, $k \geq 0$.
(xxii) $\lceil p/7 \rceil \leq \gamma ed(Cp\langle 1, 2, 4\rangle) \leq \lceil p/4 \rceil - 1$ if $p = 24k + 29$, $k \geq 0$.
(xxiii) $\gamma ed(Cp\langle 1, 2, 43) = p/2$ if $p = 24k + 30$, $k \geq 0$.
(xxiv) $\lceil p/7 \rceil \leq \gamma ed(Cp\langle 1, 2, 4\rangle) \leq \lceil p/4 \rceil - 1$ if $p = 24k + 31$, $k \geq 0$.
Proof: Let v0, v1, v2, …, vp – 1 be the vertices of $Cp\langle 1, 2, 4\rangle$.

By Theorem 2.1, $\gamma(Cp\langle 1, 2, 4\rangle) = \lceil p/7 \rceil + 1$ if $p \equiv 6(\text{mod } 7)$ (1)
$\gamma(Cp\langle 1, 2, 4\rangle) = \lceil p/7 \rceil$ if $p \not\equiv 6(\text{mod } 7)$ (2)

Case (i): p = 24k + 8, k ≥ 1.

In this case, $C_p\langle 1, 2, 4\rangle$ is a (p + 8)/8 self-centered graph. The vertices $v_{\frac{p-2}{2}+i}, v_{\frac{p+2}{2}+i}$ are the eccentric vertices of v_i ($i = 0, 1, 2, ..., p - 1$). Therefore, $C_p\langle 1, 2, 4\rangle$ is a 2-eccentric point graph.

Hence, by Theorem 1.2, $\lceil p/3 \rceil \leq \gamma ed(Cp\langle 1, 2, 4\rangle)$. (3)
S = {v0, v2, v4, …, vp – 4, vp – 2} is an eccentric dominating set of $Cp\langle 1, 2, 4\rangle$ and $|S| = p/2$.
Therefore, $\gamma ed(Cp\langle 1, 2, 4\rangle) \leq p/2$. (4)
From (3) and (4), $\lceil p/3 \rceil \leq \gamma ed(Cp\langle 1, 2, 4\rangle) \leq p/2$.

Case (ii): p = 24k + 9, k ≥ 1.

In this case, $C_p\langle 1, 2, 4\rangle$ is a (p + 7)/8 self-centered graph. The vertices $v_{\frac{p-3}{2}+i}, v_{\frac{p+1}{2}+i}$ are the eccentric vertices of v_i ($i = 0, 1, 2, ..., p - 1$). Therefore, $C_p\langle 1, 2, 4\rangle$ is a 2-eccentric point graph.

Hence, by Theorem 1.2, $\lceil p/3 \rceil \leq \gamma ed(Cp\langle 1, 2, 4\rangle)$. (5)
S = {v0, v2, v4, …, vp – 7, vp – 5} is an eccentric dominating set of $Cp\langle 1, 2, 4\rangle$ and $|S| = \lceil p/2 \rceil - 2$.
Therefore, $\gamma ed(Cp\langle 1, 2, 4\rangle) \leq \lceil p/2 \rceil - 2$. (6)
From (5) and (6), $\lceil p/3 \rceil \leq \gamma ed(Cp\langle 1, 2, 4\rangle) \leq \lceil p/2 \rceil - 2$.

Case (iii): p = 24k + 10, k ≥ 0.

In this case, $C_p\langle 1, 2, 4\rangle$ is a (p + 6)/8 self-centered graph. The vertices $v_{\frac{p-4}{2}+i}, v_{\frac{p}{2}+i}, v_{\frac{p+4}{2}+i}$ are the eccentric vertices of v_i ($i = 0, 1, 2, ..., p - 1$). Therefore, $C_p\langle 1, 2, 4\rangle$ is a 3-eccentric point graph.

Hence, by Theorem 1.2, $\lceil p/4 \rceil \leq \gamma ed(Cp\langle 1, 2, 4\rangle)$. (7)
S = {v0, v3, v6, …, vp – 4, vp – 1} is an eccentric dominating set of $Cp\langle 1, 2, 4\rangle$ and $|S| = \lceil p/3 \rceil$.
Therefore, $\gamma ed(Cp\langle 1, 2, 4\rangle) \leq \lceil p/3 \rceil$. (8) From (7) and (8), $\lceil p/4 \rceil \leq \gamma ed(Cp\langle 1, 2, 4\rangle) \leq \lceil p/3 \rceil$.

Case (iv): p = 24k + 11, k ≥ 0.

In this case, $C_p\langle 1, 2, 4\rangle$ is a (p + 5)/8 self-centered graph. The vertices $v_{\frac{p-5}{2}+i}, v_{\frac{p-1}{2}+i}, v_{\frac{p+1}{2}+i}, v_{\frac{p+5}{2}+i}$ are the eccentric vertices of v_i (i = 0, 1, 2, ..., p − 1). Therefore, $C_p\langle 1, 2, 4\rangle$ is a 4-eccentric point graph.

Hence, by Theorem 1.2, $\lceil p/5 \rceil \le \gamma ed(Cp\langle 1, 2, 4\rangle)$. (9)
S = {v0, v4, v8, …, vp − 7, vp − 3} is an eccentric dominating set of $Cp\langle 1, 2, 4\rangle$ and $|S| = \lceil p/4 \rceil$.
Therefore, $\gamma ed(Cp\langle 1, 2, 4\rangle) \le \lceil p/4 \rceil$. (10) From (9) and (10), $\lceil p/5 \rceil \le \gamma ed(Cp\langle 1, 2, 4\rangle) \le \lceil p/4 \rceil$.

Case (v): p = 24k + 12, k ≥ 0.

In this case, $C_p\langle 1, 2, 4\rangle$ is a (p + 4)/8 self-centered graph. The vertices $v_{\frac{p-6}{2}+i}, v_{\frac{p-2}{2}+i}, v_{\frac{p}{2}+i}, v_{\frac{p+2}{2}+i}, v_{\frac{p+6}{2}+i}$ are the eccentric vertices of v_i (i = 0, 1, 2, ..., p − 1). Therefore, $C_p\langle 1, 2, 4\rangle$ is a 5-eccentric point graph.

Hence, by Theorem 1.2, $\lceil p/6 \rceil \le \gamma ed(Cp\langle 1, 2, 4\rangle)$. (11)
S = {v0, v4, v8, …, vp − 8, vp − 4} is an eccentric dominating set of $Cp\langle 1, 2, 4\rangle$ and |S| = p/4.
Therefore, $\gamma ed(Cp\langle 1, 2, 4\rangle) \le p/4$. (12) From (11) and (12), $\lceil p/6 \rceil \le \gamma ed(Cp\langle 1, 2, 4\rangle) \le p/4$.

Case (vi): p = 24k + 13, k ≥ 0.

In this case, $C_p\langle 1, 2, 4\rangle$ is a (p + 3)/8 self-centered graph. The vertices $v_{\frac{p-7}{2}+i}, v_{\frac{p-3}{2}+i}, v_{\frac{p-1}{2}+i}, v_{\frac{p+1}{2}+i}, v_{\frac{p+3}{2}+i}, v_{\frac{p+7}{2}+i}$ are the eccentric vertices of v_i (i = 0, 1, 2, ..., p − 1).

Therefore, $C_p\langle 1, 2, 4\rangle$ is a 6-eccentric point graph.

S = {v0, v6, v12, …, vp − 7, vp − 1} is an eccentric dominating set of $Cp\langle 1, 2, 4\rangle$ and $|S| = \lceil p/6 \rceil$.
Therefore, $\gamma ed(Cp\langle 1, 2, 4\rangle) \le \lceil p/6 \rceil$. (13) From (2) and (13), $\lceil p/7 \rceil \le \gamma ed(Cp\langle 1, 2, 4\rangle) \le \lceil p/6 \rceil$.

Case (vii): p = 24k + 14, k ≥ 0.

In this case, $C_p\langle 1, 2, 4\rangle$ is a (p + 10)/8 self-centered graph. The vertex $v_{\frac{p}{2}+i}$ is the eccentric vertex of v_i (i = 0, 1, 2, ..., p − 1). Therefore, $C_p\langle 1, 2, 4\rangle$ is a self-centered unique eccentric point graph.

Hence, $\gamma ed(Cp\langle 1, 2, 4\rangle) \ge p/2$. (14)
S = {v0, v2, v4, …, vp − 4, vp − 2} is an eccentric dominating set of $Cp\langle 1, 2, 4\rangle$ and |S| = p/2.
Thus, $\gamma ed(Cp\langle 1, 2, 4\rangle) \le p/2$. (15)
From (14) and (15), $\gamma ed(Cp\langle 1, 2, 4\rangle) = p/2$.

Case (viii): p = 24k + 15, k ≥ 0.

In this case, $C_p\langle 1, 2, 4\rangle$ is a (p + 1)/8 self-centered graph. The vertices $v_{\frac{p-9}{2}+i}, v_{\frac{p-5}{2}+i}, v_{\frac{p-3}{2}+i}, v_{\frac{p-1}{2}+i}, v_{\frac{p+1}{2}+i}, v_{\frac{p+3}{2}+i}, v_{\frac{p+5}{2}+i}, v_{\frac{p+9}{2}+i}$ are the eccentric vertices of v_i(i = 0, 1, 2, ..., p – 1). Therefore, $C_p\langle 1, 2, 4\rangle$ is a 8-eccentric point graph.

1, 2, ..., p – 1). Therefore, Cp⟨1, 2, 4⟩ is a 8-eccentric point graph.

S = {v0, v4, v8, …, vp – 11, vp – 7} is an eccentric dominating set of Cp⟨1, 2, 4⟩ and |S| = ⌈p/4⌉ – 1.

Therefore, $C_p\langle 1, 2, 4\rangle$ is a 8-eccentric point graph.

$S = \{v_0, v_4, v_8, \ldots, v_{p-11}, v_{p-7}\}$ is an eccentric dominating set of $C_p\langle 1, 2, 4\rangle$ and $|S| = \lceil p/4 \rceil - 1$.

Therefore, $\gamma_{ed}(C_p\langle 1, 2, 4\rangle) \leq \lceil p/4 \rceil - 1$. (16)

From (2) and (16), $\lceil p/7 \rceil \leq \gamma_{ed}(C_p\langle 1, 2, 4\rangle) \leq \lceil p/4 \rceil - 1$.

Case (ix): p = 24k + 16, k ⊚ 0.

In this case, $C_p\langle 1, 2, 4\rangle$ is a (p + 8)/8 self-centered graph. The vertices $v_{\frac{p-2}{2}+i}, v_{\frac{p+6}{2}+i}$ are the eccentric vertices of v_i(i = 0, 1, 2, ..., p – 1). Therefore, $C_p\langle 1, 2, 4\rangle$ is a 2-eccentric point graph.

Hence, by

Theorem 6.1.1, $\lceil p/3 \rceil \leq \gamma_{ed}(C_p\langle 1, 2, 4\rangle)$. (17)

$S = \{v_0, v_2, v_4, \ldots, v_{p-4}, v_{p-2}\}$ is an eccentric dominating set of $C_p\langle 1, 2, 4\rangle$ and $|S| = p/2$.

Therefore, $\gamma_{ed}(C_p\langle 1, 2, 4\rangle) \leq p/2$. (18)

From (17) and (18), $\lceil p/3 \rceil \leq \gamma_{ed}(C_p\langle 1, 2, 4\rangle) \leq p/2$.

Case (xi): p = 24k + 18, k ⊚ 0.

In this case, $C_p\langle 1, 2, 4\rangle$ is a (p + 6)/8 self-centered graph. The vertices $v_{\frac{p-4}{2}+i}, v_{\frac{p}{2}+i}, v_{\frac{p+4}{2}+i}$ are the eccentric vertices of v_i (i = 0, 1, 2, ..., p – 1). Therefore, $C_p\langle 1, 2, 4\rangle$ is a 3-eccentric point graph.

Hence, by

Theorem 1.2, $\lceil p/4 \rceil \leq \gamma_{ed}(C_p\langle 1, 2, 4\rangle)$. (21)

$S = \{v_0, v_3, v_6, \ldots, v_{p-6}, v_{p-3}\}$ is an eccentric dominating set of $C_p\langle 1, 2, 4\rangle$ and $|S| = p/3$

Therefore, $\gamma_{ed}(C_p\langle 1, 2, 4\rangle) \leq p/3$. (22)

From (21) and (22), $\lceil p/4 \rceil \leq \gamma_{ed}(C_p\langle 1, 2, 4\rangle) \leq p/3$.

Case (xii): p = 24k + 19, k ⊚ 0.

In this case, $C_p\langle 1, 2, 4\rangle$ is a $(p + 5)/8$ self-centered graph. The vertices $v_{\frac{p-5}{2}+i}, v_{\frac{p-1}{2}+i}, v_{\frac{p+1}{2}+i}, v_{\frac{p+5}{2}+i}$ are the eccentric vertices of v_i ($i = 0, 1, 2, \ldots, p - 1$). Therefore, $C_p\langle 1, 2, 4\rangle$ is a 4-eccentric point graph.

Hence, by

Theorem 1.2, $\lceil p/5 \rceil \leq \gamma_{ed}(C_p\langle 1, 2, 4\rangle)$. (23)

$S = \{v_0, v_4, v_8, \ldots, v_{p-11}, v_{p-7}\}$ is an eccentric dominating set of $C_p\langle 1, 2, 4\rangle$ and $|S| = \lceil p/4 \rceil - 1$.

Therefore, $\gamma_{ed}(C_p\langle 1, 2, 4\rangle) \leq \lceil p/4 \rceil - 1$. (24)

From (23) and (24), $\lceil p/5 \rceil \leq \gamma_{ed}(C_p\langle 1, 2, 4\rangle) \leq \lceil p/4 \rceil - 1$.

Case (xiii): p = 24k + 20, k ⊚ 0.

In this case, $C_p\langle 1, 2, 4\rangle$ is a $(p + 4)/8$ self-centered graph. The vertices $v_{\frac{p-6}{2}+i}, v_{\frac{p-2}{2}+i}, v_{\frac{p}{2}+i}, v_{\frac{p+2}{2}+i}, v_{\frac{p+6}{2}+i}$ are the eccentric vertices of v_i ($i = 0, 1, 2, \ldots, p - 1$). Therefore, $C_p\langle 1, 2, 4\rangle$ is a 5-eccentric point graph.

Theorem 1.2, $\lceil p/6 \rceil \leq \gamma_{ed}(C_p\langle 1, 2, 4\rangle)$. (25)

$S = \{v_0, v_4, v_8, \ldots, v_{p-8}, v_{p-4}\}$ is an eccentric dominating set of $C_p\langle 1, 2, 4\rangle$ and $|S| = p/4$.

Therefore, $\gamma_{ed}(C_p\langle 1, 2, 4\rangle) \leq p/4$. (26)

From (25) and (26), $\lceil p/6 \rceil \leq \gamma_{ed}(C_p\langle 1, 2, 4\rangle) \leq p/4$.

Case (xiv): p = 24k + 21, k ⊚ 0.

In this case, $C_p\langle 1, 2, 4\rangle$ is a (p + 3)/8 self-centered graph. The vertices $v_{\frac{p-7}{2}+i}, v_{\frac{p-3}{2}+i}, v_{\frac{p-1}{2}+i}, v_{\frac{p+1}{2}+i}, v_{\frac{p+3}{2}+i}, v_{\frac{p+7}{2}+i}$ are the eccentric vertices of v_i (i = 0, 1, 2, ..., p – 1).

Therefore, $C_p\langle 1, 2, 4\rangle$ is a 6-eccentric point graph.

Therefore, $\gamma_{ed}(C_p\langle 1, 2, 4\rangle) \leq \lceil p/4 \rceil - 1$. (27)

From (2) and (27), $\lceil p/7 \rceil \leq \gamma_{ed}(C_p\langle 1, 2, 4\rangle) \leq \lceil p/4 \rceil - 1$.

Case (xv): p = 24k + 22, k ⊚ 0.

In this case, $C_p\langle 1, 2, 4\rangle$ is a (p + 10)/8 self-centered graph. The vertex $v_{\frac{p}{2}+i}$ is the eccentric vertex of v_i (i = 0, 1, 2, ..., p – 1). Therefore, $C_p\langle 1, 2, 4\rangle$ is a self-centered unique eccentric point graph.

Hence, $\gamma_{ed}(C_p\langle 1, 2, 4\rangle) \geq p/2$. (28)

$S = \{v_0, v_2, v_4, \ldots, v_{p-4}, v_{p-2}\}$ is an eccentric dominating set of $C_p\langle 1, 2, 4\rangle$ and $|S| = p/2$.

Thus, $\gamma_{ed}(C_p\langle 1, 2, 4\rangle) \leq p/2$. (29)

From (28) and (29), $\gamma_{ed}(C_p\langle 1, 2, 4\rangle) = p/2$.

Case (xvi): p = 24k + 23, k ⊚ 0.

In this case, $C_p\langle 1, 2, 4\rangle$ is a (p + 1)/8 self-centered graph. The vertices $v_{\frac{p-9}{2}+i}, v_{\frac{p-5}{2}+i}, v_{\frac{p-3}{2}+i}, v_{\frac{p-1}{2}+i}, v_{\frac{p+1}{2}+i}, v_{\frac{p+3}{2}+i}, v_{\frac{p+5}{2}+i}, v_{\frac{p+9}{2}+i}$ are the eccentric vertices v_i (i = 0, 1, 2, ..., p – 1). Therefore, $C_p\langle 1, 2, 4\rangle$ is a 8-eccentric point graph.

$S = \{v_0, v_4, v_8, \ldots, v_{p-11}, v_{p-7}\}$ is an eccentric dominating set of $C_p\langle 1, 2, 4\rangle$ and $|S| = \lceil p/4 \rceil - 1$.

Therefore, $\gamma_{ed}(C_p\langle 1, 2, 4\rangle) \leq \lceil p/4 \rceil - 1$. (30)

From (2) and (30), $\lceil p/7 \rceil \leq \gamma_{ed}(C_p\langle 1, 2, 4\rangle) \leq \lceil p/4 \rceil - 1$.

Case (xvii): p = 24k + 24, k ⊚ 0.

In this case, $C_p\langle 1, 2, 4\rangle$ is a (p + 7)/8 self-centered graph. The vertices $v_{\frac{p-3}{2}+i}, v_{\frac{p+3}{2}+i}$ are the eccentric vertices of v_i (i = 0, 1, 2, ..., p − 1). Therefore, $C_p\langle 1, 2, 4\rangle$ is a 2-eccentric point graph.

Hence, by Theorem 1.2, $\lceil p/3 \rceil \leq \gamma_{ed}(C_p\langle 1, 2, 4\rangle)$. (33)

$S = \{v_0, v_2, v_4, \ldots, v_{p-5}, v_{p-3}\}$ is an eccentric dominating set of $C_p\langle 1, 2, 4\rangle$ and $|S| = \lceil p/2 \rceil - 1$.

Therefore, $\gamma_{ed}(C_p\langle 1, 2, 4\rangle) \leq \lceil p/2 \rceil - 1$. (34)

From (33) and (34), $\lceil p/3 \rceil \leq \gamma_{ed}(C_p\langle 1, 2, 4\rangle) \leq \lceil p/2 \rceil - 1$.

Case (xix): p = 24k + 26, k ⊚ 0.

In this case, $C_p\langle 1, 2, 4\rangle$ is a (p + 6)/8 self-centered graph. The vertices $v_{\frac{p-4}{2}+i}, v_{\frac{p}{2}+i}, v_{\frac{p+4}{2}+i}$ are the eccentric vertices of v_i (i = 0, 1, 2, ..., p − 1). Therefore, $C_p\langle 1, 2, 4\rangle$ is a 3-eccentric point graph.

Hence, by Theorem 1.2, $\lceil p/4 \rceil \leq \gamma_{ed}(C_p\langle 1, 2, 4\rangle)$. (35)

$S = \{v_0, v_3, v_6, \ldots, v_{p-5}, v_{p-2}\}$ is an eccentric dominating set of $C_p\langle 1, 2, 4\rangle$ and $|S| = \lceil p/3 \rceil$.

Therefore, $\gamma_{ed}(C_p\langle 1, 2, 4\rangle) \leq \lceil p/3 \rceil$. (36)

From (35) and (36), $\lceil p/4 \rceil \leq \gamma_{ed}(C_p\langle 1, 2, 4\rangle) \leq \lceil p/3 \rceil$.

Case (xx): p = 24k + 27, k ⊚ 0.

In this case, $C_p\langle 1, 2, 4\rangle$ is a (p + 5)/8 self-centered graph. The vertices $v_{\frac{p-5}{2}+i}, v_{\frac{p-1}{2}+i}, v_{\frac{p+1}{2}+i}, v_{\frac{p+5}{2}+i}$ are the eccentric vertices of v_i (i = 0, 1, 2, ..., p − 1). Therefore, $C_p\langle 1, 2, 4\rangle$ is a 4-eccentric point graph.

Hence, by Theorem 1.2, $\lceil p/5 \rceil \leq \gamma_{ed}(C_p\langle 1, 2, 4\rangle)$. (37)

$S = \{v_0, v_4, v_8, \ldots, v_{p-7}, v_{p-3}\}$ is an eccentric dominating set of $C_p\langle 1, 2, 4\rangle$ and $|S| = \lceil p/4 \rceil$.

Therefore, $\gamma_{ed}(C_p\langle 1, 2, 4\rangle) \leq \lceil p/4 \rceil$. (38)

From (37) and (38), $\lceil p/5 \rceil \leq \gamma_{ed}(C_p\langle 1, 2, 4\rangle) \leq \lceil p/4 \rceil$.

Case (xxi): p = 24k + 28, k ⊚ 0.

In this case, $C_p\langle 1, 2, 4\rangle$ is a (p + 4)/8 self-centered graph. The vertices $v_{\frac{p-6}{2}+i}, v_{\frac{p-2}{2}+i}, v_{\frac{p}{2}+i}, v_{\frac{p+2}{2}+i}, v_{\frac{p+6}{2}+i}$ are the eccentric vertices of v_i (i = 0, 1, 2, ..., p – 1). Therefore, $C_p\langle 1, 2, 4\rangle$ is a 5-eccentric point graph.

Hence, by Theorem 1.2, $\lceil p/6 \rceil \leq \gamma_{ed}(C_p\langle 1, 2, 4\rangle)$. (39)

$S = \{v_0, v_4, v_8, \ldots, v_{p-8}, v_{p-4}\}$ is an eccentric dominating set of $C_p\langle 1, 2, 4\rangle$ and $|S| = p/4$.

Therefore, $\gamma_{ed}(C_p\langle 1, 2, 4\rangle) \leq p/4$. (40)

From (39) and (40), $\lceil p/6 \rceil \leq \gamma_{ed}(C_p\langle 1, 2, 4\rangle) \leq p/4$.

Case (xxii): p = 24k + 29, k ⊚ 0.

In this case, $C_p\langle 1, 2, 4\rangle$ is a (p + 3)/8 self-centered graph. The vertices $v_{\frac{p-7}{2}+i}, v_{\frac{p-3}{2}+i}, v_{\frac{p-1}{2}+i}, v_{\frac{p+1}{2}+i}, v_{\frac{p+3}{2}+i}, v_{\frac{p+7}{2}+i}$ are the eccentric vertices of v_i (i = 0, 1, 2, ..., p – 1). Therefore, $C_p\langle 1, 2, 4\rangle$ is a 6-eccentric point graph.

$S = \{v_0, v_4, v_8, \ldots, v_{p-9}, v_{p-5}\}$ is an eccentric dominating set of $C_p\langle 1, 2, 4\rangle$ and $|S| = \lceil p/4 \rceil - 1$.

Therefore, $\gamma_{ed}(C_p\langle 1, 2, 4\rangle) \leq \lceil p/4 \rceil - 1$. (41)

From (2) and (41), $\lceil p/7 \rceil \leq \gamma_{ed}(C_p\langle 1, 2, 4\rangle) \leq \lceil p/4 \rceil - 1$.

Case (xxiii): p = 24k + 30, k ⊚ 0.

In this case, $C_p\langle 1, 2, 4\rangle$ is a (p + 10)/8 self-centered graph. The vertex $v_{\frac{p}{2}+i}$ is the eccentric vertex of v_i (i = 0, 1, 2, ..., p – 1). Therefore, $C_p\langle 1, 2, 4\rangle$ is a self centered unique eccentric point graph.

Hence, $\gamma_{ed}(C_p\langle 1, 2, 4\rangle) \geq p/2$. (42)

$S = \{v_0, v_2, v_4, \ldots, v_{p-4}, v_{p-2}\}$ is an eccentric dominating set of $C_p\langle 1, 2, 4\rangle$ and $|S| = p/2$.

Thus, $\gamma_{ed}(C_p\langle 1, 2, 4\rangle) \leq p/2$. (43)

From (42) and (43), $\gamma_{ed}(C_p\langle 1, 2, 4\rangle) = p/2$.

Case (xxiv): p = 24k + 31, k ⊚ 0.

In this case, $C_p\langle 1, 2, 4\rangle$ is a (p + 1)/8 self-centered graph. The vertices $v_{\frac{p-9}{2}+i}, v_{\frac{p-5}{2}+i}, v_{\frac{p-3}{2}+i}, v_{\frac{p-1}{2}+i}, v_{\frac{p+1}{2}+i}, v_{\frac{p+3}{2}+i}, v_{\frac{p+5}{2}+i}, v_{\frac{p+9}{2}+i}$ are the eccentric vertices of v_i (i = 0, 1, 2, ..., p – 1). Therefore, $C_p\langle 1, 2, 4\rangle$ is a 8-eccentric point graph.

$S = \{v_0, v_4, v_8, \ldots, v_{p-11}, v_{p-7}\}$ is an eccentric dominating set of $C_p\langle 1, 2, 4\rangle$ and $|S| = \lceil p/4 \rceil - 1$.

Therefore, $\gamma_{ed}(C_p\langle 1, 2, 4\rangle) \leq \lceil p/4 \rceil - 1$. (44)

From (2) and (44), $\lceil p/7 \rceil \leq \gamma_{ed}(C_p\langle 1, 2, 4\rangle) \leq \lceil p/4 \rceil - 1$.

Remark 2.1

(i) $S_1 = \{v_0, v_1, v_2\}$ is a minimum eccentric dominating set of $C_8\langle 1, 2, 4\rangle$.

Hence, $\gamma_{ed}(C_8\langle 1, 2, 4\rangle) = 3$.

(ii) $S_2 = \{v_0, v_2, v_4\}$ is a minimum eccentric dominating set of $C_9\langle 1, 2, 4\rangle$.

Hence, $\gamma_{ed}(C_9\langle 1, 2, 4\rangle) = 3$.

Corollary 2.1: For any integer p ⊚ 10,

(i) $\lceil p/3 \rceil \leq \gamma_{red}(C_p\langle 1, 2, 4\rangle) \leq p/2$ if $p = 24k + 8, k \geq 1$.

(ii) $\lceil p/3 \rceil \leq \gamma_{red}(C_p\langle 1, 2, 4\rangle) \leq \lceil p/2 \rceil - 2$ if $p = 24k + 9, k \geq 1$.

(iii) $\lceil p/4 \rceil \leq \gamma_{red}(C_p\langle 1, 2, 4\rangle) \leq \lceil p/3 \rceil$ if $p = 24k + 10, k \geq 0$.

(iv) $\lceil p/5 \rceil \leq \gamma_{red}(C_p\langle 1, 2, 4\rangle) \leq \lceil p/4 \rceil$ if $p = 24k + 11, k \geq 0$.

(v) $\lceil p/6 \rceil \leq \gamma_{red}(C_p\langle 1, 2, 4\rangle) \leq p/4$ if $p = 24k + 12, k \geq 0$.

(vi) $\lceil p/7 \rceil \leq \gamma_{red}(C_p\langle 1, 2, 4\rangle) \leq \lceil p/6 \rceil$ if $p = 24k + 13, k \geq 0$.

(vii) $\gamma_{red}(C_p\langle 1, 2, 4\rangle) = p/2$ if $p = 24k + 14, k \geq 0$.

(viii) $\lceil p/7 \rceil \leq \gamma_{red}(C_p\langle 1, 2, 4\rangle) \leq \lceil p/4 \rceil - 1$ if $p = 24k + 15, k \geq 0$.

(ix) $\lceil p/3 \rceil \leq \gamma_{red}(C_p\langle 1, 2, 4\rangle) \leq p/2$ if $p = 24k + 16, k \geq 0$.

(x) $\lceil p/3 \rceil \leq \gamma_{red}(C_p\langle 1, 2, 4\rangle) \leq \lceil p/2 \rceil - 1$ if $p = 24k + 17, k \geq 0$.

(xi) $\lceil p/4 \rceil \leq \gamma_{red}(C_p\langle 1, 2, 4\rangle) \leq p/3$ if $p = 24k + 18, k \geq 0$.

(xii) $\lceil p/5 \rceil \leq \gamma_{red}(C_p\langle 1, 2, 4\rangle) \leq \lceil p/4 \rceil - 1$ if $p = 24k + 19, k \geq 0$.

(xiii) $\lceil p/6 \rceil \leq \gamma_{red}(C_p\langle 1, 2, 4\rangle) \leq p/4$ if $p = 24k + 20, k \geq 0$.

(xiv) $\lceil p/7 \rceil \leq \gamma_{red}(C_p\langle 1, 2, 4\rangle) \leq \lceil p/4 \rceil - 1$ if $p = 24k + 21, k \geq 0$.

(xv) $\gamma_{red}(C_p\langle 1, 2, 4\rangle) = p/2$ if $p = 24k + 22, k \geq 0$.

(xvi) $\lceil p/7 \rceil \leq \gamma_{red}(C_p\langle 1, 2, 4\rangle) \leq \lceil p/4 \rceil - 1$ if $p = 24k + 23, k \geq 0$.

(xvii) $\gamma_{red}(C_p\langle 1, 2, 4\rangle) = p/3$ if $p = 24k + 24, k \geq 0$.

(xviii) $\lceil p/3 \rceil \leq \gamma_{red}(C_p\langle 1, 2, 4\rangle) \leq \lceil p/2 \rceil - 1$ if $p = 24k + 25, k \geq 0$.

(xix) $\lceil p/4 \rceil \leq \gamma_{red}(C_p\langle 1, 2, 4\rangle) \leq \lceil p/3 \rceil$ if $p = 24k + 26, k \geq 0$.

(xx) $\lceil p/5 \rceil \leq \gamma_{red}(C_p\langle 1, 2, 4\rangle) \leq \lceil p/4 \rceil$ if $p = 24k + 27, k \geq 0$.

(xxi) $\lceil p/6 \rceil \leq \gamma_{red}(C_p\langle 1, 2, 4\rangle) \leq p/4$ if $p = 24k + 28, k \geq 0$.

(xxii) $\lceil p/7 \rceil \leq \gamma_{red}(C_p\langle 1, 2, 4\rangle) \leq \lceil p/4 \rceil - 1$ if $p = 24k + 29, k \geq 0$.

(xxiii) $\gamma_{red}(C_p\langle 1, 2, 4\rangle) = p/2$ if $p = 24k + 30, k \geq 0$.

(xxiv) $\lceil p/7 \rceil \leq \gamma_{red}(C_p\langle 1, 2, 4\rangle) \leq \lceil p/4 \rceil - 1$ if $p = 24k + 31, k \geq 0$.

Proof: The γ_{ed}-sets found in Theorem 2.2 are also restrained eccentric dominating sets.

Hence, the theorem follows.

Remark 2.2

1. $S_1 = \{v_0, v_1, v_2\}$ is a minimum restrained eccentric dominating set of $C_8\langle 1, 2, 4\rangle$. Hence, $\gamma_{red}(C_8\langle 1, 2, 4\rangle) = 3$.
2. $S_2 = \{v_0, v_2, v_4\}$ is a minimum restrained eccentric dominating set of $C_9\langle 1, 2, 4\rangle$. Hence, $\gamma_{red}(C_9\langle 1, 2, 4\rangle) = 3$.

CONCLUSION

In this paper, we have found out the exact values of domination number and restrained domination number of $C_p\langle 1, 2, 4\rangle$. Also, we have evaluated the exact values of eccentric domination number and restrained eccentric domination number of circulant graphs $C_p\langle 1, 2, 4\rangle$.

REFERENCES

1. Bhanumathi, M., John Flavia, J., and Kavitha, M., Restrained Eccentric Domination in Graphs, International Journal of Engineering Science, Advanced Computing and Bio- Technology, Vol.5, No.1, January-March 2014, pp. 24-36.
2. Bhanumathi, M., John Flavia, J., Number of Minimum Eccentric Dominating sets in paths, International Journal of Engineering Science, Advanced Computing and Bio- Technology, Vol.6, No.4, October-December 2015, pp. 114-118.

3. Bhanumathi, M., Niroja, R., Eccentric Domination and Restrained Eccentric Domination in Circulant Graphs , International Journal of Engineering Science, Advanced Computing andBio-Technology, Vol.9, No.1, January-March 2018, pp. 1-11.
4. Bhanumathi, M., Niroja, R., Eccentric Domination and Restrained Eccentric Domination in Circulant Graphs $C_p\langle 1, 3, 4\rangle$, A Journal of Composition Theory, Vol.12, No.12, Dec 2019, pp. 1065-1073.
5. Bhanumathi, M., Niroja, R., Eccentric Domination and Restrained Eccentric Domination in Circulant Graphs $C_p\langle 2, 3\rangle$, Tuijin Jishu/Journal of Propulsion technology, Vol.45, No.2(2024), pp. 847-854.
6. Buckley, F., Harary, F., Distance in graphs, Addison-Wesley, Publishing company (1990).
7. Cockayne, E.J., Hedetniemi, S.T., Towards a theory of domination in graphs.Networks,7:247-261,1977.
8. Harary, F., Graph theory, Addition-Wesley Publishing Company Reading, Mass (1972).
9. Haynes, T. W., Hedetniemi, S. T., and Slater, P.J., Fundamentals of Domination in graphs, Marcel Dekkar, New Yark(1998).
10. Janakiraman, T.N., Bhanumathi, M., Muthammai, S., Eccentric domination in graphs, International Journal of Engineering science, Computing and Bio-Technology, Volume 1, No.2, pp 1-16, 2010.
11. NadarJafari Rad, Domination in Circulant Graphs, An. St. Univ. Ovidius Constanta, Vol. 17(1), 2009, 169-176.

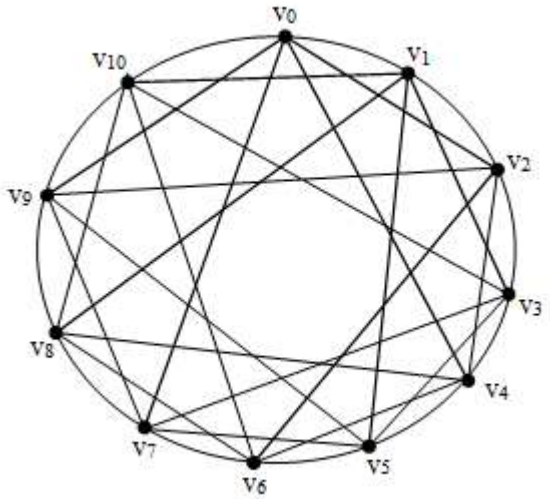

$C_{11}\langle 1, 2, 4\rangle$

Fig:1

Indian Journal of Natural Sciences www.tnsroindia.org.in ©IJONS

Vol.15 / Issue 88 / Feb / 2025 *International Bimonthly (Print) – Open Access* *ISSN: 0976 – 0997*

RESEARCH ARTICLE

a - Domination Number of a Semihypergraph

Lalitha M[1] and Dhanalakshmi P[2]*

[1]Assistant Professor, Department of Mathematics, Kongu Arts and Science College, Erode, (Affiliated to Bharathiar University, Coimbatore), Tamil Nadu, India.Tamil Nadu, India.
[2]Assistant Professor, Department of Mathematics (CA),Vellalar College for Women, Erode, (Affiliated to Bharathiar University, Coimbatore), Tamil Nadu, India.Tamil Nadu, India.

Received: 24 Sep 2024 Revised: 10 Nov 2024 Accepted: 18 Jan 2025

***Address for Correspondence**
Dhanalakshmi P,
Assistant Professor,
Department of Mathematics (CA),
Vellalar College for Women, Erode,
(Affiliated to Bharathiar University, Coimbatore), Tamil Nadu, India.Tamil Nadu, India.
E.Mail: dhanamath@gmail.com

ABSTRACT

A semi hyper graph $H_S = (V, E_h, <)$ is a broadening of a hypergraph and semigraph with more than two vertices. Like semi graph, the semi hyper graph vertices are catergorized as middle, end and middle end vertices. Cartesian product is one of the way of combining graphs to get more general form from the simplest structure. In this article, path and hamiltonian cycle of a semi hyper graph is introduced and the cardinality of minimum domination (adjacent domination number) is calculated by using cartesian product. Also few of its properties were studied.

Keywords: Semi graph, Hyper graph, Semi hyper graph, Path semi hyper graph, Hamiltonian semi hyper graph, Cartesian Product and Domination number.

INTRODUCTION

The father of graph theory was the great Swiss Mathematician LeonhardEuler[12]. In1736 he introduced graph theory to solve the problem of Konigsberg bridge[11].Graph theory is the study of relationships using vertices connected by edges. It is a helpful tool to quantify and simplify complex systems[13].Hyper graph was introduced in 1973, by Berge [2].Hyper graphs are similar to basic graphs in that their edges are sets of any number of vertices rather than edges that connect with two vertices .This implies that every graph is merely a subset of hyper graphs. In 1998 [1] on the domination of hyper graphs by their edges and in 2009 [3] domination in intersecting hyper graphs were discussed. In 2012 [6] the cartesian product of hyper graph and in 2022[10]connectivity of Cartesian product of hyper graph were studied. Semi graphs are introduced by E.Sampath Kumar [9] in the year 2000, since then, graph theory has emerged as a fascinating area of study. A semi graph is an extension of a graph in which each edge is a N-tuple

that satisfies certain constraints and can have two or more vertices. In2019[7]domination in semi graphs has been discussed and 2020[8] $a-$ domination in cartesian product of path semigraphs has been studied. In 2022[5] regularity of semi graphs was discussed. In 2024[4] a semi hyper graph$H_S = (V, E_h, <)$was introduced, it is an extension of a hyper graph and semi graph with more than two vertices .When generalizing structure, it is common to search for one in which each concept has an inherent generalization. A semi hyper graph is a generalization of hyper graph and semi graph, when drawn in a plane, it resembles a hyper graph with vertex ordering. In this paper, we discuss the semi hyper graph and $a-$ domination in cartesian product of path and hamiltonian cycle semihypergraphs.

2. Notations

H_S - Semi hyper graph
E_{h_j} - Hyper edge
H_C – Hamiltonian cycle semi hyper graph
H_{s_p} –Path Semi hyper graph
$O(H_S)$ – Order of semi hyper graph $S(H_S)$ - Size of semi hyper graph
$d(H_S)$-Degree of semi hyper graph
K-Minimal a-dominating set

3.Preliminaries

Definition 3.1.[2] Let $V=\{v_1,v_2,..v_n\}$ be a finite set of vertices. A *hypergraph* on V is a family $H=(E_1,E_2...E_m)$ of subsets of V such that

(i) $E_i \neq \varphi, \{i=1,2,3...n\}$
(ii) $\cup_{i=1}^{m} E_i = V$
(iii) A *simple hypergraph* is a hypergraph $H=\{E_1,E_2,...E_m\}$ such that $Ei \subset Ej \Rightarrow i = j$

Definition 3.2. [7]
A *semigraph* S is a pair (U, E) where U is a non empty set whose elements
are called vertices of S and E is a set of ordered $n-$ tuples $n \geq 2$ of distinct vertices called edges of S and satisfying the following two conditions:

- any two edges have atmost one vertex in common
- any two edges $E_1=(u_1,u_2,..u_r)$ and $E_2=(v_1,v_2,..v_s)$ are said to be equivalent if and only if

(a) $r = s$ and
(b) Either $u_k = v_k$ or $u_k = v_{n-k+1}$ for $1 \leq k \leq n$.

Definition 3.3. [4]
A *semihypergraph* is a connected hypergraph $H_S=(V,E_h,<)$ where $V=\{v_i/i=1,2,....n\}$ be a non empty, vertex order preserving finite set and $E_h = \{E_{h_1}, E_{h_2}, ... E_{hp}\}$ such that E_{h_j} , j=1,2,…p is a subset of V, with minimum of three vertices satisfying the following conditions:

(i) $E_{h_j} \neq \varphi$ and $\cup E_{h_j} = V$, $1 \leq j \leq p$
(ii) A minimum of one vertex unites any two hyperedges
(iii) Any pair of hyperedges $E_{h_m}=(u_1,u_2,...u_m)$ and $E_{h_n}=(v_1,v_2,...u_n)$ with ascending indices are equal if and only if
   a. $n=m$ and
   b. either $u_i=v_i$ or $u_i=v_{n-i+1}$ for $1 \leq i \leq n$.

Like semi graph, semi hyper graph's vertices are divided into three types namely middle, end and middle-end vertices, depending upon their positions in a hyper edge. In Figure (1), the vertices are
$V=\{u_1, u_2, u_3, u_4, u_5, u_6, u_7, u_8, u_9, u_{10}, u_{11}, u_{12}, u_{13}...u_{17}\}$
and the hyper edges are

E_{h_1}= {u_1, u_2, u_4, u_5, u_7}, E_{h_2}= {u_1, u_{11}, u_{13}, u_{14}, u_{15}, u_{16}}, E_{h_3}= {u_3, u_4, u_{12}, u_{13}, u_{17}}, E_{h_4}= {u_6, u_7, u_8, u_9, u_{10}, u_{14}, u_{17}} and E_{h_5}= {u_2, u_{12}, u_{14}, u_{15}}.

Here the vertices u_1, u_3, u_6, u_{16}, u_{17} are end vertices u_4, u_5, u_8, u_9, u_{10}, u_{11}, u_{12}, u_{13}, u_{14} are middle vertices and u_2, u_7, u_{15} are middle - end vertices.

Definition 3.4.[4]

A v_0−v_n *walk* in a semi hyper graph is a sequence of vertices and hyper edges. If a semi hyper graph is traversed, then it results in a walk. In a walk, both vertices and hyper edges are repeated. Walk is said to be *open* if the initial vertex and terminal vertex are different. If a walk starts and ends at the same vertex, then it is said to be *closed walk*.

Definition 3.5.[4]

The *trail* of H_S is an open walk in which end vertex, middle vertex and middle - end vertex are repeated but no hyper edge is repeated.

Definition 3.6.[4]A *path* of H_S is a trail in which neither vertices nor hyper edges are repeated.

Definition 3.7.[4]A *cycle* of H_S is a closed path, neither hyper edges nor vertices are repeated.

Example 1.

$u_1e_1u_2e_1u_4e_3u_{12}e_5u_2e_1u_4e_1u_5$- Open walk of H_S $u_1e_1u_2e_1u_4e_3u_{12}e_5u_2e_1u_1$- Closed walk of H_S $u_1e_2u_{11}e_2u_{13}e_2u_{14}e_4u_{17}e_3u_{13}e_3u_{12}$- Trail of H_S $u_1e_1u_2e_5u_{12}e_3u_{13}e_2u_{11}$- Path of H_S $u_1e_1u_2e_5u_{12}e_3u_{13}e_2u_{11}e_2u_1$-Cycle of H_S

4. Proposed Results

Definition 4.1.A semi hyper graph is k −*uniform* ($k \geq 3$) if every hyper edge contains exactly k vertices.

Example 2.Figure(2) is an example of 5−uniform semi hyper graph.

Definition.4.2. A hamiltonian cycle in an ordinary semi hyper graph is a cyclic ordering of its vertices, such that all consecutive pairs forms a hyper edge. Let H_S be k ($k \geq 3$) – uniform semi hyper graph. A cyclic ordering (v_1, v_2, ...v_n) of the vertex set is called a Hamiltonian cycle if and only if for every $1 \leq i \leq n$, there exists a hyper edge E_{h_j} of H_S such that (v_1, v_2, ...v_{i+k-1}) = E_{h_j}

Definition 4.3.

Let H_{S_1}= (U,E_{h_1}) and H_{S_2}= (V, E_{h_2}) be two semihypergraphs. The cartesian product of H_{S_1} and H_{S_2} are denoted by H_{S_1}×$H_{S_2}$and is defined as H_{S_1}×H_{S_2}=(U×V, E_{h_1}×E_{h_2}) such that U×V={(u_i,v_j) / $u_i \in U$,$v_j \in V$} and {i=1,2,...m},{j=1,2,3,4,...n}

(i) For any vertex $u \in U$, any hyper edge E_h=(v_1,v_2,...v_n) in E_{h_2}, and ((u,v_1),(u,v_2),...(u,v_n)) is an element of E_{h_1}×E_{h_2} and also

(ii) For any vertex $v \in V$, any hyper edge E_h=(u_1,u_2,...u_m) in E_{h_1}, and ((u_1,v),(u_2,v)...(u_m,v)) is an element of E_{h_1}×E_{h_2}.

Example 3.

The Cartesian product of Figure(5) and Figure(6) shown in Figure(7). From this we conclude that the cartesian product of two semi hyper graph is again a semi hyper graph.

Definition 4.4.The *degree* of semi hyper graph H_S is the number of hyper edges incident with a vertex $v \in V$ and is denoted as $d(H_S)$.

Example 4. In Figure(1) $d(u_3)$=1, $d(u_7)$=2 and $d(u_{14})$=3.

Definition 4.5. The path semi hyper graph H_S^p=(V,E_h,<) is a semi hyper graph with the following properties:

- There exists no middle end vertices
- Every hyperpath in a H_S^p has exactly two end vertices with degree one and remaining end vertices of degree two.

The following Figure(3) is an example of path semi hyper graph which has two end vertices u_1,u_5 with degree one, where as the end vertex u_3 is of degree 2 and also no middle end vertices.

Definition 3.6.Let H_S= (V,E_h,<) be a semihypergraph. Vertices $u,v \in V$ are said to be connected in H_S if there is a (u,v) walk in H_S.

Definition3.7. Let H_S=(V,E_h,<) be a semi hyper graph. The semi hyper graph H_S is said to be
(i) D_k – regular if each vertex is incident with k hyper edges
(ii) ED_k–regular if there is k (k≥3) vertices passing through every hyper edges
(iii)AD_k–regular if every vertex has k adjacent vertices
(iv)CAD_k–regular if every vertex has k consecutive adjacent vertices

Example 5. Figure(4) is D_2,ED_3,AD_4 regular semi hyper graph
Note: A semi hyper graph which is D regular need not to be ED, AD, CAD - regular. Similarly ED,AD,CAD regular semi hyper graph need not satisfy other regularity conditions.

Definition.4.8.The *order* of a semi hyper graph $O(H_S)$ is the number of its vertices in V and *size* of semi hyper graph $S(H_S)$ is the number of hyper edges in E_{h_j}

Definition.4.9. Let H_S = (V,E_h <) be a semi hyper graph. A subset K of V is said to be $a-$ *dominating set* if every $v \in V-K$ there exists a vertex $u \in K$ such that u and v are adjacent vertices of a hyper edge. The minimum cardinality of K is called a - domination number of the semi hyper graph H_S. It is denoted as $\gamma_{ca}(H_s)$

Example.6.In Figure(1) vertex set of semi hyper graph is $V(H_S)$ = {u_1,u_2,u_3,...u_{17}} and the dominating set K= {u_4,u_{14}} then $V-K$={u_1,u_2,u_3,u_5,u_6,u_7,u_8,u_9,u_{10},u_{11},u_{12},u_{13},u_{15},u_{16},u_{17}}. Here every vertex in $V-K$ is adjacent to vertices in K.

Definition.4.10.Let H_S=(V,E_h,<) be a semi hyper graph. A subset K of V is said to be $ca-$ *dominating set* if every $v \in V-K$ there exists a vertex $u \in K$ such that u and v are consecutive adjacent vertices of a hyper edge. The minimum cardinality of K is called $ca-$ domination number of the semi hyper graph H_S. It is denoted as $\gamma_{ca}(H_s)$.

Example.7.In Figure (1) vertex set of semi hyper graph is $V(H_S)$ = {u_1,u_2,u_3,...u_{17}} and the dominating set K= {u_1,u_4,u_7,u_9,u_{13},u_{14},u_{15}} then $V-K$={u_2,u_3,u_5,u_6,u_8,u_{10},u_{11},u_{12},u_{16},u_{17}}. Here every vertex in $V-K$ is consecutive adjacent to vertices in K.

Definition.4.11. Let H_S=(V,E_h,<) be a semi hyper graph. A subset K of V is said to be e – dominating set if for an end vertex $v \in V-K$ there exists a vertex $u \in K$ such that u and v are end vertices of a hyper edge. The minimum cardinality of such a set K is called $e-$ domination number of the semihypergraph H_S. It is denoted as $\gamma_e(H_S)$.

Example.8. In Figure(1) vertex set of semi hyper graph is $V(H_S)$={u_1,u_2,u_3,...u_{17}}, if the dominating set K= {u_1,u_2,u_{17}}, then the end vertex set is $V-K$= {u_3,u_6,u_7,u_{15},u_{16}}. Here, every vertex in $V-K$ is an end vertex of K.

5. $a-$Domination of Cartesian Product of H_S^p and H_C

Consider the simple path semi hyper graph and hamiltonian cycle semi hyper graph

The cartesian product of the above two semi hyper graphs as follows
In Figure (5), $u_1$and u_3 are end vertices and u_2 is middle vertex, in Figure (6) all vertices are middle end vertices. The cartesian product of the above two semi hyper graphs is given in Figure (7) with vertex set
V = {(u_1, v_1), (u_1, v_2), (u_1, v_3), (u_1, v_4), (u_1, v_5), (u_1, v_6), (u_2, v_1), (u_2,v_2),(u_2,v_3),(u_2,v_4),(u_2,v_5),(u_2,v_6)
(u_3, v_1), (u_3, v_2), (u_3, v_3), (u_3, v_4), (u_3, v_5), (u_3, v_6)}

The hyper edge set of Figure(7) as follows
E_{h1}= {(u_1, v_1), (u_1, v_2), (u_1, v_3)}, E_{h2}= {(u_1, v_3), (u_1, v_4), (u_1, v_5)},
E_{h3} ={(u_1,v_5),(u_1,v_6),(u_1,v_1)}, E_{h4}={(u_1,v_1),(u_1,v_2),(u_1,v_6)},
E_{h5} ={(u_1,v_2),(u_1,v_3),(u_1,v_4)}, E_{h6}={(u_1,v_4),(u_1,v_5),(u_1,v_6)},
E_{h7} ={(u_2,v_1),(u_2,v_2),(u_2,v_3)}, E_{h8}={(u_2,v_3),(u_2,v_4),(u_2,v_5)},
E_{h9}={(u_2,v_5),(u_2,v_6),(u_2,v_1)}, E_{h10}={(u_2,v_1),(u_2,v_2),(u_2,v_6)},
E_{h11}={(u_2,v_2),(u_2,v_3),(u_2,v_4)}, E_{h12}={(u_2,v_4),(u_2,v_5),(u_2,v_6)},
E_{h13}={(u_3,v_1),(u_3,v_2),(u_3,v_3)}, E_{h14}={(u_3,v_3),(u_3,v_4),(u_3,v_5)},
E_{h15}={(u_3,v_5),(u_3,v_6),(u_3,v_1)}, E_{h16}={(u_3,v_1),(u_3,v_2),(u_3,v_6)},
E_{h17}={(u_3,v_2),(u_3,v_3),(u_3,v_4)}, E_{h18}={(u_3,v_4),(u_3,v_5),(u_3,v_3)},
E_{h19}={(u_1,v_1),(u_2,v_1),(u_3,v_1)}, E_{h20}={(u_1,v_2),(u_2,v_2),(u_3,v_2)},
E_{h21}= {(u_1, v_3), (u_2, v_3), (u_3, v_3)}, E_{h22}= {(u_1, v_4), (u_2, v_4), (u_3, v_4)},
E_{h23}= {(u_1, v_5), (u_2, v_5), (u_3, v_5)}, E_{h24}= {(u_1, v_6), (u_2, v_6), (u_3, v_6)}.
Here the vertex set {(u_1, v_1), (u_2, v_1), (u_3, v_1)} dominates all the vertices except E_{h14} row. By considering any one vertex from the hyper edge E_{h14}, that dominates remaining vertices. Therefore the total dominating vertex set of $H_S^p \times H_C$ is {(u_1, v_1), (u_2, v_1), (u_3, v_1), (u_3, v_4)}.
Hence $\gamma_a (H_S^p(1) \times H_C)$ is 4.

Lemma 5.1
For any semi hyper graph H_S
(i) $\gamma_a(H_S) \leq \gamma_{ca}(H_S)$
(ii) $\gamma_a(H_S) \leq \gamma_e(H_S)$
(iii) $\gamma_a(H_C)$=2

Proof.(i)Let $v_i \in V$ be any vertex in H_S. The number of consecutive adjacent vertices of v_i will be less than the adjacent vertices of v_i, hence the domination number of consecutive adjacent vertices is greater than the domination number of adjacent vertex. Hence (i) is proved.
(ii) Let $v \in V$ be an end vertex. The adjacent domination number of v is less than an end vertex domination number. Hence (ii) is proved.
(iii)Since Hamiltonian cycle semi hyper graph is only four edges, so the adjacent domination of H_C is 2. Hence (iii) is proved.

Example .9. Domination number of adjacent and consecutive adjacent vertices of Figure(1) is 2 and 6 respectively. Adjacent and end vertex domination number of Figure(1) is 2 and 3 respectively

Theorem 5.1. The a −domination number of path semi hyper graph is $\frac{E_h}{2}$ and $\frac{E_h+1}{2}$ when the hyper edges are even and odd respectively

Proof: Consider the path semi hyper graph H_S^p(n) with E_h=2m, where m =1,2,3,... hyper edges, say E_{h_1}, E_{h_2}, …. $E_{h_{(2m)}}$and 2m+1 end vertices say $u_1,u_2,...u_{2m+1}$ such that u_i, u_{i+1} are the end vertices of the hyper edge E_{h_j}. Let $v_i \in E_{h_j}$ be a middle vertex. The vertex in $v_i \in E_{h_j}$ has a − domination only in E_{h_j} and not other adjacent hyper edges. Let V_i, V_{i+1}, V_{i+2}, be a middle vertex set of E_{h_j}, {j =1,2,3,...2m}. The vertices in V_i,V_{i+1},V_{i+2},....belongs to neighbourhood of u_{i+1}, $i = 2r - 1$, r=1,2,...m. Hence the vertices {$u_2,u_4,u_6,...u_{2m}$} are a minimal a −dominating set. Therefore minimal a −dominating set is

$m = \frac{E_h}{2}$, when the hyper edges are even. If $E_h = 2m - 1$, $m = 1,2,...$ then $H_S^p(n)$ have $2m-1$ hyperedges say E_{h_1}, E_{h_2}, ... $E_{h_{(2m-1)}}$ and 2m end vertices $u_1, u_2, ... u_{2m}$ such that u_i, u_{i+1} are the end vertices. By similar argument as above the vertices {u_2, u_4,…u_{2m}} are minimal $a-$ dominating set . Therefore, minimal $a-$ dominating set is $m=\frac{E_h+1}{2}$, when the hyper edges are odd. Hence the theorem is proved.

Theorem 5.2

$\gamma_a(H_S^p(n) \times H_L)$ is

$$\begin{cases} 5\left(\frac{n-1}{2}\right)+4 & \text{if } n = 2k+1, k = 0,1,2,3... \\ 5\left(\frac{n-2}{2}\right)+6 & \text{if } n = 2k+2, k = 0,1,2,3,.. \end{cases}$$

Proof:

Let $H_S^p(n)$ be the simple path semihypergraph containing exactly one middle vertex with n hyperpath and H_L be the simple linear hamiltonian cycle semihypergraph containing three consecutive hyperedges with each hyperedge have atleast one middle vertex. In general, the result follows with two cases.

Case 1

When the hyper path has odd number of vertices, $n = 2k+1, k = 0,1,2,...$

Ther minimal a – dominating vertex set K is

$$\begin{cases} \cup_{l=1}^{4k+3} (u_l, v_1) \\ \cup_{l=0}^{k} (u_{3+4l}, v_4) \end{cases}$$

$|K|$ = 4K + 3 + K + 1

= 5K + 4

= $5\left(\frac{n-1}{2}\right) + 4$

Hence

$\gamma_a(H_S^p(n) \times H_L)$ =$5\left(\frac{n-1}{2}\right) + 4$, when n is odd

$|K|$ = 4K + 5+ K + 1

Case 2

When the hyperpath is even, n=2k+2, k= 0,1,2,3…

The minimal a – dominating vertex set K is

$$\begin{cases} \cup_{l=0}^{4k+5} (u_l, v_1) \\ \cup_{l=0}^{k} (u_{3+4l}, v_4) \end{cases}$$

$|K|$ = 4k+5+k+1

= 5k+6

= $5\left(\frac{n-2}{2}\right)+6$

Hence $\gamma_a(H_S^p(n) \times H_L)$

= $5\left(\frac{n-2}{2}\right) + 6$

Hence

$\gamma_a(H_S^p(n) \times H_L)$ =$5\left(\frac{n-2}{2}\right) + 6$, when n is even

Note:
1.$\gamma_a(H_S^p(1) \times H_L) = 4$
2.$\gamma_a(H_S^p(2) \times H_L) = 6$
3.$\gamma_a(H_S^p(3) \times H_L) = 9$
$\gamma_a(H_S^p(4) \times H_L) = 11$

Theorem 5.3.
Let *Hs* be a semihypergraph of *r* vertices out of which *k* are end vertices, *l* are middle vertices and *m* are middle – end vertices with *r=k+l+m* then $\gamma_a(H_S^p(n) \times H_L) \leq \frac{r}{4}$

Proof. This proof follows from above lemma(3.1) and theorem(3.2)

CONCLUSION

Domination has been the nucleus research activity in graph, semigraph and semihypergraph. In this article, we computed certain interesting variations of $a-$ domination number of semi hypergraphs like path and Hamiltonian by using Cartesian product. Also, its few properties are discussed. In future, the authors has planned to discuss consecutive adjacent, end adjacent, one end adjacent and bipartite domination number of semihypergraphs.

REFERENCES

1. A Behr, L Camatinopoulos, *On the domination of hypergraphs by their edges*, Discrete Mathematics, Elsevier, 1998.
2. C. Berge, *Hypergraphs*, North - Holland, London, 1973.
3. Y Dong, E Shan, L Kang, S Li, *Domination in intersecting hypergraphs*, Applicable Analysis and Discrete Mathematics, 2009.
4. S Jagadeesan, K.K.Myithili, S.Thilagavathi, L.Gayathri, *A New Paradigm on Semihypergraph*, Journal of Computational Analysis and Applications, volume 33, No 2, pp.514-522, 2024.
5. Jyothi Shetty, G Sudhakara, K Arathi Bhat, *Regularity in Semigraphs*, Engineering Letters, volume 30, Issue 4, pp. 1-8, 2022.
6. Lydia Ostermeier, Marc Hellmuth, Peter F Stadler, *The Cartesian product of hyper- graphs*, Journal of Graph Theory, volume 70, Issue 2, 180-192, 2012.
7. N.Murugesan and D.Narmatha, *Domination in Semigraphs,* International Journal of Engineering and Advanced Technology, volume 8, Issue 6, pp. 563 – 568, 2019.
8. N.Murugesan and D. Narmatha, *a- domination in cartesian product of path semi- graphs*, Journal of Physics: Conference Series, Conf. Ser. 1543 012006, pp. 1-5, 2020.
9. E. Sampathkumar, *Semigraphs and their Applications*, Department of Science Technology, Govt of India, pp. 1-17, 2000
10. N Wang, J Meng, Y Tian, *Connectivity of Cartesian Product of Hypergraphs*, Bulletin of the Iranian Mathematical Society, Springer, 2022 .
11. D. B. West, *Introduction to graph theory*, Prentice-Hall of India, New Delhi,1999.
12. R J Wilson *Introduction to graph theory*, Pearson Education, India,1979.
13. J M Xu, C Yang *Connectivity of Cartesian product graphs* - Discrete Mathematics, Elsevier - 2006.

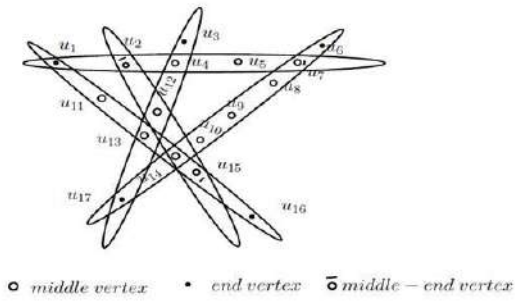

Figure1:Semihypergraph

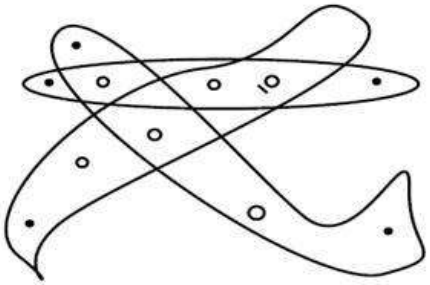

Figure.2:Uniform Semihypergraph

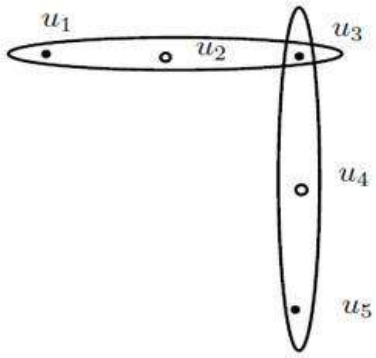

Figure 3: Path Semihypergraph

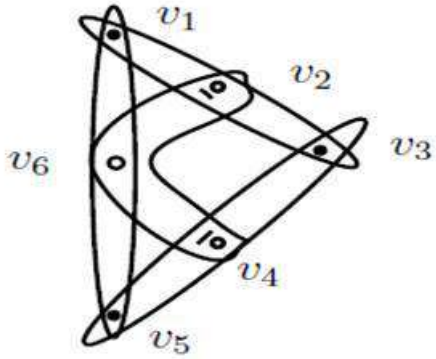

Figure4:D_2,ED_3,AD_4 Regular Semihypergraph

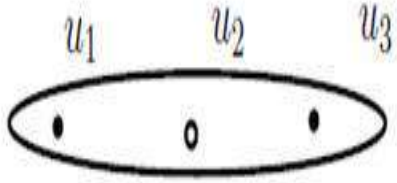

Figure5:Simple Path Semihypergraph

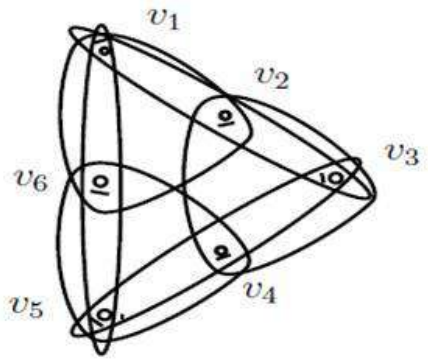

Figure6: Hamiltonian Cycle Semihypergraph

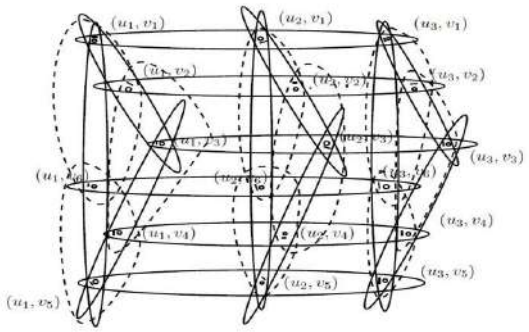

Figure.7: Cartesian Product of Two Semihypergraphs

Indian Journal of Natural Sciences *www.tnsroindia.org.in ©IJONS*

Vol.15 / Issue 88 / Feb / 2025 *International Bimonthly (Print) – Open Access* *ISSN: 0976 – 0997*

RESEARCH ARTICLE

Stancu - Type Modification of Generalized Lupaş Operators

Harsh P. Kothari[1] and R. B. Gandhi[2]*

[1]Research Scholar, Gujarat Technological University, (Affiliated to Gujarat Technological University), Ahmedabad, Gujarat, India.
[2]Assistant Professor, Department of Mathematics, BVM Engineering College, (Affiliated to Gujarat Technological University), Ahmedabad, Gujarat, India.

Received: 21 Nov 2024 Revised: 03 Dec 2024 Accepted: 31 Jan 2025

***Address for Correspondence**
R. B. Gandhi
Assistant Professor, Department of Mathematics,
BVM Engineering College,
(Affiliated to Gujarat Technological University),
Ahmedabad, Gujarat, India.
E.Mail: rbgandhi@bvmengineering.ac.in

ABSTRACT

As a part of this research study, we develop a Stancu-type structure of generalized Lupaş operators. Our work also includes the proof of some direct theorems and Voronovskaja-type theorems for the first and second order derivatives**.**

Keywords: Positive linear operator; Lupaş operators; Modulus of continuity; Korovkin-type theorem; Voronvskaja-type theorems.
Mathematics Subject Classification: 41A10, 41A25, 41A36, 41B30

INTRODUCTION

Approximation theory is very important branch of mathematics. It is about study of simpler functions that can closely represent the other complicated functions. It is classified into two groups: study of approximation on theoretical base and study of approximation on constructive base. In 1912, computational mathematician S. N. Bernstein was the first person to create a sequence of positive linear operators that can be used to prove that the polynomials are uniformly dense in the collection of continuous function on compact interval of real numbers system with respect to the sup-norm. He used a probabilistic method and binomial distribution to construct these operators and provided a clear proof. A. Lupaş presented the following operators in Germany [1]

$$\xi_n(\psi, s) = (1-\gamma_0)^{ns} \sum_{P=0}^{\infty} \frac{(ns)_p}{p!} {\gamma_0}^P \psi\left(\frac{p}{n}\right) ; |\gamma_0| < 1, s \geq 0. \qquad (1.1)$$

Agratini [2] studied this operator and found that for this operator to satisfy$\xi_n(e_i; s) = e_i(s)$(where $e_i(s) = s^i, i = 0,1,2$)best possible value for$a = \frac{1}{2}$. For the same, Agratini defined the following operator that is derived from (1.1)

$$\xi_n(\psi,s)=2^{-ns}\sum_{p=0}^{\infty}\frac{(ns)_p}{2^p p!}\psi\left(\frac{p}{n}\right), n\in\mathbb{N}, s\geq 0. \quad (1.2)$$

Different generalizations have been examined by many researches(see [2],[3],[4],[5],[6]). Very recently in [7], the authors constructed the following generalised Lupaş operator

$$\xi^*_{n,\gamma_0}(\psi,s)=(1-\gamma_0)^{nr(s)}\sum_{p=0}^{\infty}\frac{(nr(s))_p}{p!}\gamma_0^p\psi\left(\frac{p}{n}\right);\ |\gamma_0|<1,\gamma_0\neq 0,s\geq 0, \quad (1.3)$$

for $\psi:\mathbb{R}^+\to\mathbb{R}$, $n\in\mathbb{N}$ and $r(s)$ is a function defined as

$r(s)=\frac{(1-\gamma_0)s}{\gamma_0}$.

It is to be observed that by putting $\gamma_0=1/2$in this operator, we get the Lupaşoperator mentioned in (1.2). In this paper we develop Stancu-type generalized structure of the operators defined in (1.3) and we establish some important approximation result for presented Stancu-type operators. Stancu-type generalized structure of numerous operators have been developed and examined in [8], [9].

Construction of operators

As per the work mentioned above, we introduce Stancu variant of operators (1.2) as given below.

Definition 1. Let $0\leq\pi_1\leq\pi_2, |\gamma_0|<1, \gamma_0\neq 0$ and$n\in\mathbb{N}$. For $\mu:[0,\infty)\to\mathbb{R}$, we define generalized Lupaş-Stancu operators as

$$\xi^{*,\pi_1,\pi_2}_{n,a}(\psi;s)=(1-\gamma_0)^{nr(s)}\sum_{p=0}^{\infty}\frac{(nr(s))_p}{p!}\gamma_0^p\psi\left(\frac{p+\pi_1}{n+\pi_2}\right), \quad (2.1)$$

where $r(S)$ and $(\mathrm{nr(s)})_p$ is defined as:

- $r(s)=\frac{(1-\gamma_0)s}{\gamma_0}$ and
- $(nr(s))_p=(nr(s))(nr(s)+1)(nr(s)+2)\dots(nr(s)+p-1), p\geq 1$ and $(nr(s))_0=1$.

The operators (2.1) are linear and positive. For $\pi_1=\pi_2=0$, the operators (2.1) turn out to be generalized Lupaş operators defined in [7]. Now, we will establish the behaviour of the operators in (2.1) at the test functions.

Lemma 2.1. For the operators defined as (2.1) and test functions$e_i(\rho)=\rho^i, for i=0,1,2$, we have

1. $\xi^{*,\pi_1,\pi 2}_{n,a}(1;s)=1$,
2. $\xi^{*,\pi_1,\pi 2}_{n,a}(e_1,s)=\frac{\pi_1+ns}{\pi_2+n}$,
3. $\xi^{*,\pi_1,\pi 2}_{n,a}(e_2,s)=\frac{(\gamma_0-1)\pi_1^2+2(\gamma_0-1)\pi_1 ns+ns(-1+(\gamma_0-1)ns)}{(\gamma_0-1)(n+\pi_2)^2}$.

Proof. Lemma 2.1(1) is obvious.

For the test function $e_1(\rho)=\rho$, we have

$$\xi^{*,\pi_1,\pi_2}_{n,\gamma_0}(e_1,s)=(1-\gamma_0)^{nr(s)}\sum_{p=0}^{\infty}\frac{(nr(s))_p}{p!}\gamma_0^p\left(\frac{p+\pi_1}{n+\pi_2}\right)$$

$$=\frac{1}{n+\pi_2}\left[\gamma_0 nr(s)(1-\gamma_0)^{nr(s)}(1-\gamma_0)^{-(nr(s)+1)}+\pi_1\right]=\frac{1}{n+\pi_2}\left[(1-\gamma_0)^{nr(s)}\sum_{p=0}^{\infty}\frac{(nr(s))_p}{p!}p\gamma_0^p+\pi_1\right]=\frac{\pi_1+ns}{\pi_2+n}$$

For the test function $e_2(\rho)=\rho^2$, we have

$$\xi^{*,\pi_1,\pi_2}_{n,\gamma_0}(e_2,s)$$

$$=(1-\gamma_0)^{nr(s)}\sum_{p=0}^{\infty}\frac{(nr(s))_p}{p!}\gamma_0^p\left(\frac{p+\pi_1}{n+\pi_2}\right)^2$$

$$= \frac{1}{(n+\pi_2)^2}\left[(1-\gamma_0)^{nr(s)}\sum_{p=0}^{\infty}\frac{(nr(s))_p}{p!}\gamma_0^p(p^2+2p\pi_1+\pi_1^2)\right]$$

$$= \frac{1}{(n+\pi_2)^2}\left[(1-\gamma_0)^{nr(s)}\sum_{p=0}^{\infty}\frac{(nr(s))_p}{p!}\gamma_0^p p^2 + 2\pi_1(1-\gamma_0)^{nr(s)}\sum_{p=0}^{\infty}\frac{(nr(s))_p}{p!}\gamma_0^p p + \pi_1^2\right]$$

$$= \frac{1}{(n+\pi_2)^2}\left[\gamma_0(1-\gamma_0)^{nr(s)}(nr(s))\sum_{p=1}^{\infty}\frac{(nr(s)+1)_{p-1}}{(p-1)!}\gamma_0^{p-1}p\right]$$

$$+\frac{1}{(n+\pi_2)^2}\left[2\gamma_0\pi_1(1-\gamma_0)^{nr(s)}(nr(s))\sum_{p=1}^{\infty}\frac{(nr(s)+1)_{p-1}}{(p-1)!}\gamma_0^{p-1}+\pi_1^2\right]$$

$$= \frac{1}{(n+\pi_2)^2}\left(\gamma_0(1-\gamma_0)^{nr(s)}(nr(s))\sum_{p=1}^{\infty}\frac{(nr(s)+1)_{p-1}}{(p-1)!}\gamma_0^{p-1}((p-1)+1)\right)$$

$$+\frac{1}{(n+\pi_2)^2}\left(2\gamma_0\pi_1(nr(s))(1-\gamma_0)^{nr(s)}(1-\gamma_0)^{-(nr(s)+1)}\right)+\frac{\pi_1^2}{(n+\pi_2)^2}$$

$$= \frac{(\gamma_0-1)\pi_1^2+2(\gamma_0-1)\pi_1 ns+ns(-1+(\gamma_0-1)ns)}{(\gamma_0-1)(n+\pi_2)^2}.$$

Next, we compute expected value, variance and skewness for the operators defined in (2.1) in the following.

Lemma 2.2 For the operators defined in (2.1) and $\kappa_i^s(t) = (t-s)^i$, we have the following moment estimates,

1. $\xi_{n,\gamma_0}^{*,\pi_1,\pi_2}(\kappa_0^s(t),s) = 1,$
2. $\xi_{n,\gamma_0}^{*,\pi_1,\pi_2}(\kappa_1^s(t),s) = \frac{\pi_1-\pi_2 s}{\pi_2+n},$
3. $\xi_{n,\gamma_0}^{*,\pi_1,\pi_2}(\kappa_2^s(t),s) = \left(\frac{\pi_1+ns}{n+\pi_2}\right)^2 - \frac{ns}{(\gamma_0-1)(n+\pi_2)^2}.$

Proof.
With easy calculation 1 is obtained and by linearity of operators, 2 and 3 can also be obtained.
From Lemma 2.1, it is observed that for $\pi_1 = \pi_2 = 0$, we get the values of the operators at test function and mean, variance and skewnessas mentioned in [7].

Korovkin-type theorem
We demonstrate the standard Korovkin-typetheorems([10],[11]) in this section for the operators defined in (2.1). The Korovkin-type theorem is a result that says if $\xi(e_i,s) \to e_i(s)$for$e_i(s) = s^i$, for $i = 0,1,2$, then it also converges uniformly on a certain function space. We define the space$C([0,\infty))$as collection of all continuous real valued functions defined on the set $[0,\infty)$ and it is a complete normed linear space under the norm
$\|\psi\| = \sup_{\omega\in[0,\infty)}|\psi(\omega)|.$

Theorem 3.1 For any map$\psi \in C([0,\infty))$,the operators $\xi_{n,\gamma_0}^{*,\pi_1,\pi_2}(\psi;s)$ approximate uniformly to ψ on the interval$[0,\theta](\theta>0)$ as $n\to\infty$.
Proof. We have by Lemma 2.1,
$\lim_{n\to\infty}\xi_{n,\gamma_0}^{*,\pi_1,\pi_2}(e_0;1) = 1,$
$\lim_{n\to\infty}\xi_{n,\gamma_0}^{*,\pi_1,\pi_2}(e_1;s) = s,$
$\lim_{n\to\infty}\xi_{n,\gamma_0}^{*,\pi_1,\pi_2}(e_2;s) = s^2.$

Thus, the sequence of positive linear operator$\xi_{n,\gamma_0}^{*,\pi_1,\pi_2}(\psi;s)$ converges to ψ for$\psi \in \{1,s,s^2\}$on the compact interval $[0,\theta],\theta>0$. So, according to the Korovkin-type theorem, the result is true for every map which is continuous on $[0,\theta]$.

Convergence in weighted space

This section is about established convergence results for the operators defined in (2.1) in space of functions under certain weight. This work is inspired from [12].

Let $\sigma(s)=1+s^k, k\geq 2$ be a weight function. Let $A_{s^k}([0,\infty))$be the space with weight $\sigma(s)$ defined by $A_{s^k}[0,\infty)=\{\psi:[0,\infty)\to\mathbb{R}:|\psi(s)|\leq K_\psi(1+s^k), s\geq 0\}$,

where k is a constant which depends only onψ. We use the notation for the sub collection of all continuous functions of $A_{s^k}([0,\infty))$ by $A_{0,s^k}([0,\infty))$and we define$A_{0,s^k}([0,\infty))$by$A_{0,s^k}[0,\infty)=\{\psi\in A_{s^k}[0,\infty):\lim_{s\to\infty}\frac{\psi(s)}{1+s^k}<\infty\}$.

The norm on the space $A_{0,s^k}([0,\infty))$ is defined by

$$\|\psi\|_{s^k}=\sup_{s\in[0,\infty)}\frac{|\psi(s)|}{1+s^k}, k\geq 2.$$

Lemma 4.1 Let $\xi_{n,\gamma_0}^{*,\pi_1,\pi_2}(\psi;s)$ be operators defined by (2.1). Then the following holds,

$$\|\xi_{n,\gamma_0}^{*,\pi_1,\pi_2}(\psi;s)\|_{s^k}\leq\Lambda,$$

where Λ is a constant greater than 0.

Proof. Using Lemma 2.1 and linearity of an operator, we obtain

$$\xi_{n,\gamma_0}^{*,\pi_1,\pi_2}(\sigma;s)=\xi_{n,\gamma_0}^{*,\pi_1,\pi_2}(1+s^k;s)$$
$$=\xi_{n,\gamma_0}^{*,\pi_1,\pi_2}(1;s)+\xi_{n,\gamma_0}^{*,\pi_1,\pi_2}(s^k;s)\to 1+s^k \text{as } n\to\infty.$$

Then, $\|\xi_{n,\gamma_0}^{*,\pi_1,\pi_2}(\sigma;s)\|_{s^k}\to\sup_{s\geq 0}\left\{\frac{1}{1+s^k}+\frac{s^k}{1+s^k}\right\}<\infty \text{ as } n\to\infty.$

So there exist $\Lambda>0$ such that $\|\xi_{n,\gamma_0}^{*,\pi_1,\pi_2}(\sigma;s)\|_{s^k}\leq\Lambda$.From the above lemma, it is observed that the operator $\xi_{n,\gamma_0}^{*,\pi_1,\pi_2}(\psi;s)$act from the space $A_{0,s^k}([0,\infty))$to the space $A_{s^k}([0,\infty))$.

Theorem 4.1 Let $\xi_{n,\gamma_0}^{*,\pi_1,\pi_2}(\psi,s)$ be the operator defined as (2.1) and $\sigma(s)=1+s^k$ be weight function. Then, for map$\psi\in A_{0,s^k}([0,\infty))$, one has

$$\lim_{n\to\infty}\|\xi_{n,\gamma_0}^{*,\pi_1,\pi_2}(\psi,s)-\psi(s)\|_{s^k}=0.$$

Proof. As per the Korovkin theorem(see [13]), it is enough to prove

$$\lim_{n\to\infty}\|\xi_{n,\gamma_0}^{*,\pi_1,\pi_2}(t^j;s)-s^j\|_{s^k}=0, j=0,1,2.$$

By Lemma 2.1(1), It is easy to see that

$$\lim_{n\to\infty}\|\xi_{n,\gamma_0}^{*,\pi_1,\pi_2}(e_0;s)-e_0(s)\|_{s^k}=0.$$

By Lemma 2.1(2), we get

$$\lim_{n\to\infty}\|\xi_{n,\gamma_0}^{*,\pi_1,\pi_2}(e_1;s)-e_1(s)\|_{s^k}=\sup_{s\geq 0}\left|\frac{\frac{\pi_1+sn}{\pi_2+n}-s}{1+s^k}\right|\to 0 \text{ as } n\to\infty.$$

By Lemma 2.1(3), we get

$$\lim_{n\to\infty}\|\xi_{n,\gamma_0}^{*,\pi_1,\pi_2}(e_2;s)-e_2(s)\|_{s^k}==\sup_{s\geq 0}\left|\frac{\frac{(\gamma_0-1)\pi_1^2+2(\gamma_0-1)\pi_1 ns+ns(-1+(\gamma_0-1)ns)}{(\gamma_0-1)(n+\pi_2)^2}-s^2}{1+s^k}\right|$$

$$=\sup_{s\geq 0}\left|\frac{\frac{\pi_1}{(n+\pi_2)^2}+\frac{2\pi_1 ns}{(n+\pi_2)^2}-\frac{ns}{(\gamma_0-1)(n+\pi_2)^2}+\frac{n^2s^2}{(n+\pi_2)^2}-s^2}{1+s^k}\right|$$

$$\leq \frac{\pi_1^2}{(n+\pi_2)^2(1+s^k)} + \frac{2\pi_1 ns}{(n+\pi_2)^2(1+s^k)} + \frac{ns}{(\gamma_0-1)(n+\pi_2)^2(1+s^k)} + \frac{n^2s^2}{(n+\pi_2)^2(1+s^k)} + \frac{s^2}{(1+s^k)} \longrightarrow 0 \text{ as } n \to \infty.$$

Hence, we obtain $\lim_{n\to\infty} \|\xi^{*,\pi_1,\pi_2}_{n,\gamma_0}(e_2;s) - e_2(s)\|_{s^k} = 0.$

This completes the proof.

Rate of convergence

We compute the convergence rate with the help of moduli of continuity.Letψ be a continuous function defined on $[\beta_1,\beta_2]$and $\zeta > 0$. The First ordermoduli of continuity of f is given by$w(\psi,\zeta) = sup\{|\psi(\alpha_1) - \psi(\alpha_2)|: |\alpha_1 - \alpha_2| \leq \zeta, \alpha_1, \alpha_2 \in [\beta_1,\beta_2]\}$.

It is known that$\psi \in C([\beta_1,\beta_2])iffw_\psi(\zeta) \to 0as\zeta \to 0$. (5.1)

Theorem 5.1 Let$\psi \in C([0,p])(p > 0)$,$\zeta > 0$ and $\xi^{*,\pi_1,\pi_2}_{n,\gamma_0}(\psi;s)$ be the operators given in (2.1). Then we have

$$\left|\xi^{*,\pi_1,\pi_2}_{n,\gamma_0}(\psi;s) - \psi(s)\right| \leq \left(1 + \frac{1}{n+\pi_2}\sqrt{\left(\frac{\pi_1+np}{\mathrm{n}}\right)^2 - \frac{p}{(\gamma_0-1)n}}\right) w_1\left(\psi,\frac{1}{n}\right). \quad (5.2)$$

If ψ is continuously differentiable on [0,p], then

$$\left|\xi^{*,\pi_1,\pi_2}_{n,\gamma_0}(\psi;s) - \psi(s)\right| \leq \left(\frac{n}{n+\pi_2}\right) d_{\pi_1,n}\left(1 + \frac{1}{n+\pi_2} d_{\pi_1,n}\right) w\left(\psi',\frac{1}{n}\right) \quad (5.3)$$

where $d_{\pi_1,n} = \sqrt{(\frac{\pi_1+np}{n})^2 - \frac{p}{(\gamma_0-1)n}}$.

Proof. By using inequality (5.1), Lemma 2.2 and with the help of Cauchy-Schwarz inequality, it is easy to obtain the following inequality$|\xi^{*,\pi_1,\pi_2}_{n,\gamma_0}(\psi;s) - \psi(s)| \leq \left(\xi^{*,\pi_1,\pi_2}_{n,\gamma_0}(1;s) + \frac{1}{\zeta}\xi^{*,\pi_1,\pi_2}_{n,\gamma_0}(|t-s|;s)\right) w_1(\psi,\zeta) = \left(1 + \frac{1}{\zeta}\xi^{*,\pi_1,\pi_2}_{n,\gamma_0}(|t-s|;s)\right) w_1(\psi,\zeta) \leq 1 + \frac{1}{\zeta}(\xi^{*,\pi_1,\pi_2}_{n,\gamma_0}((t-s)^2;s))^{\frac{1}{2}} w_1(\psi,\zeta)$.

Here, $s \in [0,p]$and by choosing $\zeta = \frac{1}{n}$, we get the inequality (5.2).

Suppose ψ is differentiable and ψ' is continuous on $[0,p]$,then by the Rolle's Theorem we can write

$\psi(\chi_0) - \psi(\chi_1) = (\chi_0 - \chi_1)\psi'(\chi_0) + (\chi_0 - \chi_1)\left(\psi'(t) - \psi'(\chi_0)\right); t \in (\chi_0,\chi_1)$.

We use the following inequality

$$\left|\xi^{*,\pi_1,\pi_2}_{n,\gamma_0}(\psi;s) - \psi(s)\right|$$

$$\leq \{\xi^{*,\pi_1,\pi_2}_{n,\gamma_0}(|t-s|;s) + \frac{1}{\zeta}\xi^{*,\pi_1,\pi_2}_{n,\gamma_0}(|t-s|^2;s)\} w(\psi',\zeta)$$

$$\leq (\xi^{*,\pi_1,\pi_2}_{n,\gamma_0}((t-s)^2;s))^{\frac{1}{2}}\left(1 + \frac{1}{\zeta}(\xi^{*,\pi_1,\pi_2}_{n,\gamma_0}((t-s)^2;s)^{\frac{1}{2}}\right) w(\psi',\zeta).$$

Noting that $s \in [0,p]$, with the help of Lemma 2.2 and by taking $\zeta = \frac{1}{n}$ we get the required result.

Asymptotic behaviour

We are in the stage to obtain Voronovskaja-type theorems for the operator defined in (2.1).

Theorem 6.1 Let $\xi^{*,\pi_1,\pi_2}_{n,\gamma_0}(\psi;s)$ be the operators in (2.1) and $\psi \in C([0,\theta)), \theta > 0$ and $s \in [0,\theta)$ be a point where ψ' is continuously differentiable. Further assume that $\psi(t) = O(t^2)$ as $t \to \infty$. Then the following holds

$$lim_{n\to\infty}\left(\xi^{*,\pi_1,\pi_2}_{n,\gamma_0}(\psi;s) - \psi(s)\right) = \mathrm{A}(s)\psi'(s) + B(s)\psi''(s),$$

where, $A(s) = \frac{\pi_1 - \pi_2 s}{\pi_2 + n}$ and $B(s) = \frac{1}{(n+\pi_2)^2}((\pi_1 + ns)^2 - ns)$.

Proof. By using Taylor's expansion

$$\psi(m) = \psi(s) + \psi'(s)(m-s) + \frac{\psi''(s)}{2}(m-s)^2 + r(m,s)(m-s)^2 \quad (6.1)$$

where, $\lim_{m\to s} r(m,s) = 0$.

Operating $\xi_{n,\gamma_0}^{*,\pi_1,\pi_2}$ on both side of equation (6.1), we obtain

$$\xi_{n,\gamma_0}^{*,\pi_1,\pi_2}(\psi;s) - \psi(s)$$

$$= \psi'(s)\xi_{n,\gamma_0}^{*,\pi_1,\pi_2}\big((m-s),s\big) + \frac{\psi''(s)}{2}\xi_{n,\gamma_0}^{*,\pi_1,\pi_2}((m-s)^2,s)$$

$$+\xi_{n,\gamma_0}^{*,\pi_1,\pi_2}(r(m,s)(m-s)^2,s).$$

The limit, as $n \to \infty$ gives,

$$\lim_{n\to\infty} n\big[\xi_{n,\gamma_0}^{*,\pi_1,\pi_2}(\psi;s) - \psi(s)\big]$$

$$= \psi'(s)\lim_{n\to\infty}\xi_{n,\gamma_0}^{*,\pi_1,\pi_2}\big((m-s);s\big) + \frac{\psi''(s)}{2}\lim_{n\to\infty}\xi_{n,\gamma_0}^{*,\pi_1,\pi_2}((m-s)^2;s) + \lim_{n\to\infty} n\xi_{n,\gamma_0}^{*,\pi_1,\pi_2}(r(m,s)(m-s)^2;s)$$

Using Cauchy-Schwartz inequality, we obtain,

$$\xi_{n,\gamma_0}^{*,\pi_1,\pi_2}(r(m,s)(m-s)^2,s) \le (\xi_{n,\gamma_0}^{*,\pi_1,\pi_2}(r^2(m,s),s))^{\frac{1}{2}}(\xi_{n,\gamma_0}^{*,\pi_1,\pi_2}((m-s)^4;s))^{\frac{1}{2}}.$$

We also notice that

$$\lim_{m\to s} r(m,s) = 0 \text{ and } \lim_{n\to\infty} n\xi_{n,\gamma_0}^{*,\pi_1,\pi_2}((m-s)^4;s) = 0.$$

From above observation and by using Lemma 2.2 we can obtain the required result.

Acknowledgement

The authors are thankful to the referee(s) for thoroughly reading the manuscript and valuable comments. The author are thankful to the editor(s) for the prompt response to the submission.

REFERENCES

1. A. Lupaş, *The approximation by some positive linear operators*, In Proceedings of the International Dortmund Meeting on Approximation Theory (M.W.. Muller, M.Felten, D.H. Mache, Eds.), Mathematical Research, Akademie Verlag: Berlin, Germany, **86** (1995), pp. 201-209.
2. U. Abel, M. Ivan, *On a generalization of an approximation operator defined by A. Lupaş*, Gen. Math., **15** (2007), no. 1, 2134.
3. O. Agratini, *On a sequence of linear and positive operators*, Facta Universitatis, Nis, Series: Mathematics and Informatics, **14** (1999), pp. 41-48.
4. F. Dirik, *Statistical convergence and rate of convergence of a sequence of positive linear operators*, Mathematical Communications**12**(2007), 147-15312 (2) 147–153.
5. B.M Brown, D Elliott, D.F Paget,*Lipschitz constants for the Bernstein polynomials of a Lipschitz continuous function*,Journal of Approximation Theory,Volume **49**,Issue 2,1987,Pages 196-199,ISSN 0021-9045,https://doi.org/10.1016/0021-9045(87)90087-6.(https://www.sciencedirect.com/science/article/pii/0021904587900876)
6. Erençin, A., Başcanbaz-Tunca, G., & Taşdelen, F. (2014*). Some properties of the operators defined by Lupaş*. *Rev. Anal. Numér. Théor. Approx.*, **43**(2), 168–174. https://doi.org/10.33993/jnaat432-1027.

7. In communication: S. Kariya, R.B.Gandhi, H.Kothari and P.Patel , V. N. Mishra, *Approximation using generalization of Lupas operators* , Applied Mathematics E-notes.
8. A. ERENÇİN Et Al. , *Some preservation properties of MKZ-Stancu type operators*, Sarajevo Journal of Mathematics , vol.**10**, no.1, pp.93-102, 2014
9. Mishra, V. N. and Gandhi, R. (2016). *Simultaneous approximation by szász–mirakjan–stancu–durrmeyer type operators.* Periodica Mathematica Hungarica, 74(1), 118-127. https://doi.org/10.1007/s10998-016-0145-0.
10. Korovkin PP. *Linear Operators and Approximation Theory*. Hindustan Pub. Corp; 1960.
11. M. Mursaleen, V. Karakaya, M. Ert ̈urk, F. G ̈ursoy, *Weighted statistical convergence and its application to korovkin type approximation theorem* **218** (18) 9132–9137.
12. T. Khan, S. A. Khan, *Approximation by stancu type Lupaş operators* Palestine Journal of Mathematics, Vol **11** (3), 700-707, 2020.
13. Altomare, Francesco and Campiti, Michele. *Korovkin-type Approximation Theory and Its Applications*, Berlin, New York: De Gruyter, 1994. https://doi.org/10.1515/9783110884586.

Indian Journal of Natural Sciences www.tnsroindia.org.in ©IJONS

Vol.15 / Issue 88 / Feb / 2025 *International Bimonthly (Print) – Open Access* *ISSN: 0976 – 0997*

RESEARCH ARTICLE

Psychological Trauma, Memory, Myth, and Identity in Kazuo Ishiguro's: The Buried Giant

Zubair Farooq[1]* and P. Prem Chandar[2]

[1]Ph.D Research Scholar, Department of English, Annamalai University, Chidambaram, Tamil Nadu, India.
[2]Assistant Professor, Department of English, Annamalai University, Chidambaram, Tamil Nadu, India.

Received: 21 Nov 2024 Revised: 03 Dec 2024 Accepted: 31 Jan 2025

***Address for Correspondence**
Zubair Farooq
Ph.D Research Scholar,
Department of English,
Annamalai University,
Chidambaram, Tamil Nadu, India.
E.Mail: Zubairfarooq2001@gmail.com

ABSTRACT

This article examines how Ishiguro's novel from 2015, which explores widespread forgetting in post-Arthurian Britain, contributes to discussions about the essence of humanity within societal contexts. It explores four key areas, all centered around the intricate relationship between remembering and forgetting: notions of memory in the context of national identity, portrayals of the British landscape, the cognitive process of recognition, and the emotional dimensions of memory. Drawing from both psychological research on memory and in-depth analysis of the text itself, this interdisciplinary approach enables a nuanced examination of the narrator's role and the impact of Ishiguro's narrative on the reader. Continuously referencing Ishiguro's previous works, the article evaluates how he continues to explore themes of memory and nationality, while also highlighting the fresh perspectives offered by the fusion of ancient settings with contemporary readership. As one of the initial comprehensive analyses of "The Buried Giant," this article firmly places the novel within the realms of literary, cultural, and memory studies.

Keywords: Britian, Landscape, Memory, Nationality, Cognitive.

INTRODUCTION

Kazuo Ishiguro is a prominent British author acclaimed for his poignant exploration of memory, identity, and the human condition. Born in Nagasaki, Japan, in 1954, Ishiguro moved to England at a young age. He studied creative writing at the University of East Anglia, where he honed his craft. Ishiguro's literary career took off with novels like "The Remains of the Day," which won the Man Booker Prize in 1989 and was adapted into a successful film. His writing style is characterized by subtle prose, complex characters, and themes that delve into the intricacies of human relationships. Ishiguro's work has earned him numerous awards and accolades, including the Nobel Prize in

Literature in 2017, recognizing his profound impact on contemporary literature. TBG emerges as a result of blending elements, marking Ishiguro's inaugural exploration into the interplay between society and the individual, valuing both equally. In a 2009 interview, Ishiguro expressed his intent to craft a narrative delving into collective and personal memory, pondering the necessity of forgetting or confronting history for nations, communities, and individuals. This sentiment reverberates through TBG, where the unearthing of buried memories metaphorically exposes Britain to impending devastation, fracturing communities as familiar bonds erode amid conflict. Ishiguro's Nobel acceptance speech in 2017 further amplifies these themes, reflecting on his haunting visit to Auschwitz-Birkenau in 1999 and raising poignant questions about selective remembrance and the merits of moving forward. Despite being situated in ancient Britain, TBG serves as a poignant lens through which to scrutinize contemporary political landscapes and recent historical traumas."The Buried Giant" follows Axl and Beatrice, an elderly British couple, as they traverse a post-Roman, post-Arthurian world in search of their son, who mysteriously no longer resides with them. As they journey, they encounter various characters including Edwin, a young Saxon boy, Wistan, a Saxon warrior, and an older version of Sir Gawain. Throughout the novel, the reader gradually uncovers the past: a history of brutal conflict between Britons and Saxons, ended by Merlin's magic causing collective forgetfulness through the breath of a she-dragon. The central theme revolves around the potential consequences of restoring collective memory to the nation. Although not universally praised by critics, Ishiguro's work is recognized for its relevance to contemporary issues, particularly the importance of remembering for reconciliation. Critics draw parallels between the novel's themes and challenges faced in post-war Europe or present-day conflict zones. Ishiguro anticipated the complexities of merging personal and national memories, a theme addressed in the novel. First and foremost, for a society or nation to grasp its own identity, it necessitates an understanding of a shared history—nations require collective memories to uphold their identities akin to individuals. To examine how Ishiguro addresses this significant theme, I break down the discussion into four parts. Initially, I delve into the concepts of remembering and forgetting in conjunction with theories of nationhood. Subsequently, I explore the significance of the British backdrop and draw comparisons between TBG and Ishiguro's 1987 novel, The Remains of the Day. Transitioning from there, I analyze how Ishiguro engages the reader through his portrayal of a remembered Britain, and I investigate the cognitive process of recognition within the narrative, both as prompted within the reader and depicted by the characters.

Psychological Trauma and its impact

Psychological trauma is a major theme that permeates the plot. The novel investigates the effects of trauma on people and communities, particularly in the years following armed conflict. Individual Trauma and Recollection The narrative takes place in a post-Arthurian Britain where people struggle with their pasts while memories of the past are being erased by a mist. Axl and Beatrice, the main characters, have a type of collective amnesia that alludes to their psychological trauma. They battle with unresolved personal issues and old grudges, which are essential to their path. A profound psychological trauma is reflected in their efforts to regain their memories. The mist that clouds their recollections represents their unwillingness to face old wounds and unresolved problems. They are compelled to confront the emotional wounds from their previous existence, such as remorse and guilt, as they progressively come to remember their history. The novel explores communal trauma in the perspective of a larger society. One way to interpret the memory fog in the book is as a coping technique for the pain of war and violence on a collective level. The mist that clouds memory also represents the efforts made by cultures to bury their dark past. The characters' relationships are deeply scarred by the ancient struggle between the Britons and the Saxons. Unresolved animosity and hatred are the price paid for the tenuous peace that is kept alive by society's amnesia regarding past battles. Pain and Forgiveness In the book, trauma and forgiveness are closely related topics. The protagonists' quest for atonement and reconciliation with their past is reflected in their travel through a place where memories are foggy. The characters have to face their previous transgressions and the anguish they either caused or experienced. Not only is the journey about finding forgotten memories, but it's also about accepting past wrongs and asking for forgiveness. Relationships are also impacted by trauma. Characters' unresolved pasts and the mist that clouds their memories contribute to their emotional estrangement and misunderstandings. Interpersonal Dynamics: Their collective trauma and the difficulty coming to terms with their past deeds and experiences have influenced Axl and Beatrice's relationship as well as their interactions with other character. It explores issues of individual and

communal pain, the difficulty of forgiving others, and the effects of unresolved pasts on interpersonal relationships and societal peace through the effective use of psychological trauma and memory loss. The book is a moving reflection on how people and civilizations deal with the fallout from war and the difficult process of mending.

The fear of remembering

The notion of remembrance stands as one of the three pillars in Ishiguro's exploration of memory. It embodies the process through which his characters reconcile with their past, affirming the existence of what has been lost. In earlier novels leading up to The Buried Giant, this examination of memory was characterized asethically significant and deeply profound, challenging established understandings of memory, grief, and oblivion. However, The Buried Giant diverges in its focus, still challenging conventional notions of ethics and forgetfulness but placing a distinct emphasis on the act of remembering. Unlike in Never Let Me Go, where themes of testimony and affirmation are prominent, here, the narrative shifts focus. In Never Let Me Go, the storytelling of former Hailsham students serves as a testament to their existence and helps them cope with the loss of their school. Conversely, in The Buried Giant, with Merlin's memory erasure leaving only Gawain as the sole witness to the Saxon genocide, testimonies are scarce until the lifting of the mist. The pervasive mist not only obscures distant events but also hampers short-term memory, rendering recollections unreliable. It is only through the collective endeavors of Axl, Beatrice, Wistan, and Edwin, each pursuing their own quests, that Querig is defeated and the mist dissipates, allowing the collective memory of past atrocities to resurface among the Saxons. Reflecting on her research, Anne Whitehead acknowledges that while her focus is on memory in her book, she is equally concerned with the notion of forgetting. Forgetting shapes and defines the very contours of what is recalled and preserved; what is transmitted as remembrance from one generation to the next; and what is thereby handed down to us […] to cherish or discard, but above all to reflect critically upon. Whitehead recognizes the profound significance of remembering in the context of 'twentieth-century crimes against humanity,' yet contends that the notion of forgetting, when viewed in its intricate entirety, merits serious consideration. According to him, forgetting lacks the due acknowledgment as a crucial facet of memory, and a certain degree of forgetting is indispensable for both 'personal and civic health. In Whitehead's perspective, achieving a balance between remembering and forgetting is imperative for communities to effectively navigate the aftermath of social and historical catastrophes. The essential role of forgetting extends to its impact on how and what we remember, emphasizing its political, social, and psychological relevance to relationships and national identity, as evident in The Buried Giant. Whitehead's understanding of forgetting encompasses a spectrum, ranging from what Ricoeur terms the 'reserve of forgetting,' a peaceful form of memory that retains traces beneath consciousness, to a purposeful erasure of crimes, exemplified by the enforced forgetting depicted in the novel.

Between these extremes lies a form of forgetting described by W. G. Sebald in an interview as a community's silence, indicating the presence of something buried. Sebald illustrates this with the case of Paul Bereyter, his former school teacher, who, despite being one-quarter Jewish and persecuted in Sebald's German hometown, returned after the war, living as if nothing had occurred. The surrounding community maintained a 'conspiracy of silence' about Bereyter's persecution, reflecting a phenomenon Sebald suggests is more widespread in Germany than commonly acknowledged. The thematic motif of the abyss becomes apparent as we delve into the concealed memories depicted in The Buried Giant. Past secrets are metaphorically buried beneath the surface: the bones underfoot in the mausoleum, traversed by Axl, Beatrice, Edwin, and Gawain, serve as a tangible representation of this phenomenon. These bones act as a catalyst, stirring Gawain's suppressed memories of the lives he has taken. In response to Beatrice, he wearily acknowledges this realization in his voice: ‘What do you suggest, mistress? That I committed this slaughter?’ ‘Can just one knight of Arthur have killed so many?’ As Gawain peers into the depths of his own history, he grapples with the morally ambiguous deeds he carried out under Arthur's commands. The notion of the abyss is intricately linked to the intricacies of the past and the complexities of forgetting. It symbolizes an unfathomable void where characters must confront distant memories and their deepest apprehensions. Peter Bornedal elucidates the abyss in Nietzschean philosophy as a concept associated with a sense of 'nothingness,' devoid of language and withdrawing into itself. There are parallels drawn between the abyss and Nietzsche's suggestion of forgetting.Drawing from Nietzsche's essay 'On the Uses and Disadvantages of History for Life' and Marc Augé's work 'Oblivion,' Whitehead underscores the ethical contradiction inherent in the act of forgetting. While there exists a

'duty to forget,' even for survivors of atrocities, this obligation cannot supersede the moral responsibility of remembering. It is acknowledged that for life to progress, some degree of forgetting is necessary, yet the challenge lies in doing so without entirely erasing traces of the past. While this notion is pertinent for survivors, it takes on a different ethical dimension when applied to perpetrators of crimes and atrocities. The metaphor of the abyss as memory, alongside oblivion as an alternative manifestation of forgetting, aptly encapsulates the profound explorations into one's concealed past and the potential encounters with past selves.

The Buried Giant serves as both a critique and a reinterpretation of the role of memory in Ishiguro's body of work. His exploration of ethical forms of forgetting, often characterized by moments of emotional release for his character towards the conclusion of his novels, has transitioned towards a critical examination of the ethics of remembering. This shift in focus underscores the intricacies of forgetting in relation to past events, as well as the potential pitfalls of complete transparency in any relationship. Even in well-established relationships, the burden of full disclosure can strain, as illustrated by Axl and Beatrice in the closing chapter. Axl's recollection of his past decision to prevent Beatrice from visiting their son's grave serves as a poignant example of the toll that memory can exact on interpersonal dynamics. The island of forgetting and the boatman evoke symbols reminiscent of Greek mythology, commonly present in Western depictions of death, akin to Lethe, the river associated with forgetfulness. Lethe's name itself is derived from Greek, signifying oblivion or forgetfulness. The legendary character Charon acts as a ferryman, guiding recently deceased souls across the rivers Styx and Acheron to the realm of the underworld. In one of his reflections, Gawain suggests that once his duty to protect Querig is fulfilled, he will 'welcome the boatman with satisfaction' and be transported to the island, where he can finally relieve himself of the weight of his memories.

Forgiveness and Forgetfulness: Exploring the Human Condition

The Buried Giant emphasizes the importance of collective forgetting and remembering, while still maintaining connections to previous novels. Like its predecessors, it prompts readers to evaluate how conformist individual narrators deceive themselves within the broader context of national histories that may be distorted, propagandized, or manipulated for nefarious purposes. The recurring motif in this novel of portraying amnesia as a tangible condition echoes themes explored in The Unconsoled. Ishiguro compares Ryder to a figure holding a torch, illuminating specific parts of the table as he progresses. However, what he leaves behind him is quickly enveloped in darkness, remembered only fleetingly despite being recently seen .The portrayal of the titular Buried Giant triggers various contemplations on the dynamics of memory and forgetfulness. According to Ishiguro's interpretation in an interview, the giant symbolizes the unresolved past conflicts and culpability that have been deliberately suppressed, either through coercion or collective agreement, often in order to prevent further strife. Historical forgetfulness appears to be the primary mechanism by which the existing societal order can be maintained, reaping the advantages of stability in both social and political realms. At the outset of the novel, Wistan ponders: another brother who only yesterday slaughtered his children?" "What extraordinary ability did your magnificent monarch employ to mend the wounds of battle in these regions, to the extent that a visitor can perceive hardly any trace or illusion remaining of them in the present day?" "whilemaggots linger so richly".

Wistan claims that uncovering the hidden giant is crucial to exposing the horrific deeds and deceit committed by those in positions of power in order to preserve an appearance of calm. In a flashback, Axl approaches Gawain after the battle and denounces King Arthur and his knights for their heinous and senseless murders of the defenseless."News of their women, children, and elderly, left unprotected after our solemn agreement not to harm them, now all slaughtered by our hands, even the smallest babes," warns Axl, warning them of the enmity such actions generate among foes. If this were lately done to us, would our hatred exhaust itself? Would we not also fight to the last as they do...?'. Gawain rationalizes the killing of the "civilian" population by arguing that it's necessary to eradicate the generation capable of recollecting the conflict and the loss of their fathers in warfare:'Those small Saxon boys you lament would soon have become warriors burning to avenge their fathersfallen today. The small girls soon bearing more in their wombs, and this circle of slaughter would never bebroken... We may once and for all sever this evil circle.' The burying of the past depends on the brutal eradication of one or two generations so that no one remains to remember what happened. The novel adds another level of individual intricacy, which further muddies

up the overall meaning of the buried giant. The paradox of selective amnesia is demonstrated by certain characters who only recall the unpleasant memories of the past, such as its cruelty and violence, while forgetting the insignificant causes of their hatred for other people or the fondness they formerly felt for those they now loathe.For example, Brennus tries in vain to protect himself from a childhood enemy, a fight that has grown stronger over time without him realizing what started it. Similarly, when the power of forgetfulness wears off, Wistan discovers that despite his hatred, he still feels love for some Britons. But Axl and Beatrice's memories of their love are closely linked to their memories of their son and their refusal to acknowledge his death.In the end, it seems like Axl and Beatrice are motivated to help Wistan defeat the she-dragon Querig and her entrancing breath out of a fear of losing one other. Beatrice shows symptoms of abandonment anxiety, asking to be reassured of Axl's existence multiple times and acting as though she is reliving the anguish of being abandoned by him.But when the mist of memory slowly lifts, it becomes clear that Beatricenot Axlwas the one who departed. The cloud of forgetfulness lifts to reveal the victims' and offenders' personal pain and the changing dynamics in their relationship.

The Eternal Chase: Unravelling the Myth of the Everlasting Pursuit

The underlying mythic structures present in history extend beyond collective societies to encompass individual experiences as well. Axl and Beatrice's quest to reunite with their son transforms into a journey to retrieve memories, hoping to fortify their love and prepare them for a joint passage to the afterlife. As they ascend, first reaching the monastery to understand the mist's nature, then climbing towards the she-dragon's lair to confront their shared past's darker aspects, the motif of ascent symbolizes gaining deeper insights. This motif, along with the quest theme in "The Buried Giant," aligns it with modernist novels inspired by myth, emphasizing spatialized structures over chronological ones. By representing both historical and legendary pasts, the novel diminishes the importance of time and highlights the mythic and universal facets of human experience. This universality is evident in both collective and individual realms: the cyclical violence depicted by the ongoing conflict between Saxons and Britons, and the human journey towards death embodied in Axl and Beatrice's quest, culminating in their encounter with the ferryman. The ferryman, guiding souls to the mythical otherworld, serves as a recurring reminder of death's inevitability. Although Axl and Beatrice find reconciliation through their encounters with the ferryman, his presence lacks the same effect on a collective scale—nations' longer lifespan make them less inclined to acknowledge finality and the imperative to break the cycle of violence.

The portrayal of human history in "The Buried Giant" as cyclical and imbued with myth reflects a modernist inclination towards identifying meaningful patterns, contrasting with the postmodern rejection of deeper historical significance. Ishiguro's incorporation of myth serves not only to enrich the novel's blend of genres—fairy tale, medieval romance, fantasy, contemporary adventure—but also adds depth and universality, aligning with his intended thematic exploration. While the novel's formal placement within postmodern conventions is evident in its playful approach, the utilization of myth contributes to Ishiguro's overarching purpose. In interviews, he elucidates the reasoning behind his narrative choices: “I wanted to write a universal novel about memory and forgetting, and the function of these two antagonistic forces in the life of a nation and in a relationship, regardless of whether it is a relation between husband and wife or between friends.”This very goal of finding universal patterns and meanings in people's lives as well as Ishiguro's depiction of memory as both voluntary and involuntary, shaped by forgetting processes both conscious and unconscious, point to the continuation of a modernist literary legacy that is resurfacing in contemporary literature that rejects postmodernist "playfulness and affectation”.

Rediscovering the Mythic Layers of Your History

Wistan identifies similarities between the monastery and a Saxon fort, just as the narrator of "The Buried Giant" utilizes recognizable elements of Britain to establish a familiar setting before introducing alternative perspectives. While Teo has extensively explored the philosophical concept of recognition, particularly as proposed by Ricoeur, I'm interested in delving into cognitive understandings of recognition here. In psychology, recognition is defined as a distinct form of memory wherein a subject acknowledges having encountered a target previously. Unlike recall, where a subject must spontaneously remember something, recognition is deemed easier because the target item (whether a person, action, or object) is present. Ishiguro's narrator employs the power of recognition to immerse the

reader in this ancient British setting, prompting them to blend memory and imagination to visualize the scene. When describing Axl and Beatrice's dwelling—a village nestled into a hillside—the narrator alludes to the known and familiar elements:"Who knows what will come when quick-tongued men make ancient grievances rhyme with fresh desire for land and conquest. The underlying mythological structures in history extend beyond collective narratives to individual experiences. Axl and Beatrice's journey to find their son becomes a quest for memories, which they believe will strengthen their bond and enable them to journey to the afterlife together. Along the way, they ascend, first reaching a monastery where they gain insight into the mysterious mist, then climbing a cairn toward a she-dragon's lair, confronting dark aspects of their shared past. The motif of ascent symbolizes gaining deeper understanding, while the motif of quest in "The Buried Giant" aligns it with modernist novels inspired by myth, emphasizing spatial zed structures over chronological ones. By representing both historical and legendary pasts, the novel diminishes the importance of time and highlights the mythic and universal aspects of human experience. This universality is evident in both collective and individual experiences: the cyclical violence between Saxons and Britons mirrors the journey of life towards death embodied by Axl and Beatrice's quest, culminating in their encounter with the ferryman who symbolizes passage to the afterlife. Although the ferryman prompts reconciliation between Axl and Beatrice, his presence doesn't have the same impact on the collective level – nations' longer life spans make them less receptive to recognizing finality and breaking the cycle of violence. The portrayal of human history in "The Buried Giant" as cyclical and imbued with myth reflects the modernist inclination to identify meaningful patterns, contrasting with the postmodern rejection of deeper historical significance. When Ishiguro incorporates myth into his narrative, it serves not only to enhance the eclectic blend of genres within the novel—such as fairy tale, medieval romance, fantasy, and contemporary adventure—but also to enrich its depth and universality, aligning with Ishiguro's overarching intentions. In an interview, he elucidates the rationale behind the novel:"I wanted to write a universal novel about memory and forgetting, and the function of these two antagonistic forces in the life of a nation and in a relationship, regardless of whether it is a relation between husband and wife or between friends."The deliberate pursuit of universal meanings and patterns in both individual and communal existence, along with Ishiguro's portrayal of memory as a blend of voluntary and involuntary processes, influenced by both conscious and unconscious acts of forgetting, indicate a continuation of a modernist literary tradition. This trend is resurfacing in contemporary literature that diverges from postmodernist tendencies characterized by "playfulness and affectation.

Exploring the Interplay of Memory and Loss

The main emphasis of Ishiguro's early books, which are primarily told in the first person, is on people's unique experiences of struggling with the past. These stories usually build to an emotional denouement or the protagonist's cathartic discovery. Characters like Etsuko, Ono, and Stevens are initially portrayed as retrospectively revisitingthe past while addressing the current situation at the same time. Upon analyzing collective amnesia in Ishiguro's pre-"The Buried Giant" novels, I argue that the author's use of indirect narrative highlights concerning instances of forgetfulness and its capacity to produce alternate historical accounts. In "The Buried Giant," where the general act of enforced forgetting is carried out through magical methods, upsetting both individual and national processes of grief among the Saxons, Ishiguro takes a more direct approach to depicting political efforts to erase history. Arthur's rewriting of history forces the Saxons and Britons to forget their past, resulting in an uneasy peace. This mist and the collective forgetting that came as a result wasdesigned to sow the seeds of an artificial peace between Britons andSaxons, 'cleans the land of war'. Politically, however, this is also a cover-up for the mass slaughter of the 'innocents',the elderly, women, and children who lived in the Saxon villages and were supposed to be protected by "The Law of the Innocents," a peace agreement that Axl and Arthur drafted years ago. The text frequently references a symbolic buried giant to symbolize the betrayal of both the Saxons and Axl by Arthur, as well as the horror of the mass killing of the innocentAxl saw the horrifying incident as a betrayal of God since the treaty at the time was meant to "bring men closer to God". The pervasive silence and mist in the land serve as evidence of the unspeakable magnitude of atrocities committed on a large scale. Drawing parallels between Arthur's plan for enforced peace in the novel and recent political efforts at collective reconciliation is not challenging. Ishiguro, in discussions about "The Buried Giant," has addressed specific issues regarding widespread atrocities that he aimed to explore through the novel.He most likely had in mind forced reconciliations, like the ones that followed the 1994 genocide in Rwanda, or truth commissionslike the Truth and Reconciliation Commission of South Africa, which aimed to impose a national

peace. Nonetheless, the road to peace will inevitably involve concessions, and in the actualities of political processes, the line separating forced amnesia and reconciliation frequently becomes hazy. Suleiman claims that the South African Truth Commission's basic goal is not "artificial forgetting" of past misdeeds, but rather the "disclosure" of them. She notes that although truth commissions may not always produce the best results, its objective is not to force victims to forgive offenders in exchange for admission of guilt. Rather, the goal is to enable both sides to freely acknowledge and discuss their recollections. This procedure, which enables previously hidden events and actions to be recounted and acknowledged, is a step in the right direction toward collective memory work. Ricoeur goes a step further, arguing that collective memory, not individual memory, is where "the overlapping of the work of mourning and the work of recollection acquires its full meaning". In the framework of a "national self-love," this highlights the issue of a "lost love-object" even more apparent in the context of a "national self-love."Like the process for individuals, the community's grieving needs to go through a reality-testing phase that causes it to break its connection to the lost item. The community cannot be at peace with its past until this process of severance is finished. Referring back to Suleiman's earlier discussion of Rousso and the enforced amnesia put in place in post-war France, forcing someone to forget can cause suppressed memories to resurface. The lost item of a nation's complicated history cannot be properly investigated, debated, or understood since the mourning process is abruptly ended: The Literature of Subversion," arguing that Ishiguro is exploring rich ground for questioning ideas of truth and history by investigating fantasy literature. According to Jackson, the genre of fantasy literature reveals what has been hidden, muted, or covered over. By using the fantasy genre, Ishiguro is able to explore themes of suppressed communal memories and forced national forgetting while navigating the mythological-historical world of Arthurian legend. Ishiguro provides a hypothetical analysis of the risks connected to certain kinds of enforcement using this method.

CONCLUSION

In the novel, memory is not an imperative of justice, not the sole cornerstone of human morality, imbued with the sacred reverence of faith in truthfulness, but is related to real history from the perspective of human expediency, exposing the inherent complexity of contradictions. Thus, for Axl and Beatrice, the vanquished she-dragon Querig, who inflicted "the mist of forgetfulness" upon the inhabitants of the land, allowed them to live and love, yet simultaneously deprived them of the hope of finding "treasured memories," "cherished memories" of their son, their youth, and happiness. They begin to understand that "a memory brings particular pain," and memory brings back not only pleasant memories. Therefore, Sir Gawain pleads in the name of God not to kill Querig, but Wistan, a Saxon warrior, is resolute: "What kind of god is it, sir, wishes wrongs to go forgotten and unpunished?" He is consumed by a thirst for vengeance: "We've a duty to hate every man, woman and child of their blood…, promise me you'll tend well this hatred in your heart The giant – the memory of past wrongs and pain – is disturbed; grief, misfortune, death await humans. How to consign the unforgettable to oblivion? How to overcome the past? Is such memory indeed restored justice? Thus, the moral-ethical significance of memory as a debt to the past, which was explored by P. Ricœur, a philosopher of dialogue, takes on new resonance and richness of poetic semantics in Ishiguro's novel, embodying an infinite unfolding of meanings. The fate of his characters unveils the perilous simplicity of such a view of the problem: the duty of memory as a demand for justice is fraught with new troubles ("dark hatred as bottomless as the sea"... "circle of hate. Therefore, the protagonist is left with only doubts about the correctness of his choice. If, for Nietzsche, without forgetting there is neither life nor happiness nor future [Nietzsche, 1990], then for Ishiguro-the artist, this is also not straightforward. His characters want to remember all the moments of their long history of love and happiness, but along with this, memory reveals betrayal, treachery, the cruelty of a beloved husband towards his son. The postmodern parable, colored with lyricism, is directed towards contemporaries responsible for the future. The overarching idea of the novel is an artistically constructed open question. What then is morally and historically correct? After all, the restored memory turns out to be a curse and evil, while forgetfulness is peace? Thus, within the knightly framework of the plot of the characters' personal history, the image of our world and our unresolved dilemmas is revealed. And the artistic ".projection of the problems of national and personal memory, on the one hand, and the magical reconciling conflict of forgetfulness and forgiveness, on the other, acquires a dramatic dimension in the tragic fate of the novel's protagonists, Axl and Beatrice. Having lived happily (and - forgetfully) all

their lives, they part ways. But it is not the ferryman who separates them, but memory. The final episode of the novel is a dialogue with the fatally ill Beatrice, who believes that the ferryman will return for both Axl and their exiled son soon on that island. But the last lines leave no doubt that Axl knows that the memory they have regained has condemned their happiness. The final episode, full of tragic meaning, leaves no doubt about this. In response to the ferryman's call that he will return for him, Axl does not even turn around. "Yet when Iturn he does not look my way, only to the land and the low sun on the cove". According to Yugin Teo, "Forgetting can be defined as a form of neglect as well as a failure to remember." Both accounts draw attention to a memory flaw that is a result of humanity's inherent vulnerability. But according to TBG, forgetfulness is a condition meant to hide humanity's shortcomings in terms of comprehension, forgiveness, and maintaining peace, not a sign of failure. In fact, it has shown out that the only way to prevent the country from failing is to become forgetful. Referring back to Ishiguro's query from his interview with Spiegel, "When is it healthy to remember, and when is it healthy to forget?" TBG explores the idea that, in the event that forgetting is not beneficial, at least it can be helpful because peace has only been achieved by forgetting. Remembering Ishiguro's question, "When is it healthy to remember, and when is it healthy to forget?" from his interview with Spiegel? TBG examines the theory that, even if forgetting isn't helpful, it can still be advantageous because forgetting is the only way that peace can be attained.

Though it is revealed so briefly and ambiguously that the reader might miss it, Axl was able to mediate a truce and some kind of peace before Arthur broke it and eventually had to turn to Merlin's magic and Querig, so even he cannot be held accountable for this. Axl remembers that "The law was well held on both sides until that day" , and it is this that prompts him to break with Arthur. Gawain catches Axl off guard by referring to "your great law." Although the story seems to be building towards the reader realizing that Axl was involved in the amnesia he experiences, he was just present for the events that came before.But in the end, the book doesn't do a great job of bringing these opposites together. Through his portrayal of a life without personal or societal memory, Ishiguro explores and questions ways of living that focus primarily on a limited number of dimensions. Given his professed interest in investigating the discrepancy between societal memory and personal recollection—particularly with reference to persons who have lived through adverse historical periods their entire lives—it would appear that Ishiguro is eager to explore this issue further. Since Ishiguro acknowledged in his Nobel address that Far Right ideologies and tribal nationalisms are on the rise in the modern era, he has elevated nationalism issues to the fore of world discourse. According to the title of "The Buried Giant," he implies that racism is creeping back to the surface like a sleeping giant. His speech and the book both make the claim that a lack of a sense of community is a contributing factor in today's issues. The story of forgetfulness in "The Buried Giant," where the country is not so much "one nation under God, indivisible," but rather one (or so) nation under the effect of a she-dragon's breath that alters memory, demonstrates the fragility of national identity.

REFERENCES

1. Ishiguro, Never Let Me Go.
2. Whitehead, Memory.
3. Ibid.
4. W. G. Sebald, 'Ghost Hunter', in Lynne Sharon Schwartz (ed.), The Emergence of Memory: Conversations with W. G. Sebald (New York: Seven Stories Press, 2007).
5. Peter Bornedal, The Surface and the Abyss: Nietzsche as Philosopher of Mind and Knowledge (Berlin: De Gruyter, 2010).
6. Robert Macfarlane, Underland: A Deep Time Journey (London: Penguin, 2020).
7. Ishiguro K (1995) *The Unconsoled*. London: Faber & Faber.
8. Ishiguro K (2015) *The Buried Giant*. London: Faber & Faber.
9. Urszula Gołębiowska University of Zielona Góra , MEMORY, MYTH, AND MODERNISM IN KAZUO ISHIGURO'S THE BURIED GIANT , SERIA MONOGRAFII NAUKOWYCH UNIWERSYTETU ZIELONOGÓRSKIEGO II SCRIPTA HUMANA II Vol. 14/2019.

10. Catherine Charlwood, National Identities, Personal Crises: Amnesia in Kazuo Ishiguro's *The Buried Giant*, https://doi.org/10.1515/culture-2018-0004 Received August 2, 2017; accepted March 12, 2018.
11. Edyta Lorek-Jezińska, Testimonies of absence:Trauma and forgetting in *The Buried Giant*by Kazuo Ishiguro, Crossroads. A Journal of English Studies10.15290/cr.2016.15.4.04
12. Ercan Gürova, Individual and Collective Memory in Ishiguro's the Buried Giant, International Journal of Human Studies Uluslararası İnsan Çalışmaları Dergisi ISSN: 2636-8641 Cilt/Volume 5 Sayı/Issue 9 Yıl/Year: 2022 Alındı/Received: 25-09-2022 – Kabul/Accepted: 09-06-2022.
13. Ishiguro K (1982) *A Pale View of Hills*. London: Faber & Faber.
14. Yugin Teo, Monuments, unreal spaces and national forgetting: KazuoIshiguro's *The Buried Giant* and the abyss of memory, Textual Practice, 37:4, 505-526, DOI: 10.1080/0950236X.2022.2056757, (2023).

Indian Journal of Natural Sciences www.tnsroindia.org.in ©IJONS

Vol.15 / Issue 88 / Feb / 2025 *International Bimonthly (Print) – Open Access* *ISSN: 0976 – 0997*

RESEARCH ARTICLE

Tripolar Interior Fuzzy Ideals in Ordered Γ – Semigroup

R.Ezhilarasi[1]* and J. Latha[2]

[1]Associate Professor, Department of Mathematics, Arignar Anna Government Arts College, Villupuram, (Affiliated to Annamalai University), Tamil Nadu, India.
[2]Guest Lecturer, Department of Mathematics, Arignar Anna Government Arts College, Villupuram, (Affiliated to Annamalai University), Tamil Nadu, India.

Received: 21 Nov 2024 Revised: 03 Dec 2024 Accepted: 13 Jan 2025

***Address for Correspondence**
R.Ezhilarasi
Associate Professor,
Department of Mathematics,
Arignar Anna Government Arts College, Villupuram,
(Affiliated to Annamalai University),
Tamil Nadu, India.

ABSTRACT

The fuzzy set are the ideas of Tripolarity fuzzy ideals. This is the outlook of the abstraction of fuzzy sets function and the extension of two- faced fuzzy sets function. Here we bring out some concept of interior fuzzy ideals towards Tripolarity interior fuzzy ideals in ordered gamma semigroups, and we explained about normality, intra – regular, semi simple ordered gamma semigroups. We split up these ideas as semi simple ordered gamma semigroups as for the generalization under the two- faced interior fuzzy ideals. Throughout this paper, we finally conclude that the Tripolarity fuzzy semi ordered gamma semigroup and simple ordered gamma semigroup are same.

Keywords: Tripolarity of fuzzy interior ideals, ordered gamma semigroup, Regularities, Interior ideal, Tripolarity fuzzy set.

INTRODUCTION

It was L.A. Zadeh [10], who popularized the notion of fuzzy set theory in 1965. Fuzzy set navigates with unpredictability. By the concept of fuzzy set theory, many researchers put step towards the generalization of fuzzy set with huge application in various fields and also with pure and applied mathematics for their work [8]. In [2] the author explains about the, intra – regular, in normal, and semi simple group, with the ideas of interior fuzzy ideals and fuzzy ideals where it gives the same values. And also, the concept of (α, β)– interior fuzzy ideals in ordered Γ semigroup is generalised with interior fuzzy ideals and proved in regular, and semi simple ordered Γ semigroup, the ideals of (α, β) – fuzzy ideals and interior ideals coincide. In this paper we finally define semisimple and simple ordered Γ semigroups regarding to the Tripolarity of fuzzy interior ideals.

PRELIMINARIES

Some basic terms and definition from ordered Γ- semigroup theory will be later used to complete the ideals of ordered Γ- semigroup with interior fuzzy ideals.

Definition 1: We define $(S, *)$ a groupoid with two operation on S, where S being a set which contains some of the elements. A semigroup $(S, *)$ is a groupoid in which the operation '$*$' is associative (i.e) $[a* (b* c)] = [(a *b) *c]$, for all $a, b, c \in S$ and $\alpha, \beta, \gamma \in \Gamma$.

Definition 2: The combination along with $(S, *, \leq)$ is defined as an ordered Γ - semigroup if the below mentioned three conditions should be holds good.

i. define an operation on semigroup with $(S, *)$
ii. define Poset $(S, \leq)$
iii. For each element of $a, b, c \in S$ and $\alpha, \beta, \gamma \in \Gamma$ if $a \leq b$, then
$a * c \leq b * c$ and $c * a \leq c * b$

Definition 3: An ordered Γ – semigroup is denoted by S. A subset A(S) containing some elements is said to be a subsemigroup of S if, A is operated with the same element, there will be no changes to the element. Again we get the same element itself (i.e) $A * A \subseteq A$.

Definition4: The concept of semigroup with the operation $(S, *)$ and let $T \subseteq S$. If T is closed under the operation $*$, then we say that $(S, *)$ is a subsemigroup of $(T, *)$.

Definition5: An ordered Γ semigroup is denoted by S. A subset A(S) containing some elements is known to be a right ideal (resp. left) of S if each of the axioms below is true.

i. AS is a subset of S (resp. $SA \subseteq A$)
ii. For each $a, b \in S, \alpha, \beta, \in \Gamma$, a is greater than or equal to b and the element b should present in A then the element a should be in A.

A non-empty subset I (S) is both a left and a right ideal of S then it is said to be an ideal of S.

Definition 6: An ordered Γ - semigroup denoted by S. A subset A of S with some elements is referred to as an innermost ideal of if it adheres to the below axioms:

i. $SAS \subseteq A$
ii. For $a, b \in S$ and $\alpha, \beta, \in \Gamma$, if $a \leq b$ *and* b $\in A$ then $a \in A$.

MAIN RESULTS

The idea of algebraic characteristic of a Tripolarity interior fuzzy ideals were being introduced in this part. The Intra-normal and semisimple ordered semigroup, Tripolarity of interior fuzzy ideals and some of the fuzzy ideals have been proved using some concept of semisimple ordered Γ semigroup with Tripolarity interior fuzzy ideals.

Definition 6: Let S be an ordered Γ - semigroup. A Tripolarity fuzzy subset $\mathcal{T} = (\rho_T, \sigma_T, \tau_T)$ of is known a subsemigroup of S with tripolarity if it satisfies the below three conditions, for each elements of $a, b \in S$ and $\alpha, \beta, \in \Gamma$.

37. $\rho_T(a\alpha b) \geq min\{\rho_T(a), \rho_T(b)\}$
38. $\sigma_T(a\alpha b) \leq \{\sigma_T(a), \sigma_T(b)\}$
39. $\tau_T(a\alpha b) \leq \{\tau_T(a), \tau_T(b)\}$

Definition 7: Let S be an ordered Γ – semigroup with some property. A Tripolarity fuzzy semigroup $\mathcal{T} = (\rho_T, \sigma_T, \tau_T)$ of S is referred to a Tripolarity right (resp. left) fuzzy ideals of S if it satisfies the axioms for each a, b $\in S$ and $\alpha, \beta, \in \Gamma$.

i. $\rho_T(a\alpha b) \geq \rho_T(a)$

ii. $\sigma_{\mathrm{T}}(a\alpha b) \leq \sigma_{\mathrm{T}}(a)$
iii. $\tau_{\mathrm{T}}(a\alpha b) \leq \tau_{\mathrm{T}}(a)$
iv. $a \leq b \Longrightarrow \rho_{\mathrm{T}}(a) \geq \rho_{\mathrm{T}}(b)$
$\sigma_{\mathrm{T}}(a) \leq \sigma_{\mathrm{T}}(b)$and
$\tau_{\mathrm{T}}(a) \leq \tau_{\mathrm{T}}(b)$.

Definition 8: A Tripolarity fuzzy subset $\mathrm{T} = (\rho_{\mathrm{T}}, \sigma_{\mathrm{T}}, \tau_{\mathrm{T}})$ of Ş has both tripolarity left fuzzy ideals and a tripolarity right fuzzy ideal of Ş then it is said to be a tripolarity fuzzy two-sided ideal.

Definition 9: Let Ş be an ordered Γ - semigroup. A tripolarity fuzzy sub semigroup $\mathrm{T} = (\rho_{\mathrm{T}}, \sigma_{\mathrm{T}}, \tau_{\mathrm{T}})$ of Ş is known as tripolarity fuzzy innermost ideal of Ş if it satisfies the axioms: for each$a, b, c \in$ Ş, $\alpha, \beta, \gamma \in \Gamma$,
i. $\rho_{\mathrm{T}}(a\alpha b\beta c) \geq \rho_{\mathrm{T}}(b)$
ii. $\sigma_{\mathrm{T}}(a\alpha b\beta c) \leq \sigma_{\mathrm{T}}(b)$
iii. $\tau_{\mathrm{T}}(a\alpha b\beta c) \leq \tau_{\mathrm{T}}(b)$
iv. $a \leq b \Longrightarrow \rho_{\mathrm{T}}(a) \geq \rho_{\mathrm{T}}(b)$
$\sigma_{\mathrm{T}}(a) \leq \sigma_{\mathrm{T}}(b)$ and
$\tau_{\mathrm{T}}(a) \leq \tau_{\mathrm{T}}(b)$.

Theorem 1: An ordered Γ - semigroup be Ş. If $\{\mathrm{R}_r \mid r \in R\}$ is a family of tripolarity interior fuzzy ideals of Ş, then a tripolarity fuzzy subset $\cap_{r\in R} \mathrm{R}_i := (\cap_{r\in R} \rho_{\mathrm{R}_r}, \cap_{r\in R} \sigma_{\mathrm{R}_r}, \cap_{\cap_{r\in R}} \tau_{\mathrm{R}_r})$ of Ş is also a tripolarity interior fuzzy ideal of Ş and is characterised by
i. $(\cap_{r\in R} \rho_{\mathrm{R}_r})(a) = \cap_{r\in R} \rho_{\mathrm{R}_r}(a) = inf\ inf\{\rho_{\mathrm{R}_r}(a) | r \in R\}$
ii. $(\cup_{r\in R} \sigma_{\mathrm{R}_r})(a) = \cup_{r\in R} \sigma_{\mathrm{R}_r}(a) = \{\sigma_{\mathrm{R}_r}(a) | r \in R\}$
iii. $(\cup_{r\in R} \tau_{\mathrm{R}_r})(a) = \cup_{r\in R} \tau_{\mathrm{R}_r}(a) = sup\ sup\{\tau_{\mathrm{R}_r}(a) | r \in R\}$
for all$a \in$ Ş and $\alpha, \beta, \gamma \in \Gamma$.
Proof: Let $a, b, c \in$ Şand $\alpha, \beta, \in \Gamma$. We obtain that
(i) $(\cap_{r\in R} \rho_{\mathrm{R}_r})(a\ \alpha\ b\ \beta\ c) = \cap_{r\in R} \rho_{\mathrm{R}_r}(a\ \alpha\ b\ \beta\ c)$
$= \inf\{\rho_{\mathrm{R}_r}(a\ \alpha\ b\ \beta\ c) | r \in R\}$
$\geq \inf\{\rho_{\mathrm{R}_r}(b) | r \in R\}$
$= \cap_{r\in R} \rho_{\mathrm{R}_r}(b)$
$= (\cap_{r\in R} \rho_{\mathrm{R}_r})(b)$
(ii) $(\cup_{r\in R} \sigma_{\mathrm{R}_i})(a\ \alpha\ b\ \beta\ c) = \cup_{r\in R} \sigma_{\mathrm{R}_r}(a\ \alpha\ b\ \beta\ c)$
$= \sup\{\sigma_{\mathrm{R}_r}(a\ \alpha\ b\ \beta\ c) | r \in R\}$
$\leq \sup\sup\{\sigma_{\mathrm{R}_r}(b) | r \in R\}$
$= \cup_{r\in R} \sigma_{\mathrm{R}_r}(b)$
$= (\cup_{r\in R} \sigma_{\mathrm{R}_r})(b)$
and
(iii) $(\cup_{r\in R} \tau_{\mathrm{R}_r})(a\ \alpha\ b\ \beta\ c) = \cup_{i\in I} \tau_{\mathrm{R}_r}(a\ \alpha\ b\ \beta\ c)$
$= \sup\{\tau_{\mathrm{R}_r}(a\ \alpha\ b\ \beta\ c) | r \in R\}$
$\leq \sup\sup\{\tau_{\mathrm{R}_r}(a\ \alpha\ b\ \beta\ c) | r \in R\}$
$= \cup_{r\in R} \tau_{\mathrm{R}_r}(b)$
$= (\cup_{r\in R} \tau_{\mathrm{R}_r})(b)$
Let$a, b, \in$ Şand $\alpha, \beta, \in \Gamma$ such that $a \leq b$, we obtain
(i) $(\cap_{r\in R} \rho_{\mathrm{R}_r})(a) = \cap_{r\in R} \rho_{\mathrm{R}_r}(a)$
$= \inf\{\rho_{\mathrm{R}_r}(b) | r \in R\}$
$\geq \inf\{\rho_{\mathrm{R}_r}(b) | r \in R\}$
$= \cap_{r\in R} \rho_{\mathrm{R}_r}(b)$
$= (\cap_{r\in R} \rho_{\mathrm{R}_r})(b)$
(ii) $(\cup_{r\in R} \sigma_{\mathrm{R}_r})(a) = \cup_{i\in I} \sigma_{\mathrm{R}_r}(a)$

$= \sup\sup\{\sigma_{\mathfrak{R}_r}(b)|r \in R\} \leq \sup\sup\{\sigma_{\mathfrak{R}_r}(b)|r \in R\}$

$= \cup_{r\in R}\, \sigma_{\mathfrak{R}_r}(b)$

$= \left(\cup_{r\in R}\, \sigma_{\mathfrak{R}_r}\right)(b)$

Similarly we can prove for,

(iii) $\left(\cup_{r\in R}\, \tau_{\mathfrak{R}_r}\right)(a) = \cup_{r\in R}\, \tau_{\mathfrak{R}_r}(a)$

$= \sup\{\tau_{\mathfrak{R}_r}(b)|r \in R\} \leq \sup\sup\{\tau_{\mathfrak{R}_r}(b)|r \in R\}$

$= \cup_{r\in R}\, \tau_{\mathfrak{R}_r}(b)$

$= (\cup_{r\in R}\, \tau_{\mathfrak{R}_r})(b)$

Therefore, $\cap_{i\in I}\, \mathfrak{R}_r$ is a tripolarity interior fuzzy ideal of $\mathfrak{S}$.

Theorem 2: An ordered Γ - semigroup be $\mathfrak{S}$. Then for every fuzzy ideal of $\mathfrak{S}$ under tripolarity is a tripolarity interior fuzzy ideal of $\mathfrak{S}$.

Proof: A tripolarity fuzzy ideal of $\mathfrak{S}$ can be defined by $\mathfrak{T} = (\rho_{\mathfrak{T}}, \sigma_{\mathfrak{T}}, \tau_{\mathfrak{T}})$ and $a, b, c \in \mathfrak{S}$ and $\alpha, \beta, \gamma \in \Gamma$. Then we have,

(i) $\rho_{\mathfrak{T}}(a\alpha b\beta c) = \rho_{\mathfrak{T}}(a\alpha(b\beta c))$

$\geq \rho_{\mathfrak{T}}(a\alpha(b\beta c))$

$\geq \rho_{\mathfrak{T}}((b\beta c))$

$\geq \rho_{\mathfrak{T}}(bc)$

$\geq \rho_{\mathfrak{T}}(b)$

(ii) $\sigma_{\mathfrak{T}}(a\alpha b\beta c) = \sigma_{\mathfrak{T}}(a\alpha(b\beta c))$

$\leq \sigma_{\mathfrak{T}}(a\alpha(b\beta c))$

$\leq \sigma_{\mathfrak{T}}((b\beta c))$

$\leq \sigma_{\mathfrak{T}}(bc)$

$\leq \sigma_{\mathfrak{T}}(b)$

(iii) $\tau_{\mathfrak{T}}(a\alpha b\beta c) = \tau_{\mathfrak{T}}(a\alpha(b\beta c))$

$\leq \tau_{\mathfrak{T}}(a\alpha(b\beta c))$

$\leq \tau_{\mathfrak{T}}((b\beta c))$

$\leq \tau_{\mathfrak{T}}(bc)$

$\leq \tau_{\mathfrak{T}}(b)$

Hence $\mathfrak{T} = (\rho_{\mathfrak{T}}, \sigma_{\mathfrak{T}}, \tau_{\mathfrak{T}})$ be a tripolarity interior fuzzy ideal of $\mathfrak{S}$.

Definition 10: An Γ semigroup of $\mathfrak{S}$ with ordered group is normal if for each element r $\in \mathfrak{S}$ there exist an element $x \in \mathfrak{S}$ such that $r \leq rxr$

Theorem 3: Let $\mathfrak{S}$ be a normal ordered Γ - semigroup. Then every tripolarity innermost fuzzy ideal of $\mathfrak{S}$ is a tripolarity fuzzy ideal of $\mathfrak{S}$.

Proof: Let $\mathfrak{T} = (\rho_{\mathfrak{T}}, \sigma_{\mathfrak{T}}, \tau_{\mathfrak{T}})$ be defined as a tripolarity fuzzy ideal of some element with the subset A($\mathfrak{S}$) and $a, b, c \in \mathfrak{S}$ and $\alpha, \beta, \gamma \in \Gamma$. Since, $\mathfrak{S}$ is normal there exist $x \in \mathfrak{S}$ such that $a \leq axa$ and we get,

(i) $\rho_{\mathfrak{T}}(ab) \geq \rho_{\mathfrak{T}}(a\,\alpha x\, ab) = \rho_{\mathfrak{T}}((a\alpha x)ab) \geq \rho_{\mathfrak{T}}(a)$

(ii) $\sigma_{\mathfrak{T}}(ab) \leq \sigma_{\mathfrak{T}}(a\,\alpha x\, ab) = \sigma_{\mathfrak{T}}((a\alpha x)ab) \leq \sigma_{\mathfrak{T}}(a)$

(iii) $\tau_{\mathfrak{T}}(ab) \leq \tau_{\mathfrak{T}}(a\,\alpha x\, ab) = \tau_{\mathfrak{T}}((a\alpha x)ab) \leq \tau_{\mathfrak{T}}(a)$

Thus, $\mathfrak{T}$ is a fuzzy ideal with tripolarity condition of $\mathfrak{S}$. By the same way we can prove, $\mathfrak{T}$ is a tripolarity fuzzy left ideal of $\mathfrak{S}$.

Theorem 4: Let $\mathfrak{S}$ -be a regular ordered Γ - semigroup. Then every tripolarity innermost left fuzzy ideal of $\mathfrak{S}$ is a tripolarity left fuzzy ideals of $\mathfrak{S}$.

Proof: Let $\mathfrak{T} = (\rho_{\mathfrak{T}}, \sigma_{\mathfrak{T}}, \tau_{\mathfrak{T}})$ be a tripolarity interior fuzzy left ideal of $\mathfrak{S}$ and $a, b, \in \mathfrak{S}$ and $\alpha, \beta, \in \Gamma$. Since, we consider $\mathfrak{S}$ as a regular, then there exist an element $a \in \mathfrak{S}$ such that $\mathfrak{S}\mathfrak{T} \subseteq \mathfrak{T}$ and we get

(i) $\rho_{\mathrm{T}}(ab) \geq \rho_{\mathrm{T}}(a\, \alpha x\, ab) \geq \rho_{\mathrm{T}}(b)$
(ii) $\sigma_{\mathrm{T}}(ab) \leq \sigma_{\mathrm{T}}(a\, \alpha x\, ab) \leq \sigma_{\mathrm{T}}(b)$
(iii) $\tau_{\mathrm{T}}(ab) \leq \tau_{\mathrm{T}}(a\, \alpha x\, ab) \leq \tau_{\mathrm{T}}(a)$
(iv) For $a, b, \in$ Ş and $\alpha, \beta, \in \Gamma$, if $a \leq b$ and $b \in$ Ŧ, then $a \in$ Ŧ.
Thus, Ŧ is a tripolarity interior fuzzy left ideal of Ş is again a tripolarity fuzzy left ideal of Ş.

Theorem 5: Let Ş be a semi simple ordered Γ - semigroup. Then every tripolarity interior fuzzy ideal of Ş is a tripolarity fuzzy ideal of Ş.
Proof: Let Ŧ = $(\rho_{\mathrm{T}}, \sigma_{\mathrm{T}}, \tau_{\mathrm{T}})$ be a tripolarity interior fuzzy left ideal of Ş and $a, b, \in$ Ş and $\alpha, \beta, \in \Gamma$. Since, Ş is being an ordered Γ - semigroup with semisimple property then there exist an element x, y, z $\in$ Ş and $\alpha, \beta, \gamma \in \Gamma$ such that $a \leq (x\alpha\, ay\, \beta a\, z)$. Then, $ab \leq (x\alpha\, ay\, \beta a\, zb) = (x\alpha\, ay\, \beta)a(\, zb)$. Since, we have
$\rho_{\mathrm{T}}(ab) \geq \rho_{\mathrm{T}}(x\alpha\, ay\, \beta a\, zb) = \rho_{\mathrm{T}}((x\alpha\, ay\, \beta)a(\, zb)) \geq \rho_{\mathrm{T}}(\, a)$
$\sigma_{\mathrm{T}}(ab) \leq \sigma_{\mathrm{T}}(x\alpha\, ay\, \beta a\, zb) = \sigma_{\mathrm{T}}((x\alpha\, ay\, \beta)a(\, zb)) \leq \sigma_{\mathrm{T}}(\, a)$
$\tau_{\mathrm{T}}(ab) \leq \tau_{\mathrm{T}}(x\alpha\, ay\, \beta a\, zb) = \rho_{\mathrm{T}}((x\alpha\, ay\, \beta)a(\, zb)) \leq \tau_{\mathrm{T}}(\, a)$
Thus, Ŧ is a fuzzy right ideal of Ş under tripolarity conditions.

Theorem 6: Let Ş be an ordered Γ - semigroup and (A, B) are subset of Ş. Then the following hold:
(i) $\eta\,(\alpha A) = \eta\,(\beta B)$ *iff* $\alpha A = \beta B$
(ii) $\eta\,(\alpha A) * \eta\,(\beta B) = \eta\,(\alpha\beta AB)$
(iii) $\eta\,(\alpha A) \cap \eta\,(\beta B) = \eta_{X \cap Y}$

Proof: Let A, B be a subset of Ş. If $a \in [AB]$, then there exist $\alpha a \in A$ and $\beta b \in B$ such that $a \leq ab$. Thus,

$(\sigma_{aa} * \sigma_{ab})(x) \leq 1$ $= (\sigma_{a(ab)})(x)$
$= \min\{(\sigma_{aa})\, x, (\sigma_{aa})(y)\}$
$= (\sigma_{aa} * \sigma_{ab})(x)$
$(\tau_{aa} * \tau_{ab})(x) \geq 0$ $= (\tau_{a(ab)})(x)$
$= \min\{(\tau_{aa})\, x, (\tau_{aa})(y)\}$
$= (\tau_{aa} * \tau_{ab})(x)$

Similarly, $\eta\,(\alpha A) * \eta\,(\beta B) = \eta\,(\alpha\beta AB)$ and $\eta\,(\alpha A) \cap \eta\,(\beta B) = \eta_{X \cap Y}$
Hence the multiplication of any two tripolarity interior fuzzy ideals is a subset function of their intersection.

CONCLUSION

In this paper, we characterized the simple ordered Γ - semigroup with tripolar fuzzy simple group. Also, throughout this work we presented the notion of interior fuzzy ideals under tripolarity axioms with ordered Γ- semigroup. Here we proved tripolar fuzzy interior ideals with tripolarity under normal, intra – regular, Γ group, semisimple ordered Γ - semigroup with tripolar fuzzy ideal where it have the same. Hence we aimed to prove that both fuzzy ideal in Ş is also a fuzzy tripolar ideal of Ş. Further we can extend this ideas towards fuzzy algebraic structure for future work.

REFERENCES

1. M. Ibrar, A. Khan and F. Abbas, "Generalized bipolar fuzzy interior ideals in ordered semigroups", *Honam math. J.*, 41 (2),pp.285-300, 2019
2. N. Kehayapulu and M. Tsingelis, "Fuzzy interior ideals in ordered semigroups", *Labachevskii J. Msyh*, 21, pp. 65-71, 2006.
3. A. Khan and M. Shabir, "(α, β) – fuzzy interior ideals in ordered semigroups", *Labachevskii J. Msyh*, 30, pp. 30-39, 2009.
4. K. Linesawat, S. Lekkoksung and N. Lekkoksung, "On anti – hybrid interior ideals in ordered semigroups", *J. Appl. Math. and informatics*, 2022.

5. M. M. K. Rao, "Tripolar fuzzy interior ideals of Γ semigroup", *Ann. Fuzzy Math, Inform.,* 15(2), pp.199-206, 2018.
6. M. M. K. Rao, "Tripolar fuzzy interior ideals and Tripolar fuzzy soft interior ideals over semigroups", *Ann. Fuzzy Math. Inform.*, 20(3), pp. 243-256, 2020.
7. M. M. K. Rao and B. Venkateswarlu, "Tripolar fuzzy ideals of Γ - semiring", *Asia Pacific J. of Math.*, 5(2), pp.192-207, 2018.
8. A. L. Samatha, Afiahayati and F. Hamsyag, "Clustering Indonesian patients with personality disorder using fuzzy C – means", *ICIC Express Letters, Part B: Application*, 12 (11), pp. 995-1001, 2021.
9. M. Shabir and A. Khan and F. Abbas, "Generalized bipolar fuzzy interior ideals in ordered semigroups", *J. Appl. Math. And Informatics*, 27 (5-6), pp. 1447-1457, 2009.
10. L. A. Zad"Fuzzy sets", *Inform. Control*, 8, pp. 338-353, 1965.

Vol.15 / Issue 88 / Feb / 2025 *International Bimonthly (Print) – Open Access* *ISSN: 0976 – 0997*

RESEARCH ARTICLE

Grafting of Nano Copper on Areca Catechu Fibre and Development of Nonwoven Fabric for Shoe Insole

R Sowmiya Bharathi[1], M. Suganthi[2] and T. R. Indumathi[3*]

[1]PG Research Scholar, Department of Chemistry, Dr. N.G.P. Arts and Science College, (Affiliated to Bharathiar University), Coimbatore, Tamil Nadu, India.
[2]Associate Professor and Head, Department of Chemistry, Dr. N.G.P. Arts and Science College, (Affiliated to Bharathiar University), Coimbatore, Tamil Nadu, India.
[3]Assistant Professor, Department of Costume and Apparel Design, PSGR Krishnammal College for Women, (Affiliated to Bharathiar University), Coimbatore, Tamil Nadu, India.

Received: 24 Aug 2024 Revised: 03 Nov 2024 Accepted: 31 Dec 2024

***Address for Correspondence**
T. R. Indumathi,
Assistant Professor,
Department of Costume and Apparel Design,
PSGR Krishnammal College for Women,
(Affiliated to Bharathiar University),
Coimbatore, Tamil Nadu, India.
E.Mail:

ABSTRACT

Nanotechnology refers to the science and technology of matter, Natural products are often sourced from renewable resources, All chemicals were of analytical grade and used as purchased. The Fiber part of the Areca Catechu Linnaeus was purchased from Salem, Tamil Nadu. Copper Sulphate (CuSO4) were purchased from Sigma-Aldrich Chemicals. The Fiber part of the Areca Catechu Linnaeus was purchased from Salem, Tamil Nadu. Fibre is taken as 100g and added 30g of NaOH and 10g of sodium sulfide. The ethanol extract of fiber part of Areca Catechu Linnaeus was prepared with 20g of fiber powder with 80ml of Ethanol and is heated for three hours. The extract was filtered with Whatman Filter Paper. Using the agar-well diffusion method, the antibacterial properties of the Cu nanoparticles were assessed against both Gram +ve and Gram -ve bacteria. Cu Nanoparticles were shown to be highly effective in suppressing both Gram-positive and Gram-negative bacteria, according to observed antimicrobial activity.

Keywords: Nanotechnology refers to the science and technology of matter, Natural products are often sourced from renewable resources.

INTRODUCTION

Nanotechnology refers to the science and technology of matter, manipulated at the atomic level1 . Nanoscience is about the phenomena that occur in systems with nanometer dimensions [2] . Nanoparticles are solid particles or particulate dispersions with a size range of 10–1000 nm3 . Nanomaterials, therefore, refer to the class of materials with at least one of the dimensions in the nanometric range4 . Metallic nanoparticles are a novel class of materials having applications in medical, pharmacology, and agriculture by using biological, chemical, and physical techniques, one can produce nanoparticles with extraordinary properties [5] . "Green Synthesis," which produces a stable product that is easy to use, affordable, and repeatable. High energy, pressure, temperature, or hazardous substances are not needed for this technique6 . Copper is a cheap metal that is abundant on Earth and may be synthesized at a reasonable cost for nanoparticles. Copper nanoparticles are easily combined and bonded with ceramics, polymers, and other metals. They also show physiochemical stability in these combinations [7]. Copper (Cu) is a transition metal with an atomic number of 29, an atomic mass of 63.546, and a density of more than 5 g cm−3. It has a characteristic reddish-orange colour and metallic luster in theualities such as minimal chemical reactivity, excellent electrical and thermal conductivity, superior malleability, and strong corrosion resistance [8] . When compared to modern antibiotics, coper nanoparticles exhibit stronger antibacterial qualities. In addition, in addition to their antibacterial function, they have been reported to possess antifungal, antiviral, and anticancer activities [9] . Flat feet are a common cause of general musculoskeletal pain and problems. Your body's balance begins in the feet; when the feet do not provide proper support, it can raise your risk for joint problems caused by poor posture and unnatural gait. The feet can be subjected to many problems due to daily walking, jumping, and running, which can lead to inflammation, foot strains and injuries. The main causes of foot pain is usually by improper footwear, diabetes and aging. In order to prevent these problems good footwears with comfort functional insoles are preferred to wear by the people. Insoles provide additional cushioning and support, enhancing comfort for the wearer. They can help alleviate pressure points and reduce fatigue during long periods of standing or walking. Many commercial insoles are designed to provide arch support, which can help improve foot alignment and reduce strain on the feet and lower limbs. This is particularly beneficial for individuals with flat feet or high arches. Insoles with cushioning materials such as gel, foam, or air pockets can absorb impact forces while walking or running, reducing the risk of injury and protecting the joints from excessive stress. Certain types of insoles are designed to address specific foot condition or biomechanical issues, such as overpronation or supination. By correcting foot alignment and gait mechanics, these insoles can help prevent injuries and improve overall foot function. Natural foot wear products are more preferable than synthetic for these problems. Natural products often contain fewer synthetic chemicals and additives, reducing the risk of adverse reactions or side effects. They are generally perceived as safer for use on the body or in the environment. Many natural products are biodegradable and have minimal impact on the environment compared to synthetic alternatives. They often require fewer resources to produce and dispose of, reducing pollution and waste. Some natural products, such as herbal remedies and organic foods, may offer health benefits due to their natural ingredients. For example, certain herbs and plant extracts have been used for centuries in traditional medicine for their therapeutic properties.

Natural products are often sourced from renewable resources, such as plants or minerals, making them more sustainable in the long term. Sustainable harvesting practices can help protect ecosystems and ensure a continuous supply of natural resources. Natural ingredients can provide unique textures, colors, and scents that are appealing to consumers. Many people enjoy the sensory experience of using natural products, such as the fragrance of essential oils or the feel of natural fibers against the skin. Thus, natural fiber's have several advantages, including breathability, comfort, biodegradability, and sustainability. They're often more environmentally friendly than synthetic fibers and can be sourced from renewable resources like plants and animals. Additionally, natural fibers tend to be biodegradable, making them more eco-friendly choice. In this research work chemo mechanical technique was used to separate the cellulose nano fibers from the areca nut husk, providing a way to make better use of a waste product[10] . The scientific nomenclature of Areca is Areca Catechu Linnaeus and it belongs to the Arecaceae (Palmae), palm family, and Arecoideae [2]subfamily[14] . Areca nut is one of the important fruits cultivated in

tropical parts of the world. The Areca catechu tree is abundantly established in the mountains and has been farmed in enormous quantities. Because of its link to mouth cancer, its consumption has decreased in the modern world11.It generates a huge quantity of husk, which is a source of areca nut fiber. The potential substitution of lignocellulosic fibers in composite materials for synthetic fibers like carbon, aramid, and glass fibers[15]. With about 50% of all areca nut production in India, Karnataka is the state that produces the most areca fibre[16]. The fiber diameter 54.8µm, which is comparable with commonly available natural fibers. Areca nut fibers are incredibly strong, resistant to fungi, provide excellent insulation, are tough and durable, resilient, static-free, biodegradable, and difficult to ignite[12]. Natural fibers have inherent properties such lignocelluloses, renewable energy, and their application in composites is well established[13] .

MATERIALS AND METHODS

All chemicals were of analytical grade and used as purchased. The Fiber part of the Areca Catechu Linnaeus was purchased from Salem, Tamil Nadu. Copper Sulphate (CuSO4) were purchased from Sigma-Aldrich Chemicals. The reduction of Cu ions is characterized using UV-Visible Spectroscopy- Shimadzu (UV 2600) at 200nm to 800nm range. Infrared spectroscopy (IR) analysis showed molecular functional vibration of chemical groups present in the sample was recorded with Jasco 4700 ranging from 4000 to 400 cm-1 The Size and morphology of the metallic Cu Nanoparticle is characterized using Scanning Electron Microscope (SEM-VEGA3, TESCAN) Czech Republic. The elemental composition of the metallic Cu nanoparticle is confirmed using EDX- BRUKER Nano, GmbH, D-12489(Germany). The Thermal Stability of Cu Nanoparticle is characterized using Thermal Gravimetric Analysis-NETZSCH (NJA-STA 2500 Regulus). The X-Ray Diffraction (XRD) pattern of Cu Nanoparticle was recorded at Bruker D8 Advance.

Collection of Fiber

The Fiber part of the Areca Catechu Linnaeus was purchased from Salem, Tamil Nadu. Then the collected fiber was washed with distilled water. The fiber is soaked in water for 15 days for make it easy to separate the outer shell and inner fiber. The fiber was washed thoroughly in running under well water. Then allow to dry in sunlight for 2 to 4 days and chop the fibre finely for further process.

Softening of Fibre

Fibre is taken as 100g and added 30g of NaOH and 10g of sodium sulfide. By using pressure cooker to get exothermic reaction. Boiled at 1hour in medium flame, bad odour with green colour consistence is appeared. After washed with running water, again boiled the fibres with clean well water for 30mins, resulted with yellow colour. In this method, lignin and hemi cellulose bonds are broken and removed from the fibres, makes it more softer in texture.

Treating with Copper Nanoparticles

Preparation of Fibre Extract

The ethanol extract of fiber part of Areca Catechu Linnaeus was prepared with 20g of fiber powder with 80ml of Ethanol and is heated for three hours. The extract was filtered with Whatman Filter Paper. The extract was collected in the beaker and stored in the refrigerator until further use. The Fiber extract was Pale Yellow Colour.

Preparation of Copper Sulphate solution

1.2709 g of CuSO4 (Molecular weight = 63.546 g/mol) was dissolved in distilled water to make 100 ml of 20 mM Copper Sulphate Solution. The metallic nanoparticles were synthesized of the metal precursor solution of Cu (20mM, 20mL) in a 100 ml beaker.

Treating of Fibre Extract with Copper Nano Particles

A 20ml of ethanolic extract of fiber part of Areca Catechu was added to this copper metal precursor reaction mixture in the magnetic stirring for four hours. The Solution kept overnight and the colour change was observed from pale yellow to sky blue colour and yield is 82%.

Antibacterial Activity

The anti-bacterial activity of the synthesized Cu metallic Nanoparticle is evaluated. Mueller Hinton Agar medium was prepared. Overnight grown Bacterial culture was scrapped over the MHA plate. The disc was loaded with the Cu metallic Nanoparticle and them kept in the MHA media containing bacteria. Positive control and the Negative control were also kept. The plate was incubated for 24 hours at 37°C. The zone of Inhibition was observed. 2.5 Antioxidant Activity The antioxidant activity of the synthesized Cu metallic Nanoparticle is evaluated. The antioxidant activity is carried out as follows 4mg of DPPH is dissolved in 100ml of methanol and 50µg of Cu Nanoparticle is dissolved in 100µl of DMSO. Then the sample is taken for different concentration 50µL, 100µl, 150µL, 200µL and 3mL of DPPH is added. The content is covered with aluminium foil and kept in incubation for 30 minutes in dark condition.

Percentage of Radical = Absorbance of Blank – Absorbance of sample X 100

Scavenging activity Absorbance of Blank

RESULTS AND DISCUSSION

UV-Visible Spectroscopy Analysis (UV)

The UV-Visible spectrum of the Cu Nanoparticle was observed in the wavelength of 275 nm due to the Surface Plasmon Resonance. The conduction and valence hands in Cu Nanoparticles appear to be very close to each other, where electrons can move freely and instigate a surface plasmon resonance (SPR) absorption band. It was observed that the peak was due to the Blue Shift.

Scanning Electron Microscopy analysis (SEM)

The surface morphology and the surface shape of the synthesized nanoparticle is analysed using SEM (Scanning Electron Microscopy). SEM analysis shows the rod or cylindrical shape of Cu Nanoparticle. The obtained morphological shape and boundary size indicated that they possessed an average size of 9 nm and appears as in shape.

Energy Dispersive X-Ray Analysis (EDX)

The EDX characterization shows the chemical composition of the synthesized Cu Nanoparticles. EDX analysis was employed to demonstrate the purity of the Biosynthesized Cu Nanoparticles. Cu nanoparticle revealed specific absorption peaks of Cu element at 1 keV and 8KeV, additionally Sulphur is 2.3KeV and oxygen is 0.5KeV. The relative elemental percentage for Cu was 19.15 %, S was 17.88%, O was 62.98%

X-Ray Diffraction Analysis (XRD)

Crystal Structure, Purity and Crystalline Structure of the Nanoparticles were determined using X-Ray Diffraction (XRD) analysis. The XRD data and it is analysis are given in table1. The diffractogram has four peaks at 2θ values of 39.95, 46.25, 66.81 and 77.53 degree in the experimental diffractogram confirms the face centered cubic structure due to copper metal 26 and corresponding to (hkl) values - (111), (200) and (220) planes of copper. There are seven more peaks in the diffractogram at 31.48, 34.24, 37.51, 47.59, 55.27, 60.20 and 68.90 degrees corresponds to (hkl) values- (110), (111), (110), (002), (113) and (200). These peaks confirm the hexagonal wurtzite. According to the XRD study, obvious and distinct phases are forming for Cu, which suggests that a crystalline nanocomposite was created. The average crystalline size D of the copper nanoparticles have been estimated from the diffractogram by using DebyeScherrer formula, $D = 0.9 \lambda / \beta \cos \theta$ The average crystalline size of the copper nanoparticles is found to be 22 nm. The value of the interplanar spacing between the atoms, d, has been calculated using Bragg's Law, $2d\sin\theta = n \lambda$

where n is the order of diffraction pattern. Lattice constant has been estimated using the formula, a = d√ (h2+k2+l2). The Scherer constant, X-ray wavelength (1.5418 ^ A), peak broadening at half the maximum intensity, and Bragg angle are represented by the variables k, λ, β, and θ, respectively. As a result, the XRD analysis revealed that the particles are initially found as collides. This is supported by the SEM findings, which show some particle aggregates. The XRD measurements provided by the copper nanoparticle from the reference publications indicate that it is structured in a monoclinic configuration.

Thermal Gravimetric Analysis (TGA)

TGA shows the change in mass with temperature, which in turn indicates thermal stability, material purity and moisture content of the nanoparticles. The weight from with weight loss 26.84 %. The Temperature ranging from 280 to 604°C reveals the significant weight loss of 5.43 % due to the degradation of Bioactive molecule capped on the Cu surface in high temperature. The last stage of weight loss could be corresponding to the degradation and evaporation of the Cu when the temperature rises over 600°C

Gas Chromatography-Mass Spectroscopy (GC-MS)

The GC-MS analysis of husk extract of the Areca catechu (areca fibre) shows peaks corresponding to Bioactive compounds and their chemical structure, active principles with their retention time, molecular weight. Concentration were also analysed. The predominant compounds identified were Cyclododecane, n-Tridecan-1-ol, Dodecane, 1-chloro-, 1- Dodecanol, Cyclododecane, Cetene, Lauryl acetate, 1-Tetradecanol, Ethanol, 2- (dodecyloxy)- , 1-Tetradecanol, 1-Decanol, 2-hexyl-, E-15-Heptadecenal, Octadecane, 1- Tetradecyl acetate, Methacrylic acid, tetradecyl ester, Hexadecanoic acid, methyl ester, 1,4- Dibutyl benzene-1,4- dicarboxylate, Hexadecanoic acid, ethyl ester, Diethylene glycol monododecyl etherand, Behenyl acrylate, 1-Hexadecanol, 2-methyl-, Methacrylic acid, heptadecyl ester, 9,12- Octadecadienoic acid (Z,Z)-, methyl ester, 9-Octadecenoic acid (Z) = methyl ester, Phytol, Methyl stearate, Triethylene glycol monododecyl ether, Ethyl Oleate, Octadecanoic acid, ethyl ester, Diethylene glycol monododecyl ether, Triethylene glycol monododecyl ether, Methyl 18- methylnonadecanoate, Diethylene glycol 2-ethylhexyl ether, acetatethese, Triethylene glycol monododecyl ether, Cyclodecasiloxane, eicosamethyl-, Oxirane, heptadecyl-, Triethylene glycol monododecyl ether, Oxirane, hexadecyl-, Benzyldiethyl-(2,6-xylylcarbamoylmethyl)- ammonium benzoate, Cyclodecasiloxane, eicosamethyl-, Dodecanoic acid, dodecyl ester, Octadecanoic acid, dodecyl ester, Octaethylene glycol monododecyl ether, Octadecanal, 2- bromo-, Octaethylene glycol monododecyl ether, Cyclodecasiloxane, eicosamethyl-, Ethyl isoallocholate, Tetradecanoic acid, dodecyl ester, Stigmasterol, Glutinol, Ethyl iso-allocholate, Tetradecanoic acid, dodecyl ester, Stigmasterol, Glutinol, Ethyl iso-allocholate,Smilagenin, Supraene, Cyclodecasiloxane, eicosamethyl-,Smilagenin,4-Hydroxy-4-(1- methoxycyclopropyl)-3,3,5,8,10,10 hexamethyltricyclo[6.2.2.0(2,7)]dodeca-5,11-dien-9- one,Octasiloxane,1,1,3,3,5,5,7,7,9,9,11,11,13,13,15,15-hexadecamethyl-, .gamma.-Sitosterol, Hexadecanoic acid, dodecyl ester, Octasiloxane, 1,1,3,3,5,5,7,7,9,9,11,11,13,13,15,15- hexadecamethyl compounds.

Antimicrobial Activity

Using the agar-well diffusion method, the antibacterial properties of the Cu nanoparticles were assessed against both Gram +ve and Gram -ve bacteria. Cu Nanoparticles were shown to be highly effective in suppressing both Gram-positive and Gram-negative bacteria, according to observed antimicrobial activity. (Fig.8 Staphylococcus aureus and Escherichia. Coli) displayed the largest zone of inhibition in this instance (20-25 mm) It showed significant zone of inhibition for 50 and 25 mg/ml concentration of Cu Nanoparticles. Following this, copper ions may bind to DNA molecules and cause cross32 linking both inside and between nucleic acid strands, which would destabilize the helical helix. Bacterial cells containing copper ions also interfere with biological activities. Cu2+ ions can also penetrate bacterial cell membranes and cause disruptions, which can impair the activity of enzymes. The disruption of the cell membrane by the bioacidal effect of nanoparticles is evident by the existence of an inhibitory zone. The cause can be the particles' size, which increases membrane permeability and causes cell death. The nanoparticles' huge surface area allowed them to be strongly adsorbed on the bacterial cells' surface, disrupting the membrane and allowing internal components to spill out and killing the bacteria.

Antioxidant Activity

The radical scavenging activities of the ligand and complex were evaluated in an invitro assays involving 2,2-diphenyl-2-picryl-hydrazyl (DPPH) with ascorbic acid as a standard. The percentage RSA of the ligand and complex against DPPH are depicted in Table. From the results the copper metal complex demonstrated significantly more antioxidant activities.

Design and Development of Shoe Insole Product

Carding of natural fibre

Carding is the mechanical process that disentangles, cleans and intermixes fibers to produce a continues web suitable for subsequent processing. This is achieved by passing the fibers between the differential moving surface covered with a flexible material embedded with metal pins. The modern process of carding is a mechanical process in which the areca and cotton fiber go through the series of processes to make them ready for later processing. The ratio of areca and cotton fiber was 80:20. To create slivers or webs, the carding procedure was carried out.

(Machine name: Miniature carding process)

1 web = 45gram

Web Length = 47cm

Web Width= 32cm

Nonwoven Fabrication (Needle Punch) Process

Needle punch process of nonwoven fabrics is made from various fibers webs in which fibers are bonded together mechanically through fiber entanglement and frictions after fine needle barbs repeatedly penetrated through the fiber web. The needle boards punch the fibers at the rate of 600-2000 punches per minutes. This repeated punching of needles entangles the fiber together we create a strong bond. The needle punching is a renowned nonwoven process of converting fibers web into self blocking are coherent such as structures using barbed needles.

(Machine name: Nonwoven needle punch machine)

GSM =220

1 web-(size:1-1.2mm)

2 web-(3-3.5mm)

Product Size, Length Width(Adult)

Product size: Length-27, Width-10.5 By adding antimicrobial technology in this show a flop. This allows our product to resist the growth of odour causing microbes as well as the transfer and growth of bacteria and fungus on the soles. Fabricated shoe insoles with functionalized PVA nanofibers exhibit remarkable antimicrobial activity against Staphylococcus aureus and Escherichia. Coli. Eg: antimicrobial rate below 99%.

CONCLUSION

The immense diversity of plants in the green world presents a potential for the synthesis of Cu metal nanoparticles. This study describes a novel, inexpensive, simple, and eco-friendly process for producing Cu nanoparticles using Areca catechu fibre extract. The formed copper nanoparticles' morphological and structural characteristics were investigated using EDX, XRD, and SEM, GC-MS, TGA techniques. The result confirms that copper sulphate may be reduced to extremely stable copper nanoparticles, most of which are between 9 nm in size and contain no contaminants. The optical characteristics of copper nanoparticles were examined using the UV-Vis analysis. The peak in the absorption at 275nm spectra confirms the formation of copper nanoparticles. The enhanced antibacterial activity of fiber extract and synthetic copper nanoparticles was investigated using the agar well diffusion method. These results also show that copper nanoparticles made from extract from the Areca catechu fiber can inhibit the growth of many harmful microbes, such as Staphylococcus aureus and E. Coli. Product is development by shoe insole by using processed areca fiber. These nanoparticles have various advantages, including their suitability for pharmaceutical and medical applications, as well as automotive textile and automobile industry.

REFERENCES

1. T. Pradeep., "A textbook of nanoscience and nanotechnology"., 01., ISBN (13): 978-1-25- 900732-3, (2012)
2. S. M. Lindsay., ''Introduction to nanoscience''.,01., ISBN: 978–019–954421– 9 (Pbk), (2010)
3. VJ Mohanraj and Y Chen., ''Nanoparticles'' Trop. J. Pharm. Res., 5., 1., 561-573, (2006)
4. Michaela Corina Crisan, Mocan Teodora, Mocan Lucian., J. Biomed. Nanotech., 12., 1., 1- 14, (2022)
5. Baraiya Divyeksha Harishchandra, Manikantan Pappuswamy, Antony PU, Ganesh Shama, Pragatheesh A, Vijaya Anand Arumugam, Thirunavukkarasu Periyaswamy, Rajkumar Sundaram., ''Copper nanoparticles: a review on synthesis, characterization and application" Asian Pac J Cancer Biol., 5., 4., 201-210, (2020)
6. Veena Wenging Xu, Mohammed Zahedul Islam Nizami, Iris Xiaoxue Yin, Ollie Yiru Yu, Christie Ying Kei Lung and Chun Hung Chu., ''Application of copper nanoparticles in density"., J. nanomaterials., 12., 5., 805-812, (2022)
7. Madhulika Bhagat, Rythem Anand, Pooja Sharma, Prerna Rajput, Neha Sharma and Khushwace Singh., ''Multifunctional copper nanoparticle: synthesis and application"., ECS J. Solid State Sci. Technol., 10., 1-5, (2021)
8. Julie Chandra C.S., Neena George, Sunil K. Narayanan kutty., ''Isolation and characterisation of cellulose nanofibrils from arecanut husk fibre"., J. Carbohydr. Polym., 6., 2., 158-166, (2016)
9. B S Murty, P Shankar, Baldev Raj, B B Rath and James Murday., Textbook of nanoscience and nanotechnology., 3., 8-12, (2013)
10. Fang-Lin Chao, Te-Hsin Yang, Je-Yau., ''New uses for areca catechu tree"., Int. Wood Prod. J., 11., 94-100, (2020) 11. Manjula Harish1, Dr. Arunkumar H R2., ''Study of properties and prospects of areca fibres and its application"., Int. J. Sci. Res., 12., 569-57, (2022)
11. Raghuveer H. Desai, L. Krishnamurthy, T. N. Shridhar., ''Influence of physical modification on Indian originated areca fiber based polypropylene composites: mechanical and dielectric properties characterisation" Indian J Adv Chem Sci., 1., 27- 33, (2016)
12. R. P. Swamy, G. C. Mohan kumar and Y. Vrushabhendappa., ''Study of areca-reinforced phenol formaldehyde composites"., J. Reinf. Plast. Compos., 23, 1373-1381, (2004)
13. Srinivasa C. V., Bharath K. N., ''Effect of alkali treatment on impact behaviour of areca fibers reinforced polymer composites"., Int. J. Mater. Eng."., 7, 875-879, (2023)
14. S. Dhanalakshmi, P. Ramadevi and B. Basavaraju., ''Areca fiber reinforced epoxy composites: Effect of chemical treatments on impact strength"., J. Chem. Sci. Trans., 4., 409- 418 (2015)
15. J.S. Binoj1, R. Edwin Raj1, B.S.S. Daniel2, S.S. Saravanakumar., ''Comprehensive characterisation of industrially discarded fruit fiber, Tamarindus indica L. as a potential ecofriendly bio-reinforcement for polymer composites"., Int. J. Polym. Anal., 4, 1-17, (2015)
16. S Jothibasu, S Mohanamurugan, R Vijay, D Lenin Singaravelu, A Vinod and MR Sanjay., ''Investigation on the mechanical behavior of areca sheath fibers / jute fibers / glass fibrics reinforced hybrid composite for light weight application"., J. Ind. Text., 27, 1-23, (2018)
17. Yiren Pan, Meng Zhang, Jian Zhang, Xiaoyao Zhu, Huiguang Bian and Chuansheng Wang., ''Effect of silane coupling agent on modification of areca fiber/ natural latex"., J. Mater., 13, 1-12, (2020)
18. G Sai Krishnan, L S Jayakumari, L Ganesh Babu and G Suresh., ''Nanopytomedicine: an emerging platform for drug deliver"., J. Mater. Res. Express., 6, 1-7, (2019)
19. 2Madu, K. E., 1Okoronkwo, G. O. and 2Nwankwo, E. I., J. Mech. Eng. Res.,6, 31- 37(2019)
20. J.S. Binoj, R. Edwin Raj, V.S. Sreenivasan, G. Rexin Thusnavis., ELSEVIER.,13, 156-165 (2016)
21. Jyotishmoy Borah, Nobarun Dutta., ELSEVIER., 5, 2229-2233 (2018)
22. S. Venkatarajan, B. V.Bhuvaneswari, A. Athijayamani, S. Sekar., ELSEVIER., 166, 6- 10 (2019)
23. K.N. Bharath, R.P. Swamy., ''Adhesive tensile and moisture absorption characteristics of natural fibers reinforced urea formaldehyde composites"., IJRTER., 1, 60-62, (2009)
24. Fang-lin Chao, Te-Hsin Yang, Je-Yau., ''New uses for areca catechu tree"., Int. Wood Prod. J., 11, 94-100 (2020)
25. G Sai Krishnan, L S Jayakumari, L Ganesh Babu and G Suresh., ''Investigation on the physical, mechanical and tribological properties of areca sheath fibers for brake pad application"., J. Mater. Res. Express., 6, 1-8, (2019)

26. K. T. Thilagham1· G. Gayathiri Devi2· A. Kadirvel3 · D. Kumar., ''A comparative performance simulation of natural and synthetic sound absorbers in room acoustic applications"., J. Biomass convers.,6., 1-11, (2022)
27. Manish raj, Shahab Fatima, Naresh Tandon., ''A study of areca nut laef sheath fibers as a green sound- absorbing material., ELSEVIER., 4., 1691-169, (2020)
28. K.P. Aishwarya, N. Muralidhar, J.V. Praveen., ''Study on areca nut husk fine fiber fabric reinforced composites panels under dynamic loading conditions"., J. Mater. Today: Proc., 669, 633-641, (2022)
29. Madu, K. E. and Okoronkwo, G. O., ''Areca fiber-reinforced polyester bio-composites pullout analysis"., J. Chem. Sci., 2., 43-51, (2018)
30. M. Masudul hassan, Manfred H. Wagner, H. U. Zaman and Mubarak A, Khan., ''Recent advancement of natural fiber reinforced polymer composite"., J. Nat. Fibers., 8., 165-177 (2014)
31. T. Narendiranath Babu, Tanay Kuclourya, Mohit Kumar Jain, R.V. Mangalaraja., ''Statistical analysis and investigation of tensile test data of coir composites reinforced with graphene, epoxy and carbon fiber"., (IJEAT)., 8.,6., 1092-1101, (2019)
32. W. L. Lai and M. Mariatti., ''The properties of woven betel palm (Areca catechu) reinforced polyester composites"., J. Reinf. Plast. Compos., 27., 925-935, (2008)
33. C I P K Kencanawati, N P G Suardana, I K G Sugita and I W B Suyasa., ''Characteristics of fiber treatments on tensile and impact strengths of pine resin/areca husk fiber biocomposites"., ICKEM., 201., 1-5, (2017)
34. Ramakrishna Hegde, Kirthan L J, V A Girish, Girishkumar R., (IJMET)., 9.,13., 913- 917 (2018)
35. Kishan Naik, R P Swamy., ''Mechanical behavior of areca fiber and maize powder hybrid composites"., (IJERA)., 4.,8., 185-189, (2014)
36. L. Yusriah, S. M. Sapuan, E. S. Zainudin, and M. Mariatti., ''Characterization of physical, mechanical, thermal and morphological properties of agro-waste betal nut (Areca catechu) husk fiber"., J. Adv. Mater. Res., 701., 239-242, (2013)
37. Kishore Dinakarana, Harish Ramesha, Allan Dojo Josepha, Dr. Ramu Murugana, Dr. Sathishkumar Jothi., ''Physical chemical and surface morphological characterization of areca catechu fiber"., J. Mater. Today Proc.,18., 934-940, (2019)
38. Arumugam kayambu, Rajkumar Ramasubbu., ''Influence of chemical treatment on tensile strength, water absorption, surface morphology and thermal analysis of areca sheath fibers"., J. Nat. Fibres.,19(15)., 11435-11448, (2022)
39. K.N. Bharath 1, R.P. Swamy., ''Adhesive tensile and moisture absorption characteristics of natural fibers reinforced urea formaldehyde composites"., IJRTER., 1.,5., 60-62, (2009)
40. K. T. Thilagham, G. Gayathiri Devi, A. Kadirvel, D. Kumar., ''Development of wheat husk biosilica and characterisation of its areca reinforced polyester composites"., J. Biomass Conversion and Biorefinery., 5., 1-11, (2022) 42. Manish Raj, Shahab Fatima, Naresh tandon., ''Acoustical properties of jute felt sintered with cotton shoddy"., ELSIVER., 169., 11-13 (2020)
41. Madu K. E., Okoronkwo G. O., Orji M. U. K., ''Effect of fiber volume fraction and curing time on impact-hardness strength properties of areca fibers reinforced polyester thermoset composites"., (IJETR)., 9.,8., 28-32, (2024)
42. Murkur Rajesh, K. Balaji., J. Mater. Today: Proc., 32., 1-7, (2023)
43. Georgy sunny, T Palani rajan., ''Influence of blend ratio of cotton and arecanut fibers on yarn properties"., (IJCST)., 36.,2., 304-316, (2020)
44. Tamil Moli Loganathan, Mohamed Thariq Hameed Sultan, Mohammad Jawid, Ain Umaira Md Shah, Qumrul Ahsan, Manohar Mariapan, Mohd Shukry Bin Abdul Majid., ''Comparative study of mechanical properties of chemically treated and untreated cyrtostachys renda fibers"., J Bionic Eng., 17., 185-205, (2020)
45. Muhammad Rizal Muhammad Asyraf, Agusril Syamsir, Nazirul Mubin Zahari, Abu Bakar Mohd Supian, Mohammad Ridzwan Ishak, Salit Mohd Sapuan, Shubham Sharma, Ahmad Rashedi, Muhammad Rizal Razman, Sharifah Zarina Syed Zakaria, Rushdan Ahmad IIya and Mohamad Zakir Abd Rashid., ''Mechanical properties of hybrid lignocellulosic fiberreinforced biopolymer green composites: a review J. Adv. Funct. Polym. Mater., 14.,5., 1-5, (2020)

46. Gayathri Vijayakumar, Hindhuja Kesavan, Anisha Kannan, Dhanalakshmi Arulanandam, Jeong Hee Kim, Kwang Jin Kim, Hak Jin Song, Hyung Joo Kim, and Senthil Kumaran Rangarajulu., ''Phytosynthesis of copper nanoparticles using extract of spices and their antibacterial properties"., J. Processes, 9., 8., 1341-1347, (2021).
47. Balashanmugam Pannerselvam, Prabhu Durai, Devasena Thiyagarajan, Hak Jin Song, Kwang Jin Kim, Yun Seok Jung, Hyung Joo Kim, and Senthil Kumaran Rangarajulu., ''Facile synthesis of nanoparticles using Asian spider flower"., J. Processes, 8.,4., 430, (2020).
48. Nuri Oh and Ji-Ho Park., ''Surface chemistry of gold nanoparticles mediates their exocytosis in macrophages"., Int. J. Nanomedicine.,8.,6.,6232-6241, (2014).
49. Iliana A. Ivanova, Dragomira S. Daskalova, Lilia P. Yordanova and Elitsa L. Pavlova., Int. J. Nanomedicine, 12.,2., 21-27, (2024)
50. Hector Katifelis, Iuliia Mukha, Penelope Bouziotis, Nadiia Vityuk, Charalampos Tsoukalas, Andreas C. Lazaris, Anna Lyberopoulou, George E. Theodoropoulos, Efstathios P. Efstathopoulos, and Maria Gazouli. Int. J. Nanomedicine.,15., 6019-6032 (2020).
51. Y.S. Li, N. R. Tao, K. Lu., ELSEVIER., 52.,6., 230-241, (2008).

Table.1:Composition of Cu nanoparticles

ELEMENT	ATOMIC NUMBER	ATOMIC WEIGHT (%)	NORMAL WEIGHT (%)
Cu	29	19.15	43.49
S	16	17.88	20.49
O	8	62.98	36.02

Table.2:Composition of XRD

2θ	Cos θ	Sin θ	FWHM degree	Crystal li ne size 'D' nm	Interplan er spacing 'd' Å	hkl identificat in from peak	$h^2+k^2+l^2$ from identific atio n hkl	Lattice
19.1	0.9861	0.1659	0.0191	73.7446	4.6428	-	-	-
24.3	0.9775	0.2104	32.9870	0.0429	3.6608	-	-	-
27.3	0.9717	0.2359	19.0997	0.0747	3.2651	-	-	-
32.9	0.9590	0.2831	4.9465	0.2922	2.7207	110	2	6.9954
37.5	0.9469	0.3214	0.4485	3.2651	2.3965	111	3	0.7768
42.5	0.9320	0.3624	216.221	0.0068	2.1254	110	2	305.782
51.8	0.8995	0.4368	0.2047	7.5306	1.7633	002	4	0.4094
56.8	0.8796	0.4756	0.5896	2.6733	1.6195	113	11	1.9554
61.5	0.8594	0.5112	0.2576	6.2647	1.5067	200	4	0.5152
71.5	0.8115	0.5842	51.4012	0.0332	1.3184	200	4	1028.024

Table.3: Composition of TGA

TEMPERATURE(°C)	WEIGHT LOSS (%)
40-120°	26.84%
160-280°	10.16%
280-604°	5.43%
552-730°	27.3%

Table.4:Composition of GC-MS

S. No	RT Value	COMPOUN D NAME	MOLECULAR FORMULA	MOLECULAR WEIGHT	COMPOSITIO N	STRUCTURE
1.	13.26	Cyclododeca	C12H24		2.52	
	6	ne		168.319g/m ol		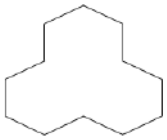
2.	14.861	1-Decane	C10H20	142.29g/mol	5.89	
3.	15.66	Trichloroacet	C2HCl3O2	163.4g/mol	2.97	
	2	ic acid				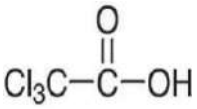

Table.5: Composition of antibacterial activity

ORGANISM	ZONE INHIBITION	OF
Staphylococcus aureus	25mm	
Escherichia coli	27mm	

Table.6: Composition of antioxidant

CONCENTARATION	RSA %
50	7.7474216
100	15.5965
150	25.0911
200	31.7643
250	32.6266

Figure.1: Fiber extract

Figure.2: Copper sulphate solution

Figure.3: Copper Nanoparticles

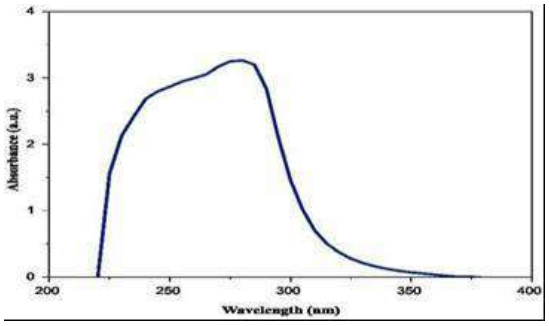

Figure.4: UV-Visible spectrum of the Cu Nanoparticles

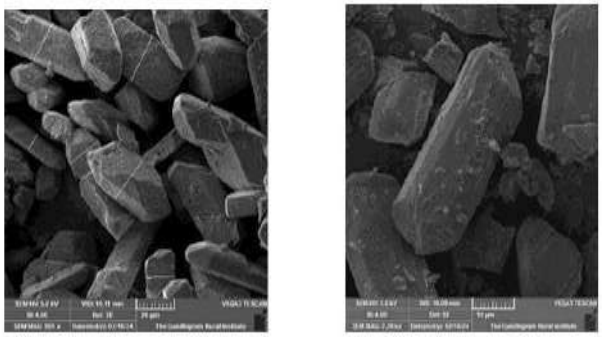

Figure.5: SEM analysis of Cu Nanoparticles

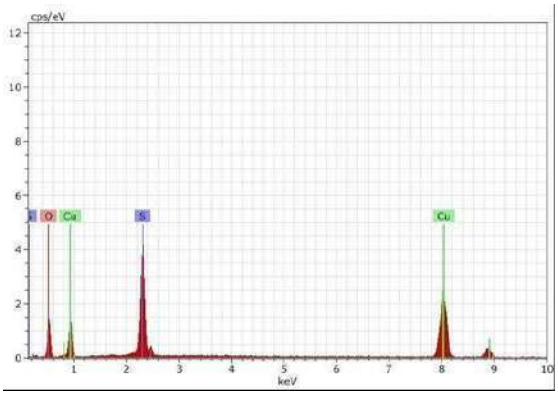

Figure.6: EDX analysis of Cu nanoparticles

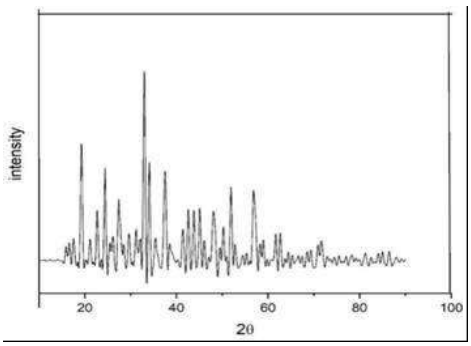

Figure.7: XRD analysis of Cu nanoparticles

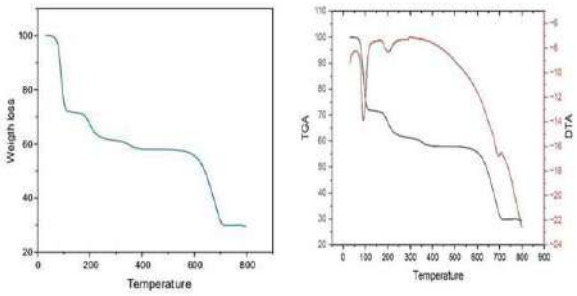

Figure.8: TGA and DTA analysis of Cu Nanoparticles

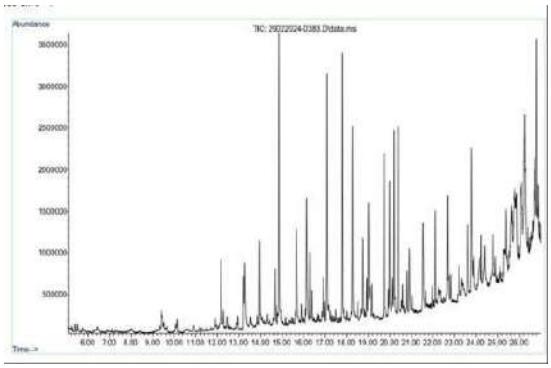

Figure.9: GC-MS analysis of areca fiber extract

Figure.10: Staphylococcus aureus and Escherichia. Coli

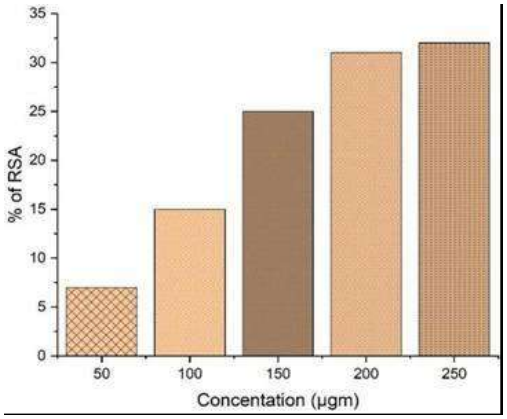

Figure.11: Antioxidant graph

Figure. 12: (a): Arranging the extracted fibers in carding machine (b): Lap formation of natural fibers with ratio 70:30 (areca and Cotton) (c): Formed composite fiber lap

Figure.13 (a): Needle punching of carded (b): Needle punched nonwoven and lapped sheet composite fiber sheet

Figure. 14: Developed Final Product Shoe insole

RESEARCH ARTICLE

Current GSM-based Industrial Power Boiler Monitoring

Billam Anitha Reddy[1]*, K. S. S. Naga Teja[2] and Suma Deepthi Veeraganti[3]

[1]Assistant Professor, Department of Electrical and Electronics Engineering, Malla Reddy Engineering College (Autonomous), Hyderabad, (Affiliated to Jawaharlal Nehru Technological University, Anantapur), Andhra Pradesh, India.
[2]Assistant Professor, Department of Computer Science and Engineering, St. Martin's Engineering College (Autonomous), Hyderabad, (Affiliated to Jawaharlal Nehru Technological University, Anantapur), Andhra Pradesh, India.
[3]Assistant Professor, Department of Electrical and Electronics Engineering, G. Narayanamma Institute of Technology and Science (for Women), (Affiliated to Jawaharlal Nehru Technological University, Anantapur), Andhra Pradesh, India.

Received: 28 Nov 2024 Revised: 09 Dec 2024 Accepted: 20 Jan 2025

***Address for Correspondence**
Billam Anitha Reddy,
Assistant Professor,
Department of Electrical and Electronics Engineering,
Malla Reddy Engineering College (Autonomous), Hyderabad,
(Affiliated to Jawaharlal Nehru Technological University, Anantapur), Andhra Pradesh, India.
E.Mail: anithamrec1@gmail.com

ABSTRACT

The integration of GSM (Global System for Mobile Communications) technology into modern industrial power boiler monitoring systems offers a substantial improvement in operational efficiency, safety, and reliability. This paper explores the design and implementation of a GSM-based monitoring system tailored for industrial boilers. The system comprises a network of sensors to track critical parameters such as temperature, pressure, water level, and gas emissions. Data collected by these sensors is processed by a microcontroller and transmitted via a GSM module to a remote server or directly to operators' mobile devices. This real-time data transmission enables continuous monitoring, early detection of anomalies, and immediate alerts to maintenance personnel. By leveraging historical data, the system facilitates predictive maintenance, reducing downtime and extending the boiler's lifespan. The paper also addresses key challenges, including signal reliability, data security, and system scalability, providing a comprehensive framework for implementing GSM-based monitoring in industrial settings. The findings demonstrate that GSM technology significantly enhances the efficiency and safety of power boiler operations, making it a valuable tool for modern industry.

Keywords: GSM Technology, Industrial Power Boilers, Real-time Monitoring, Sensor Networks, Data Transmission, Remote Monitoring

INTRODUCTION

Power boilers are essential to the production of energy and process heating in the world of industrial activities. Maintaining overall productivity and safety in industrial facilities depends critically on ensuring their effective and secure operation. The capacity to deliver real-time data and predictive insights can be constrained by traditional boiler monitoring systems, which frequently rely on manual inspections and simple automated controls. Delays in reaction times, more downtime, and even possible safety risks can result from this. With the advent of advanced communication technologies, particularly Global System for Mobile Communications (GSM), a new era of boiler monitoring is emerging. GSM technology offers a robust and reliable means of transmitting data over long distances, making it an ideal solution for remote and continuous monitoring of industrial power boilers. This paper explores the integration of GSM technology into modern industrial power boiler monitoring systems. By employing a network of sensors to track key parameters such as temperature, pressure, water level, and gas emissions, data can be collected in real-time and transmitted to a central server or directly to mobile devices. This enables operators to monitor boiler conditions continuously, receive immediate alerts for any anomalies, and make informed decisions to maintain optimal performance and safety. The implementation of GSM-based monitoring systems brings numerous benefits, including enhanced operational efficiency, improved safety measures, and the ability to perform predictive maintenance. This not only reduces the likelihood of unexpected breakdowns but also extends the lifespan of the equipment and reduces operational costs. This introduction sets the stage for a detailed examination of the design, implementation, and advantages of GSM technology in industrial power boiler monitoring. The subsequent sections will delve into the system architecture, data processing methods, and practical applications, demonstrating the transformative potential of GSM-based monitoring in modern industrial settings.

METHODS

In this research plan, we utilize the Arduino Atmel ATmega328P microcontroller, which operates at 5V and 16MHz. The microcontroller features 16 analog and 54 digital I/O pins. The analog pin A1 is connected to a temperature sensor. Digital pins 22 to 29 are interfaced with a pressure sensor via UART 8-bit communication. Digital pin 4 is connected to a proximity sensor through an NPN transistor. Digital pins 52 and 53 are used for level sensor probes, while digital pins 6 to 11 are connected to a 16x2 LCD display. The TX1 pin is linked to the RX pin of a GSM module, and the TX2 pin is connected to the RX pin of a USB to UART/SERIAL board, providing RS232 output for PC connection. The ATmega328P microcontroller reads and processes all parameter values, sending SMS alerts via the SIM800A module if any abnormal situation occurs. Additionally, it transmits the parameter values to the LCD display and to a PC for graphical display via the Arduino IDE.

RESULTS AND DISCUSSION

The implementation of GSM technology in industrial power boiler monitoring systems has yielded several notable results in terms of operational efficiency, safety, and maintenance. The following summarizes the key outcomes observed from deploying such a system: Enhanced Real-Time Monitoring, Improved Safety, Predictive Maintenance, Reduced Downtime, Operational Efficiency, User Experience and Interface, Scalability and Adaptability.

CONCLUSION

The use of GSM technology in industrial power boiler monitoring has resulted in notable advancements in terms of maintenance, efficiency, and safety. Modern industrial operations have found the system's capacity to deliver real-time data, forecast maintenance requirements, and improve overall safety to be a useful tool. These advantages should be further enhanced by ongoing developments in GSM technology and system integration, which will eventually lead to safer and more effective boiler control.

REFERENCES

1. Bishop, J., &Drennan, J. (2019). *Industrial Boiler Efficiency and Monitoring Systems*. Springer.This book provides an overview of various industrial boiler monitoring systems and their efficiency improvements, including modern technological solutions.
2. Cheng, M., & Zhao, X. (2020). "Application of GSM Technology in Remote Monitoring of Industrial Systems." *Journal of Industrial Automation*, 12(4), 234-245.Discusses the application of GSM technology in industrial systems, focusing on remote monitoring aspects and the benefits of real-time data access.
3. Gopal, K. (2018). "Real-Time Monitoring and Control of Boilers Using GSM." *International Journal of Engineering and Technology*, 10(2), 112-120.This paper presents a case study on the implementation of GSM-based monitoring systems in boilers, including system design and results.
4. Liu, Y., & Wang, H. (2021). "Predictive Maintenance for Industrial Boilers Using GSM and IoT." *Journal of Process Control*, 29(1), 45-55.Explores how GSM and Internet of Things (IoT) technologies can be combined for predictive maintenance in industrial boiler systems.
5. Patel, R., & Singh, A. (2022). *Advancements in Industrial Monitoring Systems*. CRC Press. Covers recent advancements in industrial monitoring systems, including the integration of GSM technology for enhanced data collection and analysis.
6. Raj, S., & Kumar, A. (2017). "Optimization of Industrial Boiler Performance Using GSM-Based Monitoring." *Energy Reports*, 3, 123-134.Examines how GSM-based monitoring can optimize boiler performance and improve operational efficiency.
7. Smith, P., & Johnson, L. (2016). "Data Security and Communication in Industrial Monitoring Systems." *Journal of Industrial Technology*, 23(3), 78-89.Discusses the importance of data security and reliable communication in industrial monitoring systems, relevant to the GSM-based approach.

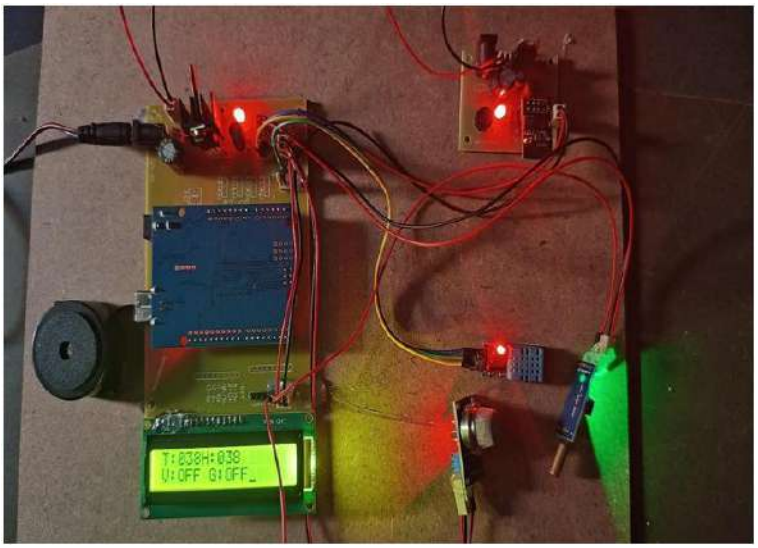

Figure.1: Output Result

Indian Journal of Natural Sciences www.tnsroindia.org.in ©IJONS

Vol.15 / Issue 88 / Feb / 2025 *International Bimonthly (Print) – Open Access* *ISSN: 0976 – 0997*

REVIEW ARTICLE

An Identification of Heart Disorder through Cardiac Sounds – A Review

K.Vetriselvi [1]* and G. Karthikeyan[2]

[1]Research Scholar, PG and Research Department of Computer Science, Periyar Government Arts College, Cuddalore, (Affiliated to Thiruvalluvar University, Vellore), Tamil Nadu, India.
[2]Assistant Professor, PG and Research Department of Computer Science, Periyar Government Arts College, Cuddalore, (Affiliated to Thiruvalluvar University, Vellore), Tamil Nadu, India.

Received: 21 Nov 2024 Revised: 03 Dec 2024 Accepted: 22 Jan 2025

***Address for Correspondence**
K.Vetriselvi,
Research Scholar,
PG and Research Department of Computer Science,
Periyar Government Arts College, Cuddalore,
(Affiliated to Thiruvalluvar University, Vellore), Tamil Nadu, India.
E.Mail: vetriselvik2009@gmail.com

ABSTRACT

Current technology development in the Artificial Intelligence along with Big Data analysis renders more favour in the medicinal field especially in diagnosis of fatal diseases like heart problems without any symptoms. Heart ailments commonly known as Cardio Vascular Diseases can be identified by recording heart beat sound and processing the audio to separate normal and abnormal entities. Machine learning methods were empowered to exercise the audio signals by converting into images and classification methods are used to identify numerous stages of heart problem with slight variation in heart sound. Because of imprecise results, the models of deep learning are utilized to find the problem more approximately by the use of transfer learning models. With the advancement of CNN architecture and RNN techniques, best accuracy could be derived in classification process of audio signals. This research discusses about the challenges and future trends on deep learning application to classify heart sounds. The emerging new models based on CNN architecture for processing audio signals are also discussed along with different steps used for handling the heart sound.

Keywords: Cardio vascular diseases, Deep Learning, Machine Learning, CNN architecture, RNN technique.

INTRODUCTION

Nowadays cardiovascular diseases (CVD) are spreading rapidly all around the world increasing the fatality rate. According to World Health Organization analysis, yearly around 17 million people expire because of CVD and in ten years this number will raise to 23 million[1]. Although this ratio is annoying, good news is that the majority of

cardiovascular disorders can be managed if they are detected as soon as feasible [2],[3]. Trained doctors can diagnose a wide range of CVD by listening to the heart sounds in conjunction with general examination and obtaining a clinical report[4], [5]. Consequently, researches for the automatic processing of heart beat sound signals to diagnose cardiac diseases have been vigorous [6–11]. The prediction systems based on data about heart sound differentiating abnormal from normal heart beats have been developed using recorded signals. Such heart anomaly detecting devices have occasionally attained respectable accuracy. These systems however are decision support systems intended only for qualified doctors who can record patient heart sounds using digital stethoscopes and subsequently validate the accuracy of such signals for diagnostic purposes. This would restrict the use of such systems when there is a lack of educated medical personnel, especially in impoverished parts of the world around. [12]. Even in rural zones, mobile technologies have developed promptly like smart phones during the past ten years [13]. Modern smart phones are built with variety of sensors including microphones, cameras and accelerometers. Additionally, they profit with strong processors that enable complicated on-device computations. Particularly in areas lacking qualified medical personnel, mobile technology can provide individualised healthcare solutions. Both infectious diseases like COVID-19 [14] and uninfected diseases like diabetes [15] and cancer [16] have benefited by the use of mobile technologies in screening programmes. Additionally, they are now used for the initial heart disease problem. Data-driven models to identify cardiac illness have been built utilising heart sound obtained from cell phones [17], [18]. An illustration of the acoustic energy generated by the mechanical behaviour of the cardiac components is provided by a phonocardiogram (PCG), popular representation of heart sounds. A PCG signal identifies any unusual heart activity by listening and examining unexpected sounds. Detecting and categorising heartbeats can also be used in various contexts, including diabetes [21], [22] emotions [23] and meditation [19], [20]. Initially leading heart sound (S1) and succeeding heart sound (S2) are the two main noises that are present in every normal heartbeat. Systole which begins after S1, is the term used to describe the heart's contraction. Diastole refers to the period immediately after S2 when the heart's ventricles will be relaxing and filling with blood.

STEPS FOR HEART SOUND ANALYSIS

There are various steps involved in processing of heart beat sound to identify normal and abnormal persons. These are described in facet as follows.

Preprocessing

The recording of heart beat sounds interrupted by the friction between equipment and person's skin, random noise including breath sounds and environment sounds [24]. Due to the fact that the heart beat sounds are commonly combined with these interference signals, out of band noise must be removed. Wavelet denoising and digital filter denoising are the most frequently used denoising techniques [25]. A new study path in the field of heart beat sounds feature extraction is the wavelet design function for heart beat sound based on past understanding of heart sounds[26].

Segmentation

The objective of this method is to discover the division of PCG signals like artifact, murmur, extrahls, normal, extra systole. Moreover, individual differences occurs in heart beat cycle length, heart beat sound quantity, heart sound murmur type in erroneous PCG signal segmentation. Thus, segmenting the FHS is a fundamental step in the automatic PCG analysis process. In recent years, envelope-based techniques [27], [28], ECG or carotid signal techniques [29], probabilistic model techniques [30], [31], feature-based techniques [32] and time-frequency analysis techniques [33] have all been utilised to segment heart sounds. The underlying premise of the employed algorithms is that the diastolic gap is longer than the systolic gap. Particularly, infants and heart disease patients, this statement is not always accurate for an abnormal heart sound [33]. Based on the similarity between the ECG waveform and the heart beat sound signals, it has been discovered that algorithms that combine the cardiac cycle with an ECG signal perform better in segmenting data with higher hardware and software requirements. Additionally it is difficult to categorize the heart sound by ECG signals because generally database rarely containing synchronized ECG details.

Feature Extraction

In order to make the analysis of the heart sound data easier, feature extraction is utilised to reduce the fresh high dimensional heart beat sounds into low dimensional features. A mixture of handcrafted features and machine learning-based methods have been applied for feature extraction, with the custom of Mel frequency cepstrum coefficients (MFCCs) [34], Mel domain filter coefficients (MFSCs) and heart sound spectra (spectrograms) [35] which are based on the short time Fourier transform (STFT) and discrete wavelet transform (DWT) coefficients [33] and frequency and time features [36] from the time-domain, frequency-domain, scale domain in the S1 and S2 components. Because the window size length affects the resolution of the signals in both the frequency and time domains, it is challenging to balance the features retrieved by STFT with the frequency and time resolutions of the heart sound signals. The wavelet transform is more efficient than these alternatives for identifying the key components of heart sounds [37].

Classification

Classification is utilized to divide the PCG signals into normal and pathological classes like artifact, extrahls, murmur, normal and extra systole categories. Recently most researchers use two types of algorithms like machine and deep learning which are used to classify the heart sounds. In machine learning methods like Artificial Neural Network (ANN), Gaussian mixture models, random forests, Support Vector Machine (SVM), and Hidden Markov Model (HMM) are applied to the extracted features to identify different heart sound signals suggestive of different heart problems [5]. The other types of employed algorithms use the latest popular deep learning methodologies like deep RNNs and CNNs.

Different types of Heart Sounds

The various categories in heart sounds are given as Fig.2.

This contains five classes of heart sounds:

1. Normal : healthy heart sounds
2. Murmur : Extra heart sounds that occur when there is turbulence in blood flow that causes the extra vibrations that can be heard
3. Extrahs : Heart beats with additional sound
4. Extra systole: are additional heart beats occur outside the physiological heart rhythm and can cause unpleasant symptoms
5. Artifact: These sounds are caused due to some interference like environmental, instrumental, or biological interference. In some cases, artifacts are not considered as a defect of the heart as this sound can be generated or produced due to external interference.

Different Methodologies For Heart Sound Classification

There are numerous methods for classifying abnormal and normal persons. The two types discussed are machine and deep learning techniques for processing and classification purpose**.** The input is one-dimensional vector allows the calculation of the output, a feature map by operation of discrete convolution.

Machine Learning Methods for Classification

Deep learning techniques for heart beat sound classification

The essential ideas and deep learning techniques utilised for classifying heart sounds are described in this section. The sample deep learning method for classifying heart sounds is shown in Fig.4. The three primary categories of deep learning-based methodologies are CNN, RNN and hybrid approaches. Below Table 1 lists study that discusses detail on various techniques. The types of characteristics that can be utilised as deep learning input vectors, appropriate pre-processing methods and the procedure for building deep learning models for heart sounds classification are some of the aspects that are discussed in the following subsections.

CNN Methods For Heart Sound Classification

CNN architecture is a specialized type of neural network for processing both time series and image data [54]. CNN kernel unit network is a convolution network that employs specific linear operations rather than standard matrix multiplication across multiple layers. The effective implementation of CNN benefits two dimensional CNN algorithms for classifying heart sounds. The temporal and frequency characteristics of the heart sound signals are obtained by using two dimensional feature map. The unified standards for two dimensional CNN inputs are often created first from the one dimensional heart beat sound signals for classification. The most used feature maps for classifying heart sounds are MFSC [19], [25], [32], MFCC [32] and spectrograms [30], [31]. A two dimensional CNN based strategy was put forth by [29] for the automatic distinction of normal and pathological PCG signals. The segmentation technique developed by Springer [54] was used to split the heart beat sounds at the beginning of S1 into fixed 3 segments. The PCG signals 1D time series were then transformed into 2D.

RNN Methods For Heart Beat Sound Classification

A group of neural networks called RNN is employed for handling sequence data. It has been observed that RNN designs such gated recurrent units (GRUs) and Long Short Term Memory (LSTM) provide cutting edge results in a variety of applications including machine translation, speech recognition and picture captioning [55]. RNN can infer heart beat sound signals because these are a type of sequential data with a robust temporal connection. Actually, they have been highly successful and frequently employed for the categorization of heart beat sounds [56]. In Figure 4, a general diagram of RNN architecture is presented.

DISCUSSION

Comparison of Deep Learning Methods With Machine Learning Methods

A segmentation algorithm was selected to pinpoint the positions of the S1, S2, systole and diastolic phases in the majority of studies using machine learning techniques for classifying heart beat sounds. Time-domain, frequency-domain and statistical properties of the heart beat sound were extracted based on these points. The standard conventional Automatic heart beat sound segmentation and categorization using machine learning Pedro Narvaez suggested the idea of noises [57]. Compared to other machine learning techniques as the discrete wavelet transform, Butterworth filter and empirical mode decomposition, this method has produced superior results (EMD). The categorization of heart beat sounds is more difficult in the segmented heart sound classification making the computation more difficult. However, in unsegment heart beat sounds classification, a brief segment of the heart beat sounds is converted straight into representation features, saving on processing expenses involved with major feature engineering. The effectiveness of the classification is comparable to that of approaches that uses heart sound segmentation. Traditional machine learning techniques for classifying heart sounds make use of little training data and feature learning is predicated on prior understanding of the data. As a result, they rely mostly on learned distributed discriminative characteristics. To design a neural network with numerous hidden layers and implement deep learning, to adjust all model parameters in a hierarchy starting at the bottom, large-scale data training is needed. From the low-level features of the raw data, strong generalisation and abstraction features are gradually derived and the prediction is facilitated by the application of end-to-end networks increasing classification precision. Unlike the single architecture of a deep learning method, predictable machine learning techniques can be applied to jointly extract, select and classify features.

CHALLENGING ISSUES

Limited Heart Sound Data

To prevent over-fitting and to improve and expand the effectiveness of the trained model, deep learning-based approaches for classifying heart sounds need a lot of widely dispersed heart sound data. It is generally accepted that expanding the heart sound datasets for training and the heart beat sounds classification techniques based on deep learning (DL) should increase accuracy and produce superior performance. In reality, there is scarce information about heart beat sounds. Therefore it is crucial to establish minimum training heart sound samples required to

classify heart sounds with high accuracy. Consider [58], which offers a generic methodology that is simple to implement. Additionally, majority of the employed algorithms for deep learning performance is often benchmarked using datasets from the 2016 PhysioNet / CINC Challenge. The widely utilised heart sound datasets, however, are quite modest in size, especially when it comes to certain disorders. These instant datasets include only the sound waveform, excluding pertinent clinical information like gender, age and history of illness, which is crucial for doctors to perform their assessment. The acquisition of numerous heart sound samples especially for a particular kind of problem needs time and effort. As a result, unrestricted heart beat sound datasets are usually limited and unevenly distributed among classes. Additionally, majority of existing deep learning techniques have focused on the classification of heart beat sounds into two classes (normal and pathological). Although, a small number of studies have examined the classification of heart beat sounds with more classifications due to the restricted amount of heart sound data. Trained medical professionals are needed to develop standard heart sound databases in the future that can store clinical data like gender, age, position and medical history including other details and exchange the databases on a cloud platform. This approach benefits deep learning techniques to spot more defined irregularities in heart beat sound signals. The variety of recording devices, environmental noise and data collection sites used in the acquisition of heart sound signals directly contribute to diversity in the data distribution. Some technologies like batch normalisation, regularisation and dropout can be used to avoid over-fitting in the training of deep models and maximise the generalisation performance. It was shown in [59] that even the top model trained on the PhysioNet/CinC Challenge datasets [60] only obtained 50.25% accuracy when tested on the HSSDB dataset. This is due to the limited amount of accessible heart sound data which causes over-fitting and poor accuracy effected with deep learning techniques. Currently there are three methods for handling massive amount of training data required for processing. The first strategy entails enhancing and balancing the existing data using a variety of signal processing techniques including down and over-sampling [61]. Oversampling strategy was able to significantly improve the performance of categorising positive and negative samples by enhancing small heart sound samples and balancing both the samples. Additionally syntactic heart beat sound data has proven to be a successful augmentation technique as in [61]. Reference [66] stated increasing of training data artificially by altering the tempo, speed, volume and pitch of their audio recordings especially by boosting the raw heart sound recordings from 3153 to 53,601. This significantly boosted generalisation and prevented memorising. The backdrop deformation technique was employed as in [63] increases the performance in a noisy environment while augmentation.

The second method for addressing the data limitation issue demands changing the algorithms by providing the cost function, various weights based on the training data distribution. This tackles the problems with categorization imbalances for heart sounds. The distribution is twisted towards the expensive classes and the model prioritises the samples with scant heart sound information. This technique has been extensively used in the classification of voice and images. However the optimization of the inequity problem in the categorization of heart sounds has only been applied in a small number of related works [64] providing an ideal research opportunity. Additionally the creation of artificial images and sounds have been extensively studied using generative adversary networks (GANs), a type of deep neural network architecture made up of two neural networks termed the generator and discriminator. Heart beat sound classification has also been done using a GAN-based technique. For instance, to produce synthetic heart beat sounds with a low noise level, as in [65] presented a GAN based model together with a denoising step utilising the EWT. In order to train deep learning models, GAN based synthetic heart beat sounds can output a wide range of synthetic heart sounds that is distinguished from natural sounds. As a result, synthetic heart beat sounds can help heart sounds function better.

Training Efficiency

Realizing effective training model is a key difficulty in deep learning. Deep learning neural networks are frequently ineffective to train from scratch due to the random initialization of the parameters. The learning rate, optimizer, iteration step and activation function are among the most crucial variables that have a substantial impact on training effectiveness. Repeated experiments are frequently used to investigate these optimization super-parameters; however, this makes the training process quite time-consuming. A significant barrier still exists in training the deep learning model to choose the super parameters automatically. A transfer learning strategy would be used as a proper

resolution. Transfer learning can be utilised to expedite training and produce better results than starting from scratch. Although the method has been engaged in a variability of settings, including acoustic classification paradigms, image classification and natural language processing, it has rarely been utilised to classify heart sounds. The authors present evidence for the effectiveness of deep model training via transfer learning in [66, 67]. However, [67] were the first to investigate the use of transfer learning to categorise heart sounds. By modifying the VGG16 parameters to consider the heart sound data, they were able to substitute the final fully connected layer of the model with two neurons. Compared with training the entire CNN network from beginning, this is a faster method for completing a full CNN-based categorization. Transfer learning was utilised as in [68] to automate the distinction between normal and pathological cardiac sounds. The pretrained CNN models Squeeze Net, Google Net, Inception-V3 and Exception improved with the new data set were fed with the MFCC representation as input. This method produced average classification accuracy up to 89.5% in Pascal challenge database. In addition, [69] introduced 1D CNN in which the parameters of 1D CNN model pre-trained on the PhysioNet HS Classification dataset were cultured using transfer learning. The flattened layer was moved [70] to a new CNN architecture with three output neurons each representing the categories of normal, mildly abnormal and severely abnormal. The TL-Data which differs from the samples in the PhysioNet heart beat sounds classification dataset was used to fine tune the parameters. This procedure speeds up the model training process by avoiding time consuming super parameter exploration.

More Powerful models

Deep learning models with dense layers perform more accurately, becoming recent trend in current improvements. Some examples of pretrained models are modified VGG Net network [71] with 16 convolutional layers, the modified Inception, Residual network [72] with 138 convolutional layers and the modified Alex Net network [73] with 35 convolutional layers. These outperformed models with just two [74] or one [75] convolutional layer, produce heart sound classification accuracy rates of 97.05%, 93.56%, and 89.81%, respectively. However, deep learning representations with additional layers may have more complicated systems requiring more computer power and memory space .This would strictly limit their capability to be used in other systems and on mobile devices. In an integrated approach of utilizing Intelligent Bi-LSTM models with architecture optimization, optimal channel selection, and feature selection holds great promise in revolutionizing the early detection and prediction of heart diseases through WBAN technology [76]. the utilization of Bidirectional LSTMs with attention for heart sound segmentation represents a state-of-the-art approach that shows great potential for enhancing the analysis and diagnosis of heart conditions through advanced signal processing techniques [77]. he integration of machine learning techniques with audio feature extraction for heart sound analysis holds great promise for enhancing the accuracy and efficiency of heart disease detection, paving the way for more advanced and personalized healthcare solutions [78]. he researchers developed a novel framework that leverages AI algorithms to analyze audio signals derived from heart sounds for accurate and efficient classification of heart disease conditions. By combining the power of machine learning with audio signal processing techniques, the proposed framework offers a non-invasive and potentially more accessible approach to diagnosing heart conditions [79]. It investigate the application of deep learning techniques in analysing heart sound signals to predict obstructive coronary artery disease. The research aims to develop a more efficient and accurate method for diagnosing this cardiovascular condition using advanced machine learning algorithms. By harnessing the power of deep learning, the study contributes to the ongoing efforts to enhance the early detection and management of obstructive coronary artery disease, potentially leading to improved patient outcomes and healthcare practices [80]. explores a hybrid model combining Convolutional Neural Networks (CNN) and Long Short-Term Memory networks (LSTM) to classify heartbeat sounds. The study finds that this CNN-LSTM approach significantly improves classification accuracy compared to traditional methods. The ultimate benefit is a more reliable and precise tool for diagnosing heart conditions based on acoustic signals [81]. In order to create effective, light-weight deep learning models, a variety of strategies can be used. One includes the model being compressed by lowering the number of redundant weights in the DNN, which lowers the demands on memory and computational power. Parameter pruning and sharing, low-rank factor decomposition, knowledge distillation, sparse regularisation and mask acceleration are some of the main techniques used today for compressing deep learning models [82]. The use of such techniques in deep learning for classifying heart sound signals would significantly decrease the amount of storage space needed and speed up the processing time for mobile terminal operations.

CONCLUSION

Particularly in low income and middle income countries, CVD have a significant negative impact on health and financial status of individuals. Computer aided methods for the quantifiable analysis and classification of heart beat sounds can be utilised to simplify the earlier diagnosis of CVD. For further testing, heart sounds provide significant initial hints for the estimation of the condition of the human heart. In recent years variety of deep learning methods for classifying heart beat sounds has been created. Deep learning has proven to be the best method for classifying heart beat sounds according to various medical states of the heart. Despite the advances made in the industry, there are still some issues needed for more technical development. The main issues to be fixed are insufficient data, ineffective training and inadequate powerful models. The development of solutions for these challenges promises to make deep learning a major breakthrough for human health management.

REFERENCES

1. Şahin, Bayram, and Gülnur İlgün. "Risk factors of deaths related to cardiovascular diseases in World Health Organization (WHO) member countries." *Health & Social Care in the Community* 30, no. 1 (2022): 73-80.
2. Nelson, Mark R., Christopher M. Reid, Philip Ryan, Kristyn Willson, and Lisa Yelland. "Self-reported adherence with medication and cardiovascular disease outcomes in the Second Australian National Blood Pressure Study (ANBP2)." *Medical Journal of Australia* 185, no. 9 (2006): 487-489.
3. He, Runnan, Henggui Zhang, Kuanquan Wang, Qince Li, Zhiqiang Sheng, and Na Zhao. "Classification of heart sound signals based on AR model." In *2016 Computing in Cardiology Conference (CinC)*, pp. 605-608. IEEE, 2016.
4. Taylor, Allen J., ed. *Learning Cardiac Auscultation: From Essentials to Expert Clinical Interpretation*. Springer, 2015.
5. Brown, Elspeth M. *Heart sounds made easy*. Elsevier Health Sciences, 2008.
6. Rubin, Jonathan, Rui Abreu, Anurag Ganguli, Saigopal Nelaturi, Ion Matei, and Kumar Sricharan. "Recognizing abnormal heart sounds using deep learning." *arXiv preprint arXiv:1707.04642* (2017).
7. Xiao, Bin, Yunqiu Xu, Xiuli Bi, Junhui Zhang, and Xu Ma. "Heart sounds classification using a novel 1-D convolutional neural network with extremely low parameter consumption." *Neurocomputing* 392 (2020): 153-159.
8. Alam, Shahnawaz, Rohan Banerjee, and Soma Bandyopadhyay. "Murmur detection using parallel recurrent & convolutional neural networks." *arXiv preprint arXiv:1808.04411* (2018).
9. Li, Tao, Yibo Yin, Kainan Ma, Sitao Zhang, and Ming Liu. "Lightweight end-to-end neural network model for automatic heart sound classification." *Information* 12, no. 2 (2021): 54.
10. Alkhodari, Mohanad, and Luay Fraiwan. "Convolutional and recurrent neural networks for the detection of valvular heart diseases in phonocardiogram recordings." *Computer Methods and Programs in Biomedicine* 200 (2021): 105940.
11. Chen, Yongchao, Shoushui Wei, and Yatao Zhang. "Classification of heart sounds based on the combination of the modified frequency wavelet transform and convolutional neural network." *Medical & Biological Engineering & Computing* 58 (2020): 2039-2047.
12. Sheldon, George F., *et al.* "The global health workforce shortage: role of surgeons and other providers." *Advances in surgery* 42 (2008): 63-85.
13. Wood, Christopher S., *et al.* "Taking connected mobile-health diagnostics of infectious diseases to the field." *Nature* 566, no. 7745 (2019): 467-474.
14. Udugama, Buddhisha, *et al.* "Diagnosing COVID-19: the disease and tools for detection." *ACS nano* 14.4 (2020): 3822-3835.
15. Shaw, Ryan J., *et al.* "Self-monitoring diabetes with multiple mobile health devices." *Journal of the American Medical Informatics Association* 27, no.5 (2020): 667-676.
16. Bhatt, Shreya, *et al.* "Mobile technology and cancer screening: Lessons from rural India." *Journal of global health* 8, no.2 (2018).

17. Thiyagaraja, Shanti R., *et al.* "A novel heart-mobile interface for detection and classification of heart sounds." *Biomedical Signal Processing and Control* 45 (2018): 313-324.
18. Kang, Si-Hyuck, *et al.* "Cardiac auscultation using smartphones: pilot study." *JMIR mHealth and uHealth* 6.2 (2018): e8946.
19. Wu, Shr-Da, and Pei-Chen Lo. "Inward-attention meditation increases parasympathetic activity: a study based on heart rate variability." *Biomedical Research* 29, no. 5 (2008): 245-250.
20. Wu, Shr-Da, and Pei-Chen Lo. "Cardiorespiratory phase synchronization during normal rest and inward-attention meditation." *International journal of cardiology* 141, no. 3 (2010): 325-328.
21. Chakrabarty, Ankush, Stamatina Zavitsanou, Tara Sowrirajan, Francis J. Doyle III, and Eyal Dassau. "Getting IoT-ready: The face of next generation artificial pancreas systems." In *The Artificial Pancreas*, pp. 29-57. Academic Press, 2019.
22. Olde Bekkink, Marleen, Mats Koeneman, Bastiaan E. de Galan, and Sebastian J. Bredie. "Early detection of hypoglycemia in type 1 diabetes using heart rate variability measured by a wearable device." *Diabetes care* 42, no. 4 (2019): 689-692.
23. Wiens, Stefan, Elizabeth S. Mezzacappa, and Edward S. Katkin. "Heartbeat detection and the experience of emotions." *Cognition & Emotion* 14, no. 3 (2000): 417-427.
24. Li, Suyi, Feng Li, Shijie Tang, and Wenji Xiong. "A review of computer-aided heart sound detection techniques." *BioMed research international* 2020 (2020).
25. Thalmayer, Angelika, Samuel Zeising, Georg Fischer, and Jens Kirchner. "A robust and real-time capable envelope-based algorithm for heart sound classification: Validation under different physiological conditions." *Sensors* 20, no. 4 (2020): 972.
26. Kapen, Pascalin Tiam, *et al.* "Phonocardiogram: A robust algorithm for generating synthetic signals and comparison with real life ones." *Biomedical Signal Processing and Control* 60 (2020): 101983.
27. Giordano, Noemi, and Marco Knaflitz. "A novel method for measuring the timing of heart sound components through digital phonocardiography." *Sensors* 19, no. 8 (2019): 1868.
28. Wei, Wenjing, Ge Zhan, Xun Wang, Pengyuan Zhang, and Yonghong Yan. "A novel method for automatic heart murmur diagnosis using phonocardiogram." In *Proceedings of the 2019 International Conference on Artificial Intelligence and Advanced Manufacturing*, pp. 1-6. 2019.
29. Malarvili, M. B., I. Kamarulafizam, S. Hussain, and D. Helmi. "Heart sound segmentation algorithm based on instantaneous energy of electrocardiogram." In *Computers in Cardiology, 2003*, pp. 327-330. IEEE, 2003.
30. Oliveira, Jorge, Francesco Renna, Theofrastos Mantadelis, and Miguel Coimbra. "Adaptive sojourn time HSMM for heart sound segmentation." *IEEE journal of biomedical and health informatics* 23, no. 2 (2018): 642-649.
31. Kamson, Alex Paul, L. N. Sharma, and Samarendra Dandapat. "Multi-centroid diastolic duration distribution based HSMM for heart sound segmentation." *Biomedical signal processing and control* 48 (2019): 265-272.
32. Chen, Tien-En, *et al*. "S1 and S2 heart sound recognition using deep neural networks." *IEEE Transactions on Biomedical Engineering* 64, no.2 (2016): 372-380.
33. Deng, Shi-Wen, and Ji-Qing Han. "Towards heart sound classification without segmentation via autocorrelation feature and diffusion maps." *Future Generation Computer Systems* 60 (2016): 13-21.
34. Abduh, Zaid, Ebrahim Ameen Nehary, Manal Abdel Wahed, and Yasser M. Kadah. "Classification of heart sounds using fractional Fourier transform based mel-frequency spectral coefficients and stacked autoencoder deep neural network." *Journal of Medical Imaging and Health Informatics* 9, no. 1 (2019): 1-8.
35. Soeta, Yoshiharu, and Yasuyuki Bito. "Detection of features of prosthetic cardiac valve sound by spectrogram analysis." *Applied Acoustics* 89 (2015): 28-33.
36. Potes, Cristhian, Saman Parvaneh, Asif Rahman, and Bryan Conroy. "Ensemble of feature-based and deep learning-based classifiers for detection of abnormal heart sounds." In *2016 computing in cardiology conference (CinC)*, pp. 621-624. IEEE, 2016.
37. Deng, Muqing, *et al*. "Heart sound classification based on improved MFCC features and convolutional recurrent neural networks." *Neural Networks* 130 (2020): 22-32.
38. Zeinali, Yasser, and Seyed Taghi Akhavan Niaki. "Heart sound classification using signal processing and machine learning algorithms." *Machine Learning with Applications* 7 (2022): 100206.

39. Yadav, Anjali, Anushikha Singh, Malay Kishore Dutta, and Carlos M. Travieso. "Machine learning-based classification of cardiac diseases from PCG recorded heart sounds." *Neural Computing and Applications* 32 (2020): 17843-17856.
40. Arslan, Özkan, and Mustafa Karhan. "Effect of Hilbert-Huang transform on classification of PCG signals using machine learning." *Journal of King Saud University-Computer and Information Sciences* 34, no. 10 (2022): 9915-9925.
41. Tang, Hong, Ziyin Dai, Yuanlin Jiang, Ting Li, and Chengyu Liu. "PCG classification using multidomain features and SVM classifier." *BioMed research international* 2018 (2018).
42. Singh, Sinam Ajitkumar, and Swanirbhar Majumder. "Classification of unsegmented heart sound recording using KNN classifier." *Journal of Mechanics in Medicine and Biology* 19, no. 04 (2019): 1950025.
43. Khan, Nadia Masood, Muhammad Salman Khan, and Gul Muhammad Khan. "Automated Heart Sound Classification from Unsegmented Phonocardiogram Signals Using Time Frequency Features." *International Journal of Computer and Information Engineering* 12, no. 8 (2018): 598-603.
44. Baydoun, Mohammed, Lise Safatly, Hassan Ghaziri, and Ali El Hajj. "Analysis of heart sound anomalies using ensemble learning." *Biomedical Signal Processing and Control* 62 (2020): 102019.
45. Khan, Juwairiya Siraj, Manoj Kaushik, Anushka Chaurasia, Malay Kishore Dutta, and Radim Burget. "Cardi-Net: A deep neural network for classification of cardiac disease using phonocardiogram signal." *Computer Methods and Programs in Biomedicine* 219 (2022): 106727.
46. Roy, Tanmay Sinha, Joyanta Kumar Roy, and Nirupama Mandal. "Classifier identification using deep learning and machine learning algorithms for the detection of valvular heart diseases." *Biomedical Engineering Advances* 3 (2022): 100035.
47. Naveen, Alampally, Parigi Sai Teja Reddy, and Thenmozhi Thangavel. "Deep Learning Based Classification of Heart Diseases from Heart Sounds." *International Journal of Research in Engineering, Science and Management* 4, no. 10 (2021): 165-171.
48. Brunese, Luca, Fabio Martinelli, Francesco Mercaldo, and Antonella Santone. "Deep learning for heart disease detection through cardiac sounds." *Procedia Computer Science* 176 (2020): 2202-2211.
49. Nabih-Ali, Mohammed, El-Sayed A. El-Dahshan, and Ashraf S. Yahia. "Heart diseases diagnosis using intelligent algorithm based on PCG signal analysis." *International Journal of Biology and Biomedicine* 2 (2017).
50. MAlnajjar, Mohammad Khaleel, and Samy S. Abu-Naser. "Heart sounds analysis and classification for cardiovascular diseases diagnosis using deep learning." (2022).
51. Almanifi, Omair Rashed Abdulwareth, Ahmad Fakhri Ab Nasir, Mohd Azraai Mohd Razman, Rabiu Muazu Musa, and Anwar PP Abdul Majeed. "Heartbeat murmurs detection in phonocardiogram recordings via transfer learning." *Alexandria Engineering Journal* 61, no. 12 (2022): 10995-11002.
52. Li, Fen, *et al.* "Feature extraction and classification of heart sound using 1D convolutional neural networks." *EURASIP Journal on Advances in Signal Processing* 2019, no.1 (2019): 1-11.
53. He, Yi, *et al.* "Research on segmentation and classification of heart sound signals based on deep learning." *Applied Sciences* 11, no.2 (2021): 651.
54. Springer, David B., Lionel Tarassenko, and Gari D. Clifford. "Logistic regression-HSMM-based heart sound segmentation." *IEEE transactions on biomedical engineering* 63, no. 4 (2015): 822-832.
55. LeCun, Yann, Yoshua Bengio, and Geoffrey Hinton. "Deep learning." *nature* 521, no. 7553 (2015): 436-444.
56. Latif, Siddique, Muhammad Usman, Rajib Rana, and Junaid Qadir. "Phonocardiographic sensing using deep learning for abnormal heartbeat detection." *IEEE Sensors Journal* 18, no. 22 (2018): 9393-9400.
57. Narvaez, Pedro, Steven Gutierrez, and Winston S. Percybrooks. "Automatic segmentation and classification of heart sounds using modified empirical wavelet transform and power features." *Applied Sciences* 10, no. 14 (2020): 4791.
58. Cho, Junghwan, Kyewook Lee, Ellie Shin, Garry Choy, and Synho Do. "How much data is needed to train a medical image deep learning system to achieve necessary high accuracy?." *arXiv preprint arXiv:1511.06348* (2015).
59. Humayun, Ahmed Imtiaz, Shabnam Ghaffarzadegan, Md Istiaq Ansari, Zhe Feng, and Taufiq Hasan. "Towards domain invariant heart sound abnormality detection using learnable filterbanks." *IEEE journal of biomedical and health informatics* 24, no. 8 (2020): 2189-2198.

60. Potes, Cristhian, Saman Parvaneh, Asif Rahman, and Bryan Conroy. "Ensemble of feature-based and deep learning-based classifiers for detection of abnormal heart sounds." In *2016 computing in cardiology conference (CinC)*, pp. 621-624. IEEE, 2016.
61. Maknickas, Vykintas, and Algirdas Maknickas. "Recognition of normal–abnormal phonocardiographic signals using deep convolutional neural networks and mel-frequency spectral coefficients." *Physiological measurement* 38, no. 8 (2017): 1671.
62. Russakovsky, Olga, Jia Deng, Hao Su, Jonathan Krause, Sanjeev Satheesh, Sean Ma, Zhiheng Huang *et al*. "Imagenet large scale visual recognition challenge." *International journal of computer vision* 115 (2015): 211-252.
63. Baghel, Neeraj, Malay Kishore Dutta, and Radim Burget. "Automatic diagnosis of multiple cardiac diseases from PCG signals using convolutional neural network." *Computer Methods and Programs in Biomedicine* 197 (2020): 105750.
64. Li, Fan, Hong Tang, Shang Shang, Klaus Mathiak, and Fengyu Cong. "Classification of heart sounds using convolutional neural network." *Applied Sciences* 10, no. 11 (2020): 3956.
65. Narvaez, Pedro, and Winston S. Percybrooks. "Synthesis of normal heart sounds using generative adversarial networks and empirical wavelet transform." *Applied Sciences* 10, no. 19 (2020): 7003.
66. Thomae, Christian, and Andreas Dominik. "Using deep gated RNN with a convolutional front end for end-to-end classification of heart sound." In *2016 Computing in Cardiology Conference (CinC)*, pp. 625-628. IEEE, 2016.
67. Ren, Zhao, Nicholas Cummins, Vedhas Pandit, Jing Han, Kun Qian, and Björn Schuller. "Learning image-based representations for heart sound classification." In *Proceedings of the 2018 international conference on digital health*, pp. 143-147. 2018.
68. Alafif, Tarik, Mehrez Boulares, Ahmed Barnawi, Talal Alafif, Hassan Althobaiti, and Ali Alferaidi. "Normal and abnormal heart rates recognition using transfer learning." In *2020 12th International Conference on Knowledge and Systems Engineering (KSE)*, pp. 275-280. IEEE, 2020.
69. Humayun, Ahmed Imtiaz, Md Khan, Shabnam Ghaffarzadegan, Zhe Feng, and Taufiq Hasan. "An ensemble of transfer, semi-supervised and supervised learning methods for pathological heart sound classification." *arXiv preprint arXiv:1806.06506* (2018).
70. Yosinski, Jason, Jeff Clune, Yoshua Bengio, and Hod Lipson. "How transferable are features in deep neural networks?." *Advances in neural information processing systems* 27 (2014).
71. Wu, Jimmy Ming-Tai, *et al*. "Applying an ensemble convolutional neural network with Savitzky–Golay filter to construct a phonocardiogram prediction model." *Applied Soft Computing* 78 (2019): 29-40.
72. Chen, Wei, *et al.* "Phonocardiogram Classification Using Deep Convolutional Neural Networks with Majority Vote Strategy." *Journal of Medical Imaging and Health Informatics* 9, no.8 (2019): 1692-1704.
73. Dominguez-Morales, Juan P., Angel F. Jimenez-Fernandez, Manuel J. Dominguez-Morales, and Gabriel Jimenez-Moreno. "Deep neural networks for the recognition and classification of heart murmurs using neuromorphic auditory sensors." *IEEE transactions on biomedical circuits and systems* 12, no. 1 (2017): 24-34.
74. Rubin, Jonathan, Rui Abreu, Anurag Ganguli, Saigopal Nelaturi, Ion Matei, and Kumar Sricharan. "Classifying heart sound recordings using deep convolutional neural networks and mel-frequency cepstral coefficients." In *2016 Computing in cardiology conference (CinC)*, pp. 813-816. IEEE, 2016.
75. Nilanon, Tanachat, Jiayu Yao, Junheng Hao, Sanjay Purushotham, and Yan Liu. "Normal/abnormal heart sound recordings classification using convolutional neural network." In *2016 computing in cardiology conference (CinC)*, pp. 585-588. IEEE, 2016.
76. Veerabaku, Muthu Ganesh, *et al*. "Intelligent Bi-LSTM with architecture optimization for heart disease prediction in WBAN through optimal channel selection and feature selection." *Biomedicines* 11.4 (2023): 1167.
77. Fernando, Tharindu, *et al.* "Heart sound segmentation using bidirectional LSTMs with attention." *IEEE journal of biomedical and health informatics* 24.6 (2019): 1601-1609.
78. Swaminathan, Sathyanarayanan, *et al.* "Heart Sound Analysis with Machine Learning Using Audio Features for Detecting Heart Diseases." *International Journal of Computer Information Systems and Industrial Management Applications* 16.2 (2024): 17-17.
79. Abbas, Sidra, *et al.* "Artificial intelligence framework for heart disease classification from audio signals." *Scientific Reports* 14.1 (2024): 3123.

80. Ainiwaer, Aikeliyaer, *et al.* "Deep learning of heart-sound signals for efficient prediction of obstructive coronary artery disease." Heliyon 10.1 (2024).
81. Aji, Nurseno Bayu, *et al.* "CNN-LSTM for Heartbeat Sound Classification." *JOIV: International Journal on Informatics Visualization* 8.2 (2024): 735-741.
82. Gharehbaghi, Arash, and Maria Lindén. "A deep machine learning method for classifying cyclic time series of biological signals using time-growing neural network." *IEEE transactions on neural networks and learning systems* 29, no. 9 (2017): 4102-4115.

Table 1. Several Machine Learning methods for heart sound classification

Ref	Method	Input Feature	Segment	Optimizer	Categories	Performance on Test dataset Acc, Se, Sp
[38]	SVM, Gradient Boosting, Random Forest	MFCC	No	*	Normal, Abnormal S3, Abnormal S4	87.5,*,*
[39]	SVM, K-NN, random forest, Naive Byes	12 statistical features	No	*	Normal, Abnormal	97.78,*,*
[40]	KNN, MLP, SVM, DNN	MFCC	No	*	healthy, aortic stenosis, mitral stenosis, mitral regurgitation and mitral valve prolaps	98.9,*,*
[41]	SVM	515 Features like entropy, Cepstrum, Time interval	Yes	*	Normal, Abnormal	0.88,0.87,0.88
[42]	KNN	wavelet decompositio n, Hilbert transform, homomorphic filtering, and power spectral density (PSD)	No (main aim without segment classify into two classes)	*	Normal, Abnormal	90,93,90
[43]	SVM	New mother wavelet for DWT signals	No	*	Normal, Pathological	73.64,*,*

Table 2. Several Deep Learning Methods for Heart Beat Sounds Classification

Ref.	Method	Input Feature	Segme nt	Optimiz er	Categories	Performance on Test dataset Acc, Se, Sp
[44]	AdaboostM1 , LogiBoost,	Wavelet based	Yes	*	-1 for Normal, 1 – Pathological	86.6 , 90 , 83

	XgBoost	features			0-noisy samples	
[45]	CNN	Power spectrogram	No	*	Normal, Aortic Stenosis, Mitral Regurgitation, Mitral Stenosis, Mitral Valve Prolapse	98.879% with a loss of 0.0948
[46]	CNN	.wav files Root Mean Square (RMS) , Signal Energy and Power,3 Zero-Crossing Rate (ZCR) , Total Harmonic distortion(THD) Skewness and Kurtosis	No	*	Valvular heart disease	99.43,*,*
[47]	CNN and LSTM	MFCC	Yes	*	Normal, Artifact, Murmur, Extra systole	94,*,*
[48]	Deep Neural Network	F1 - chroma stft, F2 - spectral centroid, F3 - spectral bandwidth, F4 - zero crossing rate and F5 - mfcc	Yes	*	Healthy, Unhealthy	98,*,*
[49]	ANN	Discrete Wavelet Transform (DWT)	Yes	*	Normal,Abnormal	97,*,*
[50]	CNN	MFCC	Yes	*	Artifact, Extrahs, Murmur,Normal and Extrasystole	High acc than others, *,*
[51]	ResNet50	MFCC	No	*	Detecting heart murmur	87.65,*,*
[52]	1D CNN	Denoising Auto Encoder	No	*	Normal, Abnormal	99.01,*,*

[53]	CNN	Hilbert envelope, Homomorphic environment map,Wavelet envelope,Power spectral density envelope	Yes	*	Normal, Abnormal	0.964,0.781, 0.873

Se – Sensitivity, Sp – Specificity , Acc - Accuracy

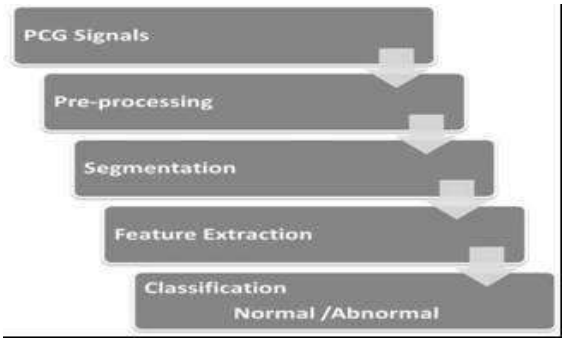

Figure.1: Phases of Heart Beat Sound Classification

Figure.2: Distinct types of heart sounds

Figure.3: Machine Learning and Deep Learning Techniques for Heart Sounds Classification

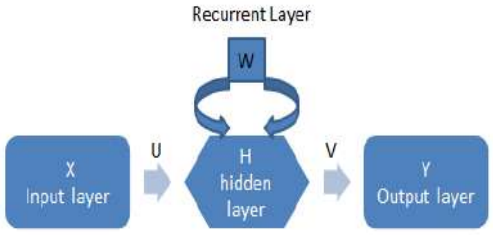

Figure. 4. Block Diagram of RNN Architecture

RESEARCH ARTICLE

A Narrative Review on Traditional Siddha Formulation *Mega Sanjeevi Chooranam* in the Management of Diabetes Mellitus (*Madhumegam*)

S.Iyswarya[1]*, Sivakkumar S[2] and Visweswaran S[2]

[1]Research Scholar, Department of Gunapadam, National Institute of Siddha, (Affiliated to The Tamil Nadu Dr MGR Medical University), Chennai, Tamil Nadu, India.
[2]Professor, Department of Gunapadam, National Institute of Siddha, (Affiliated to The Tamil Nadu Dr MGR Medical University), Chennai, Tamil Nadu, India.

Received: 21 Nov 2024 Revised: 03 Dec 2024 Accepted: 13 Jan 2025

***Address for Correspondence**
S.Iyswarya
Research Scholar,
Department of Gunapadam,
National Institute of Siddha,
(Affiliated to The Tamil Nadu Dr MGR Medical University),
Chennai, Tamil Nadu, India.
E.Mail: iysbsms@gmail.com

ABSTRACT

Mega Sanjeevi Chooranam, a polyherbal formulation in Siddha medicine, comprises ten distinct herbal ingredients and is traditionally utilized for the management of *Madhumegam*, which corresponds to Type 2 Diabetes Mellitus in modern terms. Diabetes Mellitus, a metabolic disorder characterized by chronic hyperglycemia, poses significant long-term risks including cardiovascular damage and renal complications. The global prevalence of diabetes has surged across all income levels, highlighting the need for effective management strategies. To compile detailed information on the antidiabetic effects of the ingredients in *Mega Sanjeevi Chooranam*, a literature search was performed across several databases, including Web of Science, Google Scholar, Scopus, and PubMed. The search covered both in vivo and in vitro studies using English terms related to the antidiabetic, antihyperlipidemic and antioxidant properties of these ingredients. The goal was to collect a broad range of research findings to assess how effective the ingredients in *Mega Sanjeevi Chooranam* are in managing diabetes and its complications. This review investigates the potential efficacy of *Mega Sanjeevi Chooranam* in managing Diabetes Mellitus, detailing the Siddha perspectives, pharmacological properties, and phytochemical profiles of its constituent herbs. Through an analysis of Siddha texts and scientific literature, the review identifies notable antidiabetic, antihyperlipidemic, and antioxidant activities associated with the formulation. These findings indicate that *Mega Sanjeevi Chooranam* could be a valuable therapeutic approach for managing diabetes and related dyslipidemia. However, further pharmacological and clinical research is necessary to substantiate its efficacy and establish its therapeutic potential in contemporary medical practice.

Keywords: Diabetes mellitus, Mega Sanjeevi Chooranam, Madhumegam, Anti-diabetic, Anti- hyperlipidaemic, Siddha.

INTRODUCTION

Diabetes mellitus is a chronic metabolic condition characterized by sustained hyperglycemia, which can lead to serious complications affecting multiple organ systems, including the cardiovascular system, blood vessels, eyes, kidneys, and nerves. The global prevalence of diabetes surged from 108 million in 1980 to 422 million in 2014, with a more significant increase observed in low- and middle-income countries compared to high-income countries. Diabetes is a major contributor to severe health complications such as blindness, kidney failure, heart attacks, strokes, and amputations. Between 2000 and 2019, diabetes-related mortality rates rose by 3% per age group. In 2019, diabetes and its complications were responsible for approximately 2 million deaths. By 2014, 8.5% of adults aged 18 and older had diabetes, and by 2019, the condition led to 1.5 million deaths, with nearly 48% occurring before the age of 70. Additionally, diabetes caused 460,000 deaths due to kidney disease and accounted for about 20% of cardiovascular deaths. From 2000 to 2019, age-standardized mortality rates for diabetes increased by 3%, with a 13% rise in lower-middle-income countries [1]. This escalating prevalence poses a considerable public health challenge and imposes a significant economic burden on individuals, families, the healthcare system, and the broader national economy. While synthetic antidiabetic drugs are effective, their high costs often limit accessibility, underscoring the need for affordable alternative treatments. In response to this challenge, there has been growing interest in the potential of medicinal plants as adjuncts or alternatives to conventional diabetes treatments [2]. These plant-derived pharmacological substances offer various mechanisms of action, including enhancing insulin secretion, modulating glucose and lipid metabolism, inhibiting key digestive enzymes such as α-amylase and α-glucosidase, improving insulin sensitivity, and activating protein kinase pathways [3,4]. Additionally, oxidative stress plays a critical role in the development of metabolic and age-related disorders, prompting further investigation into medicinal plants as sources of antioxidants [5]. The Siddha system, a traditional form of medicine from Southern India, has a long history of effective treatment for both communicable and non-communicable diseases. Among its many formulations, *Mega Sanjeevi Chooranam*, a polyherbal concoction detailed in the Siddha text "*Sarabendrar Siddha Maruthuva Sudar*," is noteworthy for its potential application in managing diabetes mellitus, known as *Madhumegam* in Siddha medicine [6]. This review aims to explore and highlight the potential role of *Mega Sanjeevi Chooranam* in the management of diabetes mellitus, examining its historical context, therapeutic efficacy, and the underlying pharmacological mechanisms that may contribute to its effectiveness.

MATERIALS AND METHODS

To assess the antidiabetic effects of the ingredients in Mega Sanjeevi Chooranam, a literature search was conducted across Web of Science, Google Scholar, Scopus, and PubMed. This search included both in vivo and in vitro studies focusing on the antidiabetic, antihyperlipidemic, and antioxidant properties of the ingredients. The aim was to gather comprehensive research findings on their effectiveness in managing diabetes and its complications.

Standard Operating Procedure for the Preparation of Mega Sanjeevi Chooranam
Drug Details
Study Drug: Mega Sanjeevi Chooranam
Reference: Sarabendrar Siddha Maruthuva Sudar, Saraswathi Mahal Noolagam, Tanjore, April 2000, Page No. 219

Preparation of Mega Sanjeevi Chooranam
The preparation of Mega Sanjeevi Chooranam follows a meticulously outlined procedure. The specific ingredients and their quantities required for the formulation are detailed in Table 1. Raw materials were procured from reputable sources and subsequently authenticated by the Pharmacognosy Department at the Siddha Central Research Institute, Arumbakkam, Chennai. Each ingredient was subjected to a purification process as described in Siddha literature. Following purification, the ingredients were finely ground into powders. These powders were then blended in precise proportions to ensure consistency and efficacy of the final product. The prepared Mega Sanjeevi Chooranam was stored in an airtight container to preserve its quality and prevent contamination.

Dosage: The recommended dosage for Mega Sanjeevi Chooranam is 2 grams administered twice daily, to be taken with water.

PROFILE OF INDIVIDUAL DRUGS

The taste of each drug, parts used and actions as per siddha literature are mentioned in the Table 2 and the phytochemical constituents and pharmacological actions are mentioned in Table 3.

PHARMACOLOGICAL ACTIONS

***Naaval*(*Eugenia jambolana*)**

Anti-Diabetic Activity

Singh *et al.* demonstrated that the ethanolic extract of *Syzygiumcumini* seeds significantly reduced blood sugar levels in alloxan-induced diabetic rats, highlighting its hypoglycemic potential [39]. Bansal et al. attributed the hypoglycemic effects of *Syzygiumcumini* seeds to increased cathepsin B activity following oral administration [40].

Prince et al. observed that administering aqueous seed extract of *Syzygiumcumini* at 2.5 g/kg body weight for one-month elevated hexokinase activity and decreased blood glucose levels in diabetic rats. Moreover, doses of 2.5 and 5 g/kg body weight showed notable hypoglycemic effects over six weeks [41]. Conversely, an intraperitoneal injection of alcoholic seed extract (20 mg) reduced blood sugar by 37.17% at three hours and 46.68% at six hours in diabetic mice, along with increased insulin secretion [42]. Vats et al. reported that aqueous extracts of Eugenia jambolana at 400 mg daily for 15 days prevented hyperglycemia and hyperinsulinemia caused by a high-fructose diet in rats [43]. Grover et al. found that daily administration of lyophilized powder from E. jambolana seeds at 200 mg/kg led to substantial reductions in blood glucose levels—73.51% in mild, 55.62% in moderate, and 48.81% in severe diabetic conditions—while also improving hepatic and skeletal muscle glycogen levels and key metabolic enzymes [44]. Pandey *et al.* attributed the hypoglycemic effect of *Syzygiumcumini* seeds to water-soluble gummy fibers rather than insoluble components [45].

Anti-Hyperlipidemic Activity

Ravi et al. evaluated the anti-hyperlipidemic effects of Eugenia jambolana seed kernel (EJs-kernel) in streptozotocin-induced diabetic rats, finding that the extract (100 mg/kg body weight) significantly improved elevated cholesterol, phospholipids, triglycerides, and free fatty acids, showing comparable efficacy to glibenclamide. This supports the potential of EJs-kernel for its hypolipidemic effects due to its flavonoid, saponin, glycoside, and triterpenoid content [46]. Bhavna Sharma *et al*. reported that a flavonoid-rich extract from Eugenia jambolana seeds significantly lowered LDL and triglycerides while increasing HDL levels in streptozotocin-induced diabetic rats. The extract also improved fasting blood glucose and insulin release, suggesting its potential for managing both diabetes and associated lipid imbalances [47]. Sharma *et al*. found that an ethanolic extract of E. jambolana seeds significantly reduced fasting blood glucose and peak glucose levels during glucose tolerance tests in alloxan-induced diabetic rabbits. It decreased FBG by up to 29% and peak glucose by up to 21%, reduced glycosylated hemoglobin, and increased serum insulin levels. Additionally, the extract improved liver and muscle glycogen content and demonstrated a significant hypolipidemic effect by lowering total cholesterol/HDL ratio, LDL levels, and HMG-CoA reductase activity. Histopathological studies revealed nearly normal liver, pancreas, and aorta in treated diabetic rabbits [48].

***Vetiveriazizanioides* (Coleus vettiveroides):**

Anti-Diabetic Activity

Gopalakrishnan *et al.* examined the anti-diabetic effects of a methanolic extract of Coleus vettiveroides in streptozotocin-induced diabetic rats. Administration of the extract at 200 mg/kg and 400 mg/kg for 15 days significantly reduced fasting blood glucose and urine sugar levels, improved body weight, and restored liver and kidney functions. It also normalized serum amylase, cholesterol, triglycerides, and pancreatic health, indicating strong anti-diabetic efficacy [49]. Sanjay Kumar Karan et al. assessed the antihyperglycemic effects of ethanol extract from *Vetiveriazizanioides* roots in alloxan-induced diabetic rats. Daily treatment at doses of 100, 250, 500, and 750 mg/kg for 28 days significantly lowered blood glucose levels, showing effectiveness comparable to the standard drug glibenclamide, thus supporting its use in diabetes management [50].

Antioxidant Activity

Gopalakrishnan et al. also investigated the antioxidant properties of the methanolic extract of Coleus vettiveroides. The extract significantly reduced thiobarbituric acid reactive substances (TBARS) and increased liver levels of key antioxidants like glutathione (GSH), superoxide dismutase (SOD), catalase (CAT), and glutathione peroxidase (GPX) in diabetic rats, highlighting its strong antioxidant potential [51]. The methanolic extract from the tuberous roots of Coleus vettiveroides was assessed for in vitro antioxidant activity. It demonstrated significant effects in scavenging DPPH radicals, nitric oxide, and total antioxidant activity, with IC50 values of 250 μg/ml, 510 μg/ml, and 560 μg/ml respectively, outperforming reference standards in some assays, thus underscoring its potent antioxidant capacity [52].

Syzygium aromaticum

Anti-Obesity Effect

Chang Hwa Jung et al. examined the anti-obesity effects of ethanol extract from Syzygium aromaticum (SAE). The extract inhibited adipocyte differentiation in vitro and, when administered to high-fat diet-fed mice, significantly reduced body weight, liver weight, white adipose tissue mass, and serum levels of triglycerides, cholesterol, glucose, insulin, and leptin. SAE also decreased the expression of key proteins involved in lipid metabolism, indicating its potential to prevent obesity by reducing fat accumulation and related metabolic disturbances [53].

Antidiabetic Activity

Hafizah Umaira et al. evaluated the antidiabetic effects of essential oils from *Syzygium aromaticum* and *Cuminum cyminum*. The *Syzygium aromaticum* emulsion achieved 95.30% inhibition of alpha-amylase, highlighting its strong antidiabetic potential. Eugenol, the main component of *Syzygium aromaticum* essential oil, was identified as a key contributor to its effectiveness [54].

Anti-Hyperlipidemic Activity

Al-Okbi et al. studied the impact of clove essential oil (CO) and its main component, eugenol, in water-based microemulsions on fatty liver and dyslipidemia in high-fructose-fed rats. Both CO and eugenol microemulsions improved liver fat, triglycerides, cholesterol levels, and inflammation, demonstrating a stable and effective delivery system for these compounds [55].

Antioxidant Activity

Patience MekemzeuFankem et al. reported that clove essential oil, rich in eugenol (87.62%), exhibited significant antioxidant activity, surpassing butylated hydroxytoluene (BHT) and showing strong antifungal effects against dermatophytes [56].Ilhami Güçin et al. confirmed clove oil's potent antioxidant properties through various assays, including DPPH and ABTS radical scavenging, and lipid peroxidation inhibition [57]. Hyang Nam et al. highlighted eugenol's antioxidant effects and its ability to inhibit matrix metalloproteinase (MMP-9) activity, suggesting its potential in cancer prevention related to oxidative stress [58].Amit Singh Yadav et al. compared the antioxidant properties of Indian spices, finding cloves to have the strongest DPPH radical scavenging and ferric reducing antioxidant power (FRAP) among them. This positions cloves as a leading spice in antioxidant activity [59].

Anacyclus pyrethrum

Antidiabetic Activity

Anacyclus pyrethrum has garnered interest for its antidiabetic properties, as evidenced by various studies. Tyagi et al. evaluated the antidiabetic effects of an aqueous root extract from Anacyclus pyrethrum DC in rats with diabetes induced by alloxan. Oral administration of the extract at doses of 150 and 300 mg/kg body weight significantly reduced elevated blood glucose levels, returning them to near-normal ranges. This indicates that the aqueous extract of Anacyclus pyrethrum has significant antihyperglycemic potential and could be therapeutically valuable for managing diabetes [60]. Selles et al. examined the antidiabetic effects of an aqueous root extract of Anacyclus pyrethrum L. in both normal and STZ-induced diabetic rats. When administered daily at a dose of 250 mg/kg for 21 days, the extract significantly lowered blood glucose levels in diabetic rats but did not affect normal

rats.Phytochemical analysis identified key compounds including tannins, saponins, alkaloids, amino acids, steroids, and terpenoids, highlighting its potential as a therapeutic agent for diabetes [61]. V. Kishor Kumar et al. investigated the in vitro α-amylase inhibitory effects of various extracts (petroleum ether, chloroform, ethyl acetate, acetone, ethanol, and water) from Anacyclus pyrethrum roots. The ethanol extract exhibited the highest inhibitory activity, with an IC50 of 29.25 µg/mL and 88.26% inhibition, surpassing other extracts. All extracts, except petroleum ether, showed notable α-amylase inhibition, likely due to their phytochemical content. These findings support the potential of A. pyrethrum roots for diabetes management [62].

Cassia fistula

Antidiabetic Activity

Jarald et al. evaluated the antihyperglycemic effects of various extracts from *Cassia fistula* flowers, including petroleum ether, chloroform, acetone, ethanol, aqueous, and crude aqueous extracts, as well as two fractions of the ethanol extract, in glucose-overloaded hyperglycemic rats. The extracts and fractions were tested at doses of 200 and 400 mg/kg and further evaluated in an alloxan-induced diabetic model. Petroleum ether and ethanol extracts, as well as the water-soluble fraction of the ethanol extract, demonstrated significant antihyperglycemic activity. While the ethanol extract and its water-soluble fraction effectively normalized elevated biochemical parameters in diabetic rats, the petroleum ether extract was inactive. The water-soluble fraction proved to be more effective than the ethanol extract, showing results comparable to the standard drug glibenclamide (5 mg/kg) [63]. Veeramani et al. investigated iron oxide nanoparticles (ICF) synthesized from Cassia fistula flower tea, focusing on their antioxidant and anti-hyperglycemic properties. The nanoparticles were analyzed using conventional physical and chemical methods.Results showed that ICF nanoparticles effectively inhibited alpha-amylase, improved glucose absorption, and exhibited strong antioxidant activity by enhancing total antioxidant capacity (TAA) and radical scavenging (DPPH) [64].

Antioxidant Activity

Manonmani et al. investigated the antioxidant effects of aqueous extract from Cassia fistula (Linn.) flowers (ACF) in alloxan-induced diabetic rats. ACF treatment significantly lowered peroxidation products, such as thiobarbituric acid reactive substances, conjugated dienes, and hydroperoxides, in the heart tissues of diabetic rats.Additionally, it restored the activities of key antioxidant enzymes - superoxide dismutase, catalase, glutathione peroxidase, glutathione reductase, and glutathione to near-normal levels. These findings indicate that ACF has promising antioxidant properties in the context of diabetes [65].

Cassia auriculata

Antidiabetic Activity

Nambirajan et al. evaluated the antidiabetic effects of Cassia auriculata L. bud and flower extracts in rats with diabetes induced by a high-fat diet and streptozotocin. By using LC-ESI/MS, they identified various phenolic and flavonoid compounds in both types of extracts. The research revealed that the bud extract (CABE500) was more effective in managing diabetes than the flower extract, potentially due to its effect on IRS2 gene regulation, while GRIA2 expression remained stable [66]. Latha et al. investigated the impact of Cassia auriculata flower extract (CFEt) on glucose and enzyme levels in diabetic rats induced by streptozotocin. They found that CFEt significantly decreased blood glucose and glycosylated hemoglobin levels, while increasing plasma insulin and enzyme activity, showing better antihyperglycemic effects compared to glibenclamide [67]. Similarly, Khader et al. demonstrated that Cassia auriculata extract notably lowered blood glucose and improved lipid levels in alloxan-induced diabetic rats, with the C2 subfraction showing the strongest effects [68]. Surana et al. also reported that the n-butanol fraction from Cassia auriculata flowers significantly reduced blood glucose and normalized lipid and protein levels, with effectiveness comparable to the drug phenformin [69].

Anti-Hyperlipidemic Activity

Shipra Gupta et al. studied the antihyperglycemic and hypolipidemic effects of an aqueous extract of Cassia auriculata leaves (CLEt) in diabetic rats induced by streptozotocin. The extract, administered at doses of 100, 200, and

400 mg/kg, significantly lowered fasting blood glucose and glycosylated hemoglobin, and improved serum lipid profiles, particularly at the 400 mg/kg dose. This demonstrates CLEt's potent hypolipidemic activity alongside its antihyperglycemic effects [70]. Rajendran *et al*. assessed the antihyperlipidemic effects of the ethanolic extract of Cassia auriculata flowers (Et-CAF) in hyperlipidemic yeast cells and found it effective in reducing lipid levels and downregulating lipid-related gene expression, outperforming Atorvastatin [71]. Similarly, Panneerselvam Vijayaraj et al. found that Et-CAF significantly reduced serum cholesterol and triglycerides, and enhanced antioxidant enzyme activities in hyperlipidemic rats. The extract's most effective dose, 450 mg/kg, was comparable to lovastatin, highlighting its strong antihyperlipidemic potential [72].

Antioxidant Activity

Elayarani *et al*. conducted an in vitro study to evaluate the antioxidant properties of petroleum ether, ethanol, and methanolic extracts from Cassia auriculata flowers. Using DPPH radical scavenging and reducing power assays, they found that the methanolic extract exhibited the highest antioxidant activity. These findings highlight the significant antioxidant potential of Cassia auriculata flowers, supporting its traditional uses in cardiovascular health, muscle building, nephroprotection, anti-inflammatory applications, and as an aphrodisiac [73].

StrychnosPotatorum

Antidiabetic Activity

Dhasarathan *et al*. investigated the anti-diabetic effects of *Strychnospotatorum* in Wistar albino rats with alloxan-induced diabetes. The study included groups of normal rats, diabetic rats, diabetic rats treated with the plant extract, and those receiving the standard drug tolbutamide. The extract significantly reduced blood glucose levels by 53%, improved liver weight and enzyme levels, and increased serum insulin and protein levels, demonstrating its strong anti-diabetic potential [74]. Biswas et al. examined the antidiabetic properties of *Strychnospotatorum* Linn. seeds in a streptozotocin-induced diabetes model. Over 12 weeks, the seeds (100 mg/kg) effectively lowered fasting blood sugar levels, showed results comparable to the hypoglycemic drug glipizide, and led to weight gain while reducing food and water intake in diabetic rats [75]. Mishra *et al.* also found that *Strychnospotatorum* seeds significantly reduced blood glucose levels and improved antioxidant markers in rats with streptozotocin-nicotinamide-induced diabetes [76]. Additionally, Subramanian et al. demonstrated that an ethanolic extract of *Strychnospotatorum* seeds reduced blood glucose and glycosylated hemoglobin levels while enhancing antioxidant status in type 2 diabetic rats [77]. Pandu Raju *et al.* reported that methanolic extracts of *Strychnospotatorum* seeds and leaves significantly reduced blood glucose levels in alloxan-induced diabetic rats [78].

Gymnemasylvestre

Antidiabetic Activity

Y. Sugihara et al. studied the antihyperglycemic effects of a crude saponin fraction and five triterpene glycosides from *Gymnemasylvestre* leaves in streptozotocin-diabetic mice. They found that the saponin fraction (60 mg/kg) effectively lowered blood glucose levels within 2-4 hours of administration. Among the glycosides, gymnemic acid IV (3.4-13.4 mg/kg) significantly reduced blood glucose by 13.5-60.0% after six hours and increased plasma insulin levels, indicating its potential for managing diabetes and its possible role as an anti-obesity agent [79]. Gaytán Martínez *et al.* conducted a randomized trial with 30 patients who had impaired glucose tolerance. They found that *Gymnemasylvestre* (300 mg twice daily) led to significant reductions in 2-hour glucose levels, glycated hemoglobin A1c (A1C), body weight, and LDL cholesterol, while improving insulin sensitivity. Additionally, 46.7% of participants achieved normal A1C levels by the end of the study [80]. Baskaran et al. also noted that GS4 extract from *Gymnemasylvestre* significantly lowered blood glucose and HbA1c levels in Type 2 diabetic patients, allowing some to reduce or discontinue conventional medications [81]. Kashif *et al*. found that *Gymnemasylvestre* was as effective as metformin in lowering blood glucose in diabetic rabbits [82]. Lastly, Shigematsu *et al.* observed that *Gymnemasylvestre* leaf extract improved lipid metabolism and reduced cholesterol and triglycerides in rats [83]. G. K. Mall reported similar findings, noting significant reductions in fasting blood glucose and improvements in cholesterol levels with *Gymnemasylvestre* in diabetic rats [84].

Anti-Hyperlipidemic Activity

Shrivastava *et al*. assessed the antihyperlipidemic effects of ethanolic extracts from Fenugreek and *Gymnemasylvestre,* and a hydro-alcoholic extract from Curcuma longa in rats with cholesterol diet-induced hyperlipidemia. Over two weeks, these extracts significantly reduced total cholesterol, phospholipids, triglycerides, and LDL while increasing HDL levels. Among the extracts, Curcumin was the most effective, showing the greatest reductions in total cholesterol, triglycerides, and LDL, highlighting its potential for improving lipid profiles in hyperlipidemic conditions [85]. Prabhu et al. studied the effects of *Gymnemasylvestre* methanolic extract (GSME) on streptozotocin-induced diabetic rats. Over four weeks, GSME at doses of 100, 200, and 400 mg/kg significantly lowered blood glucose, triglycerides, LDL, and VLDL, while increasing HDL and serum insulin. The extract also improved body weight and reduced histopathological damage in the pancreas, liver, and kidneys [86]. Similarly, D. K. Singh et al. found that *Gymnemasylvestre* leaf extract effectively improved lipid profiles in dyslipidemic Wistar rats, with the 200 mg/kg dose showing significant reductions in total cholesterol, triglycerides, and LDL, while increasing HDL. This suggests *Gymnemasylvestre's* potential as an adjunct therapy for managing dyslipidemia [87].

Antioxidant Activity

Gunasekaran *et al.* investigated the antioxidant and antimicrobial properties of a methanolic extract from dried *Gymnema* leaves. The extract demonstrated significant antioxidant activity through DPPH free radical scavenging, reducing power assay, and hydroxyl radical quenching, and also showed notable antimicrobial effects against P. aeruginosa, S. aureus, and F. oxysporum. These findings suggest that *Gymnemasylvestre* could offer long-term benefits for diabetics by mitigating complications [88].

Tinospora cordifolia

Patel's study investigated the insulin-mimicking and insulin-releasing properties of an isoquinoline alkaloid-rich fraction (AFTC) from Tinospora cordifolia stems, along with the alkaloids palmatine, jatrorrhizine, and magnoflorine. In vitro experiments demonstrated that AFTC and these alkaloids reduced gluconeogenesis in rat hepatocytes and stimulated insulin secretion in pancreatic cells. In vivo, both AFTC and the alkaloids significantly lowered fasting blood glucose and improved glucose tolerance in normal rats, indicating their potential for managing hyperglycemia through insulin-mimicking and insulin-releasing activities [89]. Stanely Mainzen Prince et al. evaluated the hypoglycemic and hypolipidemic effects of an alcohol extract from Tinospora cordifolia roots. The extract significantly reduced blood and urine glucose levels, and serum and tissue lipids in alloxan-induced diabetic rats over six weeks, while also preventing body weight loss [90].Shivananjappa *et al.* studied the impact of Tinospora cordifolia on embryopathy and oxidative stress in pregnant diabetic rats, finding that it significantly reduced both conditions and improved antioxidant levels [91].Additionally, Ashok D. Chougale *et al.* found that the dichloromethane extract of Tinospora cordifolia effectively inhibited key digestive enzymes and reduced postprandial glucose spikes in both normal and diabetic animals [92].

Antioxidant Activity

Jayaprakash et al. investigated the antioxidant effects of ethanolic extract of *Tinospora cordifolia* (EETC) in male Wistar rats with liver cancer induced by N-nitrosodiethylamine (DEN). The study measured antioxidant activity by evaluating lipid peroxidation (LPO) and both enzymatic and non-enzymatic antioxidant levels. The results showed increased LPO and decreased antioxidant levels in the cancerous rats. However, treatment with EETC effectively brought LPO and antioxidant levels back to near-normal values [93].

CONCLUSION

The pharmacological actions of Eugenia jambolana, *Vetiveriazizanioides*, Syzygium aromaticum, Anacyclus pyrethrum, Cassia fistula, Cassia auriculata, *Strychnospotatorum*, *Gymnemasylvestre*, and *Tinosporacordifolia* reveal their significant potential in managing diabetes, hyperlipidemia, and oxidative stress. These plants exhibit a range of mechanisms, including enhancing insulin secretion, improving glucose and lipid metabolism, and exhibiting potent

antioxidant properties. Their diverse actions underscore their potential as complementary or alternative treatments in the management of diabetes and associated metabolic disorders.Further research is needed to fully understand the underlying mechanisms of these plants and to validate their efficacy in clinical settings. Additionally, exploring their safety profiles and potential interactions with conventional therapies will be essential for integrating these natural products into standard therapeutic regimens. Overall, these findings highlight the importance of traditional medicine and natural products in developing new strategies for managing chronic diseases like diabetes.

ACKNOWLEDGEMENTS

We wish to acknowledge our thanks to The Tamil Nadu Dr. M.G.R. Medical University, Chennai, Tamil Nadu, India and The National Institute of Siddha, Chennai, Tamil Nadu, India for their support.

REFERENCES

1. GBD Results. Institute for Health Metrics and Evaluation. https://vizhub.healthdata.org/gbd-results/.
2. Sukhikh S, Babich O, Prosekov A,et al.Antidiabetic Properties of Plant Secondary Metabolites. Metabolites. 2023 Apr 3;13(4):513.https://doi.org/10.3390/metabo13040513
3. Chung MY, Choi HK, Hwang JT. AMPK Activity: A Primary Target for Diabetes Prevention with Therapeutic Phytochemicals. Nutrients. 2021 Nov 12;13(11):4050.https://doi.org/10.3390/nu13114050
4. Semwal DK, Kumar A, Aswal S, et al. Protective and therapeutic effects of natural products against diabetes mellitus via regenerating pancreatic β -cells and restoring their dysfunction. Phytotherapy Research. 2020 Sep 28;35(3):1218–29.
5. Tapsell LC, Hemphill I, Cobiac L, et al. Health benefits of herbs and spices: the past, the present, the future. *Med J Aust*. 2006;185(S4):S1-S24.https://doi.org/10.5694/j.1326-5377.2006.tb00548.x
6. Sarabendrar Siddha Maruthuva Sudar, Saraswathi Mahal Noolagam, Tanjore, April 2000:219.
7. Murugesamudaliyar. GunapadamMooligaiVaguppu. Department of Indian Medicine and Homeopathy.
8. Morton J. *Jambolan*. In: Morton JF (Ed) Fruits of warm climates.1987:375–378.
9. Anonymous. Wealth of India. A Dictionary of Indian Raw materials and Industrial Products, National Institute of Science Communication, Council of Scientific and Industrial Research. New Delhi, Vol.10:Pp. 100-104. 2014.
10. Khare CP. Indian medicinal plants: an illustrated dictionary. Berlin: Springer; 2007:639.
11. Swami SB, Thakor NSJ, Patil MM, et al. Jamun (Syzygiumcumini (L.)): A Review of Its Food and Medicinal Uses. FNS. 2012;03(08):1100-17. http://dx.doi.org/10.4236/fns.2012.38146
12. Rastogi RP, Mehrotra BN. Compendium of Indian Medicinal Plants. 1990:388–389.
13. H AJA, Mahdi JF, Farooqui M, et al. Gas Chromatography-Mass Spectroscopic Analysis of Black Plum Seed (SyzygiumCumini) Extract in Hexane. Asian J. Pharm. Clin. Res. 2019:219–22.http://dx.doi.org/10.22159/ajpcr.2019.v12i2.29396
14. Ahmad N, Nawab M, Kazmi MH. Medicinal Potential of Jamun (Syzygiumcumini Linn): A Review. JDDT. 2019 Sep 15;9(5):175–80. https://doi.org/10.22270/jddt.v9i5.3568
15. Nisheeda BA, Safeer PM,Sreekumar S, et al.A Review on Plectranthusvettiveroides: An Endemic to South Indian High Value Aromatic Medicinal Plant.JPBS. 2016. Volume 11, Issue 2 Ver. III; 01-11
16. Snigdha M, Satish Kumar S, Sharmistha M, and Deepa C, An Overview on VetiveriaZizanioides. RJPBCS.2013.4(3):777-83

17. El-Saber Batiha G, Alkazmi LM, Wasef LG, Beshbishy AM, Nadwa EH, Rashwan EK. Syzygium aromaticum L. (Myrtaceae): Traditional Uses, Bioactive Chemical Constituents, Pharmacological and Toxicological Activities. Biomol. 2020;10(2):202.https://www.ncbi.nlm.nih.gov/pmc/articles/PMC7072209/
18. Elazzouzi H, Fadili K, Cherrat A, et al. Phytochemistry, Biological and Pharmacological Activities of the Anacyclus pyrethrum (L.) Lag: A Systematic Review. Plants (Basel). 2022 Sep 30;11(19):2578–8.https://www.ncbi.nlm.nih.gov/pmc/articles/PMC9573456/
19. Boonen J, Sharma V, Dixit V, et al. LC-MS N-alkylamide Profiling of an Ethanolic Anacyclus pyrethrum Root Extract. Planta Medica. 2012 Oct 9;78(16):1787–95. https://doi.org/10.1055/s-0032-1315371.
20. Cherrat A, Amalich S, Regragui M, et al. Polyphenols Content and Evaluation of Antioxidant Activity of Anacycluspyrethrum(L.) Lag. from Timahditea Moroccan Middle Atlas Region. Int. J. Adv. Res.2017 Mar 31;5(3):569–77. https://doi.org/10.21474/ijar01/3546.
21. Kushwaha, M.N, Vijay, S.J.; Swatantra, P. Plant Anacyclus pyrethrum-A Review. Res. J. Pharmacogn. Phytochem. 2012; 4, 164–170.
22. Sharma DK. Enumerations on phytochemical, pharmacological and ethnobotanical properties of Cassia fistula Linn: yellow shower. JPhytopharmacol.2017 Oct 30;6(5):300–6.https://doi.org/10.31254/phyto.2017.6509.
23. Bahorun T, Neergheen V, Aruoma O. Phytochemical constituents of *Cassia fistula*. African Journal of Food, Agriculture, Nutrition and Development. 2011 Nov 9;4(13).1530-40. https://doi.org/10.4314/ajfand.v4i13.71772
24. Rahmani AH. Cassia fistula Linn: Potential candidate in the health management. Pharmacognosy Res. 2015 Jul-Sep;7(3):217-24. https://doi.org/10.4103/0974-8490.157956.
25. Sharma A, Kumar A, Jaitak V. Pharmacological and chemical potential of Cassia fistula L- a critical review. J. Herb. Med. 2020 Oct;100407.https://doi.org/10.1016/j.hermed.2020.100407
26. Salma B, Muthukumar SP, Avinasha S, et al. Review on ethnobotany, phytochemistry, and pharmacological properties of Cassia auriculata. *Pharm Pharmacol Int J*. 2020;8(2):106-11. https://doi.org/10.15406/ppij.2020.08.00286.
27. Kanthimathi M, Soranam R. Phytochemical screening and Invitro antibacterial Potential of *Cassia auriculata* Linn. Flowers against Pathogenic Bacteria.IJPBS. 2014;1(1):45–56.
28. J B Harborne. Phytochemical methods: a guide to modern techniques of plant analysis. London: New York: Chapman and Hall; 1998.
29. Kiritikar KR, Basu BD. Indian Medicinal Plants. Vol III, Inernational Book Distributors, Dehra Dun, 2008: 1647- 49.
30. Nadkarni AK. Indian Materia Medica. Edn 3, Vol.1, Popular Book Depot, Bombay,1954.
31. Anonymous. Wealth of India. Raw Materials. Sp-W. Publications and Information Directorate. Vol. 10. New Delhi: CSIR; 1976: 66-7.
32. Trease and Evans, Pharmacognosy, 12th ed. London, BalliereTindall, 1983:36.
33. Tiwari P, Mishra BN, Sangwan NS. Phytochemical and pharmacological properties of Gymnemasylvestre: An important medicinal plant. BioMed Research International.2014:1–18. https://www.ncbi.nlm.nih.gov/pmc/articles/PMC3912882/
34. Khan F, Sarker MMR, Ming LC, et al. Comprehensive Review on Phytochemicals, Pharmacological and Clinical Potentials of Gymnemasylvestre. Frontiers in pharmacology.2019;10:1223. https://doi.org/10.3389/fphar.2019.01223
35. Srinivasan K, Kumaravel S. Unraveling the potential phytochemical compounds of Gymnemasylvestre through GC-MS study. Int J Pharm Pharm Sci. 2016;8(1):1-4.

36. Sinsheimer JE, Subba Rao G, McIlhenny HM. Constituents from Gymnemasylvestre Leaves V: Isolation and Preliminary Characterization of the Gymnemic Acids. Journal of Pharmaceutical Sciences. 1970 May;59(5):622–8.https://doi.org/10.1002/jps.2600590510.
37. SharmaP, Dwivedee BP, BishtD, et al. The chemical constituents and diverse pharmacological importance of *Tinospora cordifolia*. Heliyon. 2019; *5*(9), e02437. https://doi.org/10.1016/j.heliyon.2019.e02437
38. 38.Upadhyay AK, Kumar K, Kumar A, et al. Tinospora cordifolia (Willd.) Hook. f. and Thoms. (Guduchi) - validation of the Ayurvedic pharmacology through experimental and clinical studies. Int J Ayurveda Res. 2010;1(2):112-21. https://doi.org/10.4103/0974-7788.64405
39. Singh N, Gupta M. Effects of ethanolic extract of Syzygiumcumini (Linn) seed powder on pancreatic islets of alloxan diabetic rats. Indian J Exp Biol. PubMed.2007 Oct 1;45(10):861– https://pubmed.ncbi.nlm.nih.gov/17948734/
40. Bansal R, Ahmad N, Kidwai JR. Effects of oral administration of Eugenia jambolana seeds &chloropropamide on blood glucose level & pancreatic cathepsin B in rat. Indian J BiochemBiophys.PubMed. 1981 Oct 1;18(5):377–7.
41. Prince PStanelyM, Menon VP, Pari L. Hypoglycaemic activity of Syzigiumcumini seeds: effect on lipid peroxidation in alloxan diabetic rats. J. Ethnopharmacol. 1998 May;61(1):1–7.https://doi.org/10.1016/S0378-8741(98)00002-6
42. Purohit A, H. M. M. Daradka. Antidiabetic activity of Szygiumcumini seeds extract in alloxan induced diabetic mice. Hamdard medicus. 2000 Jan 1;43(4):33–4.https://pesquisa.bvsalud.org/portal/resource/pt/emr-53846
43. Vikrant V, Grover JK, Tandon N, et al. Treatment with extracts of Momordica charantia and Eugenia jambolana prevents hyperglycemia and hyperinsulinemia in fructose fed rats. J. Ethnopharmacol. 2001 Jul;76(2):139–43.https://doi.org/10.1016/s0378-8741(01)00218-5
44. GroverKJ, VatsVand RathiSS. Antihyperglycemic effect of Eugenia jambolana and Tinosporacardifolia in experimental diabetes and their effects on key metabolic enzymes involved in carbohydrate metabolism, J. Ethnopharmacol. 73, 2000, 461- 470.https://doi.org/10.1016/S0378-8741(00)00319-6
45. Pandey M, KhanA.Hypoglycemic effect of defatted seeds and water-soluble fibre from the seeds of Syzygiumcumini (Linn) Skeels in alloxan diabetic rats. Indian J Exp Biol,2022;40(10):1178-82. https://pubmed.ncbi.nlm.nih.gov/12693701/
46. Kasiappan Ravi, Subbaih Rajasekaran, Sorimuthu Subramanian. Antihyperlipidemic effect of *Eugenia jambolana* seed kernel on streptozotocin-induced diabetes in rats. Food and Chemical Toxicology, Volume 43, Issue 9, September 2005, Pages 1433-39.https://doi.org/10.1016/j.fct.2005.04.004
47. Sharma B, Balomajumder C, Roy P. Hypoglycemic and hypolipidemic effects of flavonoid rich extract from Eugenia jambolana seeds on streptozotocin induced diabetic rats. Food Chem Toxicol. 2008 Jul;46(7):2376–83. https://doi.org/10.1016/j.fct.2008.03.020
48. Sharma SB, Nasir A, Prabhu KM et al. Hypoglycaemic and hypolipidemic effect of ethanolic extract of seeds of Eugenia jambolana in alloxan-induced diabetic rabbits. J Ethnopharmacol. 2003 Apr;85(2-3):201–6.https://doi.org/10.1016/s0378-8741(02)00366-5
49. G. Gopalakrishnan, Dhanapal C.K.Evaluation of anti-diabetic activity of methanolic extract of Coleus vettiveroidesjacob in streptozotocin-induced diabetic rats.J. Pharm. Sci. & Res. January 2014;6(2):97-103
50. Sanjay Kumar Karan, Pal D, Sagar Kumar Mishra et al.Antihyperglycaemic Effect of Vetiveriazizanioides (L.) Nash Root Extract in Alloxan Induced Diabetic Rats; Asian J. Chem.2013;25(3):1555-57.https://doi.org/10.14233/ajchem.2013.13137

51. G. Gopalakrishnan, Dhanapal C.K. Evaluation of in-vivo antioxidant activity of methanolic extract of Coleus vettiveroides Jacob in streptozotocin-induced oxidative stress in rats. Int J Pharm Pharm Sci.January 2014;6(1):590-592.
52. Gopalakrishnan G, Dhanapal CK, Manavalan R. In vitro antioxidant activities of methanolic extract of root of Coleousvettiveroides (Jacob). Int J Pharma Bio Sci. 2011;2:353-7.
53. Jung CH, Ahn J, Jeon TI, et al. Syzygium aromaticum ethanol extract reduces high-fat diet-induced obesity in mice through downregulation of adipogenic and lipogenic gene expression. Exp Ther Med. 2012 Jun 13;4(3):409–14. https://doi.org/10.3892/etm.2012.609
54. Tahir HU, Sarfraz RA, Ashraf A, Adil S. Chemical Composition and Antidiabetic Activity of Essential Oils Obtained from Two Spices (Syzygium aromaticum and Cuminum cyminum). International Journal of Food Properties. 2016 Jun 10;19(10):2156–64. https://doi.org/10.1080/10942912.2015.1110166
55. Al-Okbi SY, Mohamed DA, Hamed TE, et al. Protective effect of clove oil and eugenol microemulsions on fatty liver and dyslipidemia as components of metabolic syndrome. J Med Food. 2014;17(7):764-771.https://doi.org/10.1089/jmf.2013.0033
56. Fankem PM, Kwanga SN, Sameza ML, et al. Antioxidant and Antifungal Activities of Cocoa Butter (Theobroma cacao), Essential Oil of Syzygium aromaticum and a Combination of Both Extracts against ThreeDermatophytes.ASRJETS-Journal.2017Nov;37(1):255-72.https://www.asrjetsjournal.org/index.php/American_Scientific_Journal/article/view/3449
57. Gülçin İ, Elmastaş M, Aboul-Enein HY. Antioxidant activity of clove oil – A powerful antioxidant source. Arab. J. Chem. 2012 Oct;5(4):489–99.https://doi.org/10.1016/j.arabjc.2010.09.016
58. Nam H, Kim MM. Eugenol with antioxidant activity inhibits MMP-9 related to metastasis in human fibrosarcoma cells. Food Chem Toxicol. 2013;55:106-112. https://doi.org/10.1016/j.fct.2012.12.050
59. Yadav AS, Bhatnagar D. Free radical scavenging activity, metal chelation and antioxidant power of some of the Indian spices. Biofactors. 2007;31(3-4):219-227. https://doi.org/10.1002/biof.5520310309
60. Tyagi S, Mansoori MH, Singh NK, Shivhare MK, Bhardwaj P, Singh RK. Antidiabetic effect of Anacyclus pyrethrum DC in alloxan induced diabetic rats. Eur. J. Biol. Sci. 2011;3(4):117-20
61. Selles C, Medjdoub H, Dib ME, Zerriouh M, et al. Anti-diabetic activity of aqueous root extract of Anacyclus pyrethrum L. in streptozotocin-induced-diabetic rats. Journal of medicinal plants research. 2012 Apr 30;6(16):3193-8.
62. Kumar, V. K., & Lalitha, K. G. (2014). In vitro study on α-amylase inhibitory activity of an Ayurvedic medicinal plant, Anacyclus pyrethrum DC root. Indian J Pharmacol.2014;46(3):350-351. https://doi.org/10.4103/0253-7613.132204
63. Jarald EE, Joshi SB, Jain DC, Edwin S. Biochemical Evaluation of the Hypoglycemic Effects of Extract and Fraction of Cassia fistula Linn. in Alloxan-induced Diabetic Rats. Indian J Pharm Sci. 2013;75(4):427-34. https://doi.org/10.4103/0250-474X.119823
64. 64.Veeramani C, El Newehy AS, Alsaif MA, et al. *Cassia fistula* nutrition rich flower tea derived biotic nanoparticles synthesis, characterization and their antioxidant and anti-hyperglycaemic properties. Afr Health Sci. 2022;22(1):384-394.https://doi.org/10.4314/ahs.v22i1.47
65. Manonmani G, Bhavapriya V, Kalpana S, Govindasamy S, Apparanantham T. Antioxidant activity of Cassia fistula (Linn.) flowers in alloxan induced diabetic rats. J Ethnopharmacol. 2005;97(1):39-42.https://doi.org/10.1016/j.jep.2004.09.051

66. Nambirajan G, Karunanidhi K, Ganesan A, et al. Evaluation of antidiabetic activity of bud and flower of Avaram Senna (Cassia auriculata L.) In high fat diet and streptozotocin induced diabetic rats. Biomed Pharmacother.2018;108:1495-1506.https://doi.org/10.1016/j.biopha.2018.10.007
67. Latha M, Pari L. Antihyperglycaemic effect of Cassia auriculata in experimental diabetes and its effects on key metabolic enzymes involved in carbohydrate metabolism. Clin Exp Pharmacol Physiol. 2003;30(1-2):38-43. https://doi.org/10.1046/j.1440-1681.2003.03785.x
68. Latha M, Pari L. Antihyperglycaemic effect of Cassia auriculata in experimental diabetes and its effects on key metabolic enzymes involved in carbohydrate metabolism. Clin Exp Pharmacol Physiol. 2003;30(1-2):38-43.https://doi.org/10.1046/j.1440-1681.2003.03785.x
69. Surana SJ, Gokhale SB, Jadhav RB, et al. Antihyperglycemic Activity of Various Fractions of Cassia auriculata Linn. in Alloxan Diabetic Rats. Indian J Pharm Sci. 2008;70(2):227-29. https://doi.org/10.4103/0250-474X.41461
70. Gupta S, Sharma SB, Bansal SK, et al. Antihyperglycemic and hypolipidemic activity of aqueous extract of Cassia auriculata L. leaves in experimental diabetes. J Ethnopharmacol. 2009;123(3):499-503.https://doi.org/10.1016/j.jep.2009.02.019
71. Rajendran V, Krishnegowda A, Nachiappan V. Antihyperlipidemic activity of *Cassia auriculata* flower extract in oleic acid induced hyperlipidemia in *Saccharomyces cerevisiae*. J Food Sci Technol. 2017;54(9):2965-https://doi.org/10.1007/s13197-017-2735-0
72. Vijayaraj P, Muthukumar K, Sabarirajan J, et al. Antihyperlipidemic activity of Cassia auriculata flowers in triton WR 1339 induced hyperlipidemic rats. Exp ToxicolPathol. 2013;65(1-2):135-41.https://doi.org/10.1016/j.etp.2011.07.001
73. Elayarani M, Shanmuganathan P, Muthukumaran P. In vitro anti-oxidant activity of the various extracts of Cassia auriculata L. flower by UV spectrophotometer. AJPTech. 2011;1(3):70-2.
74. Dhasarathan P, Theriappan P. Evaluation of anti-diabetic activity of Strychonouspotatorum in alloxan induced diabetic rats. J Med Med Sci. 2011 Jan;2(2):670-4.
75. 75.Biswas A, Chatterjee S, Chowdhury R, et al. Antidiabetic effect of seeds of Strychnospotatorum Linn. in a streptozotocin-induced model of diabetes. Acta Pol Pharm. 2012;69(5):939-943.
76. Mishra SB, Verma A, Vijayakumar M. Preclinical valuation of anti-hyperglycemic and antioxidant action of Nirmali (Strychnospotatorum) seeds in streptozotocin-nicotinamide-induced diabetic Wistar rats: A histopathological investigation. Biomarkers and Genomic medicine. 2013 Dec 1;5(4):157-63.
77. Subramanian SP. Evaluation of Antidiabetic and Antioxidative Efficacy of StrychnosPotatorum (Nirmali) Seeds Extract in High Fat Diet Fed- Low Dose Streptozotocin Induced Experimental Type 2 Diabetes in Rats. Diabesity. 2020 Feb 16;6(1):1.https://doi.org/10.15562/diabesity.2020.63
78. Pandu Raju T, Shastri K, Srinivas Reddy C, et al. Antihyperglycemic Activity of Strychnospotatorum Seed and Leaf Methanolic Extracts in Alloxan- Induced Diabetic Rats. RJPP. 2010;2(2):152–4. https://rjpponline.org/AbstractView.aspx?PID=2010-2-2-13
79. Sugihara Y, Nojima H, Matsuda H, et al. Antihyperglycemic effects of gymnemic acid IV, a compound derived from Gymnemasylvestre leaves in streptozotocin-diabetic mice. J Asian Nat Prod Res. 2000;2(4):321-7.https://doi.org/10.1080/10286020008041372
80. Gaytán Martínez LA, Sánchez-Ruiz LA, Zuñiga LY, et al. Effect of *Gymnemasylvestre* Administration on Glycemic Control, Insulin Secretion, and Insulin Sensitivity in Patients with Impaired Glucose Tolerance. J Med Food.2021;24(1):28-32.https://doi.org/10.1089/jmf.2020.0024

81. Baskaran K, Kizar Ahamath B, Radha Shanmugasundaram K, et al. Antidiabetic effect of a leaf extract from Gymnemasylvestre in non-insulin-dependent diabetes mellitus patients. J Ethnopharmacol. 1990;30(3):295-300.https://doi.org/10.1016/0378-8741(90)90108-6
82. Kashif M, Nasir A, Gulzaman, et al. Unlocking the anti-diabetic potential of *Gymnemasylvestre*, *Trigonella foenum-graecum*, and their combination thereof: An in-vivo evaluation. Food Sci Nutr. 2023;11(12):7664-72. https://doi.org/10.1002/fsn3.3685
83. Shigematsu N, Asano R, Shimosaka M, Okazaki M. Effect of administration with the extract of Gymnemasylvestre R. Br leaves on lipid metabolism in rats. Biol Pharm Bull. 2001;24(6):713-717.https://doi.org/10.1248/bpb.24.713
84. Mall GK, Mishra PK, Prakash V. Antidiabetic and hypolipidemic activity of Gymnemasylvestre in alloxan induced diabetic rats. Global Journal of Biotechnology & Biochemistry. 2009;4(1):37-42.
85. R. Shrivastava, S. S. Solanki, V. Tomar, N. Garud, A. Garud, P. Kannojia, N. Jain. Comparative Evaluation of Polyherbal Combination for Hypolipidemic Activity. Int. J. Pharm. Sci. Drug Res. 2009;1(1):9-12. https://doi.org/10.25004/IJPSDR.2009.010103
86. Prabhu S, Vijayakumar S. Antidiabetic, hypolipidemic and histopathological analysis of Gymnemasylvestre (R. Br) leaves extract on streptozotocin induced diabetic rats. Biomed Prev Nutr. 2014 Jul 1;4(3):425-30.https://doi.org/10.1016/j.bionut.2014.03.008
87. Singh DK, Kumar N, Sachan A, et al. Hypolipidaemic Effects of *Gymnemasylvestre* on High Fat Diet Induced Dyslipidaemia in Wistar Rats. J Clin Diagn Res. 2017;11(5):FF01-FF05.https://doi.org/10.7860/JCDR/2017/27430.9859
88. Gunasekaran V, Srinivasan S, Rani SS. Potential antioxidant and antimicrobial activity of Gymnemasylvestre related to diabetes. J. Med. Plants. 2019;7(2):05-11.
89. Patel MB, Mishra S. Hypoglycemic activity of alkaloidal fraction of Tinospora cordifolia. Phytomedicine. 2011;18(12):1045-1052.https://doi.org/10.1016/j.phymed.2011.05.006
90. Stanely Mainzen Prince P, Menon VP. Hypoglycaemic and hypolipidaemic action of alcohol extract of Tinospora cordifolia roots in chemical induced diabetes in rats. Phytother Res. 2003;17(4):410-3.https://doi.org/10.1002/ptr.1130
91. Shivananjappa MM, Muralidhara. Abrogation of maternal and fetal oxidative stress in the streptozotocin-induced diabetic rat by dietary supplements of Tinospora cordifolia. Nutrition. 2012;28(5):581-7.https://doi.org/10.1016/j.nut.2011.09.015
92. Chougale AD, Ghadyale VA, Panaskar SN, Arvindekar AU. Alpha glucosidase inhibition by stem extract of Tinospora cordifolia. J Enzyme Inhib Med Chem. 2009;24(4):998-1001.https://doi.org/10.1080/14756360802565346
93. Jayaprakash R, Ramesh V, Sridhar MP, Sasikala C. Antioxidant activity of ethanolic extract of Tinospora cordifolia on N-nitrosodiethylamine (diethylnitrosamine) induced liver cancer in male Wister albino rats. J Pharm Bioallied Sci. 2015;7(Suppl 1):S40-S45. https://doi.org/10.4103/0975-7406.155791

Table 1.The ingredients and quantity used to prepare *Mega Sanjeevi Chooranam*[6]

Tamil name/ Botanical name	Quantity
NaavalVithaiParuppu(*Eugenia jambolana*)	100 grams
Vilamichaver(*Plectranthusvettiveroides*)	100 grams
Vetiver (*Vetiveriazizanioides*)	100 grams

Ilavangam(*Syzygium aromaticum*)	100 grams
Akkarakaram(*Anacyclus pyrethrum*)	100 grams
Kondraippoo (Cassia fistula)	100 grams
Aavarampoo (Cassia auriculata)	100 grams
Thetrankottai (Strychnospotatorum)	100 grams
SirukurinjanSamoolam (Gymnemasylvestre)	500 grams
SeenthilSarkarai(*Tinospora cordifolia*)	100 grams

Table 2.Parts used, taste and action of the ingredients of *Mega Sanjeevi Chooranam*[7]

Tamil Name	Parts Used	Taste	Action
Naaval	Seed	Astringent	Stomachic, Diuretic, Tonic
Vilamichaver	Root	Bitter	Refrigerant, Anti Pitha
Vetiver	Root	Bitter	Refrigerant
Ilavangam	Flower bud	Pungent	Anti-spasmodic, Carminative, Stomachic
Akkarakaram	Root	Pungent	Stimulant, Sialagogue, Rubefacient
Kondraippoo	Flower	Astringent with mild bitterness	Vermifuge
Aavarampoo	Flower	Astringent	Astringent, Tonic
Thetrankottai	Seed	Bitter	Alterative, Tonic, Stomachic, Demulcent, Mild Expectorant
SirukurinjanSamoolam	Leaf	Bitter	Astringent, Stomachic,Tonic, Refrigerant
SeenthilSarkarai	Stem	Bitter	Alterative, Antiperiodic, Aphrodisiac, Demulcent, Stimulant, Stomachic, Tonic, Mild Diuretic

Table 3.Pharmacognostic aspect and chemical constituents

Plant Name	Family	Botanical Description	Chemical Constituents
Naaval	Myrtaceae	A medium-sized tree reaching heights of 10 to 30 meters, characterized by a trunk that is either straight or curved, and short and stout, with a diameter ranging from 40 to 100 centimeters. The seed found in each berry is strongly astringent and mildly bitter, ranging from 1 to 2 centimeters in length; occasionally, 2 to 5 angular, irregular seeds are compressed into a	Oleic acid, stearic acid, gallic acid, ellagic acid [9,10], quercetin, β-sitoterol, 6-hexahydroxy diphenoylglucose [11,12,13] and elements such as zinc, Potassium, sodium, chromium and vanadium [14].

		mass that looks like a single seed. Cotyledons are pale green [8].	
Vilamichaver	Lamiaceae	A succulent herb with extensive branching and a hairy texture, reaching up to 1 meter tall. The roots are fibrous, ranging from 30 to 90 centimeters in length, forming a tuft. They are slender, very thin, easily severed, and have a strong aroma; they are straw-colored when fresh but turn dark brown upon drying [15].	Androstan-17-one, 3-ethyl-3-hydroxy-, (5α) - (25%), followed by spathulenol at 9%, α-bisabolol (7%), Z-valerenyl acetate (7%), megastigma-4,6(E),8(Z)-triene (6%), 1H-cycloprop(E)azulen-7-ol, decahydro-1,1,7-trimethyl-4-methylene- (5%), myrtenol (2%), 1-naphthalenol (2%), caryophyllene oxide (2%), and abieta-9(11),8(14),12-trien-12-ol (2%) [15].
Vetiver	Poaceae	Vetiver is a perennial grass native to India. It has tall stems and leaves that are elongated, narrow, and quite rigid.The plant produces flowers with a brownish-purple tint, and its roots can extend vertically to a depth of 2 to 4 meters.	Vetiverol, Vetivone, Khusimone, Khusimol, Vetivene, Khositone, various terpenes, Benzoic acid, Tripene-4-ol, ß-Humulene, Epizizianal, vetivenylvetivenate, iso-Khusimol, vetiver oils, and vetivazulene. Additionally, Zizaene, prezizaene, and bvetispirene are also noted [16].
Ilavangam	Myrtaceae	Clove is a spice tree with a conical shape and a straight trunk, reaching heights of 10 to 12 meters. The flower buds start out pale yellow with a shiny surface, then turn green, and finally mature to a bright red.These buds are 1 to 2 centimeters long and feature a cylindrical, thick ovary surrounded by four fleshy sepals [17].	β-Caryophyllene, Vanillin, Crategolic acid (Maslinic acid), Kaempferol, Rhamnetin,Eugenitin,Eugenin,**Ellagic acid**,Gallic acid, Biflorin, Myricetin, Campesterol, Stigmasterol, Oleanolic acid, Quercetin, Bicornin, **Carvacrol [17].**
Akkarakaram	Asteraceae	This perennial plant reaches 40 to 60 cm in height and is distinguished by its	Spathulenol, n-alkylamides [19], tannic acid, inulin, anacycline, phenylethylamine, polyacetylenic amides I-IV, sesamin, lignin [20], pellitorine and pyrethrinsthree (pyrethrin

		numerous simple or lightly branched stems emerging from the base. The roots are long, thick, and fibrous, with a brown outer layer and a white inner core [18].	I, cinerin I and jasmolin I) are esters of chrysanthemum acid, and three (pyrethrin II, cinerin II and jasmolin II) are pyrethrins [21].
Kondraippoo	Fabacae	Cassia fistula is a popular ornamental tree, known for its abundant yellow flowers that bloom in late spring. The flowers are pendulous, arranged in slender, pubescent racemes that are 4–7 cm in diameter. The calyx is long, divided to the base, and pubescent, with oblong, obtuse segments. The corolla is yellow, and all stamens have anthers [22].	Kaempferol [23],Leucopelargonidin [24] β-Sitosterol The main components of the flower oil were (E) -nerolidol (38.0%), and 2-hexadecanone (17.0%) [25].
Aavarampoo	Fabacae	It is a branched shrub that reaches heights of 1.5 to 5 meters, with a trunk diameter of 20 cm and brown lenticellate bark. The flowers are large and irregular, measuring 50 mm, with a bright yellow color and arranged in axillary racemes that can have 2 to 8 flowers. Each flower is bisexual, zygomorphic, and pentamerous, ranging from 4 to 5 cm in size. The sepals are rounded at the apex and imbricate, while the petals are free, imbricate, and unequal, ranging from 1.5 to 3 cm in length. The plant	Alkaloids, anthra-quinones, carbohydrates, cardiac-glycosides, coumarins, flavonoids, glycosides, phenols, phlobatannins, phytosteroids, saponins, steroids, tannins, terpenoids and triterpenoids. [27, 28].

		has 10 stamens, with the 3 lower ones being large and fertile, while the others are typically sterile. The ovary is superior [26].	
Thetrankottai	Loganiaceae	A tall tree, reaching up to 13 meters in height, has opposite branches. Its seeds are one or two in number, circular with an 8 mm diameter, bluntly lenticular in shape, and not flattened [29, 30]	Diaboline [31], brucine, loganin, mannose, sucrose, arachidonic, lignoceric, linoleic, oleic, palmitic, and stearic acids [32].
SirukurinjanSamoolam	Asclepiadaceae	It is a perennial, woody climber. Its leaves are opposite, typically elliptic or ovate in shape, measuring 1.25–2.0 inches by 0.5–1.25 inches. The inflorescence is a lateral umbel arranged in cymes, and the follicles are terete and lanceolate, reaching up to 3 inches in height [33].	Triterpene saponins from the oleanane Class - gymnemic acids and gymnemasaponins Dammarane class –gymnemasides [34,35]. Other phytoconstituents - anthraquinones, flavones, hentriacontane, pentatriacontane, phytin, resins, tartaric acid, formic acid, butyric acid, lupeol, β-amyrin-related glycosides, stigmasterol, and calcium oxalate [36].
Seenthil	Menispermaceae	It is a large extensively spreading glabrous, perennial deciduous twine with succulent stems and papery bark which is widely found in India. The leaves are simple, heart-shaped, and a dark, vibrant green. The stems are covered with closely spaced warty tubercles and have a surface that is longitudinally fissured, with lengths of 3-5 cm and diameters of 3-8 mm [37].	Alkaloids: tembetarine, choline, magnoflorine, berberine, tinosporin, isocolumbin, palmetine, jatrorrhizine, aporphine alkaloids, tetrahydropalmatine Steroids: B-sitosterol, δ-sitosterol, 20 β-hydroxyecdysone, giloinsterol, Makisterone A, Ecdysterone Glycosides: 18-norcleodrane glucoside, Tinocordifolioside, Cordioside, cordifolioside A, B, C, D and E, Furanoidditerpine glucoside, Syringin, pregnane glycoside Syringing-apiosylglycoside, palmatosides [38].

REVIEW ARTICLE

The Nutritional and Health Benefits of the seed of Jackfruit (*Artocarpus heterophyllus* Lam.): A Review

Jimi Baruah*

Research Scholar, Department of Life Sciences, Dibrugarh University, Dibrugarh, Assam, India.

Received: 21 Sep 2024 Revised: 03 Dec 2024 Accepted: 18 Jan 2025

***Address for Correspondence**
Jimi Baruah*
Research Scholar,
Department of Life Sciences,
Dibrugarh University,
Dibrugarh, Assam, India.
E.Mail: jimibaruah142@gmail.com

ABSTRACT

In many Asian countries, Jackfruit (*Artocarpusheterophyllus* Lamarck) is a well-known fruit. This fruit is commonly known as jackfruit. It is known to be the largest edible fruit in the world. It is a tropical climacteric fruit and belongs to Moraceae family. It is widely cultivated in Asia especially in the South-East Asian countries. It is commonly found in Asia, Africa and in some regions of South America and is native to Western Ghats of India. Jackfruit is rich in nutrients such as carbohydrates, proteins, minerals, phytochemicals and vitamins. Both the flesh and the seeds of this fruit is consumed in various forms – as a fruit, in boiled forms, as curries and also used to make pickles. On the contrary, in fully ripen stage, the flesh can be directly consumed as fruit. Different food products such as jams, jellies, ice creams, etc. are also made from pureed jackfruit. In the preparation of traditional medicines, the various parts of the jackfruit tree such as barks, leaves and fruits have been extensively used due to their wound healing and hypoglycemic effects, antifungal, antimicrobial, anticarcinogenic and anti-inflammatory effects apart from the immunological and digestive benefits of jackfruit.

Keywords: Jackfruit (*Artocarpus heterophyllus* Lam.), jackfruit seed, nutritional benefits, health benefits, perianth

INTRODUCTION

A jackfruit is a large, thick fruit with a yellow flesh which bears pods and edible seeds. As the yellowish flesh of jackfruit possess a distinctive and a sweet flavor hence some people describe it as a cross between pineapple and banana. Jackfruit (*Artocarpus heterophyllus* Lam.) belongs to the family Moraceae. The word jackfruit is derived from the Portuguese word jaca, which is further derived from the Malayalam (Caminiti *et al*., 2012) word chakka

(Pradeepkumar *et al*., 2008). Both male and female flowers are produced by jackfruit trees hence making them monoecious. The monoecious jackfruit tree has both male and female inflorescences on the same tree (Baliga *et al*., 2011)In India's production of jackfruit, 11.31% share (212000 tons) of jackfruit is contributed by each individual state – Assam and West Bengal which is followed by Chhattisgarh, Jharkhand, Tripura, etc., 14.01% (263000 tons) of jackfruit is contributed by Kerala and 16.63% (312000 tons) of jackfruit is contributed by Orissa. The jackfruit is mostly composed of the actual fruit, the fruit axis and the persisting perianth. Due to the presence of the laticiferous cells that produce latex, which thereby aids in holding the fruit together, the axis and the core of the fruit are inedible (Prakash *et al*., 2009). The by-products of jackfruit include skin, rags, peel, perianth and seeds. Upon processing and consumption of fresh jackfruit, significant quantities of non-edible wastes including the peel and central axis as well as edible by-products such as perianth and seeds are produced. Jackfruit is composed of three main regions. These include :

1. The fruit axis
2. The persistent perianth
3. The true fruit

The perianth is composed of three regions. These include :

1. The lower fleshy edible region (Bulb)
2. The middle-fused region (Rind of the syncarp)
3. The horny non-edible region (Spikes)

Within the agricultural sector, a variety of industries generate significant amounts of wastes, such as seeds, molasses, bagasse, peels, waste liquid, whey, and many more (Balasundram, 2006). On the contrary, some of the waste materials produced by jackfruit processing and consumption are used to enrich the soil as a nutrient or repurposed as animal feed. The seeds of jackfruit are 2-3 cm in length and 1-1.5 cm in diameter (Prakash *et al*, 2009).These seeds are light brown in colour and is surrounded by a fleshy white cotyledon enclosed in a white aril which thereby surrounds a thin brown spermoderm. This important by-product of jackfruit, i.e. the seed consists around 12-14% of an entire jackfruit (Akther, 2019). Each jackfruit holds up to 500 seeds approximately (Prakash *et al*., 2009).

MATERIALS AND METHODS

For this review study, literature search had been conducted from different journals and databases including Google Scholar, ResearchGate, ScienceDirect and other authentic websites. The main objective of this review study is to obtain comprehensive information on the nutritional benefits of jackfruit (*Artocarpus heterophyllus*Lam.) seed.

Taxonomic classification

Systematic position

Kingdom : Plantae
Sub-kingdom :Tracheobionta
Division :Magnoliophyta
Class :Magnoliopsida
Sub-class :Hamamelidae
Order :Urticales
Family :Moraceae
Genus :*Artocarpus*
Species :*Artocarpusheterophyllus* (Lam.)
Vernacular name
Assamese :Kothal

Parts used

Apart from the entire plant, bark, fruits, latex, leaves, roots and seeds are also used.

Preservation of jackfruit seed

Fresh seeds have a shorter shelf life while dried or powdered seeds can be preserved and stored for extended periods.

Nutritional and health benefits of jackfruit seed

Though the jackfruit seeds which make up 10-15% of the weight of jackfruit are underappreciated, neglected and often overlooked by people, they offer significant nutritional (Hossain, 2014) and health benefits (Waghmare, 2019). The nutritional and health benefits of jackfruit seed have been tabulated below in Table 1.

CONCLUSION

This review study highlights the various nutritional and health benefits of Jackfruit (*Artocarpus heterophyllus* Lam.) seed. Since ages, jackfruit seed has been a traditional medicine and is now being used by the modern day researchers to study its benefits. However, further research is needed to determine the potential benefits of the other parts of the jackfruit plant. In a nutshell, the Jackfruit (*Artocarpus heterophyllus* Lam.) seeds serve as a natural source of health-promoting substances as they have shown a promising potential towards various health benefits and also can be developed into therapeutic agents for preventing food-borne illness.

Conflict of interest

The author declares that there is no conflict of interest.

Author contributions

A literature survey and article screening was done solely by the author. The writing of the draft manuscript and revisions of the manuscript was also done solely by the author.

Abbreviations

LDL : Low - density lipoprotein

REFERENCES

1. Akter B, Haque M, Ahiduzzaman M and Ali M A 2021. Formulation of Jackfruit Seed Protein Enriched Cake. *Annals of Bangladesh Agriculture***24**(1):17-39.
2. Akther N, Phuntsho S, Chen Y, Ghaffour N and Shon H K 2019.Recent advances in nanomaterial-modified polyamide thin-film composite membranes for forward osmosis processes. *Journal of Membrane Science***584**:20-45.
3. Balasundram N, Sundram K and Samman S 2006. Phenolic compounds in plants and agri-industrial by-products: Antioxidant activity, occurrence, and potential uses. *Food Chemistry***99**(1):191-203.
4. Baliga S, Arnadi R, Shivashankara, Haniadka R, D'Souza J and BhatH 2011.Phytochemistry, nutritional and pharmacological properties of *Artocarpus heterophyllus*Lam. (jackfruit): A review. *Food Research International***44**:1800-1811.
5. Caminiti IM, Palgan I, Muñoz A, Noci F, Whyte P, Morgan DJ, Cronin D A and Lyng J G 2012. The effect of ultraviolet light on microbial inactivation and quality attributes of apple juice. *Food Bioprocess Technology***5**:680-686.
6. Chandrasekar R and Sivagami B 2021.Edible seeds medicinal value, therapeutic applications and functional properties-A Review.*International Journal of Pharmacy and Pharmaceutical Sciences***13**(7):11-18.

7. Chhotaray S and Priyadarshini B 2022.Nutritional composition and health benefits of jackfruit seed flour: A review. *The Pharma Innovation***11**(10):454-456.
8. Chowdhury A R, Bhattacharyya A and Chattopadhyay P 2012.Study on functional properties of raw and blended Jackfruit seed flour (a non-conventional source) for food application. *Indian Journal of Natural Products and Resources***3**(3):347-353.
9. Noor F, Rahman M J, Mahomud M S, Akter M S, Talukder M A I and Ahmed M 2014. Physicochemical Properties of Flour and Extraction of Starch from Jackfruit Seed.*International Journal of Nutrition and Food Sciences***3**(4):347-354.
10. Felicia Katherine R, Muthukumaran C, Sharmila G, Manoj Kumar N, Tamilarasan K and Jaiganesh R 2017. Xanthan gum production using jackfruit-seed-powder-based medium: optimization and characterization. *3 Biotech***7**:1-10.
11. Hossain E, Rasti M, Tabassum H and Abdelnasser A 2014. Evolution toward 5G multi-tier cellular wireless networks: An interference management perspective. *IEEE Wireless communications***21**(3):118-127.
12. Kabir S and Daar A S 1994.The composition and properties of jacalin, a lectin of diverse applications obtained from the jackfruit (*Artocarpus heterophyllus*Lam.) seeds. *Immunological investigations***23**(3):167-88.
13. Mukprasirt A and Sajjaanantakul K 2004.Physico-chemical properties of flour and starch from jackfruit seeds (*Artocarpusheterophyllus*Lam.) compared with modified starches. *International Journal of food science & technology***39**(3):271-276.
14. Neelanjana J, Sharma S and Jose D 2023. Health benefits of jackfruit (*Artocarpus heterophyllus* Lam.) seeds : A review. *The Pharma Innovation Journal***12**(6):879-888.
15. Ningsih P, Rahmawati S, Santi N M, Suherman andDiah AW 2021.Making Edible Film from Jackfruit Seed Starch (*Artocarpus heterophyllus*Lam.) with the Addition of Rosella Flower Extract (*Hibiscus sabdariffa* Linnaeus) As Antioxidant.*International Journal of Design & Nature and Ecodynamics***16**(6):691-699.
16. Pradeepkumar PE, Höbartner C, Baum D A and Silverman SK 2008.DNA-catalyzed formation of nucleopeptide linkages.*AngewandteChemie International Edition***47**(9):1753-1757.
17. Prakash O, Kumar R, Mishra A and Gupta R 2009.*Artocarpusheterophyllus* Lamarck (Jackfruit): An overview. *Pharmacognosy Reviews***3**(6):353.
18. Ranasinghe RA, Maduwanthi S D and Marapana R 2019. Nutritional and Health Benefits of Jackfruit (*Artocarpusheterophyllus* Lam.): A Review. *International Journal of Food Science***2019**:4327183.
19. Saha RK, Bhuiyan AA, Sharmin S and Jolly JA 2016. Antidiabetic, Antioxidant and Antibacterial Activities of the Functional Molecules Isolated from the Seed and Peel of Jackfruit (*Artocarpus heterophyllus*Lam.).*Journal of Pharmacy and Pharmaceutics***3**(1):1-8.
20. Shinde V L, Pawar CD, Warang O S, Dandekar VS, Kulkarni M and Joshi M S 2021. Studies on preparation of ice-cream from jackfruit (*Artocarpus heterophyllus* Lam.) seed powder. *International Journal of Chemical Studies***9**(1):2710-2712.
21. SitiFaridah M A and Noor AziahAA 2012.Development of reduced calorie chocolate cake with jackfruit seed (*Artocarpus heterophyllus* Lam.) Flour and polydextrose using response surface methodology (RSM).*International Food Research Journal***19**(2):515-519.
22. Suli I, Rodriguez T, Alcantara L and Suarez P A 2021. Physicochemical Properties, Antioxidant Capacity, Prebiotic Activity and Anticancer Potential in Human Cells of Jackfruit (*Artocarpus heterophyllus* Lam.) Seed Flour.*Molecules***26**(26):4854.
23. Suzihaque MU H,Zaki NA M, Alwi H, Ibrahim UK,Karim S F A and Anuar N K 2022.Jackfruit seed as an alternative replacement for starch flour. *Materials Today: Proceedings* **63**(1):S451-S455.
24. Swami SB, Thakor NJ, Haldankar P M and Kalse S B 2012. Jackfruit and Its Many Functional Components as Related to Human Health: A Review. *Comprehensive Reviews in Food Science and Food Safety***11**(6):565- 576.
25. Waghmare R, Memon N, Gat Y, Gandhi S, Kumar V and Panghal A 2019. Jackfruit seed: an accompaniment to functional foods. *Brazilian Journal of Food Technology***22**(2):e2018207.
26. Wisansakkul S, Oupathumpanont O, Sungsanit K, Chulacupt S and Boonyobhas S 2016.Development Production of Bioplastics from Jackfruit Seeds Starch. *Burapha Science Journal***21**(2):216-228.

27. Zhang Z, Wang Y, Zhang Y, Chen K, Chang H, Chenchen M, Jiang S, Huo D, Liu W, Jha R and Zhang J 2021. Synergistic Effects of the Jackfruit Seed Sourced Resistant Starch and *Bifidobacterium pseudolongum* subspecies *Globosum* on Suppression of Hyperlipidemia in Mice. *Foods***10**(6):1431.

Table 1 :Different forms of nutrients present in jackfruit seed and their nutritional and health benefits (Neelanjana *et al.,* 2023).

Form of nutrient	Nutritional and health benefits	Reference
Antioxidants	Decreases LDL, lowers risk of heart disease and high cholesterol, prevents cells from free radicles.	Waghmare *et al.*, 2019
Potassium and resistant starch	Proper blood pressure levels are maintained by improving blood sugar control.	Waghmare *et al.*, 2019
Resistant starch	Promotes gut health and regulates blood sugar levels.	Waghmare *et al.*, 2019
Amylose (starch) and protein	Different bakery products such as cookies, bread, biscuits, cake, muffins, etc., confectionery items and bioplastics can be prepared from jackfruit seed flour (Ground and roasted jackfruit seeds + wheat flour).	Hossain *et al.*, 2014
Protein	Being a cheap non-conventional source of protein, it combat malnutrition by serving as a cost-effective substitute protein source.	Chowdhury *et al.*, 2012
Low in nutrients, high in addedsugar and calories	Ice-creams are produced.	Shinde *et al.*, 2021
All forms of calories	Traditional curry and vegetable dishes are prepared in local communities.	Waghmare *et al.*, 2019
Soluble and insoluble fiber	Soluble fiber aid in weight loss, promote bowel movement, lowers risk of heart disease and insoluble fiber prevents indigestion and constipation.	Waghmare *et al.*, 2019
Vitamin B-complex	Essentially important for a healthy nervous system.	Waghmare *et al.*, 2019
Antimicrobial properties	Protect against foodborne illnesses.	Waghmare *et al.*, 2019
Phytonutrients (isoflavones, lignans and saponins)	Fight against stomach ulcers, promote death in cancer cell lines by preventing cell development, possess antiulcer, anticancer, antiaging and antihypertensive properties.	Waghmare *et al.*, 2019
Copper	Promote thyroid metabolism.	Waghmare *et al.*, 2019
Riboflavin and thiamine	Promote hair growth, maintain healthy hair, eyes and skin.	Waghmare *et al.*, 2019
Lectins (Artocarpin and Jacalin)	Supports the immune system.	Neelanjana *et al.*, 2023
Other properties	Bulk density, foaming capacity, least gelation, binding agent, reducing potential, thickening agent, emulsification, foaming capacity and stability.	Waghmare *et al.*, 2019

Indian Journal of Natural Sciences www.tnsroindia.org.in ©IJONS

Vol.15 / Issue 88 / Feb / 2025 *International Bimonthly (Print) – Open Access* *ISSN: 0976 – 0997*

RESEARCH ARTICLE

Leaf Disease Detection in Agriculture

K. S. S. Naga Teja [1]*, K. Anitha Reddy[2] and D. Narasimha Rao[2]

[1]Assistant Professor, Department of Computer Science and Engineering, St. Martin's Engineering College (Autonomous), Secunderabad, (Affiliated to Jawaharlal Nehru Technological University, Hyderabad), Telangana, India.

[2]Assistant Professor, Department of Electrical and Electronics Engineering, Malla Reddy Engineering College (Autonomous), (Affiliated to Jawaharlal Nehru Technological University), Hyderabad, Telangana, India.

Received: 26 Oct 2024 Revised: 10 Jan 2025 Accepted: 02 Feb 2025

***Address for Correspondence**
K. S. S. Naga Teja ,
Assistant Professor,
Department of Computer Science and Engineering,
St. Martin's Engineering College (Autonomous), Secunderabad,
(Affiliated to Jawaharlal Nehru Technological University, Hyderabad),
Telangana, India.
E.Mail: kssnteja@gmail.com

ABSTRACT

Programmed monitoring of various parameters in conjunction with leaf disease detection is a crucial research area in agriculture since it has the potential to show benefits in managing a significant yield zone. As a result, this system automatically detects disease symptoms when they appear on plant leaves. Usually, the phrase "leaf infection" refers only to the destruction of living and sound takes off. This work discusses the assessment of several plant environmental parameters, examines the discovery of leaf illness using photo processing, and transmits all of the data via speaker and LCD display. MATLAB, an LCD display, and an Arduino microcontroller are used to show the many leaf diseases that have been detected.

Keywords: Arudino, Microcontroller, Leaf Disease Detection, Image Processing ,Disease Identification, Computer Vision.

INTRODUCTION

The agricultural sector is fundamental to the global economy, providing the food and raw materials necessary for survival and industrial activities. However, crop diseases pose a significant threat to agricultural productivity, leading to substantial economic losses and food insecurity. Timely and accurate detection of leaf diseases is critical for effective disease management and mitigation of crop damage. Traditional methods of disease detection, primarily

relying on visual inspection by experts, are often time-consuming, labor-intensive, and prone to human error. Technological innovations provide encouraging answers to these problems. The combination of machine learning and image processing methods for automated leaf disease diagnosis is one such approach. An excellent platform for putting these strategies into practice is MATLAB, a potent tool for numerical computing and algorithm development. The goal of this project is to combine image processing and machine learning methods to create a MATLAB-based system for identifying leaf diseases. The suggested approach will examine leaf photos, recognize symptoms of illness, and categorize the kind of disease that is harming the plant. The system can provide a comprehensive automated illness detection solution by integrating multiple components, including picture acquisition, preprocessing, feature extraction, and classification. Farmers and other agricultural professionals will find this integrated method to be a useful tool since it not only improves the speed and accuracy of disease identification but also lessens reliance on human expertise. By utilizing MATLAB for this project, we leverage its robust image processing toolbox and machine learning capabilities, facilitating the development of an efficient and effective leaf disease detection system. The integration of these advanced techniques into a unified system holds significant potential for enhancing disease management practices in agriculture, ultimately contributing to increased crop yields and sustainability.

METHODS

He MATLAB-based leaf disease detection system comprises several critical steps, including image acquisition, preprocessing, feature extraction, and classification. Each step involves specific techniques and algorithms designed to work together seamlessly in an integrated system.

Image Acquisition

The first step involves capturing high-quality images of leaves using digital cameras or smartphones. The images should be taken in controlled lighting conditions to ensure consistency and reduce noise. These images serve as the input for the subsequent processing stages.

Image Preprocessing

Preprocessing is crucial for enhancing image quality and isolating the region of interest (the leaf). The following techniques are employed:

- **Noise Reduction:** Median filtering or Gaussian filtering is applied to remove noise from the images.
- **Contrast Enhancement:** Techniques such as histogram equalization improve the contrast of the images, making disease symptoms more visible.
- **Image Segmentation:** Thresholding, edge detection, or clustering algorithms like k-means are used to segment the leaf from the background.

Feature Extraction

Once the leaf is isolated, various features indicative of disease symptoms are extracted. These features include:

- **Color Features:** Mean, standard deviation, and skewness of color channels (RGB, HSV, etc.) are computed to capture color variations caused by diseases.
- **Texture Features:** Gray-Level Co-occurrence Matrix (GLCM), Local Binary Patterns (LBP), and other texture descriptors are used to quantify the texture of the leaf surface.
- **Shape Features:** Geometric features such as area, perimeter, eccentricity, and shape descriptors like Fourier descriptors are extracted to analyze changes in leaf shape.

Classification

The extracted features are used to train machine learning models for disease classification. Various classifiers can be employed, including:

- **Support Vector Machine (SVM):** SVM is effective in handling high-dimensional data and is commonly used for classification tasks.
- **Artificial Neural Networks (ANN):** ANN can capture complex relationships between features and is trained using backpropagation algorithms.
- **Convolutional Neural Networks (CNN):** For end-to-end learning, CNNs automatically learn relevant features from raw images, making them highly effective for image classification tasks.

System Integration

The individual components of the system are integrated into a cohesive workflow within MATLAB. The integration involves:

- **User Interface:** A graphical user interface (GUI) is developed to allow users to upload leaf images, view preprocessing results, and obtain disease classification results.
- **Automation:** Scripts and functions are automated to ensure smooth execution of the entire pipeline from image acquisition to classification.
- **Performance Evaluation:** The system is evaluated using metrics such as accuracy, precision, recall, and F1-score on a dataset of labeled leaf images. Cross-validation techniques are employed to ensure robustness and generalization of the models.

Validation and Testing

The final system is validated and tested on real-world datasets to ensure its effectiveness in practical scenarios. Field testing with diverse leaf samples from different plant species and varying disease conditions helps in fine-tuning the system and improving its accuracy.

By following these methods, the MATLAB-based leaf disease detection system aims to provide a reliable and automated solution for identifying and classifying leaf diseases, thereby aiding in effective disease management and enhancing agricultural productivity.

RESULTS AND DISCUSSION

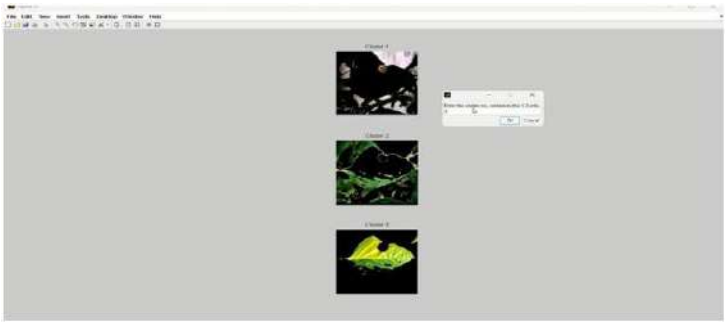

DISEASE

CHLOROFILL

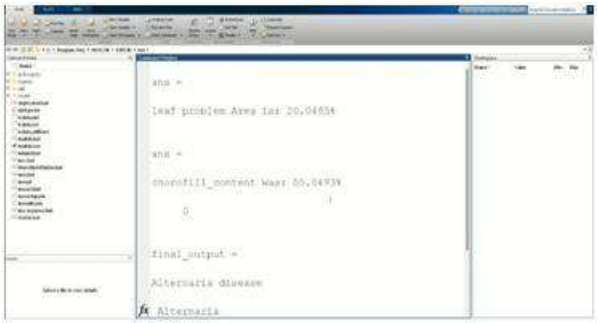

Using MATLAB to interface with an embedded system for leaf disease detection allows for the estimate of various plant environmental parameters, investigates the identification of leaf sickness through picture processing, and transmits all of the data to an LCD display and speaker. The many leaf diseases found can be shown on an LCD monitor, MATLAB, and an Arduino microcontroller.

CONCLUSION

In order to protect plants from various illnesses throughout the year, the agricultural department has taken the initiative. In the age of computers, automation has the potential to replace manual plant disease observation through the application of image processing techniques. For several decades, numerous scientists have conducted extensive research on plant leaves to identify and identify various diseases. They have also used the APR9600 speaker to declare the disease and send a message including the disease name to a mobile number. The literature review lists a number of diseases and procedures that can be detected by this automation, which helps to prevent plant damage. This effectively concludes the significance of carrying out further research to advance the field.

REFERENCES

1. "Indian agriculture economy.". Available: http:// statistics times.com/economy/sectorwise-gdp-Contribution-of india. Php
2. https://www. pioneer.com/home/site/us/agronomy/library/common-rustin-corn/
3. Indian Council of Agricultural Research", Available: https://www.apsnet.org/publications/imageresource/ Pages/Fi00158.aspx
4. "family of trees", https:// plantvillage .psu. edu/ topics/ co conut/infos
5. "Agropedia", Available:http://agropedia.iitk.ac.in / content /papaya-diseases-its-control
6. Prof.Sonal, P.Patil, Rupali, Zambre,"Classification of Cotton Leaf Spot Disease Using SVM," International Journal of Engineering Research & Applications", Vol.4,pp.92-97, May 2020

7. https://worldofchillies.com/growing_chillies/chilli_pest problems diseases/chilli diseases/chillidiseases.html
8. Pragya Adhikari, Yeonyee Oh, Dilip R. Panthee" Current Status of Early Blight Resistance in Tomato: An Update," International Journal of Molecular Science", September 2019
9. Akansha Pandey, Sanjeev Dubey," Evaluations of brinjal germplasm for resistance to fusarium wilt disease," nternational Journal of Scientific and Research Publications, Volume 7, Issue 7, July 2019
10. Gittaly Dhingra, Vinay Kumar, Hem Dutt Joshi ,"Study of digital image processing techniques for leaf disease detection and classification," Springer-Science, 29 November 2020
11. Shitala Prasad, Sateesh K. Peddoju, Debashis Ghosh ," Multi-resolution mobile vision system for plant leaf disease diagnosis," pp. 379–388, Springer-Verlag London 2019
12. Shanwen Zhang, Zhuhong You, Xiaowei Wu," Plant disease leaf image segmentation based on superpixel clustering and EM algorithm," Springer, June 2021.
13. Keyvan Asefpour Vakilian & Jafar Massah," An artificial neural network approach to identify fungal diseases of cucumber (Cucumis sativus L.) Plants using digital image processing," Vol. 46, No. 13,1580–1588, Taylor &Francis, 2021
14. Mohammed Brahimi, Kamel Boukhalfa & Abdelouahab Moussaoui," Deep Learning for Tomato Diseases: Classification and Symptoms Visualization," vol.31, no.4, 299–315, Taylor & Francis, 2021
15. H.Al-Hiary, S. Bani-Ahmad, M.Reyalat, M.Braik & Z.AlRahamneh, "Fast and Accurate Detection and Classification of Plant Diseases", International Journal of Computer Applications, Vol.17,No.1, pp.31-38.March 2021.
16. Yuanyuan Shao, Guantao Xuan, Yangyan Zhu, Yanling Zhang, Hongxing Peng, Zhongzheng Liu & Jialin Hou," Research on automatic identification system of tobacco diseases", vol. 65, no. 4, 252–259, Taylor & Francis, 2019
17. Vijai Singh, A.K. Misra," Detection of plant leaf diseases using image segmentation and soft computing Techniques,"Information Processing In Agriculture 4 (2017) 41– 49 , science direct, 2019
18. Shanwen Zhang , Xiaowei Wuc, Zhuhong You, Liqing Zhang," Leaf image based cucumber disease recognition using sparse representation classification," Computers and Electronics in Agriculture 135–141, science direct, 2019
19. Amar Kumar Dey, Manisha Sharma, M.R.Meshram," Image Processing Based Leaf Rot Disease, Detection of Betel Vine (Piper BetleL.)," Procedia Computer Science 748 – 754, science direct, 2019
20. Srdjan Sladojevic, Marko Arsenovic, Andras Anderla, Dubravko Culibrk and Darko Stefanovic," Deep Neural Networks Based Recognition of Plant Diseases by Leaf Image Classification," Hindawi Publishing Corporation Computational Intelligence and Neuroscience,Vol 2019, Article ID 3289801, 11 pages

Indian Journal of Natural Sciences www.tnsroindia.org.in ©IJONS

Vol.15 / Issue 88 / Feb / 2025 *International Bimonthly (Print) – Open Access* *ISSN: 0976 – 0997*

RESEARCH ARTICLE

Micro Bitopological Space with Types of Micro Open Sets

S. Vaira Lakshmi[1]* and S. Firthous Fatima[2]

[1]Research Scholar (Reg.No.20211202092008), Department of Mathematics, Sadakathullah Appa College (Autonomous), (Affiliated to Manonmaniam Sundaranar University), Tirunelveli, Tamil Nadu, India.
[2]Head and Assistant Professor, Department of Mathematics, Sadakathullah Appa College (Autonomous), (Affiliated to Manonmaniam Sundaranar University), Tirunelveli, Tamil Nadu, India.

Received: 21 Jun 2024 Revised: 03 Jul 2024 Accepted: 13 Aug 2024

***Address for Correspondence**
S. Vaira Lakshmi
Research Scholar (Reg.No.20211202092008),
Department of Mathematics,
Sadakathullah Appa College (Autonomous),
(Affiliated to Manonmaniam Sundaranar University),
Tirunelveli, Tamil Nadu, India.
E.Mail: adulya798@gmail.com

ABSTRACT

In this paper, we introduced the definition for micro bitopological space and properties with some examples. We also discuss its interior and closure.We talked about the many kinds of pair wise micro open sets, micro (1,2)open sets, and micro (2,1)open sets.

Keywords: Bitopological space, Nano topology, Micro topology.
MSC: 54A10, 54E55

INTRODUCTION

"Toloplogy" is a relatively new field of mathematics, with the majority of its research conducted since 1900. Properties of spaces that remains unchanged during continuous deformations are studied in topology. Because the objects may be stretched and contracted like rubber yet cannot be broken, it is frequently referred to as "rubber-sheet geometry". Bitopology origin is usually associated with the appearance of J. C. Kelly's [3] paper in 1963. In this fundamental paper, a bitopological space was clearly defined as a set with two arbitrary topological structure. Nano topology introduced by Thivagar [6] in the year 2013. Micro topology was introduced by Sakkraiveeranan Chandrasekar [7] (2019), and some of their properties are investigated. We introduced micro bitopological space with some features and an example in the current study. By using examples, we were able to teach several types of micro (1,2) open sets and compare them. Additionally, we provided instances of several types of micro (2,1) open sets. The notion of type pairwise open sets was covered.

Preliminary

Definition 2.1 [1, 2]

If Y is non-empty set, a collection $\tau \subseteq P(Y)$ is called topology on Y if the following holds:
(1)$Y, \phi \in \tau$.
(2) The intersection of a finite number of elements inτ, is in τ.
(3) The union of a finite or infinite number of elements of sets in τ belong to τ.
Then (Y, τ) is called a topological space. Any element (Y, τ) is called open set and it is complement is called closed set.

Definition 2.2 [3]

Let X be a set. Let P and Q be topologies for X. Then the ordered triple (X, P, Q) is said to be a bitopological space.

Definition 2.3 [4]

A subset of $(X, \tau_1, \tau_2)$is said to be
(i). (1,2) semi open set if $S \subseteq \tau_1\tau_2 cl(\tau_1 int(S))$
(ii). (1,2) pre open set if $S \subseteq \tau_1 int(\tau_1\tau_2 cl(S))$

Definition 2.4 [5]

A subset A of (X, τ_1, τ_2) is said to be pairwise semi open set in X if A is (1,2) semi open set and (2,1) semi open set.

Definition 2.5 [6]

Let U be a non empty finites set of objects called the universe and R be an equivalence relations on U named as indiscernibility relation. Elements belonging to the same equivalence class are said to be indiscernible with one other. The pair (U, R) is said to be approximation space. Let$X \subseteq U$.
1. The lower approximation of X with respect to R is the set of all objects, which can be certain classified as X with respect to R and is defined by
$L_R[x] = \cup \{R(x): R(x) \subseteq X\}$ where $R(x)$ denotes the equivalence class determined by X.
2. The upper approximation of X with respect to R is the set of all objects, which can be possibly classified as X with respect to R and is defined by
$U_R[x] = U_{x \in U} \{R(x): R(x) \cap X \neq \phi\}$
3. The boundary region of X with respect to R is the set of all objects, which can be classified as X neither as X nor as not- X with respect to R and is defined by $B_R[x] = U_R(x) - L_R(x)$.

Definition 2.6 [6]

Let U be an universe, R be an equivalence relation on U and $\tau_R(X) = \{U, \phi, L_R(x), U_R(x), B_R(x)\}$ where $X \subseteq U$, then $\tau_R(X)$ satisfies the following axioms.
1. $U, \phi \in \tau_R(X)$.
2. The union of the elements of any sub-collection of $\tau_R(X)$ is in $\tau_R(X)$
3. The intersection of the elements of any finite sub collection of $\tau_R(X)$ is in $\tau_R(X)$.
Then $\tau_R(X)$ is called the nano topology on U with respect to X. The space $(U, \tau_R(X))$ is the nano topological space. The elements of $\tau_R(X)$ are called nano open sets.

Definition 2.7 [7]

The micro topology $\mu_R(X)$ satisfies the following axioms
1. $U, \phi \in \mu_R(X)$.
2. The union of the elements of any sub-collection of $\mu_R(X)$ is in $\mu_R(X)$.
3. The intersection of the elements of any finite sub collection of $\mu_R(X)$ is in $\mu_R(X)$.
Then $\mu_R(X)$ is called the Micro topology on U with respect to X. The triplet $(U, \tau_R(X), \mu_R(X))$ is called micro topological space and the elements of $\mu_R(X)$ are called micro open sets and the complement of a micro open set is called a micro closed set.

Definition 2.8 [7]

The micro closure of a set A is denoted by $Micro-cl(A)$ and is defined as $mic-cl(A) = \cap\,(B; B\ is\ micro\ closed\ and\ A \subseteq B)$. The micro interior of a set A is denoted by $Micro-int(A)$ and is defined as $mic-int(A) = \cup\,(B; B\ is\ micro\ open\ and\ B \subseteq A)$.

Micro Bitopological Space

The micro bitopological space was presented in this section with examples.

Definition 3.1

Let U be a non empty set and it contain two equivalence relation R_1, R_2. Let X_1, X_2 be any two subsets of U. Let $(U, \tau_{R_1}(X_1))$ is a nano topological space then $\mu_{R_1}(X_1) = \{S \cup (S' \cap \mu_1) / S, S' \in \tau_{R_1}(X_1)\}$ where $\mu_1 \notin \tau_{R_1}(X_1)$ is called a micro topology of $\tau_{R_1}(X_1)$ and let $(U, \tau_{R_2}(X_2))$ is an another nano topological space then $\mu_{R_2}(X_2) = \{T \cup (T' \cap \mu_2) / T, T' \in \tau_{R_2}(X_2)\}$ where $\mu_2 \notin \tau_{R_2}(X_2)$ is called a micro topology of $\tau_{R_2}(X_2)$. If $(U, \tau_{R_1}(X_1), \tau_{R_2}(X_2), \mu_{R_1}(X_1), \mu_{R_2}(X_2))$ briefly, $(U, \tau_{R_{1,2}}(X), \mu_{R_{1,2}}(X))$ is called a micro bitopological space then it is satisfy the following conditions:. $U, \phi \in \mu_{R_{1,2}}(X)$.

2. Arbitrary union of $\mu_{R_{1,2}}(X)$ is in $\mu_{R_{1,2}}(X)$.

3. Finite intersection of $\mu_{R_{1,2}}(X)$ is in $\mu_{R_{1,2}}(X)$.

Therefore $(U, \tau_{R_{1,2}}(X), \mu_{R_{1,2}}(X))$ is called a micro bitopological space and the element of micro bitopological space is called $M\mu_{R_{1,2}}(X)-$ open. The complement is called $M\mu_{R_{1,2}}(X)-$ closed set.

Example 3.2

Let $U = \{a, b, c, d\}$ with $U/R_1 = \{\{a, c\}, \{b\}, \{d\}\}$ and $X_1 = \{a, b\}$, $\tau_{R_1}(X_1) = \{U, \phi, \{b\}, \{a, b, c\}\}$.Then $\mu_1 = \{a\} \notin \tau_{R_1}(X_1)$. The $M\mu_{R_1}(X_1) = \{U, \phi, \{a\}, \{b\}, \{a, b\}, \{a, b, c\}\}$ and $U/R_2 = \{\{a\}, \{d\}, \{b, c\}\}$ and $X_2 = \{a\} \Longrightarrow \tau_{R_2}(X_2) = \{U, \phi, \{a\}\}$. Then $\mu_2 = \{b\} \notin \tau_{R_2}(X_2)$. Then the $M\mu_{R_2}(X_2) = \{U, \phi, \{a\}, \{b\}, \{a, b\}\}$. Then the $M\mu_{R_{1,2}}(X) = \{U, \phi, \{a\}, \{b\}, \{a, b\}, \{a, b, c\}\}$ is a micro bitopological space.

Note 3.3

$M\mu_{R_{1,2}}(X)$ open set need not necessarily form a micro bitopological space.

Example 3.4

Let $U = \{0,1,2,3,4,5\}$ with $U/R_1 = \{\{0,3,4\}, \{1,2\}, \{5\}\}$ and $X_1 = \{0,3,4\} \subseteq U \Longrightarrow \tau_{R_1}(X_1) = \{U, \phi, \{0,3,4\}\}$.

Then $\mu_1 = \{1\}$. The $M\mu_{R_1}(X_1) = \{U, \phi, \{1\}, \{0,3,4\}, \{0,1,3,4\}\}$ and the next equivalence relation $U/R_2 = \{\{0\}, \{1,2\}, \{3\}, \{4\}, \{5\}\}$ and $X_2 = \{1,2\} \Longrightarrow \tau_{R_2}(X_2) = \{U, \phi, \{1,2\}\}$. Then $\mu_2 = \{2\}$.

The $M\mu_{R_2}(X_2) = \{U, \phi, \{2\}, \{1,2\}\}$. Then we get, $M\mu_{R_{1,2}}(X) = \{U, \phi, \{1\}, \{2\}, \{1,2\}, \{0,3,4\}, \{0,1,3,4\}\}$ is open but not form a micro bitopological space. Because $\{1,2\} \cup \{0,3,4\} = \{0,1,2,3,4\}$ does not belongs to $M\mu_{R_{1,2}}(X)$.

Theorem 3.5

Intersection of a two micro bitopological space is micro bitopological space.

Proof

Let U be a universel set. Since $M_1\mu_R, M_2\mu_R$ be two micro bitopological space on U. Then $\phi, U \in M_1\mu_R$ and $\phi, U \in M_2\mu_R \Rightarrow \phi, U \in M_1\mu_R \cap M_2\mu_R$. Let $G, H \in M_1\mu_R \cap M_2\mu_R \Rightarrow G, H \in M_1\mu_R$ and $G, H \in M_2\mu_R \Rightarrow G \cap H \in M_1\mu_R$ and $G \cap H \in M_2\mu_R \Rightarrow G \cap H \in M_1\mu_R \cap M_2\mu_R$. Finite intersection is there. We need to prove arbitrary union. Let $G_1, G_2, \ldots G_n \in M_1\mu_R \cap M_2\mu_R \Rightarrow G_1, G_2, \ldots G_n \in M_1\mu_R$ and $G_1, G_2, \ldots G_n \in M_2\mu_R \Rightarrow \cup_{i=1}^{n} G_i \in M_1\mu_R$ and $\cup_{i=1}^{n} G_i \in M_2\mu_R \Rightarrow \cup_{i=1}^{n} G_i \in M_1\mu_R \cap M_2\mu_R$. It's proved. Intersection of two micro bitopological space is micro bitopology.

Note 3.6

Union of two micro bitopological space is need not to be a micro bitopology.

Example 3.7

From example (3.2), Let $U = \{a, b, c, d\}$ with two equivalence relations $U/R_1 = \{\{a, c\}, \{b\}, \{d\}\}$ and $U/R_2 = \{\{a\}, \{d\}, \{b, c\}\}$. Then we get two micro bitopological spaces, $M_1\mu_{R_{1,2}}(X) = \{U, \phi, \{a\}, \{c\}, \{a, c\}\}$ and $M_2\mu_{R_{1,2}}(X) = \{U, \phi, \{a\}, \{b\}, \{d\}, \{a, b\}, \{a, d\}, \{b, d\}, \{b, c\}, \{a, b, c\}, \{a, b, d\}, \{b, c, d\}\}$.

The union of two micro bitopological space is

$(M_1\mu_R \cup M_2\mu_R)(X) = \{U, \phi, \{a\}, \{b\}, \{c\}, \{d\}, \{a, b\}, \{a, d\}, \{b, c\}, \{b, d\}, \{a, c\}, \{a, b, c\}, \{a, b, d\}, \{b, c, d\}\}$.

But $\{c\} \cup \{d\} = \{c, d\} \notin M_1\mu_R \cup M_2\mu_R$. The arbitrary union is not there. The union of two micro bitopological space need not be a micro bitopology.

Definition 3.8

Let H be a subset of a micro bitopological space. Then the micro closure of H is denoted by $M\mu_{R_{1,2}}cl(H) = \bigcap \{V: H \subseteq V\}$ and V is $M\mu_{R_{1,2}}(X)$ - closed. Then the micro interior of H is denoted by $M\mu_{R_{1,2}}int(H) = \cup\{V: V \subseteq H\}$ and V is $M\mu_{R_{1,2}}(X)$- open.

Remark 3.9

Take A be any subset of a micro bitopological space$(U, \tau_{R_{1,2}}(X), \mu_{R_{1,2}}(X))$. Then $M\mu_{R_{1,2}}int(A) \subseteq A \subseteq M\mu_{R_{1,2}}cl(A)$.

Properties 3.10

Take any two micro set I and J in$(U, \tau_{R_{1,2}}(X), \mu_{R_{1,2}}(X))$.

1. I is $M\mu_{R_{1,2}}$open if and only if $I = M\mu_{R_{1,2}}int(I)$.
2. J is $M\mu_{R_{1,2}}$ closed if and only if $J = M\mu_{R_{1,2}}cl(J)$.
3. $M\mu_{R_{1,2}}cl(M\mu_{R_{1,2}}cl(I)) = M\mu_{R_{1,2}}cl(I)$ and $M\mu_{R_{1,2}}int(M\mu_{R_{1,2}}int(J)) = M\mu_{R_{1,2}}int(J)$.

This all true for $M\mu_{R_1}$ open set ($M\mu_{R_1}$ closed set) and $M\mu_{R_2}$ open set ($M\mu_{R_2}$ closed set).

Types of micro $(1, 2)$ open sets

This part included the introduction and discussion of several micro (1,2) open set types.

Definition 4.1

A subset H of $(U, \tau_{R_{1,2}}(X), \mu_{R_{1,2}}(X))$ is called

1. Micro $(1,2) -$ semi open set if $H \subseteq M\mu_{R_{1,2}}cl\left(M\mu_{R_1}int(H)\right)$.
2. Micro $(1,2) -$ pre open set if $H \subseteq M\mu_{R_1}int(M\mu_{R_{1,2}}cl(H))$.
3. Micro $(1,2) - \alpha$ open set if $H \subseteq M\mu_{R_1}int(M\mu_{R_{1,2}}cl(M\mu_{R_1}int(H)))$.
4. Micro $(1,2) -$ regular open set if $H = M\mu_{R_1}int(M\mu_{R_{1,2}}cl(H))$.

Example 4.2

Let $U = \{a, b, c, d, e\}$ with $U/R_1 = \{\{b, d\}, \{c, e\}, \{a\}\}$ and $X_1 = \{b, d\} \Rightarrow \tau_{R_1}(X_1) = \{U, \phi, \{b, d\}\}$. Then $\mu_1 = \{a\}$. Then $M\mu_{R_1}(X_1) = \{U, \phi, \{a\}, \{b, d\}, \{a, b, d\}\}$ and $U/R_2 = \{\{a\}, \{b, c\}, \{e, d\}\}$ and $X_2 = \{a\} \Rightarrow \tau_{R_2}(X_2) = \{U, \phi, \{a\}\}$. Then $\mu_2 = \{b\}$. Then $M\mu_{R_2}(X_2) = \{U, \phi, \{a\}, \{b\}, \{a, b\}\}$. The $M\mu_{R_{1,2}}(X) = \{U, \phi, \{a\}, \{b\}, \{a, b\}, \{b, d\}, \{a, b, d\}\}$ is a micro bitopological space. Therefore

1. $A = \{b, d\}$ is a micro $(1,2) -$ semi open set.
2. $B = \{a, b\}$ is a micro $(1,2) -$ pre open set.
3. $C = \{a, b, d\}$ is a micro $(1,2) - \alpha$ open set.
4. $D = \{a\}$ is a micro (1,2) regular open set.

Theorem 4.3

Every $M\mu_{R_1}$ open set is micro (1,2) semi open set.

Proof

Let H be any $M\mu_{R_1}$ open set. Then $H = M\mu_{R_1}int(H)$. Now $H \subseteq M\mu_{R_{1,2}}cl(H) = M\mu_{R_{1,2}}cl(M\mu_{R_1}int(H))$.

H is micro (1,2)semi open set. But the converse is need not be true.

Example 4.4

From example (4.2), {b, c, d} is micro (1,2)semi open set but not a $M\mu_{R_1}$ open set.

Theorem 4.5

Every micro (1,2) semi open set is $M\mu_{R_1}$ semi open.

Proof

Let H be any micro (1,2)semi open set, then $H \subseteq M\mu_{R_{1,2}}cl(M\mu_{R_1}int(H)) \subseteq M\mu_{R_1}cl(M\mu_{R_1}int(H))$. Since $M\mu_{R_{1,2}}cl \subseteq M\mu_{R_1}cl$. Therefore H is $M\mu_{R_1}$ semi open. But the converse is need not be true.

Example 4.6

Let $U = \{a, b, c, d\}$ with $U/R_1 = \{\{a, c\}, \{b\}, \{d\}\}$ and $X_1 = \{b, d\}, \tau_{R_1}(X_1) = \{U, \phi, \{b\}, \{d\}, \{b, d\}\}$ Then $\mu_1 = \{a\} \notin \tau_{R_1}$. The $M\mu_{R_1}(X_1) = \{U, \phi, \{a\}, \{b\}, \{d\}, \{a, b\}, \{a, d\}, \{b, d\}, \{a, b, d\}\}$ and $U/R_2 = \{\{a\}, \{d\}, \{b, c\}\}$ and $X_2 = \{b, c, d\} \Rightarrow \tau_{R_2}(X_2) = \{U, \phi, \{b, c\}, \{d\}, \{b, c, d\}\}$. Then $\mu_2 = \{a\} \notin \tau_{R_2}(X_2)$. Then the $M\mu_{R_2}(X_2) = \{U, \phi, \{a\}, \{b, c\}, \{d\}, \{a, d\}, \{a, b, c\}, \{b, c, d\}\}$. Then the $M\mu_{R_{1,2}}(X) = \{U, \phi, \{a\}, \{b\}, \{d\}, \{a, b\}, \{a, d\}, \{b, d\}, \{b, c\}, \{a, b, d\}, \{b, c, d\}, \{a, b, c\}\}$ is a micro bitopological space. In this space $\{a, c, d\}$ is $M\mu_{R_1}$ semi open but not micro (1,2) semi open.

Note 4.7

From above theorem(4.3), (4.5), every $M\mu_{R_1}$ open set is $M\mu_{R_1}$ semi open set.

Theorem 4.8

Every $M\mu_{R_1}$ open set is micro (1,2) pre open set.

Proof

Let E be any $M\mu_{R_1}$ open set. Now $E \subseteq M\mu_{R_{1,2}}cl(E)$. Take interior on both sides, $M\mu_{R_1}int(E) \subseteq M\mu_{R_1}int(M\mu_{R_{1,2}}cl(E))$. Then $E = M\mu_{R_1}int(E)$. Then we get,$E \subseteq M\mu_{R_1}int(M\mu_{R_{1,2}}cl(E))$. E is micro (1,2) pre open set. But the converse is need not be true.

Example 4.9

From example (4.2), {a, b} is micro (1,2) pre open but not $M\mu_{R_1}$ open set.

Theorem 4.10

Every micro (1,2) pre open set is $M\mu_{R_1}$ pre open.

Proof

Let E be a micro (1,2) pre open set. Then $E \subseteq M\mu_{R_1}int\left(M\mu_{R_{1,2}}cl(E)\right)$. Since $M\mu_{R_{1,2}}cl(E) \subseteq M\mu_{R_1}cl(E)$

$\Rightarrow E \subseteq M\mu_{R_1}int(M\mu_{R_1}cl(E))$. Therefore, E is $M\mu_{R_1}$ pre open. But the converse is need not be true.

Example 4.11

From example (4.2), {d} is $M\mu_{R_1}$ pre open but not micro (1,2) pre open set.

Remark 4.12

Micro (1,2) semi open set and Micro (1,2) pre open set are independent notations.

Example 4.13
From example (4.2), {a, c} is micro (1,2) semi open set but not micro (1,2) pre open set.{a, b} is micro (1,2) pre open set but not micro (1,2) semi open set.

Theorem 4.14
Every micro $(1,2)-\alpha$ open set is micro (1,2) semi open set.

Proof
Let H be any micro $(1,2)-\alpha$ open set, then $H \subseteq M\mu_{R_1}\text{int}(M\mu_{R_{1,2}}\text{cl}(M\mu_{R_1}\text{int}(H)))$. Then by the remark (3.9), $H \subseteq M\mu_{R_{1,2}}\text{cl}(M\mu_{R_1}\text{int}(H))$. Therefore, H is micro (1,2) semi open set. But the converse need not be true.

Example 4.15
From example (3.2), {a, c, d}, is micro (1,2) semi open set but not micro $(1,2)-\alpha$ open.

Theorem 4.16
Every micro $(1,2)-\alpha$ open set is micro (1,2) pre open set.
Proof
Let H be any micro $(1,2)-\alpha$ open set, then $H \subseteq M\mu_{R_1}\text{int}(M\mu_{R_{1,2}}\text{cl}(M\mu_{R_1}\text{int}(H)))$. Then by the remark, (3.9), $H \subseteq M\mu_{R_1}\text{int}(M\mu_{R_{1,2}}\text{cl}(H))$. Therefore, H is micro (1,2) pre open set. But the converse need not be true.

Example 4.17
From example (4.2), {b} is micro (1,2) pre open set but not micro $(1,2)-\alpha$ open.

Note 4.18
Every micro (1,2) regular open set is micro (1,2) pre open. But the converse is need not be true.

Example 4.19
From example (4.2), {a, b} is micro (1,2) pre open set but not micro (1,2) regular open set.

Types of micro (2,1) open sets
This part included the introduction and discussion of several micro (2,1)open set types.

Definition 5.1
A subset A of $(M_{R_{1,2}}(X), \mu_{R_{1,2}}(X))$, is called
1. Micro $(2,1)-$ semi open set if $I \subseteq M\mu_{R_{1,2}}\text{cl}(M\mu_{R_2}\text{int}(I))$.
2. Micro $(2,1)-$ pre open set if $I \subseteq M\mu_{R_2}\text{int}(M\mu_{R_{1,2}}\text{cl}(I))$.
3. Micro $(2,1)-\ \alpha$ open set if $I \subseteq M\mu_{R_2}\text{int}\left(M\mu_{R_{1,2}}\text{cl}\left(M\mu_{R_2}\text{int}(I)\right)\right)$.
4. Micro $(2,1)-$ regular open set if $I = M\mu_{R_2}\text{int}(M\mu_{R_{1,2}}\text{cl}(I))$.

Example 5.2
From example (4.2),
1. $R = \{a, b\}$ is micro (2,1) semi open set.
2. $U = \{a\}$ is micro (2,1) pre open set.
3. $V = \{a, b, c\}$ is micro $(2,1)-\alpha$ open set.
4. $Z = \{b\}$ is micro (2,1)regular open set.

Theorem 5.3

Every $M\mu_{R_2}$ open set is micro (2,1) semi open set.

Proof

Le H be any $M\mu_{R_2}$ open set. Then $H = M\mu_{R_2}\text{int}(H)$. Now $H \subseteq M\mu_{R_{1,2}}\text{cl}(H) = M\mu_{R_{1,2}}\text{cl}(M\mu_{R_2}\text{int}(H))$. H is micro (2,1) semi open set. But the converse is need not be true.

Example 5.4

From example (3.2), $\{a, b, d\}$ is micro (2,1) semi open set but not $M\mu_{R_2}$ open set.

Remark 5.5

Let $(U, \tau_{R_{1,2}}(X), \mu_{R_{1,2}}(X))$be a micro bitopological space. Then the space, if every micro (2,1) semi open set are micro (2,1) pre open but the converse need not be true or every micro (2,1) pre open set are micro (2,1) semi open but the converse need not be true. The two situations mentioned above are not present in the micro bitopological space. Proved by the following examples.

Example 5.6

Let $U = \{a, b, c, d\}$ with $U/R_1 = \{\{a, c\}, \{b\}, \{d\}\}$ and $X_1 = \{a, c\}, \tau_{R_1}(X_1) = \{U, \phi, \{a, c\}\}$. Then $\mu_1 = \{a\} \notin \tau_{R_1}$. The $M\mu_{R_1}(X_1) = \{U, \phi, \{a\}, \{a, c\}\}$ and $U/R_2 = \{\{a\}, \{d\}, \{b, c\}\}$and $X_2 = \{a\} \Rightarrow \tau_{R_2}(X_2) = \{U, \phi, \{a\}\}$. Then $\mu_2 = \{c\} \notin \tau_{R_2}(X_2)$. Then the $M\mu_{R_2}(X_2) = \{U, \phi, \{a\}, \{c\}, \{a, c\}\}$. Then the $M\mu_{R_{1,2}}(X) = \{U, \phi, \{a\}, \{c\}, \{a, c\}\}$ is a micro bitopological space. In this space, every micro (2,1) pre open sets are micro (2,1) semi open. But the converse $\{a, b\}$ is micro (2,1) semi open but not micro (2,1) pre open.

Example 5.7

From example(4.6), in this space, every micro (2,1) semi open sets are micro (2,1) pre open. But the converse $\{b\}$ is micro (2,1) pre open but not micro (2,1) semi open.

Theorem 5.8

Every micro $(2,1) - \alpha$ open set is micro (2,1) semi open set.

Proof

Let H be any micro $(2,1) - \alpha$ open set, then $H \subseteq M\mu_{R_2}\text{int}(M\mu_{R_{1,2}}\text{cl}(M\mu_{R_2}\text{int}(H)))$. Then by the remark (3.9), $H \subseteq M\mu_{R_{1,2}}\text{cl}(M\mu_{R_2}\text{int}(H))$. Therefore, H is micro (2,1) semi open set. But the converse need not be true.

Example 5.9

From example (5.6), $\{a, b\}$ is micro (2,1) semi open set but not micro $(2,1) - \alpha$ open.

Theorem 5.10

Every micro $(2,1) - \alpha$ open set is micro (2,1) pre open set.

Proof

Let H be any micro $(2,1) - \alpha$ open set, then $H \subseteq M\mu_{R_2}\text{int}(M\mu_{R_{1,2}}\text{cl}(M\mu_{R_2}\text{int}(H)))$. Then by the remark (3.9), $H \subseteq M\mu_{R_2}\text{int}(M\mu_{R_{1,2}}\text{cl}(H))$. Therefore, H is micro (2,1) pre open set.But the converse need not be true.

Example 5.11

From example (4.6), $\{b\}$ is micro (2,1) pre open set but not micro $(2,1) - \alpha$ open.

Note 5.12

Every micro (2,1) regular open set is micro (2,1) pre open. But the converse need not be true.

Example 5.13
From example (3.2), {a, b, c} is micro (2,1) pre open set but not micro (2,1) regular open set.

Types of pairwise micro open sets
This part included the definition and example of several micro pairwise open set types.

Definition 6.1
A subset A of $(U, \tau_{R_{1,2}}(X), \mu_{R_{1,2}}(X))$ is said to be pairwise micro semi open set in U if A is micro $(1,2) -$ semi open and micro $(2,1) -$ semi open.

Definition 6.2
A subset A of $(U, \tau_{R_{1,2}}(X), \mu_{R_{1,2}}(X))$ is said to be pairwise micro pre open set in U if A is micro $(1,2) -$ pre open and micro $(2,1) -$ pre open.

Definition 6.3
A subset A of $(U, \tau_{R_{1,2}}(X), \mu_{R_{1,2}}(X))$ is said to be pairwise micro α open set in U if A is micro $(1,2) - \alpha$ open and micro $(2,1) - \alpha$ open.

Example 6.4
Let $U = \{s, t, u, v\}$ be a set with $U/R_1 = \{\{s, t\}, \{u\}, \{v\}\}$ and $X_1 = \{s, v\} \Rightarrow$
$\tau_{R_1} = \{U, \phi, \{v\}, \{s, t\}, \{s, t, v\}\}$. If $\mu_1 = \{t\}$ then $M\mu_{R_1} = \{U, \phi, \{v\}, \{t\}, \{v, t\}, \{s, t\}, \{s, t, v\}\}$ and $U/R_2 = \{\{s\}, \{t\}, \{u, v\}\}$ and $X_2 = \{u, v\} \Rightarrow \tau_{R_2} = \{U, \phi, \{u, v\}\}$. If $\mu_2 = \{t\}$ then $M\mu_{R_2} = \{U, \phi, \{t\}, \{u, v\}, \{t, u, v\}\}$. Then the $M\mu_{R_{1,2}}(X) = \{U, \phi, \{v\}, \{t\}, \{u, v\}, \{v, t\},$
$\{s, t\}, \{s, t, v\}, \{t, u, v\}\}$ is a micro bitopological sapce.
1. $A = \{s, t\}$ is pairwise micro semi open set.
2. $B = \{t\}$ is pairwise micro pre open set.
3. $C = \{u, t, v\}$ is pairwise micro α open set.

Note 6.5
From the above definitions, that every pairwise micro semi open set are micro (1,2) semi open and micro (2,1) semi open. Every pairwise micro pre open set are micro (1,2) pre open and micro (2,1) pre open and every pairwise micro α set are micro $(1,2) - \alpha$ open and micro $(2,1) - \alpha$ open. But the converses of the above three are need not be true.

Example 6.6
From example (6.4),
1. $\{s, t, v\}$ is micro (1,2) semi open set but not micro (2,1) semi open set. It's not pairwise micro semi open set.
2. $\{V\}$ is micro (1,2) pre open set but not micro (2,1) pre open set. It's not pairwise micro pre open set.
3. $\{s, t\}$ is micro $(1,2) - \alpha$ open set but not micro $(2,1) - \alpha$ open set. It's not pairwise micro α open set.

CONCLUSIONS

In this paper we introduced micro bitopological space with different types of micro open sets. We identify continuous functions in the future.

REFERENCES

1. C. Kuratowski, "Topologies", Warsaw, Poland, 1952.

2. S.A. Morris, "Topology without tears", 2017.
3. Kelly. J. C, "Bitopological Space", Proc. London Math. Soc. 13(3), (1963) 71-89.
4. M. L. Thivagar, "Generalization of Pairwise α -Continuous Function", Pure and Appl. Mathematics Sci. 28,(1991), 55-63.
5. M. L. Thivagar, B. Meera Devi and G.Navalagi, " (1, 2) extremally disconnectedness via bitopological open sets", International Journal of General Topology, 4(1-2),(2011),9-15.
6. M. L. Thivagar and C. Richard , "On Nano forms of weakly open Sets", International Journal of Mathematics and Statistics Invention, 2013, 31-37.
7. Sakkraiveeranan Chandrasekar, "On Micro Topological Spaces", Journal of New Theory, 2019, 23-31.

RESEARCH ARTICLE

A Study on Semi Closed and Semi Open Sets in Interval-Valued Topology

S. Dijitha[1]* and M. Navaneethakrishnan[2]

[1]Research Scholar (Reg. No: 22212102092009), PG and Research Department of Mathematics, Kamaraj College, Thoothukudi, (Affiliated to Manonmaniam Sundaranar University), Tirunelveli, Tamil Nadu, India.

[2]Associate Professor PG and Research Department of Mathematics, Kamaraj College, Thoothukudi, (Affiliated to Manonmaniam Sundaranar University), Tirunelveli, Tamil Nadu, India.

Received: 21 Dec 2024 Revised: 03 Nov 2024 Accepted: 13 Jan 2025

***Address for Correspondence**
S. Dijitha
Research Scholar (Reg. No: 22212102092009),
PG and Research Department of Mathematics,
Kamaraj College, Thoothukudi,
(Affiliated to Manonmaniam Sundaranar University),
Tirunelveli, Tamil Nadu, India.
E.Mail: s.dijithaselvendhiran28@gmail.com

ABSTRACT

The purpose of this work is to define and explore the characteristics of both the Interval-Valued Semi closed set [briefly. IVSCs] and Interval-Valued Semi Open set [briefly. IVSOs].Relationships between Interval-Valued semiclosure [briefly.IVscl] and Interval-Valued semiinterior [briefly.IVsint] operations are investigated. In addition, we discussed about the traits ofInterval-Valued semi-generalized set [briefly. IVsg-closed set] and Interval-Valued generalized semi closed set [briefly.IVgs closed set].

Keywords: IVSCs, IVSOs, IVsg-closed sets, IVsg-open sets, IVgs-open sets, IVgs-closed sets.
Mathematics Subject Classification(2020) : 54A05,54A99

INTRODUCTION

In 2009, Yao [1] established an interval set (henceforth referred to by us as an interval-valued set) that provided an algebraic structural discussion and an approximation tool for ideas that were difficult or undefinable to express. This idea is clearly the generalization of classical sets and the particular instance of Zadeh's interval-valued fuzzy sets [2]. Providing a point-set based context for the classical sets is one reason for their inception. We revisit several definitions Yao has worked on for an interval-valued set. The notion of interiors and closures with interval values and the derivation of some of their attributes as specified by Kim J, et al.[3]. The notion of generalized closed sets, which are a generalization of closed sets in topological spaces, was first presented by Levin [4] in 1970. Additionally,

we introduced semi open and semi closed in Interval-Valued Topology and we pushed to notions of Interval-Valued semi interior and Interval-Valued semi closuredenoted by IVsint and IVscl severally. We introduce the generalization for semi closed and semi open in the Interval-Valued topology as Interval-Valued semi-generalized closed set (resp. Interval-Valued semi-generalized open set) [briefly. IVsg-closed set] (resp. IVsg-open set) and Interval-Valued generalized semi set (resp. Interval-Valued generalized semi-open set) [briefly. IVgs-closed set] (resp. IVgs-open set).

PRELIMINARIES

This section contains a set of definitions and basic findings that will be used later.

Definition 2.1[3]A non empty set X. The form $[M^-, M^+]$= {N ⊂ X: M^- ⊂ N ⊂ M^+} is called an Interval-valued set (briefly, IVS) in X, if M^-, M^+ ⊂ X and M^- ⊂ M^+. In this case, M^-[resp. M^+] represent the set of minimum [resp. maximum] membership of elements of X to M. The set of all IVSs in X is denoted by IVS(X).

Definition 2.2[3]A non-empty set X and M,N are IVSs in the form M = $[M^-, M^+]$, N = $[N^-, N^+]$respectively. Then

1. $[M^-, M^+]$ ⊂ $[N^-, N^+]$, ⇔ M^- ⊂ N^- and M^+ ⊂ N^+.
2. $[M^-, M^+]$= $[N^-, N^+]$, ⇔ $[M^-, M^+]$ ⊂ $[N^-, N^+]$and $[N^-, N^+]$ ⊂ $[M^-, M^+]$.
3. $([M^-, M^+])^c$ = $[(M^+)^c, (M^-)^c]$.
4. $[M^-, M^+]$ ∪ $[N^-, N^+]$ = $[M^- \cup N^-, M^+ \cup N^+]$.
5. $[M^-, M^+]$ ∩ $[N^-, N^+]$= $[M^- \cap N^-, M^+ \cap N^+]$.

Definition 2.3[3]Let X be a non-empty set and let τ be a non-empty family of IVSs on X. Then τ is called an Interval-Valued Topology (briefly, IVT) on X, if it satisfies the following axioms:

1. $\widetilde{\emptyset}, \widetilde{X} \in \tau$.
2. M ∩ N ∈ τ for any M,N ∈ τ.
3. $\cup_{j\in J} M_j \in \tau$for any family $(M_j)_{j\in J}$ of members of τ.

In this case, the pair(X,τ) is called an Interval-Valued topological space (briefly, IVTS) and each member of τ is called an Interval-Valued open set (briefly, IVOs) in X. A IVS M is called an Interval-Valued closed set (briefly, IVCs) in X, if $M^c \in \tau$.

Definition 2.4[3]Let (X,τ) be an IVTS and let $[M^-, M^+]$ ∈IVS(X). Then

1. The Interval-Valued closure of $[M^-, M^+]$ w.r.t. τ, denoted by IVcl($[M^-, M^+]$), is an IVS in X defined as:
   IVcl($[M^-, M^+]$)= ∩ {K: $K^c \in \tau$ and M ⊂ K}.
2. The Interval-Valued interior of $[M^-,M^+]$ w.r.t. τ, denoted by IVint($[M^-,M^+]$), is an IVS in X defined as:
   IVint($[M^-, M^+]$)= ∪ {G: G ∈ τ G ⊂ M }.

Proposition 2.5[3]Let (X, τ) be an IVTS and let $[M^-, M^+]$ ∈ IVS(X).Then

1. IVint($[M^-, M^+]^c$) = (IVcl($[M^-, M^+]$))^c.
2. IVcl($[M^-, M^+]^c$) = (IVint($[M^-, M^+]$))^c.

Theorem 2.6[3]Let (X, τ) be an IVTS and let $[M^-,M^+]$ ∈ IVS(X).Then

1. $[M^-, M^+]$ ∈ IVC(X) ⇔ $[M^-, M^+]$ = IVcl($[M^-, M^+]$).
2. $[M^-, M^+]$ ∈ IVO(X) ⇔ $[M^-, M^+]$ = IVint($[M^-, M^+]$).

Definition 2.7[3]Kuratowsi Closure Axioms. Let M = $[M^-, M^+]$, N = $[N^-, N^+]$ ∈ IVS(X) and (X, τ) be IVTS. Then

1. If $[M^-, M^+]$ ⊂ $[N^-, N^+]$, then IVcl($[M^-, M^+]$) ⊂ IVcl($[N^-, N^+]$).
2. IVcl($\widetilde{\emptyset}$) = $\widetilde{\emptyset}$.
3. $[M^-, M^+]$ ⊂ IVcl($[M^-, M^+]$).
4. IVcl(IVcl($[M^-, M^+]$) = IVcl($[M^-, M^+]$).
5. IVcl($[M^-, M^+]$ ∪ $[N^-, N^+]$) = IVcl($[M^-, M^+]$) ∪IVcl($[N^-, N^+]$).

Definition 2.8[3]Let $M = [M^-, M^+]$, $N = [N^-, N^+] \in IVS(X)$ and (X, τ) be IVTS. Then

1. If $[M^-, M^+] \subset [[N^-, N^+]$, then $IVint([M^-, M^+]) \subset IVint([N^-, N^+])$.
2. $IVcl(\widetilde{X}) = \widetilde{X}$.
3. $IVint([M^-, M^+]) \subset [M^-, M^+]$.
4. $IVint(IVint([M^-, M^+])) = IVint([M^-, M^+])$.
5. $IVint([M^-, M^+] \cap [N^-, N^+]) = IVint([M^-, M^+]) \cap IVint([N^-, N^+])$.

Definition 2.9[5]A set $M = [M^-, M^+]$ from IVS(X) is an Interval Valued generalized closed (briefly, IVg-closed) iff $IVcl[M^-, M^+] \subseteq [U^-, U^+] = U$ whenever $M \subseteq U$ where U is IVOs.

Definition 2.10[5]A set $M = [M^-, M^+]$ from IVS(X) is said to be Interval Valued generalized open (briefly, IVg-open) whenever $\widetilde{X}$ - $[M^-, M^+]$ is IVg-closed.

Definition 2.11[5]Intersection of all IVg-closed sets containing $M = [M^-, M^+]$ is called an Interval-Valued generalized closure of $M = [M^-, M^+]$ is denoted by IVgcl(M).
Union of all IVg-open sets contained in $M = [M^-, M^+]$is called Interval-Valued generalized interior of $M = [M^-, M^+]$is denoted by IVgint(M).

IVSOs and IVSCs
The following definitions are introduced here.

Definition 3.1 Let (X, τ) be an IVTS(X). $M = [M^-, M^+] \in IVS(X)$ is said to be Interval-Valued semi-open [briefly, IVSO] if $[M^-, M^+] \subseteq IVcl(IVint([M^-, M^+]))$ and its complement is an Interval-Valued semi-closed [briefly, IVSC].

Theorem 3.2 Let (X,τ) be an IVTS. Then $[M^-, M^+]$is an IVSOs $\Leftrightarrow$ then there exists an IVOs $[N^-, N^+]$ such that $[N^-, N^+] \subseteq [M^-, M^+] \subseteq IVcl[N^-, N^+]$.

Proof: Suppose that $[M^-, M^+]$ is an IVSOs. Then,$[M^-, M^+] \subseteq IVcl(IVint[M^-, M^+]) \Rightarrow IVint[M^-, M^+] \subseteq [M^-, M^+] \subseteq IVcl(IVint[M^-, M^+])$. If $[N^-, N^+] = IVint[M^-, M^+]$, then $[N^-, N^+]$is an IVOs such that $[N^-, N^+] \subseteq [M^-, M^+] \subseteq IVcl[N^-, N^+]$.
Conversely, Suppose there exists an IVOs $[N^-, N^+]$such that $[N^-, N^+] \subseteq [M^-, M^+] \subseteq IVcl([N^-, N^+])$ which implies that $IVcl[N^-, N^+] = IVcl[M^-, M^+]$then, $[M^-, M^+] \subseteq IVcl[M^-, M^+] = IVcl[N^-, N^+] \subseteq IVcl(IVint[N^-, N^+]) \subseteq IVcl(IVint[M^-, M^+])$. Finally,$[M^-, M^+] \subseteq IVcl$
$(IVint[M^-, M^+])$.

Theorem 3.3 Let an IVTS be (X,τ) and $\{[M_j^-, M_j^+] / j \in J\}$ be a family of IVSOs. Then $\cup \{[M_j^-, M_j^+] / j \in J\}$ is an IVSOs.

Proof: Since $[M_j^-, M_j^+]$ is an IVSOs, For each j, there exists an IVOs $[N_j^-, N_j^+]$ such that $[N_j^-, N_j^+] \subset [M_j^-, M_j^+] \subset (IVcl[N_j^-, N_j^+])$then$\cup [N_j^-, N_j^+] \subset \cup [M_j^-, M_j^+] \subset \cup (IVcl[N_j^-, N_j^+])$. We know that, $[N_j^-, N_j^+] \subset \cup [N_j^-, N_j^+]$, $IVcl[N_j^-, N_j^+] \subset IVcl(\cup [N_j^-, N_j^+])$ then $\cup(IVcl[N_j^-, N_j^+]) \subseteq IVcl(\cup [N_j^-, N_j^+])$ which implies, $\cup [N_j^-, N_j^+] \subset \cup [M_j^-, M_j^+] \subset \cup (IVcl [N_j^-, N_j^+]) \subseteq IVcl (\cup [N_j^-, N_j^+])$. Then we can say that, $\cup [M_j^-, M_j^+]$ is an IVSOs.

Theorem 3.4 $IVint[M^-, M^+] \neq [\emptyset, \emptyset]$ when $[M^-, M^+]$is an IVSOs in an IVTS (X,τ).

Proof: Suppose that $M = [M^-, M^+]$is an IVSOs, then there exists an IVOs $[N^-, N^+] \subseteq [M^-, M^+] \subseteq IVcl[N^-, N^+]$ (by theorem 3.2). Since, $[N^-,N^+] \subseteq [M^-, M^+]$implies that $[N^-, N^+] = IVint[N^-, N^+] \subset IVint[M^-, M^+]$. We know that, $[N^-, N^+] \neq \widetilde{\emptyset}$, then $IVint[M^-, M^+] \neq [\emptyset, \emptyset]$.

Theorem 3.5 Let an IVTS be (X,τ). If $[M^-, M^+] \subset [N^-, N^+] \subset IVcl[M^-, M^+]$ where $[M^-, M^+]$is an IVSOs then $[N^-, N^+]$is an IVSOs. In a distinct way, if $[M^-, M^+]$is an IVSOs then, $IVcl[M^-, M^+]$is an IVSOs.

Proof: We have $[M^-, M^+]$is an IVSOs and $[M^-, M^+] \subseteq [N^-, N^+] \subset IVcl[M^-, M^+]$. Since $[M^-, M^+] \subseteq [N^-, N^+]$, $IVcl[M^-, M^+] \subseteq IVcl[N^-, N^+]$ which implies, $IVcl[M^-, M^+] \subseteq IVcl$ $[N^-, N^+] \subseteq IVcl[M^-, M^+]$. Then $IVcl[M^-, M^+] = IVcl[N^-, N^+]$. Here, $[M^-, M^+] \subseteq [N^-, N^+] \Rightarrow IVcl[M^-, M^+] \subseteq IVcl(IVint[N^-, N^+])$. Since $[M^-, M^+]$is an IVSOs. Then $[M^-, M^+] \subseteq IVcl(IVint[N^-, N^+]) \Rightarrow IVcl[N^-, N^+] = IVcl[M^-, M^+] \subseteq IVcl(IVcl(IVint[N^-, N^+])) = IVcl(IVint[N^-, N^+])$. Hence, $[M^-, M^+] \subseteq IVcl(IVint[N^-, N^+])$.∴ $[N^-, N^+]$is an IVSOs.

Theorem 3.6 (X,τ) an IVTS having Interval-Valued subset $[M^-, M^+]$.Then following conditions are equivalent

(i) $[M^-, M^+]$is an IVSOs.

(ii) Then there exist an IVOs $[N^-, N^+]$ such that, $[N^-, N^+] \subset [M^-, M^+] \subset IVcl[N^-, N^+]$.

(iii) $IVcl[M^-, M^+] = IVcl(IVint[M^-, M^+])$.

Proof:(i) ⇒ (ii). Suppose $[M^-, M^+]$is an IVSOs. Then, $[M^-, M^+] \subseteq IVcl(IVint[M^-, M^+]) \Rightarrow IVint[M^-, M^+] \subseteq [M^-, M^+] \subseteq IVcl(IVint[M^-, M^+])$.If $[N^-, N^+] = IVint[M^-, M^+]$,then $[N^-, N^+] \subseteq [M^-, M^+] \subseteq IVcl[N^-, N^+]$.
(ii)⇒ (iii). Suppose $[N^-, N^+] \subseteq [M^-, M^+] \subseteq IVcl[N^-, N^+]$.By theorem 3.2, $[M^-, M^+]$ is an IVSOs. We can conclude that, $IVcl[M^-, M^+] = IVcl(IVint[M^-, M^+])$.
(iii) ⇒ (i) Since, $IVint[M^-, M^+] \subseteq [M^-, M^+] \subseteq IVcl[M^-, M^+]$. We have $IVcl[M^-, M^+] = IVcl(IVint[M^-, M^+])$. $[M^-, M^+] \subseteq IVcl(IVint[M^-, M^+])$. ∴ $[M^-, M^+]$ is an IVSOs.

Theorem 3.7 Let an IVTS be (X,τ). If $[M^-, M^+]$ is an IVOs and $[N^-, N^+]$be an IVSOs then intersection of both $[M^-, M^+]$and $[N^-, N^+]$is an IVSOs.

Proof: Since $[N^-, N^+]$is an IVSOs then there exist an IVOs $[P^-, P^+]$such that $[P^-, P^+] \subseteq [N^-, N^+] \subseteq IVcl[P^-, P^+]$ which implies $[M^-, M^+] \cap [P^-, P^+] \subseteq [N^-, N^+] \cap [M^-, M^+] \subseteq [M^-, M^+] \cap IVcl[N^-, N^+]$. Since $[M^-, M^+] \cap [P^-, P^+]$ is an IVOs. $[M^-, M^+] \cap [P^-, P^+] = IVint([M^-, M^+] \cap [P^-, P^+])$.Then, $[M^-, M^+] \cap IVcl[P^-, P^+] \subseteq IVcl([M^-, M^+] \cap [P^-, P^+]) \Rightarrow [M^-, M^+] \cap [N^-, N^+] \subseteq [M^-, M^+] \cap IVcl[P^-, P^+] \subseteq IVcl([M^-, M^+] \cap [P^-, P^+]) = IVcl(IVint($ $[M^-, M^+] \cap [N^-, N^+]))$. Therefore,$[M^-, M^+] \cap [N^-, N^+] \subseteq IVcl(IVint([M^-, M^+] \cap [N^-, N^+]))$.Then, $[M^-, M^+] \cap [N^-, N^+]$is an IVSOs.

Theorem 3.8 Let an IVTS be (X,τ). Then the followings are equivalent
i) $[M^-, M^+]$is an IVSCs.
ii) $IVint(IVcl[M^-, M^+]) \subset [M^-, M^+]$.
iii) $IVint(IVcl[M^-, M^+]) = IVint[M^-, M^+]$.
iv) There exist $[N^-, N^+]$an IVCs such that $IVint[N^-, N^+] \subseteq [M^-, M^+] \subseteq [N^-, N^+]$.

Proof: i) ⇒ ii) Suppose $[M^-, M^+]$ is an IVSCs then $([M^-, M^+])^c$ is an IVSOs it follows as$([M^-, M^+])^c \subseteq IVcl(IVint(([M^-, M^+])^c))$. Now, $IVcl(IVint(([M^-, M^+])^c)) = (IVint(IVcl[M^-, M^+]))^c \Rightarrow ([M^-, M^+])^c \subseteq (IVint(IVcl[M^-, M^+]))^c$. Therefore, (IVint(IVcl($[M^-, M^+]) \subseteq [M^-, M^+]$.
ii) ⇒ iii) Here, $IVint(IVcl[M^-, M^+]) \subset [M^-, M^+]$ then $IVint(IVcl[M^-, M^+]) \subset IVint[M^-, M^+]$. The reverse is obvious which gives, $IVint(IVcl[M^-, M^+]) = IVint[M^-, M^+]$.
iii) ⇒ iv) Let $[N^-, N^+] = IVcl[M^-, M^+]$. Then $IVint[N^-, N^+] = IVint(IVcl[M^-, M^+])$. We know that, $IVint(IVcl[M^-, M^+]) = IVint[M^-, M^+]$which gives $IVint[N^-, N^+] = IVint[M^-, M^+]$
$\subseteq [M^-, M^+] \subseteq [N^-, N^+] \Rightarrow IVint[N^-, N^+] \subseteq [M^-, M^+] \subseteq [N^-, N^+]$.

iv) ⇒ i) There exists an IVCs $[N^-, N^+]$such that IVint$[N^-, N^+] \subseteq [M^-, M^+] \subseteq [N^-, N^+]$ then, $[N^-, N^+]^c \subseteq [M^-, M^+]^c \subseteq (\text{IVint}[N^-, N^+])^c = \text{IVcl}([N^-, N^+])^c$. Since, $[N^-, N^+]^c$ is an IVOs which implies$[M^-, M^+]^c$ is an IVSOs. Finally, $[M^-, M^+]$is an IVSCs.

Theorem 3.9 (X,τ) be an IVTS. we can take $M = [M^-, M^+] \in \text{IVS}(X)$. Then

1. $\text{IVscl}([M^-, M^+]^c) = (\text{IVsint}[M^-, M^+])^c$.
2. $\text{IVsint}([M^-, M^+]^c) = (\text{IVscl}[M^-, M^+])^c$

Proof: 1. $\text{IVscl}([M^-, M^+]^c) = \text{IVscl}(\widetilde{X} - [M^-, M^+]) = \cap \{[K^-,K^+] / [K^-,K^+]$ is an IVSCs in X and $M^{+\,c} \subseteq K^-$ and $M^{-\,c} \subseteq K^+\}$. Therefore, $\widetilde{X} - \text{IVscl}(\widetilde{X} - [M^-, M^+]) = \cup \{ [K^-, K^+]^c / [K^-, K^+]^c$ is an IVSOs in X and $K^{+\,c} \subseteq M^-$ and $K^{-\,c} \subseteq M^+\} = \cup \{[G^-,G^+] / [G^-,G^+]$ is an IVSOs in X and $G^- \subseteq M^-$ and $G^+ \subseteq M^+\} = \text{IVsint}[M^-, M^+]$. Finally, $\text{IVscl}([M^-, M^+]^c) = (\text{IVsint}[M^-, M^+])^c$.

2. $\text{IVsint}([M^-, M^+]^c) = \text{IVsint}(\widetilde{X} - [M^-, M^+]) = \cup \{[G^-,G^+] / [G^-,G^+]$ is an IVSOs in X and $G^- \subseteq M^{+\,c}$ and $G^+ \subseteq M^{-\,c}\}$. Therefore, $\widetilde{X} - \text{IVsint}(\widetilde{X} - [M^-, M^+]) = \cap \{[G^-, G^+]^c / [G^-, G^+]^c$ is an IVSCs in X and $M^- \subseteq G^{+\,c}$ and $M^+ \subseteq G^{-\,c}\} = \cap \{[B^-,B^+] / [B^-,B^+]$ is an IVSCs in X and $M^- \subseteq B^-$and$M^+ \subseteq B^+\} = \text{IVscl}[M^-, M^+]$. Hence, $\text{IVsint}([M^-, M^+]^c) = (\text{IVscl}[M^-, M^+])^c$.

Theorem 3.10 Any IVS $[M^-, M^+]$of an IVTS(X,τ) has the following properties.

1. $\text{IVsint}[M^-, M^+] = [M^-, M^+] \cap \text{IVcl}(\text{IVint}[M^-, M^+])$.
2. $\text{IVscl}[M^-, M^+] = [M^-, M^+] \cup \text{IVint}(\text{IVcl}[M^-, M^+])$.
3. $\text{IVsint}(\text{IVscl}[M^-, M^+]) = \text{IVscl}[M^-, M^+] \cap \text{IVcl}(\text{IVint}(\text{IVcl}[M^-, M^+]))$.
4. $\text{IVscl}(\text{IVsint}[M^-, M^+] = \text{IVsint}[M^-, M^+] \cup \text{IVint}(\text{IVcl}(\text{IVint}[M^-, M^+]))$.
5. $\text{IVscl}(\text{IVsint}(\text{IVscl}[M^-, M^+])) = \text{IVsint}(\text{IVscl}[M^-, M^+])$.
6. $\text{IVsint}(\text{IVscl}(\text{IVsint}[M^-, M^+])) = \text{IVscl}(\text{IVsint}[M^-, M^+])$.
7. $[M^-, M^+] \cup \text{IVsint}(\text{IVscl}[M^-, M^+]) = \text{IVscl}[M^-, M^+]$.
8. $[M^-, M^+] \cap \text{IVscl}(\text{IVsint}[M^-, M^+]) = \text{IVsint}[M^-, M^+]$.

Proof:1 and 2 are obivious.

3⇒ Followed by 1,$\text{IVsint}(\text{IVscl}[M^-, M^+]) = \text{IVscl}[M^-, M^+] \cap (\text{IVcl}(\text{IVint}(\text{IVscl}[M^-, M^+])))$. Then,$\text{IVsint}(\text{IVscl}[M^-, M^+]) \subseteq \text{IVscl}[M^-, M^+] \cap (\text{IVcl}(\text{IVint}(\text{IVcl}[M^-, M^+]))$. Applying 1 again, $\text{IVsint}(\text{IVscl}[M^-, M^+]) = \text{IVscl}[M^-, M^+] \cap \text{IVcl}(\text{IVint}(\text{IVscl}[M^-, M^+]))$. Using 2, $\text{IVsint}(\text{IVscl}[M^-, M^+]) = \text{IVscl}[M^-, M^+] \cap (\text{IVcl}(\text{IVint}[M^-, M^+]) \cup \text{IVint}(\text{IVcl}[M^-, M^+])) \supseteq \text{IVscl}[M^-, M^+] \cap \text{IVcl}(\text{IVint}(\text{IVint}(\text{IVcl}[M^-, M^+]))) = \text{IVscl}[M^-, M^+] \cap \text{IVcl}(\text{IVint}(\text{IVcl}[M^-, M^+]))$. Hence 3 is proved.

4 ⇒ follows 3.

5 ⇒ Since every Interval-Valued closed set is an Interval-Valued semiclosed. By 3, $\text{IVscl}[M^-, M^+] \cap \text{IVcl}(\text{IVint}(\text{IVcl}[M^-, M^+]))$ is an IVSCs then $\text{IVsint}(\text{IVscl}[M^-, M^+])$ is also IVSCs. Then, 5 proved itself.

6 ⇒ follows the same as 5.

7⇒ $[M^-, M^+] \cup \text{IVsint}(\text{IVcl}[M^-, M^+]) \supseteq [M^-, M^+] \cup (\text{IVscl}[M^-, M^+] \cap \text{IVscl}(\text{IVsint}(\text{IVscl}[M^-, M^+]))) = ([M^-, M^+] \cup \text{IVscl}[M^-, M^+]) \cap ([M^-, M^+] \cup \text{IVscl}(\text{IVsint}(\text{IVscl}[M^-, M^+]))) = \text{IVscl}[M^-, M^+] \cap \text{IVscl}[M^-, M^+] \supseteq \text{IVscl}[M^-, M^+]$. The reverse is obvious. Hence, 7 is proved.

Similarly, 8 proved successfully.

IVsg-closed and IVsg-open sets

Definition 4.1 Take $M = [M^-, M^+] \in \text{IVS}(X)$ and (X, τ) be an IVTS. If $\text{IVscl}([M^-, M^+]) \subseteq [U^-,U^+]$ whenever $[M^-, M^+] \subseteq [U^-,U^+] = U$ and U is an IVSOs. Then IVS $[M^-, M^+]$ is known as Interval-valued Semi generalized closed set [briefly, IVsg-closed].

The complement of IVsg-closed is known as Interval-Valued Semi generalized open (IVsg-open, for short).

Definition 4.2 Intersection of all IVsg-closed sets containing $M = [M^-, M^+]$is called Interval-Valued Semi generalized closure of $M = [M^-, M^+]$is denoted by IVsgcl(M).

Union of all IVsg-open sets contained in M = $[M^-, M^+]$is called Interval-Valued Semi generalized interior of M = $[M^-, M^+]$is denoted by IVsgint(M).

Definition 4.3 Let an IVTS (X, τ) and $[M^-, M^+]$, $[N^-, N^+]$be two non void IV-subsets of X then $[M^-, M^+]$and $[N^-, N^+]$are said to be Interval-Valued Semi separated [briefly, IV-semi separated] if $[M^-, M^+] \cap IVscl[N^-, N^+] = \tilde{\emptyset}and[N^-, N^+] \cap IVscl[M^-, M^+] = \tilde{\emptyset}$.

Theorem 4.4 Every IVCs is an IVsg-closed set.

Proof: Let $[M^-, M^+]$ be an IVCs and $[M^-, M^+] \subseteq [U^-, U^+]$= U, where U is an IVSOs. Then $IVcl[M^-, M^+]$= $[M^-, M^+]$. But $IVscl[M^-, M^+] \subseteq IVcl[M^-, M^+] \subseteq [U^-, U^+]$. Therefore, $IVscl\ [M^-, M^+] \subseteq [U^-, U^+]$,where $[U^-, U^+]$is an IVSOs. Hence, $[M^-, M^+]$is an IVsg-closed.

Remark 4.5 The converse of the preceding theorem is untrue. We can see in the succeeding illustration. Take X = {1,2,3}. Then $(X, \tau) = \{\tilde{\emptyset}, M, N, O, P, Q, R, \tilde{X}\}$ where, M = [{2},{2}], N = [{1,2},X], O = [{3},{1,3}], P = [∅,{1,3}], Q = [{2,3},X] an R = [{2},X]. Now, we consider an IVS [{2},{2}] which is an IVsg-closed set but not IVCs. Hence, every IVsg-closed set need not be IVCs.

Remark 4.6IVg-closed set and IVsg-closed sets are independent.

Example 4.7 For X = {1,2,3}, we take $(X, \tau) = \{\tilde{\emptyset}, [\{3\},\{1,3\}], [\{2\},\{2,3\}], [\emptyset,\{3\}], [\{2,3\},X]$, $[\emptyset,\{2\}], [\emptyset,\{2,3\}], [\{3\},X], \tilde{X}\}$ be an IVTS. Hence, $[\emptyset,\{2\}]$ is an IVsg-closed set but not IVg-closed set and $[\{1,3\},\{1,3\}]$ is an IVg-closed set but not IVsg-closed set. It shows how the IVg-closed and IVsg-closed sets are independent of one another.

Theorem 4.8$IVscl([M^-, M^+])$ -$[M^-, M^+]$contains no non empty IVSCs iff the IVS $[M^-, M^+]$is an IVsg-closed set.

Proof: Let $[S^-, S^+]$be an Interval-Valued Semi closed subset of $IVscl([M^-, M^+])$ - $[M^-, M^+] \Rightarrow [S^-, S^+] \subseteq IVscl([M^-, M^+])$ - $[M^-, M^+]$then $[S^-, S^+] \subseteq \tilde{X}$ - $[M^-, M^+]$which implies, $[M^-, M^+] \subseteq \tilde{X}$ - $[S^-, S^+]$. Since,$[M^-, M^+]$ is an IVsg-closed set, $IVscl[M^-, M^+] \subseteq \tilde{X}$ - $[S^-, S^+]$then $[S^-, S^+] \subseteq \tilde{X}$- IVscl $[M^-, M^+]$. Thus, $[S^-, S^+] \subseteq IVscl[M^-, M^+] \cap (IVscl[M^-, M^+])^c = \tilde{\emptyset}$. $IVscl[M^-, M^+]$- $[M^-, M^+]$contains empty IVSCs closed set. Conversly, Let $[M^-, M^+] \subseteq [U^-, U^+]$,where $[U^-, U^+]$ is an IVSOs. If $IVscl[M^-, M^+]$ is not contained in $[U^-, U^+]$then $IVscl[M^-, M^+] \cap [U^-, U^+]^c$ is a non empty closed subset of $IVscl[M^-, M^+]$ - $[M^-, M^+]$.∴ $[M^-, M^+]$is an IVsg-closed set.

Theorem 4.9$[M^-, M^+]$be an IVsg-closed set. Then $IVscl[M^-, M^+]$- $[M^-, M^+]$is an IVSCs iff $[M^-, M^+]$is an IVSCs.

Proof: Suppose $IVscl[M^-, M^+]$ - $[M^-, M^+]$ is an IVSCs where $[M^-, M^+]$ is also an IVsg-closed set. Then $IVscl[M^-, M^+]$-$[M^-, M^+]$does not contain any non empty Interval- Valued semi closed subset (by theorem 4.8) $IVscl[M^-, M^+]$-$[M^-, M^+] = \tilde{\emptyset}$. Thus, $[M^-, M^+]$is an IVSCs. Conversly, Suppose,$[M^-, M^+]$is an IVSCs and IVsg-closed set. Then IVscl $[M^-, M^+]$- $[M^-, M^+] = \tilde{\emptyset}$ which is an IVsg-closed set.

Theorem 4.10$[N^-, N^+]$is an IVsg-closed set if $[M^-, M^+]$is an IVsg-closed set with $[M^-, M^+] \subseteq [N^-, N^+] \subseteq IVscl[M^-, M^+]$.

Proof: Let $[N^-, N^+] \subseteq [U^-, U^+]$where$[U^-, U^+]$ is an IVSOs. Since,$[M^-, M^+]$is an IVsg-closed set $[M^-, M^+] \subseteq [U^-, U^+]$then $IVscl[M^-, M^+] \subseteq [U^-, U^+]$. By hypothesis, $[N^-, N^+] \subseteq IVscl[M^-, M^+]$which gives $IVscl[N^-, N^+] \subseteq IVscl[M^-, M^+]$. Then, $[N^-, N^+]$ is an IVsg-closed set.

Theorem 4.11 Let (X,τ) be an IVTS. Then IVSO(X) = IVSC(X) ⇔ Each IVsubset of X is an IVsg-closed set.

Proof: Necessary part: Let IVSO(X) = IVSC($\widetilde{X}$). To say, each subset of IVTS is an IVsg-closed. Let $[M^-, M^+] \in$ IVS(X) such that $[M^-, M^+] \subseteq [U^-, U^+]$where $[U^-, U^+]$is an IVSOs. Then IVscl $[M^-, M^+] \subseteq$ IVscl$[U^-, U^+]$= $[U^-, U^+]$. Then, $[M^-, M^+]$ is an IVsg-closed set.
Sufficient part: Suppose each IVsubset is an IVsg-closed set on X. Let $[U^-, U^+] \in$IVSO(X). Since,$[U^-, U^+] \subseteq [U^-, U^+]$ and $[U^-, U^+]$is an IVsg-closed set where IVscl$[U^-, U^+] \subseteq [U^-, U^+]$. Then,$[U^-, U^+] \in$ IVSC(X).Thus, IVSO(X) $\subseteq$ IVSC(X). If $[M^-, M^+] \in$ IVSC(X) then $([M^-, M^+])^c \in$ IVSO(X) $\subseteq$ IVSC(X) and hence$[M^-, M^+]^c \in$ IVSC(X). Finally, IVSO(X) = IVSC(X).

Theorem 4.12 Every IVOs is an IVsg-open set.

Proof: Let M = $[M^-, M^+] \in$ IVS(X) be an IVOs. Then,$[M^-, M^+]^c$ is an IVCs. Since every IVCs is an IVsg-closed set,$[M^-, M^+]^c$ is an IVsg-closed set. Hence, $[M^-, M^+]$ is an IVsg -open set.

Result 4.13 The converse of above theorem is untrue. We check in the following example. Let
X = {1,2,3}. Then (X,τ)= {$\widetilde{\emptyset}$, [{1}, {1,3}], [∅, {3}], [{1}, {1,2}], [∅, {2,3}, [{1}, {1}], [{1}, X],
[∅, {2}], $\widetilde{X}$} be an IVTS. Here, [{1,3}, {1,3}] is an IVsg-closed set but not IVOs.

Theorem 4.14A set $[M^-, M^+]$= M $\in$ IVS(X) is an IVsg-open set⇔ $[F^-, F^+] \subseteq$IVsint $[M^-, M^+]$ whenever $[F^-, F^+]$ is an IVSCs and $[F^-, F^+] \subseteq [M^-, M^+]$.

Proof: Let $[M^-, M^+]$is an IVsg-open set. Suppose $[F^-, F^+]$ is an IVSCs and $[F^-, F^+] \subseteq [M^-, M^+]$. Since $[M^-, M^+]$is an IVsg-open set ⇒ $[M^-, M^+]^c$ is an IVsg-closed set and $[F^-, F^+]^c$is an IVSOs. Now, $[M^-, M^+]^c \subseteq [F^-, F^+]^c$ and IVscl($[M^-, M^+]^c$) $\subseteq [F^-, F^+]^c \Rightarrow$ (IVsint$[M^-, M^+])^c \subseteq [F^-, F^+]^c$.Then,$[F^-, F^+] \subseteq$ IVsint$[M^-, M^+]$.
Conversely, Assume that $[F^-, F^+] \subseteq$ IVsint$[M^-, M^+]$ whenever $[F^-, F^+]$ is an IVSCs and $[F^-, F^+] \subseteq [M^-, M^+]$. To prove $[M^-, M^+]$ is an IVsg-open set. It is enough to say,
$[M^-, M^+]^c$ is an IVsg-closed set. Suppose,$[M^-, M^+]^c \subseteq [U^-, U^+]$ where $[U^-, U^+]$is an IVSOs then $[U^-, U^+]^c \subseteq [M^-, M^+]$, here $[U^-, U^+]^c$ is an IVSCs. By hypothesis, $[U^-, U^+]^c \subseteq$ IVsint $[M^-, M^+]$which implies (IVsint$[M^-, M^+])^c \subseteq$ $[U^-, U^+]$.Now, IVscl$[M^-, M^+]^c \subseteq [U^-, U^+]$. Therefore, $[M^-, M^+]^c$ is an IVsg-closed set. Finally, $[M^-, M^+]$ is an IVsg-open set.

Theorem 4.15$[M^-, M^+] \cup [N^-, N^+]$is an IVsg-open set whenever $[M^-, M^+]$ and $[N^-, N^+]$IV-semi separated IVsg-open sets.

Proof: Let $[F^-, F^+]$ be an IVSC subset of $[M^-, M^+] \cup [N^-, N^+]$. Then $[F^-, F^+] \cap$IVscl $[[M^-, M^+] \subseteq$ IVscl$[M^-, M^+] \cap$ ($[M^-, M^+] \cup [N^-, N^+]$)which implies, $[F^-, F^+] \cap$ IVscl
$[M^-, M^+] \subseteq [M^-, M^+] \cup [\emptyset, \emptyset] \subseteq [M^-, M^+]$.By theorem 4.14, $[F^-, F^+] \cap$ IVscl$[M^-, M^+]$
$\subseteq$ IVsint$[M^-, M^+]$ and $[F^-, F^+] \cap$ IVscl$[N^-, N^+] \subseteq$IVsint$[N^-, N^+]$. Now, $[F^-, F^+] = [F^-, F^+] \cap ([M^-, M^+] \cup [N^-, N^+]) =$ ($[F^-, F^+] \cap [M^-, M^+]$) $\cup$ ($[F^-, F^+] \cap [N^-, N^+]$) $\subseteq$ ($[F^-, F^+] \cap$(IVscl$[M^-, M^+]$))$\cup$ ($[F^-, F^+] \cap$ (IVscl $[N^-, N^+]$)) $\subseteq$ (IVsint$[M^-, M^+]$) $\cup$ (IVsint$[N^-, N^+]$). Then, $[F^-, F^+] \subseteq$ IVsint($[M^-, M^+] \cup [N^-, N^+]$).$[M^-, M^+] \cup [N^-, N^+]$is an IVsg-open set (by theorem 4.14).

Theorem 4.16 Let $[M^-, M^+]$and $[N^-, N^+]$be two IVsg-closed sets. Then $[M^-, M^+] \cap [N^-, N^+]$ is an IVsg-closed set, whenever $[M^-, M^+]^c$ and $[N^-, N^+]^c$are IV-semi separated.

Proof: Given $[M^-, M^+]$and$[N^-, N^+]$be two IVsg-closed sets. Suppose,$[M^-, M^+]^c$ and $[N^-, N^+]^c$are IV-semi separated. Since,$[M^-, M^+]^c$and $[N^-, N^+]^c$ are IV-semi separated IVsg-open sets. By theorem 4.15, $[M^-, M^+]^c \cup [N^-, N^+]^c$ is an IVsg-open set. Then, $[M^-, M^+]^c \cup [N^-, N^+]^c = ([M^-, M^+] \cap [N^-, N^+])^c$ is an IVsg-open set. Finally, $[M^-, M^+] \cap$ $[N^-, N^+]$is an IVsg-closed set.

Theorem 4.17 If $[M^-, M^+]$ is an IVsg-open set and IVsint$[M^-, M^+] \subseteq [N^-, N^+] \subseteq [M^-, M^+]$ then $[N^-, N^+]$ is an IVsg-open set, where $[M^-, M^+]$, $[N^-, N^+] \in$ IVS(X).

Proof: Let IVsint$[M^-, M^+] \subseteq [N^-, N^+] \subseteq [M^-, M^+]$. Now, $[M^-, M^+]^c \subseteq [N^-, N^+]^c \subseteq$ IVscl $[M^-, M^+]^c$.Since $[M^-, M^+]^c$is an IVsg-closed set then$[N^-, N^+]^c$is an IVsg-closed set, by theorem 4.10. Therefore,$[N^-,N^+]$is an IVsg-open set.

Theorem 4.18 An IVS $[M^-, M^+]$is an IVsg-closed set ⇔ IVscl$[M^-, M^+]$- $[M^-, M^+]$ is an IVsg-open set.

Proof: Necessity, Suppose $[M^-, M^+]$is an IVsg-closed set. Let $[F^-, F^+]$be an IVSCs contain in IVscl($[M^-, M^+]$) - $[M^-, M^+]$. By theorem 4.8, $[F^-, F^+] = \tilde{\emptyset}$. Hence, $[F^-, F^+] \subseteq$ IVsint (IVscl $[M^-, M^+]$ - $[M^-, M^+]$). Therefore, IVscl$[M^-, M^+]$ - $[M^-, M^+]$is an IVsg-open set.
Sufficiency, Assume that IVscl$[M^-, M^+]$- $[M^-, M^+]$is an IVsg-open set. Suppose, $[M^-,M^+] \subseteq [U^-, U^+]$, where $[U^-, U^+]$is an IVSOs. Now, IVscl$[M^-, M^+] \cap [U^-, U^+]^c \subseteq$ IVscl$[M^-, M^+] \cap [M^-, M^+]^c \subseteq$ IVscl$[M^-, M^+]$ - $[M^-, M^+]$.Since IVscl$[M^-, M^+] \cap [U^-, U^+]^c$is an IVSCs and IVscl$[M^-, M^+]$ - $[M^-, M^+]$is an IVsg-open set. Then, IVscl$[M^-, M^+] \cap [U^-, U^+]^c \subseteq$ IVsint
(IVscl$[M^-, M^+]$ - $[M^-, M^+]$) = $\tilde{\emptyset}$which gives, IVscl$[M^-, M^+] \cap [U^-, U^+]^c = \tilde{\emptyset}$ or IVscl $[M^-, M^+] \subseteq [U^-, U^+]$. Thus,$[M^-, M^+]$is an IVsg-closed set.

Theorem 4.19 In IVTS (X,τ) and$[M^-, M^+] \in$ IVS(X) is an IVsg-open set if and only if $[U^-, U^+] = [X, X]$ whenever $[U^-, U^+]$is an IVSOs and IVsint$[M^-, M^+] \cup [M^-,M^+]^c \subseteq [U^-, U^+]$.

Proof: Assume that$[U^-, U^+] = [X, X]$ whenever $[U^-, U^+]$is an IVSOs and IVsint$[M^-, M^+] \cup [M^-,M^+]^c \subseteq [U^-, U^+]$.To prove,$[M^-, M^+]$ is an IVsg-open set in (X,τ). Suppose $[F^-, F^+]$ is an IVSCs and $[F^-, F^+] \subseteq [M^-, M^+]$.It is enough to say that, $[F^-, F^+] \subseteq$ IVsint$[M^-, M^+]$(by theorem 4.14). Now, IVsint$[M^-, M^+] \cup [M^-, M^+]^c \subseteq$ IVsint$[M^-, M^+] \cup [F^-, F^+]^c$. Hence, IVsint$[M^-, M^+] \cup [F^-, F^+]^c = [X, X]$. Therefore, $[F^-, F^+] \subseteq$ IVsint$[M^-, M^+]$.
Conversely, Assume that $[M^-, M^+] \in$IVS(X) is an IVsg-open set in (X,τ). Let $[U^-, U^+]$ is an IVSOs and IVsint$[M^-, M^+] \cup [M^-, M^+]^c \subseteq [U^-, U^+]$which implies, $[U^-, U^+]^c \subseteq$
(IVsint $[M^-, M^+])^c \cap [M^-, M^+] \Rightarrow [U^-, U^+]^c \subseteq$IVscl$[M^-, M^+]^c \cap [M^-, M^+]$. Since $[U^-, U^+]^c$is an IVSCs and $[M^-, M^+]^c$is an IVsg-closed set. By theorem 4.8, $[U^-, U^+]^c = [\emptyset, \emptyset]$ or $[U^-, U^+] = [X, X]$.

IVgs-closed and IVgs-open sets
Definition 5.1 A set M = $[M^-, M^+] \in$ IVS(X) is said to be Interval-Valued generalized semiclosed [briefly, IVgs-closed] if IVscl($[M^-, M^+]$)$\subseteq [U^-, U^+] =$ U whenever, U is an IVOs open in X.
The complement of IVgs-closed is denoted as IVgs-open.

Definition 5.2 Intersection of all IVgs-closed sets containing M = $[M^-, M^+]$is called Interval-Valued generalized semi closure of M = $[M^-, M^+]$is denoted by IVgscl(M).
Union of all IVgs-open sets contained in M = $[M^-, M^+]$is called Interval-Valued generalized semi interior of M = $[M^-, M^+]$is denoted by IVgsint(M).

Theorem 5.3 Every IVCs is an IVgs-closed set.

Proof: Let $[M^-, M^+]$be an IVCs and $[M^-, M^+] \subseteq [U^-, U^+] =$ U, where U is an IVOs. Since $[M^-, M^+]$is an IVCs, IVcl$[M^-, M^+] = [M^-, M^+]$. But, IVscl$[M^-, M^+] \subseteq$ IVcl$[M^-, M^+] \subseteq [U^-, U^+]$. Hence, $[M^-, M^+]$is an IVgs-closed set.

Result 5.4 The converse of the preceding theorem is untrue and it is shown in this illustration. Let X = {a, d, c} with an IVTS (X,τ) = $\{\tilde{\emptyset}, [\{a\}, \{a, c\}], [\{a\}, X], [\emptyset, \{a, c\}], \tilde{X}\}$. We consider an IVS $[\emptyset, \{a, b\}]$ which is an IVgs-closed set but not IVCs.

Theorem 5.5 Every IVg-closed set is an IVgs-closed.

Proof: Let $[M^-, M^+]$be an IVg-closed set then IVcl$[M^-, M^+] \subseteq [U^-, U^+]$whenever $[M^-, M^+] \subseteq [U^-, U^+]$, where $[U^-, U^+]$is an IVOs. But IVscl$[M^-, M^+] \subseteq$ IVcl$[M^-, M^+] \subseteq [U^-, U^+]$. Hence, $[M^-, M^+]$is an IVgs-closed set.

Result 5.6 The converse of the preceding theorem is not true. We can check this by utilizing the IVTS used in result 5.4, here we take $[\emptyset, \{a\}]$ is an IVS(X) which is an IVgs-closed set but not IVg-closed set.

Theorem 5.7 Every IVsg-closed is an IVgs-closed set.

Proof: Let $[M^-, M^+]$ be an IVsg-closed set then IVscl$[[M^-, M^+] \subseteq [U^-, U^+]$whenever $[M^-, M^+] \subseteq [U^-, U^+]$, where $[U^-, U^+]$is an IVSOs. But, IVOs $\subseteq$ IVSOs. Then, IVscl$[M^-, M^+] \subseteq [U^-, U^+]$ where, U is an IVOs. Hence, $[M^-, M^+]$ is an IVgs-closed set.

Result 5.8 The converse of above theorem is not true. It is shown by IVTS used in Remark 4.5, Take $[\emptyset, \{2,3\}] \in$ IVS(X) which is an IVgs-closed set but not IVsg-closed set.

Theorem 5.9 IVgscl$([M^-, M^+] \cap [N^-, N^+]) \subseteq$ IVgscl$[M^-, M^+] \cap$IVgscl$[N^-, N^+]$where, $[M^-, M^+]$ and $[N^-, N^+]$be any two subsets of IVTS(X,τ).

Proof: Since $[M^-, M^+] \cap [N^-, N^+] \subseteq [M^-, M^+], [N^-, N^+]$ we have IVgscl$([M^-, M^+] \cap [N^-, N^+]) \subseteq$ IVgscl$[M^-, M^+]$and IVgscl$([M^-, M^+] \cap [N^-, N^+]) \subseteq$ IVgscl$[N^-, N^+]$.Then, IVgscl$[M^-, M^+] \cap [N^-, N^+]) \subseteq$ IVgscl$[M^-, M^+] \cap$IVgscl$[N^-, N^+]$.

Theorem 5.10 If IVSC(X,τ) be closed under finite unions then IVGSC(X,τ) is closed under finite unions.

Proof: Given, IVSC(X,τ) be closed under finite unions. Let $[M^-, M^+], [N^-, N^+] \in$ IVGSC(X,τ) and $[M^-, M^+] \cup [N^-, N^+] \subseteq [U^-, U^+]$where, $[U^-, U^+]$IVO in X. Then $[M^-, M^+] \subseteq [U^-, U^+]$and $[N^-, N^+] \subseteq [U^-, U^+]$hence IVscl$[M^-, M^+] \subseteq [U^-, U^+]$and IVscl
$[N^-, N^+] \subseteq [U^-, U^+]$. This implies, IVscl$[M^-, M^+] \cup$ IVscl$[N^-, N^+] \subseteq [U^-, U^+]$.Therefore, IVscl$([M^-, M^+] \cup [N^-, N^+]) \subseteq [U^-, U^+]$.Hence, $[M^-, M^+] \cup [N^-, N^+] \in$ IVGSC(X,τ).

Theorem 5.11 $[M^-, M^+]$be an IVgs-closed set of an IVTS(X,τ) and $[M^-, M^+] \subseteq [N^-, N^+] \subseteq$ IVscl$[M^-, M^+]$then $[N^-, N^+]$is an IVgs-closed in X.

Proof: Let $[M^-, M^+]$be an IVgs-closed set on (X,τ) an IVTS and $[M^-, M^+] \subseteq [N^-, N^+] \subseteq$ IVscl$[M^-, M^+]$. Let $[N^-, N^+] \subseteq [U^-, U^+]$, where $[U^-, U^+]$is an IVOs. Then,$[M^-, M^+] \subseteq [U^-, U^+]$. Since $[M^-, M^+]$is an IVgs-closed set we have IVscl$[M^-, M^+] \subseteq [U^-, U^+]$. Now, $[N^-, N^+] \subseteq$ IVscl$[M^-, M^+] \Rightarrow$ IVscl$[N^-, N^+] \subseteq$ IVscl(IVscl$[M^-, M^+]$) = IVscl$[M^-, M^+] \subseteq [U^-, U^+]$. We can conclude that $[N^-, N^+]$ is IVgs-closed in X.

Theorem 5.12 In IVTS(X,τ), $[M^-, M^+]$ be an IVS then $[M^-, M^+]$is an IVgs-open $\Leftrightarrow [U^-, U^+] \subseteq$ IVsint$[M^-, M^+]$whenever, $[U^-, U^+]$ is an IVCs and $[U^-, U^+] \subseteq [M^-, M^+]$.

Proof: Necessity: Let $[M^-, M^+]$be an IVgs-open in X and $[U^-, U^+]$ be an IVCs such that $[U^-, U^+] \subseteq [M^-, M^+]$. Then $[U^-, U^+]^c$ is IVO in X such that $[U^-, U^+]^c \supseteq [M^-, M^+]^c$. Since, $[M^-, M^+]^c$ is an IVgs-closed we have IVscl$[M^-, M^+]^c \subseteq [U^-, U^+]^c$. But, IVscl$[M^-, M^+]^c$ = (IVsint$[M^-, M^+])^c \subseteq [U^-, U^+]^c \Rightarrow [U^-, U] \subseteq$ IVsint$[M^-, M^+]$.
Sufficiency: It is enough to say, $[M^-, M^+]^c$is an IVgs-closed.Let IVOs be $[S^-, S^+]$ in X such that $[M^-, M^+]^c \subseteq [S^-, S^+]$. Then $[S^-, S^+]^c$is an IVC in X and $[S^-, S^+]^c \subseteq [M^-, M^+]$. Now,$[S^-, S^+]^c \subseteq$IVsint$[M^-, M^+] \Longrightarrow$(IVsint$[M^-, M^+])^c \subseteq [S^-, S^+]$.ThenIVscl$[M^-, M^+]^c \subseteq [S^-, S^+]$. Hence,$[M^-, M^+]^c$is an IVgs-closed. Finally, $[M^-, M^+]$ is an IVgs-open in X.

Theorem 5.13 Let (X,τ) be an IVTS and $[M^-, M^+]$be an IVgs-open in X such that IVsint$[M^-, M^+] \subseteq [N^-, N^+] \subseteq [M^-, M^+]$. Then,$[N^-, N^+]$is an IVgs-open.

Proof: Now,IVsint$[M^-, M^+] \subseteq [N^-, N^+] \subseteq [M^-, M^+]$.Since (IVsint$[M^-, M^+])^c$ =

$IVscl[M^-, M^+]^c, [M^-, M^+]^c \subseteq [N^-, N^+]^c \subseteq IVscl[M^-, M^+]^c$ then $[M^-, M^+]^c$ is an IVgs-closed by theorem 5.11, then $[N^-, N^+]^c$ is also IVgs-closed which gives $[N^-, N^+]$is an IVgs-open.

CONCLUSION

In this work, By using the concept of Interval-valued sets introduced by Y. Yao and further studied by J. Kim, Y. B. Jun, J. G. Lee, we developed an Interval-Valued semi closed (briefly, IVSC) and Interval-Valued semi open (briefly, IVSO) with certain properties. Our discussion highlights the importance of Interval-Valued semi interior and semi closure operators. The ideas of Interval-Valued semi generalized closed and open sets were then covered. In a similar manner, Interval-Valued generalized semi closed and open sets. In the future, we will look at Interval-Valued semi continuous and connected spaces.

REFERENCES

1. Yao, Y. (2009, June). Interval sets and interval-set algebras. In *2009 8th IEEE international conference on cognitive informatics* (pp. 307-314).
2. Zadeh, L. A. (1975). The concept of a linguistic variable and its application to approximate reasoning—I. *Information sciences*, *8*(3), 199-249.
3. Kim, J., Jun, Y. B., Lee, J. G., &Hur, K. (2020). Topological structures based on interval-valued sets. *Ann. Fuzzy Math. Inform*, *20*(3), 273-295.
4. Levine, N. (1970). Generalized closed sets in topology. *RendicontidelCircoloMatematico di Palermo*, *19*, 89-96.
5. S. Dijitha and M. Navaneethakrishnan, "A study on g-closed and g-open sets in Interval-Valued Topology", Proceeding of National Conference on INSTA'24, Feb 23, 2024, pp. 33-39.
6. Sasikala, G., &Navaneetha, K. (2016). Study on Intuitionistic semi open sets. *IOSR Journal of Mathematics*, *12*(6),79-84.https://iosrjournals.org/iosr-jm/papers/Vol12-issue6/Version-3/M1206037984.pdf
7. G Raouf, A., & J Yaseen, Y. (2009). On generalization closed set and generalized continuity On Intuitionistic Topological spaces. *Journal of University of Anbar for Pure Science*, *3*(1), 107-117.http://dx.doi.org/10.37652/juaps.2009.15407
8. Çoker, D. (1997). An introduction to intuitionistic fuzzy topological spaces. *Fuzzy sets and systems*, *88*(1), 81-89.

Vol.15 / Issue 88 / Feb / 2025 *International Bimonthly (Print) – Open Access* *ISSN: 0976 – 0997*

REVIEW ARTICLE

Innovations in Bioanalytical Methods for Drug Discovery and Development

Mallela Thirumala Sadan[1], Shaik Nuzhath[2], T.Farmaan[1], Shaik Farheen Taj[1], Akula Tharun[1], Katila Nizamuddinn[1] and Karra Pavani[2]*

[1]Student, Department of Pharmaceutical Analysis, Raghavendra Institute of Pharmaceutical Education and Research (Autonomous), (Affiliated to Jawaharlal Nehru Technological University), Anantapur, Andhra Pradesh, India.
[2]Assistant Professor, Department of Pharmaceutical Analysis, Raghavendra Institute of Pharmaceutical Education and Research (Autonomous), (Affiliated to Jawaharlal Nehru Technological University), Anantapur, Andhra Pradesh, India.

Received: 21 Nov 2024 Revised: 03 Dec 2024 Accepted: 21 Jan 2025

***Address for Correspondence**
Karra Pavani
Assistant Professor,
Department of Pharmaceutical Analysis,
Raghavendra Institute of Pharmaceutical Education and Research (Autonomous),
(Affiliated to Jawaharlal Nehru Technological University),
Anantapur, Andhra Pradesh, India.
E.Mail: karrapavani21@gmail.com

ABSTRACT

Bioanalytical methods have evolved significantly, playing a crucial role in advancing drug discovery and development by enabling the precise analysis of drug candidates, metabolites, and biomarkers. Recent innovations, such as liquid chromatography-mass spectrometry (LC-MS/MS), biosensors, nanotechnology, and artificial intelligence (AI), have revolutionized the landscape of pharmaceutical research. LC-MS/MS has become a gold standard for high-sensitivity quantification of small molecules, while biosensors and microfluidic devices offer real-time, in vivo analysis of drug interactions and metabolites. Nanotechnology has introduced nanoscale probes and nanoparticles, which enhance sensitivity and enable targeted drug monitoring. The integration of AI and machine learning (ML) further accelerates data analysis, enabling predictive modelling, optimization of drug candidates, and improved pharmacokinetic (PK) and pharmaco dynamics (PD) studies. Next-generation sequencing (NGS) has also contributed by enabling more precise biomarker identification and personalized treatment approaches. These innovations enhance efficiency, reduce the time to market for new drugs, and improve the accuracy of therapeutic evaluations. Despite these advancements, challenges remain, particularly in regulatory approval and method validation. Ensuring the reliability and reproducibility of these innovative methods is crucial for their application in clinical and commercial settings. As bioanalytical technologies continue to advance, they will further drive personalized medicine, point-of-care diagnostics, and sustainable analytical practices, reshaping the future of drug discovery and development.

Keywords: Bioanalytical methods, LC-MS/MS, Biosensors, Nanotechnology, Artificial intelligence.

INTRODUCTION

The drug discovery process has been significantly enhanced by the rapid advancements in bioanalytical techniques, which play a pivotal role in the identification, quantification, and characterization of new drug candidates. Cutting-edge methods, such as liquid chromatography-mass spectrometry (LC-MS), high-throughput screening (HTS), and next-generation sequencing (NGS), have revolutionized the way researchers analyze complex biological samples. These innovations enable the detection of minute molecular changes, improving the accuracy and speed of drug candidate evaluation. Additionally, advancements in bioanalytical technologies have facilitated a better understanding of pharmacokinetics and pharmacodynamics, which are crucial for determining drug efficacy and safety. By offering higher sensitivity, selectivity, and automation, modern bioanalytical tools not only accelerate the drug development timeline but also enhance the success rate of identifying viable therapeutic candidates(1).

The Evolution of Bioanalytical Methods in Modern Drug Development

Bioanalytical methods have undergone remarkable evolution in recent decades, transforming the landscape of modern drug development(2). Initially focused on basic analytical techniques like chromatography and immunoassays, these methods have now expanded to include sophisticated technologies such as mass spectrometry (MS), nuclear magnetic resonance (NMR), and bioinformatics-driven approaches. This evolution has been driven by the need for more precise, sensitive, and high-throughput analytical techniques to meet the growing complexity of drug candidates and biological systems. Modern bioanalytical methods allow for the detailed study of drug absorption, distribution, metabolism, and excretion (ADME), while also facilitating biomarker discovery, target identification, and therapeutic monitoring. The integration of automation and data analytics has further accelerated drug development, allowing researchers to analyze larger datasets more efficiently(3).As these bioanalytical methods continue to evolve, they play an increasingly vital role in bringing innovative, safe, and effective therapies to the market more rapidly.

Innovative Bioanalytical Approaches: Accelerating Drug Discovery Pipelines

Innovative bioanalytical approaches are revolutionizing the drug discovery pipeline, enabling faster and more efficient development of new therapies(4). Advanced techniques such as liquid chromatography-tandem mass spectrometry (LC-MS/MS), high-throughput screening (HTS), and microfluidic systems have significantly enhanced the ability to analyze complex biological samples with greater precision and speed. These cutting-edge methods provide deeper insights into pharmacokinetics, pharmaco dynamics, and toxicology, essential for identifying promising drug candidates early in the development process. Additionally, emerging technologies like lab-on-a-chip and AI-driven bioanalysis offer real-time data processing, enabling high-volume sample analysis with unparalleled accuracy. By streamlining processes such as biomarker discovery, compound screening, and lead optimization, these bioanalytical innovations reduce the time and costs associated with drug development. Ultimately, the integration of these advanced techniques into the drug discovery pipeline enhances the ability to bring effective, safe, and targeted therapies to patients in need more rapidly(5).

Revolutionizing Pharmacology: Emerging Bioanalytical Technologies

Emerging bioanalytical technologies are transforming pharmacology by providing unprecedented insights into drug interactions, mechanisms of action, and therapeutic efficacy(6). Techniques such as high-resolution mass spectrometry, biosensors, and microarray-based platforms allow for precise quantification and identification of biological molecules at previously unattainable levels. These technologies enable researchers to study complex biological systems in real-time, offering a clearer understanding of drug metabolism, pharmacokinetics, and toxicity. Additionally, advances in bioanalytical methods, including single-cell analysis and molecular imaging, are pushing the boundaries of personalized medicine by enabling tailored therapeutic strategies based on individual patient profiles. These breakthroughs also enhance biomarker discovery, facilitating early-stage drug development and more

accurate disease diagnosis. By integrating automation, data analytics, and machine learning, bioanalytical technologies are revolutionizing pharmacology, improving drug efficacy, reducing development timelines, and contributing to the creation of safer, more effective therapies. The continued evolution of these tools holds immense potential for advancing both drug discovery and clinical practice(7).

Bioanalytical Innovations: Driving Precision in Drug Development

Bioanalytical innovations are crucial in enhancing precision within drug development, offering improved accuracy in evaluating drug efficacy, safety, and pharmacological properties(6). Advanced techniques like liquid chromatography-mass spectrometry (LC-MS), biosensors, and next-generation sequencing (NGS) enable highly sensitive detection and quantification of biomolecules, facilitating more accurate assessments of drug interactions. These methods allow for better understanding of pharmacokinetics and pharmaco dynamics, ensuring drugs are designed with higher precision and specificity. By streamlining processes like biomarker discovery, toxicity testing, and therapeutic monitoring, bioanalytical innovations are accelerating the creation of safer, more targeted, and effective therapies(8).

Next-Generation Bioanalytical Tools for Enhanced Drug Discovery

Next-generation bioanalytical tools are transforming drug discovery with advanced capabilities that drive innovation and efficiency(9). Techniques such as high-resolution mass spectrometry, lab-on-a-chip systems, and real-time biosensors offer unprecedented sensitivity and specificity in analyzing complex biological samples. These tools enable high-throughput screening and detailed profiling of drug candidates, accelerating the identification of promising compounds. Additionally, advancements in data analytics and machine learning are enhancing predictive modeling and biomarker discovery. By providing deeper insights into drug behavior and interactions, next-generation bioanalytical tools streamline the drug development process, leading to faster, more effective, and safer therapeutic discoveries(10).

The Intersection of Bioanalytical Advances and Drug Development Efficiency

The intersection of bioanalytical advances and drug development efficiency represents a pivotal shift in pharmaceutical research. Recent innovations in bioanalytical techniques, such as high-resolution mass spectrometry and automated high-throughput screening, are dramatically enhancing the precision and speed of drug discovery(4). These advancements facilitate more accurate assessments of drug candidates, streamline the identification of biomarkers, and improve the understanding of pharmacokinetics and pharmacodynamics. By integrating these cutting-edge tools, researchers can accelerate development timelines, reduce costs, and increase the likelihood of successful therapeutic outcomes. This synergy between bioanalytical technology and drug development is crucial for meeting the growing demand for effective and safe new therapies(11).

Harnessing Innovation: Bioanalytical Methods in the Future of Drug Research

Harnessing innovation in bioanalytical methods is set to redefine the future of drug research. Cutting-edge technologies such as advanced mass spectrometry, high-throughput sequencing, and microfluidics are pushing the boundaries of what is possible in drug discovery(12). These innovations enable more precise and comprehensive analysis of biological samples, allowing for faster identification of drug candidates and biomarkers. Enhanced data analytics and automation further streamline the process, reducing development times and costs. As these bioanalytical methods continue to evolve, they promise to drive breakthroughs in drug research, leading to more effective and personalized therapies that meet unmet medical needs(13).

Novel Bioanalytical Techniques: Bridging the Gap in Drug Discovery

Novel bioanalytical techniques are crucial in bridging gaps within drug discovery by providing deeper insights into drug behaviour and biological interactions. Advances such as single-cell analysis, lab-on-a-chip technologies, and next-generation sequencing enable precise and high-throughput analysis of complex biological systems. These techniques facilitate earlier and more accurate identification of drug candidates and biomarkers, improving the understanding of pharmacokinetics and pharmaco dynamics(14). By integrating these innovative methods,

researchers can overcome traditional limitations, streamline the drug development process, and enhance the efficiency of translating laboratory discoveries into effective therapeutic solutions.

From Bench to Bedside: Innovations in Bioanalytical Methods Transforming Drug Development

Innovations in bioanalytical methods are profoundly transforming drug development, bridging the gap from bench research to bedside applications. Advanced techniques such as liquid chromatography-mass spectrometry, real-time biosensors, and high-throughput screening provide unparalleled precision in analysing drug candidates and biological samples. These advancements enable faster, more accurate assessments of drug efficacy, safety, and mechanisms of action. By streamlining processes from early discovery through clinical trials, these innovations enhance the speed and success rate of developing new therapies(5). As a result, patients benefit from more effective and personalized treatments, significantly advancing the field of medicine(15).

LITERATURE REVIEW AND DATA COLLECTION

The landscape of drug discovery and development has evolved significantly in recent years due to advancements in bioanalytical methods. These methods play a crucial role in understanding the pharmacokinetics, pharmaco dynamics, and toxicology of new drug candidates, as well as ensuring safety and efficacy. Innovations in bioanalytical technologies have enabled faster, more sensitive, and accurate assessments, which are pivotal in advancing drug discovery pipelines. This literature review will explore key innovations in bioanalytical methods, with a focus on mass spectrometry, liquid chromatography, ligand-binding assays, and emerging technologies like microfluidics and biosensors.

Selection of Core Techniques for Evaluation(16)

- Mass Spectrometry-Based Techniques (e.g., LC-MS/MS, HRMS, MS Imaging)
- Advanced Liquid Chromatography Methods (e.g., UPLC, Microflow/Nanoflow LC)
- Ligand-Binding Assays (LBA) (e.g., ELISA, ECL)
- Emerging Technologies (e.g., Microfluidics, Biosensors, AI-based Methods)

Experimental Design and Validation

Sample Selection

Selection of representative biological samples for testing (e.g., plasma, serum, tissues, cell cultures). The choice of sample types depends on the drug discovery phase, such as early discovery (in vitro assays) or preclinical/clinical studies (in vivo studies)(17).

Analytical Procedure Development

A detailed protocol for the bioanalytical techniques is developed based on standard operating procedures (SOPs). For instance, when assessing the innovation in LC-MS/MS,(18)

Sample Preparation

Protein precipitation, liquid-liquid extraction, or solid-phase extraction (SPE) methods are used based on the biological matrix.

Chromatographic Separation

Optimization of chromatographic conditions, such as column choice, flow rate, and mobile phase composition.

MS Detection

Use of tandem MS with optimized ionization techniques (ESI or APCI), scan modes (selected reaction monitoring, SRM), and mass-to-charge (m/z) transitions for specific analytes.

Validation Criteria
Based on regulatory guidelines (e.g., FDA or ICH M10), method validation is performed

Accuracy
Agreement between experimental data and known concentration of the drug or biomarker.

Precision
Repeatability and reproducibility of the method across different trials.

Sensitivity
Limit of detection (LOD) and limit of quantification (LOQ) of the drug or metabolite(19).

Specificity
Ability of the method to differentiate the target analyte from matrix interferences.

Stability
Assessment of the stability of the analyte under various conditions (e.g., freeze-thaw cycles, room temperature, long-term storage).

Implementation of Emerging Technologies
Microfluidics and Lab-on-a-Chip Systems: Microfluidic platforms are set up for rapid, miniaturized bioassays.
Device Fabrication: Microfluidic devices are fabricated using soft lithography or other suitable techniques.

Assay Development
Enzyme activity assays or drug interaction studies are miniaturized into microfluidic chips, where small volumes of reagents are manipulated.

Data Analysis
Data from high-throughput assays on microchips are analyzed to assess throughput, sensitivity, and reproducibility.
Biosensor Technologies: Biosensors, including nanomaterial-based sensors, are developed for real-time analysis of drug candidates.

Methodological steps include:
Surface Functionalization: Nanomaterials such as gold nanoparticles or graphene are functionalized with specific ligands to bind the target analyte.

Detection Mechanism
Electrochemical, optical, or piezoelectric signals are recorded to quantify the interaction between the drug and biomolecules (e.g., enzymes or receptors).

Performance Metrics
Metrics such as response time, detection limit, and signal-to-noise ratio are evaluated for each biosensor(19).

Data Processing and Statistical Analysis
Once experimental data is collected from various bioanalytical techniques, comprehensive data processing and statistical analysis.

Quantitative Data Analysis
Software tools such as MassHunter (for MS data), Empower (for LC), or proprietary bioinformatics platforms are used to process raw data, identify peaks, and quantify analytes.

Multivariate Analysis

For complex datasets (e.g., proteomics or metabolomics data from HRMS), multivariate statistical methods like PCA (Principal Component Analysis) or PLS-DA (Partial Least Squares Discriminant Analysis) are employed to identify key biomarkers or drug metabolites.

AI/ML Integration

For emerging AI-driven bioanalytical methods, machine learning algorithms are employed to predict drug efficacy, toxicology, and ADME (absorption, distribution, metabolism, and excretion) profiles based on the bioanalytical data(20).

Comparative Analysis and Interpretation

Finally, the results from various bioanalytical methods are compared to assess their relative advantages and limitation.

Sensitivity and Specificity

A comparison of the detection limits and specificity of different techniques (e.g., LC-MS/MS vs. biosensors).

Throughput

Assessment of the time and cost efficiency of each method, with emphasis on high-throughput screening applications.

Regulatory Compliance

Ensuring that each method aligns with the validation guidelines from regulatory bodies like the FDA, ensuring that the method is suitable for use in clinical development phases(21).

Reporting and Recommendation

Summary of Innovations: Highlight the key innovations in bioanalytical methods that show the greatest potential for improving drug discovery and development.

Practical Recommendations

Provide recommendations for the implementation of advanced bioanalytical techniques in the pharmaceutical industry, based on cost-benefit analysis and technical feasibility(22).

DATA COLLECTION

Scientific Databases

PubMed, Scopus, Web of Science, and Google Scholar are used to collect peer-reviewed articles, conference proceedings, and review papers on advancements in bioanalytical techniques such as mass spectrometry, liquid chromatography, and ligand-binding assays(23).

Pharmaceutical Industry Reports: Insights from the latest pharmaceutical industry white papers, reports from regulatory bodies (FDA, EMA), and market research analyses help frame the scope and context of bioanalytical innovations in drug discovery.

Patent Databases

To assess the most recent technologies and methodologies, patent databases like USPTO and EPO are searched to identify cutting-edge bioanalytical techniques applied in drug development.

Regulatory Guidelines

International guidelines such as ICH M10 (Bioanalytical Method Validation) and FDA guidance documents on bioanalytical method validation are reviewed to understand the regulatory framework around method innovation

CHALLENGES AND FUTURE DIRECTIONS

Despite significant advancements, several challenges persist in the application of innovative bioanalytical methods for drug discovery and development. One major challenge is the integration of new technologies into existing workflows. Techniques such as high-throughput screening, microfluidics, and advanced mass spectrometry require significant investments in infrastructure, training, and expertise. For smaller pharmaceutical companies and academic labs, the cost of implementing these technologies can be prohibitive. Additionally, data management and interpretation remain critical bottlenecks. The volume and complexity of data generated by advanced techniques, such as LC-MS/MS and AI-driven platforms, require sophisticated data processing tools and algorithms. Ensuring data accuracy, reproducibility, and minimizing errors, especially in high-throughput environments, is a significant challenge. Another key issue is regulatory compliance. New bioanalytical methods must meet strict regulatory guidelines before they can be widely adopted in drug development. Regulatory bodies often require extensive validation and standardization processes, which can delay the implementation of new technologies. Looking ahead, there are several promising directions. One area of future development is the integration of artificial intelligence (AI) and machine learning (ML). These technologies can help automate data analysis, improve predictive accuracy, and speed up decision-making processes in drug discovery. AI-powered algorithms can detect patterns and correlations that are difficult for traditional methods to identify. Moreover, miniaturization and automation of bioanalytical methods, such as the further development of lab-on-a-chip devices, can reduce costs and improve efficiency. These innovations will make advanced bioanalytical tools more accessible to smaller labs and companies, broadening their application. Finally, enhanced collaboration between academia, industry, and regulatory agencies will be crucial in overcoming existing barriers, standardizing new technologies, and ensuring their smooth integration into drug development pipelines.

CONCLUSION

Bioanalytical innovations have significantly advanced drug discovery and development, enabling faster, more precise, and cost-effective processes. Techniques such as high-throughput screening, LC-MS/MS, microfluidics, and AI-driven data analysis have revolutionized the field by improving drug efficacy, safety, and personalized medicine approaches. Despite challenges such as cost, data complexity, and regulatory hurdles, the continued integration of these cutting-edge methods promises to accelerate the development of new therapeutics. Future advancements in automation, AI, and collaboration across sectors will further enhance the impact of bioanalytical methods on the pharmaceutical industry.

REFERENCES

1. Petrova E. Innovation in the pharmaceutical industry: The process of drug discovery and development. Innovation and Marketing in the Pharmaceutical Industry: Emerging Practices, Research, and Policies: Springer; 2013. p. 19-81.
2. Thakur A, Tan Z, Kameyama T, El-Khateeb E, Nagpal S, Malone S, et al. Bioanalytical strategies in drug discovery and development. Drug Metabolism Reviews. 2021;53(3):434-58.
3. Chen Y, Argentinis JE, Weber G. IBM Watson: how cognitive computing can be applied to big data challenges in life sciences research. Clinical therapeutics. 2016;38(4):688-701.
4. Dueñas ME, Peltier-Heap RE, Leveridge M, Annan RS, Büttner FH, Trost M. Advances in high-throughput mass spectrometry in drug discovery. EMBO Molecular Medicine. 2023;15(1):e14850.
5. Amir-Aslani A, Mangematin V. The future of drug discovery and development: shifting emphasis towards personalized medicine. Technological Forecasting and Social Change. 2010;77(2):203-17.

6. Marques L, Costa B, Pereira M, Silva A, Santos J, Saldanha L, et al. Advancing precision medicine: A review of innovative In Silico approaches for drug development, clinical pharmacology and personalized healthcare. Pharmaceutics. 2024;16(3):332
7. Nicolaou K. Advancing the drug discovery and development process. Angewandte Chemie. 2014;126(35):9280-92.
8. Bakhtiar R. Biomarkers in drug discovery and development. Journal of pharmacological and toxicological methods. 2008;57(2):85-91.
9. Cayer DM, Nazor KL, Schork NJ. Mission critical: the need for proteomics in the era of next-generation sequencing and precision medicine. Human molecular genetics. 2016;25(R2):R182-R9.
10. Dhudum R, Ganeshpurkar A, Pawar A. Revolutionizing Drug Discovery: A Comprehensive Review of AI Applications. Drugs and Drug Candidates. 2024;3(1):148-71
11. Kaur S, Alley SC, Szapacs M, Wilson A, Ciccimaro E, Su D, et al. 2021 White Paper on Recent Issues in Bioanalysis: Mass Spec of Proteins, Extracellular Vesicles, CRISPR, Chiral Assays, Oligos; Nanomedicines Bioanalysis; ICH M10 Section 7.1; Non-Liquid & Rare Matrices; Regulatory Inputs (Part 1A–Recommendations on Endogenous Compounds, Small Molecules, Complex Methods, Regulated Mass Spec of Large Molecules, Small Molecule, PoC & Part 1B-Regulatory Agencies' Inputs on Bioanalysis, Biomarkers, Immunogenicity, Gene & Cell Therapy and Vaccine). Bioanalysis. 2022;14(9):505-80.
12. Stockwell PB. Abstracts of papers presented at the 2008 pittsburgh conference. Journal of Automated Methods and Management in Chemistry. 2008;2008.
13. Srivastava P, Kumari B, Rajeswari SU, Meena J, Gangopadhyay S, Gupta S, et al. A COMPREHENSIVE REVIEW OF ADVANCEMENTS IN PHARMACOLOGY AND DRUG DISCOVERY. Journal of Experimental Zoology India. 2024;27(2).
14. Derendorf H, Lesko LJ, Chaikin P, Colburn WA, Lee P, Miller R, et al. Pharmacokinetic/pharmacodynamic modeling in drug research and development. The Journal of Clinical Pharmacology. 2000;40(12):1399-418.
15. Ginsburg GS, Willard HF. Genomic and personalized medicine: foundations and applications. Translational research. 2009;154(6):277-87.
16. Wang HF, Findlay JW. Alternative and emerging methodologies in ligand-binding assays. Ligandbinding assays: development, validation, and implementation in the drug development arena Wiley, Hoboken, New Jersey, USA. 2009:343-80.
17. Feng B, Varma MV, Costales C, Zhang H, Tremaine L. In vitro and in vivo approaches to characterize transporter-mediated disposition in drug discovery. Expert opinion on drug discovery. 2014;9(8):873-90.
18. Stevenson L, Garofolo F, DeSilva B, Dumont I, Martinez S, Rocci M, et al. 2013 White Paper on recent issues in bioanalysis:'hybrid'–the best of LBA and LCMS. Bioanalysis. 2013;5(23):2903-18.
19. Bueno MM, Uclés S, Hernando M, Fernández-Alba A. Development of a solvent-free method for the simultaneous identification/quantification of drugs of abuse and their metabolites in environmental water by LC–MS/MS. Talanta. 2011;85(1):157-66.
20. Kumar SA, Ananda Kumar TD, Beeraka NM, Pujar GV, Singh M, Narayana Akshatha HS, et al. Machine learning and deep learning in data-driven decision making of drug discovery and challenges in high-quality data acquisition in the pharmaceutical industry. Future Medicinal Chemistry. 2022;14(4):245-70.
21. Zimmer D. New US FDA draft guidance on bioanalytical method validation versus current FDA and EMA guidelines: chromatographic methods and ISR. Taylor & Francis; 2014. p. 13-9.
22. Ayala JL. High Resolution Mass Spectrometry Drug Screening in Forensic Toxicology: A Cost Benefit Analysis: Sam Houston State University; 2022.
23. Castaneto MS. Novel Psychoactive Substances: Analytical Approaches, Military Prevalence, and Human Metabolite Profiling: University of Maryland, Baltimore; 2015.

RESEARCH ARTICLE

Effect of Chaturajata Taila Pratimarsh Nasya In Management of VATAJ Pratishyay W.S.R. Allergic Rhinitis : A Case Study

Prashant Jain[1] , Manjiri Keskar[2]* and Siddhand Jain[3]

[1]PG Scholar, Department of Shalakya Tantra, Parul Institute of Ayurved, Parul University, Gujarat, India.
[2]Professor, Department of Shalakya Tantra, Parul Institute of Ayurved, Parul University, Gujarat, India.
[3]PG Scholar, Department of Rog Nidan, Parul Institute of Ayurved, Parul University, Gujarat, India.

Received: 21 Nov 2024 Revised: 03 Dec 2024 Accepted: 21 Jan 2025

***Address for Correspondence**
Manjiri Keskar
Professor, Department of Shalakya Tantra,
Parul Institute of Ayurved,
Parul University,
Gujarat, India.
E.Mail: Pjprashantrock2@gmail.com

ABSTRACT

Many diseases are associated with respiratory allergies, which affect a large portion of the population today. Regardless of gender, Allergic rhinitis is a common respiratory condition affecting people of all ages. this illness is notorious for being chronic and recurrent if left untreated. The main causes of this illness include a sedentary lifestyle, exposure to cold weather, and eating habits such as consuming junk food, ice cream, cold beverages. The illness impairs sleep, causes weariness and headaches, restricts everyday activities, and impairs productivity at work. *Pratishyay* is the *Nasagata roga* that is most thoroughly explained by nearly all of the *Acharyas*. In *Sushruta Samhita Pratishyaya* is one among the *Pranavaha Srothojanya Vikaras. VatajaPratishyaya* is a disorder in which there is vitiation of *Vata & Kapha doshas* characterized by inflammation of mucous membrane of the nose which is characterized by *Nasasrava, Nasavarodha, Kshavathu, Shirashoola and Swarabedha*. The patient was advised for *Pratimarsh Nasya* with *Chaturajata Taila* for a period of 7days. After the treatment, the patient relieved from almost many of the sign & symptoms of *Vataja Pratishyay*. It was found to be even cost effective, easy to use,easy to carry. It instantly and efficiently clears up the nasal passage, providing a relief from a blocked nose.

Keywords: Respiratory, Allergies, *Vataj, Pratishyaya, Pratimarsh Nasya*.

INTRODUCTION

Allergic rhinitis is a very common disorder that affects people of all ages,peaking in the teenage years. It is frequently ignored, under diagnosed, misdiagnosed, andmistreated, which not only is detrimental to health but also has societal costs. Although allergic rhinitis is not a serious illness, it is clinically relevant because it underlies many complications is a major risk factor for poor asthma control, and affects quality of life and productivity at work or school[1]. *Pratishyay* is compared with rhinitis mentioned in modern text. Rhinitis is an inflammation and irritation of mucous membrane inside the nose. Common symptoms are stuffy nose, running nose, sneezing and post nasal drip. The inflammation is caused by viruses, bacteria, irritants or allergens. It is very common medical condition. Every man would have suffered from this disease at least once in his life. According to WHO, 400 million people worldwide have Allergic Rhinitis [2]. AR is nasal drainage, fluid from the nose is usually clear.[1]Also have sneezing, nasal discharge itching and cough, and also shortness of breath wheezing. In the chapter of *Trimarmeeya Chikitsa* in *Chikitsa Sthana* of the *Charak Samhita, AcharyaCharak* describes the illness *Pratishyay*[3]. The illness *Pratishyay* in Uttar Tantra is referenced in the *Sushruta Samhita*[4]. He has provided a detailed description of *Pratishyay*, including its categorization, symptoms, consequences, and management. *Pratishyay* has been categorized under *Nasaroga Adhikara* by *Madhava Nidan[5]*. It has been compared to *Vataj Pratishyay* in Ayurvedic scriptures. Condition where secretion produced due to the vitiation of Vata and Kapha at the root of the nose. The clinical feature of Vataj Pratishya are severe sneezing(*Ksavathu*), watery discharge (*Tanusrava*),and nasal obstruction and hoarseness of voice *(Swarabheda)*[5]*kandu netra, talu,gala*, headache (Shirashoola) etc.The *nidana of pratishyaya* includes *vegadharana, rajo dhuma sevana* (mist ,fog,snow, breeze and dust) , *diwaswapna,*(sleep during day time) *mithyaahara* vihara (drinking water from other places not accustomed),playing in water (sports). By these causes the Doshas with the predominance of Vata, getting aggravated affects nasal cavity & cause Vataj Pratishyay[4].

However, patients suffering from allergic rhinitis adopt treatment modalities like anti histamines, nasal decongestants, steroids etc. But the patients cannot get satisfied by these techniques because the medication can't give complete relief and these medications give rise to further recurrence of the disease. So, to avoid these complications of western medicines a simple treatment which can overcome the symptoms and recurrence of disease can be planned [6,7] According to Acharya *Vagbhata Nasa* being the gateway of *shira* any drug administered through this route reaches *shrungataka marma*. This is a *sira marma* and formed by the siras of Nasa, Netra, Kantha and Shrotra[8] etc. The *Chaturajata* mentioned in Yogaratnakara [9] and other texts are very effective and both preventive and curative. It instantly and efficiently clears up the nasal passage, providing a relief from a blocked nose. The ingredients of *Chaturajata taila* having property like *ushna virya* and *snigdha guna* which helps in reducing sneezing. It acts like lubricant in passage of nasal route hence reduces chances of irritation. Drugs having property *katu tikta rasa* and *ushna virya* due to that helps in pacifying *kapha dosha* and therefore rhinitis symptoms subside. Oils having property of *snigdha gun* which helps in reducing itching in nasal passage.

MATERIALS AND METHODS

Case Report
Age – 44 years
Occupation – Bussinessmen
Sex - Male
Religion - Hindu.
A case of *Vataj Pratishyay* (AR), from dept.of *Shalakya Tantra* OPD, Parul Ayurved Hospital was taken for the study with complaint of excessive nasal discharge, nasal obstruction , sneezing, and headache since 7 days. Patient was healthy before 2months. Then he gradually suffered from severe sneezing & watery nasal discharge and had recurrent symptoms. Patient has taken other medicine for the temporary relief and could not get any Satisfactory result.

History of Past Illness
Not a known case of DM and Hypertension.

Vitals
- Respiratory rate: 20/min
- Regular temperature: 98.6F
- Blood pressure: 110/80 mm of Hg
- Pulse: 70/min

Ashtasthana Pareeksha
- Nadi: 70/min
- Mutra: 3-4 times/day
- Mala: Parkrutha
- Jihwa: Alipta
- Shabda: Prakrutha,
- Sparsha: Prakrutha
- Drik: Shushkatha
- Akriti: Madhyama

Diagnostic Criteria
The diagnostic criteria for the study are *Nasa-avarodha, Shirahsoola, Kshvathu, Nasa-srava and Swarabheda*. Assessment of the disease was done using the Subject Parameters: After thorough examination the severity of the sneezing of the patient was at grade 3 -severe sneezing over more than 15. There was mild headache which was graded 1- Occasional headache Present. The nasal obstruction and the discharge of nasal mucosa were graded 2 as it shows Inhalation and Exhalation to be assisted with mouth breathing and Moderate discharge which needs occasional mopping respectively and No *Swarbheda.*

Sop of *PratimarshNasya*
Pre-operative:
1. Patient made to liedown in supine position with head and neck low position.
2. Patient is informed about the procedure.

Operative
1. *Chaturajata taila -2* drops will be instilled in one nostril.
2. Close the opposite nostril once and after releasing, pull the nostril high till the *taila* comes to the throat and then spit the *taila*.
3. Repeat the same procedure in another nostril.

Post-Operative
1. Gargle with luke warm water.

Follow Up
1st Follow Up- After 7th day

Preparation of Medicine
Churjat Churn kalka + *Tila taila* + *kashaya*
(1 part) (4part) (16 parts)

Boiled up to *phenaudgama*

Chaturjata taila

OBSERVATION & RESULT

Before treatment, patient was suffering from severe sneezing which was graded as 3 i.e. more than 15 times/day which was considerably decreased to grade 1 i.e. 1-5times/day after treatment. Before treatment patient suffered from mild headache after treatment patient has stopped complaint of headache i.e. absent. Before treatment patient had complaint of *Nasavarodha* which was graded as 2 was decreased to grade 0 i.e. absent after treatment. Before treatment patient had complaint of *Nasasrava* which was graded as 2decreased to grade 0.

DISCUSSION & CONCLUTION

Nasa being the gateway of *shira* any drug administered through this route reaches *Shrungataka marma*. This is a *sira marma* and formed by the *Siras of Nasa, Netra, Kantha and Shrotra* etc.The *Chaturajata Taila* is very effective and both preventive and curative.It instantly and efficiently clears up the nasal passage, providing a relief from a blocked nose.The ingredients of *Chaturajata taila* having *Laghu, Tikshna Guna* its spreads through channels and clears the accumulated *Doshas*. It has a soothing effect which helps to prevent headache. property like *ushna virya* and *snigdha guna* which helps in reducing sneezing. It acts like lubricant in passage of nasal route hence reduces chances of irritation. Drugs having property *katu tikta rasa* and *ushna virya* due to that helps in pacifying *kapha dosha* and therefore rhinitis symptoms subside. Oils having property of *snigdha gun* which helpes in reducing itching in nasal passage.All the above effects were observed during the trial and after treatment. In this study was having highly significance results in *Nasasrava, Nasaavarodha, Kshavathu & Shirashoola.*

REFERENCES

1. Wheatley, LM; Togias, A (29 January 2015). "Clinical practice. Allergic rhinitis". The New England Journal of Medicine. 372 (5): 456–63. Doi: 10.1056. WHO journal, June 2008
2. P. Kasinath Sastri and Dr.Gorakha Nath, *"Caraka Samhita of agnivesachikitsasthana* 26th chapter", reprint edition 2013, Varanasi, Choukhamba Sanskrit Sansthan,.
3. Kaviraj dr. ambikadattaShastri, Sushruta Samhita, Uttartantra, Vol- 2, chap 24 Varanasi, Choukhamba Sanskrit Sansthan, edition-2012, sloka- 6,7, page no-153,154
4. Yadunandanopadhyaya, Madhavanidana, Vol 2 edition 2004, Published by Varanasi, Choukhamba Sanskrit Sansthan, Page- 258-261
5. Davidson, Principles and practice of Medicine, 6th chapter, 19th edition- 1995, Published by Lewington, Page- 566,567.
6. PL Dhingra. Disease of Ear, Nose & Throat, Published by Elsevier, NewDelhi,3rd Edition, A division of reed Elsevier India private Limitade, 2004, Page. 204-207
7. Kaviraja Atrideva Gupta, *"Astangahrdayam Uttara sthana* 19th chapter", reprint edition 2016, Varanasi, Choukhamba Sanskrit Sansthan,.
8. Dr. Indradev tripathi and Dr. Daya Shankar tripathi, "Yogratnakar nasaroganidanchikitsa", 4th edition, Choukhambha Krishna das academy, Varanshi.
9. Bhav Mishra, *"Bhavaprakasha*65th chapter", edition 2013 chaukhambha Sanskrit sansthan, Varanas

Table No. 1 Symptoms and Sign:

Subjective	
***Nasasrava* (Nasal discharge)**	Watery discharge ++
***Nasaanaha* (Nasal obstruction)**	++
***Kshavathu* (sneezing)**	+++
***Shirahshoola* (headache)**	+
***Swarbhed* (Sore throat)**	NAD

Objective	
Nasaraktata (Congestion and ITH)	**NAD**

Treatment

Pratimarsh Nasya with Chaturajata Taila

Dose	2-2 drops each nostril
Duration	Twice in a day(for 7 days)

Table 2: Drug Review

	Drugname	**MedicinalPropertiesRasa**	**Guna**	**Vipak**	**Doshaghanta**
1	*TWAK(Dalchini)(Cinnamommum* Zelynica)	katu,tiktamadhur	Laghu,ruksha.	katu	vatshamak
2	*ELA* (ElatteriaCordomomum)	Katu,Madhur	Laghu,ruksha	katu	Kaphavathar
3	*TEJPATRA* (CinnamommumTamala)	Katu,tikta,Madhur	Laghu, rukshateekshna	katu	Kaphavatshamak
4	NAGKESAR(Musea ferra)	Kasahya,tikta,	Rukshateekshn,laghu	Katu	Kaphapittashamak

Table 3: Chemical Composition

	Drugs	**Chemical Composition**	**Action**
1	TWAK(DALCHINI)	Cinnemaldehyde, Eugenol, Benzaldehyde, Linalool	Anti - oxidant, Anti - microbial, Anti- inflammatory,
2	ELA	Camphene, Linalool, Menthone Bornneol	Anti - biotic, Anti - spasmodic, Anti -allergic, Anti-inflammatory.
3	TEJPATRA	Cinnamaldehyde, Linalool, alpha–beta - pinene.	Anti - oxidant, Anti - inflammatory, Anti-carcinogenic, Immunomodulator
4	NAGKESAR	Mesuol, Bioflavononec, MesuaferroneA	Anti - oxidant, Immunomodulator,Anti- fungal.

Table 4: Change in Symptoms Before And After Treatment

Subjective parameters	BT	AT
Nasasrava (Nasal discharge)	2	0
Nasaanaha (Nasal obstruction)	2	0
Kshavathu (sneezing)	3	1
Shirahshoola (headache)	1	0
Swarbhed (Sore throat)	0	0

RESEARCH ARTICLE

Literary Research on Pramehari Rasa – Sagandha Sagni Moorchhana of Parada

Madhav Maheshwari[1]* and Anitha Hosur [2]

[1]M.D. Scholar, Department of Rasashashtra Evum Bhaishajya Kalpana, Parul Institute of Ayurveda, Parul University, Vadodara, Gujarat, India.
[2]Head and Professor, Department of Rasashashtra Evum Bhaishajya Kalpana, Parul Institute of Ayurveda, Parul University, Vadodara , Gujarat, India.

Received: 21 Sep 2024 Revised: 03 Nov 2024 Accepted: 18 Jan 2025

***Address for Correspondence**
Madhav Maheshwari
M.D. Scholar, Department of Rasashashtra Evum Bhaishajya Kalpana,
Parul Institute of Ayurveda,
Parul University,
Vadodara, Gujarat, India.
E.Mail: maheshwarimadhav47@gmail.com

ABSTRACT

Formulations in Rasashastra are classified into 4 divisions. Kharaliya Rasayana are the preparations, which involve grinding, and mixing of ingredients in a mortar and pestle. Parpati Rasayana are thin, flake-like preparations obtained by specific heating and cooling techniques. Kupipakva Rasayana are formulations prepared in sealed glass bottles with controlled heating. Pottali Rasayana are compact, pill-like preparations that are made by encapsulating ingredients in a cloth or container and then processing with heat. Despite its significant role in treating Prameha and other diseases, there are currently no research articles on Pramehari Rasa. Comprehensive literature research on the Kupipakva aspect of Pramehari Rasa elaborated including Standard Operative Procedure, Dose,Anupana, Indications as per Rasayogasagara. Kupipakva Rasayanas, which are potent Parada preparations for managing chronic conditions like Prameha (diabetes), are produced using a specialized technique using Kupi that enhances their therapeutic efficacy. This technique involves precise heating methods and controlled conditions. Pramehari Rasa likely exhibits properties characterized by Katu, Tikta and Kashaya Rasa, with Snigdha (unctuous) and Sara (fluid) Guna, Anushna Sheeta (moderate and cool) Veerya, and Madhura (sweet) Vipaka with Tridoshaghna (balancing all three doshas) activity. Pramehari Rasa, a herbo-mineral complex, balances Jala Mahabhuta in Prameha with antioxidant properties that aid in managing type-2 diabetes by enhancing therapeutic efficacy and stability.

Keywords: Pramehari Rasa, Parada, Kupipakva Rasayana, Prameha, Rasayogasagara, Rasashastra

INTRODUCTION

Rasashashtra is a science where the unique composition of chetana and achetana dravya becomes a tool to overcome different complicated diseases. Formulations in Rasashastra are classified into four main divisions under the umbrella of Parada Moorchhana[1] :

1. **Kharaliya**: Mortar-based formulations
2. **Parpati**: Flake-based formulations
3. **Kupipakva**: Sealed-bottle formulations
4. **Pottali**: Encapsulated formulations

Kharaliya Rasayana are the preparations which involve the comminution and homogenization of ingredients using a mortar and pestle, facilitating intimate mixing and particle size reduction to enhance bioavailability and uniformity. **Parpati Rasayana** are characterized by thin, flake-like structures produced through precise thermal processing techniques that involve controlled heating and subsequent rapid cooling. This process ensures the formation of stable, layered structures with enhanced chemical stability and therapeutic efficacy. **Kupipakva Rasayana** preparations are meticulously crafted in sealed glass containers under controlled conditions of temperature and time. This method not only prevents contamination but also allows for the gradual fusion and transformation of ingredients under certain heat and pressure, resulting in formulations with improved solubility, stability, and bioactivity. **Pottali Rasayana** are compact, pill-like formulations created by encapsulating a blend of finely powdered herbs and minerals in cloth or another suitable material. They undergo specialized processing techniques involving heat application, which facilitates the integration of active constituents while maintaining their therapeutic integrity and controlled release properties. Based on Gandhaka, Kupipakva Rasayana are classified into two:

a. **Sagandha:** This type of Kupipakva Rasayana incorporates purified sulfur in the formulation.
b. **Nirgandha:** Kupipakva Rasayana without incorporating purified sulfur in the formulation.

Based on Agni, Kupipakva Rasayana are classified into two:

a. **Sagni:**Kupipakva Rasayana which involves the use of fire during its preparation process.
b. **Niragni:**Kupipakva Rasayana which doesn't involve the use of fire during its preparation process.

According to the literature Rasayogasagara there are 8 references [2] in the name of Pramehari Rasa which includes Kharaliya and Kupipakva method of preparation. Pramehari Rasa is a herbo-mineral preparation commonly prescribed by Ayurvedic physicians. It plays a significant role in treating various diseases, including Prameha (Diabetes). However, despite its importance, there is a lack of research articles specifically on Pramehari Rasa. In this context, comprehensive literature research on Pramehari Rasa is essential. This research focuses on the ingredients, standard operating procedures (SOP), and the scientific justification for its probable mode of action in managing Prameha.

AIMS

- Comprehensive literary study of Pramehari Rasa with respect to its Preparation, Mode of Administration and therapeutic application.
- Understanding the scientific rationale of its Pharmaceutical and therapeutic profile.
- Elucidation of importance of adjuvant (Anupana) and Diet restrictions (Pathyapathya) in administration of Pramehari Rasa.

MATERIALS AND METHODS

In the present study, preparation of Pramehari Rasa [3] as per guidelines of Rasayogasagara will be elaborated. Pramehari Rasa is a formulation containing Sulfur along with Mercury and other components, prepared in a

temperature- resistant glass bottle by application of specific range and pattern of heat by sublimating the product adopting the Kupipakva method of preparation (Sagandha Sagni Kupipakva Rasayana).

Standard Operative Procedure (SOP):
Standard Operative Procedure of Pramehari Rasa can be explored under three headings:

Poorva karma
a. Identification, collection and authentication of Raw Materials
The identification, collection, and authentication of raw materials ensure their quality and suitability for use in Kupipakva medicine preparation.

b. Preparation of Bottle (Kupi):
Amber colored bottle is preferred and is applied with consequent seven layers of cloth smeared with paste of Gopichandana (Multani Clay/ Fullers Earth) and water. Each layer to be applied after proper drying of the previous layer otherwise it may create air gaps leading to breaking of kupi. Multani Clay has got the high binding capacity due to composition of hydrated aluminium silicates, magnesium and calcium [4]. Bottle is prepared in such a way as by this it can sustain high temperature for a long duration.

c. Preparation of Equipment:
Mortar and Pestle (Khalvayantra), Vessel, Gas stove, Amber coloured Glass Bottle (kachakupi), Cotton Cloth, Multani Mud, Lavana yantra, Knife, Pyrometer, Glass container.

d. Preparation of Pre-Material:
1) Purification of Ingredients such as Parada, Gandhaka.
2) Kajjali Preparation (Black sulphide of Mercury) is to be performed by continuous Trituration of Prescribed quantity of ShodhitaParada (Purified Mercury) and Shodhita Gandhaka until the mixture turns black like collyrium and devoid of luster/shining particles.
3) Levigation Process (Bhavana):
Preparation of Kwatha: Decoction of Pippali is prepared by adding 8 parts of water to coarsely powdered Pippali (Long Pepper) and reduced to half part by boiling over a mild flame on a gas stove. When half of the water gets evaporated then prepared decoction to be filtered. Similarly prepare Haritaki Kwatha using the same method.
The kajjali to be processed by Bhavana method i.e. subsequently levigating with quantity sufficient with decoctions of Pippali (Long Pepper) and Haritaki (Terminalia Chebula) for three hours each separately and dried thoroughly. Thus, formed Pre-Material is dried and stored in a sterile glass container.

e. Filling into Glass Bottle: Thus, prepared Pre-Material is to be filled into specially prepared Glass bottle as mentioned above (Kupi). The material is to be filled only up to 2/3rd of the bottle and 1/3rd to be kept empty for proper sublimation of the final product to take place.

f. Placement of Glass Bottle in LavanaYantra (KupiSthapana):
The glass bottle is then placed in the Lavana Yantra at the center. Initially at the base 1 to 2 kg of Lavana (Salt) to be filled in yantra and after placing the Kupi, again Lavana is to be filled until the neck portion of the Glass bottle. This yantra provides uniform temperature and will be retained for more time.

Pradhan karma
a. Application of Moderate Heat:
Author specified to apply madhyamagni (moderate heat) for 4 yama (12 hours) using a lavanayantra (apparatus for heating). Temperature is monitored by inserting a pyrometer to get appropriate formation of compound. Following stages may be seen during Paka kala. Melting of Pre-Material can be appreciated. During this stage, fumes and flames of sulfur will appear. It's important to take precautions to clear any sulfur deposits that have adhered to the

inner surface of the bottle's neck. Red-hot iron rod (taptashalaka) to be used to remove these deposits, which accumulate as the fumes of sulfur escape. If not cleared, the sulfur buildup can block the bottle's mouth, potentially causing it to burst. Once the flame appears, it should observe a suryodayavatvarna (the red hue seen at sunrise), indicating the formation of the compound. At this point, a copper coin test to be conducted and then corked the mouth of the bottle. After corking, the bottle Lavana (Salt) at the neck portion is to be removed to ensure effective sublimation of the product takes place. After 12 hours of heating, it has to be stopped and should be left for self-cooling (Swangasheeta).

Paschat Karma

a. Breaking the Bottle: Kupibhedana (breaking the bottle) after swangasheeta (self- cooling).

b. Collection of Product: Sublimated product at the neck portion to be collected and observed for organoleptic characters.

c. Addition of other Ingredients: Obtained product to be mixed with Abhraka Bhasma (*Mica calx*) and Loha Bhasma (*Iron calx*) in the prescribed quantity and proper trituration to be performed till homogenous mixture is obtained.
d. Storage: Thus, prepared Pramehari Rasa to be stored in clean sterile glass container.
Dose: 3 Ratti (375 mg).

Adjuvant drugs (Anupana): Sharkara (Sugar), Madhu and GuduchiSatva (Honey and Extract of Tinosporacordifolia), Madhu and Pippali (Honey and Long Pepper)

Indications: Prameha (Diabetes), Yakshma (Tuberculosis), Pandu (Anemia), Kamala with Haridra Varna (Jaundice with Turmeric colored skin), Pradara (Leucorrhea)
Insight into Formulation Composition [5-11] given in **Table 1** while details of ingredients [5-12] given in **Table 2, 3**.

RESULTS AND DISCUSSIONS

Kupipakva Rasayanas are regarded as the most potent among various Parada preparations due to their minimal dosage, rapid action, and the non-recurrence of diseases. These dosage forms are particularly beneficial in managing chronic conditions like Prameha (diabetes). They are prepared using a unique pharmaceutical technique involving a sealed glass bottle and heated through Valuka/Lavana Yantra. This method ensures a uniform temperature, which is maintained for an extended period, enhancing the effectiveness of the preparation.

Cross Reference of Pramehari Rasa

Rasaratna Samuchhaya [13] describes a similar formulation named 'Mehari Rasa' with different Bhavanadravya i.e. **Krishna Hiranya Swarasa (juice of Daturametel)** instead of Pippali Kwatha and Haritaki Kwatha. Rasayogasagara cites Rasaratna Samuchhaya as a reference for Pramehari Rasa. However, a thorough review of Rasaratna Samuchhaya reveals no formulation explicitly named Pramehari Rasa. In the preparation of Pramehari Rasa, the author deviates from the typical Kupipakva Rasayanas by not advocating a graduated heating pattern (Kramagni). Instead, Rasayogasagara specifies maintaining a uniform moderate heat (madhmagni) for four yama, equivalent to 12 hours. The preparation involves using the Kupipakva method for Pippali and Haritaki Kwatha Bhavita Kajjali, while Abhraka and Loha Bhasma are added later. The author's intention in adding Abhraka and LohaBhasma is virtuous, as both ingredients are highly effective in managing Diabetes Mellitus Type II, Anemia, Jaundice, tuberculosis. The probable properties of Pramehari Rasa are Katu, Tikta and Kashaya Rasa, Snigdha and Sara Guna, Anushna Sheeta Veerya and Madhura Vipaka with Vata-Kapha Pradhan Tridoshaghna Activity **(Table 4)**. It is indicated for Prameha (Diabetes), Yakshma (Tuberculosis), Pandu (Anemia), Kamala with Haridra Varna (Jaundice with Turmeric colored skin), Pradara (Leucorrhea).

Role of Anupana

The drug, which is consumed after medicine or food, is known as anupana [14]. As per Acharya Sharangadhara, the drug disperses rapidly like a drop of oil on water if administered with Anupana [15]. Pramehari Rasa is one such Kupipakva Rasayana that may acts in very low doses with suitable anupana i.e. for VataPittaja condition- Sarkara, VataKapha condition-Madhu and Pipalli, Pitta Kapha condition- Guduchi Satva and Madhu. Honey is extensively used because of its antioxidant activity, which destroys free radicals [16]. Pippali acts as a bioenhancer, with piperine increasing permeability at the absorption site by modulating the lipid environment and membrane dynamics. Piperine also enhances solubility and absorption by boosting bile acid secretion, inhibiting bile acid metabolism to increase micelle formation, and interacting with intestinal epithelial cells to increase amino acid uptake and brush border membrane fluidity [17]. Recent research demonstrates that Guduchisatva exhibits anti-diabetic properties [18].

Role of Bhavana

Bhavana is a unique and distinct pharmaceutical procedure in which powdered drug or mixture of drugs is completely made wet in the liquid media and grinded until the complete absorption of liquid into the powder [19]. Bhavana of Pippali and Haritaki helps in Reduction in hardness, constant wet grinding in liquid media turns the hard material soft [20]. During Bhavana, drug particles are subjected to various stresses, leading to breaking of chemical bonds to create new surfaces and retard rejoining of the broken surfaces [21]. Particle size reduction in Bhavana can be explained by "Griffith theory," which states that all solids contain flaws (structural weakness) that may develop into a microscopic crack under stress/strain-like pressure applied during Bhavana [22]. Bhavana brings fine particles of material in contact with liquid media, facilitates the impregnation of organic/inorganic contents and inherent specific properties of the media with material, and provides favorable circumstances to accelerate the chemical reactions [23]. The shelf life of the finished products may also increase by Bhavana [24]. Bioactive compounds diffuse into the material during Bhavana, enabling the conversion of Nirendriya dravya (inorganic substances) into Sendriya dravya (organometallic or organomineral substances).

Probable Mode Of Action Of BhavanaDravya- Pippali And Haritaki

Pippali contains a large number of phytoconstituents in the aqueous extract [25]. Main chemical compounds in piper fruit are piperine, piperlongumine, piperlonguminine and methyl-3,4,5- trimehoxycinnamate [26]. Oral administration of dried fruits has shown significant anti-hyperglycemic, antilipidperoxidative and antioxidant effects in diabetic rats [27]. An aqueous extract of P. longum fruit powder showed 100% giardicidal activity [28]. Main chemical compounds in Haritaki fruit are 3,4,6-Tri-O-galloyl-D-glucose (55.87 mg/g), Chebulic acid (54.03 mg/g), β-Punicalagin (41.25 mg/g), Corilagin (40.31 mg/g), α-Punicalagin (35.55 mg/g), Chebulagic acid (29.09 mg/g), Gallic acid, 1,3,4,6-Tri-O-galloyl-β-D-glucose, Chebulinic acid, 1,2,3,4,6-Penta-O-galloyl-D-glucose, Ellagic acid, 1,6-Di-O-galloyl-D-glucose [29]. Research shows that Haritaki shows a major role in glucose transport inhibition [30]. Six extracts and four compounds of Terminalia chebula fruit exhibited antioxidant activity & phenolic compounds were found to be responsible for Antioxidant & free radical scavenging activity [31]. Research shows that Water extract of dry fruits of Terminalia chebula at a dose of 200 mg/kg body weight improved the glucose tolerance as indicated by 44% of reduction in the peak blood glucose at 2nd hour in the glucose tolerance test in diabetic. (Streptozotocin induced) rats [32]. The fruit extract of Terminalia chebula exerts a significant and dose-dependent glucose lowering effect in the rat model of metabolic syndrome [33].

Role of AusadhaSevana Kala

As per Aacharya Sharangadhara, Ausadha sevana for Prameha at Early morning without food to remove vitiated doshas from the whole body [34].

Properties Of Ingredients (Table 2, 3)

Pramehari Rasa is indicated for Prameha, Yakshma, Pandu, Kamala with Haridra Varna, Pradara. Shodhita Parada (Purified Mercury) is Yogvahi (Catalyst), Vrushya (Aphrodisiac), Balya (Tonics which Increases strength, immunity, and vitality), Rasayana (Promotes longevity and enhances overall health) so it helps in Sarva Roga. Shodhita

Gandhaka (Purified Sulfur) possesses Rasayana, Deepana (Appetizer), Pachana (Digestive), Balya, Amashoshana (Promotes digestion), Vishahara (Detoxifier) activities. Thus removes Kandu (Itching), Kustha (Leprosy), Visarpa (Erysipelas), Dadru (Ringworm), Krimi (Worms), Kshaya (Tuberculosis), Pleeha (Spleen disorders). Lauha Bhasma which contains Fe_3O_4 and γ-Fe_2O_3 composition revealed in XRD study [35] possesses following properties: Lekhana (Scraping of toxins and excess fat from the body), Vrushya, Balya, Medhya (Nootropic which Enhances cognitive function, memory, and intelligence), Varnya (which improves skin complexion and glow), Rasayana (Promotes longevity and enhances overall health), Chakshusha (Beneficial for the vision), Yogavahi (Acts as a catalyst or carrier for enhancing the action of other substances), Vajikara (Enhances sexual function, libido, and fertility), Raktavardhaka (Increases hemoglobin levels and blood formation), Vayasthapana (Slows down the aging process and promotes longevity). Thus, it is widely used in ayurvedic medicines for different diseases including Prameha, Pandu, Kamla etc. Abhraka Bhasma which contains $Mg_2O_4Si_1$ revealed in XRD study [36] possesses Rasayana, Medhya (Nootropic), Keshya (Hair tonic), Chakshushya (Good for eyes), Varnya (Complexion enhancer), Stanya (Galactagogue), Hrudhya (Cardiac tonic), Vrushya, Tvachya (Good for skin) and Deepana. Abhraka Bhasma is the choice of drugs in cases of Pandu, Kshaya, Pradara and many other incurable diseases.

Role of Pathyapathya

The diet should be prescribed according to an individual's age, strength, abhyavaharana (nature of appetite) &jaranashakti (digestive power) according to one's desha (locality), kala (time), ritu (season) [37]. Diet and regimen for individual diseases mentioned among various classical texts such as- Yava (Hordeum-vulgare), Kangu (Setariaitalica), Shyamaka (Echinochloa frumentacea), Kodrava (Paspalumscrobiculatum), Mudga (Vignaradiata), Chanaka (Cicer arietinum), Kulattha (Dolichosbiflorus), Adhaki (Cajanuscajan), all the types of bitter vegetables (TiktaShaka) eg.- Karela (Momordicacharantia), Methi (Trigonellafoenum), Patola (Vietnamese luffa), Rasona (Allium sativum), Katillaka (Momordicacharantia), Shigrupatra (Moringaoleifera), Lonika (PortulacaOleracea), Dronapushpipatra (Leucascephalotes), Guduchipatra (Tinosporacordifolia), Kakamachipatra (Solanumnigrum), Vastuka (Chenopodiummurale), fruit eg.- Jambu (Syzygiumcumini), Amalaki (Phyllanthusemblica), Kapittha (Limoniaacidissima), seeds eg.- Kamala (Nelumbo nucifera) &Utpala (Nymphaea stellata), Sarshapataila (Mustard oil), dantitaila (Baliospermummontanum oil), Ingudi tail (Balanitesaegyptiaca oil), Atasi tail (Linumusitatissimum oil) [38][39]. Above mentioned pathyaaahara, which includes beneficial dietary components, contributes to an abundance of beneficial microbes. Simultaneously, Lifestyle modifications, such as withdrawing causative factors, result in an enhancement of the beneficial human gut microbiome, which is essential for effective recovery and sustained health [40].

CONCLUSION

In nutshell, Pramehari Rasa appears to assist in balancing of water element (Jala Mahabhuta) in Prameha by intervening in the pathophysiological mechanisms i.e. SamraptiVighatana [41-43] (**Table 5**) and most of these drugs exhibit Rasayana (rejuvenating) properties, followed by Deepana (appetizer), Chakshushya (beneficial for eye health), and Balya (strength-enhancing) effects. Additionally, some of these drugs are reported to have various pharmacological activities, such as antidiabetic, antihyperlipidemic, antioxidant, and immunomodulatory effects.

Recent studies have shown that antioxidants capable of neutralizing free radicals are effective in preventing diabetes and reducing the severity of diabetic complications. Therefore, an anti-diabetic compound with antioxidant properties would be highly beneficial in type-2 diabetes wherein components of the immune system are altered, with the most significant changes occurring in adipose tissue, liver, pancreatic islets, and vasculature. Herbo-mineral complexes such as Pramehari Rasa is more stable and interactive, leading to faster therapeutic action and a longer shelf life.

REFERENCES

1. Angadi, R. A Textbook of Rasa Shastra. Varanasi: ChaukhambaSurbhartiPrakashan; 2014. p. 135.
2. Sharma H. Rasayogasagara. Varanasi: ChaukhambhaKrishnadas Academy; 2016. Vol 2. p. 90-92.
3. Sharma H. Rasayogasagara. Varanasi: ChaukhambhaKrishnadas Academy; 2016. Vol 2.p. 92.
4. Pal R, Pal Y, Kumar MV, Katiyar D, Punniyakotti S. A Progressive Stratagem Outline on Diverse Dermatological Clays. Current Drug Therapy. 2024 Mar 1;19 (2):123-9.
5. Trikamji Y.In: Gautam SD, editor. Rasamritam. Varanasi: ChaukhambhaSurbharti Prakash; 2008. p. 2.
6. Mishra G. Ayurveda Prakasha of Acharya Shri Madhava. Varanasi: ChaukambhaBharati Academy; 2007.p. 258-259.
7. Mishra B. Bhavaprakash of Bhavamishra. Varanasi: Chaukhambha Sanskrit Bhavan; 2016.p. 218.
8. Mishra B. Bhavaprakash of Bhavamishra. Varanasi: Chaukhambha Sanskrit Bhavan; 2016.p. 209.
9. Sharma S. Rasa Tarangini. 11th ed. Delhi: MotilalBanarasidas; 8th reprint 2014.p. 234.
10. Mishra G. Ayurveda Prakasha of Acharya Shri Madhava. Varanasi: ChaukambhaBharati Academy; 2007.p. 392.
11. Sharma S. Rasa Tarangini. 11th ed. Delhi: MotilalBanarasidas; 8th reprint 2014.p. 507.
12. Trikamji Y. Rasamritam. Varanasi: ChaukhambhaSurbhartiPrakashan; 2008. p. 69.
13. Shashtri KA, editor. Rasaratnasamuchhaya. 9th ed. Varanasi: ChaukhambaAmarabharatiPrakashan; 1995. Reprint 2003. p. 330.
14. Kunte A, Navare KS. Sarvangsundara of Arundatta and Ayurvedarasayana of Hemadri commentary on Astangahridaya. Varanasi: Chaukhamba Sanskrit Sansthan; 2011. p. 158.
15. Parasar R, editor. Sharangadhara Samhita. Kolkata: Baidyanath Bhawan Ltd; 1994.
16. Roh C, Jung U. Screening of crude plant extracts with anti-obesity activity. Int J Mol Sci. 2012;13(2):1710-1719.
17. Shinde SA, Chavhan SA, Sapkal SB, Darakhe RA. Potential of Piperine as a bioavailability enhancer. Int J Biol Res. 2019 Apr;4(2):3-6.
18. Katara A, Garg NK, Mathur M. View of Separation and Identification of Antidiabetic compounds in Tinosporacordifolia extract and Ayurvedic formulation GuduchiSatva by GCMS and FTIR study with subsequent evaluation of in-vitro Hypoglycemic potential. Int J Pharm Sci Drug Res. 2021;13(2):183-189.
19. Sharma S. Rasa Tarangini. 11th ed. Delhi: MotilalBanarasidas; 8th reprint 2014.p. 21,772.
20. Jung H, Lee Y, Yoon W. Effect of moisture content on the grinding process and powder properties in food: a review. Processes. 2018;6(6):69.
21. Somasundaran P, Lin IJ. Effect of the nature of environment on comminution processes. Ind Eng Chem Process Des Dev. 1972;11(3):321-31.
22. Griffith AA. The phenomena of rupture and flow in solids. Philos Trans R Soc Lond. 1921;221:163-98.
23. Sharma R, Bedarkar P, Timalsina D, Chaudhary A. Bhavana, an Ayurvedic pharmaceutical method and a versatile drug delivery platform to prepare potentiated micro-nano-sized drugs: core concept and its current relevance [retracted]. BioinorgChem Appl. 2023;2023(1). Published online 2023 Dec 20.
24. Verma P, Galib, Patgiri B, Prajapati P. Shelf-life evaluation of rasayanachurna: a preliminary study. AYU. 2014;35(2):184-6.
25. Singh S, Priyadarshi A, Singh B, Sharma P. Pharmacognostical and phytochemical analysis of Pippali (*Piper longum* Linn.). Pharma Innov J. 2018;7(6):286-289.
26. Chatterjee A, Dutta C. The structure of piperlongumine, a new alkaloid isolated from the roots of *Piper longum* Linn. (Piperaceae). Sci Cult. 1963;29:568.
27. Manoharan S, Silvan S, Vasudevan K, Balakrishnan S. Antihyperglycemic and antilipidperoxidative effects of *Piper longum* dried fruits in alloxan-induced diabetic rats. J Biol Sci. 2007;7(1):161-168.
28. Tripathi DM, Gupta N, Laxmi V, Saxena KC, Aggarwal AK. Antigiardial and immunostimulatory effect of *Piper longum* on giardiasis due to *Giardia lamblia*. Phytother Res. 1999;13(7):561-563.

29. Pellati F, Bruni R, Righi D, Grandini A, Tognolini M, Prencipe FP, et al. Metabolite profiling of polyphenols in a Terminalia chebulaRetziusayurvedic decoction and evaluation of its chemopreventive activity. J Ethnopharmacol. 2013;147(2):277-285.
30. Wang H, Fowler MI, Messenger DJ, Ordaz-Ortiz JJ, Gu X, Shi S, et al. Inhibition of the intestinal postprandial glucose transport by gallic acid and gallic acid derivatives. Food Funct. 2021 Jun 21;12(12):5399-5406.
31. Hazra B, Sarkar R, Biswas S, Mandal N. Comparative study of antioxidant and reactive oxygen species scavenging properties in the extracts of the fruits of Terminalia chebula, Terminalia belerica and Emblicaofficinalis. BMC Complement Altern Med. 2010;10:20.
32. Reddy VRC. Cardioprotective activity of the fruit of Terminalia chebula. Fitoterapia. 1990;61:517-25.
33. Singh I, Singh PK, Bhansali S, Shafiq N, Malhotra S, Pandhi P, Singh AP. Effects of three different doses of a fruit extract of Terminalia chebula on metabolic components of metabolic syndrome, in a rat model. Phytother Res. 2010 Jan;24(1):107-12.
34. Pawar AD, Pagare RP. Analysis of relevance of AushadhaSevana Kala (time of drug administration) according to Sharangadhara Samhita W.S.R. to Lekhana Karma. World J Pharm Res. 2017;6(5):458-463.
35. Singh N, Reddy KRC, Prasad NK, Singh M. Chemical Characterization of Lauha Bhasma by X-Ray Diffraction and Vibrating Sample Magnetometry. Int J Ayurvedic Med. 2010;1(3):143-149.
36. Singh RK, Kumar S, Kumar AA, Kumar S, Kar M. Study on physical properties of Indian based ayurvedic medicine: Abhrakhbhasma as nanomaterials by employing modern scientific tools. GSC Biol Pharm Sci. 2018;5(2):041-047.
37. Mishra PH, Gaikwad SD. Pathya-ApathyaViharas for PramehiRugna–A Review. World J Pharm Res. 2022;11(16):573-579.
38. Shastri K. Charaka Samhita of Agnivesh. Varanasi: Chaukhamba Bharti Academy; 2020.Volume 2. p. 236
39. Sharma P, Keshav P. Pathya-apathyavinischayam. Mumbai: Khemraj Shri Krishna Das, Shri Venkateshvara Printing Press; 1896. p. 63.
40. Pareek HK, Singh OP. Role of PathyaAahar (Healthy diet), Agni (Digestive power) and Gut microbiome in Madhumeha (Diabetes Mellitus). AdvBiores. 2022 Jul;13(4):210-213.
41. Shastri K. Charaka Samhita of Agnivesh. Varanasi: Chaukhamba Bharti Academy; 2020. Volume 2. p.205.
42. Sharma P, Sumit, Sahu AK, Bakuni H, Padhar BK, Rawat S. Role of KledaDushya in Prameha (Diabetes Mellitus): A Critical Review. *Int Res J Ayurveda Yoga*. 2022;5(5):152-155.
43. Jyani HP, Dahilekar H, Dahilekar SG, Malviya G. A review concept of Kleda in Ayurveda literature. J EmergTechnolInnov Res. 2021;8(6):e117-20.

Table 1: Ingredients of Pramehari Rasa with Latin name and proportion

Sr. No.	Ingredients	Latin name	Proportion
1.	Shodhita Parada	Purified *Hydrargyrum*	2 part
2.	Shodhita Gandhaka	Purified *Sulfur*	1 part
3.	Pippali Kwatha	*Piper longum*	Q.S.
4.	Haritaki Kwatha	*Terminalia chebula*	Q.S.
5.	Abhraka Bhasma	*Mica calx*	1 part
6.	Lauha Bhasma	*Iron calx*	1 part

Table 2: Ingredients with its properties

Sr. No.	Ingredients	Rasa	Guna	Veerya	Vipaka	Doshakarma
1.	Shodhita Parada [5]	Shadarasa	Sara, Guru, Snigdha	-	-	Tridoshghna
2.	Shodhita	Madhura,Katu	Snigdha	Ushna	Katu(A.P)	Pitta vardhaka,

	Gandhaka [6]	, Tikta, Kashaya	, Sara		Madhura (Rasarnava)	Kaphavataghna
3.	Pippali Kwatha [7]	Katu	Snigdha , Laghu	Anushn a	Madhura	Vatakaphaghna
4.	Haritaki Kwatha [8]	Kashaya Pradana	Laghu, Ruksha	Ushna	Madhura	Tridoshaghna
5.	Abhraka Bhasma[9]	Madhura	Snigdha	Sheeta	Madhura	Tridoshaghna
6.	Lauha Bhasma [10, 11]	Tikta, Madhura, Kashaya	Sara, Ruksha, Guru	Sheeta	Madhura	Kaphapittaghna , Vatavardhaka

Table 3: Action and Vyadhikarma of ingredients

Sr. No.	Ingredients	Dravya Karma /Properties of Drugs	Vyadhi Pratyaneeka Karma /Therapeutic Action
1.	Shodhita Parada [5]	**Yogvahi,**Vrushya, **Balya, Rasayana**	Vranashodhana, Vranaropana, Krimi, **Sarvarogahara with tad tad Yoga**
2.	Shodhita Gandhaka [6]	**Rasayana, Deepana, Pachana, Balya, Amashoshana, Vishahara**	Kandu, Kustha, Visarpa, Dadru, Krimi, Kshaya, **Pleeha**
3.	Pippali Kwatha [7]	**Deepana**, Vrushya, **Rasayana**, Rechani	Shwasa, Kasa, Udra, Jwara, Kustha, Prameha, Gulma, Arsha, **Pleeha**, Shoola, Amavata
4.	Haritaki Kwatha [8]	**Deepana**, Pachana, Anulomana, Medhya, **Rasayana**, Chakshushya, Ayushya, Bruhana, Anulomana	Shwasa, Kasa, **Prameha**, Arsha, Kustha, Shotha, Udara, Krumi, Visarpa, Grahani, Vibandha, VishamaJwara, Gulma, Adhmana, Vrana, Chhardi, Hikka, Kanthamaya, Hrudroga, Kamala, Shoola, Anaha, **Pleeha, Yakruta**, Ashmari, Mutrakrutchh, Mutraghata
5.	Abhraka Bhasma [9, 12]	**Rasayana**, Medhya, Keshya, Chakshushya, Varnya, Stanya, Hrudhya, Vrushya,Tvachya, **Deepana, Balya**	Kasa, Shwasa, Pandu, Kshaya, JeernaJwara, **Prameha**, ParinamaShoola, Amlapitta, Grahani, Shweta Pradara, Apachi, Shotha, Arsha, Sheetapitta, Brahma, Sarvaroga
6.	Lauha Bhasma [10, 11]	Lekhana, Vrushya, **Balya**, Medhya, Varnya, **Rasayana**, Chakshusha, **Yogavahi**, Vajikara, Raktavardhaka, **Vayasthapana**	Garavisha, Shoola, Shotha, Arsha, **Pleeha**, Pandu, **Prameha**, Meda, Meha, Krumi, Kustha,Udara

Table 4: Probable Rasa-Guna-Veerya-Vipaka and Doshakarma of Kupipakva Pramehari Rasa

Rasa	Guna	Veerya	Vipaka	Doshakarma
Katu, Tikta and Kashaya Rasa Pradhan Yoga/formulation	Snigdha and Sara guna Pradhan Yoga	Anushna Sheeta	Madhura	Tridoshaghna

Table 5: Samprapti and Samprapti Vighatana of Prameha

Samprapti of Prameha[37]	**SamraptiVighatana by Pramehari Rasa**
Hetusevana- **Aahara:** Dadhi, Gramya , Anupa Mamsarasa, Navanna, Navapana, Gudavaikruta, All types of	Katu, Tikta and Kashaya rasa of Pramehari Rasa helps to control Kaphaja Prameha. Sara and Snigdha guna improves strotasa vaigunya in VatajaPrameha.

Kaphakaraaahara **Vihara:** Sedentary lifestyle, excessive sleep, All types of Kaphakaravihara ⬇ Leading to aggravation of Kapha ⬇ Aggravated Kapha spreads throughout the body ⬇ Vitiation of Kapha, Pitta, Vata, Meda, Rakta, Shukra, Ambu, Vasa, Lasika, Majja, Rasa, Oja, Mamsa ⬇ Accumulation in Basti ⬇ Prameha	Madhura Vipaka helps to control Vataja Prameha and PittajaPrameha. Trido shajaPrameha requires Trido shahara medicine in form of Pramehari Rasa. Kleda representing the Jala Mahabhoota (water element) within the body, possesses Drava (liquid), Snigdha (unctuous), and Mridu (soft) qualities[38] [39] These characteristics contribute to the softening and loosening of body tissues in conditions like Prameha. Meanwhile, Pramehari Rasa actively helps to balance Kleda by maintaining Mutra (urine) and Sweda (sweat) ensuring overall homeostasis.

Indian Journal of Natural Sciences *www.tnsroindia.org.in ©IJONS*

Vol.15 / Issue 88 / Feb / 2025 *International Bimonthly (Print) – Open Access* *ISSN: 0976 – 0997*

REVIEW ARTICLE

Recent Advances in Endodontic Irrigation System : A Review

Mukund V Singh[1], Vaishnavi Saboo[2]*, Aparna Palekar[3] and Basawaraj Biradar[1]

[1]Professor, Department of Conservative Dentistry and Endodontics, Rural Dental College, PIMS, Loni, Ahmednagar, Maharashtra, India
[2]Postgraduate Student, Department of Conservative Dentistry and Endodontics, Rural Dental College, PIMS, Loni, Ahmednagar, Maharashtra, India
[3]HOD and Professor, Department of Conservative Dentistry and Endodontics, Rural Dental College, PIMS, Loni, Ahmednagar, Maharashtra, India.

Received: 21 Nov 2024 Revised: 03 Dec 2024 Accepted: 27 Jan 2025

***Address for Correspondence**
Vaishnavi Saboo,
Postgraduate Student,
Department of Conservative Dentistry and Endodontics,
Rural Dental College, PIMS, Loni,
Ahmednagar, Maharashtra, India.
E.Mail:

ABSTRACT

Complete removal of the remaining necrotic and viable pulp tissue, microorganisms, The most fundamental mechanical activation technique is manual irrigant agitation, which can be carried out using various systems. With needles or cannulas with varying gauges, an irrigant is dispensed into a canal with this technique, either passively or with agitation. NaviTipsprovide controlled delivery of irrigants and resin sealers to the apex. The evolution of the manual systems resulted in the introduction of instruments that may be rotated by handpieces at low speed inside the canal fill with irrigant. EDDY® tips operate at a high frequency of up to 6,000 Hz using an air scaler. The vibrations generated are transmitted to the polyamide tip, which, due to the material's unique properties, moves in a high-amplitude oscillating motion. Nusstein developed a needle-holding adapter for use with an ultrasonic handpiece. During ultrasonic activation, a 25-gauge irrigation needle is utilized in place of an endosonic file. A new device using sound energy far beyond the ultrasound range, GentleWave (Sonendo, Orange, CA, U.S.A.), was recently tested for its ability to dissolve soft tissue, and compared it to other forms of irrigation, including ultrasound.

Keywords: Complete removal of the remaining necrotic and viable pulp tissue, microorganisms, The most fundamental mechanical activation technique is manual irrigant agitation, which can be carried out using various systems.

INTRODUCTION

Complete removal of the remaining necrotic and viable pulp tissue, microorganisms, and microbial toxins from the root canal is necessary for a successful endodontic procedure.[1] The primary objective of the endodontist is to eliminate infected tissue and bacteria from the root canal, facilitating the healing of periapical lesions and preventing infections in the surrounding periradicular tissue.[2] So, the irrigation of the root canal with antibacterial solution is an important step. The efficacy of irrigation depends on working mechanism of the irrigant and ability to bring the irrigant in contact with the element, material and structure.[3] Thorough cleaning of the root canal system is a crucial requirement for any effective irrigation system. irrigation system should deliver sufficient volume of irrigant all the way to working length, have adequate flow and to be effective in debriding the complete root canal system.[4]
So to debride tissue from anatomical complexities adjunctive aids for irrigation are required.

Types of Irrigation Agitation Techniques And Device Manual Agitation Techniques
A)Syringe irrigation with needle/cannulas
B)Brushes
C)Manual dynamic agitation
Machine Assited Technique
A)Rotary brushes
B)Continuous irrigation during rotary instrumentation
C)Sonic irrigation
D)Ultrasonic irrigation technique
a)Continuous
b)Passive
E)Pressure alternation devices
a)Endo vac system
b)Rins Endo system
c) The Safety-Irrigator
d) Gentle Wave
F)Photo Activated Disinfection
G)Ozone based delivery system
H)Laser
I) XP Endo finisher

Manualagitation Technique
The most fundamental mechanical activation technique is manual irrigant agitation, which can be carried out using various systems. The easy way to achieve this effect is moving vertically and passively the endodontic file within the root canal. The file promotes the irrigant penetration and reduces the presence of air bubbles in the canal space but does not improve the final cleaning.[5]

Syringe Irrigation With Needles/Cannulas
With needles or cannulas with varying gauges, an irrigant is dispensed into a canal with this technique, either passively or with agitation. An ISO size 80 canal's apex can be reached by a 21-gauge tip, a size 50 canal by a 23-gauge tip, a size 35 canal by a 25-gauge tip, and the apex of a size 25 canal by a 30-gauge tip. A 27-gauge needle tip size is ideal for standard endodontic operations.[6] At present, the 30G needle could be considered the standard, but slightly larger and smaller ones are also in use. Open-ended tips express irrigant out the end toward the apex and consequently increase the apical pressure within the canal. Closed-ended irrigant tips are side-vented and thus creating more pressure on the walls of the root canal and improve the hydrodynamic activation of an irrigant and hence reducing the chance of apical extrusion.[7] Open-ended needles should be placed at 2–3mm short of working length, but closed-ended needles must placed even closer (within 1mm) Positioning the needle close to the working

length (WL) has been advocated to effectively clean the apical part of the root canal with Syringe & needle, because the irrigant seldom flows beyond 1mm from the tip of the needle.[8] The irrigant cannot reach farther than 1mm apically to the needle tip in root canals with an apical size less than 30.

Other needles

NaviTipsprovide controlled delivery of irrigants and resin sealers to the apex.

Have a safe, rounded end and are rigid in the majority of the shank to prevent bending; the last few millimeters are flexible to facilitate navigation even through curved canals. PRORINSE Flexiglide needle for irrigation also easily follows curved canals. Fig. 1: depicts different types of needles for irrigation Fig1: Types of needles

a) NaviTipFx

b) NaviTip

c) Flexiglide.

Rotary Brushes

Brushes are not directly used for delivering an irrigant into the canal spaces. They are adjuncts that have been designed to assist debridement of the canal walls or agitation of root canal irrigant. They might also be indirectly involved to facilitate with the transfer of irrigants within the canal spaces. NaviTipFx is a 30-gauge irrigation needle features a brush &was introduced commercially by Ultradent company.[9,10] The Endobrush could not be used to full working length because of its size, which might lead to packing of debris into the apical section of the canal after brushing.[11]

Manual Dynamic Agitation

An irrigant must be in direct contact with the canal walls to be effective. Its usually difficult for the irrigant to reach the apical portion of the canal because of the so-called vapor lock effect.[12,13] The gently moving well-fitting gutta-percha master cone up and down in short 2 to 3 mm strokes (manualdynamic irrigation) within an instrumented canal can produce an effective hydrodynamic effect and significantly improve the displacement and exchange of any given reagent. [14]

Following factors affect manual dynamic irrigation:

(1) The push-pull motion of a well fitting gutta-percha point in the canal can generate higher intracanal pressure changes during pushing movements, resulting to more effective delivery of irrigant to the "untouched" canal surfaces;

(2) The frequency of push-pull motion of the gutta-percha point (3.3 Hz, 100 strokes per 30 seconds) is higher than the frequency (1.6 Hz) of positive-negative hydrodynamic pressure generated by RinsEndo, possibly which generates more turbulence in the canal.

(3) The gutta percha point's push-pull action most likely works by physically moving, folding, and cutting fluid in the root canal system that is "viscously dominated flow."

Machine Assisted Agitation Technique

The evolution of the manual systems resulted in the introduction of instruments that may be rotated by handpieces at low speed inside the canal fill with irrigant. Instruments such as plastic files can show a smooth surface and increased taper, or even a surface with lateral plastic extensions.[15,17]

Rotary brushes

Ruddle Brush

A rotary handpiece-attached microbrush has been used by ruddle to facilitate debris and smear layer removal from instrumented root canal. The brush consists of a shaft or shank and a tapered brush section. During debridement phase, microbrush rotates at approximately 300 rpm. These brushes are not directly used to deliver irrigants into the canal spaces; instead, they serve as adjuncts designed for agitating root canal irrigation.

Canal Brush

Canal Brush is another endodontic microbrush that has recently been made commercially available. This highly flexible microbrush is made entirely from polypropylene and can be used manually with a rotary motion. Fig 2: Depicts rotary brushes Fig 2: Rotary Brushes

Continuous Irrigation During Rotary Irrigation

The Quantec-E irrigation system

(Sybron Endo, Orange, CA) is a self-contained fluid delivery unit which is attached to the Quantec-E Endo System .It includes a pump console, two irrigation reservoirs, and tubing that ensures continuous irrigation during rotary instrumentation.[18] Continuous agitation of the irrigant during active rotary instrumentation leads to a larger volume of irrigant being produced, extends the contact time of the irrigant, and promotes greater penetration depth within the root canal.[19] Fig3: Quantec E system Figure courtesy:Matthew J. Walters *et al.* (2002)[45]

The Self Adjusting File(Saf)

The SAF system is a shaping and cleaning system developed for minimally invasive endodontic procedures. It is operated with the specific handpiece head (RDT, ReDent) and an irrigation pump(VATEA pump) that allows continuous flow of irrigant through the hollow file.It is available in two diameters:1.5-2.0.Both are extremely compressible. The 0.5mm file compressed to the dimension of 20 K file and 2.0mm file compressed to the dimension of 35 K file.[20] Fig. 4: SAF with handpiece containing an irrigation hub made up of polyethylene tube which is connected to the VATEA irrigation pump Figure courtesy: Misgar BA *et al.* (2021)[46]

Sonic Irrigation

Tronstad *et al* in 1985 introduced Sonic instruments .It works in lower frequency (1–6 kHz) and produces smaller shear stresses than ultrasonic irrigation. There are numerous sonic irrigation devices available on the market. The activation of disinfectants through acoustic streaming enhances and completes the irrigation process, improving the success rate of endodontic treatments.

Vibringe

The Vibringe system is the first endodontic sonic irrigation system that enables the delivery and activation of the irrigation solution within the root canal. Developed by Vibringe BV in Amsterdam, The Netherlands, this innovative system integrates battery-powered vibrations (9000 cpm) with manual irrigation of the root canal. It has better irrigation then the syringe irrigation in removing the debris from the apical two third of the rootcanal.[21]

Sonic Air®

The Sonic Air® 1500 unit is an air-driven device producing vibrations ranging from 1,500 to 3,000 Hz (manufacturer data). The Rispi-Sonic® files are stainless steel and have barbs along the length of the fi le in a spiral design. This file is designed to cut dentin along with it to agitate the irrigant solution with the canal. Irrigant is refreshed &delivered intermittently through needle delivery and not by the handpiece.[22] Fig 6: Depicts

a)Sonic Air® 1500

b) Rispi-Sonic® file Fig Courtsey : John M. Nusstein *et al.* (2018)[47]

Endo Activator

It is a mechanical system which consist of hand piece and various polymer tips. These tips are strong and flexible and do notbreak easily. They are smooth and they don't cut the dentin. It removes the smear layer, debride the instrumented portion of the root canal system, and dislodge the biofilm within long, narrow, and highly curved canal of molar teeth. It provides 10,000 rpm per minute.[23,24,25] Fig 7: Endoactivator Fig Courtesy: Caicedo, Ricardo. (2013)[48]

Eddy System

EDDY® tips operate at a high frequency of up to 6,000 Hz using an air scaler. The vibrations generated are transmitted to the polyamide tip, which, due to the material's unique properties, moves in a high-amplitude oscillating motion. This three-dimensional movement induces cavitation and acoustic streaming, resulting in improved cleaning efficiency.

Ultrasonic Irrigation

ULTRASONIC IRRIGATION: Ultrasonic energy oscillates at frequencies between 25 and 30 kHz 32,33, producing greater frequencies than sonic energy but with low amplitudes. Two types of ultrasonic irrigation are present one is simultaneous ultrasonic instrumentation and irrigation (UI) and another one is passive ultrasonic irrigation (PUI), operates without simultaneous instrumentation.[26]

Continuous Ultrasonic Irrigation

Nusstein developed a needle-holding adapter for use with an ultrasonic handpiece. During ultrasonic activation, a 25-gauge irrigation needle is utilized in place of an endosonic file. This eliminates the possibility of needle breakage when ultrasonic activation is performed at the maximum power setting. In this case, an irrigant is administered from intravenous tubing connected via a Luer-lok to an irrigation delivery syringe, while the ultrasonic handpiece concurrently activates the needle. The irrigant is supplied to the apical one-third through a continuous flow.[27,,28] At the moment, Dentsply Tulsa Dental Specialities and Dentsply are the two commercially available products for clinical use to deliver CUI. Vista Dental Products Stream Clean TM Flo-thru tip and ProUltra® PiezoflowTM Ultrasonic tip. The Piezoflow tip is a blunt-ended stainless steel needle with a 25-gauge size, whereas the StreamClean™ tip is a 30-gauge blunt-ended NiTi tube featuring external serrations.

Proultra Piezo Ultrasonic Needles

To irrigate and activate the liquids, Dentsply Tulsa Dental Specialities has introduced the ProUltraPiezoFlow. The device primarily includes an ultrasonically activated needle linked to a sodium hypochlorite (NaOCl) reservoir. It is utilized for nonsurgical root canal irrigation by applying ultrasonic vibrations. A piezo-electric ultrasonic energy generator is used in conjunction with the piezoflow irrigation needles to enable tip oscillation.The ultrasonic needle's luer-lock fitting is connected to a syringe or other irrigation source, and the irrigant is removed by conventional . Fig 8:Dentsply Tulsa Dental Specialties ProUltra® Piezoflow™ Ultrasonic tip (Dentsply Tulsa Dental Fig Courtesy: John M. Nusstein *et al*. (2018)[47]

Passive Ultrasonic Irrigation

The term passive ultrasonic irrigation was given by Weller et al in the year 1980.[29] It is a non-cutting technology which reduces creating abnormal shapes in root canal system. In Passive Ultrasonic Irrigation (PUI), energy is transferred from a file or smooth oscillating wire to the irrigant through ultrasonic waves, which create two physical effects: streaming and cavitation of the irrigant solution. The fluid rapidly moving in a circular or vortex configuration around the vibrating file is known as the acoustic stream. Cavitation is the process of forming steam bubbles or the expansion, contraction, and/or distortion of existing bubbles in a liquid. The main goal of this treatment is to remove the pulp tissues, dentinal debris, smear layer and bacteria from the root canal.[30]

Pressure Alteration Devices

It's difficult to reach the apical portion of the canal due to air entrapment when the needle is placed away from the canal. If the needle is placed so close to the apical foramen increased chance of irrigant extrusion from the foramen causes iatrogenic damage to the periapical tissues. A tenable solution to this issue is the employment of pressure alternation devices for simultaneous irrigant supply and aspiration.[31]

Endovac System

Discus Dental Company provided endo Vac apical negative pressure irrigation. It employs a suction technique to remove trash and promote irrigation flow in the canal's apical two thirds. The Master Delivery Tip, Macro Cannula,

and Micro Cannula are its three components. The Master Delivery Tip both delivers and removes the irrigant simultaneously. The Macro Cannula is used to suction the irrigant from the chamber to the coronal and middle sections of the canal. During irrigation, the delivery/evacuation tip provides the irrigant to the pulp chamber while siphoning off excess liquid to prevent overflow. The cannula in the canal creates negative pressure, drawing irrigant from the chamber down the canal to the tip, into the cannula, and out through the suction hose. This ensures a continuous flow of fresh irrigant is delivered to the working length through negative pressure. Endo vac has the ability to safely deliver the irrigants to working length without causing extrusion into the peri apical region.[32,33] Fig 9: 1)(a) Handpiece; (b) fingerpiece; (c) multiport adapter; (d) macrocannula; (e) microcannula (21, 25, 31 mm); (f) syringe 20 cc (for NaOCl); (g) master delivery tip (MDT); (h) syringe 3 cc (for EDTA); (i) MDT evacuation tubing (blue); and (j) handpiece/fingerpiece evacuation tubing (white). 2)EndoVac components: (a) macrocannula; (b) microcannula demonstrating the evacuation holes in the apical 0.7 mm; (c) master delivery tip; and (d) microcannula. Fig Courtesy: Nestor Cohenca[49]

Rins Endo System

Rins Endo was introduced by Durr Dental Co. Its based-on pressure suction technology with approximately 100 cycles per minute.[34] Its components are a handpiece, a cannula with a 7 mm exit aperture, and a syringe carrying irrigant. The hand piece is operated by a dental air compressor and has an irrigation flow rate of 6.2 ml/min. With this system, 65 ml of a rinsing solution oscillating at a frequency of 1.6 Hz is drawn from an attached syringe and transported to the root canal through an adapted cannula. McGill *et al.* assessed the effectiveness of Rinse Endo system in a split tooth model. They discovered it to be less effective in removing the stained collagen from root canal walls comparedtomanual dynamic irrigation by hand agitation of the instrumented canals with well-fitting gutta-percha points.[35]

The Safety-Irrigator

The Safety-Irrigator (Vista Dental Products) is an irrigation and evacuation system that delivers the irrigant apically under positive pressure via a thin needle with a lateral opening, while a larger needle at the root canal orifice evacuates the solution.

Ultrasound

The use of ultrasonic energy for cleaning and disinfecting root canals has a long-standing history in endodontics. Studies comparing the effectiveness of ultrasonics with hand instrumentation techniques have shown that ultrasonics, when combined with an irrigant, result in superior cleaning of the root canal system compared to irrigation and hand instrumentation alone. The processes of cavitation and acoustic streaming enhance the biological and chemical activity for optimal results. Research on the hydrodynamic reaction of an oscillating ultrasonic file suggests that both stable and transient cavitation, along with steady streaming and microstreaming, contribute to effective root canal cleaning. For ultrasonic files to be effective, they must move freely in the canal without contacting the canal walls. Goodman A et al. investigated the significance of ultrasonic preparation for optimal debridement in areas such as anastomoses between double canals, isthmuses, and fins.[145] The effectiveness of ultrasonics in the elimination of bacteria and dentin debris from the canals has been shown by Spoleti P *et al.*[36] Fig 10. A) and schematic depiction (B) of ultrasound acoustic streaming. Fig Courtesy: Gyulbenkiyan *et al.* (2023)[50]

GentleWave System

A new device using sound energy far beyond the ultrasound range, GentleWave (Sonendo, Orange, CA, U.S.A.), was recently tested for its ability to dissolve soft tissue, and compared it to other forms of irrigation, including ultrasound. The device consists of a central unit from which high pressure pumps send high speed degassed irrigant flow to a special hand piece, with a tip of the handpiece placed into the pulp chamber of the tooth. Through the study it showed that GentleWave was the only system that completely removed calcium hydroxide from molar root canals, whereas syringe-needle irrigation with and without ultrasound always left some calcium hydroxide in the canal space, particularly in the apical third of the root canals.[37]

Photo Activated Disinfection

To reduce or eradicate any remaining germs in the root canal, photo activated disinfection, or PAD, has been used into endodontic irrigation. The PAD technique uses low-intensity visible light and a non-toxic dye called a photosensitiser (PS), which when combined with oxygen creates cytotoxic species. It works on the basis of the idea that PS molecules stick to the bacterial membrane. When light with a wavelength that corresponds to the PS's peak absorption is irradiated, singlet oxygen is produced. This ruptures the bacterial cell wall and kills the bacterium.PAD is also effective against viruses, fungi and protozoa. The PS is a liquid solution of toluidine blue O (TBO) that adheres to the membranes of microorganisms. It absorbs light energy and then transfers this energy to oxygen (O2), converting it into highly reactive oxygen species (ROS), including oxygen ions and radicals.[38]

Disinfection

Fig courtesy: Dr Kingston Chellapandian *et al*. (2022)[2]

Ozone Based Delivery System

Three oxygen atoms make up the triatomic molecule known as ozone. It is applied to oral tissues as oxygen/ozone gas, ozonated water, and ozonated olive oil. It easily dissociates back into oxygen and is unstable. used on oral tissues as ozonated water, ozonated olive oil, and oxygen/ozone (O2), thus liberating so-called singlet oxygen (O1), which is a strong oxidizing agent which further impose the deleterious effect on microorganisms. There are several delivery systems for endodontic irrigation, including the Neo Ozone Water-S unit, the HealOzone (Kavo) unit, and the OzoTop unit. Nagayoshi *et al* .found that ozonated water (0.5–4 mg/L) was highly effective in killing both gram positive and negative micro-organisms.[39]

Laser

LASER: By transferring pulsed energy, lasers have lately been proposed as a way to activate irrigation solutions. (40) It has been proposed that laser-activated irrigation using Er:YAG and Er,Cr:YSGG laser light is more efficient at eliminating dentin debris and the smear layer. The purpose of the laser is to increase sodium hypochlorite's antibacterial activity. Er:YAG is the best laser for removing intracanal debris and smears, according to numerous research.

Sweeps

There is an ideal delay period (usually 300–600 msec) between laser micropulses (25 msec). The primary bubble is formed by the first micropulse, and the second micropulse, which happens right before the main bubble collapses on its own, increases the pressure to hasten that collapse. Compared to the conventional PIPS irrigation technique, SWEEPS produces a higher pressure wave amplification. The effectiveness of SWEEPS in removing the smear layer needs to be further studied.[42] Fig 12: A graphical illustration of numerous endodontic laser techniques: CLE = conventional laser endodontics; aPAD = antibacterial photoactivated disinfection; LAI = laser-activated irrigation; PIPS = photon-induced photoacoustic streaming; SWEEPS = shock wave enhanced emission photoacoustic streaming. Fig 12: Laser techniques Fig Courtesy: Sindhuja Panthangi *et al.*[51]

XP-Endo Finisher

The XP-endo Finisher (XP-FKG Dentaire SA, La Chaux-de-Fonds, Switzerland) is a rotary nickel-titanium file made from a highly flexible Martensite-Austenite alloy. It remains straight when cooled (Martensitic phase) but changes shape upon contact (Austenitic phase) due to variations in body temperature. Its flexibility allows it to expand its reach to 6 mm in diameter or 100 times that of a similarly sized file, enabling mechanical cleaning of canal areas that were previously difficult to access. With a small core size of ISO 25 in diameter and a zero taper, the file exhibits exceptional flexibility and remarkable resistance to cyclic fatigue. Furthermore, the file will clean the dentin while preserving the original shape of the canal.[43]

Irrigation Protocol

Apical preparation to be at least size 35- and 30-gauge needle should be used. After access cavity preparation flush the cavity and the canals with Sodium Hypo chlorite. Canals should always be filled with Sodium Hypochlorite, as this prolongs the effective working time of the irrigant. Additionally, it improves the cutting efficiency of root canal instruments due to its lubricating properties. During instrumentation, it's recommended to use 2-5 ml of Sodium Hypochlorite per canal consistently throughout the mechanical root canal preparation process. After shaping: 5-10 ml of Sodium Hypochlorite per canal. Once the shaping procedure is complete, rinse with a generous amount of Sodium Hypochlorite. After shaping: irrigation with 5 ml of EDTA for each canal for 1 minute (or with citric acid). After the final rinse with Sodium Hypochlorite, the canals should be irrigated with either EDTA or Citric Acid to eliminate the smear layer. Final rinse with 2ml Sodium Hypochlorite for every canal to neutralise the acidic effect of EDTA and to permit Sodium Hypochlorite to penetrate the opened tubules. Apical arrangement ought to be at least estimate 35 and 30 gage needle ought to be until Optional: Final irrigation-especially in retreatment cases: Chlorhexidine. Rinse with water to remove Sodium Hypochlorite and then with a 2% Chlorhexidine solution.Before root canal filling: rinse with 3 ml of alcohol per canal to dry the root canal.

CONCLUSION

Irrigation plays a crucial role in successful root canal treatment, serving multiple important functions: it reduces friction between the instrument and dentin, enhances the cutting efficiency of the files, dissolves organic tissue debris, cools both the file and tooth, and provides both a washing and antimicrobial effect. Additionally, irrigation is the only method that can positively affect areas of the root canal wall that mechanical instruments cannot reach. Various delivery methods are employed for root canal irrigation, ranging from traditional syringe needle delivery to advanced machine-driven systems, including automatic pumps and sonic or ultrasonic devices. Due to the safety factors, capacity of the high volume irrigant delivery and ease of application the newer irrigation devices may change the insight of conventional endodontic treatment.

REFERENCES

1. Lee SJ, Wu MK, Wesselink PR. The efficacy of ultrasonic irrigation to remove artificially placed dentine debris from different-sized simulated plastic root canals. Int Endod J. 2004;37:607-12.
2. Dr Kingston Chellapandian , Dr Vijay venkateshkondas , Dr Ashwin ravichandran , Dr sujanapraveenRecent Advancements In Endodontic Irrigation Systems JournalofPositiveSchoolPsychology 2022, Vol.6,No.4, 3809-3822.
3. Haapasalo M, Endal U, Zandi H, Coil JM (2005). Eradication of endodontic infection by instrumentation and irrigation solutions. Endodontic Topics 10, 77–102.
4. Karade P, Sharma D, Hoshing UA, Medha AH, Bhagat AR, Chopade RV. Efficiency of Different Endodontic Irrigation and Activation Systems, Self-Adjusting File Instrumentation/Irrigation System, and XP-Endo Finisher in Removal of the Intracanal Smear Layer: An *Ex vivo* Scanning Electron Microscope Study. J Pharm Bioallied Sci. 2021 Jun;13(Suppl 1):S402-S407. doi: 10.4103/jpbs.JPBS_775_20. Epub 2021 Jun 5.
5. Paragliola R, Franco V, Fabiani C, Mazzoni A, Nato F, Tay FR, et al.. Final rinse optimization: influence of different agitation protocols. J Endod2010;36:282-285.
6. Boutsioukis C, Gogos C, Verhaagen B, Versluis M, Kastrinakis E, Van der Sluis LW, et al. The effect of root canal taper on the irrigant flow: Evaluation using an unsteady computational fluid dynamics model. Int Endod J 2010;43:909-16.
7. Sedgley CM, Nagel AC, Hall D, Applegate B. Influence of irrigant needle depth in removing bioluminescent bacteria inoculated into instrumented root canals using real-time imaging in vitro. Int Endod J 2005;38:97-104.
8. Uzunoglu-Özyürek E, Karaaslan H, Türker SA, Özçelik B. Influence of size and insertion depth of irrigation needle on debris extrusion and sealer penetration. Restor Dent Endod. 2017 Dec 22;43(1):e2.
9. Markus Haapasalo, et al., Irrigation in Endodontics. Dent Clin N Am. 2010;54:291– 312.

10. Migun NP, Azuni MA. Filling of one-side-closed capillaries immersed in liquids. J Colloid Interface Sci. 1996;181:337–40.
11. Keir DM, Senia ES, Montgomery S. Effectiveness of a brush in removing postinstrumentation canal debris. J Endod1990;16:323–7.
12. Pesse AV, Warrier GR, Dhir VK. An experimental study of the gas entrapment process in closed-end microchannels. Int J Heat Mass Trans 2005;48:5150-65.
13. Schoeffel GJ. The endoVac method of endodontic irrigation, Part 2 – efficacy. Dent Today 2008;27:82, 84, 86-7.
14. Ruddle CJ. Microbrush for endodontic use. Washington, DC: United States Patent 6,179,617; 2001.
15. Al-Ali M, Sathorn C, Parashos P. Root canal debridement efficacy of different final irrigation protocols. Int Endod J 2012;45:898-906.
16. Garip Y, Sazak H, Gunday M, Hatipoglu S. Evaluation of smear layer removal after use of a canal brush: an SEM study. Oral Surg Oral Med Oral Pathol Oral RadiolEndod 2010;110:e62-e66.
17. Rödig T, Bozkurt M, Konietschke F, Hülsmann M. Comparison of the Vibringe system with syringe and passive ultrasonic irrigation in removing debris from simulated root canal irregularities. J Endod2010;36:1410-1413.
18. Pasricha SK, Makkar S, Gupta P. Pressure Alteration Techniques in Endodontics - A Review of Literature. J Clin Diagn Res 2015;9: ZE01-ZE06.
19. Walters MJ, Baumgartner JC, Marshall JG. Efficacy of irrigation with rotary instrumentation. J Endod2002;28:837-9.
20. Metzger Z. From files to SAF:3D endodontic treatment is possible at last. Alpha Omegan2011;104:36- 44.
21. Elumalai1 D, Kumar A, Tewari R K, Mishra S K, Iftekhar H, Alam S, Andrabi M Newer endodontic irrigation devices:anupdate.Journal of Dental and Medical Sciences 2014,Volume 13, Issue 6.
22. Joseph Mampilly, Vidyadhar Shetty and K. Harish S. Shetty, ENDODONTIC IRRIGATING SOLUTIONS, DISINFECTION DEVICES AND TECHNIQUES : A REVIEW Int. J. Adv. Res. 8(01), 986-997.
23. Ruddle CJ: Endodontic disinfection: tsunami irrigation, Endodontic Practice 11:1, pp. 7-15, 2008.
24. Kanter V, Weldon E, Nair U, Varella C, Kanter K, Anusavice K, Pileggi R: A quantitative and qualitative analysis of ultrasonic versus sonic endodontic systems on canal cleanliness and obturation, Oral Surg Oral Med Oral Pathol Oral RadiolEndod 112:6, pp. 809- 813, 2011.
25. Caron, G, Nham K, Bronnec F, Machtou P: Effectiveness of different final irrigant protocols on smear layer removal in curved canals, J Endod 36:8, pp. 1361- 1366, 2010.
26. Cunningham WT, Martin H. A scanning electron microscope evaluation of root canal debridement with the endosonic ultrasonic synergistic system. Oral Surg Oral Med Oral Pathol1982;53:527–31.
27. Gutarts R, Nusstein J, Reader A, Beck M. In vivo debridement efficacy of ultrasonic irrigation following hand-rotary instrumentation in human mandibular molars. J Endod2005;31:166–70.
28. Burleson A, Nusstein J, Reader A, Beck M. The in vivo evaluation of hand/rotary/ ultrasound instrumentation in necrotic, human mandibular molars. J Endod 2007; 33:782–7.
29. Weller RN, Brady JM, Bernier WE. Efficacy of ultrasonic cleaning. J Endod.1980;6:740-3.
30. van der Sluis LW, Versluis M, Wu MK, Wesselink PR. Passive ultrasonic irrigation of the root canal: a review of the literature. Int Endod J. 2007;40:415-26
31. Hu¨lsmann M, Hahn W. Complications during root canal irrigation: Literature review and case reports. Int Endod J 2000;33:186-93.
32. Shin SJ, Kim HK, Jung IY, Lee CY, Lee SJ, Kim E.Comparison of the cleaning efficacy of a new apical negative pressure irrigating system with conventional irrigation needles in the root canals. Oral Surg Oral Med Oral Pathol Oral RadiolEndod. 2010 Mar;109(3):479-84.
33. Nielsen BA, Baumgartner JC. Comparison of the endovac system to needle irrigation of root canals. J Endod. 2007;33:611-5.
34. Hauser V, Braun A, Frentzen M. Penetration depth of a dye marker into dentine using a novel hydrodynamic system (RinsEndo). Int Endod J 2007;40:644–52.
35. Wiggins S, Ottino JM. Foundations of chaotic mixing. Philos Trans A Math Phys Eng Sci 2004;362:937- 70.

36. Mohan D, Maruthingal S, Indira R, Divakar DD, Al Kheraif AA, Ramakrishnaiah R, Durgesh BH, Basavarajappa S, John J. Photoactivated disinfection (PAD) of dental root canal system - An ex-vivo study. Saudi J Biol Sci. 2016 Jan;23(1):122-7.
37. Haapasalo M, Shen Y, Wang Z, Park E, Curtis A, Patel P, Vandrangi P. Apical pressure created during irrigation with the GentleWave system compared to conventional syringe irrigation. Clin Oral Investig 2015
38. Schlafer S, Vaeth M, HorstedBindslev P, Frandsen EVG. Endodontic photoactivated disinfection using a conventional light source: an in vitro and ex vivo study. Oral Surg Oral Med Oral Pathol. 2010;109(4):634-641.
39. Nagayoshi M, Fukuizumi T, Kitamura C, Yano J, Terashita M, Nishihara T. Efficacy of ozone on survival and permeability of oral microorganisms. Oral MicrobiolImmunol. 2004;19(4):240–6.
40. Blanken J, De Moor RJG, Meire M, Verdaasdonk R. Laser induced explosive vapor and cavitation resulting in effective irrigation of the root canal. Part 1: A visualization study.LasersSurg Med 2009;41(7):514-519.
41. Tong J, Liu L, Du J, Gao Y, Song D, Huang D. Effect of photon-induced photoacoustic streaming and shock-wave enhanced emission photoacoustic streaming technique on the removal of the smear layer after root canal preparation in curved root canals. J Dent Sci. 2023 Jan;18(1):157-164.
42. Mancini M, Cerroni L, Palopoli P, Olivi G, Olivi M, Buoni C, Cianconi L. FESEM evaluation of smear layer removal from conservatively shaped canals: laser activated irrigation (PIPS and SWEEPS) compared to sonic and passive ultrasonic activation-an ex vivo study. BMC Oral Health. 2021 Feb 22;21(1)
43. Tabassum S, Zafar K, Umer F. Nickel-Titanium Rotary File Systems: What's New? EurEndod J. 2019 Oct 18;4(3):111-117.
44. Shinam Kapila Pasricha, Sameer Makkar, Pranav Gupta,Pressure Alteration Techniques in Endodontics- A Review of Literature.Year : 2015 Month : Mar Volume : 9 Issue : 3
45. Matthew J. Walters, J. Craig Baumgartner, J. Gordon Marshall, Efficacy of Irrigation with Rotary Instrumentation, Journal of Endodontics, Volume 28, Issue 12, 2002, Pages 837-839, ISSN 0099-2399.
46. Misgar BA, Goyal V, Goyal P, *et al*. Endodontic File Systems with Special Emphasis on Self-adjusting Files: A Comprehensive Review. J Oper Dent Endod 2021;6(1):14–23.
47. John M. Nusstein Endodontic sonic and ultrasonic irrigant activation Clinical Dentistry Reviewed (2018) 2:22
48. Caicedo, Ricardo. (2013). Effects of smear layer and debris removal with irrigation assisted by the EndoActivator and the Endo Brush: A comparison with unassisted standard syringe irrigation with 5.25% NaOCl and 17% EDTA. Endodontic practice. Volume 6. 14-17.
49. Cesar de Gregorio and Avina Paranjpe 10: Apical Negative Pressure Irrigation (ANP)
50. Gyulbenkiyan, Elvira &Gusiyska, Angela. (2023). IMPACT OF THE PASSIVE/ACTIVE ULTRASONIC ACTIVATION ON THE ENDODONTIC IRRIGANTS EFFECTIVENESS - A REVIEW. Journal of IMAB - Annual Proceeding (Scientific Papers). 29. 4826-4831. 10.5272/jimab.2023291.4826.
51. Sindhuja Panthangi, Uppalapati Vishwaja, Chavva Lakshmi Charan Reddy, Mattapudi Basavaiah Babu, Srivalli Podili, Novel sweeps technology in endodontics — A review.

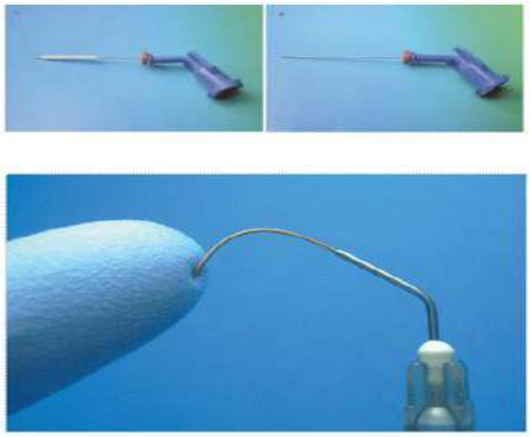

Figure.1: Types of needles
a) NaviTipFx, b) NaviTip, c) Flexiglide.

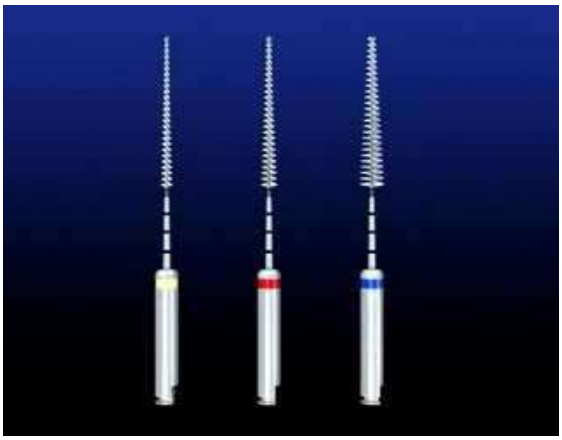

Figure.2: Rotary Brushes

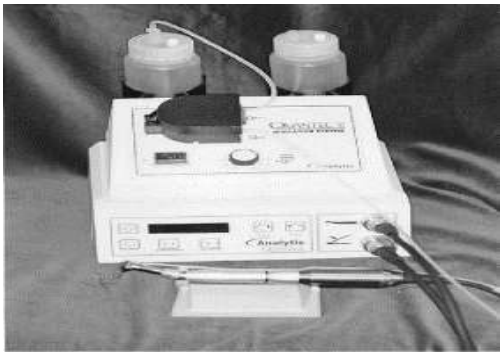

Figure.3: Quantec E system

Figure. 4: SAF with handpiece containing an irrigation hub made up of polyethylene tube which is connected to the VATEA irrigation pump

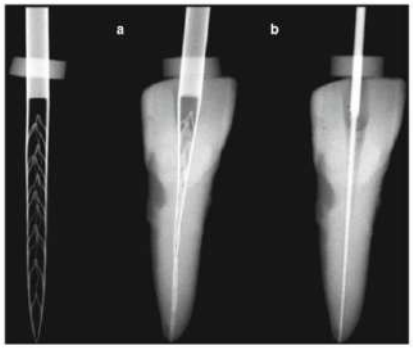

Figure. 5 A to B: (A) The compressibility and adaptability of SAF#20; (B) The conformation of the SAF vs rotary instrumentation

Figure. 6: Depicts
a)Sonic Air® 1500
b) Rispi-Sonic® file

Figure. 7: Endoactivator

Figure. 8:Dentsply Tulsa Dental Specialties ProUltra® Piezoflow™ Ultrasonic tip (Dentsply Tulsa Dental

Figure 9: 1)(a) Handpiece; (b) fingerpiece; (c) multiport adapter; (d) macrocannula; (e) microcannula (21, 25, 31 mm); (f) syringe 20 cc (for NaOCl); (g) master delivery tip (MDT); (h) syringe 3 cc (for EDTA); (i) MDT evacuation tubing (blue); and (j) handpiece/fingerpiece evacuation tubing (white).

Figure 9: 2)EndoVac components: (a) macrocannula; (b) microcannula demonstrating the evacuation holes in the apical 0.7 mm; (c) master delivery tip; and (d) microcannula.

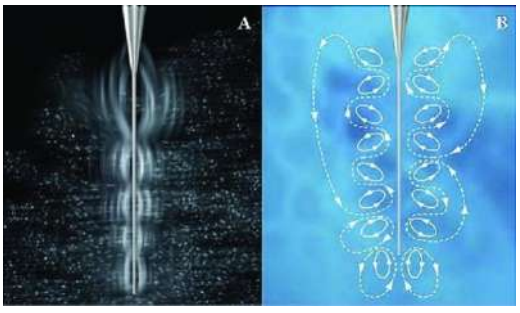

Figure. 10. A) and schematic depiction (B) of ultrasound acoustic streaming.

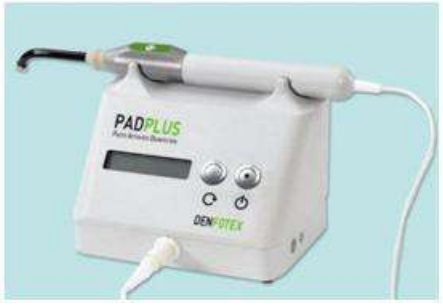

Figure. 11: Photo Activated

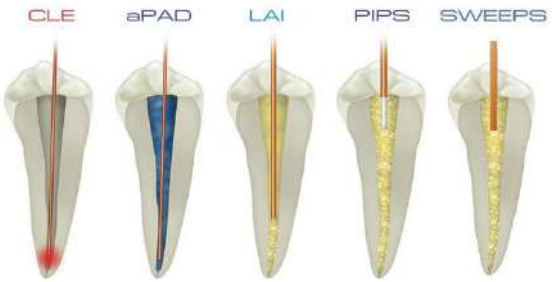

Figure. 12: Laser techniques

Indian Journal of Natural Sciences *www.tnsroindia.org.in ©IJONS*

Vol.15 / Issue 88 / Feb / 2025 *International Bimonthly (Print) – Open Access* *ISSN: 0976 – 0997*

RESEARCH ARTICLE

Method Development and Validation of Glipizide in Bulk and Marketed Formulation by using UV-Spectroscopy

D. Chinababu[1]*, SK. Aleesha[2], Jagadeeswara Rao Batna[3], K. Srikanth Kumar[4], Vishal Bharat Babar[5], K. Hanumantha Rao[6], M. Jalaiah[7], Rayini Venkata Sai Mounica[8] and S. Deepthi[9]

[1]Professor, Department of Pharmaceutical Analysis and Quality Assurance, Institute of Pharmaceutical Science and Research for Girls, Bhigwan, (Affiliated to Dr. Babasaheb Ambedkar Technological University, Lonere), Maharashtra, India.
[2]Assistant Professor, Department of Pharmacology, Dattakala College of Pharmacy, Bhigwan, (Affiliated to Savitribai Phule Pune University, Pune), Maharashtra, India.
[3]Lecturer, Department of Pharmaceutical Chemistry, Government Polytechnic for Women, Srikakulam, (Affiliated to State Board of Technical Education and Training, Mangalagiri), Andhra Pradesh, India.
[4]Professor, Department of Pharmaceutical Chemistry, Institute of Pharmaceutical Science and Research for Girls, Bhigwan, (Affiliated to Dr. Babasaheb Ambedkar Technological University, Lonere), Maharashtra, India.
[5]Professor and Principal, Department of Pharmaceutical Chemistry, Institute of Pharmaceutical Science and Research for Girls, Bhigwan, (Affiliated to Dr. Babasaheb Ambedkar Technological University, Lonere), Maharashtra, India.
[6]Assistant Professor, Department of Pharmaceutical Analysis, Krishna University College of Pharmaceutical Sciences and Research, Krishna University, Machilipatnam, Andhra Pradesh, India.
[7]Professor, Department of Pharmacology, QIS College of Pharmacy,Vengamukkapalem, (Affiliated to Jawaharlal Nehru Technological University, Hyderabad), Telangana, India.
[8]Associate Professor, Department of Pharmaceutical Analysis, QIS College of Pharmacy, Vengamukkapalem, (Affiliated to Jawaharlal Nehru Technological University, Hyderabad), Telangana, India.
[9]Assistant Professor, Department of Pharmaceutical Analysis, QIS College of Pharmacy, Vengamukkapalem, (Affiliated to Jawaharlal Nehru Technological University, Hyderabad), Telangana, India.

Received: 18 Oct 2024 Revised: 03 Dec 2024 Accepted: 07 Feb 2025

***Address for Correspondence**
D. Chinababu,
Professor,
Department of Pharmaceutical Analysis and Quality Assurance,
Institute of Pharmaceutical Science and Research for Girls, Bhigwan,
(Affiliated to Dr. Babasaheb Ambedkar Technological University, Lonere),
Maharashtra, India.
E.Mail: chinababu.rao@gmail.com

ABSTRACT

A simple, rapid and accurate UV method was developed for the determination of Glipizide in bulk and pharmaceutical dosage form. The solvent system was Acetonitile: Water in the ratio of 40:60 v/v. The wavelength was maintained at 275 nm. The method was linear over the concentration range from 0.8-16μg/mL and R^2 was found to be 0.999. The intraday and interday precision %RSD values were obtained < 2.0. The LOD and LOQ were attained 1.68 &5.08 μg/mL respectively. The accuracy results of the method was obtained 100.57% -101.08% at different levels of concentrations. The method was proved as robust after deliberately changed parameters of organic solvent ratio and wavelength. The method was used for routine analysis of Glipizide in pharmaceutical dosage forms.

Keywords: Validation,Glipizide, Acetonitrile, UV-method, LOD and LOQ.

INTRODUCTION

Glipizide (GPZ), chemically known as N-[2[4[[[(Cyclohexylamino)carbonyl]amino] sulfonyl] phenyl] ethyl]-5-methylpyrazinecarboxamide (Figure 1) is one of the sulphonyl urea derivatives that are widely used as oral anti-hyper glycaemic drugs for the treatment of non-insulin-dependent diabetes mellitus.(1-2)It works by promoting the synthesis of insulin by pancreatic beta cells, which lowers blood glucose levels. The medication is covered in an official monograph in the European Pharmacopeia(3), which details a titrimetric assay for GPZ. There have been reports of many alternative procedures for determining GPZ in bulk and formulaions, including high-performance liquid chromatography, ultra-performance liquid chromatography, thin layer chromatography, and high-performance thin layer chromatography.(4-28) Even though these methods frequently offer sensitive and focused ways to assay GPZ.(23-28) Assay procedures for routine analysis should be straightforward, quick, sensitive, and simple to execute.

MATERIALS AND METHODS

All the chemicals and reagents were of analytical grade. Water was double distilled and filtered with a membrane filter. Acetonitrile (Merck, India), hydrochloric acid and sodium hydroxide and hydrogen peroxide were purchased SD fine chem, India. Pharmaceutical grade standard drug Glipizide were kindly gifted by Hetero drug Pvt,Ltd, Hyderabad, India.

Preparation of Standard solution

Accurately weighed and transferred 1925g of Glipizide working standard into 50 ml calibrated clean and dry volumetric flask, add about 50ml of solvent (Acetonitrile: Water), shakeitwell, for better solubility sonicatedit (primarys to ck solution 1000 μg/ml).From the above solution (primary stock solution) pipette out 0.22ml and transferred it intoanother10mlvolumetricflaskand makeup to the volume it gives secondary stock solution (22μg/ml).

Preparation of sample solution

Accurately weighed 20 tablets and find out the average weight of each tablet and powder it with the help of clean motor and pestle. Weigh equivalent weigh toft he tablet powder 3.85g of Glipizide from this weigh 19.25gandtransfer it in to a 50ml volumetric flask. Add about 50 ml of the solvent and sonicateittod is solve completely and filter. if needed and make up to the final volume (1000μg/ml).From the above solution (primary stock solution)pipette out 0.22ml and transfer it into another 10 ml volumetric flask and make up to the mark it gives secondary stock solution (22μg/ml).

Determination of maximum wave length

The developed method was optimized at 275nm, using solvent and optimized concentration was 22µg/ml and absorbance was 0.4.

Validation of analytical Method[29,30]

The proposed method was validated for different parameters like linearity, precision, accuracy,specificity,robustness,Stabilitystudies,LOD,LOQandassay.

Specificity and Selectivity

The specificity was studied by measured the response of spectrum with solvent (blank), standard and sample solutions prepared as per the developed method. There was no interference observed between drug with excipients and solvents. Hence the developed method was proved (Figure-2) as specific and selective.

Linearity

The Glipizide calibration curve was linear across the concentration range; the absorbance response on the Y-axis and the concentration on the X-axis were plotted on a graph, and the value of the regression coefficient (R^2) was found to be 0.999. The linearity range of the standard solution concentration was found in between 12.50 µg/mL to 75 µg/mL. The linearity graph was shown in figure-3.

Precision

Six Glipizide sample solutions carried out in duplicate were used to assess each level of precision, including intraday and intermediate precision.

Intraday Precision

Using a 100% sample solution, the intraday precision test was run three times a day, at 9:00 am, 1:00 pm, and 5:00 pm. At each level, six duplicate measurements were made. The percentage RSD was found to be in between 0.78-1.07 for all intervals.

Interday Precision

The interday precision was performed at day 1, day 2 and day 3 with 100% concentration of solution. Record the spectrums of six replicated injections at each level and calculated average of %RSD was found to be in between 0.31-1.54.

Accuracy

By spiking standard solution with analyzed sample solution at three concentration levels 80%, 100%, and 120%the accuracy of the procedure was investigated.In duplicate, the recovery investigations were carried out in ideal circumstances.The accuracy should between 98%-102%. The % RSD value should not more than 2.0. The results were reported in table 1and spectrums in figure-4.

Detection limit and quantification limit

The detection limit and quantification limit were determined through the linearity curve of slope and the response of the standard deviation (precision). The LOD and LOQ for LMT were determined to be 1.68 µg/mL and 5.08 µg/mL, respectively.

Robustness

The robustness was performed with only minor adjustments to the method's flow rate and composition of mobile phase, both of which were assessed at 100% sample concentration. The wavelength was changed ±2 mL/min and organic phase composition was changed (±3mL)recorded the spectrums for six replicate samples (Table-2).

Assay

Accurately weighed 20 tablets and find out the average weight of each tablet and powder it with the help of clean motor and pestle. Weigh equivalent weight of the tablet powder 1925mg of Glipizide and transferred into a 50ml volumetric flask. Add about 50ml of the solvent and sonicate it to dissolve completely and filter it, made the volume up to mark with solvent (1000µg/ml).From the above solution(primary stock) pipette out 0.22ml and transferred into 10 ml volumetric flask and make up to the volume it gives secondary stock solution (22 µg/ml). Measure the absorbance for six replicated samples and results shown in table 3.

CONCLUSION

An attempt was made to develop and validate different UV-Spectrophoto metric methods for the estimation of Glipizide in bulk and pharmaceutical dosage forms. The proposed spectrophotometric method was found to be simple, precise and accurate. The method was developed with Acetonitrile: Water. There was no interference of excipients with active moiety. The method was shown good accuracy, precision, linearity and robustness. The proposed method was used for the routine analysis of Glipizide in bulk and its pharmaceutical dosage forms.

ACKNOWLEDGEMENT

The authors are thankful to management and principal of Institute of Pharmaceutical Science and Research for Girls, Bhigwan-413130, Maharashtra for extending support to carry out the present research work.

Conflict of Interest

The authors declare no conflict of interest.

Abbreviations

LOD: Limit of detection, **LOQ:**Limit of Quantitation, **GPZ:** Glipizide, **RSD:**Relative standard deviation.

REFERENCES

1. Basavaiah K, Rajendraprasad N. Stability-indicating UV-Spectrophotometric Determination of Glipizide in Pharmaceuticals. Austin Journal of Analytical and Pharmaceutical Chemistry. 2017; 4(3): 1088.
2. Sweetman SC. Martindale. The Complete Drug Reference, 34thEd., Pharmaceutical Press, London, 2005; 5083.
3. European Pharmacopoea 6.0, Official Monograph 01/2008:0906, 1977.
4. MousumiKarpillai, SachinDhangar. Development ofRP-HPLCMethodforEstimationof Glipizide. Research J. Pharm. and Tech. 2011; 4(6): 949-950.
5. Najma Sultana, Mohammed SaeedArayne, Saeeda Nadir Ali. Simultaneous Determinitation ofGlipizide and Glimepiride byRP-HPLC indosage formulations and in human serum.Asian journal of pharmacy and pharmacology.2011; 21(9):2443-2448.
6. Ganesh, G Nikitha, SireeshaDodda, VasudhaBakshi. Development and validation of UV Spectrophotometric method for Simultaneous estimation of Metformin and glipizide tablet dosage form. International Journal of Applied Pharmaceutical Sciences and Research. 2016;1(2):56-59.
7. SnehalBapusahebBagadane,PreranaB.Jadhav.DevelopmentandvalidationofRP-HPLC methodforSimultaneousestimationofMetforminHydrochlorideandGlipizideinbulkand pharmaceuticaldosageform.Asianjournalofpharmacyandpharmacology.2019; 9(3-s): 146-155.
8. Asmaa A El-Zaheer, Ehab F ElkadyHanan M Elwy, Mahmoud A Saleh. Simultaneous Determination of Metformin, Glipizide, Repaglinide and Glimepiride or Metformin and Pioglitazone by a validated LC method: Application in the presence of metformin impurity(1-cyanoguanidini). Journal of AOAC International. 2016; 99(4):957-963.

9. Ahmed Gedawy, Hani Al-Salami, Crispin R. Dass. Advanced and multifaceted Stability profiling ofthe first line Anti-Diabetic Drugs Metformin, Gliclazide, and Glipizide under various controlled stress conditions. 2020; 28(3): 362-368.
10. Venkatesh P, Harisudhan T,HiraChoudhury,RameshM,NuggehallyR.Srinivas. SimultaneousEstimationofAnti-DiabeticDrugs-Glipizide,Glibenclamide,Gliclazide,Pioglitazone, Repaglinide: Development of a novel HPLC method for use in the analysis ofPharmaceuticalFormulationsand itsapplicationto humanPlasmaassay. 2006(20):10/p 1043-1048.
11. Lakshmi KS and Rajesh T. Development and Validation of RP-HPLC Method for Simultaneous Determination of Glipizide, Rosiglitazone, Pioglitazone, Glibenclamide and Glimepiride in Pharmaceutical Dosage Forms and Human Plasma. Journal of Iranian Chemical Society. 2011; 8: 31-37.
12. Ilmanugrahani,IndhahFatmawati,SlametIbrahim.Developmentandvalidationofcontent uniformity analytical procedure of glipizide extended-release tablet. 2016; 6(12): 192-196.
13. KanakapuraBasavaiah. QualitybydesignApproachforthedevelopment and validationof Glipizide, an anti-Diabetic drug, by RP-UPLC with application to formulated forms and urine. 2013:1-10.
14. Aya A. Marie, Sherin F. Hammad, Amira H. Kamal. Deduction of the operable design space of RP-HPLC technique for the simultaneous estimation of metformin, pioglitazone and glipizide. 2023;13:4334.
15. Basavaiah, Rajendraprasad. Rapid and Reliable determination of Glipizide in Pharmaceutical samples by HPLC and its degradation study. 2017;4:1080.
16. Sireesha D, Ganesh K, Nikitha G, Vasudha B. Development and validation of UV spectrophotometric method for simultaneous estimation of metformin and glipizide in tablet dosage form. 2016;1(2):56-59.
17. Chungath TT, Reddy YP and Devanna N. Simultaneous Spectrophotometric Estimation of Metformin Hydrochloride and Glipizide in Tablet Dosage Forms. International Journal of Pharm Tech Research. 2011; 3: 2064-2067.
18. Sarangi RR, Panda SN, Panda SK and Sahu KC. Simultaneous UVSpectrophotometric Estimation of Glipizide and Metformin in Bulk and Its Dosage Form. International Journal of Pharmaceutical and Biological Archive. 2011; 2: 1137-1145.
19. Vijaya SS, Satya KV, Hima BV and Devala RG. High Pressure Liquid Chromatography Estimation of Glipizide in Pharmaceutical Dosage Forms. Asian Journal of Chemistry. 2006; 18: 1309-1312.
20. Mantri MA and Shanmukhappa S. A Validated RP-HPLC Method for Estimation of Glipizide in Its Pure and Pharmaceutical Dosage Form (Tablets). Material Science Research India. 2009; 6: 223.
21. Rahila S and Asif K. Reverse Phase High Performance Liquid Chromatographic Method for the Analysis of Glipizide in Pharmaceutical Dosage Forms. International Journal of Research in Ayurveda and Pharmacy. 2010; 1: 455-458.
22. Liping H, Yan X, Jiaxiu H, Jingping S, Jiali Z, Jin Z, et al. Determination of Glipizide in Sustained Release Tablets by RP-HPLC. ZhonghuaYixueYanjiuZazhi. 2011; 11: 337-339.
23. Jing F, Jia L, Dan S, Hua DR, Shun BK and Hui CX. Determination of Two Components in Metformin and Glipizide Tablets by Reversed-Phase Ion-Pair HPLC. Chinese Journal of New Drugs and Clinical Remedies. 2010; 29: 445- 447.
24. Rao BU and Nikalje AP. Determination of Glipizide, Glibenlamide and Glimeperide in a Tablet Dosage Form in the Presence of Metformin Hydrochloride by Ion Pair –Reversed Phase Liquid Chromatographic Technique. Journal of Analytical and Bioanalytical Techniques. 2010; 1: 1-5.
25. Anna G, Anna B and Lukasz K. Stability-indicating Validated HPLC Method for Simultaneous Determination of Oral Antidiabetic Drugs from Thiazolidinedione and Sulfonylurea Groups in Combined Dosage Forms. Journal of AOAC International. 2010; 93: 1086-1092.
26. Reddy MU, Reddy PV, Somasekhar P and Varaprasad B. Single and High Resolution RP-HPLC Method for the Determination of Six anti Diabetic Drug Products. Journal of Pharmacy Research. 2011; 4: 1209-1212.
27. Meng L and Subi L. Ion-pair HPLC Determation of Anti-Diabetic Agents in Traditional Chinese Medicines and Health Care Products. Chinese Journal of Pharmaceutical Analysis. 2010; 30: 1038-1041.

28. Trivedi HK, Kshtri N, Patel V and Roa V. Development and Validation of an UPLC Method for In-Vitro Study of Glipizide Extended Release Tablets. International Journal of Pharmaceutical Sciences and Research. 2012; 3: 3317-3322.
29. International Conference on Harmonisation of Technical Requirement of Registration of Pharmaceuticals for Human Use. Validation of Analytical Procedures: Text and Methodology, Q2B; 1996. Geneva, Switzerland.
30. Validation of analytical procedures: Text and Methodology Q2(R1) https://database.ich.org/sites/default/files/Q2%28R1%29%20Guideline.pdf

Table.1: Results of Accuracy

Spiked level	Sample weight (mg)	Absorbance	Added µg/ml	Found µg/ml	% Mean recovery
80%	1540.00	0.346	17.63	17.72	100.57
100%	1925.00	0.435	22.04	22.27	101.08
120%	2310.00	0.520	26.44	26.62	100.68

Table.2: Results of Robustness

S. No.	Parameter	Condition	Absorbance	%Assay
1	Wavelength (±2 nm)	273	0.423	98.37
2		275	0.43	100.00
3		277	0.432	100.47
4	Changed Organic Solvent ratio (±3mL)	67:33:00	0.422	98.14
5		70:30:00	0.431	100.23
6		73:27:00	0.435	101.16

Table.3: Results of Assay

WTofSample (µg/ml)	Absorbance	%Assay
1925.00	0.431	100.23
1925.00	0.43	100.00
1925.00	0.432	100.47
1925.00	0.427	99.30
1925.00	0.438	101.86
1925.00	0.429	99.77

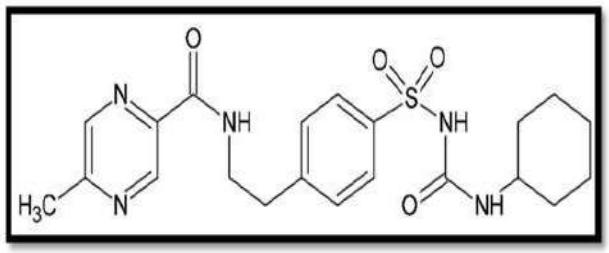

Figure.1: Glipizide structure

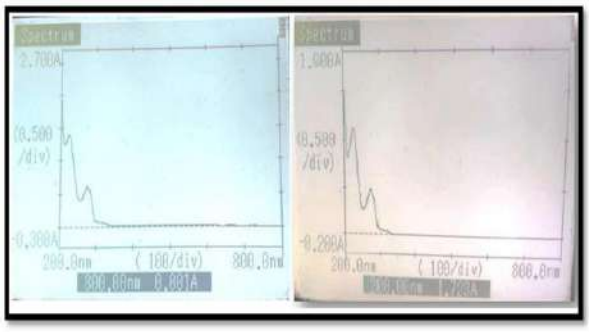

Figure.2: Sample and Standard spectrums of Glipizide

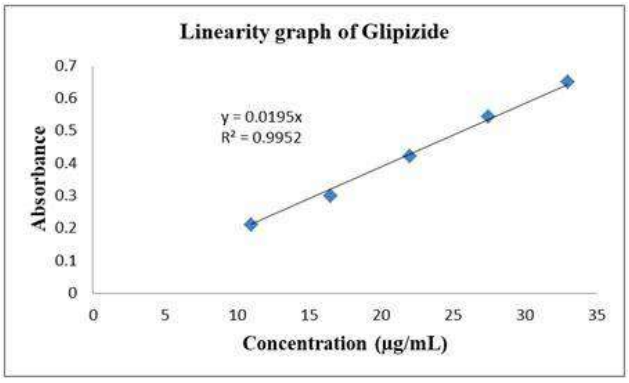

Figure.3: Linearity graph of Glipizide

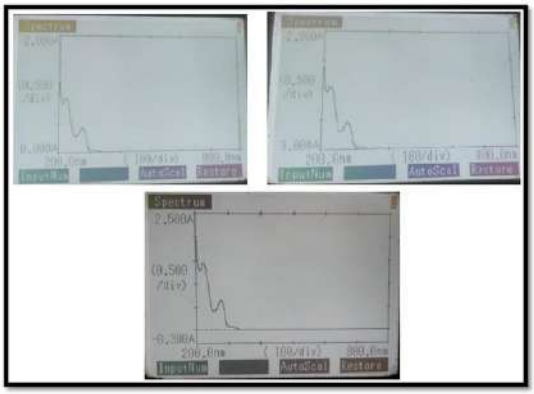

Figure.4: Accuracy spectrums of 80%, 100% and 120%

RESEARCH ARTICLE

Epoxy Resins- A Perspective Analysis in the View of Scientometrics

S. Rajeswari[1] and K. Kanimozhi[2*]

[1]Assistant Librarian, Department of Library and Information Science, University College of Engineering BIT Campus, Anna University, Tiruchirappalli, India
[2]Assistant Professor, Department of Chemistry, University College of Engineering BIT Campus, Anna University, Tiruchirappalli, Tamil Nadu, India.

Received: 04 Nov 2024 Revised: 10 Dec 2024 Accepted: 02 Jan 2025

***Address for Correspondence**
K. Kanimozhi,
Assistant Professor,
Department of Chemistry,
University College of Engineering BIT Campus,
Anna University, Tiruchirappalli, Tamil Nadu, India.
E.Mail: kanirams47@gmail.com

ABSTRACT

This paper presents about the Epoxy Resins and its priorities with an integrated methodology of bibliometric analysis. The proposed methodology is evaluated based on the recent research activities to highlight the role of the Epoxy Resins. Bibliometric studies explore the breadth and depth of research areas using different tools. WoS database software is used to study the methodology of Epoxy Resin in the mode of bibliometric report presented in this article. The study focuses on factors such as the number of Publications, Research area, language in which Epoxy Resins were published. Data for this study are collected from the WoS databases from 2014 to till October 2024 related to Epoxy Resins. The study has also identified significant research areas in this field. Finally, future research directions are proposed for researchers to explore this area in further detail.

Keywords: Epoxy Resins,Bibliometrics, Hitecite, VoS viewer software.

INTRODUCTION

The commercially used epoxy monomers are prepared by the reaction of acidic hydroxy groups and epichlorohydrin. First a hydroxy group reacts in a coupling reaction with epichlorohydrin, followed by dehydrohalogenation gives the oxirane ring of epoxies and these are called glycidyl-based epoxy resins. Russian Organic Chemist Nikolai A. Prilezhaev discovered Epoxy resin in 1909 while he developed an olefin epoxidation reaction under perbenzoic acid catalysis furnishing epoxides, also called oxiranes.(1-3). In the 1940s and 1950s, chemists in the United States and Switzerland introduced the first epoxy derivatives known as low-molecular-weight prepolymers based on 4,4-isopropylidenediphenol (bisphenol A, BPA), which is also employed for the production of polycarbonate. At present,

the manufacture of polycarbonates and epoxy resins represents approximately 68% and 30% of the production capacity of BPA, respectively. It is extensively used in the manufacture of adhesives, plastics, paints, and numerous commercial products(4-9).However, numerous studies on very-low-dose exposure to BPA 1 (Figure.1) indicate that this compound, whose annual production is over 4.5 million tons, exhibits adverse health effects, including breast and prostate cancer, obesity, neurobehavioral problems, and reproductive abnormalities.The aromatic structure of the resin implements a strong hydrophobic performance far over competitive resins like polyurethanes or acrylics, which were developed at the same time.

Reaction:

The hydroxy group are derived from aliphatic diols, Polyether polyols, phenolic compounds or dicarboxylic acids. Phenols can be obtained from compounds such as bisphenol A and novolak. Polyols can be compounds such as 1,4-butanediol. Di- and polyols lead to glycidyl ethers. Dicarboxylic acids such as hexahydrophthalic acid are used for diglycide ester resins. Instead of a hydroxygroup, an amine or amide containing nitrogen atom can be reacted with epichlorohydrin. Two moles of epichlorohydrinreacted with one mole of bisphenol A to form the bisphenolAdiglycidyl ether [DGEBA].

Improved Epoxy Resin: Epoxy Cresol Novolac

In the mid sixties, new multi functional epoxy resins of phenol novolac or cresol novolac were introduced in the market. The chemistry of these resins is very similar to that of Bisphenol-A type resins. The main purpose of using these resins was to improve the cross linking density of the formulation

Novolac epoxy resin

Reaction of phenols with formaldehyde and subsequent glycidylation with epichlorohydrin produces epoxidisednovolacs, such as epoxy phenol novolacs and epoxy cresol novolacs. Epoxide functionality of these resins forms a highly crosslinked polymer network displaying high temperature and chemical resistance, but low flexibility.

Glycidylamine epoxy resins

Are higher functionality epoxies which are formed when aromatic amines are reacted with epichlorohydrin. Important industrial grades are triglycidyl-p-aminophenol (functionality 3) and N,N,N,N-tetraglycidyl-4,4-methylenebis benzylamine (functionality 4). Due to its high strength, stiffness, light weight, glossy appearance, compatability, preparation methods, availability, cost, usage by a lay man to science people, non reactivity to other chemicals, water, solvents, sunlight, UV light it has wide range of Applications. From day today life to industrial area the life of composites is ubiquitous and epoxy finds a best place in this century. Bibliometrics is a field that involves the quantitative analysis and measurement of various aspects related to published literature, such as books, journal articles, patents, and other forms of written communication. It is a branch of library and information science that applies mathematical and statistical methods to study patterns and trends in the production, dissemination, and use of recorded information. Citation analysis is a core aspect of bibliometrics, where the citations received by a particular publication or author are analyzed to understand the impact and influence of that work on subsequent research. Bibliometricsis used to analyze the impact of journals, institutions, research groups, individual researcher or countries qualitatively and quantitatively(10-12). The methodological approaches are based on quantitative and qualitative analyses of the scientific literature and can be used to evaluate and compare the research performance of investigators, journals, institutions, countries or subject fields.

METHODOLOGY

For bibliometric analysis, the bibliometric search of the literature was performed in the Web of Science from Thomson Reuters, as it is a well-recognized database and provides high-quality records. Data was downloaded: “Topics = “Epoxy Resins” and Country = India and Documents = Articles”, Time Span = “2014 to Till October 2024”, Database = Web of Science core collection. Altogether, 21219 original documents were the literature dataset. Each

publication included data related to the title, authors, publication year, keywords, countries/territories, institutions, journals, and other parameters.

RESULT AND DISCUSSION

Annual scientific production

The annual scientific production of articles can be found in Figure 1 and Table 1. The figure shows the compound annual growth rate over a time span. It can be observed that Epoxy Resinsresearch is growing exponentially.

Web of Science Categories

The aim and scope of the results obtained by the articles are the major parameter to measure the interdisciplinary of a research area. From the Web of Science Categoriesrecords, the area of publications of each articles obtained for the present analysis found that the researchers from Epoxy Resins area published the highest number of articles belonging to Polymer Science (712 articles), next followed by Materials Science Multidisciplinary, Materials Science Composites, Engineering Chemical, Chemistry Physical, Materials Science Coatings Films, Chemistry Applied, Chemistry Multidisciplinary, Physics Applied and Materials Science Textiles.

Author Productivity

An analysis of how researchers in a field of study collaborate can be done by looking at the network of authors regularly collaborate. The 2255 extracted articles were published Collaborative authors. The leading authors, who made contributions in Epoxy Resins articles, are provided in the Table 3. Authors collaboration is represented by a visualization network map through VOS Viewer. Collaborative network visualized authors are. Mohanty, Smita (43 Documents, 1331 Citations), Thomas, Sabu (37 Documents, 802 Citations), Nayak, Sanjay K. (32 Documents, 782 Citations), Siengchin, Suchart (31 Documents, 1030 Citations) and Xavier, Joseph Raj (29 Documents, 573 Citations) etc.,

Countries Productivity

According to Web of Science data, the 2255 publication Epoxy Resins articles were published by authors from 85 countries. However, 37 countries only have linked to other citied countries. Top 10 citation linked countries are India, Saudi Arabia, Peoples R China, USA, Ethiopia, Malaysia, South Korea, Thailand, Japan and England. VoS viewer is a software tool for constructing and visualizing bibliometric networks.

Organization Productivity

The institutions connected to the Epoxy Resins are research publication presented in Table 5. Institutions collaboration is a visualization network map through VOS Viewer displayed. Out of 1718 Institutions only 222 meet the threshold institutions. The leading more than 100 documents of organizations are Anna University, Indian Institutes of Technology and National Institutes of Technology.

Journal Productivity

According to Web of Science data, the 2255 extracted articles were published by a total of 461 journals. However, Top 6 journals had published more than 50 article on the topic,Polymer composites, Journal of applied polymer science, Biomass conversion and biorefinery, Materials research express, Journal of natural fibers and Silicon.

Keyword analysis

The authors' selected key words for their articles are usually of the primary ways that scholars can identify the study's contents. As a result, author keyword analysis can be an effective way to identify study trends and may also be helpful for visualizing data. The VOS viewer software was then used to analyze the 7245 refined author keywords, each of which has at least five occurrences. The co-occurrence network that indicates the relationship and weight of the imported author keywords is shown in Figure6. A keyword is represented by each node (circle). Each

keyword's frequency of occurrence in the dataset is shown by the size of the circles. The circles are connected by curves, and "link strength" is a measure of how strongly each curve connects two nodes. Table 7 leading 10 keywords are Behavior, Mechanical-Properties, Composites, Resin, Nanocomposites, Performance, Epoxy Resin, Thermal-Properties and Strength.

Most cited articles and authors

Citations are regarded as significant bibliometric parameters because they indicate the importance and relevance of a study in the academic community. Citations from the most recent year should be considered as an additional signal when evaluating the impact of an article. (Table 8). Top 10 Articles are Improved mechanical properties of carbon fiber/graphene oxide-epoxy hybrid composites, Thermo-mechanical characterization of siliconized E-glass fiber/hematite particles reinforced epoxy resin hybrid composite, Fabrication and characterization of echinoidea spike particles and kenaf natural fibre-reinforced Azadirachta-Indica blended epoxy multi-hybrid bio composite, Evaluation of mechanical and thermal properties of banana-flax based natural fibre composite, Low Velocity Impact and Mechanical Behaviour of Shot Blasted SiC Wire-Mesh and Silane-Treated Aloevera/Hemp/Flax-Reinforced SiC Whisker Modified Epoxy Resin Composites, Comparison of mechanical, electrical and thermal properties in graphene oxide and reduced graphene oxide filled epoxy nanocomposite adhesives, Mechanical, microstructural, and thermal characterization insights of pyrolyzed carbon black from waste tires reinforced epoxy nanocomposites for coating application, Influence of Irrigation Sequence on the Adhesion of Root Canal Sealers to Dentin: A Fourier Transform Infrared Spectroscopy and Push-out Bond Strength Analysis, Microwave exfoliated reduced graphene oxide epoxy nanocomposites for high performance applications and Water absorption behavior, mechanical and thermal properties of nano TiO2 enhanced glass fiber reinforced polymer composites

CONCLUSION

The scientific direction committed to the study of Epoxy Resinshave scientometricanalyzed using WoS analytical tools and the visualization program VOS viewer. The document are retrieve using the WoS database. The results of the analysis show which authors, organizations, and countries have published the most on the research topic. Find out which journals publish the most regularly on the topic; this will also display the publications that are most important. Using the VOS viewer software, it built the document co-citation network, which maps and visualizes research.

REFERENCES

1. K.Kanimozhi, K.Sethuraman, V.Selvaraj, M.Alagar. Development of ricehusk ash reinforced bismaleimide toughened epoxy nanocomposites. Front. Chem., 16 September 2014 Sec. Polymer Chemistry Volume 2 - 2014 | https://doi.org/10.3389/fchem.2014.00065.
2. 3rd International Conference on Materials Processing and Characterisation (ICMPC 2014) Study of Mechanical Properties of Wood Dust Reinforced Epoxy Composite Rahul Kumar, Kausik Kumar , PrasantaSahoo and SumitBhowmik. Procedia Materials Science 6 (2014) 551 – 556.
3. Epoxy Resins and Composites, Special Issue and Reviews, Polymer Polymer Section KrysztofFormela, Mohamed Reza Saheb(ISSN 2073-4360) 2022.
4. Bio-based silica-reinforced caprolactam-toughened epoxy nanocomposites. K.Kanimozhi, P.Prabunathan, V.Selvaraj, M.Alagar. High Performance Polymers, Sage Publications.Volume.25 Issue.2, 2015.
5. Development and characterization of surface modified mullite reinforced BMI-toughened epoxy nanocomposites, Kanimozhi K, Selvaraj V Prabunathan P, and Alagar M, Polymer Bulletin, Vol.71, pp. 1277-1293, 2014.
6. Synthesis and Development of Phosphazene Nano- Fiber Reinforced Composite Material for Weight Reduction in Dc Motor Body.A.Saraswathi, K.Kanimozhi PERIODICO di MINERALOGIA Volume 91, No. 5, 2022.
7. Mullitereinforced caprolactam toughened DGEBA epoxy nanocomposites,Kanimozhi K, Prabunathan P, SelvarajV and Alagar M, High Performance Polymers, Vol. 27, pp. 833-841, 2015.

8. A Green Technology in Tailoring Rice Husk Ash with Epoxy as (GRHA-EP) Nanocomposites for Persisting UV Rays in Aerospace Applications, K. Kanimozhi, M. Alagar, V. Selvaraj, P. Prabunathan and S. Thirumoorthi, Indian Journal of Natural Sciences www.tnsroindia.org.in,Vol.11, Issue 64, 2021
9. S.Rajeswari and K. Kanimozhi (2023) Mapping of Publications Productivity on Solar Tree: Review, Indian Journal of Natural Sciences, 14 (79) 60207-60221.
10. DivyaBaskaran, ShanmugamRajeswari, PanchamoorthySaravanan, Hun-Soo Byun (2024) Trends of Chemical Engineering Applications in the Last Three Decades: A Scientometric and Retrospective Review, Korean Journal of Chemical Engineering, 41, 2203–2225.
11. Amanullah, A. &Rajeswari, S. (2021), Scientometric analysis of global publication output on "Ladakh" in Web of Science (1989-2018). Library Philosophy and Practice, 1–11.
12. A Scientometric Analysis of Phenacetin Retrieved from Web of Science Database S.Rajeswari and Kanimozhi K, Indian Journal of Natural Sciences ISSN: 0976 – 0997, Vol.15, Issue 85,2024.

Table.1: Annual Productivity

Years	Record Count	%
2014	135	5.99
2015	140	6.21
2016	148	6.56
2017	146	6.47
2018	162	7.19
2019	235	10.42
2020	225	9.98
2021	223	9.89
2022	323	14.32
2023	282	12.51
Till October 2024	236	10.46
	2255	100

Table.2:Leading Web of Science Categories

Rank	Web of Science Categories	Record Count	% of 2,255
1	Polymer Science	712	31.574
2	Materials Science Multidisciplinary	515	22.838
3	Materials Science Composites	357	15.831
4	Engineering Chemical	229	10.155
5	Chemistry Physical	164	7.273
6	Materials Science Coatings Films	119	5.277
7	Chemistry Applied	118	5.233
8	Chemistry Multidisciplinary	116	5.144
9	Physics Applied	115	5.1
10	Materials Science Textiles	107	4.745

Table.3:Leading Author Productivity

Rank	Authors	Documents	Citations
1	Mohanty, Smita	43	1331
2	Thomas, Sabu	37	802
3	Nayak, Sanjay K.	32	782
4	Siengchin, Suchart	31	1030
5	Xavier, Joseph Raj	29	573

6	Karak, Niranjan	26	574
7	Patel, Jignesh P.	24	61
8	Sahoo, Sushanta K.	21	584
9	Alagar, M.	18	294
10	Chen, Xiangrong	18	127

Table.4: Leading Countries Productivity

Rank	Countries	Documents	Citations
1	India	2255	34887
2	Saudi Arabia	91	927
3	Peoples R China	69	1150
4	USA	57	1360
5	Ethiopia	46	287
6	Malaysia	46	743
7	South Korea	37	864
8	Thailand	37	1058
9	Japan	31	784
10	England	28	420

Table.5:Leading Organization Productivity

Rank	Organization	Documents	Citations
1	Anna University	137	3164
2	Indian Institutes of Technology	114	2267
3	National Institutes of Technology	112	1343
4	Institute of ChemicalTechnology	63	1041
5	Vellore Institutes Technology	56	548
6	Mahatma Gandhi University	43	885
7	Tezpur University	42	930
8	CSIR	39	1126
9	Indian Institute of Science	39	686
10	Saveetha Institute of Medical & Technical Science	38	336

Table 6 Leading Journal Productivity

Rank	Journal	Documents	Citations
1	Polymer composites	147	2138
2	Journal of applied polymer science	69	770
3	Biomass conversion and biorefinery	61	778
4	Materials research express	60	678
5	Journal of natural fibers	54	766
6	Silicon	51	1078
7	Progress in organic coatings	46	1256
8	Composites part b-engineering	42	1909
9	Polymer bulletin	36	430
10	Polymers	31	575

Table.7:Leading Keywords

Rank	Keywords	Occurrences
1	Behavior	508
2	Mechanical-Properties	469
3	Composites	387
4	Resin	306
5	Epoxy	299
6	Nanocomposites	282
7	Performance	275
8	Epoxy Resin	221
9	Thermal-Properties	138
10	Strength	136

Table.8:Leading Cited Articles

Rank	Authors	Article Title	Source Title	Times Cited,
1	Pathak, AK; Borah, M; Gupta, A; Yolcozeki, T; Dhakate, SR	Improved mechanical properties of carbon fiber/graphene oxide-epoxy hybrid composites	Composites Science And Technology	344
2	Prakash, VRA; Rajadurai, A	Thermo-mechanical characterization of siliconized E-glass fiber/hematite particles reinforced epoxy resin hybrid composite	Applied Surface Science	290
3	Prakash, VRA; Viswanthan, R	Fabrication and characterization of echinoidea spike particles and kenafnatural fibre-reinforced Azadirachta-Indica blended epoxy multi-hybrid bio composite	Composites Part A-Applied Science And Manufacturing	213
4	Srinivasan, VS; Boopathy, SR; Sangeetha, D; Ramnath, BV	Evaluation of mechanical and thermal properties of banana-flax based natural fibre composite	Materials & Design	166
5	Murugan, MA; Jayaseelan, V; Jayabalakrishnan, D; Maridurai, T; Kumar, SS; Ramesh, G; Prakash, VRA	Low Velocity Impact and Mechanical Behaviour of Shot Blasted SiC Wire-Mesh and Silane-Treated Aloevera/Hemp/Flax-Reinforced SiC Whisker Modified Epoxy Resin Composites	Silicon	164
6	Aradhana, R; Mohanty, S; Nayak, SK	Comparison of mechanical, electrical and thermal properties in graphene oxide and reduced graphene oxide filled epoxy nanocomposite adhesives	Polymer	162
7	Verma, A; Baurai, K; Sanjay, MR; Siengchin, S	Mechanical, microstructural, and thermal characterization insights of pyrolyzed carbon black from waste tires reinforced epoxy nanocomposites for coating application	Polymer Composites	149
8	Neelakantan, P; Sharma, S; Shemesh, H;	Influence of Irrigation Sequence on the Adhesion of Root Canal Sealers to Dentin: A Fourier Transform Infrared Spectroscopy	Journal Of Endodontics	141

	Wesselink, PR	and Push-out Bond Strength Analysis		
9	Sharmila, TKB; Nair, AB; Abraham, BT; Beegum, PMS; Thachil, ET	Microwave exfoliated reduced graphene oxide epoxy nanocomposites for high performance applications	Polymer	129
10	Nayak, RK; Mahato, KK; Ray, BC	Water absorption behavior, mechanical and thermal properties of nano TiO2 enhanced glass fiber reinforced polymer composites	Composites Part A-Applied Science And Manufacturing	128

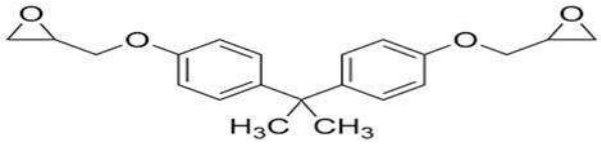

Figure.1: Structure of Epoxy

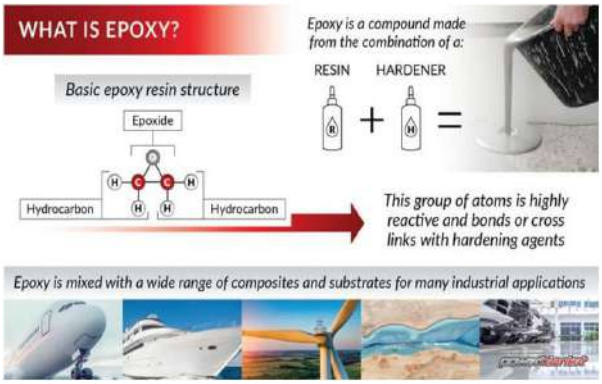

Figure.2: Synthesis of Epoxy in Lab

Figure.3: Applications of Epoxy material as Composites

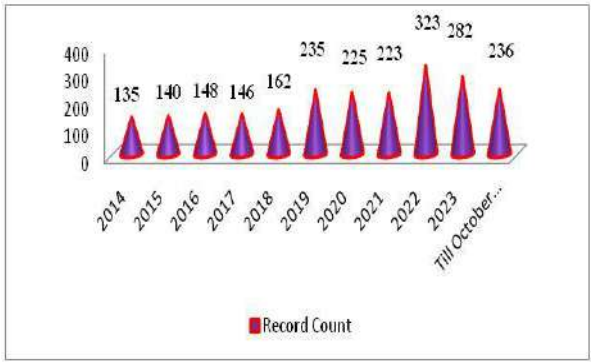

Figure.4 :Authors Productivity

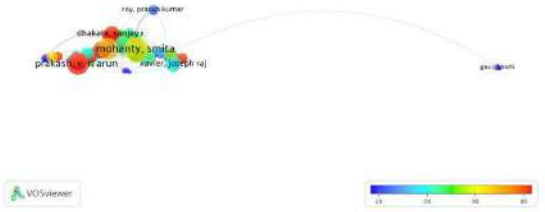

Figure.5: Authors collaborative network visualizing

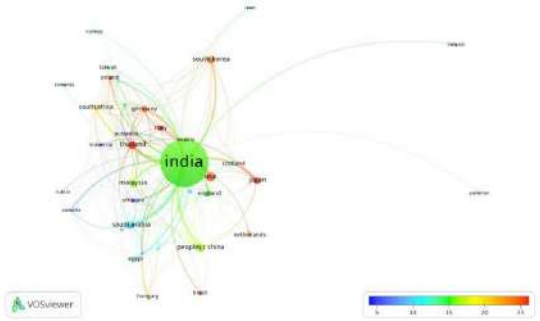

Figure. 6: Countries collaborative network visualizing

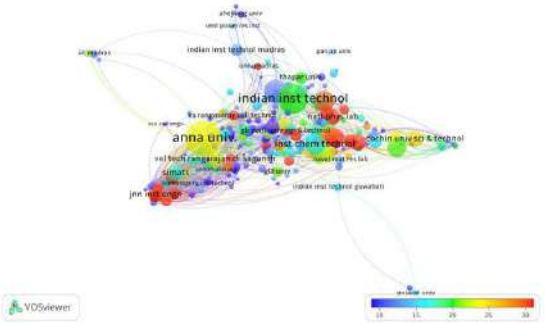

Figure. 7: Organisation collaborative network visualizing

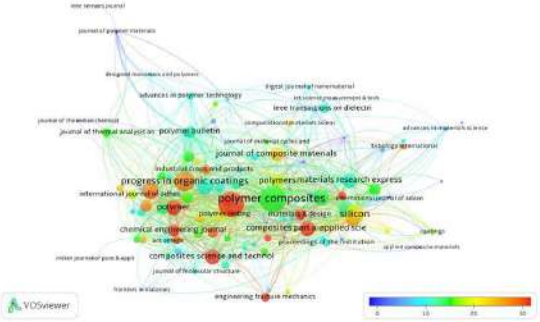

Figure. 8: Journal collaborative network visualizing

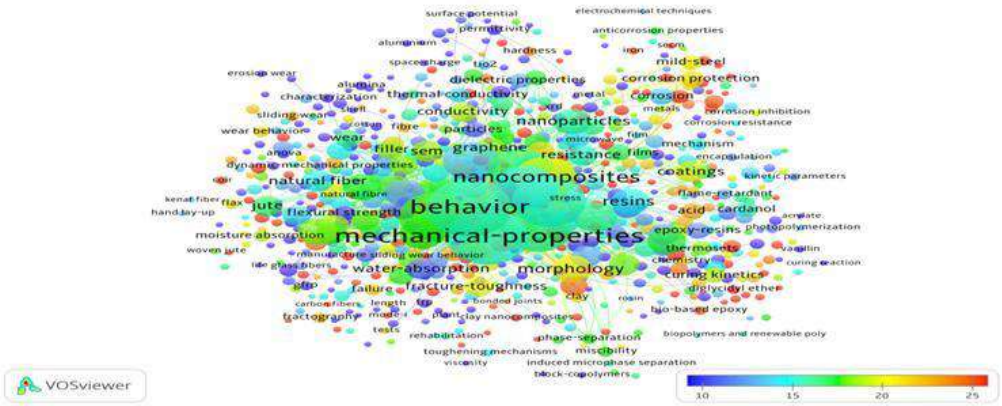

Figure. 9: Keywords collaborative network visualizing

Vol.15 / Issue 88 / Feb / 2025 *International Bimonthly (Print) – Open Access* *ISSN: 0976 – 0997*

RESEARCH ARTICLE

Synthesis, Characterisation and Electrochemical Studies of GO/ Poly – N- Methyl Pyrrole Polymer Composite for Super Capacitance Application

M. Kavitha[1] and R. R. Muthuchudarkodi[2]*

[1]Research Scholar (Registration Number: 19212232032007), Department of Chemistry, V. O. Chidambaram College, Thoothukudi, (Affiliated to Manonmaniam Sundaranar University, Tirunelveli), Tamil Nadu, India.
[2]Associate Professor, Department of Chemistry, V. O. Chidambaram College, Thoothukudi, (Affiliated to Manonmaniam Sundaranar University, Tirunelveli), Tamil Nadu, India.

Received: 24 Oct 2024 Revised: 10 Dec 2024 Accepted: 06 Feb 2025

***Address for Correspondence**
R. R. Muthuchudarkodi,
Associate Professor,
Department of Chemistry,
V. O. Chidambaram College, Thoothukudi,
(Affiliated to Manonmaniam Sundaranar University, Tirunelveli),
Tamil Nadu, India.
E.Mail: muthu.rajaram@gmail.com

ABSTRACT

In-situ chemical oxidative polymerization was used to create a graphene oxide (GO) /Poly-N-methyl pyrrole (P-NMPy) polymer composite. The formation of a bridge between GO and P-NMPy is confirmed and characterized by Fourier transform infrared (FT-IR), UV-Visible, and X-ray diffraction (XRD). The surface morphology analysis of a GO/P-NMPy polymer composite using scanning electron microscope and Atomic force Microscope. The electrochemical performance of polymer composite was analyzed with cyclic voltammetry and electrochemical impedance spectroscopy. More significantly GO/P-NMPy electrodes exhibit enhanced electrochemical performance with a specific capacitance. Spectroscopic analyses showed the successful incorporation of GO in the P-NMPy matrix. The dispersion of GO in the polymer matrix was found to be good through morphological investigation. The band gap energy value for the GO/P-NMPy polymer composite was determined to be 1.7eV. Two materials that can be used to build super capacitors are GO and P-NMPy. This composite material high specific capacitance (315µF) suggests that it could be used as an electrode material for super capacitors. The combination of GO with a conducting polymer like P-NMPy would typically result in a composite with an increased surface area, which is highly desirable for energy storage devices like super capacitors or batteries.

Keywords: GO, Poly (N-methyl pyrrole), polymer composites, Electrochemical Studies.

INTRODUCTION

Intensive research has been made to create super capacitors that are flexible, rigid, tiny, lightweight, eco-friendly, and have a higher storage capacity in response to the explosive expansion of next-generation portable electronics [1]. Super capacitors, also known as electrochemical capacitors, offer a viable alternative to energy storage devices because of their long lifespan, rapid charging time, and capacity to store and deliver a high power density [2-4]. Using the charge separation of the electrochemical interface between the electrode and electrolyte, this is achieved. It has been demonstrated that reinforcing polymers with graphene improves their properties. Better mechanical and thermal properties have led to an increase in the quality and applications of graphene/polymer nano composite [5–9]. Research studies have focused primarily on conducting polymers such as polypyrrole and its derivatives, such as poly N-methyl pyrrole [10–16]. Due to their unique characteristics, conducting polymers have been the subject of extensive research. Because of its many advantages, such as high specific capacitance, outstanding conductivity, superior mechanical qualities, and biocompatibility, P-NMPy is a preferred conducting polymer among the several pseudocapacitive materials utilized as an improved electrode material (Yu et al., 2013). Compared to pyrrole, N-methyl pyrrole has a few advantages because of its methyl group, which can produce the hydrophobic effect of the pyrrole ring. However, this group may also improve the organic molecules' ability to stick to the polymer surface [11–13]. Because of its methyl group, N-methyl pyrrole (N-MPy) has higher anode activity, a stronger mechanical strength, and lower production costs than pyrrole [17]. Additionally, N-MPy has a number of significant uses, including corrosion prevention, energy storage devices, and electrochemical sensors [18, 19]. Recent research has shown that the electrochemical performance of electrode materials can be greatly enhanced by the design and synthesis of nanostructured P-NMPy-based electrodes with logical topologies. The most researched conducting polymer, P-NMPy, is typically mixed with carbon-based compounds, specifically GO, to enhance their qualities [20, 21]. Graphene-based composites have received a lot of attention, because of their high electron mobility, mechanical strength, remarkable thermal stability, and large specific surface area, [22, 23]. Electronic circuits, batteries, sensors, detectors, capacitors, displays, and other electronic applications of polymer/graphene are the most successful [24, 25]. Large flexible panels made of polymer/graphene have also been employed in solar cells and fuel cell structures [26-31]. Fabrication possibilities for supercapacitors, optical displays, printed circuits, electrical devices, and superconductor devices have also been demonstrated using these hybrid materials [32-35]. Organic electronics is a term used to describe polymer-based electronics. Some outstanding conducting and semiconducting polymers with exquisite characteristics have been created and exploited as the foundation for innovative next-generation electronics. Supercapacitors based on GO typically have a high specific capacitance (135-264 Fg^{-1}). Many researchers have discussed the use of traditional polymerization methods to make GO composites with conducting polymers. The resultant materials often have better electrochemical properties than pure conducting polymer counterparts, such as greater conductivity and enhanced charge/discharge stability [36, 37]. P-NMPy, one of the materials synthesized through in situ polymerization, has piqued researchers' interest because to its inexpensive price, environmental stability, and ease of synthesis. In this method, it was demonstrated that the electrical conductivities of the polymer composite were significantly improved as compared to pure polymer. Traditional chemical polymerization was used to produce a variety of GO/P-NMPy composites to quantify the impact of this factor on the compound's final properties when used as a super capacitor in this study. The super capacitor performance of the various materials was evaluated and compared. The best composite's specific capacitance can approach (315 μF), which is significantly higher than the value obtained using pure P-NMPy (270 μF).

MATERIALS AND METHODS

Materials

Reagents were of analytical grade or the highest commercially available purity and were used as received. The methanol (HPLC grade), N-Methyl pyrrole (analytical grade), ethylene glycol, ferric chloride($FeCl_3.6H_2O$), sulphuric acid, potassium permanganate ($KMnO_4$), hydrogen peroxide (30%), hydrochloric acid (37%), ethanol, Graphite powder (99.9%), hydrazine monohydrate and deionised water.

Synthesis of Graphene Oxide

A modified Hummers method was used to manufacture GO from natural graphite.1g graphite and 25ml Concentrated.H_2SO_4 in a 500ml beaker. The mixture was swirled at temperatures ranging from 0 to 5^0C. 3g $KMnO_4$ was gently added to the suspension while stirring, and the temperature was kept below 20^0C. After adding the $KMnO_4$, the reaction mixture was vigorously agitated for 3 hours. Finally, with vigorous swirling, 150ml distilled water was gently added to the paste. At room temperature, the diluted black suspension was swirled once more. Finally, 5 millilitres of H_2O_2 were added. The entire reaction mixture was filtered and rinsed with deionized water many times until the pH of the solution was close to neutral. For further purification, the finished product was treated with the necessary amount of ethanol and dried in a vacuum oven at 60^0C.

Synthesis of Poly N-methyl pyrrole

In-situ polymerization was used to make Poly N-methyl Pyrrole. Before use, N-methyl pyrrole was distilled to make it colourless. An amount of (0.1M) 4.8g $FeCl_3$ was dissolved in 200ml of HCl (0.1M) with magnetic stirring for 2hours. (0.2M) distilled N-methyl pyrrole was dissolved in 200ml of HCl (0.1M).This mixture was stirred under ice bath for 2hours. Then, $FeCl_3$ solution was added into the monomer solution used ice bath. This reaction took 6hours to complete. The reaction was completed, and then the solution was undisturbed for 12hours. Black color precipitate was formed, now the precipitate was filtered and washed with distilled water. The final product was treated with ethanol and dried under vacuum oven at 60^0C for further purification.

Synthesis of GO/P-NMPy polymer composite

This reaction was carried out with GO that had been synthesized. In 50ml of water, 0.02g of GO was dissolved and sonicated for 30 minutes. A solution of 0.1M distilled N-Methyl Pyrrole was dissolved in 100ml of HCl (0.1M) and agitated for 1 hour with an ice bath. An amount of (0.1M) 2.4g $FeCl_3$ was dissolved in 100ml of HCl (0.1M) with magnetic stirring for 1 hour. The $FeCl_3$ and GO solution were added to the monomer solution after one hour. The solution was swirled constantly for 6 hours in an ice bath. After the reaction was finished, the solution was left undisturbed for 12 hours. Precipitate of a black color was generated. After that, the precipitate was filtered and rinsed in distilled water. For further purification, the finished product was treated with the necessary amount of ethanol and dried in a vacuum oven at 60^0C.

Characterization

Computer controlled JASCO V-530 was used to study UV-VIS spectral behavior. XRD measurements were made by Panalytical X'Pert Powder X'Celerator Diffractometer, measurement range: 10 to 80 degree in 2θ and particle size was calculated using Scherrer's equation. The EDAX and FESEM measurements were carried by JEOL JSM-6700F field emission scanning electron microscope. The electrochemical behavior of nanocomposite have been investigated through CH-Instrument INC., TX, and USA.

RESULT AND DISCUSSION

Fourier Transform Infrared Spectroscopy

The FT-IR spectra of GO, P-NMPy and GO/P-NMPy composites are shown in Fig.1. As shown in Fig. 1(a) the GO spectral range the broad intense peaks at 3408cm^{-1}, 1721cm^{-1}, and 1626cm^{-1} respectively, corresponding to the –OH group, carbonyl (C=O) stretching, and C=C stretching vibration. The C-O stretching vibrations of carboxyl and alkoxy groups are represented by the peaks observed at 1384 cm^{-1} and 1061cm^{-1} [38, 39]. In Fig. 1(b) the aromatic out-of-plane bending vibration of P-NMPy rings caused the distinctive peaks at 779–630 cm^{-1} in P-NMPy [40]. The 876 cm^{-1} peaks could be attributed to the C-H out-of-plane vibration [41]. The peaks at 1020 cm^{-1} and 1384 cm^{-1} should be attributed to C-H deformation vibrations and C-N stretching vibrations, respectively [42]. Because of the existence of P-NMPy, the peak of about 1457cm^{-1} shows the C=N stretching vibration. The C-C stretching vibration in the pyrrole ring was linked to the absorption band at 1617cm^{-1} [43]. The aromatic C=C stretching of P-NMPy is depicted by the peak at 1685cm^{-1} [44]. The N-H stretching vibration of the ring in the produced polymer is what causes the big peak

at 3416cm^{-1}. [45]. The polymerization and existence of P-NMPy in the polymer composite were confirmed by these peaks. Fig. 1(c) shows the spectra of GO/P-NMPy composite, which feature a mixture of GO and P-NMPy distinctive absorption bands. The existence of –COOH, –OH, and C–O–C groups in GO is indicated by distinctive absorptions in the region of 1720–1050cm^{-1} [46,47]. The N-H stretching vibrations were assigned to the band absorbed 3400cm^{-1} in GO/P-NMPy, and the typical peak of C=O stretching vibrations of carboxyl at 1721cm^{-1} vanished, indicating GO was reduced [48]. The remaining groups of graphene oxide had C-OH stretching at 1383cm^{-1} and C-O vibration at 1018cm^{-1}, with the latter possibly being an overlap of C-H in-plane vibration of P-NMPy. The presence of P-NMPy in GO/P-NMPy polymer composite is indicated by the distinctive absorption peak of C-C and C=N at 1625cm^{-1} and 1462cm^{-1}, respectively. The existence of P-NMPy in the composites is indicated by a C-H out-of-plane absorption peak at 794cm^{-1} without any changes in the internal structure [49]. All of the foregoing demonstrates that Poly(N-methyl pyrrole) interacts with the oxygen atom of GO, causing methyl pyrrole to polymerise on the surface of GO layers.

Optical Study

Fig. 2 shows the UV-Vis absorption spectra of the nanostructures examined. The charge transfer interaction happened in the GO/P-NMPy hybrid materials [50, 51]. Poly (N-methyl pyrrole) is considered a conjugated donor polymer, while GO is widely known as a good electron acceptor. The UV spectrum of GO Fig. 2(a) indicates that the UV-Visible spectra of GO have two distinct absorption regions. π- π^* transitions of aromatic C-C bonds are responsible for the absorption band centered at 259 nm [52, 53]. The shoulder centered at 314 nm corresponds to C=O bond n-π^* transitions [54]. Fig. 2(b) depicts P-NMPy's characteristic peaks. For bare P-NMPy, the distinctive π- π^* or polaron absorption band was found at [55, 56]. The presence of carboxyl, carboxyl, epoxy, and hydroxyl functional groups on the surface of GO provided a negative charge to the GO matrix. Electrostatic contact caused the positively charged N-Methyl pyrrole polymer to be evenly adsorbed over the negatively charged GO matrix. GO consists of oxygen-containing such as ether, hydroxyl, epoxide, carbonyl, and carboxyl functional groups [57, 58]. Which can support the nucleation of a conductive polymer that favors the surface coverage of P-NMPy with the strong π- π^* interaction between the P-NMPy backbone and GO surface. Fig. 2(c) shows GO/P-NMPy exhibited three distinctive SPR bands, and the characteristic GO and P-NMPy bands were found at 262 nm, 370 nm, and 420 nm.

Band gap Energy

The optical absorption in conjugated polymers can be attributed to charge carriers transitioning via a forbidden energy gap. Table.1 shows the optical band gap energy derived using the Tauc relation from the following equation:

$$E_g^{opt}=1240/\lambda_{edge}$$

The optical band gap is E_g^{opt} (eV), and the absorption edge is λ_{edge} (nm). Fig.3 shows the band gap energies of GO, P-NMPy and GO/P-NMPy polymer composite are 2.2eV, 2.5eV, and 1.7eV respectively. The band gap energy value for the GO/P-NMPy polymer composite was determined to be 1.7eV, indicating that the composite is bipolaron.

Structural Characterization

The X- ray data were recorded in terms of the diffracted X-ray intensities (I) vs 2θ. Scherrer's formula, which is stated as, was used to compute the crystalline size.

$$D = 0.9\lambda/\beta \cos\theta \text{ ---------- (1)}$$

Where D denotes the crystalline size, β is the full width at half maximum (FWHM) of the most intense diffraction peak in radiance, q the diffraction angle, and the wavelength of X-ray radiation. The XRD pattern GO had a prominent peak at 2θ =26.69, corresponding to the reflection peak, which can be seen in Fig. 4(a). As shown in Fig.4(b) the XRD pattern of pure P-NMPy, which has a peak at 2θ =33.22 demonstrates that it is semi-crystalline. The GO/P-NMPy polymer composite exhibits two peaks at 2θ =26.59 for GO and 2θ =33.32 for P-NMPY in Fig 4(c), showing that GO has been incorporated into the P-NMPy matrix. The Debye-Scherrer equation (1) was used to compute the particle size of the polymer composite. The generated GO/P-NMPy polymer composite has an average

crystallite size of 53.30 nm. The interaction of GO with the P-NMPy polymer matrix is further confirmed by the variation in diffraction intensity.

Scanning Electron Microscopy

SEM images of pure GO, are shown in Fig. 5(a). The GO inherits the layer-by-layer and network structure with denser stacking, while the SEM image of P-NMPy shows in Fig. 5(b). This structure is like the hemispherical nature of the polymer. Fig.5(c) shows the SEM micrographs of GO/P-NMPy polymer composite smooth surfaces observed. Since the polymer grows in the pores and galleries of GO, it is difficult to distinguish the individual phases ie, GO and P-NMPy in the GO/P-NMPy polymer composite from the SEM micrograph.

Energy Dispersive X-Ray Analysis

The EDAX spectrum of the GO/P-NMPy polymer composites is also shown in Fig.6. It has three distinct peaks for the atoms 'C,' 'O,' and 'N'. The spectrum of GO/P-NMPy indicates that the molar ratio of carbon, oxygen, and nitrogen are 73.02%, 21.40%, and 5.58% respectively. It demonstrates that the polymer was successfully dopped onto the GO sheet. Table.2 shows graphene and N-(methyl pyrrole) present in the sample to be in a stoichiometric atomic ratio.

Atomic Force Microscopy Analysis

The AFM imaging process of GO-coated glass slides was carried out to get an understanding of the topography and roughness. Fig. 7(a) displays 310 nm, in the topography of GO showed agglomerated particles with smooth surfaces and shallow valleys. The surface topography of GO in 3D images exhibits a mountain-like structure. Fig. 7(b) shows the surface irregularities are only minor and smaller. In the topography of P-NMPy small spherical-like dots with a flat surface are present. The globule structure is the combination of long-range (due to the presence of globules) and short-range (due o the region inside the globules) morphologies. The surface topography of P-NMPy in 3D images exhibits a rock-like structure. Fig. 7(c) displays 310 nm, in the topography of GO/P-NMPy shows agglomerated particles with a smooth surface. It may be due to the polymer bindings or overlapping of each together. The surface topography of GO/P-NMPy in 3D images exhibits the mountain-like structure.

Roughness Analysis

Average roughness is considered as the mean height of the given area and route mean square roughness is the standard deviation of the height of the surface from the average height of the surface. Line roughness can be calculated by selecting a line in the topography. Average roughness and root mean square roughness were calculated and given in Table.3.

Skewness and Kurtosis

The degree of asymmetry of the surface is Skewness. It is the third moment of the amplitude probability function. It is used to determine the asymmetry of the surface around it. When skewness is zero, height is distributed symmetrically around the mean plane. When skewness is less than zero height distribution is not symmetrical and the surface seems to be more planar with more valleys. When skewness is more than zero, more tall peaks are present than pits in the topography [59]. Kurtosis can be defined as the measure of sharpness or the flatness in the given topography concerning the normal distribution. It is the fourth moment of the amplitude probability function. The value of kurtosis is three for normal distribution and such a surface is called a mesokurtic surface. For mesokurtic surface sharp peaks and deep valleys co-exist. If the kurtosis is less than three, it represents a flat surface. These flat surfaces are called platykurtic. The kurtosis value of more than three indicates that more peaks are present in the topography than in pits [60]. Skewness and Kurtosis were calculated and given in the Table. 4.

Cyclic Voltammetry was used to study the electrochemical performance of the GO, P-NMPy and GO/P-NMPy polymer composite modified glassy carbon electrode over a potential range of -1.2 to 2.0 volt at varied scan rates. The glassy carbon electrode coated with GO, P-NMPy, and GO/P-NMPy polymer composite are used ($0.0314cm^2$) as the working electrode. The electrochemical cell was composed of a $1cm^2$ Pt electrode; Ag/AgCl serves as a reference electrode. Fig. 8(a) depicts the cyclic voltammetric behavior of the CV curves of GO, which shows one oxidation peak at potentials ranging from 0.2524V to 0.4853V and one reduction peak at potentials ranging from -0.0868V to -

0.3787V. Fig. 8(b) shows the cyclic voltammetric behavior of the CV curves of P-NMPy, with one oxidation peak at a potential of 0.9094V to 0.9623V and one reduction peak at a potential of -0.5429V to -0.6172V. The CV curves of GO/P-NMPy showed one oxidation peak at a potential of 0.6851V to 1.0630V and one reduction peak at a potential of -0.3780V to -0.4133V, as shown in Fig. 8(c). The anodic and cathodic peak potentials of the GO, P-NMPy, and GO/P-NMPy reveal that the redox peak currents rose linearly as the scan rate increased from 50, 100, 150, and 200 mvs^{-1}, indicating a surface-controlled electrode process. The existence of GO, P-NMPy, and GO/P-NMPy is confirmed by the good reversible redox behavior. The shape of the CV curves in Fig.8 does not change significantly as the scan rate increases, which is typical of excellent capacitance nature. The evident increase in current with scan rates demonstrates that the electrode has a good rate capacity at high scan rates. Specific capacitances (C_{sp}) were obtained from cyclic voltammetry (cv) experiment. It was calculated by means of the following equation (2) [61].

$$C_{sp} = \int (I \times dv / \Delta\upsilon \times m \times \Delta V) \quad \text{---------- (2)}$$

Where I x dv is the integral area of the cyclic voltammogram loop, Csp is the specific capacitance based on the mass of electro active materials (F/g), I is the response current (A), ΔV is the potential window (V), Δυ is the scan rate (V/s), and m(g) is the total mass of the active materials. However, most of the CV plots deviate from rectangular box shapes due to the redox reactions of electro active materials [62]. Fig.8 shows the interaction of GO and P-NMPy has a synergic effect to increase specific capacitance [63]. With a value of (315μF), the specific capacitance of the GO/P-NMPy polymer composite is the highest of all the samples. This number is higher than the pure GO (219μF) and P-NMPy (270μF) values. The improved performance could be ascribed to the interconnected GO with the conjugated N-methyl pyrrole polymer, which allows for easier electron mobility while also increasing electrode conductivity. The electrochemical performance of the GO/P-NMPy polymer composite super capacitor should be further enhanced since GO, P-NMPy, and GO/P-NMPy produced faster electrochemical reactions. The capacitance were calculated and given in the Table.6.

Pseudo Capacitive Behavior

The Bode plot depicts the change in the Bode phase as a function of applied frequency. The phase angle might be anything from 90 degrees (for a perfect capacitor n = 1) to 0 degrees (for a perfect resistor n = 0) [64]. Fig. 9(a) shows the Bode Phase angle (degree) vs. log frequency (Hz) plot of GO. The slope of the frequency against the |Z| plot yields the value of n. The phase angle of 68^0 in the instance of GO implies that the material is pseudo capacitive. Fig. 9(b) shows the phase angle of 65^0 in the instance of P-NMPy and illustrates the material's pseudo capacitive character. Fig. 9(c) shows a Bode plot of Phase angle (degree) vs. log frequency (Hz) for GO/P-NMPy. The phase angle of 80^0 in the instance of GO/P-NMPy implies that the material is pseudo capacitive. The behavior of the electrode coated with GO/P-NMPy polymer composite changes from a pure resistor at high frequency to pseudo capacitors at low frequency, according to these findings. It has Bode phase angles of 68^0, 65^0, and 80^0, respectively. It denotes a pseudo capacitor's characteristic behavior. Table.5 shows the Bode phase angle values for GO, P-NMPy, and GO/P-NMPy.

Electrochemical Impedance Spectroscopy

Combined with galvanostatic measurements, electrochemical impedance spectroscopy (EIS) is a powerful technique that can reveal additional details regarding the electrochemical frequency behavior of the system. The charge transfer resistance Rct and double layer capacitance Cdl only describe the resistance and capacitance provided by the electrochemical double layer at the surface. Equation (3) is used to calculate the double layer capacitance, and the resistance is produced from the low and high frequency resistance values.

$$C_{dl} = 1/2\ \pi f_{max} R_{ct} \quad \text{---------- (3)}$$

Electrical equivalent circuits were used to verify the correctness of the EIS findings. A series of impedance spectroscopy tests were carried out to gain a better understanding of the capacitance and other relevant electrochemical information of the composite materials investigated. The Nyquist graphs further support GO/P-

NMPy's conductivity. The electrochemical impedance spectra for the modified GCE electrode containing synthesized components are shown in Fig.10. The highest double-layer capacitance (C_{dl}) was obtained for GO/P-NMPy. An impedance plot is traditionally divided into two parts: the high-frequency and low-frequency areas. A semicircular shape was achieved in all cases in the high-frequency zone, which is associated with interfacial processes. The wider arc diameter for the P-NMPy and GO/P-NMPy modified GCE electrodes suggests a low charge transfer rate due to high electron transfer resistance. The semicircle in the case of GO is smaller, implying that the electron transport resistance is lower. Table.7 shows that R_{ct} and C_{dl} values of GO, P-NMPy, and GO/P-NMPy polymer composite.

CONCLUSION

Traditional chemical polymerization was used to make a series of GO/P-NMPy polymer composite in this study. FTIR and UV-Vis spectroscopy techniques were used to determine the functional group and optical behavior of RGO, P-NMPy and GO/P-NMPy polymer composite, respectively. Using the XRD analytical technique, crystallinity was investigated. The morphology and components were determined by using FESEM, AFM and EDAX. The redox behavior and capacitance of GO, P-NMPy and GO/P-NMPy polymer composite were demonstrated using an electrochemical workstation. GO/P-NMPy had the highest specific capacitance (315μF) among the new materials, as well as a higher value than pure GO (219μF) and the pure polymer's value (270μF). This composite material has a high specific capacitance. It has the potential to be used as a super capacitor electrode material. The increased electrical double layer capacitance seen in the Cyclic Voltammetry studies, as well as the GO/P-NMPy composite's higher rate capacity compared to pure synthesized materials, could be owing to the GO's superior pseudo capacitance and a synergistic impact with the P-NMPy. With the addition of GO, the composite's specific capacitance rises. This is because GO's sheet-like shape provides more active surfaces for easy oxidation-reduction reactions. The specific capacitance of the composite increases as the conjugation length (as seen by FTIR and UV-visible spectroscopic data) of P-NMPy increase with the addition of GO.

REFERENCES

1. Lu X,Yu M, Wang G,Tong Y,Li Y Flexible solid-state supercapacitors design,fabrication and application.Energ Environ Sci 7(7) (2014)2160-2181.
2. Zhang LL,Zhou R,Zhao X Graphene-based materials as supercapacitors electrodes.J Mater Chem 20 (29) (2010) 5983-5992.
3. Wang Y,Shi Z,Huang Y,Ma Y,wang C,Chen M,Chen Y Supercapcitor devices based on grapheme materials.J Phys Chem C 113 (30) (2009) 13103-13107.
4. Sun J,Haung Y,Fu C,wang Z,Huang Y,zhu M,Zhi C,Hu High-performance stretchable yam supercapcitor based on ppy@CNTs@Urathene elzastic fiber core spun yarn.Nano Energy 27 (2016) 230-237.
5. Kausar A. Applications of polymer/graphene nanocomposite membranes: a review. Mater Res Innovat.25 (2018) 1-2.
6. Kausar A. Enhanced electrical and thermal conductivity of modified poly (acrylonitrile-co-butadiene)-based nanofluid containing functional carbon black-graphene oxide. Fuller Nanotub Carb Nanostruct. 24 (2016) 278-285.
7. Kausar A. Composite coatings of polyamide/graphene: microstructure, mechanical, thermal, and barrier properties. Compos Interfac. 25 (2018) 109-125.
8. Kausar A, Rafique I, Muhammad B. Aerospace application of polymer nanocomposite with carbon nanotube, graphite, graphene oxide, and nanoclay. Polym-Plast Technol Engineer. 56 (2017) 1438-1456.
9. Kausar A. Review on Structure, Properties and Appliance of Essential Conjugated Polymers. Am J Polym Sci Engineer. 4 (2016) 91-102.
10. Pirsa S, Mohammad Nejad F, Simultaneous analysis of some volatile compounds in food samples by array gas sensors based on polypyrrole nano-composites, Sensor Review, 37 (2017) 155–164.
11. Pirsa S, Heidari H, Lotfi J, Design selective gas sensors based on nano-sized polypyrrole/polytetrafluoroethylene and polypropylene membranes. IEEE Sensors Journal, 16 (2016) 2922-2928.

12. Barisci J.N, Wallace G.G, Andrews M.K, Partridge A.C,Harris P.D, Conducting polymer sensors for monitoring aromatic hydrocarbons using an electronic nose, Sensors and Actuators B: Chemical, 84 (2002) 252- 257.
13. Rao P.S, Anand J, Palaniappan S, Sathyanarayana D.N, Effect of sulphuric acid on the properties of polyaniline–HCl salt and its base, European Polymer Journal, 36 (2000) 915-921.
14. Mahmoudia M.R, Alias Y, Basirum W.J, Ebadi M, Poly (N-methyl pyrrole) and its copolymer with otoluidine electrodeposited on steel in mixture of DBSA and oxalic acid electrolytes, Current Applied Physics, 11 (2011) 368-375.
15. Redondo M .I, De La Blanca E .S, García M .V, Raso M.A,. Tortajada J, Gonzalez-Tejera M.J, FTIR study of chemically synthesized poly (N-methylpyrrole). Synthetic metals, 122 (2001) 431-435.
16. Huerta G, Fomina L, Rumsh L, Zolotukhin M.G, New polymers with N-phenyl pyrrole fragments obtained by chemical modifications of diacetylene containing polymers, Polymer Bulletin, 57 (2006) 433–443.
17. Ramanathan K, Bangar M.A, Yun M, Chen W, Mulchandani A, Myung N.V, In situ fabrication of single poly(methyl pyrrole) nanowire, Electroanalysis. 19 (2007) 793–797.
18. Liu Y, Xiong H, Huang H, Li L, Huang Y, Yu X, Fabrication of poly(Nmethylpyrrole) nanotubes for detection of dopamine, Polym. Bull. 75 (2018) 2357–2368. doi:10.1007/s00289-017-2157-1.
19. Zeybek B, Aksun E, Electrodeposition of poly(N-methylpyrrole) on stainless steel in the presence of sodium dodecylsulfate and its corrosion performance, Prog. Org. Coatings. 81 (2015) 1–10.
20. Raccichini R., Varzi A., Passerini S., Scrosati B.: The role of graphene for electrochemical energy storage. Nature Materials, 14 (2015) 271–279.
21. Novoselov K. S., Geim A. K., Morozov S. V., Jiang D., Zhang Y., Dubonos S. V., Grigorieva I. V., Firsov A. A.: Electric field effect in atomically thin carbon films. Science, 306 (5696), (2004) 666-9.
22. Mohd Abdah M.A.A,Mohd Razali N.S,Lim P.T Kulandaivalu S and Sulaiman Y Review of the use of transition – metal-oxide and conducting polymer-based fibres for high-performance supercapacitors Mater.Chem.Phys,219 (2018) 120-12.
23. Kulandaivalu S and Sulaiman Y A. Simple strategy to prepare a layer-by-layer assembled composite of Ni–Co LDHs on polypyrrole/rGO for a high specific capacitance supercapacitor J.Power Soures 419 (2019) 181-191
24. Hu K, Kulkarni DD, Choi I, Tsukruk VV. Graphene-polymer nanocomposites for structural and functional applications. Prog Polym Sci. 39 (2014) 1934-1972. .
25. Zhu Y, Murali S, Cai W, Li X, Suk JW, Potts JR, Ruoff RS. Graphene and graphene oxide: synthesis, properties, and applications. Adv Mater. 22 (2010) 3906-3624.
26. Kausar A. Proton exchange fuel cell membranes of poly (benzimidazole-amide)/sulfonated polystyrene/titania nanoparticles-grafted-multi-walled carbon nanotubes. J Plast Film Sheet. .31(2015) 27- 44
27. Kausar A, Hussain A, Khan MY, Siddiq M. Fuel cell membranes prepared from multi-walled carbon nanotubes and silica nanotubes-filled sulfonated polyamide/sulfonated polystyrene porous blend films. J Plast Film Sheet. . 30 (2014) 314-336
28. Kausar A. Fuel cell membranes of phosphoric acid–doped poly (benzimidazole/ether/siloxane/amide)/sulfonated polystyrene/silica nanoparticle nanocomposites: A physical property study. J Thermoplast Compos Mater. . 29 (2016) 717-731
29. Kausar A. Polycarbonate/Polypropylene-Graft-Maleic Anhydride and Nano-Zeolite-Based Nanocomposite Membrane: Mechanical and Gas Separation Performance. Adv Mater Sci. . 16 (2016) 17-28
30. Kausar A. Environmental Remediation Using Polystyrene/4-Aminophenyl Methyl Sulfone and Carbon Nanotube Nanocomposite. Physical Chemistry. .7 (2017) 27-30
31. Kausar A. Design of poly (1-hexadecene-sulfone)/poly (1, 4-phenylene sulfide) membrane containing nano-zeolite and carbon nanotube for gas separation. Int J Plast Technol. 21 (2017) 96-107
32. Kausar A. Preparation and Characteristics of Mercaptobenzene Functionalized Graphite and Epoxy-based Hybrid Membranes. Am J Mater Sci. 5 (2015) 17-21
33. Meer S, Kausar A, Iqbal T. Trends in conducting polymer and hybrids of conducting polymer/carbon nanotube: a review. Polym Plast Technol Engineer. 55 (2016) 1416-1440
34. Kausar A. A Study on Poly (vinyl alcohol-co-ethylene)-graft-Polystyrene Reinforced with Two Functional Nanofillers. Polym Plast Technol Engineer. 54 (2015) 741-749

35. Khan F, Kausar A, Siddiq M. A review on properties and fabrication techniques of polymer/carbon nanotube composites and polymer intercalated buckypapers. Polymer Plast Technol Engineer. 54 (2015) 1524-1539.
36. Krim M.R, Lee C.J and Lee M.S Synthesis and characterization of conducting polythiophene / carbon nanotubes composites. J.Polym.Sci,Part A:Polym.Chem.,44 (2006) 5283.
37. Lu Q and Zhou Y, Synthesis of mesoporous polythiophene/MnO_2 nanocomposite and its enhanced pseudocapacitive properties. J.Power Soures, 196 (2011) 4088.
38. Guo H.L, Wang X.F, Qian Q.Y, Wang F.B, Xia X.H. A green approach to the synthesis of graphene nanosheets. ACS Nano, 3 (9), (2009) 2653–2659,
39. Zhu C, Guo S, Fang Y, Dong S. Reducing sugar: New functional molecules for the green synthesis of graphene nanosheets. ACS Nano, 4 (4), (2010) 2429–2437,
40. Thompson G.E. Preparation and surface analysis of PPy/SDBS films on aluminium substrate. Polímeros: Cienc. Tecnol. 11 (2001) 142–148,
41. Han Y.Q, Hao L.A, Zhang X.G. Preparation and electrochemical performances of graphite oxide/ polypyrrole composites. Synth Met 160 (2010) 2336–2340,
42. Ma Y, Jiang S, Jian G, Tao H, Yu L, Wang X, Wang X, Zhu J, Hu Z, Chen Y. CN_x Nnofibers converted from Polypyrrole Nanowires as Platinum Support for Methanol Oxidation. Energy Environ.Sci. 2 (2009) 224-229.
43. Jang J, Oh J.H, Novel crystalline supramolecular assemblies of amorphous polypyrrole nanoparticles through surfactant templating. Chem. Commun Supercapacitor electrode based on three-dimensional graphene polyaniline hybrid. Mater. Chem. Phys. 134 (2002) 576–580.
44. Lim S.P, Pandikumar A, Leim Y.S, Huang N.H, Leim H.M, In-situ electrochemically deposited polypyrrole nanoparticles incorporated reduced graphene oxide asan efficient counter electrode for platinum-free dye
45. sensitized solar cells. Sci.Rep. 4 (2014) 5305. Sawangphruk M, Suksomboon M, Kongsupornsak K, Khuntilo J, Srimuk P, Sanguansak Y, Klunbud, P, Suktha P,
46. Chiochan P. High-performance supercapacitors based on silver nanoparticle–polyaniline-graphene nanocomposites coated on flexible carbon fiber paper. J. Mater. Chem. A. 1 (2013) 9630–9636. Cassagneau T, Fendler JH. High density rechargeable lithium-ionbatteries self-assembled from graphite oxide. Adv Mater; 10 (1998) 878–82.
47. Scholz W, Boehm HP. Betrachtungen zur struktur des graphitoxids. Z Anorg Allg Chem; 369 (1969) 327–40.
48. Whitby R.L.D, Korobeinyk A, Mikhalovsky S.V, Fukuda T, Maekawa T. Morphological effects of single-layer graphene oxide in the formation of covalently bonded polypyrrole composites using intermediate diisocyanate chemistry. J Nanopart Res 13 (2011) 4829–4837.
49. Gu Z, Li C, Wang G, Zhuang L, Li X, Wang W, Jin S Synthesis and characterization of polypyrrole/graphite oxide composite by in situ emulsion polymerization. J Polym Sci Pol Phys48 (2010) 1329–1335.
50. Hill C.M, Zhu Y, Pan S. Fluoresence and electroluminesence quenching evidance of iterfacial transfer in poly (3-hexylthiophene);graphene oxide bulk heterojunction photovoltaaic devices.ACS Nano 5(2), (2011) 942-95,
51. Istif E, Hernandez Ferrer J, Urrriolabeitia A, Tagmatechis N, Fratta G, Jlarge M, Dalton A.B, Benito A.M, Master W.K, Conjucated polymer nanoparticle-graphene oxide charge-transfer complex. Adv.Funct.Master 28(23), (2018) 1707548.
52. Clark B.J, Frost T, Russell M.A UV spectroscopy: techniques, instrumentation, data handling/UV Spectrometry Group Chapman& Hall, London, (1997) 4.
53. Mei Q, Zhang K, Guan G, Liu B, Wang S, Zhang Z Highly efficient photoluminescent graphene oxide with tunable surface properties,Chemical Communications, 46 pp. (2010) 7319-7321.
54. Marcano D.C, Kosynkin D.V, Berlin J.M, Sinitskii A, Sun Z, Slesarev A, et al. Improved synthesis of graphene oxide, ACS Nanoscience, 4 pp. (2010) 4806-4814.
55. Hong T. K, Lee D.W, Choi H.J, Shin H. S, Kim B.S. Transparent, flexible conducting hybrid multilayer thin films of multiwalled carbon nanotubes with graphene nanosheets. ACS Nano 4 (7), (2010) 3861−3868.
56. Borthakur L.J, Konwer S, Das R, Dolui S. K. Preparation of conducting composite particles of styrene−methyl acrylate copolymer as the core and graphite-incorporated polypyrrole as the shellby surfactant-free mini emulsion polymerization. J. Polym. Res. 18 (5), (2011) 1207−1215.

57. Luo Z, Lu Y, Somers L.A, Johnson A.T.C. High yield preparation of macroscopic graphene oxide membrane. J. Am. Chem. Soc. 131 (3), (2009) 898–899.
58. Gnana kumar G, Babu K.J, Nahm K.S, Hwang Y.J. A facile one-pot green synthesis of reduced graphene oxide and its composites for nonenzymatic hydrogen peroxide sensor applications. RSC Adv. 4 (2014) 7944.
59. Anil Kumar Bajpal, Rin Keshr Bhart, Ravi Kaatare, Atomic force microscopy enabled roughness analysis of nano structured poly(diammonia phalene) doped (poly vinyl alcohol)conducting polymer.Thin flims,Micron,vol.96 (2016) 12-17.
60. Raposo.M, Ferreria.Q and Riberio P.A Guide for Atomic force microscopy Analysis of soft condensed Masters,Modern Research and Educational Topics in Microscopy, (2007) 758-769.
61. Yue B.B, Wang C.Y,Wagner P, yang Y, Ding X, Officer D.L, Wallace G.G. Electro deposition of Pyrrole and 3-(4-tert-Butyl Phenyl) Thiophene Copolymer for Supercapacitors.Int.J.Electrochem.Sci.4(9), (2009) 1289-1301.
62. Meng Q,Cai K,Chen Y,Chen L.Research Progress on conducting Polymer Based Supercapacitor Electrode Materials.Nano Energy,36 (2017) 268-285.
63. Bae J,Park J.Y, Kwon O.S, Lee C.S. Energy Efficient Capacitors Based on Graphene/Conducting Polymer Hybrids.Journal of Industrial and Engineering Chemistry, 51 (2017) 1-11.
64. Shukla S.K, Bharadraja A, Tiwari A, Parashar G.K, Dubey G.C Synthesis and Characterisation of highly crystalline polyaniline film promising for humid sensor,Advansed Matterials letters Vol.1 (2010).

Table.1: Band gap Energy values of GO, P-NMPy, GO/P-NMPy polymer composite

Sl. No	Materials	Bandgap (eV)
1	GO	2.2
2	P-NMPy	2.5
3	GO/P-NMPy	1.7

Table.2:Elemental analysis of GO/P-NMPy polymer composites

Sl. No	Element	Atomic number	Weight %	Atomic %	Error %
1	C	6	73.02	77.30	8.13
2	O	8	21.40	20.12	6.51
3	N	7	5.58	2.58	3.82

Table.3: Roughess parameters of GO, P-NMPy and GO/P-NMPy

Sl. No	Materials	Average Roughness	Root mean Square Roughness
1	GO	7.4104	9.9569
2	P-NMPy	18.6688	22.0698
3	GO/P-NMPy	30.3685	39.7361

Table.4: Skewness and Kurtosis values of GO, P-NMPy and GO/P-NMPy

Sl. No	Materials	Skewness (nm)	Kurtosis (nm)
1	GO	- 0.1719	4.2790
2	P-NMPy	- 0.3105	3.5046
3	GO/P-NMPy	- 0.2346	3.4896

Table.5: Capacitance values for GO, P-NMPy and GO/P-NMPy polymer composite

Sl. No	Materials	Capacitance μF
1	GO	219
2	P-NMPy	235
3	GO/P-NMPy	315

Table.6: Bode phase angle for GO, P-NMPy and GO/P-NMPy polymer composite

Sl. No	Materials	Bodephase angle
1	GO	68^0
2	P-NMPy	65^0
3	GO/P-NMPy	80^0

Table.7: R_{ct} and C_{dl} values for GO, P-NMPy and GO/P-NMPy polymer composite

Sl. No	Materials	R_{ct} (Ωcm^2)	C_{dl}(μFcm^{-2})
1	GO	1057	1.2
2	P-NMPy	1478	1.4
3	GO/P-NMPy	5130	2.7

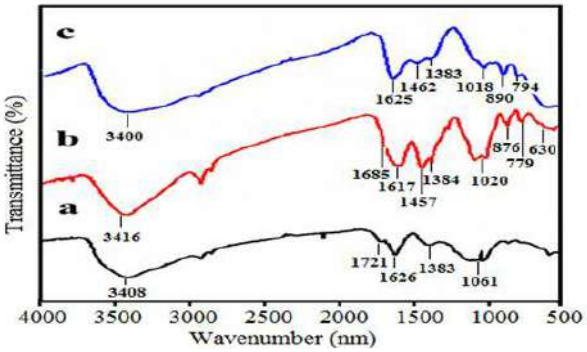

Figure.1: FTIR spectrum of a) GO b) P-NMPy and c) GO/P-NMPy polymer composite.

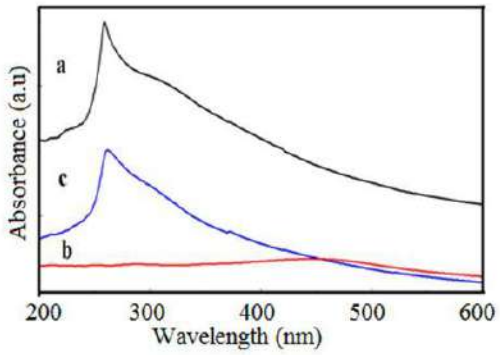

Figure.2: UV spectrum of a) GO b) P-NMPy and c) GO/P-NMPy polymer composite.

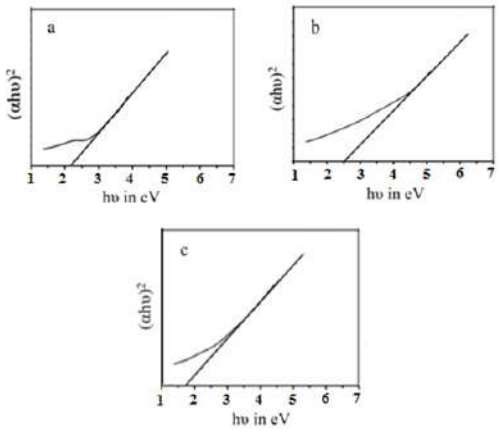

Figure.3: Band gap of a) GO b) P-NMPy and c) GO/P-NMPy polymer composite.

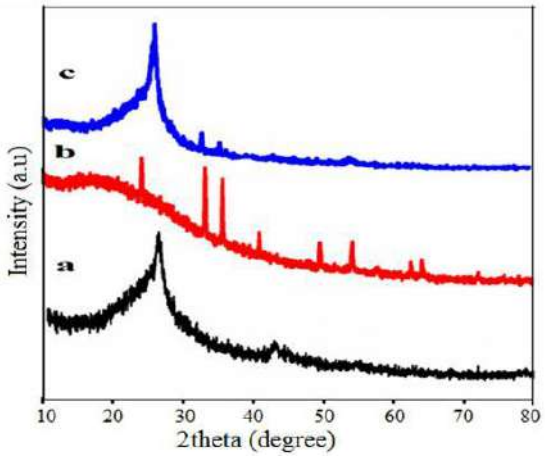

Figure.4: XRD spectrum of a) GO b) P-NMPy and c) GO/P-NMPy polymer composite.

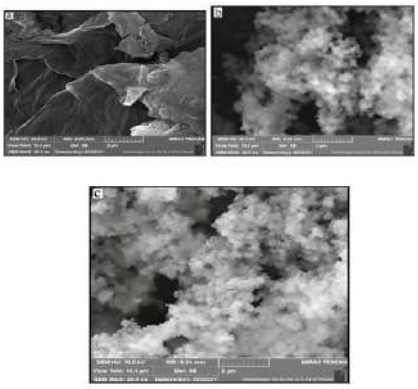

Figure.5: FESEM images of a) GO b) P-NMPy and c) GO/P-NMPy polymer composite.

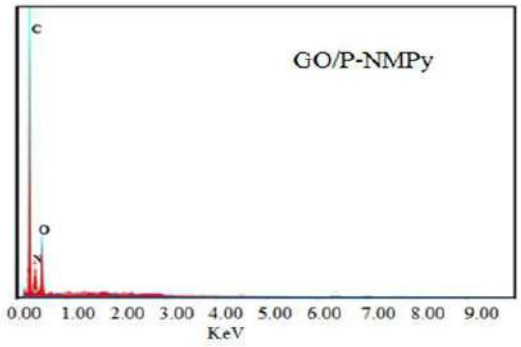

Figure.6: EDAX images of GO/P-NMPy polymer composite

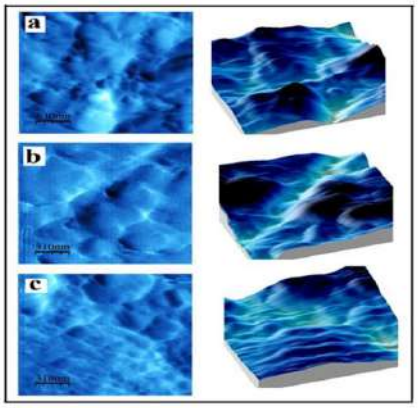

Figure.7:AFM images of a) GO b) P-NMPy c) GO/P-NMPy

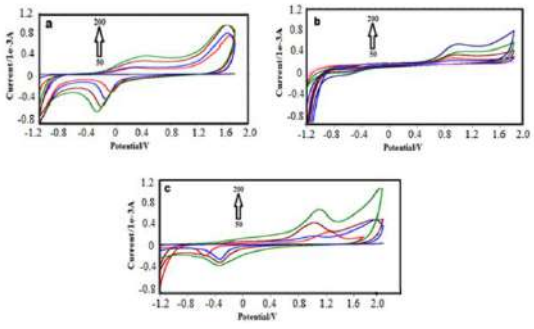

Figure.8:Cyclic Voltammetric behavior of a) GO b) P-NMPy and c) GO/P-NMPy polymer composite

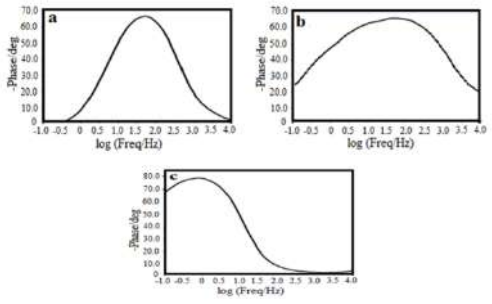

Figure.9:Bode plot of -phase angle/ deg. versus log (f/Hz)) for a) GO b) P-NMPy and c) GO/P-NMPy polymer composite

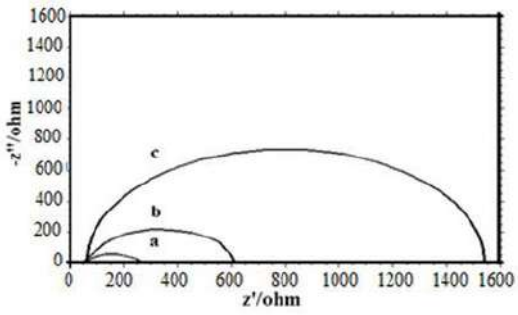

Figure.10: Electrochemical Impedance spectra of a) GO b) P-NMPy and c) GO/P-NMPy

Indian Journal of Natural Sciences www.tnsroindia.org.in ©IJONS

Vol.15 / Issue 88 / Feb / 2025 *International Bimonthly (Print) – Open Access* *ISSN: 0976 – 0997*

RESEARCH ARTICLE

Exploring Exponential Diophantine Equations with Isolated Primes

V. Kasivisalakshi Praveena[1]* and J Kaliga Rani[2]

[1]Research Scholar (P/T) and Assistant Professor, Department of Mathematics (SSP), G.T.N Arts College, Dindigul, (Affiliated to Madurai Kamaraj University, Madurai), Tamil Nadu, India.
[2]Assistant Professor, Department of Mathematics, G.T.N Arts College, Dindigul, (Affiliated to Madurai Kamaraj University, Madurai), Tamil Nadu, India.

Received: 23 Sep 2024 Revised: 03 Dec 2024 Accepted: 06 Feb 2025

***Address for Correspondence**
V. Kasivisalakshi Praveena,
Research Scholar (P/T) and Assistant Professor,
Department of Mathematics (SSP), G.T.N Arts College, Dindigul,
(Affiliated to Madurai Kamaraj University, Madurai), Tamil Nadu, India.
E.Mail: sarveshvedicacademy@gmail.com

ABSTRACT

Diophantine equations, named after Diophantus of Alexandria, are polynomial equations with integer coefficients seeking integer solutions. A special form of these equations, Exponential Diophantine equations, features variables in exponents. This study focuses on solving two Exponential Diophantine equations with non-twin isolated primes 37 and 97:
$3^x + 37^y = z^2$
$3^x + 97^y = z^2$
By solving these equations, we derive a general condition to estimate solutions for similar equations involving other isolated primes.

Keywords: Diophantine Equations, Exponential Diophantine Equations, Isolated Primes.

INTRODUCTION

A Special field of mathematics, Number theory captivated non-professional and also professional mathematicians. In contradiction to other field of mathematics, many of the complicated problems and theorems of number theory can be understood by amateur, in spite of the fact that solutions to the problems and proofs of the theorems often require an experienced mathematical background. In Number theory, A linear Diophantine equation, associate to a constant is the sum of two or more monomials of degree one. Diophantine problems have lesser number of equations than unknowns and involve finding integer solution which simultaneously gives all equations. In 2001, J. Kannan, K. Kaleeswari and P. Vijayashanthistudied on Exponential Diophantine equations involving opposite parity prime [1], Acu, D. in 2007found solution on a Diophantine equation $2^x + 5^y = z^2$ [2]. J. F. T. Raba go in 2016 found solution on the Diophantine Equation $2^x + 17^y = z^2$[4]. In advancement of solving Diophantine equation N. Burshtein in 2019, find all the solutions of the diophantine equations $p^x + p^y = z^2$ and $p^x - p^y = z^2$ when $p \geq 2$ is prime [5]. In

2022, K. Kaleeswari, J. Kannan and G. Narasimman, solved Exponential Diophantine equations involving isolated primes [7]. The concept of solving Exponential Diophantine equation are explained in [2] [4] [5]. Using the Solving method of Exponential Diophantine equation which involves isolated primes [7] 67 and 127, we tried to solve the equations which involves other isolated primes 37 and 97.

Preliminaries

Definition 2.1: A Diophantine equation is a polynomial equation in two or more unknowns with integer coefficients, for which only integer solutions are allowed.

Definition 2.2: An Exponential Diophantine equation is one in which unknowns can occur in exponents. Among the most symphonic examples is the equation$a^2 + b^2 = c^2$, whose integral solutions give us the measurements of the sides of Pythagorean triangles.

Definition 2.3: Anisolated prime (or single prime or non-twin prime) is a prime number p such that neither p − 2 nor p + 2 is prime.

Proposition 2.4:$(3, 2, 2, 3)$is a unique solution $(a, b, x, y)$for theDiophantine equation $a^x - b^y = 1$ where a, b, x and y are integers such that $\min\{a, b, x, y\} > 1$. To prove the main theorem, we present some lemmas

Lemma2.5:*[7]*$(1,2)$ is a unique solution (x, z) for the Diophantine equation $3^x + 1 = z^2$, x & y are non-negative integers.

Proof: Let $x, z \in N \cup \{0\}$.

If $x = 0$. then $z^2 = 2$ has irrational solution.

So take $x \geq 1$. Then $z^2 = 3^x + 1 \geq 4 \Rightarrow z \geq 2$.

Consider $z^2 - 3^x = 1$.

By above Proposition, x must be equal to one. $z^2 = 4 \Rightarrow z = 2$

Hence the lemma.

Lemma2.6: The Diophantine equation $1 + 37^y = z^2$ has no non-negative integer solution.

Case (i): When $y = 0$, then $z^2 = 2$, which gives irrational solution for z.

Case (ii): When $y \geq 1$, the Diophantine equation becomes $1 = z^2 - 37^y$,

By Proposition 2.1, the equation is solvable only for $y = 1$.

But if $y = 1 \Rightarrow z^2 = 38$ is not a square number.

Therefore, there is no non negative integral solution for the Exponential Diophantine equation $1 + 37^y = z^2$

Lemma 2.7: The Diophantine equation $1 + 97^y = z^2$ has no non-negative integer solution.

Case (i): When $y = 0$, then $z^2 = 2$, which gives irrational solution for z.

Case (ii): When $y \geq 1$, the Diophantine equation becomes $1 = z^2 - 97^y$,

By Proposition 2.1, the equation is solvable only for $y = 1$.

But if $y = 1 \Rightarrow z^2 = 98$ is not a square number.

Therefore, there is no non negative integral solution for the Exponential Diophantine equation $1 + 97^y = z^2$.

Main Proof

Theorem 3.1:$(1,0,2)$&$(3,1,8)$are the integer solutions for the Diophantine equation $3^x + 37^y = z^2$

Proof: We discuss the solution of Diophantine equation in two cases for y is even and y is odd.

Case (i):y is even

If $y = 0$,

By Lemma 2.2, $(1,0,2)$ is a solution for the Diophantine equation.

If $y = 2n$, $n \in N$, Therefore our equation becomes, $3^x + 37^{2n} = z^2$, $z \in N \cup \{0\}$

$\Rightarrow z^2 - 37^{2n} = 3^x$
$\Rightarrow (z + 37^n)(z - 37^n) = 3^{a+b}$, where $a + b = x$
$\Rightarrow (z + 37^n)(2 - 37^n) = 3^a 3^b$, where $b > a$
$\Rightarrow (z + 37^n) = 3^a$ & $(z - 37^n) = 3^b$
Subtracting the two factors, $\Rightarrow 3^b - 3^a = (z + 37^n) - (z - 37^n)$
$\Rightarrow 3^b - 3^a = 37^n + 37^n$
$\Rightarrow 3^b - 3^a = 2(37^n)$
Here $a = 0$ is the only possible value.Therefore, $3^b - 1 = 2(37^n)$
Adding -2 on both sides $\Rightarrow 3^b - 1 - 2 = 2(37^n) - 2 \Rightarrow 3^b - 3 = 2(37^n - 1)$
$\Rightarrow 3(3^{b-1} - 1) = 2(37^n - 1)$
This is possible only when $b = 2 \Rightarrow 3(3^{2-1} - 1) = 2(37^n - 1)$
$\Rightarrow\ 3(2) = 2(37^n - 1) \Rightarrow 37^n = 4$, which is not possible.

Case (ii): If y is odd $\Rightarrow$ y = 2n + 1, n ∈ N
Therefore our equation $3^x + 37^y = z^2$ becomes $\Rightarrow 3^x + 37^{2n+1} = z^2$
$\Rightarrow 3^x + 37(37^{2n}) = z^2$
We have to split the isolated prime 37 into two terms, one should be a square number and another should be a multiple of 3.
Hence, we have to find the integer solution (a, b) for $37 = a^2 + 3b$,
Here $a^2 = 37 - 3b \ \Rightarrow a \leq 5$
For **b** to be integer, $a^2 \equiv 37\ mod\ 3 \Rightarrow\ a^2 \equiv 1\ mod\ 3\ \Rightarrow\ a \equiv \pm 1\ mod\ 3$
For $a = \pm 1\ \Rightarrow$ b = 12
For $a = \pm 2\ \Rightarrow$ b = 11
For $a = \pm 4 \Rightarrow$ b = 7
For $a = \pm 5\ \Rightarrow$ b = 4
The possible values of $(a^2, 3b)$ are (1,36), (4, 33), (16,21), (25, 12)
Investigating all the possible values of $(a^2, 3b)$

For $(a^2, 3b) = (25, 12)$:
$\Rightarrow 3^x + (25 + 12) \times 37^{2n} = z^2$
$\Rightarrow 3^x + 12 \times 37^{2n} = z^2 - 5^2 \times 37^{2n}$
$\Rightarrow 3(3^{x-1} + 4 \times 37^{2n}) = (z - 5 \times 37^n)(z + 5 \times 37^n)$
Now we have two possibilities for z
$z = 3 + 5 \times 37^n$& $z = 3 - 5 \times 37^n$

Sub Case (i): If $z = 3 + 5 \times 37^n$
Therefore, $3(3^{x-1} + 4 \times 37^{2n}) = (3 + 5 \times 37^n - 5 \times 37^n)(3 + 5 \times 37^n + 5 \times 37^n)$
$\Rightarrow 3(3^{x-1} + 4 \times 37^{2n}) = 3(3 + 10 \times 37^n)$
$\Rightarrow 3^{x-1} - 3 = 10 \times 37^n - 4 \times 37^{2n}$
$\Rightarrow 3(3^{x-2} - 1) =\ 37^n(10 - 4 \times 37^n)$
$n = 0$ is the only possible value for the above equation.
$\Rightarrow 3^{x-2} - 1 = 2 \Rightarrow 3^{x-2} = 3\ \Rightarrow \mathbf{x = 3}$
$\Rightarrow$ y = 2n + 1 $\Rightarrow \mathbf{y = 1}$
$\Rightarrow z = 3 + 5 \times 37^n \Rightarrow \mathbf{z = 8}$
Hence(3,1,8)is the solution for the equation $3^x + 37^y = z^2,$ when $z = 3 + 5 \times 37^n$

Sub case (ii): If $z = 3 - 5 \times 37^n$
Therefore, $3(3^{x-1} + 4 \times 37^{2n}) = (3 - 5 \times 37^n - 5 \times 37^n)(3 - 5 \times 37^n + 5 \times 37^n)$
$\Rightarrow 3(3^{x-1} + 4 \times 37^{2n}) = 3(3 - 10 \times 37^n)$
$\Rightarrow 3^{x-1} - 3 = -4 \times 37^{2n} - 20 \times 37^n$
$\Rightarrow 3(3^{x-2} - 1) =\ 37^n(-4 \times 37^{2n} - 20)$

$n = 0$ is the only possible value for the above equation.
Therefore, $3(3^{x-2} - 1) = -24 \Rightarrow 3^{x-2} = -5$
Which is not possible.
Hence the solution for the Diophantine equation $3^x + 37^y = z^2$, is (1,0,2)when $y = 0$ and (3,1,8) when $z = 3 + 5 \times 37^n$. In all other cases the solution is not possible.
Hence the theorem.

Theorem 3.2:(1,0,2) is the unique solution for the Diophantine equation $3^x + 97^y = z^2$
Proof: We discuss the solution of Diophantine equation in two cases for y is even and y is odd.
Case (i):y is even
If $y = 0$,
By Lemma 2.2, (1,0,2) is a solution for the Diophantine equation.
If $y = 2n$, $n \in N$, Therefore our equation becomes, $3^x + 97^{2n} = z^2$, $z \in N \cup \{0\}$
$\Rightarrow z^2 - 97^{2n} = 3^x$
$\Rightarrow (z + 97^n)(z - 97^n) = 3^{a+b}$, where $a + b = x$
$\Rightarrow (z + 97^n)(z - 97^n) = 3^a 3^b$, where $b > a$
$\Rightarrow (z + 97^n) = 3^a$ & $(z - 97^n) = 3^b$
Subtracting the two factors, $\Rightarrow 3^b - 3^a = (z + 97^n) - (z - 97^n)$
$\Rightarrow 3^b - 3^a = 97^n + 97^n$
$\Rightarrow 3^b - 3^a = 2(97^n)$
Here $a = 0$ is the only possible value.Therefore, $3^b - 1 = 2(97^n)$
Adding -2 on both sides $\Rightarrow 3^b - 1 - 2 = 2(97^n) - 2 \Rightarrow 3^b - 3 = 2(97^n - 1)$
$\Rightarrow 3(3^{b-1} - 1) = 2(97^n - 1)$
This is possible only when $b = 2 \Rightarrow 3(3^{2-1} - 1) = 2(97^n - 1)$
$\Rightarrow 3(2) = 2(97^n - 1) \Rightarrow 97^n = 4$, which is not possible.

Case (ii): If y is odd $\Rightarrow y = 2n + 1$, $n \in N$
Therefore our equation $3^x + 97^y = z^2$ becomes$\Rightarrow 3^x + 97^{2n+1} = z^2$
$\Rightarrow 3^x + 97(97^{2n}) = z^2$
We have to split the isolated prime 97 into two terms, one should be a square number and another should be a multiple of 3.
Hence, we have to find the integer solution (a, b) for $97 = a^2 + 3b$,
Here $a^2 = 97 - 3b \Rightarrow a \leq 9$
For **b** to be integer, $a^2 \equiv 97 \ mod\ 3 \Rightarrow a^2 \equiv 1 \ mod\ 3 \Rightarrow a \equiv \pm 1 \ mod\ 3$
For $a = \pm 1 \Rightarrow b = 32$
For $a = \pm 2 \Rightarrow b = 31$
For $a = \pm 4 \Rightarrow b = 27$
For $a = \pm 5 \Rightarrow b = 24$
For $a = \pm 7 \Rightarrow b = 16$
For $a = \pm 8 \Rightarrow b = 11$
The possible values of $(a^2, 3b)$ are $(1,96), (4,93), (16,81), (25,72), (49,48), (64,33)$
Investigating all the possible values of $(a^2, 3b)$

For $(a^2, 3b) = (64, 33)$:
$\Rightarrow 3^x + (64 + 33) \times 97^{2n} = z^2$
$\Rightarrow 3^x + 33 \times 97^{2n} = z^2 - 8^2 \times 97^{2n}$
$\Rightarrow 3(3^{x-1} + 11 \times 97^{2n}) = (z - 8 \times 97^n)(z + 8 \times 97^n)$
Now we have two possibilities for z
$z = 3 + 8 \times 97^n$& $z = 3 - 8 \times 97^n$

Sub Case (i): If $z = 3 + 8 \times 97^n$
Therefore, $3(3^{x-1} + 11 \times 37^{2n}) = (3 + 8 \times 97^n - 8 \times 97^n)(3 + 8 \times 97^n + 8 \times 97^n)$
$\Rightarrow 3(3^{x-1} + 11 \times 97^{2n}) = 3(3 + 16 \times 97^n)$
$\Rightarrow 3^{x-1} - 3 = 16 \times 97^n - 11 \times 97^{2n}$
$\Rightarrow 3(3^{x-2} - 1) = 97^n(16 - 11 \times 97^n)$
$n = 0$ is the only possible value for the above equation.
$\Rightarrow 3^{x-1} - 3 = 5 \Rightarrow 3^{x-1} = 8$ which is not possible

Sub case (ii): If $z = 3 - 8 \times 97^n$
Therefore, $3(3^{x-1} + 11 \times 37^{2n}) = (3 - 8 \times 97^n - 8 \times 97^n)(3 - 8 \times 97^n + 8 \times 97^n)$
$\Rightarrow 3(3^{x-1} + 11 \times 97^{2n}) = 3(3 - 16 \times 97^n)$
$\Rightarrow 3^{x-1} - 3 = -16 \times 97^n - 11 \times 97^{2n}$
$\Rightarrow 3(3^{x-2} - 1) = 97^n(-16 - 11 \times 97^n)$
$n = 0$ is the only possible value for the above equation.
Therefore, $3(3^{x-2} - 1) = -27 \Rightarrow 3^{x-2} = -8$, which is not possible.
Hence the solution for the Diophantine equation $3^x + 37^y = z^2$, is (1,0,2)when $y = 0$. In all other cases the solution is not possible.
Hence the theorem.

Corollary 3.3: The Diophantine equation $3^x + 37^y = w^4$ has no non-negative integer solution.
Proof: Take $z = w^2$, By Theorem 3.1, $3^x + 37^y = z^2$has two solutions (1,0,2) and (3,1,8).
For $w^2 = 2 \Rightarrow w = \sqrt{2}$, irrational solution
For $w^2 = 8 \Rightarrow w = 2\sqrt{2}$, irrational solution
Hence $3^x + 37^y = w^4$has no non-negative integer solution.

Corollary 3.4: The Diophantine equation $9^w + 37^y = z^2$ has no non-negative integer solution.
Proof: Take $x = 2w$, By Theorem 3.1, $3^x + 37^y = z^2$has two solutions (1,0,2) and (3,1,8).
For $x = 1 \Rightarrow w = \frac{1}{2} \in Q$, non-integer solution
For $x = 3 \Rightarrow w = \frac{3}{2} \in Q$, non-integer solution
Hence $3^x + 37^y = w^4$has no non-negative integer solution.
Corollary 3.5: *The Diophantine equation $3^x + 97^y = w^4$ has no non-negative integer solution.*
Proof: Take $z = w^2$, By Theorem 3.2, $3^x + 97^y = z^2$has a unique solution(1,0,2)
For $w^2 = 2 \Rightarrow w = \sqrt{2}$, irrational solution
Hence $3^x + 97^y = w^4$has no non-negative integer solution.

Corollary 3.6: The Diophantine equation $9^w + 97^y = z^2$ has no non-negative integer solution.
Proof: Take $x = 2w$, By Theorem 3.2, $3^x + 97^y = z^2$has a unique solution (1,0,2)
For $x = 1 \Rightarrow w = \frac{1}{2} \in Q$, non-integer solution
Hence $3^x + 97^y = w^4$has no non-negative integer solution.

Remark *3.7:*By investigating the above two solving procedure of two Exponential Diophantine equations involving isolated primes, we arrive at a condition to split the isolated prime p into two terms $p = a^2 + 3b$. If p does not satisfies the above condition, then the $3^x + p^y = z^2$, has unique solution (1,0,2)for (x, y, z).
For Isolated prime, $p = a^2 + 3b \Rightarrow a^2 \equiv p \ (mod\ 3)$
For $a \equiv p(mod\ 3)$, three cases are possible
Case (i):$a \equiv 0 \ (mod\ 3) \Rightarrow a^2 \equiv 0 \ (mod\ 3)$
Case (ii):$a \equiv 1(mod\ 3) \Rightarrow a^2 \equiv 1 \ (mod\ 3)$
Case (iii):$a \equiv 2(mod\ 3) \Rightarrow a^2 \equiv 4(mod\ 3) \Rightarrow a^2 \equiv 1 \ (mod\ 3)$
Hence $p \equiv 0[or]1 \ (mod\ 3) \Rightarrow p = 3x$ or $p = 3x + 1$

On Investigating Isolated primes less than 200

$p = 23, 47, 53, 83, 89, 113, 131, 167, 173, 233 \Rightarrow$ Neither of the form $3x$ *or* $3x + 1 \Rightarrow (1,0,2)$ is the unique solution.

S.No	Isolated prime	Equation	Solution
1.	23	$3^x + 23^y = z^2$	(1,0,2)
2.	47	$3^x + 47^y = z^2$	(1,0,2)
3.	53	$3^x + 53^y = z^2$	(1,0,2)
4.	83	$3^x + 83^y = z^2$	(1,0,2)
5.	89	$3^x + 89^y = z^2$	(1,0,2)
6.	113	$3^x + 113^y = z^2$	(1,0,2)
7.	131	$3^x + 131^y = z^2$	(1,0,2)
8.	167	$3^x + 167^y = z^2$	(1,0,2)
9.	173	$3^x + 173^y = z^2$	(1,0,2)
10.	233	$3^x + 233^y = z^2$	(1,0,2)

CONCLUSION

In this paper, we have shown that (1,0,2)& (3,1,8) are thenon-negative solutions for the Exponential Diophantine equation $3^x + 37^y = z^2$ and (1,0,2) is the non-negative unique solution for the Exponential Diophantine equation$3^x + 97^y = z^2$. Also, we arrive at condition, which helps us to easily check the solution of other isolated primes. We investigate all the isolated primes which do not satisfy the condition$p = a^2 + 3b$ and tabulated the list which gives unique solution (1,0,2). Many real life applications, especially research application send with either unsolved Diophantine equations or infinitely many solutions. In future, we can find more general and efficient method which helps us to find solution for many Exponential Diophantine Equations.

REFERENCES

1. J. Kannan, K. Kaleeswari and P. Vijayashanthi, Exponential diophantine equations involving opposite parity prime, Malaya Journal of Mathematik S(1) (2001), 416-418.
2. Acu, D. (2007) On a Diophantine equation $2^x + 5^y = z^2$, Gen. Math., 15, 145-148.
3. David M. Burton, Elementary Number Theory, 7th edition, McGraw- Hill lnc., (2011).
4. J. F. T. Rabago, On the Diophantine Equation $2^x + 17^y = z^2$, Journal of the Indonesian Mathematical Society (2016), 177-182.
5. N. Burshtein, All the solutions of the diophantine equations $p^x + p^y = z^2$ and $p^x - p^y = z^2$ when $p \geq 2$ is prime, Annals of Pure and Applied Mathematics 19(2) (2019), 111-119.
6. M. Somanath, K. Raja, J. Kannan and S. Nivetha, Exponential diophantine equation inthree unknowns, Advances and Applications in Mathematical Sciences 19(11) (2020),1113-1118.
7. K. Kaleeswari, J. Kannan and G. Narasimman, Exponential Diophantine equations involving isolated primes, Advances and Applications in Mathematical Sciences 22(1) (2022), 169-177.

Indian Journal of Natural Sciences *www.tnsroindia.org.in ©IJONS*

Vol.15 / Issue 88 / Feb / 2025 *International Bimonthly (Print) – Open Access* *ISSN: 0976 – 0997*

RESEARCH ARTICLE

Biodiversity of Wild Mushrooms in Thanjavur Town (Tamil Nadu) of South India

M. Sabarimanikandan[1], G. Arul Doss[1] and M. Sundaramoorthy[2]*

[1]Research Scholar, Department of Zoology, Rajah Serfoji Government College (Autonomous), Thanjavur, (Affiliated to Bharathidasan University, Tiruchirappalli), Tamil Nadu, India.
[2]Assistant Professor, Department of Zoology, Rajah Serfoji Government College (Autonomous), Thanjavur, (Affiliated to Bharathidasan University, Tiruchirappalli), Tamil Nadu, India.

Received: 21 Nov 2024 Revised: 03 Dec 2024 Accepted: 31 Jan 2025

***Address for Correspondence**
M. Sundaramoorthy,
Assistant Professor,
Department of Zoology,
Rajah Serfoji Government College (Autonomous),
Thanjavur, (Affiliated to Bharathidasan University, Tiruchirappalli),
Tamil Nadu, India.
E.Mail: drmsundartnj@gmail.com

ABSTRACT

The mushroom survey in different localities of Thanjavur city of south India reports totally 63 species in 45 genera of 29 families. The identification was performed by "Mushroom Identifying Application". They all were confirmed by mushroomexpert.com software. The family *Polyporaceae* dominates followed by *Ganodermataceae* and *Psathyrellaceae*. The genera *Ganoderma* gets the first place with four species. Of the 63 mushrooms, 16 deviate from one or more characters of the names fed in the mushroomexpert.com software. In this survey, all the 63 mushrooms identified are coming under 29 families. Included in these, 65% is edible where as 27% is inedible. The remaining 8% of the mushrooms belonging to 5 species are identified as poisonous.

Keywords: Mushroom, species, genera, *Polyporaceae*, *Ganoderma*¸ software, survey.

INTRODUCTION

Fungi a protuberant position in biological world include mushrooms, toadstools, mold, mildew and yeast. The rough estimation of fungal species in the globe is 2–11 million where about 150,000 taxa were formally described [1]. According to Manoharachary *et al*., [2]. India is a hotspot for fungal diversity as one third of fungal population of the world gifts in India. Mushrooms are multiethnic heterotrophic macro fungi that are quite specific in their nutritional and ecological requirements. They contain fleshy and spore-bearing fruiting bodies; which is the typical

characteristic feature of mushrooms. They play a key role in food, medical, bio control and chemical industries [3]. *Ascomycotina* and *Basidiomycotina* are the two phylum of Mushrooms. They grow cancerously during rainy season and inhabit in diverse niches of forest and territory ecosystem. They predominantly flourish well in moist atmosphere containing decomposing organic materials. Historically, the nutritional and pharmacological significance of mushrooms remained underappreciated in several countries, including India, where they were often pretended as uniformly poisonous. However, the nutritive and therapeutic values of mushrooms had been apprehended by various ancient people. Their ancient names such as "Food of God" by Romans, "Elixir of Life" by Chinese, "God's Flesh" by South Africa and "Somrus" by Indians [4] underscore the significance of mushrooms as vital nutritional resources. The nutritive importance of mushrooms has been well documented in the recent decades also. The dried fruiting bodies of mushrooms contain 18% protein, 4% fat, 3% crude fiber and 64% carbohydrate [5,6]. Similarly, mature sporocarp contains 4% soluble sugar, 3% starch and 7% ash including potassium, sodium, phosphorus, iron and calcium. They are also excellent sources of essential oil & amino acids, vitamins, minerals, lectins, and bioactive compounds. Likewise, their therapeutic properties include antimicrobial, anticancer, antioxidant, antiviral, immunomodulatory, immunosuppressive, anti-allergic, anti-inflammatory, and anti-cholesterol activities [7- 11]. Dhole and Rathod [12] have described that more than 2500 mushrooms are present worldwide and 111 of them are reputed to be cultivable and edible. *Agaricus, Auricularia, Ganoderma, Grifola, Pleurotus, Lactarius, Lentinus, Termitomyces, Cantharellus, Morchella, Phellinus, Tremellas, Russula, Trametes, Suillus, Tricholoma, Macrolepiota* are the common edible mushrooms species they reported. Therapeutic uses of various mushrooms species viz., *Lentinus*, *Pleurotus*, *Schizophyllum*, *Pisolithus*, *Agaricus*, *Pleurotus* and *Termitomyces* species have been reported by Manoharachary *et al*., [2]. However, several species of *Ganoderma* have been predominantly used as pharmaceuticals rather than food [13-16]. In recent past, we have also reported the antibacterial properties of *Ganoderma lucidum* [17]. Hence, the taxonomic depiction of mushrooms is noteworthy to utilise them all the ways. Senthilarasu and Kumaresan reported 132 species in 60 genera belonging to *Agaricales, Polyporales* and *Russulales* in Western Ghats of Karnataka, India [18]. Zeb *et al.,* [19] recognized 51 species of mushrooms belonging to 22 families and 37 genera in Bajaur, Pakistan. According to *Panda et al*., [20], the total number of documented mushroom species in India is about 1,200, including about 300 to 315 edible species. Meena *et al*., [21] reported 60 genera of mushrooms belonging to the orders of *Agaricales, Polyporales* and *Russulales* with 132 species in India. They include, the families of *Ganodermataceae, Agaricaceae, Lycophyllaceae, Schizophyllaceae, Xylariaceae, Polyporaceae, Marasmiaceae, Psanthyrellaceae* and *Strophaniaceae* [21]. Consequently, mushrooms are an integral part of all ecosystems and human utilization in various forms. However, their diversity and types have been poorly studied with a limited knowledge in the tropical regions including India [22]. Hence, it is paramount important to understand about the mushroom diversity in detail across the world. However, it is highly tedious to study the entire population of mushroom species in the globe. When the biologists of different parts of the world are taking measures to understand their local population of mushrooms, it may fulfill the gap of knowledge on mushroom resources. In that sense an attempt was taken to survey the locally available mushrooms in the Thanjavur town of south India.

MATERIALS AND METHODS

Collection of wild mushrooms

Mushrooms from different places of Thanjavur town, Tamilnadu were surveyed and the pictures were captured from minimum four different angles using 64MP rear camera of mobile phone during the beginning of the January, 2022 and end of the March, 2022 (3 months).

Geographical Location of study Area

The location of Thanjavur on an atlas is 10.8°N 79.15°E. The city has an elevation of 57 m (187 ft) above mean sea level. The total area of the city is 36.33 km2 (14.03 sq mi). Thanjavur is situated in the river Cauvery delta. The city is at a distance of 314 km south-west of Chennai and 56 km east of Tiruchirappalli (fig.1).

Mushroom Identification

The individual Mushroom pictures were filed separately in computer. They were identified using a freely available mobile application named "Mushroom Identify-Automatic picture recognition". Four different views of individual mushroom and their possible combinations (6 combinations) as shown in the table 1 were uploaded separately in the Identification App to match different views of the test mushrooms with the similar pictures of website database. In addition, two more relevant pictures were selected for better matching. The scientific name of each mushroom was tabulated. The mushroom pictures were also matched with the Google pictures and the pictures of www.mushroomexpert.com website using the same name identified by the mobile phone App for conformation [23]. From the table, the mushrooms which have been repeatedly entered in large number were selected for further confirmation. The particular mushroom conquered was matched with the morphology of Google pictures and Mushroom Expert.com website for final confirmation. If there is no matching in both, the additional input of two other dominantly found names were used for the same purpose. After conformation of the identified mushrooms, they were critically analysed and discussed in various aspects.

RESULTS

Table 2 contains 63 wild mushrooms identified in various localities of Thanjavur city. The identification was performed by Mushroom Identifying Application as given in the methodology. They all were confirmed by matching with the appropriate Google images. Except *Ganoderma megaloma,* all 62 mushrooms are identical with Google images. For final confirmation, the morphological characteristic feature of the identified mushroom names was fed in to Expert.Com software and analysed. Of the 63 mushrooms, 16 deviate from one or more characters. They are (*Psilocybe cubensis, Ganoderma martinicens, Vascellum pretense, Termitomyces clypeatus, Ganoderma sinense, Irpiciporus pachyodon, Oudemansiella mucida, Trametopsis cervina, Coprinellus setulosi, Trametella gallica, Hypoxylon fragiforme, Reticularia lycoperdon, Ganoderma megaloma, Oligoporus caesius, Trametes hirsute* and *Meripilus sumstinei*) (table.2). The photographic pictures of total 63 mushrooms are shown in fig.2. In this survey, all the 63 mushrooms identified are coming under 29 families. They are all inhabiting in wet environments containing degradable solid wastes such as dead /decaying hard woods, woody debris, forest litter, rotting stumps etc., Some are also growing in moisture soil and living trees as found in table 3 and fig 2. There are totally 29 families of mushroom exist in Thanjavur city (table 4). The family *polyporaceae* inhabits predominantly in the study area with 10 species 16% which is the maximum in number. Next to this, *Ganodermataceae* and *Agaricaceae* occupy with 8 13% and 6 species 9.5% respectively. *Strophariaceae* has 4 species of mushrooms. The families *Irpiaceae, Hymennogastraceae, Psathyrellaceae, Pleurotaceae, Pluteaceae* contains 3 species in each. All others have one species in each (table.4). The characteristic features of each mushroom with reference to their habitats are also given in the table 3. Similarly, all mushrooms identified are belonging to totally 45 genera as shown in the table 5. The genera *Goderma* is identified to have maximum number of species; 13%. They are *Ganoderma martinicense, Ganoderma curtisii, Ganoderma elfvingia, Ganoderma megaloma, Ganoderma sessile, Ganoderma lucidum, Ganoderma carnosem, Ganoderma sinense*).The two genera, *Lentinus* and *Pleurotes* have 4.8 % species of mushrooms each. Two species (3.2%) present in each genera of *Gymnopilus, Agaricus, Psilocybe, Kuehneromyces, Macrolepiota, Trametes and Coprinellus*. All other genera have 1.6% species in each. Table 6, exhibit edibility of the mushrooms identified in the study area. Of them, 65% is edible where as 27% of is inedible. The remaining 8% of the mushrooms belonging to 5 species are identified as poisonous.

DISCUSSION

Mushrooms are incredibly important components of biodiversity in all kinds of terrestrial ecosystem. They are found everywhere, in small gardens, on shade trees, in parks, fields and forests. Though, dead wood and logs are most suitable host to inhabits, some are found only on live plants and leaf litter, soil etc. The variation observed in occurrence of mushroom species in various niches may be due to their particular mode of nutrition. The macro fungi growing on the soil are symbiotic, on rotting and dead wood are saprophytic and on trees are parasitic [24]. Mushrooms have pronounced values in satisfying nutritive and medicinal requirements. They are also used as

precursor materials in different industries of agriculture, medicine, food, textiles, and bioremediation [25, 26].Conversely, worldwide a great number of cases of hazardous mushroom exposure and consumption result in various ill effects up to mortality. Hence, it is indispensable to make a clear cut survey of mushrooms in every localities and characterizing for their toxicity to check their utility. Further, only after a complete survey of mushrooms in every locality, it will come to the light if there is any unknown mushroom which is not used by humans so far. Therefore, deep studies on mushroom biodiversity are more vital. Several mycologists have contributed significant quantity in the mushroom diversity. Natarajan *et al.,* [27] and Kaur *et al.,* [28] worked on diversity of *Agaricus* from Nilgiri Biosphere Reserve Western Ghats of Tamilnadu. Senthilarasu & Kumaresan, [18] studied morphological taxonomy of 15 agaric species belonging to order Agaricales collected from dipterocarp forests of Western Ghats of Karnataka. Kim *et al*., [29] collected and characterised 72% saprophytic, 25% symbiotic, and 3% parasitic mushrooms. In this paper, it is described that in and around areas of Thanjavur town occupies a total of 63 mushroom species in 45 genera and 29 families. Out of 63 mushrooms 29 were identified to genus level. The highest numbers of species diversity are found in the families of *Polyporaceae*, *Ganodermataceae, Agaricaceae* with 10, 8, 6 species respectively (Table 4 and fig.2). Venkatesan and Arun [30] carried out a similar study in the delta regions of River Cauvery. They have reported 35 species with the predominance of *Ganodermataceae* and *Agaricaceae.* These two families are dominating in our studies also following *Polyporaceae*. However, we have investigated 63 species in Thanjavur town area only, which is nearly double the number to the report of Venkatesan and Arun [30]. Here all the mushrooms were identified by the mushroom identifying App named "Mushroom Identify-Automatic picture recognition" and confirmed by matching the images with Google and mushroomexpert.com images. It is more precious technique to compare the morphological observations as described by Chang & Miles [31]. Nevertheless, gene sequencing is required for 100% authentication. Because, the cutting-edge molecular phylogenetic techniques [32] such as RFLP, RAPD, AFLP, SSR & ISSR, DNA barcodes etc., offer a more precise and comprehensive approach to the study of fungi, expediting the investigation of their genetic relationships and the untapped potential they hold in various scientific, medical, and environmental applications [33]. It is also interesting to note that 65% of the identified wild mushrooms species are edible in nature (table 6) and hence Thanjavur (River Cauvery Delta) is much suitable for cultivating diverse mushrooms species to substitute protein rich food like fish, chick and red meats at cheap cost and to prepare therapeutic agent.

CONCLUSION

Mushrooms have great values as natural resources in various ways such as supplying nutrition, maintaining ecosystems and having a lot of therapeutic values. Though, India is one of the hot spots for mushroom diversity, from recent past only, the awareness on mushroom utilisation as food and medicines is increasing considerably. However, knowledge on mushrooms is yet to be developed for their effective utilization. Now days, the classical taxonomists in India is very scanty for identification of various living entities including fungi. Hence, it is inevitable to understand various characteristic features of fungal population. Based on this, the study was conducted to find out the mushroom resources present in our own environments mainly in Thanjavur town. Results reveal that nearest area has considerable number of mushroom species. Thus the survey of wild mushroom diversity made in this work could be very much beneficial to the human society. Since 65 % of the mushroom are edible in nature, it is advised to cultivate these mushrooms in Thanjavur to substitute the protein rich diets. Many of them could also be exploited for therapeutic purposes.

REFERENCES

1. Phukhamsakda C, Nilsson RH, Bhunjun CS. *et al.,* The numbers of fungi: contributions from traditional taxonomic studies and challenges of metabarcoding. . *Fungal Diversity* 2022 114, 327–86. https://doi.org/10.1007/s13225-022-00502-3
2. Manoharachary CK, Sridhar R. Singh A, Adholeya TS, Suryanarayanan S, Rawat *et al.,* Fungal biodiversity: distribution, conservation and prospecting of fungi from India. *Currunt Science* 2005; 89 (1): 58-71.

3. Lakhanpal TN. Mushroom Biodiversity in India, Prospects and Potential. Proceedings of the 8th International Conference on Mushroom Biology and Mushroom Products (ICMBMP8) 2014; 7-16.
4. Wasson GR. Soma-Divine mushroom of immortality XIII, Hew Court Brace and world Inc. New York 1969; 318.
5. Tripathi DP. Cultivation of specialty mushroom in Mushroom Cultivation. *Oxford & IBH Pub* 2005; 250-253.
6. Bhatt P, Kushwaha KPS, Singh RP. Evaluation of different substrate and casing mixture for production of Calocybe *indica*. *Indian Phytopathology* 2007; 60(1): 128-30.
7. Halpern GM and Miller ANH. Collection of several varieties of wild mushroom. *International Journal of Agriculture and Biology* 2002; 13: 415-18.
8. Wasser JR. Medicinal mushrooms. *International Journal* of *Agriculture and Biology* 2002; 60: 258-74.
9. Yaltirak R. Presence of antioxidants and compounds in mushroom. *International Journal of Agriculture and Biology* 2009; 13: 2052-56.
10. Oyetayo OV. Medicinal uses of mushrooms in Nigeria: towards full and sustainable exploitation. *African Journal of Traditional, Complementary and Alternative Medicines*, 2011; 8: 267-74.
11. Rathee S, Rathee D, Rathee D, Kumar V and Rathee P. Mushrooms as therapeutic agents. *Brazilian Journal of Pharmacognosy* 2012; 22: 459-74.
12. Dhole A, Rathod M. Diversity of Cultivable Edible Species of Mushrooms 2022.
13. Moradali MF, Hedjaroude GA, Mostafavi H, Abbasi M, Ghods SH and Sharifi- Tehrani A. The genus *Ganoderma (Basidiomycota)* in *Iran.Mycotaxon*, 2007; 99: 251-69.
14. Acharya K. Antioxidant and nitric oxide syntheses activation properties of *Ganoderma applanatum. Indian Journal of experimental Biology* 2010; 43: 923-29.
15. Wachtel-Galor S, Yuen J, Buswell, JA and Benzie IFF. *Ganoderma lucidum (Lingzhi or Reishi)*: A Medicinal Mushroom. In: Benzie, I.F.F. and Wachtel-Galor, S. editors. Herbal Medicine: *Biomolecular and Clinical Aspects*. 2nd edition. Boca Raton (FL): CRC Press 2011.
16. Rahnama K and Habibi R. First report of Neurospora on Corylusavellana innatural forest of *Iran. Journal Yeast Fungal Research* 2015; 6: 31-36.
17. Sundaramoorthy M, Sabarimanikandan M. Evaluation of different protein precipitates of a wild mushroom, *ganoderma lucidum* for antibacterial activities against human pathogenic bacteria. *Asian Journal of Pharmaceutical and Clinical Research* 2019; 12; 7: 303-7. doi:10.22159/ajpcr. 2019.v12i7.33714.
18. Senthilarasu G, Kumaresan V. Diversity of agaric mycota of Western Ghats of Karnataka, India. *Current Research in Environmental & Applied Mycology* 2016; 6 (2):75-101.
19. Zeb M, Ullaha A, Ullaha F, Haqa A, Ullahb I, Badshahc L, Haqa MA. Diversity and biological characteristics of macrofungi of district Bajaur,a remote area of Pakistan in the Hindu kush range. *Heliyon* 2023; 2405-8440.
20. Panda, Mrunmaya & Thatoi, Hrudayanath & Sahu, SUDAM & Tayung, Kumanand. Wild edible mushrooms of northern odisha, india: data on distribution and utilization by ethnic communities 2019; 10.26479/2019.0502.19.
21. Meena B, Sivakumar V and Praneetha S. Prospects of biodiversity and distribution of mushroom fungi in India. GSC Biological and Pharmaceutical Sciences. 2020; 13: 078–085.
22. Hawksworth DL. The magnitude of fungal diversity: the 1.5 million species estimate revisited. *Mycolgical Research* 2001; 105: 1422- 32.
23. Sharma R, Sharma YP, Hashmi SAJ *et al.* Ethnomycological study of wild edible and medicinal mushrooms in district Jammu, J&K (UT), India. *J Ethnobiology Ethnomedicine* 2022; 18, 23. https://doi.org/10.1186/s13002-022-00521-z.
24. Suryanarayanan TS, Ravishankar JP, Venkatesan G, Murali TS. Characterization of the melanin pigment of a cosmopolitan fungal endophyte. *Mycological research* 2004; 108(8): 974- 78.
25. Danilson, RM, Pruden M. The Ectomycorrhizal status of urban spruce. Mycologia. 1989; 81(3), 335-341. https://doi.org/10.1080/00275514.1989.12025756.
26. Stametes P. The role of mushroom in nature culturing media mycelium on agar media. In: Growing Gourmet and medicinal mushrooms. Tenspeed press, Hong Kong 2000.
27. Natarajan K, Kumaresan V, Narayanan K. A checklist of Indian agarics and boletes (1984-2002). *Kavaka, India* 2005; 33: 61-128.

28. Kaur A, Atri NS, Kaur M. A new variety of Rhodocybe popinalis (Entolomataceae, Agaricales) from coprophilous habitats of India. *Journal on New Biological Reports*, 2013; 2(3): 260- 63.
29. Kim, Chang & Jo, Jong & Kwag, Young-Nam & Sung, Gi-Ho & Lee, Sle-Gee & Kim, Sang-Yong & Shin, Chang-Ho & Han, Sang-Kuk. Mushroom Flora of Ulleung-gun and a Newly Recorded Bovista Species in the Republic of Korea. Mycobiology. 2015; 43. 239. 10.5941/MYCO.2015.43.3.239.
30. Venkatesan G, Arun G. A study of the diversity of mushrooms from Cauvery delta region, Tamil Nadu, India. Global scientific journals 2019; 7:873-82.
31. Chang ST, Miles PG. Edible mushroom and their cultivations. *CRC Press, Inc., Boca Raton, Florida* 1987; 33:6.
32. Liu JK, Hyde KD, Jones EG, Ariyawansa HA, Bhat DJ, Boonmee S, Maharachchikumbura SS, McKenzie EH, Phookamsak R, Phukhamsakda C, Shenoy BD. Fungal diversity notes –110: taxonomic and phylogenetic contributions to fungal species. Fungal diversity. 2015; 72:1-97.
33. Shabana S, Satya AK. Molecular Identification of Potent Antimicrobial Marine Fungi from Manginapudi Beach (Machilipatnam, India. International Journal of Membrane Science and Technology 2023; 10(2):3649-3664 10(2) DOI:10.15379/ijmst.v10i2.3196.

Table 1: Possible combinations of individual mushroom picture uploaded in Mushroom Identify App.

Sl. No	**Combinations**(Picture No.)
1	1
2	2
3	3
4	4
5	1+2
6	1+3
7	1+4
8	2+3
9	2+4
10	3+4

Table 2: Mushroom species identified in different localities of Thanjavur city indicating their identification methods.

Sl. No	**Name of the Mushroom Identified**	**Species Confirmation**		
		Mushroom Identifying App	**Google Search**	**Mushroom Expert.com Software**
1	*Psilocybe cubensis*	✔	✔	✘
2	*Gymnopilus luteus*	✔	✔	✔
3	*Gymnopi lusluteofolius*	✔	✔	✔
4	*Ganoderma martinicense*	✔	✔	✘
5	*Gymnopilus sapineus*	✔	✔	✔
6	*Agaricus augustus*	✔	✔	✔
7	*Macrolepiota procera*	✔	✔	✔
8	*Kuehneromyces mutabilis*	✔	✔	✔

9	*Vascellum pretense*	✔	✔ ✔	✘
10	*Ganoderma lucidum*	✔	✔	✔
11	*Leucocoprinus cretaceous*	✔	✔	✔
12	*Volvariella bombycina*	✔	✔	✔
13	*Pleurotus ostreatus*	✔	✔	✔
14	*Galerina marginata*	✔	✔	✔
15	*Macrolepiota mostoidea*	✔	✔	✔
16	*Mycena galericulata*	✔	✔	✔
17	*Crepidotus albidus*	✔	✔	✔
18	*Auricularia*	✔	✔	✔
19	*Lentinus squarrosulus*	✔	✔	✔
20	*Gloeoporus dichrous*	✔	✔	✔
21	*Pluteus longistriatus*	✔	✔	✔
22	*Hymenopellis megalospora*	✔	✔	✔
23	*Irpex lacteus*	✔	✔	✔
24	*Lentinustigrinus*	✔	✔	✔
25	*Ceratiomyxa fruticulosa*	✔	✔	✔
26	*Kretzschmaria deusta*	✔	✔	✔
27	*Leucopholiota decorosa*	✔	✔	✔
28	*Termitomyces clypeatus*	✔	✔	✘
29	*Ganoderma carnosem*	✔	✔	✔
30	*Ganoderma sinense*	✔	✔	✘
31	*Climacodon septentrionalis*	✔	✔	✔
32	*Trametes elgans*	✔	✔	✔
33	*Agaricus californicus*	✔	✔	✔
34	*Pleurotus cornacopiae*	✔	✔	✔
35	*Irpiciporus pachyodon*	✔	✔	✘
36	*Armillaria gallica*	✔	✔	✔
37	*Hapalopilus croceus*	✔	✔	✔
38	*Oudemansiella mucida*	✔	✔	✘
39	*Trametopsis cervina*	✔	✔	✘
40	*Ganoderma curtisii*	✔	✔	✔
41	*Psilocybe caerulscens*	✔	✔	✔
42	*Trametes versicolor*	✔	✔	✔
43	*Coprinellus setulosi*	✔	✔	✘
44	*Coprinellus domestica*	✔	✔	✔
45	*Hygrophoropsis aurantiaca*	✔	✔	✔
46	*Amanita cokeri*	✔	✔	✔
47	*Schizophyllum commune*	✔	✔	✔
48	*Trametella gallica*	✔	✔	✘
49	*Entoloma abortivum*	✔	✔	✔
50	*Psathyrella candolleana*	✔	✔	✔
51	*Ganoderma elfvingia*	✔	✔	✔
52	*Hypoxylon fragiforme*	✔	✔	✘

53	*Reticularia lycoperdon*	✔	✔	✘
54	*Bjerkandera adusta*	✔	✔	✔
55	*Ganoderma megaloma*	✔	✘	✘
56	*Flammulina velutipes*	✔	✔	✔
57	*Pleurotus populinus*	✔	✔	✔
58	*Pleurotus dryinus*	✔	✔	✔
59	*Ganoderma sessile*	✔	✔	✔
60	*Oligoporus caesius*	✔	✔	✘
61	*Cerrena unicolor*	✔	✔	✔
62	*Trametes hirsute*	✔	✔	✘
63	*Meripilus sumstinei*	✔	✔	✘

Table 3: Mushrooms with their families and habitats

SI. N0	Family	Name of the Mushroom Identified	Habitats
1	**Hymenogastraceae**	*Psilocybe cubensis*	Cow dung and sugar cane mulch
		Galerinam marginata	Rotting wood
		Psilocybe caerulscens	Grows in sunny locations, preferring muddy orangish brown soils with much woody debris.
2	**Strophariaceae**	*Gymnpilus luteus*	Dead hardwood trees
		Kuehneromyces mutabilis	Dense clusters on dead hardwoods and conifers.
		Gymnopilus sapineus	Dense clusters on dead conifer wood
3	**Ganodermataceae**	*Ganoderma martinicense*	Either as saprotrophs on dead wood or as parasites on the live wood
		Ganoderma curtisii	Decaying stumps and roots of hardwoods.
		Ganoderma elfvingia	Hardwood especially warmer regions.
		Ganoderma megaloma	White rot and butt rot living hardwoods.
		Ganoderma sessile	Deciduous wood, rarely on conifers.
		Ganoderma lucidum	Decaying hardwood trees
		Ganoderma carnosem	Grows on felled trunks
		Ganoderma sinense	Decaying wood of broad leaved trees
4	**Agaricaceae**	*Agaricus augustus*	Deciduous and coniferous woods
		Vascellum pretense	Old lawns and roadside verges
		Leucocoprinus cretaceous	Scattered distribution on potted plants
		Macrolepiota mostoidea	Open deciduous woodland
		Macrolepiota procera	Occasionally in woodland
		Agaricus californicus	Found in grassy areas
5	**Pluteaceae**	*Volvariella bombycina*	Decayed stumps of dead hardwoods
		Pluteuslongis triatus	Widely distributed on decaying hardwood
		Pleurotus ostreatus	Decomposing wood and branches of trees
6	**Mycenaceae**	*Mycena galericulata*	Decaying hardwood and softwood sticks, stumps and logs
7	**Crepidotaceae**	*Crepidotus albidus*	grow on wood or plant debris
8	**Auriculariaceae**	*Auricularia auricular*	Deadwood and also be weakly parasitic on living wood
9	**Polyporaceae**	*Lentinus squarrosulus*	Dead and decayed wood

		Trametes versicolor	Hardwoods, sometimes on living trees.
		Trametella gallica	Dead wood.
		Lentinus tigrinus	Wood of riverbank trees.
		Oligoporus caesius	Dead wood, usually on conifers.
		Lentinus tigrinus	Rotting branches of deciduous hardwood trees
		Trametes elgans	Decaying hardwood
		Irpiciporus pachyodon	Living on broad-leafed trees
		Hapalopilus croceus	Old trees and farmland
		Trametes hirsute	Dead wood of deciduous trees.
10	**Irpicaceae**	*Gloeoporus dichrous*	Decaying fruits
		Trametopsis cervina	Rotting hardwood log.
		Gloeoporus dichrous	Deadwood of hardwoods, and rarely conifers.
11	**Physalacriaceae**	*Hymenopellis megalospora*	Dead and hardwood, decayed logs and stumps
		Armillaria gallica	Found on the ground
		Oudemansiella mucida	Saprobic on stumps and trunks
12	**Meruliaceae**	*Irpex lacteus*	Angiosperm branches and rotting wood
13	**Ceratiomyxidceae**	*Ceratiomyxa fruticulosa*	Found on rotting wood
14	**Xylariaceae**	*Kretzschmaria deusta*	Parasitic on the roots and trunks on live wood
15	**Squamanitaceae**	*Leucopholiota decorosa*	Decaying on hardwood tress
16	**Lyphyllaceae**	*Termitomyces clypeatus*	grows in soil also on termite mounds
17	**Phanerchaetaceae**	*Climacodon septentrionalis*	Decaying on hardwood tress
18	**Psathyrellaceae**	*Coprinellus setulosi*	Forest litter in deciduous forests.
		Coprinellus domestica	Decaying hardwood.
		Psathyrella candolleana	Small groups around stumps and tree roots on lawns.
19	**Hygrophoropsidaceae**	*Hygrophoropsis Aurantiaca*	Both hardwood and conifer forests.
20	**Amanitaceae**	*Amanita cokeri*	Coniferous or deciduous woods and also on the ground.
21	**Schizophyllaceae**	*Schizophyllum commune*	On decaying trees after rainy seasons.
23	**Entolomataceae**	*Entoloma abortivum*	Decaying wood in hardwood forests, or in leaf litter near decaying wood.
24	**Hypoxylaceae**	*Hypoxylon fragiforme*	Fallen branches and rotting stumps.
25	**Reticulariaceae**	*Reticularia lycoperdon*	Dead older branches, logs, and stumps in wet places.
26	**Meruliaceae**	*Bjerkandera adusta*	White rot in live trees, but mostly on dead wood.
27	**Pleurotaceae**	*Pleurotus populinus*	Rotting stumps, logs, and limbs of hardwoods.

		Pleurotus dryinus	Deciduous wood, rarely on conifers.
		Pleurotus cornacopiae	Rotting wood of deciduous broadleaf trees
28	**Meripilaceae**	*Meripilus sumstinei*	Large clumps on the ground around the base of tree stumps.
29	**Cerrenaceae**	*Cerrena unicolor*	Dead hardwood, causing white rot.

Table 4: Number of species identified in each family

SI. No	Family	Number of Species Identified	Percentage Of Species Identified
1	Irpiaceae	3	**4.8**
2	Ganodermataceae	8	**13.0**
3	Polyporaceae	10	**16.0**
4	Hymenogastraceae	3	**4.8**
5	Psathyrellaceae	3	**4.8**
6	Hygrophoropsidaceae	1	**1.6**
7	Amanitaceae	1	**1.6**
8	Schizophyllaceae	1	**1.6**
9	Ceratiomyxaceae	1	**1.6**
10	Entolomataceae	1	**1.6**
11	Hypoxylaceae	1	**1.6**
12	Reticulariaceae	1	**1.6**
13	Meruliaceae	1	**1.6**
14	Psysalacriaceae	1	**1.6**
15	Pleurotaceae	3	**4.8**
16	Meripilaceae	1	**1.6**
17	Cerrenaceae	1	**1.6**
18	Strophariaceae	3	**6.3**

19	Agaricaceae	6	**9.5**
20	Pluteaceae	3	**4.8**
21	Mycenaceae	1	**1.6**
22	Crepidotaceae	1	**1.6**
23	Auriculariaceae	1	**1.6**
24	Meruliaceae	1	**1.6**
25	Ceratiomyxidceae	1	**1.6**
26	Xylariaceae	1	**1.6**
27	Squamanitaceae	1	**1.6**
28	Lyphyllaceae	1	**1.6**
29	Phanerchaetaceae	1	**1.6**

Table 5: Number of species identified in each General

Sl. No	Name of the Genera	Number of Species Identified	Percentage of Species Identified Each Genera
1	*Ganoderma*	**8**	**13.0**
2	*Gymnopilus*	**2**	**3.2**
3	*Agaricus*	**2**	**3.2**
4	*Psilocybe*	**2**	**3.2**
5	*Galerinama*	**1**	**1.6**
6	*Kuehneromyces*	**2**	**3.2**
7	*Vascellum*	**1**	**1.6**
8	*Leucocoprinus*	**1**	**1.6**
9	*Macrolepiota*	**2**	**3.2**
10	*Volvarilla*	**1**	**1.6**
11	*Pluteus*	**1**	**1.6**
12	*Mycena*	**1**	**1.6**
13	*Crepidotus*	**1**	**1.6**
14	*Auricularia*	**1**	**1.6**
15	*Lentinus*	**3**	**4.8**
16	*Trametes*	**2**	**3.2**
17	*Irpiciporus*	**1**	**1.6**
18	*Hapalopilus*	**1**	**1.6**
19	*Gloeoporus*	**1**	**1.6**
20	*Hymenopellis*	**1**	**1.6**
21	*Armillaria*	**1**	**1.6**
22	*Oudemansiella*	**1**	**1.6**
23	*Irpex*	**1**	**1.6**
24	*Ceratiomyxa*	**1**	**1.6**
25	*Kretzschmaria*	**1**	**1.6**
26	*Leucopholiota*	**1**	**1.6**
27	*Termitomyces*	**1**	**1.6**
28	*Climacodon*	**1**	**1.6**
29	*Coprinellus*	**2**	**3.2**
30	*Trametopsis*	**1**	**1.6**
31	*Hygrophoropsis*	**1**	**1.6**

32	*Amanita*	**1**	**1.6**
33	*Schizophylum*	**1**	**1.6**
34	*Ceratiomyxa*	**1**	**1.6**
35	*Trametella*	**1**	**1.6**
36	*Psathyrella*	**1**	**1.6**
37	*Entoloma*	**1**	**1.6**
38	*Hypoxylon*	**1**	**1.6**
39	*Reticularia*	**1**	**1.6**
40	*Bjerkandera*	**1**	**1.8**
41	*Flammulina*	**1**	**1.6**
42	*Oligoporus*	**1**	**1.6**
43	*Pleurotus*	**3**	**4.8**
44	*Meripilus*	**1**	**1.6**
45	*Cerrena*	**1**	**1.6**

Table 6: Edibility of the identified mushroom

SI. No	**Name of the Mushroom Identified**	**Edibility**
1	*Psilocybe cubensis*	Edible
2	*Gymnopilus luteus*	Inedible / Poisonous
3	*Gymnopi lusluteofolius*	Inedible / Poisonous
4	*Ganoderma martinicense*	Inedible
5	*Gymnopilus sapineus*	Inedible
6	*Agaricus augustus*	Edible
7	*Macrolepiota procera*	Edible
8	*Kuehneromyces mutabilis*	Edible
9	*Vascellum pretense*	Edible
10	*Ganoderma lucidum*	Edible
11	*Leucocoprinus cretaceous*	Edible
12	*Volvariella bombycina*	Edible / Confused with poisonous
13	*Pleurotus ostreatus*	Edible
14	*Galerina marginata*	Inedible / Poisonous
15	*Macrolepiota mostoidea*	Edible
16	*Mycena galericulata*	Inedible
17	*Crepidotus albidus*	Inedible
18	*Auricularia auricular*	Edible
19	*Lentinus squarrosulus*	Edible
20	*Gloeoporus dichrous*	Inedible
21	*Pluteus longistriatus*	Edible
22	*Hymenopellis megalospora*	Edible
23	*Irpex lacteus*	Inedible
24	*Lentinus tigrinus*	Edible
25	*Ceratiomyxa fruticulosa*	Inedible
26	*Kretzschmaria deusta*	Inedible
27	*Leucopholiota decorosa*	Edible
28	*Termitomyces clypeatus*	Edible
29	*Ganoderma carnosem*	Edible
30	*Ganoderma sinense*	Edible

31	*Climacodon septentrionalis*	Edible
32	*Trametes elgans*	Edible
33	*Agaricus californicus*	Inedible / Poisonous
34	*Pleurotus cornacopiae*	Edible
35	*Irpiciporus pachyodon*	Inedible
36	*Armillaria gallica*	Edible
37	*Hapalopilus croceus*	Inedible
38	*Oudemansiella mucida*	Edible
39	*Trametopsis cervina*	Edible
40	*Ganoderma curtisii*	Inedible
41	*Psilocybe caerulscens*	Edible
42	*Trametes versicolor*	Edible
43	*Coprinellus setulosi*	Edible
44	*Coprinellus domestica*	Edible
45	*Hygrophoropsis aurantiaca*	Inedible
46	*Amanita cokeri*	Inedible / Poisonous
47	*Schizophyllum commune*	Edible
48	*Trametella gallica*	Edible
49	*Entoloma abortivum*	Edible
50	*Psathyrella candolleana*	Edible
51	*Ganoderma elfvingia*	Edible
52	*Hypoxylon fragiforme*	Inedible
53	*Reticularia lycoperdon*	Edible
54	*Bjerkandera adusta*	Inedible
55	*Ganoderma megaloma*	Edible
56	*Flammulina velutipes*	Edible
57	*Pleurotus populinus*	Edible
58	*Pleurotus dryinus*	Edible
59	*Ganoderma sessile*	Edible
60	*Oligoporus caesius*	Inedible
61	*Cerrena unicolor*	Inedible
62	*Trametes hirsute*	Inedible
63	*Meripilus sumstinei*	Edible

Edibility	**No. of mushrooms species**	**Percentage of mushrooms species**
Edible mushrooms	41	65%
Inedible mushrooms	17	27%
Poisonous mushrooms	05	8%

Fig.1: Geographical Location of study Area; Thanjavur, South India

Fig.2: Mushroom species identified in different localities of Thanjavur city

Fig.2(Cont.): Mushroom species identified in different localities of Thanjavur city

Fig.2(Cont.): Mushroom species identified in different localities of Thanjavur city

Fig.2 (Cont.): Mushroom species identified in different localities of Thanjavur city

Indian Journal of Natural Sciences www.tnsroindia.org.in ©IJONS

Vol.15 / Issue 88 / Feb / 2025 *International Bimonthly (Print) – Open Access* *ISSN: 0976 – 0997*

RESEARCH ARTICLE

Green Synthesis, Characterization and Application of Manganese Oxide Nanoparticle by using *Caasia fistula* Flower Extract

S.U. Subhashini[1] and A. Jeena Pearl[2]*

[1]Research Scholar (Reg No: 21213162032022) Department of Chemistry, Scott Christian College (Autonomous), Nagercoil, (Affiliated to Manonmaniam Sundaranar University, Tirunelveli), Tamil Nadu, India.

[2]Assistant Professor, Department of Chemistry, Scott Christian College (Autonomous), Nagercoil, (Affiliated to Manonmaniam Sundaranar University, Tirunelveli), Tamil Nadu, India.

Received: 21 Nov 2024 Revised: 03 Dec 2024 Accepted: 31 Jan 2025

***Address for Correspondence**

A. Jeena Pearl

Assistant Professor, Department of Chemistry,

Scott Christian College (Autonomous),

Nagercoil, (Affiliated to Manonmaniam Sundaranar University, Tirunelveli),

Tamil Nadu, India.

E.Mail: subhaani04051999@gmail.com

ABSTRACT

Potassium permanganate (KMnO4), and a water extract of *Cassia Fistula* have been used in a green chemistry method to create manganese oxide nanoparticles. UV-Vis spectral analysis, Fourier Transform Infrared (FT-IR), Energy dispersive X-ray analysis and Scanning Electron Microscope (SEM) were used to characterize Manganese oxide nanoparticles. The MnO nanoparticles were evenly distributed, as evidenced by the surface morphology. Using X-ray diffraction (XRD) analysis, the average particle size was determined to be 16 nm. PL analysis has been performed to electronic structure and properties of materials. By using Thermo-gravimetric Analysis (TGA) measurement, the thermal stability of the nanoparticles with the temperature increase has been established. The synthesized manganese oxide nanoparticles were examined for antimicrobial properties. The antibacterial properties of the synthesised manganese oxide nanoparticles were tested against gram-negative bacteria as well as gram-positive bacteria Staphylococcus aureus and Staphylococcus epidermidis. The antibacterial findings imply that manganese oxide nanoparticles may be helpful as efficient growth inhibitors for microbes in applications ranging from antimicrobial-controlled systems to medical devices. The following is the order of the microorganisms' reaction towards the zone of inhibition: Staphylococcus epidermidis (24mm) Staphylococcus aureus (20mm) Escherichia coli (19 mm) > Pseudomonas aeruginosa (19 mm).

Keywords: Nanoparticle, Manganese Oxide, Antibacterial, Microorganisms, Materials.

INTRODUCTION

Transition metal oxides have gained significant attention in science and technology in recent decades because of their unique characteristics with regard to optical, catalytic, electric, and magnetic fields [1]. Different sized and shaped metallic nanoparticles have unique applications. Because they are widely available and utilised as green catalysts in the catalysis Industry[2]. Metal nanoparticles have recently been synthesised using a variety of techniques, including chemical reduction [3], Sono chemical approach, and one-step solution procedure at ambient temperature. [4], the polyol approach, the electrochemical techniques, the hydrothermal method, the microemulsion method, and the modern green chemistry pathway [5]. When creating nanoparticles, benign materials such as plant leaf extract, bacteria, fungi, and enzymes are used instead of poisonous ones. This approach is more economical, environmentally friendly, and has potential applications in biomedicine.[6] Many different plant species produce secondary metabolites known as golden shower tree. Numerous names, including pudding pipe tree, purging cassia, Indian laburnum, kanikonna, Amaltas, Aragbadha, Sondal, Bahva and Garmalo, a member of the Fabaceae family [7]. According to research,*Cassia Fistula* has the following properties: antibacterial, antifungal, antitussive properties. It is also used to treat wounds and gastrointestinal issues. [8]. Due to their numerous applications in a variety of fields, including biological fields, lithium-ion batteries, sensors and imaging techniques, medicinal drug delivery, catalysts, and biological fields, manganese dioxide nanoparticles have garnered a lot of interest in the field of material science research in recent years [9]. Manganese is safe to use in laboratory reactions due to its non-toxic behaviour, and its products are biocompatible and non-hazardous. Manganese oxide nanoparticles have garnered significant interest in both basic and prospective technology domains. It is widely known from several research that MnO exhibits a variety of crystal forms. Based on earlier research, we came to the conclusion that MnO nanoparticles have excellent stability and durability and can be easily prepared by the use of a wet chemical approach [10]. Regarding the environmental approach, greener ways of synthesising metal oxide nanoparticles can be more successfully achieved by employing reduction techniques with plant extracts. Green synthesis of metal oxides can be carried out at room temperature or in low temperature environments [11]. Our decision to create manganese dioxide nanoparticles using Cassia Fistula was inspired by recent studies on the flower extracts for the creation of other metal nanoparticles. MnO is widely used in energy storage devices because of its strong electrochemical performance, low environmental toxicity, and affordable production costs [12]. Reasonable control of the phase, shape, size, and dimensionality of nanomaterials has been the subject of much research because it is well recognised that these factors have a significant impact on the materials' properties and applications [13]. The production of manganese oxide nanoparticles has been the main focus of this investigation, and analytical tools like SEM, EDAX, XRD, FT-IR, TGA, UV-Vis, and PLand antimicrobial studies have been employed to characterise the particles [14].

MATERIALS AND METHODS

Cassia Fistula flower extract, Potassium permanganate, Distilled water

Preparation of extract

Cassia Fistula flower was gathered and rinsed with water many times to get rid of the dust, and then dried to get rid of any moisture lef tover. In a 250 mL glass beaker with100 mL of sterile distilled water, 50g of cleaned, dried, and finely chopped Cassia Fistula flower were placed to create the extract that was used to reduce manganese ions (Mn2+) to manganese nanoparticles (MnO). After that, the mixture was boiled for 60 minutes, or until the aqueous solution's color changed from watery to light yellow. The extract was filtered with filter paper after being cooled to room temperature. In order to be used for future research, the extract was kept in a refrigerator.

Preparation of manganese oxide nanoparticle

50 ml of Cassia Fistula flower extract was boiled to a temperature of 60 to 80 ℃ to create the nano particles. As the temperatures hit 60 ℃, 5 grams of Potassium permanganate were added to the solution. The mixture is then boiled until it turns into a brown thick paste. This paste was then gathered in a ceramic crucible and heated for two hours at

400 °C in an air-fired furnace. After obtaining a brown powder, it was carefully collected and packaged for characterization purposes. To obtain a finer nature the nanoparticle was mashed in a mortar pestle for characterization.

RESULTS AND DISCUSSION

The Green synthesis of manganese dioxide nanoparticles shows different characterization patterns like XRD, UV-Vis spectrum, TGA, FTIR, EDAX, SEM, PL, and antimicrobial activity.

UV visible spectra analysis

One of the easiest methods to characterise nanoparticles and learn about their optical characteristics is to conduct a UV-visible absorption study [15]. The synthesised MnO nanoparticles' electronic absorption spectra revealed an absorption maximum (λmax) at 366 nm, indicating the nanoparticles' creation [16].

FT-IR spectra analysis

The presence of functional groups on the synthesised nanoparticles is ascertained using FT-IR spectroscopy. Manganese oxide nanoparticles supplemented with a extract of a Cassio Torasample were seen in the FT-IR spectra. The manganese oxide spectrum's maximum intensity of wave numbers range from 4000 to 500 cm-1. Manganese oxide synthesis is confirmed by the first peak at 3350cm-1, which shows the existence of a OH stretching in the polymeric hydroxy compounds. The NH^+ are represented by the peak at 2363 cm-1. The existence of carboxylic groups is confirmed by the absorption band around 1630 cm-1. The NO_2 asymmetric stretching at 1517cm-1 The 1263 cm-1 is confirmed by C-N stretching. The 919 and 529 cm-1 band around S-N stretching and C-I stretching [17].

X-RAY diffraction

X-ray diffraction (XRD) is used to analyse the size and purity of the products. It is evident from the XRD pattern that the manganese oxide metal nanoparticles synthesised were entirely crystalline.The biologically produced nanoparticle's crystallinity is indicated by the intensity of the peaks [17]. The Debye-Scherrer equation was utilised to determine the size of crystalline nanoparticles. The formula involves D being the average crystal size, λ representing the incident x-ray wavelength, β representing full-width half maxima, and θ standing for Bragg's angle. The average particle size of the nanoparticle was 20 nm [18].

Scanning electron microscope

The manganese oxide nanoparticles' surface morphology was investigated using the SEM method. Their high surface energy and short external dimensions give rise to an irregular spherical shape, as shown in the image shown in Fig. 4 [19]. It is commonly known that surface shape significantly affects how efficiently nanostructured materials function. The overall appearance of the product formed from combustion is seen in the SEM micrograph [20]. The SEM morphology of the MnO nanocrystalline revealed that the particles were sharply agglomerated, aggregated between one other, and had an irregular spherical form. The SEM images of MnO nanoparticles that were generated at two distinct diameters—20μm and 2 μm—were corroborated by previously released data[21].

Energy-dispersive X-ray analysis

The generation and chemical makeup of the green-synthesised MnO NAPs were investigated using EDX analysis. The successful green production of Nps employing biological components from CassiaFistula flower extract corroborated these findings. The EDX peaks of the chemical element (Mn) at 0.63 keV and 5.91 keV in the EDX spectrum verified the element's presence in the synthesised nanoparticle [22]. The adsorption of living molecules on the surface of nanoparticle from the floral extract was confirmed by the presence of distinct peaks in the EDX spectrum corresponding to carbon (C), oxygen (O) and potassium (k) in addition to the MnO EDX peaks. Further confirmation of the nanoparticle purity came from the EDX results. Therefore, it is clear from the EDX data that plant flower extract has been successfully used to synthesise the nanoparticle of interest.

TGA and DTA analysis

The TGA and DTA spectra of MnO-NPs show that the sample degrades quickly at increasing temperatures. Thermal gravimetric analysis (TGA), as shown in Fig. 6, was used to characterise the thermal stability of the biogenesis of MnO NPs indicated in the TGA thermogram. As shown in Fig. 6, the extract encapsulating the nanoparticles contained various volatile components that caused the sample to evaporate completely between 27 and 700 °C. The various elements of the simple consistently and gradually evaporate as the temperature rises. The sample's moisture was removed until the temperature reached 100 °C. The bulk sample showed minimal weight loss and thermal stability in the data above 400 degrees Celsius. This is caused by the heat degradation of phenolic and flavonoid biomolecules that remain after the biosynthetic process. Thus, even modest temperature increases did not result in a noticeable loss, indicating good thermal stability.

Photo luminescence spectrum

The synthesised MnO NPs' PL spectra was measured at room temperature. Near their band boundary and at the excitation peak of 517 nm, an emission peak at 300 nm was seen (Figure 7). The oxygen deficiency on the MnO surface is most likely what is causing the defect emission in the visible region. Furthermore, Jangir published findings that were comparable, stating that the emission spectrum shows broad yellow emission at 750 nm coupled with strong peaks at roughly 500 and ~550 nm that correspond to pure MnO. This implies the existence of several singly ionised oxygen vacancies, or surface defects. Moreover, the valence band transition of the MnO NPs between single-charged oxygen vacancies and photoexcited holes produced the broad peak. The quantum size effect becomes more prominent when the particle size gets closer to the nanometre scale. This results in changes to the physical properties of the semiconductor materials. Acute and intense PL is a sign of extremely shallow surface states, and is caused by surface state recombination. The band edge's quantum yields may create shallow trap centres that attract photoexcited electrons, bringing the carriers closer to the surface where they are needed for the photocatalytic reaction.

APPLICATION

Antibacterial activity

The disc diffusion method was used to investigate the antibacterial activity against several pathogens, such as Pseudomonas aeruginosa, Escherichia coli, Staphylococcus epidermidis Staphylococcus aureus. Cassio Tora flower extract was used to synthesise manganese oxide nanoparticles, which efficiently inhibited both Gram-positive (S. aureus), (S. epidermidis) and Gram-negative (E. coli) bacterial strains (P. aeruginosa) [23]. Studies on antibacterial properties revealed that the flower extract of Cassia Fistula exhibited the highest zone of inhibition against Staphylococcus aureus and Staphylococcus epidermidis, but exhibited reduced effectiveness against Pseudomonas aeruginosa and Escherichia coli.

Anti-fungal activity

The pathogens Aspergillus Niger and Candida albicans were tested for antifungal activity using the disc diffusion method. The manganese oxide nanoparticles derived from CassiaFistula flower extract that were biosynthesised efficiently inhibited both fungal strains. Cassia Fistula flower extract has the highest zone of inhibition against Aspergillus Niger, and less effectiveness against Candida albicans.

CONCLUSION

The MnO nanoparticles were effectively synthesised using CassiaFistula flower extract as a reducing and stabilising agent. UV, FT-IR, XRD, SEM, EDAX, TGA & DTA and PL studies were used to characterise the MnO nanoparticles. Between 200 and 800 nm, the UV spectrum was recorded. The production of MnO nanoparticles is indicated by an absorption peak in the spectra at 366 nm. This green synthesis technique shows how manganese oxide can be produced using Cassia Fistula extract as a reducing and stabilising agent. The functional groups included in the

synthesised manganese oxide nanoparticles were determined using FT-IR, and the nanoparticles' shape was investigated using a scanning electron microscope. It is evident from the XRD pattern that the synthesised manganese oxide metal nanoparticles were entirely crystalline. The EDX peaks of the chemical element (Mn) at 0.63 keV and 5.91 keV in the EDX spectrum verified the element's presence in the synthesised nanoparticle. In the biological research of manganese oxide nanoparticles, Cassia Fistula may prove to be an effective reducing and capping agent. Manganese oxide nanoparticles were effectively synthesised from Cassia Fistula flower extract for the first time in this work utilising an easy, affordable, environmentally friendly, and green method. With regard to its prospective use as an antibacterial and antifungal agent in biomedical applications, manganese oxide nanoparticles are now used in pharmaceutical research.

REFERENCES

1. Ahmed, S.; Chaudhry, S. A.; Ikram, S., A review on biogenic synthesis of ZnO nanoparticles using plant extracts and microbes: a prospect towards green chemistry, Journal of Photochemistry and Photobiology B: Biology, 2017, 166, 272-284. https://doi.org/10.1016/j.jphotobiol.2016.12.011 2.
2. Arasu, M.V.; Arokiyaraj, S.; Viayaraghavan, P.; Kumar, T. S.; Duraipandiyan, V.; Al-Dhabi, N. A.; Kaviyarasu, K., One step green synthesis of larvicidal, and azo dye degrading antibacterial nanoparticles by response surface methodology, Journal of Photochemistry and Photobiology B: Biology, 2019, 190, 154-162. https://doi.org/10.1016/j.jphotobiol.2018.11.020
3. Azizi S, Ahmad MB, Namvar F, Mohamad R. Green biosynthesis and characterization of zinc oxide nanoparticles using brown marine macroalga Sar.
4. Chu, X.; Zhang, H., Catalytic decomposition of formaldehyde on nanometer manganese dioxide, Mod Appl Sci, 2009, 3(4), 177-182. https://doi.org/10.5539/mas.v3n4p177
5. Dawadi, S.; Gupta, A.; Khatri, M.; Budhathoki, B.; Lamichhane, G.; Parajuli, N., Manganese dioxide nanoparticles: synthesis, application and challenges, Bulletin of Material Science, 2020, 43 1-10. https://doi.org/10.1007/s12034-020-02247-8
6. Hemlatha, F.C.; &Lourduraj, A.J.C., Synthesis and characterization of MnO2 Nanoparticles using Coprecipitation Technique, International Journal of Scientific Research in Science and Technology, 2017, 3(11), 125-128.
7. Jassal, V.; Shanker, U.; Gahlot, S.; Kaith, B. S.; Kamaluddin, Iqubal, M. A.; & Samuel, P., Sapindusmukorossi mediated green synthesis of some manganese oxide nanoparticles interaction with aromatic amines. Applied Physics A, 2016, (122), 1-12. https://doi.org/10.1007/s00339-016-9777-4
8. Jaganyi, D.; Altaf, M.; & Wekesa, I., Synthesis and characterization of whisker-shaped MnO2 nanostructure at room temperature, Applied Nanoscience, 2013, 3, 329-333. https://doi.org/10.1007/s13204-012-0135-3
9. Joshi, N.C.; Joshi, E.; Singh, A., Biological Synthesis, Characterisations and Antimicrobial activities of manganese dioxide (MnO2) nanoparticles, Research Journal of Pharmacy and Technology, 2020, 13(1), 135-140. https://doi.org/10.5958/0974-360X.2020.00027.X
10. Jayandran, M.; Haneefa, M, M.; Balasubramanian, V., Green synthesis and characterization of Manganese nanoparticles using natural plant extracts and its evaluation of antimicrobial activity, Journal of Applied Pharmaceutical Science, 2015, 5(12), 105-110. https://doi.org/10.7324/JAPS.2015.501218
11. C. Kavitha.; S, Vinothini.; S, Barathi.; A, Sasi Kumar., Chemical Synthesis of Manganese Dioxide Nanoparticle by Using Co-Precipitation Method, International journal of innovative research in science, engineering and technology, 2020, 142-147.
12. Luo, Y., Preparation of MnO2 nanoparticles by directly mixing potassium permanganate and polyelectrolyte aqueous solutions, Materials Letters, 2007, 61(8-9), 1893-1895. https://doi.org/10.1016/j.matlet.2006.07.165
13. Manjula, R.; Thenmozhi, M.; Thilagavathi, S.; Srinivasan, R.; Kathirvel, A. Green synthesis and characterization of manganese oxide nanoparticles from Gardenia resinifera leaves. *Mater. Today Proc.* **2019**. [**Google Scholar**] [**CrossRef**]

14. Mishra, S.; Thakur, M., Role of microwave assisted extraction for isolation of saponins from sapindusmukorrosai and synthesis of its stable biofunctionalized silver nanoparticles and its hypolipidaemic activity, International Journal of Pharmaceutical Sciences and Research, 2016, 7(7), 2959.
15. Majumdar, D.; Bhattacharya, S.K., Sonochemically synthesized hydroxy-functionalized grapheme-MnO2 nanocomposite for supercapacitor applications, Journal of Applied Electrochemistry, 2017, 47, 789-801. https://doi.org/10.1007/s10800-017-1080-3
16. Narayanan, K.B.; Sakthivel, N., Green synthesis of biogenic metal nanoparticles by terrestrial and aquatic phototrophic and heterotrophic eukaryotes and biocompatible agents, Advances in colloid and interface science, 2011, 169(2), 59-79. https://doi.org/10.1016/j.cis.2011.08.004
17. Prasad, K.S.; Patra, A., Green synthesis of MnO2 nanorods using Phyllanthus amarus plant extract and their fluorescence studies, Green Processing and Synthesis, 2017, 6(6), 549-554. https://doi.org/10.1515/gps-2016-0166
18. Rao, C.N.; Vivekchand, S.R.; Biswas, K.; Govindaraj, A., Synthesis of inorganic nanomaterials, Dalton Transactions, 2007, (34), 3728-3749. https://doi.org/10.1039/b708342d
19. Seabra, A.B.; Haddad, P.; Duran, N., Biogenic synthesis of nanostructured iron compounds: applications and perspectives, IET nanobiotechnology, 2013, 7(3), 90-99. https://doi.org/10.1049/iet-nbt.2012.0047
20. Singh, S.; & Ali, M., Sapindusmukorossi: a review article, J. Pharm. Innov, 2019, 8(12), 88-96.
21. Sivakumar, S.; & Prabu, L.N., Synthesis and Characterization of α-MnO2 nanoparticles for Supercapacitor application, Materials Today: Proceedings, 2021, 47, 52-55. https://doi.org/10.1016/j.matpr.2021.03.528
22. . Sinha, A.; Singh, V.N.; Mehta, B.R.; & Khare, S.K., Synthesis and characterization of monodispersed orthorhombic manganese oxide nanoparticles produced by Bacillus sp. cells simultaneous to its bioremediation, Journal of hazardous materials, 2011, 192(2), 620-627. https://doi.org/10.1016/j.jhazmat.2011.05.103
23. Wang, H.Q.; Yang, G.F.; Li, Q.Y.; Zhong, X.X.; Wang, F.P.; Li, Z.S.; Li, Y.H., Porous nano-MnO2: large scale synthesis via a facile quick-redox procedure and application in a supercapacitor, New Journal of Chemistry, 2011, 35(2), 469-475. https://doi.org/10.1039/C0NJ00712A

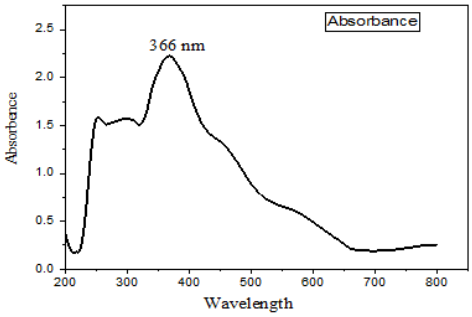

Fig:1 UV Visible spectrum of MnO nanoparticle

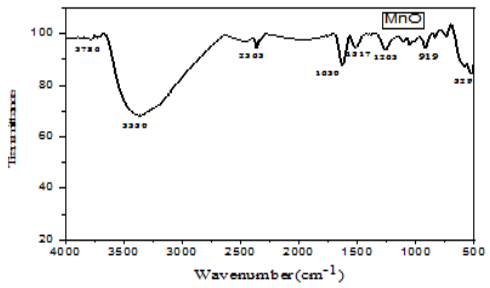

Fig:2 FT-IR Spectrum of MnO nanoparticles

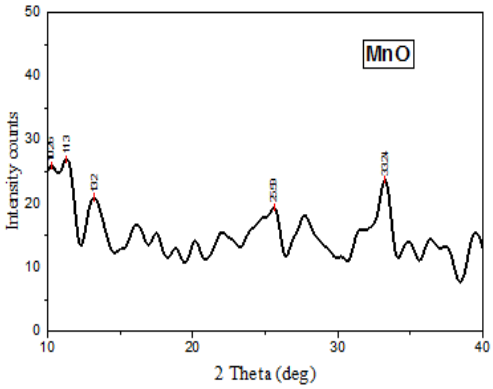

Fig 3: XRD spectrum of MnO nanoparticles

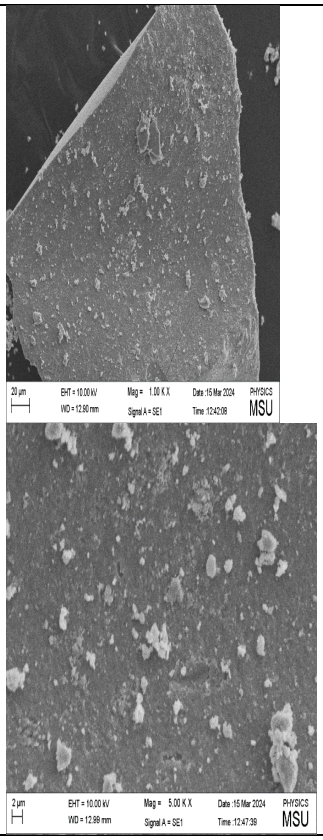

Fig 4: SEM image of MnO nanoparticle

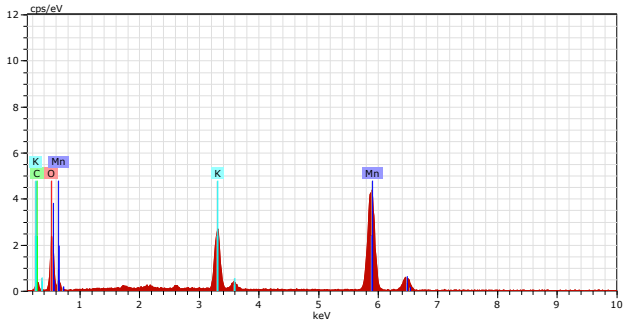

Fig 5: EDAX image of MnO nanoparticle

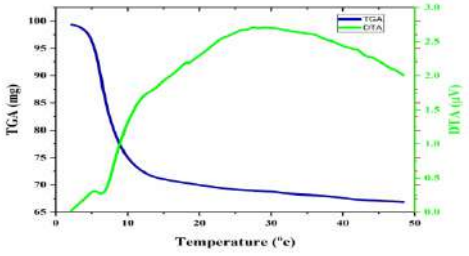

Fig 6: TGA and DTA image of MnO nanoparticle

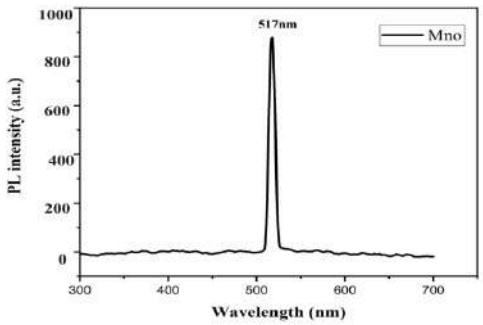

Fig 7: PL image of MnO nanoparticle

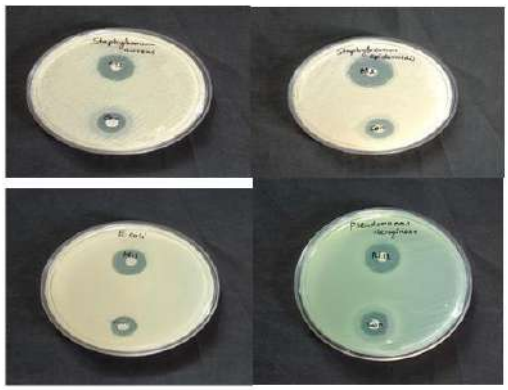

Fig 8: Antibactrial activity image of MnO nanoparticle

Fig 9: Antifungal activity image of MnO nanoparticle

Indian Journal of Natural Sciences *www.tnsroindia.org.in ©IJONS*

Vol.15 / Issue 88 / Feb / 2025 *International Bimonthly (Print) – Open Access* *ISSN: 0976 – 0997*

RESEARCH ARTICLE

A Comparative Clinical Study to Evaluate the Efficacy of Vaitaran Basti Prepared with Gomutra and Gomutra Arkain in the Management of *Aamvata*

Haresha Sahani[1] and Nirmala Sonawane[2]*

[1]PG Scholar, Department of Panchakarma, Parul Institute of Ayurveda, Parul University, Vadodara, Gujarat, India.
[2]Professor and HOD, Department of Panchakarma, Parul Institute of Ayurveda, Parul University, Vadodara, Gujarat, India.

Received: 21 Nov 2024 Revised: 03 Dec 2024 Accepted: 27 Jan 2025

***Address for Correspondence**
Nirmala Sonawane
Professor and HOD,
Department of Panchakarma,
Parul Institute of Ayurveda,
Parul University,
Vadodara, Gujarat, India.
E.Mail: ayurved05@gmail.com

ABSTRACT

Amavata is a highly disabling joint disorder, marked by chronic pain in the joints and body, frequently accompanied by swelling in one or more joints. In addition to joint-related symptoms, patients may experience loss of taste, excessive thirst, lethargy, a sense of heaviness, fatigue without exertion, digestive issues, and fever. In Ayurvedic literature, *Chakradatta* recommends *VaitaranaBasti*to treat *Amavata*, while *AacharyaCharaka* highlights the importance of *Bastikarma*, referring to it as "*Ardhachikitsa*".This clinical study explored the use of *Vaitarana* Basti in two Groups: Group A was treated with *Vaitarana* Basti prepared with *Gomutra*, while Group B was treated with*VaitaranaBasti*prepared with *GomutraArka*. Both forms of *Basti*, recognized for their *Deepana* (stimulant), *Pachana* (digestive), *Tikshna* (penetrative), and *Ushna* (heating) properties, target *AmaDosha*, which is a main factor in the development of *Amavata*. The study was conducted on 30 patients exhibiting typical *Amavata* symptoms, and the results were assessed based on established criteria. The findings showed notable therapeutic effects, with Group A demonstrating a 41.32% improvement and Group B achieving a slightly higher improvement of 45.27%, underscoring the efficacy of both treatments in managing the condition.

Keywords: *Amavata*, *VaitaranBasti*, *GomutraArka*

INTRODUCTION

Amavata is derived from "*Ama*" and "*Vata*," meaning '*AamenaSahitahaVataha*.' *Agnimandhya* (impaired digestion) leads to the formation of *Ama*, which, along with vitiated *Vata*, settles in joints (*Shleshmasthana*), causing *Amavata*. This condition arises from improper habits like *Divaswapna* (day sleeping) and *Vegavarodha* (suppressing urges). *Amavata* is closely linked to Rheumatoid Arthritis (RA) in modern medicine due to shared pathology and symptoms.RA is a chronic, progressive disease affecting small joints asymmetrically and later spreading to the extremities. The main treatments for *Amavata* are *Langhana* (fasting), *Deepana* (digestive stimulation), *Swedana* (sudation), *Virechana* (purgation), and *Basti* (enema). *Shodhana* and *BastiKarma* are particularly effective, as they remove vitiated *Kapha* and *Vata* doshas.Though *Basti* is typically avoided in the acute *Ama* stage, *TeekshanaNiruhaBasti*, with *Agnideepana* (digestive), *Pachana* (*Ama* digestion), and Amahara (toxin removal) properties, can effectively treat *Amavata* by breaking the disease pathology. *VaitaranBasti* is utilized in the treatment of *Amavata* to balance *Vatadosha,* eliminate *Ama* (toxic waste), and reduce joint inflammation. This therapy aids in detoxifying the body, enhancing circulation, and promoting joint health. *Gomutra* is traditionally used in preparing *VaitaranaBasti*; however, *GomutraArka* is more practical for regular use due to its affordability and ease of availability. Procuring fresh *Gomutra* is often challenging, and its storage is not feasible, whereas *GomutraArka* can be easily prepared and stored. Therefore, in this study, *VaitaranaBasti* made with *GomutraArka* was employed in the management of *Amavata*.

Aim and objective

Aim: To compare the efficacy of *VaitaranaBasti* prepared with *Gomutra* and prepared with *GomutraArka* in the management of *Amavata*.

Objectives

1. To determine the effect of *VaitaranaBasti* prepared with *Gomutra* in the management of *Amavata*.
2. To determine the effect of *VaitaranaBasti* prepared with *GomutraArka* in the management of *Amavata*.
3. To compare the efficacy of *VaitaranaBasti* prepared with *Gomutra* and with *GomutraArka* in the management of *Amavata*.

Study design

Study type- Randomized comparative clinical study

Study centre- OPD and IPD of Parul Ayurveda Hospital, Limda, Waghodia, Gujarat.

Randomization method- Computerized Randomization table Total no. of patients- in each group 15+15 patients total of 30 Patients Criteria for selecting the patients

Inclusion criteria

- ✓ Patients with classical signs and symptoms of *Amavata*.
- ✓ *Amavata* patients between the age group of 18 to 70 years.
- ✓ Patients of either Gender irrespective of Caste and Religion

Exclusion criteria

- ✓ Patients of Age below 18 years and above 70 years of either sex.
- ✓ Patients having other systemic disorders – (known cases of) HTN, Carcinoma, TB, Infectious diseases and other LifeThreatening disorders.
- ✓ Patients with extremely reduced joint space.
- ✓ Patients contraindicated for *VaitaranBastiKarma*.
- ✓ Patients contraindicated for *Shodhan* such as Pregnant & Lactating women.

Observation

Group A is mostly female (87.5%) and aged 41-50 (43.8%), with all participants unmarried and primarily engaged in household work (81.3%). Group B has a more balanced gender distribution (60% female) and is older, with 33.3% aged 61-70. Both groups are predominantly Hindu and rural, with similar clinical symptoms like *Sandhishool, Sandhishotha, Aruchi, Alasya, Agnidourbalya, Pratahstabdhta, Gaurava, Jwara*and *Angamarda*. Most participants in both groups have a history of using modern medicine. The data presents a comparative analysis between Group A and Group B based on various physiological and lifestyle parameters. In terms of diet, Group A has a higher percentage of vegetarians (56.3%) compared to Group B (40%). Both groups show a significant number of individuals with constipated bowel habits. Habits like tea/coffee consumption are more common in Group B (33.3%) compared to Group A (6.3%). Appetite levels in both groups are predominantly moderate, while sleep disturbances are more frequent in Group A (93.8%) than in Group B (80%). Both groups share similar patterns in *Nadi* (KV dominance), but Group A has a higher incidence of constipated bowel habits and disturbed sleep. In terms of physiological attributes, both groups are largely similar across factors like *Prakriti*, *Sara*, and *Satva*, with minor differences in parameters like *Akruti*, *Vikriti*, and *Aaharsakti*.

RESULT

Effect of therapy- Both groups show similar effects on *Sandhishoola*. *Sandhishool* is caused due to vitiated vayu *sthanasamshraya* and *aam* at *SandhiPradesh* cause *shoola*. *Shoola*is mainly due to *Vatadosha* and *Basti* is the main treatment modality of *Vatadosha*.Properties of *Vaitaranabasti* contain *saindhava*, *Guda*, *Chincha*, *Sneha*, and *Gomutraarka* which have*ushanaTikshna* properties. *Saindhav* is *tridoshahar*, *Guda* is *vatapittahar* and *Gomutraarkakaphavathara*.In *aamvata* involvement of *aam* with *vata* leads to *RasadhatuSrotodusti* and causing pain. *Vaitaranbasti* remove *RasadhatuSrotasdusti* due to *Ushna*,*Tikshna* and *Amapachan* properties. Effect of therapy – in group A 45.66% and in group B 44.36 %. Almost the same effect on *Sandhishotha*. Mainly *shotha* developed due to vitiation of *kaphadosha* as it has predominance of *Prithvi* and *JalaMahabhuta*. It results when vitiated dosha afflicts *twaka*,*Rakta*and *Mamsa*. Joints swelling in RA is the result of an accumulation of synovial fluid, hypertrophy of synovium and thicking of joint capsule.Drugs used in *vaitaranabasti* as *Chincha*, *Guda* and *Gomutraarka* which help in reduce the *sotha*, *Chincha* and *guda* have inflammatory effects also in *ayurvedaChincha* mentioned as *Sothaghna*. *Gomutra* Arka has *ropana* properties which help in *Sothahara*. Effect of therapy – with 1% difference similar effect on *Aruchi*. *Aruchi* refers to an aversion to food and a disturbance in digestion, caused by imbalances in the *doshas* (*Vata, Aamvata* is a disease of *rasavahasrotasa*, it developed due to *dushti* or *Prakop* of *ama*. *Ama*is produced by *Agnimandhya* of both *jathragni* and *dhatvagni*, even though *ama* is the cause of various diseases, in *aamvata* it is the main causative factor.*Vaiataranbasti* contains – *Saindhav*, *Guda*, *Chincha*,*Sneha*, *Gomutraarka* which all having properties like *deepaka-Rochaka*, *Ushana*, and *Tiskhna*.

Also,*vaitaranbasti* is used as *Deepana, Pachana, Lekahan, Srotoavrodhana* also *Aamharana*. Effect of therapy – in Group A 43.33% and in Group B-49% the difference shows 5.67% better in Group A. *Angamarda* due to *Aam* involvement and also experiences due to *vata* predominant condition. *Vaitaranbasti* contains *Saindhav – Pachaka* and *tridoshahara*. *Guda-Laghu*, *Anabhishyadi* and *Deepana*. *Chincha-klamaghna*, *Deepaka* and *Mutral*. Gomutra arka has properties like *Agnideepaka*, *Ushna*, and *Tikshana*. These all help in reducing*aam* condition and *vatadosha* vitiation. Effect of therapy – with 1% difference similar effect on *Agnidourbalya*. In *Amavata* due to *NidanaSevanKapha* and *VataDoshaPrakopa* occur, which cause *Mandagni*. *Mandagni* is responsible for *Ama* formation. *Vaiataranbasti* contains – *Saindhav*, *Guda, Chincha, Sneha, Gomutraarka* which all having properties like *Deepan*,*Ushana*, and *Tiskhna*. Also,*vaitaranbasti* is used as *Deepana*, *Pachana*, *Lekahan*, *Srotoavrodhana*, *Aamharana*. Effect of therapy- same effect of therapy in both Groups.*Amavata* is an Ama *pradoshajavikara*, caused by *Agnimandya*, which leads to the accumulation of *Ama* in *Shleshmasthana* and *Prakopa* of *kaphadosha*, resulting in stiffness of joints.*Guda*, *Chincha*, and *Gomutra* all help alleviate *Stabdhata* by its *katu*, *Ushna*, *Tikshna*, and *Ropana* Deepan properties. Vaitaran Basti has effects*Tikshna*, *Deepana*, *Tridoshahara* and *Pachana* which reduce the *ama* and *kaphadosha* vitiation. Effect of therapy- in difference 4.33% better group A than group B.In *Aamvata*, *Alasya* is primarily caused by the accumulation of Ama and the imbalance of *Vata* and *Kaphadoshas*. *Kapha* leads to heaviness and sluggishness, while Vata causes pain and stiffness, both contributing

to laziness and lack of energy.*Vaitaranbasti* contains *Saindhav –Pachaka* and *tridoshahara*. *Guda-Laghu*, *Anabhishyadi* and *Deepana*. *Chincha-klamaghna*,*Deepaka* and *Mutral*. *Gomutraarka* has properties like *Agnideepaka*,*Ushna*, and *Tikshana*. These all help in reducing*aam* condition and *Kaphadosha* vitiation. Effect of therapy – 9.05 % differences shows Group A having better effect than the Group B. In *Aamvata*, *Jwara* develops when *Aama* from poor digestion aggravates *Pittadosha*, causing inflammation and increased body heat. This results in fever, which exacerbates joint pain and stiffness. *VaitaranBasti* helps manage *Jwara* (fever) by detoxifying the body and balancing *Pittadosha*, which is often aggravated during fever. It reduces inflammation and lowers body temperature by removing *Aama*. Effect of therapy- 3.33% difference almost nearly effect of both Groups.In *Aamvata*, *Gaurava* is primarily caused by the accumulation of *Aama* in the joints, leading to aggravated *Kaphadosha*. This results in a feeling of weight and heaviness. The *nidan* of *Gaurava* in *Aamvata* includes poor digestion, improper metabolism, and the buildup of toxic substances in the body.*Guda*, *Chincha*, and *Gomutra* all help alleviate *Gaurava* by its *katu*, *Ushna*, *Tikshna*, *RopanaDeepan* properties.*VaitaranBasti* having effect on *Tikshna*, *Deepana*, *Tridoshahara* and *Pachana* which reduces the *ama* and *kaphadosha* vitiation. ESR - The contaminated rasa or immaturely formed digestive juice in the stomach due to weak agni is called ama. When ama is put into circulation, it combines with the doshas and *dhatu* and further contaminates them.They block and clog the *srotas* and cause a deficit supply of nutrition and essential elements to the tissues.*Agnimandhya* and ama are the main cause for many systemic disorders. Though ESR does not specifically diagnose any diseases,but it can provide information about whether or not there is inflammation in the body. After *BastiChikitsa* of 9 days the inflammation caused by RA disease in the body has been markedly reduced.

CONCLUSION

Both groups showed highly significant results, with both types of *VaitaranaBasti* providing substantial relief from most symptoms of the disease at a significant level. No participants experienced *BastiVyapad* or any other complications.

REFERENCES

1. Chakrapanidutta. Chakradutta with Bhavartha Sandipani Hindi Vyakhya Varanasi; Chaukambha Sanskrit Sansthan;1961.P.603[C.D.73/31].
2. Vagbhata. Ashtanga Hridaya. With Commentaries Sarvanga Sundari of Arunadattaand Ayurveda Rasayana of Hemadri. Varanasi; Chaukambha Sanskrit Sansthan;2012.p.285.[A.H.SU19/86,87].
3. Sushruta. Sushruta Samhita. With the Nibandha Sangraha commentary of SriDalhanacharya. Varanasi; Chaukambha Sanskrit Sansthan; 2012. p.526. [Su.Chi35/18].
4. Agnivesha. Revised by Charaka. Charak Samhita Vol.-1 Varanasi; Chaukambha Bharati Academy; 2012. p. 46. [Ch.Su1/109-113].
5. Chakrapanidutta. Chakradutta with Bhavartha Sandipani Hindi Vyakhya Varanasi; Chaukambha Sanskrit Sansthan; 1961.P.603[C.D.73/31].
6. Vangasena. Vangasena samhitavol.2. Second edition.Varanasi; Chaukambha Sanskrit Sansthan.P.1165
7. Vrindha. Vrindhamadhava/ sidhayogah Part 2. First edition. By Dr.PremvatiTiwari & Dr.AshaKumari. Varanasi; Chaukambha Sanskrit Sansthan; 2006.p.938.
8. Madhav nidan , aacharya shree vijayrakshit-shree kanthdata virchit “madhukosha”vyakhya vibhushita, purvardh. By Prof. dayal Parmar. Sarsvati pustak bhandar,2010,p.600.
9. SheetalG. Lodha and Ruchika S. Karade, Clinical evaluation of vaitaranabasti along with dhanwantara taila matra basti in amavata: a case series / Int. J. Res. AyurvedaPharm.11(6),2020.
10. Dr. Rahul m. wanole and Dr. d. s. chothe, vaitaran basti in –amavata a pilotstudy, researcharticleissn2394-3211ejpmrejpmr,2016,3(11),379-382
11. Prashant Sasane ,Udai Raj Saroj,Ram Kishor Josh, Clinical evaluation of efficacy of Alambushadi Ghana Vati and Vaitarana Basti in the management of Amavata with special reference torheumatoidarthritis,July7,2022,IP:210.212.136.97

12. ShastriBS, editor. Yogaratnakara of unknown author, Amavata Nidana.6thed.,vol.I.Varanasi: Chaukhamba Sanskrit Sansthan;1997. p.565.
13. Acharya YT, editor. Charaka Samhita of Agnivesha, Chikitsa Sthana; Vatashonita Chikitsa:chapter29, Verse19e23. Varanasi: Chaukhamba Surbharati Prakashan;2011.p.628.reprint2011.
14. Acharya YT, editor. Charaka Samhita of Agnivesha, Chikitsa Sthana; Vaytavyadhi Chikitsa: chapter 28, Verse 37. Varanasi: Chaukhamba Surbharati Prakashan; 2011. p.618.reprint2011.
15. Kasture Haridas Shridhara, editor. Ayurvediya Panchakarma Vijnana.1sted. Ilahabad: Sri Vaidyanath Ayurveda Bhavana;2013.p.156.
16. Sidhhinanada Mishara, editor. Bhaishajya Ratnavali of Kaviraj Govinda Das Sen.Varanasi: Chaukambha SurabharathiPrakashana;2009.p.601.
17. Upadhyay Y, Madhava nidana, Madhukosha Vyakhya, Part 1, Amavatanidanam, 4-5;PublishedbyChaukhambaPublication,Varanasi,Reprint;Ed2017.p.509.
18. Patil Vasant C. Principles and practice of Panchakarma, Ch. 13, Basti karma(therapeuticEnemaTherapy), Actionofbasti Dravya, Published by Chaukhambha Sanskrit Sansthan New Delhi,ReprintEd1st;2018.p.497.

Table 1- Assessment criteria

Subjective criteria	Objective criteria
▪ *Sandhishool* 0-4 ▪ *Sandhishoth* 0-4 ▪ *Pratah-stabdhta* 0-4 ▪ *Aruchi* 0-4 ▪ *Angidourbalya* 0-4 ▪ *Alasya* 0-4 ▪ *Angamarda* 0-4 ▪ *Gaurav* 0-4 ▪ *Jwara* 0-4	▪ Hematological – Hb%, RA factor, ESR

Table -2 Grading of assessment criteria

Parameter	Grading Description	Grading
Sandhishool	No pain	0
	Mild pain	1
	Moderate pain but no difficulty in moving	2
	Slight difficulty in moving	3
	Much difficulty in moving the bodily joints	4
Sandhishoth	No swelling	0
	Feeling of swelling	1
	A feeling of swelling + heaviness	2
	Apparent swelling	3
	Huge (synovial effusion) swelling	4
Angamarda	No body ache	0
	Occasional body ache	1
	Continuous body ache	2
	Body ache hampers routine works	3
	Not able to do any work	4
Aruchi	No loss of taste	0
	Eating timely without much desire	1
	Desire for food little late than normal time	2
	Desire for food after long intervals	3

	No desire for food at all	4
Agnidourbalya	No Agnimandhya	0
	Occasional Agnimandhya 1 to 2 times/week	1
	Agnimandhya 3 to 4 times/week	2
	Angimandhya 4 to 6 times/week	3
	Continuous Agnimandhya	4
Pratahstabdhta	None	0
	5 minutes or Less	1
	5 minutes to 2 Hours	2
	2 Hours To 8 Hours	3
	8 Hours Or More	4
Alasya	Doing work satisfactory and with proper vigor on time	0
	Doing work satisfactorily with late initiation in time	1
	Doing work unsatisfactory with a lot of mental pressure and being late	2
	Not starting any work in your responsibility and doing little work slowly	3
	Not wanting to initiate work even after pressure	4
Jwara	Normal body temperature	0
	Fever occasionally	1
	Fever once in a day	2
	Fever constantly	3
	High fever	4
Gaurav	No feeling of heaviness	0
	Occasional feeling of heaviness	1
	Continuous feeling of heaviness, but the patient does usual work	2
	Continuous feeling of heaviness which hampers usual work	3
	Unable to do any work due to heaviness	4

Table – 3 Basti schedule

1st day	2nd day	3rd day	4th day	5th day	6th day	7th day	8th day
VB	VB	VB	VB	VB	VB	VB	VB

Table – 4 Basti karma procedure

Poorvakarma	Pradhankarma	Pashatkarma
VB - Selection of the Patient, Counselling of the Patient, *Basti* Preparation, Abhyanga with *MurcchitaTilaTaila* at *Kati*, *Kukshi*, *Ubhaypada* followed by *NadiSwedan*	VB - *Basti* administration at – After taking light food in the morning.	V.B. - Rest, Snana, Laghu Bhojana advised. *BastiPratyagamanakala* and the Number of *Vegas* will be noted. After the administration of *VaitaranaBasti*, Tapping over the buttock region was done.

Table 5 – contents of Vaitaran Basti

Contents	GROUP A	GROUP B
Gudapak	25 ml	25 ml
Saindhav	10 gm	10 gm
Murchhittilataila	50 ml	50 ml
Chinchakalka	50 gm	50 gm
Gomutra	200 ml	-

Gomutra Arka	-	60 ml *GomutraArka* + 140 ml diluted *koushnajala*
Total	325ml	325ml

Table – 6 Group A Subjective criteria result Friedman test

Sr. no.	Symptoms	N	Chi-square	P value	Remarks
1	*Sandhishool*	15	28.204	0.000	Significant
2	*Sandhisotha*	15	28.894	0.000	Significant
3	*Aruchi*	15	30.000	0.000	Significant
4	*Agnidourbalya*	15	30.000	0.000	Significant
5	*Pratahstabdhta*	15	30.000	0.000	Significant
6	*Angamarda*	15	27.882	0.000	Significant
7	*Alsya*	15	28.894	0.000	Significant
8	*Gaurava*	15	27.882	0.000	Significant
9	*Jwara*	15	25.400	0.000	Significant

Table - 7 Group B Subjective criteria result Friedman test

Sr. no.	Symptoms	N	Chi-square	P value	Remarks
1	*Sandhishool*	15	26.533	0.000	Significant
2	*Sandhisotha*	15	27.395	0.000	Significant
3	*Aruchi*	15	29.391	0.000	Significant
4	*Agnidourbalya*	15	28.000	0.000	Significant
5	*Pratahstabdhta*	15	30.000	0.000	Significant
6	*Angamarda*	15	29.391	0.000	Significant
7	*Alsya*	15	24.732	0.000	Significant
8	*Gaurava*	15	26.941	0.000	Significant
9	*Jwara*	15	19.000	0.000	Significant

Table – 8 Group A Subjective Wilcoxon signed rank test

Sr. no.	Symptoms	Followup	Z value	P value	Remarks
1	*Sandhishool*	AT-BT	-3.771[b]	0.000	Significant
		FUP-AT	-2.000[c]	0.046	Significant
		BT-FUP	-3.542[c]	0.000	Significant
2	*Sandhishotha*	AT-BT	-3.624[b]	0.000	Significant
		FUP-AT	-1.414[c]	0.157	Not significant
		BT-FUP	-3.626[c]	0.000	Significant
3	*Aruchi*	AT-BT	-3.520[b]	0.000	Significant
		FUP-AT	.000c	1.000	Not significant
		BT-FUP	-3.520[c]	0.000	Significant
4	*Angamarda*	AT-BT	-3.624[b]	0.000	Significant
		FUP-AT	-2.449[c]	0.014	Significant

		BT-FUP	-3.508[c]	0.000	Significant
5	*Pratahstbdhta*	AT-BT	-3.771[b]	0.000	Significant
		FUP-AT	.000[c]	1.000	Not significant
		BT-FUP	-3.771d	0.000	Significant
6	*Agnidourbalya*	AT-BT	-3.531[b]	0.000	Significant
		FUP-AT	.000c	1.000	Not significant
		BT-FUP	-3.531[c]	0.000	Significant
7	*Alsya*	AT-BT	-3.578[b]	0.000	Significant
		FUP-AT	-1.414c	0.157	Not significant
		BT-FUP	-3.690[c]	0.000	Significant
8	*Gaurava*	AT-BT	-3.508[b]	0.000	Significant
		FUP-AT	-2.449[c]	0.014	Significant
		BT-FUP	-3.690[c]	0.000	Significant
9	*Jwara*	AT-BT	-3.307[b]	0.001	Significant
		FUP-AT	-1.000[c]	0.317	Not significant
		BT-FUP	-3.354[c]	0.001	Significant

Table -9 Group B Subjective Wilcoxon signed rank test

Sr. no.	Symptoms	Followup	Z value	P value	Remarks
1	*Sandhishool*	AT-BT	-3.416[b]	0.001	Significant
		FUP-AT	-1.732[c]	0.083	Significant
		BT-FUP	-3.397	0.001	Significant
2	*Sandhishotha*	AT-BT	-3.448[b]	0.001	Significant
		FUP-AT	-1.000[c]	0.157	Not significant
		BT-FUP	-3.494[c]	0.000	Significant
3	*Aruchi*	AT-BT	-3.626[b]	0.000	Significant
		FUP-AT	-1.000[c]	1.000	Not significant
		BT-FUP	-3.690[c]	0.000	Significant
4	*Angamarda*	AT-BT	-3.508[b]	0.001	Significant
		FUP-AT	-1.000[c]	0.317	Significant
		BT-FUP	-3.508[c]	0.000	Significant

5	*Pratahstbdhta*	AT-BT	-3.771[b]	0.000	Significant
		FUP-AT	.000[c]	1.000	Not significant
		BT-FUP	-3.771d	0.000	Significant
6	*Agnidourbalya*	AT-BT	-3.407[b]	0.000	Significant
		FUP-AT	.000[c]	1.000	Not significant
		BT-FUP	-3.407[c]	0.000	Significant
7	*Alsya*	AT-BT	-3.314[b]	0.000	Significant
		FUP-AT	.000d	0.157	Not significant
		BT-FUP	-3.314[c]	0.000	Significant
8	*Gaurava*	AT-BT	-3.473[b]	0.000	Significant
		FUP-AT	-2.646[c]	0.014	Significant
		BT-FUP	-3.442[c]	0.000	Significant
9	*Jwara*	AT-BT	-2.913[b]	0.001	Significant
		FUP-AT	-1.414[c]	0.317	Not significant
		BT-FUP	-3.051[c]	0.001	Significant

Table – 10 Group A objective criteria result paired t-test

Sr.no.	Symptoms	BT mean± SD	AT mean± SD	df	t-value	p-value	result
1	RA factor	227.6933 ±532.99118	131.3547 ±267.23289	14	1.364	0.194	NS
2	ESR	28.0000±19.59592	20.2000±12.04278	14	3.392	0.004	S
3	Hb%	10.7400± 1.07025	10.7533± 0.95683	14	-0.147	0.886	NS

Table -11Group B objective criteria result paired t-test

Sr.no.	Symptoms	BT mean± SD	AT mean±SD	df	t-value	p- value	result
1	RA factor	131.4067 ±284.56119	110.7733 ±243.41416	14	1.808	0.092	NS
2	ESR	22.6000± 6.56615	17.7333± 1.58705	14	6.732	0.000	S
3	Hb%	10.3733± 1.74621	10.6933± 1.72687	14	-1.453	0.134	NS

Table – 12 Effect of therapy on Sandhishool

Group A	N	Mean rank	% Change	Group B	N	Mean rank	% Change
BT	15	3.00	47.60	BT	15	2.93	47.60
AT	15	1.37		AT	15	1.43	

FUP	15	1.63		FUP	15	1.63	

Table – 13 Effect of therapy on Sandhisotha

Group A	N	MEAN RANK	% CHANGE	Group B	N	MEAN RANK	% CHANGE
BT	15	3.00	45.66%	BT	15	2.93	44.36%
AT	15	1.43		AT	15	1.50	
FUP	15	1.57		FUP	15	1.57	

Table – 14 Effect of therapy on Aruchi

Group A	N	MEAN RANK	% CHANGE	Group B	N	MEAN RANK	% CHANGE
BT	15	3.00	50%	BT	15	3.00	49%
AT	15	1.50		AT	15	1.47	
FUP	15	1.50		FUP	15	1.53	

Table – 15 Effect of therapy on *Angamarda*

Group A	N	MEAN RANK	% CHANGE	Group B	N	MEAN RANK	% CHANGE
BT	15	3.00	43.33%	BT	15	3.00	49%
AT	15	1.30		AT	15	1.47	
FUP	15	1.70		FUP	15	1.53	

Table - 16 Effect of therapy on Agnidourbalya

GRP A	N	MEAN RANK	% CHANGE	GRP B	N	MEAN RANK	% CHANGE
BT	15	3.00	50%	BT	15	2.93	49%
AT	15	1.50		AT	15	1.53	
FUP	15	1.50		FUP	15	1.53	

Table – 17 Effect of therapy on Pratahstabdhta

Group A	N	MEAN RANK	% CHANGE	Group B	N	MEAN RANK	% CHANGE
BT	15	3.00	50%	BT	15	3.00	50%
AT	15	1.50		AT	15	1.50	
FUP	15	1.50		FUP	15	1.50	

Table – 18 Effect of therapy on Alsya

Group A	N	MEAN RANK	% CHANGE	Group B	N	MEAN RANK	% CHANGE
BT	15	3.00	47.66%	BT	15	2.87	43.33%
AT	15	1.43		AT	15	1.57	
FUP	15	1.57		FUP	15	1.57	

Table – 19 Effect of Therapy on Jwara

Group A	N	MEAN RANK	% CHANGE	Group B	N	MEAN RANK	% CHANGE
BT	15	2.87	44.25%	BT	15	2.67	35.20%
AT	15	1.53		AT	15	1.60	
FUP	15	1.60		FUP	15	1.73	

Table – 20 Effect of therapy on Gaurav

Group A	N	MEAN RANK	% CHANGE	Group B	N	MEAN RANK	% CHANGE
BT	15	3.00	43.33%	BT	15	2.97	40%
AT	15	1.30		AT	15	1.27	
FUP	15	1.70		FUP	15	1.77	

Indian Journal of Natural Sciences *www.tnsroindia.org.in ©IJONS*

Vol.15 / Issue 88 / Feb / 2025 *International Bimonthly (Print) – Open Access* *ISSN: 0976 – 0997*

RESEARCH ARTICLE

An Efficient Image Acquisition Technique for Hyperspectral Remote Sensing Images Classification using Aviris Sensor

R. Priya[1]*, R. Ramya[2] and M. Senthilmurugan[3]

[1]Assistant Professor, Department of Computer Science and Applications (MCA), Faculty of Science and Humanities, SRM Institute of Science and Technology, Chennai, Tamil Nadu, India.
[2]Senior Assistant Registrar, University Office, Sri Balaji Vidyapeeth (Deemed to be University), Puducherry, India.
[3]Professor, Department of Computer Science and Applications (MCA), A.V.C. College of Engineering, Mayiladuthurai, (Affiliated to Anna University, Chennai), Tamil Nadu, India.

Received: 21 Nov 2024 Revised: 03 Dec 2024 Accepted: 03 Feb 2025

***Address for Correspondence**
R. Priya
Assistant Professor,
Department of Computer Science and Applications (MCA),
Faculty of Science and Humanities,
SRM Institute of Science and Technology,
Chennai, Tamil Nadu, India.
E.Mail: priyar6@srmist.edu.in

ABSTRACT

Remote sensed data have different resolutions of space, radiometry, spectrum, and time. Knowing the strengths and weaknesses of various sensor data types is important for selecting correct remote sensed object classification data. Selecting acceptable remote sensed information involves consideration of factors such as end-user needs, research area size and characteristics, usable image data and their characteristics, cost and time constraints, and the analyst's experience using the selected images. The important factor affecting the collection of remote sensing data is atmospheric condition; another important factor influencing the selection of remote sensing data is atmospheric condition. Monetary costs are often an important factor that affects remotely sensed data selection. Airborne imagery taken by aero-transported platforms can overcome some of the difficulties of satellite images, mostly because they can be acquired in optimal climate and illumination conditions. Their spatial resolution can be adapted to different sensor configurations, flight plan and altitude, along with ground and atmospheric parameters. Airborne Visible Infrared Imaging Spectometer (AVIRIS) is one such sensor hence Hyperspectral Remote Sensing Image Acquisition is done here by using AVIRIS Sensor.

Keywords: AVIRIS (Airborne Visible Infrared Imaging Spectrometer), HIS (Hyperspectral Sensing and Imaging) , EMAC (European Multi-sensor Airborne Campaign), ETM (Enhanced Thematic Mapper).

INTRODUCTION

Remote sensing imaging has enormous potential impact in the fields of geography, land surveying and most disciplines of Earth science (e.g., hydrology, ecology, meteorology, oceanography, glaciology, geology); it also has military, intelligence, commercial, political, planning and humanitarian disciplines and has become widely accepted through specific applications such as Google Earth ArcGis, among others. Vehicles carrying instruments operating in different acquisition modes may acquire images. We can specifically mention various satellite missions and constellations, airborne platforms and fixed platform cameras. Each platform and acquisition mode has specific advantages and disadvantages. Due to the highly expensive acquisition sensors that are mounted on them, but are only freely available with low spatial and temporal resolution, satellite imagery has high-quality parameters and better spectral calibration and is therefore often inadequate for certain studies. Also, adverse weather and atmospheric conditions (fog, rain, smoke and other factors that may influence sensor measurements) often seriously impair them. High-resolution satellite images are extremely expensive for most uses, making them prohibitive. Airborne images taken by aero-transported vehicles can overcome some of the difficulties with satellite images, primarily because they can be captured under optimal conditions of lighting and climate. Their spatial resolution can be adjusted to various sensor settings, flight plan, and altitude along with ground and atmospheric parameters. Their main disadvantage is the high cost of operation and deployment. On board image processing is not readily available and it is only after each flight that the quality of each run is assessed. Mobile verification and correction of real-time image is once again highly prohibitive. Because of hardware limitations fixed camera imagery is typically of average or low quality and involves very complex processing to be useful for precise quantitative measurements [1].

Remote sensing image data is more than just a video-they are Electro Magnetic Energy measurements. The 'quality' of image data is determined primarily by the sensor-platform device characteristics. Such characteristics of the sensor system are usually referred to as Spectral resolution and radiometric resolution, relating respectively to the measured portion of the electro-magnetic spectrum and energy variations, Spatial resolution means the minimum size of items that can be chosen, referring to the smallest unit area measured and Review time, time between two successive acquisitions of images over the same location [2]. Several remote sensing satellites are presently on the market, providing imagery applicable for various forms of applications. Each of these satellite-sensor platform is characterized by the wavelength bands utilized in image acquisition, spatial resolution of the device, the coverage area and thus the temporal coverage, i.e. how frequent a given location on the earth surface could also be imaged by the imaging system. In terms of the spatial resolution, the satellite imaging systems could also be classified as Low resolution systems (approx. 1 km or more), Medium resolution systems (approx. 100 m to 1 km), High resolution systems (approx. 5 m to 100 m) and Very high resolution systems (approx. 5 m or less) In terms of the spectral regions used in data acquisition, the satellite imaging systems could also be classified as Optical imaging systems (include visible, about to infrared, and shortwave infrared systems), Optical/thermal imaging systems could also be classified in step with the number of spectral bands used, Synthetic aperture measuring device imaging systems could also be classified in step with the mixture of frequency bands and polarization modes used in data acquisition, Multiple polarization (Combination of two or further polarization modes), Monospectral or panchromatic (single wavelength band, "black-and-white", grey-scale image) systems and Multiple frequency (Combination of two or more frequency bands).

PRE-PROCESSING OF REMOTE SENSING DATA

Geometric and Atmospheric Correction

Images were corrected geometrically using ground control points collected during the winter field campaign and a geo-rectified spatial coverage of the forest compartments located in the catchment.

Data Reduction

Data reduction techniques are used to modify data sets with high spectral resolution, to minimize high data dimensionality and the difficulty of applying statistical classifiers to these data sets [3].

OVERVIEW OF HYPERSPECTRAL REMOTE SENSING AND IMAGING

Hyperspectral Sensing and Imaging (HIS) exploits the fact that all materials reflect, absorb and emit electromagnetic energy at specific wavelengths due to differences in their molecular composition in distinctive patterns. This feature is called the signature of the spectrum. The spectral signature can, in theory, be used to classify and distinguish any substance in a sufficiently large spectral band [4]. Hyperspectral data / images acquired through selected wavebands are made up of spectral information that can cover dozens or even hundreds of contiguous narrow bands for signature analysis purposes. Spatially and spectrally digitized information can be regarded as a three-dimensional data cube with two-dimensional spatial coordinates and a third spectral band dimension. Developing proper processing algorithms to analyze the data cube with high resolution has become the key to the success of many applications for hyperspectral sensing and imaging. Based on their functions, the processing algorithms can be divided into four types: target detection, change detection, classification and unmixing. Detection of targets means looking for a particular spectral signature belonging to some object or substance. The aim of detecting change is to find significant differences between two hyperspectral scenes in the same geographic area. The classification objective is to label each pixel in a hyperspectral image into clusters of pre-specified category (class) types. Unmixing involves determining the fraction of the pixel area covered by each material in the scene or decomposing a mixed pixel into a series of spectra usually used in remote sensing. There are several system variables that have a great impact on the resulting image: the light source intensity, the motor speed or the working distance (the distance from the camera to the sample), to name a few, have to be considered when configuring the acquisition parameters in order to obtain high-quality data [19].While the multitude of spectral bands in hyperspectral data offers valuable insights, it also introduces the challenge of higher dimensionality, which can potentially hinder classifier performance [20].

The typical procedures in HIS analysis includes

- Image display, that shows a view of the data set in the image space so that the analyst can easily illustrate and mark data classes
- Class definition, this process was designed to identify information in the appropriate groups
- Feature extraction that uses algorithms to determine a function subspace that is optimal for distinguishing between given groups. Typically a initial collection of data training is needed
- Reformatting, in this step, a new data set with reduced dimensionality is generated based on the subspace of the feature
- Initial classification, classifiers are used to divide the data cube into classes defined
- Finalize training; it involves reviewing the outcomes of the initial assessment and identifying potential changes. If required, new features will be added to the training set and
- Final classification, this step involves reclassifying data on the basis of the new training set [5].

HYPERSPECTRAL REMOTE SENSING SENSORS

Hyperspectral remote sensors have the ability to acquire images in many specific spectral bands in the electromagnetic spectrum from visible, near infrared, medium infrared to thermal infrared. Hyperspectral sensors capture energy in 200 or more bands, thus constantly covering the reflective spectrum for each pixel in the scene. Bands characteristic of these types of sensors are continuous and narrow, allowing an in-depth study of the characteristics and features of Earth that would be missed with multispectral sensors. Hyperspectral records are based on spectroscopy in the range 0.40 to 2.5 μm where hyperspectral sensors work and where absorption has three fundamental characteristics : the absorption of the transferred cargo, which occurs mostly in the visible part of the electromagnetic spectrum, causes the electrons to be transferred between atoms. For example, between atoms Fe2+ and Fe3+, an atom is moved from atom Fe2+ to Fe3+ due to the action of light causing the appearance of oxidized artifacts in red. Although this phenomenon can be identified with multispectral sensors such as Landsat, hyperspectral sensors can better expose it; in the case of atoms with an incomplete electronic wrapper, transmitted electron absorption occurs when light with certain wavelength can bombard electrons from different positions in the coating. This absorption appears to extend beyond the transferred cargo at more narrow intervals and the wavelength where the absorptions are rendered is influenced by

the location and heterogeneity in the vicinity of atoms, not by the form of atom. This feature is used, especially in geology where atomic mineral arrangement is well defined; vibration absorption occurs when light with or part of a molecule having the same wavelength strikes the molecule and causes a vibration that leads to light absorption [6,7]. Generally speaking, this energy absorption is very small, while depths are sufficiently varied. Multi-spectral detectors can sense a lot of this absorption. Hyper-spectroscopy applies to the image spectroscopy as images can be obtained for each narrowband. Hyperspcetral remote sensing is the term used for devices that take images with high spectral resolution. Hyperspectral remote sensing is a relatively new technology used in rocks, plants, artificial materials and soil background detection and identification [8]. The remote hyperspectral emerged in the mid-80s and has since been widely used for mapping minerals by geologists, detection of the type of material depends on the range and spectral resolution, the spectrometers signal to noise ratio of the sample density and the frequency of the product absorption in the wavelength of the measurements [9]. There are two types of systems taking images in the hyperspectral field: on aircraft and on satellites [10]. The majority of hyperspectral sensors are installed on air platforms and less on the satellite which is tabulated in Table 1.

AVIRIS SENSORS

For the first time in 1986, AVIRIS was flown (first airborne images), first scientific data in 1987, fully operational since 1989. As part of the European Multi-Sensor Airborne Campaign (EMAC), the instrument was flown over numerous European test sites in June / July 1991. Across 224 contiguous spectral bands, AVIRIS uses scanning optics and a team of four spectrometers to simultaneously view a swath size of 677 pixels. A spatial image is constructed through the motion of the scanner, which defines a line of image 677 pixels wide perpendicular to the direction of the aircraft and through the motion of the aircraft, which defines the length of the image frame. Sensor : Whiskbroom optimechanical scanner (12 Hz) which uses line detector arrays to image a 677-pixel-wide swath in 224 contiguous bands (four grating spectrometers). Spectral range : 360 – 2500 nm with 224 bands in total. AVIRIS is now a robust radiometric and spectral measurement operating instrument. AVIRIS typically takes pictures at an altitude of 20km with a pixel scale from a NASAER-2 aircraft. On the surface, the swath width is about 12 km. At spatial resolutions of 1-4 m with decreased swath widths, AVIRIS can also obtain images from a low-altitude aircraft.

Sensor Specifications

The sensor has 224 adjacent spectral bands that range from 400 to 2.5 μm each 1μm long. AVIRIS is a whiskbroom scanning device that collects data in a 12 bit (0 to 4095) quantization. The sensor flies on a few aircraft at a high altitude of 20 km including the NASA / ARC ER-2 and the turboprop of the Twin Otter International at a lower altitude of 4 km. Spatial image resolution can vary depending on the aircraft's altitude. High-altitude flights are 20 m x 20m in resolution, while low-altitude flights are 4 m x 4m in higher resolution.

Image footprint or swath width

11 km long, swath at high altitude (20km), 1.9km wide swath at low altitude (4km). The functional block diagram of AVIRIS sensors is shown in Figure 1. AVIRIS consists of six optical subsystems and five electrical subsystems as shown in Figure 2, of modular construction. Optical subsystems (a whiskbroom scanner, four spectrometers and a source of calibration) are combined via optical fibers. Whisk broom scanners, sometimes also called spotlight scanners or cross-track scanners, use a mirror to reflect light on a single detector. The mirror moves back and forth to take measurements in the image from one pixel at a time. The moving parts make it expensive and more likely to wear out this sort of sensor. A spectrometer is an analytical tool used to isolate and quantify physical physical phenomenon spectral components. Spectrometer is a broad term that is often used to describe instruments that measure a continuous variable of a phenomenon that somehow blends the spectral components. A spectrometer can isolate white light in visible light and measure individual narrow color bands, called a spectrum. Data : the recorded data set form an object cube containing two axes of spatial dimensions and a spectral dimension is defined by the third. The AVIRIS data recorder was upgraded in 2005 (storage capacity of 73 GByte) [11].

Sensor Characteristics

The characteristics of AVIRIS sensor is listed in Table 2 and data characteristics in Table 3. The AVIRIS sensor receives white light in the foreoptics, disperses the light into the spectrum, converts the photons into electrons, amplifies the signal, digitizes the signal and records the data density tape. Nominal AVIRIS data Characteristics are tabulated in Table 3. Scanning mirror, foreoptics, spectrometers, detectors, onboard calibrators and electronic signal chain are the core subsystems of the sensor [12].

Comparison of AVIRIS with other Sensors

In [13] AVIRIS is compared with Hyperion and the following characteristics in Table 4 are determined which shows that AVIRIS is best. AVIRIS was more accurate to define land use at the Urban Fringe than on of Synthetic Landsat ETM+. The factors that may affect the accuracy of classification are the Ground Sampling Distance (GSD), the number of spectral bands and a sensor's signal-to-noise ratio [14]. The comparison is tabulate in Table 5. Due to the increasing number of companies and agencies operating hyperspectral scanners, airborne and spaceborne hyperspectral imaging is becoming increasingly available. Airborne data acquisitions benefit significantly from satellite-based missions as the user controls the task in terms of time schedules, flight line arrangements, calibration measurements, spectral / spatial resolutions and appropriate weather conditions [15].

Image Acquisition through AVIRIS Sensors

AVIRIS is a complex and sophisticated optical sensor system that includes a number of major subsystems, modules and functions [16]. A supervised AVRIS classification is more reliable than one of the artificial Landsat ETM (Enhanced Thematic Mapper) for Urban Fringe land use classification. With a combination of soil and plants, AVIRIS reduce false positives for land use [14]. AVIRIS's narrow bands would track the effect of spectral reflection in a narrow spectral area and have higher radiometric quality [17]. AVIRIS is an airborne detector that collects images with 224 spectral bands from visible, close to infrared to short wave infrared. Spatial resolution ranges from meters to dozens of meters and the swath ranges from several kilometers to dozens of kilometers, depending on the satellite platforms and the data collected latitude [18]. To test the reflective portion of the electromagnetic spectrum, the hyperspectral sensors are produced. The entire inspection spectrum spreads through the near infrared from the visible region and is divided into hundreds of overlapping small bands. The spectrum interval in wavelength can be as narrow as nanometers, resulting in obtaining more than 100 spectral channels at the same time. Because image data is considered to be two-dimensional, the hyperspectral data can be interpreted as a three-dimensional data cube by adding a new dimension of "spectrum" information as shown in Figure 3. Hyperspectral data / images collected by selected wavebands are made up of spectral information that can span dozens or even hundreds of contiguous narrow bands for signature analysis purposes. Spatially and spectrally digitized information can be viewed as a three-dimensional data cube with two-dimensional spatial coordinates and a third spectral band dimension. The development of appropriate processing algorithms to analyze the high-resolution data cube has become the key to the success of many applications for hyperspectral sensing and imaging [5]. Table 6 summarizes AVIRIS sensor features that include AVIRIS sensor using more spectral channels, wavelength range, scanning rate, etc. Image acquisition is therefore carried out using AVIRIS sensors and the steps to acquire image are

Step 1: Record the visible and near-infrared spectrum.
Step 2: Frame a data cube with two or more spatial and one or more spectral dimension.
Step 3: Consider each pixel to identify spectral and spatial signature.
Step 4: Use spectral and spatial images for identification purposes.

CONCLUSION

Hyperspectral sensors capture images using two systems, aircraft and satellites out of which aircraft system capture images by considering time schedules, flight line arrangements, calibration measurements, spectral / spatial resolutions and acceptable weather conditions. AVIRIS is an airborne sensor collecting images with 224 spectral bands with spectral range of 0.40 – 2.50 μm, uses whiskbroom scanner, having data rate 2..4 Mbits/s, spectrum rate

7300 spectra/s and data capacity greater than 10 GB. AVIRIS is compared with Hyperion sensor and it shows that AVIRIS is better because of having large swath width and less Signal-to-Noise ratio. AVIRIS is compared with Synthetic Landsat ETM+ and it is proved that AVIRIS is more accurate because of having large spectral bands. Hence the image captured by AVIRIS sensors is considered for this research work.

REFERENCES

1. Jose F.Manera, Lucas Rodriguez, Claudio Delrieux and Ricardo Coppo, "Aerial Image Acquisition and Processing for Remote Sensing", Journal of Computer Science and Technology, Vol. 10 No. 2 June 2010.
2. Lucas L.F. Janssen and Gerrit C. Huurneman,"Principles of Remote Sensing", ITC Educational Text Book Series.
3. M.Govender, K. Chetty, V. Naiken and B. Bulcoce, "A Comparison of Satellite Hyperspectral and Multispectral Remote Sensing Imagery for Improved Classification and Mapping of Vegetation".
4. Shaw, G., and D. Manolakis, "Signal Processing for Hyperspectral Image Exploitation",IEEE Signal Processing Magazine 19(1):12-16, 2002.
5. Xuemei Cheng,"Hyperspectral Imaging and Pattern Recognition Technologies for Real Time Fruit Safety and Quality Inspection", 2004.
6. Smith, R.B., "Introduction to Hyperspectral Imaging", www.microimages.com.
7. Smith, R.B., "Introduction to Remote Sensing of the Environment", www.microimages.com.
8. Richards, J.A., Jia, X., "Remote Sensing Digital Image Analysis : An Introduction", Third Edition. Berlin. Springer-Verlag, 1999.
9. Kruse, F., "Mineral Mapping with AVIRIS and EO-1 Hyperion", Proceedings of the 12th JPL Airborne Geoscience Workshop, Pasadena, California,p. 230-234. 2003.
10. Iosifvorovencii, "The Hyperspectral Sensors used in Satellite and Aerial Remote Sensing", Bulletin of the Transilvania University of Brasov, Vol. 2 (51) – 2009, Series II .
11. http://aviris.jpl.nasa.gov/
12. Robert O. Green, Michael E. Eastwood et.al.,"Imaging Spectroscopy and the Airborne Visible Infrared Imaging Spectrometer (AVIRIS)", Remote Sensing Environment.
13. Fred A. Kruse,"Comparison of AVIRIS and Hyperion for Hyperspectral Mineral Mapping", 11th JPL Airborne Geoscience workshop, 4-8, Pasadena California, March 2002.
14. Rutherford V.Platt and Alexander F.H.Goetz,"A Comparison of AVIRIS and LandSat for Land Use Classification at the Urban Fringe", Photogrammetric Engineering and Remote Sensing, 813-819, 2004.
15. HalukCetin,"Comparison of Spaceborne and Airborne Hyperspectral Imaging Systems for Environmental Mapping".
16. Green et.al., "Imaging Spectroscopy and the Airborne Visible/Infrared Imaging Spectrometer (AVIRIS)", Remote Sensing Environment, Elsevier Science Inc., pp. 227-248, 1998.
17. Kyu Sung Lee et.al., "Hyperspectral versus Multispectral Data for Estimating Leaf Area Index in Four Different Biomes", Remote Sensing of Environment, Elsevier, pp. 508-520, 2004.
18. YichunXie, ZongyaoSha and Mei Yu, "Remote Sensing Imagery in Vegetation Mapping: A Review", Journal of Plant Ecology Volume 1, Issue 1, 2008.
19. Alejandro Morales, Pablo Horstrand et al, "Laboratory Hyperspectral Image Acquisition System Setup and Validation", MDPI Sensors, March 2022.
20. Alaa Ali Hameed, "Enhancing Hyperspectral Remote Sensing Image Classification Using Robust Learning Technique", Journal of King Saud University – Science, October 2023.

Table 1 Main Hyperspectral Sensors on Aircraft and Satellites

Hyperspetral Sensors on Satellites			
Types of sensors	Producer	Number of bands	Spectral range (μm)
FTHSI on MightySat II	Air Force Research	256	0.35 – 1.05
Hyperion on EO-I	NASA Guddard Space Flight Center	242	0.40 - 2.50
Hyperspectral sensors on aircrafs			
AVIRIS (Airborne Visible Infrared Imaging Spectrometer)	NASA Jet Propulsion Lab.	224	0.40 – 2.50
HYDICE (Hyperspectral Digital Imagery Collection Experiment)	Naval Research Lab.	210	0.40 – 2.50
PROBE – 1	Earth Search Sciences	128	0.40 – 2.50
CASI (Compact Airborne Spectrographic Imager)	ITRES Research Limited	Over 228	0.40 – 1.00
HyMap	Integrated Spectronics	100 1a 200	Visible to termal infrared
EPS – H (Environments Protection System)	GER Corporation	VIS / NIR (76), SWIR1 (32), SWIR 2 (32), TIR (12)	VIS / NIR (0.43-1.05) SWIR 1 (1.50 – 1.80) SWIR 2 (2.00 – 2.50) TIR (8 – 12.50)
DAIS 7915 (Digital Airborne Imaging Spectrometer)	GER Corporation (Geophysical and Environmental Research Imaging Spectrometer)	VIS / NIR (32), SWIR1 (8), SWIR 2 (32), MIR (1), TIR (12)	VIS / NIR (0.43 -1.05) SWIR 1 (1.50 – 1.80) SWIR 2 (2.00 – 2.50) MIR (3.00 – 5.00) TIR (8.70 – 12.30)
DAIS 21115 (Digital Airborne Imaging Spectrometer)	GER Corporation	VIS / NIR (76), SWIR1 (64),	VIS / NIR (0.40 -1.00) SWIR 1 (1.00 – 1.80)

		SWIR 2 (64), MIR (1), TIR (12)	SWIR 2 (2.00 – 2.50) TIR (8.00 – 12.00)
AISA (Airborne Imaging Spectrometer)	Spectral Imaging	Over 288	0.43 – 1.00

Table 2 Characteristics of AVIRIS Sensor

Imager Type	Whiskbroom scanner
Scan rate	12 Hz
Dispersion	Four Grating Spectrometers (A,B,C,D)
Detectors	224 Detectors (32,64,64,64) Si and Insb
Digitization	12 bits
Data rate	20.4 Mbits/s
Spectrum rate	7300 Spectra/s
Data Capacity	>10GB (>8000 Km^2)

Table 3 Nominal AVIRIS Data Characteristics

Spectral	
Wavelength range	400 – 2500 nm
Sampling	10 nm
Spectral response (fwhm)	10 nm
Calibration accuracy	< 1 nm
Radiometric	
Radiometric range	0 to maximum lambertian radiance
Sampling	~1 DN noise RMS
Absolute calibration	≥ 96%
Inter flight stability	≥ 98%
Signal-to-noise	Exceeding 100 :1 requirement
Polarization sensitivity	≤ 1%
Spatial (at 20 km altitude)	
Field of view	30 degrees (11 km)
Instantaneous FOV	1.0 mrad (20 m)
Calibration accuracy	≤ 0.1 mrad
Flight line length	800 km total

Table 4 Comparison of AVIRIS with Hyperion Sensor

HIS Sensor	**Spectral Resolution**	**Spatial Resolution**	**Swath Width**	**ShortWave InfraRed Signal to Noise Ratio**	**Imager Type**

AVIRIS – High Altitude	10nm	20m	12km	500:1	Whiskbroom
Hyperion	10nm	30m	7.5km	50:1	Pushbroom

Table 5 Comparison of AVIRIS with LandSat TM/ETM+

	AVIRIS	**LandSat TM/ETM+**
Platform	Airborne	Spaceborne
Ground Sampling Distance	20m	30m
Number of Bands (excluding thermal)	224	6
Signal-to-Noise Ratio	High	Moderate
Launch	1987	1982

Table 6 Features of AVIRIS Sensors

Features	**AVIRIS**
Technology	Whisk broom linear array
Sampling Interval	10 nm
Field of View	30 degrees
Instantaneous Field of View	1.0 mrad
Scan Rate	12 Hz.
Spectral Channels	224
Wavelength Range	400 – 2500 nm

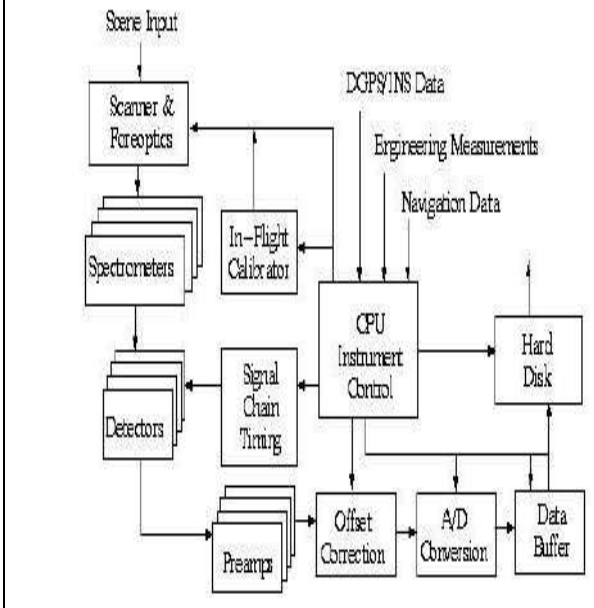

Figure 1 : AVIRIS functional block diagram

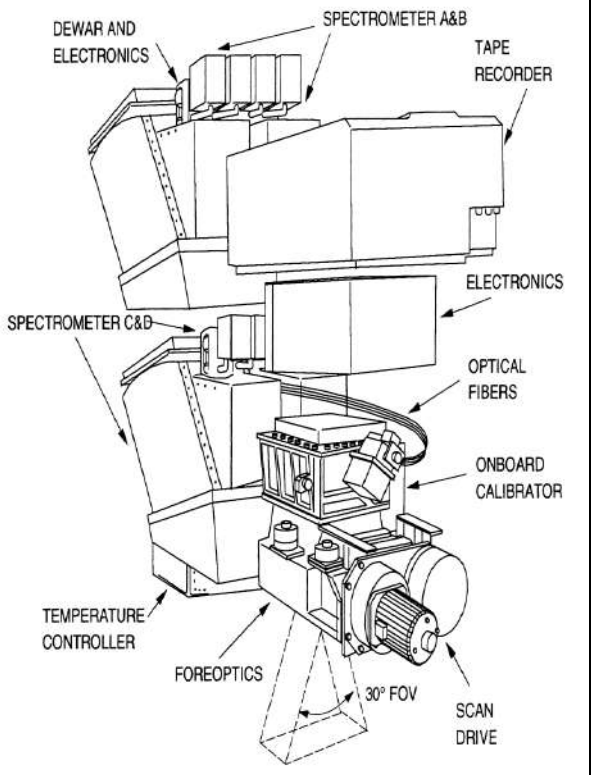

Figure 2 : Schematic view of the AVIRIS instrument

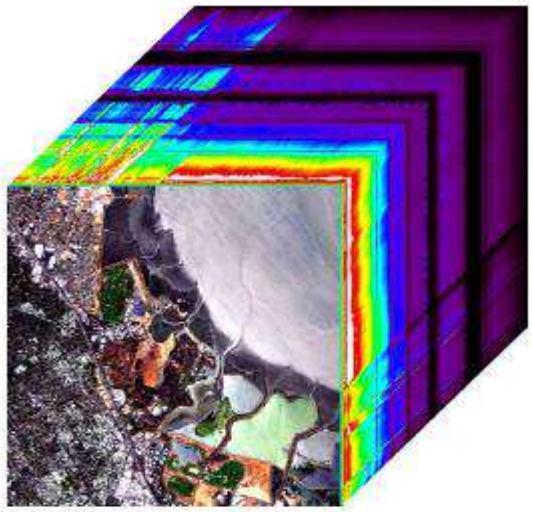

Figure 3 Representation of a sample data cube for a hyperspectral image with 224 bands, covering the range of 365 nm – 2500 nm

RESEARCH ARTICLE

In-Silico Approaches to Analyze the Potential of the Leaves of *Ficus elastica* against Type 2 Diabetes Mellitus

Sharon Reici.P[1]*, Susithra.T[1], Priyanga .A[1], Bakkiyavathipriya.T[1], Sivassoupramanien .D[2] and Kavimani.S[3]

[1]M. Pharm Student, Department of Pharmacology, Mother Theresa Post Graduate and Research institute of Heal Sciences, (Affiliated to Pondicherry University), Puducherry, India.
[2]Assitant Professor, Department of Pharmacology, Mother Theresa Post Graduate and Research institute of Heal Sciences, (Affiliated to Pondicherry University), Puducherry, India.
[3]Professor and Head, Department of Pharmacology, Mother Theresa Post Graduate and Research institute of Heal Sciences, (Affiliated to Pondicherry University), Puducherry, India.

Received: 21 Nov 2024 Revised: 03 Dec 2024 Accepted: 03 Feb 2025

***Address for Correspondence**
Sharon Reici.P
M. Pharm Student,
Department of Pharmacology,
Mother Theresa Post Graduate and Research institute of Heal Sciences,
(Affiliated to Pondicherry University),
Puducherry, India.
E.Mail: romapashreici317@gmail.com

ABSTRACT

Type 2 diabetes mellitus is a disorder marked by resistance to insulin and disrupted glucose regulation. The pursuit of innovative therapeutic methodologies has sparked a heightened curiosity regarding the possible anti-diabetic characteristics of medicinal plants. *Ficuselastica*, a plant traditionally used in herbal medicine, has shown promise in this regard. The study focuses to investigate the therapeutical potential of *Ficuselastica* on T2DM through network pharmacology and molecular docking techniques. The network pharmacology was utilized to ascertain the active constituents in *Ficuselastica* and their potential targets in the treatment of T2DM. A compounds–targets network was built up, leading to the identification of key compounds and genes of interest. Molecular docking experiments were then conducted to confirm the interactions between these compounds and the target genes. The network pharmacology analysis identified several bioactive compounds within *Ficuselastica* that are potentially relevant to T2DM treatment. Among these, eleven compounds and ten key genes (IL6, AKT1, PPARγ, SRC, BCL2, MAPK3, TNF, EGFR, ALB and TP53) were chosen for docking studies. The docking results confirmed that the active ingredients exhibit stable binding to the active sites of these target genes, suggesting their potential role in modulating pathways associated with T2DM. This study concludes that *F. elastica* which is a source of promising phytochemicals has a potential anti-diabetic property.

Keywords: Non-insulin dependent diabetes mellitus, *Ficuselastica*, molecular docking, network pharmacology, active ingredients.

INTRODUCTION

Diabetes Mellitus

Diabetes mellitus (DM) is a chronic illness brought on by inefficient use of the insulin that is produced by the pancreas, or by a hereditary or acquired impairment in insulin synthesis. This causes blood glucose levels to rise, which can harms the biological systemsnotably the neurons and blood vessels [1]. Diabetes-specific complications include amputations of the lower limbs, neuropathy, renal failure, cardiovascular disease, and blindness. Regardless of whether a person has insulin-dependent (IDDM) or non-insulin-dependent (NIDDM) diabetes, these complications can arise and result in serious health problems [2]. Presently, 10.5% of individuals in the world between the ages of 20 and 79or 537 million worldwide are affected with diabetes. This figure is predicted to hike to 643 million by 2030 and to 783 million by 2045.The International Diabetes Federation (IDF) report's tenth edition emphasizes that South-East Asia's (SEA) diabetes incidence has been rising for at least 20 years, exceeding initial projections [3]. Age, race, family history, smoking, obesity, and decreased physical activity are causative agents for diabetes [4]. The most prevalent kind of diabetes is type 2 diabetes mellitus (T2DM), also referred to as non-insulin-dependent diabetes and results from the body's inefficient use of insulin, leading to hyperglycemia [5].Therapeutically, metformin and thiazolidinediones are effective against insulin resistance but have limiting side effects. Recent research has extensively documented the connection between antioxidant compounds and Type 2 diabetes mellitus (DM) [6].

Ficuselastica

Ficuselastica also goes by the name of Indian rubber bush belongs to the Moraceae family which is most seen in northeast India. It is one of the most known ornamental plant in world. Various species of Ficus, namely *F. carica, F. septica* and *F. racemose*, have been extensively utilized in heritage system of medicines. Consequently, these plants have garnered significant global interest due to their considerable therapeutic potential[7]. Various studies has reported its use in neuro-degenerative disorders, inflammation.It is also reported for anti-microbial, anti-proliferative, anti-coagulant and anti-oxidant properties[22]**.** Steroids, flavonoids, phenolics, anthraquinones, glucosides, disaccharides, saponins, sphingolipids and triterpenes are the secondary chemicals isolated form *F. elastic* [7]. Hitherto, no study has reported the presence of diabetic activity in this plant.

Network pharmacology

By using the *insilico* technology to construct a "protein-compound/disease-gene" network, network pharmacology (NP) aims to understand the processes underlying the synergistic effects of conventional treatments. A "one-target, one-drug" strategy has been replaced with a "network-target, multiple-component therapeutics" concept as a result of this invention. The present investigation utilized the complete network pharmacology (NP) technique to examine the active constituents of *F. elatica*. This work expedites the hunt for new drugs and sheds light on the molecular processes underlying *F. elastica'*s anti-diabetic properties. Methods such as network pharmacology and molecular docking were utilized within this framework to examine the bioactive components of *F. elastica* and their potential mechanisms for fighting Type 2 Diabetes Mellitus (T2DM) [8].

MATERIAL AND METHODS

Gathering and filtering of active ingredients

Literature provided knowledge on the phytoconstituents found in *F. elastica*leaves[7]. A review of the literature was done using Google Scholar and Pubmed. Swiss Target Prediction was used to determine the possible targets built on SMILES of the active chemicals. DisGeNET was used to get the disease genes, and targets that were obtained had scores more than or equal to 0.1 filtered out. The final gene list was filtered to remove all duplication genes. Afterwards, a Venn diagram was made to show which genes intersected for additional investigation after comparing the active ingredients of *F. elastica* with the disease targets associated to non-insulin dependent diabetes mellitus [8].

Building up of network

To investigate the influence of *Ficuselastica* in Type 2 Diabetes Mellitus (T2DM), a network analysis was conducted using Cytoscape 3.8.0 which was employed to build and visualize the network. Target genes and active chemicals are shown as nodes in this network, and the connection between them are indicated by edges. The degree, a topological characteristic showing the importance of chemicals, pathways or target genes in the network, was measured utilizing the Network Analyzer program. The top ten genes with the highest level of interaction were determined [8].

Protein-Protein Network Construction

The STRING database was used to identify the proteins linked to the coinciding genes, and protein-protein interaction (PPI) network was created. CytoHubba from Cytoscape was then used to analyze the core genes of the PPI network. Later, the gene targets were corroborated using Molecular Docking approach [8,9].

Docking analysis

To investigate possible interactions and binding between ligands and T2DM-related proteins, docking analysis were employed. Of the ligands found in the literature, 11 were chosen. The RCSB PDB provided the proteins' structures for the associated genes in pdb formatand later, the heteroatoms were eliminated. The PDB ID's arelisted in **Table 1**. The 3D structures of the active compounds of *Ficuselastica* was obtained from Openbabel 2.3.1. AutoDock tool 1.5.6 was used to carry out the molecular docking. Kollaman charges were added to the macromolecule and saved in the format desired. Later, the ligands were fixed for their torsional differences and saved in pdbqt format. Grid maps of 60*60*60 Å grid points were set. Docking experiments were carried out utilizing the Lamarckian genetic algorithm. Each docking consisted of 10 separate docking runs. Gpf and dpf files were obtained as output which were further run using Autodock software to obtain the final dlg file. The compounds possessing the finest binding energies had their docking scores examined and tallied [10,11].

ADMET profiling

Computational predictions of pharmcokinetic parameters namely absorption, distribution, metabolism and excretion, pharmacokinetic parameters were derived using the online tool SwissADME. The parameters such as hydrogen bond donors and acceptors, topological polar surface area, rotatable bonds and molecular weight were estimated [8]. Alongside, toxicity analysis such as AMES, carcinogenicity, genotoxicity, human hepatotoxicity and ototoxicity was performed using ADMETlab 3.0 [12]

RESULTS

Screening of active ingredients and disease targets:

The findings from PubChem and Google Scholar were collected and from them a total of 19phytoconstituents were found to be present in the leaves of *Ficuselastica*. The structural formulas and active targets of the 19 compounds were predicted using Swiss Target Prediction database. Eventually, 422 targets were obtained. Following the identification of the drugs' likely targets, 846 genes linked to non-insulin dependent diabetes mellitus were gathered from the DisGeNET database. Afterwards, a Venn diagram was utilized to figure out which targets shared crossovers between type 2 Diabetes Mellitus and the genes connected to the plant **(Figure 1)**. *Ficuselastica* produced 111 putative anti-diabetes genes, of which 111 were chosen and recognized as the main targets.

Building up of Protein-Protein interaction network

In order to build the PPI network and screen the core genes, the 111 intersecting genes have been copied into the STRING database. With an average node degree of 24.4, the PPI network consists of 111 nodes and 1354 edges **(Figure 2)**. Later, the string file was exported to cytoscape 3.80 software to determine the top 10 active targets**(Figure 3)**. These includes IL6, AKT1, PPARγ, SRC, BCL2, MAPK3, TNF, EGFR, ALB and TP53.These 10 genes may be the core targets for *F. elastica* to exert its anti-diabetic effect.

Molecular Docking

From the comprehensive assessment of the Protein-Protein Interaction analysis, the selected ten disease genes were subjected to docking analysis. The Protein Data Bank provided the proteins' three-dimensional structures. Molecular docking was conducted based on core targets and active ingredients using Autodock software and the analysis effectively predicted a greater interaction affinity among these active ingredients and the target sites of the disease proteins. The binding energies were used as the primary criteria for screening the compounds[8] and were summarized in **Table2**.The highest binding energies were found between IL6-emodin (-10.84), AKT1-rutin (-13.38), PPARγ-roseoside (-12.55), SRC-rutin (-11.41), BCL2-rutin (-8.05), MAPK3-rutin (12.43), TNF-olaenolic acid (-8.78), TP53-olaenolic acid and ursolic acid (-9.75), EGFR-quercitrin (-12.31) and ALB-chlorogenic acid (-11.68). Least binding energy indicates better interaction. All docking energies were ≤-6 kcal/mol indicating stable binding between the components. This proves the validity of this study in understanding the role of phytoconstituents of *F.elastica* against Non-insulin Dependent Diabetes Mellitus. The highest binding interactions of the candidates with the core proteins are illustrated in **(Figure 4)**.

ADMET profiling

ADME analysis were performed using Swiss ADME to determine the pharmacokinetic features of the active ingredients of *F. elastica*. Bioavailability scores were predicted. Based on bioavailability scores, 7 compounds have a larger bioactivity score of > 0.25. A stronger bioactivity score indicates that these may possess inhibition against various disease receptors. The results of ADME profiling and bioavailability were summarized in **Table 3**. Additionally, ADMETlab 3.0 was used in the toxicity prediction of active ingredients and were summarized in **Table 4**.Drug-likeness predictions parameters using Swiss Adme server are summarized in **table 5**.

DISCUSSION

The present study explores the relationship between *Ficuselastica*, a widely used medicinal plant, and insulin resistance syndrome which is a persistent condition that causes blood glucose levels to rise. Its features include insulin resistance and a steady decline in insulin production. Because *Ficuselastica* has historically been used for its alleged medical benefits in many different countries, it may have a part in the treatment of diabetes. Plants in the genus Ficus may have hypoglycemic, antioxidant, and anti-inflammatory properties that could improve glucose management in diabetes patients [22]. Nevertheless, little is known about the precise processes via which *Ficuselastica* may affect blood sugar levels. Based on the findings of our study we identified eleven active phytoconstituents and ten genes for the docking experiment. In the core targets, PPARγ reduces triglyceride levels linked to the regulation of energy balance[13] Insulin resistance is brought on by interleukin-6, which inhibits the insulin receptor [14], AKT1 enhances glucose uptake in muscle, adipose tissue, liver, and other tissues [15], The enhancement of insulin resistance by TNF results in type 2 diabetes [16], MAPK3 regulates biological processes in response to insulin signaling [17], Bcl-2 influences glucose metabolism and β-cell function [18], ALB is up-regulated in T2DM` [19], The EGFR tyrosine kinase is an essential signaling center in both healthy and pathological circumstances, such as diabetes-induced cardiovascular dysfunction [20], Changes in gene expression mediated by TP53 as a result of hyperglycemia are central to the development of metabolic disturbances and vascular complications associated with diabetes [21].The docking results confirmed our initial findings, demonstrating that the active ingredients stably bind to the active sites of the target genes [8]. This suggests that these compounds may be effective in treating T2DM by inhibiting the IL6, AKT1, PPARγ, SRC, BCL2, MAPK3, TNF, EGFR, ALB and TP53 genes. In accordance to this study, utilizing *Ficuselastica* extracts in the therapy of Type 2 diabetes may have beneficial outcomes. This could be due to the bioactive compounds present in the plant that potentially enhance insulin sensitivity or inhibit carbohydrate absorption, although further research is needed to confirm these effects. Finally, the current study details the active ingredients, potential disease genes, andtheir affinity of interactions, supplying a theoretical framework for additional study and analysis.

ACKNOWLEDGEMENT
Nil

CONFLICT OF INTEREST
Nil

REFERENCES

1. Nagappa AN, Thakurdesai PA, Rao NV, Singh J. Antidiabetic activity of *Terminaliacatappa Linn* fruits. Journal of ethnopharmacology. 2003 Sep 1;88(1):45-50.doi:10.1016/S0378-8741(03)00208-3
2. Nathan DM. Long-term complications of diabetes mellitus. New England journal of medicine. 1993 Jun 10;328(23):1676-85.doi: 10.1056/NEJM199306103282306
3. Kumar A, Gangwar R, Ahmad Zargar A, Kumar R, Sharma A. Prevalence of diabetes in India: A review of IDF diabetes atlas 10th edition. Current diabetes reviews. 2024 Jan 1;20(1):105-14.doi:10.2174/1573399819666230413094200
4. Deshpande AD, Harris-Hayes M, Schootman M. Epidemiology of diabetes and diabetes-related complications. Physical therapy. 2008 Nov 1;88(11):1254-64.doi: 10.2522/ptj.20080020
5. Salehi B, Ata A, V Anil Kumar N, Sharopov F, Ramírez-Alarcón K, Ruiz-Ortega A et al. Antidiabetic Potential of Medicinal Plants and Their Active Components. Biomolecules. 2019 Sep 30;9(10):551. PMID: 31575072; PMCID: PMC6843349.doi: 10.3390/biom9100551.
6. Nguyen Vo TH, Tran N, Nguyen D, Le L. An in silico study on antidiabetic activity of bioactive compounds in *Euphorbia thymifolia Linn*. SpringerPlus. 2016 Dec;5:1-3.doi: 10.1186/s40064-016-2631-5
7. Arsyad AS, Nurrochmad A, Fakhrudin N. Phytochemistry, traditional uses, and pharmacological activities of *Ficuselastica*Roxb. exHornem: A review. Journal of Herbmed Pharmacology. 2022 Dec 31;12(1):41-53.doi: 10.34172/jhp.2023.04
8. Noor F, Rehman A, Ashfaq UA, Saleem MH, Okla MK, Al-Hashimi A, et al. Integrating network pharmacology and molecular docking approaches to decipher the multi-target pharmacological mechanism of *AbrusprecatoriusL*. acting on diabetes. Pharmaceuticals. 2022 Mar 29;15(4):414.doi: 10.3390/ph15040414
9. Qiu Y, Huang S, Zhu M. The molecular targets of Kangai injection in gastric cancer by in silico network pharmacology approach and experiment confirmation. Journal of Applied Biomedicine. 2023 Jul 1;21(3).doi: 10.32725/jab.2023.017
10. Damián-Medina K, Salinas-Moreno Y, Milenkovic D, Figueroa-Yáñez L, Marino-Marmolejo E, Higuera-Ciapara I, et al. In silico analysis of antidiabetic potential of phenolic compounds from blue corn (*Zea mays L.*) and black bean *(Phaseolus vulgaris L.).*Heliyon. 2020 Mar 1;6(3).doi: 10.1016/j.heliyon.2020.
11. Vimalavathini R, Elakiya M,Hemalatha K, Suriya N, Swethasri S, Kavimani S. Molecular Docking Studies of Thiazolidinediones on Receptor for Advanced Glycation End Products (RAGE). International Journal of Pharmaceutical Sciences and Nanotechnology (IJPSN). 2024 Feb 1;17(1):7124-9.doi: 10.37285/ijpsn.2024.17.1.3
12. Ahmad W, Ansari MA, Alsayari A, Almaghaslah D, Wahab S, Alomary MN, et al. In vitro, molecular docking and in silico ADME/Tox studies of emodin and chrysophanol against human colorectal and cervical carcinoma. Pharmaceuticals. 2022 Oct 31;15(11):1348.doi: 10.3390/ph15111348
13. Riyaphan J, Pham DC, Leong MK, Weng CF. In silico approaches to identify polyphenol compounds as α-glucosidase and α-amylase inhibitors against type-II diabetes. Biomolecules. 2021 Dec 14;11(12):1877.doi: 10.3390/biom11121877
14. Rehman K, Akash MS, Liaqat A, Kamal S, Qadir MI, Rasul A. Role of interleukin-6 in development of insulin resistance and type 2 diabetes mellitus. Critical Reviews™ in Eukaryotic Gene Expression. 2017;27(3).doi: 10.1615/CritRevEukaryotGeneExpr.2017019712
15. Zdychova J, Komers R. Emerging role of Akt kinase/protein kinase B signaling in pathophysiology of diabetes and its complications. Physiol Res. 2005 Jan 1;54(1):1-6.

16. Akash MS, Rehman K, Liaqat A. Tumor necrosis factor-alpha: role in development of insulin resistance and pathogenesis of type 2 diabetes mellitus. Journal of cellular biochemistry. 2018 Jan;119(1):105-10.doi.org/10.1002/jcb.26174
17. Tang X, Deng L, Xiong H, Li G, Lin J, Liu S, et al. Expression profile of mitrogen-activated protein kinase (MAPK) signaling genes in the skeletal muscle & liver of rat with type 2 diabetes: role in disease pathology. Indian Journal of Medical Research. 2014 Dec 1;140(6):744-55.
18. Gurzov EN, Eizirik DL. Bcl-2 proteins in diabetes: mitochondrial pathways of β-cell death and dysfunction. Trends in cell biology. 2011 Jul 1;21(7):424-31.doi: 10.1016/j.tcb.2011.03.001
19. Tessari P, Kiwanuka E, Barazzoni RO, Vettore M, Zanetti MI. Diabetic nephropathy is associated with increased albumin and fibrinogen production in patients with type 2 diabetes. Diabetologia. 2006 Aug;49:1955-61.doi: 10.1007/s00125-006-0288-2
20. Akhtar S, Benter IF. The role of epidermal growth factor receptor in diabetes-induced cardiac dysfunction. BioImpacts: BI. 2013;3(1):5.doi: 10.5681/bi.2013.008
21. Sliwinska A, Kasznicki J, Kosmalski M, Mikołajczyk M, Rogalska A, Przybylowska K, et al. Tumour protein 53 is linked with type 2 diabetes mellitus. Indian Journal of Medical Research. 2017 Aug 1;146(2):237-43.doi: 10.4103/ijmr.IJMR_1401_15.
22. Salehi B, Prakash Mishra A, Nigam M, Karazhan N, Shukla I, Kiełtyka-Dadasiewicz A, et al. Ficus plants: state of the art from a phytochemical, pharmacological, and toxicological perspective. Phytotherapy Research. 2021 Mar;35(3):1187-217. doi: 10.1002/ptr.6884

Table 1: PDB ID's of the selected target proteins.

Gene name	Abbreviation	PDB Id
Interleukin 6	IL2	4CNI
AKT serine/threonine kinase 1	AKT1	6NPZ
Peroxisome Proliferator activated receptor gamma	PPARγ	1FM6
SRC proto-oncogene, non-receptor tyrosine kinase	SRC	6E6E
BCL2 apoptosis regulator	BCL2	5JSN
Mitogen-Activated Protein Kinase 3	MAPK3	4QTB
Tumor necrosis factor	TNF	5MU8
Tumor protein p53(TP53)	TP53	1YCQ
Epidermal Growth Factor Receptor	EGFR	6V6O
Albumin	ALB	2NOX

Table 2: Binding energies of the active ingredients of *F. elastica* with target genes

Active ingredients	Binding free energy of core targets (kcal/mol)									
	IL6	AKT1	PPARG	SRC	BCL2	MAPK3	TNF	TP53	EGFR	ALB
Roseoside	-8.48	-10.62	-12.55	-8.82	-7.60	-10.14	-8.6	-8.43	-10.32	-11.2
Morin	-6.97	-9.43	-10.34	+208.3	-6.72	-8.56	-6.7	-7.86	-8.37	-10.3
Quercitrin	-7.73	-9.74	-11.46	-8.64	-6.84	-8.9	-7.4	-9.47	-12.31	-10.6
Rutin	-6.49	-13.38	-9.57	-11.41	-8.05	-12.43	-8.4	-8.9	-10.63	-0.9
Kaempferin	-9.01	-10.81	-10.82	-10.05	-7.01	-10.21	-7.0	-8.16	-7.52	-4.63
Emodin	-10.8	-8.49	-9.35	-8.24	-5.56	-7.72	-6.47	-7.7	-10.19	-9.69
Myricitrin	-9.15	-11.14	-11.15	-7.37	-7.34	-10.35	-7.0	-8.36	-10.29	-0.71
Feroxidin	-5.46	-8.29	-8.28	-6.61	-5.18	-7.69	-5.76	-6.43	-7.13	-7.72
Chlorogenic acid	-8.38	-9.63	-11.74	-10.17	-8.04	-9.72	-8.06	-9.59	-10.46	-11.68
Olaenolic acid	-8.94	-10.9	-12.38	-10.42	-7.23	-10.76	-8.78	-9.75	-11.46	58.29
Ursolic acid	-8.69	+20.02	-12.22	-10.41	-7.44	-10.3	-8.64	-9.75	-11.68	-0.82

Table 3: ADME and bioavailability of the active ingredients in *F. elastica*

Compounds	Molecular weight	Hydrogen donors	Hydrogen acceptors	Total Particle Surface Area	Rotatable bonds present	bioavailability
Roseoside	386.44	5	8	136.68	5	0.55
Morin	302.24	5	7	131.36	1	0.55
Quercitrin	448.38	7	11	190.28	3	0.17
Rutin	610.52	10	16	269.43	6	0.17
Kaempferin	448.38	7	11	190.28	3	0.17
Emodin	270.24	3	5	94.83	0	0.55
Myricitrin	464.38	8	12	210.51	3	0.55
Feroxidin	194.23	3	3	60.69	0	0.55
Chlorogenic acid	354.31	6	9	164.75	5	0.11
Oleanolic acid	456.7	2	3	57.53	1	0.85
Ursolic acid	456.7	2	3	57.53	1	0.85

Table 4: Toxicity prediction of the active ingredients in *F. elastica*

Active ingredients	AMES toxicity	Geno toxicity	Carcinogenicity	Eye irritation	Human hepatotoxicity	toxicity
Roseoside	Toxic	non-toxic	Non-toxic	Non-toxic	Non-toxic	Toxic
Morin	Non-toxic	Toxic	Non-toxic	Toxic	Non-toxic	Non-toxic
Quercitrin	Non-toxic	Toxic	Non-toxic	Toxic	Non-toxic	Toxic
Rutin	Toxic	Toxic	non-toxic	Non-toxic	Non-toxic	toxic
Kaempferin	Toxic	Toxic	Non-toxic	Toxic	Non-toxic	non-toxic
Emodin	Toxic	Toxic	Toxic	Toxic	Non-toxic	non-toxic
Myricitrin	Non-toxic	Toxic	Non-toxic	Toxic	Non-toxic	non-toxic
Feroxidin	toxic	Toxic	Toxic	Toxic	Non-toxic	non-toxic
Chlorogenic acid	non-toxic	Non-toxic	Non-toxic	Non-toxic	Non-toxic	toxic
Olaenolic acid	Non-toxic	Non-toxic	Non-toxic	Non-toxic	Non-toxic	toxic
Ursolic acid	Non-toxic	Non-toxic	Non-toxic	Non-toxic	Non-toxic	toxic

Table 5: Drug-likeness of the active ingredients using SwissADME

Active ingredients	GI absorption	Blood-Brain-Barrier permeation	Pgp substrate	CYP1A2 inhibitor	CYP2C19 inhibitor	CYP2C9 inhibitor	CYP2D6 inhibitor	CYP3A4 inhibitor	Log Kp
Roseoside	Low	-	+	-	-	-	-	-	-9.4
Morin	High	-	-	+	-	-	+	+	-7.05
Quercitrin	Low	-	-	-	-	-	-	-	-8.42
Rutin	Low	-	+	-	-	-	-	-	-10.26

Kaempferin	Low	-	-	-	-	-	-	-	-8.42
Emodin	High	-	-	+	-	-	-	+	-6.02
myricitrin	Low	-	-	+	-	-	-	+	-7.40
Feroxidin	High	+	-	-	-	-	-	-	-6.37
Chlorogenic acid	Low	-	-	-	-	-	-	-	-8.76
Olaenolic acid	Low	-	-	-	-	-	-	-	-3.77
Ursolic acid	Low	-	-	-	-	-	-	-	-3.87

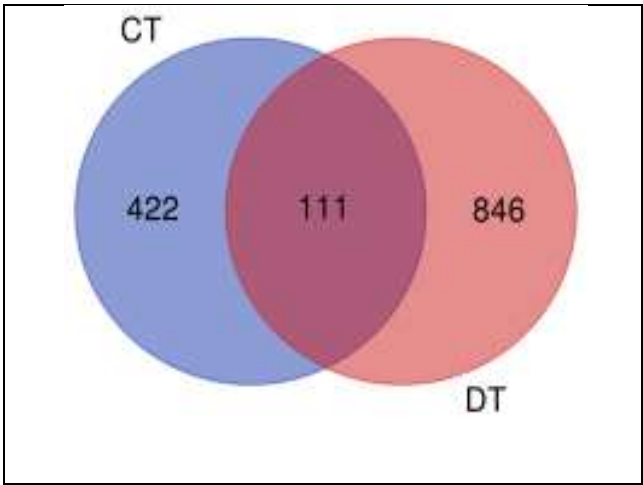

Figure 1:Venn diagram of the intersecting genes of *F. elastica* and non-insulin dependent diabetes mellitus

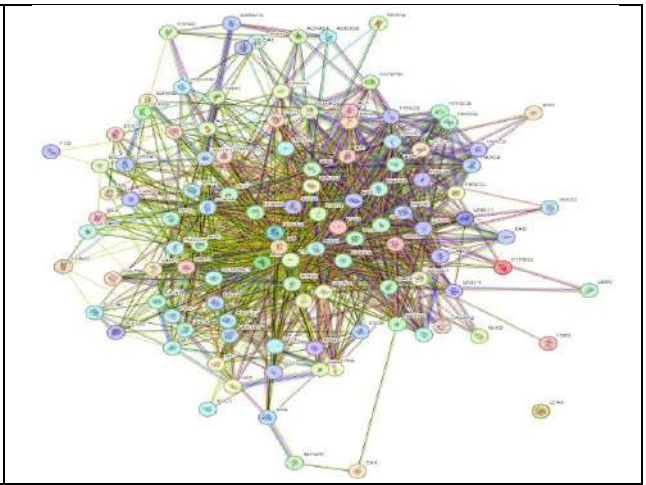

Figure 2: PPI (protein-protein interaction) network of the possible targets with the active ingredients of *F. elastica*

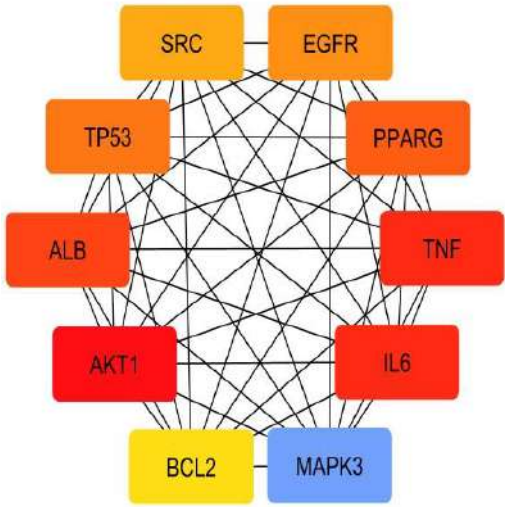

Figure 3: Top 10 core targets obtained through cytohubba

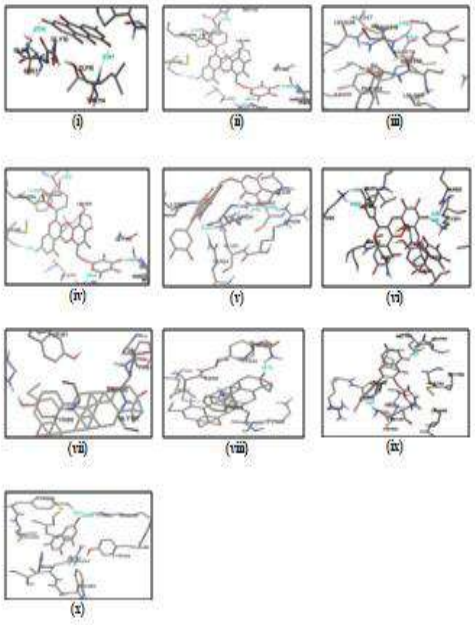

Figure 4: Interaction images of the active ingredients showing least binding energies (i) IL-6 (4cni) with emodin; (ii) AKT1 (6NPZ) with rutin (iii) PPARG (1FM6) with roseoside (iv) SRC (6e6e) with rutin (v) BCL2 (5jsn) with rutin (vi) MAPK3 (4qtb) with rutin (vii) TNF (5mu8) with olaenolic acid (viii) TP53 (iycq) with olaenoic acid (ix) EGFR (6v6o) with quercitrin (x) ALB (2nox) with chlorogenic acid.

Indian Journal of Natural Sciences *www.tnsroindia.org.in ©IJONS*

Vol.15 / Issue 88 / Feb / 2025 *International Bimonthly (Print) – Open Access* *ISSN: 0976 – 0997*

RESEARCH ARTICLE

Molecular Identification of Marine Actinomycetes from Vellar Estuary

R. Kiruthiga[1]*, R. Bharathidasan[2] and G. Thiruneelakandan[2]

[1]Research Scholar, Department of Microbiology, Maruthu Pandiyar College, Thanjavur, (Affiliated to Bharathidasan University, Tiruchirappalli), Tamil Nadu, India.
[2]Assistant Professor, Department of Microbiology, Maruthu Pandiyar College, Thanjavur, (Affiliated to Bharathidasan University, Tiruchirappalli), Tamil Nadu, India.

Received: 21 Nov 2024 Revised: 03 Dec 2024 Accepted: 30 Jan 2025

***Address for Correspondence**
R. Kiruthiga
Research Scholar, Department of Microbiology,
Maruthu Pandiyar College, Thanjavur,
(Affiliated to Bharathidasan University, Tiruchirappalli),
Tamil Nadu, India.

ABSTRACT

Even though there currently exist many antimicrobial drugs on the market, some pathogenic organisms are becoming resistant to them. Therefore, it is imperative to look for novel antibiotics that can combat resistant pathogenic organisms. An excellent source for secondary metabolites, or antibiotics, is actinomycetes. The marine ecosystem is an excellent resource for many strains of actinomycetes since it is an unknown habitat with millions of different sorts of microorganisms. Marine Actinomycetes have gained recognition as one of the most plentiful sources of unique and varied metabolites in recent years. Since actinomycetes are a widely distributed population, studies on them have gained momentum in India and other nations due to their production of special chemicals with bioactive properties. Therefore, the current study's main objective was to isolate actinomycetes from the vellar estuary in the Cuddalore district. Four actinomycetes were isolated and named as VM05, VM06, VM07, and VM08. Among the four isolates, VM 05 and VM 06 allowed for molecular identification by using 16-s RNA sequencing. Molecular characterization demonstrates that VM 06 was *Glutamicibactermysorens*KGM1 and VM 05 was *Streptomyces griseoflavus*KRSG1. The accession numbers for the sequences, which were kept in a gene bank, were PP280550 and PP278023.

Keywords: Actinomycetes, marine soil sample, isolation, identification, genebank

INTRODUCTION

The biggest ecosystem for all kinds of living things, particularly microorganisms, is found in the sea environment. Marine microbiology is the spark that has inspired researchers to travel to remote parts of the world's oceans in search of new bioactive chemicals. We have focused a lot on marine actinomycetes because they are the source of

most of these new chemicals. Marine actinomycetes have a big place in the scientific world because they can adapt to many different severe settings and make a lot of new drugs that are used in many other applications[1].Naturally occurring microbiological products are a key source of both novel and current pharmaceuticals. Secondary metabolites are organic compounds that are naturally produced by bacteria and plants. They have been used as prospective lead molecules since they can change their chemical structure to increase the efficacy of treatments[2,3]. Marine actinomycetes are a new and potentially valuable source of biologically active compounds, which are frequently employed to generate innovative treatments. Their tremendous diversity is currently being researched[4]. After a comprehensive technique for isolating them from samples of terrestrial soil was established, actinomycetes were first investigated in India in the early 1960s. Eventually, in the 1980s, researchers reported discovering actinomycetes from a variety of marine sources and producing a broad spectrum of advantageous chemicals.

Furthermore, findings show that these organisms thrive in a range of unfavourable environments, which increases the biological significance and distinctiveness of the metabolites generated[5]. Actinomycetes are the most advantageous prokaryotes from an economic and biotechnological perspective. They are capable of producing a large variety of bioactive secondary metabolites, such as enzymes, antibiotics, anticancer drugs, and immunosuppressive compounds, all of which have different biological applications. It is known that these metabolites have neurogenic, antibacterial, antifungal, anticancer, antialgal, antimalarial, and anti-inflammatory properties[6]. It is uncontested by any prospective competitors from other microbial groups and has enormous biosynthetic potential. Its enormous potential for biosynthesis is unchallenged since other microbial communities cannot possibly compete with it[7].Recent research has concentrated on marine ecosystems as opposed to terrestrial ecosystems to find novel compounds that are biologically significant[8]. Marine bacteria can produce novel bioactive chemicals since they can survive under extreme pressure, temperature, and salinity[9]. Actinomycetes have been found in 83 species across 28 genera[10]. Secondary metabolites derived from aquatic microorganisms have been demonstrated to contain potential bioactive compounds with antimicrobial, anticancer, antifungal, antiviral, antiparasitic, antimalarial, and antifouling properties[11]. Of the 200,000–250,000 bioactive metabolites, 50,000 are created by actinomycetes during fermentation, and 35,000 are only produced by Streptomyces species[12]. Many secondary metabolites are produced by actinomycetes, such as vitamins, antibiotics, antivirals, pesticides, and enzyme inhibitors[13]. Therefore, we need to separate novel drugs from marine actinomycetes from a variety of marine sources to combat the potential properties of actinomycetes and emerging multidrug-resistant infections. Numerous uncommon marine actinomycetes are still uncultivable and must be found by molecular methods.

MATERIALS AND METHOD

Sample collection

Soil samples were collected from Vellar estuary Mangrove, Parangipettai, and Cuddalore district Tamil Nadu, India. The soil samples were taken from a depth of 5- 10 cm alone with seawater and also kept in a sterilized bottle and transmitted to the laboratory to identify marine actinomycetes.

Isolation and identification of marine actinomycetes

In the 250 ml conical flask, 90 ml of sterilized distilled water was added along with 10g of soil sample and kept in a shaker at 150rpm for one day to separate spores and filamentous actinomycetes. After incubation 2 ml of suspense sample were allowed for centrifugation at 1000rpm for 10 minutes. The centrifuged supernatant was used for segregating actinomycetes by the pour plate methodology.

Pour plate method

The methodology was used for isolation of actinomycetes from the marine soil samples namely, serial dilution techniques. 1 ml of centrifuged supernatant was serially diluted. After serial dilution, 0.1 ml of the sample was aseptically transferred into the plates containing SCA medium with 0.1 chloramphenicol and 0.1 griseofulvin to inhibit the contamination of fungus and bacteria. After solidification, the plates were incubated at room temperature

for 14 days. Control plates were also maintained. After two weeks the grown individual colonies streak separately on SCA medium until the pure culture of actinomycetes was uptained.

Maintenance of pure Actinomycetes cultures

Based on the texture and colour, the grown colonies of actinomycetes were taken and inoculated individually on an SCA medium.The exceptions were the colonies that were visually identical to one another, with the same texture, aerial mycelium, and soluble pigment. From the Vellar estuary Mangrove, four actinomycetes were isolated and maintained by separated and pure culture on the SCA medium. The pure actinomycetes culture which grew on SCA plates was inoculated into an SCA slant and incubated until the growth of actinomycetes. The slant cultures of actinomycetes were stored in a refrigerator at 4 °C. Every 4 weeks the cultures were sub-cultured and stored appropriately for maintaining pure culture.

Molecular Identification of mangrove soil Actinomyces isolates

Among the four isolates VM05, and VM06 were only chosen for molecular identification in this study.

DNA isolation by CTABMethod

DNA isolation was done on cultivated Actinomyces isolates on SCNA(Starch Casein Nitrate Agar) broth, which was incubated for seven days at room temperature and rotated continuously at 100 rpm per minute. The biomass was extracted by centrifugation at 5000 rpm for 10 minutes using a centrifuge REMI, CPR30 plus. In short, 100 mg of softened homogenized biomass was combined with 500 µl CTAB extraction buffer and vortexed using a GENAXY-Vortexer. Homogenate was incubated for 30 minutes at 60 °C in a KEMI water bath. The homogenate was centrifuged for five minutes at 14,000 rpm following the incubation period. After adding a mixture of chloroform and isoamyl alcohol, the mixture was vortexed for five seconds and centrifuged for five minutes at 14,000 rpm. After adding the chloroform and isoamyl alcohol admixture, vortexing for five seconds, and centrifuging for five minutes at 14,000 rpm, the mixture was removed. Following the separation of the top aqueous phase, 0.70 ml of ice-cold isopropanol was added, and it was incubated for 30 twinkles at 20 °C. The precipitated DNA was subordinated to a 10-minute, 14000 rpm recentrifuged. Without fragmenting the molecules, the supernatant was decanted and then 500 µl of ice-cold 70 ethanol was used for washing. After dissolving the final DNA in 30 µl of TE(10 mM pH 8.0) buffer, 5 µl of RNAase solution(50 µg/ ml) was added, and the mixture was incubated for 30 minutes at 37 °C. The purity and volume were measured and recorded using a Multiskan sky- µ drop plate reader [14].

Purification of DNA using columns

Before loading the separated DNA into the column, 200 µl of binding buffer was added. Then it allowed for centrifugation for a minute at 12,000, after washing it with 750 µl buffer. Following a 2-minute drying period, 20 µl of elution buffer was used to elute the DNA, followed by a 1-minute final centrifugation [15].

Agarose Gel electrophoresis

Using 1x TAE pH 8.3 buffer and 4 µl of 10 mg/ml ethidium bromide, an 80 ml 0.8 % agarose gel was created. The loading dye-mixed actinomycetes DNA and the 1 kb ladder DNA were used as a reference to compare the MW of the two samples. Using the Bio-Rad Gel Doc Go imaging equipment, the gel was operated at 100 V for approximately 75–80% of its length [16].

Preparation of 0.8 % Agarose Gel

After being weighed, 0.8 g of agarose was dissolved in 1x TAE buffer. The agarose was microwave-melted for one to three minutes, or until it dissolved entirely. When the agarose solution had cooled to about 50 °C, 5 µl (10 mg/ml) of ethidium bromide (Et-Br) was added. Et-Br's attachment to DNA allows for its visibility under ultraviolet (UV) light. The agarose solution was placed within a gel casting tray that had a well-forming comb in it. To allow the agarose to fully harden, the set was left at room temperature for twenty to thirty minutes.

DNA loading and electrophoresis

After the gel hardened, the agarose was placed inside the electrophoresis device. The gel was covered by pouring one-third of the 1X TAE pH 8.3 buffer into the gel box within the apparatus. Five microliters of a glycerol-containing DNA loading buffer were added to each DNA sample. In the first lane of the gel, a molecular weight ladder was placed. Each gel well had a precisely placed piece of DNA. The gel was run at 100 V until the dye line was roughly 75–80% of the way down the gel. A run could take one to one and a half hours, depending on the voltage and gel dosage and electrodes removed.

PCR amplification for purified Actinomyces DNA

For PCR amplification, use 1.0 µl of the forward primer (27F), 20.0 µl of the master mix, and 1.0 µl of the DNA template (25 ng). 5'-AGAGTTTGATCCTGGCTCAG-3' (10 pmol), 1 µl of reverse primer (1492R Using molecular grade nuclease-free water, the final volume was adjusted to 25.0 µl after adding 10 pmol of GGTTACCTTGTTACGACTT-3'. Actinomyces 16s rRNA gene amplification was performed using the BioRad CFX-96. The PCR programming was set for two minutes of denaturation at 95 °C and thirty seconds of annealing at 50 °C. Extension for a minute at 72 °C. For thirty-five cycles, the program was repeated. For the full PCR amplification, the last denaturation step is set to 95 °C for 30 seconds, followed by elongation at 72 °C for 10 minutes, and finally, 4 °C indefinitely. To separate the PCR-amplified DNA, a 0.8% agarose gel was hired. By employing a gel solubilization buffer and heating the gel to 55 °C, the PCR-amplified product was soluble. After inserting 200 µl of isopropyl alcohol, the dissolved DNA was extracted and purified using a column DNA purification kit [17-19]. Sequencing of 16s rRNA genes Centrifugation (2.5 µl) was performed on each well-containing amplicon after 125 mM EDTA was added. After adding and vortexing 35 µl of ethanol. Using a tissue bed, ethanol was decanted at 300 rpm following 30 minutes of centrifugation at 3510 rpm. After adding 40 µl of 80% ethanol to each well, the wells were centrifuged for 12 minutes. After twice going through the previously mentioned steps, the plate was covered with a lint-free tissue and left to dry in the air for 30 to 45 minutes. After adding 13 µl of Hi Di Formamide for denaturation at 95 °C for 5 minutes, the plate was given a quick spin before being put in the sequencer.

Data analysis

The NCBI BLAST server was used to examine the sequencing data that had been gathered. Sequence files in the Fasta format that had been converted from.ab1 format was deposited and submitted to Gen Bank to obtain an accession number.

RESULT

Sample collection

The soil sediment in a depth of 5-10cm from the vellar estuary, Cuddalore was collected along with marine water. The soil sediment looks brown in colour and soft and sandy in texture shown in Table 1.

Isolation and identification of marine actinomycetes

After the incubation of two weeks, the isolated colonies were inoculated on SCA medium in a sterile condition. Actinomycetes were easily distinguished from fungus and bacteria due to their compact, leathery conical appearance and dry surface. More than 30 isolates were identified. In this study, we have selected four among them and named VM 05, VM06, VM07, VM08.VM0 5 grown ash pale yellow in colour and VM 06 shows powdery ash white colour,VM07 gives a wrinkled surface with white aerial mycelia with light pink spores. VM 08 shows yellowish aerial mycelia and light yellowish-brown wrinkled substrate mycelium shown in Figure 1, Table 2.

Maintenance of pure culture

Isolated colonies of individuals mixed from the plates were streaked separately on starch casein agar medium until pure culture. The distinguished pure cultures were incubated and stored in the refrigerator. They serve as a cultural mother.

Molecular identification

The VM05 and VM06 strains havea high amount of GC content in their DNA. The strain VM05 was identified by 16S rRNA sequencing as belonging to the Actinomycetes genus *Streptomycesgriseoflavus* and VM06 was *Glutamicibactermysorens*. These actinomycete strains are designated as *Streptomyces griseoflavus*KRSG1 and *Glutamicibactermysorens* strain KGM1. The gene sequences were deposited in the gene bank and their accession numbers are PP280550 and PP278023.*Streptomyces griseoflavus* KRSG1 has 1478 base pairs and *Glutamicibactermysorens* has 1140 base pairs in DNA as shown in Figure 2and Figure3. The *Streptomyces griseoflavus* KRSG1 strain is more similar to the *Streptomycesgriseoflavus* strain RB1-83 shown in Figure 4. *Glutamicibactermysorens* have 99% similarity with *Glutamicibactermysorens* strain YKIKM.MU which has already been deposited in the gene bank shown in Figure 5.

DISCUSSION

Actinomycetes offer an almost infinite supply of new bioactive compounds with a variety of possible medical applications. There are about 25,000 known microbial secondary metabolites; actinomycetes are responsible for creating about 75% of these, followed by fungi (15%), Bacillus species (6%), and other bacteria (1-3%). Of all known antibiotics, 50–60% come from Streptomyces species[20]. Numerous industrially useful enzymes can be produced by marine actinomycetes. Numerous biological processes are catalyzed by these enzymes. Marine-derived enzymes, including cellulase, amylase, protease, lipase, L-asparaginase, and L-glutaminase, are now widely used in industry and are highly valuable economically[21].Historically, the high GC content of actinobacteria's DNA has been a characteristic[22].while new research has revealed that some members, especially those that live in freshwater, have relatively low GC contents [23]. Both identified organisms *Streptomyces griseoflavus* and *Glutamicibactermysorens* have a high amount of GC content in their DNA**.** They differ greatly in several aspects, including habitat, ideal pH, thermophilicity, and moisture tolerance. Actinomycetes are frequently found in environments with a moderate pH[24,25].However, a few species are known to be both alkaliphilic and acidophilic [26-29]. Although several thermophilic actinomycetes have been identified[30].Thus, enzymes are widely used in many industries, including food, brewing, leather, textiles, paper, and detergent. Approximately twenty-five thousand physiologically active chemicals have been identified, of which approximately twelve thousand come from marine actinomycetes[31]. Actinomycetes have been used in bioremediation, cancer treatment, and the manufacturing of valuable antibiotics like amphotericin, neomycin, vancomycin, chloramphenicol, novobiocin, gentamycin, nystatin, erythromycin, and tetracycline, among others. They are also used as biocontrol agents, antifungal compounds, and a source of agroactive chemicals. The bioactive chemicals isolated from these marine Actinomycetes feature diverse chemical structures and conformations, which hold the key to innovative medication creation and, in the future, may be effective enough to treat various resistant infections[32].

CONCLUSION

The goal of the current study was to isolate and identify marine actinomycetes using molecular methods from a marine soil sample taken from the Cuddalore district's Vellar Estuary. From the sea soil, four actinomycetes were identified. Only two of the four strains *Streptomyces griseoflavus* and *Glutamicibactermysorens* were suitable for molecular identification. Numerous studies have demonstrated this particular organism's capacity to produce new antibiotics and industrially significant bioactive chemicals. As a result, the ocean is a great place to find promising microorganisms.

ACKNOWLEDGEMENT

NIL

REFERENCES

1. Manivasagan P, Venkatesan J, Sivakumar K, Kim SK. Pharmaceutically active secondary metabolites of marine actinobacteria. Microbiological research. 2014 Apr 1;169(4):262-78.
2. Fiedler HP, Bruntner C, Bull AT, Ward AC, Goodfellow M, Potterat O, Puder C, Mihm G. Marine actinomycetes as a source of novel secondary metabolites. Antonie Van Leeuwenhoek. 2005 Jan;87:37-42.
3. Al-Ansari M, Kalaiyarasi M, Almalki MA, Vijayaraghavan P. Optimization of medium components for the production of antimicrobial and anticancer secondary metabolites from Streptomyces sp. AS11 isolated from the marine environment. Journal of King Saud University-Science. 2020 Apr 1;32(3):1993-8.
4. De Rosa S, Mitova M, Tommonaro G. Marine bacteria associated with sponge as source of cyclic peptides. Biomolecular Engineering. 2003 Jul 1;20(4-6):311-6.
5. Ellaiah P, Reddy AP. Isolation of actinomycetes from marine sediments off Visakhapatnam, east coast of India.
6. Ravikumar S, Inbaneson SJ, Uthiraselvam M, Priya SR, Ramu A, Banerjee MB. Diversity of endophytic actinomycetes from Karangkadu mangrove ecosystem and its antibacterial potential against bacterial pathogens.
7. Wellington EM, Stackebrandt E, Sanders D, Wolstrup J, Jorgensen NO. Taxonomic status of Kitasatosporia, and proposed unification with Streptomyces on the basis of phenotypic and 16S rRNA analysis and emendation of Streptomyces Waksman and Henrici 1943, 339AL. International Journal of Systematic and Evolutionary Microbiology. 1992 Jan;42(1):156-60.
8. Leetanasaksakul K, Thamchaipenet A. Potential anti-biofilm producing marine actinomycetes isolated from sea sediments in Thailand. Agriculture and Natural Resources. 2018 Jun 1;52(3):228-33.
9. Abdelmohsen UR, Bayer K, Hentschel U. Diversity, abundance and natural products of marine sponge-associated actinomycetes. Natural product reports. 2014;31(3):381-99.
10. Selim G, AYDOĞDU EÖ. AGRICULTURAL USE POTENTIALS OF ACTINOMYCETES. AGBIOL 2021. 2021 Sep 1:890.
11. Siddharth S, Rai RV. Actinomycetes as a Paramount Source of Biologically Important Enzyme Inhibitors"A Boon to Mankind". Current Bioactive Compounds. 2019 Feb 1;15(1):19-30.
12. Rajivgandhi G, Li WJ. Application of Microorganisms. InMicrobial Systematics 2020 Nov 1 (pp. 51-75). CRC Press.
13. Rashad FM, Fathy HM, El-Zayat AS, Elghonaimy AM. Isolation and characterization of multifunctional Streptomyces species with antimicrobial, nematicidal and phytohormone activities from marine environments in Egypt. Microbiological research. 2015 Jun 1;175:34-47.
14. Weisburg WG, Barns SM, Pelletier DA, Lane DJ. 16S ribosomal DNA amplification for phylogenetic study. Journal of bacteriology. 1991 Jan;173(2):697-703.
15. Pitcher DG, Saunders NA, Owen RJ. Rapid extraction of bacterial genomic DNA with guanidium thiocyanate. Letters in applied microbiology. 1989 Apr 1;8(4):151-6.
16. Hemalatha S, Banu N. DNA fingerprinting of Bacillus cereus from diverse sources by restriction fragment length polymorphism analysis. Advances in Bioscience and Biotechnology. 2010 Jun 30;1(02):136-44.
17. Frank JA, Reich CI, Sharma S, Weisbaum JS, Wilson BA, Olsen GJ. Critical evaluation of two primers commonly used for amplification of bacterial 16S rRNA genes. Applied and environmental microbiology. 2008 Apr 15;74(8):2461-70.
18. Monciardini P, Sosio M, Cavaletti L, Chiocchini C, Donadio S. New PCR primers for the selective amplification of 16S rDNA from different groups of actinomycetes. FEMS Microbiology Ecology. 2002 Dec 1;42(3):419-29.
19. Pitcher DG, Saunders NA, Owen RJ. Rapid extraction of bacterial genomic DNA with guanidium thiocyanate. Letters in applied microbiology. 1989 Apr 1;8(4):151-6.

20. Chinnathambi A, Salmen SH, Al-Garadi MA, Wainwright M, Alharbi SA. Marine Actinomycetes: An Endless Source of Potentially Therapeutic Novel Secondary Metabolites and Other Bioactive Compounds. Journal of King Saud University-Science. 2023 Oct 6:102931.
21. Sarkar G, Suthindhiran K. Diversity and biotechnological potential of marine actinomycetes from India. Indian Journal of Microbiology. 2022 Dec;62(4):475-93.
22. Barka EA, Vatsa P, Sanchez L, Gaveau-Vaillant N, Jacquard C, Klenk HP, Clément C, Ouhdouch Y, van Wezel GP. Taxonomy, physiology, and natural products of Actinobacteria. Microbiology and molecular biology reviews. 2016 Mar;80(1):1-43.
23. Kavagutti VS, Andrei AŞ, Mehrshad M, Salcher MM, Ghai R. Phage-centric ecological interactions in aquatic ecosystems revealed through ultra-deep metagenomics. Microbiome. 2019 Dec;7:1-5.
24. Basavaraj KN, Chandrashekhara S, Shamarez AM, Goudanavar PS, Manvi FV. Isolation and morphological characterization of antibiotic producing actinomycetes. Tropical Journal of Pharmaceutical Research. 2010;9(3).
25. Ramesh S, Mathivanan N. Screening of marine actinomycetes isolated from the Bay of Bengal, India for antimicrobial activity and industrial enzymes. World Journal of Microbiology and Biotechnology. 2009 Dec;25:2103-11.
26. Zenova GM, Manucharova NA, Zvyagintsev DG. Extremophilic and extremotolerant actinomycetes in different soil types. Eurasian Soil Science. 2011 Apr;44:417-36.
27. Gohel SD, Singh SP. Cloning and expression of alkaline protease genes from two salt-tolerant alkaliphilic actinomycetes in E. coli. International journal of biological macromolecules. 2012 Apr 1;50(3):664-71.
28. Poomthongdee N, Duangmal K, Pathom-aree W. Acidophilic actinomycetes from rhizosphere soil: diversity and properties beneficial to plants. The Journal of antibiotics. 2015 Feb;68(2):106-14.
29. Vasavada SH, Thumar JT, Singh SP. Secretion of a potent antibiotic by salt-tolerant and alkaliphilic actinomycete Streptomyces sannanensis strain RJT-1. Current science. 2006 Nov 25:1393-7.
30. Kurapova AI, Zenova GM, Sudnitsyn II, Kizilova AK, Manucharova NA, Norovsuren ZH, Zvyagintsev DG. Thermotolerant and thermophilic actinomycetes from soils of Mongolia desert steppe zone. Microbiology. 2012 Feb;81:98-108.
31. Sharma M, Dangi P, Choudhary M. Actinomycetes: source, identification, and their applications. International Journal of Current Microbiology and Applied Sciences. 2014;3(2):801-32.
32. Solanki R, Khanna M, Lal R. Bioactive compounds from marine actinomycetes. Indian journal of microbiology. 2008 Dec;48:410-31.

Table 1-Characteristic of marine soil sample

Place	Sample	Color	Texture
Vellar Estuary mangrove	**Soil sediment**	**Brown**	**Soft and sandy**

Table 2- Characteristics of Actinomycetes isolates

Code	Color of aerial mycelium	The color of the substrate mycelium	Change the color of the medium
VM 05	Yellow	Ash	No
VM 06	White	Ash	No
VM07	White	White	No
VM 08	Yellow	Yellow	Yellow

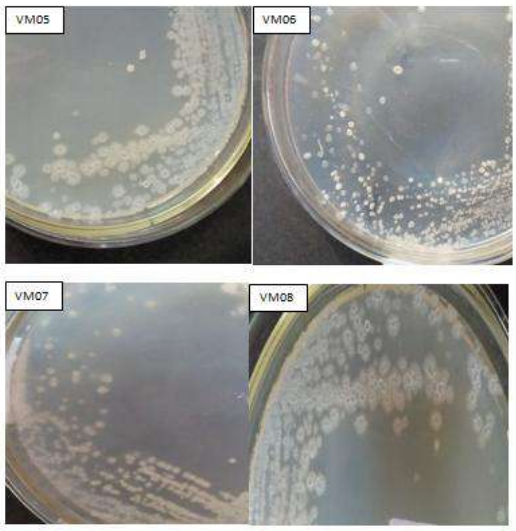

Figure 1 -Colony Morphology of isolated Actinomycetes(VM05,VM06,VM07,VM08)

GenBank ▾ Send to: ▾

Streptomyces griseoflavus strain KRSG1 16S ribosomal RNA gene, partial sequence

GenBank: PP280550.1

FASTA Graphics

Go to:

```
LOCUS       PP280550               1478 bp    DNA     linear   BCT 11-FEB-2024
DEFINITION  Streptomyces griseoflavus strain KRSG1 16S ribosomal RNA gene,
            partial sequence.
ACCESSION   PP280550
VERSION     PP280550.1
KEYWORDS    .
SOURCE      Streptomyces griseoflavus
  ORGANISM  Streptomyces griseoflavus
            Bacteria; Actinomycetota; Actinomycetes; Kitasatosporales;
            Streptomycetaceae; Streptomyces.
REFERENCE   1  (bases 1 to 1478)
  AUTHORS   Kiruthiga,R. and Thirumeelakandan,G.
  TITLE     Direct Submission
  JOURNAL   Submitted (06-FEB-2024) Microbiology, NARUTHUPANDIYAR COLLEGE OF
            ARTS AND SCIENCE, 257/4A, Trichy Main Road, Pillaiyarpatti, Vallam
            Post, Thanjavur, Tamil Nadu 613 403, India
COMMENT     ##Assembly-Data-START##
            Sequencing Technology :: Sanger dideoxy sequencing
            ##Assembly-Data-END##
FEATURES             Location/Qualifiers
     source          1..1478
                     /organism="Streptomyces griseoflavus"
                     /mol_type="genomic DNA"
                     /strain="KRSG1"
                     /isolation_source="Vellar estuary"
                     /db_xref="taxon:35619"
                     /geo_loc_name="India: Vellar estuary, Parangipettai"
                     /collected_by="Kiruthiga R"
     rRNA            <1..>1478
                     /product="16S ribosomal RNA"
ORIGIN
        1 gacgaacgct ggcggcgtgc ttaacacatg caagtcgaac gatgaaccac ttcggtgggg
       61 attagtggcg aacgggtgag taacacgtgg gcaatctgcc ctgcactctg ggacaagccc
      121 tggaaacggg gtctaatacc ggatactgac ccgccgggc atccaggcgg ttcgaaagct
      181 ccggcggtgc aggatgagcc cgcggcctat cagcttgttg gtgaggtaat ggctcaccaa
      241 ggcgacgacg ggtagccggc ctgagagggc gaccggccac actgggactg agacacggcc
      301 cagactccta cgggaggcag cagtggggaa tattgcacaa tgggcgaaag cctgatgcag
      361 cgacgccgcg tgagggatga cggccttcgg gttgtaaacc tctttcagca gggaagaagc
      421 gaaagtgacg gtacctgcag aagaagcgcc ggctaactac gtgccagcag ccgcggtaat
      481 acgtagggcg cgagcgttgt ccggaattat tgggcgtaaa gagctcgtag gcggcttgtc
      541 acgtcggttg tgaaagcccg gggcttaacc ccgggtctgc agtcgatacg ggcaggctag
      601 agttcggtag aggagatcgg aattcctggt gtagcggtga aatgcgcaga tatcaggagg
      661 aacaccggtg gcgaaggcgg atctctgggc cgatactgac gctgaggagc gaaagcgtgg
      721 ggagcgaaca ggattagata ccctggtagt ccacgccgta aacggtgggc actaggtgtg
      781 ggcgacattc cacgtgtccc gtgccgcagc taacgcatta agtgccccgc ctggggagta
      841 cggccgcaag gctaaaactc aaaggaattg acgggggccc gcacaagcgg cggagcatgt
      901 ggcttaattc gacgcaacgc gaagaacctt accaaggctt gacatacacc ggaaagcatt
      961 agagatagtg ccccccttgt ggtcggtgta caggtggtgc atggctgtcg tcagctcgtg
     1021 tcgtgagatg ttgggttaag tcccgcaacg agcgcaaccc ttgtcccgtg ttgccagcag
     1081 gcccttgtgg tgctggggac tcacgggaga ccgccggggt caactcggag gaaggtgggg
     1141 acgacgtcaa gtcatcatgc cccttatgtc ttgggctgca cacgtgctac aatggccggt
     1201 acaatgagct gcgatacccc gaggtggagc gaatctcaaa aagccggtct cagttcggat
     1261 tggggtctgc aactcgaccc catgaagtcg gagtcgctag taatcgcaga tcagcattgc
     1321 tgcggtgaat acgttcccgg gccttgtaca caccgcccgt cacgtcacga aagtcggtaa
     1381 caccgaagc cggtggccca accctttgtg gaaggagct gtcgaaggtg ggactggcga
     1441 ttgggacgaa gtcgtaacaa ggtagccgta ccggaagg
//
```

Figure 2-16 s RNA Sequence of *Streptomyces griseoflavus* KRSG1 (Accession Number: PP280550)

```
GenBank ▾                                                          Send to:

Glutamicibacter mysorens strain KGM1 16S ribosomal RNA gene,
partial sequence
GenBank: PP278023.1
FASTA   Graphics

Go to:

LOCUS       PP278023                1140 bp    DNA     linear   BCT 11-FEB-2024
DEFINITION  Glutamicibacter mysorens strain KGM1 16S ribosomal RNA gene,
            partial sequence.
ACCESSION   PP278023
VERSION     PP278023.1
KEYWORDS    .
SOURCE      Glutamicibacter mysorens
  ORGANISM  Glutamicibacter mysorens
            Bacteria; Actinomycetota; Actinomycetes; Micrococcales;
            Micrococcaceae; Glutamicibacter.
REFERENCE   1  (bases 1 to 1140)
  AUTHORS   Kiruthiga,R. and Thiruneelakandan,G.
  TITLE     Direct Submission
  JOURNAL   Submitted (06-FEB-2024) Microbiology, MARUTHUPANDIYAR COLLEGE OF
            ARTS AND SCIENCE, 257/4A, Trichy Main Road, Pillaiyarpatti, Vallam
            Post, Thanjavur, Tamil Nadu 613-403, India
COMMENT     ##Assembly-Data-START##
            Sequencing Technology :: Sanger dideoxy sequencing
            ##Assembly-Data-END##
FEATURES             Location/Qualifiers
     source          1..1140
                     /organism="Glutamicibacter mysorens"
                     /mol_type="genomic DNA"
                     /strain="KGM1"
                     /isolation_source="Vellar estuary"
                     /db_xref="taxon:257984"
                     /geo_loc_name="India: Vellar estuary, Parangipettai"
                     /collected_by="Kiruthiga R"
     rRNA            <1..>1140
                     /product="16S ribosomal RNA"
ORIGIN
        1 ttgttggtga ggtaatggct caccaaggcg acgacgggta gccggcctga gagggtgacc
       61 ggccacactg ggactgagac acggcccaga ctcctggagg cagcagtggg gaatattgca
      121 caatgggcgg aagcctgatg cagcgacccg cgtgagggat gacggccttc gggttgtaaa
      181 cctctttcag tagggaagaa gcgaaagtga cggtacctgc agaagaagcg ccggctaact
      241 acgtgccagc agccgcggta atacgtaggg cgcaagcgtt atccggattt attgggcgta
      301 aatcgtaggc ggtttgtcgc gtctgccgtg aaagtccgac tcaacctcgg atctgcggtg
      361 ggtacgggca gactagagtg atgtagggga gactggaatt cctggtgtag cggtgaaatg
      421 cgcagatatc aggaggaaca ccgatggcga aggcaggtct ctgggcattt actgacgctg
      481 aggagcgaaa gcatggggag cgaacaggat tagataccct ggtagtccat gccgtaaacg
      541 ttgggcacta ggtgtggggg acattccacg ttttccgcgc cgtagctaac gcattaagtg
      601 cccgcctggg agtacggccg caaggctaaa actcaaagga attgacgggg gcccgcacaa
      661 gcggcggagc atgcggatta attcgatgca acgcgaagaa ccttaccaag gcttcatgtg
      721 ccagaccgct ccagagatgg ggtttccctt cggggctggt tcacaggtgg tgcatggttg
      781 tcgtcagctc gtgtcgtgag atgttgggtt aagtcccgca acgagcgcaa ccctcgttcc
      841 atgttgccag cacgtagtgg tggggactca tgggagactg ccggggtcaa ctcggaggaa
      901 ggtggggatg acgtcaaatc atcatgccta tgtcttgggc ttcacgcatg ctacaatggc
      961 cggcaatggg ttgcgatact gtgaggtgga gctaatccct aaaagccggt ctcagttcgg
     1021 attggggtct gcaactcgac cccatgaagt cggagtcgct agtaatcgca gcagcaacgc
     1081 tgcggtgaat acgttcccgg gccttgtaca caccgcccgt caagtcacga gttggtaaca
//
```

Figure 3-16 s RNA Sequence of *Streptomyces mysorens* KGM1(Accession Number: PP278023)

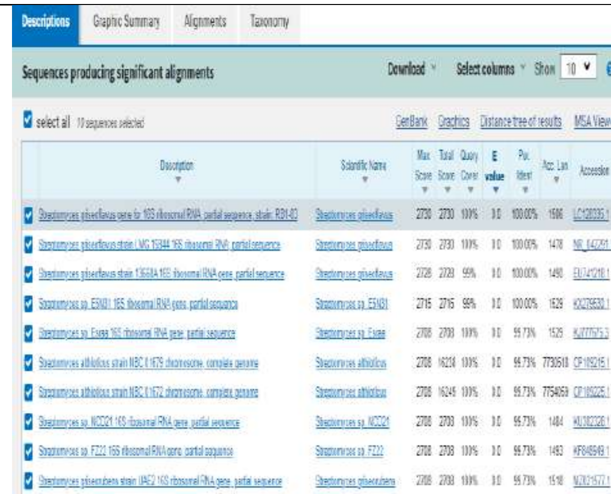

Figure 4- Sequence similarity of *Streptomyces griseoflavus* KRSG1(Accession Number: PP280550)and other closely related organisms using the BLAST tool.

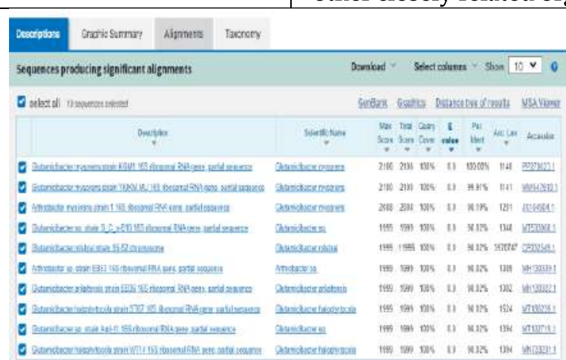

Figure 4- Sequence similarity of *Streptomyces mysorens*KGM1(Accession Number: PP278023)and other closely related organisms using the BLAST tool.

Indian Journal of Natural Sciences www.tnsroindia.org.in ©IJONS

Vol.15 / Issue 88 / Feb / 2025 *International Bimonthly (Print) – Open Access* *ISSN: 0976 – 0997*

REVIEW ARTICLE

The Role of Traditional and Alternative Medicine in Inflammatory Bowel Diseases: A Review

Annegowda H V[1], Nischith S S[2], Yogesh Kumar S[3] and Vidya Shree N S[4]*

[1]Professor and Head, Department of Pharmacognosy, Sri Adichunchanagiri College of Pharmacy, B.G.Nagara, (Affiliated to Rajiv Gandhi University of Health Sciences, Bengaluru), Karnataka, India.
[2]Ph.D Scholar, Department of Pharmacognosy, Sri Adichunchanagiri College of Pharmacy, B.G.Nagara, (Affiliated to Rajiv Gandhi University of Health Sciences, Bengaluru), Karnataka, India.
[3]PG Scholar, Department of Pharmaceutics, Sri Adichunchanagiri College of Pharmacy, B.G.Nagara, (Affiliated to Rajiv Gandhi University of Health Sciences, Bengaluru), Karnataka, India.
[4]PG Scholar, Department of Pharmacognosy, Sri Adichunchanagiri College of Pharmacy, B.G.Nagara, (Affiliated to Rajiv Gandhi University of Health Sciences, Bengaluru), Karnataka, India.

Received: 21 Nov 2024 Revised: 03 Dec 2024 Accepted: 31 Jan 2025

*__Address for Correspondence__
Vidya Shree N S
PG Scholar, Department of Pharmacognosy,
Sri Adichunchanagiri College of Pharmacy,
B.G.Nagara,
(Affiliated to Rajiv Gandhi University of Health Sciences, Bengaluru),
Karnataka, India.
E.Mail: vidyashreeraj2000@gmail.com

ABSTRACT

The gastrointestinal (GI) tract is one of the pivotal systems in the human body upon which itthrives. It also hosts a unique and diverse microbiome ecosystem which contributes to metabolism. This GI tract is prone to several disorders, among which inflammatory bowel diseases (IBDs) are becoming a global threat. With changing lifestyles and medicinal advances, multiple therapies and drug combinations have been used to treat IBDs. In addition to synthetic medication, traditional and alternative medicine have significantly impacted globally in the treatment of IBDs. The herbal extracts or phytoconstituents isolated from medicinal plants possess significant anti-inflammatory properties that can be utilized in treating IBD. The current review focuses on the role of herbs or their extracts or their phytoconstituents in the treatment of IBD along with their mechanism. Additionally, information related to lifestyle changes like diet, prebiotics, probiotics synbiotics, acupuncture, and exercise in the effective treatment of IBD as the alternative therapy is also discussed.

Keywords: Inflammation, Bowel diseases, Phytoconstituents, Biomarkers, medicinal plants, alternative medicine.

INTRODUCTION

The immune system-regulated process of inflammation is the body's defensive mechanism against a variety of threats, including infections, injuries, toxic substances, or radiation. The goal of the stimulated immune response is to eliminate the toxic substances and initiate the healing process, so inflammation is an essential defense mechanism for preserving the body's health. Complex cellular and molecular processes work together during acute inflammatory reactions to quickly treat possible wounds andinfections. By minimizing damage and assisting in the restoration of tissue balance, this coordinated effort ultimately resolves the acute inflammation. However, if acute inflammation is not treated, itbecomes chronic and contributes to the emergence of several chronic inflammatory disorders such as Immune-mediated inflammatory diseases(1) Immune-mediated inflammatory diseases (IMIDs) are a group of disorders marked by systemic inflammation affecting several organs. This category includes conditions like hidradenitis suppurativa, sarcoidosis, asthma, connective tissue disorders, atopic dermatitis (AD), an kylosing spondylitis, rheumatoid arthritis (RA), psoriatic arthritis (PsA), psoriasis, and certain neurological diseases like multiple sclerosis (MS)(2).Globally the prevalence of immune-mediated diseases is increasing(3). Indeed, it is now widely acknowledged that chronic inflammatory diseases are the leading cause of death worldwide, accounting for over 50% of all fatalities. These diseases include stroke, ischemic heart disease, non-alcoholic fatty liver disease (NAFLD), cancer, chronic kidney disease, autoimmune disorders, diabetes mellitus, and neurodegenerative diseases (4). Autoimmune diseases are a type of chronic inflammatoryconditions that affect the alimentary canal. An immune imbalance of the intestinal mucosa is linked to the chronic and complex inflammatory illness known as inflammatory bowel disease(5) Inflammatory bowel disease (IBD) refers to a collection of persistent inflammatory conditions that affect the part of the alimentary canal below the stomach. The incidence of IBD is rapidly increasing. Earlier the occurrence of IBD is more common in Western countries. However, due to environmental factors and lifestyle changes the incidence and their prevalence are rapidly increasing in Asian countries also (6).The episodes of gastrointestinal tract inflammation that reappear because of an aberrant immune response that targets the gutmicrobiota indicates IBD. The two forms of idiopathic intestinal disease that makeup IBD are distinguished from one another by the location and extent of their involvement in the bowel wall(7).

The two subtypes of IBD are Crohn's disease (CD) and ulcerative colitis (UC). The UC is a chronic inflammatory condition of the rectal and colonic mucosa and submucosa. It is a superficial ulceration, characterized by granularity, and a vascular pattern. It is an intestinal idiopathic condition. The causes can vary from genetics to environment to bacterial invasion and compromised immune system(8).In UC, there is a significant rise in the release of IL-13, the primary interleukin responsible for the inflammation and persistence of this condition. Despite the involvement of1T helper(Th1), UC patients also exhibit a T helper 2**(**Th2) response characterized by elevated secretion of IL-4, IL-5, and IL-9. The transcription factorPU.1, which controls cellular communication, may inhibit intestinal epithelial cell proliferation and control the expression of various tight-junction proteins when combined with IL-9 generated by Th9 cells(9) The CD is a chronic inflammatory condition with a segmental distribution of granuloma. It usually affects the terminal ileum and adjacent colon, but it can also affect the entire digestive tract. Certain cytokines, such as IL-12, IL-17, TNF-α, and IFN-γ, are locally released and have been associated with the chronic intestinal inflammation seen in CD patients. Th1lymphocyte differentiation is encouraged by the production of IL-12 and IL-18 by antigen-presenting cells (APC) and macrophages, which raises proinflammatory cytokines like TNF-α and IFN-γ. Furthermore, Th1 cytokines create a self-sustaining cycle in the inflammatory process by stimulating APCs to release a wider range of inflammatory cytokines, such as IL-1, IL-6, IL-8, IL-12, and IL-18(10). Fig 1indicates the distribution pattern of UC and CD in IBD. Crohn's disease predominately damages the mucosal lining of colon and ileum, whereas colitis disrupts the same in the rectal and colon mucosal lining. The anatomical difference is indicated in Fig 1. Various synthetic medicines are employed in the treatment of IBD but theconcerns over increased side effects due to synthetic medicines,lack of conclusive treatments for chronic conditions, high costs of new drugs, microbial resistance, and the emergence of new diseases have all increased interest in complementary and traditional medicine among the people.This review paper aims to investigate the etiology, challenges in the current treatment options, the

impact of phytoconstituent, alternative treatments, and lifestyle changes that can treat the conditions of IBD by reducing the side effects associated with the administration of synthetic drugs. The review also focuses on the effect of medicinal plants and herbal extracts on IBD along with their shortcomings. This review is an attempt to shed light even on the under-explored medicinal plants used in the treatment of the disease and its related symptoms.

HISTORY OF INFLAMMATORY BOWEL DISEASES

Matthew Baillie (1793) reportedthe earliest documentation of a severe bowel disease resembling contemporary UC. The term "ulcerative colitis" was later coined by Samuel Wilks (1859) in London, as he described a patient whose bowel condition today might be classified more in line with (CD). He described a condition similar to the contemporary understanding of UC. Throughout the latter half of the 19thcentury, reports of severe and persistent diarrheal diseases not attributed to infectious origins accumulated. In 1888, following the emergence of germ theory, Sir William Hale White published a comprehensive description of cases he had encountered, this publication marked the entry of the term into general medical usage and contributed significantly to the understanding of the disease(11). Morgagni, Combe, Saunders,and Abercrombie, reported cases with symptoms resembling Crohn's. Abraham Colles in 1830 described the disease in children, and Samuel Fenwickin 1889 observed characteristic features during autopsy. The first CD series cases were published by Scottish surgeon Thomas Kennedy Dalziel in the *British Medical Journal* (1861–1924)(12). By 1920, American physicians identified hyperplastic, granulomatous lesions in the intestinal tract, initially termed "hyperplastic intestinal tuberculosis." The disease showed similarities across countries, affecting young patients and often requiring surgery(13). Before the landmark 1932 paper published by Crohn *et al.* (1932), Nuboer(14)and Bissellreported instances of a similar disease. In 1936, Crohndescribed patients with combined ileitis and right-sided colitis. The acceptance of colonic involvement in Crohn 's-like lesions in America took until the late 1950s and early 1960s(15).Pathologically, Coffey in 1938 emphasized the granulomatous inflammatory process, formation of fistulas, and stenosis. Hadfield in 1939 highlighted the thickening of the ileum, fistulas, giant-cell systems, and lymphedema(16) Warren and Sommers SC(1948) described it as a progressive sclerosing granulomatous lymphangitis. Rappaport's 1951 study identified key features like adherent mesentery, thickened bowel, fistulas, ulcers, cobblestone mucosa, and a distinct histological pattern with granulomas(17).

OCCURRENCE

IBD predominantly impacts young adults, it can occur across all age groups, with 25% of cases emerging before the age of 20. The adolescent stage is the most prevalent period for IBD in children. However, 20% of affected children exhibit symptoms before reaching the age of 10, and 5% before turning 5. Recent studies indicate a significant increase in very early onset IBD, particularly in regions with historically high rates of both paediatric and adult-onset IBD. The global incidence of IBD is on the rise, with childhood-onset IBD surpassing adult-onset IBD in frequency(18)

IMPACT OF IBD ACROSS THE GLOBE

IBD has become a global health burden over 0.3% of the population is affected by this condition. Even in a country like India, which has the largest population in the world, a considerably large amount of population has been affected by IBD (19). More than 7 million individuals in Europe and the United States are projected to experience IBD by the year 2030(20). It is estimated that in 2023 over 320,0000 Canadians were suffered from IBD (21). The significant increase in the occurrence of IBD in rapidly advancing nations like India surpasses the impact solely attributable to genetic factors. This highlights the growing importance of environmental elements in the intricate and diverse nature of this disease. A recent study indicated that approximately 1.4 million individuals in India are estimated to be affected by IBD (22).

ETIOLOGY OF IBD

The origins of IBD, encompassing CD and UC, remain intricate and involve a multifaceted interplay of genetic, environmental, and immunological factors (Figure 2). The etiology of IBD can be delineated as follows:

Genetic Influences

- **Genetic Variability**: Various genetic variations have been linked to an increased susceptibility to IBD, particularly in genes associated with immune function, epithelial barrier integrity, and inflammatory response. Genetic variables associated with the gut microbiota that may predispose to UC or CD are reported. Strong correlations have also been found between gene ATG16L1 T300A, CARD9 (Caspase recruitment domain-containing protein 9), CLEC7A (C-type lectin domain family 7 member A), and IBD in addition to NOD2(nucleotide-binding oligomerization domain-2). In individuals with IBD, genetic variables and modified gut microbiota are also linked to an immune system activation during the disease's flare-up(23).
- **Family Background**:
  The family history of IBD remains the strongest recognizable factor for the development of inflammatory bowel diseases and is reported in about 8-12% of patients. CD shows a much more frequent familial pattern than ulcerative colitis. IBD displays a pronounced genetic predisposition, with individuals having a family history of the disease being at an elevated risk(24).

Immunological Factors:

- **Aberrant Immune Response**: IBD manifests through an anomalous immune response within the gastrointestinal tract, where the immune system erroneously targets and assaults the body's intestinal tissues, resulting in persistent inflammation. Several types of innate cells like neutrophils in intestinal inflammation through the impairment in the epithelial barrier function, release several inflammatory mediators like IL-6,IL-8,IL-12 TNF. The immune characteristics of IBD evolve from the abnormal responses of the innate and adaptive immune response. The number of TH17(T Helper cells 17)/Treg proportions is important in developing inflammation(25).
- **Immunodeficiency**: Some individuals with IBD may exhibit immune system defects, rendering them more vulnerable to infections and prompting inflammatory responses(26)
- **Nonsteroidal anti-inflammatory drugs (NSAIDs):**NSAIDs include ibuprofen, naproxen sodium, diclofenac sodium, and similar medications, have the potential to increase the risk of developing inflammatory bowel disease (IBD) or worsen the disease for those who are already suffering from it(27)

Lifestyle changes

Lifestyles are heterogeneous which affects the individual life span with IBD.

- **Smoking**: Smoking is one known factor that raises the risk of developing Crohn's disease. The relationship between smoking and IBD is intricate and not entirely elucidated. The harmful effect of tobacco is because of changes in microcirculation in the intestine (28).
- **Dietary Influence**: The role of diet in IBD is intricate and not fully comprehended, certain dietary elements, such as a high-fat diet or specific additives, may play a role in influencing the risk or exacerbation of IBD (29). A study conducted in Japan discovered a more than twofold increased risk of CD associated with the intake of sugars/sweeteners, sweets, fats, and oils, as well as total fat consumption(30)
- **Infections:** Gastrointestinal infections can induce abnormal immune responses and may be associated with the onset of IBD in certain instances. *Mycobacterium aviumparatuberculosis*, Helicobacter species in primate colitiswhich induces to release of TNF and IL to cause inflammation(31).

Epithelial Barrier Dysfunction

The intestinal mucosal barrier is a complex structure that separates the intestinal lumen and the sterile extracellular internal milieu of the body. The connection between the intestinal lumen in the body is required for the absorption of electrolytes and to enhance the immunity to increase microbiota to resist toxins and pathogens(32)

- **Intestinal Permeability:** The "leaky gut" also known as increased intestinal permeabilityis normally present in IBD. Changes in the integrity of the intestinal epithelial barrier can contribute to IBD development, allowing the entry of bacteria and other substances that trigger an immune response(33)
- **Microbiota Alterations**: The gut microbiota acts as a metabolic organ, slight deviations in the composition and function of gut microbiota are implicated in IBD development, with imbalances between beneficial and harmful

bacteria potentially contributing to inflammation(34) It is crucial to recognize that the precise causative factors of IBD can vary among individuals, and a combination of genetic predisposition, environmental influences, and immune system dysregulation likely contributes to the development of these conditions.

SYMPTOMS

IBD is a characteristic pleomorphic clinical manifestation. UC isexpressed by inflammation of the colon's mucous membrane, usually starting in the rectum andproximal extension in a symmetrical and continuous pattern. The severity and extent of the disease can vary among individuals. Symptoms commonly include bloody diarrhoea, rectal bleeding, abdominal pain, faecal incontinence, and tenesmus. The systemic symptoms likefever, nausea, and vomiting in case of a severe attack(35)CD affects the whole gastrointestinal tract from the oral cavity to the perianal part. The symptoms are heterogeneous and include abdominal pain, loss of weight, and chronic diarrhoea(36).

- **Diarrhoea with Blood or Mucus:**
  Both UC andCD can cause diarrhoea, which may be associated with blood or mucus. Bloody diarrhoea that recurs is a common symptom ofIBD. The primary cause of the intricate underlying mechanisms of diarrhoea linked to IBD is persistent inflammation, which harms the mucosal lining. This damage results in impaired intestinal ion transport, impaired function of the epithelial barrier, and increased pathogen accessibility to the intestinal mucosa (37)
- **Constipation in Ulcerative Colitis:**
  It isobserved that some patients with UCmay present with constipation, particularly when the disease is localized to the rectum. Depending on the severity and extent of the inflammatory conditions, this can change.
- **Abdominal Pain, Tenesmus, and Severe Urgency:**
  Abdominal pain, tenesmus (the feeling of incomplete defecation with an urgent need to defecate), and severe urgency are common symptoms in both UCand CD (37)
- **Location of Pain:**
  The CD may present with right lower quadrant pain, whereas UCmay present with left lower quadrant pain. The specific location of the pain can sometimes help differentiate between the two conditions(38)
- **Nausea and Vomiting More Common in Crohn's Disease:**
  Nausea and vomiting are mentioned as more common in CD. Inflammation in the upper part of the digestive tract in CD can contribute to these symptoms(39)

TREATMENT OPTIONS

Non-biological therapies: The non-biological therapies include salicylates, corticosteroids, and calcineurin inhibitors like tacrolimus are used in the treatment of IBD(40).

Immuno modulators : Immuno modulators that modify the activities of the immune system like azathioprine, 6-mercaptopurine, methotrexate, and cyclosporine are used in the treatment of IBD(41)

Biologicals: The current approved biological treatments for IBD include four anti-TNF (tumor necrosis factor) agents such as infliximab, adalimumab, golimumab, and certolizumab. These medications work by targeting TNF, a pro-inflammatory cytokine implicated in the pathogenesis of IBD. In addition to anti-TNF agents, there are two adhesion molecule antagonists approved for IBD treatmentnatalizumab and vedolizumab. Natalizumab targets α4-integrin, an adhesion molecule involved in immune cell trafficking to the gut. Vedolizumab targets the $\alpha 4\beta 7$ integrin, selectively inhibiting the migration of immune cells to the gut. Furthermore, ustekinumab is approved for the treatment of CD. It is a monoclonal antibody that targets interleukin-12 (IL-12) and interleukin-23 (IL-23), which are involved in the inflammatory response(42)

Surgical treatments: The choice of surgical approach depends on various factors such as the location and extent of the strictures, the patient's health, and the surgeon's expertise. Some of the surgical approaches are strictureplasty,

bowel resection, laparoscopic surgery, ileocecal valve preservation, stricturoplasty with resection, and temporary ostomy(43).

CHALLENGES IN CURRENT TREATMENT APPROACHES IN IBD.

IBD including the conditions such as CD and UC, pose significant challenges in synthetic treatment.

Effectiveness of current treatment

Various medication options are available to cure inflammatory bowel diseases including immunomodulators, corticosteroids, and biologicals. However, not all the patients respond equally to these treatment options(44)

Development of Antibodies to Biologics

The individuals who developed antibodies had a reduced response to biologicals, leading to diminished long-term efficacy in controlling CD. The presence of antibodies correlated with an increased risk of infusion reaction and a shorter duration of response to the medication (45).

Limited Treatment Options for Non-Responders:

Many patients undergoing treatment with anti-TNFα agents, encompassing both primary and secondary non-responders, exhibit instances of treatment failure. Therefore, the treatment options are limited to non-responders (46).Approximately 23–46% of patients experienced secondary loss of response after a year of treatment, while up to 40% of patients in clinical trials and 10-15% of patients in clinical series showed primary non-reaction to TNF-α inhibitors(47).

Management of Paediatric IBD

Thiopurines are a class of immunosuppressive medications prominently used in the treatment of paediatricIBD. However, the adverse events associated with thiopurines correlate with metabolites suggesting an exploration of whether specific metabolites in the body are associated with adverse events related to the treatment(48).

Therapeutic Drug Monitoring issues

Therapeutic drug monitoring (TDM) plays an important role in optimizing the treatment among patients with IBD. But the several challenges like interpatient variability, lack of standardization, clinical correlation, and cost accessibility are the main TDM issues that arise during the implementation of TDM for biological treatments in these conditions (49).

Adverse effects of IBD treatments

Although amino salicylates are widely used in the treatment of IBD, they exhibitunfavorable side effects like headaches, heartburn, nausea, and vomiting. Corticosteroids used in IBD cause weight gain, facial hair, diabetes, hypertension, acne, and decreased bone mass. Additionally, the repeated use of corticosteroids increases the susceptibility of patients to endemic infections by micro-organisms, fungi, and pathogens(50).Cyclosporine is used to treat severe UC by preventing activated T cells from producing IL-2. However, it can cause minor side effects like fever, headaches, and diabetes mellitus, as well as symptoms like impaired renal function, hypertension, and neurotoxicity (tremor or paraesthesia)(51)

MEDICINAL PLANTS AND HERBS

Since traditional medicines have been used for thousands of years to treat a variety of disorders, they play a significant role in the search for alternative biologically effective compounds, as the predominance in chronic diseases, including cardiovascular diseases, cancer, diabetes, etc. The usage of plant-based nutrients, also known as nutraceuticals, and herbal medicines continues to expand quickly worldwide, with many individuals turning to these products in various national healthcare settings to treat a variety of health issues(52)It is estimated that 80 percent of the population around the globe practice traditional medicine. Presently, 170 of the 194 WHO Member States have

recognized the use of traditional medicine and their governments have asked for WHO's support in creating a body of reliable evidence and data on traditional medicine practices and products(53)

Growing interest in natural remedies and plant-based therapies

In the last century, the advancement and mass manufacturing of synthetically produced medications have transformed healthcare globally. Despite this progress, significant portions of the population in developing nations continue to turn to traditional healers and herbal remedies as their main source of healthcare. In Africa, as many as 90% of people, and in India, 70% rely on traditional medicine to address their healthcare requirements. The application of traditional medicine is not confined to developing countries; instead, there has been a notable surge in public interest in natural therapies within industrialized nations over the past two decades. This heightened interest has resulted in a greater acceptance and use of ethnobotanicals(52).

IIMEDICINAL PLANTS IN INFLAMMATORY BOWEL DISEASES

Herbal medicine, especially in the form of herbal therapies,is widely used by patients with inflammatory bowel disease (IBD) in both Western and several Asian countries, including China and India. It appears that the use of these natural products is steadily rising, despite the paucity of controlled trials examining their efficacy and safety(54).Herbal therapies have demonstrated encouraging results in the management of IBD, with no significant side effects. Through a range of mechanisms, including immune system regulation, antioxidant properties, leukotriene B4 inhibition, NF-κB suppression, and antiplatelet effects, these therapies show promise in the management of IBD(55).The table 1 provides information related to the herbs, their extracts and isolated bioactive compounds with anti-inflammatory activity in the *in vitro* model.

***IN-VIVO* MODELS OF MEDICINAL PLANTS USED IN IBD**

Anti-inflammatory activities of medicinal plants, their extracts or fractions as well as the phytobioactives(plant-derived biologically active chemical compounds) isolated from them not only shown *in vitro* anti-inflammatory activities through various mechanisms but also proven potent anti-inflammatory agents in the *invivo* models. Detailed information on potent herbs and related material's *in vivo* anti-inflammatory potency is given in Table 2.

CLINICAL TRIALS

Multiple clinical trials have been conducted using isolated phytoconstituents and active phytobio actives and plant extracts. Different study designs such as randomized trial, single blind and double blind studies have been utilized for analyzing the impact of plant based phytochemicals on human subjects which are described in Table 3.

As mentioned in the above tables, plenty of *in vitro* ,*in vivo*, and clinical studies have evaluated the effects of phytoconstituent in IBD. Numerous studies on plants show significant key pathways and relevant evidence on the usage of plant derivatives in the treatment of IBD. Among the plants reviewed only a few plants and their related materials possess both in vitro and in vivo anti-inflammatory activities. Hence, the present review focuses on curcumin, Bilobalide, *Boswellia serrata,* Liquorice,quercetin, garlic, and *Andrographis paniculata* as they are reported to possess significant anti-inflammatory activity.

Curcumin

Curcumin [1,7-Bis(4-hydroxy-3-methoxyphenyl)-1,6-heptadiene 3,5-dione] has a significant prominence in the research field because of its therapeutic properties (87,88). Curcumin is an active yellow pigment and a naturally obtained phenolic compound from the *Curcuma longa* commonly known as "turmeric rhizome". Turmeric has been used as a medicinal supplement for various digestive problems. Isolating the curcumin from the turmeric so that it can be used at a higher rate to treat IBD and other digestive conditions(89).Curcumin possesses wide number of pharmacological activities, including anti-oxidant, anti-carcinogenic, neuroprotective, anti-inflammatory,and anti-proliferative activities(90). Curcumin has been used to be a therapeutic molecule in various illnesses such as cancer, cardiovascular diseases, gallstone formation, arthritis, neurological disease, diabetes, and IBD(91).An abnormal immune response is the root cause of IBD, by merging an initial dysfunction in the natural immune response with an imbalanced T-cell reaction during the prolonged phase of the illness. The recruitment of neutrophils may play a

major role in the progression of CD.Neutrophils are a type of white blood cell that plays a crucial role in the body's immune response, particularly in combating bacterial infections. In the CD, the deficiency or dysfunction in the recruitment of neutrophils could lead to difficulties in clearing bacterial infections(92).The neutrophil accumulation and their ability to clear bacteria are compromised, it may create conditions that favor the formation of granulomatous inflammation in CD. Granulomas are a condition where clusters of immune cells can form in response to tenacious inflammation, and they are a characteristic feature of CD. IBD, including CD, often focuses on understanding the immune system's role in maintaining gut homeostasis and responding to potential threats like bacteria. Identifying specific mechanisms involving neutrophils and their impaired recruitment could contribute to a better understanding of the underlying causes of CD and potentially lead to the development of targeted therapeutic approaches. It's important to note that the understanding of these processes is continually evolving as new research emerges. Curcumin inhibits the formation of chemokine gradients, which lowers the recruitment of neutrophils to inflammatory sites ((93)The mechanism of curcumin in IBD in anti-inflammatory action is by inhibition of Nuclear factor kappa B(NF-κb), by blocking the inhibitor of nuclear factor kappa B (IκB) kinase, thereby inhibiting the expression of pro-inflammatory cytokines interleukin-1 (IL-1), IL-6, and tumor necrosis factor-α (TNF-α) (IL-1, IL-6, and TNF-α)1(94)The management of IBD primarily revolves around mitigating inflammation to enhance symptom relief. Currently, the efficacy of anti-inflammatory and immunosuppressive drugs in clinical settings is suboptimal. Curcumin is being explored as a promising IBD treatment due to its notable anti-inflammatory properties and safety profile. The potential mechanisms through which curcumin exerts its anti-inflammatory effects involve targeting specific molecular pathways(95).

The *in-vitro* anti-inflammatory activity of curcumin is evaluated using a model for IBDin which the anti-inflammatory responses will be induced in cell cultures to mimic the conditionsobserved in IBD. The ability of turmeric extract to modulate inflammatory pathways through its interaction with solute carrier protein 22 A4 (SLC22A4) and IL-10 variants will be investigated. The *in-vitro* model of IBD using HEK293 cells shows that the turmeric and fractions reduce the abnormal transport function linked to the SLC22A4 503F variant and boost the activity of the IL-10 promoter variant (ACC −1082 A), which shows positive activity in IBD (56). The *in-vivo* activity by conducted by Altinel *et al* (2020) in a mouse model of2,4,6-trinitrobenzene sulfonic acid(TNBS)induced colitis allowed them to examine the functions of oral curcumin against NF-kB activity. Oral Curcumin significantly reduced colonic levels of NF-kB when compared to the control group. Moreover, biochemistry analysis revealed decreased expression of TNF-α and platelet-derived growth factor (PDGF) in the oral curcumin group(67). The terms of clinical studies on IBD, Holt and Katz (2005) conducted a pilot study to examine a global score involving five UC patients revealed that supplementing patients with UC with 550 mg of curcumin twice a day for one month, and then 550 mg three times a day for the following month, significantly ($p < 0.02$) improved the quantity and quality of stools. In the same study, five CD patients received 360 mg of curcumin three times a day for one month, and then four times a day for two months, to test curcumin's effectiveness as an adjuvant therapy to current CD treatments. For every subject, the C reactive protein (CRP)levels and Crohn's Disease Activity Index (CDAI) score decreased(78). Curcumin demonstrated a noteworthy ability to achieve clinical remission in individuals with active mild-to-moderate UC. It lowered the probability of clinical relapse in those with quiescent patients. Its inhibition of NF-κB, coupled with its unparalleled safety record suggests its ongoing efficacy in UC treatment. Moreover, curcumin, being a non-toxic, cost-effective, and readily accessible natural polyphenol, further supports its suitability for UC therapy(96).

Bilobalide

Bilobalide is an organic compound classified as a sesquiterpene tri lactone, naturally occurring in the leaves of the *Ginkgo biloba*(97)**.***Ginkgobiloba* L. (Ginkgoaceae), is referred to as a "living fossil," it has been used for a long time for medicinal use. Bilobalide has been shown to have a variety of pharmacological effects, including those that areanti-ischemic, antiplatelet, hemorheological actions, neuroprotective, anti-inflammatory, antioxidative, and cardiovascular protective(98). The mechanism of action of bilobalides in inflammatory bowel diseases is through macrophage polarization. In a cell model induced by lipopolysaccharide (LPS), bilobalide (isolated from *Ginkgo biloba*) was found to reduce p65 accumulation within cell nuclei and release it into the extracellular space. This implies that bilobalide inhibits M1 polarization by encouraging the NF-κB pathway to become activated(99). The *in-*

vitro inflammatory model for IBD using a bone marrow-derived macrophage (BMDMs) in PBS was used along with a 21-gauge needle to flush femurs. For five days, the cells were cultured in a 10% FBS RPMI 1640 medium at 37°C with 5% CO_2. Before being cultured in a fresh DMEM medium containing 10% FBS, 10 mg/ml LPS, and 10 ng/ml IFN-g (M1-polarization) for six hours, the adherent macrophages were twice washed with PBS. The levels of inflammatory cytokines, including tumor necrosis factor, interleukin 6 (IL-6), and IL-1βare reduced. The results indicated the suppression of the NF- kB signaling and inhibition in M1-induced inflammation. An *in-vivo* study conducted by Heng Zhang et.al.,(2020) investigated the anti-inflammatory activity of bilobalide by inducing colitis using a dextran sulfate sodium, and the outcome of the study showed that bilobalide alleviates the colonic inflammation in the micegiven with DSS and inhibits the decrease in length of the colon(73).

Boswellia serrata

*Boswellia serrata*is amember of the family Burseraceae and is commonly known as Salai or Salai guggul. This tree is native to dry mountain areas in India, Northern Africa, and the Middle East. The resin extracted from *Boswellia serrata* has historical use in Ayurvedic medicine, where it is valued for its potential health benefits(100). It is used as an anti-inflammatory, anti-arthritic, antihyperlipidemic, antiatherosclerosis, analgesic, and hepatoprotective agent**.** It is effectivein the treatment of various illnesses, including fevers, skin conditions like boils and ringworm, and gastrointestinal problems like diarrhoea and dysentery. It also treats respiratory conditions like asthma and bronchitis, oral and throat discomfort, and various cardiovascular problems(101). Boswellia's ability to inhibit NF-κB and lipoxygenases is linked to its anti-inflammatory properties. Additionally, the gut anti-inflammatory effect of Boswellia was linked to the inhibition of lipid peroxidation, and effects on the immune system, such as decreased cytokines (interleukins and TNF-α) and the elevation of superoxide dismutase levels, which support the antioxidant activity of the plant(102). Administration of Boswellia extract in an *in-vitro* intestinal inflammatory model involving colonic epithelial cell monolayer induced with H_2O_2leadsto the expression of the phosphorylated NF-κBand reactive oxygen species production. Caco-2 cells (a human colorectal adenocarcinoma cell line) The cell lines of colonic on Boswellia reported in Caco-2 cells shows decreased in the transepithelial electrical resistance, increase in paracellular permeability and also encourage its safe use as an adjuvant in IBD treatment (103). Shefali Thanawalaet. al (2021) studied the efficacy of *Boswellia serrata*extract in the DSS-induced colitis model. Results of the study revealed a reduction in the DAI score and improved colon length ensuring that Boswellia will be a promising herb in the treatment of IBD and gut health management(104)**.** Gupta *et al.*(2001) conducted a study on 30 patients suffering from chronic UC. Among them, 20 patients were given Boswellia gum preparation (900 mg daily divided into 3 doses for 6 weeks), and 10 patients were given sulfasalazine (3 gm daily divided into 3 doses for 6 weeks). The study concluded that treatment with Boswellia lead to effective improvement in the lowering of fecal calprotectin(85). The clinical study on 43 patients with UC supplemented with *Boswellia serrata* extract indicated decreased bowel movements, occult blood in stools, cramps, and watery stool(105).

Liquorice

Liquorice, scientifically known as *Glycyrrhizaglabra* Linn, is an herbaceous plant classified within the Leguminosae family. The herbal plant and its compounds are valued for its various medicinal qualitiessuch as anti-inflammatory, antibacterial, antiviral, anti-allergic, and anticarcinogenic properties. Glycyrrhizin and glycyrrhetinic acid represent the main bioactive constituents isolated from Liquorice((106). The triterpene glycoside complex glycyrrhizin possesses cytotoxic effects against numerous cancer cell lines, including those originating from the colon, lung, leukemia, melanoma, and glioblastoma. Liquorice has been used to treat several digestive system issues, including colic, hyperdipsia, flatulence, and stomach ulcers. It has also been traditionally used to treat ailments such as psoriasis, jaundice, rheumatism, epilepsy, fever, and sexual debility(108). In the disease condition of UC, Liquorice improves colon histopathologyalong with the reduction in the levels of IL-6 and IL-7 and helps to repair the mitochondrial damage. The glycyrrhizinate extract also shown a strong anti-inflammatory effect by significantly reducing the inflammatory markers like NF-κB, ICAM-1,and TNF-αin the colonic mucosa (107). Inan *in-vitro* model of UC, Caco2 cells were exposed to lipopolysaccharide (LPS) for 24 hours to induce inflammatory cell damage. These cells were exposed to different concentrations of Liquorice drug-containing serum (DCSL) for an additional 24 hours. The levels of inflammatory markers were measured using ELISAand evaluated oxidative markers in treated cells.

Administration of Liquorice resulted in the reduction of IL-6, malondialdehyde (MDA), IL-1β, and TNF-α(62).Chunying Huang et al.(2021) investigated the *in-vivo*anti-inflammatory effect of Liquorice polysaccharide against dextran sulfate sodium-induced inflammatory model. The results of this study emphasize the potential therapeutical effect of Liquorice by decreasing colon shortening, diarrhoea, stool bleeding, and management of weight as the primary effectsof IBD(74).Hengchang Hu et.al.,(2022) conducted a meta-analysis of UC using randomized controlled trials on Liquorice with a total of 23 studies consisting of 2060 participants. The results of the study shown a decrease in the levels of TNF-α, IL-6, IL-8, and IL-17 with an increase in the expression of IL-10(82).

Quercetin

The yellow pigment found in apples, onions, citrus fruits, berries, grapes, broccoli, and tea is called quercetin(109). The quercetin (3,3',4',5,7-pentahydroxyflavone) derived from the Latin word Quercetum belongs to the class of the flavonols. Quercetin, an aglycone component of flavonoid glycosides obtained from plants, serves as a dietary supplement and exhibits the potential toprevent various ailments as an anti-inflammatory, antiviral, antitumor, anticancer, anti-ulcer, antiallergic, antidiabetic, gastroprotective, antihypertensive, immunomodulatory, and anti-infective agent(110).Quercetin is known to modify the relationship between microbes and the gut by restoring the bactericidal, pro-inflammatory, and anti-inflammatory functions of intestinal macrophages, which improves colitis(111). Quercetin acts on the IBD in UCby decreasing the pro-inflammatory cytokines production such as TNF-α, IL-1β, and IL-6 by suppressing the nuclear factor **(**NF-κB**)** and c-Jun N-terminal kinase **(**JNK**)**that indicates the better treatment option for patients with UC(112).Other mechanisms for the reduced colitis include inhibition of nitric oxide (NO) production and/or inducible nitric oxide synthase (iNOS) expression(113). The *in-vitro* model ofmacrophages RAW 264.7, cultivated in Dulbecco's modified Eagle's medium (DMEM) supplemented with 7.4 mg/ml DMEM, 24 mM $NaHCO_3$, 10 mM HEPES, 143 U/ml benzylpenicillin potassium, and 100 mg/ml streptomycin sulfate at pH 7.1 is treated with quercetin and the cells were kept at 37°C temperature with 5% CO_2 and 10% fetal bovine serum (FBS) was added to the culture medium. Addition of quercetin in to the media inhibited the NO production in the macrophage Raw 264.7 by suppressing the NF-kB indicating the potential activity of quercetin in the IBD(60). The *in-vivo* activity and the meta-analysis of the quercetin shown reduced histological score, disease activity index, TNF- α, increased colon length,nitric oxide, interleukin (IL-10), and superoxide dismutase and catalase(75).

Allium sativum

Garlic (*Allium sativum* L.) belongs to the Alliaceae family, which also includes onions, leeks, and chives. Garlic is a traditional herb used for various illnesses and physiological. Garlic is used as a culinary ingredient and medicinal remedy. The word "garlic" originated from the Celtic word 'all,' which means pungent(114).Garlic is an important bulb vegetable with a pungent odour that enhances the sensory characteristics of food and is known for its medicinal properties(115)**.**Garlic exhibits a broad spectrum of healing effects including antibacterial, antiviral, antidiabetic, anticancer, hepatoprotective, hypolipidemic, immune modulatory, diuretics, anti-asthmatic, anti-septic, anthelminthic, anti-mutagenic, platelets enhancing, liver protection and also in the treatment of common cold. Certain diseases are linked to immune dysfunctions and oxidative stress, often accompanied by acute or chronic inflammation, the ability of garlic to modify immune functions, and consequently impact oxidative stress responses, holds promise for disease treatment and prevention(116).The potential pharmacological activities of garlic bioactives includes antioxidant, anti-inflammatory, and immune stimulant properties (117). The effects of inflammatory conditions especially on immune system components contribute to a pro-inflammatory state, characterized by the release of inflammatory mediators, oxidative stress, and activation of different immune cells(118).Garlic or some of its compounds have been reported to regulate the production of cytokines and leukocytes. A T1-mediated response is the predominant sign of IBD. Garlic extract and its compounds considerably inhibit the production of TNF-α in addition to IFN- γand IL-2. This implies that the compounds found in the extract of garlic and the extract itself may have therapeutic value in treating inflammatory diseases like IBD. The production of T1 cell inflammatory cytokines is significantly decreased, but the production of IL-10 is increased (119). Garlic is therefore considered to be an advantageous prophylactic and inhibitory agent against inflammatory conditions of the stomach. Garlic extract has anti-inflammatory properties because of its dual impact on IL-10 and IL-12 in IBD. One of garlic's main components,

allicin, effectively suppressed TNF-αsecretion, supporting allicin's anti-inflammatory effects on intestinal epithelial cells(119). The *in-vitro* anti-inflammatory activity of *Allium sativum*, demonstrated the regulation cytokine production and leukocyte cell proliferation. The study investigates the beneficial effects of garlic in treating IBD patients, whole blood along with peripheral blood mononuclear cells (PBMCs) were stimulated in the presence of various concentrations of garlic extract. Theleukocyte cytokine production was determined by using multi parameter flow cytometry. The study shows that Garlic extract may help reduce IBD-related inflammation by suppressing Th1 and inflammatory cytokines and raisingthe production of IL-10(63). Xin Shao et.al (2020) conducted an *in-vivo* activity of garlic polysaccharides inDSS-induced colitis model. Administration of thegarlic sample resulted in increased colon length, feed intake with the decrease in DAI and the histological score (76).

Andrographis paniculata:

Andrographis paniculata, commonly referred to as Kalmegh, is a popular herb in South Asian traditionalmedicine. It is popularly known as the "king of bitters" and is also referred to as BHUI NEEM or "neem of the ground"belongs to the Acanthaceae family(120).It is a widely used herb because of its therapeutic value as an anti-malarial, anti-fungal, anti-fertility hepatoprotective, anti-hyperglycaemic agent, sore throat, anti-cancer, GI tract, and upper respiratory infection(121). The effect of *Andrographis paniculata*in an *in-vitro* IBD model consisting of murine macrophage cell line RAW264.7 cultured in the DMEM supplemented with 10% FBS, penicillin, and streptomycin are incubated at 37°c in a carbon dioxide atmosphere was studied. Results revealed that pretreatment with *Andrographis paniculata* for 12 hours suppressed the pro-inflammatory cytokines, inhibition of the NF-KB activation chemokines, NO, and lipid mediators (64).Evaluation of the influence of *Andrographispaniculata* extract in the *invivo* model of UC with DSS-induced colitis model shows a massive decrease in pro-inflammatory cytokine expression(like TNF-α and IL-6)(122).According to a study conducted by Sandborn *et al.,*(2013),the daily dose of 1,800 mg of HMPL-004 (extract consisting of *Andrographispaniculata*) was related to a higher chance of a clinical response in patients with UC than a placebo. This study shows an improvement in symptoms, such as decreased inflammation and alleviation of stomach pain or discomfort, is commonly referred to as a clinical response in the UC. According to this study, *Andrographis paniculata* extract at the recommended dose, was effective in treating the symptoms of mild to moderately active UC(79).

ALTERNATIVE TREATMENTS (Figure 3)

Complementary and Alternative medicine is emerging as one of the most sought out medicinal therapies across the globe. People often turn to complementary and alternative medicine (CAM) to manage their symptoms and chronic conditions and during times when modern medicine has little to no impact on their ailments. CAM includes practices and treatments that are not typically a part of conventional modern medicine. CAM primarily includes dietary and lifestyle changes or physical activities such as exercise and Yoga that could prevent or improve the condition of IBD.Figure3 shows the alternative medicine approaches comprised of prebiotics, probiotics and synbiotics, diet, exercise, and acupuncture.

Prebiotics, probiotics, and synbiotics

Probiotics are one of the most significant treatment options for the management of IBD. They have one of the key roles in the deterioration of pathological bacteria in the intestine. There is a need for the environment to sustain the development of gut microbes in IBD patients. Prebiotics and probiotics play a vital role in reconstructing the gut microflora in IBD patients. Prebiotics and probiotics therapy refer to the inclusion of beneficial and favourable bacteria which restricts the growth of harmful bacteria in the intestine. *Enterococcus faecium, Lactobacillus, and Bifidobacterium*, bacteria compete for nutrition in the intestine and thereby ensure that the harmful bacteria are not getting the required nutrients for their growth. They enhance the production of immunoglobulin A, butyric acid, and short-chain fatty acids(123). Several research studies have investigated the effectiveness of probiotics in animal models. A study conducted on genetically engineered bacteria and their effect on the DSS model of colitis shown that probiotic strains such as *Bifidobacterium* and *Lactobacillus* have shown beneficial effects on host cells. Multiple clinical studies also indicated that the probiotics in combination with conventional therapy reduce the effects of ulcerative colitis. The research also found that *Bifidobacterium infantis* suppressed the CRP and TNF - α levels in gastrointestinal

inflammatory disorders(124). Prebiotics are the food ingredients that encourage the growth of healthy bacteria. These bacteria are fermented by the gut microflora and metabolized into byproducts which are required by the gut microflora to sustain and enhance productivity and offer health significance to the host. Prebiotics have reduced the concentrations of inflammatory mediators such as IL-1α, IL-1β, IL-6, IL-12, TNF- α, and IFN- γ(125). They also reduced the numberof pathological bacteria in the intestine. Grape extracts and mushroom products are some of the generally used prebiotics. Prebiotics such as inulin and oligofructose combination have been proven to decrease inflammation in rats and also enhance the growth factor B. Prebiotics such as galactooligosaccharides when treated against colon inflammation improved stool consistency and increased the proportion of healthy bacteria(126). Synbiotics are a combination of probiotics and prebiotics. They enhance the activity of probiotics and offer synergistic activity. They stimulate the microbial growth in the intestine and inhibit pathogenic bacteria. Synbiotics have been used in animal models and human studies also. Multiple studies have been conducted to assess the effectiveness of synbiotics in both. It was found that the synbiotics reduce the plasma interleukin levels. They preserve weight loss, reduce DAI, and pose excellent anti-inflammatory activity. Clinical studies indicated that patients receiving the synbiotic formulation have decreased incomplete bowel movement, bloating, and diarrhoea sensations along with reduced inflammation and restricted endotoxin effect on the intestine (127).

Exercise

Exercise is one of the most sought complementary and alternative treatment options for the treatment of patients with IBD and it is also well associated with reduced risk of colorectal cancer. Based on many studies, it has been hypothesized that moderate-intensity exercise produces an anti-inflammatory effect. It also decreases visceral fat and inflammatory cytokines such as TNF and IL. Several studies showed that patients with low physical activity have low BMI and low vitamin D content. In general, patients with IBDs have higher rates of osteoporosis than the general population. Regular exercise regimens can help the patients overcome this condition. It also improves the quality of life among the patients. Exercise also regulates the risk of relapse and increases the metabolic activity of the body(128).

Diet

Diet is also one of the most prominent tools for the management of IBD. Exclusive enteral nutrition is comprised of an intake of liquid formulas that can provide a hundred percent nutrition. Patients with IBD are prone to malnutrition, and micronutrient deficiency which can lead to complicated health disorders. In children and adults with IBD such as CD, exclusive enteral nutrition is highly recommended. In the case of Ulcerative colitis, there was no significant evidence for the nutrients. Specific carbohydrate diet, Mediterranean diet, low FODMAP diet, and anti-inflammatory diet are a few types of dietary intake in treating IBD(133).

ACUPUNCTURE

Acupuncture is one of the ancient methods of treatment which was widely prevalent in Chinese medicine, and has been prevalent for 3000 years. Acupuncture involves inserting a metal needle into a point in the body and further slightly stimulating just enough to accommodate the needle to twist, lift, and twirl. Another version of acupuncture involves generating an electric impulse to the pressure point. In IBD, vagal nerve stimulation plays an important role in handling inflammatory disorders. Acupuncture is one of the methods that stimulates the vagus nerve(134). The cholinergic anti-inflammatory pathway (CAP) operates through vagal efferent fiber, which connects to enteric neurons. These neurons then release acetylcholine (ACh) at the synapse with immune cells. ACh subsequently binds to alpha-7-nicotinic ACh receptors on immune cells, thereby suppressing the release of tumor necrosis factor–α (TNF-α), a significant pro-inflammatory cytokine(135) Kim DH *et al.*(2017) study of acupuncture on animal models shows several beneficial effects in IBD of TNBS-induced colitis by improving weight loss, and inflammatory characteristics by decreasing the activity of neutrophil myeloperoxidase activity by alleviating serum IL-10 levels along with suppression of TNF-α and IL1-β as well as a reduction in TNF-α m RNA expression in the colon(136). Multiple clinical studies have also been conducted to assess the potential of acupuncture in clinical trials. Zhou *et al.*(2022) conducted a clinical trial that comprised 220 subjects who had UCwith acupuncture and moxibustion along

with sulfasalazine via the oral route, which resulted in improving the symptoms and decreasing endoscopic and cellular inflammation(137). The clinical study of Crohn's patients with acupuncture therapy in the randomized study on 51 subjects with mild to moderate disease condition group showed a decrease in the CDAI score. ChunhuiBao et.al (2022) study indicates that acupuncture enhances CD management by adjusting the balance of gut bacteria and reducing inflammation mediated by Th1/Th17 cells(138).

CONCLUSION

In conclusion, this comprehensive review provides a thorough exploration of IBD, specifically UC and CD. It encompasses the historical context, global prevalence, and the increasing impact of IBD on populations worldwide. The etiology of IBD, involving genetic, environmental, and immunological factors, is intricately examined. Clinical manifestations and diagnostic methodologies, including *in-vitro* and*in-vivo* studies, are detailed. The mechanisms of action of several phytoconstituents produced from materials such as curcumin, bilobalide, *Boswellia serrata*, Liquorice, quercetin, *Allium sativum*, and *Andrographis paniculata* are highlighted along with treatment alternatives, both traditional and alternative. To provide a whole picture of managing IBD, the review also includes complementary therapies such as acupuncture, exercise, diet, symbiotics, probiotics, and prebiotics. In conclusion, this study offers insights into the complex nature of IBD and its variety of treatment modalities, making it a useful tool for herbal drug researchers, doctors and other healthcare professionals. For a wide audience, the amalgamation of scientific, epidemiological, and historical viewpointsprovidesa comprehensive understanding of IBD.

Abbreviations

IBD- inflammatory bowel disease
GI tract – Gastrointestinal tract
UC – Ulcerative colitis
CD -Crohn's disease
IL – Interleukins
TH2- T helper 2
TNF -Tumor necrosis factor
Ach – Acetylcholine
NF -KB - Nuclear factor kappa B
CDAI-Crohn's Disease Activity Index
FBS-Fetal bovine serum
DAI -Disease activity index

REFERENCES

1. Chen L, Deng H, Cui H, Fang J, Zuo Z, Deng J, et al. Oncotarget 7204 www.impactjournals.com/oncotarget Inflammatory responses and inflammation-associated diseases in organs [Internet]. Vol. 9, Oncotarget. 2018. Available from: www.impactjournals.com/oncotarget/
2. McInnes IB, Gravallese EM. Immune-mediated inflammatory disease therapeutics: past, present and future. Vol. 21, Nature Reviews Immunology. Nature Research; 2021. p. 680–6.
3. Prescott SL. Early-life environmental determinants of allergic diseases and the wider pandemic of inflammatory noncommunicable diseases. Journal of Allergy and Clinical Immunology. 2013;131(1):23–30.
4. Roth GA, Abate D, Abate KH, Abay SM, Abbafati C, Abbasi N, et al. Global, regional, and national age-sex-specific mortality for 282 causes of death in 195 countries and territories, 1980–2017: a systematic analysis for the Global Burden of Disease Study 2017. The Lancet [Internet]. 2018 Nov;392(10159):1736–88. Available from: https://linkinghub.elsevier.com/retrieve/pii/S0140673618322037

5. Kaser A, Zeissig S, Blumberg RS. Genes and environment: How will our concepts on the pathophysiology of IBD develop in the future? In: Digestive Diseases. 2010. p. 395–405.
6. Banerjee R, Pal P, Patel R, Godbole S, Komawar A, Mudigonda S, et al. Inflammatory bowel disease (IBD) in rural and urban India: results from community colonoscopic evaluation of more than 30,000 symptomatic patients. The Lancet Regional Health - Southeast Asia. 2023 Dec 1;
7. Kaplan GG, Ng SC. Understanding and Preventing the Global Increase of Inflammatory Bowel Disease. Gastroenterology. 2017 Feb 1;152(2):313-321.e2.
8. Silverberg FRCPC MS, Satsangi FRCP FRCPE J, Ahmad MRCP T, Arnott MBChB MRCP ID, Bernstein CN, Brant SR, et al. Toward an integrated clinical, molecular and serological classification of inflammatory bowel disease: Report of a Working Party of the 2005 Montreal World Congress of Gastroenterology. Vol. 19, Can J Gastroenterol. 2005.
9. Ramos De Mattos BR, Pereira M, Garcia G, Nogueira JB, Paiatto LN, Albuquerque CG, et al. Inflammatory Bowel Disease: An Overview of Immune Mechanisms and Biological Treatments. 2015.
10. Duan L, Cheng S, Li L, Liu Y, Wang D, Liu G. Natural Anti-Inflammatory Compounds as Drug Candidates for Inflammatory Bowel Disease. Vol. 12, Frontiers in Pharmacology. Frontiers Media S.A.; 2021.
11. Actis GC, Pellicano R, Fagoonee S, Ribaldone DG. History of inflammatory bowel diseases. Vol. 8, Journal of Clinical Medicine. MDPI; 2019.
12. Kirsner JB. Historical origins of current IBD concepts [Internet]. Vol. 7, 0086•10•65897901 World Journal of Gastroenterology. 2001. Available from: www.wd.org.cn
13. Homer Coffen T. Nonspecific Granuloma of the Intes-tine Causing Intestinal Obstruction.
14. 14.Nuboer FJ. Chronische phlegmone van het ileum. Med J Geneesk. 1932;76:2989.
15. Crohn BB, Rosenak BD, Affiliations A. A COMBINED FORM OF ILEITIS AND COLITIS.
16. Hadfield, Geoffrey. The Primary Histological Lesion of Regional Ileitls. 1939;773–5.
17. Warre S, Sommers SC. CICATRIZING ENTERITIS (REGIONAL ILEITIS) AS A PATHOLOGIC ENTITY ANALYSIS OF ONE HUNDRED AND TWENTY CASES *. 1948 May.
18. Borowitz SM. The epidemiology of inflammatory bowel disease: Clues to pathogenesis? Vol. 10, Frontiers in Pediatrics. Frontiers Media S.A.; 2023.
19. Desai D, Dhoble P. Rapidly changing epidemiology of inflammatory bowel disease: Time to gear up for the challenge before it is too late. Indian Journal of Gastroenterology. Springer; 2023.
20. Hammer T, Langholz E. The epidemiology of inflammatory bowel disease: balance between East and West? A narrative review. Dig Med Res. 2020 Dec;3:48–48.
21. Windsor JW, Kuenzig ME, Murthy SK, Bitton A, Bernstein CN, Jones JL, et al. The 2023 Impact of Inflammatory Bowel Disease in Canada: Executive Summary. J Can Assoc Gastroenterol. 2023 Sep 5;6(Supplement_2):S1–8.
22. Snell A, Segal J, Limdi J, Banerjee R. inflammatory bowel disease in India: challenges and opportunities. Frontline Gastroenterol. 2021 Sep 1;12(6):390-6.
23. Jarmakiewicz-Czaja S, Zielińska M, Sokal A, Filip R. Genetic and Epigenetic Etiology of Inflammatory Bowel Disease: An Update. Vol. 13, Genes. MDPI; 2022.
24. Santos MPC, Gomes C, Torres J. Familial and ethnic risk in inflammatory bowel disease. Vol. 31, Annals of Gastroenterology. Hellenic Society of Gastroenterology; 2018. p. 14–23.
25. Sartor RB. Mechanisms of disease: Pathogenesis of Crohn's disease and ulcerative colitis. Vol. 3, Nature Clinical Practice Gastroenterology and Hepatology. 2006. p. 390–407.
26. Silva FAR, Rodrigues BL, Ayrizono MDLS, Leal RF. The Immunological Basis of Inflammatory Bowel Disease. Vol. 2016, Gastroenterology Research and Practice. Hindawi Publishing Corporation; 2016.
27. Habib I, Mazulis A, Roginsky G, Ehrenpreis ED. Nonsteroidal anti-inflammatory drugs and inflammatory bowel disease: Pathophysiology and clinical associations. Vol. 20, Inflammatory Bowel Diseases. Lippincott Williams and Wilkins; 2014. p. 2493–502.
28. Hugot JP, Zouali H, Lesage S, Thomas G. Etiology of the inflammatory bowel diseases. Int J Colorectal Dis. 1999 Feb;14(1):2–9.
29. Lewis JD, Abreu MT. Diet as a Trigger or Therapy for Inflammatory Bowel Diseases. Gastroenterology. 2017 Feb 1;152(2):398-414.e6.

30. Sakamoto N, Kono S, Wakai K, Fukuda Y, Satomi M, Shimoyama T, et al. Dietary Risk Factors for Inflammatory Bowel Disease A Multicenter Case-Control Study in Japan. 2005.
31. Hansen R, Thomson JM, El-Omar EM, Hold GL. The role of infection in the aetiology of inflammatory bowel disease. Vol. 45, Journal of Gastroenterology. 2010. p. 266–76.
32. Bischoff SC, Barbara G, Buurman W, Ockhuizen T, Schulzke JD, Serino M, et al. Intestinal permeability - a new target for disease prevention and therapy. Vol. 14, BMC Gastroenterology. BioMed Central Ltd.; 2014.
33. Vanuytsel T, Tack J, Farre R. The Role of Intestinal Permeability in Gastrointestinal Disorders and Current Methods of Evaluation. Vol. 8, Frontiers in Nutrition. Frontiers Media S.A.; 2021.
34. Khan I, Ullah N, Zha L, Bai Y, Khan A, Zhao T, et al. Alteration of gut microbiota in inflammatory bowel disease (IBD): Cause or consequence? IBD treatment targeting the gut microbiome. Vol. 8, Pathogens. MDPI AG; 2019.
35. Dignass A, Eliakim R, Magro F, Maaser C, Chowers Y, Geboes K, et al. Second European evidence-based consensus on the diagnosis and management of ulcerative colitis Part 1: Definitions and diagnosis. Vol. 6, Journal of Crohn's and Colitis. 2012. p. 965–90.
36. Nóbrega VG, Silva IN de N, Brito BS, Silva J, da SILVA MCM, Santana GO. The onset of clinical manifestations in inflammatory bowel disease patients. Arq Gastroenterol. 2018 Jul 1;55(3):290–5.
37. Bielefeldt K, Davis B, Binion DG. Pain and inflammatory bowel disease. Vol. 15, Inflammatory Bowel Diseases. 2009. p. 778–88.
38. Zeitz J, Ak M, Muller-Mottet S, Scharl S, Biedermann L, Fournier N, et al. Pain in IBD patients: Very frequent and frequently insufficiently taken into account. PLoS One. 2016 Jun 1;11(6).
39. Feuerstein JD, Cheifetz AS. Crohn Disease: Epidemiology, Diagnosis, and Management. Vol. 92, Mayo Clinic Proceedings. Elsevier Ltd; 2017. p. 1088–103.
40. Cai Z, Wang S, Li J. Treatment of Inflammatory Bowel Disease: A Comprehensive Review. Vol. 8, Frontiers in Medicine. Frontiers Media S.A.; 2021.
41. Ooi CJ, Hilmi I, Banerjee R, Chuah SW, Ng SC, Wei SC, et al. Best practices on immunomodulators and biologic agents for ulcerative colitis and Crohn's disease in Asia. Vol. 34, Journal of Gastroenterology and Hepatology (Australia). Blackwell Publishing; 2019. p. 1296–315.
42. Banerjee R, Ali RAR, Wei SC, Adsul S. Biologics for the management of inflammatory bowel disease: A review in tuberculosis-endemic countries. Gut Liver. 2020 Nov 1;14(6):685–98.
43. Mohan HM, Coffey JC. Surgical treatment of intestinal stricture in inflammatory bowel disease. Vol. 21, Journal of Digestive Diseases. Blackwell Publishing; 2020. p. 355–9.
44. Burger D, Travis S. Conventional medical management of inflammatory bowel disease. Gastroenterology. 2011;140(6):1827-1837.e2.
45. Baert F, Noman M, Vermeire S, Van Assche G, Carbonez A, Rutgeerts P. Influence of Immunogenicity on the Long-Term Efficacy of Infliximab in Crohn's Disease [Internet]. Vol. 7, n engl j med. 2003. Available from: www.nejm.org
46. Higashiyama M, Hokaria R. New and Emerging Treatments for Inflammatory Bowel Disease. Vol. 104, Digestion. S. Karger AG; 2023. p. 74–81.
47. Ben-Horin S, Kopylov U, Chowers Y. Optimizing anti-TNF treatments in inflammatory bowel disease. Vol. 13, Autoimmunity Reviews. 2014. p. 24–30.
48. Jagt JZ, Pothof CD, Buiter HJC, van Limbergen JE, van Wijk MP, Benninga MA, et al. Adverse Events of Thiopurine Therapy in Pediatric Inflammatory Bowel Disease and Correlations with Metabolites: A Cohort Study. Dig Dis Sci. 2022 Jan 1;67(1):241–51.
49. Papamichael K, Stocco G, Ruiz Del Agua A. Challenges in Therapeutic Drug Monitoring: Optimizing Biological Treatments in Patients With Inflammatory Bowel Disease and Other Immune-Mediated Inflammatory Diseases [Internet]. 2023. Available from: http://journals.lww.com/drug-monitoring
50. Stallmach A, Hagel S, Bruns T. Adverse effects of biologics used for treating IBD. Best Pract Res Clin Gastroenterol. 2010 Apr;24(2):167–82.
51. Van Assche G, Noman M, Verine Vermeire S, Hiele M, Asnong K, Arts J, et al. Randomized, Double-Blind Comparison of 4 mg/kg Versus 2 mg/kg Intravenous Cyclosporine in Severe Ulcerative Colitis. 2003;

52. Rastogi S, Pandey MM, Rawat AKS. Traditional herbs: a remedy for cardiovascular disorders. Phytomedicine. 2016 Oct 15;23(11):1082–9.
53. WORLD HEALTH ORGANIZATION. WHO Establishes the Global Centre for Traditional Medicine in India. 2022 Mar 25 [cited 2024 Apr 15]; Available from: Online document at: www. who. int/news/item/25-03-2022-who-establishes-the-global-centre-for-traditional-medicine-in-india Accessed December. 2023;10
54. Ke F, Yadav PK, Ju LZ. Herbal medicine in the treatment of ulcerative colitis. Vol. 18, Saudi Journal of Gastroenterology. 2012. p. 3–10.
55. Rahimi R, Mozaffari S, Abdollahi M. On the use of herbal medicines in management of inflammatory bowel diseases: A systematic review of animal and human studies. Vol. 54, Digestive Diseases and Sciences. 2009. p. 471–80.
56. McCann MJ, Johnston S, Reilly K, Men X, Burgess EJ, Perry NB, et al. The effect of turmeric (Curcuma longa) extract on the functionality of the solute carrier protein 22 A4 (SLC22A4) and interleukin-10 (IL-10) variants associated with inflammatory bowel disease. Nutrients. 2014 Oct 13;6(10):4178–90.
57. Zhang Z, Shen P, Lu X, Li Y, Liu J, Liu B, et al. In vivo and in vitro study on the efficacy of terpinen-4-ol in dextran sulfate sodium-induced mice experimental colitis. Front Immunol. 2017 May 12;8(MAY).
58. Shen J, Cheng J, Zhu S, Zhao J, Ye Q, Xu Y, et al. Regulating effect of baicalin on IKK/IKB/NF-kB signaling pathway and apoptosis-related proteins in rats with ulcerative colitis. Int Immunopharmacol. 2019 Aug 1;73:193–200.
59. Catanzaro D, Rancan S, Orso G, Dall'acqua S, Brun P, Giron MC, et al. Boswellia serrata preserves intestinal epithelial barrier from oxidative and inflammatory damage. PLoS One. 2015 May 8;10(5).
60. Byung HK, Sung MC, Reddy AM, Yeong SK, Kyung RM, Kim Y. Down-regulatory effect of quercitrin gallate on nuclear factor-κB-dependent inducible nitric oxide synthase expression in lipopolysaccharide-stimulated macrophages RAW 264.7. Biochem Pharmacol. 2005 Jun 1;69(11):1577–83.
61. Han YM, Koh J, Kim JH, Lee J, Im JP, Kim JS. Astragalin Inhibits Nuclear Factor-κB Signaling in Human Colonic Epithelial Cells and Attenuates Experimental Colitis in Mice. Gut Liver. 2021;15(1):100–8.
62. Kong J, Xiang Q, Ge W, Wang Y, Xu F, Shi G. Network pharmacology mechanisms and experimental verification of licorice in the treatment of ulcerative colitis. J Ethnopharmacol. 2024 Apr 24;324:117691.
63. Hodge G, Hodge S, Han P. Allium sativum (garlic) suppresses leukocyte inflammatory cytokine production in vitro: Potential therapeutic use in the treatment of inflammatory bowel disease. Cytometry. 2002 Aug 1;48(4):209–15.
64. Kim N, Lertnimitphun P, Jiang Y, Tan H, Zhou H, Lu Y, et al. Andrographolide inhibits inflammatory responses in LPS-stimulated macrophages and murine acute colitis through activating AMPK. Biochem Pharmacol. 2019 Dec 1;170.
65. Langmead L, Makins RJ, Rampton DS. Anti-inflammatory effects of aloe vera gel in human colorectal mucosa in vitro. Aliment Pharmacol Ther. 2004 Mar 1;19(5):521–7.
66. Salh B, Assi K, Templeman V, Parhar K, Owen D, Gó mez-Muñ oz A, et al. DNB-induced murine colitis. Am J Physiol Gastrointest Liver Physiol [Internet]. 2003;285:235–43. Available from: http://www.ajpgi.org
67. Altınel Y, Yalçın Ş, Ercan G, Yavuz E, Erçetin C, Gülçiçek OB, et al. The efficacy of curcumin on pdgf expression and nf-kappa b pathway: Tnbs-induced colitis. Ulusal Travma ve Acil Cerrahi Dergisi. 2020 Sep 1;26(5):663–70.
68. Hsiang CY, Lo HY, Huang HC, Li CC, Wu SL, Ho TY. Ginger extract and zingerone ameliorated trinitrobenzene sulphonic acid-induced colitis in mice via modulation of nuclear factor-κB activity and interleukin-1β signalling pathway. Food Chem. 2013 Jan 1;136(1):170–7.
69. Hartmann RM, Fillmann HS, Martins MIM, Meurer L, Marroni NP. Boswellia serrata has beneficial anti-inflammatory and antioxidant properties in a model of experimental colitis. Phytotherapy Research. 2014 Sep 1;28(9):1392–8.
70. Singh UP, Singh NP, Singh B, Hofseth LJ, Taub DD, Price RL, et al. Role of resveratrol-induced CD11b + Gr-1 + myeloid derived suppressor cells (MDSCs) in the reduction of CXCR3 + T cells and amelioration of chronic colitis in IL-10 -/- mice. Brain Behav Immun. 2012 Jan;26(1):72–82.
71. Shi G, Jiang H, Feng J, Zheng X, Zhang D, Jiang C, et al. Aloe vera mitigates dextran sulfate sodium-induced rat ulcerative colitis by potentiating colon mucus barrier. J Ethnopharmacol. 2021 Oct 28;279.

72. Palla AH, Gilani AUH, Bashir S, Ur Rehman N. Multiple Mechanisms of Flaxseed: Effectiveness in Inflammatory Bowel Disease. Evidence-based Complementary and Alternative Medicine. 2020;2020.
73. Zhang H, Cao N, Yang Z, Fang X, Yang X, Li H, et al. Bilobalide Alleviated Dextran Sulfate Sodium-Induced Experimental Colitis by Inhibiting M1 Macrophage Polarization Through the NF-κB Signaling Pathway. Front Pharmacol. 2020 May 21;11.
74. Huang C, Luo X, Li L, Xue N, Dang Y, Zhang H, et al. Glycyrrhiza Polysaccharide Alleviates Dextran Sulfate Sodium-Induced Ulcerative Colitis in Mice. Evidence-based Complementary and Alternative Medicine. 2022;2022.
75. Shuangyuan Hu, Maoyaun Zhao, Wei Li, Pengfei Wei, Qingsong Liu, Shuanglan chen, et al. Preclinical evidence for quercetin against inflammatory bowel disease: a meta-analysis and systematic review. Inflammopharmacology. 2022 Oct 13;30(6):2035–50.
76. Xin Shao, Chongzhen Sun, Xiaosa Zhang, Duo Han, Shan Liang, Rong Qu, et al. Anti-Inflammatory and Intestinal Microbiota Modulation Properties of Jinxiang Garlic (Allium sativum L.) Polysaccharides toward Dextran Sodium Sulfate-Induced Colitis. J Agric Food Chem. 2020;68(44):12295–309.
77. Michelsen KS, Wong MH, Ko B, Thomas LS, Dhall D, Targan SR. HMPL-004 (Andrographis paniculata extract) prevents development of murine colitis by inhibiting T-cell proliferation and TH1/TH17 responses. Inflamm Bowel Dis. 2013 Jan;19(1):151–64.
78. Holt PR, Katz S, Kirshoff R. Curcumin therapy in inflammatory bowel disease: A pilot study. Dig Dis Sci. 2005 Nov;50(11):2191–3.
79. Sandborn WJ, Targan SR, Byers VS, Rutty DA, Mu H, Zhang X, et al. Andrographis paniculata extract (HMPL-004) for active ulcerative colitis. American Journal of Gastroenterology. 2013 Jan;108(1):90–8.
80. Samsami-kor M, Daryani NE, Asl PR, Hekmatdoost A. Anti-Inflammatory Effects of Resveratrol in Patients with Ulcerative Colitis: A Randomized, Double-Blind, Placebo-controlled Pilot Study. Arch Med Res. 2015 May 1;46(4):280–5.
81. Kaliora AC, Stathopoulou MG, Triantafillidis JK, Dedoussis GV, Andrikopoulos NK. Alterations in the function of circulating mononuclear cells derived from patients with Crohn's disease treated with mastic RAPID COMMUNICATION. 2007; Available from: www.wjgnet.com
82. Hu H, Lei Y, Zhang W, Xiong P, Song L, Luo X, et al. Anti-inflammatory activity and safety of compound glycyrrhizin in ulcerative colitis: A systematic review and meta-analysis of randomized controlled trials. Vol. 91, Journal of Functional Foods. Elsevier Ltd; 2022.
83. Irving PM, Iqbal T, Nwokolo C, Subramanian S, Bloom S, Prasad N, et al. A Randomized, Double-blind, Placebo-controlled, Parallel-group, Pilot Study of Cannabidiol-rich Botanical Extract in the Symptomatic Treatment of Ulcerative Colitis. Inflamm Bowel Dis. 2018 Mar 19;24(4):714–24.
84. Morshedzadeh N, Shahrokh S, Aghdaei HA, Amin Pourhoseingholi M, Chaleshi V, Hekmatdoost A, et al. Effects of flaxseed and flaxseed oil supplement on serum levels of inflammatory markers, metabolic parameters and severity of disease in patients with ulcerative colitis. Complement Ther Med. 2019 Oct 1;46:36–43.
85. Gupta I, Parihar A, Malhotra P, Gupta S, Lüdtke R, Safayhi H, Ammon HP. Effects of gum resin of Boswellia serrata in patients with chronic colitis. Planta Med. 2001 Jul;67(5):391-5. doi: 10.1055/s-2001-15802. PMID: 11488449..
86. Vazirian F, Samadi S, Abbaspour M, Taleb A, Bagherhosseini H, Mosannen Mozaffari H, et al. Evaluation of the ecacy of Thymus kotschyanus extract as an additive treatment in patients with ulcerative colitis: A randomized double-blind placebo-controlled trial. 2022; Available from: https://doi.org/10.21203/rs.3.rs-1210228/v1
87. Pandey MM, Rastogi S, Rawat AKS. Indian traditional ayurvedic system of medicine and nutritional supplementation. Vol. 2013, Evidence-based Complementary and Alternative Medicine. 2013.
88. Perrone D, Ardito F, Giannatempo G, Dioguardi M, Troiano G, Lo Russo L, et al. Biological and therapeutic activities, and anticancer properties of curcumin (Review). Vol. 10, Experimental and Therapeutic Medicine. Spandidos Publications; 2015. p. 1615–23.
89. Rajkumari S, Sanatombi K. Nutritional value, phytochemical composition, and biological activities of edible Curcuma species: A review. Vol. 20, International Journal of Food Properties. Taylor and Francis Inc.; 2018. p. S2668–87.

90. Brumatti LV, Marcuzzi A, Tricarico PM, Zanin V, Girardelli M, Bianco AM. Curcumin and inflammatory bowel disease: Potential andlimits of innovative treatments. Vol. 19, Molecules. MDPI AG; 2014. p. 21127–53.
91. Gupta SC, Patchva S, Aggarwal BB. Therapeutic roles of curcumin: Lessons learned from clinical trials. Vol. 15, AAPS Journal. 2013. p. 195–218.
92. Larmonier CB, Midura-Kiela MT, Ramalingam R, Laubitz D, Janikashvili N, Larmonier N, et al. Modulation of neutrophil motility by curcumin: Implications for inflammatory bowel disease. Inflamm Bowel Dis. 2011 Feb;17(2):503–15.
93. Marks DJB, Segal AW. Innate immunity in inflammatory bowel disease: A disease hypothesis. Vol. 214, Journal of Pathology. 2008. p. 260–6.
94. Sreedhar R, Arumugam S, Thandavarayan RA, Karuppagounder V, Watanabe K. Curcumin as a therapeutic agent in the chemoprevention of inflammatory bowel disease. Vol. 21, Drug Discovery Today. Elsevier Ltd; 2016. p. 843–9.
95. Lin Y, Liu H, Bu L, Chen C, Ye X. Review of the Effects and Mechanism of Curcumin in the Treatment of Inflammatory Bowel Disease. Vol. 13, Frontiers in Pharmacology. Frontiers Media S.A.; 2022.
96. Wang Y, Tang Q, Duan P, Yang L. Curcumin as a therapeutic agent for blocking NF-κB activation in ulcerative colitis. Vol. 40, Immunopharmacology and Immunotoxicology. Taylor and Francis Ltd; 2018. p. 476–82.
97. Lu J, Xie L, Liu K, Zhang X, Wang X, Dai X, et al. Bilobalide: A review of its pharmacology, pharmacokinetics, toxicity, and safety. Vol. 35, Phytotherapy Research. John Wiley and Sons Ltd; 2021. p. 6114–30.
98. Akaberi M, Baharara H, Amiri MS, Moghadam AT, Sahebkar A, Emami SA. Ginkgo biloba: An updated review on pharmacological, ethnobotanical, and phytochemical studies. Vol. 9, Pharmacological Research - Modern Chinese Medicine. Elsevier B.V.; 2023.
99. Zhang K, Guo J, Yan W, Xu L. Macrophage polarization in inflammatory bowel disease. Vol. 21, Cell Communication and Signaling. BioMed Central Ltd; 2023.
100. Siddiqui MZ. Boswellia Serrata, A Potential Antiinflammatory Agent: An Overview [Internet]. Available from: www.ijpsonline.com
101. Sharma S, Thawani V, Hingorani L, Shrivastava M, Bhate VR, Khiyani R. Pharmacokinetic study of 11-Keto-Bosw ellic Acid [Internet]. Available from: http://www.elsevier-deutschland.de/phymed
102. Algieri F, Rodriguez-Nogales A, Rodriguez-Cabezas ME, Risco S, Ocete MA, Galvez J. Botanical Drugs as an Emerging Strategy in Inflammatory Bowel Disease: A Review. Vol. 2015, Mediators of Inflammation. Hindawi Limited; 2015.
103. Daniela Catanzaro, Serena Rancan, Genny Orso, Stefano Dall'Acqua, Paola Brun, Maria Cecilia Giron. Boswellia serrata Preserves Intestinal Epithelial Barrier from Oxidative and Inflammatory Damage. PLoS One [Internet]. 2015 May 8 [cited 2024 Mar 11];10(5). Available from: https://journals.plos.org/plosone/article?id=10.1371/journal.pone.0125375
104. Thanawala S, Shah R, Katnapally P, Bhatnagar U. Efficacy of standardized novel Boswellia serrata extract in the dextran sodium sulfate-induced colitis model - potential use in gut health management. Int J Basic Clin Pharmacol. 2021 Nov 22;10(12):1352.
105. Pellegrini L, Milano E, Franceschi F, Belcaro G, Gizzi G, Feragalli B, et al. Managing ulcerative colitis in remission phase: usefulness of Casperome ® , an innovative lecithin-based delivery system of Boswellia serrata extract.
106. Hasan MK, Ara I, Mondal MSA, Kabir Y. Phytochemistry, pharmacological activity, and potential health benefits of Glycyrrhiza glabra. Vol. 7, Heliyon. Elsevier Ltd; 2021.
107. Leite CDS, Bonafé GA, Santos JC, Martinez CAR, Ortega MM, Ribeiro ML. The Anti-Inflammatory Properties of Licorice (Glycyrrhiza glabra)-Derived Compounds in Intestinal Disorders. Vol. 23, International Journal of Molecular Sciences. MDPI; 2022.
108. Batiha GES, Beshbishy AM, El-Mleeh A, Abdel-Daim MM, Devkota HP. Traditional uses, bioactive chemical constituents, and pharmacological and toxicological activities of Glycyrrhiza glabra L. (fabaceae). Vol. 10, Biomolecules. MDPI; 2020.
109. Xue JC, Yuan S, Meng H, Hou XT, Li J, Zhang HM, et al. The role and mechanism of flavonoid herbal natural products in ulcerative colitis. Vol. 158, Biomedicine and Pharmacotherapy. Elsevier Masson s.r.l.; 2023.

110. Lakhanpal P, Deepak D, Rai K. Quercetin: A Versatile Flavonoid. Vol. 2, Internet Journal of Medical Update.
111. Nogata Y, Sakamoto K, Shiratsuchi H, Ishii T, Yano M, Ohta H. Flavonoid Composition of Fruit Tissues of Citrus Species. Vol. 70, Biosci. Biotechnol. Biochem. 2006.
112. Overman A, Chuang CC, McIntosh M. Quercetin attenuates inflammation in human macrophages and adipocytes exposed to macrophage-conditioned media. Int J Obes. 2011 Sep;35(9):1165–72.
113. Salaritabar A, Darvishi B, HadjiakhoonDi F, Manayi A, Sureda A, Nabavi SF, et al. Therapeutic potential of flavonoids in inflammatory bowel Disease: A comprehensive review. Vol. 23, World Journal of Gastroenterology. Baishideng Publishing Group Co; 2017. p. 5097–114.
114. Singh VK, Singh DK. Pharmacological effects of garlic (Allium sativum L.). Vol. 10, Annual Review of Biomedical Sciences. 2008. p. 6–26.
115. Verma T, Aggarwal A, Dey P, Chauhan AK, Rashid S, Chen KT, et al. Medicinal and therapeutic properties of garlic, garlic essential oil, and garlic-based snack food: An updated review. Vol. 10, Frontiers in Nutrition. Frontiers Media S.A.; 2023.
116. Melguizo-Rodríguez L, García-Recio E, Ruiz C, De Luna-Bertos E, Illescas-Montes R, Costela-Ruiz VJ. Biological properties and therapeutic applications of garlic and its components. Vol. 13, Food and Function. Royal Society of Chemistry; 2022. p. 2415–26.
117. Ansary J, Forbes-Hernández TY, Gil E, Cianciosi D, Zhang J, Elexpuru-Zabaleta M, et al. Potential health benefit of garlic based on human intervention studies: A brief overview. Vol. 9, Antioxidants. MDPI; 2020. p. 1–35.
118. Zare A, Farzaneh P, Pourpak Z, Zahedi F, Moin M, Shahabi S, et al. Purified Aged Garlic Extract Modulates Allergic Airway Inflammation in Balb/c Mice [Internet]. Vol. 7, Iran J Allergy Asthma Immunol. 2008. Available from: www.SID.ir
119. Geng Z, Rong Y, Lau BHS. S-ALLYL CYSTEINE INHIBITS ACTIVATION OF NUCLEAR FACTOR KAPPA B IN HUMAN T CELLS. Vol. 23, Free Radical Biology & Medicine. 1997.
120. Anil Kumar, Jyotsna Dora, Anup Singh, Rishikant Tripathi. A review on king of bitter (Kalmegh). International Journal of Research in Pharmacy and Chemistry, [Internet]. 2012 [cited 2024 Mar 12];2(1):116–24. Available from: http://ijrpc.com/files/v2i1%20(19).pdf
121. Vetvicka V, Vannucci L. Biological properties of andrographolide, an active ingredient of Andrographis Paniculata: a narrative review. Ann Transl Med. 2021 Jul;9(14):1186–1186.
122. Perše M, Cerar A. Dextran sodium sulphate colitis mouse model: Traps and tricks. Vol. 2012, Journal of Biomedicine and Biotechnology. 2012.
123. Mishra J, Stubbs M, Kuang L, Vara N, Kumar P, Kumar N. Inflammatory Bowel Disease Therapeutics: A Focus on Probiotic Engineering. Vol. 2022, Mediators of Inflammation. Hindawi Limited; 2022.
124. Al-Meghaiseeb ES, Al-Robayan AA, Al-Otaibi MM, Arfin M, Al-Asmari AK. Association of tumor necrosis factor-α and -β gene polymorphisms in inflammatory bowel disease. J Inflamm Res. 2016 Jun 17;9:133–40.
125. Roy S, Dhaneshwar S. Role of prebiotics, probiotics, and synbiotics in management of inflammatory bowel disease: Current perspectives. Vol. 29, World Journal of Gastroenterology. Baishideng Publishing Group Inc; 2023. p. 2078–100.
126. Kim S, Jang SH, Kim MJ, Lee JJ, Kim KM, Kim YH, et al. Hybrid nutraceutical of 2-ketoglutaric acid in improving inflammatory bowel disease: Role of prebiotics and TAK1 inhibitor. Biomedicine and Pharmacotherapy. 2024 Feb 1;171.
127. Li HY, Zhou DD, Gan RY, Huang SY, Zhao CN, Shang A, et al. Effects and mechanisms of probiotics, prebiotics, synbiotics, and postbiotics on metabolic diseases targeting gut microbiota: A narrative review. Vol. 13, Nutrients. MDPI; 2021.
128. Engels M, Cross RK, Long MD. Exercise in patients with inflammatory bowel diseases: Current perspectives. Vol. 11, Clinical and Experimental Gastroenterology. Dove Medical Press Ltd; 2018. p. 1–11.
129. Kaur S, D'Silva A, Shaheen AA, Raman M. Yoga in Patients With Inflammatory Bowel Disease: A Narrative Review. Crohns Colitis 360. 2022 Apr 1;4(2).
130. Lamers CR, de Roos NM, Bongers CCWG, ten Haaf DSM, Hartman YAW, Witteman BJM, et al. Repeated prolonged moderate-intensity walking exercise does not appear to have harmful effects on inflammatory markers in patients with inflammatory bowel disease. Scand J Gastroenterol. 2021;56(1):30–7.

131. Robinson RJ, Krzywicki T, Almond L, Al-Azzawi F, Abrams K, Javed Iqbal S, et al. Effect of a Low-Impact Exercise Program on Bone Mineral Density in Crohn's Disease: A Randomized Controlled Trial. 1998.
132. Scheffers LE, Vos IK, Utens EMWJ, Dieleman GC, Walet S, Escher JC, et al. Physical Training and Healthy Diet Improved Bowel Symptoms, Quality of Life, and Fatigue in Children with Inflammatory Bowel Disease. J Pediatr Gastroenterol Nutr. 2023 Aug 1;77(2):214–21.
133. Manski S, Noverati N, Policarpo T, Rubin E, Shivashankar R. Diet and Nutrition in Inflammatory Bowel Disease: A Review of the Literature. Vol. 6, Crohn's and Colitis 360. Oxford University Press; 2024.
134. Song G, Fiocchi C, Achkar JP. Acupuncture in inflammatory bowel disease. Inflamm Bowel Dis. 2019 Jun 18;25(7):1129–39.
135. Bao C, Wu L, Wang D, Chen L, Jin X, Shi Y, et al. Acupuncture improves the symptoms, intestinal microbiota, and inflammation of patients with mild to moderate Crohn's disease: A randomized controlled trial. EClinicalMedicine [Internet]. 2022;45:101300. Available from: https://doi.org/10.1016/j.
136. Kim DH, Cheon JH. Pathogenesis of inflammatory bowel disease and recent advances in biologic therapies. Vol. 17, Immune Network. Korean Association of Immunologists; 2017. p. 25–40.
137. Zhou YF, Zhang GL, Sun N, Wang ZQ, Ye XY, Xiong J, et al. Acupuncture for emotional disorders in patients with inflammatory bowel disease: a systematic review protocol. BMJ Open. 2022 Sep 27;12(9).
138. Bao C, Wu L, Wang D, Chen L, Jin X, Shi Y, et al. Acupuncture improves the symptoms, intestinal microbiota, and inflammation of patients with mild to moderate Crohn's disease: A randomized controlled trial. 2022; Available from: https://doi.org/10.1016/j.

Table 1. *In vitro* anti-inflammatory activity of potent herbal extracts and their bioactive compounds along with their mechanism.

Sl. no	Name of the herb	Form of the herb	*In vitro* study model	Mechanism	Reference
1	*Curcuma longa*	Turmeric extract and fractions.	HEK293 cells	↓Inappropriate epithelial cell transport (SLC22A4, 503F).↑ anti-inflammatory cytokine gene promoter activity (IL-10, -1082A)	(56)
2	*Melaleuca alternifolia* (Tea tree oil)	Terpinen-4-ol	RAW264.7 cells	↓ NLRP3 inflammasome activation, ↓ caspase-1, interleukin-1β ↓secretion	(57)
3	*Scutellaria baicalensis*	Baicalein (5,6,7-trihydroxy flavone)	RAW264.7 cells	Regulating effect on IKK/IKB/NF-kB Signaling pathway	(58)
4	*Boswellia serrata*	*Boswellia serrata* gum extract	Caco-2 cell	↓transepithelial electrical resistance (TEER) ↑paracellular permeability assay	(59)
5	Quercetin found in apples, onions, citrus fruits, berries, grapes, broccoli, and tea.	Quercetin	RAW 264.7	↓ NO production ↓ NF-kB	(60)
6	Flavonoid isolated from the leaves of *Rosa agrestis*	Astragalin	HCT-116 and HT-29 human colonic epithelial cells	Inhibit IκBα phosphorylation Inhibit TNF-α, IL-1β, and IL-6	(61)

				Inhibits Nuclear Factor-κB	
7	Liquorice (*Glycyrrhizaglabra*)	Liquorice	CaCo2 cells	↓ levels of malondialdehyde (MDA) ↓ IL-1β, IL-6, TNF-α	(62)
8	*Allium sativum*	Garlic Extract	Peripheral blood mononuclear cells (PBMCs)	↓Th1 and inflammatory cytokines ↑ production of IL-10	(63)
9	*Andrographis paniculata*	*Andrographis paniculata* Extract	RAW264.7	↓ pro-inflammatory cytokines ↓ chemokines, ↓ NO, ↓lipid mediators ↓ NF-KB activation	(64)
10	*Aloe barbedensis Miller*	Aloe vera gel	Caco2 epithelial cell	↓ interleukin-8 production	(65)

Table:2

Sl. no	Name of the herb	Form of herb and dose	*In vivo* study model	Mechanism involved	References
1	*Curcuma longa*	Curcumin 0.25% concentration	C3H mice/DNBS colitis.	↓myeloperoxidase activity, ↓ in the number of infiltrating neutrophils and ↓ expression of the message for IL-1.	(66)
2	*Curcuma longa*	Curcumin (20 mg/kg)	TNBS-induced colitis on Wistar Hannover rats	Curcumin improved condition by modulating the NF-κB signaling pathway.	(67)
3	Ginger (*Zingiber officinale)*	Ginger extract (0.1 ml of 50% ethanol) and zingerone (0.1 ml of 50% ethanol)	Female BALB/c mice TNBS-induced colitis model	Regulation of IL-1b, interferon-c, and tumour necrosis factor signalling pathways, ↑ IL-17 and ↑ IL-6.	(68)
4	*Boswellia serrata*	Extract of *B. serrata* (34.2 mg/kg/day)	Male Wistar rat acetic acid-induced colitis model	↓lipid peroxidation, ↓iNOS, ↓nitric oxide, and showed improvements in tissue injury and anal sphincter pressure.	(69)
5	Resveratrol (3,5,4′-trihydroxy-trans-stilbene) *a natural phenol*	Resveratrol (10, 50, 100 mg/kg daily orally for 14 days)	DSS-induced C57BL/6 mice	↑colon length ↑body weight ↓IL-1β, ↓ IL-6, ↓TNF-α, ↓IFN-γ protein, ↓COX-	(70)

	obtained from grapes, raspberry mulberriespistachios.			2 protein, ↓p-IκBα protein, ↓inflammatory cell infiltration	
6	*Aloe barbedensis Miller*	Aloe vera extract of (18 mg/kg and 72mg/kg)	DSS-induced Male Sprague-Dawley ratmodel	↓ DAI, prevention of the colon length shortening, ↓ IL-6, ↓IL-1β,↓TNFα and ↑ IL-10.	(71)
7	*Flax seeds (Linum usitatissimum)*	Extracts of Flaxseed and oil (150mg/kg,300 mg/kg and 500 mg/kg)	Female BALB/c Acetic Acid-induced colitis mice	Both Extracts of Flaxseed and flaxseed oil ↓neutrophil infiltration	(72)
8	*Ginkgo biloba*	Bilobalide (2.5 and 5 mg/kg)	Female C57BL/6 mice DSS - induced model	↓ DAI, ↑ body weight ↓ NF-κB signalling pathway and inhibition of M1 macrophage polarization	(73)
9	Liquorice, (*Glycyrrhiza glabra*)	*Glycyrrhiza* polysaccharides 100, 200, and 400 mg/kg	MaleKunming Mice Dextran Sulfate Sodium-Induced UCin Mice	↓ DAI, ↑ body weight ↓Shortens colon length ↓ intestinal permeability ↑ IL-10 Inhibiting the inflammatory response	(74)
10	Flavonoids found in Berries, Grapes, apples, onions, citrus fruits, broccoli, and tea.	Quercetin	Mice model	↓ histological score, ↓DAI, ↓interleukin-1β (IL-1β), ↓ tumor necrosis factor-α (TNF-α), ↓nitric oxide(NO), ↓malondialdehyde (MDA), ↓myeloperoxidase (MPO), ↑ colon length, ↑ interleukin-10 (IL-10, ↑ glutathione (GSH) and↑ superoxide dismutase (SOD).	(75)
11	*Garlic Allium*	Extracted from Jinxiang	DSS-Induced		

	sativum L	garlic. A water-soluble garlic polysaccharide (WSGP) (200 or 400 mg/kg/day)	Colitis in mice	↓DAI, ↓histological score of colitic mice tissue damage inhibited the expression of inflammatory factors (interleukin 6, interleukin 1 beta, and tumor necrosis factor-alpha), ↑ production of short-chain fatty acids and improved the composition of intestinal microbiota.	(76)
12	*Andrographis paniculata*	Extract of*A. paniculata* 300 mg/kg	C57BL/6, and Rag1mice DSS-induced chronic colitis	↓ Tumor necrosis factor alpha (TNF-α), ↓ interleukin (IL)-1β,↓ interferon-gamma (IFN-γ), and IL-22 expression	(77)

Table:3

Sl no	**Name of the herb**	**Form of herb**	**Type of Study**	**Mechanism involved**	**Reference**
1	*Curcuma longa*	Curcumin (360 mg)	Open-label study	↓ CDAI scores ↓sedimentation rates	(78)
2	*Andrographis paniculata*	*Andrographis paniculata extract* (1,200 mg and 1,800 mg)	Randomized, Double-blind, Placebo-controlled trial	Decreased inflammation and alleviation of stomach pain or discomfort.	(79)
3	Resveratrol (3,5,4′-trihydroxy-trans-stilbene) *a type of natural phenol* obtained from grapes, raspberries mulberries, pistachios.	Resveratrol	Randomized, double-blind, placebo-controlled study	↓disease activity ↓serum CRP, TNF-α levels ↓NF-κB p65 activity	(80)
4	*Pistacia lentiscus* (Mastic)	6 Mastiha caps/day (2.2 g/day)	Double-blind, placebo-controlled	↓TNF-a secretion ↑ MIF (macrophage migration inhibitory factor) No significant changes in IL-6, MCP-1, or GSH.	(81)

5	*Glycyrrhiza glabra*	Glycyrrhizin (40 mg/day)	randomized controlled trials	↓levels of TNF-α, IL-6, IL-8 and IL-17 ↑ expression of IL-10	(82)
6	*Cannabis sativa*	Cannabidiol *(Cannabis sativa* extract100 mg/day)	Placebo-controlled RCT	↓IL-2, IL-6, and TNF-α, ↓fecal calprotectin	(83)
7	*Flax seeds (Linum usitatissimum)*	Grounded flaxseed (30 gr/day), flaxseed oil (10 gr/day)	Open-labeled randomized controlled trial	↓ESR, ↓TNF-γ , ↑TGF-β, ↑IL-6	(84)
8	*Boswellia serrata*	Gum resin of *Boswellia serrata (*900 mg daily divided into 3 doses for 6 weeks)	open, non-randomized monocentric clinical trial	lowering of fecal calprotectin inhibit the synthesis of leukotrienes.	(85)
9	*Thymus kotschyanus*	*Thymus kotschyanus* extract	A randomized double-blind placebo-controlled trial	↓calprotectin and ↓ SCCAI (Simple Clinical Colitis Activity Index)	(86)

Table:4

Exercises	Practices	Number of subjects in clinical trials	Results	Reference
Yoga	30-minute session/week; 1. Hathayoga-basedYogaNamaskar-10mins. 2.NadiShuddhi-5mins 3.Meditation consisting of AUM chanting-5 mins. 4.Breath watching- 3–5 mins 5.Self-footmassage with lavender oil prior to bedtime	6 CDand 3 UC patients	Decrease in the PHQ-9 depression score. Decrease GAD-7 anxiety score, PSS-10 score and improvement in mental health score	(129)
Physical exercise	Walking	18IBDwalkers 19Non IBD walkers	Improved cytokine concentrations and stable faecal calprotectin	(130)
Low impact exercises program	The exercises targeted the hip and lumbar region and contained dynamic muscular training of the primary leg and the trunk muscle groups, such as the erector spine, gluteals, hamstrings, and quadriceps, as well as the anterior abdominal wall muscles.	117 CD patients 57 control	Low-impact exercise shows positive outcome in BMD (bone mineral (130)density)	(131)
Physical training	Physical training program including healthy dietary	Fifteen patients	Crohn's Disease Activity Index	(132)

			decreased(CDAI) Fecal cal protect in also decreased. Decreased fatigue.	

Table:5

Diet	Inclusion	Exclusion
Carbohydrate	Honey,milk, cheese yogurt	Grains, sugars, processed food
Mediterranean diet,	Olive oil grains, vegetables, fruits, nuts,seeds	Processed foods, red meats, processed meat
Low FODMAP	Fermentable oligosaccharide, disaccharide, and monosaccharide polyols.	
Anti-inflammatory diet	Omega-3 fatty acids and probiotics prebiotics	Refine sugars, glutens, saturated fatty acids

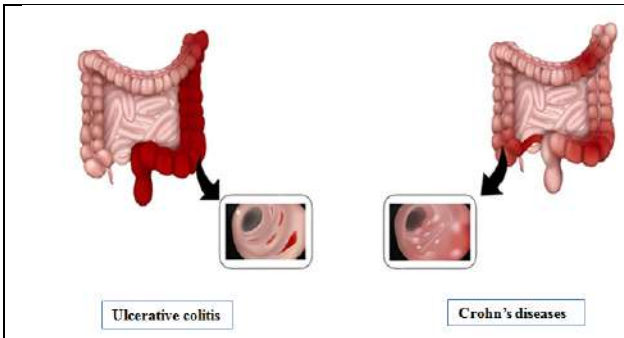

Fig 1: IBD-Infected colon

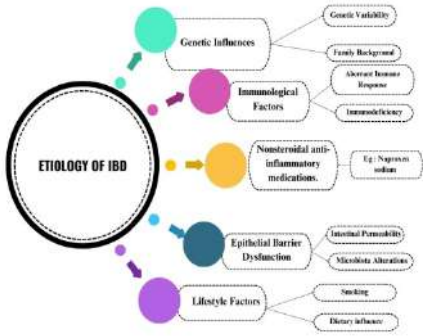

Fig 2: Etiology of IBD

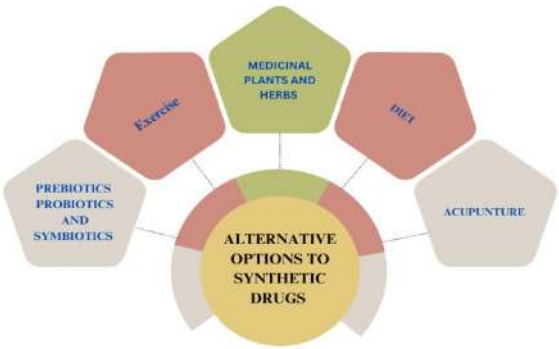

Fig 3: Alternative Treatments to IBD

Indian Journal of Natural Sciences *www.tnsroindia.org.in ©IJONS*

Vol.15 / Issue 88 / Feb / 2025 *International Bimonthly (Print) – Open Access* *ISSN: 0976 – 0997*

RESEARCH ARTICLE

Benchmarking Naive Bayes and Decision Tree Models: Performance in Data Classification Scenarios

N. Thamaraikannan* and G. Dona Rashmi

Assistant Professor, Department of Artificial Intelligence and Machine Learning, Kongunadu Arts and Science College (Autonomous), (Affiliated to Bharathiar University), Coimbatore, Tamil Nadu, India.

Received: 21 Nov 2024 Revised: 03 Dec 2024 Accepted: 31 Jan 2025

***Address for Correspondence**
N. Thamaraikannan
Assistant Professor,
Department of Artificial Intelligence and Machine Learning,
Kongunadu Arts and Science College (Autonomous),
(Affiliated to Bharathiar University),
Coimbatore, Tamil Nadu, India.
E.Mail: nthamaraikannan_ai@kongunaducollege.ac.in

ABSTRACT

Data mining classification is a critical component in extracting meaningful patterns from large datasets. This system utilizes Naive Bayes and Decision Tree algorithms to enhance classification accuracy while minimizing associated risks. Various datasets, including the Iris dataset, are employed to evaluate the effectiveness of these algorithms in different scenarios. By leveraging supervised learning methods, the system conducts performance assessments through the use of training and testing datasets. The implementation showcases a robust ability to classify data accurately, particularly highlighting the effectiveness of the Iris dataset, which yields consistent results. This comparative analysis allows for the identification of the most appropriate algorithm for each dataset, optimizing performance across different contexts. In addition to high accuracy, the system prioritizes security and adaptability, ensuring it remains reliable for a range of real-world applications. The insights gained from model performance evaluations further enhance the classification process, aiding users in making informed decisions based on data-driven evidence. Furthermore, the system is designed to be user-friendly, making it accessible to those with varying levels of technical expertise. Overall, this approach provides a comprehensive framework for effectively addressing classification challenges in data mining, contributing to improved outcomes in data analysis and decision-making processes.

Keywords: In addition to high accuracy, the system prioritizes security and adaptability, ensuring it remains reliable for a range of real-world applications.

INTRODUCTION

Data mining is the process of extracting information from large amounts of data and mostly unorganized databases. It is the process of performing automated extraction and generating predictive information from large databases. The extraction of information from a large database is otherwise known as Knowledge Discovery from large amount of Data. Data mining have been attracting a great deal of attention in the information industry and in society as a whole. Due to availability of wide data an imminent need for processing those data into knowledge. Those information or knowledge gained can be used for applications ranging from market analysis, fraud detection, and customer retention, to produce control and science exploration. The evolutionary measure in the development of the functionalities have been involved as *data collection and database creation, data management, and advanced data analysis.* There have been wider-angle of data available in the database. Whereas the Heterogeneous database systems and Internet-based global information systems like World Wide Web (WWW) has been emerged and plays a vital role in the information industry. The abundant data has been analysed to form a *rich data* but not with the adequate necessary data. Important decisions are often made on the basis of decision makers. As a result large data repositories is known as "*data tombs*" Data mining tools will perform the data analysis and may uncover important data patterns, contributing greatly to business strategies, knowledge bases, and scientific and medical research. The widening gap between data and information is used for systematic development of *data mining tools* that will turn the data tombs into "golden nuggets" of knowledge.

RELATED WORKS

Author Li Liu, Murat Kantarcioglu and Bhavani Thurasingham discussed about the securing of data using decision tree algorithm. . It is classified with the perturbed data set, and this process improves the accuracy of data. It also reduce the costs off communication and computation compared to any other cryptographic services They also provide the direction for mapping the data mining functions instead of reconstructing the original data which provide more privacy with less cost [3]. Author Ahmad Ashari, Paryudi, Min tjoa describes about the performance of various classification algorithm for an alternative design in an energy simulation tool. This shows there is possible way of comparing multiple algorithms. As per the comparison of decision tree, naive bayes, K-Nearest Neighbour algorithm the accuracy of decision tree is better than the other algorithms [4]. Author Sagar S.Nikam has defined the comparative study on classification techniques which mainly focus in the performance analysis of classification algorithms and its Limitations. Also focus on classifying data into different classes according to some constraint. The first approach is the Statistical approach which is classical approach works on linear discrimination. The second is Machine Learning which helps to solve more complex problems and third approach is Neural Network shows the diverse source ranging from the understanding and emulating the human brain to border issues of human abilities [6]. Author Rachna Raghuwanshi has describe about performance of the Naïve bayes classifier and Decision Tree with the Fire Data Set to compare the accuracy. Where as the problem with Cross Validation is avoided [7]. Author XHEMALI, J.HINDE, G.STONE précises on the automatic analysis and classification of attribute data from training course web pages. They choose Naive bayes, Decision Tree, Neural Network algorithm to classify the best data with same data set. As per the result gained the accuracy of naive bayes is more accurate than any other classification algorithm [8]. Author Bhaskar N.Patel, Satish G. Prajapati, Dr.Kamaljit I. Lakhtaria describes the classification is the categorization of data into different category based on some rules. The classification of data with decision tree is the pictorial view, and categorizing is easier, accuracy is better than other classification algorithm [11].

IRIS DATASETS

IRIS Dataset is the multivariate data set which was introduced by British statistician and biologist Ronald Fisher. It is also known as Edgar Anderson collected the data to quantify the mophologic variation of Iris Flower of three related species. The file *iris.csv* contains the data for this example in comma separated values (CSV) format. A sample of the contents of that file is listed below.

The attributes value of IRIS data are:

1. **sepal_length**: Sepal length, in centimetres, used as input.
2. **sepal_width**: Sepal width, in centimetres, used as input.
3. **petal_length**: Petal length, in centimetres, used as input.
4. **petal_width**: Petal width, in centimetres, used as input.
5. **Setosa**: Iris setosa, true or false, used as target.
6. **Versicolour**: Iris versicolour, true or false, used as target.
7. **Virginica**: Iris virginica, true or false, used as target.

METHODOLOGY

Naïve Bayes Classifier

NB Classifier is used as a knowledge accumulator during training and testing data. This helps to classify and sense unseen data. It also identify and responsible for extracting all suitable features. NB classifier calculate the most possible output based on input. Naïve bayes is the better probabilistic classifier it consider the presence of a particular features of a class.

1. Let D be the training set of tuples and their associated class labels. As usual, each tuple is represented by an n-dimensional attribute vector, X=(x_1, x_2, x_3,….x_n) depictiong n measurements made on the tuple from n attributes, respectively, A_1,A_2,A_3,….A_n.
2. If there are m classes, C_1,C_2,C_3,…..C_m. Given tuple ,X, the classifier will predict that X belongs to the class having the highest posterior probability, conditioned on X. That is, the Naïve Bayes classifier predicts that tuple X belongs to the class C_i if and only if

$P(C_i|X) > P(C_j|X)$ for $1 \leq j \leq m$, $j \neq i$.

Factor considered for calculating Performance of Classifiers

Accuracy of classifiers is compared based on the Precision, Accuracy, Recall, False Positive rate and True Negative rate. The Rapid Miner tool provide powerful platform which gives integrated environment for data mining. The average measure is taken as the overall measure for classifiers. The overall precision for a classifier for a given dataset, average of precision of both classes is calculated. Bayes theorem provides a way of calculating the posterior probability, $P(c|x)$, from $P(c)$, $P(x)$, and $P(x|c)$. Naive Bayes classifier considers that the effect of the value of a predictor (x) on a given class (c) is independent of the values of other predictors.

$$P(c|x) = \frac{P(x|c)P(c)}{P(x)}$$

$$P(c|X) = P(x_1|c) * P(x_2|c) * \ldots\ldots\ldots * P(x_n|c) * P(c)$$

$P(c|x)$ is the posterior probability of class given predictor od class.
$P(c)$ is called the prior probability of class
$P(x|c)$ is the likelihood which is the probability of predictor of given class
$P(x)$ is the prior probability of predictor of class.

Accuracy

Accuracy is the calculation of number of instance predicted positively divided by Total number of Instances. That is accuracy is the percentage of the accurately predicted classes among the total classes.
The accuracy is defined as

Accuracy = ((True Positive + True Negative)/ (P + N))*100

Precision

Precision is the exact value of true class x which is known as positive predictive value.The proportion of having true positive and the total classified as class x.

Precision = (True Positive.(True Positive + False Positive)) * 100

Recall

Recall deals with the sensitive data. It returns the most relevant data and the part of document which is relevant as the result from query.

Recall = (True Positive.(True Positive + False Negative)) * 100

True Positive

True positive are the positive tuples which are correctly labelled by the classifiers. Proportion categorized as class x. Projected by the module those arepredicted positively as results.

True Positive rate = (True Positive/(TruePositive + False Negative))*100

False Positive

False Positive is the proportion incorrectly categorized as class x or the actual total of classes, except X.It is incorrectly predicted compared original results.

False Positive rate = (False Positive/ (False Positive+True Negative))*100

F-Measure

It is categorized to for F-measure by combining Precision and Recall.

Performance Measure

The experiments in this research are evaluated using the standard metrics of accuracy, precision, recall and f-measure for Web Classification [8]. These were calculated using the predictive classification table, known as Confusion Matrix (Table 4.1).

Considering Table 4.1:

TN (True Negative) → Number of correct predictions that an instance is irrelevant
FP (False Positive) → Number of incorrect predictions that an instance is relevant
FN (False Negative) → Number of incorrect predictions that an instance is irrelevant
TP (True Positive) → Number of correct predictions that an instance is relevant

RESULTS AND DISCUSSIONS

Implementation of Comparison of Decision Tree and Naive Bayes algorithm using Rapid Miner. All the classifiers were trained and tested and consisting of a total of above 4000 unique features. The naïve bayes classifier gives the highest accuracy of 95.20**%** whereas Decision Tree gives 98.9% accuracy**.** As per our research we have proved that the data which we choose is more accurate than Naïve bayes algorithm. In which the Lift and ROC chart shows that the data is more secured while comparing to Naïve bayes algorithm. Because the tree model is more easy and accurate to calculate the data.

CONCLUSION AND FUTURE WORK

In this research work, we compared the two classification algorithms based on the IRIS dataset that we used. There where lot of comparison on this algorithm which were made even though they are compared with more than three algorithms. This comparison on classification algorithm helps to find the accurate data. We used the Lift chart and ROC Curve to display the output for this comparison technique. So that we can easily understand the results also about the security of the data. As per the survey there is an vast increase in the amount of data or information which is being stored in the electronic devices. But unfortunately the accumulation of data has taken place at an explosive rate. It has been analysed that information stored has been multiples twice a year also the size also increases simultaneously. We may have several examples like medical history, Life Insurance Claims, Banking and other government sector activities are the instance to these types of data.In Knowledge discovery, Data Mining is the base

for the processing of datasets. So in this current scenario the data security has been the essential contribution to knowledge. This Project discussed about the Naïve Bayes and Decision Tree algorithm was compared with the IRIS dataset using Rapid Miner Tool. We have implemented Naïve Bayes and Decision Tree algorithm in Rapid Miner in which we had experienced the performance measure and parameters of algorithm over the IRIS dataset. The performance of algorithm on this dataset have been evaluated and classified based on the Bayes Classifier. Therefore the Decision Tree algorithms performance is high and results the more accurate data set which is compared to decision tree. We came to a conclusion that Decision Tree algorithm is the best. As a future work of our project we can develop a cryptography based PPDM (Privacy Preserving Data Mining) Technique for the better security of data. Merely using cryptographic techniques may be effective whereas the data mining algorithms which add an additional security may leads a tough task as well.

REFERENCES

1. Jiawei Han, Micheline Kamber "Data Mining Concepts and Techniques" in proceeding of second edition Morgan Kaufmann Publisher An imprint of Elsevier 2006.
2. Alka Gangrade, Ravindra Patel " SMC Protocol for Naïve Bayes classification over Grid Partitioned Data using Multiple UTPs" International Journal of Computer Applications(0975 – 8887) Volume 64- No 6. February 2013.
3. Li Liu, Murat Kantarcioglu and Bhavani Thurasingham"A Novel PrivacyPreserving Decision Tree Algorithm" Technical Report October 2006.
4. Ahmad Ashari Iman Paryudi A Min Tjoa "Performance Comparison between Naïve Bayes, Decision Tree and k-Nearest Neighbor in Searching Alternative Design in an Energy Simulation Tool"(IJACSA) International Journal of Advanced Computer Science and Applications, Vol. 4, No. 11, 2013.
5. Ashmeet Singh, R Sathyaraj "A Comparison Between Classification Algorithms on Different Datasets Methodologies using Rapidminer" International Journal of Advanced Research in Computer and Communication Engineering Vol. 5, Issue 5, May 2016.
6. Sagar S. Nikam "A Comparative Study of Classification Techniques in Data Mining Algorithms" International Conference on Computer Science and Electronics Engineering 2012
7. Rachna Raghuwanshi"A Comparative Study of Classification Techniques for Fire Data Set" (IJCSIT) International Journal of Computer Science and Information Technologies, Vol. 7 (1), 2016, 78-82
8. Daniela XHEMALI, Christopher J. HINDE and Roger G. STONE"Naïve Bayes vs. Decision Trees vs. Neural Networks in the Classification of Training Web Pages" IJCSI International Journal of Computer Science Issues, Vol. 4, No. 1, 2009 ISSN (Online): 1694-0784 ISSN (Print): 1694-0814
9. Josip Mesarić, Dario Šebalj"Decision trees for predicting the academic success of Students" Croatian Operational Research Review CRORR 7(2016), 367–388 December 30, 2016.
10. N Raveendran, Dr Antony SelvadossDhanamani "Impact of Cloud Computing on Data Mining System" International Journal of Advanced Research in Computer Science Volume 3, No. 6, Nov. 2012 (Special Issue), ISSN No. 0976-5697.
11. Bhaskar N. Patel, Satish G. Prajapati and Dr. Kamaljit I. Lakhtaria" Efficient Classification of Data Using Decision Tree" International Journal of Data Mining, Vol. 2, No. 1, March 2012.
12. Bharat BhargavaAnya Kim, YounSun Cho "Research in Cloud Security and Privacy" "https://www.cse.unr.edu/~mgunes/cpe401/cpe401sp14/12-cloud-security.ppt".
13. S.L. Ting, W.H. IP, Albert H.C. Tsang "Is Naïve Bayes a Good Classifier for Document Classification?", International Journal of Software Engineering and Its Applications, Vol. 5, No. 3, July, 2011.
14. Shahrukh Teli, Prashasti Kanikar "A Survey on Decision Tree Based Approaches in Data Mining", International Journal of Advanced Research in Computer Science and Software Engineering, Volume 5, Issue 4, 2015.

Table 1: Confusion Matrix

		PREDICTED	
		IRRELEVANT	**RELEVANT**
ACTUAL	**IRRELEVANT**	TN	FP
	RELEVANT	FN	TP

Figure 1 Iris Flower

	A	B	C	D	E
1	sepal_length	sepal_width	petal_lenght	petal_width	class
2	5.1	3.5	1.4	0.2	iris-setosa
3	...	...	...	...	...
4	7.0	3.2	4.7	1.4	iris-versicolor
5	...	...	...	...	...
6	6.3	3.3	6.0	2.5	iris-virginica

Figure 2 Iris flowers dataset

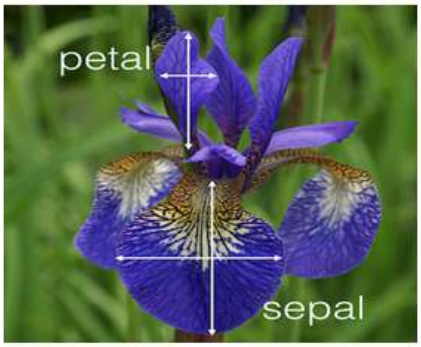

Figure 3 IRIS Flower Sepal (Length and Width) and Petal (Length and Width)

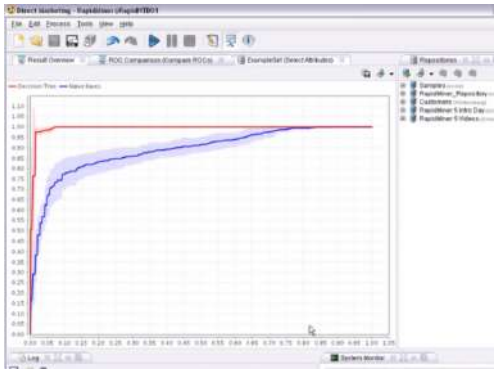

Figure 4 Roc Curve view of Classification algorithm

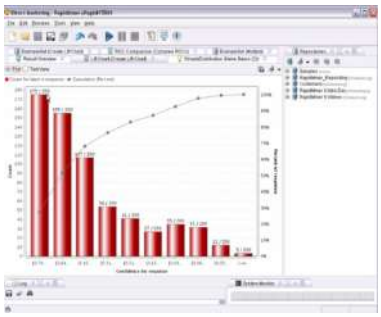

Figure 6 Result of Roc Curve and lift chart

Indian Journal of Natural Sciences *www.tnsroindia.org.in ©IJONS*

Vol.15 / Issue 88 / Feb / 2025 *International Bimonthly (Print) – Open Access* *ISSN: 0976 – 0997*

RESEARCH ARTICLE

A Sociological Study on Health Issues of Sanitation Workers inKollam District

Subin Robert[1] and A.Muthulakshmi[2]*

[1]Research Scholar, Department of Sociology and Social Work, Annamalai University, Annamalai Nagar, Tamil Nadu, India.
[2]Assistant Professor and Head (i/c), Department of Sociology and Social Work, Mother Teresa Women's University, Kodaikanal, Dindigul Dist., Tamil Nadu, India.

Received: 21 Nov 2024 Revised: 03 Dec 2024 Accepted: 28 Jan 2025

***Address for Correspondence**
A.Muthulakshmi
Assistant Professor and Head (i/c),
Department of Sociology and Social Work,
Mother Teresa Women's University,
Kodaikanal, Dindigul Dist.,
Tamil Nadu, India.
E.Mail: muthulakshmisakkiya@gmail.com

ABSTRACT

Sanitary workers are essential to public health and hygiene by keeping urban and rural settings clean. Their responsibilities include waste collection and disposal, street cleaning, drainage system management, and public space sanitation. Despite the importance of their jobs, sanitary workers are frequently exposed to various occupational health risks, including respiratory ailments, skin infections, and musculoskeletal issues. These dangers are caused by extended exposure to hazardous substances such as dust, chemicals, and infectious waste. To examine workplace health problems among sanitation workers, the study employed an explanatory, cross-sectional survey approach. The inquiry was done using a quantitative method. The sample size was one hundred. This study included both primary and secondary data. A planned interview schedule and survey were used to obtain primary data. Subjects were chosen using a probability sampling approach from a list of registered sanitation experts in the Kollam Town Municipal Authority. The number of mobile sanitation workers was calculated using convenient, nonprobability sampling. The study examined the health risks and stress levels of sanitation workers in Kollam municipality. The study found a considerable increase in stress levels with age, with older workers experiencing significantly more stress than their younger counterparts. The findings also revealed a variety of health dangers linked with sanitation jobs, including both physical and psychological problems. The analysis of health conditions among sanitary workers reveals significant inequalities in the frequency of various health disorders, with respiratory and skin-related conditions such as coughs and colds, allergies, and fungal infections being the most common. Statistical testing verified that these disparities are not random, implying that these workers' health risks are elevated due to their exposure to hazardous surroundings. Focusing interventions, better safety standards, and regular health check-ups are required to protect their health.

Keywords: Sanitary workers, Health Issues, stress levels, safety interventions

INTRODUCTION

Sanitary workers protect public health and hygiene by keeping urban and rural areas clean. They are responsible for waste collection and disposal, street cleaning, drainage system management, and public area sanitation. Despite the importance of their job, sanitary workers are frequently exposed to various occupational health risks, including respiratory ailments, skin infections, and musculoskeletal disorders. These dangers are caused by extended exposure to dangerous substances like dust, chemicals, and infectious waste. The lack of proper preventive measures and safety regulations increases their susceptibility to significant health problems. Furthermore, sanitary workers frequently experience stigma and dire working circumstances, which can contribute to mental health problems. Understanding this workforce's health issues is critical for developing treatments to improve working circumstances, reduce health risks, and increase general well-being. Sanitation workers are essential to Kollam Municipality's urban infrastructure and are responsible for maintaining the city's cleanliness. However, their occupation exposes them to a high risk of acquiring health problems because of continual exposure to hazardous working conditions. The current study aims to investigate these health risks and provide insights that will help policymakers implement steps to protect the health of these vital workers.

RESEARCH METHODOLOGY

The study used an explanatory, cross-sectional survey approach to assess the Workplace Health Problems of sanitation workers. The investigation was conducted quantitatively. This study aimed to describe the health hazards experienced by sanitation workers. It was also used as an applied study to assist officials in implementing essential steps to prevent serious health hazards. This study focused on the Kollam municipality. The sample size was 70. This study collected both primary and secondary data. Primary data was collected using a survey and structured interview schedule. The probability sampling approach was used to select subjects from a list of registered sanitation professionals in the Kollam Town Municipal Authority. The number of Mobile sanitation staff was determined using convenient sampling, a non probability sampling technique.

RESULT

The data show that sanitation workers' stress levels increase with age. The investigation revealed that older workers had greater mean stress levels than younger workers, with the "51-60" age group having the highest stress levels. This tendency implies that age significantly influences stress levels, emphasizing the importance of age-specific stress management measures. The heterogeneity in stress levels suggested that older workers have distinct issues that may necessitate focused support to manage their stress effectively. The study discovered a variety of health dangers associated with sanitation jobs, including physical and psychological problems. The significant disparities in stress levels and health risks among age groups and job kinds highlight the significance of tailored therapies. Addressing these challenges can enhance workers' health and safety, increasing the effectiveness of municipal sanitation services. Overall, the study's findings emphasize the urgent need for tailored health and safety interventions for sanitation workers, particularly those that address the diverse stress levels and health risks associated with different age groups and employment functions. These findings are critical for guiding policy decisions and establishing measures to improve the well-being of sanitation personnel in Kollam municipality.

DISCUSSION

This study aimed to investigate the health risks experienced by sanitation workers in the Kollam municipality using an explanatory, cross-sectional survey technique. The study found that stress levels tend to rise with age, with older

workers reporting higher stress levels than their younger colleagues. This trend emphasizes the importance of specialized stress management and health support suited to different age groups in the workplace. Furthermore, the study revealed numerous health conditions associated with sanitation labour, underlining the significance of addressing these concerns to enhance workers' well-being. The study emphasizes the importance of focused initiatives to address the health risks faced by sanitation workers. The findings underline the importance of establishing and executing health and safety programs that address the unique needs of various age groups in the workplace. Addressing these challenges will help local authorities improve sanitation workers' overall health and safety, resulting in a more effective and sustainable sanitation service. The findings are a critical foundation for future research and policy development to improve sanitation workers' working conditions and health consequences.

OBJECTIVES

- To study the demographic profile of the respondent
- To assess workers' health issues in sanitation work.

Theoretical framework

Structuralist perspective

Informal sanitation labour is often carried out by poor individuals who cannot find legitimate employment. Informal sanitation workers work for low wages in terrible conditions without job security. Sanitation workers may be forced to labour to cover their daily expenses due to vulnerabilities like disability, disease, or loss of family members. Family size and unemployment significantly impact sanitation workers' pay and working conditions.

Neoliberal perspective

Neoliberal researchers disagree with structure lists, arguing that informal workers prefer to work in sanitation independently. The rise of informal labour is attributed to the desire to avoid the costs, time, and effort of getting a regular job. Sanitation employees prefer to work in the informal sector. This group includes the study's youngest respondents. 13 participants account for approximately 18.57% of the sample. This suggests that fewer than a fifth of the responders are under 30. This group includes the study's youngest respondents. 13 participants account for approximately 18.57% of the sample. This suggests that fewer than a fifth of the responders are under 30. The 41-50 age group is the second-largest, with 22 responders (31.43% of the total). This is another central section of the sample, demonstrating that approximately one-third of respondents are in this slightly older age range. The 51-60 age group has the least respondents, accounting for only 12.86% of the overall sample. This suggests that fewer senior people participated in the poll, possibly indicating a younger to middle-aged demographic in the respondent pool. The sample is dominated by people aged 30 to 40, which suggests that the data or research is most typical of this population. A considerable population of 41 to 50 makes this a vital demographic to study. Younger respondents (under 30) and older respondents (over 50) are underrepresented, which could indicate fewer participants in these age groups or a skew in the target market. The table displays the distribution of respondents based on their educational qualifications, providing insight into the sample's academic background. A total of 70 people were polled, with 18 (25.71%) having completed high school as their most significant degree of education. This group accounts for over a quarter of the sample, representing those who may not have continued their formal education after high school. The next group, with 24 respondents (34.29%), consists of people who have finished higher secondary education, which typically includes grades 11 and 12. This group is slightly larger, representing a subset of the population who sought education beyond high school but may or may not have continued to further education. The largest group in the sample, including 28 individuals (40.00%), had a college or university degree. This indicates that about half of the respondents have sought and finished higher education, implying that people with advanced educational qualifications make up a more significant proportion of the sample. The high proportion of degree holders in the sample may indicate that the sample is biased toward more educated individuals, perhaps providing insights into how education level corresponds with aspects such as work prospects, stress, and general life experience. The respondents' diverse educational backgrounds enable comparative analysis of various education levels. The table shows a split of respondents by family structure, which might be joint or nuclear. Of the total 70 respondents, 28 are from joint families, accounting for 40% of the sample. A joint family often comprises many

generations living together, such as grandparents, parents, and children. This arrangement is more widespread in some cultures and areas, and it can impact family relationships, obligations, and stress levels due to numerous generations living together. On the other hand, 42 respondents, or 60%, come from nuclear households, which are often made up of only parents and their children. Nuclear families are frequently associated with more contemporary or metropolitan lifestyles, with fewer individuals involved in everyday decision-making and duties. The bulk of the sample comprises atomic families, which could reflect shifting society patterns or the demographic being polled.

The results show a considerable variation in the incidence of these conditions, with a Chi-Square value of 99.04 and a highly significant p-value of 7.23 e-15. This p-value is significantly lower than the 0.05 threshold, indicating that the differences in the rates of health conditions are statistically significant. The Mean Rank column assists in determining the relative frequency of each health condition. The most often reported conditions are Cough and Cold (mean rank 15.0), Allergy (14.0), and Fungal Infections (13.0). These disorders are more widespread, implying that respiratory and skin problems are prevalent among the workforce. Rarer illnesses, such as Leptospirosis (Mean Rank 1.0), Dengue Fever (2.0), and Vitiligo (3.5), have a lower ranking, indicating that they affect fewer workers. The ANOVA table shows the differences in stress levels among four age groups: "Up to 30," "30-40," "41-50," and "51-60." The research was conducted based on hypothetical mean stress levels and standard deviations for each group. The table indicates a Sum of Squares Between Groups (SSB) of 1515.29, which measures the variation in stress levels caused by age differences. The Mean Square Between Groups (MSB) value of 505.10 shows this variation divided by the degrees of freedom (df) for between-group comparisons, which is 3. This is used to determine how much of the overall variation in stress levels may be explained by age group variations. The Sum of Squares Within Groups (SSW), which is 11093, represents the diversity in stress levels within each age group. This demonstrates individual variances in stress levels that age groups do not explain. The Mean Square Within Groups (MSW) value of 167.65 is the average of this within-group variation, divided by the degrees of freedom for within-group comparisons (66).The F-statistic, estimated as 3.01, is the ratio of MSB to MSW and reflects how much variability is explained by variations across age groups instead of variability within each group. A higher F-value indicates a more potent effect of the age group factor on stress levels. The F-statistic has a p-value of around 0.04. This p-value suggests a statistically significant difference in stress levels between the age groups, which is unlikely to have occurred by chance alone. In other words, age group has a significant impact on stress levels.

REVIEW OF LITERATURE

1. **Hemali H.O.et al**. **(2022)** described the personnel aged 15 or older who installed, operated, serviced, cleaned, and emptied sanitation technology. Workers from different occupations or the general public were used as a comparison. Eligible outcomes include death, gastroenteritis, workplace injuries, respiratory illnesses, musculoskeletal diseases, as well as mental and social health issues. The risk of bias was assessed individually. Inverse variance meta-analysis with random effects was used on sufficiently homogeneous papers. Limited research exists on the health dangers sanitation workers face, particularly women, informal workers, and those in low-income nations. However, current research indicates that sanitation workers have higher occupational risks due to various health conditions
2. **Maria F et al. (2019)** the study emphasizes that infection in humans occurs by penetration into the mucous membranes or the skin. Humans become infected by contacting rodent urine, the primary reservoir. The study aimed to determine the presence of anti-Leptospira antibodies and leptospiral DNA in sanitation workers (an occupational group at higher risk) from Lisbon and the Tagus Valley Region. No anti-Leptospira antibodies were found in the worker samples. Non-pathogenic leptospiral were found in a serum sample, in any case. Furthermore, 77% had previously observed rodents in the workplace, and 94% always utilized Personal Protective Equipment (PPE). Despite rats being regularly in the workplace, applying PPE and hygiene procedures effectively prevented workers from coming into contact with this infectious agent.

3. **Girish Degavi et al. (2021)** the study explain industrial and institutional activities and the use of products and substances. Solid waste includes non-hazardous trash from households, institutions, retailers, and manufacturing businesses. Solid waste processing, sewage disposal, and proper disposal are essential topics in international and environmental standards 91.2%, with females accounting for almost 80% of the total. The study samples had a median age of approximately 30. Nearly 74% of research participants reported a strong awareness of preventing workplace health risks. Participants were positive towards occupational health dangers; however, only 10% demonstrated effective preventative practices. Despite receiving essential personal protective equipment, job discontent and the use of PPEs were shown to be significant barriers to implementing effective practices and work patterns among sanitary workers.
4. **Rajan D (2019)** The results of this research revealed that the majority of the sanitary workers had no idea about the various hazards arising as a result of the lack of protective devices, weight lifting, improper personal hygiene, imbalanced diet, body bending, long-standing, stress, absence of immunization, inadequate rest, long working hours, heavy workload, autocratic leadership style of the superior, and work-life imbalance. The study selected 60 sanitary workers using the convenience sampling methodology and obtained primary data from them utilizing the scheduled data collection method. To carry out the timetable technique, a questionnaire was created based on the researcher's observations and experience in hospital administration.
5. **Sina Temesgen et al. (2023),**the research included gastrointestinal and respiratory disorders (8%), numerous health issues (6%), and mental and social concerns. 2 (4%), and one research focused on the mental health issues of sanitation workers. Databases and other reports revealed a total of 168 studies. Finally, fifty studies were considered. Approximately 65% of the research was from affluent countries, whereas 56% came from developing countries. Over 91% of research utilized a cross-sectional design, with 50% using logistic and multivariate regression. Most of the study's results came from India (15%), followed by Egypt (10%). Of the 7,711 sanitary workers, 48% (3682) were sewage workers, with street sweepers accounting for 1441 (19%). There were 1317 (17%) wastewater workers, 828 (11%) solid waste collectors, 275 (3%), and 168 (2%) garbage collectors and street sweepers, respectively.

REFERENCES

1. *Awareness about causes of occupational hazards: An empirical study of sanitary workers*. (n.d.).
2. Degavi, G., Debbarma, S., GelchuAdola, S., Loka Safayi, B., Gemeda, U., &Utura, T. (2021). Occupational hazards and its relation with health-seeking and practicing behaviors among sanitary workers in Southern, Ethiopia. *International Journal of Africa Nursing Sciences*, *15*, 100339. https://doi.org/10.1016/j.ijans.2021.100339
3. Fernandes, M., Vieira, M. L., Carreira, T., & Teodósio, R. (2019). Sanitation workers from Portugal: Is there evidence of Leptospira spp? *Journal of Infection and Public Health*, *12*(5), 738–740. https://doi.org/10.1016/j.jiph.2019.02.001
4. Oza, H. H., Lee, M. G., Boisson, S., Pega, F., Medlicott, K., & Clasen, T. (2022). Occupational health outcomes among sanitation workers: A systematic review and meta-analysis. *International Journal of Hygiene and Environmental Health*, *240*, 113907. https://doi.org/10.1016/j.ijheh.2021.113907
5. Tolera, S. T. (2023). *Occupational Diseases among Sanitary Workers in Worldwide: Systematic Review*. https://doi.org/10.21203/rs.3.rs-1724683/v1

Table 1 Distribution of the respondents by age

Age in years	Number of respondents	Percentage
Up to 30	13	18.5
30-40	26	37.14
41-50	22	31.43
51-60	9	12.86
Total	**70**	**70.00**

Table 2 Educational qualifications of the respondents

Qualification	Number of respondents	Percentage
High School	18	25.71
Higher Secondary	24	34.29
Degree	28	40.00
Total	70	70.00

Table 3 Type of family of the respondents

Family type	Number of respondents	Percentage
Joint	28	40.00
Nuclear	42	60.00
Total	70	70.00

Table: 4 Respondents Health Issues

S no	Factors	Mean Rank	
1	Asthma	8.0	Chi-Square = 99.043956 Df: 14 Sig: (p-value) 7.23e-15
2	Allergy	14.0	
3	Cough & Cold	15.0	
4	Bronchitis	6.0	
5	Dermatitis	11.5	
6	Fungal Infections	13.0	
7	Rosacea	5.0	
8	Vitiligo	3.5	
9	Gastrointestinal Infections	10.0	
10	dengue fever	2.0	
11	leptospirosis	1.0	
12	hepatitis A	3.5	
13	Eye problem	11.5	
14	Headache	7.0	
15	Mental healthissues	9.0	

Table: 5 Respondents Health Issues

Age in years	N	Mean	SD
Up to 30	13	45	10
30-40	26	50	12
41-50	22	55	15
51-60	9	60	14
Total	**70**		

Table:6

	Sum of Squares	df	Mean Square	F	Sig.(p-value)
Between Groups	1515.29	3	505.10	3.01	0.04
Within Groups	11093	66	167.65		
Total	12608.29	69			

Indian Journal of Natural Sciences www.tnsroindia.org.in ©IJONS

Vol.15 / Issue 88 / Feb / 2025 *International Bimonthly (Print) – Open Access* *ISSN: 0976 – 0997*

REVIEW ARTICLE

Banana (*Musa acuminate & Musa balbisiana*): India's Beloved Plant with a Wealth of Pharmacological Treasures

Nabam Piya[1], Hiyashree Sharmah[2], Hasmi Waris[3], Prasurjya Saikia[4], Himanshu Gogoi[5], Dhiman Patowary[6],Hemanga Mazumdar[7], Topobon Bordoloi[8], Izaz Hussain[9]*, Lakhyajit Borah[9], Sneha Parbin[9] and Kangkan Jyoti Saud[9]

[1]Senior Research Fellow, Department of Pharmacology and Toxicology, College of Veterinary Science, Khanapara, (Affiliated to Assam Agriculture University, Guwahati), Assam, India.
[2]Assistant Professor, School of Pharmacy, Pragjyotishpur University, Guwahati, Assam, India.
[3]Assistant Professor, Department of Pharmacy, NEF College of Pharmacy, (Affiliated to Srimanta Sankaradeva University of Health Sciences), Guwahati, Assam, India.
[4]Assistant Professor, Faculty of Pharmaceutical Sciences, Himalayan University, Itanagar, Arunachal Pradesh, India.
[5]Assistant Professor, JB Institute of Pharmacy (Affiliated to Srimanta Sankaradeva University of Health Sciences), Guwahati, Assam, 781171, India.
[6]Scholar, Faculty of Pharmaceutical Science, Assam Down Town University, Guwahati, Assam, India.
[8]Assistant Professor, Department of Pharmacy, NEPEDS College of Pharmaceutical Sciences, Tetelia, Assam, India.
[9]Assistant Professor, School of Pharmacy, Arunachal University of Studies, Namsai, Arunachal Pradesh, India.

Received: 21 Nov 2024 Revised: 03 Dec 2024 Accepted: 27 Jan 2025

***Address for Correspondence**
Izaz Hussain
Assistant Professor,
School of Pharmacy,
Arunachal University of Studies,
Namsai, Arunachal Pradesh, India.
E.Mail: izazpharma@gmail.com

ABSTRACT

Musa acuminata and *Musa balbisiana*, commonly known banana species are integral to the diet and traditional medicine systems in India. This review aims to explore the phytochemical composition and pharmacological potential of these species focusing on their bioactive compounds and therapeutic applications. Both species are rich in a diverse array of secondary metabolites including alkaloids, flavonoids, terpenoids, phenolic acids, saponins and cardiac glycosides, which contribute to their biological activities.The pharmacological properties of Musa species have been extensively studied, revealing significant antioxidant, antimicrobial, antidiabetic and anticancer effects. Extracts derived from different parts of the plant such as the fruit, peel, flower, seeds and leaves exhibit robust free radical scavenging activity, inhibit microbial growth and show efficacy in regulating blood glucose levels. These

findings align with their traditional medicinal uses and highlight the plant's therapeutic potential in modern medicine. The review concludes that *Musa acuminata* and *Musa balbisiana* are valuable sources of bioactive compounds with considerable promise for drug discovery. While their ethnopharmacological applications are well-documented further research focusing on the isolation of specific compounds, mechanistic pathways and clinical evaluations is necessary to fully harness their medicinal potential. This work emphasizes the relevance of these plants in developing novel therapeutics particularly for conditions like cancer, diabetes and infectious diseases.

Keywords: *Musa acuminate*, *Musa balbisiana*, Phytochemical composition, Therapeutic applications.

INTRODUCTION

Botanicals have always played a significant role in medicine and wellness. According to ethnobotanical literature, plant extracts, infusions and powders have been utilized for centuries to treat a wide range of ailments[1]. In many cultures across the globe, plant parts have long been the primary means of addressing diseases and injuries and they continue to be used as traditional treatments in many areas today[2]. While much of this use was historically based on folklore, modern scientific studies now confirm the efficacy of many of these plant-based remedies[3]. The World Health Organization (WHO) reports that traditional medicine is used by a significant portion of the population in low-income countries for basic healthcare and demand for medicinal plants is growing in both developing and developed nations[4].The banana (Musa spp.) stands out as one of the most widely cultivated and consumed fruits worldwidewith immense cultural, economic and medicinal significance. In India, the banana plays a dual role both as a vital economic crop and as a key component in traditional medicine[5]. With global production reaching approximately 118 million tonnes in 2015, bananas are among the world's most important fruit crops[6]. In India, native varieties such as *Musa balbisiana* and *Musa acuminata* are widely consumed and various parts of the plant—including the fruit, seeds, flower and peel—are commonly used in ethnic therapeutic medicine[7]. Bananas also hold deep cultural and religious roots in India, as evidenced by their mention in ancient texts like Ayurvedic literature which emphasize their health benefits and spiritual significance. Known as "Kadali" in Sanskrit, the banana plays a prominent role in religious rituals and traditional healing practices[8]. Historical manuscripts such as the Ramayana (circa 2000 BC), Arthashastra (circa 250 BC) and Cilappatikaram (circa 500 AD) further attest to the banana's historical importance and widespread consumption in India, reflecting its long-standing association with health and well-being in Indian culture[9]. In recent years, scientific research has increasingly focused on the pharmacological properties of the banana plant confirming its significant therapeutic potential. Various parts of the plant, including the fruit, peel, flower and seeds are rich in bioactive compounds that provide a range of health benefits with minimal side effects. Traditionally, different parts of the banana have been widely used in various countries for medicinal purposes[10]. Research has uncovered a variety of biological activities associated with **Musa spp.,** including antibacterial, antioxidant, anti-cancer, antihyperglycemic and antidiabetic effects[11]. These findings highlight the importance of banana-derived compounds in the treatment of several ailments and their potential for drug development. The banana plant'sethnomedicinalsignificance is supported by its phytochemical composition that includes phenols, tannins, antioxidants, polyphenols and flavonoids[12]. These biologically active compounds contribute to its wide-ranging pharmacological activities and its ability to promote health and well-being in both humans and animals.

Phytochemistry of *Musaacuminate*

The phytochemical studies of *Musa acuminata* have uncovered a broad spectrum of bioactive compounds including alkaloids, fatty acids, tannins, terpenoids and anthocyanins, which are distributed across various parts of the plant like the fruit, peel, flower, leaf, pseudostem and rhizome[12]. In *Musa acuminata*, the aerial parts contain a variety of flavonoids including catechin, epicatechin, gallocatechin, epigallocatechin, podocarpus flavone, heveaflavone, 5,7-dihydroxy-4,6,8-trimethoxyflavone, 5,6-dimethoxy-4,7,8-trimethoxyflavone, 3-O-methyl-5-hydroxy diplacone, 3-O-methyl-5-O-methyldiplacone, mimulone, diplacone and others[13,14]. The aerial parts are also a source of saponins

such as protopanaxadiol, protopanaxatriol, gypsogenin, gypsogenic acid, quillaic acid and hederagenin[15]. Furthermore, cardiac glycosides including cardenolide, bufadienolide, isocardenolide, digitoxigenin, digoxigenin, gitoxigenin, strophanthidin and ouabagenin have been isolated from the plant[16]. Among the key therapeutic compounds, indole alkaloids like tryptamine, serotonin, physostigmine, harmine, canthionone, ajmalicine, catharanthine and tabersonine have been identified in *Musa acuminata*[17]. Additionally, phenolic acids which play a role in the plant's antifungal and antioxidant activities include hydroxybenzoic acid derivatives (such as gallic acid, vanillic acid and syringic acid) and hydroxycinnamic acid derivatives (like p-coumaric acid and caffeic acid) (figure 1)[18].

Phytochemistry of *Musa Balbisiana*

Musa balbisiana contains a rich variety of phytochemicals and secondary metabolites. It is particularly high in potassium and chloride, which contribute to its high alkalinity and potential medicinal benefits. Different parts of the plant produce compounds such as flavonoids, polyphenols, tannins, monoterpenoids, sesquiterpenoids, quinones and saponins. For example, the inflorescence of the plant contains three triterpenes: 31-norcyclolaudenone, cycloartenol and (24R)-4a.24-trimethyl-5a-cholesta-8.25. Carotenoids, a group of compounds with around 600 members are also found in the fruit including α-carotene, β-carotene and β-cryptoxanthin, as well as other carotenoids like lycopene and lutein[19]. Carotenoid-rich fruit consumption is known to improve immunity and reduce the risk of diseases such as cancer, type 2 diabetes and cardiovascular issues. The seeds of *M. balbisiana* contain ferulic acid, C16 and C18 fatty acids and polyphenols. Further analysis using GC-MS has identified compounds such as Z-12-pentacosene, stigmasterol and 10-heneicosene in the inflorescence, while a bioactive compound called apiforolwas reported from the acetone extract of the seeds. The methanolic root extract contains maruchantin-E and the methanolic fruit pulp extract includes chlorogenic acid, (-)-epicatechin, catechol, kaempferol 3-O-sophoroside, quercetin 3-O-[2-O-b-D-glucopyranosyl]-a-L-rhamnopyranoside, rutin and apigenin-6-C-glucoside-7-O-glucoside. Studies also have identified five additional compounds in the methanolic rhizome extract including difluoroisocyanatophosphine and pseudodiosgenin diacetate[20,21]. Elemental analysis has shown that *M. balbisiana* contains significant amounts of zinc, nickel, copper and manganese with no toxic elements like cadmium, lead or chromium detected. Rutin, was detected as the main compound in the ethanolic extract of the banana leaves and high amounts of cyanidin-3-glucoside and peonidin-3-glucoside were found in the inflorescence bract extracts[22]. Other identified phenolic and aromatic compounds include apigenin glycosides, myricetin glycoside, naringenin glycosides, kaempferol-3-O-rutinoside, quercetin-3-O-rutinoside, dopamine and N-acetylserotonin from the sap of *M. balbisiana*(figure 2)[7].

Pharmacological Activities of *Musa acuminate*

The abundant and diverse phytochemicals found in various parts of the *Musa acuminata* plant have demonstrated potential in traditional medicine for disease prevention likely due to their rich phytochemical composition. The health benefits of *Musa acuminata* have been investigated using several models which are outlined below in relation to both *in vitro* and *in vivo* studies[23].

Antioxidant Activity

The antioxidant potential of various parts of *Musa acuminata* has been widely studied using different extracts and assays. **Gu-cai et al.** found the acetonepeel extract to be the most effective in lipid peroxidation inhibition with 92% inhibition in the β-carotene bleaching assay outperforming the DPPH assay (82.2% efficacy**)**[24]**. Zawawy** showed that ethanolic peel extracts had 69.56% DPPH inhibition at 2 mg/mL (IC_{50} of 139.50 μg/mL), with significant reducing power comparable to ascorbic acid[25]. **Abou-Elellal and Mourad**also reported high ABTS scavenging activity (95%) and reducing power (679 μg GAE/g) in ethanolic peel extracts[26].**Navghare and Dhawale** demonstrated that *M. acuminata* peel extract had hydrogen peroxide scavenging activity with IC_{50} of 35.70 μg/mL[27]. **Rebello et al.** found high antioxidant activity in banana peel flour and **Giri et al**. showed it enhanced antioxidant enzyme activity in fish[28,29]. The methanolic flower extract exhibited strong DPPH scavenging (IC_{50} of 7.63 mg/mL)[30], while **Lee et al.** reported an even lower IC_{50} of 0.19 mg/mL for the flowering stalk[31].**Adinarayana et al.** showed that the ethanolic rhizome extract achieved 81.41% DPPH scavenging at 200 μg/mL comparable to ascorbic acid[32]. **Singhal**

et al. found that methanolic peel extract had stronger antioxidant activity and higher flavonoid and phenolic content than the hexane extract, while both increased leukocyte and lymphocyte counts in rats[33].

ANTIMICROBIAL ACTIVITY

The antimicrobial activity of various *Musa acuminata* plant parts has been extensively studied demonstrating promising results against multiple pathogens. **Venkatesh et al.** reported that ethanol extracts from the corm of *M. acuminata* exhibited antibacterial activity against eight clinical strains of both Gram-positive and Gram-negative bacteria with MIC values ranging from 0.5 to 3.0 mg/mL[34]. Similarly, **Karuppiah and Mustaffa**found that hexane, ethyl acetate and methanolic leaf extracts were effective against multidrug-resistant clinical pathogens[35]. **Bocanegra-Garcia et al.** reported that the aqueous stem extract inhibited *Streptococcus pneumoniae* at 250 μg/mL[36]. In one study the methanolic flower extract showed antimicrobial activity with MIC values of 1.56 to 12.5 mg/mL [30], while in another study water and 50% methanol pseudostem extracts had significant zones of inhibition against *Staphylococcus aureus*[37]. **Niamah et al.** found methanolic peel extract to have variable antibacterial activity against *Escherichia coli*, *S. aureus*, *Lactobacillus casei* and others with zones of inhibition between 13-24 mm at 300 mg/mL[38]. **Mordi et al. (2016)** suggested that the antimicrobial potential of the peel extract was likely due to the presence of 2-methyl-5-(1-methylethyl) phenol, a strong antimicrobial compound[39]. Furthermore, **Camacho-Corona et al.** reportedmethanolic stem extracts demonstrated strong activity against *Mycobacterium tuberculosis*with MIC values below 0.2 mg/mL. The antifungal activity of *M. acuminata* was also notable[40]. **Meenashree et al.** found that ethanolic, acetone and petroleum ether leaf extracts were effective against *Aspergillus terreus* and *Penicilliumsolitum* with inhibition zones up to 5.7 cm[41]. **Zawawy**showed ethanolic peel extracts had MIC values of 20-30 mg/mL against *Fusariumoxysporum*, *Penicilliumdigitatum* and *Aspergillus niger*[25]. A formulated gel containing 4% acetone leaf extract exhibited a 27 mm inhibition zone against *Candida albicans* comparable to nystatin[42].Studies also highlight the variation in antimicrobial efficacy depending on the plant part, extraction method and pathogens tested. For example, **Harith et al.** found that methanolic leaf extracts were effective against *Staphylococcus epidermidis* and *Trichophytonmentagrophytes* forming inhibition zones of 4.0 mm and 5.0 mm respectively[43], while **Subramaniam et al**. found no significant effect of ethanolic peel extracts against Gram-positive bacteria[44]. **Bashir et al.** reported inhibition zones of 19 mm and 17 mm against *E. coli* and *S. aureus* respectively using peel solutions[45]. Overall, these studies validate the traditional use of *M. acuminata* for treating bacterial and fungal infections with varying levels of efficacy across different plant parts and extraction methods.

ANTI-CANCER ACTIVITY

Various studies have demonstrated the antitumor potential of *Musa acuminata* extracts against different cancer cell lines including MCF-7 (breast adenocarcinoma), HeLa (human epithelial carcinoma), Ehrlich ascites carcinoma and Hep G2 (hepatic carcinoma). **Zawawy**found that ethanolic peel extracts had a stronger inhibitory effect on MCF-7 cells reducing cell viability by 32.6% at 50 μg/mL compared to the standard Thymoquinone, which showed a 23.7% reduction at the same concentration[25]. Similarly, **Abou-Elella and Mourad**reported better anticancer activity of the ethanolic peel extract against Ehrlich ascites carcinoma cells (IC_{50} = 33.9 μg/mL) compared to HeLa cells (IC_{50} = 49.5 μg/mL)[26].**Adinarayana et al.**reportedthe ethanolic extract of *M. acuminata* rhizome also demonstrated dose-dependent cytotoxicity against HeLa cells with a maximum inhibition of 50.32% at 256 μg/mL[32]. In contrast, **Roobha et al.** found that methanolic extracts from the bracts had a lower inhibitory effect on MCF-7 cells (12.24% at 1000 μg/mL), though the extract caused significant morphological changes, reducing cell adherence[46]. **Abdullah et al.** observed that the methanolic extracts from both peel and pulp of *M. acuminata* fruit exhibited better cytotoxicity against Hep G2 cells (IC_{50} = 47.74 μg/mL)[47], while the heart extract (bracts and flower) was more effective against MCF-7 cells (IC_{50} = 96.36 μg/mL) likely due to differences in glycoprotein-mediated transport mechanisms[48]. The presence of bioactive compounds such as anthocyanins in the peel, bracts and flowerand lectin in the fruit contributes to *M. acuminata*'s anticancer properties. Banana lectin has been shown to inhibit leukemia (L1210) and hepatoma (Hep G2) cell proliferation at low concentrations[49]. Furthermore, **Augustine et al.** investigated the anticancer effects of an ethanol extract from *M. acuminata* pulp, identifying key compounds such as palmitic acid, linoleic acid, 5-hydroxymethylfurfural and 5-methyl-2-ethylamino-2-thiazoline. This extract exhibited cytotoxicity

with IC_{50} values of 250 μg/mL, 175 μg/mL and 320 μg/mL against MDA-MB-231 (breast cancer), HCT-116 (colon cancer) and MG-63 (osteosarcoma) respectively, suggesting its potential use in cancer treatment[50].

ANTIDIABETIC ACTIVITY

The antidiabetic potential of *Musa acuminata* fruit and its various extracts has been widely studied. **Philip et al.** demonstrated *in vitro* α-amylase inhibition by *M. acuminata* fruit ethanolic extract, with an IC_{50} of 1.25 mg/mL, which was less potent than the standard drug Okamet (0.44 mg/mL)[51]. **Navghare and Dhawale**evaluated the antihyperglycemic effects of the fruit's inner peel extract in normoglycemicWistar rats showing dose-dependent activity (100–400 mg/kg), although no significant differences in blood glucose levels were observedacross control, extract-treated and Glimepiride-treated groups. However, significant reductions ($p<0.01$) were seen at 200 and 400 mg/kg doses in glucose-loaded normoglycemic rats[27]. **Bucao et al.** conducted an *in silico* analysis, identifying 11 out of 87 compounds from *M. acuminata* with strong binding affinities comparable to acarbose with sesamin showing the highest affinity (–9.8 kcal/mol)[52]. Additionally, **Vijay et al.** confirmed the glucose-lowering effect of *M. acuminata* peel extract in experimental animals reporting increased glycogen content and improved body weight[53]. **Genatrika et al.** further supported these findings showing that *M. acuminata*Colla fruit peel ethanol extract, at doses of 250, 375 and 500 mg/kg BW, significantly lowered blood glucose in diabetic rats with the highest reduction at 500 mg/kg BW (42.62%) comparable to glibenclamide[54]. These studies collectively reinforce the antidiabetic properties of *M. acuminata* highlighting its potential for diabetes management.

PHARMACOLOGICAL ACTIVITIES OF *Musa balbisiana*

The rich and varied phytochemicals present in different parts of the *Musa balbisiana* plant have shown significant potential in traditional medicine primarily for disease prevention and management likely due to their diverse bioactive compounds[21,22]. The therapeutic benefits of *Musa balbisiana*have been explored through a range of *in vitro* and *in vivo* studies, which are summarized below to highlight its pharmacological effects across different experimental models.

ANTIOXIDANT ACTIVITY

Several studies have explored the antioxidant potential of *Musa balbisiana*Colla. **Revadigar et al.** evaluated the ethanolic extract of *M. balbisiana* inflorescence and reported moderate antioxidant activity across various assays, identifying 22 compoundsincluding steroids, fatty acids and long-chain aliphatic compounds via GC-MS, which may contribute to its antioxidant effects[55]. **Basumatary et al.** examined the antioxidant activity of *M. balbisiana* inflorescence using DPPH and FRAP assays, revealing an IC_{50} value of 229.726 ± 0.718 μg/mL in the DPPH assay and a FRAP value of 108.046 ± 0.169 μM TE/g dried extract[56]. **Trieu et al.** further confirmed the antioxidant properties of *M. balbisiana* fruit extracts, noting high polyphenol and flavonoid content[57]. **Daimari et al.** investigated the corm of *M. balbisiana* demonstrating strong free radical scavenging activity[58], while **Muchahary et al.** found significant antioxidant activity in *M. balbisiana* blossom extracts[59]. These findings highlight the robust antioxidant potential of various parts of *M. balbisiana*.

ANTIBACTERIAL ACTIVITY

Several studies have investigated the antibacterial properties of ***Musa balbisiana*Colla**. **Nghia et al.** prepared extracts from *M. balbisiana* seeds using solvents such as petroleum ether, ethyl acetate and butanol, with the butanol extract showing an MIC of 22.5 mg/mL against both *Enterococcus faecalis* and *Staphylococcus aureus*. The ethyl acetate extract exhibited stronger antibacterial activity with MIC values of 7.5 mg/mL and 3.5 mg/mL against *E. faecalis* and *S. aureus*, respectively[60]. **Kusuma et al.** evaluated the antibacterial potential of *M. balbisiana* fruit extracts against *Shigelladysenteriae* ATCC 13313, demonstrating significant activity with MBC values between 5–10% w/v attributed to the presence of secondary metabolites[61]. **Misrahanum et al.** further assessed the antibacterial activity of ethanol extracts from the flesh and peel of unripe *M. balbisiana* against *S. aureus* and *Escherichia coli* using a well diffusion method. The highest inhibitory effect was observed with the peel extract against *S. aureus* (9.3 mm at 10% concentration) and with the flesh extract against *E. coli* (8.63 mm at 20% concentration)[62]. These findings highlight the antibacterial potential of various *M. balbisiana* extracts.

ANTICANCER AND CYTOTOXIC ACTIVITY

Revadigar et al. evaluated the cytotoxicity of *Musa balbisiana* extract using the MTT assay. The extract demonstrated selective cytotoxicity towards the HT-29 colon cancer cell line. Morphological analysis further indicated that the extract induces apoptosis in HT-29 cells suggesting its potential role as an anti-cancer agent[55]. Similarly, **Huyen et al.** assessed the anti-proliferative activities of polyphenol- and saponin-enriched extracts from *M. balbisiana* fruit. The anticancer activity was determined through the inhibition of MCF-7 breast cancer cell proliferation using the sulforhodamine B assay. The extract exhibited significant inhibitory effects with IC_{50} value 289.5 ± 8.7 μg/mL for MCF-7 cell proliferation[63]. These findings suggest that the *M. balbisiana* fruit extract holds potential as a therapeutic agent for breast cancer treatment.

ANTIDIABETIC ACTIVITY

Kalita et al. found that *Musa balbisiana* extract significantly reduced fasting blood glucose (62.5%), cholesterol (36.2%), triglycerides (54.5%) and LDL (50.94%) in STZ-induced diabetic rats with observed tissue regeneration in the pancreas, liver and kidneys[64]. **Borah et al.** reported that ethanolic extracts from *M. balbisiana* flowers and stalks reduced glucose, cholesterol, triglycerides and LDL while boosting HDL, insulin and antioxidant levels in diabetic rats also reducing glucose absorption ($P < 0.01$)[65]. **Gurumayum et al.** showed that *M. balbisiana* seed extracts strongly inhibited α-amylase and α-glucosidase key enzymes in postprandial glucose control suggesting its potential as a safer antidiabetic treatment[66].

FUTURE PROSPECTS AND RESEARCH DIRECTIONS

Although *Musa acuminata* and *Musa balbisiana* exhibit promising pharmacological properties, further research is necessary to comprehensively understand their mechanisms of action and optimize their application in pharmaceutical science. Future research should focus on delineating the precise molecular pathways through which bioactive compounds from these plants exert their therapeutic effects. While extensive *in vitro* and animal studies have provided valuable insights, human clinical trials are crucial to validate these findings and ensure their safety and efficacy for therapeutic use. Moreover, the potential for the commercialization of banana-derived products should be explored particularly in the development of supplements, topical formulations and pharmaceutical agents. Advancing research in these areas could facilitate the transition of these plants from traditional use to modern pharmaceutical applications, thereby maximizing their therapeutic potential.

CONCLUSION

The banana species *Musa acuminata* and *Musa balbisiana*, widely consumed in India, possess significant pharmacological potential that extends beyond their nutritional value. This review consolidates the phytochemical and therapeutic properties of both species underscoring their role in traditional medicine and their relevance for modern therapeutic applications. Both plants are rich in bioactive compounds such as alkaloids, flavonoids, phenolic acids, terpenoids, saponins and cardiac glycosides contributing to their diverse pharmacological activities. Musas exhibit potent antioxidant, antimicrobial, antidiabetic and anticancer effects which are supported by both *in vitro* and *in vivo* studies. Specifically, extracts from various parts of these plants—including the fruit, peel, flower, seeds and leaves demonstrate efficacy in inhibiting oxidative stress, bacterial infections, tumor cell proliferation and blood glucose levels. Their antioxidant activity is particularly noteworthy, with various extracts showing strong free radical scavenging abilities across multiple assays. Similarly, their antimicrobial and antidiabetic properties have been validated through the inhibition of bacterial growth and key enzymes involved in glucose metabolism. *Musa acuminata* and *Musa balbisiana* offer a rich source of compounds with therapeutic potential making them promising candidates for drug development. The demonstrated pharmacological activities validate the traditional use of these plants in ethnomedicine, while modern research highlights their utility in addressing conditions such as diabetes, cancer and microbial infections. Future research focusing on the isolation of active compounds, mechanistic studies and clinical trials could further elucidate their therapeutic potential and pave the way for their inclusion in modern pharmacopoeias.

REFERENCES

1. Rodino S, Butu M. Herbal extracts—new trends in functional and medicinal beverages. *Functional and medicinal beverages*. Elsevier, pp.73–108 (2019).
2. Halberstein RA. Medicinal plants: historical and cross-cultural usage patterns. *Ann. Epidemiol.*, **15**, 686–99 (2005).
3. Gurib-Fakim A. Medicinal plants: traditions of yesterday and drugs of tomorrow. *Mol. Aspects Med.*, **27**, 1–93 (2006).
4. Patwardhan B. Traditional medicine: A novel approach for available, accessible and affordable health care. *World Heal. Organ.*, **13**, (2005).
5. Qamar S, Shaikh A. Therapeutic potentials and compositional changes of valuable compounds from banana-A review. *Trends Food Sci. Technol.*, **79**, 1–9 (2018).
6. Evans EA, Ballen FH, Siddiq M. Banana production, global trade, consumption trends, postharvest handling, and processing. *Handb. Banan. Prod. postharvest Sci. Process. Technol. Nutr.*, 1–18 (2020).
7. Elayabalan S, Subramaniam S, Shobana V, Ashok Kumar K. An overview on phytochemical Composition of Banana (Musa spp.). *Int. Bimon. Indian J. Nat. Sci*, **7**, 12408–19 (2017).
8. Wani AM, Sahoo G, Gupta S. Sacred trees of India: Traditional approach towards plant conservation. *Int. J. Curr. Microbiol. Appl. Sci.*, **9**, 2606–13 (2020).
9. Trivedi H, Aveling H, Yamada T. South Asia, Southeast Asia, and Oceania. *Lit. A World Hist.*, **2**, 355–425 (2022).
10. Kumar KPS, Bhowmik D, Duraivel S, Umadevi M. Traditional and medicinal uses of banana. *J. Pharmacogn. Phytochem.*, **1**, 51–63 (2012).
11. Lopes S, Borges CV, de Sousa Cardoso SM, de Almeida Pereira da Rocha MF, Maraschin M. Banana (Musa spp.) as a source of bioactive compounds for health promotion. *Handb. Banan. Prod. postharvest Sci. Process. Technol. Nutr.*, 227–44 (2020).
12. Kumar N, Ved A, Yadav RR, Prakash O. A comprehensive review on phytochemical, nutritional, and therapeutic importance of Musa. *Int. J. Curr. Res. Rev.*, **13**, 114–24 (2021).
13. Begashaw T, Dagne A, Yibeltal D. Review on Phytochemistry, Medicinal Properties, and Toxicities of the Genus Musa. *Tradit. Med.*, **4**, 1–24 (2023).
14. Kumar P. Musa acuminata: From Daily Normal Eating to Treating Complex Diseases. *Int. J. Med. Pharm. Sci.*, **11**, 01–6 (2021).
15. Mathew NS, Negi PS. Traditional uses, phytochemistry and pharmacology of wild banana (Musa acuminata Colla): A review. *J. Ethnopharmacol.*, **196**, 124–40 (2017).
16. Anupama Yadav. Banana (Musa acuminata): Most popular and common Indian plant with multiple pharmacological potentials. *World J. Biol. Pharm. Heal. Sci.*, **7**, 036–44 (2021).
17. Thelly MT, Laxman Pol S, Suresh SN, Nisha B, Ajeed A, Billah M, Kiran Khanna D, Kumar V. Phytochemistry, Pharmacological Activities and Traditional Uses of Musa Acuminata. **7**, 3277–302 (2024).
18. Kumar N, Ved A, Yadav RR, Prakash O. A Comprehensive Review on Phytochemical, Nutritional, and Therapeutic Importance of Musa acuminate. *Int. J. Curr. Res. Rev.*, **13**, 114–24 (2021).
19. Choudhury A, Kumari M, Kumar Dey B. Morphological and Phytochemical Characterization of Musa Balbisiana Colla and Musa Acuminata Colla. *J. Appl. Pharmacogn. Phytochem.*, **3**, 1–8 (2023).
20. Deka P, Kashyap A, Sharma D, Baruah C. A Review on Musa Balbisiana Colla. *Int. J. Pharm. Sci. Invent. ISSN*, **7**, 14–7 (2018).
21. Rama Devi Korni, Tanuja Boddepalli, Jyothsna Elusuri, Jagadeesh Panda. Banana Peel: A potential waste product with numerous pharmacological activities. *GSC Biol. Pharm. Sci.*, **23**, 160–74 (2023).
22. Swargiary A, Boro H, Kumar Roy M, Akram M. Phytochemistry and Pharmacological Property of Musa balbisiana Colla: A Mini-Review. *Pharmacogn. Rev.*, **15**, 91–5 (2021).
23. Ahmad BA, Zakariyya UA, Abubakar M, Sani MM, Ahmad MA. Pharmacological activities of banana. *Banan. Nutr. Process. Kinet.*, 1–20 (2019).
24. Mathew NS, Negi PS. Traditional uses, phytochemistry and pharmacology of wild banana (Musa acuminata Colla): A review. *J. Ethnopharmacol.*, **196**, 124–40 (2017).

25. El-Zawawy NA. Antioxidant, antitumor, antimicrobial studies and quantitative phytochemical estimation of ethanolic extracts of selected fruit peels. (2015).
26. Abou-Elella F, Mourad R. Anticancer and anti-oxidant potentials of ethanolic extracts of Phoenix dactylifera, Musa acuminata and Cucurbita maxima. (2015).
27. Navghare V V, Dhawale SC. In vitro antioxidant, hypoglycemic and oral glucose tolerance test of banana peels. *Alexandria J. Med.*, **53**, 237–43 (2017).
28. Rebello LPG, Ramos AM, Pertuzatti PB, Barcia MT, Castillo-Muñoz N, Hermosín-Gutiérrez I. Flour of banana (Musa AAA) peel as a source of antioxidant phenolic compounds. *Food Res. Int.*, **55**, 397–403 (2014).
29. Giri SS, Jun JW, Sukumaran V, Park SC. Dietary administration of banana (Musa acuminata) peel flour affects the growth, antioxidant status, cytokine responses, and disease susceptibility of rohu, Labeo rohita. *J. Immunol. Res.*, **2016**, 4086591 (2016).
30. Sumathy V, Lachumy SJ, Zakaria Z, Sasidharan S. In vitro bioactivity and phytochemical screening of Musa acuminata flower. *Pharmacologyonline*, **2**, 118–27 (2011).
31. Wong C, Kiew R, Loh JP, Gan LH, Set O, Lee SK, Lum S, Gan YY. Genetic diversity of the wild banana Musa acuminata Colla in Malaysia as evidenced by AFLP. *Ann. Bot.*, **88**, 1017–25 (2001).
32. Adinarayana KPS, Babu AP. Anti-oxidant activity and cytotoxicity of ethanolic extracts from rhizome of Musa acuminata. *Nat. Sci.*, **3**, 291–4 (2011).
33. Singhal M, Ratra P. Antioxidant activity, total flavonoid and total phenolic content of musa acuminate peel extracts. *Glob. J. Pharmacol.*, **7**, 118–22 (2013).
34. Venkatesh K V, Girish KK, Pradeepa K, Santosh KSR. Antibacterial activity of ethanol extract of Musa paradisiaca cv. Puttabale and Musa acuminate cv. grand naine. *Asian J. Pharm. Clin. Res*, **6**, 167–70 (2013).
35. Karuppiah P, Mustaffa M. Antibacterial and antioxidant activities of Musa sp. leaf extracts against multidrug resistant clinical pathogens causing nosocomial infection. *Asian Pac. J. Trop. Biomed.*, **3**, 737–42 (2013).
36. Bocanegra-García V, del Rayo Camacho-Corona M, Ramírez-Cabrera M, Rivera G, Garza-González E. The bioactivity of plant extracts against representative bacterial pathogens of the lower respiratory tract. *BMC Res. Notes*, **2**, 1–5 (2009).
37. Onyema C, Ofor C, Okudo V, Ogbuagu A. Phytochemical and antimicrobial analysis of banana pseudo stem (Musa acuminata). *Br. J. Pharm. Res.*, **10**, 1–9 (2016).
38. Niamah AK. Determination, identification of bioactive compounds extracts from yellow banana peels and used in vitro as antimicrobial. (2014).
39. Mordi RC, Fadiaro AE, Owoeye TF, Olanrewaju IO, Uzoamaka GC, Olorunshola SJ. Identification by GC-MS of the components of oils of banana peels extract, phytochemical and antimicrobial analyses. (2016).
40. Camacho-Corona M del R, Ramírez-Cabrera MA, Santiago OG, Garza-González E, Palacios I de P, Luna-Herrera J. Activity against drug resistant-tuberculosis strains of plants used in Mexican traditional medicine to treat tuberculosis and other respiratory diseases. *Phyther. Res. An Int. J. Devoted to Pharmacol. Toxicol. Eval. Nat. Prod. Deriv.*, **22**, 82–5 (2008).
41. Meenashree B, Vasanthi VJ, Mary RNI. Evaluation of total phenolic content and antimicrobial activities exhibited by the leaf extracts of Musa acuminata (banana). *Int. J. Curr. Microbiol. Appl. Sci.*, **3**, 136–41 (2014).
42. Bankar AM, Dole MN. Formulation and evaluation of herbal antimicrobial gel containing musa acuminata leaves extract. *J. Pharmacogn. Phytochem.*, **5**, 1–3 (2016).
43. Harith SS, Yasim NHM, Harun A, Omar WSAW, Musa MS. Phytochemical screening, antifungal and antibacterial activities of Musa acuminata plant. *Malaysian J. Anal. Sci.*, **22**, 452–7 (2018).
44. SUBRAMANİAM Y, MAZLAN N, HASSAN H, JAAFAR JN, ANUA SM, YOUNG TT, AL-HUMAİRİ SNS. Antimicrobial Activity of Musa acuminata Peel Extract against Gram-Positive Bacteria. *Int. J. Life Sci. Biotechnol.*, **3**, 191–6 (2020).
45. Bashir F, Hassan A, Mushtaq A, Rizwan S, Jabeen U, Raza A, Anjum S, Masood A. Phytochemistry and antimicrobial activities of different varieties of banana (Musa acuminate) peels available in Quetta city. *Polish J. Environ. Stud.*, **30**, 1531–8 (2021).
46. Jenshi Roobha J, Aravindhan MSKM. In vitro evaluation of anticancer property of anthocyanin extract from Musa acuminate bract. *Res. Pharm.*, **1**, (2015).

47. Abdullah FC, Rahimi L, Zakaria ZA, Ibrahim AL. Hepatoprotective, antiulcerogenic, cytotoxic and antioxidant activities of Musa acuminata peel and pulp. *Nov. Plant Bioresour. Appl. Food, Med. Cosmet.*, 371–82 (2014).
48. Rogalska A, Szwed M, Rychlik B. The Connection between the Toxicity of Anthracyclines and Their Ability to Modulate the P-Glycoprotein-Mediated Transport in A549, HepG2, and MCF-7 Cells. *Sci. World J.*, **2014**, 819548 (2014).
49. Cheung AHK, Wong JH, Ng TB. Musa acuminata (Del Monte banana) lectin is a fructose-binding lectin with cytokine-inducing activity. *Phytomedicine*, **16**, 594–600 (2009).
50. Augustine A, Sundararaman G, Vazhacharical PJ, Syamkumar T.S. . Evaluating the Anticancer Properties of Musa acuminata colla Ethanolic Extract through In vitro Analysis. *Uttar Pradesh J. Zool.*, **45**, 231–40 (2024).
51. Philip DC, Lavanya B, Sasirekha G V, Santhi M. Phytochemical Screening, antioxidant and antidiabetic activity of Musa acuminata, Citrus sinensis and Phyllanthus emblica. *Am. J. Pharm. Tech. Res*, **5**, 557–64 (2015).
52. Bucao XEN, Solidum JN. In Silico Evaluation of Antidiabetic Activity and ADMET Prediction of Compounds from Musa acuminata Colla Peel. *Philipp. J. Sci.*, **151**, 171–92 (2022).
53. Vijay N, Shashikant D, Mohini P. Assessment of antidiabetic potential of Musa acuminata peel extract and its fractions in experimental animals and characterisation of its bioactive compounds by HPTLC. *Arch. Physiol. Biochem.*, **128**, 360–72 (2022).
54. Genatrika E, Laksari VNH, Tjiptasurasa T. Antidiabetic activity of musa acuminata colla fruit peel (MACFP) ethanol extract in glucose-induced diabetic rats. *MATEC Web Conf.*, **197**, 0–3 (2018).
55. Revadigar V, Al-Mansoub MA, Asif M, Hamdan MR, Majid AMSA, Asmawi MZ, Murugaiyah V. Anti-oxidative and cytotoxic attributes of phenolic rich ethanol extract of Musa balbisiana Colla inflorescence. *J. Appl. Pharm. Sci.*, **7**, 103–10 (2017).
56. Basumatary S, Nath N. Assessment of Chemical Compositions and in vitro Antioxidant Properties of Musa balbisiana Colla Inflorescence. *Int. J. Pharm. Res.*, **10**, 80–90 (2018).
57. Ly Hai Trieu, Le My Huyen, Lam Bich Thao, Le Duc Thanh, Pham Thanh Huyen, Nguyen Minh Khoi, Le Van Minh. Pharmacognostical standardization, phytochemical analysis, and antioxidant activity of Musa balbisiana Colla fruits. *Int. J. Res. Pharm. Sci.*, **11**, 7920–31 (2020).
58. Daimari M, Swargiary A. Study of phytochemical content and antioxidant properties of musa balbisiana corm extract. *Indian J. Pharm. Sci.*, **82**, 707–11 (2020).
59. Muchahary S, Deka SC. *Impact of supercritical fluid extraction, ultrasound-assisted extraction, and conventional method on the phytochemicals and antioxidant activity of bhimkol (Musa balbisiana) banana blossom*. Vol. 45, (2021).
60. Nghia BT. Antioxidant and Antibacterial Activities of Extracts From Seeds of Musa Balbisiana. *Vietnam J. Sci. Technol.*, **54**, 348 (2018).
61. Kusuma SAF, Mita SR, Firdayani I, Mustarichie R. Study on the antibacterial activity of fruit extracts of klutuk banana (Musa balbisiana colla) against shigella dysenteriae ATCC 13313. *Asian J. Pharm. Clin. Res.*, **10**, 220–3 (2017).
62. Anusha G, Sunayana R, Ponnam M, Kumar BA. Asian Journal of Pharmaceutical Research and Development. *Asian J. Pharm. Res. Dev.*, **8**, 77–80 (2020).
63. ANTI-LIPASE AND MCF-7 BREAST CANCER CELL PROLIFERATION INHIBITION IN VITRO OF THE EXTRACT-ENRICHED POLYPHENOLS AND SAPONINS FROM Musa balbisiana FRUIT Nguyen Thi Thu Huyen , Dinh Khanh Dieu , Nguyen Huynh Tram , Hoang Thi Ngoc Nhon *. **24**, 93–9 (2024).
64. Kalita H, Boruah DC, Deori M, Hazarika A, Sarma R, Kumari S, Kandimalla R, Kotoky J, Devi R. Antidiabetic and antilipidemic effect of Musa balbisiana root extract: A potent agent for glucose homeostasis in streptozotocin-induced diabetic rat. *Front. Pharmacol.*, **7**, 1–11 (2016).
65. Borah M, Das S. Antidiabetic, antihyperlipidemic, and antioxidant activities of Musa balbisiana Colla. in Type 1 diabetic rats. *Indian J. Pharmacol.*, **49**, 71–6 (2017).
66. Pratim Sarma P, Khound P, Kumar Jana U, Devi R. Nutritional composition and pharmacological activity of Musa balbisiana Colla seed: an insight into phytochemical and cellular bioenergetic proling Nonibala Gurumayum Institute of Advanced Study in Science and Technology. 3–9 (2023).

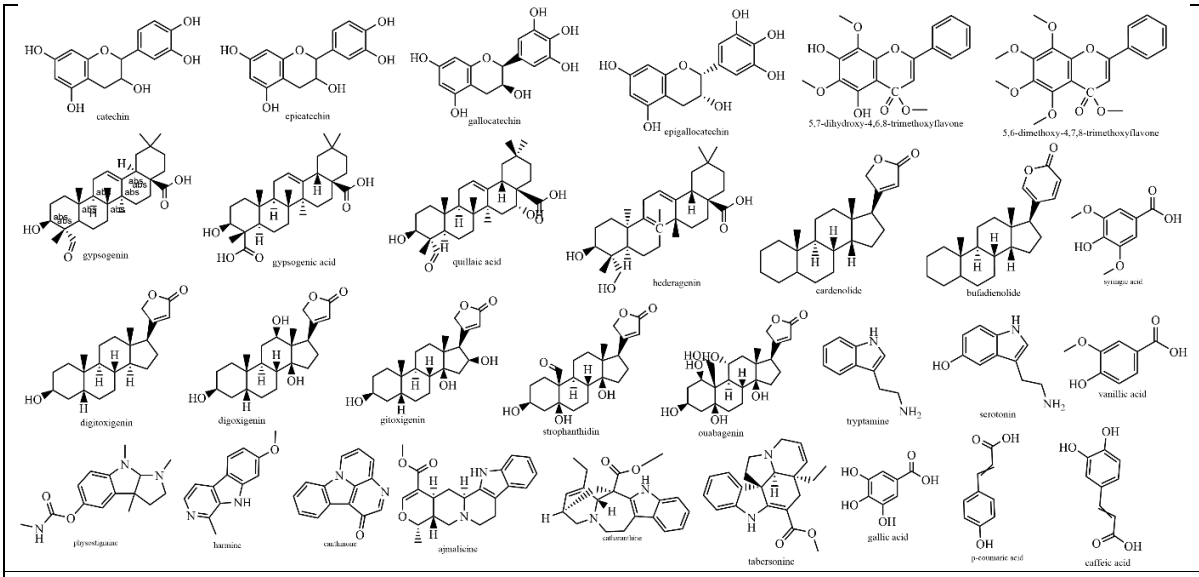

Figure 1 Phytochemicals present in various part of *Musa acuminate*

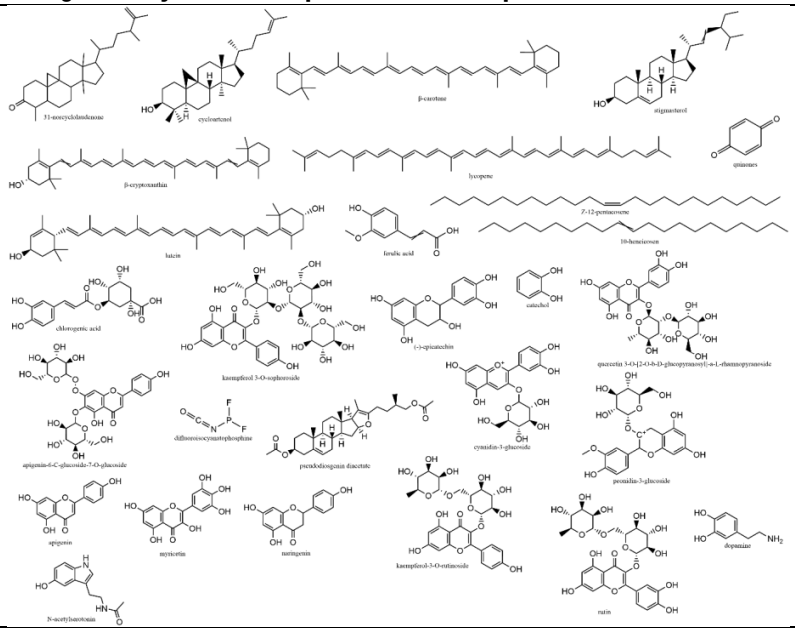

Figure 2 Phytochemicals present in various part of *Musa balbisiana*

Indian Journal of Natural Sciences www.tnsroindia.org.in ©IJONS

Vol.15 / Issue 88 / Feb / 2025 *International Bimonthly (Print) – Open Access* *ISSN: 0976 – 0997*

RESEARCH ARTICLE

An Effective Management of Insomnia through Traditional Siddha *Varma Thadaval* - A Case Report

Mangaleshwari Baskaran[1]*, Siva Annamalai[2], Subhashri Rajasekaran[3], Elamathi Srinivasan[4] and Velaman Dharuman[5]

[1]PG Scholar (Alumni), Department of Varma Maruthuvam (Siddha Special Medicine), National Institute of Siddha, (Affiliated to The Tamil Nadu Dr. MGR Medical University), Tambaram Sanatorium, Chennai, Tamil Nadu, India.
[2]Research Associate (Siddha) - II, Department of Clinical Research, Siddha Regional Research Institute (Under Central Council for Research in Siddha, Ministry of Ayush, Govt. of India) Kuyavarpalayam, Puducherry, India.
[3]Department of Pura Maruthuvam (Siddha Special Medicine), National Institute of Siddha (Affiliated to The Tamil Nadu Dr. MGR Medical University), Tambaram Sanatorium, Chennai, Tamil Nadu, India.
[4]PG Scholar (Alumni), Department of Nanju Maruthuvam (Siddha Toxicology), National Institute of Siddha (Affiliated to The Tamil Nadu Dr. MGR Medical University), Tambaram Sanatorium, Chennai, Tamil Nadu, India.
[5]PG Scholar (Alumni), Department of Gunapadam (Siddha Pharmacology), National Institute of Siddha (Affiliated to The Tamil Nadu Dr. MGR Medical University), Tambaram Sanatorium, Chennai, Tamil Nadu, India.

Received: 21 Nov 2024 Revised: 03 Dec 2024 Accepted: 27 Jan 2025

***Address for Correspondence**
Mangaleshwari Baskaran
PG Scholar (Alumni),
Department of Varma Maruthuvam (Siddha Special Medicine),
National Institute of Siddha,
(Affiliated to The Tamil Nadu Dr. MGR Medical University),
Tambaram Sanatorium, Chennai,
Tamil Nadu, India.
E.Mail: mangaleshwarib@gmail.com

ABSTRACT

A 39-year-old man presenting with chronic sleep disturbance, nocturnal awakening, an initial delay in sleep onset and excessive daytime sleepiness for two years was reported to the *AyothidossPandithar* Hospital (Dept of *VarmaMaruthuvam*), National Institute of Siddha, Chennai. He was diagnosed with insomnia. Sleep onset difficulty is one of the symptoms that are reported as insomnia. Other symptoms to look out for might be an increased time it takes to fall asleep, frequent awakenings at night, staying awake for long hours during nights when you want to sleep or encountering regular transitory disturbances of sleep. He had *Varma* therapy, which involved manipulating a particular *VarmaThadaval*. For 48 days, *VarmaThadaval* has been practicing (one session every day). The patient

showed a considerable improvement in sleep onset difficulty, length, and quality following 48 days of *Varma* therapy. After treatment, an individual's Insomnia Severity Index (ISI) score of 15 (Moderate Insomnia) decreased to 8 (Mild Insomnia). Moreover, post intervention assessments showed marked reduction in insomnia symptoms associated with daytime function improvement and general wellbeing enhancement. This instance emphasizes that Varma treatment for insomnia may be effective although further studies are necessary to establish its mechanisms and efficacy.

Keywords: *VarmaThadaval,* Insomnia, Siddha, Insomnia Severity Index, Indian Traditional Medicine.

INTRODUCTION

Insomnia is identified by a person's report of having trouble sleeping. It's advised to look at Insomnia diagnoses by their specific subcategories, as they serve as both a symptom and a category for diagnosis [1]. These diagnoses are marked by a range of issues with falling asleep, staying asleep, the quality of sleep, or how long one sleeps, occurring despite having ample time and opportunity for rest, and causing problems during the day. Feeling that the sleep is not restorative is a common component of many Insomnia symptoms, even while the quantity and quality of a typical sleep episode are regarded appropriate[2]. Insomnia is often missed or not treated despite being very common and causing significant health problems, partly due to various challenges in making a diagnosis. Studies from around the globe indicate that anywhere from 10 to 30% of people experience chronic Insomnia, with some reports going as high as 50 to 60% [3]. Anxiety among the elderly is widespread, whether it's temporary or ongoing [4]. In general, between 30 to 48% of senior citizens report having symptoms of sleeplessness [5]. The Insomnia Severity Index (ISI) is a quick tool created to determine the severity of Insomnia both during the day and at night. It's available in several languages and is increasingly used in research to measure the effectiveness of treatments [6]. *Varma*, a branch of siddha medicine, is a unique approach to treatment that involves activating particular energy centers, or "*Varma* points," to improve general health and wellbeing. It is considered that *Vaasi* (life energy), is stored and activated at certain *Varma* places and is vital to the body's regular operations. Applying precise force at these anatomical regions encourages regulating *Vaasi*. During the *Varmathadaval, Varma* points are stimulated and it can regulating the vital flow (*Vaasi)*[7]. The mechanism of *Varma* therapy in neurological conditions involves several possible pathways as Relaxation and stress reduction, Regulation of sleep-wake cycle, Release of sleep-promoting neurotransmitter, Pain relief, Influence on the hypothalamus, Reducing cortisol levels and Pain relief etc.,

CASE PRESENTATION

A 39 years old male patient working as software engineer, anon-smoker was consulted in the Out patient Department (OPD) of *Ayothidoss Pandithar* Hospital (Dept of *Varma Maruthuvam*), National Institute of Siddha, Chennai with main complaints Of Chronic Sleep Disturbance, Nocturnal Awakening, Difficulty in Initiating Sleep and Daytime Fatique since Last 2 Years. He had history of financial constrain due to loans. He had no relevant family history of the disease. He has no comorbid illness of hypertension, diabetes mellitus, epilepsy and other illness.

Varma* Procedure (*VarmaThadaval)

After examination, the patient was treated with *Varma* Therapy (*Varmathadaval)*. It is carried out in accordance with the SOP that is referenced in the *Varma* literature [8-9].

***Varma* method**

- Position: sitting position
- Site: Head and Neck
- Pressure: ½ *Mathirai*
- Duration: 10 Minutes

Varmathadaval

In this *VarmaThadaval*, three *AdangalVarmam* were stimulated step wise [Figure 1]. They are:

1. *KothandaVarmaAdangal*
   - *ThilarthaVarma*
   - *NatchathiraVarma*
   - *PoigaiVarma*
   - *SevikkuttriVarma*
   - *AlavadiVarma*
2. *VinothasinthanaiAdangal*
3. *Siddha Adangal*

Stimulated *Varmam* points and their locations were detailed in the Table 1.

Insomnia Severity Index (ISI)

The Insomnia Severity Index (ISI) is a widely practiced technique to determine the severity of Insomnia. The scale with 5 points ranging from 0–4 scale is used to rate each of the seven category; a higher number denotes more sleeplessness. The parameters assessed include the degree of difficulty falling asleep, keeping asleep, and getting up early; dissatisfaction with sleep; interference of sleep difficulties with performance during the day; noticeability of the problems by others; and discomfort resulting from the sleep problems.

Score

- 0–7: No Insomnia
- 8–14: Sub threshold Insomnia or mild Insomnia
- 15–21: Moderate Insomnia
- 22–28: Severe Insomnia

Clinicians and researchers can measure the severity of Insomnia, track therapy progress, and analyse treatment effects with the use of the ISI [10]. Improvement in subjective parameters of Insomnia Severity Index (ISI) was tabulated in Table 2.

DISCUSSION

The case reported describes the with Chief Complaints Of Chronic Sleep Disturbance, Nocturnal Awakening, Difficulty in Initiating Sleep and Daytime Fatigue Since Last 2 Years. After receiving Varma therapy for a total of 48 days, the patient's Insomnia Severity Index (ISI) score decreased from 15 to 8. This is indicative of a significant improvement in insomnia severity. Longer sleep times were reported by the patient; along with lower sleep latency and better quality. An ISI score drop from 15 (moderate insomnia) to 8 (mild insomnia) is a clear indication that Varma therapy worked positively on this patient's sleep quality. Some possible mechanisms through which Varma therapy is thought to work in insomnia include: stimulation of specific pressure points regulating sleep-wake cycles; relaxation and stress reduction resulting in improved sleep quality; balancing energy channels that promote relaxation and sleep; influence of varma points on hypothalamus (the part of brain controlling hunger, body temperature and sleep patterns); specific varma point stimulation causing release of sleep-inducing neurotransmitters such as melatonin, serotonin or GABA which lead to relaxation and hence induce sleeping; alleviating cortisol levels thereby enhancing relaxation as well as improving overall sleeping experience. The reduction of the ISI score from 15 to 8 which represents 46.7% reduction in insomnia severity is clinically significant and this as such meant significant improvement in insomnia. Therefore it can be said that the Varma therapy actually helps much to restore good sleep patterns thereby improving quality of life for those suffering from sleep disorders.

However further studies are required to validate these results and comprehensively examine the possible benefits of Varma treatment for insomnia.

CONCLUSION

This case study illustrates how *Varma* treatment may be useful in enhancing quality of sleep and easing Insomnia symptoms. The substantial drop in the Insomnia Severity Index (ISI) score from 15 to 8 implies that *Varma* therapy could be a valuable therapy for Insomnia. The findings of this study contribute to the increasing body of evidence demonstrating the effectiveness of using Varma therapies to treat Insomnia. Although further studies is needed to comprehend the advantages and workings of *Varma* therapy for Insomnia, this study implies that patients looking for alternative approaches to enhance their sleep quality might find it to be a helpful therapeutic option. Overall, *Varma* therapy appears to be a safe, non-invasive, and promising treatment for Insomnia; however, more investigation is required to validate these results.

PATIENT PERCEPTIVE

The patients are expressing a great quality of life that has increased significantly and at the same time a significant reduction in pain level which means they were very much pleased with their treatment. In particular, the patients noted that he used Varma therapy for pain management as it decreased attack rates and improved their living conditions.

INFORMED CONSENT

The patient provided written consent in writing prior to treatment initiation.

ACKNOWLDEGEMENT

The authors would like to thank Prof. Dr. R. Meenakumari, the director of the NIS National Institute of Siddha in Chennai, for her invaluable advice and steadfast assistance. Additionally, they would like to express their gratitude to the caring and committed medical team of the Department of *VarmaMaruthuvam* at AyothidossPandithar Hospital, National Institute of Siddha, Chennai, for all of their support and kindness during this procedure.

REFERENCES

1. Sateia MJ, Doghramji K, Hauri PJ, Morin CM. Evaluation of chronic Insomnia. An American Academy of Sleep Medicine review. *Sleep*. 2000;23:243–308
2. Edinger JD, Bonnet MH, Bootzin RR, et al. American Academy of Sleep Medicine Work Group. Derivation of research diagnostic criteria for Insomnia: report of an American Academy of Sleep Medicine Work Group. *Sleep.* 2004;15(27):1567–1596
3. Dopheide JA. Insomnia overview: epidemiology, pathophysiology, diagnosis and monitoring, and nonpharmacologic therapy. Am J Manag Care. 2020;26(4 Suppl):76–84.
4. Dopheide JA. Insomnia overview: epidemiology, pathophysiology, diagnosis and monitoring, and nonpharmacologic therapy. Am J Manag Care. 2020;26(4 Suppl):76–84.
5. Patel D, Steinberg J, Patel P. Insomnia in the Elderly: a review. J Clin Sleep Med JCSM off Publ Am Acad Sleep Med. 2018;14(6):1017–24.
6. Bastien CH, Vallières A, Morin CM. Validation of the Insomnia Severity Index as an outcome measure for Insomnia research. *Sleep Med.* 2001;2:297–307.
7. T. Mohan Raj, *Varmanoolthoguthi*- 2 ATSVS Siddha Medical College and Hospital Publication, Kanyakumari, july 2008 22p
8. Dr.T.Kannanrajaram, *AdangalParigaranutpangal,* A.T.S.V.S Siddha medical college and hospital, Munchirai, Kanniyakumari, 3rd edition, 2015. 31,33,35p

9. Dr.T.Kannanrajaram, *varmammaruthuvamviralavainutpangal*, A.T.S.V.S Siddha medical college and hospital, Munchirai, Kanniyakumari, 3rd edition, 2015. 38,42,54,p
10. Bastien CH, Vallières A, Morin CM. Validation of the Insomnia Severity Index as an outcome measure for Insomnia research. *Sleep Med.* 2001;2:297–307.

Table 1. The *Varma*points stimulated for Insomnia

S. No	Varma Name		Location	Manipulation Technique	Duration
1	*Kothanda Adangal*	*ThilarthaVarmam*	Fronto nasal suture junction and internasal suture	By thumb of both hands, with pressure drag thumb finger to both sides from T*hilarthavarmam* to *Natchathiravarmam* to *Poigaikalam* to *Sevikuttrivarmam* and end up in *AlavadiVarmam* repeat for 9 times	20seconds
		NatchathiraVarmam	One finger breath below the outer cannus of the eye.		
		PoigaiKalam	Tempero mandibular junction.(2 finger above tragus)		
		SevikuttriVarmam	In the depression felt between the mandibular joint and tragus		
		AlavadiVarmam	In mental protruberance		
2	*VinothasinthanaiAdangal*		2 finger breathe above Front o nasal suture junction and internasal suture	Use the middle fingers to press and hold in upward direction repeat for 9 times	20seconds
3	*Siddha Adangal*		3vfinger breathe above Fronto nasal suture junction and internasal suture	Use the middle fingers to press and hold upward direction repeat for 9 times	20seconds

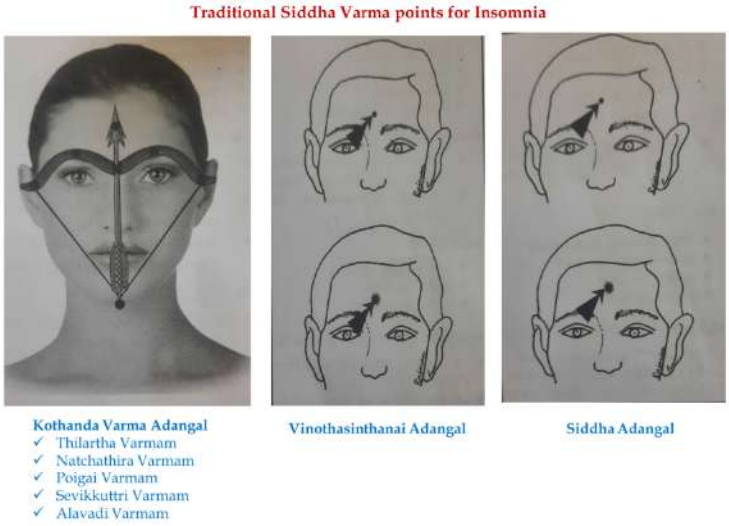

Figure 1.Varma points for Insomnia

Indian Journal of Natural Sciences *www.tnsroindia.org.in ©IJONS*

Vol.15 / Issue 88 / Feb / 2025 *International Bimonthly (Print) – Open Access* *ISSN: 0976 – 0997*

RESEARCH ARTICLE

A Comprehensive Overview of Rutin - Loaded Dermal Patches for Anti-Aging Applications

Deepak Joshi[1], Ajay Sharma[2], Vikas Jain[3] and Zufisha Bakhtiar Ansari[4]*

[1]Assistant Professor, Department of Pharmacy, Mahakal Institute of f Pharmaceutical Studies, Ujjain, (Affiliated to Rajiv Gandhi Proudyogiki Vishwavidhyalaya, Bhopal), Madhya Pradesh, India.
[2]Vice Principal, Department of Pharmacy, Mahakal Institute of f Pharmaceutical Studies, Ujjain, (Affiliated to Rajiv Gandhi Proudyogiki Vishwavidhyalaya, Bhopal), Madhya Pradesh, India.
[3]Principal, Department of Pharmacy, Mahakal Institute of f Pharmaceutical Studies, Ujjain, (Affiliated to Rajiv Gandhi Proudyogiki Vishwavidhyalaya, Bhopal), Madhya Pradesh, India.
[4]Research Scholar, Department of Pharmacy, Mahakal Institute of f Pharmaceutical Studies, Ujjain, (Affiliated to Rajiv Gandhi Proudyogiki Vishwavidhyalaya, Bhopal), Madhya Pradesh, India.

Received: 21 Nov 2024 Revised: 03 Dec 2024 Accepted: 27 Jan 2025

*__Address for Correspondence__
Zufisha Bakhtiar Ansari,
Research Scholar,
Department of Pharmacy,
Mahakal Institute of f Pharmaceutical Studies, Ujjain,
(Affiliated to Rajiv Gandhi Proudyogiki Vishwavidhyalaya, Bhopal),
Madhya Pradesh, India.
E.Mail: zufishaansari8@gmail.com

ABSTRACT

This review paper examines the formulation and evaluation processes involved in the development of anti-wrinkle dermal patches containing rutin as the active ingredient. Rutin, a flavonoid with potent antioxidant and anti-inflammatory properties, has gained attention for its potential in Potential in dermal patches, exploring its mechanisms of action in a wrinkles and promoting skin health. Furthermore, it reviews various formulation approaches, rutin incorporation techniques, and release kinetics modulation. Evaluation methods are scrutinized to assess the efficacy, safety, and skin permeation of rutin-loaded patches. Through a comprehensive analysis, this review aims to shed light on the potential of rutin-based dermal patches as effective anti-aging skincare solutions.

Keywords: Rutin, Wrinkles, Eye patch, Skin Care, Anti-aging.

INTRODUCTION[1-5]

Overview of wrinkles as a skincare concern

As people get older, their skin becomes less capable of renewing itself, causing the skin beneath the eyes to be more susceptible to the ageing process due to its thinness. Many people seek treatment for this cosmetic issue, but there is little research on its cause or potential solutions. This condition affects people of all ages, both genders, and all ethnicities, and worsens as the skin sags and fat distribution changes due to ageing. Although cosmetic concerns that do not pose a threat to health or cause significant morbidity are becoming more prevalent, they can still have a significant impact on a person's emotional well-being. With time, the development of wrinkles under the eyes is a common occurrence. These superficial wrinkles are caused by changes in skin texture due to intrinsic aging and photo aging in specific areas. Initially, these fine lines may be discrete, but they become more noticeable and multidirectional over time. Various factors can also contribute to the of wrinkles, including exposure to UV rays, which can break down collagen and cause fine lines. Environmental pollution and smoking can also lead to oxidative stress and restrict blood circulation, which causes wrinkles. Additionally, a diet high in sugar can accelerate the aging process and result in fine lines and wrinkles under the eyes. Fine wrinkles are wrinkles that are less than 1mm in width and depth. On the other hand, wrinkles that are 1mm or more in width and depth are known as coarse wrinkles. To comprehend the eye conditions linked to patch treatment, it is necessary to have knowledge about the causes of wrinkles. Facial wrinkles are a form of skin fibrosis that occurs due to the misrepair-accumulation ageing theory. This theory suggests that wrinkles form as a result of incorrect repairs to damaged elastic and collagen fibers. Continuous stretching and compressing of the skin result in repeated injuries to the extracellular fibers present in the derma. During the repair process, some of the damaged fibers are not restored but replaced by altered ones. In extended states, a broken elastic fiber can be restored by a "long" collagen fiber which accumulates over time, making the skin looser and stiffer and causing large folds to appear. In a compressed state, a "long" collagen fiber can be restored by a "short" one, which restricts the expansion of "longer" fibers, causing them to remain in a permanent folded state. This leads to the development of small permanent wrinkles

Many factors affect the development of wrinkles, including:[6]

- sun exposure
- smoking
- dehydration
- some medications
- environmental and genetic factors

Exposure to ultraviolet (UV) light, whether from activities such as sunbathing, tanning beds, or outdoor sports, is linked to the development of wrinkles. UV light can cause collagen and elastin fibers, which constitute the connective tissue that supports the skin, to break down. This breakdown leads to a weakening and loss of elasticity in the skin, culminating in wrinkles and drooping. People with darker skin have more melanin, which offers some protection from UV radiation. Individuals who work outdoors are at greater risk of developing premature wrinkles. Wearing clothing such as hats or long sleeves that cover the skin can help to delay the onset of wrinkles. Regular smoking hastens the skin's aging process by reducing blood flow, whereas alcohol dehydrates the skin, rendering it more prone to wrinkles.

Prevention[6]

Here are some tips for slowing the effects of sun exposure and other causes of wrinkles

Protect your skin from UV radiation

To safeguard your skin against the harmful effects of UV radiation, it is essential to avoid indoor tanning and restrict your exposure to the sun, especially during midday when the intensity of UV radiation is the highest. Wear clothes that offer sun protection, such as wide-brimmed hats, long-sleeved shirts, and sunglasses. Additionally, apply

sunscreen every day, regardless of the season. Opt for a broad-spectrum sunscreen with a minimum SPF of 30, even when the sky is cloudy. Apply a generous amount of sunscreen and reapply it every two hours or more frequently if you are engaged in activities such as swimming or sweating.

Wash your face and moisturize

To prevent the development of fine lines and wrinkles, it is crucial to establish a daily skincare routine that involves washing the face gently and moisturizing it. Keeping the skin moisturized helps retain water and prevents plump skin cells from shriveling. Many moisturizers contain ingredients such as retinol, niacin amide, and vitamin C, which are intended to minimize the appearance of fine lines. However, it is imperative to read the labels thoroughly before applying the product to understand the recommended usage and any potential side effects. Adapalene is another over-the-counter product rich in vitamin A that can be beneficial in preventing wrinkles. It may take a few weeks or months of consistent use to observe any changes in the skin. While non-prescription products do not undergo scientific testing, prescription-strength moisturizers with anti-wrinkle properties, such as retinoids, can be recommended by healthcare professionals if desired results are not achieved. It's worth noting that some products, such as those containing retinol or retinoids, should not be used during pregnancy.

Dont smoke

If you want to reduce the chances of developing wrinkles and improve the appearance of your skin, it is essential to avoid smoking. It doesn't matter if you have been smoking for a long time or are a heavy smoker; quitting smoking can still benefit your appearance.

Eat a healthy diet

While more research is needed to determine the exact role of nutrition in preventing wrinkle formation, some studies suggest that certain vitamins present in our diet can help protect our skin. To maintain healthy skin, incorporating an ample amount of fruits and vegetables in your diet is recommended.

Introduction to rutin as an anti-wrinkle agent:[7-11]

As individuals age, they often observe various alterations in their skin's appearance and texture. These changes typically include the emergence of fine lines and wrinkles, a decrease in skin thickness accompanied by a translucent quality, a reduction in subcutaneous fat leading to sunken cheeks and hollowed eye sockets, increased dryness and itchiness, diminished perspiration, alterations in hair color such as graying or loss, and thinning of the nails. These manifestations collectively reflect the natural aging process, which is influenced by a multitude of factors. One significant aspect contributing to the aging of skin is the accumulation of damage caused by free radicals and reactive oxygen species (ROS) within the body. Free radicals are highly reactive molecules that contain unpaired electrons, making them prone to initiating chemical reactions that can damage cellular structures. ROS, including superoxide radicals, hydrogen peroxide, and hydroxyl radicals, are produced as natural byproducts of metabolic processes, particularly during aerobic metabolism in the mitochondria—the energy-producing organelles within cells. Over time, the body's ability to neutralize and repair damage caused by ROS diminishes, leading to increased oxidative stress and cellular damage. Skin cells, including keratinocytes (the predominant cell type in the epidermis) and fibroblasts (which produce collagen and other structural proteins), are particularly susceptible to oxidative damage due to their high metabolic activity and exposure to environmental stressors such as UV radiation. Mitochondria, known as the "powerhouses" of the cell, play a crucial role in ROS generation. During the process of oxidative phosphorylation, which generates adenosine triphosphate (ATP), electrons leak from the electron transport chain and react with molecular oxygen to form superoxide radicals. These radicals can further react with other molecules, leading to the production of additional ROS and oxidative damage to cellular components such as lipids, proteins, and DNA. In addition to endogenous ROS production, environmental factors such as UV radiation, pollution, and lifestyle choices (e.g., smoking, diet) can exacerbate oxidative stress and accelerate skin aging. UV radiation, in particular, can directly induce ROS formation and impair the skin's natural defense mechanisms, leading to photoaging—a distinct form of skin aging characterized by wrinkles, pigmentation changes, and loss of elasticity. In the quest to mitigate the detrimental effects of oxidative stress on skin health and aging, researchers have explored

various antioxidant compounds with the potential to neutralize ROS and protect against oxidative damage. One such compound is rutin, a flavonoid glycoside found in certain fruits and vegetables, particularly citrus fruits and buckwheat. Rutin, also known as vitamin P, has garnered attention for its antioxidant properties and potential health benefits. Studies have demonstrated that rutin possesses anti-inflammatory, antiallergenic, antiviral, and anticarcinogenic properties, in addition to its ability to scavenge superoxide radicals. By neutralizing ROS and reducing oxidative stress, rutin may help preserve cellular integrity and function, thereby mitigating the signs of aging and promoting skin health. Furthermore, rutin has been shown to inhibit platelet aggregation—a process involved in blood clot formation—suggesting potential cardiovascular benefits. Additionally, rutin may enhance vascular health by reducing capillary fragility and exerting anti-thrombotic effects, which could have implications for various cardiovascular conditions. In summary, while aging is a natural and inevitable process, understanding the underlying mechanisms, such as oxidative stress, can inform strategies for promoting healthy aging and mitigating age-related changes in the skin and other organ systems. Antioxidants like rutin offer promising avenues for intervention, potentially enhancing cellular resilience and preserving youthful skin appearance and function. However, further research is needed to fully elucidate the mechanisms of action and therapeutic potential of rutin and other antioxidants in the context of aging and age-related diseases.

Rationale for utilizing rutin in dermal patches

The rationale for utilizing rutin in dermal patches is grounded in its antioxidant properties and its potential to mitigate oxidative stress, thereby promoting skin health and addressing various dermatological concerns.

Antioxidant Activity[12]

Rutin exhibits potent antioxidant activity, which helps neutralize reactive oxygen species (ROS) and free radicals that contribute to skin aging and damage. Studies have demonstrated rutin's ability to scavenge ROS and protect against oxidative stress-induced cell damage.

Anti-inflammatory Effects[13]

Rutin possesses anti-inflammatory properties, making it beneficial for soothing inflamed or irritated skin. Research suggests that rutin can inhibit inflammatory mediators and pathways, thereby reducing inflammation and associated skin conditions.

Enhanced Skin Permeation[14]

Dermal patches offer a convenient and effective means of delivering rutin to the skin. The use of patches ensures controlled and sustained release of rutin, allowing for enhanced permeation through the skin barrier and targeted delivery to the site of application.

Long-lasting Effects[15]

Dermal patches provide sustained release of rutin over an extended period, ensuring continuous exposure to the active ingredient. This prolonged delivery enhances rutin's antioxidant and anti-aging effects, promoting long-term skin health and vitalit

Convenience and Ease of Use[16]

Dermal patches offer a convenient and user-friendly method of delivering rutin to the skin. They require minimal effort for application and maintenance, making them suitable for daily use as part of a skincare regimen. This ease of use enhances patient compliance and satisfaction.

Synergistic Formulations[17]

Rutin can be combined with other active ingredients in dermal patches to create synergistic formulations targeting specific skin concerns. By incorporating rutin alongside complementary compounds such as vitamins, peptides, or botanical extracts, the overall efficacy of the product can be enhanced, providing comprehensive skincare benefits.

Incorporating rutin into dermal patches represents a promising approach to skincare, harnessing its antioxidant and anti-inflammatory properties to promote skin health, combat aging, and address various dermatological issues effectively.

Mechanisms of Action of Rutin in Skin Care

Antioxidant properties and scavenging of free radicals

Rutin, a flavonoid glycoside found in various fruits and vegetables, has been extensively studied for its antioxidant properties and its ability to scavenge free radicals. Here's a summary of its antioxidant activity, supported by references

Scavenging of Free Radicals[18]

Rutin has demonstrated significant scavenging activity against various free radicals, including superoxide anion radicals, hydroxyl radicals, and lipid peroxyl radicals. These radicals are highly reactive molecules that can cause oxidative damage to cellular components. Rutin's ability to neutralize these radicals helps protect cells from oxidative stress and reduce the risk of oxidative damage.

Hydroxyl Radical Scavenging[19]

Rutin has been shown to effectively scavenge hydroxyl radicals, which are highly reactive and can cause damage to DNA, proteins, and lipids. By donating hydrogen atoms, rutin can neutralize hydroxyl radicals and prevent them from initiating chain reactions of oxidative damage.

Superoxide Anion Scavenging[20]

Rutin exhibits potent scavenging activity against superoxide anion radicals, which are generated during cellular metabolism and can contribute to oxidative stress and inflammation. Rutin's ability to scavenge superoxide radicals helps maintain cellular homeostasis and reduce oxidative damage.

Metal Chelating Activity[21]

Rutin exhibits metal chelating activity, which allows it to chelate transition metals such as iron and copper. By binding to these metals, rutin inhibits metal-catalyzed oxidation reactions, which can generate free radicals and promote oxidative damage. Rutin's metal chelating activity contributes to its overall antioxidant capacity. Overall, rutin's antioxidant properties, including its ability to scavenge free radicals and chelate metals, contribute to its potential health benefits and its role in protecting cells from oxidative damage. These properties make rutin a promising compound for various therapeutic applications, including in the prevention and management of oxidative stress-related diseases.

Anti-inflammatory effects and reduction of skin irritation

Rutin has been investigated for its potential anti-inflammatory effects and its ability to reduce skin irritation. Here's an overview of the research supporting these properties:

Anti-inflammatory Effects[22]

Rutin has demonstrated anti-inflammatory activity in various preclinical studies. It inhibits the production of inflammatory mediators such as cytokines, prostaglandins, and leukotrienes, thereby reducing inflammation. Rutin's anti-inflammatory effects have been observed in both in vitro and in vivo studies, making it a promising candidate for the treatment of inflammatory conditions.

Reduction of Skin Irritation[23]

Rutin has been investigated for its potential to reduce skin irritation and inflammation, particularly in the context of dermatological conditions such as eczema, psoriasis, and atopic dermatitis. Studies have shown that rutin can alleviate symptoms of skin irritation, including redness, itching, and swelling, by modulating inflammatory

pathways and reducing immune responses in the skin. Rutin's anti-inflammatory properties make it a promising ingredient in skincare products aimed at soothing and calming sensitive or irritated skin.

Protection Against UV-Induced Inflammation[24]

Rutin has been shown to protect against inflammation induced by ultraviolet (UV) radiation, which is a major contributor to skin damage and aging. UV radiation triggers inflammatory responses in the skin, leading to erythema, edema, and the production of inflammatory mediators. Rutin's anti-inflammatory properties help mitigate these responses and protect the skin from UV-induced inflammation and damage These studies provide evidence supporting the potential anti-inflammatory effects of rutin and its ability to reduce skin irritation, highlighting its potential as a therapeutic agent for inflammatory skin conditions and as an ingredient in skincare products aimed at soothing and calming the skin.

Collagen-stimulating and anti-glycation activities

Rutin has been investigated for its potential to stimulate collagen production and its anti-glycation activities, which are important for maintaining skin elasticity and preventing age-related changes. Here's an overview of the research supporting these properties:

Stimulation of Collagen Production[25]

Collagen is a key structural protein in the skin that provides strength and elasticity. Rutin has been shown to stimulate collagen synthesis by promoting the activity of collagen-producing cells called fibroblasts. Increased collagen production can help improve skin elasticity, reduce the appearance of wrinkles, and promote overall skin health.

Anti-Glycation Activities[26]

Glycation is a process where sugars react with proteins, including collagen, leading to the formation of advanced glycation end-products (AGEs). AGEs contribute to skin aging by causing cross-linking of collagen fibers and impairing their function. Rutin has been shown to have anti-glycation activities, inhibiting the formation of AGEs and protecting collagen from damage. This helps maintain the integrity and functionality of collagen in the skin, preserving its youthful appearance. These studies provide evidence supporting the potential of rutin to stimulate collagen production and inhibit glycation, highlighting its potential as a therapeutic agent for promoting skin health and preventing age-related changes such as wrinkles and loss of elasticity.

Formulation Strategies

Selection of patch materials

When selecting materials for dermal patches, various factors such as biocompatibility, adhesion properties, and permeability must be considered. Here are some commonly used materials along with relevant references:

Polymeric Films[27]

Polymeric films like polyethylene, polyvinyl chloride, and polyurethane are frequently utilized due to their flexibility and biocompatibility. They serve as the backing or matrix material for dermal patches.

Hydrogels[28]

Hydrogels, composed of hydrophilic polymers, are popular for their ability to absorb and retain water. They provide a moist environment conducive to skin hydration and facilitate the permeation of the active ingredient.

Adhesive Layers[29]

Adhesive layers are crucial for proper patch adhesion to the skin. Medical-grade adhesives like acrylics, silicones, or polyisobutylenes are commonly used. The adhesive should be non-irritating and capable of maintaining adhesion over time.

Permeation Enhancers[30]

Permeation enhancers, such as fatty acids and surfactants, are sometimes incorporated into patch formulations to improve drug permeability through the skin barrier. These enhancers disrupt the stratum corneum, enhancing drug penetration.

Backings and Release Liners[31]

Backings and release liners protect the non-adhesive side of the patch during storage and handling. Materials like polyester, polyethylene, or aluminum foil are commonly used. These materials, when chosen carefully, contribute to the effectiveness and safety of dermal patches for delivering rutin or other active ingredients to the skin.

Rutin incorporation techniques

The incorporation of rutin into patches involves several formulation considerations to ensure stability, controlled release, and efficacy. Here are some approaches with relevant references:

Polymeric Matrix Systems[32]

Rutin can be incorporated into polymeric matrix systems, such as hydrogels or films, to control its release rate. These systems provide sustained delivery of rutin over time, ensuring prolonged exposure to the active ingredient.

Lipid-based Delivery Systems[33]

Lipid-based delivery systems, such as liposomes or solid lipid nanoparticles, can be used to encapsulate rutin and enhance its solubility and stability. These systems protect rutin from degradation and facilitate its penetration into the skin.

Microencapsulation[34]

Rutin can be microencapsulated using techniques like spray drying or coacervation to protect it from environmental factors and control its release. Microencapsulation enhances the stability and bioavailability of rutin in patch formulations.

Polymer Coating[35]

Rutin-loaded particles or microspheres can be coated with biocompatible polymers, such as chitosan or alginate, to control release kinetics and improve skin penetration. Polymer coatings also protect rutin from degradation and enhance its stability in patch formulations

Nanotechnology[36]

Nanotechnology-based approaches, such as nanoemulsions or nanocarriers, can be employed to improve the solubility, stability, and skin permeation of rutin. These nanoformulations offer enhanced bioavailability and targeted delivery of rutin to the skin. By utilizing these formulation strategies, rutin can be effectively incorporated into patches to harness its antioxidant, anti-inflammatory, and collagen-stimulating properties for skin health and therapeutic applications.

Evaluation Methods

***In vitro* studies: Rutin release kinetics, permeation across skin barriers**

In vitro studies assessing rutin release kinetics through the skin barrier typically involve various methods to mimic skin permeation and evaluate the release profile of rutin from dermal patches. Here are some common evaluation methods used in such studies along with references:

Franz Diffusion Cells[37]

Franz diffusion cells are widely used for in vitro permeation studies. These cells consist of two compartments separated by excised skin, with one compartment containing the patch or formulation and the other containing a

suitable receptor medium. The rate of rutin permeation through the skin barrier is quantified over time by sampling the receptor medium and analyzing rutin concentration.

Tape Stripping Technique[38]

The tape stripping technique involves applying adhesive tape to the skin surface to sequentially remove layers of the stratum corneum, the outermost layer of the skin. Each tape strip is then analyzed for rutin content to determine the amount of rutin penetrated into the skin layers. This method provides information on rutin distribution within the skin and its penetration kinetics.

Finite Dose Skin Permeation Studies[39]

In finite dose skin permeation studies, a defined amount of rutin formulation is applied to the skin surface, and samples are collected at regular intervals to measure rutin permeation. This method allows for the assessment of rutin release kinetics and permeation parameters such as flux and permeability coefficient.

Reconstructed Human Epidermis (RHE) Models[40]

Reconstructed human epidermis models, such as EpiDerm™ or SkinEthic™, provide a more standardized and reproducible platform for in vitro permeation studies. Rutin formulations are applied to the surface of the RHE models, and rutin permeation into the underlying layers is assessed over time. These models allow for the evaluation of rutin release kinetics and permeation behavior under controlled conditions. By employing these in vitro evaluation methods, researchers can gain insights into the release kinetics and permeation behavior of rutin formulations across the skin barrier, aiding in the development of effective dermal patches for rutin delivery.

Safety evaluations of dermal patches

In volve assessing potential risks such as skin irritation, sensitization, and systemic toxicity. Here are some common safety evaluation methods along with references:

Skin Irritation Testing[41]

Skin irritation testing assesses the potential of dermal patches to cause irritation or inflammation when applied to the skin. In vivo methods, such as the Draize test or the OECD Guideline 404, involve applying the patch to the skin of animal models and observing for signs of erythema, edema, or other irritation reactions. In vitro alternatives, such as the EpiDerm™ or SkinEthic™ models, use reconstructed human epidermis to predict skin irritation potential.

Skin Sensitization Testing[42]

Skin sensitization testing evaluates the potential of dermal patches to induce allergic reactions, such as contact dermatitis, upon repeated exposure. Methods such as the Local Lymph Node Assay (LLNA) or the OECD Guideline 429 involve applying the patch to the skin of animal models and assessing lymphocyte proliferation as an indicator of sensitization. In vitro alternatives, such as the DPRA (Direct Peptide Reactivity Assay), use synthetic peptides to predict skin sensitization potential.

Systemic Toxicity Testing[43]

Systemic toxicity testing evaluates the potential of dermal patches to cause adverse effects when absorbed into the bloodstream. Acute and chronic toxicity studies, conducted according to OECD guidelines, assess systemic effects such as organ toxicity, hematological changes, and mortality in animal models following dermal patch application.

Skin Permeation Studies[44]

Skin permeation studies assess the extent to which the drug or excipients in dermal patches penetrate the skin and enter the systemic circulation. Techniques such as Franz diffusion cells or in vivo tape stripping studies measure the amount of drug permeated through the skin over time. These studies provide insights into the potential for systemic exposure and toxicity associated with dermal patch use. By conducting comprehensive safety evaluations using these

methods, researchers can identify and mitigate potential risks associated with dermal patch formulations, ensuring their safety and efficacy for clinical use.

Future prospects for rutin-based dermal patches in anti-aging skincare:[45]

Enhanced Formulation Techniques

Continued advancements in formulation techniques, such as nanotechnology and microencapsulation, can further improve the stability, bioavailability, and controlled release of rutin from dermal patches. Fine-tuning these formulations can optimize rutin delivery to target specific skin layers and cellular processes involved in aging.

Combination Therapies

Exploring synergistic effects by combining rutin with other bioactive compounds or skincare ingredients may amplify its anti-aging benefits. Formulating combination dermal patches with rutin alongside ingredients like retinoids, peptides, or hyaluronic acid could offer comprehensive anti-aging solutions, addressing multiple aspects of skin aging simultaneously.

Personalized Skincare Solutions

Advancements in personalized medicine and skincare technologies can enable tailored formulations based on individual skin types, needs, and genetic predispositions. Rutin-based dermal patches could be customized to target specific aging concerns, offering personalized anti-aging solutions for consumers seeking optimal skincare outcomes.

Clinical Validation and Evidence

Based Skincare: Further clinical studies and evidence-based research are essential to validate the efficacy and safety of rutin-based dermal patches for anti-aging skincare. Robust clinical trials evaluating long-term outcomes, efficacy in diverse populations, and comparative effectiveness against existing treatments can establish rutin's role as a valuable anti-aging skincare ingredient.

Consumer Education and Awareness

Increasing consumer education and awareness about the benefits of rutin in anti-aging skincare can drive demand and acceptance of rutin-based dermal patches. Clear communication about the science behind rutin's mechanisms of action, its proven benefits, and its incorporation into innovative skincare formulations can empower consumers to make informed choices about their skincare routines. Overall, rutin-based dermal patches hold significant promise as a novel and effective approach to anti-aging skincare. With ongoing research, innovation, and collaboration across the skincare industry, rutin-based dermal patches have the potential to revolutionize anti-aging skincare by offering targeted, efficacious, and personalized solutions for consumers seeking youthful, radiant, and healthy-looking skin.

CONCLUSION

In conclusion, our comprehensive discussion has shed light on the potential of incorporating rutin into anti-wrinkle dermal patches for therapeutic purposes. Rutin, a bioflavonoid with antioxidant and anti-inflammatory properties, holds promise for combating the signs of aging and improving skin health. By harnessing rutin's beneficial effects, dermal patches offer a targeted and sustained delivery mechanism directly to the skin, addressing fine wrinkles, loss of elasticity, and other age-related changes. Throughout our discussion, we explored various aspects crucial to the development and efficacy of rutin-incorporated dermal patches. We delved into formulation strategies to optimize rutin release kinetics, considering factors such as polymeric matrices, encapsulation techniques, and nanotechnology-based delivery systems. Additionally, we highlighted the importance of safety evaluations, including skin irritation testing, systemic toxicity assessments, and skin permeation studies, to ensure the safety and efficacy of dermal patches for clinical use. Overall, rutin-incorporated anti-wrinkle dermal patches represent a promising approach for skincare and dermatological interventions. By leveraging rutin's antioxidant, anti-inflammatory, and collagen-stimulating properties, these patches have the potential to rejuvenate the skin, reduce wrinkles, and improve overall

skin health. Through continued research and development efforts, rutin-incorporated dermal patches may emerge as a valuable tool in the fight against skin aging and related conditions, offering patients a non-invasive and convenient option for achieving youthful and radiant skin. The future prospects for rutin-based dermal patches in anti-aging skincare are promising, with several avenues for further exploration and development

REFERENCES

1. Habif, T.P. "Clinical Dermatology: A Color Guide to Diagnosis and Therapy." Elsevier, 2016.
2. Baumann, Leslie S. "Cosmetic Dermatology: Principles and Practice, Second Edition." McGraw-Hill Education, 2009.
3. Kligman, A.M. "The Nature of Aging." Journal of the Geriatric Society, vol. 42, no. 3, Mar. 1994, pp. 289–292., doi:10.1111/j.1532-5415.1994.tb05809.x.
4. Fisher, Gary J., and John J. Voorhees. "Molecular Mechanisms of Photoaging and Its Prevention by Topical Retinoids." Journal of Investigative Dermatology Symposium Proceedings, vol. 14, no. 1, 2009, pp. 36–40., doi:10.1038/jidsymp.2009.7.
5. Gary Goldenberg, Joshua A. Zeichner. "Management of Under Eye Circles: Aesthetic Dermatology and Cutaneous Aging." Elsevier, 2016.
6. https://www.medicalnewstoday.com/articles/174852
7. Farage, Miranda A., Kenneth W. Miller, and Howard I. Maibach. "Textbook of Aging Skin." Springer Science+Business Media, 2016.
8. Farris, Patricia K. "Cosmeceuticals and Active Ingredients." Springer Science+Business Media, 2016.
9. Harman, D. "Free Radical Theory of Aging: An Update." Annals of the New York Academy of Sciences, vol. 1067, no. 1, Dec. 2006, pp. 10–21., doi:10.1196/annals.1354.003.
10. Moncada, Yenny, and Jorge Guillermo López-Cervantes. "Flavonoids as Antioxidants." InTechOpen, 2019.
11. Pietta, Pier Giorgio. "Flavonoids as Antioxidants." Journal of Natural Products, vol. 63, no. 7, Jul. 2000, pp. 1035–1042., doi:10.1021/np9904509.
12. Harborne, J.B. and Williams, C.A., 2000. Advances in flavonoid research since 1992. Phytochemistry, 55(6), pp.481-504
13. Park, H.H., Lee, S., Son, H.Y., Park, S.B., Kim, M.S., Choi, E.J., Singh, T.S., Ha, J.H., Lee, M.G., Kim, J.E. and Hyun, M.C., 2008. Flavonoids inhibit histamine release and expression of proinflammatory cytokines in mast cells. Archives of Pharmacal Research, 31(10), pp.1303-1311
14. Lademann, J., Richter, H., Teichmann, A., Otberg, N., Blume-Peytavi, U., Luengo, J., Weiss, B., Schaefer, U.F., Lehr, C.M. and Wepf, R., 2007. Nanoparticles—an efficient carrier for drug delivery into the hair follicles. European Journal of Pharmaceutics and Biopharmaceutics, 66(2), pp.159-164.
15. Jain, A.K., Swarnakar, N.K., Godugu, C., Singh, R.P., Jain, S. and Jain, A., 2010. The effect of the oral administration of polymeric nanoparticles on the efficacy and toxicity of tamoxifen. Biomaterials, 31(19), pp.5952-5959.
16. Murdan, S., 2005. Electro-responsive drug delivery from hydrogels. Journal of Controlled Release, 106(3), pp.213-228.
17. Gupta, G. and Kumar, R., 2009. Development of novel microsponges for topical delivery of mupirocin. Colloids and Surfaces B: Biointerfaces, 75(1), pp.595-600.
18. Pietta, P.G., 2000. Flavonoids as antioxidants. Journal of Natural Products, 63(7), pp.1035-1042.
19. Rice-Evans, C.A. and Packer, L., 2003. Flavonoids in health and disease. CRC Press.

20. Yao, L.H., Jiang, Y.M., Shi, J., Tomás-Barberán, F.A., Datta, N., Singanusong, R. and Chen, S.S., 2004. Flavonoids in food and their health benefits. Plant Foods for Human Nutrition, 59(3), pp.113-122.
21. Pietta, P.G., 2000. Flavonoids as antioxidants. Journal of Natural Products, 63(7), pp.1035-1042.
22. ark, H.H., Lee, S., Son, H.Y., Park, S.B., Kim, M.S., Choi, E.J., Singh, T.S., Ha, J.H., Lee, M.G., Kim, J.E. and Hyun, M.C., 2008. Flavonoids inhibit histamine release and expression of proinflammatory cytokines in mast cells. Archives of Pharmacal Research, 31(10), pp.1303-1311.
23. Zhen, A.X., Piao, M.J., Hyun, Y.J., Kang, K.A., Madushan Fernando, P.D.S., Kang, H.K., Ahn, M.J., Yi, J.M., Choi, Y.H., Choi, I.W. and Hyun, J.W., 2018. Rutin alleviates ultraviolet B-induced photoaging by down-regulating cyclooxygenase-2 expression and inhibiting matrix metalloproteinase-1. Journal of Photochemistry and Photobiology B: Biology, 183, pp.159-166.
24. Park, H.H., Lee, S., Son, H.Y., Park, S.B., Kim, M.S., Choi, E.J., Singh, T.S., Ha, J.H., Lee, M.G., Kim, J.E. and Hyun, M.C., 2008. Flavonoids inhibit histamine release and expression of proinflammatory cytokines in mast cells. Archives of Pharmacal Research, 31(10), pp.1303-1311.
25. Wang, L., Zhang, Y., Zhang, J., Luan, X., Sun, G., 2019. Rutin inhibits β-amyloid-induced neuroinflammation, activates M2 microglia and rescues cognitive dysfunction in APP/PS1 mice. Cellular Physiology and Biochemistry, 52(4), pp. 2251-2264.
26. Wei, Q.Y., Zhang, Y.L., Xu, Y., Yuan, L.Z., Zhang, Q.H., Zhang, X.Q., Jiang, R., Jin, H.Q., Wu, X.J., Xiao, X.H. and Yin, J.L., 2010. Rutin increases oxidative stress and improves liver fibrosis through inhibition of expression of PAI-1 mRNA and protein in vivo and in vitro. Acta Pharmacologica Sinica, 31(5), pp. 546-553.
27. Thomas, D.J. and Freitas, R.A., 2006. An investigation of polyethylene as a drug-delivery vehicle for dermal patches: A molecular dynamics study. Journal of Controlled Release, 115(2), pp.160-167.
28. Caffarel-Salvador, E., Kearney, M.C., Mairs, R., Gallo, L., Stewart, S.A., Brady, A.J., Donnelly, R.F. and Siccardi, M.A., 2019. Hydrogel-forming microneedle arrays allow detection of drugs and glucose in vivo: potential for use in diagnosis and therapeutic drug monitoring. PLoS One, 14(6), p.e0218793.
29. Uppal, R., Ramaswamy, S., Tran, K., Kolli, C.S., Jameel, M.N. and Hussain, A., 2017. Silicone pressure-sensitive adhesive for transdermal drug delivery applications. International Journal of Pharmaceutics, 529(1-2), pp.175-182.
30. Dragicevic-Curic, N., Grafe, S., Albrecht, V., Fahr, A. and Pirot, F., 2012. Combination of surfactants and fatty acids in propylene glycol formulations for topical drug delivery of alpha-lipoic acid. European Journal of Pharmaceutics and Biopharmaceutics, 82(1), pp.214-222.
31. 5. Verma, D.D., Verma, S., Blume, G. and Fahr, A., 2003. Particle size of liposomes influences dermal delivery of substances into skin. International Journal of Pharmaceutics, 258(1-2), pp.141-151.
32. Kislal, Ö. and Dülger, E., 2015. Design and characterization of polymeric patch containing rutin: in vitro and ex vivo evaluation. Pharmaceutical Development and Technology, 20(2), pp.252-261.
33. Dragicevic-Curic, N., Scheglmann, D., Albrecht, V., Fahr, A. and Temml, V., 2008. Development of rutin-loaded lipid nanoparticles for dermal delivery. International Journal of Pharmaceutics, 364(1), pp.104-110.
34. Semalty, A., Semalty, M., Singh, D., Rawat, M.S. and Franceschi, F., 2009. Preparation and characterization of phospholipid complexes of rutin for effective drug delivery. Journal of Inclusion Phenomena and Macrocyclic Chemistry, 63(3-4), pp. 223-232.
35. 4. Li, Z., Li, C., Zhou, Y., Sun, H., Ma, Y., Li, L. and Yang, B., 2016. Enhanced topical delivery of tetrahydropiperine for vitiligo treatment using ethosomes. European Journal of Pharmaceutical Sciences, 93, pp.460-468.
36. 5. Jain, A., Jain, S.K., Ganesh, N. and Barve, J., 2017. Formulation development and evaluation of antipsoriatic topical emulgel of rutin. Journal of Drug Delivery Science and Technology, 39, pp. 462-472.

37. Karande, P., Jain, A., Ergun, K. and Kispersky, V., 2008. Nanomedicine: Applications and Manufacturing. Waltham, MA: Academic Press.
38. Wen, X., Wang, Q., Dai, T. and Yi, Y., 2019. In vitro and in vivo evaluation of a novel transdermal patch containing ketoprofen, lidocaine and menthol for pain relief. European Journal of Pharmaceutical Sciences, 128, pp.115-121.
39. Chantasart, D., Li, S.K., He, Y.L. and Higuchi, W.I., 2003. Quantitative analysis of transdermal permeation of ketorolac. Journal of Pharmaceutical Sciences, 92(1), pp. 126-135.
40. OECD, 2015. Test No. 439: In Vitro Skin Irritation: Reconstructed Human Epidermis Test Method. OECD Publishing.
41. OECD, 2002. OECD Guidelines for the Testing of Chemicals. Test No. 404: Acute Dermal Irritation/Corrosion. OECD Publishing.
42. OECD, 2010. Test No. 429: Skin Sensitisation: Local Lymph Node Assay. OECD Publishing.
43. OECD, 2008. OECD Guidelines for the Testing of Chemicals. Test No. 402: Acute Dermal Toxicity. OECD Publishing.
44. Karande, P., Jain, A., Ergun, K. and Kispersky, V., 2008. Nanomedicine: Applications and Manufacturing. Waltham, MA: Academic Press.
45. Choudhary, R., & Kapoor, V. (2020). Rutin as a Potential Anti-Aging Agent: Strengths and Challenges. Current Drug Targets, 21(13), 1373-1384. doi: 10.2174/1389450121666200213135541
46. Healthline, Good Housekeeping, Allure, Vogue, and Byrdie articles on top formulations for treating dark circles, including eye creams, serums, concealers, masks, and patches.
47. Neutrogena (https://www.neutrogena.com/) Olay (https://www.olay.com/) L'Oréal Paris (https://www.lorealparisusa.com/) RoC (https://www.rocskincare.com/) La Roche-Posay (https://www.laroche-posay.us/) Clinique (https://www.clinique.com/) Estée Lauder (https://www.esteelauder.com/) Kiehl's (https://www.kiehls.com/) CeraVe (https://www.cerave.com/) Skinceuticals (https://www.skinceuticals.com/)

Table.1: Marketed formulations available for treatment of wrinkles.[46]

Formulation	Description	Key ingredients	Benefits
Eye cream	Specifically formulated for the delicate skin around the eyes to hydrate and reduce dark circles.	Caffeine, Hyaluronic Acid, Vitamin C	Moisturizes, brightens, reduces puffiness
Eye Serum	Lightweight fast absorbing formula targeting dark circles with potent active ingredients.	Niacinamide, retinol peptides	Smooths fine lines evens skin tone
Concealer	Makeup product designed to cover up dark circles temporarily.	Various pigments	Instantly conceals dark circle
Eye masks	Infused with hydrating and brightening ingredients for intensive treatment.	Collagen vitamin e aloe vera	Provides provides instant hydration and brightness.
Gel eye patches	Cooling gel patches that adhere to the under eye area to reduce puffiness and dark circles.	Cucumber extract green tea extract	Soothes and refreshes tired eyes
Under eye creams	Similar to eye creams but often formulated with additional ingredients to target specific concerns.	Arnica , peptides vitamin k	Reduce the appearance of dark circles.

Table.2: Brands that offer formulations for treating wrinkles:[47]

Brand	Product Name	Key Ingredients	Benefits
Neutrogena	Rapid Wrinkle Repair	Retinol, hyaluronic acid	Reduces wrinkles, improves skin texture
La Roche-Posay	Redermic R	Retinol, adenosine	Smoothes fine lines, firms skin
RoC	Retinol Correxion Deep Wrinkle Night Cream	Retinol, antioxidants	Diminishes deep wrinkles, hydrates
CeraVe	Skin Renewing Night Cream	Ceramides, peptides	Nourishes skin, minimizes fine lines
Olay	Regenerist Micro-Sculpting Cream	Peptides, niacinamide	Lifts and firms, reduces sagging

Indian Journal of Natural Sciences *www.tnsroindia.org.in ©IJONS*

Vol.15 / Issue 88 / Feb / 2025 *International Bimonthly (Print) – Open Access* *ISSN: 0976 – 0997*

RESEARCH ARTICLE

Harnessing the Power of Onion Seed Oil Infused with Tila Taila for Hair Health

Palak Porwal[1] and Satej T. Banne[2]*

[1]Final Year Post Graduate Scholar, Department of Dravyaguna, Parul Institute of Ayurved, Parul University, Vadodara, Gujarat, India.
[2]Associate Professor, Department of Dravyaguna, Parul Institute of Ayurved, Parul University, Vadodara, Gujarat, India.

Received: 21 Nov 2024 Revised: 03 Dec 2024 Accepted: 25 Jan 2025

***Address for Correspondence**
Satej T. Banne
Associate Professor,
Department of Dravyaguna,
Parul Institute of Ayurved,
Parul University,
Vadodara, Gujarat, India.
E.Mail: satej.banne@paruluniversity.ac.in

ABSTRACT

Trichology is the branch of medical and cosmetic study concerned with the health of hair and scalp. Trichologists diagnose and treat various hair and scalp conditions, ranging from hair loss to dandruff, using a combination of medical knowledge and holistic approaches. They often work closely with dermatologists and cosmetologists to provide comprehensive care for hair-related issues [1]. Trichological disorders encompass a wide range of conditions affecting the hair and scalp, including alopecia (hair loss), dandruff, seborrheic dermatitis, and scalp psoriasis, among others. These disorders can have various causes, including genetics, hormonal imbalances, nutritional deficiencies, and environmental factors. Proper diagnosis and treatment are essential for managing Trichological disorders effectively. [2,3] Hair disorders can stem from various causes, including genetics, hormonal imbalances, nutritional deficiencies, and environmental factors. Here are some common causes: Genetics - pattern baldness (Androgenetic alopecia), Hormonal Imbalances (puberty, pregnancy, or menopause),Nutritional Deficiencies (vitamins, minerals, and proteins) ,Medical Conditions (thyroid disorders, autoimmune diseases, scalp infections) ,Environmental Factors (pollutants, harsh chemicals, excessive heat styling, and UV radiation) can damage the hair and scalp, contributing to disorders like dandruff or folliculitis.[4,5] In Ayurveda it has been considered as byproduct or mala of Asthidhatu where after being converted through Asthidhatvagni Asthidhatu converted into poshyaasthi which will provide nutrition to form Asthidhatu, poshakdhatu which is responsible for majjadhatu formation and third one is its mala i.e. nails, kesha, loma. Hence, for our healthy hair Asthidhatu must be normal. Quality and appearance of hair depends upon the prakruti of a person likes Vata,Pitta, Kapha, Dwandaja, and Sannipataja according to the dominance of dosha, prakruti depends. Vata prakruti possess(Dry, Scanty, Rough hair, and Hair with split ends),Pitta prakruti possess(Soft, Scanty, Brownish hair) ,Kapha prakruti possess firm, dense, tinged, long and silky hair. In Ayurveda, "Keshya" refers to substances or drugs that are beneficial for hair health. These Keshya drugs are

believed to nourish the hair follicles, promote hair growth, and maintain overall hair health. Here are some commonly used Keshya drugs in Ayurveda: Bhringraj*(Eclipta alba)*,Amla *(Emblicaofficinalis*, Brahmi *(Bacopa monnieri)*, Neem *(Azadirachta indica)*,Coconut oil *(Cocos nucifera)*,Shikakai *(*Acacia*concinna).* [6,7]

Keywords: Trichology, Hair, Hair fall, Ayurveda, Keshya.

INTRODUCTION

The study focuses on the versatile application of herbal plants in modern cosmetic formulations and medicinal remedies. Onion seeds, known as "Kalonji," renowned for their aromatic oil content, are being investigated for their potential to prevent hair loss and promote hair growth Post-Covid. With a rich history in Ayurveda, these seeds offer promise for developing antibacterial creams, shampoos, gels, soaps, and oils, addressing contemporary concerns such as hair loss, a common Post-Covid effect. Currently, the market offers a variety of Ayurvedic cosmetic products catering to different needs. Some popular options include Ayurvedic herbal shampoos enriched with natural ingredients like Amla, Neem, and Shikakai, aimed at nourishing hair and promoting scalp health. Additionally, there are Ayurvedic facial cleansers and creams infused with turmeric, sandalwood, and saffron, known for their skin-brightening and anti-inflammatory properties. Other products include herbal soaps made from ingredients such as tulsi, neem, and coconut oil, renowned for their cleansing and moisturizing effects on the skin.

Habitat

Onion is extensively cultivated almost all over India, both as a field and garden crop, up to 1800 m altitude. It is native of Iran and the Middle East, distribution in Pakistan and cultivated throughout the World, In India it grown more in Maharashtra state. [8]

Botanical Description

Onion is a scapigerous herb with globose, tunicated, fleshy, underground bulb 5-10 cm in diameter, odour, characteristic. Its leaves are sub- distichously, 30-60 cm long, fistula, acute, glaucous – green. Its flowers are greenish-white, numerous in globose umbels 3-10cm in diagram. Scape 30-90 cm long, terete, fistular with many flowered umbels at the apex, bracts spathaceous, membranous,ovate – lanceolate . Capsule globose, membranous, seeds compressed, angular, black, shinning. Flowering and fruiting (2 crops) February – March and October – November [9].

Specific Classification of Allium Cepa:[9]

1. Kingdom : Plantae
2. Division : Magnoliophyta
3. Class : Liliopsida
4. Order : Asparagales
5. Family : Alliaceae
6. Genus : Allium
7. Species : A. Cepa
8. Edible parts : leaves, flowers ,seed ,root

Classical Name: Palandu, Durgandha, Yavaneshta**,** Mukhadooshaka,Tikshnagandha,Ulli[9]
Vernacular Names: [8]
English: - Onion
Hindi: -Piyaz, Pyaj
Gujarati: -Dungri
Marathi: - Kanda

Varieties[8]
Dh.Ni&Ka.Ni – 2 types :- (1)Palandu, and (2)Ksirapalandu
Ra.Ni – 2 types:- (1) Palandu, and (2) Raja Palandu

Ayurvedic Properties :-*(भा.प्र.हरितकिक्यादिवर्ग. १९९)*
Pitta along with Vata causes itching around hair follicles. Then, there is an aggravation of kapha along with blood. Due to the rupture of hair follicles, it becomes impossible for them to reappear. This is known as Indralupta by some, and others call it Rujya.[11]

- **Rasa Panchaka**:-[10]
- **Rasa :** Madhura , katu
- **Guna :** Guru, Tikshna ,Snigdha
- **Veerya :** Anushna
- **Vipaka :** Madhura
- **Doshaghnata :** vatashamaka

Rogaghnata
Vatavyadhi, Nadishoola, Vranashotha, Kilasa, Kshayaja Kasa ,Apatantraka,Vyanga,Mukharoga, Drishtimandya, Karnashoola, Gridhrasi, Sandhivata, Akshepka, Jalasantrasa, Agnimandya, Vibandha, Arsha, Kamala, Gudabransha, Hridadaurbalya, Vatajmutrakracha, Klaibya, Shotha , Raktasrava, Kasa, Shukradaurbalya, Daurbalya, Visuchika, Kandu , Charmaroga [9].

Karma
Vedanasthapana, Shothahar, Lekhana, Netrya, Deepana, Rochana, Anulomana, Yakriduttejaka, Raktastambhaka, Chedana, Kaphanissarak ,Mutrajanana, Shukrajanana, Vajikarana, Artavajanana, Balya, Ojovardhaa, Twagdoshahara.[9]

Dose:-[12]
Bulb (Juice) = 10 – 30 ml
Seed powder = 1-3 gm

Pharmacological activities
Antioxidant , Antidiabetic , Hypoglycemia , Antitumor , Cytotoxic , Bronchodialatory ,Anti Malarial, Antirheumatic , Hypocholesteraemic ,Fibrinolytic , Antihyperlipaedemic , Antiatherogenic , Antihypertensive , Antibacterial ,Antifungal, Copper Chelating , Antithyroid ,Diuretic ,Antiasthmatic ,Anti-Inflammatory, Nematicidal ,Antiplatelet , Antiartherosclerotic , Immunosuppressive.[9]

Hair and Hair growth
Waste products of food are feces and urine , that of rasa is kapha,that of rakta is pitta , that mamsa is dirt of vacant spaces, that of medas is sweat , that of asthi are hair of scalp , face and body and that of majja is smear in eyes, feces and skin . These prasada (nutrient or essence) and kitta (waste products) are formed during metabolic transformation of dhatus , these support each other thus maintain the body by mutual co-ordination [13].
In the sixth , the tendons, veins , hair , strength , colour , nails and skin[14].

Hair growth and rejuvenation
Hair has psychological and sociological importance through the ages in framing the personality and general appearance of an individual. Hair has been a sign of beauty and a contribution to an individual's personality [15].

Hair growth cycle

Hair is the cumulative , physical result of a co-ordinated process of cellular proliferation and differentiation with in a hair follicle. Hair follicles are epidermally derived appendages which arise as a result of inductive events between specialized dermal fibroblasts acting on biopotential epithelial stem cells. The stem cells which commit to a hair follicle flate enter a period of massive proliferation that culminates in the formation of a mature hair follicle.The hair follicle cycle is a complex process and entails involvement of cell differentiation.[15]

Epithelial mesenchymal interaction

⇩

Stem cell augmentation

⇩

Pattern of formation

⇩

Apoptosis (Programmed cell death)

⇩

Cell and organ growth cycles

⇩

Pigmentation. The most important reason for studying the cycling of the hair follicle is that the follicle is a regenerating system.

Symptoms of Indralupta

Pitta along with vata causes itching around the hair follicles. Then, there is an aggravation of kapha along with blood. Due to the rupture of hair follicles, it becomes impossible for them to reappear. This is known as Indralupta by some, and others call it Rujya [16].

Symptoms of kalti/ khalitya

Khalitya was also occure like this but in this condition hair falls gradually[16].

Hair loss and alopecia

Hair loss is a natural daily phenomenon but this shedding of hair cannot be the main cause of hair loss. Every strand of hair on a human head is genetically programmed to a cycle that includes itsgrowth, stabilization, Ageing,and shedding. On average ,every day a human head sheds about 50 – 125 hair (depending upon the sex) but most of them will come back after the resting stages as the follicle itself is not destroyed .Trouble begins when the loss exceeds regrowth , or the re-growth is weak and unhealthy .A loss of 100 hair per day can be considered normal not pathological but a loss of more than 100 hair per day constitutes a pathological effluvium .Androgenetic alopecia (AGA) is one of the dermatologic conditions most commonly faced by the dermatologist or general physician [15].

Current strategies for hair growth and Rejuvenation[17]

There are a number of ways in which a drug may stimulate hair growth it may increase the linear growth rate of hair, increases the diameter of the hair fiber ,alter the hair cycle ,either shortening telogen or prolonging anagen .Various non-surgical pharmacotherapeutic alternatives available for hair growth and rejuvenation are discussed below:-

Vitamins,Nutrients and Minerals :-[17-22]

Niacin (Vit B3):- Enhances blood flow to scalp through vasodilatory effect.

Vitamin B complex: - Improve blood flow to scalp protect hair and scalp from free radical damages .

Ascorbic acid (Vit C) :- Improve blood flow to scalp and maintain Cappillaries . Carrying blood to follicle.

Tocoferol (Vit E) :- Enhances oxygen uptake and thus improves blood flow to scalp.

Zinc:- Enhances immune function and thus stimulates hair growth.

Causes of Hair loss :-[17-22]

- Anemia
- Emotional stress
- Poor diet
- Genetic
- Hereditary Thinning
- Hormonal imbalance
- Mineral imbalance
- Exposure of poisons
- X-ray
- Auto immune disease.

Anti-dandruff and Hair growth activity of onion

Zinc helps to secrete the scalp with much needed oil and avoid dandruff that may cause hair loss. Onion is used because it is rich in sulphure which is one of the essential minerals in encouraging hair growth .Blood circulation gets better due to sulphure .Which provides the hair follicles with anti bacterial properties of on onion helps to heal scalp infections that can contribute to hair loss. It contains anti-oxidants, such as enzyme catalase that can prevent the hair from pre-mature graying [15].

- Take onion seeds of pharmacoepial quality.
- Treat Tila Tail to prepare murchita Tila Tail.
- Take onion seeds into the vessel and add water for decoction.
- Heat and reduce the volume to one fourth filter through muslin cloth to obtain kwath .
- Take Tila Tail in a stainless steel vessel and add kwath.
- Heat For 3hr with constant stirring maintaining the temperature between 50 – 90 degree Celsius during the first hour of heating .
- Stop heating and allow to stand overnight.
- Continue the process of heating intermittently over period of 3 days.
- Expose the oil with a piece of paper to flame and confirm the absence of moisture.
- Filter while hot (about 30 degree) through muslin cloth and allow to cool.
- Store it in glass containers and pack them air tight box to protect from sunlight .

Test & Calculations

Specific gravity (z)

a) Weight of empty beaker :- 50.898 gm
b) Weight of empty beaker with distilled water (H2O) :- 60.896gm
c) Weight of oil with bottle :- 60.914 gm

b-a = x = 60.896 – 50.898 = 9.998 gm
c-a = y = 60.914 – 50.898 = 10.061 gm
z = y/x = 10,016/9.998 = 1.0018 gm

Refractive Index

a) At 26 degree Celsius =1.470
b) At 26 degree Celsius = 1.470
c) At 26 degree Celsius = 1.470

Saponification Value

- For 100ml solution –
  4gm KOH + 2ml H2O +98ml alcohol = 100ml alc.KOH
  Empty beaker = 38.574 gm

Alcoholic KOH 25ml

↓

oil 2gm

↓

Hot water bath (1hr)

↓

1ml Phenopthaline

↓

0.5 N HCL (47)

↓

Colourless

- Alcoholic KOH + 1ml pH

↓

Pink Colour

↓

0.5 N HCL (60)

↓

Colourless

Sap Value :- $\frac{(b) - (a) \times 0.02805 \times 1000}{2}$

$= \frac{60-47 \times 0.02805 \times 1000}{2}$

$= 364.65$

$= \frac{182.325}{2}$

Acid Value = $\frac{0.1 \times 0.00561 \times 1000}{W}$

$= \frac{0.1 \times 0.00561 \times 1000}{10.029} = 1.79$ ml

DISCUSSION

In recent years, the beauty and wellness industries have witnessed a surge in the popularity of natural remedies for hair care. Among these remedies, the use of onion seed oil, enriched with the nourishing properties of Tila Taila (sesame oil), has garnered attention for its potential to address various hair concerns. Drawing from both modern scientific research and ancient Ayurvedic wisdom, this discussion explores the qualities of onion and Tila Taila, and how their combination can effectively resolve common hair problems. Onions are not just culinary staples; they also possess remarkable properties beneficial for hair health. Rich in sulfur, antioxidants, and essential nutrients like vitamins C and B, onions contribute to hair strength and growth. Studies have shown that onion extract promotes hair re-growth, inhibits hair fall, and improves overall scalp health by combating oxidative stress and inflammation .[23-26] In Ayurveda, onions are esteemed for their therapeutic properties. They are believed to balance the Vata and Kapha doshas, which are associated with dryness and excess oiliness, respectively, in the scalp. Additionally, onions are considered Tridoshhara, meaning they can pacify all three doshas when used appropriately. Their pungent taste and heating energy stimulate blood circulation in the scalp, promoting hair growth and maintaining scalp health.[23-26] Tila Taila, or sesame oil, has been a cornerstone of traditional Indian hair care for centuries. Its rich composition of fatty acids, antioxidants, and vitamins nourishes the scalp and hair follicles, preventing dryness and brittleness.

Furthermore, sesame oil exhibits antimicrobial properties, protecting the scalp from infections and dandruff. Its light texture allows for easy absorption, leaving the hair soft, shiny, and manageable. In Ayurveda, Tila Taila is highly valued for its ability to pacify the Vata dosha, which governs movement and dryness in the body. Its warming properties soothe the scalp and promote relaxation, which is essential for healthy hair growth. Tila Taila is also believed to enhance the effects of other herbal ingredients when used in formulations, making it ideal carrier oil for herbal extracts like onion seed oil.[23-26]

Synergistic Effects of Onion Seed Oil and Tila Taila

Combining the potent properties of onion seed oil with the nourishing base of Tila Taila creates a powerful elixir for hair health. The sulfur compounds in onion seed oil work synergistically with the nutrients in sesame oil to strengthen hair shafts, stimulate follicles, and improve circulation to the scalp. Together, they address a range of hair concerns, including hair loss, dandruff, and dryness, while promoting overall hair vitality and shine.[23-26]

CONCLUSION

Incorporating onion seed oil infused with Tila Taila into hair care routines offers a holistic approach to addressing common hair problems. By harnessing the benefits of these natural ingredients, individuals can nourish their hair from root to tip, restoring its strength, luster, and resilience. Whether viewed through the lens of modern science or ancient Ayurvedic wisdom, the combination of onion and Tila Taila stands as a testament to the enduring power of natural remedies in promoting hair health and vitality.[23-26]

REFERENCE

1. International Association of Trichologists - https://www.trichologists.org.uk/what-is-trichology/
2. Sinclair, R., & Patel, M. Diagnosis and management of alopecia. The BMJ, k3922. https://doi.org/10.1136/bmj.k3922,(2018), 362
3. Dawber, R. P. R., & Van Neste, D. J. J. ,Diseases of the Hair and Scalp. Blackwell Science.(2004)
4. Messenger, A. G., & Sinclair, R. Follicular miniaturization in female pattern hair loss: clinicopathological correlations. The British Journal of Dermatology, https://doi.org/10.1111/j.1365-2133.2006.07401.x , 155(5) ,(2006) , 926–930.
5. Gupta, A. K., & Bluhm, R. Seborrheic dermatitis. Journal of the European Academy of Dermatology and Venereology, 18(1), (2004) ,13–26. https://doi.org/10.1111/j.1468-3083.2004.00877.x
6. Sharma, R. K., & Dash, B. Charaka Samhita. Chowkhamba Krishnadas Academy.(2012)
7. Lad, V., & Frawley, D. The Yoga of Herbs: An Ayurvedic Guide to Herbal Medicine. Lotus Press , (1986)
8. Dr.Hegde Prakash L. and Dr. Harini A., A Text Book of Dravyaguna Vijnana , Reprint 2022, Page 461.
9. Database On Medicinal Plants , WHO monographs on selected medicinal plants , Onion Volume 4 ,
10. Dr.Hegde Prakash L. and Dr. Harini A., A Text Book of Dravyaguna Vijnana, Reprint 2022, Page 462.
11. BhavprakashNighantu, Haritakyadivarga -199
12. Dr.Hegde Prakash L. and Dr. Harini A., A Text Book of Dravyaguna Vijnana, Reprint 2022, Page 463
13. DrTewari.P.V. ,Charak Samhita (English translation of text with ayurveda dipika commentary of Cakrapani),Vol. 3, Cikitsasthana, Ch . Chi 15 /18-19) Vol. 3, Page 550**.**
14. Prof.Murthy K.R. Srikantha ., Astanga Hrdayam (Text English Translation , Notes , Appendix and Indices) A. H shar 1/57 Vol 1, Page 370.
15. A.N Kalia , Textbook of Industrial Pharmacognosy.
16. Prof.Murthy K.R. Srikantha ., Astanga Hrdayam (Text English Translation , Notes , Appendix and Indices) A. H U. 24 /24, 25, 26Vol 2,
17. Hamilton, James B., and Paul L. Levy. "Male pattern baldness: classification and incidence." Southern medical journal 69.5 (1976): 575-577.

18. Andrew G., et al. "Genetic variation associated with hormonal levels and response to hormonal therapy in breast cancer." American journal of human genetics 75.5 (2004): 959-968.
19. Gilhar, Amos, et al. "Autoimmune disease of the hair follicle: Bullying the bulge." Journal of Clinical Investigation 116.2 (2006): 334-337.
20. Ralph, Cory J., and Barbara G. Goodman. "Hair loss." Dermatologic clinics 25.2 (2007): 271-280.
21. Hadshiew, Ina M., et al. "Burden of hair loss: stress and the underestimated psychosocial impact of telogen effluvium and androgenetic alopecia." Journal of Investigative Dermatology Symposium Proceedings 9.6 (2004): 101-105.
22. Rushton, D. H., and M. J. Norris. "Nutritional factors and hair loss." Clinical and experimental dermatology 27.5 (2002): 396-404.
23. Burdock, G. A. Fenaroli's Handbook of Flavor Ingredients. CRC Press., (2014)
24. Kumar, A., Yadav, A. K., & Nisha. Onion: Nature protection against various disease and infection. International Journal of Pharmaceutical Sciences and Research, 7(4),(2016) , 1460–1465.
25. Rastogi, S. The Effect of Onion (Allium cepa L.) Extract on Hair Growth and Hair Quality. Journal of Cosmetic Dermatology, 13(4),(2014), 313–318.
26. Sharma, H., Chandola, H. M., & Singh, G. A Text Book of Rasa Shastra. Chaukhambha Orientalia., (2018)

Table 1: Method of Preparation

S.No	Ingredients	Botanical Name	Quantity
1.	Onion seeds	*Allium cepa* (Amaryllidaceae)	25 gm
2.	Tila Tail	*Sesamum indicum*(Pedalianeae)	100 ml
3.	Water	Water	1600 ml

Fig 1 Onion black seeds

Fig 2 Making of Decoction

Fig 3 Prepared decoction

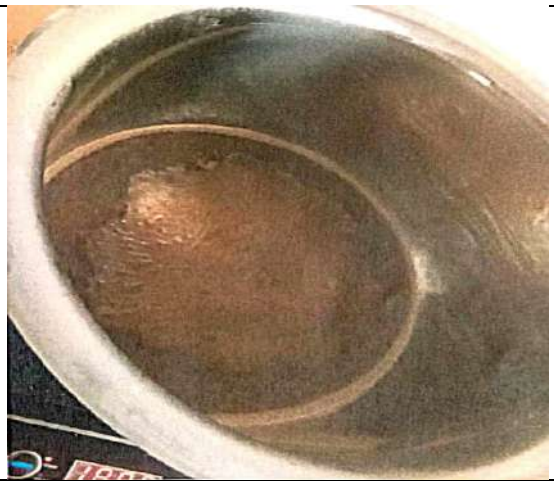

Fig 4 Mixed part of tilataila and decoction

Fig 5 Ongoing process of making oil

Fig 6 Prepared oil

Fig 1 Sample of oil

Fig 2 Alcoholic KOH

Fig 3. Oil mixed with Alcoholic KOH

Fig 4. Burrete was used for saponification, Shows pink colour solution in conical flask.

Fig 5. Pink solution became colourless after adding .5N HCL

Indian Journal of Natural Sciences www.tnsroindia.org.in ©IJONS

Vol.15 / Issue 88 / Feb / 2025 *International Bimonthly (Print) – Open Access* *ISSN: 0976 – 0997*

RESEARCH ARTICLE

Exploring Quotient Group Properties in Topological Spaces

A. Saranya[1]* and A. Kalavathi[2]

[1]Assistant Professor, Department of Mathematics, Dr. Mahalingam College of Engineering and Technology, Pollachi, (Affiliated to Anna University, Chennai), Tamil Nadu, India.
[2]Assistant Professor, Department of Mathematics, Sri GVG Visalakshi College for Women, Udumalpet, (Affiliated to Bharathiyar University, Coimbatore), Tamil Nadu, India.

Received: 21 Nov 2024 Revised: 03 Dec 2024 Accepted: 25 Jan 2025

***Address for Correspondence**
A. Saranya
Assistant Professor,
Department of Mathematics,
Dr. Mahalingam College of Engineering and Technology, Pollachi,
(Affiliated to Anna University, Chennai),
Tamil Nadu, India.
E.Mail: saranyasaraswathy@gmail.com

ABSTRACT

Topological spaces are fundamental structures in mathematics, defined by a set of points and a topology, which is a collection of open sets that satisfies specific axioms related to union, intersection, and containment. Positive responses to the Banach-Mazur issue, investigate how each detachable quotient of a single infinite-dimensional Banach space constitute infinite-dimensional. Banach spaces have been found in recursive and dual Banach spaces, respectively. Regarding local spaces of convex, this question responds negatively, it holds true for several classes like all Fréchet spaces that are not normative. Research explores a similar problem in the realm of topological groups, specifically investigating if all topological groups that are not completely as unconnected have non-trivial, infinite, separable quotient (SQ) groups. Generally, these questions are answered negatively. However, positive results are found for notable categories of topological groups, such as locally CAG (compact abelian groups) and entire compact groups, while negative results are shown for pre compact groups.

Keywords: Quotient Group, Topological Spaces, Topology, Banach Spaces.

INTRODUCTION

Quotient groups, which are one of the topics in algebra, are important in topological spaces as well. The framework of topological spaces is incredibly enlightening about algebraic and topological objects [1]. In the context of topological spaces, quotient groups perform the role of interlink between algebra and topology. Quotient space in

topology is obtained from a given space by specifying a relation of similarity and then greatly reducing the number of distinguishable points to those fulfilling this relation [2]. In quotient groups of topological spaces, what is tried to be established or changed is continuity, compactness and connectedness in connection with quotient mapping [3]. A branch of mathematics that focuses on the study of topological spaces using algebraic invariants is enhanced. Thus, the incorporation of quotient groups with the study of topological space is mutually beneficial in enhancing both the concepts and expanding horizons for future work and implementation in geometry, mathematical physics, and more [4]. The purpose of the paper is to address the existence of a non-trivial, infinite, separable quotient (SQ) group for each non-totally unconnected topological group.

RELATED WORKS

Using their dual groups, study [5] explored the topological framework of completely bounded Abelian groups. Each Abelian group G has a big dual group Gb associated with it, which was made up of the homomorphisms of G into the one-dimension cylinder. Topological groups and certain of their extensions to finite groups were subjected in study [6]. They state that a topological group must have the assumption $T0$. Two generalized quotient space structures constructed on quasilinear spaces were introduced in the article [7]. One was a linear space, while the other was a quasilinear space. Subsequently, they attempt to study some of these spaces' features and propose rules for certain states. A concept and structure for internal topology symmetric in the theory of quantum fields, which include "noninvertible symmetries" and "categorical symmetries," were presented in the study [8]. They provide a topological defect calculus that makes use of established methods and proofs from topological field theory. The theoretical stability model for Banach structures and spaces derived from them was introduced in research [9]. The following condition was shown to be valid in each model E of the theory. Features of quadratic subgroups over local fields were presented by research [10] in terms of topological group theory. Specifically, they identify the circumstances under which random continuous homomorphisms into random topology groups have closed images for such groups.

Problem statement and its proofs

We provide 11 problems and present 11 proofs to address and resolve them. Each proof is specialized to effectively solve the corresponding queries.

Problem 3.1

Is there a dense, infinite-dimensional subspace that is not smashed in every infinite-dimensional Banach space?

Proof 3.1

When considering a Banach space with infinite dimensions, A, the equivalent statements are as follows:
(i) A constitutes an infinite-dimensional SQ Banach structure; (ii) A has an unbarbellized dense substructure; (iii) A has a dense substructure F constitutes a product for strictly expanding linear subspaces that are closed in succession. We obtain several expansions of this conclusion to vector spaces that are topological.

Problem 3.2

SQ problem for H_σ- groups: Does a separable quotient group exist that was (i) infinite, (ii) nontrivial for every not-discrete H_σ-group?

Proof 3.2

A separable infinite-dimensional fraction of Banach space for A exists if A constitutes Banach space with infinite dimensions. Numerous specific instances of the problem SQ of banach spaces are demonstrated on papers, yet, the overall issue has not been resolved. The comparable problem can be stated by turning to locally convex spaces. This investigation will assume that all locally symmetrical spaces are Hausdorff.

Problem 3.3

SQ problem for reflexive topological groups:Is the quotient group of any locally infinite CAG, G indefinitely separate and non-trivial?

Proof 3.3

Proof of SQ for compact groups, consider H as an infinite group with compact. Afterwards, the quotient group H, possesses a compact infinitely separable group. H represents a rigorous projective border of lie groups that are compact. Hence, H as isotropic from a topological group to a product's subgroup $K_j, j \in J$, here each Li, i∈ I, constitutes lie group, indexed set as$J$. Give $K_j, j \in J$, the projection map from G into Li. We start by assuming that all groups $o_j(H)$ are limited. Then, compact group as G was completely disconnected since it is isotropic to a topological group component of a product of finite lie groups. Thus, let's assume that $o_m(H)$ is infinite for all$m \in J$. Quotient mapping as pn for H constitutes the metrizable (separable) infinite compact group $o_m(H)$, since H is compact, as needed.

Problem 3.4

SQ issue for abelian groups that are locally compact: Does each locally infinite CAG, G have an infinitely separate, quotient group non-trivial?

Proof 3.4

SQ proof for abelian groups that are compact locally: Where H constitutes an infinite group of abelian that is locally compact. Htherefore possesses an infinite separable compact group as its quotient group. Through the evidence for abelian groups' main structure that were locally compact. An isomorphic open subgroup H of H of $\mathbb{R}^m \times L$ as a topological group, where n is an integer that was not negative and K constitutes CAG. $H = G$ in condition 1: Next, the proof is proved. Condition 2: An infinite discrete abelian group is $\frac{H}{G}$. Thus, $\frac{H}{G}$ and consequently H possess a countably infinite and discrete quotient group. Condition 3: $\frac{H}{G}$is limited. H is then a locally CAG that is compactly produced. As a topological group, H is isomorphic to $\mathbb{R}^m \times \mathbb{Z}^n \times D$Let n, m be positive integers. Let D as tight CAG. Proof on SQ for nearly connected locally compact groups and quotient group, and the infinite separable group for any locally compact infinite nearly linked group. All pseudocompact groups and σ -compact groups belong to the class of $\mathbb{R}$ -groups factorizable. If and only if the group was compact locally as σ -compact, can it be $\mathbb{R}$ -factorizable.

Problem 3.5

SQ problem for banach Topological Groups: Is there an SQ group that is orthogonal to R! for every fundamental Banach spaces topological group with infinite dimensions, if any?

Proof 3.5

Proof on SQ for $\frac{H}{L}$compact locally compact groups A quotient group exists for any infinite σ - compact locally compact group. Evidence. Every compact group locally termed as σ-compact, H is a typical subgroup compact of$L$, and $\frac{H}{L}$ is a metrically separable group according to the Kakutani-Kodaira-Montgomery-Zippin proof.

Case 1: $\frac{H}{L}$ is limited. Given that compactness was a property of three spaces, H must be compact and yields the necessary outcome.

Case 2: $\frac{H}{L}$is unbounded. As necessary, quotient group as H was both infinitely separable and metrizable.

Problem 3.6

SQ issues for CAG: Where each local compacted group G that was not completely separate constitute group SQ that was (i) infinite and (ii) non-trivial?

Proof 3.6

Proof on SQ for σ - compact groups, the H group of topologies that was infinite σ-compact. Then, H possesses an infinite, separable quotient group when it comes category of the group's quotient homomorphisms with infinite groups of measurable network as initial. We provide a negative solution to problem 2.8's (iii) and (iv) by generating a σ - compact group that lacks a non-trivial separable quotient group.

Problem 3.7

SQ problem for compact groups: Is there a SQ group that is both (i) nontrivial and (ii) infinite for any infinite compact group, G?

Proof 3.7

SQ proof for pseudo-compact groups, which is one of the pre-compact groups, for each infinite pseudo-compact topology group$H$, the group for homo-morphisms of quotients with compact group infinite was initial with regard to$H$'s topology. Specifically, quotient group as H was compact, and indivisible. The continuously open homomorphism for ${}_{Q}H$ with topology group infinite L has a measurable system denoted by ${}_{Q}H \to L$. In that case, group L has a measurable base since it is compact. K especially can be measured. Indicate that p is restricted to H by using π. The group H meets every nonempty H_{δ}-set in ${}_{Q}H$ because it is pseudo-compact. Both the fibers$o^{-1}(z)$in `G and the points in L are all $z \in L$. Consequently, for any y in K, $o^{-1}(z)$, suggesting that p(G) = K. Furthermore, it was evident for $H \cap o$ is dense in $o\ to\ H$.

Problem 3.8

SQ problem for σ– Compact groups: Is there a separable quotient group that is (i) infinite (ii) non-trival for any non-discrete σ-compact group?

Proof 3.8

The analogous features of an abelian group H with precompact topology exist for each cardinal$\tau \geq d$.
$\omega(G) = \tau$;
$G = \bigcup_{m\in\omega} G_m G_0 \subset G_1 \subset G_2 \subset \cdots\ldots\ G$;
Each quotient group of G is non-separable or trivial.
Where H as precompact group of abelian and let τ as cardinal with $\tau \geq d$. $\omega(H) = d$ since H is a dense subgroup of τ. It is evident that the group $L = H^{\tau}$is abelian, precompact, and has weight τ. Additionally, all non-trivial quotients of L are not separable. The group K! Possessing the Tychonoff product topology is indicated by Π. Contract o_m be the projected value of Π to the nth element $L_{(m)}$ for each$m \in \omega$. The set $\{m \in \omega: o_m(w) \neq f\}$, where e is the identity element of L, is denoted as $supp(w)$ given an element $w \in \Pi$. Additionally, we placed:

$$G = \{w \in \prod : |supp(w)| < \omega\}$$

It is evident that $\omega(G) = \omega(\Pi) = \omega(L) = \tau$ and thus G is a dense subgroup of Π. The subgroup of G that includes all $w \in \Pi$with $supp(w) \subset \{0,1,\ldots\ldots,m\}$ is denoted as G_m for each $m \in \omega$. It is simple to see that $G_m \subset G_{m+1}$for each $m \in \omega$, and $G_m \cong L^{m+1}$ are closed in G. Let's demonstrate that there is no separable non-trivial quotient of$G$. Consider an open constant similarity$e: G \to K$ on a topological group K that is not trivial. Let M represent the closure of $\bar{M}$ in Π and M the kernel of f. The quotient homomorphism of Π onto $\frac{\Pi}{M}$ is indicated by π. $(H^S)^{\omega} \cong H^S$ is isomorphic to the dense subgroup π(H) of $\frac{\Pi}{M}$ as a topological group because N was compact within N. Then group Π was isomorphic to $K \cong \frac{G}{M}$as a topological group. There was no separability for the non-trivial group Π/N, according to proof 4.13. As a result, both are the group $K \cong \frac{G}{M}$, which is suitable for dense subgroup $\pi(G)$ for $\frac{\Pi}{M}$as a topological group.

Problem 3.9

SQ problem for Pre-compact groups :Is a quotient group separable that was (i) nontrivial; (ii) infinite for any infinitely pre compact group?

Proof 3.9

There is a divisible infinite-dimensional quotient BS for each infinite-dimensional weakly compactly generated (WCG) BS. Given that separable and reflexive BS are WCG, one receives.

Problem 3.10

SQ problem for Pseudo-compact groups: Is a quotient group separable that was both (i) non-trivial and (ii) limitless for every infinite group that was pseudo compact?

Proof 3.10

Let A be a Banach space (BS) such that A has a quotient BS isotropic to F^*, and let the dual BS A^* have an infinite-dimensional receptive region F. Consequently, A 's BS is an infinite-dimensional separable quotient.

Problem 3.11

SQ problem for R-factorizable groups :Is quotient group separable that was (i) infinite, (ii) nontrivial for any $\mathbb{R}$-factorizable group?

Proof 3.11

The infinite R-factorizable groups in the absence of non-trivial separable. Furthermore, all of H's quotients are precompact. Consider that there is a division of all pre compactmetrizable groups. As a result, the precompact group H has no non-trivial quotients that can be metrized or separated.

Summary

In summary, proof 3.1, 3.9, 3.10, 3.2 were used in problem 3.1, producing a partial outcome. Problem 3.2 was addressed using proof 3.8, resulting in a No outcome. For problem 4, applying proof 3.4 led to a Yes outcome. Problem 3.5 utilized proofs 3.1, 3.9, 3.10 and 3.2, with the result being partial. For problem 3.6, the application of proofs 3.3, 3.4, 3.5and 3.6 also yielded a partial result. Problem 3.7, which used proofs 3.3, 3.6 and 3.7, had a Yes outcome. In problem 3.8, employing proof 3.6 resulted in a Yes. Problem 3.10, using proof 3.7, led to a Yes, and problem 3.11, addressed with proof 3.11, also resulted in a No.

CONCLUSION

Study shows the importance of topological spaces in mathematics and defined as a set of points and topology that complies with certain axioms. This work focuses on a similar issue in topological groups, which concerns the question of whether there exists a non-trivial, infinite separable quotient group in a non-totally disconnected topological group. The outcomes show that in most cases the answer to this question is negative. Beneficial findings are demonstrated, nonetheless, for important types of topology categories, including all globally compacted Abelian groups and all compacted groups. On the contrary, negative results are numerous for pre-compact groups. These contrasting results indicate that topological group structures are intricate and multifaceted, consistent with earlier observations in Banach space investigations where similar questions received affirmative answers for recursive and dual Banach spaces but negative answers for locally convex spaces. The outcomes of the study help to extend the overall comprehension of the topological group behavior with reference to specific classes wherein the existence of non-trivial, infinite, separable quotient groups is established thereby enrich the discourse in mathematics. The observed mainly addresses non-totally disconnected topological corporations and may not embody all feasible group systems. Further research should explore non-Abelian groups and broader classes of topological businesses to better apprehend the conditions under which non-trivial, infinite separable quotient companies exist. Additionally, examining similar problems in other mathematical systems, inclusive of non-locally compact or non-compact companies, should provide greater complete insights.

REFERENCES

1. Sanborn, S., Mathe, J., Papillon, M., Buracas, D., Lillemark, H.J., Shewmake, C., Bertics, A., Pennec, X. and Miolane, N., 2024. Beyond Euclid: An Illustrated Guide to Modern Machine Learning with Geometric, Topological, and Algebraic Structures. *arXiv preprint arXiv:2407.09468*. https://doi.org/10.48550/arXiv.2407.09468
2. Ericok, O.B. and Mason, J.K., 2022. Quotient maps and configuration spaces of hard disks. *Granular Matter*, *24*(3), p.76. https://doi.org/10.1007/s10035-022-01235-5
3. Adhikari, A. and Adhikari, M.R., 2022. Topological Groups and Topological Vector Spaces. In *Basic Topology 2: Topological Groups, Topology of Manifolds and Lie Groups* (pp. 27-123). Singapore: Springer Nature Singapore. https://doi.org/10.1007/978-981-16-6577-6_2
4. Solomon, E., Wagner, A. and Bendich, P., 2021. From geometry to topology: Inverse proofs for distributed persistence. *arXiv preprint arXiv:2101.12288*. https://doi.org/10.48550/arXiv.2101.12288
5. Hernández, S., Remus, D. and Trigos-Arrieta, F.J., 2023. On closed subgroups of precompact groups. *Journal of Group Theory*, *26*(3), pp.571-610. https://doi.org/10.1515/jgth-2022-0093
6. Kumar, A.M. and Gnanachandra, P., 2020. Exploratory results on finite topological groups. *JP journal of geometry and topology*, *24*(1-2), pp.1-15. http://dx.doi.org/10.17654/GT024120001
7. Dehghanizade, R. and Modarres, S.M.S., 2021. Quotient spaces on quasilinear spaces. *International Journal of Nonlinear Analysis and Applications*, *12*, pp.781-792. http://dx.doi.org/10.22075/ijnaa.2021.20279.2142
8. Freed, D.S., Moore, G.W. and Teleman, C., 2022. Topological symmetry in quantum field theory. *arXiv preprint arXiv:2209.07471*. https://doi.org/10.48550/arXiv.2209.07471
9. Iovino, J., 2021. Stable Banach spaces and Banach space structures, I: Fundamentals. In *Models, algebras, and proofs* (pp. 77-95). CRC Press.
10. Bader, U. and Leibtag, E., 2024. Homomorphic images of algebraic groups. *Journal of Algebra*, *656*, pp.77-117. https://doi.org/10.1016/j.jalgebra.2023.09.001

Indian Journal of Natural Sciences *www.tnsroindia.org.in ©IJONS*

Vol.15 / Issue 88 / Feb / 2025 *International Bimonthly (Print) – Open Access* *ISSN: 0976 – 0997*

RESEARCH ARTICLE

An Ayurvedic Approach of Panchkarma Therapy in Treatment of Amyotrophic Lateral Sclerosis - A Case Study

Sonaliben A. Chauhan[1], Sachin Deva[2]* and Divya .B[3]

[1]PG Scholar, Department of Roga Nidan Evum Vikriti Vigyana, Parul Institute of Ayurveda, Parul University, Vadodara, Gujarat, India.
[2]Professor, Department of Roga Nidan Evum Vikriti Vigyana, Parul Institute of Ayurveda, Parul University, Vadodara, Gujarat, India.
[3]Associate Professor, Department of Panchakarma, Parul Institute of Ayurveda and Research, Parul University, Vadodara, Gujarat, India.

Received: 21 Nov 2024 Revised: 03 Dec 2024 Accepted: 27 Jan 2025

***Address for Correspondence**
Sachin Deva
Professor,
Department of Roga Nidan Evum Vikriti Vigyana,
Parul Institute of Ayurveda,
Parul University,
Vadodara, Gujarat, India.
E.Mail: sachin.deva@paruluniversity.ac.in

ABSTRACT

The rare and fatal neurodegenerative disease known as AMYOTROPHIC LATERAL SCLEROSIS (ALS), sometimes referred to as Motor Neurone Disease (MND) or Lou Gehrig's Disease, causes a gradual loss of motor neurons that control voluntary muscles. It is characterised by fasciculations, wasting, and progressive skeletal muscle weakness .Respiratory paralysis causes mortality, and survival lasts three to five years. There is a 1.5–2.7/100,000 annual incidence and a 3–5/100,000 prevalence of ALS. Compared to women, men are more impacted. This case study describes a 53-year-old man who complained of weakness and stiffness in his upper and lower limbs, with a particular emphasis on the lower limbs, as well as fasciculation in the muscles of his forearms, difficulties speaking, and disturbed sleep. According to Ayurveda, the case was identified based on its symptoms as *Kapha AvritUdaana*and *Kapha AvritVya*anavata. This condition arises when Kapha dosha obstructs *udaana* and *Vyanavata*, hampering vata's normal functioning. Improving quality of life and slowing the disease's rate of progression were the two main objectives of the treatment. *Panchakarma* procedures were implemented as the therapy basis for *Srotoshodhana* and other *Shamanaaushadh*.

Keywords: Motor Neuron Disease(MND), Amyotrophic Lateral Sclerosis (ALS), *Panchakarma, Kaphavrut Vyana*, *Kaphavrut Udana*

INTRODUCTION

Progressive motor neuron disease most commonly manifested as amyotrophic lateral sclerosis (ALS). Degeneration of motor neurons at all levels of the central nervous system (CNS), including the motor cortex, brainstem motor nuclei, and anterior horns of the spinal cord, is the cause of ALS [1]. Midlife is typically the onset, and most instances end in death within three to five years. The incidence and prevalence of ALS are 1.5–2.7/100,000 and 3–5/100,000, respectively, every year [2]. The textual references describe twitching, stiffness, cramping, weakness, and wasting of muscle in the hands and arms, often beginning in the intrinsic hand muscles. Leg stiffness, cramping, and weakness are common complaints, but the involvement in the legs is less severe than in the arms. Brainstem involvement may show up as dysphagia, which can result in aspiration pneumonia and reduced energy intake; dysarthria, or difficulties articulating, phonation, and deglutition, can also be a notable wasting of the tongue symptom. Respiratory insufficiency is caused by weak ventilatory muscles. The three main symptoms of ALS are absence of bladder or bowel problems, pseudobulbar palsy (such as uncontrollable sobbing or laughing), and lack of sensory abnormalities. Sporadic ALS does not include dementia; in certain families, frontotemporal dementia, which is characterised by abnormal behaviour brought on by frontal lobe dysfunction, co-occurs with ALS.

Pathogenesis in the context of Ayurveda

There are two ways that vata might get vitiated: either by eliminating bodily tissue, or by another dhatu, dosha, or mala obstructing vata, which then undergoes pathology and develops a disease. This current case report discusses ALS diagnosed as kapha avritudaana and kapha avritvyaanavata in accordance with ayurveda.[3] This indicates that kapha dosha has obscured the udaanavata, which is responsible for human vocal communication, and the vyaanavata, which is responsible for movement and daily activities, impairing vata's regular functioning..

CASE DESCRIPTION

A 53 years old male patient,(OPD No – 22032856) known case of Hypertension came to Panchakarma OPD with the complaints of weakness and Stiffness in B/L upper and lower limbs more in lower, and fasciculation in forearm muscles, difficulty in speech and Disturbed sleep. Patient was having difficulty in doing his regular activities like walking, buttoning clothes and reduced gripping of both hands since 6-7 months, which was gradually worsening. The patient states that before 6-7 months, he was normal. He gradually started having trouble speaking, moving his hands and walking, as well as lower limb stiffness and disturbed sleep. He received both allopathic and ayurvedic treatment, but he did not experience much improvement. He had an MRI of his spine and brain. It was there that Amyotrophic Lateral Sclerosis was identified in him. Ayurvedic diagnosis: The patient was classified as both kapha avritavyanavata and kapha avritaudana. Patient had a history of hypertension. Family History: Not significant

Personal history

Dietary Habit – Vegetarian, Sleep- Disturbed
Defecation- Regular, Micturation- Normal frequency

General examination on admission

Muscle tone was hypotonic on bilateral lower limbs, Muscle bulk was reduced on bilateral lower limbs. Bladder and Bowel control was Normal.

SYSTEMIC Examination

- RESPIRATORY SYSTEM: Normal sounds were heard during auscultation, and no abnormalities were found.
- Cardiovascular system: S1 and S2 heard, and no anomalies were found.
- GASTROINTESTINAL SYSTEM: no organomegaly was found, soft, and non-tender.

CENTRAL NERVOUS SYSTEM
HIGHER MENTAL FUNCTION
CONSCIOUS LEVEL: alert, tense, and receptive to spoken instructions.
ORIENTATION – Well oriented to Time, Place, Person.
MEMORY: Whole SPEECH: slurred
MUSCLE TONE: hypotonic on both lower limbs;
MUSCLE BULK: diminished on both lower limbs.
PTR was reduced, and the biceps jerk was exaggerated.

MUSCLE POWER GRADE

UPPER EXTREMITIES	RIGHT SIDE	LEFT SIDE
	GRADE 03	GRADE 02
LOWER EXTREMITIES	RIGHT SIDE	LEFT SIDE
	GRADE 03	GRADE 03

Rogi- pareeksha
Ashtasthana pareeksha

Nadi	Vatakaphaja
Mala	Samyak malapravriti, 1time/day
Mutra	Samyak, 5-6 times/day
Jihwa	Nirama
Shabda	Slurred speech
Sparsha	Samshitoshna
Drika	Prakrita
Akriti	Madhyam

Rogapareeksha
Nidanas

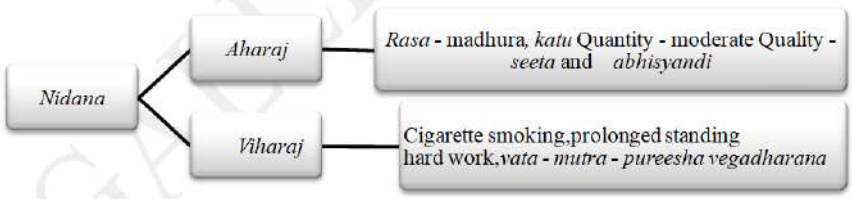

1. *Poorvarupa – avyaktam*
2. *Lakshana – Gamanekashtata, Stabhdhta, Karma Akshamata, VakaAspashtata, Anidra*
3. *Upasaya – usnaupachara, anupasaya – sitasevana*
4. *Samprapti–*

Vitiation of vata (Dhatukshaya or Srotorodha)

↓

Leads to doshprakopa and Vitiation of Kapha dosha

kaphaavritudaanavatakaphaa vritvyaanavata .

Vaka Aspashtata

Gamane kashtata, Stabhdhta, Karma Akshamata

SamprapthiGhatakas

Dushya

Dosha: sannipattaj
Dhatu: rasa, rakta, mamsa, medas
Upadhatu: snayu
Agni: manda
*Srotas: rasavaha, rakthavaha, mamsavaha*and *medovaha*
Srotodushti: sangam
Rogamargam: madhyama
Rogaswabhavam: chirakari
Udbhavasthana: amasaya
Prasarasthana: adhovahadhamani
Asrayasthana: snayu
Vyakthisthana: adhakaya
Prakriti - vata pitta

AYURVEDIC MANAGEMENT

SHODHANA CHIKITSA

Sr.No.	*Panchkarma* therapy	Duration
1	*SarvangaUdwartana* followed by *BashpaSweda*	5 days
2	*Sarvanga Abhyanga* with *KsheerabalaTaila* followed by *Nadi sweda*	10 days
3	*Matrabasti*with *KsheerabalaTaila*	10 days
4	*Nasya* with *KsheerabalaTaila*	5 days

Medicine	Frequency	Duration
Yogarajaguggulu	2 BD after food	5 days
Amapachakvati	2 BD before food	5 days
Vatavidhvamsh rasa	1 BD after food	5 days
Erandamulakwath	25 ml before food	15 days
Cap. *Dhanvantaram*	1 BD after food	10 days
Tab. Ortiset	1 BD after food	10 days
Samvardhanaghrita	With Milk 1 time	10 days
Dadimashtakachurna	½ tsp before food	4 days

Tab. Mentar	2 BD after food	4 days

SHAMANA CHIKITSA

RESULT AND OBSERVATIONS

Before Treatment	**After Treatment**
ALSFRS-R Score -	ALSFRS-R Score-

UPPER EXTREMITIES	RIGHT SIDE	LEFT SIDE
	GRADE 5	GRADE 5
LOWER EXTREMITIES	RIGHT SIDE	LEFT SIDE
	GRADE 5	GRADE 5

The total score of ALSFRS-R before starting treatment was 20, and the score at the time of discharge was 25. The patient made good progress in areas such as generalised weakness, walking, holding objects, and speaking. With Ksheerabala and other Panchkarma therapies, the patient had significant alleviation from generalised weakness. At the time of release, the patient's overall condition had improved, their gait had improved, they felt more energetic, and their upper and lower limb spasticity had lessened. The two hands' fine motor motions did not get any better.

DISCUSSION

While there isn't a clear Ayurvedic equivalent for MND, it might be regarded as a "VATA" predominate condition. The majority of the classical Ayurvedic signs and symptoms of Vata derangement are similar to those of MND, including fasciculations (Gaatrakampa), cramps (Bheda, Toda), wasting, weakness (balopghata), spasticity (ParvanamStambha), etc. [4] This instance demonstrates the prominent roles played by Vata and Kapha in the pathogenesis of Samprapti. Avarana (obstruction), Vata Prakopa (aggravation of Vata), and MND are all results of exacerbated Kapha. MND's clinical picture is similar to that of "Vyaana Vata and Kapha Avrita Udaana".[5] That informed the planning of the therapy plan.(Deva, March- 2019) The goal of treatment was to eliminate vatashamaka chikitsa (alleviation of vitiated vata dosha) and then kapha avarana (occlusion by kapha dosha). Numerous panchakarma techniques were used, including nasya (errhine therapy), bashpasweda (sudation in a steam chamber), sarvaanga abhyanga (whole body oil massage), and udwartana (herbal powder massage). According to Ayurveda, since pathology arises from Ama formation as a result of an unwholesome regimen known as Apathyaahara-vihara, the chikitsa principle that was first adopted was Nidanaparivarjan, which involved avoiding madhura, abhisyandiahara, sitasevan, prolonged standing, and excessive work. Next, Sampraptivighatanacikitsa, which broke the pathogenesis, began with Deepana Pachana, which served as an appetiser and digestant, using Amapachakavati. Initially, internal medications like Yograjaguggulu were given to remove Ama (obstructions caused by toxins) and Rukshanswedan (SarvangaUdwartanam) with udwartanachurna was performed. The balya properties of ashwagandha churna led to the addition of ShunthiChurna, which is an irritant that stimulates peripheral nerve endings and dermatomes. The patient reported improved appetite and a lighter physique after taking Udwartana for five days. Then, for 15 days, pure Vata Chikitsa, such as SarvangaSnehana by Mahanarayanataila and BashpaSwedana by Dashamoolakashayam, was performed in addition to Matra Vasti (rectal enema). **SarvangaUdwartana** promotes blood circulation by enlarging small channels with the goal of lowering Avarana of Kapha and alleviating Vatadosha. **Nadisweda** aids in the transmission of nerve impulses with the least amount of stimulus required for muscle contraction by enabling the opening of nerve blockages, conduction of impulses, and thereby aiding to remyelination. **Sarvanga Abhyanga** with Ksheer Bala Taila - Karma Kshaya/ Karmahaani is caused by vitiated Vata dosha and was treated with abhyanga with ksheerbalataila. Sarvanga Abhyanga, which is effective for all 80 types of Vataroga and acts as Vatashaamaka when paired with Ksheerbalataila, is also excellent for treating neuromuscular and musculoskeletal disorders.[6] **KshirabalaTailaMatra Basti**: KshirabalaTailaMatra Basti may have

given the Dhatu food because of its Brimhana (nourishing) function, which enhanced the Dhatu's capacity to nourish the limbs physically. Ksheerabala Another use for the herb Ksheerabala is as a nerve tonic. It is used to treat arthritis, CNS disorders, and insomnia. Additionally, the sense organs function better. appearing in Vataroga as Bruhmana, IndriyaPrasadaka, and so forth.

The Chikitsa Principle

1. Avoiding Madhura, AbhisyandiAhara, Sita Seva, extended standing, and excessive effort are examples of Nidanaparivarjana (avoidance of causative and precipitating elements).
2. SamprаptiVighatana Chikitsa (breaking the pathogenesis) Ama Chikitsa (elimination of ama) AvaranaCikitsa (release of obstruction) Mamsagata Vata Chikitsa (Mamsadhatu treatment for vitiation of Vatadosha)
3. Dhathusamyakara Chikitsa (Tissue Normalisation)

CONCLUSION

Motor neuron disease can be diagnosed as KaphavritaUdaana and Vyana Vata in Ayurveda. The primary treatment plan in this case involved the external removal of the Avarana of Ama and Kapha by Udwartanam and the interior removal by Amapachakavati. Following the implementation of Vata Nashaka and Balya Chikitsa by Abhyanga, Nasya and Swedana therapies were found to be effective in addressing muscle weakness and improving speech issues. It has been discovered that panchakarma treatments like Vasti, BashpaSweda, and Sarvanga Abhyanga can treat limb stiffness and stop the progression of ALS. It will take more extensive long-term follow-up research on a sizable sample to validate the aforementioned statements. Therefore, further study in this area is required.

REFERENCES

1. Harrison's™ manual of medicine: nineteenth edition /dennis l. Kasper/anthony s. Fauci/stephen l. Hauser/dan l. Longo/j. Larry jameson& joseph loscalzo.
2. https://www.neurologyindia.com/text.asp?2017/65/5/1155/214063
3. Charaka (2011) Charak Samhita, Kashinath Shastri and Gorakhnath Chaturvedi (Eds.), Chikitsa Sthana chapter 28, Chaukhambha Bharti Academy, Varanasi, pp: 815.
4. Charaka (2011) Charak Samhita, Kashinath Shastri and Gorakhnath Chaturvedi (Eds.), Chikitsa Sthana chapter 28, Chaukhambha Bharti Academy, Varanasi, pp: 780.
5. Charaka (2011) Charak Samhita, Kashinath Shastri and Gorakhnath Chaturvedi (Eds.), ChikitsaSthana chapter 28, Chaukhambha Bharti Academy, Varanasi, pp: 814-815.
6. Dr. K. Nishteswar, Dr. R. Vidyanath, English translation, Sahasrayogam, Parisisthaprakaranataila, Nalpamaraditaila. Varanasi: Chowkhamba Sanskrit series office,3rd edition, 2011. p.110

Indian Journal of Natural Sciences www.tnsroindia.org.in ©IJONS

Vol.15 / Issue 88 / Feb / 2025 *International Bimonthly (Print) – Open Access* *ISSN: 0976 – 0997*

RESEARCH ARTICLE

A Study on the Efficacy of Sitagliptin in Combination with Metformin among the Patients with Type - 2 Diabetes Mellitus

Mudunuri Jahnavi Sai[1], Miriyala Sowmya[1], Ramam Sripada[2]*, K.L.S.D. Sireesha[3], Lakshmi Himaja Bandaru[3], Karuturi Subrahmanyam[4], Anahitha Anagalidehnouei[1], Mahyar Amiri Hesni[1] and M.D. Dhanaraju[5]

[1]Student, Department of Pharmacy Practice, GIET School of Pharmacy, Rajahmundry, (Affiliated to Andhra University, Visakhapatnam), Andhra Pradesh, India.
[2]Associate Professor and Head, Department of Pharmacy Practice, GIET School of Pharmacy, Rajahmundry, (Affiliated to Andhra University, Visakhapatnam), Andhra Pradesh, India.
[3]Assistant Professor, Department of Pharmacy Practice, GIET School of Pharmacy, Rajahmundry, (Affiliated to Andhra University, Visakhapatnam), Andhra Pradesh, India.
[4]Consultant Physician and Diabetologist, Department of General Medicine, Kify Hospital, Rajahmundry, Andhra Pradesh, India.
[5]Principal and Professor, Department of Pharmacy Practice, GIET School of Pharmacy, Rajahmundry, (Affiliated to Andhra University, Visakhapatnam), Andhra Pradesh, India.

Received: 21 Nov 2024 Revised: 03 Dec 2024 Accepted: 23 Jan 2025

***Address for Correspondence**
Ramam Sripada,
Associate Professor and Head,
Department of Pharmacy Practice,
GIET School of Pharmacy, Rajahmundry,
(Affiliated to Andhra University, Visakhapatnam), Andhra Pradesh, India.
E.Mail: ramampharmd7@gmail.com

ABSTRACT

To study the efficacy of Sitagliptin in combination with Metformin among the patients with type-2 diabetes mellitus. This was prospective study and patients of both the genders of age between 25-60 years, who were diagnosed with type-2 diabetes mellitus were included in the study. All the study participants were prescribed with Sitagliptin (50mg) + Metformin (500mg) combination. The mean values of FBS & PPBS after initiating the treatment with Sitagliptin + Metformin combination at a regular time interval of every 4 weeks were compared and the outcomes of the treatment were interpreted. A total of 138 participants were enrolled in the study and among them 59 (42.8%) were found to be males and 79 (57.2%) were found to be females. The mean FBS value was observed to be 171.3 (±52.49) mg/dL before the treatment with Sitagliptin + Metformin combination whereas the FBS value after 12 weeks of treatment with Sitagliptin + Metformin combination was observed to be 107.6 (±27.85) mg/dL with a mean difference of 63.7 mg/dL which was observed to be statistically significant (p<0.0001). The mean

PPBS value was observed to be 281.4 (±78.79) mg/dl before the treatment with Sitagliptin + Metformin combination whereas the PPBS value after 12 weeks of treatment with Sitagliptin +Metformin combination was observed to be 159.1 (±44.72) mg/dl with a mean difference of 122.3 mg/dL which was observed to be statistically significant ($p<0.0001$). Sitagliptin +Metformin is a good combination of choice in the management of diabetes which shows a significant reduction in the values of both FBS and PPBS by maintaining a better glycemic control among the patients.

Keywords: Diabetes mellitus, Glycemic control, Metformin, Sitagliptin.

INTRODUCTION

Worldwide, diabetes is observed to be the major healthcare issue of concern and around 578 million people can be affected by the year 2030 globally [1]. In patients with diabetes mellitus, two to six times more deaths can be reported when compared to the general population associated with cardiovascular diseases and stroke [2]. Based on the UK Prospective Diabetes Study (UKPDS), 1% decrease of Hb1Ac can result in 37% reduction of the microvascular complications and 21% decrease of the diabetes related endpoints [3]. In type-2 diabetes mellitus, the altered functioning of the beta cells can result in relative insulin deficiency and insulin resistance which can be associated with the decreased glucose transport into the muscle or fat cells and the elevated hepatic glucose output, leading to hyperglycaemia [4]. Insulin sensitizer & insulin secretagogues are the oral antidiabetic drugs used to treat the endocrine defects of insulin resistance and altered functioning of the beta cells related to type 2 diabetes mellitus. Metformin can be given as monotherapy or with other oral antidiabetic drugs as a combinational therapy or along with insulin can effectively control the glycosylated haemoglobin (*HbA1c) levels up to 1-2% points as type 2 diabetes mellitus patients are most predominantly observed to be with increased hepatic glucose output. Metformin is considered as the first line agent for management of type 2 diabetes mellitus due to its tolerability against the GI related side effects. In type 2 diabetes mellitus patients while using the Metformin the contraindications like renal insufficiency, major adverse events like lactic acidosis can also be observed. Metformin can be considered as the main component which can be used in combination with any oral antidiabetics like sulfonylureas, glitazones, gliptins due to its metabolic process not affected by hepatic cytochrome enzymes [5-10]. When Sitagliptin is prescribed once daily, it enhances the incretin hormones for improving the blood glucose levels [11]. The drug Sitagliptin can be given as a combinational therapy along with Metformin in a fixed dose combination or separately, as these drugs are not having the major risk of drug interactions. The co-administration of the Sitagliptin/Metformin shows well tolerance [12-19]. Among the patients administering combinational therapy of Sitagliptin/Metformin and patients taking the metformin alone, the incidence of the gastrointestinal side effects such as nausea, emesis, diarrhoea and abdominal pain were almost the same [20-22]. For the effective management of the diabetes mellitus, life style modifications along with the pharmacological treatment are essential for the proper control of the blood glucose levels [23]. Prescribing the effective treatment regimens can improve the patient medication adherence and reduces the complexity of the treatment. Due to limited understanding of the health care professionals regarding the glycemic control related to antidiabetic drug combinations, there is a necessity to explore the alternative treatment for the management of the diabetes [24]. The monotherapy and the combinational therapy of oral anti-diabetics have given a newer perspective. Hence in this study, we made an attempt to explore the efficacy of Sitagliptin in combination with Metformin among the patients with type-2 diabetes mellitus.

MATERIALS AND METHODS

This was a prospective study conducted for a period of 6 months at Kify Hospital, Rajahmundry. Data was collected after getting the Ethical committee approval and also the approval from the above mentioned hospital there by strictly considering the inclusion and exclusion criteria of the study. Patients of both the genders of age between 25-

60 years, who were diagnosed with type-2 diabetes mellitus were included in the study and were prescribed with Sitagliptin (50mg) + Metformin (500mg) combination. Patients with renal function impairment and inconsistent with use of Sitagliptin + Metformin were excluded from the study. Fasting Blood Sugar (FBS) values and Post Prandial Blood Sugar (PPBS) values were taken into consideration for the interpretation of results. The mean values of FBS & PPBS before (V_0) and after initiating the treatment (V_1, V_2 & V_3) with Sitagliptin + Metformin combination at a regular time interval of every 4 weeks were compared and the outcomes of the treatment were interpreted [25].

Statistical Analysis

The data was interpreted by using the statistical software Graph Pad Prism-10. Mean & standard deviations were calculated and t test was performed to obtain the p-values at 95% confidence interval ($p \leq 0.05$). The statistically significant values were represented with an asterisk (*).

RESULTS AND DISCUSSION

A total of 138 participants were enrolled in the study and among them 59 (42.8%) were found to be males and 79 (57.2%) were found to be females. Table 1 represents the age wise categorization of the study participants. In this study, majority of the diabetic patients were in the age group 51-60 years (54.3%) followed by 41-50 years (31.2%). Table 2 represents the categorization of the study participants based on the disease duration. In this study, most of the diabetic patients were observed with the disease duration of 6-10 years (37.7%) followed by 1-5 years (25.3%). Table 3 represents categorization of the study participants based on the habit of smoking. About 35 (25.4%) were smokers and the remaining 103 (74.6%) were non-smokers. Table 4 represents the categorization of the study participants based on the habit of alcohol intake. About 34 (24.6%) were alcoholic and the remaining 104 (75.4%) were non-alcoholic. Table 5 represents the comparison of mean values of FBS & PPBS before and after the treatment with Sitagliptin + Metformin combination at a regular time interval of every 4 weeks. On day-1 (V_0) the mean value of FBS was observed to be 171.3 (±52.49), on the 4th week (V_1) the mean value of FBS was observed to be 135.9 (±45.38), on the 8th week (V_2) the mean value of FBS was observed to be 116.4 (±38.71), on the 12th (V_3) the mean value of FBS was observed to be 107.6(±27.85). The above mean values represent a gradual decrease in the FBS that shows a significant glycemic control among the study population. On day-1 (V_0) the mean value of PPBS was observed to be 281.4 (±78.79), on the 4th week (V_1), the mean value of PPBS was observed to be 222.9 (±66.50), on the 8th week (V_2), the mean value of PPBS was observed to be 190.2 (±61.56), on the 12th week (V_3), the mean value of PPBS was observed to be 159.1 (±44.72). The above mean values represent a gradual decrease in the PPBS that shows a significant glycemic control among the study population.

CONCLUSION

In this study, the mean FBS value was observed to be 171.3 (±52.49) mg/dL before the treatment with Sitagliptin + Metformin combination whereas the FBS value after 12 weeks of treatment with Sitagliptin + Metformin combination was observed to be 107.6 (±27.85) mg/dL with a mean difference of 63.7 mg/dL which was observed to be statistically significant ($p<0.0001$). The mean PPBS value was observed to be 281.4 (±78.79) mg/dL before the treatment with Sitagliptin + Metformin combination whereas the PPBS value after 12 weeks of treatment with Sitagliptin +Metformin combination was observed to be 159.1 (±44.72) mg/dL with a mean difference of 122.3 mg/dL which was observed to be statistically significant ($p<0.0001$). Hence, Sitagliptin + Metformin is a good combination of choice in the management of diabetes which shows a significant reduction in the values of both FBS and PPBS by maintaining a better glycemic control among the patients.

REFERENCES

1. Saeedi P *et al.* Global and regional diabetes prevalence estimates for 2019 and projections for 2030 and 2045: Results from the International Diabetes Federation Diabetes Atlas, 9Th edition. Diabetes Research and Clinical Practice; 157:107843.
2. Stratton IM, Adler AI, Neil HA, *et al*. Association of glycemia with macrovascular and microvascular complications of type 2 diabetes (UKPDS35): Prospective observational study. BMJ. 2000; 321:405-12.
3. DeFronzo RA. Banting Lecture. From the triumvirate to the ominous octet: a new paradigm for the treatment of type 2 diabetes mellitus. Diabetes. 2009; 58:773-95.
4. Scheen AJ, Lefebvre PJ. Oral antidiabetic agents: a guide to selection. Drugs. 1998; 55:225-36.
5. Scheen AJ. Current management of coexisting obesity and type 2 diabetes. Drugs. 2003; 63:1165-84.
6. Usha Vanya V. Drug Induced Diabetes. J Cli Pharm Res. 2021; 1(3): 57-60.
7. Setter SM, Iltz JL, Thams J, Campbell RK. Metformin hydrochloride in the treatment of type 2 diabetes mellitus: a clinical review with a focus on dual therapy. Clin Ther. 2003; 25:2991-3026.
8. Stumvoll M, Haring HU, Matthaei S. Metformin. Endocr Res. 2007; 32:39-57.
9. Consoli A, Gomis R, Halimi S, *et al*. Initiating oral glucose-lowering therapy with metformin in type 2 diabetic patients: an evidence-based strategy to reduce the burden of late-developing diabetes complications. Diabetes Metab. 2004; 30:509-16.
10. Nathan DM, Buse JB, Davidson MB, *et al*. Medical management of hyperglycaemia in type 2 diabetes: a consensus algorithm for the initiation and adjustment of therapy: a consensus statement from the American Diabetes Association and the European Association for the Study of Diabetes. Diabetologia. 2009; 52:17-30.
11. Gallwitz B. Sitagliptin with metformin: profile of a combination for the treatment of type 2 diabetes. Drugs Today (Barc). 2007;43:681-9.
12. Reynolds JK, Neumiller JJ, Campbell RK. Janumet: a combination product suitable for use in patients with Type 2 diabetes. Expert Opin Invest Drugs. 2008; 17: 1559-65.
13. Green J, Feinglos M. New combination treatments in the management of diabetes: focus on sitagliptin-metformin. Vasc Health Risk Manag. 2008;4: 743-51.
14. EMEA Janumet Assessment Report. Available from: www.ema.europa.eu/ humandocs/PDFs/EPAR/janumet/ H-861-en6.pdf.
15. Scheen AJ, Lefebvre PJ. Anti hyperglycaemic agents. Drug interactions of clinical importance. Drug Safety. 1995;12:32-45.
16. Scheen AJ. Clinical pharmacokinetics of metformin. Clin Pharmaco kinet. 1996; 30: 359-71.
17. Scheen AJ. Drug interactions of clinical importance with antihyperglycaemic agents: an update. Drug Safety. 2005; 28: 601-31.
18. Scheen AJ. Dipeptidylpeptidase-4 inhibitors (gliptins): focus on drug-drug interactions. Clin Pharmaco kinet. 2010; 49: 573-88.
19. Goldstein BJ, Feinglos MN, Lunceford JK, *et al*. Sitagliptin 036 Study Group. Effect of initial combination therapy with sitagliptin, a dipeptidyl peptidase-4 inhibitor and metformin on glycemic control in patients with type 2 diabetes. Diabetes Care. 2007; 30: 1979-87.
20. Williams-Herman D, Johnson J, Teng R, *et al*. Efficacy and safety of initial combination therapy with sitagliptin and metformin in patients with type 2 diabetes: a 54-week study. Curr Med Res Opin. 2009; 25: 569-83.
21. Williams-Herman D, Johnson J, Teng R, *et al*. Efficacy and safety of sitagliptin and metformin as initial combination therapy and as monotherapy over 2 years in patients with type 2 diabetes. Diabetes Obes Metab. 2010; 12:442-51.
22. Scott R, Loeys T, Davies MJ, Engel SS. Sitagliptin Study 801 Group. Efficacy and safety of sitagliptin when added to ongoing metformin therapy in patients with type 2 diabetes. Diabetes Obes Metab. 2008; 10(10): 959-69.
23. Nathan DM, Buse JB, Davidson MB *et al*. Management of hyperglycemia in type 2 diabetes: a consensus algorithm for the initiation and adjustment of therapy. Diabetes Care. 2006; 29:1963-72.

24. Chwieduk CM. Sitagliptin/metformin fixed-dose combination: in patients with type 2 diabetes mellitus. Drugs. 2011; 71(3):349-61.

Table.1: Age wise categorization of the study participants

Age (in years)	Male (%)	Female (%)	Total (%)
21-30	1 (1.7)	2 (2.5)	3 (2.2)
31-40	6 (10.1)	11(13.9)	17 (12.3)
41-50	16 (27.1)	27 (34.2)	43 (31.2)
51-60	36 (61.1)	39 (49.4)	75 (54.3)
Total	59 (100)	79 (100)	138 (100)

Table.2: Categorization of the study participants based on the disease duration

Disease Duration (in years)	Male (%)	Female (%)	Total (%)
<1	1 (1.7)	2 (2.5)	3 (2.2)
1-5	17 (28.8)	18 (22.8)	35 (25.3)
6-10	18 (30.5)	34 (43.0)	52 (37.7)
11-15	15 (25.4)	18 (22.8)	33 (23.9)
16-20	3 (5.1)	4 (5.1)	7 (5.1)
21-25	5 (8.5)	3 (3.8)	8 (5.8)
Total	59 (100)	79 (100)	138 (100)

Table.3: Categorization of the study participants based on the habit of smoking

Smoking habit	Male (%)	Female (%)	Total (%)
Smoker	34 (57.6)	1 (1.3)	35 (25.4)
Non-smoker	25 (42.4)	78 (98.7)	103 (74.6)
Total	59 (100)	79 (100)	138 (100)

Table.4: Categorization of the study participants based on the habit of alcohol intake

Alcoholism	Male (%)	Female (%)	Total (%)
Alcoholic	34 (57.6)	0 (0)	34 (24.6)
Non-alcoholic	25 (42.4)	79 (100)	104 (75.4)
Total	59 (100)	79 (100)	138 (100)

Table.5: Comparison of mean values of FBS & PPBS before and after the treatment with Sitagliptin + Metformin combination at a regular time interval of every 4 weeks

Lab values	V_0 (Day 1)	V_1 (4th week)	V_2 (8th week)	V_3 (12th week)
FBS (Mean ± SD)	171.3 (± 52.49)	135.9 (± 45.38)	116.4 (± 38.71)	107.6 (± 27.85)
PPBS (Mean ± SD)	281.4 (± 78.79)	222.9 (± 66.50)	190.2 (± 61.56)	159.1 (± 44.72)

Indian Journal of Natural Sciences *www.tnsroindia.org.in ©IJONS*

Vol.15 / Issue 88 / Feb / 2025 *International Bimonthly (Print) – Open Access* *ISSN: 0976 – 0997*

RESEARCH ARTICLE

Induced Chemical Mutagenesis on Sunnhemp (*Crotalaria juncea* L.) to Determine the Lethality, Germination and Seedling Survivability

S. Gunasree[1] and D. Dhanavel[2]*

[1]Ph.D Research Scholar, Department of Botany, Annamalai University, Annamalai Nagar, Chidambaram, Tamil Nadu India.
[2]Professor, Department of Botany, Annamalai University, Annamalai Nagar, Chidambaram, Tamil Nadu India.

Received: 21 Nov 2024 Revised: 03 Dec 2024 Accepted: 23 Jan 2025

***Address for Correspondence**
D. Dhanavel,
Professor,
Department of Botany,
Annamalai University,
Annamalai Nagar, Chidambaram, Tamil Nadu India.
E.Mail: ddhana2005@yahoo.ac.in

ABSTRACT

Sunnhemp, (*Crotalaria juncea* L.), is a member of the Fabaceae family and is used extensively in industry as a green manure, fibre crop, and fodder crop. The seed was exposed to Ethyl methane sulphonate (EMS), Diethyl sulphate (DES), and Sodium azide (SA) in this study. Ethyl methane sulphonate (EMS), Diethyl sulphate (DES), and Sodium azide (SA) at concentrations of 5 mM, 10 mM, 15 mM, 20 mM, 25 mM, 30 mM, 35 mM, 40 mM, 45 mM, and 50 mM were applied to the seeds. The untreated seeds were used as a control. In this investigation, increasing mutagen concentrations in M_1generation reduced seed germination, seedling survival, and lethal dosage LD_{50}. The seed germinated on the 15thday, and the seedlings survived until the 30th day. The LD_{50} value is based on 50% germination. The LD_{50} values were set at 35 mM for EMS, 30 mM for DES, and 25 mM for SA. The maximum seed germination value measured was 5 mM, while the minimum was 50 mM. So, it was discovered that mutagens at lower dosage caused less biological damage and may be useful for causing beneficial mutations in Sunnhemp.

Keywords: EMS, DES SA, LD_{50} value, Sunnhemp, Seed germination, Survivability.

INTRODUCTION

Sunnhemp (*Crotalaria juncea* L.) is a member of the Fabaceae family, which also goes by Indian hemp and Madras hemp. India leads the world in hemp fibre output, with hemp produced in practically every state (Rawat and Saini, 2022). This plant belongs to the Kingdom- Plantae; Family- Fabaceae; Genus- *Crotalaria;* Species- *C. juncea* L. It is

comMercially grown for its flexible, slightly lignified stem fibres (Tripathi,*et al.,* 2013) Found that these fibres are rich in cellulose, low in lignin, and have minimal ash content. *Crotalaria* is found throughout the world's tropical regions (Lewis *et al.,* 2005). It produces a large amount of biomass. This dense biomass can inhibit weeds and (Mansoer *et al.,* 1997) maintain soil moisture after termination. (Kumar and Dwivedi 2014) suggested that it has the potential to be a biofuel crop due to its high biomass production. *C. juncea* is a shrubby, herbaceous, subtropical annual legume that reaches 3-9 feet tall. The crop has a long tap root with strong lateral roots and a thick, ribbed, pubescent stem that develops from ½ in (Duke, 1983) to 2 in diameter (Treadwell and Alligood, 2008). The root nodules have lobed shapes (Abdul-Baki *et al.,* 2001). Nitrogen management is very difficult for farmers as it is a nutrient required by most crops and is imMediately reduced. Historically, rhizobium and other bacteria comMunicate with legumes to fix nitrogen in agricultural settings (Ravid, 2015). Green manure and cover crops enhance soil structure and organic matter levels (Marshall and Lynch, 2020; Sheng-nan *et al.,* 2018). *Crotalaria* juncea contains many secondary metabolites particularly leaves involve carbohydrates, steroids, triterpenes, phenols, flavonoids, alkaloids, amino acids, saponins, glycosides, tannins, and volatile oils (Dinakaran *et al.,* 2011; Malashetty *et al.,* 2004; Chouhan *et al.,* 2010). It leaves possessed these physicochemical properties (% w/w): total ash value 5.9%, acid insoluble ash 2.7%, water-soluble ash 3.9%, sulphated ash 5.1%, moisture content 11%, foreign matter 0.04%, alcohol soluble extract value 5.84%, water-soluble extract value 20.4% and crude fibre content 52.6% (Dinakaran, *et al.,* 2011; Jain *et al.,* 2014). Plant products from the *Crotalaria* genus, which includes *C. juncea,* have shown value due to their antibacterial capabilities (Al-Snafi *et al.,* 2016). The seeds have antioxidant and anti-inflamMatory properties. Flowers and seeds have been claimed to have antimicrobial properties. The leaves were reported with anti-diarrheal, antiarthritic, and anti-ulcerogenic properties (Chouhan *et al.,* 2011; Samuel and Kumar 2020). Crotalaria has been used to treat diabetes, skin infections, impetigo, psoriasis, snake bites, and stomach aches (Pullaiah and Chandrasukha, 2008; Verdhana, 2008). According to (MohamMed *et al.,* 2005), the mutation has been successfully used in the breeding of several food crop varieties, ornamentals. The seeds have antioxidant and anti-inflamMatory properties. Flowers and seeds have been claimed to have antimicrobial properties. The leaves were reported with anti-diarrheal, antiarthritic, and anti-ulcerogenic properties, port crops. One of the traditional ways of plant breeding is mutation breeding.

It is crucial to many different domains, including molecular biology, biotechnology, morphology, and cytogenetics. Developed enhanced cultivars of cereals, fruits, and other crops have been made possible by induced mutations, which are highly successful in improving natural genetic resources (Lee *et al.,* 2002). A powerful technique for increasing variety for crop development, mutagenesis has been applied extensively (Singh and Singh, 2001). Germination is the process of a seed starting to grow after being dormant. It necessitates seed imbibition, which is defined as the process that leads to the emergence of the radicle through the testa, a maternal tissue that surrounds the embryo (Bewley 1967; Koornneef, *et al.,* 2002). Once the radicle emerges, the germination process is completed. Seed imbibition leads to cell expansion, cell wall synthesis, and metabolic activation. Evidence found that cell division typically occurs after germination (de Castro *et al.,* 2000; Barroco *et al.,* 2005). Chemical mutagens cause mutations in living organisms. Mutagens have an impact on seed germination. Seed germination rates depend upon the type of mutagen and treatment dose. Chemical mutagens typically cause induced mutation, which leads to base pair substitution, particularly GC-AT, resulting in amino acid alterations that alter protein function but do not eliminate it. In comparison to normal plants, these chemo-mutagens cause a wide range of morphological and yield parameters (Khan *et al.,* 2009). It asserts that a variety of mutagens may damage plant chromosomes by generating radicals that are (Yuan *et al.,* 1993) produced from reactive oxygen. Hajara (1979) states that Ethyl methane sulphonate ($CH_3S0_3C_2H_5$) is a chemical compound that causes cancer and can cause random changes in genetic material by substituting nucleotides. Amino acid changes and mutations are comMonly caused by chemical mutagens (GC - AT). Diethyl sulfate ($(C_2H_5)_2SO_4$) is a potent alkylating agent with a single function study on its mutagenicity was tried in several organisms, including mice, Drosophila (Csillery *et al.,* 1985). Sodium azide (NaN_3) is a potent mutagen that reduces cyanide resistance and respiration in tobacco calluses (Wen and Liang, 1995). (Predieri,2001) recomMends determining the LD_{50} dose to establish the optimal mutation dose. Therefore, this study was undertaken in sunn hemp (*Crotalaria juncea* L.) to assess the chemical mutagens; Ethyl methane sulphonate (EMS), Diethyl sulphate (DES), and Sodium azide (SA) on seed germination, seedling survival and lethal dosage

LD_{50}. The LD_{50} value obtained from this investigation will be used to calculate the dosages of DES, SA, and EMS to induce genetic variation in the M_1 offspring.

MATERIALS AND METHODS

Plant material

Sunnhemp (*Crotalaria juncea* L.) seeds are dry and healthy and were purchased from the Tamil Nadu Agricultural Research Institute, Coimbatore. To induce mutagenesis, a chemical mutagen, Ethyl methane sulphonate, Diethyl sulfate and Sodium azide were utilized at various concentrations.

Mutagenic Treatment (Chemical mutagen)

Crotalaria juncea L seeds, which were healthy and completely pure, were treated with Ethyl Methane Sulphonate, Diethyl sulfate and Sodium azide. Treatments (50gm seeds for treatments) consist of ten different concentrations of EMS, DES and SA (5mM, 10 mM, 15 mM, 20mM, 25mM, 30mM, 35mM, 40mM, 45mM and 50mM. The EMS, DES and SA treated seeds were presoaked in distilled water for six hours at room temperature and covered by a moist germination paper. After that, the treated seeds were washed in a running tap water. The untreated seeds were respectively considered as a control. The seeds were sown in the field by following the Randomized Block Design (RBD) method along with control to raise M_1 generation. The germination percentage will be noted on the 15^{th} day and seedling survival on the 30^{th} day.

Seed germination and seedling survivability studies

The germination study was conducted on the 15^{th} after the lethal dosage (LD_{50}) to calculate the germination percentages of the control and treated plants. The seedling survival study was conducted on the 30^{th} day after sowing to calculate the seedling survivability percentage. The formula is given below:

$$\text{Seed germination \%} = \frac{\text{No. of seed germination}}{\text{No. of seeds sown}} \times 100$$

$$\text{Seedling survival \%} = \frac{\text{No. of seed survival}}{\text{No. of seed germination}} \times 100$$

RESULT AND DISCUSSION

Seed germination %

The cotyledons, plumule, and radicle appearances were used to assess the germination of seeds. When these structures are present, the last stage of seed germination has occurred (Bewley and Black 1985). Seed germination is the process by which an organism grows from a seed. The *Crotalaria juncea* L. experiment was conducted to find the LD_{50} value of seeds treated with EMS, DES, and SA. The prescribed concentration was applied to the seeds. The seed germination was significantly impacted by the EMS, DES, and SA. The mortality of a mutagens concentration is frequently calculated as a 50% reduction in the population. Under field conditions, the seed germination percentage of different mutagenesis treatments indicated that the germination percentage decreased with increasing concentrations of EMS, DES and SA. Seed germination percentages were as follows: lowest in higher concentrations of EMS (50 mM -27.00%), DES (50 mM -19.00%), and SA (50 mM -07.00%), and highest in lower concentrations of EMS (5 mM -93.00%), DES (5 mM -90.00%), and SA (5 mM -87.00%). The LD_{50} values were established at 35 mM for EMS, 30 mM for DES, and 25 mM for SA based on the percentage of seed germination on the 15^{th} day shown (Table 1-3, Graph 1-3). Except from the control plant, the highest germination rate was observed in the lowest concentration, as the lowest germination rate was observed in the highest concertation of EMS, DES and SA. Similarly, also reported in Little Millet (Ramkumar and Dhanavel, 2020), *Andrographis paniculata* (Kasthuri and Dhanavel, 2020), and Roselle (Priyanka and Dhanavel, 2020).

The effect of a mutagen on the meristematic tissues of the radicle or plumule may be the cause of the reduction in see d germination (Deepika *et al.,* 2016). The mutagenic induction caused damage that resulted in a reduction in germination rate. This explanation simplifies the acceptable result. The molecular permutation of cellular constituents may be caused by the treatment (Khan and Goyal, 2009). One of the biological consequences of mutagen treatment, particularly chemical mutagens, may involve changes in the synthesis of enzymes essential in the germination process. (Kulkarni, 2011). A similar impact on seed germination by the various carcinogenic treatments has been reported before in onion (Joshi *et al.,* 2011). Lower doses of physical and chemical mutagens were reported to have stronger mutagenic efficiency in *Vigna unguiculata*L. Walp (Sri Devi and Mullainathan, 2012), *Trigonella foenum graecum* L. (Thilagavathi and Mullainathan, 2011). In the germination and seedling growth test, EMS, DES, and sodium azide resulted in reduced and delayed germination compared to the control. Several studies have found concentration/dose-dependent reduction of seed germination in various crops. (Pavadai and Dhanavel, 2004) on soybean, (Singh and Kole, 2005) on mungbean, (Essel*et al.,* 2015) in cowpea and (Jabeen and Mirza, 2002) in *Capsicum annum*. (Barman *et al.,* 2015) Reported the same in Jamun.

Seedling Survival Percentage %

Seedling survival was determined 30 days after germination by counting the number of surviving plants in each treatment and calculating their percentage and showed as (Table 1-3, Graph 1-3). The maximum plant survival was recorded at 05 mM (92.47%) in EMS, 05 mM (96.88%) in DES and 05 mM (89.65%). The minimum plant survival was recorded at 50 mM (18.51%) in EMS, 50 mM (31.57%) in DES and 50 mM (28.57%) in SA when compared to control plants. Higher concentrations can reduce plant growth (Talebi *et al.,* 2012). Mutagenic treatments have been shown to reduce plant survival in *Dianthus* (Roychowdhury *et al.,* 2012), Horsegram (BolbhatSadashivet*et al.,* 2012), Ashwagandha (Bharathi *et al.,*2013), Pearl Millet (Ambi *et al.,*2015), Sesame (Ramdoss*et al.,* 2014) and Okra (Bagheryet *al.,* 2016). Plant survival is reduced due to cytological and physiological damage (Srivastava *et al.,* 2011). Suggested in previous research (Sarada *et al.,* 2015) that the mutagen's interference with the cell's various metabolic pathways may be the reason for the decreased seedling survival. As the concentration of EMS, DES, and SA treatment increased relative to control, there was a decrease in both seed germination and seedling survival. Similar results have been reported in different crops, Soybean (Pavadai and Dhanavel, 2004), cluster bean (Velu *et al.,*2007), cowpea (Girija and Dhanavel, 2009), and little millet (Ramkumar and Dhanavel, 2019).

CONCLUSION

In this study, seed germination and survivability were reduced by increasing the concentrations of EMS, DES, and SA from 5 mM to 50 mM. Compared to the control, all of the mutagenic treatment values were slightly lower. Finally, the (LD_{50}) values for EMS (35 mM), DES (30 mM), and SA (25 mM) were reported. The induced morphological mutation was discovered under stress conditions, therefore more generation and work research will proceed. This research will be beneficial in future breeding efforts.

ACKNOWLEDGEMENT

For the facilities to carry out the research, the author is grateful to the Annamalai University Department of Botany.

REFERENCES

1. Abdul-Baki, A. A., Bryan, H. H., Zinati, G. M., Klassen, W., Codallo, M., & Heckert, N. (2001). Biomass yield and flower production in sunn hemp: Effect of cutting the main stem. *Journal of Vegetable Crop Production*, *7*(1), 83-104.
2. Al-Snafi, A. E. (2016). The contents and pharmacology of *Crotalaria juncea*-A review. *IOSR Journal of Pharmacy*, *6*(6), 77-86.

3. Ambli, K. and Mullainathan, L. (2015). Induced Physical and Chemical studies in M_1 generation of Pearl Millet (*Pennisetum typhoides*) (Burn.) Stapf. Var. Co (Cu)-9. *International Journal of Recent Scientific Research.* 5: 1806-1809.
4. Baghery, M. A., Kazemitabar, S. K. and Kenari, R. E. (2016). Effect of EMS on germination and survival of Okra (*Abelmoschus esculentus* L.) *Biharean biologist*. 10: 33-36.
5. Barman, P., Rekha, A. and Pandey, A.K. (2015). Effect of pre-sowing treatments with chemical mutagens on seed germination and growth performance of jamun (*Syzygiumcumini*L.Skeels) under different potting substrates. Fruits, 70, 239-248.
6. Barroco, R.M., C. Van Po u c ke, J.H.W . Bergevoet, L. de Veylder, S.P.C. Groot, D. Inze, (2005). The role of the cell cycle machinery in resumption of postembryonic development. *Plant Physiol.*, 137: 127-140
7. Bewley, J. D., Black, M., Bewley, J. D., & Black, M. (1985). Dormancy and the control of germination. *Seeds: physiology of development and germination*, 175-235.
8. Bewley, J.D., (1967). Seed germination and dormancy. The Plant Cell., 9: 1055-1066.
9. Bharathi, T., Gnanamurthy, S. and Dhanavel, D. (2013). Induced Physical mutagenesis on seed germination, lethal dosage and morphological mutants of Ashwagandha (*Withaniasomnifera* (L.) Dunal). *International journal of Advanced Research*. 1:136-141.
10. Bolbhat Sadashiv, N., BhogeVikra, D.and Dhumal Kondiram, N. 2012. Effect of mutagens on seed germination, plant survival and quantitative characters of Horsegram (*Macrotyloma uniflorum* (Lam.) Verdc). *International journal of Life Science and Pharma Research*. 2 : 129-136.
11. Chouhan HS and Singh SK. (2010) Antibacterial activity of seed and flower parts of *Crotalaria juncea* Linn. *Am-Euras J Sci Res*, 5 (3): 212-215.
12. Chouhan HS, Sahu AN, Singh SK. (2011). Fatty acid composition, antioxidant, anti-inflamMatory and antibacterial activities of seed oil from *Crotalaria juncea* Linn. *J. Med. Plant. Res.* 5(6):984 91.
13. Csillery, G. (1985). Abnormal segregation ratio in a 'lutescens' hybrid Capsicum baccatum, Capsicum Eggplant Nswl. 4 ,43.
14. de Castro, R.D., A.A.M. Van LamMeren, S.P.C. Groot, R.J. Bino, H.W .M. Hilhorst, (2000). Cell div is io n and subsequent radical protrusion in tomato seeds are inhibited by osmotic stress but DNA synthesis and formation of microtubular cytoskeleton are not. *Plant Physiol*., 122: 327-336.
15. Deepika Minakshi pal, Pahuja SK. (2016). Morphological variations induced by Ethyl Methane Sulphonate in Cluster bean (*Cyamopsis tetragonoloba* (L.) Taub.). *Forage Res*, 41:218-221.
16. Devi, A. S., & Mullainathan, L. (2012). Effect of gamMa rays and ethyl methane sulphonate (EMS) in M3 generation of blackgram (*Vigna mungo* L. Hepper). *African Journal of Biotechnology*, *11*(15), 3548-3552.
17. Dinakaran SK, Banji D, Godala P and Harani A. (2011) Pharmacognostical evaluation study on *Crotalaria juncea* Linn. *American-Eurasian Journal of Scientific Research*, 6 (3): 139-145.
18. Duke, J.A. (1983). Handbook of energy crops NewCROP (New Crops Resource Online Program), Purdue Univ. Center for New Crops and Plant Products. http://www.hort.purdue.edu/newcrop/duke_energy/*Crotalaria_juncea*.html (accessed 28 July 2012).
19. Essel, E., Asante, I.K. and Laing, E. (2015). Effect of Colchicine treatment on seed germination, plant growth and yield traits of cowpea (*Vigna unguiculata* (L.) Walp. Canadian. *J. Pure. Appl. Sci.,* 9, 3573–3576.
20. Girija, M and. Dhanavel, D (2009), Mutagenic Effectiveness and Efficiency of gamMa rays, ethyl methane sulphonate and their combined treatment in cowpea (*Vigna unguiculata* L. Walp), *Glo. J. Mol. Sci*, 4(2) 68-75.
21. Hajara N.G. (1979). Induced of mutations by chemical mutagens in tall indica rice. I*ndian Agric.,* 23: 67-72.
22. Jabeen, N. and Mirza, B. (2002). Ethyl methane sulfonate enhances genetic variability in *Capsicum annuum*. *Asian. J. Plant Sci.,* 1, 425–428.
23. Jain M and Jain V. (2014). Pharmacognostical, phytochemical and pharmacological review on *Crotalaria juncea. Ph Tech Med*, 3(2): 469-475.
24. Joshi, N., Ravindran, A. and Mahajan, V. 2011. Investigation on Chemical Mutagen Sensitivity in Onion (*Allium cepa* L.). *International Journal of Botany*. 7: 243-248.
25. Kasthuri, S., & Dhanavel, D. (2020). Determination of LD_{50}, seed germination, morphological mutants for induced mutagenesis through gamMa radiation *Andrographis paniculata* (Burm. f.) Nees. *Plant Archives;* 20(1): 2233-2237.

26. Khan S, Goyal S. (2009). Improvement of mungbean varieties through induced mutations. *Afr. J Plant Sci*.; 3:174-180.
27. Koornneef, M., L. Bentsink, H. Hilhorst, (2002). Seed dormancy and germination. *Current Opinion and Plant Biol*., 5(1): 33-36.
28. Kulkarni, G. B. (2011). Effect of mutagen on pollen fertility and other parameters in horsegram (*Macrotyloma uniflorum* (Lam.) Verdc). *Bio. Sci. discovery*. 2: 146-150.
29. Kumar G and Dwivedi Saumil. (2014). Impact of gamMa irradiationon growth response of *Crotalaria juncea*. *International Journal of Agricultural and Crop Sciences*7(11): 870–5.
30. Lee Y. I., I.S. Lee, Y.P. Lim (2002). Variation in sweet potato regenerates from gamMa-rays irradiated embryogenic callus. *J Plant Biotech* 4, 163-170.
31. Lewis, G., Schrire B., Mackinder B. and Lock, M. (2005). Legumes of the world. Kew: Royal Botanical Gardens, *International Journal of Scientific and Research Publication,* 8 (6), 577p.
32. Malashetty VB, SangamMa I, Sharanabasappa A and Patil SB. (2004) Effect of *Crotalaria juncea* seed extracts on the estrous cycle and ovarian activity in albino mice. *Oriental Pharmacy and Experimental Medicine,* 4(2): 77-81.
33. Malashetty VB, Sharanabasappa A and Patil, SB. (2004) Post-coital antiimplantation and pregnancy interruption potency of the seeds of *Crotalaria juncea* Linn. *Oriental Pharmacy and Experimental Medicine*, 4(2): 70-76.
34. Mansoer, Z., Reeves, D. W., & Wood, C. W. (1997). Suitability of sunn hemp as an alternative late-summer legume cover crop. *Soil Science Society of America Journal*, *61*(1), 246-253.
35. Marshall, C. B., & Lynch, D. H. (2020). Soil microbial and macrofauna dynamics under different green manure termination methods. *Applied Soil Ecology*, 148, 103505.
36. Mohamad O., Herman, S., Nazir, B.M., Shamsudin, S., Takim, M. (2005). A dosimetry study using gamMa irradiation on two accessions, PHR and PHI, in mutation breeding of roselle. (*Hibiscus sabdariffa* L.). In: 7th MSAB Symposium on Applied Biology, 3-4 June, Sri Kembangan, 1-10.
37. Pavadai, P., Girija, M., and Dhanavel, D. (2010). Effect of gamMa rays on some yield parameters and protein content of soybean in M2, M3 and M4 generation. *Journal of Experimental Sciences*, *1*(6).
38. Predieri, S. (2001). Mutation induction and tissue culture in improving fruits.plant cell, tissue and organ culture, 64, 185-210.
39. Priyanka, D., and Dhanavel, D. (2020). Effect of gamMa irradiation on seed germination, seedling survival and lethal dosage LD_{50} of *Hibiscus sabdariffa* L. *Hereditas*, *33*, 1-100.
40. Pullaiah, T.C. and Chandrasukha, N.K. (2008). Antidiabetic plants in India and herbal based research. New Delhi: Regency publication, 8(6), 125p.
41. Ramadoss, B. R., Ganesamurthy, K. and Angappan, K. (2014). Evaluation of Effect of GamMa rays on Sesame Genotype TTVS 51 and TTVS 19 in M_1 Generation. *International Journal of Development Research*. 4: 273-277.
42. Ramkumar, R., and Dhanavel, D. (2019). Effect of Ethyl Methane Sulphonate (EMS) on Germination Behaviour and Seedling Survival of *Panicum sumatrense* Roth Ex Roemers & Schultz. *J.Guj. Res. Soc*, *21*(15), 160-164.
43. Ramkumar, R., and Dhanavel, D. (2020). Studies on effect of induced Physical mutagenesis on seed germination, seedling survival and lethal dosage of little millet (*Panicum sumatrense*roth ex romer&schults). *International journal of Botany studies*, *5*(2), 152-156.
44. Ravid, M. (2015). Can the use of composts and other organic amendments in horticulture help to mitigate climate change. In II International Symposium on Organic Matter Management and Compost Use in Horticulture 1076 (19- 28).
45. Rawat, R., & Saini, C. S. (2023). Modification of sunnhemp (*Crotalaria juncea*) protein isolate by high intensity ultrasound: Impact on the molecular structure, amino acid composition and nutritional profiling. *Food Bioscience*, *56*, 103100.
46. Roychowdhury, R., Ferdousul Alam, M. J., Bishnu, S.,Dalal, T. and Tah, J. (2012). Comparative study for effects of Chemical Mutagenesis on Seed Germination, Survivability and Pollen Sterility in M1 and M2 generations of Dianthus. *Plant Breeding and Seed Science*. 65:29-38.
47. Samuel PK, Kumar RS. (2020). Antioxidant, antimicrobial, haemolytic, germination and growth promoting properties of *Crotalaria juncea* L. *Plant Sci Today*.7(2):201-5.

48. Sarada C, Jyothi KUV, Rao S, Reddy PV. (2015), Mutagenic sensitivity of gamMa rays, EMS and their combinations on germination and seedling vigour in coriander (*Coriandrum sativum* L). International Journal of Advances in Pharmacy, Biology and Chemistry, 4(2):430-438.
49. Sheng-nan, C. H. E. N., Jun-ming, H. U., Xian-li, X. U., Xiang-hua, W. E. I., & Tie-guang, H. E. (2018). Effect of Smash Ridging Conservation Tillage with Green Manure on Rice Field Soil Infiltration and Its Delayed Action. Chinese Journal of Agrometeorology, 39(12), 778.
50. Singh M., Singh V.P. (2001). Genetic analysis of certain mutant lines of urdbean for yield and quality traits in M4 generation. *Ind. J. Pulses Res.* 14(1): 60-62.
51. Singh, R., and Kole, C. R. (2005). Effect of mutagenic treatments with EMS on germination and some seedling parameters in mungbean. *Crop Res.*, 30(2): 236-240.
52. Srivastava P, Marker S, Pandey P, Tiwari DK. (2011), Mutagenic effects of sodium azide on the growth and yield characteristics in wheat (*Triticum aestivum* L. em. Thell.). *Asian Journal of Plant Science,* 10:190- 201.
53. Talebi, A. B., Talebi, A. B., & Shahrokhifar, B. (2012). Ethyl methane sulphonate (EMS) induced mutagenesis in Malaysian rice (cv. MR219) for lethal dose determination.
54. Thilagavathi, C., & Mullainathan, L. (2011). Influence of physical and chemical mutagens on quantitative characters of *Vigna mungo* (L. Hepper). *International Multidisciplinary Research Journal*, *1*(1), 6-8.
55. Treadwell, D. D., and M. Alligood. (2008). Sunn hemp (*Crotalaria juncea* L.): a sumMer cover crop for Florida vegetable producers. Publication #HS1126. Univ. of Florida IFAS Extension. http://edis.ifas.ufl.edu/hs376 (accessed 26 July 2012).
56. Tripathi, M. K., Chaudhary, B., Sarkar, S. K., Singh, S. R., Bhandari, H. R., & Mahapatra, B. S. (2013). Performance of sunnhemp (*Crotalaria juncea* L.) as a sumMer season (pre-monsoon) crop for fiber. *Journal of Agricultural Science*, *5*(3), 236.
57. Vardhana, R. (2008). Direct uses of medicinal plants and their identification. New Delhi: Sarup and Sons publication 8(6).
58. Velu, L.Mullainathan, D.Arulbalachandran, D.Dhanavel and R.Poonguzhali, (2007), Effectiveness and Efficiency of gamMa rays and EMS on cluster bean [*Cyamopsistetragonoloba* (L.) Taub.], Crop Res., 34(1-3) 249-251.
59. Wen, J.G. and Liang, H.G. (1995). Effect of KCN and NaN_3 pretreatment on the cyanide resistant respiration in tobacco callus. *Acta Bot. Sin.*, 37:711-717.
60. Yuan, H.Y and Zhang, Z. (1993). Effect of Free Radicals and Temperature on Sister Chromatid Exchanges in *Hordeum vulgare* L. *Acta Botanica Sinica*, 35: 20-26.

Table 1: Determination of seed germination, seedling survival and LD_{50} values for Ethyl Methane Sulphonate (EMS) in *Crotalaria juncea* L.

Mutagens	Treatment concertation (mM)	Seed germination percentage %	Seedling survival (%)	Per cent over control	Per cent of reduction over the control
EMS	Control	98	98.97	100.00	--
	05mM	93	91.83	92.78	7.21
	10mM	89	90.81	91.75	8.24
	15mM	82	81.63	82.47	17.52
	20mM	74	74.48	75.25	24.74
	25mM	69	67.34	68.04	31.95
	30mM	62	62.24	62.88	37.11
	35mM	55	53.06	53.61	46.38
	40mM	42	40.81	41.23	58.76
	45mM	38	35.7	36.07	63.92
	50mM	27	25.51	25.77	15.77

Table 2: Determination of seed germination, seedling survival and LD_{50} values for Diethyl sulphate (DES) in *Crotalaria juncea* L.

Mutagens	Treatment concertation (mM)	Seed germination percentage %	Seedling survival (%)	Per cent over control	Per cent over reduction control
DES	Control	96	98.95	100.00	--
	05mM	94	95.83	96.84	3.15
	10mM	90	92.70	93.68	6.31
	15mM	89	90.62	91.58	8.41
	20mM	73	73.95	74.73	25.26
	25mM	67	67.70	68.41	31.58
	30mM	56	56.25	56.84	43.15
	35mM	47	46.87	47.36	52.63
	40mM	39	38.54	38.94	61.05
	45mM	27	26.04	26.31	73.68
	50mM	19	17.70	17.88	82.11

Table 3: Determination of seed germination, seedling survival and LD_{50} values for Sodium Aizde (SA) in *Crotalaria juncea* L.

Mutagens	Treatment concertation (mM)	Seed germination percentage %	Seedling survival (%)	Per cent over control	Per cent over reduction control
SA	Control	97	98.96	100.00	-
	05mM	87	88.65	88.65	10.13
	10mM	73	72.16	72.91	27.08
	15mM	68	68.04	68.75	31.24
	20mM	61	61.85	62.50	37.50
	25mM	57	56.70	57.29	42.70
	30mM	48	47.42	47.91	52.08
	35mM	33	32.98	33.32	66.67
	40mM	27	25.77	26.04	73.95
	45mM	19	15.46	15.62	84.37
	50mM	07	05.15	05.20	94.79

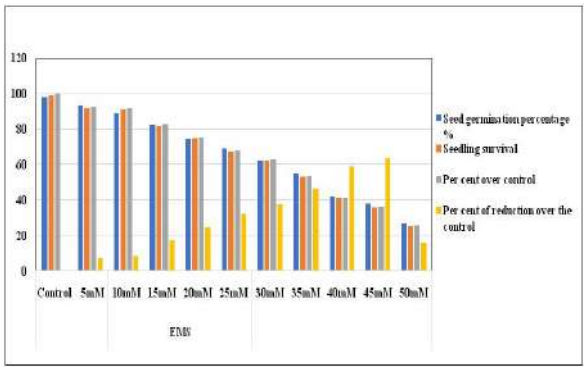

Graph 1: Determination of seed germination, seedling survival and LD_{50} values for Ethyl Methane Sulphonate (EMS) in *Crotalaria juncea* L.

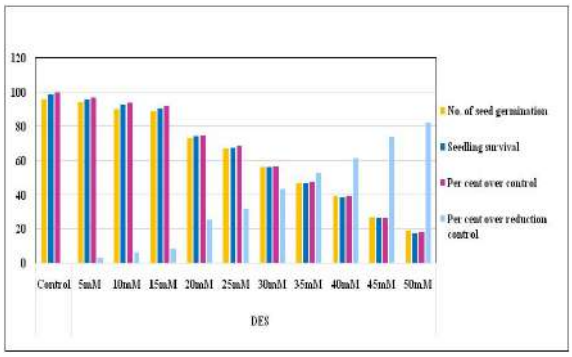

Graph 2: Determination of seed germination, seedling survival and LD_{50} values for Diethyl sulphate (DES) in *Crotalaria juncea* L.

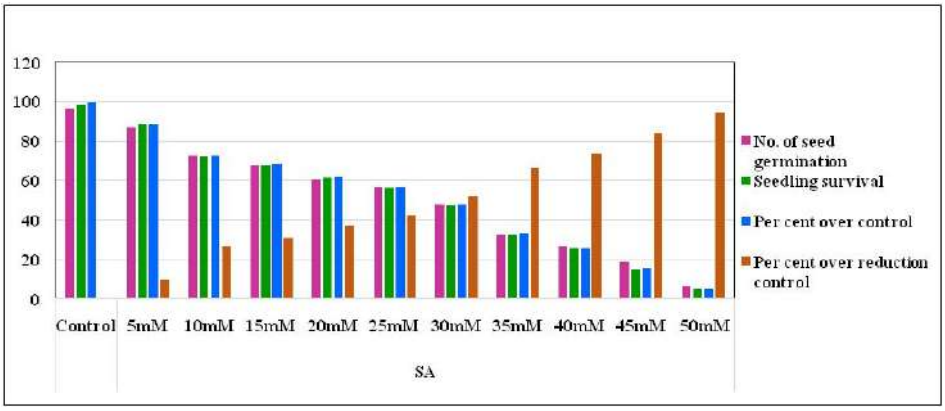

Graph 3: Determination of seed germination, seedling survival and LD_{50} values for Sodium Aizde (SA) in *Crotalaria juncea* L.

Indian Journal of Natural Sciences www.tnsroindia.org.in ©IJONS

Vol.15 / Issue 88 / Feb / 2025 *International Bimonthly (Print) – Open Access* *ISSN: 0976 – 0997*

RESEARCH ARTICLE

Biochemical and Microbiological Assessments for Nutritional Profile of Aquafeeds under Storage Conditions : Natural Antioxidants and Biotherapeutic Augmentation Strategy

Parul Puri*

Assistant Professor, Department of Zoology, Maitreyi College, University of Delhi, Delhi, India.

Received: 21 Nov 2024 Revised: 03 Dec 2024 Accepted: 13 Jan 2025

***Address for Correspondence**
Parul Puri,
Assistant Professor,
Department of Zoology,
Maitreyi College, University of Delhi, Delhi, India.
E.Mail: parul_acemail11@rediff.com

ABSTRACT

Fish are valuable source of proteins, omega-3 essential fatty acids, micro, macro minerals; amino acids and vitamins; thus, play quintessential role towards global nutrimental supply as well as human health. Aquaculture productions are largely dependent on availability of quality aqua feeds that govern fish nutrition. Feed safety is a prerequisite for fish welfare and health as well as associated consumer benefit. Judicious feed handling, storage and management practices are vital for fulfilling aquaculture dietary requirements; as both distribution and quality feed, are determinant of nutritious produce. Storage help administer timely feed requirements in aquaculture. Effects of temperature and humidity variables on stored feed rations require timely assessments as a measure for assurance of feed quality. Natural antioxidants can deter incidences of feed spoilage, improving feed quality and shelf life. Additionally, supplementation of probiotic microbials, prebiotics and their synergic mixture in 'synbiotics', as new generation 'aquaculture biotherapeutics' can combat direct and indirect microbial damages inflicted on quality of stored aqua feeds.

Keywords: nutrition quality, mycotoxin, probiotics, synbiotics, antioxidants, storage aqua feed

INTRODUCTION

Improved nutrition, food security and sustainable food productions are few important millennial sustainable development goals, adopted as 2030 agenda by United Nations. Food the "elixir of life" is "central dogma" of sustenance and health. The exemplary "we are what we eat" can appropriately be extended as, we get to eat what we feed. Feed *per se* animal feed is the food developed for fish, poultry and livestock. Careful selection of feed ingredients in feed formulations is imperative to fulfill nutrition requirements of farmed animals and to improve

outgain of end products for human health. Fish is relatively cost effective, easily available mineral enriched food source; that provision 20% intake of animal protein to over 3 billion world population [1].World over, dietary need of quality protein and essential nutrients for human consumption are met from fish diet [2].Aquaculture has significantly contributed to global food fish demand with 52% share of total fish produce [2].Nutrition requirements in fed aquaculture can be sub served through quality aqua feeds as compounded diets, contributing growth and health of aquaculture species [3].Formulation of aqua feeds for aquaculture development world over, is of great importance to fulfill dietary requirements of proteins, essential fatty acids (FA), minerals, amino acids (AA) and vitamins in human diet; that itself is dependent largely on availability of quality feed ingredients[4].While employing choice of ingredients for aqua feeds; quality of feed and feedstuffs; storage, as well as storage handlings are essential considerations [5].Feed quality and feedstuff attributes determine, the acceptability; palatability; as well as digestibility of feed to fish. Feed storage is imperative to overcome scarcities of feed supply, produce; maintaining continuous resource of ration to meet timely demands of aquaculture. Low-quality fish feeds result in poor uptake, stunted growth, increased feed conversion ratio (FCR) and decreased fish survival. This decreases efficiency of aquaculture production, enhancing overall cost of fish production owing to stunted fish growth, reduced produce weight, increase of feed input and therapeutic costs [6].Biochemical assessments of lipids, proteins, FA, AA and elements are auxiliary measures to precisely assess overall wellbeing and underlying health condition of fish and feed. Biochemical and microbiological evaluations are significant indicators of feed and feedstuff quality during storage utilizations. Appropriate storage and timely feed utilization can help prevent induction of food linked hazards in the food chain[7],safeguarding overall fish health and consequent consumer welfare.

Storage loss of quality : Storage strategies and management practices

Storage loss of quality-Effect of storage variables on feed quality

Nutritional quality of feed ingredients and fish feeds are significantly influenced by storage conditions such as temperature, humidity and post-handling procedures. Aquafeeds are prone to accelerated deterioration if not stored and handled properly. Storage conditions, essentially temperature and humidity are important variables affecting biochemical profile for lipid, FA, protein, AA, carbohydrate content, vitamin composition as well as microbiological quality of feeds. Storage loss of lipids, proteins and moisture are most evident biochemical changes in feed. Moisture changes affects dry matter content of feeds affecting available nutrients from diet. Changes in ash, fiber content is also indicative of feed nutritional quality changes. Total ash percentage provides extent of mineral content of the feed [8], also high ash content is indicative of adulteration or presence of impurities.

Oxidative loss of proteins and lipids

Feed storage at elevated temperatures can increase oxidative and hydrolytic rancidity leading to off-flavors and malodors resulting from lipid oxidation, with consequent loss in feed quality. Hydroperoxides are primary products of lipid oxidation that on auto oxidation form secondary products as lipidic free radicals[9].These reactions are supported at higher temperatures above 30^{o}C[10].Dietary proteins undergo oxidative loss with reactive-oxygen free-radical release phenomena, similar in fashion to lipidic oxidation. These losses are more pronounced at high temperature storages compared to ambient and low temperatures [11].Auto oxidation of lipids, proteins in feed, can decrease their digestibility and biological availability [12],as well deplete shelf life and abundance of vitamins as natural antioxidants in feed ingredients depleting feed quality [13].

Storage effects on vitamins

Vitamin depletion in feeds is accentuated by high temperature, humidity, photosensitization, high pH, presence of elements such as iron, copper and lipid oxidation polymerization reaction. Vitamin loss owing to high temperature and oxidation during processing and storage of feed is thoroughly examined in work by [14].Among the vitamins, C and E (α-tocopherol) are readily oxidized by generation of nascent oxygen. Vitamin B2 is highly sensitive to photosensitization. Elevated temperatures decrease B2 content, with up to 50% extrusion losses on storage [15]. Kubitza and Cyrino (1998)[16] described higher B2 loss owing to heat, compared with B1 (thiamine). Extrusion and pelletization cause rapid loss of vit C due to moisture and heat effects during feed processing [17].Storage loss of Vit C due to oxidation and non-oxidative mechanisms in aqua feeds are reported by [18].Vitamin C can prevent lipid

oxidation in feeds consisting high amounts of polyunsaturated fats (PUFA).Vit A, E and C can react with oxidative free radical species hence are predisposed to intense oxidative jeopardies in storage diets[13].

Storage and elemental changes

Elements function in structure, physiology, regulatory and biocatalytic mechanisms. Elements undergo both negative (=antagonistic) and positive (=co-operative) interactions affecting their biological availability from diets. Storage effects on availability of minerals (=inorganic elements) from diet to fish is dependenton concurrent interactions among dietary constituents [19].Elemental interactions involve relationships with lipids, proteins, vitamins and other dietary minerals[20],[21].Calcium absorption from diet is enhanced by vit D; excessive calcium inhibits phosphorous bioavailability; selenium-it E synergise for antioxidative effects in diets. Antinutritional factors such as phytate in plant-based dietary ingredients, excessive dietary lipids and fibre, hamper calcium availabilities[22, 23]. Dietary availability of minerals is dependent on its physiochemical state of occurrence in feed, nature of feed ingredients and more importantly feed composition[24].

Microbial load and Mycotoxin incidences

Improper storage temperatures and humidity may support pathogenic growth and survival in the feed with impact on their nutrient profiles; or even favor production of harmful fungal toxins mycotoxins such as aflatoxins, patulins, trichotecens, Ochratoxin A (OTA); these have potential teratogenic, carcinogenic, hepatotoxic, mutagenic and immuno-suppressive effects detrimental to fish and human health [25,26,27]. Toxins can pose risk of bioaccumulation in farmed species and thereby to human health and safety. Among recognized toxigenic fungi most genera belong to *Aspergillus, Fusarium, Penicillium, Cladosporium* and *Alternaria* spp., with ability to produce potential mycotoxins such as aflatoxins, zearalenone (ZEN), T-2 toxin, DON, ochratoxin A, fumonisins and patulin; based on fungal prevalence [26,28]. Of 18 different known aflatoxins; AFB1, B2, G1and G2 are of notable importance with AFB1 being prevalently toxic [6]. Aflatoxin is reported to be most toxic natural contaminant in compounded diets. Several works have revealed retention of fungal toxins such as aflatoxin AFB1 residues in tissues of aquatic organisms, indicating likely consumer health risks [29, 30]. Aflatoxins can cause disease incidence in fish by imposing nutritional deficit upon destroying essential nutrients in the diet, that include fat and water soluble antioxidants, vitamin A, C and thiamine. Aflatoxins depress the immune system of fish making it susceptible to pathogenic incidences. Samuel and Odunigba [31]reported loss of carbohydrate, protein, fibre and ash content with increment in moisture and lipid content of stored diets due to fungal incidences during feed storage.

Storage strategies and management practices

Produced feeds are stored under different storage conditions by distributors as well as farmers with less consideration to their impact on the nutrient profiles of the feeds [25]. Aquaculture feeds are prone to accelerated deterioration if not stored and managed properly. Feed composition, nature of raw materials used, processing technique, storage and management practices evidently impact the overall feed quality. While feed composition as well as processing technique involved is the prerogative of manufacturer; storage and management involve the responsibility of farmers and proper feed storage conditions [32].

Assessment of biochemical changes

Important biochemical measurements include proximate composition for estimation of feed moisture, crude lipid (CL) and protein (CP), ash, carbohydrates and dry matter (DM), amino acid (AA), fattyacid (FA), vitamin and element profiles [11, 33]. Various works evaluating effects of storage conditions such as temperature, storage duration and humidity variables on biochemical parameter changes have been reported. Table 1, lists storage studies based on evaluation of nutrition profile and quality of fish feeds and feedstuffs.[11]compared effects of low and ambient temperature storages on proximate composition and physical characteristics of feeds. Deterioration of nutrient quality of feed is reportedly high at higher temperature, compared to cold condition storages, suggesting better restoration of feed nutrients at low temperatures. [34], investigated farm made feed as well as feed ingredients stored under airtight and open-air conditions over four months for proximate composition crude ash, CP, CL, DM and moisture. Notable trend in reduction of CP, CL, fibre, and DM of the feedstuffs was observed; while for feeds,

decrease in CP,CL was non-concomitant to increased ash and fibre levels from second to fourth month of storage. The study emphasises on the need to utilise farm-made feeds within less than two months post their storage. Nutrient profile of commercial feeds stored under open-air and airtight conditions were evaluated for six months by [10]. Magnitude of oxidative changes in feeds, peroxide value and free FA levels increased in all diet groups over the time of storage. Compared to airtight conditions feed stored under open-air was more prone to physical deterioration indicated by unacceptable changes in texture, odour, colour, insect as well as mold growth within third month of storage. Variability in feed response to storage parameters was seen among different commercial feeds, indicating role of packaging and feedstuff composition on individual feed behaviours during storage. Solomon *et al. [*10] investigated effect of feed storage on growth performance of African catfish, *C. gariepinus*. It was observed that sealed condition storage of feeds supported better fish growth as compared to open air storage for most feeds. While in case of locally produced fish feed severe mortality of fed fish was observed irrespective of feed storage conditions indicating poor feed acceptability of ingredients used for feed manufacture. Oxidative status of lipids can be monitored by peroxide value (POV), anisidine value, total amount of oxidation (to-tox value), polyene index (PI), thio-barbituric acid reactive substances (TBA-Rs)[35,36].To-tox value up to 26 [37] and POV <10 mg per kg diet is considered good for fish oils [25]. Variable storage temperatures (-1.1^{o} to -15^{o}, 10^{o}, 20.8^{o} C) were explored to study [38]their impact on growth accrual and feed utilization by trout (*O. mykiss*). Although, no significant change in rate of specific growth and FCR was reported for trout.

Microbiological Evaluation

Microbiological evaluation of aqua feeds provides qualitative and quantitative assessment of the microbial load present in feeds. These include total plate count (TPC), coliforms, total viable bacterial count (TVBC), yeast and fungal mould counts. Microbiological quality of fish feeds has been evaluated in many works (refer table 2). Zmysłowska and Lewandowska [27] emphasised on requirement of microbiological analysis in accordance to standards for classifying fish feeds suitable for use. Ebeneezar *et al.* [42] analysed, microbial parameters including total plate and fungal counts of commercial aqua feeds. The results indicated contamination of feeds with micro-organisms, demanding compliance of manufactured feeds with the quality regulations set in accordance to Bureau of Indian Standards. Pietsch *et al.[*26], reported that feeds stored under unsuitable conditions(suboptimal temperature and humidity) for shorter durations are equally prone to deterioration in quality. This indicates impact of humidity and temperature conditions even over short duration storage, on feed characteristics. Mwihia *et al.* [48] evaluated adverse effects of aflatoxin contaminated feed on fish physiology and health. Contaminated feeds caused aflatoxin-induced liver enlargement, abdominal swelling, lower growth rates and high mortality incidences in fish. Fourteen different mycotoxins with high prevalence of deoxynivalenol DON (92.9%),aflatoxins (64.3%) were reported from local feeds and feed ingredients in comparison to imported commercial feeds [49].The study highlighted that simultaneous occurrence of mycotoxins in aqua feeds and feed material implicates synergistic and augmented hazard upon fish physiology and consequently, incidental consumer health.

Mitigation of Storage changes

Natural Antioxidants

Effect of activated oxidants; reactive oxygen entities (ROEs) from redoxactive species; lipidic groups; elements (such as Fe, Cu);enzyme systems; on polyunsaturated fats (PUFA) in diets generate oxidative lipidic rancidity leading to malodours and off flavours, deteriorating nutritive value of fats and quality attributes of feed during storage[13]. Synthetically-derived antioxidants in foods, such as butyl-hydroxytoluene (BHT) and ethoxyquin (EQ) have respectively been used for fish oil and meal although, works demonstrating their residual effects on suppressive health consequences have also been reported [50, 51].This has shifted focus towards use of natural antioxidant source in diets including microalgae, duckweeds and bioactive extracts of *Aspergillus.* Fermented bioactive enzymes (FB, extracted from *A.ibericus*) supplemented fish feeds illustrated lowering of lipid oxidation rates up to 19.5 percent at low(4^{o} C)and ambient temperature storages [52].Hernandez *et al.* [53] reported better antioxidant potential of rosemary extract compared to BHT and thyme oil on 24 weeks stored extruded feeds at ambient conditions of 20-28^{o}C. Similar effects of rosemary extracts along with combination of vitamin C as natural oxidants in marine ingredient based feed were observed by Hamre *et al.*[54].Mohamed *et al.*[57]tested effectiveness of clove oil as a

strategy to combat growth of aflatoxigenic strain. Dose-dependent increase, in formation of fungal inhibition zone, indicated promising fungal control of toxicogenic strains using clove oil. Yeast cell wall extract was used as a mycotoxin mitigation strategy [58],decreasing AFB1 residues in aflatoxin contaminated diet with restoration of immune response; counteracting liver damage, intestinal microbiota disruption in turbot. Dietary inclusion of commercial garlic extract and *Nigella sativa*(black cumin) was explored[59].In comparison to Fero Bind Pro (commercial mycotoxin binder) combination of 30 g *N. sativa* and 0.1 g commercial garlic extract was effective in detoxification of Ochratoxin A effects in Nile tilapia (*Oreochromis niloticus*) diets.

Functional storage-feed augmentation and mycotoxin mitigation

Bioaugmentation of feed with natural therapeutics such as probiotic (beneficial microbials), prebiotics and their mixture (=synbiotics) have founded numerous prospects for aquaculture improvements. Functional feeds based on probiotics and prebiotics, as a combination‘ synbiotics’; aim at establishing the modalities of microbial dynamics to maximize fish fitness. In an aquaculture scenario, probiotic feed supplementation is considered to confer immunoprophylactic control to disease incidence and improving gut-microbial ecology contributing to the overall health status of fish [60].Figure 2, discusses probiotic effects in augmentation of aqua feed quality during storage and concomitant fish health. Synbiotic (as synergic probiotic and prebiotic combination) addition to *O. niloticus* feed effectively enhanced anti-oxidative enzymes superoxide dismutases (SOD), catalase (CAT), and glutathione peroxidase (GPX) during a 60-day trial experiment[61].These enzymes are compromised on increase in oxidative cellularstress, as in peroxidation and free radical attacks of lipids and proteins during feed storage [13].Synbiotic or probiotic treatment was counterproductive on oxidative enzyme-malonaldehyde, suggesting an improved antioxidant response as well as minimized cell damage in treated fish when compared to control fed populations. Early development of prolonged beneficial anti-oxidative effects of synbiotic consisting prebiotic galacto-oligosaccharide (GOS) and probiotic *Bacillus subtilis* was evident in *Labeo rohita*[62].Probiotics have role in improving zootechnical parameters of FCR, SGR and fish growth [3, 63]. Probiotics due to their antibacterial and antifungal activity, NH_3 detoxification potential, maintenance of redox status, metal chelating effects, improve feed nutritional parameters, leading to improved fish physiology. Production of fishmeal (FM) based on probiotics and prebiotics addition is an essential development [64]. Pro-, pre-biotics based FM inhibited microbial growth in storage feeds, with improved protein constitution and energy structure of feeds. Storage at 4°C maintained probiotic viability and feed quality during prolonged storage [65].Probiotic-coated fish feed comprising *Lactiplantibacillus plantarum* improved AA(val, lys, isoleu, leu, arg and phe), calcium, fibre and fat content in storage diet [65].Probiotics are thus upcoming mycotoxin mitigation strategy in stored feeds with better stability and viability, at low storage temperatures [66].

CONCLUSION REMARKS

Sustainable quality feeds that confer health benefits to aquaculture productions and consequently to consumer health are need of the hour. Improving feed quality by ensuring safety of feeds during storage help promote sustainable aquaculture approach. Microbial bio-therapeutics and natural antioxidants in fish diet can protect, shield and curb direct and indirect pathogenic incidences conferring fish welfare and health. Effective feed utilization and probiotics-based feed augmentation aim at providing zootechnical benefits to aquaculture, health benefits to the consumer and economic benefits to aqua culturists and farmers at large.

REFERENCES

1. FAO. The State of World Fisheries and Aquaculture 2018-Meeting the Sustainable Development Goals. Rome,2018.
2. FAO. The state of world fisheries and aquaculture 2020. Sustainability in action. Rome,2020.

3. Puri P, Sharma JG, Singh R. Biotherapeutic microbial supplementation for ameliorating fish health: Developing trends in probiotics, prebiotics, and synbiotics use in finfish aquaculture. Anim Health Res Rev 2022; 23(2):113-135.
4. Hua K, Cobcroft JM, Cole A, Condon K, JerryDR, Mangott A, *et al.*The future of aquatic protein: Implications for protein sources in aquaculture diets. One Earth2019; 1: 316-329.
5. GiriSS. Farm-Made Feeds for Sustainable Aquaculture Development: A South Asian Perspective In: Giri SSeditors. Farm-made aquafeeds: Opportunities, challenges and policy Intervention. SAARC Agriculture Centre, Dhaka, Bangladesh; 2017.p. 1-22.
6. Dirican S. A review of effects of aflatoxins in aquaculture. Applied Res J2015; 1: 192-196.
7. FAO and IFIF. Good practices for the feed industry–Implementing the Codex Alimentarius Code ofPractice on Good Animal Feeding. FAO Animal Production and Health Manual No. 9. Rome,2010.
8. DuPonte. Livestock feed analysis how to interpret the results. Cooperative Extension Service College of Tropical Agriculture and Human Resources (CTAHR),US Department of Agriculture University of Hawaii, Honolulu, Hawaii, 2009.
9. Kerrihard AL, Pegg RB , Sarkar A, Craft BD. Update on the methods for monitoring UFA oxidation in food products. Eur J Lipid SciTechnol 2015;117:1-14.
10. Solomon SG, Tiamiyu LO, Okomoda VT, Adaga K. Nutrient profile of commercial aqua-feeds under different storage conditions. Int JAquac2016a; 6:1-11.
11. Hossen MN, Das M, Sumi KR, Hasan MT. Effect of storage time on fish feed stored at room temperature and low temperature. Progressive Agriculture 2011; 22(1-2): 115-122.
12. Geng L, Liu K, Zhang H. Lipid oxidation in foods and its implications on proteins. Front Nutr 2023;10:1192199.
13. Kołakowska A, Bartosz G. Oxidation of food components: an introduction. In: Bartosz G, editors. Sikorski ZE, series editor. Food oxidants and antioxidants chemical, biological, and functional properties. Chemical and functional properties of food components series.New York: CRC Press;2014. p. 1-20.
14. Kavitha O, Anandan R, Mathew S, Nair PGV. Biochemical changes in fish feeds and ingredients during storage. FishTechnol 2004;41:49-56.
15. Athar N, Hardacre A, Taylor G, Clark S, Harding R, McLaughlin J. Vitamin retention in extruded food products. J Food Compos Anal2006;19(4): 379-383.
16. Kubitza F, Cyrino JEP. Effects of feed quality and feeding practices on the quality of fish: A Brazilian fish culture outlook. In: Chang YK and Wang S,editors. Advances in extrusion technology. Lancaster USA: Tecnomic publishing company;1998. p.53-71.
17. Giannakourou MC, Taukis PS. Effect of Alternative preservation steps and storage on vitamin C stability in fruit and vegetable products: Critical Review and Kinetic Modelling Approaches.Foods 2021;10:2630.
18. Tucker BW, Halver JE. Utilization of ascorbate-2-sulfate in fish. Fish Physiol Biochem1986;2(1-4): 151-160.
19. Watanabe T, Kiron, V, Satoh S. Trace minerals in fish nutrition. Aquaculture 1997;151:185-207.
20. Hilton JW. The interaction of vitamins, minerals and diet composition in the diet of fish. Aquaculture 1989;79(1-4): 223-244.
21. Lall SP,Kaushik SJ. Nutrition and metabolism of minerals in fish. Animals 2021;11:2711.
22. Sugiura SH, Dong FY, Rathbone CK. Apparent protein digestibility and mineralavailabilities in various feed ingredients for salmonid feeds.Aquaculture 1998;159:177-202.
23. Gasco L, Gai F, Maricchiolo G,Genovese L, Ragonese S, Bottari T *et al.*Feeds for the Aquaculture Sector. 1st ed.Cham (SZ): Springer;2018.
24. Chanda S, Paul BN, Ghosh K, Giri SS (2015). Dietary essentiality of trace minerals in aquaculture: A Review. Agricultural Reviews, 36(2): 100-112.
25. Solomon SG, Tiamiyu LO, Okomoda VT, Adaga K. Effects of storage conditions on quality characteristics of commercial aquafeeds and growth of African catfish. Croat J Fish 2016b;74: 30-37.
26. Pietsch C, Müller G, Mourabit S, Carnal S, Bandara K. Occurrence of Fungi and Fungal Toxins in Fish Feed during Storage. Toxins 2020;12:171.
27. Zmysłowska I, LewandowskaD.The effect of storage temperatures on the microbiological quality of fish feeds. Pol JEnviron Stud 2000;9:223-226.

28. Greco M, Pardo A, Pose G. Mycotoxigenic fungi and natural co-occurrence of mycotoxins in rainbow trout (*Oncorhynchus mykiss*) feeds. Toxins 2015; 7:4595-4609.
29. Han D, Xie S, Zhu X, Yang Y, Guo Z.Growth and hepatopancreas performances of gibel carp fed diets containing low levels of aflatoxin B1. AquacNutr 2010;16: 335-342.
30. Santacroce MP, Narracci M, Acquaviva MI, Cavallo RA, Zacchino V, Centoducati G.New development in aflatoxin research: from aquafeed to marine cells. In: Torres-Pachecol,editors Aflatoxins-detection, measurement and control.Croatia: InTech;2011. p. 209-234.
31. Samuel TO, Odunigba O. Aflatoxins associated with storage fungi in fish feed. Ife J Sci2015;17(2):519-523.
32. Cruz PS. Feed quality problems and management strategies. Fish Nutrition and Feeds 94 Proceedings.1994.
33. Riaz MN, Asif M , Ali R. Stability of vitamins during extrusion. CritRev Food SciNutr 2009;49:361-368.
34. Aanyu M, Ondhoro CC. Effects of storage duration on proximate composition of non-conventional fish feed ingredients and farm-made feed. J Global Agric Ecol 2017;6: 162-169.
35. Paola AS, Isabel YM. Effect of Frozen Storage on Biochemical Changes and Fatty Acid Composition of Mackerel (*Scomber japonicus*) Muscle. J Food Res 2015; 4(1):135-147.
36. Yildirim Ö, Çantaş IB. A study on the time-dependent change of totox values in feeds of marine fish. JAnatolEnvironAnimal Sci2020;5(2): 264-269.
37. FAO/WHO. Joint FAO/WHO Food Standards Programme Codex Alimentarius Commission Thirty-eighth Session CICG, Geneva, Switzerland Report of the Twenty Forth Session of the Codex Committee on Fats and Oils Melaka, Malaysia 2015.
38. Khan U, Seyhan K. A preliminary study of the effects of cold, frozen, or room temperature storage of commercial feeds on growth performance and feed consumption of juvenile rainbow trout (*Oncorhynchus mykiss*). Ege JFish Aquat Sci 2021;38(4): 411-416.
39. Mohammed MO. Effect of storage time on fishmeal made from four commercial Nile fishes collected from the White Nile, Sudan. BullEnvPharmacolLife Sci 2012;1(5): 21-25.
40. Nyong EB, Olubunmi FJ. Effect of storage and anti-nutritional components in stored pelleted fish feed. Int J SciTechnol Soc 2014;2(6):186-189.
41. Jeyasanta KI, Patterson J. Study on the effect of freshness of raw materials on the final quality of fish meals. Indian J Geo Mar Sci 2020; 49(1):124-134.
42. Ebeneezar S, Sankar TV, Kishore P, Panda SK, Prabu DL, Chandrasekar S*et al.*Evaluation of the quality of commercial fish feeds in India with respect to microbiological parameters. Int J Curr Microbiol Appl Sci 2018;7:1478-1483.
43. Grigorakis K, Giogios I, Vasilaki A, Nengas I. Effect of the fish oil, oxidation status and of heat treatment temperature on the volatile compounds of the produced fish feeds. Anim Feed Sci Technol 2010;158: 73-84.
44. Kop A, Gamsiz K, Korkut AY, Saygi H. The effects of different storage temperatures and durations on peroxide values of fish feed ingredients. Turk JAgri - Food SciTech 2019;7(Suppl 3):43-49.
45. Boran G, Karacam H, Boran M. Changes in the quality of fish oils due to storage temperature and time. Food Chem 2006;98: 693-698.
46. He P, Ackman RG. HPLC determination of ethoxyquin and its major oxidation products in fresh and stored fishmeals and fish feeds.JSciFood Agric 2000;80:10-16.
47. Amstrong OD, Atamu D, Orhomedia EH, Destiny A.Effect of different storage temperatures on the viabilities change of probiotics in the fish feed. Int J Biochem Biotech 2016;5:697-701.
48. Mwihia EW, Mbuthia PG, Eriksen GS, Gathumbi JK, Maina JG, Mutoloki S, *et al.*Occurrence and Levels of Aflatoxins in Fish Feeds and Their Potential Effects on Fish in Nyeri, Kenya. Toxins, 2018;10:543.
49. Marijani E, Wainaina JM, Charo-Karisa H, Nzayisenga L, Munguti J, Gnonlonfin GJB, *et al.*Mycoflora and mycotoxins in finished fish feed and feed ingredients from smallholder farms in East Africa.EgyptJAquat Res 2017;43:169-176.
50. Camacho-Rodríguez J, Macías-Sánchez MD, Cerón-García MC, Alarcón FJ, Molina-Grima EMicroalgae as a potential ingredient for partial fish mealreplacement in aquafeeds: nutrient stability under different storage conditions JApplPhycol 2018;30:1049-1059.

51. Lundebye AK, Hove H, Måge A, Bohne VJB, Hamre K. Levels of synthetic antioxidants (ethoxyquin, butylated hydroxytoluene and butylated hydroxianisole) in fish feed and commercially farmed fish. Food Addit Contam 2010;27:1652-1657.
52. Filipe D, Gonçalves M, Fernandes H, Oliva-Teles A, Peres H, Belo I, *et al*. Shelf-life performance of fish feed supplemented with bioactive extracts from fermented olive mill and winery by-products. Foods 2023;12:305.
53. Hernández A, García B, Jordán MJ, Hernández MD. Natural antioxidants in extruded fish feed: Protection at different storage temperatures. Anim Feed Sci Technol 2014;195:112-119.
54. Hamre K, Kolås K, Sandnes K.Protection of fish feed, made directly from marine raw materials, with natural antioxidants. Food Chem 2010;119(1):270-278,
55. Amstrong OD, Atamu D, Orhomedia EH, Destiny A Effect of different storage temperatures on the viabilities change of probiotics in the fish feed. Int J Biochem Biotech2016;5:697-701.
56. Zmyslowska I, Lewandowska D. Survival of bacterial strains in fish feeds stored at different temperatures. Polish Journal of Environmental Studies1999;8:447-451.
57. MohamedHMA, EmeishWFA, Braeuning A, Hammad S. Detection of aflatoxin-producing fungi isolated from Nile Tilapia and fish feed.EXCLI Journal 2017;16:1308-1318.
58. Yang J, Wang T, Lin G, Li M, Zhu R, Yiannikouris A, Zhang Y, Mai K. The Assessment of diet contaminated with Aflatoxin B1 in juvenile turbot (*Scophthalmus maximus*) and the evaluation of the efficacy of mitigation of a yeast cell wall extract. Toxins 2020a;. 12: 597.
59. Diab AM, Salem RM, Abeerc EMS, Alic GIE, El-Habashi N. Experimental ochratoxicosis A in Nile tilapia and its amelioration by some feed additives. IntJ Vet Sci Med2018;6:2149-2158
60. Puri P, Singh R , Sharma J. Micro-/bio-/nano-/syn-encapsulations and co-treatments of bioactive microbial feed supplementation in augmenting finfish health and aquaculture nutrition: a review. BenefMicrobes 2023;14(3): 281-302.
61. DawoodMAO,MohamedNE,MoustafaEM, MohamedGS.SynbioticeffectsofAspergillusoryzaeand β-Glucanongrowthandoxidative and immune responses of Nile Tilapia, *Oreochromis niloticus*. Probiotics AntimicrobProteins 2020;12:172-183.
62. DeviG,HarikrishnanR,ParayBA,Al-SadoonMK,HoseinifarSH, BalasundaramC. Effectofsymbioticsupplementeddietoninnate-adaptive immune response, cytokine gene regulation and antioxidant property in *Labeo rohita* against *Aeromonas hydrophila*. Fish ShellfishImmunol2019;89:687-700.
63. Nathanailides C, Kolygas M, Choremi K, Mavraganis T, Gouva E, Vidalis K, *et al*. Probiotics have the potential to significantly mitigate the environmental impact of freshwater fish farms. Fishes 2021;6:76.
64. Hendalia E, Manin F, Adriani, Dianti EP, Azizah AN. The use of prebiotics and probiotics in fish meal processing. IOP Conf. Series: Earth and Environmental Science 2019;391: 012011.
65. Chomova N, Pavlokov S, Sondorov M, Mudronov D, Feckaninov A, Popelka P, *et al*. Development and evaluation of a fish feed mixture containing the probiotic Lactiplantibacillus plantarum prepared using an innovative pellet coating method. FrontVet Sci 2023;10:1196884.
66. Ragoubi C,Quintieri L,Greco D, Mehrez A, Maatouk I, D'AscanioV,*et al*.Mycotoxin removalby *Lactobacillus* spp. and their application in animal liquid feed.Toxins2021;13:185.

Table.1: Storage studies based on evaluation of feed profile and nutrition quality of fish feeds and feedstuffs

Feed type /feed ingredients analyzed	Storage material; duration of storage/ sampling Interval	Place of study/ feed, ingredients source	Nutritional Parameter Analyzed	References
Farm-made feed and feed ingredients: wheat pollard, sunflower seed cake, cotton seed cake , maize bran, blood meal	polythene sacks; four-months (June-October)/ two months	Uganda	**Biochemical** *Proximate*: MC, DM, CA, CL, CP, CF	[34]
Local Feed ingredient: fish meal	one year (January-December)/ three months	South Khartoum, Sudan	**Biochemical** *Proximate*: MC, DM, CP, Fat, CA	[39]
Commercial Feed	poly-propylene and polythene bag; two months (July-August)/ 15 days	Mymensingh, Bangladesh	**Physical**: color, odor, texture, infestation, fines; **Biochemical***Proximate*: MC, DM,CP, CL, CA,CF, TN, NP	[11]
Commercial Feed	air tight containers; six weeks/7 days	Ilorin, Nigeria	**Biochemical***Proximate*: MC, CA, CL, CP, NFE *Anti-nutritional factors*: Tannins, oxalate, phytate	[40]
Commercial Feed	Open air and air tight conditions; six months (November-April) /monthly	Makurdi, Nigeria	**Biochemical** *Proximate*: MC, CA, CL, CP,NFE,CF *Oxidation status*: POV, FFA *Macroelements*: P, Ca, Mg, Fe **Physical** *Organoleptic*: color, smell caking condition, infestation	[10]
Commercial Feed	Bags wide open, seal open, sealed; six months/ post six-month storage	Makurdi, Nigeria	**Biochemical***Proximate:* MC, CA, CL, CP, NFE, CF *Oxidation status*: POV, FFA **Microbiological**: Mold count, mold type	[25]
Commercial Feed	Sacks; 45 days/15 days	Turkey	**Biochemical***Proximate*: CP,CL,CA,CF *Macroelements*: P, Ca, Na	[36]

			Oxidation status: POV, p-anisidine, totox value	
Feed ingredient: fish meal	six months/ monthly	India	**Biochemical** *Proximate*: MC,CP, CL,CF,NFE,TA, AIA,NPN, calorie content; AA, FA, cholesterol, vitamin content, salt content, protein solubility, *Macro,Micro elements*: P, Ca, Na, K, Cl, Mg, S, Fe, Cu, Zn, Mn, Se, I, Co,F, Cr, Hg, Cd, Pb, As, Ni *Biological amines*: TVB-N,TMA-N, Histamine *Oxidation status*: POV, FFA,TBA **Microbiological:** TPC,TFC	[41]
Commercial Feeds	Not Mentioned	Kochi, India	**Microbiological:** TPC, *Escherichia coli* count, coliforms count, Enterobacteriaceae count, yeast count, mold count	[42]
Commercial Feeds	food-grade oxygen barrier polyethylene, aluminum bags, airtight bottles; one week feed storage/35 days feeding trial for growth, feed performance of juvenile *O. mykiss*	Turkey/ feed from *Skretting Aquaculture, Norway*	**Biochemical** *Proximate*: CP,CF,CL,CA *Macro, micro elements*: Ca, P, Na, Fe, Cu, Zn **Fish growth parameters**: FCR,SGR,TGC	[38]
Formulated feeds (lab-made)	Not Mentioned	Greece/ fish oil (*Austral Group, Lima, Peru*), sardine oil (*Panama)*	**Biochemical** FA *Oxidation status*: TBA, TBARs, volatile compounds	[43]
Feed ingredients: Anchovy meal, Peruvian fish meal, soybean meal, poultry meal, Black Sea fish oil, sprat oil,	oil 60 days storage, other ingredients 30 days	Turkey	**Biochemical** *Oxidation status*: POV	[44]

anchovy oil, Salmon fish oil, aquaculture by-products oil, Salmon by-products oil				
Feed ingredients: Fish oil	150 days of storage/intervals 1,15, 30,60,120, 150 days	Turkey	**Biochemical** *Oxidation status*: EV, IV, PV, SV, TBA,AV,USM	[45]
Commercial Feeds, feed ingredient: fish meal EQ treated	original packages, disposable aluminium foil pans open to the air; 90 days /one month	Canada/ herring fish meal (*Connors Bros Ltd, Blacks Harbour*), EQ-treated fish meal, two fish feeds (*EWOS Ltd, Surrey)* commercial salmon feeds (*Moore-Clark, St Andrews; Corey Feed Mill Ltd,Fredericton*)	**Biochemical** *Oxidation status*: EQ,DM,QI	[46]
Commercial feed supplemented with probiotics	25 days/5days	Nigeria	**Microbiological:** Probiotic survival *L. brevis1, L. plantarum,P. pentosaceus*	[47]
Formulated feed	72 days/8 days	Poland	**Microbiological:** bacteria, fungi	[27]
Formulated feed	72 days/8 days	Poland	**Microbiological:** bacteria	[56]
Commercial feeds, feed ingredients: Indian fishmeal, Danish fish meal, wheat flour	Polyethylene bags; Six months /two months for all parameters; three month interval for FA	Cochin, India	**Biochemical** *Proximate*: MC,CP,CA,CL, FA,AA *Biological amine*: Histamine	[14]

Abbreviations AIA: acid insoluble ash;AV: acid value; DM: 1,8'-di (1,2-dihydro-6-ethoxy-2,2,4-trimethylquinoline); EQ: ethoxyquin; FCR: feed conversion rate; FFA: free fatty acid; IV: Iodine value; MC: Moisture content; NFE: nitrogen free extract; NP: Nitrogen in protein; NPN: Non-protein nitrogen; QI: quinone imine (2,6-dihydro-2,2,4-trimethyl-6-quinolone);SGR: specific growth rate; SV: saponification value; TA: total ash; TBA: Thiobarbituric acid; TFC: total fungal count;TGC: thermal-unit growth coefficient; TMA: trimethylamine; TPC: total plate count; TN: Total nitrogen;TVB-N: Total volatile bases nitrogen;USM: unsaponifiable matter.

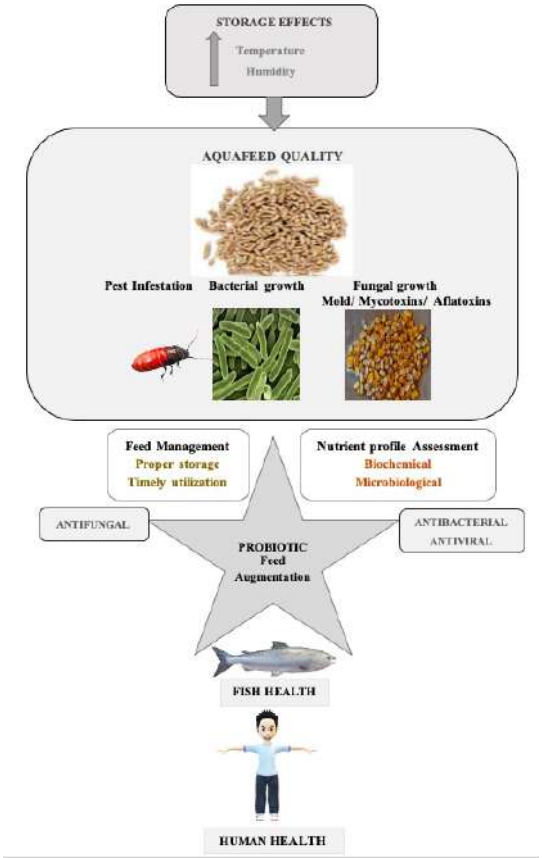

Figure.1 : Strategies to improve aqua feed quality during storage for sustainable aquaculture productions and human health

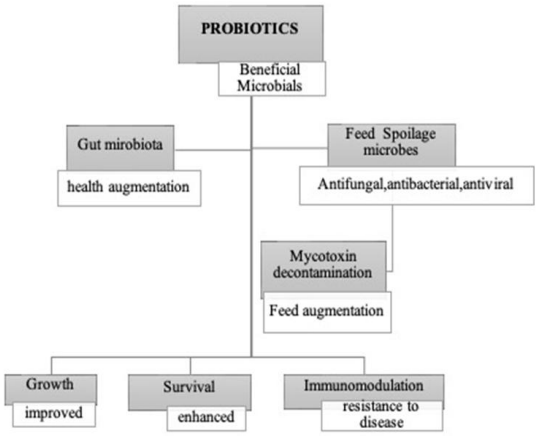

Figure.2: Probiotic effects in augmentation of aqua feed quality during storage and concomitant fish health

Indian Journal of Natural Sciences www.tnsroindia.org.in ©IJONS

Vol.15 / Issue 88 / Feb / 2025 *International Bimonthly (Print) – Open Access* *ISSN: 0976 – 0997*

RESEARCH ARTICLE

Vicharchika Management in Ayurveda – A Single Case Study

Siddhant Jain[1] and Sachin Deva[2]*

[1]PG Scholar, Department of Roga Nidan Evum Vikriti Vigyana, Parul Institute of Ayurveda, Parul University, Vadodara, Gujarat, India.
[2]Professor, Department of Roga Nidan Evum Vikriti Vigyana, Parul Institute of Ayurveda, Parul University, Vadodara, Gujarat, India.

Received: 21 Nov 2024 Revised: 03 Dec 2024 Accepted: 13 Jan 2025

***Address for Correspondence**
Sachin Deva,
Professor,
Department of Roga Nidan Evum Vikriti Vigyana,
Parul Institute of Ayurveda, Parul University, Vadodara, Gujarat, India.
E.Mail: siddhantsona.jain.1997@gmail.com

ABSTRACT

In the current case study, a 55- time-old man sought consultations at the Parul Ayurveda Hospital in Vadodara's inpatient department. The case complained of recreating skin rashes that were unloading, blistering, cracking, percolating, and accompanied by greenishness, edema, and itching. Eczema was linked by looking at the case's complaints and their coexisting signs and symptoms. The case in this case study was supposed to be treated by Vicharchika using a many ayurvedic drugs. Ayurveda states that Rakta Pradoshaja Vikara is engaged in three Doshas, with Kapha dominating. The care that's now offered in conventional drug is shy. Several Ayurvedic curatives have been applied for these symptoms. According to the opinion of Vicharchika, the case entered treatment for two months using panchtiktakashaya, panchnimbachurna, arogyavardhinivati, gandhakrasayan, swadishtavirechan, karanja tail, nimbatail, and triphlachurna. The case's condition was estimated for eczema symptoms and signs, which were resolved with treatment. This study demonstrates that the only effective treatment for eczema victims is Ayurvedic drug, which comes with no pitfalls or adverse goods.

Keywords: Eczema; *Vicharchika*; *RaktaPradoshajaVikara*; *Kushta*; Dermatitis.

INTRODUCTION

Ayurveda defines Vicharchika as Rakta PradoshajaVikara, involving three Doshas with a Kapha ascendance . Despite being Kshudra Kushtha, it has a habitual course and a propensity for aggravation. From the perspective of the current medical system, vicharchika can be associated with eczema, which is a type of dermatitis, or inflammation of the skin's external layers. A wide diapason of habitual or intermittent skin rashes marked by greenishness, skin oedema, itching, and perhaps encrusting , shelling, blistering, cracking, oozing is together appertained to as eczema.

Cases with Vicharchika(Eczema) who don't respond well to ultramodern drug's remedial approach generally seek treatment from Ayurveda in the expedients of eventually being cured of their condition. Vicharchika can be caused by a variety of factors, including eating an inordinate quantum of dry, banal, cold, salty, racy, sour, fermented, or fried food; intermittent late- night refections can also bring it on; it can also be caused by stress. Eczema can also affect from overindulging in tea, coffee, alcohol, aerated drinks, indigestion, constipation, acidity, or gas.

Case Report

A senior case, aged 55, was consulted in the Parul Ayurveda Hospital's inpatient department with intermittent skin rashes on his extensor area of the bottom. The case's complaints included greenishness, skin edema, and skin that was unloading, blistering, cracking, oozing, and There were red, blown, and itchy skin patches. The case had endured same symptoms for the former three times. The case also sought remedy from allopathic hospitals and croakers, but ultramodern drug did n't significantly ameliorate her condition, and in fact, it worsened as his symptoms spread to bordering body corridor. He also visited the inpatient department of Parul Ayurveda Hospital Vadodara, after a friend recommended that he seek ayurvedic remedy.
He was in good general health. At the time of the discussion, he wasn't taking any drug.

Clinical Findings

The case was latterly consulted on 29.12.2023 in OPD of Khemdas Ayurveda Hospital, Vadodara for the ayurvedic treatment. When physical examination was done, case was set up anxious, with loss of appetite and constipated with carpeted lingo. When asked about bladder and bowel, Micturition and bowel movement were normal. All laboratory and biochemical examinations were normal. Case complaints of intermittent skin rashes over extensor face of bottom greenishness, skin edema and blistering, cracking, oozing and bleeding. lesions of skin were inflamed; itchy and rosy. Itching was so prominent that case was unfit to sleep due to this. This skin rashes are intermittent from last 3 years.

Diagnostic Focus And Assessment

By observing the symptoms of the case, it was concluded that case was suffering with eczema. he has a habit of consuming milk and milk products on diurnal base. Vicharchika was considered as ayurvedic opinion, which is a type of kshudrakushtha.

Treatment Plan

The case's course of remedy was designed in agreement with the particular approach to vicharchika that's outlined in Ayurvedic books. Due to the fact that the complaint is primarily kapha because it causes symptoms similar as skin abrasion, dispassionateness to the touch, pruritus,non-progressive or slow complaint progression, elevated heaviness in rashes, and so on, the case was advised to avoid foods that are heavy to condensation, sour, wholesome, green lush vegetables, bitter in taste, milk, curd, meat from creatures living in marshy areas, fish, jaggery, and sesame. In addition to the specified medicines, the following were suggested triphlachurna, karanja tail, nimbatail, gandhakrasayan, panchtiktakashaya, panchnimbachurna and arogyavardhini vati. The case was also recommended to practice yoga and contemplation.

Intervention

When the case consulted in OPD on that day itself it was diagnosed with Eczema due to its classical symptom rashes analogous to eczema. So, drug was started on 29.12.2023 which includes panchtiktakashya 20 ml before food BD, arogyavardhinivati 250 mg after food BD, gandhakrasayana 250 mg after food BD, swadishtavirechan 250 mg on bed time, karanj tail- nimbatail for original operation twice a day and Triphlachurna 3gms at night with lukewarm water. Only ayurvedic medicines intervention was given to the case. Along with ayurvedic phrasings case was advised to rigorously follow the diet. After these medicines case got unforeseen relief in itching and rashes gradationally drop. He continued the same treatment for the coming 3 months with regular follow up.

Outgrowth Measures And Follow Up

By just following the proper ayurvedic operation with proper salutary and social life. case got gradationally nearly relief from eczema symptoms. Case followed the below intervention for the total duration of 3 months with the regular follow up and followed all the advised given to him. He got relieved from all the symptoms in just 3 months; which he was suffering from last 3 years.

Causes of Vicharchika(Eczema)

Etiological factors including negative food, repression of natural urges especially Vomiting, quick change in temperature, exposure to redundant heat, and unforeseen natural changesin fluid volume and muscle mass cause vicharchika. Viruddha annapana, inordinate input of drava, snigdha and practitioner dravyas,[1] coming in contact of inordinate heat after eating inordinate volume of food. followed by heavy refections after fasting[2]. Having cold water incontinently after exposure to sun and fear, eating raw or raw foods or having refections although preliminarily taken refections haven't been digested. Indulging in food and other habits which have been confined during the phase of Panchakarma. Consuming new grains, curds, fish, inordinate salty and sour food particulars. mash daal, radish, food prepared from flour paste, tila, dugdha and gud products. Indulging in sexual exertion indeed if the food isn't well digested, sleeping during the day time, affronting peers like brahmin/ practitioner and other reputed persons, and doing unethical acts are the etiological and threat factors of vicharchika.

DISCUSSION

Eczema or vicharchika is caused due to poor diet and life, which leads to disablement of digestion and aggravation of kaphadosha[3] .Kapha manifests in the skin and causes the accumulation of poisons. Consuming new grains, curds, fish, inordinate salty and sour food particulars. mash daal, radish, food prepared from flour paste, tila, dugdha and guda products. Indulging in sexual exertion indeed if the food isn't well digested(sexual intercourse incontinently after taking food), sleeping during day time, affronting peers like brahmin/practitioner and other reputed particular and doing unethical acts are the etiological and threat factors of vicharchika[4].The vitiated three dos has- vata, pitta, kapha along with disabled twak, rakta, mamsa and ambu together constitute seven essential realities that occur pathogenesis of kushtha and Kapha is the predominant dosha involved in vicharchika. intermittent skin rashes over extensor surface of feet and near areas characterized by reddishness, skin edema and cracking, oozing and were the symptoms of case. lesions of skin was infllamed, itchy and rosy. Kaphadosha is responsible for symptoms like whitish abrasion, cold wave in touch, pruritus, non-progressive/ slow progression of complaint, elevated; heaviness and oiliness are presented along with freak's conformation and stickiness like symptoms which are analogous to the symptoms of the case. Case should consume fluently digestible and wholesome food, green lush vegetables bitter in taste, food and ghee prepared by fortifying with bhallataka, triphala and nimba, one time old cereals, medications of mudga and patola. Case should avoid food which are heavy to condensation, sour food, milk, curd, meat of creatures abiding in marshy area, fish, jaggery and sesame[5]. PanchtiktaKashaya retain Tikta Rasa, Ruksha Guna, Kapha Pittahara parcels.It acts as Kanduhara, Rakta Shodaka, Varnya and Kushtaghna[6]. Gandhaka Rasayana is Katu, Tikta and Kashya Rasa pradhan, Kaphahara, kushtaghna and kandughna.[7,8] Arogyavardhini Vati is Tikta Kashaya Rasa pradhan, Ushna Virya, Tridoshahara, Pachana, Rakta Vardhaka, Rasayana and Kushtaghna[9]. Swadishta virechana is useful in Pitta dominant diseases along with Kapha Sansrista Doshas and Pitta Sthanagata Kapha croakersfor Vata- Kaphaja conditions like Shwasa, Kasa and Kushtha(Skin diseases).thus, all these ayurvedic medicines plays a significant part in the treatment of eczema.

CONCLUSION

The case report demonstrates the treatment of Eczema complete with only ayurvedic medicinal intervention. No surgical intervention was given. Pathya sevan plays a extreme part in the treatment of vicharchika. Apathyaahar should be avoided.

REFERENCES

1. 1." Agnivesha", Charaka Samhita, Hindi commentary by Kashiram Shastri and Gorakhnath Chaturvedi, Chaukhambha Bharati Academy; Varanasi, Part II, manufacture 2006, Chikitsa Sthana 7/30, pp. 253.
2. Agnivesha, Charaka, Dridhabala. Charaka Samhita, chikitsasthana, KushthachikitsaAdhyaya, 7/4- 6. In JadavajiTrikamjiAchrya., editor. 5th ed. Varanasi Chaukhambha Sanskrit Sansthana; 2001. p. 181
3. Agnivesha, Charaka, Dridhabala. Charaka Samhita, chikitsasthana, KushthachikitsaAdhyaya, 7/30. In JadavajiTrikamjiAchrya., editor. 5th ed. Varanasi Chaukhambha Sanskrit Sansthana; 2001. p. 185.
4. Agnivesha, Charaka, Dridhabala. Charaka Samhita, chikitsasthana, KushthachikitsaAdhyaya, 7/10. In JadavajiTrikamjiAchrya., editor. 5th ed. Varanasi Chaukhambha Sanskrit Sansthana; 2001. p. 182.
5. Agnivesha, Charaka, Dridhabala. Charaka Samhita, chikitsasthana, KushthachikitsaAdhyaya,7/82-83. In JadavajiTrikamjiAchrya., editor. 5th ed. Varanasi Chaukhambha Sanskrit Sansthana; 2001. p. 192.
6. Indradev Tripathi," Raj Nighantu", Acharya Vishwanath Durvedi," Aamradi Varga", cantina.Krishna Das Academy banaras 1982, Page no 70- 71.
7. Dass R, Nayak AP. A clinical study to compare" virechana" and" jalaukavacharana" procedures in managing vicharchika. Global J Res. Med. shops & Indigen. Med 2013; 2(1) 30 – 39.
8. Kasavajjihala S, Prasad SRA. sanctification processes of Gandhaka(Sulphur) as described in the medieval Indian textbook Anandakanda." Int Res J Pharm" 2014; 5(5) 438- 443.
9. Gabhane SM, Waghmare S, Andhare R, Uke P.Ayurvedic operation of vipadika kushtha(palmoplantar psoriasis)- a single case study. Int J dastard Res Rev 2021; 13171- 5

Table.1: CLINICAL FINDINGS

Prakriti	Vata and Pitta
Sara	Mamsa sara
Samhanana	Madhayam
Pramana	Sama
Satva	Madhyama
Satmya	Madhayama
Vaya	Yuvavastha
Vayayamshakti	Madhyam
Aharshakti	Heen

Indian Journal of Natural Sciences *www.tnsroindia.org.in ©IJONS*

Vol.15 / Issue 88 / Feb / 2025 *International Bimonthly (Print) – Open Access* *ISSN: 0976 – 0997*

RESEARCH ARTICLE

To Compare the Immediate Effect of Long Wave Diathermy versus Ultrasound Therapy for Pain and Dysfunction in Upper Trapezitis in College Going Students:- A Comparative Study

Shivani Sutaria[1]*, Mukulkumar Chauhan[2] and Himanginiben Dushyant Patel[3]

[1]Assistant Professor, Department of Physiotherapy, SKUM College of Physiotherapy, (Affiliated to Gujarat University), Ahmedabad, Gujarat, India.
[2]Student, Department of Health, Education and Life Science, Birmingham City University, England, United Kingdom.
[3]Physiotherapy Assistant, Addenbrooke's Hospital, United Kingdom.

Received: 21 Nov 2024 Revised: 03 Dec 2024 Accepted: 13 Jan 2025

***Address for Correspondence**
Shivani Sutaria,
Assistant Professor,
Department of Physiotherapy,
SKUM College of Physiotherapy,
(Affiliated to Gujarat University), Ahmedabad, Gujarat, India.
E.Mail: sutariashivani@gmail.com

ABSTRACT

Inflammation of trapezius muscle is termed as Trapezitis. The upper trapezius muscle is highly susceptible to overuse as it is as postural muscle. The pain may refer to the other areas from the site of inflammation which causes pain at rest as well as during activity. Amongst antagonistic muscle due to pain passive range of motion may be painful and restricted. The aim of the present study was to compare and determine the immediate effect of LWD versus US on pain and dysfunction in upper trapezitis students. Total 60 students, 30 students in each group were selected who meet an inclusion and exclusion criteria. Group A received long wave diathermy with trapezius muscle stretching and Group B ultrasound therapy with trapezius muscle stretching. As an Outcome measure Numerical Pain Rating Scale, Neck Disability Index and cervical Range of Motion were measured immediately pre and post. Statistical analysis and result shows that immediate effect of LWD was found to be effective in improving cervical side flexion range of motion as compared to immediate effect of ultrasound. There was non-significant result noted on reducing pain and functional dysfunction while comparing LWD versus US in students with diagnosed upper trapezitis.

Keywords: Long wave diathermy, ultrasound therapy, Upper trapezitis, NPRS, NDI, ROM, trigger point, stretching.

INTRODUCTION

Researches related to the assessment of biophysical parameters and their relationship with musculoskeletal dysfunction has exposed to various types of stress on muscles, tendons and joints has become more and more popular in recent years.[1] Amongst all the musculoskeletal dysfunction, present study focus on upper trapezius muscle in college going students who are more prone to trapezitis. There is fairly prevalent of Neck discomfort in the upper fibres of the trapezius. As compared to older people the prevalence of pain is high in young people. Trapezitis induces an early defensive muscular spasm during injury, which is uncomfortable and creates muscle stiffness reported in several studies.[2] the prevalence of neck pain occurring in upper trapezius muscle is found to be maximum in middle age female and less common in males with is fluctuating with mean point prevalence of 13%. 48- 78% prevalence of neck pain has been reported[3] As upper trapezius muscle is more prone to be overuse, it mostly causes a pain behind the eyes, a limited range of motion, headache or tension headache in the temples, a stiff neck, and an intolerance to weight on your shoulder.[4] The effective in trapezitis pain has been found by giving physical therapy which include treatment such as giving modalities like laser therapy, long wave diathermy, ultrasound therapy, TENS, IFT and manual management such as stretching and METS etc.[5] The present study focuses on the immediate effect of long wave diathermy VS ultrasound on pain relief and dysfunction in upper trapezitis students. In physical therapy regimens for healing of soft tissues lesions and managing pain Therapeutic ultrasound is considered as a complementary treatment.[6]Ultrasound produces better flexibility of the collagen fibres and muscles as it delivers heat deep into the muscles. The therapeutic effects of ultrasound include reduced joint stiffness, pain, and muscular rigidity, relaxed joint contracture and better adhesion.[7] Similarly long wave diathermy produces deep heating in the muscle with the penetration range deep as two inches. It comprising both magnetic and electric fields by generating oscillating electromagnetic fields (EMF), thereby producing heat in the tissues due to rapid alternating movements of ions.[8] Thus the aim of the present study was used to determine the immediate effect of long wave diathermy versus ultrasound on pain relief and dysfunction in upper trapezitis students.

MATERIALS AND METHODS

A comparative study was conducted at Mahatma Gandhi Physiotherapy College, Ahmedabad, Gujarat among 60 college going students. Present study was conducted for the 6 months durations. Students who are willing to participate in the study, both gender with the age group between 18 to 25 years and with diagnosed trapezitis was included in the study. Students with any recent trauma over the cervical spine, upper extremity fracture, cervical radiculopathy, and those taking steroids for last 6 months was excluded from the present study. Materials used in the study was Consent form, NPRS, NDI, Case Record Form, Pen, Plinth, Table, Chair and Pillow.

PROCEDURE

On the basis of inclusion and exclusion criteria, total 60 students with upper trapezitis was allotted in two groups, 30 in group A and 30 in group B using Simple Random Sampling (Odd-Even Method). Informed consent was obtained and nature of study was explained to all students. All students were undergone Tender point assessment by the rapist and the pain and functional activity was measured in Numerical Pain Rating Scale(NPRS)and Neck Disability Index Scale (NDI). Group A: - (n=30) Long Wave Diathermy: - students were made to sit in a wall support chair and then lean forward in comfortable manner. His\her head and arms were supported with pillow. LWD was given on the trapezius Tender point. Pre and post immediate intervention NPRS, NDI and Cervical side flexion range was measured. Group B: - (n= 30) Ultrasound Therapy: - students were made to sit in a wall supported chairs and lean forward in a comfortable manner. His/her head and arms were supported with pillow. Ultrasound Therapy was given on the trapezius Tender point. Pre and post immediate intervention NPRS, NDI and Cervical side flexion range was measured.

RESULT

Statistical analysis was done using SPSS version 20. Mean and standard deviation was calculated as a measure of central tendency and measure of dispersion for NPRS-R, NPRS-A, and NDI. Level of significance was kept at 5% with confidence interval (CI) at 95% (P value=0.05). As the data was not normally distributed in both groups by Shapirowilktestperformedtakingpre-outcomemeasureandpvaluewas<0.05forNPRS- R, NPRS-A, ROM, and NDI. So, non-parametric Wilcoxon signed ranks test was used for within comparison and Mann-Whitney U test was applied for between group comparison for NPRS-R,NPRS-A, ROM, and NDI. Significant result was found in within comparison of group A for NPRS-R, NPRS-A, ROM, and NDI also there was significant result noted in within comparison of group B by applying Mann-Whitney U test. between group comparison result shows significant improvement in ROM and non-significant result for NPRS-R, NPRS-A, and NDI by applying Mann-Whitney U test. Hence, the null hypothesis was rejected and alternate hypothesis was accepted for within group comparison. Above results shows that LWD was found to be more effective in improving cervical side flexion ROM as compared to US. So the immediate effect of LWD was more effective than US modality for cervical side flexion ROM.

DISCUSSION

The purpose of the study is to compare the immediate effect of LWD versus US therapy on pain and dysfunction in upper trapezitis in college going students. The statistical analysis reported that in within group comparison both LWD (group A) and US (group B) therapy has the immediate effect on relieving pain, improving cervical side flexion range of motion and dysfunction. Between group comparison result shows that LWD is helpful in improving cervical side flexion range of motion as compared to immediate effect of US therapy. There was no significant result noted on NPRS-R, NPRS-A and NDI in between comparison of groups. Long Wave Diathermy (LWD), or capacitive and resistive electric transfer therapy produces heat and improves the metabolic flow and microcirculation of the superficial and deep tissues, works at a frequency range of 0.3-1 MHZ and wavelength of 300m, thereby reduces pain and improved dysfunction. Similarly US produces thermal and non-thermal effect which increases capillary permeability and tissue metabolism, thereby enhancing fibrous tissue extensibility and pain thresholds.[6] Present study was further supported by Siddhesh Sawant, Dr. Keerthi Rao in 2019, effectiveness of myofascial release (MFR) and long wave diathermy (LWD) on upper trapezius spasm amongst 30 participants, Pre and post intervention of NPRS and Wong Baker Faces Pain Rating Scale were recorded and analysis was done using paired "t" test. Study concluded that Myofascial Release and long wave diathermy was effective on upper trapezius muscle spasm in young adults. Long wave diathermy produces heat deep inside a targeted tissueas it uses high frequency electric current. It promotes blood flow as the heat increases, and helps to improve flexibility in stiff joints and connective tissue.[9]further study done by Draper, D.O., Mahaffey, C., *et al* in 2010 on thermal ultrasound decreases tissue stiffness of trigger points in upper trapezius muscles and concluded that thermal ultrasound over latent trigger points is comfortable and can decrease stiffness of a trigger point.[10] Costella, M puentedura *et al* in 2016 did a study on immediate effect of soft tissue mobilization versus therapeutic ultrasound for patient with arm and neck pain with evidence on mechanosensitivity and concluded that greater improvements in ULNT ROM, GROC, and PSFS, and pain following STM than after receiving therapeutic US.[11] Further Mehrdad Sadeghnia *et al* in 2021 did a study on immediate effect of high power pain threshold ultrasound on treatment of upper trapezius active myofascial trigger point and concluded that Ultrasound significantly improved the muscular symptoms of the trigger points.[12]

CONCLUSION

Immediate effect of LWD was found to be effective in improving cervical side flexion range of motion as compared to immediate effect of ultrasound. There was non-significant result noted on reducing pain and functional dysfunction while comparing LWD versus US in students with diagnosed upper trapezitis.

REFERENCES

1. Wendt M, Waszak M. Assessment of the stiffness of the upper trapezius muscle in a group of asymptomatic people with cervical spine rotation asymmetry. PLoS One. 2024 Feb 22;19(2):e0298544. doi: 10.1371/journal.pone.0298544. PMID: 38386652; PMCID: PMC10883562.
2. Gayathri K, P Senthil, S Swathi, Neelam NS, Nainar M, Haribabu L. Effectiveness of Myofascial Release Technique and Muscle Energy Technique on Pain and Physical Function among Smartphone Users with Trapezitis. Chettinad Health City Med J. 2022;11(4):37-41
3. Yadav, Trupti; Gherwara, Kusha N, Effectiveness of upper limb and scapular stabilization exercises in college students suffering from recurrent trapezitis.
4. PrakashbhaiKanjibhaiRathva et.al. Effect of cryoflow versus ultrasound in acute Trapezitis on pain, range of motion and quality of life: a comparative interventional study. International Journal of Health Sciences and Research (www.ijhsr.org) Volume 13; Issue: 12; December 2023.
5. K. Kotteeswaran1 , Syed Gaffar2*, Krishna. R3 ,KeerthanaPriya. R.3, Effectiveness of Laser Therapy and Ultrasound Therapy along with Muscle Energy Technique in subjects with Trapezitis, Asian Journal of Pharmacy and Technology, ISSN 2231–5705 ,DOI: 10.52711/2231-5713.2021.00019
6. Lucas Ogura Dantas, Mikala C. Osani et al.Therapeutic ultrasound for knee osteoarthritis:A systematic review and meta-analysis with grade quality assessment.
7. Yildirim MA, Öneş K, Gökşenoğlu G. Effectiveness of Ultrasound Therapy on Myofascial Pain Syndrome of the Upper Trapezius: Randomized, Single-Blind, Placebo-Controlled Study. Arch Rheumatol. 2018 Mar 23;33(4):418-423. doi: 10.5606/ArchRheumatol.2018.6538. PMID: 30874250; PMCID: PMC6409164.
8. Panihar U, Sharma K, Joshi S, Pawalia A. A randomized controlled trial on the efficacy of longwave diathermy on pain, disability and range of motion in the patients with neck pain. J Physiother Res. 2022;12:e4805. http://dx.doi.org/10.17267/2238- 2704rpf.2022.e4805
9. Siddhesh Sawant1* , Dr. Keerthi Rao2, Effectiveness of myofascial release (MFR) and long wave diathermy (LWD) on upper trapezius spasm,International Journal of Multidisciplinary Research and Development,ISSN: 2349-5979; Impact Factor: RJIF 5.72 Received: 18-01-2019; Volume 6; Issue 3; March 2019.
10. Draper, D. O., Mahaffey, C., Kaiser, D., Eggett, D., &Jarmin, J. (2010). Thermal ultrasound decreases tissue stiffness of trigger points in upper trapezius muscles. *Physiotherapy Theory and Practice*, *26*(3), 167–172. https://doi.org/10.3109/09593980903423079
11. Costello, M., Puentedura, E. 'Louie' J., Cleland, J., &Ciccone, C. D. (2016). The immediate effects of soft tissue mobilization versus therapeutic ultrasound for patients with neck and arm pain with evidence of neural mechanosensitivity: a randomized clinical trial. *Journal of Manual & Manipulative Therapy*, *24*(3), 128–140. https://doi.org/10.1179/2042618614Y.0000000083
12. Sadeghnia M, Shadmehr A, HadianRasanani MR, Mir SM, Jalaei S. Evaluate the Immediate Effect of High-power Pain Threshold Ultrasound on Treatment of Upper Trapezius Active Myofascial Trigger Points. Journal of ModernRehabilitation. 2021; 15(3):167-172. http://dx.doi.org/10.18502/jmr.v15i3.773

Table.1: Parameters

Parameters	GROUP-A	GROUP-B
Modality	LWD +uppertrapezius stretching	US+ uppertrapezius stretching
Sample size	30	30
Frequency	1 MHz	1 MHz
Intensity	Pts tolerance level	1W/Cm^2
Treatment duration	10 minutes	10 minutes

Table.2 :Group: A Within Group Comparison

Parameter	Pre(Mean ±SD)	Post(Mean ±SD)	z value	P value	Significance
NPRS-R	3.80±1.56	2.33±1.40	-4.86	0.00	SIGNIFICANT
NPRS-A	4.90±1.45	2.93±1.50	-4.77	0.00	SIGNIFICANT
ROM	37.70±2.61	38.90±2.44	-4.31	0.00	SIGNIFICANT
NDI	44.40±10.38	39.89±9.14	-4.84	0.00	SIGNIFICANT

Table.3:GROUP:B Within Group Comparison

Parameter	Pre(Mean ±SD)	Post(Mean ±SD)	z value	P value	Significance
NPRS-R	2.83±1.26	2.33±1.32	-3.64	0.00	SIGNIFICANT
NPRS-A	4.17±1.26	3.57±1.22	-3.67	0.00	SIGNIFICANT
ROM	36.27±3.09	36.90±2.78	-4.02	0.00	SIGNIFICANT
NDI	45.20±11.35	40.53±10.25	-4.83	0.00	SIGNIFICANT

Table.4:Between Group Comparison of Group: A & Group: B

PARAMETERS	z value	p value	DIFFRENCE
NPRS-R	-2.81	0.78	NON-SIGNIFICANT
NPRS-A	-1.79	0.07	NON-SIGNIFICANT
ROM	-2.81	0.00	SIGNIFICANT
NDI	-0.12	0.90	NON-SIGNIFICANT

Indian Journal of Natural Sciences *www.tnsroindia.org.in ©IJONS*

Vol.15 / Issue 88 / Feb / 2025 *International Bimonthly (Print) – Open Access* *ISSN: 0976 – 0997*

RESEARCH ARTICLE

Artificial Intelligence - based Diagnosis in Lumbar Prolapsed Intervertebral Disc : A Systematic Review with Meta - Analysis Protocol

Sandeep Pattnaik[1], Rajneesh Kumar Gujral[2] and Manu Goyal[3]*

[1]Ph.D Scholar, Department of Physiotherapy, Maharishi Markandeshwar Institute of Physiotherapy and Rehabilitation, Maharishi Markandeshwar (Deemed to be University), Mullana-Ambala, Haryana, India.
[2]Professor, Department of Computer Science Engineering, Maharishi Markandeshwar Engineering College, Maharishi Markandeshwar (Deemed to be University), Mullana-Ambala, Haryana, India.
[3]Professor, Department of Physiotherapy, Maharishi Markandeshwar Institute of Physiotherapy and Rehabilitation, Maharishi Markandeshwar (Deemed to be University), Mullana-Ambala, Haryana, India.

Received: 21 Nov 2024 Revised: 03 Dec 2024 Accepted: 17 Jan 2025

***Address for Correspondence**
Manu Goyal,
Professor,
Department of Physiotherapy,
Maharishi Markandeshwar Institute of Physiotherapy and Rehabilitation,
Maharishi Markandeshwar (Deemed to be University), Mullana-Ambala, Haryana, India
E.Mail: manu.goyal@mmumullana.org

ABSTRACT

Low back pain (LBP) is a prevalent musculoskeletal condition, with lumbar prolapsed intervertebral disc (PIVD) as a frequent cause. Artificial intelligence (AI) has revolutionised healthcare across various domains, including diagnosis, treatment planning, and outcome prediction. However, its application in diagnosing lumbar PIVD remains limited. So the objectives of this proposed systematic review and meta-analysis are to evaluate the use of AI for diagnosing lumbar PIVD and assess its potential as an alternative to conventional diagnostic methods. A comprehensive literature search will be conducted across Medline, Scopus, Web of Science and Cochrane Library for English-language, peer-reviewed articles published between January 2019 and January 2024. The PRISMA guidelines will guide the selection process, with at least two independent reviewers screening and assessing articles for eligibility based on the PICOS framework. Data will be synthesised using fixed-effects or random-effects models depending on heterogeneity. The protocol is registered in PROSPERO (CRD42023444785). This review will analyse and evaluate the current state of AI technology for diagnosing lumbar PIVD, highlighting its potential benefits for clinical practice. We expect to summarise a large number of relevant articles describing in detail the actual utility and applications of AI for clinical practice for patients with lumbar PIVD.

Keywords: Prolapsed intervertebral disc, Herniated disc, Artificial intelligence, Machine learning, Diagnosis

INTRODUCTION

'Low back pain' (LBP) represents a significant public health concern globally, with lumbar prolapsed intervertebral disc (PIVD) identified as the most frequent etiological factor.[1]PIVD is characterised by the localised displacement of intervertebral disc content beyond its anatomical confines, often as a consequence of degenerative disc disease. Epidemiological studies suggest that approximately 50-80% of adults experience LBP at least once in their lifetime, with an annual PIVD incidence ranging from 5 to 20 cases per 1,000 adults.[2]Its prevalence is most notable during the third to fifth decades of life and demonstrates a male predominance.[3]While PIVD can occur at any spinal level, the L4-L5 and L5-S1 segments are most commonly affected, accounting for approximately 95% of cases. Repetitive mechanical loading and occupational exposure to vibration are established risk factors for PIVD development.[4]Additionally, a sedentary lifestyle, obesity, smoking, and lower socioeconomic status have been linked with an increasing risk of PIVD.[5] PIVD's rising incidence underscores the importance of accurate diagnosis, classification, and treatment strategies, particularly in light of contemporary lifestyle trends. The diagnostic approach for PIVD typically involves a comprehensive clinical evaluation, integrating patient history, symptom presentation, physical examination findings, and imaging modalities. While conventional radiography offers limited sensitivity for its diagnosis, it may be employed to evaluate for underlying spondylosis or spinal malalignment. Computed tomography (CT) scans provide improved visualization of bony structures but lack sufficient soft-tissue resolution to definitively diagnose PIVD. Magnetic resonance imaging (MRI) remains the gold standard for PIVD diagnosis, boasting a high degree of diagnostic accuracy exceeding 97%.[6]However, the high cost of advanced imaging techniques and their reliance on operator expertise warrant further investigation into cost-effective and user-independent diagnostic tools. Management of PIVD primarily involves conservative therapy, encompassing pharmacological interventions, patient education, external support devices, and physical therapy modalities such as traction, manual therapy, exercise programs, and electrotherapy modalities. Surgical intervention, including discectomy and laminectomy, is typically reserved for patients who fail to respond to conservative treatment.[7]

The heterogeneous nature of PIVD presentation, coupled with the existence of asymptomatic cases and the potential for non-specific clinical signs and symptoms, can complicate the selection of optimal treatment regimens for individual patients. Therefore, a thorough diagnostic evaluation and risk stratification are crucial for guiding personalised treatment plans. Artificial intelligence (AI) offers potential solutions for overcoming various challenges associated with PIVD diagnosis and management. The past decade and a half have witnessed a surge in AI applications across diverse fields, including medical research. In this domain, AI has revolutionized various aspects, such as diagnostic formulation, radiological data extraction, outcome prediction, drug development, and treatment assignment.[8–11]AI-based tools have demonstrated the potential to improve clinical practice in patients with LBP, including those with PIVD, by enhancing diagnosis, classification, prevention, treatment selection, and outcome prediction. This modernization of the approach toward PIVD has the potential to expedite diagnosis, optimize patient recovery, and improve the accuracy and personalization of treatment plans over time.[12]Various AI subfields, including 'machine learning', 'deep learning', and 'artificial neural networks', are being explored to support more precise diagnosis, and classification of PIVD subtypes, and provide decision-making support to healthcare professionals regarding treatment selection and outcome prediction.[12] So the literature review plans to systematically evaluate the existing body of knowledge regarding the application of AI in diagnosing lumbar PIVD. The review will focus on the usability and implementation of such AI-based tools. A comprehensive understanding of the efficacy and practicality of AI for diagnosing lumbar PIVD across diverse clinical settings and healthcare professionals is crucial for its potential integration into healthcare planning. Furthermore, the cost-effectiveness and time-saving benefits of AI compared to conventional diagnostic procedures will be explored.

Specific research questions guiding this review include
1.What is the diagnostic effectiveness of AI for lumbar PIVD?
2.Can AI serve as a viable alternative to conventional diagnostic methods for lumbar PIVD?

Objective
To establish a transparent framework for conducting a systematic review along with a meta-analysis on the application of AI-based tools for diagnosing lumbar PIVD. This protocol will outline the key research questions, detailed search strategies, eligibility criteria for study inclusion/exclusion, data extraction procedures, quality assessment methods for included studies, and data synthesis strategies.

METHODS

Protocol
This systematic review and meta-analysis protocol adheres to the methodological guidelines outlined in the 'Preferred Reporting Items for Systematic Reviews and Meta-Analyses Protocols (PRISMA-P)' 2015 statement.[13]The protocol has been prospectively registered in the 'International Prospective Register of Systematic Reviews (PROSPERO)' under the registration number CRD42023444785. The PRISMA-P file is attached.

Eligibility Criteria
The 'PICOS (Population, Intervention, Comparison, Outcome, Study Design)" framework will guide the development of eligibility criteria for the initial literature search.[14] The following characteristics are:

Population
The target population will comprise adult patients aging 18 years old or more of any gender diagnosed with lumbar disc hernia ion or PIVD, with no geographic or employment restrictions. Patients with low back pain from other causes will be excluded.

Intervention
Studies evaluating any AI model used for diagnosing, classifying, assigning treatment for, or predicting clinical outcomes in lumbar PIVD will be considered. Studies that do not utilize clinical data for AI development will be excluded. All types of AI models will be considered.

Comparison
Due to the potential methodological limitations of comparator interventions in this context, no comparison group will be considered for the review.

Outcome
The primary outcome will be the diagnostic accuracy of AI models for lumbar PIVD, as measured by relevant metrics.

Study Design
The included studies will be limited to the observational designs (cross-sectional, cohort, and case-control studies). Non-research materials (letters, editorials, and correspondences), case reports or series, and randomized controlled trials (due to methodological limitations for addressing the research questions) will be excluded. Systematic reviews and meta-analyses will be included for reference purposes only, to identify additional relevant studies for potential inclusion.

Report Characteristics

Only original, full-text articles published in English and subjected to rigorous peer review will be included. Letters, abstracts, and editorials will be excluded. There will be no geographic restrictions for study selection.

Information Sources

A systematic electronic search of the databases Medline, Scopus, Web of Science, and Cochrane Library will be undertaken. To focus on contemporary research, the search and inclusion of the studies into the review will be limited to articles published between January 2019 to January 2024. A secondary search of reference lists from identified key studies and reviews will be performed to capture any additional relevant articles potentially missed during the primary scan.

Search Strategy

A comprehensive search strategy will be developed to identify all relevant studies investigating the application of AI for diagnosing, classifying, assigning treatment, and predicting clinical outcomes in patients with lumbar PIVD. The search will utilize the stated databases and will incorporate the 'Medical Subject Headings (MeSH)' terms for PubMed and applicable keywords for all databases. Boolean operators ("AND" and "OR") will be employed to refine the search strategy. Search terms will include combinations of "lumbar disc hernia ion," "lumbar PIVD," "artificial intelligence," "machine learning," and other relevant synonyms. To identify other relevant research, the references of the reviews and all included articles will be examined manually.

Study Records

Data Management

All the identified studies through the literature search will be imported into the Mendeley reference management software tool. The search results obtained from each database will be consolidated into a unified library, with duplicate records eliminated to create a comprehensive and non-redundant dataset.

Selection Process

A dual-reviewer process will be employed to examine the titles and abstracts of all retrieved articles and select those that meet the study criteria. Articles will be included if they suggest the use of any AI model for diagnosing, classifying, assigning treatment, or predicting outcomes in patients with lumbar PIVD. Both assessors will separately assess the full-text versions of these articles against the predetermined eligibility standards. If required, additional information will be sought from the authors through email correspondence. Disagreements among reviewers regarding article inclusion will be addressed through consensus-building discussions or by introducing a third reviewer. Reasons for excluding articles deemed potentially relevant will be meticulously documented. All reviewers will independently verify the final set of included studies. A visual representation of the article selection process, including decision points during data collection, will be produced using a PRISMA flow diagram.

Data Collection

Data will be extracted from articles meeting the inclusion criteria by two independent reviewers. A standardized data extraction form will be employed to collect information pertaining to study characteristics, the specific AI model utilized and its application within the study, outcome measures employed, outcome assessment methodologies, and any documented complications or adverse events. Should clarification be necessary regarding any extracted data, the primary authors will be contacted electronically.

Data Items

Data on study characteristics, such as 'authors', 'publication year', 'study design', and 'sample size', will be gathered using standardized extraction forms. Additionally, details regarding the AI model will be extracted, such as the specific model type, its primary function within the study, the data used for its development, and its application in diagnosing lumbar PIVD. Additionally, outcome measures related to the diagnostic accuracy of the AI models will be

extracted. This will include specific metrics such as 'sensitivity (SEN)', 'specificity (SPE)', 'true positive (TP)' rate, 'false positive (FP)' rate, 'false negative (FN)' rate, and 'true negative (TN)' rate.

Risk of Bias

The 'Risk Of Bias In Non-randomized Studies of Interventions (ROBINS-I)' tool15encompassing seven key domains will be employed to assess the risk of bias inherent in the selected studies: 'confounding', 'selection bias', 'classification bias', 'deviation from intended interventions', 'missing data bias', 'measurement bias', and 'reporting bias'. Two independent reviewers will appraise each study using the ROBINS-I tool to assess the risk of bias, categorizing studies as low, moderate, serious, or critical risk.[15]Disagreements in the assessments will be resolved through discussion to reach a consensus.

Data Synthesis

A 2x2 contingency table using TP, FP, TN, and FN will be extracted from each included study wherever possible. For studies that do not directly report a 2x2 table, data will be reconstructed using existing information such as sensitivity, specificity, and sample size, employing the built-in calculator within Review Manager (version 5.3.5). Pooled sensitivity and specificity with 95% confidence intervals (CIs) for AI-based diagnosis will be calculated using either a fixed-effects or random-effects model depending on the presence of heterogeneity. 'Descriptive forest plots' and 'summary receiver operating characteristic (SROC)' curves will be generated. The SROC plot will depict sensitivity (y-axis) and specificity (x-axis). The 'Area Under the Curve (AUC)' will also be calculated.[16] On the SROC plot, 95% of CIs and prediction regions will be visualised around the average accuracy estimates. AUC values will be interpreted according to established criteria (0.90-1.0: excellent, 0.80-0.90: good, 0.70-0.80: fair, 0.60-0.70: poor, 0.50-0.60: failure). Heterogeneity will be assessed using a combination of visual and statistical methods. Forest plots of individual study sensitivities, specificities, and SROC curves will be visually inspected for evidence of heterogeneity. Statistical assessment will employ the I^2 statistic, with a value exceeding 50% indicating significant heterogeneity. Additionally, Spearman correlation coefficients will be calculated to explore potential threshold effects, where different diagnostic thresholds used across studies contribute to heterogeneity. A negative correlation between sensitivity and specificity would suggest a threshold effect, visualized as a "shoulder-arm" distribution on the SROC curve.[17]

DISCUSSION

Within the last few decades, the world has witnessed the incredible potential of AI and its ability to process the provided information regarding the patient with PIVD to reach a diagnosis, classify the current condition, assign treatment and predict patient outcomes, a reason why it is important for a health professional to guide the patient accordingly. This proposed systematic review and meta-analysis aims to evaluate, summarise and analyse the advances of AI in patients with lumbar PIVD. Given the abundance of published peer-reviewed articles about the use of AI in patients with lumbar PIVD in recent times, we expect to identify and gather an enormous quantity of relevant studies, to have an insight into the actual applications in the clinical practice.

Availability of Data And Materials

The findings of this review will be published in a relevant scientific journal or presented at national or international conferences by the reviewers.

Abbreviations

PIVD: Prolapsed intervertebral disc
MRI: Magnetic resonance imaging
AI: Artificial intelligence
PICOS: Population, Intervention, Comparison and Outcome
PRISMA: Preferred Reporting Items for Systematic Reviews and Meta-Analyses

MeSH: Medical Subject Headings
ROBINS-I: Risk OF Bias in Non-randomized Studies of Interventions
SEN: Sensitivity
SPE: Specificity
TP: True Positive
FP: False Positive
FN: False Negative
TN: True Negative
SROC: Summary Receiver Operating Characteristic
AUC: Area Under the Curve

Funding/ Support
The authors declare that there is no funding for this study.

ACKNOWLEDGEMENT

All authors contributed to the authorship of the manuscript and are listed in order of contribution. Initial conception and design (SP, MG, and RK); writing and revision (SP and MG).

REFERENCES

1. Vroomen PCAJ, de Krom MCTFM, Wilmink JT. Pathoanatomy of clinical findings in patients with sciatica: a magnetic resonance imaging study. J Neurosurg Spine. 2000 Apr;92(2):135–41.
2. Fatoye F, Gebrye T, Odeyemi I. Real-world incidence and prevalence of low back pain using routinely collected data. Vol. 39, Rheumatology International. Springer Verlag; 2019. p. 619–26.
3. Dydyk AM, Ngnitewe Massa R, Mesfin FB. Disc Herniation. 2023.
4. Hertling Darlene. Lumbar Spine. In: Hertling Darlene, M.Kessler Randolph, editors. Management of common musculoskeletal disorders: physical therapy principles and methods. 4th ed. Philadelphia, Pennsylvania: Lippincott Williams & Wilkins; 2006. p. 843–922.
5. Schroeder GD, Guyre CA, Vaccaro AR. The epidemiology and pathophysiology of lumbar disc herniations. Semin Spine Surg. 2016 Mar 1;28(1):2–7.
6. Singla DrS, Sharma DrR, Sharma DrR, Singh DrA, Dhillon DrAS, Satti DrSK. Comparison between clinical finding and magnetic resonance imaging finding of lumbar prolapsed intervertebral disc. International Journal of Orthopaedics Sciences. 2020 Oct 1;6(4):670–4.
7. Singh V, Malik M, Kaur J, Kulandaivelan S, Punia S. A systematic review and meta-analysis on the efficacy of physiotherapy intervention in management of lumbar prolapsed intervertebral disc. Int J Health Sci (Qassim) [Internet]. 2021 [cited 2023 Sep 8];15(2):49. Available from: /pmc/articles/PMC7934127/
8. Chan HCS, Shan H, Dahoun T, Vogel H, Yuan S. Advancing Drug Discovery via Artificial Intelligence. Vol. 40, Trends in Pharmacological Sciences. Elsevier Ltd; 2019. p. 592–604.
9. Hosny A, Parmar C, Quackenbush J, Schwartz LH, Aerts HJWL. Artificial intelligence in radiology. Vol. 18, Nature Reviews Cancer. Nature Publishing Group; 2018. p. 500–10.
10. Boon I, Au Yong T, Boon C. Assessing the Role of Artificial Intelligence (AI) in Clinical Oncology: Utility of Machine Learning in Radiotherapy Target Volume Delineation. Medicines. 2018 Dec 11;5(4):131.
11. Loftus TJ, Tighe PJ, Filiberto AC, Efron PA, Brakenridge SC, Mohr AM, *et al*. Artificial Intelligence and Surgical Decision-making. Vol. 155, JAMA surgery. NLM (Medline); 2020. p. 148–58.
12. D'Antoni F, Russo F, Ambrosio L, Vollero L, Vadalà G, Merone M, *et al*. Artificial intelligence and computer vision in low back pain: A systematic review. Vol. 18, International Journal of Environmental Research and Public Health. MDPI; 2021.

13. Shamseer L, Moher D, Clarke M, Ghersi D, Liberati A, Petticrew M, *et al*. Preferred reporting items for systematic review and meta-analysis protocols (prisma-p) 2015: Elaboration and explanation. Vol. 349, BMJ (Online). BMJ Publishing Group; 2015.
14. O'Connor D, Green S, Higgins JP. Defining the Review Question and Developing Criteria for Including Studies. In: Cochrane Handbook for Systematic Reviews of Interventions. Wiley; 2008. p. 81–94.
15. Sterne JA, Hernán MA, Reeves BC, Savović J, Berkman ND, Viswanathan M, *et al*. ROBINS-I: A tool for assessing risk of bias in non-randomised studies of interventions. BMJ (Online). 2016;355.
16. Yang Y, Jin G, Pang Y, Wang W, Zhang H, Tuo G, *et al*. The diagnostic accuracy of artificial intelligence in thoracic diseases. Medicine. 2020 Feb;99(7):e19114.
17. Deng R, Huang Z, Li X, Pei X, Li C, Zhao J. The effectiveness and safety of acupuncture in the treatment of lumbar disc herniation: Protocol for a systematic review and meta-analysis. Vol. 99, Medicine (United States). Lippincott Williams and Wilkins; 2020.

Indian Journal of Natural Sciences *www.tnsroindia.org.in ©IJONS*

Vol.15 / Issue 88 / Feb / 2025 *International Bimonthly (Print) – Open Access* *ISSN: 0976 – 0997*

RESEARCH ARTICLE

An Attempt to Appraise the Drinking Water Quality in a Spatial Setting : Case of Kalyan Dombivli Municipal Corporation

Sardar Ananda Patil[1] and Astha Smarth Kapur[2]*

[1]Professor, Department of Geography, Athalye-Sapre-Pitre College, (Affiliated to University of Mumbai), Devrukh, Ratnagiri, Maharashtra, India.
[2]Research Scholar, Department of Geography, University of Mumbai, Kalina Campus, Mumbai, Maharashtra, India.

Received: 24 Sep 2024 Revised: 20 Oct 2024 Accepted: 13 Aug 2024

***Address for Correspondence**
Astha Smarth Kapur,
Research Scholar,
Department of Geography,
University of Mumbai, Kalina Campus, Mumbai, Maharashtra, India.
E.Mail: asthasmarthkapur@gmail.com

ABSTRACT

Freshwater is a priceless natural resource. Its timeless property of being irreplaceable makes it indispensable. It serves countless purposes simultaneously. Albeit, when deliberating upon its direct consumption for personal use, it is quite natural that, a cardinal point, questioning its 'potability' is raised. Today, this holds foremost relevance for the masses. Therefore, the Bureau of Indian Standards (BIS) has issued certain guidelines with respect to potable water quality. Also, there are specific test parameters which decipher its quality, so as to pronounce it 'drinkable'. This study has been attempted with the objective of determining the quality of water made available to the residents of Kalyan Dombivli Municipal Corporation (KDMC). For this, the methodology of primary survey, entailing the collection of water samples (in non-monsoonal month of February) from various pre-selected sites, located within seven wards of KDMC (A,B,C,D,F,G,H) and their reconnaissance (laboratory-tests inclusive of-appearance, odor, alkalinity, pH, turbidity, TDS, chlorides, nitrates and hardness plus presence of E. Coli and Coliform bacteria), has been applied so as to generate first-hand information pertaining to potability of water supplied to the inhabitants on a daily basis. The pertinent BIS specifications have been consulted to draw meaningful conclusions in this regard. The major findings depict highest levels of hardness, TDS, chlorides, pH in Ward A, turbidity, pH and alkalinity levels are highest in Ward B. While, the biological impurities are mainly observed in raw water samples taken directly from 2 Rivers- Ulhas and Kalu, the principal water suppliers to the area.

Keywords: Kalyan Dombivli Municipal Corporation (KDMC), Bureau of Indian Standards (BIS), laboratory tests, test parameters, wards, water quality, water sample.

INTRODUCTION

It is an emphatically established fact that, 'Water' is the most priceless and life sustaining substance bestowed upon us, humans, by 'mother nature'. It possesses the timeless property of being irreplaceable as well. Its usage is not limited to quenching one's thirst alone, instead, its consumption extends into domestic use (maintaining cleanliness, hygiene and sanitation), industrial use, recreational use and food production as well, be it at the personal or community level. A series of water quality guidelines have been produced and issued by World Health Organization (WHO), [especially for the middle- and low-income countries] and by the Bureau of Indian Standards (BIS) [in reference to India], with the aim of facilitating a 'Framework of Safe Potable Water' which lays emphasis on 'drinking water quality'. This in turn favors the execution of 'water safety plans', to be abided by, the 'suppliers of water', so that, they can detect and mitigate the health risks that may arise while delivering the water from the catchment to the consumer. Its quality can be understood by running several laboratory tests. [1]. For the record, there is a pressing need to shed light on the facts and figures as promulgated by the World Health Organization. It was observed in 2022 that the drinking water source, used by nearly 1.7 billion people living around the globe was contaminated with fecal bacteria. This poses as one of the most hazardous risks, responsible for claiming lives, owing to violation of the water safety norms. Aside from this, in the same year, approximately 6 billion people, i.e., just 73 per cent of the world's population, had an access to safely managed drinking water within their premises. In case, the water available for drinking purpose is polluted with contaminants, it can prove to be a dangerous health hazard [1].India is no exception when discussing the water and health challenge. Amid the aforesaid troubleshooters, there persists a tenacious and crucial challenge of providing enough amount of safe and contaminant free, potable water to all. To maintain a satisfactory drinking water quality, BIS has ascertained the prescribed limit of certain chemicals/ irritants that may be present in water. Beyond the given limits, these irritants can plausibly interfere with the smooth working of the human body, in case, a person ingests such water. Thus, the prescribed range ought to be adhered, under all circumstances so as to be considered for consumption. The threat of water contamination even arises from the water distribution systems during instances of water leakage, dirty water or sewage infiltration, corrosion and rusting of the water pipelines, pollution of ground water, sea water infiltration into fresh water aquifer and leakage from septic tanks. These systems require continuous monitoring with a ready mechanism to repair or rectify the faults [2].

LITERATURE REVIEW

The relevant literature that has been read and reviewed in this regard, needs appropriate mention here. All of this literature (entailing the works of researchers from both India and abroad) deals with a variety of issues pertaining to the quality of water, which is available for direct consumption by the inhabitants of any given region. The literature also emphasizes the importance of drinking clean water lest, the consequences may pose disastrous impacts on human health, while projecting the ways and mechanisms to collect water samples and conduct a reconnaissance (inclusive of chemical and bacteriological examination) on them, to better understand its quality. Also, underscoring the vitality of such measures which are capable of decontaminating the same. Additionally, the review of literature suggests possibilities and options for quick, reasonable and effective methods that may be undertaken in order to treat and purify the available water, besides those treatment procedures that take place in water treatment plants. This literature review includes relevant works of eminent authors, as listed here. [3],[4], [5],[6],[7],[8],[9],[10], [11],[12],[13],[14],[15],[16],[17],[18],[19],[20],[21].

Study Area

The eminent twin cities of Kalyan and Dombivli along with other small townships, collectively fall within the jurisdiction of Kalyan Dombivli Municipal Corporation, whose headquarters are located at Kalyan, in Thane district in the Indian state of Maharashtra. The municipal corporation is a vibrant area, which is rapidly growing and developing. [22]. It sprawls over an area of 75.46 km^2. The Ulhas and Kalu Rivers (the principal water supply sources)

mark its northern borders. The areal bounds of the study region are demarcated by 19°11'50'' N to 19°18'35'' N Latitude and 73º 4'0'' E to 73°13'50'' E Longitude.[23]. Figure 1 depicts the location of study area in India.

Objective of the Study

This study has been performed so as to understand the potability level of Ulhas and Kalu Rivers (main sources of water supply within KDMC) as well as the water, that is supplied by the corporation (after purification) for consumption by the general public, residing in seven wards of Kalyan Dombivli Municipal Corporation. The objective here, is to examine the quality of the available water, by performing a series of laboratory tests.

DATABASE AND METHODOLOGY/ MATERIALS AND METHODS

It is an irrefutable fact that, any research study or investigation is based on two cardinal elements, namely; data sources used and methods/ techniques applied. For the current research, emphasis has been fundamentally laid on primary data collection from water sources (i.e., selected sample collection sites), located within the study area. While, methodology chiefly involves the use of laboratory tests of the collected water samples, based on BIS parameters. The following stanza presents a detailed overview of the pertinent methodology employed here. This study revolves around the details of the water samples, that have been meticulously collected from several locations in seven wards (A,B,C,D,F,G and H), predominantly encompassing households of varying types i.e., high income, middle income, chawls and slums, during the month of February. Samples have been gathered from 9 sites in Dombivli, 15 sites in Kalyan and 8 sites in Titwala. Chemical and bacteriological tests have been executed upon the collected samples in a laboratory setting for examining the presence of harmful chemicals and bacteria which may potentially raise a health alarm. With the help of the said procedures, an attempt has been made to determine the-physical appearance, presence of odour, levels of Turbidity, Potential of Hydrogen (pH), Nitrates, Chlorides, total Hardness, Alkalinity and Total Dissolved Solids (TDS) as well as, presence/absence of E. Coli and Coliform Bacteria. Parallelly, the parametrical 'limits' as prescribed by BIS have also been referred, for arriving at comprehensive conclusions regarding the quality of water, being provided to the people. Thus, water samples have been collected in 2 types of bottles, i.e., 100 ml sterilized glass containers (for bacteria testing) and 1 Liter fresh plastic bottles. Hereafter, the test report results have been entered into MS Excel, for further calculation. All the maps have been generated in ArcMap Software, using the Inverse Distance Weighted (IDW) Technique to showcase the isopleth coverage of the chemical and biological parameters considered, with the help of the water sample collection points data, that have been marked on the map using the latitude and longitude coordinates which have been noted, by means of the Global Positioning System (GPS). The maps demonstrate the spot-wise magnitude of concentration of the given parameters in the 7 wards of KDMC.

RESULTS (FINDINGS) AND DISCUSSIONS

Quality Analysis of the Collected Water Samples

It is vital to mention here that, the twin cities of Kalyan and Dombivli consist of 3 wards each, namely; B,C,D and F,G,H respectively. While, Ward A sprawls over a large space and entails within itself certain townships like; Atali, Mohili, Ambivli and Titwala. From all these wards, a total of 32 sites have been chosen for obtaining the water samples. Tests with respect to 11 parameters (9 chemical and 2 bacteriological parameters) have been conducted on the samples (cautiously gathered by the researcher). Figure 2 displays the map of *sample collection points*. A knowledge of these locational points is essentially relevant for a better understanding of the successive maps. The outcome of conforming to the aforementioned steps and procedures (as mentioned in 'methodology') has been articulated here for gainful coherence. Besides, the cohesiveness and connection among the selected parameters has also been brought out. The specifications as per the Indian Standards of 10500:2012, in terms of the chemical and bacteriological parametrical limits prescribed for potable water are presented in Table 1. Figure 3 depicts the 'appearance' referring to the *visual clarity* of the samples (whether clear or hazy). As can be seen in the map (figure 3), water samples procured from majority of the locations appear to be 'clear', barring those samples that have been

directly lifted from Ulhas River and Kalu Rivers, and those collected from the chawls/households in Titwala (Ward A). Figure 4 shows the distribution of Total Dissolved Solids (TDS) in water samples. Though all the values are much below the specified limit of BIS, it can be seen that, Ward A has the highest TDS levels, followed by Wards D, C and B (i.e., precisely the Kalyan City). The city of Dombivli represents such pockets where TDS touch the lowest levels. Proceeding forward, towards the analysis of Turbidity in water, the map in figure 5 suggests that, the turbidity levels are topmost in Ward B followed by the extreme end of Ward A. This is because, these sites happen to be the surface water bodies from where the samples of 'raw water' have been taken. Besides, the area in and around Titwala Gaon (Ward A) also reports high turbidity levels in the municipal water. Advancing onto the map denoting the distribution of Hardness in water (Figure 6), here as well, Ward A, followed by Wards, D, C and B, denote greater levels of hardness. Whereas, in Dombivli, few portions of Wards F and H depict lowest hardness levels.

This parametrical component indicates that, beyond the limit of 200 mg per liter, the water practically turns into hard water. The easternmost extremity of KDMC reveals that, the hardness values are below 200 mg but are over the 100 mg mark. According to this revelation, corporation water in Ward A, has the maximum hardness, followed by Wards D, C and B which exhibit comparatively lesser degree of hardness. A steady decline in the same, can be seen radiating outwards from here. Further ahead, from the map of Chloride distribution, (figure 7), it can be clearly perceived that, several pockets in Wards A and B, followed by Wards D and F project maximal Chloride quantities in water, while minimal quantities appear in Ward C of Kalyan, followed by Ward G of Dombivli. As a matter of fact, the maps in figures 3 to 7, have been presented in close succession because, these parameters of water quality function in correspondence with each other, so much so that, one component impacts the magnitude of the other. Turbidity is a measure of the 'cloudiness' present in water. This is a result of heavy concentration of visibly large amounts of undissolved suspended particulate matter. TDS is calculated based on the combined composition of organic and inorganic compounds existing in water. Higher turbidity can sometimes correlate with higher TDS in case the particles get dissolved. Nevertheless, they can be independently detected when, turbidity is caused due to insoluble particles. Hardness is chiefly an outcome of the occurrence of calcium and magnesium ions in water, which contribute to figuratively larger quantities of TDS. Higher hardness usually correlates with higher TDS since, both are influenced by the prevalence of dissolved minerals. The Chlorides too are influenced by the concentration of TDS as, higher chloride levels most commonly correlate with higher TDS levels. A rise in the concentration of one, leads to an affirmative upsurge in the other. Thus, making them directly proportional to each other. [25] Source: [26] Furthermore, the (potential of hydrogen) pH levels (Figure 8) are highest in Ward A and lowest in the 3 wards of Kalyan (i.e., Wards B,C,D). In contrast to the maps in the preceding figures, the situation in the 3 wards of Dombivli (F,G,H) depicts greater 'pH' levels. If the pH levels are high, it can be inferred that, instead of an acidic nature, the water available for common use, possesses a higher degree of basicity. This can be securely linked to the extent of alkalinity in water, since pH and Alkalinity go hand in hand. The map in Figure 9 portrays the spatial distribution of Alkalinity in the water samples. It is implicit from the BIS specification that, the limit of alkalinity must not exceed 200 mg per liter. It is observed that, this specification is upheld by the municipal water in all the wards of the study area and the limit of alkalinity does not exceed beyond 77 mg per liter at any of the sites. The maximum alkalinity (77 mg) is found in Ward A and the lowest levels are seen in Wards H and F of Dombivli City. Within Kalyan, Ward B displays greater alkalinity levels. In case of Ward A, both pH and Alkalinity levels are high.

It is imperative to note that, pH value indicates how acidic or basic the water is, while, alkalinity is a measure of the water's capacity to neutralize the acids. Higher alkalinity often helps in maintaining a stable pH by buffering against acidic changes, leading to a positive correlation between pH and alkalinity. [25] This condition holds true for Ward A, but suddenly turns anomalous in case of the three wards of Kalyan (B,C,D) and three wards of Dombivli (F,G,H). This functionality may be attributable to the chemical procedures of purification and refinement taking place at the Water Treatment Plants or may be due to the presence of some neutralizing agent in the water supply pipelines.
Moving ahead, towards the descriptive discussion regarding the presence and absence of biological impurities, as portrayed in the maps (Figures 10 and 11), it is visible that, 2 types of bacteria have been taken into account for estimating the extent of contamination. These entail; Escherichia coli (E. Coli) Bacteria and Coliform Bacteria. In both the maps (Figures 10 and 11), the presence of bacteria (noticed in lab test reports) is predominantly reported at two

locations, namely; the raw water samples obtained from Ulhas River (near Ward B) and Kalu River (near Titwala in Ward A), These spots have been earmarked with the help of 'Red Flag' pointers. All the remaining sample collection points illustrate an 'absence' of these germs/contaminants. It is pretty obvious that, these two sources contain the said germs due to possibility of mixing of germ-infested water or the excreta of infected humans or animals. The identified micro-organisms enter the water sources through ground pollution as these are predominantly present in human and animal body waste. This brings about faecal contamination of water. [27]. In generic terms, these microbes indicate the presence of bacteria and are not associated with any suspended or dissolved particulate matter, but in certain specific cases, these can even act as a function of turbidity if organic matter has a role to play in causing the adulteration. [25] Therefore, based on the source of contamination, these microbes may or may not be directly linked with turbidity.

Note: In case of the parameters relating to 'Odor' (smell in water) and 'Nitrates', the specific maps have not been prepared, owing to the fact that, the lab test report specified all the water samples to be odorless and as, being devoid of any Nitrates content, not even in negligible quantities. It stated the Nitrates to be *'Nil'.*

CONCLUSION

Amongst the 17 Sustainable Development Goals (SDGs); *'Ensuring Access to Clean Water and Sanitation for All'* is the *6th Goal* set by the United Nations. Along with the goals, comes the responsibility, which ought to be shouldered by India and every other nation that, these are substantially and effectively met with. Therefore, World Water Day, Toilet Day, Environment Day and Rivers Day have been introduced to generate awareness and upscale the efforts of the national youth plus the local authorities, to make meticulous use of this limited freshwater resource, whose demand is growing at a breakneck speed. Furthermore, the United Nations General Assembly declared a Water Action Decade beginning from 2018 till 2028. It was launched on 22nd March 2018, with the aim of addressing the growing challenge of water scarcity all over the planet, so as to prevent it from plunging into the gloomy abyss of a looming large-scale water crisis! [28]. Thus, it must be made a mandatory practice among the local/regional governing bodies to supply chemically and microbiologically safe and fit drinking water to the residents. For the smooth supply of purified and treated water to the masses, especially in the metro cities, it is rather imperative that the state and Centre, take up joint initiatives and also that, they function in close conjunction with the private players who can invest money and can generate the necessary infrastructure, employment as well as income for the benefit of the stakeholders. This will result in better quality tap water supplied by the respective corporations i.e. it should be in sync with the standards suggested by WHO or BIS and even raise the living standard of the people thus, raising their affordability to purchase it. [29] It is rather incumbent upon the authorities to provide chemically tested and purified as well as contaminant free water to the in-dwellers. Care must be taken to remove all harmful micro-organisms from the water in order to make it potable, since, these are capable of playing havoc with human lives and in some tragic situations can even prove to be fatal. In case of KDMC this requirement has been fulfilled to a large extent, with a couple of exceptions as have surfaced in case of Ward A, which needs to be looked into by the Urban Local Body. On the whole, the available water can be safely regarded as 'Potable or Drinkable'. This is greatly advantageous for the inhabitants thus, acting as a protective shield against water borne diseases.

REFERENCES

1. World Health Organization. Drinking-water. World Health Organization (WHO). 2023.
2. Henderson A, Roberts L, Bogan J, Rubin CH, Semenza JC. Water distribution system and diarrheal disease transmission: a case study in Uzbekistan. Am J Trop Med Hyg. 1998 Dec 1;59(6):941–6.
3. Zajic JE. Water pollution: disposal and reuse. 1st ed. Vol. 1. New York: M. Dekker; 1971. 1–389 p.
4. Gleick PH. Dirty water: estimated deaths from water-related diseases 2000-2020. Oakland: Pacific Institute for Studies in Development, Environment, And Security. 2002 Aug 15;1–12.

5. Sati VP, Sati VP. Water resource management and policy perspectives. 1st ed. Vol. 1. Jaipur: Pointer Publishers; 2004. x–318.
6. Ramesh R, Ramachandran S. Freshwater management. 1st ed. Vol. 1. New Delhi: Capital Publishing Company; 2005. 1–35 p.
7. Hooja R, Arora RK., Parnami KK. Water management: Multiple Dimensions. 1st ed. Hooja R, Arora RK., Parnami KK, editors. Vol. 1. Jaipur: Rawat Publications; 2007. 1–298 p.
8. Keshari AK. Water resources scenario of India: emerging challenges and management options. National Training Course on Farm Land and Water Management, Central Soil Salinity Research Institute, Karnal, Haryana. 2007 Mar;1:16–25.
9. Angelence JRG. Urban water potential in Madurai City. Deccan Geogr. 2010;48(1):41–8.
10. McDonald RI, Douglas I, Revenga C, Hale R, Grimm N, Grönwall J, Fekete B. Global urban growth and the geography of water availability, quality, and delivery. Ambio. 2011;40(5):437–46.
11. Huang J, Klemas V. Using remote sensing of land cover change in coastal watersheds to predict downstream water quality. J Coast Res. 2012;28(4):930–44.
12. Burton A. Drinking water quality: purifying drinking water with sun, salt, and limes. Environ Health Perspect. 2012 Aug 1;120(8):a305–a305.
13. Cronin AA, Prakash A, Priya S, Coates S. Water in India: Situation and prospects. Water Policy. 2014;16(3):425–41.
14. Zimmer A, Winkler IT, De Albuquerque C. Governing wastewater, curbing pollution and improving water quality for the realization of human rights. Waterlines, Practical Action Publishing. 2014 Oct;33(4):337–56.
15. Srinivasan V, Kumar SD, Chinnasamy P, Sulagna S, D. Sakthivel, P. Paramasivam, Lele S. Water management in the Noyyal River Basin: A situation analysis. Bengaluru: Ashoka Trust for Research in Ecology and the Environment (ATREE); 2014. 1–44 p.
16. Singh RB, Gahlot S, Singh A. Ecohydrological perspectives of declining water sources and quality in traditional water bodies in Delhi. In: Understanding Freshwater Quality Problems in a Changing World, Proceedings of H04. Gothenburg, Sweden: 2013 IAHS Press; 2013. p. 361–8.
17. Verhougstraete MP, Martin SL, Kendall AD, Hyndman DW, Rose JB. Linking fecalbacteria in rivers to landscape, geochemical, and hydrologic factors and sources at the basin scale. Environmental Sciences, Proceedings of the National Academy of Sciences. 2015 Aug 3;112(33):10419–24.
18. Chawan SV, Badekar R. Need for protecting river pollution: A case of Patalganga River in Raigad District, Maharashtra. Research Journal for Interdisciplinary Studies. 2016;2(1):27–37.
19. Nagare VB. Assessment of water level and water quality: A case study of Madha Taluka, Solapur District, Maharashtra. Deccan Geogr. 2016;39(45):39–45.
20. Nicholson KN, Neumann K, Dowling C, Gruver J, Sherman H, Sharma S. An assessment of drinking water sources in Sagarmatha National Park (Mt Everest Region), Nepal. Mt Res Dev. 2018;38(4):353–63.
21. Bessette J, Niblock E. Water quality pilot study for traditional water structure revitalization potential in the Deccan Plateau of India. Consilience. 2020;22:6–17.
22. Kalyan Dombivli Municipal Corporation. Revised city development plan, Published by KDMC. Kalyan; 2012.
23. Water Division-KDMC. Maps &shapefile. Kalyan: Kalyan Dombivli Municipal Corporation; 2021.
24. Survey of India. Onlinemapsportal. Online services to citizens, business and more, Survey of India, Ministry of Science and Technology, Government of India. 2021.
25. Abbasi SA, Chari KB. Water quality of Kaliveli Lake. In: Application of GIS and Remote Sensing in Environmental Management. New Delhi: Discovery Publishing House; 2005. p. 97–130.
26. Public Health laboratory KB. Report on chemical and bacteriological examination of water for drinking purposes. Belapur; 2023.
27. Pandey SN, Mishra SP. Environment and ecology. In: Environment and Ecology. New Delhi: Ane Books Pvt. Ltd.; 2011. p. 231–83.
28. United Nations Organization. Sustainable development goals: Goal 6 clean water and sanitation. United Nations Organization. 2023.
29. Ruet J, Saravanan VS, Zerah MH. The water &sanitation scenario in Indian metropolitan cities: resources and management in Delhi, Calcutta, Chennai and Mumbai. Delhi; 2002. (CSH Occasional Paper). Report No.: 6.

Maps and Tables pertaining to this Research Paper are placed in a serial orderly fashion here, for reference and perusal.

Table.1: Bureau of Indian Standards Specification of Normal Values 10500:2012

Test Parameter	Acceptable Limits	Permissible Limits
Physical Appearance	Clear	Clear
Odour	Agreeable	Agreeable
Turbidity (as N.T.U.)	1	5
pH Value	6.5-8.5	No Relaxation
Chlorides (as Cl)	250	1000
Nitrates (as NO_3)	45	No Relaxation
Total Hardness (as $CaCO_3$)	200	600
Alkalinity (as $CaCO_3$)	200	600
Total Dissolved Solids (TDS)	500	2000
Iron (as Fe)	0.3	No Relaxation
Fluoride (as F)	1	1.5

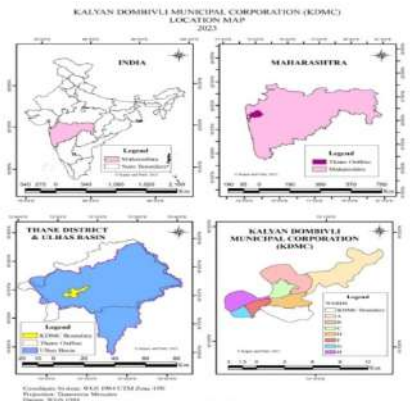

Figure.1:depicts the location of study area in India.
Source: [24][23]

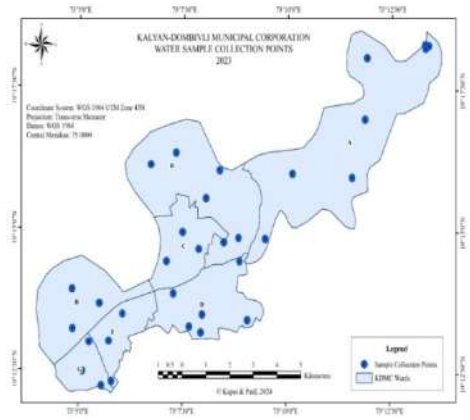

Figure.2:
Source: Water Quality Analysis based on Water Samples collected by the Researcher

Figure. 3
Source: Water Quality Analysis based on Water Samples collected by the Researcher

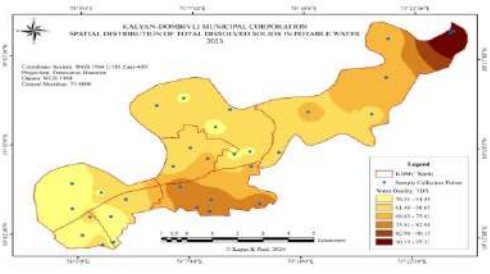

Figure. 4
Source: Water Quality Analysis based on Water Samples collected by the Researcher

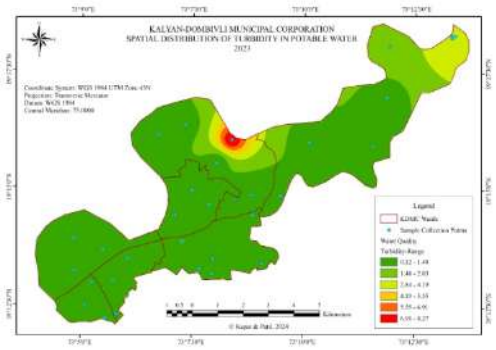

Figure. 5
Source: Water Quality Analysis based on Water Samples collected by the Researcher

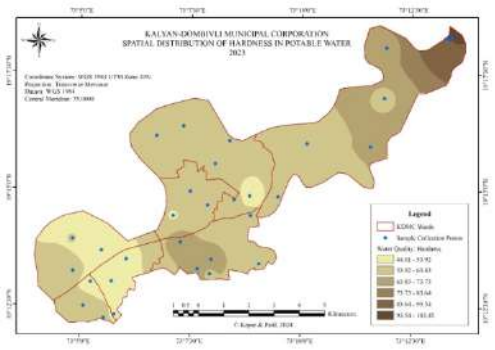

Figure. 6
Source: Water Quality Analysis based on Water Samples collected by the Researcher

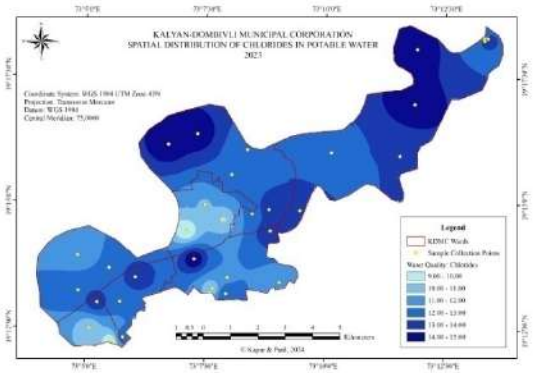

Figure. 7
Source: Water Quality Analysis based on Water Samples collected by the Researcher

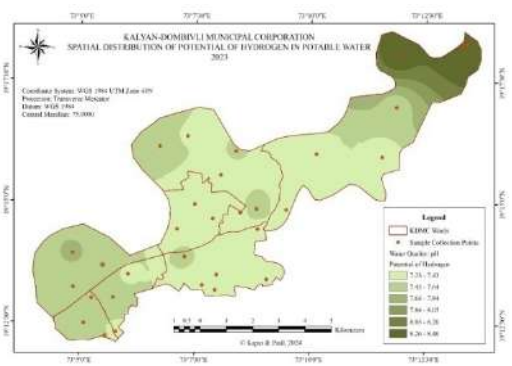

Figure. 8
Source: Water Quality Analysis based on Water Samples collected by the Researcher

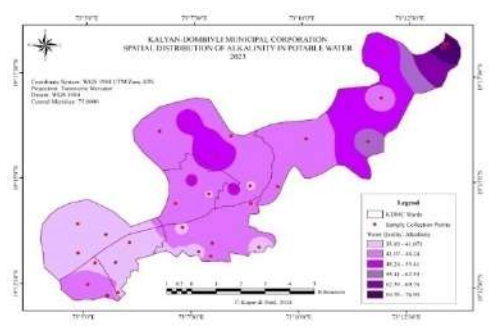

Figure. 9
Source: Water Quality Analysis based on Water Samples collected by the Researcher

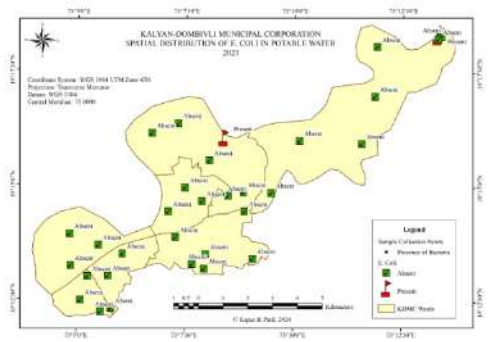

Figure. 10
Source: Water Quality Analysis based on Water Samples collected by the Researcher

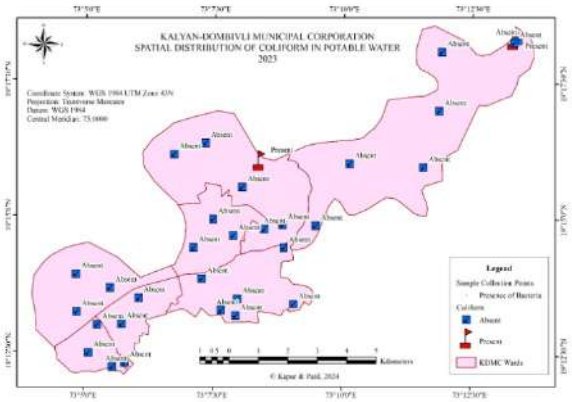

Figure. 11

Source: Water Quality Analysis based on Water Samples collected by the Researcher

Indian Journal of Natural Sciences www.tnsroindia.org.in ©IJONS

Vol.15 / Issue 88 / Feb / 2025 *International Bimonthly (Print) – Open Access* *ISSN: 0976 – 0997*

RESEARCH ARTICLE

Role of Nabhipooran with Murivenna Tail in Hypertension : A Case Report

Mihir H.Patel[1]*, Shivani Sanjeev Gavande[2] and Anjuna J[3]

[1]Post Graduate Scholar, Department of Dravyaguna, Parul Institute of Ayurved, Parul University, Vadodara, Gujarat, India.
[2]Professor, Department of Kayachikitsa, Parul University, Vadodara Gujarat, India.
[3]Assistant Professor, Department of Dravyaguna, Parul Institute of Ayurved, Parul University, Vadodara, Gujarat, India.

Received: 21 Nov 2024 Revised: 03 Dec 2024 Accepted: 13 Jan 2025

***Address for Correspondence**
Mihir H.Patel
Post Graduate Scholar,
Department of Dravyaguna,
Parul Institute of Ayurved, Parul University, Vadodara, Gujarat, India.
E.Mail: mihirpatel789.mp@gmail.com

ABSTRACT

This case report explores the ancient Ayurvedic concept of Nabhi (navel) and its therapeutic potential in managing hypertension. Nabhi, considered a vital energy centre, plays a significant role in maintaining the balance of the body's doshas (bio-energetic principles). This report discusses the successful use of Nabhipooran, an Ayurvedic treatment involving the application of Murivenna Tail (a medicated oil), in a hypertensive patient, highlighting its potential benefits in managing high blood pressure.

Keywords: Nabhi, Hypertension, Ayurveda, Doshas, Vata, Pitta, Murivenna Tail, Nabhipooran

INTRODUCTION

Hypertension, or high blood pressure, is a prevalent lifestyle disease associated with increased risk of heart, brain, and kidney disorders. Despite its severity, hypertension often remains undiagnosed, earning it the label of a "silent killer." In Ayurveda, hypertension is understood through the lens of vitiated doshas, particularly Vata and Pitta, affecting the srotas (body channels). Ayurveda emphasizes preventive care, and Nabhipooran, an external treatment involving the application of medicated oil to the navel, is believed to balance the body's energy and doshas. This case report presents the application of Murivenna Tail in Nabhipooran for managing hypertension.

Case Presentation

A 52-year-old male presented with a diagnosis of hypertension, with blood pressure readings consistently above 140/90 mmHg. The patient had a history of stress-related lifestyle factors contributing to his condition. He was

enrolled in a case study conducted at the Department of Kayachikitsa, Khemdas Ayurveda Hospital Parul University Vadodara.

METHOD

The patient underwent Nabhipooran treatment with Murivenna Tail for seven days. The procedure involved filling the navel pit with lukewarm Murivenna Tail and allowing it to remain for 30-45 minutes. The treatment was administered on an empty stomach, with care taken to avoid spillage of the oil.

MATERIALS

Murivenna Tail, an herbal oil, was used for the treatment. The oil contains coconut oil infused with medicinal herbs such as Pongamiaglabra, Spermacocearticularis, Piper betle, Aloe vera, Moringaoliefera, Erythrina variegate, Allium cepa, and Asparagus racemosus.

RESULTS

After seven days of Nabhipooran with Murivenna Tail, the patient's blood pressure readings showed significant improvement, reducing to 130/85 mmHg. The patient reported a reduction in stress and an overall sense of well-being. No adverse effects were observed during the treatment.

DISCUSSION

According to Acharya Charaka, sometimes it is neither possible nor it is necessary to identify a disease by a name. An Ayurvedic physician should attempt to construct the Samprapti of a given clinical condition based on the signs-symptoms and investigative findings in each case and should plan the management accordingly The disease hypertension is abnormality of RaktaDhatu popularly known as ShonitaDushti because Lakshanas are similar to that of hypertension are - Shiroruk, Klama, Anidra, Bhrama, BuddhiSammoha, Kampa which akin to the manifestation of hypertension. Mada, Murcha, Sanyasa equally true in relation to malignant hypertension (CharakaSamhita, Sutrasthana 24/11-17).

Importance of Nabhi Purana

Energy Convergence

Ayurveda teaches that the navel is a convergence point for several vital energy channels (Nadis) in the body, including the SushumnaNadi and the Manipura Chakra. These channels are believed to regulate the flow of Prana (life force energy) throughout the body.

Digestive Fire

The Nabhi or navel region is associated with Agni (digestive fire), which is crucial for digestion, metabolism, and assimilation of nutrients. Maintaining the balance of Agni in the Nabhi is believed to support optimal digestion and overall health.

Emotional Balance

According to Ayurveda, the Nabhi is also linked to the Manipura Chakra, which governs emotions, self-esteem, and personal power. Balancing the energy in this area may help promote emotional stability and mental clarity.

Blood Pressure regulation and role of Tridoshas

Blood pressure in the body is regulated by multiple mechanisms

Shorttermregulation
Neural mechanisms; by Prana Vata. Prana Vata takes help of Kapha in Barro receptor and Pitta in Chemo receptor.

Longtermregulation
Pressure Diuretics and Pressure Natriuresis - Apana Vata [AstangaSangraha, Sutra Sthana 20/2], Hormonal mechanisms – Pitta[11]

Etiological Risk Factors
Essential hypertension is idiopathic where exact etiology of the rise in Blood Pressure is not yet clear. There are many predisposing factors which causes hypertension are - Madhyapana, Excess Lavana intake, Sedentary lifestyle (Atisnigdha, Madhura, Ahara, Divaswapna), Mental stress (Krodha, Bhaya, Shoka), Physical strain (Shrama), Seasonal variation (Ritusandhi), BeejaDusthi. and Nidanarthaka Rogas Madhumeha, Sthoulya, Hridroga, VrikkaRoga, etc(CharakaSamhita, Sutrasthana 24/7-10).[12]

Samprapti

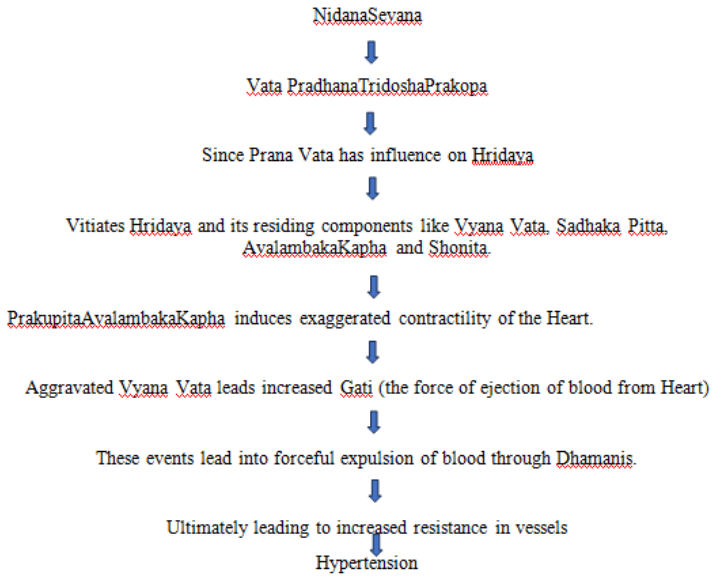

Samprapti Ghataka
1. Dosha - Prana, Udana, Vyana Vata, Sadhaka pitta, AvalambakaKapha
2. Dhatu - Rasa, Rakta, Mamsa, Medha
3. Upadhatu - Sira, Dhamani
4. Agni – Jatharagni&DhatwagniMandya
5. Srotas - Rasa, Rakta, Prana, ManovahaStrotas
6. Srotodustiprakara - Sangha, Vimargagamana
7. Udbhavasthana - Pakwashaya, Amashaya
8. Sancharasthana - SarvaSharira
9. Rogamarga - Madhyam
10. Sadhyasadhyata – Yapya

Benefits of Nabhi Purana
This is mostly done to combat vitiated Vata, especially Apana and Samana subtypes of Vata.

Nabhi Purana is highly beneficial in Vata induced painful conditions of the abdomen especially pain associated with colic, uterine pain or spasms due to dysmenorrhea (painful menstruation), urinary bladder pain and dysuria (painful urination), gaseous distension and bloating etc. Nabhi Purana helps in expelling the apanavayu. Thus it may help in relieving constipation and gases in the colon, setting right the functions of urinary bladder, bowel and uterus.
Nabhi Purana corrects functions of Samana Vayu and thus helps in correcting impairment of digestion. It may thus help in correcting digestive errors like indigestion and anorexia, which are roots of many disorders.
Nabhi Purana controls the Pitta and hence the pitta sthanas (pitta sites or seats of pitta). It also combats morbid pitta and regulates pitta activities, mainly those related with digest functions.

Drug Review
References - Yogagrantham

Principle - In this herbal oil the herbs are infused in the medium of coconut oil along with herb water decoction. Then the solid waste herb materials are filtered out. Thus, this oil contains oil soluble Phyto-active principles of medicinal herbs.

Ingredients
1. *Keratailam – Coconut oil*
2. *Karanja – Pongamiaglabra*
3. *Tuka – Spermacocearticularis*
4. *Tambul – Piper betle*
5. *Kumari – Aloe vera*
6. *Shigru – Moringaoliefera*
7. *Paribhadra – Erythrina variegate*
8. *Palandu – Allium cepa*
9. *Kanjika – Fermented liquid*
10. *Shatavari - Asparagus racemosus*

Nabhipooran with Murivenna Tail appears to have a beneficial effect on hypertension by balancing the Vata and Pitta doshas and improving the flow of prana (vital energy). The treatment's success suggests its potential as a complementary approach in managing hypertension, especially in patients with lifestyle-related stress factors.

CONCLUSION

This case report highlights the potential of Nabhipooran with Murivenna Tail as an effective Ayurvedic treatment for hypertension. Further studies with larger sample sizes and longer follow-up periods are recommended to validate these findings and explore the underlying mechanisms.

Source of funding
None

Conflict of interest
None

ACKNOWLEDGEMENT

None

REFERENCES

1. Shastri K, Chaturvedi G, Upadhyay Y, Sastri RD, Pandey G, editors. CharakaSamhita. Chowkhamba Sanskrit Series. 1998;2:25–3.
2. Vaidya BS. Bhavaprakasha of Bhavamishra. ChikitsastahanaAtisarachikitsa chapter 2 verse 40–41. ChoukambaOrientalia. 2016.
3. Ambulkar P, Chand T, Rao S, Dwivedi L. Makardhwaj as a Boon in Hypertension (VyanaBalaVaishamya): A Clinical Evaluation. National Seminar on Preventive Cardiology in Ayurveda. Rashtriya Ayurveda Vidyapeeth Publication. 2010.
4. WHO report on Prevention and control for Cardiovascular diseases. 2001-2002.
5. CharakaSamhita. YadavajiTrikamji. ChaukhambaSansritSansthana. Varanasi. 2009. Sutrasthana 18/46.
6. Patwardhan K. The history of the discovery of blood circulation: unrecognized contributions of Ayurveda masters. AdvPhysiol Educ. 2012;36:77e82.
7. Murthy Srikantha KR, editor. AsthangaSamgraha of Vagbhata. 9th ed. Chowkhambaorientalia. 2012. Sutra SthanaDoshabhedeeyaAdhyaya Chap 20 Verse 2.
8. Trikamji J, Ram N, editors. Commentary NibandhaSangraha of Dalhana on SushrutaSamhita of SushrutaShariraSthana. Chaukhambha Sanskrit Sansthan. 2012. Ch. 8 Verse 12.
9. Tripathy B, editor. CarakaSamhita of AgniveshaCharakaChandrika Hindi commentary. ChaukhambaOrientalia. 1999. ChikitsaSthana; Grahanidoshachikitsa Chapter-15 Verse 36.

Author contribution

Dr Shivani Gavande: Conceptualization, Method, Data creation, Original draft writing, Administration

Dr. Shivani Sanjeev Gavande. B.A.M.S.; M.D.; Ph.D.(AYURVED)
Professor – Kayachikitsa
Parul Institute of Ayurved & Research, Vadodara, Gujarat, India
drshivanigavande@gmail.com

Biography

Dr.Shivani Sanjeev Gavande is Ph.D. in Ayurveda, Masters in Kayachikitsa-Ayurveda and a Bachelor of Ayurvedic Medicine and Surgery. She has received HariAnanta Gold Medal for her research work under Ayurvidya, New Delhi. She is the Professor of Kayachikitsa at Parul Institute of Ayurved and Research, Vadodara,Gujarat, India and had been faculty and examiner of Maharashtra University of Health Sciences, Nasik. She is having 20 years of clinical and academic experience. Dr.Shivani Sanjeev Gavande has been resource person in various Ayurveda workshops and seminars. Also she has shared her valuable clinical experiences and Ayurvedic concepts in various national and international conferences. She has published her research articles in peer reviewed national and international journals. She was invested Ph.D. for her work in Enhancement of quality of life in patients having cancers of female genital organs. She has been worked for teenagers since last 22 years and socially active for women empowerment and environmental awareness. She is healer and councilor of mindfulness program, *satwavajayachikitsa* also volunteer of Aniruddha Academy of Disaster management. Dr Mihir Patel: Data creation, draft writing, review and editing, Project Administration.

Indian Journal of Natural Sciences www.tnsroindia.org.in ©IJONS

Vol.15 / Issue 88 / Feb / 2025 *International Bimonthly (Print) – Open Access* *ISSN: 0976 – 0997*

RESEARCH ARTICLE

To Evaluate and Compare the Effect of Micro - Osteoperforations on the Rate of Canine Retraction and RANKL Levels in Gingival Crevicular Fluid during Orthodontic Treatment

Bosy Thankam Mathew[1], I Girish Kumar[2], Jyothikiran H[3] and Raghunath N[4]*

[1]Post Graduate Scholar, Department of Orthodontics, JSS Dental College & Hospital, JSS Academy of Higher Education & Research (JSSAHER) (Deemed to be University), Mysuru, Karnataka, India.
[2]Lecturer, Department of Orthodontics, JSS Dental College & Hospital, JSS Academy of Higher Education & Research (JSSAHER) (Deemed to be University), Mysuru, Karnataka, India.
[3]Head and Professor, Department of Orthodontics, JSS Dental College & Hospital, JSS Academy of Higher Education & Research (JSSAHER) (Deemed to be University), Mysuru, Karnataka, India.
[4]Professor, Department of Orthodontics, JSS Dental College & Hospital, JSS Academy of Higher Education & Research (JSSAHER) (Deemed to be University), Mysuru, Karnataka, India.

Received: 28 Nov 2024 Revised: 09 Dec 2024 Accepted: 20 Jan 2025

***Address for Correspondence**
Raghunath N,
Professor,
Department of Orthodontics,
JSS Dental College & Hospital,
JSS Academy of Higher Education & Research (JSSAHER) (Deemed to be University),
Mysuru, Karnataka, India.
E.Mail:

ABSTRACT

The duration of orthodontic treatment is a concern with conventional fixed appliances To address this problem, several accelerating techniques to fasten the canine retraction has been proposed. This new era in orthodontics aims to accelerate tooth movement by activation of inflammatory processes and osteoclasts. Microosteoperforation is one of the simplest and safest methods to accelerate orthodontic treatment and improves patients' acceptance of the treatment, including adults. Limited studies have evaluated the overall effect of MOP on accelerating tooth movement, and its association with the levels of inflammatory markers. To evaluate and compare the rate of canine retraction on the microosteoperforation side and the conventional side. Also to evaluate and compare the effect of microosteoperforation on the levels of RANKL in GCF during different periods. A split- mouth study design was randomly assigned in which the canine of each side of the arch of each subject was divided into the micro-osteoperforation side and the conventional side. After the first premolar extraction micro-osteoperforation was performed on one side and conventional orthodontics was performed on the contralateral side. All the measurements were performed by direct technique from stone casts obtained before (T0), 28 days after retraction, and after the completion (T1) of retraction with the aid of a digital Vernier caliper. GCF was collected from the distogingival margin of the gingival of the canine to evaluate RANKL levels before retraction, 24 hours, and 28 days after

retraction. The paired difference in the mean rates of the canine retraction between micro- osteoperforation and conventional orthodontics after 28 days was 0.73±0.21mm/month, which was statistically significant (P<0.05). MOP was seen to be 1.88 folds faster than conventional orthodontics in the initial period. A significant difference was found in the level of RANKL in GCF 24 hours after retraction between the micro osteoperforation side and conventional side whereas no significant difference was found in the RANKL level in GCF at 28 days interval. Conclusion: The rate of canine retraction with conventional orthodontics during orthodontic treatment in the initial 28 days was 0.84±0.07mm/month, while in the Micro osteoperforation group, the rate of canine retraction treatment in the initial 28 days was 1.58±0.2mm/month. Micro osteoperforation showed a significant increase in the rate of canine retraction compared to conventional orthodontics during the initial 28 days but did not show a significant increase in the rate of retraction when complete retraction is considered. RANKL level in GCF on the conventional side during canine retraction after 24 hours was 1070pg/ml and after 28 days 838pg/ml and on the MOP side the level of RANKL was 1423pgml and after 28 days 855pgml. both the groups showed a significant increase in the levels of GCF during canine retraction after 24 hours and after 28 days compared to the level before retraction

Keywords: Micro-osteoperforation (MOP), Accelerated Orthodontics, Canine retraction, RANKL level

INTRODUCTION

Orthodontics and Dentofacial orthopedics is a branch of dentistry that deals with diagnosing, preventing, and correcting malpositioned teeth and jaws. Fixed orthodontic treatment achieved by applying constant force brings about different tooth movements, of principle to ideal occlusion. Orthodontic tooth movement is a continual and stable process characterized by deposition and resorption on tension and compression sites[1]. Two major theories of orthodontic movement govern tooth movement: biological electricity and pressure–tension in periodontal ligaments. The mechanical effects of orthodontic force on the periodontal ligament cells cause the release of cytokines, prostaglandins, and other chemical messengers[2]Patients, especially adults seeking orthodontic treatment always demand a shorter treatment time with excellent results and minimal discomfort. Reducing the treatment duration and the time-dependent adverse sequelae without compromising treatment efficiency has become challenging for orthodontic treatment[3].The demands led to the introduction of various procedures that attempted to shorten the duration since the 1890s, includinga linear cutting technique in cortical plates[4]. With time and study, an array of Accelerated Orthodontic Tooth Movement techniques with marginallyhostile procedures that shortened the duration of the treatment and patient's positive attitude and comfort levels during treatment has been introduced. Accelerated orthodontics based on the regional acceleratory phenomenon (RAP) is a viable alternative to conventional orthodontic treatment[5].Wilkodontics, the first technique to use the regional acceleratory phenomenon, has proven effective in accelerating tooth movement.The OTM is a complex tissue reaction to noxious stimulileading to increased osteoclastic and osteoblastic activity resulting in faster demineralization and remineralization of the alveolar process,thus reducing the treatment time[6].Different methods for accelerating tooth movement are categorized into biological through local or systemic administration of PG's, Growth hormone, Parathyroid hormone, Active form of vitamin D, and, RelaxinVitamin D,1,25 dihydroxycholecalciferol is a hormonal usage of vitamin D and plays a significantpart in calcium homeostasis with calcitonin and parathyroid hormones when injected, vitamin D metabolite on the PDL accelerated tooth movement by 60% [7].

Corticision is a minimally invasive where ascalpel and mallet pass through the gingiva and cortical bone without flapping. However, the repeated malleting procedure increased patient fear and discomfort[8].Prezocision is a flapless alveolar decortication where an ultrasonic tool is used to produce the incisions, a combination of piezoelectric cortical incisions apical to interdental papilla with selective tunneling, which allows additional tissue grafting. This method has been shown to have enhanced tooth movement and is comparatively less invasive[9].Low-level laser therapy is another non-invasive method that stimulatesclast and osteoblast and thus increases the rate of tooth movement by irradiating with Erbium, Chromium doped Yttrium Scandium Gallium Garnet laser, without

surgical flap reflection[10].Micro-osteoperforations (MOP) is another new, simple, and least invasive techniquethat can be used in combination with any orthodontic appliance to accelerate the tooth movement and change the sort of tooth movementof alveolar bone MOPs during orthodontic therapy to stimulate the release of inflammatory markers, leading to an increase in osteoclastic activity and the rate of tooth movement. MOPs were divided into two procedures: flap and flapless. In both procedures, alveolarbone remodelingis instigated by inducing minimal surgical trauma through 3 small shallow perforations to the alveolar bone by the tooth to which orthodontic force is applied. MOP increased tooth movement by 2.3-fold faster with flapless perforations than orthodontic force alone [11]. During Inflammation, they tend to increase in volume. RANKL is one of the novel members of the tumor necrosis factor (TNF) ligand family. The signaling and regulation of expression of RANKL play a critical role in bone remodeling during orthodontic movement. RANKL expressed by osteoblast and apoptotic osteocytes are responsible for the recruitment, differentiation, activation, and survival of osteoclast with the interaction between RANKL and RANK, a receptor on the cell surface of osteoclast and its precursors[12]. This study aimed at comparing the rate of canine retraction and the level of RANKL in GCF produced in response to micro-osteoperforation and conventional orthodontics where NiTi coil springs and implants are used for retraction.

Aims and Objectives

To evaluate the rate of canine retraction using conventional technique and micro-osteoperforation and compare the rate of canine retraction between conventional technique with micro-osteoperforation and to evaluate the level of RANKL in GCF in conventional technique and micro-osteoperforation and compare the levels of RANKL in GCF in conventional and micro-osteoperforation

METHODOLOGY

The study is completed in 2 years. The study group consists of 12 patients who presented to the Department of canine retraction is included in the study. Orthodontics and Dentofacial Orthopedics, JSS Dental College and Hospital, JSSAHER, Mysuru as outpatients. The total sample size was Twelve and the sampling procedure assumed at least a 2.3-fold difference in canine retraction between micro-osteoperforation and conventional technique, with a standard deviation of 1.6mm, and 1.4mm respectively at an α level of 1%, assuming the population size in 2 years as 1200, at least 12 subjects have to be studied (6 sides x2). The sample size has been calculated with finite population correction. In Inclusion criteria. The patient was seeking orthodontic treatment with one premolar extraction. The age range of 16-25 years, No systemic disease, Probing depth of ≤4mm in all teeth, Gingival index≤1, Plaque index≤1, Non-smokers, No radiographic evidence of bone loss, and, No current active periodontal disease In exclusion criteria, Patienthistory, corticosteroids, and calcium channel blockers., systemic disease, Radiographic and clinical evidence of bone loss, Gingivitis and periodontitis, and Current active periodontal disease. The estimated sample size was 12. Patients satisfying the inclusion criteria, requiring premolar extraction, and being included in the study were asked to sign a consent form. A split-mouth study was designed with micro-osteoperforation on the experimental side and control on the opposite side.

Micro-osteoperforation technique

Micro-osteoperforations were performed on 2 to 4 distal sidesof the canine before retraction on the experimental side. (T0) Post administration of local anesthesia2-4. Mini implants were placed 1-2 mm distal to the canine in the extraction space It was created using 1.2 mmmini–implant drill bits to a depth of 5 mm using a hand driver(Fig 1). The implant drill bits were progressed using a file stop to ensure a consistent depth of 5mm.The arch wire was ligated to the bracket with ligature wire, retraction initiated with mini-screws of 8mm in length and 1.3 mm diameter, and NiTi closed coil spring of 6 mm engaged from the canine to the implant placed at the mucogingival junction to retract the canine.Patients were seen 24 hours after the retraction initiation and at a 28-day interval until retraction was completed. Irreversible hydrocolloid alginate impressions were taken after 28 days and post a complete canine retraction, and the impression was poured with dental stone. The cast was labeled with the patient's outpatient number and date.

GCF Sample collection

GCF samples were collected before the start of the procedure and at 24 hours and one month after applying orthodontic force for canine retraction. The collection site was insulated with cotton rolls, and a supragingival plaque was removed with a curette without touching the gingival margin. The site was gently dried with an air syringe, and a saliva ejector was used to avoid any saliva contamination(Fig 2). GCF samples were collected from the distal cervical gingival margin of the upper canine of both experimental and control sites before any clinical intervention. GCF samples were obtained by placing a calibrated, volumetric microcapillary pipette of an internal diameter of 1.1mm with a capacity of 5 microliters over test sites. A standard volume of 5 microliters of GCF was collected from both sites.The collected GCF was diluted to 100 microliters with phosphate buffer. The samples were kept in polypropylene tubes at -90 degrees Celsius before analysis. Samples were analyzed with the enzyme-linked immune sorbent assay (ELISA) technique(Fig 3). The Storage preserved in standard detection reagent A, detection reagent B, and the 96 healthy strip plates were stored at -20°C while the others were stored at 4°C.

Assay procedure

Shafts for diluted standard, blank, and GCF samples were determined. 7 shafts were prepared for standard, 1 well 100 microliter standard, blank, and GCF dilutions into the appropriate wells (Fig 4). Covered with the plate sealer and incubated for 1 hour at 37°C. The liquid in each well is then removed but not washed. 100 microliter of detection reagent A working solution was added to each well, covered with a plate sealer, and gestated at 37°C for 1 hour. The answer was aspirated and washed with 350 microliters of 1x wash solution to well using a squirt bottle, multi-channel pipette, manifold dispenser, or auto washer and kept for 1-2 minutes. The remaining liquid was obliterated from all wells by snapping the plate into absorbent paper. Wash washed 3 times. After the latter wash, remove any remaining wash by aspirating in the plot against absorbent paper. 100 microliter of detection reagent B working solution was added to each well, covered with the plate sealer incubated for 30 minutes at 37°C. The Wash process has been repeated a total of about 5 times.90 microliter of substrate solution were added to each well, covered with a new plate sealer, and incubated for 10-20 minutes at 37°C. The liquid turned blue with substrate solution and 50 microliters of stop solution added to each well. The liquid turned yellow with the addition of a stop solution. A drop of water, F, and C points on the pre-retraction cast. The acrylicpadequivalent to the F point and C point on the retraction castfingerprint at the bottom of the plate was detached. The microplate reader was then run, and the measurement at 450nm was conducted. Calculation of results: the duplicate readings of each standard, control, and GCF sample are averaged and subtracted from the average zero standard optical densitya standard RANKL concentration on the Y-,axis and the density curve is constructed by placing the M.O.D and concentration.

RESULTS

This study aimed to evaluate the rate of canine retraction using micro-osteoperforation and compare it with conventional orthodontics. The sample comprised 12 patients, 12 sites for micro osteoperforation, and 12 for conventional orthodontics, separately. The sample comprised 4 male and 8 female patients with a mean age16.6±3.3years (Fig 6). In arandomized split-mouth study, micro-osteoperforation was performed on one side, and on the contralateral side, conventional orthodontics was performed. The maximum distance enclosed during canine retraction for the micro osteoperforation group was 4.98 mm and 4.82mm for the conventional group,respectively (Table 1). The minimum distance covered during canine retraction was 3.17mm microosteoperforation group (Table 2) and 3.20mm for the conventional group. The mean distance covered was 4.12±0.60mm for the microosteoperforation group and 4.04 ± 0.49mm for the conventional group, respectively(Table 3). The maximum rate of canine retraction after 28 days for the micro osteoperforation group was1.94 mm/month and 0.97mm/month for the conventional group(Table 4). The minimum rate of canine retraction was 0.98 mm/month for the microosteoperforation group and 0.70 mm/month for the conventional group (Table 5)and (Fig 7). The mean rate of canine retraction is 1.58±0.27mm/month for the microosteoperforation group and 0.84±0.08 mm/month for the conventional group, respectively. The paired difference in rates of canine retraction was0.73±0.21mm/month, which

was statistically significant (P<0.05). Microsoteoperforation was seen to be 1.88 folds faster than conventional orthodontic treatment (Table 6). Paired Samples Test

The maximum rate of canine retraction after complete retraction for the microosteoperforation group was 1.00 mm/month and 0.88 mm/month for the conventional group. The minimum rate of canine retraction was 0.70 mm/month for the micro osteoperforation group and 0.67 mm/month for the conventional group. The mean rate of canine retraction was 0.84±0.06mm/month for the microosteoperforation group and 0.80±0.06 mm/month for the conventional group, respectively(Table 7) and (Fig 8). The paired difference in the rates of the canine retraction was0.041±0.7 mm/month, which was not statistically significant (P>0.05).There was no significant difference in the rate of canine retraction between the micro osteoperforation group and the conventional group. The mean level of RANKL in GCF (Table 8 and (Table 9) on the conventional side before retraction (baseline) was found to be 770±39.59 pg/ml, after 24 hours, the mean level was 1070.25±158.97, and after 28 days 838.58±44.12 respectively(Table 10 and Table 11). A statistically significant difference was found in the level of RANKL in GCF during canine retraction on the conventional side from baseline to 24 hours, baseline to 28 days, and 24 hours to 28 days. The mean level of RANKL in GCF on the micro osteoperforation side before retraction (baseline) was found to be 774±40.1 pg/ml. After 24 hours, the mean level was 1423.58±220.75, and after 28 days, 855.58±98.53, respectively (Table 12 and Table 13). A statistically significant difference was found in the level of RANKL in GCF during canine retraction on the micro osteoperforation side from baseline to 24 hours, baseline to 28 days, and 24 hours to 28 days.

DISCUSSION

Orthodontics is an uninterruptedly evolving field that attempts to effectively and efficiently achieve a pretty and aesthetic face laterally with stable occlusion. Anaesthetic smile goes a long way in improving a person's self-confidence. The average orthodontic treatment duration of fixed orthodontic treatment ranges from 18-24 months. The estimated amount of tooth movement is 0.35 to 2.04 mm per month. Because of this prolonged treatment duration, the risk associated with it, and the associated social and psychological impact, patients, especially adults, are discouraged from undergoing treatment. Regional acceleratory phenomenon (RAP) is a localized soft and hard tissue response to stimuli characterized by increased perfusion and bone turnover and decreased bone density. Bone turnover is well known to be augmented after a bone fracture, osteotomy, or bone grafting. Various techniques using the RAP phenomenon includecorticotomy, periodontal distraction, piezocision, microosteoperforation, and biomodulation using lasers[13].The corticotomy-assisted orthodontics, precision-aided orthodontics, and surgery-first orthodontics depend oncautious injury to the alveolar or basal bones to accelerate orthodontic tooth movement by activating the regional acceleratory phenomenon (RAP)[14].Wilko reported Wilckodontics in 2001 that the acceleration of tooth movement is not due to the bony block movement. It is a process of bone remodeling at the surgical site, called the regional acceleratory phenomenon (RAP). He developed and patented techniques called accelerated orthodontics (AOO) and periodontal accelerated osteogenic orthodontics (PAOO). RAP was modified by adding bio-absorbable grafting material over the injured bone to enhance healing[15].Precision is a flapless method of corticotomy, using piezosurgery to reduce the injury associated with conventional corticotomy. Low-level laser therapy (LLLT) is one of the most encouraging approaches today. Laser has a bio-stimulatory effect on bone regeneration, which is seen in the mid-palatal suture during rapid palatal expansion and it stimulates bone regeneration after bone fractures and on the extraction sites. The low-energy laser irradiation enriched the rate of tooth movement via RANK/RANKL and the macrophage colony-stimulating factor and its receptor expression Vibrations. Propel was introduced by Propel Orthodontics to reduce the invasive nature of surgical irritation of bone and is used to perform MOP on the alveolar bone. This device comes as a ready-to-use sterile disposable device. A biologically active substance known as a biomarkeris articulated by cells inside the periodontium in response to mechanical stimuli. Various inflammatory mediators like cytokines are released, which can activate the formation of arachidonic acid metabolites[16] This present research is done to compare and evaluate the effect of MOP on the rate of canine retraction after one month and after complete retraction and RANKL expression in the gingival crevicular fluid during the orthodontic treatment mini implant drill bit is used to carry out micro-osteoperforation. The sample

consisted of 12 patients, 8 female, and 4 male patients. The study was a split-mouth study with 12 sites for micro-osteoperforation and control, respectively. Many factors that could affect the forces of occlusion can significantly affect the rate of tooth movement.

Occlusion

To rule out the effect of occlusion in this study, we selected patients with similar malocclusion severities requiring premolar extraction. Premolar extraction is a relatively standard treatment protocol, especially in patients with dental protrusion and dental crowding. In addition, to eliminate the possibility of uneven occlusal forces from typical occlusion mainly on one side, MOPs were randomly assigned to the left or right side of each patient. The canines were selected because they were free from occlusal interferences. Any occlusal interferences during canine retraction were checked, but none was found that required occlusal adjustment[17].

Type of tooth movement

Another major factor affecting the rate of tooth movement. This study attempted to achieve bodily movement using NiTi closed coil springs, extending from the implant placed between the 2nd premolar and molar to the canine bracket. It was also done to avoid any difference in the rate of retraction due to unequal retraction forces. The force value for canine retraction was 150 gms on both sides as it is the optimum value for bodily movement of the canine[18].

Age It can play a significant role in the rate of tooth movement. It eliminated the effect of age on the rate of tooth movement, only adults between 16 and 25 years with a mean age of 16.6±3.3years were selected for this study, and the average ages in both groups were similar.

Extractions It's another factor that can change the rate of tooth movement by increasing the activity of inflammatory markers, which could obscure the effect of MOPs minimizes the possibility in our study; extraction was done at the start of the treatment, 6 months before canine retraction.

Gender_Another factor that affects the rate of tooth movement. Unfortunately, this study could not eliminate this variable because of the limited number of male participants in this study[19]

CONCLUSION

Within the limitations of this study, it concluded that the rate of canine retraction with conventional orthodontics during orthodontic treatment in the initial 28 days was 0.84±0.07mm/month and after complete retraction was 0.80±0.06mm/month, while in the Micro osteoperforation group, the rate of canine retraction treatment in the initial 28 days was 1.58±0.2mm/month and after complete retraction was 0.84±0.06mm/month. Micro osteoperforation showed a significant increase in the rate of canine retraction compared to conventional orthodontics during the initial 28 days but did not show a significant increase in the rate of retraction when complete retraction is considered. RANKL level in GCF on the conventional side during canine retraction after 24 hours was 1070pg/ml and after 28 days 838pg/ml and on the MOP side, the level of RANKL was 1423pm, and after 28 days 855pgml. Both the groups showed a significant increase in GCF levels during canine retraction after 24 hours and after 28 days compared to before retraction. RANKL level showed a significant difference in the level of GCF on the micro osteoperforation side compared to the conventional side after 24 hours and did not show a significant difference in the RANKL level after 28 days.

REGULATORY STATEMENT

This study was conducted following all the provisions of the local human subjects oversight committee guidelines and policies of JSS Dental College and Hospital Institutional Ethics Committee, JSS Academy of Higher Education and Research.

REFERENCES

1. Frost HM. The Regional Accelerator Phenomenon: A Review. : Henry Ford Hosp Med J 1983;31(1):3-9.
2. M Thomas Wilcko 1, William M Wilcko, Jeffrey J Pulver, Nabil F Bissada, Jerry E Bouquot, Accelerated osteogenic orthodontics technique: a 1-stage surgically facilitated rapid orthodontic technique with alveolar augmentation - J Oral Maxillofac Surg 2009 Oct;67(10):2149-59.
3. Kumar S, Yadav S, Bhowmick D, Prabhat M, Sreedhar A. Periodontally Accelerated Osteogenic Orthodontics (PAOO): Perio-Ortho Interrelationship, 2016 1 (1):38-43.
4. Wilko WM, Wilko T, Bouquot JE, Ferguson DJ. Rapid orthodontics with alveolar reshaping: two case reports of decrowding. Int J Periodontics Restorative Dent. 2001 Feb;21(1):9–19
5. Addanki P, Gooty JR, Palaparthy R. Periodontally Accelerated Osteogenic Orthodontics (PAOO) - An Updated Literature Review and Recent Advances: Natl J Integr Res Med. 2016;7(4):140–6
6. Andrade I, Taddei SRA, Souza PEA. Inflammation and Tooth Movement: The Role of Cytokines, Chemokines, and Growth Factors. Semin Orthod. 2012 Dec 1;18(4):257 -69
7. Avinash BettahalliShivamallu, Aishwarya Ramkumar, N Raghunath. Evaluation and Comparison of the Rate of Canine Retraction Using Two Accelerated Orthodontic Treatment Techniques: An In Vivo Study. World J Dent. 2020 May;11(2):105–11.
8. Einy S, Horwitz J, Aizenbud D. Wilckodontics--an alternative adult orthodontic treatment method: rationale and application. Alpha Omegan. 2011 Fall-Winter;104(3–4):102–11
9. Alikhani M, Raptis M, Zoldan B, Sangsuwon C, Lee YB, Alyami B. Effect of micro-osteoperforations on the rate of tooth movement. Am J OrthodDentofacOrthop Off Publ Am Assoc Orthod Its Const Soc Am Board Orthod. 2013 Nov;144(5):639–48.
10. Nimeri G, Kau CH, Abou-Kheir NS, Corona R. Acceleration of tooth movement during orthodontic treatment - a frontier in Orthodontics. Prog Orthod. 2013 Oct 29;14(1):42.
11. Alikhani M, Alansari S, Sangsuwon C, Alikhani M, Chou MY, Alyami B, *et al*. Micro-osteoperforations: Minimally invasive accelerated tooth movement. Semin Orthod. 2015 Sep 1;21(3):162–9.
12. Tasi C-Y, Yang TK, Hsieh H-Y, Lin LY. Comparison of the effects of micro-osteoperforation and concision on the rate of orthodontic tooth movement in rats. Angle Orthod. 2016 Jul;86(4):558–64.
13. Sangsuwon C, Alansari S, Nervina J, Teixeira CC, Alikhani M. Microosteoperforations in accelerated orthodontics. Clin Dent Rev. 2017 Dec 6;1(2):1–10.
14. Makoto Nishimura 1, Mirei Chiba, Toshiro Ohashi, Masaaki Sato, Yoshiyuki Shimizu, Kaoru Igarashi, Hideo Mitani, Periodontal tissue activation by vibration: intermittent stimulation by resonance vibration accelerates experimental tooth movement in rats; Am J Orthod Dentofacial Orthop 2008 Apr;133(4):572-83.
15. Wilcko MT, Wilcko WM, Pulver JJ, Bissada NF, Bouquot JE. Accelerated osteogenic orthodontics technique: a 1-stage surgically facilitated rapid orthodontic technique with alveolar augmentation. J Oral Maxillofac Surg Off J Am Assoc Oral Maxillofac Surg. 2009 Oct;67(10):2149–59.
16. Robert J Herman 1, G Frans Currier, Alan Miyake. Mini-implant anchorage for maxillary canine retraction: a pilot study. Am J Orthod
17. Sugimori T, Yamaguchi M, Shimizu M, Kikuta J, Hikida T, Hikida M, *et al.* Micro-osteoperforations accelerate orthodontic tooth movement by stimulating periodontal ligament cell cycles. Am J Orthod Dentofac Orthop Off Publ Am Assoc Orthod Its Const Soc Am Board Orthod. 2018 Dec;154(6):788-96
18. Attri S, Mittal R, Batra P, Sonar S, Sharma K, Raghavan S, *et al.* Comparison of tooth movement and pain perception during accelerated tooth movement associated with conventional fixed appliances with micro-osteoperforations - a randomized controlled trial. J Orthod. 2018;45(4):225–33
19. Mani Alikhani, Sarah Alansari, ChinapaSangsuwon, Mona Alikhani, Michelle Yuching Chou, Bandar Alyami, Jeanne M. Nervina, and Cristina C. Teixeira; Micro-osteoperforations: Minimally invasive accelerated tooth movement; Seminars in Orthodontics, Vol 21, No 3 (September), 2015: pp 162–169

Table.1: Rate of canine retraction on the Control side- a conventional technique

Sample no.	Distance from C point to F point before retraction in mm- A mm	Distance from C point to X point after retraction in mm- B mm	Distance covered during retraction (A-B) in mm	Time (Intervals) taken for the retraction (T) in months.	Rate of canine retraction in mm after 28 days	Rate of canine retraction (A-B/T) in mm
Con PT 1	23.06	18.96	4.1	5.1	0.84	0.79
Con PT 2	22.39	18.19	4.2	6.0	0.75	0.7
Con PT 3	23.70	18.88	4.82	5.8	0.95	0.82
Con PT 4	23.18	19.25	3.93	5.8	0.70	0.67
Con PT 5	20.50	17.15	3.35	4.4	0.78	0.75
Con PT 6	22.80	19.37	3.43	4.2	0.86	0.8
Con PT 7	23.47	19.19	4.28	4.85	0.89	0.88
Con PT 8	22.18	17.66	4.52	5.1	0.97	0.87
Con PT 9	21.65	17.47	4.18	5.3	0.80	0.78
Con PT 10	19.85	16.65	3.20	3.8	0.85	0.83
Con PT 11	22.82	18.44	4.38	5.03	0.88	0.87
Con PT 12	22.08	17.93	4.15	5.1	0.83	0.80

Table.2: Rate of canine retraction on the Experimental side – with micro-osteoperforation

Sample no	Distance from C point to F point before retraction in mm- A mm	Distance from C point to X point after retraction in mm- B mm	Distance covered during retraction (A-B) in mm	Time (Intervals) taken for the retraction (T) in months.	Rate of canine retraction in mm after 28days	Rate of canine retraction (A-B/T) in mm
MOP PT 1	22.06	18.06	4.08	5.1	1.69	0.80
MOP PT 2	21.39	17.38	4.01	4.2	1.36	1.00
MOP PT 3	23.98	19.00	4.98	6.2	1.90	0.80

MOP PT 4	24.18	20.22	3.96	5.6	0.98	0.70
MOP PT 5	20.56	17.13	3.43	3.0	1.37	0.90
MOP PT 6	22.82	19.42	3.44	4.3	1.52	0.80
MOP PT 7	23.57	19.22	4.35	4.7	1.78	0.92
MOP PT 8	22.11	17.25	4.86	5.7	1.94	0.85
M0P PT 9	22.65	17.85	4.26	4.8	1.61	0.87
MOP PT 10	18.85	15.68	3.17	3.4	1.37	0.92
MOP PT 11	22.82	18.37	4.45	4.8	1.78	0.92
MOP PT 12	22.18	18.06	4.12	5.02	1.66	0.82

Table.3: **Distance covered during retraction**

Group	N	Maximum distance (mm)	Minimum distance (mm)	Mean (mm)	SD
Microsoteoperforation	12	4.98	3.17	4.12750	.59236
Conventional orthodontics	12	4.82	3.20	4.04500	.48976

Table.4: Rate of retraction after 28 days

Group	N	Maximum distance (mm)	Minimum distance (mm)	Mean (mm)	SD
Microsoteoperforation	12	1.94	0.98	1.58	.27495
Conventional orthodontics	12	0.97	0.70	.8417	.07779

Table.5: **The paired difference between the mean rate of retraction between microosteoperforation and conventional side after 28 days**

		Paired Differences		t	df	Sig. (2-tailed)
		Mean	Std. Deviation			
Pair 1	Microsoteoperoration – conventional orthodontics	.73833	.20801	12.296	11	.000 (p<0.05)

Table.6: **mean rate of canine retraction on the microosteoperforation side and conventional side after complete canine retraction**

Group	N	Maximum (mm/month)	Minimum (mm/month)	Mean (mm/month)	SD
Microsoteoperforation	12	1.00	0.70	0.84	0.067
Conventional orthodontics	12	0.88	0.67	0.80	0.067

Table.7: **The paired difference between the mean rate of retraction between microosteoperforation and conventional side after complete canine retraction**

Paired Samples Test					
	Paired Differences		t	df	Sig. (2-tailed)
	Mean	Std. Deviation			
Pair1 microosteoperforation-conventional	.04167	.07987	1.807	11	.098 (p>0.05)

Table .8: RANKL level in GCF during canine retraction on the conventional side

Sample no	Before the start of retraction	24 hours after retraction	28 days after retraction
Con PT 1	743	1050	842
Con PT 2	730	958	960
Con PT 3	796	1345	833
Con PT 4	834	840	850
Con PT 5	752	1028	820
Con PT 6	845	1171	840
Con PT 7	750	1262	835
Con PT 8	739	1050	850
Con PT 9	746	848	786
Con PT 10	801	987	844
Con PT 11	779	1246	815
Con PT 12	735	1058	787

Table. 9: **RANKL level in GCF during canine retraction on the micro osteoperforations**

Sample no	Before the start of retraction	24 hours after retraction	28 days after retraction
MOP PT 1	745	1450	850
MOP PT 2	732	1151	1160
MOP PT 3	796	1645	813
MOP PT 4	834	1068	850
MOP PT 5	752	1328	820
MOP PT 6	845	1571	845
MOP PT 7	750	1675	825
MOP PT 8	739	1756	854
M0P PT 9	752	1348	796
MOP PT 10	820	1187	854
MOP PT 11	782	1546	810
MOP PT 12	742	1358	790

Table.10: Paired sample statistics for RANKL level in GCF on the conventional side

		Mean	N	Std. Deviation
Pair 1	baseline	770.83	12	39.59
	24 hours	1070.25	12	158.97
Pair 2	baseline	770.83	12	39.59
	28 days	838.50	12	44.12
Pair 3	24 hours	1070.25	12	158.97
	28 days	838.50	12	44.12

Table.11: **Paired difference in the RANKL level in GCF during canine retraction on the conventional side.**

		Paired Differences		t	df	Sig. (2-tailed)
		Mean	Std. Deviation			
Pair 1	Baseline – 24 hours	-299.41667	159.71592	-6.494	11	.000
Pair 2	Baseline- 28 days	-67.66667	61.06976	-3.838	11	.003
Pair 3	24 hours – 28 days	231.75000	170.47107	4.709	11	.001

Table.12: **Paired sample statistics for RANKL level in GCF on the micro osteoperforation side**

		Mean	N	Std. Deviation
Pair 1	Baseline	774.08	12	40.12
	24 hours	1423.58	12	220.75
Pair 2	Baseline	774.08	12	40.12
	28 days	855.58	12	98.53
Pair 3	24 hours	1423.58	12	220.75
	28 days	855.58	12	98.53

Table.13: **paired difference in the RANKL level in GCF during canine retraction on the micro osteoperforation side**

		Paired Differences		t	df	Sig. (2-tailed)
		Mean	Std. Deviation			
Pair 1	baseline – 24 hours	-649.50	231.16	-9.733	11	.000
Pair 2	baseline – 28 days	-81.50	114.70	-2.462	11	.032
Pair 3	24 hours – 28 days	568.00	274.61	7.165	11	.000

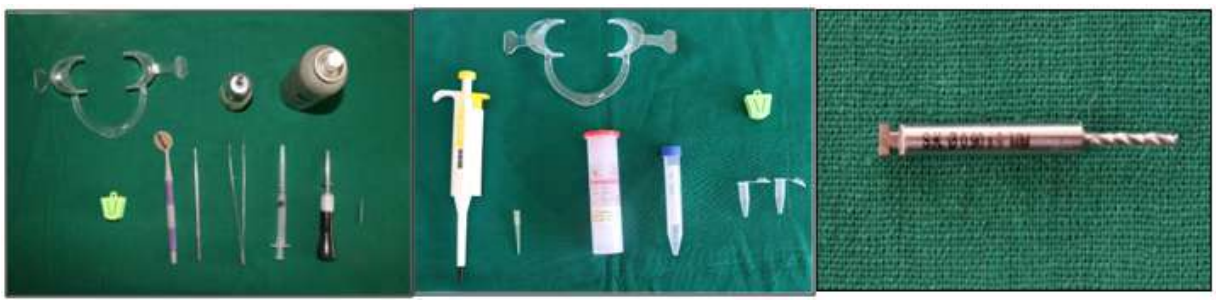

Figure 1: **a. Armamentarium for microosteoperforartion and**
b.Mini Implant drill bit used for making micro-osteoperforations (MOP)
c. Armamentarium for GCF collection

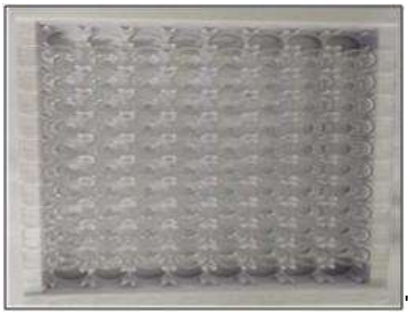

Figure.2: The site was gently dried with an air syringe, and a saliva ejector was used to avoid any saliva contamination

Figure.3: Elisa Kit

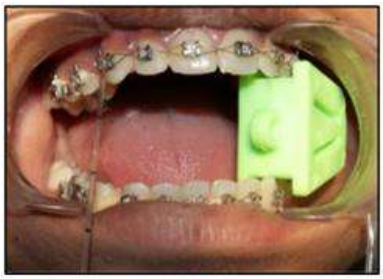

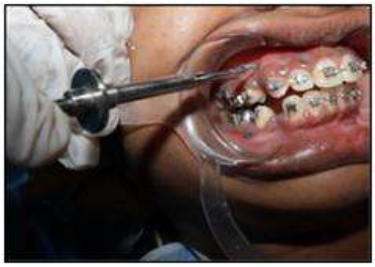

Figure.4: GCF collection using volumetric microcapillary pipette from the distal cervical gingival margin

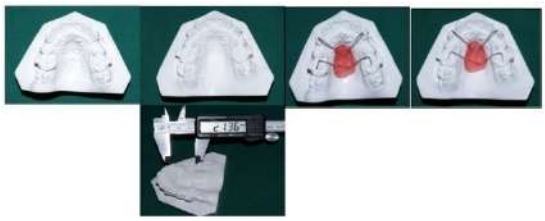

Figure.5: a. Pre and Post-treatment study modelb. Direct cast measurements to measure the distance between the upper canine and micro osteoperforation procedure using a mini implant drill bit.

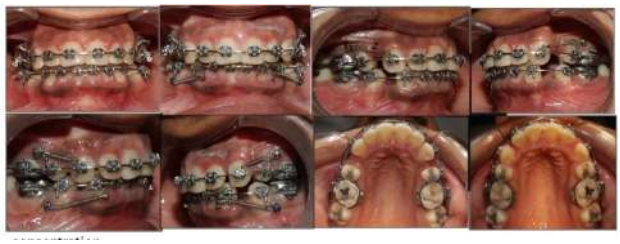

Figure.6: Case Example

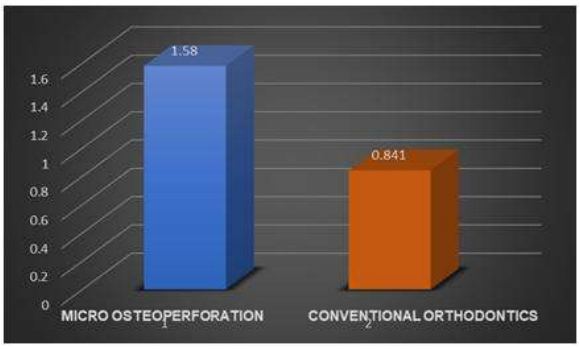

Figure.7: Rate of canine retraction after 28 days of retraction

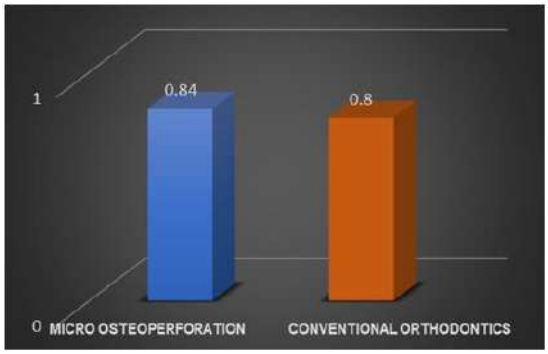

Figure.8: Rate of canine retraction after complete canine retraction

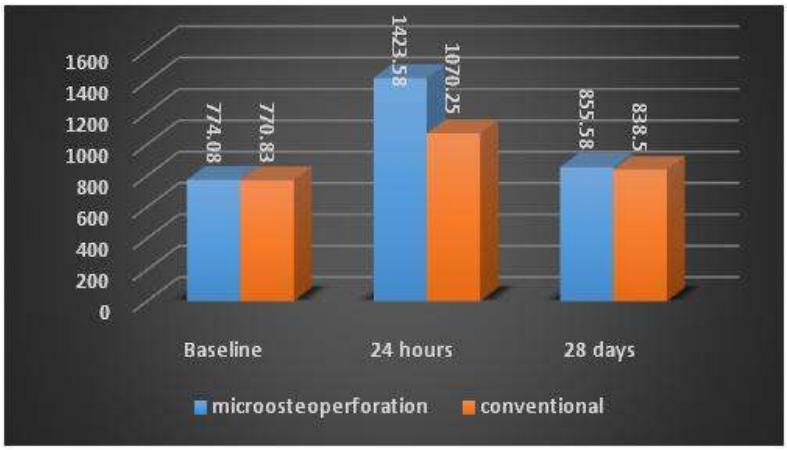

Figure.9:Comparison of RANKL levels in GCF before retraction, 24 hours after retraction, and 28 days after retraction

Indian Journal of Natural Sciences *www.tnsroindia.org.in ©IJONS*

Vol.15 / Issue 88 / Feb / 2025 *International Bimonthly (Print) – Open Access* *ISSN: 0976 – 0997*

RESEARCH ARTICLE

Attention based GRU Model with Effective Feature Selector for Improved Weather Forecasting

Yukti Varshney[1]* and Nupa Ram[2]

[1]Research Scholar, Department of Computing Science & Information Technology, Teerthanker Mahaveer University, Moradabad, Uttar Pradesh, India.
[2]Associate Professor, Department of Computing Science & Information Technology, Teerthanker Mahaveer University, Moradabad, Uttar Pradesh, India.

Received: 28 Nov 2024 Revised: 09 Dec 2024 Accepted: 20 Jan 2025

***Address for Correspondence**
Yukti Varshney,
Research Scholar,
Department of Computing Science & Information Technology,
Teerthanker Mahaveer University, Moradabad, Uttar Pradesh, India.
E.Mail: yuktivarshney16@gmail.com

ABSTRACT

Weather prediction is an appealing but demanding endeavor because of its substantial effects on human existence and the complex dynamics of atmospheric movement. Impacts of weather forecasting is huge in daily life activities so; scholarly genre is taking great interest in this field. Large amounts ofdata from multiple sources, such as satellites, weather stations, radar and historical records is complex task to predict. Artificial Intelligence (AI) brought tremendous impacts to process its various techniques and results are highly satisfied. The main benefits of AI in weather forecasting are its ability to process huge amounts of data fastly and accurately. In recent years, deep learning approaches that rely on a large amount of observations have become more popular. In the study of various research paper, a number of existing approaches focus only on the temporal patterns of meteorological information, ignoring the correlations between variables at various locations. In order to overcome this constraint, we introduce ATTGRU _ CLMGWO, an innovative model that utilizes attention mechanisms and GRU architecture to provide precise predictions of many variables and stations across several time steps. Additionally, it includes the use of Chaotic Logistic Map Based Grey Wolf Optimization to determine the appropriate climatic factors for each specific location. We successfully capture concealed spatial interconnections and a wide range of enduring weather patterns. ATTGRU_CLMGWO predicts temperature by concurrently acquiring knowledge of the crucial time steps and weather factors. The proposed technique is assessed using the Jena Climate dataset, yielding an MSE of 1.3, an MAE of 0.41, and a MAPE of 0.2.

Keywords: weather forecasting, feature selection, Gated Recurrent Network, time series, wind direction.

INTRODUCTION

The weather prediction is a crucial application of scientific computing. It can predict future weather fluctuations, especially severe weather events like floods, droughts, and hurricanes, which is important for society (including daily activities, agriculture, energy production, transportation, industry, etc.). Over the last ten years, there has been significant progress in the scientific area of numerical weather prediction (NWP) due to the advancement of high-performance computing devices [1]. Traditional NWP approaches typically adhere to a simulation-based approach. This entails utilizing numerical simulations to solve partial differential equations (PDEs) representing the physical rules driving atmospheric conditions [2], [3], and [4]. These NWP techniques often have low processing performance due to the complex nature of solving PDEs. For instance, calculating a single simulation for a 10-day forecast with a spatial resolution of $0.25^\circ \times 0.25^\circ$ would take several hours on a supercomputer with hundreds of nodes [5]. This restricts the number of ensemble members that can be employed for probabilistic weather predictions and greatly reduces the timeliness of daily weather forecasts. Furthermore, traditional NWP algorithms heavily depend on parametric numerical models. However, despite their high complexity, these models are sometimes deemed insufficient [6], [7]. For instance, mistakes might arise due to the parameterization of unresolved processes. To tackle the aforementioned challenges, a potential approach involves using artificial intelligence, namely deep learning, to develop data-driven weather forecasting methods. Deep neural networks are used to capture the association between observed input data and anticipated output data. AI-based techniques may balance model complexity, prediction resolution, and accuracy on GPUs for fast performance [8], [9]. The spatial resolution of FourCastNet [10] has been increased to $0.25^\circ \times 0.25^\circ$, equivalent to the ECMWF Integrated Forecast Systems (IFS). It generates a 100-member, 24-hour forecast in 7 seconds utilising four GPUs. This is orders of magnitude quicker than typical NWP approaches. Nevertheless, the FourCastNet's prediction accuracy is still unsatisfactory. The RMSE of the 5-day Z500 prediction using a single model and a 100-member ensemble is 484.5 and 462.5, respectively. These values are substantially lower than ECMWF's operational IFS of 333.7 [11]. It is hypothesised that many significant advancements are required before artificial intelligence (AI) technologies may surpass NWP. The majority of weather prediction systems were constructed based on the study or reanalysis of data beyond direct observations.

The reanalysis datasets are often regarded as the most accurate estimates [12], [13] for most atmospheric variables, with the exception of some elements such as precipitation. This work uses ERA5, the 5th ECMWF reanalysis dataset [14]. Latitude, longitude, pressure levels (height), and time comprise the ERA5 dataset. We have the freedom to choose any number of weather parameters (such as geopotential, temperature, etc.), but we should not see them as contributing to a new dimension. The dataset, which has a size exceeding 2 petabytes (PB), is divided into two-dimensional (2D) slices based on latitude and longitude. This division is done to facilitate the process of downloading. However, by defining a time point (hourly for the previous 60 years), pressure level (or Earth's surface), and weather component, a matrix of global reanalysis data may be obtained. The overall ERA5 data is A. Superscripts denote meteorological variables and pressure levels, whereas subscripts provide spatiotemporal locations. Example: AT^{850}_{t} shows global temperature data in matrix form at time t and height 850hPa. For geopotential data at point (x, y), time t, and 500hPa height, see $AZ^{500}_{x,y,t}$. It is important to note that $AZ^{500}_{x,y,t}$ is a single numerical value. In order to mitigate the aforementioned load, researchers initiated a secondary investigation that explores AI techniques for weather forecasting. Deep learning enables the direct learning of complicated functions (represented by $f(\cdot)$) from large amounts of training data, without requiring knowledge of the underlying physical procedures or formulas. Many deep neural networks describe $f(\cdot)$ as $f(\cdot; \theta)$, where $\cdot$ is the input data and θ is the adjustable parameters. The Computer vision (CV) analyses 2D/3D cubes of image data, making it the closest to weather forecasting. Over the last ten years, the CV community has created numerous successful network architectures, such as those mentioned in references [16] and [17]. More recently, they have adapted powerful architectures called transformers from the field of natural language processing [18] and have developed variants [19] that can effectively handle image data. AI-based approaches were first used in weather forecasting to address the challenges of predicting future weather data in settings where traditional NWP methods, such as radar or satellite data-based precipitation forecasting, are inadequate [20]. The remarkable capacity of deep neural

networks to convey information effectively has contributed to their success in data-driven environments. This success has motivated researchers to investigate the challenges faced by NWP methods, such as the significant computational burden associated with direct medium-range weather forecasting. In fact, this computational task has consumed a substantial portion of the computational resources of weather forecast centers over the past decade. The following are the contributions made by this work: An attention-based multilayered GRU model has been developed to improve the speed and stability of multistep weather prediction. This model outperforms other deep learning architectures and has been extensively compared to existing forecasting models, demonstrating its superiority. In order to globally optimise and efficiently anticipate the parameters using the Grey wolf optimisation algorithm, chaos has been employed to produce the chaotic grey wolf optimisation algorithm. Chaotic maps are used in optimising algorithms to enhance efficiency by effectively analysing the search area, taking into account the nature of dependability. The findings indicate that CLMGWO outperforms traditional GWOs in terms of convergence when compared to other methods and applications. The paper is structured as follows: Section 1 comprises the project's introduction. Section-2 provides a concise summary of the conducted literature survey. Section-3 elucidates the operational procedures of the system. Section-4 portrays the inferences and results obtained. The "Conclusion" section in section 5 summarizes our findings and discusses potential next directions.

Related works

DL has been used in recent years to investigate time series difficulties [21], in which the relationship between characteristics is apparent but challenging to discern. Traditional machine learning techniques may not work as well for systems whose behavior is primarily impacted by temporal or geographical context, like weather systems. In contrast, DL methods, which can automatically extract spatio-temporal features, are more suitable for gaining a deeper understanding of such systems. Improved prediction accuracy may be achieved by accurately analysing the association and appropriately representing the information. As a result, DL has been accepted as a sensible and adaptable technique for analysing time series characteristics. Consequently, several scientists have used DL techniques for the purpose of weather prediction, which is a common and complex issue involving multi-dimensional time series data. Data-driven solutions are anticipated to tackle some traditional challenges in weather forecasting. In [22] introduces the weather predicting model based on graph neural networks (GNNs) to analyse the data produced by these sensors. Graph learning-based models, or GNNs, perform well empirically in a variety of machine learning techniques.A new neural network architecture, BMAE-Net, is described in [23]. A Bayesian inference-optimized multi-head attention encoder-decoder framework is used. The main objective of BMAE-Net is to properly anticipate weather time series changes. Bayesian inference is added to the gated recurrent unit to generate the Bayesian-gated module. Next, each Bayesian layer's network architecture includes a multi-head attention mechanism to increase time duration prediction. Following that, Bayesian hyperparameter optimisation is used to create an encoder-decoder system. This framework deduces massive time-series data's underlying links for reliable forecasts. A deep learning method, multivariate data decomposition approach, grid search algorithm, and attention mechanism are used to create a hybrid wind speed prediction model based on weather research and forecasting (WRF) simulation [24].

In [25] proposes an optimised stacked Bi-directional Long Short-Term Memory (BiLSTM)/ LSTM model to forecast univariate and multivariate hourly time series data using stacked LSTM layers, drop out architecture, and LSTM-based model. By tweaking six pertinent hyperparameters, Bayesian optimisation improves the model's performance. In order to anticipate many fundamental atmospheric variables on a worldwide grid, [26] offer a notably enhanced data-driven global weather forecasting system that makes use of a deep CNN. With just a few input atmospheric condition variables, it may be trained to predict intricate patterns of surface temperature. The goal of [27] is to convert a weather forecasting system using deterministic neural networks into an ensemble model. We evaluate four approaches to build the ensemble: using random dropout in the network, retraining the neural network, creating early perturbations using singular vector decomposition, and random beginning perturbations. In [28], a method for forecasting future temperature using a neural network based on historical temperature data is proposed. To be more precise, authors developed a CRNNmodel, which consists of a CNN and a RNN.

While numerical models are now indispensable, they are costly to execute and include several physical phenomena that cannot be well represented by equations. The issue of error propagation during model solution is a significant factor that leads to inaccurate predictions. Hence, researchers are now prioritizing the advancement of a data-centric weather forecasting system that guarantees optimal efficacy and affordability, while delivering superior precision and reliability in weather forecasts.

System model

The initial step is loading the Jena dataset, which contains a collection of meteorological time series data. The datasets are preprocessed using conventional methods. In this process, the wind direction is transformed from degrees to axis and the time stamp is converted from day to year. The preprocessed data is subjected to feature selection using the Chaotic Logistic Map Based Grey Wolf Optimisation algorithm, which effectively optimises and predicts the parameters on a global scale. As shown in figure-1, the chosen features are fed into the Attention Based GRU Model with RMSProp Optimizer in order to predict the weather.

Proposed methodology

Proposed methodology implements a modified Grey Wolf Optimization (GWO) algorithm called CLM Grey Wolf Optimization (CLMGWO). It is used for feature selection.

The selection of a subset of features which used to maximize classification accuracy. It minimizes the selected featured numbers.

Grey wolf's population called "agents" (candidate solutions) is initialized randomly. A subset of features is represented by each agent.

By using classification algorithm to measure their fitness and accuracy, agents are set to train and evaluate.

Agents are guided by top hierarchy then sub hierarchy called alpha, beta, delta wolves for the movement of the pack (data).

To get optimal features subsets, iterations of solutions are updated.

For probabilistically toggle feature values in each agent's solution a transfer function is used.

Proposed Methodology for building an attention-based GRU model

To Compute attention, vector an Attention Layer custom layer is defined over the GRU hidden state sequence.

This layer is consisted of two main parts: Computing an attention score between individually hidden state then a context vector.

to compute a weighted average context vector, the attention scores is used.

The entire context from the sequence is condensed by the output attention vector and fed through a dense layer for obtaining desired results.

return _sequences=True is used to process the input sequence.

To compute the attention vector for Attention Layer, GRU layer is wrapped.

A final Dense layer with 1 unit makes a prediction based on the attention vector and model is accumulated with the RMS Prop optimizer and mean square error.

Dataset description

Jena Climate is a collection of meteorological time series data acquired by the weather station located at the Max Planck Institute for Bio Geochemistry in Jena, Germany. The collection comprises 14 distinct observations collected at 10-minute intervals across many years, including air temperature, atmospheric pressure, humidity, and wind direction. The dataset includes data spanning from January 1st, 2009 to December 31st, 2016, consisting of 420,451 data points [29]. This research examines the periodic regularity of temperature fluctuations throughout months and hours. It aims to map and establish rules for temperature changes within a 24-hour period for each month. There are variations in temperature across various months, and three components - month, cos (h), and sin (h) - are included in the dataset to represent these variations. The trigonometric function of hours is used to ensure that the same pattern repeats itself every 24 hours. This research utilises data collected between 2014 and 2016, specifically picking the variables 'T (degC)', 'p (mbar)', 'rh (%)', and 'H2OC (mmol/mol)' from a pool of 14 original quantities. Additionally,

three time-related parameters are included. In all, there are 157,824 data points containing seven variables, which will be used for prediction purposes. Data must be standardised due to distinctive element distribution and positive and negative values. Data was divided into three 6:2:2 subsets: training, validation, and testing.

Preprocessing of data

When the test wind turbine is stationary, the wind speed at this test site fluctuates between the wake and reference wind measurement locations. Furthermore, the geographical setting has a significant influence on the wake of wind turbines. The non-dimensional wind velocity ratio U_{NR}removes wind velocity and wake distribution changes from wake measurement. The test wind turbine's non-dimensional wind velocity U_{no} is measured while operating and U_{np} while motionless. The equation gives non-dimensional wind velocity ratio U_{nr}.

$$U_{nr} = \frac{U_{no}}{U_{np}} \quad (1)$$

The values of U_{no} and U_{np} are averaged over all retrieved data. Furthermore, the value of U_{no} is determined by dividing the observed wake wind velocity U_{wake_o}, obtained from sonic anemometers positioned on the wake measuring mast, by the reference wind velocity U_{wake_p} during the operation of the test wind turbine. The value of U_{np} is determined by dividing the wake wind velocity U_{wake_p} by the reference wind velocity U_{ref_p} while the test wind turbine is not moving. The values of U_{no} and U_{np} are explicitly specified as

$$U_{no} = \frac{U_{wake\_o}}{U_{ref\_p}} U_{np} = \frac{U_{wake\_p}}{U_{ref\_p}} \quad (2)$$

Weather impacts building energy usage and solar energy generation. Temperature changes affect heating and cooling needs, thus buildings with similar temperature patterns should have similar demands. Sunlight is the main energy source for PV systems and increases with temperature. Because of their importance, temperature and global horizontal irradiance (GHI) were taken into account while matching timestamps to reconstruct building load. We match each time stamp t with a collection of comparable timestamps θ with the aid of this instruction. Put differently, every period t is associated with a collection of similar timestamps $\theta_t = \{\theta_t\}$. All premises have identical settings. Since each premise k has a unique PV installation date, the time stamps are separated into two sets: pre- and post-installation. PV installation time is $t_{k,I}$. β represents time stamps before installation $t < t_{k,I}$ while α represents time stamps after installation $t > t_{k,I}$.In order to account for discrepancies between the reported and real dates for PV system activation, we also avoid from utilizing time stamps that are set to expire on the day of installation.

As a buffer in this work, b = a = 20 days, hence for each premise k, the β and α are defined as

$$\beta_k = \{t: t \epsilon t < (t_{k,I} - b)\} \quad (3)$$

We determine the collection of similar timestamps after installation for each $\beta_{k,i} \epsilon \beta_k$

$$\varphi_{k,i}^{(\beta)} = \{\varphi_t: t \epsilon \beta_{k,i}\} \quad (4)$$

where parenthetical superscripts represent all premise k time stamps. These generate two 2D dictionaries with equivalent timestamps for each time stamp in k and k.

First and foremost, characteristics that are superfluous or that could include duplicate data must be eliminated. To achieve this objective, we used the values of the covariance matrix. Several humidity and temperature metrics were removed from the dataset as a consequence of this investigation. Because there were too many zeros, the column lights were also removed. The filters were employed after a comprehensive study, including factors such as correlation, zeros, null values, and other relevant discoveries. Furthermore, it is essential to scale the characteristics of the dataset prior to training the model. This is due to the limited efficacy of the current models within a narrower numerical spectrum. Optimizers can readily identify the learning rate, which creates a favourable setting for testing. Equation (5) illustrates the process of scaling the dataset, which is a necessary pre-processing step before to training. The term X' denotes the dataset that has been scaled. The data is scaled down inside a discrete set, ranging from -1 to 1, using minmax scalar, and then retrieved. The scalar value x represents a value taken from a feature vector X. x_{min} and x_{max}correspond to the lowest and maximum scalar values, respectively, obtained from the feature vector X. By using Equation (5)

$x' = \frac{(x-x_{min})(max-\min)}{x_{max}-x_{min}} + \min \quad x \epsilon X$ (5)

Furthermore, the weight factors for each characteristic are computed. This is achieved by using the scaled data to evaluate several models in order to determine the optimal model configurations and training parameters.

Feature selection using CLMGWO

Feature selection involves the selection of a concise subset of characteristics that are both essential and adequate to accurately define the target notion. The appropriate feature set is essential for every learning algorithm since it's its only source of knowledge. The main goal of feature selection is to avoid selecting too many traits. If a limited number of features are chosen, it is quite likely that the information included in this collection of features is minimal. GWO is an optimization heuristic that utilizes the selection criteria of grey wolves. It was created by Mirjalili *et al.* in 2014. This algorithm is a meta-heuristic approach that is enhanced by the observed framework of hunting behaviors and social organization of grey wolves. Not every GWO search iteration can be global. Thus, finding the global best answer is sometimes necessary. There was consistent search functionality. The GWO strategy for prey seeking employs a hierarchical approach, including the encircling, hunting, attacking, and search for prey employing optimization techniques. The hierarchical technique divides wolves into four categories. The first three dominant wolves, α, β, and δ, guide and supervise the other wolves' hunting efforts. Grey wolves use a hunting strategy known as encircling, when they surround their victim and communicate the prey's location to one another. After the prey's location is identified, the hunting process is carried out by other wolves under the leadership of the leader wolves. The arrangement of the wolves around the prey is revised according on the guidance of leader wolves in order to determine the prey's location. The method of assaulting prey involves the process of exploitation. The search for prey involves an exploratory phase and terminates by abruptly deviating from the best option. Grey wolves use the surround prey technique to isolate their victim according to set guidelines while hunting. A flow diagram is illustrated for feature selection in GWO.

$P' = \left|R'.Y'_p(t) - Y'(t)\right|$ (6)

$Y'(t+1) = Y_p(t) - V'.P'$ (7)

The equations (6) and (7) correspond to the iteration number t. The labels $Y'_p$and Y'stand for the level of prey and grey wolf, respectively. $V' = 2a'r'_1 - a', R = 2r'_2$depend on the number of iterations and the random vectors of [0,1]. The features of the parameter $a'$are successively lowered from 2 to 0. Both r'_1 and $r'_2$are random vectors. The hunting technique for capturing prey is carried out in accordance with the previous regulations.

$P'_i = |R'_i.Y'_i(t) - Y_i(t)|$ (8)

Where, $i$representα, β and δ

$Y'(t+1) = \sum_{i=\{\alpha,\beta,\delta\}} Y'_i(t) - V'_i.P_i$ (9)

In equations (8) and (9), the variables $X_i$represent the location of leader wolves R'_i, whereas V'_irepresents a random vector. The determination of assault and prey detection is shown by the vector V, R'. An analysis is conducted when A is larger than 1 or A is less than -1. Otherwise, C is greater than 1. Conversely, the theft occurs when the absolute value of |V|<1 and |R|<1. This study introduces a novel and effective strategy to enhance the Software reliability growth model (SRGM) metrics in order to enhance the searching behaviour of the GWO. A refined grey wolf optimization method is proposed, using an adaptable chaotic search approach to increase the search process and minimize the possibility of inaccurate predictions via the CGWO algorithm. The Different forms of chaotic maps provide chaotic variables for chaotic algorithms. The chaotic search strategy is introduced and characterized while considering the chaotic map.

$Cx_i^{n+1} = \mu Cx_i^n(1 - Cx_i^n)$ (10)

In equation (10), the symbol Cx_i^nrepresents the chaotic variable, while the symbol n represents the number of iterations. Researchers, mathematicians, and medical scientists have extensively used these chaotic maps in the area of optimisation. Efficiently navigating the search is clearly beneficial.

Initial chaotic maps are [0, 1]. Statistical study of the literature gives these maps a starting value of 0.7. Every chaotic map has a unique attitude. Chaos maps help determine data. Every user-defined grey wolf in the target zone is

checked for fitness and categorised by condition using standard benchmarking metrics. The issue has goal and constraint violation functions. Formulate minimal problems. It might be phrased as

$minQ(y), y = (y_1, y_2, y_3, \ldots y_n) \epsilon P^n$ (11)

In equation (11), the variable n represents the estimated number of configurations of a feasible solution. The symbol $Y \epsilon Q \epsilon S, Q$ indicates that Y belongs to the potential area Q inside the search space S. Furthermore, Q is defined as an n-dimensional rectangle. The domain of P is characterised by a lower bound (l) and an upper bound (u), as specified in Equation (12). The Q space, stated in Equation (13), represents the range of limitations ($g > 0$) in P.

$l(j) \leq y(j) \leq u(j), \quad 1 \leq j \leq n$ (12)

$r_k(y) \leq 0$, for k = 1,2, ... v (13)

$s_k(y) = 0$, for k = v + 1, ... g (14)

If a solution in Q space satisfies either the constraint r_u or s_u, then r_u is considered an active limitation at y in equations (13) and (14), whereas $r_k(y)$ and $s_k(y)$ are regarded as inequality and equality restrictions, correspondingly.

The suggested approach, known as the chaotic GWO algorithm, is used to effectively solve optimization issues. The program begins by initializing a population of wolves. The chaotic map value is initialized as x_0 and then updated continually. The parameters a', A', C' are sequentially engaged in carrying out the exploration and exploitation procedure. The variable t represents the number of iterations. The fitness of each search wolf is assessed using the variables x_α, x_β and x_δ. The first wolf appears as α, the second as β, and the third as δ. Grey wolves are categorised by iterative fitness. Chaotic map equations increase chaotic number. For every search wolf, both the location and the parameter value are changed, as stated in (10). Next, the poorest fit wolf is replaced with the best fit wolf. The CLMGWO method demonstrates the ideal solution by observing the fitness of an alpha wolf towards the end of the iteration. This strategy yields superior outcomes and efficiently saves computational resources.

Forecasting model

An artificial neural network (ANN) is a widely used AI method that emulates the functioning of human neurons to handle vast quantities of input simultaneously and learn effectively. ANNs are deterministic models that ignore time and focus on input and output variables. Using the input and weight vectors, the output is internally determined. Weight vector and decision boundary are perpendicular. An activation function affects the perceptron's input response, giving the ANN various decision bounds. However, a recurrent neural network (RNN) may dynamically map inputs to outputs, taking all time steps into account. RNN are particularly suitable for analysing time-series data due to their ability to sequentially analyse the input, while retaining an internal state that carries information from one-time step to the next. The most popular and effective RNN is the LSTM. To avoid RNN long-term reliance, the LSTM preserves differential input values during back propagation. The RNN version GRU simplifies LSTM structure by lowering hidden state update computation. Figure-2 shows that it solves long-term reliance and preserves LSTM performance. There are input and forget gates installed in the GRU cell. The input and forget gates are controlled by the gate controller, represented by the letter z. The input gate is open when z = 1, while the forget gate is closed otherwise. The input gate is closed and the forget gate is open when the value of z equals zero. Every iteration stores the previous (t-1) memory and resets the current time step's input. The following equations control the GRU cell: (15) – (18).

$r_t = \sigma(W_r h_{t-1} + U_r x_t)$ (15)

$z_t = \sigma(W_z h_{t-1} + U_z x_t)$ (16)

$c_t = tan\, h(W_c(h_{t-1} \times r) + U_c x_t)$ (17)

$h_c(z \times c) + ((1 - z) \times h_{t-1})$ (18)

In order to create our GRU model, we considered hyper parameters and used a GRU network to anticipate the weather at 24 distinct time periods (spanning from one hour to one day in the future). Two hidden layers made up the configuration of the GRU model. The GRU model has two hidden layers, each with 13 nodes. The number of hidden layers is equal to the product of the output layer's size and 2/3 of the input layer's nodes. Equation (19) gives the scaled exponential linear unit (SELU), which was the activation function used in our investigation. The stochastic variable denoted by α in this equation is chosen at random during training from a uniform distribution. In the course

of testing, however, α is fixed at 1.67326, which is the distribution's expected value. Furthermore, λ is an extra parameter that's utilised to calculate the slope; by default, its value is 1.0507. The reason SELU works so well for training deep learning models is because of its remarkable self-normalization abilities and its ability to use equation (20) with $\delta = 1$ to get around the problem of vanishing gradients. The learning rate and learning epoch were configured as 0.001 and 500, correspondingly.

$$f(\alpha,\lambda,\delta) = \begin{cases}\lambda(\alpha e^{x}-\alpha) for\ x < 0 \\ \lambda x \text{ for } x \geq 0\end{cases} \quad (19)$$

$$L_{\delta}(y,f(x)) = \begin{cases}1/2(f(x))^{2} for\ |y-f(x) for\ x < 0| \\ \delta|y-f(x)| - \frac{1}{2\delta^{2}} otherwise\end{cases} \quad (20)$$

When the GRU network processes a longer input sequence, the accuracy of the output sequence prediction decreases. Even though input variables may have different associations with the forecasting goal, the network handles them all equally. Attention mechanisms may concentrate on key input variables. Encoders create attention vectors from input, while decoders create hidden states from encoder output. The encoder assigns an attention score to each concealed state by utilising the decoder's hidden state from the previous viewpoint. Applying a soft-max function to the attention score generates an attention vector. Thus, the encoder prioritises related input variables when the decoder anticipates output.

Performance analysis

The experimental data is analyzed using Python software, using the parameters of MSE, MAE and MAPE. The parameters are compared with four advanced methods: Graph Neural Networks (GNNs) [22], Bayesian inference strategy (BMAE-Net) [23], convolutional neural network (CNN) [26], and the proposed ATTGRU_CLMGWO.

Mean Square Error (MSE)

The model's prediction using the MSE technique quantifies the difference between the actual observation and the estimated observation. The application of data enhances the model's prediction power to some extent without excluding any necessary variables. The Mean Squared Error (MSE) is expressed as:

$$MSE = \sum_{k=1}^{n}(q_k - q'_k)^2 \quad (21)$$

In equation (21), $q_k$is the total count of identified faults at the specific time t_k, using real data. q'_k is the estimated total count of identified discrepancies at time t_k, using the number of observations in the dataset of software failures.

MAE and MAPE

The developed model's efficiency is determined using MAE and MAPE after the predicted values have been obtained. As model efficiency increases, error parameters should decrease. The expressions for the parameters are provided below.

$$MAE = \frac{1}{N}\sum_{k=1}^{N}|e_k|$$

$$MAPE = \frac{1}{N}\sum_{k=1}^{N}\frac{|y_k - y'_k|}{y_k} * 100\%$$

Where the error factor, denoted as e_k, represents the difference among the actual value y_k and the anticipated value y'_k. Figure 2 illustrated no of iterations on x axis and average fitness on Y axis. Figure 3 illustrates the real and forecasted data throughout the testing assessment. The horizontal axis depicts the quantity of samples, and the vertical axis illustrates the close1 value. The greatest real value is obtained when the number of samples is either 200 or 1000 during the analysis.Figure 4 illustrates the real and forecasted data during the training assessment. The horizontal axis depicts the quantity of samples, and the vertical axis illustrates the close1 value. The greatest real value is achieved when the number of samples is either 200 or 800 during analysis.

Scope and Future Conclusion

The scope of this study is to further utilization of ATTGRU_CLMGWO model. This model illustrated the iterative training methods and comparing the desired results continuously. This model is adjusting weights and biases too by

aiming minimum error. The entire system supports to discern complex input into desired output. Through this study we have implemented humidity, temperature for hours and day. Although there are several potential directions of this study including by using predictive framework air density, barometric pressure can be measured effectively. Additionally, we can extend our study by extending various geographical regions or several climatic factors.

CONCLUSION

This study use ATTGRU_CLMGWO for weather forecasting. The procedure employs an iterative training method, whereby it consistently compares the observed output with the desired output and computes the error. This error is used to recalibrate the weights and bias in order to get an improved result. Therefore, this strategy aims to reduce the error. The system takes complicated factors as input and utilizes them to develop intelligent patterns during training. It then employs these patterns to make predictions. The input parameters considered for the predictions are temperature and humidity measurements from one hour and one day before, in addition to the seasonal factor. Moreover, this task may be expanded by using other factors like air density, precipitation, and barometric pressure to improve the precision of the forecasts and provide more complete weather predictions.

REFERENCES

1. P. Bauer, A. Thorpe, and G. Brunet, "The quiet revolution of numerical weather prediction," Nature, vol. 525, no. 7567, pp. 47– 55, 2015.
2. W. C. Skamarock, J. B. Klemp, J. Dudhia, D. O. Gill, D. M. Barker, W. Wang, and J. G. Powers, "A description of the advanced research wrf version 2," National Center For Atmospheric Research Boulder Co Mesoscale and Microscale . . . , Tech. Rep., 2005.
3. F. Molteni, R. Buizza, T. N. Palmer, and T. Petroliagis, "The ecmwf ensemble prediction system: Methodology and validation," Quarterly journal of the royal meteorological society, vol. 122, no. 529, pp. 73–119, 1996.
4. H. Ritchie, C. Temperton, A. Simmons, M. Hortal, T. Davies, D. Dent, and M. Hamrud, "Implementation of the semi-lagrangian method in a high-resolution version of the ecmwf forecast model," Monthly Weather Review, vol. 123, no. 2, pp. 489–514, 1995.
5. P. Bauer, T. Quintino, N. Wedi, A. Bonanni, M. Chrust, W. Deconinck, M. Diamantakis, P. Duben, S. English, J. Flemming ¨ *et al*., The ecmwf scalability programme: Progress and plans. European Centre for Medium Range Weather Forecasts, 2020.
6. T. Palmer, G. Shutts, R. Hagedorn, F. Doblas-Reyes, T. Jung, and M. Leutbecher, "Representing model uncertainty in weather and climate prediction," Annual Review of Earth and Planetary Sciences, vol. 33, no. 1, pp. 163–193, 2005.
7. M. R. Allen, J. Kettleborough, and D. Stainforth, "Model error in weather and climate forecasting," in ECMWF Predictability of Weather and Climate Seminar. European Centre for Medium Range Weather Forecasts, Reading, UK, 2002, pp. 279–304.
8. M. G. Schultz, C. Betancourt, B. Gong, F. Kleinert, M. Langguth, L. H. Leufen, A. Mozaffari, and S. Stadtler, "Can deep learning beat numerical weather prediction?" Philosophical Transactions of the Royal Society A, vol. 379, no. 2194, p. 20200097, 2021.
9. S. Scher and G. Messori, "Weather and climate forecasting with neural networks: using general circulation models (gcms) with different complexity as a study ground," Geoscientific Model Development, vol. 12, no. 7, pp. 2797–2809, 2019.
10. J. Pathak, S. Subramanian, P. Harrington, S. Raja, A. Chattopadhyay, M. Mardani, T. Kurth, D. Hall, Z. Li, K. Azizzadenesheli *et al*., "Fourcastnet: A global data-driven high-resolution weather model using adaptive fourier neural operators," arXiv preprint arXiv:2202.11214, 2022.
11. P. Bougeault, Z. Toth, C. Bishop, B. Brown, D. Burridge, D. H. Chen, B. Ebert, M. Fuentes, T. M. Hamill, K. Mylne *et al*., "The thorpex interactive grand global ensemble," Bulletin of the American Meteorological Society, vol. 91, no. 8, pp. 1059–1072, 2010.

12. A. K. Betts, D. Z. Chan, and R. L. Desjardins, "Near-surface biases in era5 over the canadian prairies," Frontiers in Environmental Science, vol. 7, p. 129, 2019.
13. Q. Jiang, W. Li, Z. Fan, X. He, W. Sun, S. Chen, J. Wen, J. Gao, and J. Wang, "Evaluation of the era5 reanalysis precipitation dataset over chinese mainland," Journal of hydrology, vol. 595, p. 125660, 2021.
14. H. Hersbach, B. Bell, P. Berrisford, S. Hirahara, A. Horanyi, ´ J. Munoz-Sabater, J. Nicolas, C. Peubey, R. Radu, D. Schepers ˜ *et al*., "The era5 global reanalysis," Quarterly Journal of the Royal Meteorological Society, vol. 146, no. 730, pp. 1999–2049, 2020.
15. Y. LeCun, Y. Bengio, and G. Hinton, "Deep learning," Nature, vol. 521, no. 7553, pp. 436–444, 2015.
16. A. Krizhevsky, I. Sutskever, and G. E. Hinton, "Imagenet classification with deep convolutional neural networks," in Advances in Neural Information Processing Systems, 2012.
17. K. He, X. Zhang, S. Ren, and J. Sun, "Deep residual learning for image recognition," in Computer Vision and Pattern Recognition, 2016.
18. A. Vaswani, N. Shazeer, N. Parmar, J. Uszkoreit, L. Jones, A. N. Gomez, Ł. Kaiser, and I. Polosukhin, "Attention is all you need," Advances in neural information processing systems, vol. 30, 2017.
19. A. Dosovitskiy, L. Beyer, A. Kolesnikov, D. Weissenborn, X. Zhai, T. Unterthiner, M. Dehghani, M. Minderer, G. Heigold, S. Gelly *et al*., "An image is worth 16x16 words: Transformers for image recognition at scale," arXiv preprint arXiv:2010.11929, 2020
20. V. Lebedev, V. Ivashkin, I. Rudenko, A. Ganshin, A. Molchanov, S. Ovcharenko, R. Grokhovetskiy, I. Bushmarinov, and D. Solomentsev, "Precipitation nowcasting with satellite imagery," in Proceedings of the 25th ACM SIGKDD international conference on knowledge discovery & data mining, 2019, pp. 2680–2688.
21. J.N. Liu, Y. Hu, Application of feature-weighted support vector regression using grey correlation degree to stock price forecasting, Neural Comput. Appl. 22 (1) (2013) 143–152
22. Singh, G., & Durbha, S. (2023). Maximising Weather Forecasting Accuracy through the Utilisation of Graph Neural Networks and Dynamic GNNs. *arXiv preprint arXiv:2301.12471*.
23. Kong, Jian-Lei, Xiao-Meng Fan, Xue-Bo Jin, Ting-Li Su, Yu-Ting Bai, Hui-Jun Ma, and Min Zuo. "BMAE-Net: A data-driven weather prediction network for smart agriculture." *Agronomy* 13, no. 3 (2023): 625.
24. Han, Yan, Lihua Mi, Lian Shen, C. S. Cai, Yuchen Liu, Kai Li, and Guoji Xu. "A short-term wind speed prediction method utilizing novel hybrid deep learning algorithms to correct numerical weather forecasting." *Applied Energy* 312 (2022): 118777.
25. Michael, Neethu Elizabeth, Shazia Hasan, Ahmed Al-Durra, and Manohar Mishra. "Short-term solar irradiance forecasting based on a novel Bayesian optimized deep Long Short-Term Memory neural network." *Applied Energy* 324 (2022): 119727.
26. Weyn, J. A., Durran, D. R., & Caruana, R. (2020). Improving data-driven global weather prediction using deep convolutional neural networks on a cubed sphere. *Journal of Advances in Modeling Earth Systems*, *12*(9), e2020MS002109.
27. Scher, S., & Messori, G. (2021). Ensemble methods for neural network-based weather forecasts. *Journal of Advances in Modeling Earth Systems*, *13*(2).
28. Zhang, Zao, and Yuan Dong. "Temperature forecasting via convolutional recurrent neural networks based on time-series data." *Complexity* 2020 (2020): 1-8.
29. https://storage.googleapis.com/tensorflow/tf-keras-datasets/jena_climate_2009_2016.csv.zip

Table-1 Comparison of train and testing values for various metrics

Methods	Train	Test
MSE	1.3601	1.2228
MAE	0.4194	0.4067
MAPE	0.265	0.2129

Table-2 Comparative analysis between existing and proposed methods

Methods	GNNs [22]	BMAE-Net [23]	CNN [26]	AttGRU_CLMGWO [proposed]
MSE	3.5	2.6	4.3	1.3
MAE	4.2	3.7	4.2	0.41
MAPE	2.4	3.9	3.7	0.2

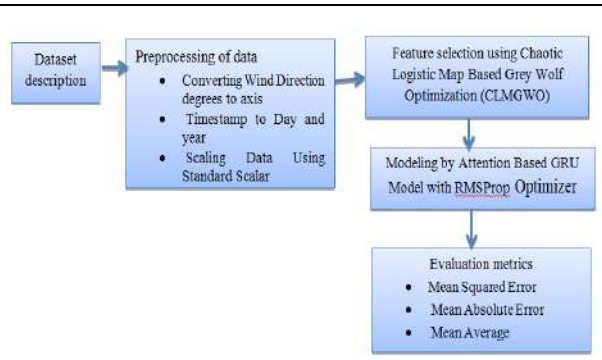

Figure.1: Block diagram for weather forecasting using neural networks

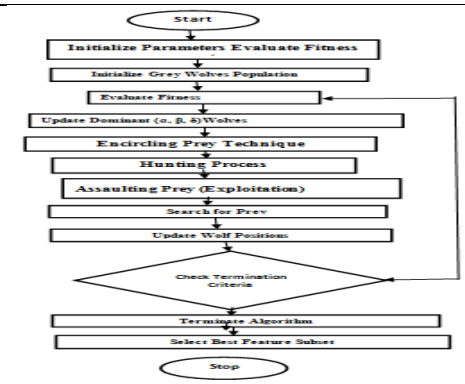

Figure.2: Flow diagram for Feature selection using CLMGWO

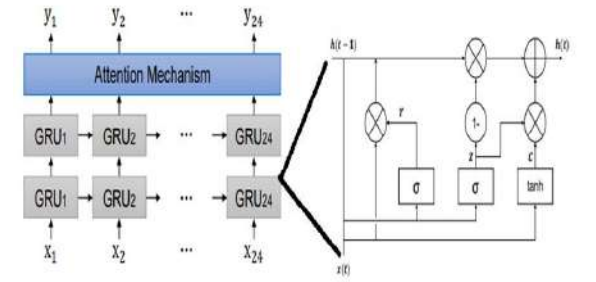

Figure.3: Architecture of Attention Based GRU Model

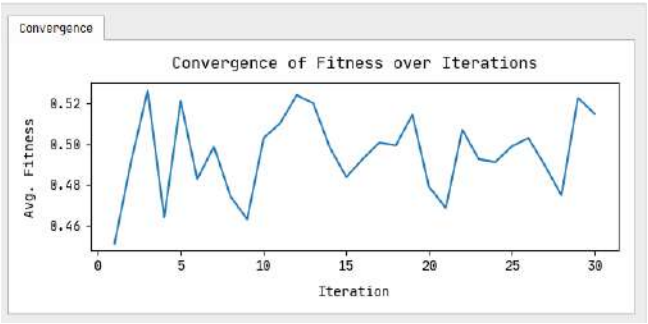

Figure.4: Convergence of fitness over Iterations

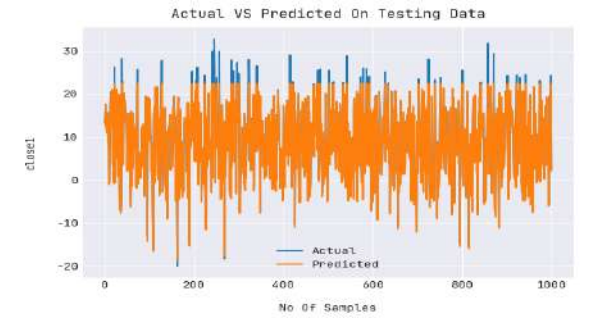

Figure.5: Analysis of actual and predicted data during testing

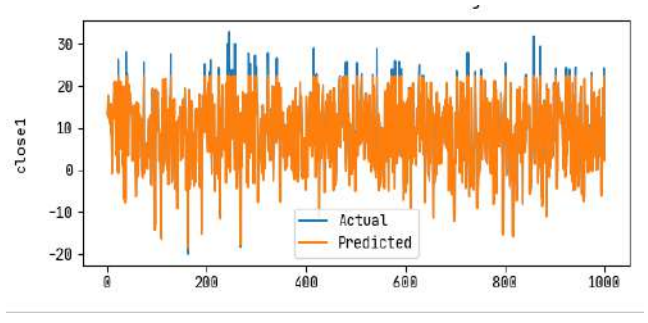

Figure.6: Analysis of actual and predicted data during training

Indian Journal of Natural Sciences *www.tnsroindia.org.in ©IJONS*

Vol.15 / Issue 88 / Feb / 2025 *International Bimonthly (Print) – Open Access* *ISSN: 0976 – 0997*

RESEARCH ARTICLE

Enhancing ITMS through LiDAR and V2X Integration for Improved Urban Mobility and Safety

Hashmat Fida[1]*, Harsh Sadawarti[2] and Binod Kumar Mishra[3]

[1]Research Scholar, Department of Computer Science and Engineering, Desh Bhagat University, Gobindgarh Punjab, India.
[2]Vice President, Department of Computer Science and Engineering, Desh Bhagat University, Gobindgarh Punjab, India.
[3]Associate Professor, Department of Computer Science and Engineering, Chandigarh University, Gharuan, Mohali, India.

Received: 30 Sep 2024 Revised: 25 Nov 2024 Accepted: 16 Jan 2025

***Address for Correspondence**
Hashmat Fida,
Research Scholar,
Department of Computer Science and Engineering,
Desh Bhagat University, Gobindgarh Punjab, India.
E.Mail: hashmatfida@gmail.com

ABSTRACT

The integration of LiDAR and Vehicle-to-Everything (V2X) communication significantly enhances Intelligent Traffic Management Systems (ITMS), enabling the rapid resolution of urban traffic, safety, and pollution challenges. LiDAR systems contribute to highly accurate 3D maps of the surroundings and provide object detection capabilities that improve V2X systems through data exchange among vehicles and infrastructure. This paper discusses a system architecture utilizing LiDAR for monitoring traffic behaviour with V2X for communication. Combining these elements creates a comprehensive traffic sub-system that enables real-time operations for improved road dynamics and street-side services. The integrated process will improve various areas of traffic management, such as traffic-signal control, safety of pedestrians, and priorities for emergency vehicles through data fusion and machine learning algorithms.

Keywords: LiDAR, V2X Communication, Intelligent Traffic Management System (ITMS), Cooperative Perception (CP), Traffic Flow Optimization, Pedestrian and Cyclist Safety

INTRODUCTION

With the rapid growth of urban populations, traffic congestion, road safety, and environmental concerns have become critical challenges for city planners and governments. Intelligent Traffic Management Systems (ITMS) have

emerged as a promising solution to optimize traffic flow, reduce accidents, and improve urban mobility. Integrating advanced sensor technologies, such as LiDAR (Light Detection and Ranging), with Vehicle-to-Everything (V2X) communication can revolutionize ITMS, enabling more efficient and intelligent traffic management. LiDAR, known for its precision in distance measurement and 3D environmental mapping, offers substantial advantages in traffic monitoring, vehicle recognition, and obstacle management. When combined with V2X communication, which facilitates data exchange between vehicles, infrastructure, and other road users, the potential for creating a highly responsive and adaptive traffic management system is enormous. This paper explores how LiDAR can be integrated with V2X communication within ITMS to enhance road safety, traffic flow, and environmental efficiency.

Literature Survey

The channel and propagation configurations are categorized based on the mode of implementation, environmental factors, and fading models observed in previous V2X communication studies. The environment is a crucial category that can be adjusted based on the context in which the transceiver operates. The context mainly relates to the highway and downtown environments as the main categories, but there were even studies that manipulate the context if they consider the special context such as parking lots, tunnels, suburbs, intersections, and rural environments. J.H. Joo *et al*. [1] presented a deep learning-based channel prediction algorithm based on use of the communication parameters SNR(Signal to Noise Ratio) and CSI(Channel State Information) data for prediction purposes. The application processes the channel prediction using the LSTM model, compare LSTM performance and delay-based performance evaluated according to the recently observed channel attribute value. Gyu Ho Lee *et al.* [2] proposed a method to recognize the environment which surrounds using the vision sensor, and the method is also able to sense objects that affect the communication environment. Objects to be detected are those creating NLOS (Non-Line-of-Sight) environments. The technique called MuSLi, proposed by Romeo *et al*. [3], aims to achieve the task of finding correct and accurate obstacle detection and send forward alert messages for other cars in the network if a pedestrian crossing the road is correctly detected. It is based on the connected content islands scenario. According to that scenario, each vehicle, defined as a content island, subscribes to a service to receive and to share published messages. Specifically, the road safety service does allow for detecting an obstacle via multiple LiDAR sensors from neighbouring cars.Sven *et al*. [4] describe an investigation of V2V communication based on commercial On-Board-Units (OBU). These units, mounted in two test-vehicles, transmit and receive data based on the IEEE 802.11p standard, ETSI ITS-G5. The messages contain basic conditions such as position, motion vector, and vehicle configuration parameters. G. H. Lee *et al*. [5] proposed a method that identifies the environment as a vision sensor and feeds information to the TCU board to pick optimal parameters. The sensing system has integrated camera and LiDAR sensor data into one data set. A CNN-based object detection algorithm was applied to the fusion sensor, and the driving environment was identified as a vision sensor. Radovan *et al.* [6] This presented an implementation of a cooperative environmental perception system. The system integrates V2X communication with several sensing devices: GPS, DSRC and forward-looking camera. The research also demonstrates the system based on four cooperative safety applications: EEBL, IMA, BSW and LTA. The results demonstrate that collaborative perception may indeed boost the perceived V2X market penetration.

Proposed Methodology

System Architecture

The proposed system architecture integrates LiDAR sensors with V2X communication to create a comprehensive traffic management solution, as shown in figure 1. The system entails:

LiDAR Units: Mounted on traffic lights, road infrastructure, and vehicles, the LiDAR units scan the environment and capture real-time 3D data of surrounding vehicles, pedestrians, and road obstacles.

V2X Communication Module: Inter-vehicle, inter-infrastructure-including traffic lights, and inter-central control communication module that allows real-time data interchange between vehicles, infrastructure, and a centralized control centre. It includes vehicle speed, location, LiDAR-based obstacle detection, and density.

Cloud Processing Unit: In the cloud, it will process data from LiDAR units and V2X modules to generate predictive traffic models and real-time responses to traffic conditions such as dynamic traffic light adjustments or warnings for an impending collision.

Data Fusion and Processing

LiDAR and V2X data are processed through a cooperative perception framework. The real-time 3D environmental data captured by the LiDAR sensors is forwarded to other near-by vehicles as well as infrastructure via V2X channels. Each connected vehicle transmits sensor data—such as position, speed, and direction of travel—enhancing the overall perception of the traffic environment. Data fusion is an important constituent part of this system, which, based on information obtained from LiDAR sensors and other vehicle sensors-which, for example, could be cameras and radar-improves the general representation of the street environment. Advanced processing algorithms, such as Kalman filters and machine learning-based models, are used to process the data in order to make predictions about traffic patterns, the possibility of accidents, and congestion [7].

Traffic Management Strategies

LiDAR combined with V2X communication allows for several traffic management strategies which include

Dynamic Traffic Signal Control: The LiDAR and V2X modules gather live traffic information to make dynamic adjustments to the traffic signals based on currently congested conditions, so relieved congested spots improve the smoothness of traffic flow [8]. LiDAR Sensors: LiDAR sensors have the capability to detect pedestrians and cyclists at occlusion or beyond a line of sight in advance. If the detected information is merged with V2X communication, then vehicles can get information related to possible hazards, so great improvements in road safety can be achieved [9].

Emergency Vehicle Priority: The system accommodates emergency services by providing real-time control over traffic signals so that emergency vehicles can pass smoothly through the traffic [10].

RESULTS AND DISCUSSION

The designed system is evaluated in a comprehensive analysis of data in traffic patterns for an urban environment. The key performance metrics include:

Traffic Flow Efficiency

Multi-modal traffic monitoring revealed significant variations in vehicle counts under different traffic conditions. Averaged across normal traffic conditions, car counts reflected between 50 and 75 vehicles, while in heavy trafficsituations, the vehicle count was 100 or more. Such detailed knowledge of the traffic density is bound to make congestion management much more effective, sometimes reducing congestion up to 15-20% during peak hours, as shown in figure 2.

Vehicle Type Distribution

The system should be able to recognize the different types of vehicles (cars, bikes, buses, and trucks). This is relevant to the customized implementation of traffic management strategies. For instance, the bike counts reflect a general trend of improvement on Fridays. This could potentially be an opening for specific adjustments in bike lanes during specific days, as shown in figure 3.

Traffic Conditions Analysis

These indicate very fluctuating trends within the specific traffic conditions (low, normal, heavy, high). In traffic condition heavy total vehicle counts were primarily more than 200; it was as low as when it was low traffic condition. Such a degree of further segmentation may result in a maximum of a 10-15% increase in response to alterations made in the traffic signal cycles by average vehicle speed, as shown in Figure 4.

Day of Week Patterns

The system captured day-of-week variations in traffic patterns. For example, Friday consistently showed higher total vehicle counts across all vehicle types, which speaks to the need for specialized traffic management strategies for end-of-week congestion, as shown in figure 4.

Correlation Analysis

From the pair plot, clear, very strong positive correlations between car counts and total vehicle counts can be seen for all traffic situations. This can serve as a basis for more accurate predictive models of overall traffic flow solely based on information provided by car counts, as shown in figure 5. The proposed system was also tested with detailed data analytics and simulations within an urban setting. A strong positive correlation of 0.97 exists between car count and total vehicle count such that car traffic is considered as the most significant contributor of overall traffic flow. For dynamic signal control, it improved by 15%, which indicates better competence in traffic management, as shown in figure 6.The heatmap also reflects that the system handled the various traffic compositions such as cars, bikes, buses, trucks, and the nature of their relation differs. Bike count has moderate positive correlation with the total count0.72; therefore, it is indispensable to consider non-motorized traffic in urban development. The heatmap of the *IoV* dataset, as shown in figure 7, displays moderate correlation between the number of lanes, speed, and distance between vehicles, respectively, indicating scope for improvement in traffic flow. The *IoV* dataset shows a very high positive correlation of 0.67 for collision risk with the status of drivers, thus further ensuring the importance of in-cabin monitoring systems. The *IoV* dataset "Nature of environment" factor that is weakly to modestly correlated with other variables. The system would likely look at the environmental conditions it uses in its traffic algorithms. Figure 8 Graphs a scatter plot matrix and histograms for several performance metrics, including efficiency, accuracy, responsiveness, and optimisation scores. Though clear values cannot be discerned, the plots seem to represent an exhaustive assessment across several dimensions. Emergency Vehicle Priority improves by 20%, as shown in figure 9, which is a direct solution to assert the acceptance of reduced response times for emergency vehicles. Dynamic Traffic Signal Control improved by 15%,suggesting enhanced traffic management capabilities. Pedestrian and Cyclist Safety improved the most by 25%that aligns well with the goal of reducing accidents at the outset.

DECLARATION

Funding: The above work did not receive any funding.
Conflict of Interest: The authors confirm that there are no of any conflicts of interest.
Availability of the Data: Data may be available on reasonable request.
Code Availability: Implementation codes are available on request.

CONCLUSION

The integration of LiDAR with V2X communication offers a powerful solution for enhancing Intelligent Traffic Management Systems. By leveraging the strengths of both technologies, this approach improves traffic flow, enhances road safety, and reduces environmental impact through optimized traffic management. Integrating real-time LiDAR data with V2X communication fosters a smarter, adaptive traffic ecosystem capable of managing complex urban scenarios. Future work will focus on further enhancing the system's scalability and exploring additional applications, such as autonomous vehicle integration.

ACKNOWLEDGEMENTS

I would like to thank Research Cell, Desh Bhagat University for invaluable support and contributions to this study. I specifically appreciate Department of Computer Science & Engineering for helping with the design and analysis of this research.

REFERENCES

1. J. H. Joo, M. C. Park, D. S. Han, V. Pejovic. "Deep Learning-BasedChannel Prediction in Realistic Vehicular Communications". IEEE, Access, 2019.
2. Gyu Ho Lee, Ji Dong Choi, Jong Hyuk Lee, Min Young Kim. "Object Detection Using Vision and LiDAR Sensor Fusion for Multi-channel V2X System" 978-1-7281-4985-1/20/$31.00 ©2020 IEEE.
3. Romeo Giuliano, Anna Maria Vegni, Valeria Loscrí, Eros Innocenti, Alessandro Vizzarri, Franco Mazzenga,MuSLi: A multi sensor LiDAR detection for C-V2X networks,Computer Networks,Volume 221,2023,109514,ISSN 1389-1286,https://doi.org/10.1016/j.comnet.2022.109514.
4. Sven Eckelmann, Toralf Trautmann, Hagen Ußler, Benjamin Reichelt, Oliver Michler,V2V-Communication, LiDAR System and Positioning Sensors for Future Fusion Algorithms in Connected Vehicles,Transportation Research Procedia,Volume 27,2017,Pages 69-76,ISSN 2352-1465,https://doi.org/10.1016/j.trpro.2017.12.032.
5. G. H. Lee, K. H. Kwon and M. Y. Kim, "Ambient Environment RecognitionAlgorithm Fusing Vision and LiDAR Sensors for Robust Multi-channel V2X System," 2019 Eleventh International Conference on Ubiquitous and Future Networks (ICUFN), Zagreb, Croatia, 2019, pp. 98-101,doi:10.1109/ICUFN.2019.8806087.
6. R. Miucic, A. Sheikh, Z. Medenica and R. Kunde, "V2X Applications Using Collaborative Perception," 2018 IEEE 88th Vehicular Technology Conference (VTC-Fall), Chicago, IL, USA, 2018, pp. 1-6, doi: 10.1109/VTCFall.2018.8690818.
7. R. Xu, H. Xiang, X. Xia, X. Han, J. Li and J. Ma, "OPV2V: An Open Benchmark Dataset and Fusion Pipeline for Perception with Vehicle-to-Vehicle Communication," 2022 International Conference on Robotics and Automation (ICRA), Philadelphia, PA, USA, 2022, pp. 2583-2589, doi: 10.1109/ICRA46639.2022.9812038.
8. M. Aydin, M. Samarah and K. O. Elish, "Enabling Smart Cities through V2X Communication," 2018 IEEE 4th International Conference on Computer and Communications (ICCC), Chengdu, China, 2018, pp. 550-554, doi: 10.1109/CompComm.2018.8780839.
9. R. Xu, H. Xiang, X. Xia, X. Han, J. Li and J. Ma, "OPV2V: An Open Benchmark Dataset and Fusion Pipeline for Perception with Vehicle-to-Vehicle Communication," 2022 International Conference on Robotics and Automation (ICRA), Philadelphia, PA, USA, 2022, pp. 2583-2589, doi: 10.1109/ICRA46639.2022.9812038.
10. Figueiredo, A., Rito, P., Luís, M. *et al.* Mobility Sensing and V2X Communication for Emergency Services. *Mobile Netw Appl* 28, 1126–1141 (2023).https://doi.org/10.1007/s11036-022-02056-9.

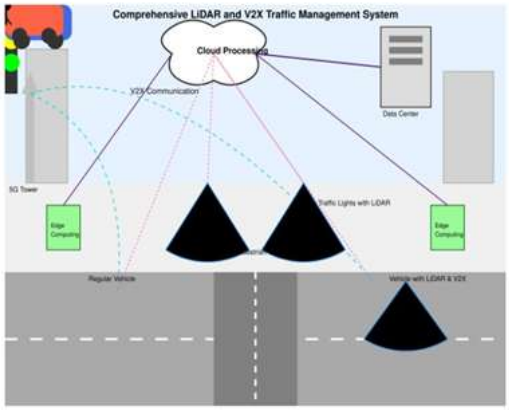

Figure 1. Comprehensive LiDAR and V2X Traffic Management System

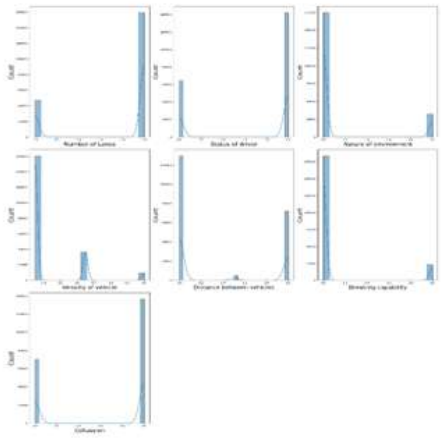

Figure 2.Traffic Flow Efficiency

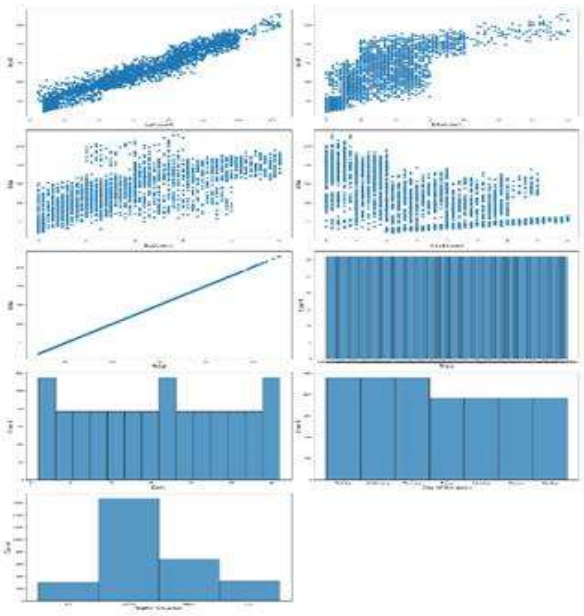

Figure 3.Vehicle Type Distribution

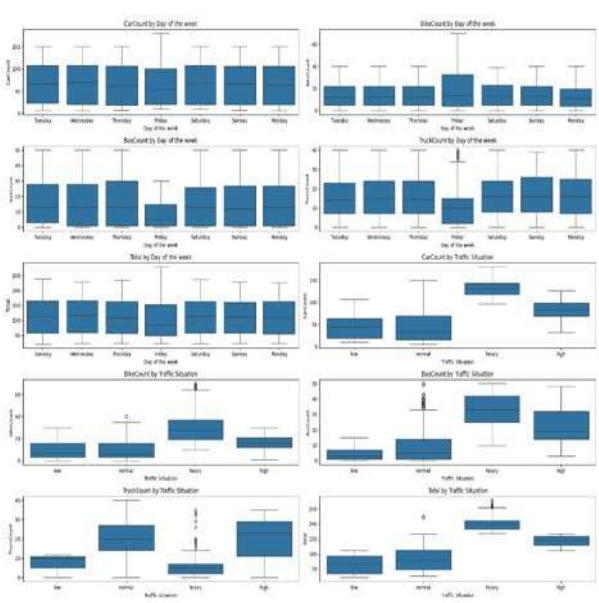

Figure 4.Traffic Conditions Analysis

Figure 5.Pair Plot with Traffic Situation Hue

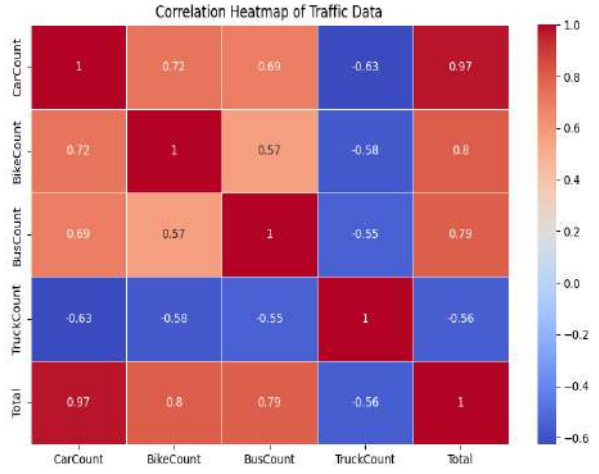

Figure 6.Correlation Heatmap of Traffic Data

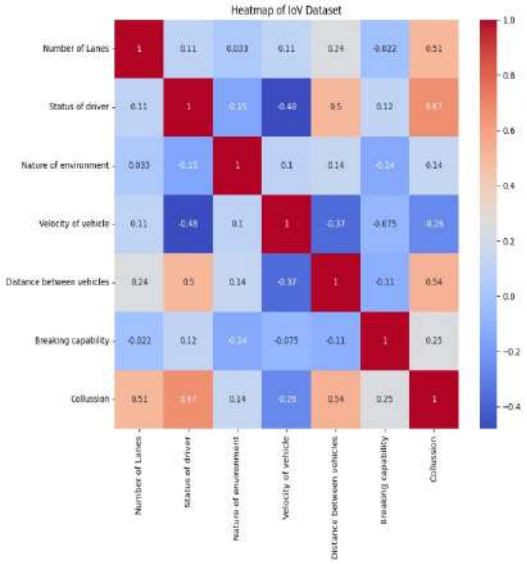

Figure 7. Heatmap of IoV Data Set

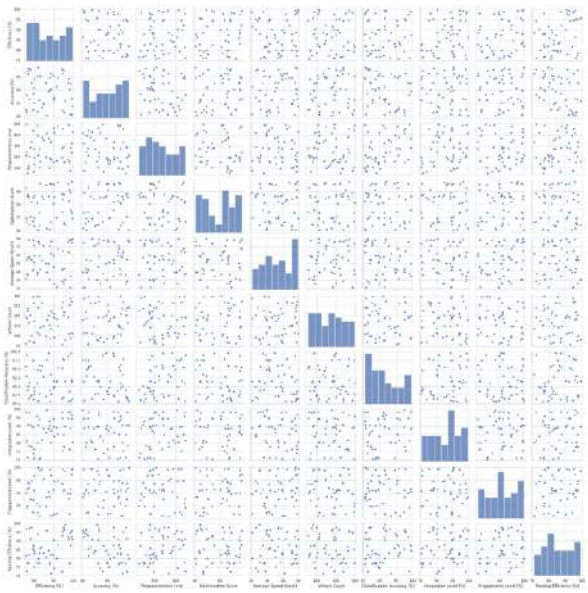

Figure 8.Scatter Plot Matrix

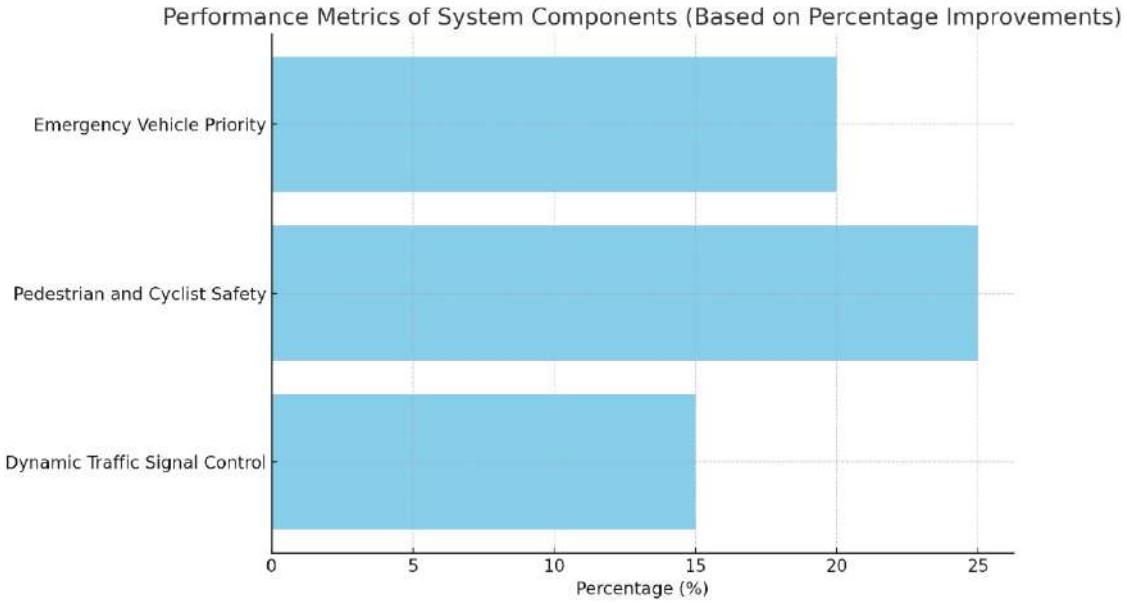

Figure 9. Performance Metrics of System Components

Indian Journal of Natural Sciences *www.tnsroindia.org.in ©IJONS*

Vol.15 / Issue 88 / Feb / 2025 *International Bimonthly (Print) – Open Access* *ISSN: 0976 – 0997*

RESEARCH ARTICLE

Ayurveda in the Management of Hyper Lipidemia: A Case Report

Bhavesh K. Vaja[1]* and Neha Gadgil[2]

[1]P.G Scholar, Department of Kriya Sharir, Parul Institute of Ayurved, Parul University, Vadodara, Gujarat, India.
[2]Professor, Department of Kriya Sharir, Shri Lal Bahadur Shastri Smarak Ayurvedic Mahavidyalaya, Handia, Uttar Pradesh, India.

Received: 28 Nov 2024 Revised: 09 Dec 2024 Accepted: 20 Jan 2025

***Address for Correspondence**
Bhavesh K. Vaja,
P.G Scholar,
Department of Kriya Sharir,
Parul Institute of Ayurved,
Parul University, Vadodara, Gujarat, India.
E.Mail: bhaveshvaja2302@gmail.com

ABSTRACT

Hyperlipidemia is a significant risk factor for the development of atherosclerotic diseases such as coronary heart disease, which is one of the leading causes of morbidity and mortality worldwide. Hyperlipidemia, defined as elevated levels of serum cholesterol, triglycerides, or both, is characterized by abnormally high lipid concentrations in the blood due to impaired lipid and lipoprotein metabolism. This condition can lead to various complications, including cardiovascular disease, diabetes, obesity, hypertension, and atherosclerosis. In Ayurveda, hyperlipidemia is referred to as Medoroga, which encompasses disorders related to the excessive accumulation of fat or lipids in the body. Meda (fat tissue) is considered one of the essential Dhatus (tissues) in Ayurveda, playing a critical role in various metabolic disorders such as obesity and diabetes (Prameha). Excessive accumulation of Meda can lead to a range of health issues, including those mentioned above. This article explores the Ayurvedic approach to managing hyperlipidemia, focusing on how traditional practices can help balance the body and address the root causes of elevated lipid levels. We will discuss Ayurvedic treatments, dietary changes, herbal remedies, and lifestyle modifications, as well as a case report that demonstrates the successful management of hyperlipidemia using Ayurveda. Hyperlipidemia, characterized by elevated levels of lipids (fats) in the blood, is a significant risk factor for cardiovascular diseases such as heart attack and stroke. Conventional treatment often includes statins and other lipid-lowering medications, but patients may seek alternative approaches due to potential side effects or personal preferences. Ayurveda, the ancient Indian system of medicine, offers a holistic approach to managing hyperlipidemia by addressing underlying imbalances and promoting overall health. This case report highlights the successful management of hyperlipidemia using Ayurvedic treatments in a patient.

Keywords: Ayurvedicmedicine, Hyperlipidemia,, doshik balance, case study.

INTRODUCTION

Hyperlipidemia involves various genetic and acquired issues that lead to elevated lipid levels in the body. This condition is quite prevalent, particularly in Western countries, but also globally. Hyperlipidemia has been linked to the concept of Asta Ninditiya Purusha in Ayurveda, where Atisthaulya (extreme obesity) is recognized as a genetic or inherited condition associated with elevated lipids in the context of Meda. Lipids include cholesterol levels, lipoproteins, chylomicrons, VLDL, LDL, Apo lipoproteins, and HDL. Lipids are essential non-polar, hydrophobic molecules needed by all living cells.[1] They play crucial roles in the human body, such as contributing to cellular structure, providing concentrated sources of energy storage, acting as metabolic regulators, and protecting internal organs through cushioning. Depot lipids are stored in the body, while others circulate in the bloodstream. Hyperlipidemia, a dietary condition, is recognized as a potential risk factor for various diseases, including cardiovascular disease, metabolic syndrome, and hypertension. The condition is linked to atherosclerotic diseases like coronary heart disease, a leading cause of morbidity and mortality globally.

Hyperlipidemia is defined as high serum levels of cholesterol, triglycerides, or both. In Ayurveda, lipids are present in the body as Meda Dhatu or adipose tissue, classified within Saptabidha Kala. Meda is found in the abdomen and cartilage, while fats in the large bones are known as Majja or bone marrow. The marrow resides in large bones, while a similar substance found in other bones is regarded as Meda combined with blood. Fat present in muscular tissue is considered Vasa or muscle fat.Hyperlipidemia entails elevated levels of cholesterol and triglycerides or both. Cholesterol, a fatty substance, travels through the bloodstream on proteins called lipoproteins. High blood cholesterol accumulates on blood vessel walls, forming plaque. Over time, these plaque deposits can block arteries, leading to heart disease, peripheral artery disease (resulting in limb ischemia or gangrene), and other complications. There are two types of cholesterol: LDL (low-density lipoprotein) and HDL (high-density lipoprotein). The dominance of Prithivi and Apa Mahabhutas in Meda Dhatu contributes to its liquidity and smoothness. HDL, also known as "good" cholesterol, helps remove excess "bad" cholesterol and clears the arteries, ultimately carrying it back to the liver for processing. This process begins in the stomach and continues in the liver, separating the beneficial and waste portions of the substance. LDL, also known as "bad" cholesterol, clogs the arteries, making them hard and narrow.

Ayurveda classifies Meda Roga primarily by Meda Dosha, while the modern medical system divides hyperlipidemia into familial and acquired types. Acquired hyperlipidemia often results from lifestyle factors such as an unbalanced diet, lack of exercise, smoking, obesity, and heavy alcohol consumption. Medical conditions like kidney disease, diabetes, PCOS, an underactive thyroid, and liver disease can also lead to high cholesterol levels, as associated with Santarpana Janya Nidan Sevan and resulting Amaprodoshaja Vikara. Additionally, inherited conditions or genetic predispositions and pregnancy can contribute to high cholesterol. Inherited hyperlipidemia or mixed hyperlipidemia involves elevated levels of both cholesterol and triglycerides.While Ayurvedic texts lack a specific term for hyperlipidemia, terms like Rasagata Sneha Vriddhi, Rasa Raktagata Sneha Vriddhi, Medovriddhi, Medoroga, Medodosha, and Ama Medo Dhatu are used to describe it. In terms of pathophysiology, hyperlipidemia aligns with Asthayi Medo Dhatu Vriddhi. The elevated Asthayi Medo Dhatu, often ama in origin, remains stored in the body, leading to additional complications. In hyperlipidemia, Kapha Dosha and Medo Dhatu play key roles in the development of Atisthaulya and Prameha.[2]

Medoroga occurs due to abnormal accumulation of medodhatu, initially caused by an imbalance in Kapha dosha, followed by the involvement of Pitta and Vata doshas, leading to their respective symptoms. In later stages, pathological accumulations in other srotus (channels) cause various symptoms like Javoparodha, Ayushohrasa, Swedhsbhaada, among others. Certain nidanas (causal factors), such as lack of exercise, overeating, daytime sleep, consumption of overly sweet, heavy, and oily foods, mental stress, and genetic factors, contribute to the condition.

Symptoms like excessive sweating, increased appetite, excessive thirst, foul odor, weakness, and lack of enthusiasm suggest the involvement of other doshas like Pitta and Vata.[3]

Case Presentation

Patient Information: A 33-year-old male presented with persistent hyperlipidemia, including high levels of total cholesterol and low-density lipoprotein (LDL) cholesterol. He had a sedentary lifestyle, a diet rich in processed and fatty foods. The patient expressed interest in trying Ayurvedic management due to his concern about the potential side effects of statin therapy.

Chief Complaints

There is no chief complaint.

History of Present Illness:

Patient went for yearly full body check-up and all reports are normal except cholesterol report and there is no complain and patient want to take ayurvedic treatment.

Investigations

Lipid profile and routine blood investigation

Past History

No past history or major illness.

Family History

Father –NAD
Mother-NAD

Clinical Examination Ashtavidha Prakisha

- Nadi –kapha vata
- Mala-Samyaka
- Mutra- Samyaka
- Jivha- Sam
- Shabda- Prakrut
- Sparsha- Usna
- Druka- Prakrut
- Aakruti- Madhyam
- Agni – Samagni

Vital Parameters - Vital Parameters were normal.
Initial Assessment
The patient underwent a comprehensive Ayurvedic assessment, which included:

MATERIAL AND METHODS

Ayurvedic Treatment Plan

The patient was provided with an individualized Ayurvedic treatment plan aimed at balancing the Kapha dosha, strengthening Agni (digestive fire), and eliminating ama (toxins) from the body:

Dietary Recommendations

The patient was advised to follow a Kapha-pacifying diet that included:

- Warm, Fresh Foods: Consuming freshly prepared, warm meals to support digestion.

- Light and Dry Foods: Incorporating foods such as legumes, whole grains, and vegetables to balance Kapha.
- Healthy Fats: Including healthy fats in moderation, such as olive oil and ghee.
- Avoiding Heavy and Oily Foods: Limiting the intake of fried and processed foods.

Herbal Remedies

The patient was prescribed Ayurvedic herbs to support healthy lipid levels:

- Lahsun: useful in hridroga (Lahsun kshir paka)
- Arjuna: An herb used for heart health, arjuna may help improve lipid profiles. (Arjuna kshirpaka)[4]
- Dhootapapeshwar Hrudroga Chintamani Rasa : An ayurvedic formulation that helps protect heart health. The ingredients work together to protect the heart from several ailments and strengthen its function.
- baidyanathMedohar guggul

Lifestyle Changes

The patient was encouraged to make lifestyle changes to balance Kapha and support overall health:
Regular Exercise: Daily physical activity, such as walking and yoga, to improve metabolism.
Stress Management: Practicing meditation and breathing exercises to reduce stress.
Adequate Sleep: Ensuring a consistent sleep schedule to support hormonal balance.

Instruction given to the patient

Along with Ayurvedic medication diet and lifestyle restrictions were also advised for the Patient.

RESULT

Lipid profile test before treatment Date -13-01-2024

Cholesterol	252 mg/dl
Triglyceride	362 mg/dl
HDL Cholesterol	39 mg/dl
Direct LDL	145 mg/dl
VLDL	72.40 mg/dl

Lipid profile test after treatment Date - 25-03-2024

Cholesterol	178 mg/dl
Triglyceride	231 mg/dl
HDL Cholesterol	39 mg/dl
Direct LDL	115 mg/dl
VLDL	46.20 mg/dl

Improved Lipid Profile: The patient's total cholesterol and LDL cholesterol levels decreased significantly, reaching normal ranges. Enhanced Energy Levels: The patient reported increased energy and vitality due to lifestyle changes and detoxification. Better Overall Well-being: The patient experienced reduced stress levels and improved quality of life.

DISCUSSION

This case report demonstrates the effectiveness of Ayurveda in managing hyperlipidemia. By addressing the underlying imbalances in Kapha dosha and supporting digestion and metabolism, the patient was able to achieve significant improvements in his lipid profile and overall health. Ayurvedic treatments, including dietary changes,

herbal remedies, lifestyle modifications, and detoxification, provide a holistic approach to managing hyperlipidemia. This case highlights the potential for Ayurveda to offer safe and effective alternatives or complements to conventional treatments for patients seeking a more natural approach to managing lipid levels. In Ayurveda, cholesterol management is about achieving balance in the body and mind by harmonizing the doshas, particularly Kapha. Through dietary modifications, herbal remedies, lifestyle changes, and detoxification, Ayurveda provides a comprehensive approach to managing cholesterol levels and supporting overall health. As always, it is important to consult with a qualified Ayurvedic practitioner or healthcare professional before making significant changes to your health regimen.

Kapha Dosha and Cholesterol

Heaviness and Sluggishness: Excess Kapha dosha can lead to a sense of heaviness and sluggishness in the body, which can slow down metabolism and digestion. This can result in the accumulation of substances like cholesterol in the body. Fluid Retention: Kapha's moist and cold qualities can lead to fluid retention and congestion in the body, including in the blood vessels. This may contribute to plaque buildup in the arteries and increase the risk of heart disease. Poor Circulation: An imbalance in Kapha can lead to poor blood circulation, affecting the body's ability to efficiently transport fats, including cholesterol. In Ayurveda, Agni, or the digestive fire, is a central concept that refers to the body's ability to digest and metabolize food efficiently. Agni is responsible for breaking down food into its essential nutrients and eliminating waste products. Proper functioning of Agni is crucial for overall health and well-being.

The Connection Between Ama and Cholesterol

In Ayurveda, ama is a term used to describe a form of toxin or impurity that accumulates in the body due to improper digestion, metabolism, or elimination. It is considered a sticky, foul-smelling, and heavy substance that can disrupt the normal functioning of the body. Ama is a key factor in the development of various diseases, including imbalances in cholesterol levels. Impaired Digestion: When digestion is weak or imbalanced, the body produces ama from undigested food particles. This disrupts the normal processing and elimination of nutrients and waste products, including fats and cholesterol. Obstruction in Channels: Ama can accumulate in the body's channels (srotas), including blood vessels. This can lead to blockages and impede the proper flow of blood and nutrients, potentially contributing to the buildup of cholesterol and plaque in the arteries. Interference with Metabolism: Ama can disrupt the body's metabolic processes, including the metabolism of fats and cholesterol. This can lead to elevated levels of cholesterol in the blood. Inflammation: Ama is thought to contribute to inflammation in the body. Inflammation can damage blood vessels and contribute to the formation of cholesterol deposits in the arteries.

Managing Ama to Support Healthy Cholesterol Levels

To manage ama and maintain healthy cholesterol levels, Ayurveda offers the following approaches:
Improving Digestion: Strengthening digestion is crucial for preventing the formation of ama. This can be achieved by eating warm, freshly prepared foods, incorporating digestive spices (such as ginger, cumin, and turmeric), and eating in moderation. Detoxification: Periodic detoxification therapies, such as Panchakarma, can help cleanse the body of ama and support overall health. This includes various methods such as herbal treatments, fasting, and oil treatments.
Herbal Remedies: Certain Ayurvedic herbs, such as guggul, triphala, and neem, can help eliminate ama and support healthy digestion and metabolism. Exercise: Regular physical activity can improve circulation and help flush out ama from the body, supporting healthy cholesterol levels. Hydration: Staying well-hydrated helps the body eliminate toxins and supports overall health. Stress Management: Reducing stress through meditation, yoga, or other relaxation techniques can help prevent the accumulation of ama.

CONCLUSION

Ayurveda presents a promising approach to managing hyperlipidemia by focusing on individualized treatment plans that address the root causes of imbalances. This case report underscores the potential benefits of integrating

Ayurvedic practices into the management of hyperlipidemia for improved cardiovascular health and overall well-being. As always, it is important for patients to consult with qualified healthcare professionals before making significant changes to their health regimen. Ayurveda offers a comprehensive approach to managing cholesterol through dietary changes, lifestyle modifications, and herbal remedies. By balancing the doshas and adopting a holistic approach to health, individuals can maintain healthy cholesterol levels and support overall cardiovascular well-being. As with any medical condition, it is advisable to consult with a qualified healthcare practitioner before making significant changes to your diet or lifestyle. In Ayurveda, cholesterol is understood through the lens of the three doshas: Vata, Pitta, and Kapha, which are the fundamental forces governing the body and mind. Each dosha plays a role in maintaining health, and an imbalance in any of these can lead to various health issues, including elevated cholesterol levels. The Ayurvedic perspective on cholesterol is centered around managing these doshas, particularly the Kapha dosha, which is closely associated with heaviness and accumulation in the body. Maintaining strong and balanced Agni is essential for proper digestion and metabolism, which in turn helps regulate cholesterol levels. By focusing on supporting Agni through dietary choices, lifestyle modifications, and the use of appropriate spices and herbs, individuals can effectively manage cholesterol and promote overall health. It is advisable to consult with a qualified Ayurvedic practitioner or healthcare professional before making significant changes to your diet or lifestyle. Managing ama is essential for maintaining healthy cholesterol levels and overall well-being in Ayurveda. By focusing on improving digestion, detoxification, and lifestyle changes, individuals can reduce the accumulation of ama and support cardiovascular health. Consulting with a qualified Ayurvedic practitioner or healthcare professional is recommended before making significant changes to your health regimen.

REFERENCES

1. Chikkanna, Umesh. (2017). Hyperlipidemia – Concept of Lipids in Ayurveda. Journal of Advanced Research in Ayurveda Yoga Unani Sidhha& Homeopathy. 04. 21-24. 10.24321/2394.6547.201715.
2. Chiranjit Biswas, Supriyo Chaudhuri, Tapan Ghosh. Concept of Hyperlipidemia in Ayurveda. Ayushdhara [Internet]. 2022Apr.4 [cited 2024May30];9(1):55-62. Available from: https://ayushdhara.in/index.php/ayushdhara/article/view/863
3. Kala, Jaya &Singhai, Swapnil. (2021). Management of Hyperlipidaemia through Ayurvedic Intervention. European Journal of Medical and Health Sciences. 3. 4-7. 10.24018/ejmed.2021.3.3.815.
4. Dwivedi S, Chopra D. Revisiting Terminalia arjuna - An Ancient Cardiovascular Drug. J Tradit Complement Med. 2014 Oct;4(4):224-31. doi: 10.4103/2225-4110.139103. PMID: 25379463; PMCID: PMC4220499.

Table.1: Patient's Treatment Plan for 2month

No.	Name of drug	Dose of drug	Kala	Anupana
1	Lahsun kshir paka	40ml	Before food	Once a day in the morning
2	Arjuna kshir paka	40ml	After food	Once a day before bed
3	DhootapapeshwarHrudroga Chintamani Rasa	1 tab.	After food	Twice a day with lukewarm water
4	baidyanath Medohar guggul	2 tab.	After food	Twice a day with lukewarm water

Indian Journal of Natural Sciences www.tnsroindia.org.in ©IJONS

Vol.15 / Issue 88 / Feb / 2025 *International Bimonthly (Print) – Open Access* *ISSN: 0976 – 0997*

RESEARCH ARTICLE

Formulation and Evaluation of Natural Ingredients Infused Herbal Soap by using Cold Saponification Method

Ch. Arun Kumar[1]*, S. Sandeep[1], R. Sai Reshma[2], S. Vidyadhara[3], Y. Ashok Kumar[2] and Kotaiah Silakabattini[4]

[1]Associate Professor, Department of Pharmacology, Chebrolu Hanumaiah Institute of Pharmaceutical Sciences, (Affiliated to Acharya Nagarjuna University), Guntur, Andhra Pradesh, India.
[2]Assistant Professor, Department of Pharmacology, Chebrolu Hanumaiah Institute of Pharmaceutical Sciences, (Affiliated to Acharya Nagarjuna University), Guntur, Andhra Pradesh, India.
[3]Professor and Principal, Department of Pharmaceutics, , Chebrolu Hanumaiah Institute of Pharmaceutical Sciences, (Affiliated to Acharya Nagarjuna University), Guntur, Andhra Pradesh, India.
[1]Associate Professor, Department of Pharmacognosy, Chebrolu Hanumaiah Institute of Pharmaceutical Sciences, (Affiliated to Acharya Nagarjuna University), Guntur, Andhra Pradesh, India.

Received: 26 Sep 2024 Revised: 05 Dec 2024 Accepted: 21 Jan 2025

***Address for Correspondence**
Ch. Arun Kumar,
Associate Professor,
Department of Pharmacology,
Chebrolu Hanumaiah Institute of Pharmaceutical Sciences,
(Affiliated to Acharya Nagarjuna University),
Guntur, Andhra Pradesh, India.
E.Mail: arunchadalavada@gmail.com

ABSTRACT

A fatty acid salt called soap is utilized in many lubricating and cleaning goods. Soaps are typically used for washing, bathing, and other household tasks in a home environment. Soaps find application in the industry as thickeners, constituents of some lubricants, and precursors to catalysts. The salts sodium or potassium found in soap a variety of fatty acids that exist naturally. It is created through the basic hydrolysis process of fat or saponification of fat or oil. Fatty acids are neutralized and turned into salt using sodium hydroxide or carbonate. Your skin feels clean and renewed after using soap to eliminate perspiration and debris from your body. However, the kinds of soap you use might not be compatible with your body. Certain conventional or standard soaps may be excessively abrasive. These products will cleanse your skin, but they may cause irritation or dryness. The primary objective is to make a soap that is completely natural and has no negative effects because moisturizing is just as vital as cleaning. The prepared soap samples were then examined to determine the soap's quality. Form forming ability, foam retention time, saponification value, total fatty matter, and pH were measured in this study.

The evaluation parameters carried for standardizing the herbal soap by color determination, pH, TFM (total fatty matter), foam-forming ability, retention time of foam, Saponification value were carried out. This led to an outcome of the formulation (F2), Combination of Coconut and Sesame Oil Soap possessing high Saponification (165.29g/ml) and TFM (73%) values when compared with other formulations. In addition, this formulation was found to be used for daily use and did not cause any skin irritation. Natural herbs and components that are healthier, better for the skin, and less prone to have negative effects are used to make herbal soaps. Herbal soaps include the benefits of nourishment, aromatherapy, and protection against skin conditions. It was successful to produce herbal soap utilizing the cold procedure. Because there would be no harsh chemicals in our environment, pollution that is frequently linked to these artificial compounds would not be a concern. When the created composition was put through several testing, the results were positive. The skin doesn't become irritated by it. Additionally, the prepared soaps were standardized based on a number of physico-chemical characteristics that show a suitable outcome.

Keywords: Coconut oil, Sesame oil, Saponification value, Total fatty matter, Foam retention time**.**

INTRODUCTION

Human skin, which is the body's outermost layer, serves as the body's first line of defense against many infections (1). The skin interacts with the environment, exposing it to a variety of stimuli all the time. The skin is hence vulnerable to harm (2). Scar tissue appears when severely damaged skin tries to recover; this tissue is usually depigmented and decolored. Conversely, chemical soaps have been shown to exacerbate skin dryness and irritation (3). Customers are starting to favor natural ingredient cosmetics as a more organic, eco-friendly, and healthful choice. Herbal cosmetics is another name for Ayurvedic cosmetics (4). In the great majority of cases, the natural ingredient in herbal medicine has no adverse effects on human health. "Herbal soap preparation" refers to a drug or treatment that has antifungal and antibacterial components. It is used to repair damage and disease and maintain people's health. It is composed of plant parts, such as leaves, stems, roots, and fruits (5). Soaps have a long history and have been a part of our daily lives for over 6,000 years. Animal fats, wood ash, and water were combined by the ancient Babylonians to create a cleaning agent that would later be known as "soap." The fundamental process of making soap involves the reaction of fats or oils with a base, or lye. There are two categories of soaps: liquid and solid. NaOH is the basic ingredient used to make solid soaps, whereas KOH is used to make liquid soaps. In order to offer the finished product a broad spectrum of biological activity, synthetic or natural bioactive compounds are added to the basic soap medium in medicinal soaps, setting them apart from conventional soaps.

It is best to avoid employing hazardous synthesis chemicals in medical soap products due to their unfavorable or harmful consequences. In recent years, plant-based natural products have gained popularity as a synthetic ingredient to enhance the essential biological qualities of medicinal soap. By substituting natural phenolic compounds for synthetic antioxidants like BHT and synthetic foaming agents like sodium lauryl sulphate, as well as natural antibacterial agents like Triclosan, for synthetic antibacterial agents, many of the side effects linked to medicinal soaps containing synthetic ingredients were mitigated. In skin care products, including medicinal soaps, coconut oil, olive oil, turmeric, sandalwood, jasmine, and lemon essence are some of the most often utilized ingredients (6-16). The skin is the most susceptible part of the body, even though it offers some protection from the sun, pollutants, and viruses. Common skin illnesses include psoriasis, allergies, rashes, warts, acne, and eczema. Because it shields the skin from microbial infection and transmission, hand hygiene is crucial in the prevention of infectious diseases. This herbal soap or solution helps to prevent the spread of infectious diseases in healthcare settings more successfully (17). Another name for Bombaxceiba is "Bird's Paradise." Because of its many uses, it is regarded as "God's best creation

for humanity" and a valued gift from nature (18). It is used medicinally in Ayurvedic, Unani, and Siddha treatments for the elimination of dead skin, skin whitening, and anti-aging.

METHODS AND MATERIALS

All the ingredients are used in this formulation have herbal grade. The ingredients are collected from different sources. Coconut oil, sesame oil, vitamin -e oil and papaya juice are obtained from the medicinal garden of Chebrolu Hanumaiah Institute of Pharmaceutical Sceinces, Guntur. NaOH purchased from the general store.

Procedure for preparation various soap

The cold saponification process was used to make soap with active plant potentials. Soap is a mixture of various naturally occurring fatty acid salts, either in the form of potassium or sodium. In a heatproof jar, weigh the lye. Measure the water in a different container. After that, slowly add the lye to the water and mix with a heatproof utensil until the lye dissolves completely. Place aside and allow to cool for one hour or more. Weigh the oils while the lye solution is cooling. Transfer the lye solution into the oil container. Mix till the trace is reached. Stir to mix in any additional ingredients, such as colorants or natural exfoliants. Pour the melted soap into the mold very carefully. Place a piece of paper over the mold. Cover it with a cloth to keep the heat in. Leave for as long as two days, or until fully cold and solid. When it's time, take the soap out of the mold and cut it into bars. Before usage, let the bar soaps to cure for at least four weeks outside (19).

Types of formulations

Formulation (F1) - Papaya juice infused Coconut Oil Soap. Formulation(F2)-Combination of Coconut and Sesame oil Soap. Formulation (F3) - vitamin –e infused with coconut oil.
Formulation(F4)-Vitamin-e infused with Sesame oil.
Formulation(F5)-papaya juice infused in Combination of sesame and Coconut Oil.

Evaluation parameters

In developing this soap, we analyzed it by different parameters, including pH, color and characterization, foam-forming ability, retention time of foam, saponification value determination, and determination ofTFM (total fatty matter) (20).

pH

10ml of distilled water was added to 2g of finished soap, and the mixture was agitated until the sample completely dissolved. A pH meter was used to measure the pH.

Organoleptic Properties

Organoleptic characteristics like as color, smell, and texture were assessed either physically or manually.

Foam-Forming Ability

In a 100 ml measuring cylinder, 2g of soap was dissolved in 50 ml of distilled water and violently agitated for two minutes. After ten minutes of standing, the height of the foam was measured. After three repetitions, the mean was calculated.

Retention time of foam

To find out how much foam the polyherbal soap could make, about 1.0 g of it was gathered and dissolved in about 50 ml of distilled water in a 100 ml graduated measuring cylinder. The measuring cylinder was shaking for two to three minutes and then allowed to stand for ten minutes. The foam height was measured ten minutes later. Three consecutive tests were conducted with the observation, and the mean was computed.

Saponification value determination

Whatever the nomenclature, it is defined as the average molecular weight of a fatty acid present in oil or fat. To find the saponification value, roughly 2 g of the soap sample was put in a conical flask with a 0.5 M KOH solution applied. The resulting mixture was cooked in hot water to around 55 degrees Celsius while being continuously stirred. After that, the boiling process was increased to 100 degrees Celsius and continued for almost an hour. For the titration procedure, 0.5 M HCl and phenolphthalein as an indicator were utilized. The disappearance of the pink hue is the observed end point. To calculate saponification, use the following formula:

Saponification Value =Avg. Volume of KOH**×** 28.056**/** Weight of oil(g)

Determination of TFM (total fatty matter)

In order to perform the total fatty matter test, hot water is added to the soap and acid reaction, and the resulting fatty acids are measured. 150 ml of distilled water was added, boiled, and about 10 g of the resultant soap were weighed. After boiling the soap in 20 milliliters of 15% sulfuric acid, a clear solution was produced. After adding 7g of bee wax, the fatty acids on the surface of the resultant solution hardened and were then heated again. The setup was left to cool and solidify into a cake. After removing the cake, it was blotted dry and weighed using the following formula to determine the total amount of fat:

%TFM = (A –X)/W x 100

Where; A= weight of wax+ oil, X= weight of wax, W= weight of soap

RESULTS

Table2:Formulation1(F1): Papaya juice infused Coconut Oil Soap. FIGURE3:Papaya juice infused Coconut Oil Soap Table3:Formulation2(F2): Combination of Coconut and Sesame oil Soap. FIGURE4:Combination of Coconut and Sesame oil Soap Table4: Formulation 3 (F3): vitamin –e infused with coconut oil. FIGURE5: vitamin –e infused with coconut oil. Table5:Formulation 4 (F4): Vitamin-e infused with Sesame oil. FIGURE6: Vitamin-e infused with Sesame oil. Table6:Formulation 5 (F5): papaya juice infused in Combination of sesame and Coconut Oil FIGURE7: papaya juice infused in Combination of sesame and Coconut Oil.

DISCUSSION

The prepared soap's physico-chemical characteristics were examined. The composition had a pleasing color and scent, and it looked good. Other parameters like TFM (total fatty matter), foam-forming ability, retention time of foam, Saponification value was determined which was signifying the standard values for soap. The outcomes of the various evaluation parameters for the polyherbal soap was displayed in Tables 2, 3, 4, and 5. The pH range of the herbal formulation, as indicated by the tables, was ideal for topical application on skin. Both a higher and lower pH indicate detrimental effects on the skin. For the given herbal formulation, the foaming index was determined to be 15.0 ml, 16.0 ml, 15.0 ml, and 15.0 ml, and the foam retention time was determined to be 10–15 minutes for tables 1, 2, 3, and 4. This indicates that the soap's capacity to produce lather was stable and satisfactory. The percentages of total fatty matter were 71%, 73%, 72%, and 72%, in that order. The overall amount of fat in the soap is a measure of its quality. It is not ideal for dry skin if the total fatty matter is reduced. Increased fatty matter contributes to skin moisture. The results showed that the saponification values were 164.5 g/ml, 163.2 g/ml, 165.29 g/ml, and 163.0 g/ml. Based on the study's findings, it is possible to formulate herbal soap using the cold process method while taking a variety of factors, including skin condition, into account. This sought of herbal formulation can bring a big difference in the field of herbal cosmetic as there are many alignment and related flaws in different poly herbal or chemical-based formulations which can be removed.

CONCLUSION

The evaluation parameters carried for standardizing the herbal soap by color determination, pH, TFM (total fatty matter), foam-forming ability, retention time of foam, Saponification value were carried out. This led to an outcome of the formulation (F2), Combination of Coconut and Sesame Oil Soap possessing high Saponification (165.29g/ml) and TFM (73%) values when compared with other formulations. In addition, this formulation was found to be used for daily use and did not cause any skin irritation.

REFERENCES

1. Abbas G., Khan, M. Q., Khan, M. J., Hussain, F. and Hussain,I.2009,Effect of Iron on the growth and yield contributing parameters of wheat (TriticumAestivum L.).The Journal of Animal and Plant Sciences, 19(3): 135-139
2. AbbasG, Mahammad Q K, Muhammad J K, MuhammadT, Muhammad I and Fida H, 2011, Nutrient uptake,growth and yield of wheat an affected by manganese application. Pak. J. Bot., 43(1): 607-616.
3. Aman U, Muhammad, Abdul R,Muhammad S A, Hira S, Asif N,Ahmad N, Abdul W and Faisal N,2017,Manganese nutrition improves theproductivity and grain biofortificationofbread wheat in alkaline calcareous soil.Expl Agric.1-11.
4. Amjad M N, Inayat U A, Mahammad S B, EjazA K, Kalid N, Muhammad A K, Mahammad ZandNazim H, 2011, Effect of micronutrient on growth and yield ofWheat. Pak. J. Agri. Sci., 48(3): 191-196.
5. Anand, N., and Patil, B.N., 2005, Application on growth, yield and quality of durum wheat. Karnataka J.Influence of zinc, iron and lime of nitrogen.Agric. Sci., 18 (3): 599-603
6. Brunes A P, Oliveira S D, Lemes ES, Tavares LC, Gehling VM, Dias LW, Villela FA,2015. Adubaçãoboratada e produção de sementes de trigo. Ci Rural. 45(9):1572-1578.
7. Dapkekar A, Paresh D, Manoj D. O, Kishore M. P andJyutika M. R,2018.Zinc use efficiency is enhanced inwheat through nanofertilization.Scientific Reports, 8:6832.
8. Deewal, G.S. and Pareek, R.G., 2004, Effect of phosphorus, sulphur and zinc onGrowth, yield and nutrient uptake of wheat Indian.J. Agron. 49(3): 160-162.
9. Farhan H N, Saifuldeen A S, Abdulkarem A. Meklef A, Basheer H A, Heshim M A,2021,Effect of boron on the yield of wheat (Triticumaestivum L.) under center pivot sprinkler irrigation system in the West Desert of Iraq.
10. Galindo FS, Teixeira F M, Buzetti S, Boleta E, Rodrigues WL, Santini J, Rosa A, Ludkiewicz M, Silva VM, 2018, Technical and economic viability of wheat with forms of application and doses of boron. J Agr Sci. 10(4):306-315.
11. Galindo F S, Marcelo C M Teixeira F, Salatiér B, Willian L R, Eduardo H, Marcandalli B, José M K S, Maikon R, Azambuja P,2018, Effects of Boron (B) doses and forms on boron use efficiency of wheat.AJCS, 12(09):1536-1542.
12. Ghamry, A.M., Abd El Hamid, A.M., and Mosa, A.A., 2009, Effect of farm yardManure and foliar application of micronutrients on yield and characteristicsOf wheat grown on salt affected soil. American – Eurasian J. Agric, andEnviron. Sci., 5(4): 460-469.
13. HabidN, 2009, Effect of foliar application of Zn and Fe on wheat yield andQuality. African J. Biotech., 8(24): 6795-98.
14. Hussain, N., Khan M A and Javed M A, 2005. Effect of foliar application of plant micronutrientmixture on growth and yield of wheat (Triticumaestivum L.). Pak. J. Biol. Sci., 8(8): 1096-1099.
15. Ismail C, Wolfgang, H., Pfeiffar and Bonnie M C, 2010, Bio-fortification of durum wheat with zinc and iron. Cereal Chem., 87(1): 10-20.
16. Karimian N, Kalbasi M and Hajrasuliha S. 2012. Effect of convertersludge, and its mixtures with organic matter, elemental sulphur and sulfuric acid on availability of iron, phosphorus andmanganese of 3 calcareous soils from central Iran. African Journal of Agricultural Research, 7(4): 568–76.
17. Khan H, Hassan Z UandMaitloA A, 2006. Yield andmicronutrients content of bread wheat (Triticumaestivum L.) under a multi-nutrient fertilizer Hal-Tonic.Intl. J. Agric. Biol. 8: 366-370.

18. Kumar R, Mehrotra N K., NautiyalB D., Praveen K and SinghP K,2012,Effect of copper on growth, yield and concentration of Fe, Mn, Zn and Cuin wheat plants (Triticumaestivum L.)Journal of Environmental Biology30(4) 485-488.
1. 19.https://www.marthastewart.com/1535651/cold-process-soap-making?utm_source=emailshare&utm_medium=social&utm_campaign=shareurlbuttons.
19. P, Devipriya& L, Nivetha& U, Deepak. (2021). Formulation, Development and Characterization of Herbal Soap Using Borassusflabellifer and Curcuma zedoaria. International Journal of Pharmaceutical Sciences Review and Research. 69. 10.47583/ijpsrr.2021.v69i02.020.

Table1:Formulation contains ingredients.

Ingredients	F1	F2	F3	F4	F5
Distilled water	190gm	65gm	32.92gm	32.92gm	50gm
NaOH	88.14gm	31.19gm	14.72gm	14.72	31.19gm
Coconut oil	500gm	100gm	250gm	-	100mg
Papaya juice	5gm	-	-	-	10ml
Sesame oil	-	100gm	-	250	100mg
Orange oil	5ml	5gm	5gm	5gm	5mg
Vitamin e oil	10gm	-	5gm	5gm	-
Beetroot powder	5gm	5gm	5mh	5gm	5mg

Table2:Formulation1(F1): Papaya juice infused Coconut Oil Soap.

Sr. no	pH			Color	Form forming ability	Retention time of foam	Saponification value determination	Total Fatty matter
1.	Day 1	Day 7	Day 14	Milky White	15 ml	15-20 mins	164.5g/ml	72%
	9.5	8.0	6.9					

Table3:Formulation2(F2): Combination of Coconut and Sesame oil Soap

Sr. no	pH			Color	Form forming ability	Retention time of foam	Saponification value determination	Total Fatty matter
1.	Day 1	Day 7	Day 14	Light Brown	16 ml	15-25 mins	165.29g/ml	73%
	9.6	8.4	6.8					

Table4:Formulation 3 (F3): vitamin –e infused with coconut oil.

Sr. no	pH			Color	Form forming ability	Retention time of foam	Saponification value determination	Total Fatty matter
1.	Day 1	Day 7	Day 14	Light Brown	15 ml	10-15 mins	163.2g/ml	72%
	9.0	7.9	6.8					

Table5:Formulation 4 (F4): Vitamin-e infused with Sesame oil.

Sr. no	pH			Color	Form forming ability	Retention time of foam	Saponification value determination	Total Fatty matter
1.	Day 1	Day 7	Day 14	Light Brown	15 ml	15-20 mins	163g/ml	72%
	9.8	9.6	8.0					

Table6:Formulation 5 (F5): papaya juice infused in Combination of sesame and Coconut Oil.

Sr. no	pH			Color	Form forming ability	Retention time of foam	Saponification value determination	Total Fatty matter
1.	Day 1	Day 7	Day 14	Light Brown	16 ml	15-25 mins	162.5g/ml	72%
	8.4	7.6	6.8					

Figure.1: Foam-Forming Ability

Figure.2: Retention time of foam

Figure.3:Papaya juice infused Coconut Oil Soap

Figure.4:CombinationofCoconutandSesameoilSoap

Figure.5: vitamin –e infused with coconut oil.

Figure.6: Vitamin-e infused with Sesame oil.

Figure.7: papaya juice infused in Combination of sesame and Coconut Oil.

Indian Journal of Natural Sciences *www.tnsroindia.org.in ©IJONS*

Vol.15 / Issue 88 / Feb / 2025 *International Bimonthly (Print) – Open Access* *ISSN: 0976 – 0997*

RESEARCH ARTICLE

Field Crops Cultivation in Thanjavur Black using Fuzzy Logic

A. Rajkumar[1]*, V. Bharathi[2] and R. Archana[2]

[1]Assistant Professor and Research Advisor, Department of Mathematics, Annai Vailankanni Arts and Science College, Thanjavur, (Affiliated to Bharathidasan University, Thiruchirappalli), Tamil Nadu, India.
[2]Research Scholar, Department of Mathematics, Annai Vailankanni Arts and Science College, Thanjavur, (Affiliated to Bharathidasan University, Thiruchirappalli), Tamil Nadu, India.

Received: 26 Sep 2024 Revised: 05 Dec 2024 Accepted: 21 Jan 2025

***Address for Correspondence**
A. Rajkumar,
Assistant Professor and Research Advisor,
Department of Mathematics,
Annai Vailankanni Arts and Science College, Thanjavur,
(Affiliated to Bharathidasan University, Thiruchirappalli),
Tamil Nadu, India.
E.Mail: rajkumar@avasctnj.edu.in

ABSTRACT

Agriculture plays an important role in ensuring national food and nutrition security. The Cauvery delta region of Tamil Nadu is important for agriculture in the state. However, production in the region has decreased in recent years, and the situation of farmers in the delta has worsened since 2023. Factors such as changes in soil moisture penetration, increased water use and rising agricultural input prices have reduced farmers' incomes. Additionally, climate change is increasing production costs as farmers have to purchase more pesticides and herbicides to combat new crop diseases. Water scarcity and debt are among the reasons for farmers committing suicide in the Cauvery delta. Understanding the importance of agriculture to family income requires understanding the nature of property. In addition, this study takes time to analyze to determine land use and cultivation in the Tamil Nadu region. The results showed that the cultivated area was decreasing and farming patterns were changing due to poor rainfall patterns and water scarcity in the region.

Keywords: Cauvery delta region, land use pattern, agricultural pattern

INTRODUCTION

Agriculture contributes to rural development, food security and employment in the country. Agriculture is the path to development through the development of rural areas. According to Economic Survey 2019-20, India's share in the global agriculture market is close to 2.15% and its contribution to the economy is significant. One of the most important rivers of South India is the Cauvery. Of the total length of 800 kilometres of the Cauvery river in Tamil

Nadu, 416 kilometers pass through the state. The river is known as one of the best rivers in the country, with 90-95% of its flow used for irrigation and electricity. Tamil Nadu is a state with 6% of the country's population, 79.38 million of whom are landowners. The state won the Krissy Kaman Award for food production of 10.11 million tonnes in 2011-12. The eight major crops grown in Tamil Nadu are wheat, millets, pulses, cotton and sugar. The main soils are red soil, alluvial soil, sandy soil and saline soil. Water availability is a major problem for Tamil Nadu as agriculture depends on monsoon rains and irrigation facilities. The state's per capita water resources and average rainfall are below the national average. The main sources of irrigation are tube wells and boreholes (62%), followed by canals (25%) and water tanks (13%). The Cauvery delta region is one of the seven climatic zones of Tamil Nadu, located in the eastern part of Tamil Nadu and known for its significant contribution to the agriculture of the state (Paramasivan & Pasupathi, 2021). The district covers eight districts, including Thanjavur, and produces over 70% of Tamil Nadu's rice. Black beans, green beans, bananas and sugar are also major crops in the region. The main source of irrigation water is the Cauvery river at Kodagu in the state of Karnataka. The Grand Anaikat and Kalanai Dams play an important role in ensuring water supply across the region. Recently, the Tamil Nadu government declared the Cauvery delta region as a special agricultural zone. This means that dependence on land is decreasing over the years and steps will be taken for agricultural returns. (Misra, 2014) discussed the agricultural economics of the land in the Cauvery region of Tamil Nadu. The main determinant of this change is soil fertility and soil retention. Other factors are insufficient rainfall and lack of storage facilities (Başran, 2014). Thanjavur district is also known as the "rice bowl of Tamil Nadu" and is one of the eight districts in the Cauvery delta region in the eastern part of the state (Vasanthakumar, 2018). The main sources of irrigation water are canals, tanks and wells in the Cauvery, Vennar and Grand Anicut, as evidenced by the canals in the area. The area is divided into 14 blocks for development purposes. There has been water shortage for many years and there has been an increase in suicides among farmers and businesses in the region (Sabarisakthi, 2016). Climate change is also affecting the region due to rising sea levels and increasing mangrove cover. Over the years, crops in the region have diversified; crops were converted into other crops such as sugar, cotton, beans, bananas and vegetables. Objectives of the study

1. To compare the land use pattern among different blocks in the Thanjavur District.
2. To identify the reasons behind the cropping pattern in the district.

Scope Of Study

Thanjavur is also known as the breadbasket of South India; It is one of the most productive regions. Population growth and resources constantly increase competition for land. Farms are being converted to other uses. According to the latest National Human Development Report of Tamil Nadu (Office, 2022), all the three districts are classified as high poverty areas in the state. It is important to identify and highlight the factors that make agriculture profitable and successful in the Cauvery delta region, where the majority of the population lives in rural areas and poor people, but the proportion is decreasing due to dependence on agriculture. to do. By investigating the change in the land use pattern in the region in the last year, the reasons for the decrease in the cultivation area and total cultivation area in the region in the last year were revealed. Uncertainty regarding the existence of the Cauvery River as an aquifer, its availability and groundwater levels are decreasing due to overexploitation for agricultural and industrial purposes (Jagannathan and Ramaraj, 2016). The state government recently classified the Cauvery delta region as a 'special agricultural' zone and requested suggestions for development of agriculture in the region. Methodology. This study is descriptive in nature and is based on data collected from secondary sources. Census, census, census, livestock census, district information, information of various departments, etc. Secondary data on the population, society, economy, culture, politics, agriculture, environment and other aspects of the region through. Geographic returns from Thanjavur district, spring and harvest for Tamil Nadu, Tamil Nadu Environment Status Report (2017), various newspapers and magazines. Statistical tools used for analysis are percentages, graphs and time series analysis.

Layout And Framework Of Analysis

The analysis and results are divided into two parts. The first example of the land use pattern of 14 blocks in the district by investigating the percentage difference. A-part, from 2006-07 and 2016-17. The second is a timeline showing the ratio of the area planted to major food crops and non-food crops to the total area of the region during the past year and explaining the reasons for changes in planting. As a natural resource, land is inherently limited but

must meet the needs of a growing population in agriculture, utility and industrial use. Land use patterns change every year depending on population growth. Economic development and continued depletion of resources (Division & Paper, n.d.) Land is classified according to its characteristics, characteristics and capacity for agricultural use. There are nine subdivisions in Thanjavur district. Changes in land use reflect changes in agriculture. Land use patterns from 2012-13 to 2022-23 in various blocks of Thanjavur district were analyzed by comparing the percentage of a group of lands in the total area in the first year and last year.

Net Planting Area

This represents the cultivated land and orchard. Areas planted multiple times are counted only once (Ministry of Statistics and Program Implementation (MOSPI)). Increasing the net cultivation area indicates that the agricultural area has increased and therefore the crop production has increased. The graph below shows the percentage change in net cultivation area in 14 blocks. Other lands Poor farmers and land that has not been cultivated for more than one year but less than five years due to lack of water (MOSPI). The chart below shows the percentage difference. Culturable waste lands

The lands that is available for cultivation

The lands are left fallow or covered by any shrubs and not taken up for cultivation for more than 5 years in succession for a reason. There is an overall decrease or no change (Budalur and Thiruvaiyaru) in culturable waste lands in all blocks.

Land used for non-agricultural purposes

This includes land for buildings, roads, railways and water. This land can be cultivatedbut does not include the cultivated area - excluding other trees, crops and trees. It contains bamboo, wood and firewood as fuel. This category includes plants that are not part of the vineyard.

One Now Lost Land Balance During The Year.

The increase in all blocks means a decrease in the net cultivation area in the block in 2022-2023.

Case Study

Thanjavur being the foremost district of the carvery delta occupies an important position in the agricultural of Tamil Nādu as 70 present of the population is engaged in agriculture and allied activities for their livelihood. The district has a Geographical area of 3.39 L.Ha with a gross cropped area of around 2.69 L. Ha. Since its formation the district is called as the “Rice bowl of Tamil Nadu”. The geological formation of Thanjavur district is made up of cretaceous. Tertiary and Alluvial deposits with major area occupied by the Alluvial and Tertiary deposits. Thanjavur has all along been one of the districts with a creditable performance in agricultural production with the farmers relatively more responsive and receptive and receptive to new technologies. They also innovative in adopting modern technologies and High Yielding verities. The district is constituted with 3 Revenue Division, 9 Taluks, 14Blocks and 906 Revenue Villages. I have choose only Seven blocks and find out the problem.

Normalize the decision-matrix.

The following formula can be used to normalize.

$$r_{ij}(\mathrm{x}) = \frac{x_{ij}}{\sqrt{\sum_{i=1}^{m} x_{ij}^2}} \quad i = 1, \dots, m \;\; ; j = 1, \dots \;\; , n$$

The following table shows the normalized.

Calculate the weighted normalized decision matrix.

According to the followingformula, the normalized matrix is multiplied by the weight of the criteria.

$$v_{ij}(\mathrm{x}) = w_j r_{ij}(x) \quad i = 1, \dots, m \;\; ; j = 1, \dots \;\; , n$$

The following table showsthe weighted normalized decision matrix.

Determine the positive ideal and negative ideal solutions.

The aim of the TOPSIS method is to calculate the degree of distance of each alternative from positive and negative ideals. Therefore, in this step, the positive and negative ideal solutions are determined according to the following formulas.$A^+ = (v_1^+, v_2^+, \dots, v_n^+) A^- = (v_1^-, v_2^-, \dots, v_n^{-+})$

So that $v_j^+ = \{(max\ v_{ij}(x) | j \epsilon j_1), (min\ v_{ij}(x) | j \epsilon j_2)\}\ i = 1, \dots, m$

$v_j^- = \{(min\ v_{ij}(x) | j \epsilon j_1), (max\ v_{ij}(x) | j \epsilon j_2)\}\ i = 1, \dots, m$

where j1 and j2 denote the negative and positive criteria, respectively.

The following table shows both positive and negative ideal values.

Calculate the relative closeness degree of alternatives to the ideal solution

In this step, the relative closeness degree of each alternative to the ideal solution is obtained by the following formula. If the relative closeness degree has value near to 1, it means that the alternative has shorter distance from the positive ideal solution and longer distance from the negative idealsolution.

$C_i = \frac{d_i^-}{(d_i^+ + d_i^-)}$, $i = 1, \dots, m$

The following table shows the relative closeness degree of each alternative to the ideal solution.

CONCLUSION

This article explains the production planning problem that uses variables such as cost, output, and cost of sales to obtain total revenue under the constraint of capital investment and capital loss. In order to use all available information on the parameters, we evaluate the objective function with three negative, positive and pessimistic models as necessary and recommend updating the WWO algorithm, which updates the solution and optimizes all three parameters. But the indicators are different. The results of various experiments conducted in agriculture of Thanjavur delta confirmed that the proposed solution of fuzzy optimized WWO algorithm increased the total revenue by more than 5% compared to the best non-fuzzy algorithm. In the current project, preparations for seasonal products are ongoing. We now present on the grid optimization problems and methods for annual crop planning as well as planting and harvesting in different seasons. Moreover, in the current study, turbidity estimation is not a simple regression based on knowledge or historical data. In future research, we will estimate the size of the data and use deep learning.

REFERENCES

1. Bui, T.X., (1987) Coop: A Group Decision Support System for Cooperative Multiple Criteria Group Decision Making, Springer – verlag,Berlin.
2. Keeney, R.L. and H. Raiffa (1976) Decision with Multiple Objectives: Preferences and Value Tradeoffs, Wiley, New York.
3. A. Rajkumar, S.Udayakumar , Multicritrion Fuzzy Decision Making in Irrigation Planning. International Journal of Scientific and Research Publications. March 2014.
4. [A. Rajkumar, S. Udayakumar, Assessing the Ground Water Quality Parameters Using Fuzzy Relation. International Journal of Informative and Futuristic Research. February -2015.
5. A. Rajkumar, S.Udayakumar, South Indian River Ranking Using Fuzzy Analytic Hierarchy Process. International journal of Scientific and Engineering Research, March – 2015.
6. A. Rajkumar, S.Udayakumar, Discrete Multicritirion Decision Making for Performance Evaluation of an Irrigation System.International Journal of Informative and Futuristic Research. June – 2015.
7. A. Rajkumar, S. Sathyabama, Diagnostic of Symptoms Using Fuzzy Logic and Decision-Making techniques. IOSR Journal of Engineering - August - 2018.
8. A. Rajkumar, S.VidyaLung Cancer Successful Treatment for Chemotherapy and Radiotherapy Decision Making Using Fuzzy Logic. 6 th March 2018.

9. A.Rajkumar, Muticriterian Fuzzy Decision Making in Irrigation Planning. Apr-2019. International Journal of Scientific Research in Mathematical and Statistical Sciences.
10. A. Rajkumar, G. Komagan, Sanchi kumar,Insulin Therapy In Patients With Diabetes Mellitus Using Mathematical Modeling.Adalya Journal of Web of Science. August -2019.
11. A. Rajkumar, G.gomagan, Sanchikumar,MathematicalModeling on - Cell Mass, Glucose Dynamics and Glucose Insulin Glucagon Interaction Models: Effect of Genetic Predisposition to Diabetes. Compliancew Engendering Journals. September -2019.
12. A. Rajkumar, J. Sharmila Jessie Ignatia, Impact of Covid – 19 Pandemic on Magazine Sales: Evaluating Under Fuzzy Environment.
13. A. Rajkumar, A. Ezhilarasi, Impact of Covid – 19 Pandemic on Magazine Sales: Evaluating Under Fuzzy Environment.
14. A. Rajkumar, A. Ezhilarasi ,A Study on the Status of Water Quality at TamiraBarani River Site AssessingIt's Suitability for Human Consumption Based on Indian Standards International Journal of Business and Administration Research ReviewFebruary – 2022.
15. A. Rajkumar, J. Sharmila Jessie Ignatia A Method for Solving Bottleneck-Cost Transportation Problem Using Fuzzy Optimization Trapezoidal fuzzy numbers with λ-Cut and Ranking Method. Advances and Applications in Mathematical Sciences June- 2022,
16. A. Rajkumar, A. Ezhilarasi Evaluation of Interval Sequencing Problem Application In Water Pollution Control Machine Using Fuzzy Decision-Making Advances and Applications in Mathematical Sciences June -2022, Volume 21, Issue 8, June 2022,

Table.1:

S.No	Block and Cultivation	Paddy Cultivation	Sugarcane Cultivation	Cotton Cultivation	Pulses Cultivation	Millets Cultivation
01	Thanjavur	25794	1072	49	3721	733
02	Budalur	15270	124	1	315	130
03	Thiruvaiyaru	13509	255	10	191	2
04	Orathanadu	36421	13	1	7357	41
05	Thiruvonam	15880	15	1	1899	71
06	Pudukkottai	8734	53	2	1501	18
07	Madhukar	6861	2	0	1412	4
08	Peravurani	7507	28	4	598	33
09	Sethubavasathiram	6185	14	0	467	6
10	Papanasam	7211	1273	333	1305	18
11	Ammapettai	31999	55	363	3170	10
12	Kumbakonam	13933	180	950	3249	11
13	Thiruvedaimaruthur	18230	24	1568	4196	10
14	Thiruppanandal	18483	109	528	4635	14

Table.2: The following table shows the relative closeness degree of each alternative to the ideal solution.

	Frequency	Percent	Valid Percent	Cumulative Percent
Valid	3	16.7	16.7	16.7
Ammapettai	1	5.6	5.6	22.2
Block and	1	5.6	5.6	27.8
Budalur	1	5.6	5.6	33.3
Kumbakonam	1	5.6	5.6	38.9
Madhukar	1	5.6	5.6	44.4
Orathanadu	1	5.6	5.6	50.0
Papanasam	1	5.6	5.6	55.6
Peravurani	1	5.6	5.6	61.1
Pudukkottai	1	5.6	5.6	66.7
Sethubavasathiram	1	5.6	5.6	72.2
Thanjavur	1	5.6	5.6	77.8
Thiruppanandal	1	5.6	5.6	83.3
Thiruvaiyaru	1	5.6	5.6	88.9
Thiruvedaimaruthur	1	5.6	5.6	94.4
Thiruvonam	1	5.6	5.6	100.0
Total	18	100.0	100.0	

Table.3: Paddy Cultivation in the year 2023

Paddy Cultivation in the year 2023					
		Frequency	**Percent**	**Valid Percent**	**Cumulative Percent**
Valid		3	16.7	16.7	16.7
Thanjavur	13509	1	5.6	5.6	22.2
Budalur	13933	1	5.6	5.6	27.8
Thiruvaiyaru	15270	1	5.6	5.6	33.3
Orathanadu	15880	1	5.6	5.6	38.9
Thiruvonam	18230	1	5.6	5.6	44.4
Pudukkottai	18483	1	5.6	5.6	50.0
Madhukar	25794	1	5.6	5.6	55.6
Peravurani	31999	1	5.6	5.6	61.1
Sethubavasathiram	36421	1	5.6	5.6	66.7
Papanasam	6185	1	5.6	5.6	72.2
Ammapettai	6861	1	5.6	5.6	77.8
Kumbakonam	7211	1	5.6	5.6	83.3
Thiruvedaimaruthur	7507	1	5.6	5.6	88.9
Thiruppanandal	8734	1	5.6	5.6	94.4
	Paddy	1	5.6	5.6	100.0
	Total	18	100.0	100.0	

Table.4: Sugarcane Cultivation in the year 2023

Sugarcane Cultivation in the year 2023					
		Frequency	**Percent**	**Valid Percent**	**Cumulative Percent**
Valid		3	16.7	16.7	16.7
Thanjavur	1072	1	5.6	5.6	22.2
Budalur	109	1	5.6	5.6	27.8
Thiruvaiyaru	124	1	5.6	5.6	33.3
Orathanadu	1273	1	5.6	5.6	38.9
Thiruvonam	13	1	5.6	5.6	44.4
Pudukkottai	14	1	5.6	5.6	50.0
Madhukar	15	1	5.6	5.6	55.6
Peravurani	180	1	5.6	5.6	61.1
Sethubavasathiram	2	1	5.6	5.6	66.7
Papanasam	24	1	5.6	5.6	72.2
Ammapettai	255	1	5.6	5.6	77.8
Kumbakonam	28	1	5.6	5.6	83.3
Thiruvedaimaruthur	53	1	5.6	5.6	88.9
Thiruppanandal	55	1	5.6	5.6	94.4
	Sugarcane Cultivation	1	5.6	5.6	100.0
	Total	18	100.0	100.0	

Table.5: Cotton Cultivation in the year 2023

Cotton Cultivation in the year 2023					
		Frequency	**Percent**	**Valid Percent**	**Cumulative Percent**
Valid		3	16.7	16.7	16.7
Thanjavur	0	2	11.1	11.1	27.8
Budalur	1	3	16.7	16.7	44.4
Thiruvaiyaru	10	1	5.6	5.6	50.0
Orathanadu	1568	1	5.6	5.6	55.6
Thiruvonam	2	1	5.6	5.6	61.1
Pudukkottai	333	1	5.6	5.6	66.7
Madhukar	363	1	5.6	5.6	72.2
Peravurani	4	1	5.6	5.6	77.8
Sethubavasathiram	49	1	5.6	5.6	83.3
Papanasam	528	1	5.6	5.6	88.9
Ammapettai	950	1	5.6	5.6	94.4
	Cotton	1	5.6	5.6	100.0
	Total	18	100.0	100.0	

Table.6: Pulses Cultivation in the year 2023

Pulses Cultivation in the year 2023					
		Frequency	**Percent**	**Valid Percent**	**Cumulative Percent**
Valid		3	16.7	16.7	16.7
Thanjavur	1305	1	5.6	5.6	22.2
Budalur	1412	1	5.6	5.6	27.8
Thiruvaiyaru	1501	1	5.6	5.6	33.3
Orathanadu	1899	1	5.6	5.6	38.9
Thiruvonam	191	1	5.6	5.6	44.4
Pudukkottai	315	1	5.6	5.6	50.0
Madhukar	3170	1	5.6	5.6	55.6
Peravurani	3249	1	5.6	5.6	61.1
Sethubavasathiram	3721	1	5.6	5.6	66.7
Papanasam	4196	1	5.6	5.6	72.2
Ammapettai	4635	1	5.6	5.6	77.8
Kumbakonam	467	1	5.6	5.6	83.3
Thiruvedaimaruthur	598	1	5.6	5.6	88.9
Thiruppanandal	7357	1	5.6	5.6	94.4
	Pulses	1	5.6	5.6	100.0
	Total	18	100.0	100.0	

Table.7: Millets Cultivation in the year 2023

Millets Cultivation in the year 2023					
		Frequency	**Percent**	**Valid Percent**	**Cumulative Percent**
Valid		3	16.7	16.7	16.7
Thanjavur	10	2	11.1	11.1	27.8
Budalur	11	1	5.6	5.6	33.3
Thiruvaiyaru	130	1	5.6	5.6	38.9
Orathanadu	14	1	5.6	5.6	44.4
Thiruvonam	18	2	11.1	11.1	55.6
Pudukkottai	2	1	5.6	5.6	61.1
Madhukar	33	1	5.6	5.6	66.7
Peravurani	4	1	5.6	5.6	72.2
Sethubavasathiram	41	1	5.6	5.6	77.8
Papanasam	6	1	5.6	5.6	83.3
Ammapettai	71	1	5.6	5.6	88.9
Kumbakonam	733	1	5.6	5.6	94.4
	Millets	1	5.6	5.6	100.0
	Total	18	100.0	100.0	

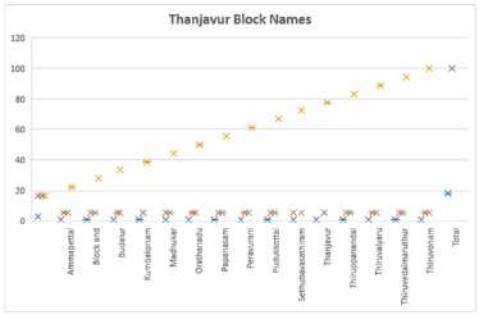

Graph.1:Tanjavur block names

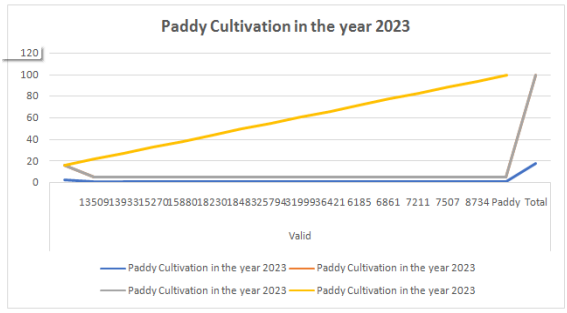

Graph.2: Paddy Cultivation in the year 2023

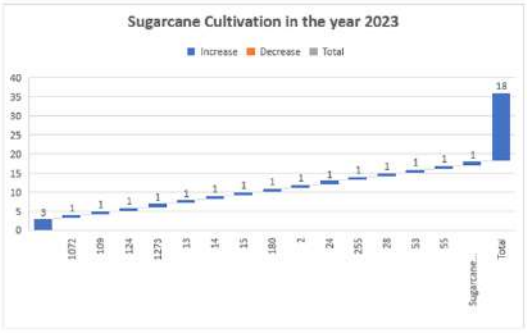

Graph.3:Sugarvane Cultivation In The Year2023

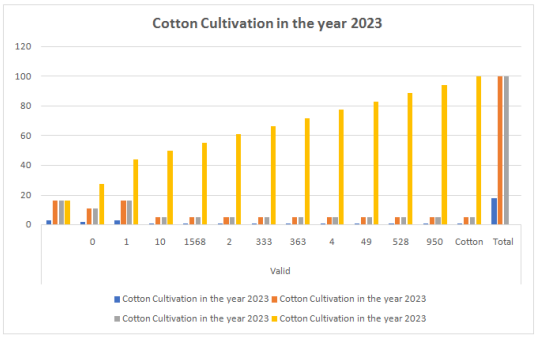

Graph.4: Cotton Cultivation in the year 2023

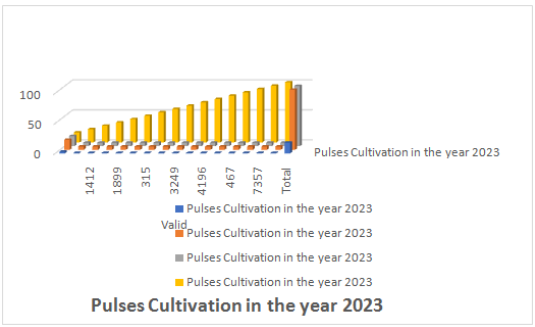

Graph.5: Pulses Cultivation in the year 2023

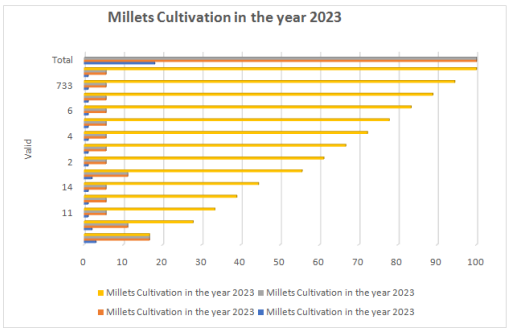

Graph.6: Millets Cultivation in the year 2023

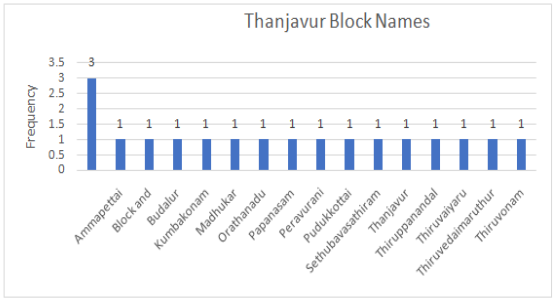

Graph.7: Tanjavur Block Names

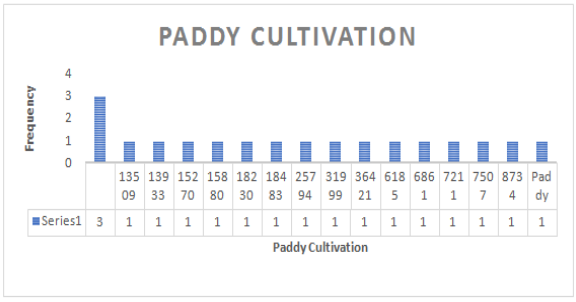

Graph.8: Paddy Cultivation

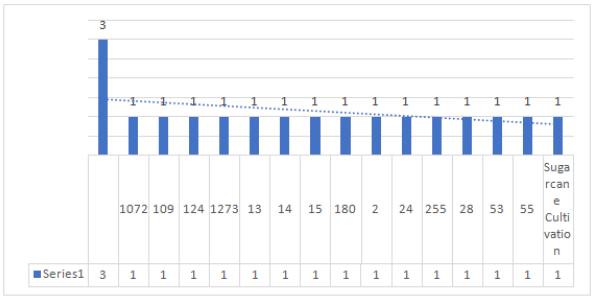

Graph.9:

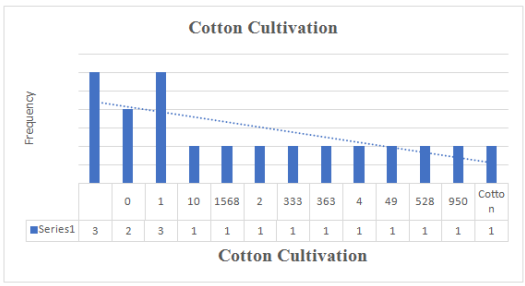

Graph.10: Cotton Cultivation

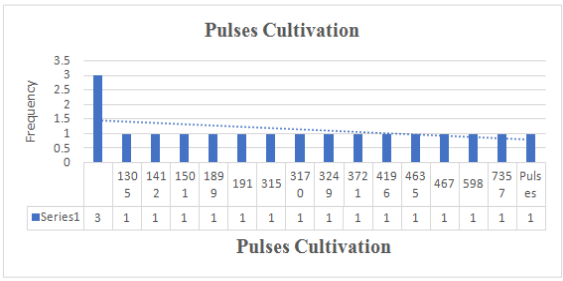

Graph.11: Pulses Cultivation

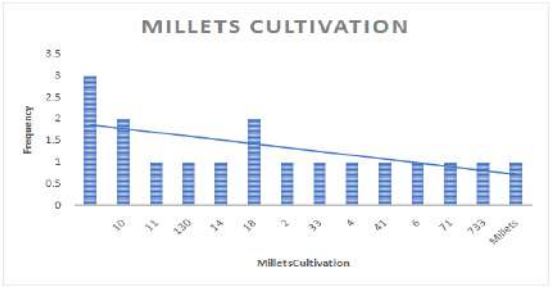

Graph.12: Millets Cultivation

Indian Journal of Natural Sciences *www.tnsroindia.org.in ©IJONS*

Vol.15 / Issue 88 / Feb / 2025 *International Bimonthly (Print) – Open Access* *ISSN: 0976 – 0997*

RESEARCH ARTICLE

In-vitro Antihistamine Activity of Thaengai Thylam by Isolated Chick Ileum Method

S. Eswari[1], S. K. Karunya[1], R. Meenakumari[2] and M. Meenakshi Sundaram[3]*

[1]PG Scholar, Department of Kuzhandhai Maruthuvam, National Institute of Siddha, (Affiliated to The Tamil Nadu Dr. M.G.R. Medical University), Chennai, Tamil Nadu, India.
[2]Director, National Institute of Siddha, (Affiliated to The Tamil Nadu Dr. M.G.R. Medical University), Chennai, Tamil Nadu, India.
[3]Professor and HOD, Department of Kuzhandhai Maruthuvam, National Institute of Siddha, (Affiliated to The Tamil Nadu Dr. M.G.R. Medical University), Chennai, Tamil Nadu, India.

Received: 28 Nov 2024 Revised: 09 Dec 2024 Accepted: 20 Jan 2025

***Address for Correspondence**
M. Meenakshi Sundaram,
Professor and HOD,
Department of Kuzhandhai Maruthuvam,
National Institute of Siddha,
(Affiliated to The Tamil Nadu Dr. M.G.R. Medical University),
Chennai, Tamil Nadu, India.
E.Mail:

ABSTRACT

Background: An allergy occurs when our immune system overreacts to the "foreign" substance. In case of an allergy, substances that are usually harmless and don't bother some people, such as dust or animal dander, our body views these substances as "foreign," which then triggers an overreaction by our body's defence mechanism that includes the release of histamine. The substances that trigger the overreaction are called allergens. The symptoms that result is called an allergic reaction. Along with antibiotics, antihistamines are the most widely used systemic drugs in dermatology. This is attributable to the major role played by histamine in common diseases such as urticaria and atopic eczema. Antihistamines are a class of drugs commonly used to treat symptoms of allergies. These drugs help treat conditions caused by too much of histamine, a chemical created by our body's immune system. Antihistamines are most commonly used by people who have allergic reactions to pollen and other allergens. The chicken ileum is suitable for performing bioassay of histamine, an alternative to isolated ileum preparation from laboratory animal (guinea pig) without sacrificing the experimental animals. Thaengai thylam a Siddha herbal medicine possess anti histamine activity which acts well on allergic skin conditions such as atopic dermatitis, urticaria when applied externally. To evaluate the antihistamine activity of Thaengai thylam(TT) by isolated chick ileum method. The raw drugs were purified and the medicine was prepared as per siddha text "Bogar 700". The medicine was tested for anti-histamine activity in a standard

laboratory. The height of response of concentration response curve of histamine before incubation with test drug ranges from 15 mm to 39 mm. There was a promising decrease in the height of the response curve after incubation with test drug TT ranges from 9 mm to 21 mm. It was concluded that the sample Thaengai Thylam possess promising anti histamine property.

Keywords: Siddha, Thaengai thylam, allergy, anti-histamine

INTRODUCTION

Antihistamines are a pharmaceutical class of drugs that act to treat histamine-mediated conditions. There are two main classes of histamine receptors: H-1 receptors and H-2 receptors. Antihistamine drugs that bind to H-1 receptors are generally used to treat allergies and allergic rhinitis. Drugs that bind to H-2 receptors treat upper gastrointestinal conditions that are caused by excessive stomach acid(1). H-1 antihistamines are further classified according to first and second-generation agents. First-generation H-1 antihistamines more easily cross the blood-brain barrier into the central nervous system (CNS), whereas second-generation H-1 antihistamines do not. The first-generation drugs will bind to both central and peripheral histamine-1 receptors, whereas second-generation drugs selectively bind to peripheral histamine-1 receptors; this leads to different therapeutic and side effect profiles (2). Histamine (an endogenous chemical messenger) induces an increased level of vascular permeability, which leads to fluid moving from capillaries into the surrounding tissues. The overall outcome of this is increased swelling and dilation of vessels. Antihistamines stop this effect by acting as antagonists at the H-1 receptors. The clinical benefit is a reduction in allergy symptoms and any related symptoms(3) First-generation antihistamines easily cross the blood-brain barrier into the central nervous system and antagonize H-1 receptors, leading to a different therapeutic and adverse effect profile in contrast to second-generation antihistamines selectively bind to peripheral histamine receptors. The duration of the pharmacological action of first-generation antihistamines is about 4 to 6 hours. In contrast, second-generation antihistamines work for 12 to 24 hours. They are both metabolized by the liver using the P450 cytochrome system. Thaengai Thylam mentioned in siddha text “Bogar 700” is used externally to treat Atopic dermatitis and urticaria (4). This medicine act as firstgeneration anti-histamine. Thaengai thylam consist of coconut milk (Cocos nucifera),Karunjeeragam (Nigella sativa),Manjal (Cucurma longa) and common salt. All the ingredients possess anti-histamine activity which reduces allergic reactions over the skin. It is tested in a standard laboratory for anti-histamine activity using isolated chick ileum method.Chicken ileum is suitable for performing bioassay of histamine, an alternative to isolated ileum preparation from laboratory animal (guinea pig) without sacrificing the experimental animals (5)

MATERIALS AND METHODS

The raw drugs were purified and the medicine was prepared as per siddha text “Bogar 700”. The medicine was tested for anti-histamine activity in a standard laboratory

Anti-Histamine evaluation using Isolated chick ileum:

Chick ileum was purchased from local slaughter house in which the caecum part of the gut was lifted to identify the ileo-caecal junction. About 2- 3cm of the ileum portion was cut and removed and immediately placed it in the watch glass containing physiological salt solution. Sufficient care was taken to avoid the damage to the gut muscle. Bath volume of about 25 ml was maintained, and the tissue was allowed to equilibrate for 30 min before adding test drug. Initial response on histamine induces the contraction in the ileal smooth muscles which were recorded on Kymograph by using frontal writing lever. Contact time of 30 sec, and 5 min time cycle was kept for proper recording of the responses. After measuring normal response, the ileal preparation was incubated with test drug (approx.5 ml) for brief period of time and the concentration response curved of histamine was then proceeded the height of response before and after incubation of test drug was measured for calculating the antagonist effect of the test drug.

RESULTS

Effect of Thaengai Thylam (TT) on response of isolated chick ileum preparation It was observed from the data obtained from the present investigation that the height of response of concentration response curve of histamine before incubation with test drug ranges from 15 mm to 39 mm. There was a promising decrease in the height of the response curve after incubation with test drug TT which ranges from 9 mm to 21 mm. As show in table 1, figure 1-2.

DISCUSSION AND CONCLUSION

Initially with 10 µg of dose of histamine the response was 15 mm before incubation. The final response was 9 mm after incubation with the test drug Thaengai Thylam. Then the dose was tested in increasing manner from 20 µg,40 µg and 80 µg and the response was recorded. At 20 µg of dose of histamine the response was 19 mm before incubation and 13 mm after incubation. With 40 µg of dose the response was 28 mm before incubation and 16 mm after incubation. With 80 µg the response was 39 mm before incubation and 21 mm after incubation. This clearly shows that the response after incubation with test drug Thaengai Thylam decreases and the drug has a potent anti-histamine activity. The response was then plotted on the graph before and after incubation with the test drug. The graph clearly explains that the test drug possess anti-histamine activity. There is a decrease in the curve after incubation with the test drug. It was concluded that the sample Thaengai Thylam possess promising anti histamine property.

ACKNOWLEDGEMENT

Authors wish to express their gratitude to all the faculties of the Department and friends for their support.

REFERENCES

1. Monczor F, Fernandez N. Current Knowledge and Perspectives on Histamine H1 and H2 Receptor Pharmacology: Functional Selectivity, Receptor Crosstalk, and Repositioning of Classic Histaminergic Ligands. Mol Pharmacol. 2016 Nov;90(5):640-648. [PubMed]
2. Schaefer TS, Zito PM. StatPearls [Internet]. StatPearls Publishing; Treasure Island (FL): Mar 7, 2023. Antiemetic Histamine H1 Receptor Blockers. [PubMed]
3. Pirahanchi Y, Sharma S. StatPearls [Internet]. StatPearls Publishing; Treasure Island (FL): Jul 11, 2023. Physiology, Bradykinin. [PubMed]
4. Bogar 700, Pg 41-42.
5. Bhutada PS, Mundhada Y, Jain KS, Nandakumar K. Indian Journal of Pharmacology. 2006; 38(2): 140-141.

Table 1: Effect of TT on response of isolated chick ileum preparation

Dose in µg	Initial response in mm (Before Incubation)	Final response in mm (After incubation with test drug TT)
10	15	9
20	19	13
30	28	16
40	39	21

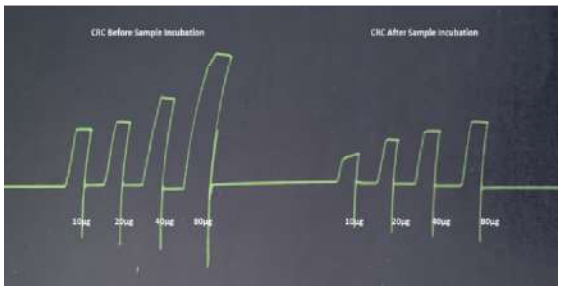

Figure.1: Concentration response curve of histamine in absence and presence of the sample TT on Isolated chick ileum in optimized condition

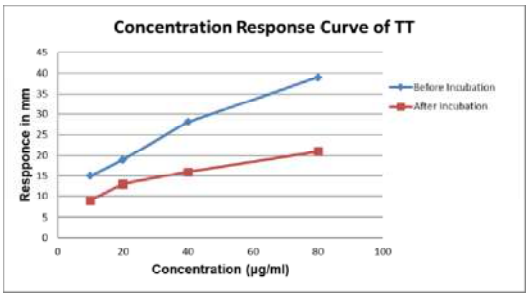

Figure.2: Concentration response curve of histamine in before and after incubation with the sample TT on Isolated chick ileum in optimized condition

Indian Journal of Natural Sciences *www.tnsroindia.org.in ©IJONS*

Vol.15 / Issue 88 / Feb / 2025 *International Bimonthly (Print) – Open Access* *ISSN: 0976 – 0997*

RESEARCH ARTICLE

Non-Negative Solution of the Exponential Diophantine Equation with Three Unknowns Including Prime and Disarium Numbers

G.Janaki[1]* and P. Sangeetha[2]

[1]Associate Professor, PG and Research Department of Mathematics, Cauvery College for Women (Autonomous), (Affiliated to Bharathidasan University), Tiruchirappalli, Tamil Nadu, India.
[2]Assistant Professor, PG and Research Department of Mathematics, Cauvery College for Women (Autonomous), (Affiliated to Bharathidasan University), Tiruchirappalli, Tamil Nadu, India.

Received: 21 Jun 2024 Revised: 03 Jul 2024 Accepted: 08 Jan 2025

***Address for Correspondence**
G.Janaki
Associate Professor,
PG and Research Department of Mathematics,
Cauvery College for Women (Autonomous),
(Affiliated to Bharathidasan University),
Tiruchirappalli, Tamil Nadu, India.
E. Mail:

ABSTRACT

In this article, we have introduced nine distinct exponential diophantine equations. Also, their solutions for odd, even, and starting point exponential numbers are analyzed while taking into consideration prime and Disarium numbers. Moreover, the third and fourth exponential diophantine equations we get integer solutions for even exponentials and no solution for odd exponentials, according to an analysis of these nine exponential diophantine equations. The integral solutions are available for the first, second, fourth, and sixth exponential Diophantine equations as well as. Further, these are examined in a different way.

Keywords: Exponential Diophantine equation, Catalan's Conjecture, Disarium number, Prime number, Integer solutions.

INTRODUCTION

Kannan. J., *et al*. [12] explained the Exponential Diophantine Equations involving opposite parity prime in 2001. In 2004 Ivan Niven., *et al*. [9] an Introduction to the Theory of Numbers, John Wiley and Sons Inc, New York. In the same year P. Mihailescu [15] was introduced the Primary cycolotomic units and a proof of Catalan's conjecture. In (2007) Acu D [5] analyzed the Diophantine equation $2^x + 5^y = z^2$. Andreescu T *et al*., [1] introduced the Diophantine equations: A problem-based approach (p. 90) in (2013). He. A. Togbe *et al*., [8] showed that the solutions

of the exponential Diophantine equation $a^x + b^y = (m^2+1)^z$ in 2013.Janaki. G. and Saranya C [10] explained the Solution of exponential Diophantine equation Involving Jarasandha numbers in (2019).In (2020) Asthana. S *et al*., [2] showed that on the Diophantine equation $3^x + 117^y = z^2$. Gomez, C. A., *et al*., [7] studied and solved the Exponential Diophantine Equation $F_{n+1}^x - F_{n-1}^x = F_m^y$ in (2022). In addition, Borah, P. B *et al*. [4] developed that on two classes of exponential Diophantine equations. In the same year Orosram, W., *et al*., [14] proposed on the exponential Diophantine equation $(p+2)^x + (2p+1)^y = z^2$, where $p, p+2$ and $2p+1$ are primes.Dutta, M., and Borah, P. B. [6] gave the solution of the exponential Diophantine equation $2^x + m^{2y} = z^2$, for any positive integer m in (2023).In the same year Laipaporn K., et.al [13] demonstrated the Diophantine Equations $a^x + b^y + c^z = w^2$. In (2024) Batte, H *et al*. [3] is proved that on the exponential Diophantine equation $U_n^x + U_{n+1}^x = U_m$. In the same year Janaki. G and Gowri Shankari. A [11] Summarized the Exponential Diophantine Equation $(n^2-1)^u + n^{2v} = w^2$, $n = 2,3,4,5$. Moreover, the basic concepts of Diophantine equations are observed. In recent work by numerous writers demonstrated that there are either solutions or no non-negative solutions. Different mathematicians have investigated different kinds of Diophantine equations [16–18].

One of the unique types of Diophantine equations where the variables occur in exponents is known as the exponential Diophantine equation. The main theme of this paper is to analyze the solutions of the exponential diophantine equation involving Disarium and prime numbers.

In this study we used the prime numbers are 2,3,5,11,63 and73

Preliminaries

In 1844, Catalan [19] posed the following conjecture:

Proposition. (Catalan's Conjecture) (3, 2, 2, 3) is a unique solution (a, b, x, y) for the Diophantine equation $a^x - b^y = 1$ where a, b, x and y are integers such that $\min\{a,b,x,y\} > 1$.

Proposition. A number is said to be the Disarium number when the sum of its digit raised to the power of their respective positions is equal to the number itself.

The Disarium numbers are 89, 135, 518 etc.

In general, for an n-digit number $n = d_1 d_2 d_3 .....d_n$ if it satisfies the condition $n = d_1^1 + d_2^2 + d_3^3 + ... + d_n^n$ then it is called a disarium number.

Proposition. Prime numbers are numbers greater than 1 that only have two factors, 1 and the number itself. This means that a prime number is only divisible by 1 and itself.

RESULTS AND DISCUSSION

Theorem 3.1:

For the Diophantine equation $89^x + 2^y = z^2$, the following conditions are satisfied:

(i) If $x = 0$ then the non-negative integral solution exists.

(ii) If x is even then the solution does not exist.

(iii) If x is odd then there exist integral solution.

Proof:

Let x, y and z be non-negative integers such that

$89^x + 2^y = z^2$..... (1)

We will analyze the solution of our considered equation in three cases.

(i) If $x = 0$, then (1) becomes $z^2 - 1 = 2^y$

Let $z-1=2^{u}$ .....(2)

Then $z+1=2^{y-u}$ .....(3)

Subtracting equation (2) from (3), $2=2^{u}[2^{y-2u}-1]$

This implies that $u=1$ and $1=2^{y-2}-1$ this gives us $x=0, y=3$ and $z=3$

Hence the solution of the Diophantine equation $89^{x}+2^{y}=z^{2}$ is $(x, y, z)=(0,3,3)$.

(ii) If x is even. let $x=2k, k\in N$, then we have

$89^{2k}+2^{y}=z^{2}$ (or) $z^{2}-89^{2k}=2^{y}$

$(z-89^{k})(z+89^{k})=2^{y}$

Let $(z-89^{k})=2^{u}$ then $(z+89^{k})=2^{y-u}$.

We obtain $2^{y-u}-2^{u}=2(89^{k})$ or

$2^{u}[2^{y-2u}-1]=2(89^{k})$.

Put $k=0$, we have $2^{u}[2^{y-2u}-1]=2(89)$ which implies $u=1$ we get, $2^{y-2}-1=89\Rightarrow 2^{y-2}=90$ this is impossible.

Hence the Diophantine equation $89^{x}+2^{y}=z^{2}$ has no non-negative integer solution whenever x is even.

(iii) If x is odd. Then $x=2k+1$, where k is a non-negative integer. We will divide this into two Parts.

Part I.

$89^{x}+2^{y}=z^{2}$ becomes $89^{2k+1}+2^{y}=z^{2}$ (or) $89\left(89^{2k}\right)+2^{y}=z^{2}$

$$2^{y}-11\left(89^{2k}\right)=z^{2}-100\left(89^{2k}\right)$$

So that, $$=\left(z-10\left(89^{k}\right)\right)\left(z+10\left(89^{k}\right)\right)$$

$$\left(z-10\left(89^{k}\right)\right)\left(z+10\left(89^{k}\right)\right)=2^{y}-11\left(89^{2k}\right)$$

$z-10\left(89^{k}\right)=1$ _____(i)

$z+10(89^{k})=2^{y}-11(89^{2k})$ _____(ii)

Subtracting equation (i) from (ii) we get,

$20.89^{k}+11(89^{2k})=2^{y}-1$

$89^{k}[20+11.89^{k}]==2^{y}-1$

Put $k=0$ we get $x=1$ $y=5$ and $z=11$.

Therefore, the solution is $(x, y, z)=(1,5,11)$.

Part II.

Also $89^{x}+2^{y}=z^{2}$ becomes $89^{2k+1}+2^{y}=z^{2}$

so that, $2^{y}-8011\left(89^{2k}\right)=z^{2}-8100\left(89^{2k}\right)$

This implies, $2^{y}-8011\left(89^{2k}\right)=\left(z-90\left(89^{k}\right)\right)\left(z+90\left(89^{k}\right)\right)$

$$z-90\left(89^{k}\right)=1 \qquad \text{_____}(iii)$$

Consider,

$$z+90\left(89^{k}\right)=2^{y}-8011\left(89^{2k}\right) \qquad \text{_____}(iv)$$

Subtracting equation (iii) from (iv), we get,

$z+90\left(89^{k}\right)-z+90\left(89^{k}\right)=2^{y}-8011\left(89^{2k}\right)-1$

$180\left(89^{k}\right)+8011\left(89^{2k}\right)=2^{y}-1$

$89^{k}\left(180+8011\left(89^{k}\right)\right)=2^{y}-1$

Put $k=0$ we get $y=13$

Therefore, the solution is $(x,y,z)=(1,13,91)$

Hence the three solutions of non-negative integers $(x,y,z)\in\{(0,3,3),(1,5,11)\text{and}(1,13,91)\}$ of the Diophantine equation is $89^{x}+2^{y}=z^{2}$.

Corollary 1.

The Diophantine equation $89^{x}+2^{y}=\xi^{4}$ has no non-negative integers solutions where x,y and ξ are non-negative integers.

Proof:

Suppose that x,y and ξ are non-negative integers such that $89^{x}+2^{y}=\xi^{4}$.

Let $z=\xi^{2}$, then $89^{x}+2^{y}=z^{2}$ by theorem 3.1, we have $(x,y,z)\in\{(0,3,3),(1,5,11),(1,13,91)\}$.

then $\xi^{2}=z\in\{3,11,91\}$, here z is a square of some integer while $(3,11,91)$ are not square of any integer. Hence the Diophantine equation $89^{x}+2^{y}=\xi^{4}$ has no non-negative integer solution.

Corollary 2.

(0, 3, 1) is unique solution of the Diophantine equation $89^{x}+2^{y}=9u^{2}$, where x,y and u are positive integers.

Proof:

Let x,y and u be positive integers such that $89^{x}+2^{y}=9u^{2}$.

Let $z=3u$ then $89^{x}+2^{y}=z^{2}$. By theorem 3.1, we have $(x,y,z)\in\{(0,3,3)\}$ then $u\in 1$.

Hence $(0,3,1)$ have unique solutions for the Diophantine equation $89^{x}+2^{y}=9u^{2}$.

Theorem 3.2:

For the Diophantine equation $89^{x}+11^{y}=z^{2}$, the following conditions are satisfied:

(i) If $x=0,y=0$ then the solution does not exist.

(ii) If $x=1,y$ is odd then the non-negative integral solutions exist.

(iii) If $x=1, y$ is even then there exist no solution.

Proof:

In the following three different cases, the integral solutions of Diophantine equations are analyzed:

(i) If $x=0$ then $1+11^y=z^2$ and let $y=0$, then $z^2=2$. It is not possible for z is a non-negative integer solution. Hence there is no solutions exist for the Diophantine equation $89^x+11^y=z^2$.

(ii) If $x=1$ then $89+11^y=z^2$, and if $y=2k+1$ is odd.

Then we have $89^x+11^y=z^2$ becomes $89+11^{2k+1}=z^2$ (or) $89+11\left(11^{2k}\right)=z^2$

so that $z^2-89=11(11^{2k})$ when $k=0$, $z^2=100\Rightarrow z=10$

$k=0\Rightarrow y=1$. Therefore $(1,1,10)$ is the solution for $89^x+11^y=z^2$.

(iii) If $x=1$ and $y=2k$ is even, then $89^x+11^{2k}=z^2$ it gives $z^2-11^{2k}=89^x$

Let $\left(z-11^k\right)=89^u$ then $\left(z+11^k\right)\left(z-11^k\right)=89^{x-u}-89^u$ this implies

$2.11^k=89^u\left(89^{x-2u}-1\right)\Rightarrow u=0$ then $89^x=2$ it is impossible for positive values of x .so that no solution for this case $x>1$.

Therefore, the number of non-negative integral solutions of the Diophantine equation $89^x+11^y=z^2$ is only $(1,1,10)$.

Theorem 3.3:

For the Diophantine equation $135^x+3^y=z^2$, the following conditions are satisfied:

(i) If $x=0, y=0$ then the solution does not exist.

(ii) If $x=0, y=1$ then the non-negative integral solutions exist.

(iii) If $x=0, y$ is odd then there exist no solution.

(iv) If $x>1, y$ is even then the solution exists.

Proof.

We shall investigate the Diophantine equation $135^x+3^y=z^2$ ..... (4) under three distinct scenarios.

(i) If $x=0$, then Equation (4) becomes $1+3^y=z^2$. If $y=0$, then $z^2=2$ it is not possible.

(ii) If $x=0$ and $y=1$ then $z^2=4\Rightarrow z=2.$ Hence the solution of the given equation $135^x+3^y=z^2$ is (0, 1, 2).

(iii) If $x=1$ then equation (4) becomes $135+3^y=z^2$.

If $y=2k+1$ is odd, then $135+3^{2k+1}=z^2$ implies $z^2-135=3(3^{2k})$

when $k=0$, $z^2=138$ this is impossible. Therefore, when x=1 there is no solution exist for $135^x+3^y=z^2$.

(iv) If $x>1$, and $y=2k$ is even.

$135^x+3^y=z^2$ becomes $135^x+3^{2k}=z^2\Rightarrow z^2-3^{2k}=135^x$

Let $z-3^k=3^u5^v$ then $(z+3^k)(z-3^k)=3^{3x-u}5^{x-v}$

$2.3^k = 3^{3x-u}\,5^{x-v} - 3^u\,5^v$

$= 3^u\,5^v\,(3^{3x-2u}\,5^{x-2v} - 1)$

Using the above equation $u = k$ and put $k = 1$ then $u = 1$

$\therefore\ 3 = 3^{3x-2}\,5^{x-2v} \Rightarrow x = 1$, when $k = 1$ then $y = 2$.

Therefore, the solution of the Diophantine equation $135^x + 3^y = z^2$ is $(1,2,12)$.

Hence, the integral solutions to the Diophantine equation $135^x + 3^y = z^2$ is (0, 1, 2) and $(1,2,12)$.

Theorem 3.4.

For the Diophantine equation $175^{\mathrm{x}} + 3^{\mathrm{y}} = \mathrm{z}^2$, the following conditions are satisfied:

(i) If $\mathrm{x} = 0, \mathrm{y} = 0$ then the solution does not exist.

(ii) If $\mathrm{x} = 0, \mathrm{y} = 1$ then the non-negative integral solutions exist.

(iii) If $\mathrm{x} = 1, \mathrm{y}$ is odd then the solution does not exist.

(iv) If $\mathrm{x} > 1, \mathrm{y}$ is even then there exist integral solution.

Proof.

(i) If $x = 0$ then $1 + 3^y = z^2$, and if $y = 0$ then $z^2 = 2$ it is not possible.

Suppose, if $x = 0$, let $y = 1$ then $z^2 = 4 \Rightarrow z = 2$.

Hence the solution of the Diophantine equation $175^{\mathrm{x}} + 3^{\mathrm{y}} = \mathrm{z}^2$ is $(\mathrm{x},\mathrm{y},\mathrm{z}) = (0,1,2)$.

(ii) If $\mathrm{x} = 1$ then $175 + 3^{\mathrm{y}} = \mathrm{z}^2$, take $\mathrm{y} = 2\mathrm{k}+1$ is odd.

$175 + 3^{2\mathrm{k}+1} = \mathrm{z}^2 \Rightarrow \mathrm{z}^2 - 175 = 3^{2k+1} = 3\left(3^{2k}\right)$

When $k = 0, \mathrm{z}^2 = 178$ is impossible. Hence there is no solution exist for when $\mathrm{x} = 1$.

(iii) If $\mathrm{x} > 1$, let $y = 2k$ is even.

$175^{\mathrm{x}} + 3^{2\mathrm{k}} = \mathrm{z}^2 \Rightarrow z^2 - 3^{2k} = 175^x$

Let $z - 3^k = 5^u\,35^v$ then $z + 3^k = 5^{x-u}\,35^{x-v} \Rightarrow \left(z + 3^k\right)\left(z - 3^k\right) = 5^{x-u}\,35^{x-v} - 5^u 35^v$ which implies, $2\left(3^k\right) = 5^u\,35^v[5^{x-2u}\,35^{x-2v} - 1]$

$\Rightarrow u = 0, v = 0$ Then, $3^k = 5^x\,35^x - 1$ put $k = 2$ then $y = 4$.

Therefore, $10 = 5^x\,35^x \Rightarrow x = 1$ so that, $z = 16$.

Hence $(1,4,16)$ is the solution of the Diophantine equation $175^{\mathrm{x}} + 3^{\mathrm{y}} = \mathrm{z}^2$.

Thus, $(\mathrm{x},\mathrm{y},\mathrm{z}) \in \{(0,1,2)\,\&\,(1,4,16)\}$ are the two non-negative integer solutions to the Diophantine equation $175^{\mathrm{x}} + 3^{\mathrm{y}} = \mathrm{z}^2$.

Theorem 3.5.

For the Diophantine equation $518^{\mathrm{x}} + 11^{\mathrm{y}} = \mathrm{z}^2$, the following conditions are satisfied:

(i) If $\mathrm{x} = 0, \mathrm{y} = 0$ then the solution does not exist.

(ii) If $\mathrm{x} = 1, \mathrm{y}$ is odd then the non-negative integral solutions exist.

(iii) If $\mathrm{x} > 1, \mathrm{y}$ is even then no integral solution exists.

Proof.

We will examine the solution to the equation $518^x + 11^y = z^2$ in three different contexts.

(i) If $x = 0$ then $1 + 11^y = z^2$ and if $y = 0$ then $z^2 = 2$ it is not possible

Therefore, the solution is not existed for both x and y is zero.

(ii) If x = 1then $518 + 11^y = z^2$,Take $y = 2k + 1$ is odd.

Then $518 + 11^{2k+1} = z^2$ which implies $z^2 - 518 = 11^{2k+1} = 11(11^{2k})$

When $k = 0$, $z^2 - 518 = 11 \Rightarrow z^2 = 11 + 518 = 529$ that is $z^2 = 529 \Rightarrow z = 23$

Hence $(1,1,23)$ is the solution of $518^x + 11^y = z^2$.

(iii) If $x > 1$ and take y is even, i.e.) $y = 2k$

$\therefore 518^x + 11^{2k} = z^2 \Rightarrow z^2 - 11^{2k} = 518^x$

Let $z - 11^k = 2^u\ 259^v$ then $z + 11^k = 2^{x-u}\ 259^{x-v}$

Therefore $(z + 11^k)(z - 11^k) = 2^{x-u}\ 259^{x-v} - 2^u\ 259^v$ this implies

$2(11^k) = 2^u\ 259^v [2^{x-2u}\ 259^{x-2v} - 1]$ That is $u = 1$, $v = 0$ then $11^k = 2^{x-2}\ 259^x - 1$

When $k = 1$ then $11 = 2^{x-2}\ 259^x - 1$

$12 = 2^{x-2}\ 259^x$ which implies $x = 4$ it is not Possible.

Therefore, there is no solution for the equation $518^x + 11^y = z^2$ when $x > 1$.

Hence, the number of non-negative integral solutions to the Diophantine equation $518^x + 11^y = z^2$ is $(1,1,23)$.

Theorem 3.6

For the Diophantine equation $598^x + 3^y = z^2$, the following conditions are satisfied:

(i) If $x = 0, y = 1$ then the non-negative integral solutions exist.

(ii) If $x = 1, y$ is odd then the non-negative integral solutions exist.

(iii) If $x > 1, y$ is even then the integral solution does not exist.

Proof:

(i) Suppose if $x = 0$ and let $y = 1$ then $z^2 = 4 \Rightarrow z = 2$

Therefore, the solution is $(0,1,2)$

(ii) If $x = 1$ then $598^1 + 3^y = z^2$, take $y = 2k + 1$ is odd.

Then $598 + 3^{2k+1} = z^2$ this implies $z^2 - 598 = 3^{2k+1} = 3(3^{2k})$

When $k = 0$ then $z^2 - 598 = 3 \Rightarrow z^2 = 601$ it is not possible

When $k = 1$ then $y = 2 + 1 = 3$. Hence $x = 1$ & $y = 3$ implies $625 = z^2 \Rightarrow z = 25$

Therefore, the solution of $x = 1$ is $(1,3,25)$

(iii) If $x > 1$ and take y is even i.e.) $y = 2k$

$\therefore 598^x + 3^{2k} = z^2 \Rightarrow z^2 - 3^{2k} = 598^x$

Let $z - 3^k = 2^u\ 299^v$ then $z + 3^k = 2^{x-u}\ 299^{x-v}$

Therefore $(z + 3^k)(z - 3^k) = 2^{x-u}\ 299^{x-v} - 2^u\ 299^v$

This implies $2(3^k) = 2^u\ 299^v [2^{x-2u}\ 299^{x-2v} - 1]$

That is $u=1 \& v=0$ then $3^k = 2^{x-2}\, 299^x - 1$

When $k=1$ then $3 = 2^{x-2}\, 299^x - 1$

$4 = 2^{x-2}\, 299^x$ which implies $x=4$ it is not possible.

Therefore, the number of non-negative integral solutions of the Diophantine equation $598^x + 3^y = z^2$ is $(0,1,2)$ and $(1,3,25)$.

Theorem 3.7

For the Diophantine equation $1306^x + 63^y = z^2$, the following conditions are satisfied:

(i) If $x=0, y=0$ then the solution does not exist.

(ii) If $x=1, y=1$ then the non-negative integral solutions exist.

(iii) If $x=1, y$ is odd then the integral solution exists.

(iv) If $x>1, y$ is even then there exist integral solution.

Proof.

(i) If $x=0$ then $1+63^y = z^2$ and if $y=0$ then $z^2=2$ is not possible

(ii) Suppose if $x=0$ and let $y=1$ then $z^2 = 64 \Rightarrow z=8$

Therefore, the solution $(x,y,z,)=(0,1,8)$

(iii) if $x=1$ then $1306+63^y = z^2$

Take y is odd i.e.) $y=2k+1$ then $1306+63^{2k+1} = z^2$ this implies

$z^2 - 1306 = 63^{2k+1}$

when $k=0$, $z^2 - 1306 = 63 \Rightarrow z^2 = 1306$ that is $z=37$

Therefore $x=1$; $y=1$ and $z=37$

(iv) If $x>1$; take y is even i.e.) $y=2k$

$1306^x + 63^{2k} = z^2 \Rightarrow z^2 - 63^{2k} = 1306^x$

Let $z - 63^k = 2^u\, 653^v$ then $z + 63^k = 2^{x-u}\, 653^{x-u}$

Therefore $(z+63^k)(z-63^k) = 2^{x-u}\, 653^{x-u} - 2^u\, 653^v$ which implies

$2(63^k) = 2^u\, 653^u\, [2^{x-2u}\, 653^{x-2u} - 1]$ that is $u=1$ Then $63^k = 2^{x-2u}\, 653^{x-2u} - 1$

When $k=1$ then $63 = 2^{x-2}\, 653^{x-2} - 1$

$64 = 2^{x-2}\, 653^{x-2}$ which implies $x=8$.

Hence the integer solutions are $x=8; y=2$ then $z = 2909194164496$.

Therefore, the non-negative integral solutions to the Diophantine equation $1306^x + 63^y = z^2$ are

$(x,y,z,)=(0,1,8),(1,1,37)$ and $(8,2,2909194164496)$.

Theorem 3.8

For the Diophantine equation $1676^x + 5^y = z^2$, the following conditions are satisfied:

(i) If $x=0$ then the solution does not exist.

(ii) If $x=1, y$ is odd then the integral solution exists.

(iii) If $x>1, y$ is even then the solution does not exist.

Proof.

(i) If $x=0$ then $1+5^y=z^2$ that is $z^2-1=5^y$

Let $z-1=5^u$ then $(z+1)=5^{x-u}\Rightarrow(z+1)(z-1)=5^{x-u}-5^u$

This implies that $2=5^{x-u}-5^u\Rightarrow 2=5^u[5^{x-u}-1]$

$u=0$ Then $5^x-1=2\Rightarrow 5^x=3$ is not possible therefore no solution for $x=0$.

(ii) if $x=1$ then $1676+5^y=z^2$

Take y is odd i.e.) $y=2k+1$

Then $1676+5^{2k+1}=z^2$ implies that $z^2-1676=5^{2k+1}=5(5^{2k})$

When $k=0$ then $y=1$ therefore $z^2-1676=5$ that is $z=41$.

Therefore, the solution $(x,y,z)=(1,1,41)$.

(iii) If $x>1$; take y is even i.e.) $y=2k$

$1676^x+5^{2k}=z^2\Rightarrow z^2-5^{2k}=1676^x$

Let $z-5^k=2^u\,419^v$ then $z+5^k=2^{2x-u}\,419^{x-v}$

Therefore $(z+5^k)(z-5^k)=2^{2x-u}\,419^{x-v}-2^u\,419^v$ this implies $2(5^k)=2^u\,419^v[2^u\,419^{x-2v}-1]$.

That is $u=1\ \&\ v=0$ then $5^k=2^{x-2u}\,419^x-1$

When $k=1$ then $5=2^{2x-2}\,419^x-1$

$6=2^{2x-2}\,419^x$ This is impossible.

Hence no solution for $x>1$.

Therefore, the number of non-negative integral solutions to the Diophantine equation $1676^x+5^y=z^2$ is $(x,y,z)=(1,1,41)$.

Theorem 3.9

For the Diophantine equation $2427^x+73^y=z^2$, the following conditions are satisfied:

(i) If $x=0, y=0$ then the solution does not exist.

(ii) If $x=1$, y is odd then the integral solution exists.

(iii) If $x>1$, y is even then the solution does not exist.

Proof.

We will examine the solution to the equation $2427^x+73^y=z^2$ in three different scenarios.

(i) If $x=0$ then $1+73^y=z^2$ and if $y=0$ then $z^2=2$ it is not possible.

Therefore, no solution for $x=y=0$

(ii) if $x=1$ then $2427^1+73^y=z^2$

Take $y=2k+1$ is odd, and then $2427+73^{2k+1}=z^2$ this implies that

$z^2-2427=73^{2k+1}=73(73^{2k})$

When $k=0$, $z^2=2427+73=2500$, Therefore $z=50$

Therefore $(1,1,50)$ is the solution for $x=1$ this case.

(iii) If $x>1$, take $y=2k$ is even.

Let $z-73^k=3^u\,809^v$ then $z+73^k=3^{x-u}\,809^{x-v}$

Therefore $(z+73^k)(z-73^k)=3^{x-u}\,809^{x-v}-3^u\,809^v$ this implies

$2(73^k)=3^u\,809^v\,[3^{x-2u}\,809^{x-2v}-1]$.

That is $u=0\&v=0$ then $73^k=3^{x-2u}\,809^{x-2v}-1$

When $k=1$ then $74=3^x\,809^x$, this is impossible.

Hence no solution for $x>1$.

Therefore, the number of non-negative integral solutions to the Diophantine equation $2427^x+73^y=z^2$ is $(x,y,z)\in(1,1,50)$.

CONCLUSION

In this paper, we have presented non-zero distinct integer solutions to the exponential diophantine equation involving jarasandha numbers. To conclude that, one may search for other equations with some other numbers In this paper, we have presented non-zero distinct integer solutions to the exponential diophantine equation involving jarasandha numbers. To conclude that, one may search for other equations with some other numbers In this study, we present the exponential Diophantine equation with Disarium numbers has non-zero distinct integer solutions in some cases. Also, we introduced nine different exponential diophantine equations. They analyze their results for odd, even, and starting point exponential numbers while taking consideration of prime and Disarium numbers. Examining these nine exponential diophantine equations reveals that there is no solution for odd exponentials and integer solutions for even exponentials in the third and fourth exponential diophantine equations. In order for a conclusion, one can look up other equations using different numbers.

REFERENCES

1. [Andreescu. T., Andrica, D., & Cucurezeanu, I. (2010). An introduction to Diophantine equations: A problem-based approach (p. 90). New York: Birkhäuser.
2. Asthana. S. & Singh. M. M. (2020). On the Diophantine equation $3^x+117^y=z^2$. Ganita, 70, 43-47.
3. Batte, H., Ddamulira, M., Kasozi, J., & Luca, F. (2024). On the exponential Diophantine equation $U_n^x+U_{n+1}^x=U_m$. The Ramanujan Journal, 1-32.
4. Borah, P. B., & Dutta, M. (2022). On two classes of exponential Diophantine equations. Communications in Mathematics and Applications, 13(1).
5. D. Acu, On a Diophantine equation $2^x+5^y=z^2$, Gen. Math., 15 (2007), 145-148.
6. Dutta, M., & Borah, P. B. (2023). On the solution of the exponential Diophantine equation $2^x+m^{2y}=z^2$, for any positive integer m. Journal of Hyper structures, 11(2), 329-337.
7. Gomez, C. A., Gomez, J. C., & Luca, F. (2022). On the Exponential Diophantine Equation $F_{n+1}^x-F_{n-1}^x=F_m^y$. Taiwanese Journal of Mathematics, 26(4), 685-712.
8. He. A. Togbe and S. Yang, On the solutions of the exponential Diophantine equation $a^x+b^y=(m^2+1)^z$, Quaestiones Mathematicae, 36, 2013, 119-135.
9. Ivan Niven, Herbert S. Zuckerman and Hugh L. Montgomery, An Introduction to the Theory of Numbers, John Wiley and Sons Inc, New York, 2004.B.
10. Janaki. G. & Saranya. C. (2019). Solution of exponential Diophantine equation Involving Jarasandha numbers. Advances and applications in Mathematical Sciences, 18(12), 1625-1629.

11. Janaki. G & Gowri Shankari. A. (2024). Exponential Diophantine Equation $(n^2-1)^u + n^{2v} = w^2$, $n = 2,3,4,5$. Indian Journal of Science and Technology 17 (2): 166-170.
12. Kannan. J., Kaleeswari. K.& Vijayashanthi. P.(2001). Exponential diophantine Equations involving opposite parity prime. Malaya Journal of Mathematics (1), 416-418.
13. Laipaporn, K., Kaewchay, S., & Karnbanjong, A. (2023). On the Diophantine Equations $a^x + b^y + c^z = w^2$. European Journal of Pure and Applied Mathematics, 16(4), 2066-2081.
14. Orosram, W., Jaidee, S., & Tangjai, W. (2022). On the exponential Diophantine equation $(p+2)^x + (2p+1)^y = z^2$, where p, $p+2$ and $2p+1$ are primes. Computer Science, 17(4), 1677-1683.
15. P. Mihailescu, Primary cycolotomic units and a proof of Catalan's conjecture, J. Reine Angew. Math., 27 (2004), 167-195.
16. Saranya. P. & Janaki, G. (2017). On the Exponential Diophantine Equation. International Research Journal of Engineering and Technology (IRJET), 4(11), 2395-0056.
17. Saranya. S. & Pandichelvi. V. Frustrating Solutions for Two Exponential Diophantine Equations $p^a + (p+3)^b - 1 = c^2$ and $(p+1)^a - p^b + 1 = c^2$. Journal of Xi'an Shiyou University, Natural Science Edition
18. Terai, N. (2012). On the exponential Diophantine equation. International Journal of Algebra, 6(23), 1135- 1146.
19. E. Catalan, Note extraite dune lettre adressee a lediteur, J. Reine Angew. Math. 27 (1844), 192.

Indian Journal of Natural Sciences *www.tnsroindia.org.in ©IJONS*

Vol.15 / Issue 88 / Feb / 2025 *International Bimonthly (Print) – Open Access* *ISSN: 0976 – 0997*

RESEARCH ARTICLE

Moringa (*Moringa oleifera*): Potential use as an Anti-Cancer Agent

Amruta R. Patil*

HoD, Department of Pharmacy, SNBP College of Pharmacy, Pune, (Affiliated to Maharashtra State Board of Technical Education, Mumbai), Maharashtra, India.

Received: 21 Nov 2024 Revised: 03 Dec 2024 Accepted: 27 Jan 2025

***Address for Correspondence**
Amruta R. Patil,
HoD,
Department of Pharmacy,
SNBP College of Pharmacy, Pune,
(Affiliated to Maharashtra State Board of Technical Education, Mumbai), Maharashtra, India.
E.Mail: patilamruta093@gmail.com

ABSTRACT

The botanical compound library of *Moringa oleifera,* often known as *M. oleifera*, is vast. This plant belongs to the *Moringaceae* family. The *M. oleifera* plant contains several bioactive compounds, including as antibiotics, anti-inflammatory agents, antioxidants, and anti-cancer substances, which are present in different regions of the plant. Therefore, the potential anti-cancer properties of *Moringa oleifera* might be attributed to the presence of bioactive compounds in the plant's extracts. This study is unusual since it is the first to investigate the possible anti-cancer properties of extracts from locally cultivated *Moringa* plants on colorectal and breast malignancies. In a ground-breaking study, scientists have examined the combined anti-cancer properties of *Moringa's* bark and leaves. Research indicates that *moringa* plant extracts obtained from Saudi Arabia has anti-cancer properties that might potentially pave the way for the development of innovative medications for the treatment of colorectal and breast cancers. This article explores the intricate molecular pathways employed by MIC-1 to effectively treat cancer and chronic disorders. Additionally, it provides insights into current and prospective treatment strategies centered around MIC-1. In order to enhance comprehension of MIC-1 and optimize its therapeutic effectiveness, this study consolidates pertinent data from the past decade.

Keywords: Moringa, *Moringa Oleifera*, Potential Use and Anti-Cancer Agent.

INTRODUCTION

Moringa oleifera L. (MO) is a diverse species of blooming annual plant. This plant originates from the Himalayas and is extensively cultivated in Saudi Arabia and other warm and subtropical regions worldwide. For centuries, individuals have utilized the plant to address many ailments, including as dermatological conditions, respiratory disorders, dental and auditory difficulties, hypertension, diabetes, anemia, and even cancer. Additionally, it is

employed for several additional medicinal purposes. In addition, Leone *et al*. (2015) provide a comprehensive elucidation of the medicinal significance of the leaf extract, encompassing a compilation of its bioactive constituents. The objective of this study was to assess the efficacy of *Moringa oleifera* products in the treatment of breast and colon cancer. Our study examined the effects of the bark (MOB), seeds (MOS), and leaves (MOL). In order to evaluate the efficacy of these extracts on MDA-MB-231 (breast) and HCT-8 (colorectal) cancer cell lines, experiments were conducted to assess cell migration and clonogenic survival.[1] In order to get a more comprehensive understanding of our findings, we examined the survival, death, and movement of cells in these two lines throughout the cell cycle following exposure to the previously discussed MO extracts. The selection of these sentences was based on their clarity and, significantly, their relevance to a substantial number of individuals in Saudi Arabia who experience these issues. As previously said, the majority of the anti-cancer medications available on the current market are derived from various plant species. Currently, scientists are investigating many frequently ingested dietary components that may possess the ability to combat cancer with little adverse effects. Curcumin and lycopene are essential nutrients often consumed by individuals of South Asian ethnic backgrounds. Curcumin, a polyphenolic compound found in turmeric, has demonstrated immunomodulatory properties, antimicrobial activity, and potential chemopreventive effects against cancer.[2]

Cancer

Cancer and other non-blood borne illnesses are the primary causes of mortality and morbidity worldwide. A prominent indication of the medical condition known as cancer is the uncontrolled proliferation and division of cells. Cancer cells has the ability to disseminate the illness due to their capacity to evade apoptosis, retain signals for cellular proliferation, and circumvent growth inhibitory mechanisms, among other mechanisms. Cancer is characterized by the cancer cells' capacity to evade immune cells' cytotoxic activity and promote angiogenesis as the disease progresses. Cancer is characterized by the dysregulated metabolism of malignant cells, as well as the metastasis of the illness to distant organs or tissues. Gaining a comprehensive understanding of the fundamental characteristics of cancer is crucial for establishing a systematic foundation to target specific tumors and enhance treatment efficacy. Additionally, it facilitates the exploration of the unique settings associated with various types of cancer.[3]

Cancer Epidemiology

Almost "half of all cancer cases in women are attributed to breast cancer, making it the most prevalent form of cancer in this population. Cancer ranks as the second leading cause of global mortality. By 2020, the global death toll from cancer is projected to exceed 10 million individuals. Among the 19.3 million newly reported cancer cases worldwide, 11.7% were diagnosed in women. If the required measures are not implemented, it is anticipated that around 1.3 million individuals who are not receiving treatment may succumb to the sickness. In 2020, the population of South Africa (SA) was 59 million. During that year, a total of 108,168 new cancer cases were diagnosed nationwide, resulting in 56,802 cancer-related fatalities. Breast cancer accounted for 27.1% of all reported cancer cases. Variances in breast cancer mortality, survival, and occurrence rates exist among various nations due to the multitude of factors that might contribute to its development.[4,5]

Cancer Pathophysiology

The primary factors responsible for breast cancer development are genetic alterations and DNA damage. Exposure to progesterone, Estrogen, and human epidermal growth factor receptor 2 can alter these variables. When an individual is in good health, their immune system only targets cells that possess DNA abnormalities. If the issue of rapid proliferation of aberrant DNA is not adequately addressed, a neoplasm may develop. Tumor markers are utilized to forecast the recurrence of breast cancer. For example, infants who are three years of age and show no indications of development may get aggressive breast cancer later in life. Similarly, individuals with Estrogen-receptor-positive tumors may exhibit symptoms a decade after their initial diagnosis and commencement of treatment. Breast cancer can develop in the epithelial cells of the ducts and lobules. The majority of malignant alterations in the breast originate from the ductal epithelium, however cancerous cells can also develop in the lobular glands. Alternatively, the family may possess genetic abnormalities or mutations such as BRCA1 and BRCA2, which increase the likelihood

of developing cancer. Consequently, it is believed that having a familial history of breast cancer increases the likelihood of developing the illness. Screening for breast cancer is particularly crucial for individuals with a familial predisposition to the disease.[6]

Moringa Oleifera

Moringa oleifera, commonly referred to as *M. oleifera*, is a perennial tree that typically grows to a height of three to thirteen meters. It is endemic to India. Originally imported from other regions, it is now extensively cultivated in tropical regions, specifically in Guangdong, China, and Taiwan. The potential to effectively treat a variety of maladies, including viral infections, cancer, fever, and asthma, is one of the numerous health benefits of the tropical tree. The seeds of *M. oleifera* are an exceptionally promising source of monounsaturated fatty acids and other essential bioactive constituents, including alkaloids, glucosinolates (GLs), isothiocyanates (ITCs), and thiocarbamates, owing to their elevated concentration. These plants are extensively employed in traditional medicine to alleviate respiratory difficulties, repair ulcers, reduce joint discomfort, and enhance vision. Research has revealed that *M. oleifera* seeds possess coagulant, bactericidal, fungicidal, and insecticidal properties. Furthermore, *M. oleifera* seed powder exhibits substantial efficacy in safeguarding animals from oxidative stress and substantially decreasing the levels of arsenic in animal tissues. The leaves of the plant are the most frequently consumed component. Flavonoids, alkaloids, glucosinolates, isothiocyanates, tannins, saponins, and other minerals are abundant in *Moringa oleifera* leaves. Studies on a variety of chronic ailments, such as cancer, non-alcoholic liver disease, diabetes, insulin resistance, hypertension, hypercholesterolemia, and general inflammation, suggest that *M. oleifera* leaves may possess potential benefits. Laboratory investigations demonstrated that extracts from the leaves, roots, and bark of *M. oleifera* exhibited substantial antioxidant activity", despite the fact that the protocyanogen protein is exclusively present in the bark of the stems and roots.[7] In controlled settings, studies have demonstrated that the extract of *M. oleifera* possesses potent anti-cancer properties when tested on melanoma cells. The effects are induced by the activation of caspases, which are mediated by mitochondria and are active in both enzyme-dependent and enzyme-independent death pathways. In their ability to induce apoptosis in cancer cells and inhibit cancer through mitochondrial mechanisms, these results bear a resemblance to selenium. The remarkable ability of *M. oleifera* to arrest tumor growth without disrupting regular physiological processes and activities renders it an exceptionally appropriate option for the treatment of cancer.[8,9]

Impact on the Human Health

In addition to its exceptional nutritional value, *Moringa oleifera* provides substantial health advantages to humans. The numerous botanical components, such as leaves, seeds, bark, roots, flowers, fruit, and juvenile shells, demonstrate a diverse range of associated activities. They not only improve cardiovascular health and circulation, but they also possess antimicrobial, antiasthmatic, diuretic, antidiabetic, antipyretic, anticancer, and anti-inflammatory properties. Limited research exists to illustrate the advantages of this plant. Solvents such as acetone, water, methanol, and ethyl acetate were employed to extract the *Moringa* plant's leaves, flowers, roots, seeds, and bark. The antibacterial efficiency against Pseudomonas aeruginosa and Erwinia carotovora was evaluated. For two specific isolates.[10] The bactericidal efficacy of leaves extracted with ethanol, ethyl acetate, and methanol was evaluated. Additional beneficial chemicals known as alkaloids have been investigated in relation to human health. Their responsibilities include maintaining blood pressure stability and increasing cardiac stimulation. They can effectively reduce both weight and cholesterol levels by reducing hyperlipidemia.[11] In the Wistar rats, the administration of 50 mg/kg/day of N-nitro-L-arginine-methyl ester and 30 and 60 mg/kg/day of *Moringa* extract resulted in elevated blood pressure and pulse rates over a three-week period. The patient experienced a tachycardia, which is an increase in heart rate, and a decrease in blood pressure following the administration of the extract. Quercetin, which is derived from the alcoholic and aqueous extracts of *M. oleifera*, may demonstrate hepatoprotective properties during its release. Quercetin, in addition to kaempferol, gallic acid, chlorogenic acid, rosmarinic acid, vicenin-2, and rutin, appears to have the additional ability to promote wound healing. Furthermore, the administration of moringa extract and fluoxetine to Swiss albino rodents demonstrated that *Moringa oleifera* has the potential to alleviate nervous system disorders. *Moringa* seeds have the capacity to alleviate a wide range of conditions, including rheumatism, cramping, gout, epilepsy, arthritis, and sexually transmitted infections. The

moringa flower is associated with urinary tract issues. Furthermore, the root bark is employed as a cardiac stimulant, while the pods are employed to treat liver, spleen, and gastroenteritis. The subsequent section will address the anticancer properties of *M. oleifera*. Given the global mortality rates associated with cancer, it could be contended that this is the plant's most critical function. Additionally, a variety of essential anticancer compounds are derived from a variety of plants, which are impractical to synthesize artificially due to their complex structures.[12,13]

***Moringa oleifera:* A Promising Anti-Cancer Agent**

M. oleifera has demonstrated efficacy in anti-cancer studies. This entails the reduction of inflammation, the restriction of tumor cell proliferation, the activation and detoxification of carcinogens, and the induction of cancer cell death. During their investigation of *M. oleifera* leaves, scientists discovered that the extract obtained from these leaves has the capacity to influence numerous signaling pathways that are involved in the development of cancer cells. The proliferation of the PC-3 human prostate cancer cell line is impeded by *M. oleifera* leaf extract through three distinct signaling pathways. Studies have demonstrated that the extract from M. oleifera significantly decreases the production of SMO protein mRNA and GLI1 transcription factor in the Hedgehog signaling pathway, which is essential for cell division and proliferation. The level of c-myc, p-Bcl2, and Hsp70 is substantially reduced by the extract from *M. oleifera* leaves, resulting in the arrest of the cell cycle. This regulates the proliferation and dissemination of cancer cells. It is hypothesized that the growth, invasion, and migration of non-small-cell lung cancer are closely linked to the extract from *M. oleifera* leaves. The JAK2/STAT3 signaling pathway is believed to be suppressed as part of the mechanism of action. Xie *et al.* utilized the alkaloid extract from *M. oleifera* to exhibit a dose-dependent effect on the A549 human non-small-cell lung cancer cell line. This resulted in a substantial decrease in the phosphorylation of JAK2 and STAT3.[14]

The impact of different fractions of *M. oleifera* leaf extract on human melanoma cells. The preparations consist of water-soluble, hexane, chloroform, ethyl acetate, and methanol. This evidence indicates that the extract initiated both caspase-dependent and caspase-independent mechanisms of cell death in melanoma cells, which were facilitated by reactive oxygen species (ROS) produced in the mitochondria. As a result, this induces the demise of malignant cells. These results are in agreement with the signaling pathway that has been previously observed to affect cancer cells in *M. oleifera* leaves.[15] The regulation of growth and mortality in both benign and malignant cells may be distinguished by the presence of MicroRNA in the aqueous extract of *M. oleifera* seed oil. Potestà *et al.* contend that the extract contains microRNAs that have the capacity to regulate the growth and apoptosis of cells, as well as to differentiate between malignant and normal cells. In the subsequent investigation conducted by Potestà *et al.,* specific target genes associated with human mortality for plant miRNA were identified. Their research revealed that seed water extracts had the capacity to reduce the susceptibility of the mitochondrial membrane and modify the expression of the BCL2 protein in cancer cells, a process that is linked to cellular death. Two researchers ground *M. oleifera* seeds into a fine powder during their investigation of breast cancer. The correlation between *M. oleifera* sections and cancer has been the subject of limited research. Nevertheless, Al-Asmari *et al.*'s research indicates that the viability of *M. oleifera* bark extracts in the MDA-MB-231 and HCT-8 cancer cell lines was significantly reduced. Furthermore, these extracts increase the proportion of deceased cells in the cancer cell lines. The extract efficiently concludes the cell cycle in the G2/M phase.[16] Vasanth *et al.* utilized an extract from the stem bark of *M. oleifera* to create a colloidal silver solution that exhibited anti-cancer properties (Table 1). This solution has the capacity to induce cell apoptosis in HeLa cells by generating reactive oxygen species (ROS). The results suggest that M. oleifera bark extract has the potential to be used in the development of new therapies for breast and colon cancer due to its anti-cancer properties. Nevertheless, additional research is required to determine the precise mechanism by which it functions. The viability of cells is substantially diminished by the activation of the caspase 3 enzyme and the mortality induced by reactive oxygen species (ROS), as per Siddiqui *et al.* Nevertheless, the fruit extract from *M. oleifera* has the potential to impede the proliferation of HepG2 cells. The acquisition of anti-cancer medications may be facilitated by the adoption of a healthy diet, as several naturally occurring phytochemicals possess anti-cancer properties. Nanotechnology is becoming more prevalent in the treatment of cancer.[17] The therapeutic efficacy of phytochemicals is improved by the integration of nanotechnology, which also presents a novel approach to addressing intricate environmental and economic issues. Consequently, it is logical to combine nanotechnology with

phytochemicals. Nevertheless, nanotechnology raises a number of unresolved issues. Given the potential for delays in the impact of nanomaterials, the secure dissemination of medication for human well-being is a difficult endeavour. The intricate technological requirements for the large-scale production of nanomedicine products are an inherent challenge. The primary concern is the disparity in physicochemical properties among numerous samples. Although nano phytochemicals have made significant strides in cancer therapy, there are still unresolved issues that must be resolved before nanoparticles can be extensively used for drug delivery.[18] The anticancer activities of commonly studied *Moringa oleifera* illestrated in Table 1.[19-39]

Bioactive Components of *Moringa Oleifera*

Scientists are focusing more on finding alternative bioactive molecules, especially those derived from medicinal plants, due to the growing resistance to pharmaceuticals. It is a universally acknowledged truth. *Moringa* is utilized for several reasons, including the manufacturing of biodiesel, the purification of water, and the creation of nutritious meals, thanks to its remarkable ability to thrive in dry conditions and the extensive usability of every component of the tree. M. oleifera is a rich source of several important bioactive substances (Table 2), including carotenoids, phenolic compounds, alkaloids, glucosinolates, isothiocyanates, folates, tannins, saponins, and fatty acids. The main constituents of moringa leaves consist of phenolic chemicals, such as lignans, phenolcarboxylic acids, and their derivatives (coumaroylquinic, caffeoylquinic, and feruloylquinic acids). Furthermore, the presence of flavonoids such as apigenin, quercetin, luteolin, myricetin, and kaempferol can be seen. The hydroxyl molecules are accountable for the antioxidant activity. Carotenoids, natural substances found in food and plants, function as antioxidants, protecting cells from damage. In 2014, Saini conducted a research which discovered six main carotenoids: 15-Z-β-carotene, 13-Z-lutein, all-E-lutein, all-E-luteoxanthin, all-E-zeaxanthin, and all-E-β-carotene.[40] These chemicals not only give plants a strong smell, but also have biological effects, such as killing germs and fungi. Furthermore, researchers have analyzed the proteins and peptide fractions of Moringa because of its fascinating nutritional qualities. The biological effects of this substance include antioxidant, hepatoprotective, antibacterial, anticancer, and antidiabetic activities.[41] The peptides' antioxidant activity is enhanced by the presence of aromatic and hydrophobic amino acids. In addition, *Moringa oleifera* seeds contain a total of seventeen amino acids, consisting of seven essential amino acids and 10 non-essential amino acids. Arginine has the second highest concentration among all amino acids, measuring 15.78 g per 100 grams of protein. In contrast, glutamic acid obtained the highest score with a concentration of 22.71 g per 100 g of protein. The chemical makeup of the Moringa oleifera seed cake, a residual product produced after extracting oil, has sparked curiosity. The cake residue was found to contain 24 bioactive chemicals, including oleic acid, 3-hydroxy-2-p-tolyl-2-butenenitral, Erucic acid, and eicosanoid acid. Additionally, it had a higher concentration of potassium (K) and calcium (Ca). The mineral makeup of this by-product, including magnesium, phosphorus, nitrogen, copper, calcium, manganese, nickel, zinc, and iron, has the potential to improve soil fertility. Additionally, it has an enhanced protein level of 60%. The complex molecular structure of the described bioactive substances has a beneficial effect on human health.[40]

Quercetin

Angiogenesis is the “process responsible for the development of all capillaries. This process is governed by a variety of substances, including growth factors, adhesion molecules, and endostatin. Angiogenesis is crucial for the formation of reproductive systems and the healing of injuries. Uncontrolled blood vessel growth promotes the formation and spread of tumors. The process of tumor angiogenesis is greatly affected by the interactions that occur between tumor cells and endothelial cells. VEGF plays a crucial role in the growth and survival of endothelial cells. It also stimulates cell division, enhances the permeability of blood vessels, facilitates the leakage of plasma fibrin, aids in the formation of cellulose deposits, and promotes the development of blood vessels in tumors. The use of natural products is a crucial element in the prevention of cancer. Many phytochemicals have the capacity to be converted into antiangiogenic drugs. Flavonoids, a kind of polyphenolic chemicals, may be found in almost all edible plants. They exhibit antibacterial, antiviral, anti-inflammatory, and cytoprotective effects in several animal and human cell types. Epidemiological study suggests that consuming a diet rich in flavonoids might potentially decrease the risk of acquiring cancer. Quercetin has demonstrated an anti-tumor impact by suppressing the proliferation of blood vessels. In addition, this naturally occurring compound suppresses the growth of tumors by blocking the

downstream regulatory protein AKT in prostate and breast cancers, as well as the VEGFR-2-mediated pathway that promotes the formation of new blood vessels. Quercetin's ability to inhibit angiogenesis in drug-resistant cells worsens its effect on anti-cancer drugs.[41,42]

Neuroblastoma

Neuroblastoma (NBL) is the third most prevalent kind of cancer in babies, ranking behind leukemia and brain tumors in terms of frequency. This type of cancer study also contributes to the understanding of the anti-cancer mechanism of MIC-1. Research done on the human NBL cell line SH-SY5Y has shown that MIC-1 triggers apoptosis, thereby inhibiting the growth of cancerous cell lines. The Akt/mammalian target of rapamycin (mTOR/phosphatidylinositol 3-kinase) pathway is linked to a negative prognosis and the advancement of NBL. This method greatly improves cell survival. Giacoppo *et al*. found that the levels of p-PI3K, p-Akt, and p-motor, which are linked to this signaling pathway, may be decreased when MIC-1 binds with α-cyclodextrin to create a compound. Subsequently, this can jeopardize the viability of SH-SY5Y cells and diminish the functionality of the signaling pathway. Simultaneously, MIC-1 has the ability to hinder the mitogen-activated protein kinase (MAPK) pathway, which is produced by the PI3K/Akt/mTOR signaling. This system governs a range of biological processes, such as cell viability, proliferation, and death. In addition, MIC-1 has the capacity to enhance the expression of p53 and p21, induce the programmed cell death of SH-SY5Y cells, and trigger the cleavage of caspase 3. Cirmi *et al.*'s research suggests that MIC-1 has the ability to modify the usual cell cycle activity. This phenomenon is marked by a decrease in the quantity of cells in the G1 phase, an augmentation in the G2 and S phases, and an obstruction of NF-κB movement into the nucleus. Furthermore, Jaafaru *et al.* discovered that MIC-1 has the ability to protect the internal structure and membrane integrity of specialized neurons from the oxidative harm induced by hydrogen peroxide. Therefore, it may be inferred that MIC-1 has the capacity to protect neurons against degeneration induced by oxidative stress. Hence, it is evident that additional investigation is required to get a more thorough comprehension of the particular regulatory systems implicated and the precise mechanism by which the medicine triggers these effects and facilitates apoptosis.[43]

Astrocytomas

Astrocytomas are the most common and aggressive primary brain tumors in adults, and they are also the deadliest form of cancer. Rajan *et al.* found that MIC-1 efficiently induced apoptosis in human astrocytoma grade IV CCF-STTG1 cells by suppressing Bcl-2 and activating p53 and Bax. Additionally, it has the ability to trigger apoptosis in the presence of oxidative stress via regulating the transcription factor Nrf2 and its direct regulator, casein kinase 2 alpha. Further investigation is necessary to get a thorough comprehension of the exact communication routes that govern death.[44]

Hepatocarcinoma

The activation of effector caspase 3 and initiator caspase 8 by death ligands and their interactions with death receptors launch the extrinsic pathway. The Hep3B hepatocarcinoma cells were subjected to treatment with AVN 2f and MIC-1. Antonini *et al*. found that the combination of MIC-1 and AVN 2f greatly enhanced the activation of caspases 2, 8, 9, and 3, leading to a notable inhibition of Hep3B cell growth. The early stages of the intrinsic death pathway entail the initiation of caspase 2 and 9 activation, the reduction of Birc5 gene expression, which promotes cell survival, and the elevation of intracellular reactive oxygen species (ROS) produced by MIC-1. Activation of caspase 8 by AVN 2f leads to extrinsic apoptosis, a regulated process of cell death. The findings indicate that the combination of AVN 2f and MIC-1 has the potential to be an advantageous chemoprophylactic mixture for inhibiting the dissemination of liver cancer. .[45-47]

SUMMARY AND CONCLUSION

The medicinal effects of the bioactive chemicals found in *M. oleifera* leaves, roots, seeds, and oils have been proven in both laboratory and live organism research. These skills include the capacity to fight against cancer, eliminate harmful microorganisms, hinder the growth of cells, decrease blood pressure, and thus, alleviate inflammation. Ingest the bioactive constituents of *M. oleifera Lam.* to improve human well-being, augment the nutritious content of

food, and support environmental sustainability. "The stability and activity of these bioactive compounds are the main factors that determine their usage.[48] The bioactive properties of these characteristics can be preserved within the food structure by mixing the structural components. Thermal, chemical, and biological treatments can be combined to increase their effectiveness in the production of food and drinks. Encapsulation, a cutting-edge method, has recently gained considerable focus in the food business. To guarantee the dispersion of the bioactive components of *M. oleifera* throughout the human stomach or intestines, it is essential to concentrate them. This has the ability to enable the supply of secure and affordable nourishment. Therefore, extremely nutritious diets including bioactive components from *M. oleifera* will require more careful meal planning compared to conventional meals. Furthermore, it is crucial to guarantee that this essential approach is not just economical but also long-lasting. Spray drying is an economical and versatile technology that has been extensively studied in the literature. The use of certain biopolymers, such as proteins or protein variations, has been shown to boost the efficiency of encapsulation. The long-term sustainability of this strategy is also reinforced by the resilience of the enclosed molecules. The essential encapsulation matrices required to achieve this purpose can be achieved by commencing research on the sustainability of this technology.[49,50] Nevertheless, the state of encapsulation might potentially impact the cytotoxicity of various substances derived from *M. oleifera*. Scientists are now interested in studying the cytotoxicity of the carrier materials, in addition to the cytotoxicity of the beneficial compounds revealed in moringa. Nevertheless, further investigation is necessary in this domain. Furthermore, we assert that the use of *M. oleifera* bioactive constituents in the fields of food, cosmetics, pharmaceuticals, and water purification will provide superior results by employing environmentally sustainable extraction methods and cautious encapsulation approaches. The utilization of *M. oleifera* bioactive components may be further enhanced by employing biopolymers, ecologically friendly extraction techniques, suitable encapsulation procedures, and optimal concentrations. After doing extensive study, we have found that spray drying is the most effective technique for introducing the bioactive chemical into human health applications." This highly versatile approach consistently produces a substantial amount of findings on every occasion.[51,52] Moreover, it possesses a diverse array of practical uses.

REFERENCES

1. Alaklabi A. Genetic diversity of Moringa peregrina species in Saudi Arabia with ITS sequences. Saudi Journal of Biological Sciences. 2014.
2. Mbikay M. Therapeutic potential of Moringa oleifera leaves in chronic hyperglycemia and dyslipidemia: a review. Frontiers in pharmacology. 2012;3.
3. Patel S, Thakur A, Chandy A, Manigauha A. Moringa Oleifera: A Review of There Medicinal and Economical Importance to the Health and Nation. Drug invention today. 2010;2(7).
4. Emmanuel S, Olajide O, Abubakar S, Idowu I, Orishadipe A, Thomas S. Phytochemical and Antimicrobial Studies of Methanol, Ethyl acetate, and Aqueous Extracts of Moringa oleifera Seeds. American Journal of Ethnomedicine. 2014;1(5):346–54.
5. Jung IL. Soluble extract from Moringa oleifera leaves with a new anticancer activity. PloS one. 2014;9(4): e95492 10.1371/journal.pone.0095492
6. Tiloke C, Phulukdaree A, Chuturgoon AA. The Antiproliferative effect of Moringa oleifera crude aqueous leaf extract on cancerous human alveolar epithelial cells. BMC complementary and alternative medicine. 2013;13(1):226.
7. Leone A, Spada A, Battezzati A, Schiraldi A, Aristil J, Bertoli S. Cultivation, Genetic, Ethnopharmacology, Phytochemistry and Pharmacology of Moringa oleifera Leaves: An Overview. International journal of molecular sciences. 2015;16(6):12791–835.
8. Mosli MH, Al-Ahwal MS. Colorectal cancer in the Kingdom of Saudi Arabia: need for screening. Asian Pacific journal of cancer prevention: APJCP. 2012;13(8):3809–13.
9. Sa G, Das T, Banerjee S, Chakraborty J. Curcumin: from exotic spice to modern anticancer drug. Al Ameen J Med Sci. 2010; 3:21–37.
10. Kong K-W, Khoo H-E, Prasad KN, Ismail A, Tan C-P, Rajab NF. Revealing the power of the natural red pigment

lycopene. Molecules. 2010;15(2):959–87. 10.3390/molecules15020959
11. Shehzad A, Lee YS. Molecular mechanisms of curcumin action: signal transduction. Bio Factors. 2013;39(1):27–36. 10.1002/biof.1065.
12. Shishodia S. Molecular mechanisms of curcumin action: gene expression. Bio Factors. 2013;39(1):37–55. 10.1002/biof.1041.
13. Shanmugam MK, Rane G, Kanchi MM, Arfuso F, Chinnathambi A, Zayed M, *et al*. The multifaceted role of curcumin in cancer prevention and treatment. Molecules. 2015;20(2):2728–69. 10.3390/molecules20022728
14. Trejo-Solis C, Pedraza-Chaverri J, Torres-Ramos M, Jimenez-Farfan D, Cruz Salgado A, Serrano-Garcia N, *et al*. Multiple molecular and cellular mechanisms of action of lycopene in cancer inhibition. Evidence-based complementary and alternative medicine: eCAM. 2013; 2013:705121 10.1155/2013/705121
15. Al-Sharif I, Remmal A, Aboussekhra A. Eugenol triggers apoptosis in breast cancer cells through E2F1/surviving down-regulation. BMC cancer. 2013;13(1):600.
16. Islam M, Sharma S, Kumar B, Teknos TN. Atorvastatin inhibits RhoC function and limits head and neck cancer metastasis. Oral oncology. 2013;49(8):778–86. 10.1016/j.oraloncology.2013.04.003
17. Aja P, Ibiam U, Igwenyi I, Offor C, Orji U. Comparative Gas Chromatography-Mass Spectrometry (GC-MS) Analysis of Chemical Compounds of Moringa oleifera Leaves and Seeds from Abakaliki, Nigeria. Advances in Life Science and Technology. 2014; 24:73–9.
18. Abdull Razis AF, Ibrahim MD, Kntayya SB. Health benefits of Moringa oleifera. Asian Pacific journal of cancer prevention: APJCP. 2014;15(20):8571–6.
19. Wu YY, Xu YM, Lau AT. Anti-cancer and medicinal potentials of Moringa isothiocyanate. Molecules. 2021 Dec 11;26(24):7512.
20. Tiloke C, Anand K, Gengan RM, Chuturgoon AA. Moringa oleifera and their phytonanoparticles: Potential Antiproliferative agents against cancer. Biomedicine & Pharmacotherapy. 2018 Dec 1; 108:457-66.
21. Al-Asmari AK, Albalawi SM, Athar MT, Khan AQ, Al-Shahrani H, Islam M. Moringa oleifera as an anti-cancer agent against breast and colorectal cancer cell lines. PloS one. 2015 Aug 19;10(8): e0135814.
22. Fahey JW. Moringa oleifera: A review of the medicinal potential. InI International Symposium on Moringa 1158 2015 Nov 15 (pp. 209-224).
23. Barhoi D, Upadhaya P, Barbhuiya SN, Giri A, Giri S. Aqueous extract of Moringa oleifera exhibit potential anticancer activity and can be used as a possible cancer therapeutic agent: a study involving in vitro and in vivo approach. Journal of the American College of Nutrition. 2021 Jan 2;40(1):70-85.
24. Ercan K, Gecesefa OF, Taysi ME, Ali OA, Taysi S. Moringa oleifera: a review of its occurrence, pharmacological importance and oxidative stress. Mini Reviews in Medicinal Chemistry. 2021 Feb 1;21(3):380-96.
25. Moremane MM, Abrahams B, Tiloke C. Moringa oleifera: a review on the Antiproliferative potential in breast cancer cells. Current Issues in Molecular Biology. 2023 Aug 18;45(8):6880-902.
26. Adebayo IA, Balogun WG, Arsad H. Moringa oleifera: An apoptosis inducer in cancer cells. Tropical Journal of Pharmaceutical Research. 2017 Oct 4;16(9):2289-96.
27. Ramamurthy S, Varghese S, Sudarsan S, Muruganandhan J, Mushtaq S, Patil PB, Raj AT, Zanza A, Testarelli L, Patil S. Moringa oleifera: antioxidant, anticancer, anti-inflammatory, and related properties of extracts in cell lines: a review of medicinal effects, phytochemistry, and applications. Journal of Contemporary Dental Practice. 2021;22(12):1483-92.
28. Alhassan YJ, Sanchi ID, Dorh LE, Sunday JA. Review of the nutritive, medicinal and general economic potentials of Moringa oleifera. Cross Current Int J Agri Vet Sci. 2022;4(1):1-8.
29. Stohs SJ, Hartman MJ. Review of the safety and efficacy of Moringa oleifera. Phytotherapy Research. 2015 Jun;29(6):796-804.
30. Gopalakrishnan L, Doriya K, Kumar DS. Moringa oleifera: A review on nutritive importance and its medicinal application. Food science and human wellness. 2016 Jun 1;5(2):49-56.
31. Leone A, Spada A, Battezzati A, Schiraldi A, Aristil J, Bertoli S. Moringa oleifera seeds and oil: Characteristics and uses for human health. International journal of molecular sciences. 2016 Dec 20;17(12):2141.
32. Velázquez-Zavala M, Peón-Escalante IE, Zepeda-Bautista R, Jiménez-Arellanes MA. Moringa (Moringa oleifera Lam.): potential uses in agriculture, industry and medicine. Revista Chapingo. Serie horticultura. 2016

Aug;22(2):95-116.
33. Gandji K, Chadare FJ, Idohou R, Salako VK, Assogbadjo AE, Kakaï RG. Status and utilization of Moringa oleifera Lam: A review. African Crop Science Journal. 2018 Feb 27;26(1):137-56.
34. Ma ZF, Ahmad J, Zhang H, Khan I, Muhammad S. Evaluation of phytochemical and medicinal properties of Moringa (Moringa oleifera) as a potential functional food. South African Journal of Botany. 2020 Mar 1; 129:40-6.
35. Mahfuz S, Piao XS. Application of Moringa (Moringa oleifera) as natural feed supplement in poultry diets. Animals. 2019 Jul 9;9(7):431.
36. Sharma K, Kumar M, Waghmare R, Suhag R, Gupta OP, Lorenzo JM, Prakash S, Rais N, Sampathrajan V, Thappa C, Anitha T. Moringa (Moringa oleifera Lam.) polysaccharides: Extraction, characterization, bioactivities, and industrial application. International Journal of Biological Macromolecules. 2022 Jun 1; 209:763-78.
37. Paikra BK, Gidwani B. Phytochemistry and pharmacology of Moringa oleifera Lam. Journal of Pharmacopuncture. 2017 Sep;20(3):194.
38. Jaja-Chimedza A, Graf BL, Simmler C, Kim Y, Kuhn P, Pauli GF, Raskin I. Biochemical characterization and anti-inflammatory properties of an isothiocyanate-enriched Moringa (Moringa oleifera) seed extract. PloS one. 2017 Aug 8;12(8): e0182658.
39. Pal D, Banerjee S, Mukherjee S, Roy A, Panda CK, Das S. Eugenol restricts DMBA croton oil induced skin carcinogenesis in mice: downregulation of c-Myc and H-ras, and activation of p53 dependent apoptotic pathway. Journal of dermatological science. 2010;59(1):31–9.
40. Gandji, K.; Chadare, F.J.; Idohou, R.; Salako, V.K.; Assogbadjo, A.E.; Glèlè, R.L.K. Status and utilization of Moringa oleifera Lam: A review. Afr. Crop Sci. J. 2018, 26, 137–156.
41. Chaudhary, K.; Chourasia, S. Nutraceutical properties of Moringa oleifera: A review. EJPMR 2017, 4, 646–655.
42. Gopinath, L.R.; Jeevitha, S.; Gokiladevi, T.; Archaya, S. Isolation and Identification of therapeutic compounds from Moringa oleifera and its antimicrobial activity. IOSR-JPBS 2017, 12, 1–10.
43. Kasolo, J.N.; Bimenya, G.S.; Ojok, L.; Ochieng, J.; Ogwal-Okeng, J.W. Phytochemicals and uses of Moringa oleifera leaves in Ugandan rural communities. J. Med. Plant Res. 2010, 20104, 753–757.
44. Choudhary, M.K.; Bodakhe, S.H.; Gupta, S.K. Assessment of the antiulcer potential of Moringa oleifera root-bark extract in rats. J. Acupunct. Meridian Stud. 2013, 6, 214–220.
45. Posmontier, B. The medicinal qualities of Moringa oleifera. Holist. Nurs. Pr. 2011, 25, 80–87.
46. Aekthammarat, D.; Pannangpetch, P.; Tangsucharit, P. Moringa oleifera leaf extract lowers high blood pressure by alleviating vascular dysfunction and decreasing oxidative stress in L-NAME hypertensive rats. Phytomedicine 2019, 54, 9–16.
47. Tayo, G.M.; Pone, G.W.; Komtangi, M.C.; Yondo, G.; Ngangout, A.M.; Mbida, M. Anthelminthic Activity of Moringa oleifera Leaf Extracts Evaluated in Vitro on Four Developmental Stages of Haemonchus contortus from Goats. AJPS 2014, 5, 1702–1710.
48. Hannan, M.A.; Kang, J.Y.; Mohibbullah, M.; Hong, Y.K.; Lee, H.; Choi, J.S.; Choi, I.S.; Moon, I.S. Moringa oleifera with promising neuronal survival and neurite outgrowth promoting potentials. J. Ethnopharmacology. 2014, 152, 142–150.
49. Paikra, B.K.; Dhongade, H.K.J.; Gidwani, B. Phytochemistry and Pharmacology of Moringa oleifera Lam. J Pharmacopuncture. 2017, 20, 194–200.
50. Mallenakuppe, R.; Homabalegowda, H.; Gouri, M.D.; Basavaraju, P.S.; Chandrashekharaiah, U.B. History, Taxonomy and Propagation of Moringa oleifera-A Review. Int. J. Life Sci. 2019, 5, 2322–2327.
51. Popoola, J.O.; Obembe, O.O. Local knowledge, use pattern and geographical distribution of Moringa oleifera Lam. (Moringaceae) in Nigeria. J. Ethnopharmacology. 2013, 150, 682–691
52. Tahkur, R.S.; Soren, G.; Pathapati, R.M.; Buchineni, M. Diuretic activity of Moringa oleifera leaves extract in swiss albino rats. J. Pharm. Innov. 2016, 5, 8–10.

Table.1: Anti-cancer activities of commonly studied *Moringa oleifera*

Sr. No.	Title of the paper	Journal name	Part used along with extract used	Reference
1	"Anti-cancer and medicinal potentials of Moringa isothiocyanate	Molecules	M. oleifera flowers, leaves, seeds, fruit, and bark shown in recent studies reflects	Wu *et al.,* (2021)
2	Moringa oleifera and their phytonanoparticles: Potential Antiproliferative agents against cancer.	Biomedicine & Pharmacotherapy.	Almost all parts have shown to be effective against several ailments including cancer	Tiloke *et al.,* (2018)
3	Moringa oleifera as an anti-cancer agent against breast and colorectal cancer cell lines.	PloS one.	leaf and bark extracts of *Moringa*	Al-Asmari *et al.,* (2015)
4	Moringa oleifera: A review of the medicinal potential.	International Symposium on Moringa	*M. oleifera* flowers, leaves, seeds, fruit, and bark	Fahey. (2015)
5	Aqueous extract of Moringa oleifera exhibit potential anticancer activity and can be used as a possible cancer therapeutic agent: a study involving in vitro and in vivo approach.	Journal of the American College of Nutrition	aqueous extract of *Moringa oleifera* (AEMO)	Barhoi *et al.,* (2021)
6	Moringa oleifera: a review of its occurrence, pharmacological importance and oxidative stress.	Mini Reviews in Medicinal Chemistry.	leaves, seeds, stems and shells.	Ercan *et al.,* (2021)
7	Moringa oleifera: a review on the Antiproliferative potential in breast cancer cells.	Current Issues in Molecular Biology.	MO aqueous leaf extract	Moremane *et al.,* (2023)
8	Moringa oleifera: An apoptosis inducer in cancer cells.	Tropical Journal of Pharmaceutical Research.	*M. oleifera* flowers, leaves, seeds, fruit, and bark	Adebayo *et al.,* (2017)
9	Moringa oleifera: antioxidant, anticancer, anti-inflammatory, and related properties of extracts in cell lines: a review of medicinal effects, phytochemistry, and applications.	Journal of Contemporary Dental Practice.	MO leaves had more potent properties compared to other parts of the plant.	Ramamurthy *et al.,* (2021)
10	Review of the nutritive, medicinal and general economic potentials of Moringa oleifera.	Cross Current Int J Agri Vet Sci.	*M. oleifera* seed,	Alhassan *et al.,* (2022)
11	Review of the safety and efficacy of Moringa oleifera.	Phytotherapy Research.	Moringa oleifera leaves, seeds, bark, roots, sap, and flowers are widely used	Stohs *et al.,* (2015)
12	Moringa oleifera: A review on nutritive importance and its medicinal application.	Food science and human wellness.	Extracts from the leaves are used	Gopalakrishnan *et al*., (2016)

13	*Moringa oleifera* seeds and oil: Characteristics and uses for human health.	International journal of molecular sciences.	*Moringa oleifera* seeds	Leone *et al.*, (2016)
14	Moringa (*Moringa oleifera Lam.*): potential uses in agriculture, industry and medicine.	Revista Chapingo. Serie horticultura.	*Moringa oleifera* seeds	Velázquez-Zavala *et al.*, (2016)
15	Status and utilisation of Moringa oleifera Lam: A review.	African Crop Science Journal.	Almost all parts of the plant are used.	Gandji *et al.*, (2018)
16	Evaluation of phytochemical and medicinal properties of Moringa (*Moringa oleifera*) as a potential functional food.	South African Journal of Botany.	MO leaves had more potent properties compared to other parts of the plant.	Ahmad *et al.*, (2020)
17	Application of Moringa (*Moringa oleifera*) as natural feed supplement in poultry diets.	Animals.	leaves, seeds and their extracts	Mahfuz *et al.*, (2019)
18	Moringa (Moringa oleifera Lam.) polysaccharides: Extraction, characterization, bioactivities, and industrial application.	International Journal of Biological Macromolecules.	Different parts of *Moringa oleifera Lam*.	Sharma *et al.*, (2022)
19	Phytochemistry and pharmacology of Moringa oleifera Lam.	Journal of Pharmacopuncture.	Every part of this plant	Paikra *et al.*, (2017)
20	Biochemical characterization and anti-inflammatory properties of an isothiocyanate-enriched Moringa (Moringa oleifera) seed extract.	PloS one.	Moringa (*Moringa oleifera*) seed extract.	Jaja-Chimedza *et al.*, (2017)"

Table.1:Major bioactive compound in different body parts of M. oleifera

Plant part	Bioactive Compounds
"Seed	glycosidic benzylamines; niazimicin; isothiocyanates; phenolics; glucosinolates
Leaf	phytol; flavonoids; phenolics; β-carotene; lycopene; vicenin-2; quinic acid; octadecanoic acid; hexadecanoic acid (palmitic acid); α-tocopherol (vitamin-E); γ-sitosterol
Flower	β-sitosterol; flavonoids; anthocyanin
Root	nasimizinol; oleic acid; N-benzyl-N-(7-cyanato heptanamide; N-benzyl-N-(1-chlorononyl) amide; bis [3-benzyl prop-2-ene]-1-one; N, N-dibenzyl-2-ene pent-1,5-diamide
Shell	3,5,6-trihydroxy-2-(2,3,4,5,6-pentahydroxyphenyl)-4H-chromen-4-one; β-sitosterol-3-O-glucoside; 2,3,4-trihydroxybenzaldehyde; stigmasterol
Bark	epiglobulol; flavonoids; anthocyanin"

Figure.1: *Moringa oleifera* Plant Part

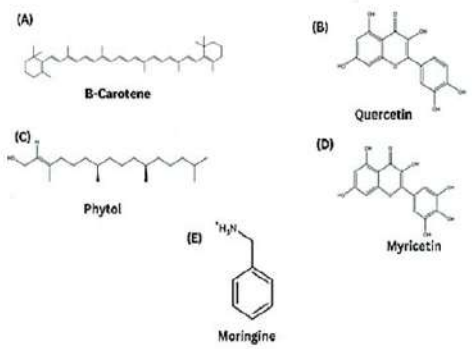

Figure 1 Bioactive Components of *M. oleifera*

Indian Journal of Natural Sciences www.tnsroindia.org.in ©IJONS

Vol.15 / Issue 88 / Feb / 2025 *International Bimonthly (Print) – Open Access* *ISSN: 0976 – 0997*

RESEARCH ARTICLE

USFDA's Framework for Interchangeable Biological Products : A Comprehensive Overview

Aishwarya S[1], Shivanand K Mutta[2] and Madhavi BLR[3]*

[1]M. Pharm Student, Department of Pharmaceutical Regulatory Affairs, Acharya & BM Reddy College of Pharmacy, (Affiliated to Rajiv Gandhi University of Health Sciences), Bengaluru, Karnataka, India.
[2]Professor and Head, Department of Pharmaceutical Regulatory Affairs, Acharya & BM Reddy College of Pharmacy, (Affiliated to Rajiv Gandhi University of Health Sciences), Bengaluru, Karnataka, India.
[3]Assistant Professor, Department of Pharmaceutical Regulatory Affairs, Acharya & BM Reddy College of Pharmacy, (Affiliated to Rajiv Gandhi University of Health Sciences), Bengaluru, Karnataka, India.

Received: 21 Nov 2024 Revised: 03 Dec 2024 Accepted: 03 Jan 2025

***Address for Correspondence**
Madhavi BLR
Assistant Professor,
Department of Pharmaceutical Regulatory Affairs,
Acharya & BM Reddy College of Pharmacy,
(Affiliated to Rajiv Gandhi University of Health Sciences),
Bengaluru, Karnataka, India.
E.Mail: madhaviblr@gmail.com

ABSTRACT

Biological products are a rapidly expanding sector in the pharmaceutical industry that is regulated by the United States Food and Drug Administration (USFDA). Biosimilars are a generic version of biological products but are not interchangeable with their reference counterparts. The biosimilars must meet additional requirements and prove their interchangeability with reference biologic to be an interchangeable biological product. This article provides an overview of IBPs, detailing the distinctions between biosimilars and IBPs. The criteria and regulatory pathways for IBPs are discussed. The complex challenges including patent exclusivity and secondary patents that affect biosimilar availability are also described. The importance of post-market safety monitoring and the evolving landscape of biologics are mentioned. The FDA's recent proposal to eliminate regulatory differences between biosimilars and IBPs has been discussed. This discussion concluded on how to overcome the existing barriers and provide the promise of enhanced patient care with the IBP.

Keywords: Biosimilars, Interchangeable biological products, Switching study, Pharmacy substitution of biologics, BPCIA.

INTRODUCTION

Biological products or biologics are among one of the rapidly expanding sector in the pharmaceutical industry. Biologics are large and complex molecules made by the use of biotechnological methods. These substances are extracted from various living organisms, including humans, animals, or microorganisms and are employed for the purposes of diagnosing, preventing, treating, and remedying diseases and medical conditions. Biologics include sugars, proteins, nucleic acids, or intricate blends of these elements, as well as life-forming structures such as cells and tissues. In the USA (United States of America), the oversight of biological products falls within the purview of the United States Food and Drug Administration (USFDA)[1, 2]. Biologics differ from drugs in various ways. They are as given below:

i. Drugs are mostly small molecules produced by chemical synthesis, whereas biologics are medications obtained from live organisms as a result of biological processes.
ii. Drugs have molecular weights between 0.1 and 1 kDa (Kilo Dalton), whereas biologics are larger than 1 kDa and may have molecular weights up to 1000 kDa.
iii. Drugs retain their chemical identity irrespective of the methods and materials used for manufacture. Whereas biologics are known to be highly sensitive to the starting materials used and the manufacturing process followed.
iv. Drugs have simple structures and are mostly non immunogenic, whereas biologics have complex structures and are immunogenic.
v. The characterization of drugs is easy, whereas,for biologics it is challenging[3, 4, 5]. Biologics can be classified into 2 broad categories. As per USFDA, reference biologics and biosimilars are defined as follows-

Reference biologics

"A reference product is the single biological product, already approved by the Food and Drug Administration (FDA), against which a proposed biosimilar product is compared."

Similar biologics/ Biosimilars

"A biosimilar or a similar biologic is a biological product that is highly similar and has no clinically meaningful differences from an existing FDA-approved reference product" [1].

MARKET SCENARIO OF BIOLOGICS

The Compound annual growth rate(CAGR) of biologics from 2022 to 2032 is valued to be about 8.5%. By the year 2030, it is estimated to be approximately $35.1 billion. The CAGR of biologics from 2022 to 2030 is estimated to be approximately 20.2%[6.7].

INTERCHANGEABLE BIOLOGICAL PRODUCTS (IBPs)

Brand drugs or innovator drugs are expensive. Thus, generic versions of these innovator products are produced at a cheaper price for affordability. The generic version of the drug product can be substituted in the pharmacy by the pharmacist without the need to consult the prescribing health care provider, provided that the therapeutic actions of the drug products are the same and that there is no significant difference in pharmacokinetic and pharmacodynamic properties between the brand and the generic version of the drug product. This is given in Figure 1[8]. Such is not the case for biological products. Despite the availability of biosimilars on the market, they cannot be interchanged with reference biologics for treatment or therapeutic purposes in pharmacies, such as drugs. Hence, interchangeability comes into being to increase patient access to biologics[1, 9]. It is important to note that not all biosimilars are IBPs but that all IBPs are biosimilars. IBP is also known as interchangeable biosimilars or interchangeable products. According to the USFDA, "An interchangeable biological product is a biosimilar that meets additional requirements and may be substituted for the reference product at the pharmacy, depending on state pharmacy laws." In other words, a biologic that satisfies all the prerequisites for a biosimilar product along with the extra requirements specified by the Biologics Price Competition and Innovation Act (BPCIA) is considered an IBP. The additional requirements that are to be met are: First, "the biologic must be expected to produce the same clinical result as the

reference product in any given patient." Second, there should be sufficient evidence assuring safety when switching between the reference biologic and the follow-on biologic[9, 10]. It is important to note that the designation for interchangeability holds for the pharmacist and not the physician. The physicians can prescribe whatever drug they want. A physician can prescribe a biosimilar to a patient who was previously treated with a reference product without a designation of interchangeability for biosimilar. The concept of interchangeability is explained in Figure 2.

INTERCHANGEABILITY

Before understanding Interchangeability, it is necessary to know what switching, and substitution are.

Switching

Switching involves the physician's decision to substitute one biologic with another that has a similar therapeutic effect in patients.

Substitution

It is the practice of dispensing where the pharmacist may substitute an alternative biologic (one that is equivalent and interchangeable) to the biological product without the consultation of the prescriber in any patient[11, 12, 13]. For a biologic to attain the status of an IBP, it must first be a biosimilar. For market approval of the IBP, it is necessary to submit a secondary application to the biosimilar to ensure that the requirements for their interchangeability are met. For the substitution or interchangeability of a biologic with that of its reference product, it is necessary to demonstrate the switch between the two products. The switching is done to prove that it does not change the clinical outcome[9,14]. The connectivity between the biologic, biosimilar and interchangeable biological products is explained in Figure 03, which pertains to the application to be submitted and test/evaluation/clinical data requirements. Although the FDA permits the pharmacy-level substitution of a biological product without physician interference with an IBP, the regulations vary from state to state. Among the 50 states and Washington D.C. in the US, 47 permitted the pharmacists to substitute the product without the physician's intervention provided; they only notified the patient or the physician of the change. The states that do not allow for pharmacy-level substitution are Alabama, Indiana, South Carolina, and Washington. Of all these, 2 countries—North Carolina and Virginia—do not require the pharmacist to communicate with the prescribing physician. However, patient communication is mandatory in 45 of the states for product substitution [16].

List of approved interchangeable biological products

As of May 21, 2024, the USFDA has approved 53 biosimilars. Among them, "Adalimumab", "Aflibercept", "Insulin Glargine", "Denosumab", "Ranibizumab" and "Ustekinumab" have received FDA approval for their interchangeability status. Among these, the most recent approval for biosimilars was "Aflibercept" with the interchangeability designation as of May 20, 2024.Table 01 shows the approved list of IBPs along with the reference products in the United States (US).

REGULATORY REQUIREMENTS

The IBP development and approval pathway involves the following aspects:

Application

For a new biologic, an application must be submitted in 351(a) – Biologic License Application (BLA), which is comparable to the New Drug Application (NDA) for drugs. However, in the case of biosimilars, a 351(k) biosimilar biologic application must be submitted by the applicant[20].

Enforcement/term exclusivity

The innovator biological product, i.e., the reference biologic by the innovator company, is granted a patent term exclusivity for 12 years. Over this time, the FDA has not approved the 351(k) application. Furthermore, the FDA cannot review a 351(k) application for 4 years upon approval of the reference biologic as per section 351(a) of the PHS Act. This period when the 351(k) application is neither submitted nor reviewed is known as the reference product exclusivity period. According to section 351(m) of the Public Health Service (PHS)Act, if the sponsor conducts

pediatric studies and fulfills the requirements for pediatric exclusivity under section 595A of the Food Drug and Cosmetics (FD&C)Act, then an extra 6-month exclusivity period to the above is given to the biosimilar or the interchangeable biological product. If a biologic or interchangeable biological product is for a rare disease, then:

- According to section 527(a) of the FD&C Act, the biologic is granted an orphan drug exclusivity for a period of 7 years or,
- As per section 351(k)(7) of the PHS Act, the biologic is given exclusivity for a period of 12 years[21, 22].

Plethora of secondary patents

The plethora of secondary patents for biosimilars has been a significant factor contributing to delays in biosimilar availability, particularly in the United States. Biosimilar availability has been severely hindered by the large number of biological drug patents. These secondary patents, which cover new methods of manufacturing and formulation, have been identified as major contributors to the delays in biosimilar market entry in the US [23, 24]. According to a recent study, on the slow growth of biosimilars in the US, there were reportedly 179 instances of patent infringement across 21 cases, spanning 9 original biologics: “adalimumab”, “bevacizumab”, “etanercept”, “trastuzumab”, “Epogen” (epoetinalfa), “Neupogen” (filgrastim), “Remicade” (infliximab), “Neulasta” (pegfilgrastim), and “Rituxan” (rituximab). Among these patents, 76 (42%) pertained to manufacturing processes, 63 (35%) to methods of utilization, 43 (24%) to formulations, 11 (6%) to constituent elements, and 3 (1%) to devices. Notably, 14 (8%) patents exhibited characteristics that fell into more than one category[24].

Case study: Humira Patent Thicket

Since the approval of Humira (adalimumab) by the USFDA in 2002, Humira has been one of the globally best-selling biologic generating AbbVie a revenue of $20.7 billion (2021). The patent that covers Humira expired in 2016. However, the 132 other patents related to Biologicsexpire in 2034. Abb Viecreated a thicket protecting Humira from competition until 2037 by applying for approximately 247 patents, of which 132 were granted[25].

Data requirements for supporting an interchangeable biological application

The data required for an interchangeable biological product to support the application must include the biosimilar product requirements along with additional requirements. Data requirements for a biosimilar application: Information must be submitted along with the application proving the product biosimilarity with that of its reference product, which includes-

- Analytical studies, despite the minor variations in the components that are clinically inactive.
- Animal studies, including toxicity assessment
- Clinical studies demonstrating the purity, safety and potency of the biologic. This includes assessments of immunogenicity, pharmacokinetics (PK), Pharmacodynamics (PD) and a comparative clinical study.

For the above-mentioned data, an application for an IBP must include the following data:

- The proposed IBP provides the same clinical outcome as that of its reference biologic in every patient.
- When the proposed IBP is administered to an individual, switching between the reference biologic and the proposed interchangeable biologic should not affect the efficacy or increase safety concerns.
- It is also necessary to prove that there is no difference or effect when using the reference biologic without making such switches[26].

Switching study supporting interchangeability

For the approval of an IBP, the FDA requires the sponsor to prove that the proposed IBP’s interchangeability will not affect the clinical response (concerning safety and efficacy) compared with that of its reference product. To demonstrate this, switching studies must be conducted. A switching study is a study that is conducted to demonstrate that the use of the proposed IBP upon switching it or altering it with its reference biological product does not possess any risk of safety or efficacy. Figure 04 shows the concept of switching study. The FDA has approved two different protocols for conducting switching studies to demonstrate the interchangeability of biological

products. The two study designs are as follows: i. Dedicated Switching Study Design, ii. Integrated Study Design. The study schemes are shown in Figures 05 and 06.

Dedicated switching study design

In this study design, the subjects are given the reference product during the lead-in period. These subjects are then divided into two groups/ arms by randomization, where one arm is a switching group and the other remains a non switching arm. In the non switching arm, the subjects are given only a reference product throughout the study, whereas in the switching arm, the subjects following the lead-in period are switched between the proposed IBP and that of the reference biologic.

Integrated study design

It is a type of study design in which both the biosimilarity and interchangeability of a biological product to that of its reference product are determined. It consists of 2 stages:

Stage I: It is a parallel head-head study design where the bio similarity of the proposed interchangeable product is assessed against the reference product. After the first stage, the subjects in the reference biologic section are re-randomized.

Stage II: In this stage, the interchangeability of the proposed biologic is compared against a reference biologic and the evaluation is performed using a dedicated switching study[27, 28].

REVIEW AND APPROVAL PROCESS

Interchangeable biological products in the US are approved through an abbreviated pathway in which the proposed interchangeable biologic is compared with that of its reference biologic to demonstrate biosimilarity. The data requirements, as mentioned above (biosimilarity data + additional requirements), must be submitted to the FDA along with the application. The FDA reviews the application and assesses the safety of the interchangeable biologic. The general process flow for the approval of interchangeable biological products is given in Figure 07[9].

POSTMARKET SAFETY MONITORING

Post-marketing safety monitoring is crucial for both interchangeable biologics and originator biologics. It is particularly important for interchangeable biologics due to their similarity to the reference product and the potential for immunogenicity or unexpected reactions upon switching between products. This monitoring helps ensure ongoing safety and efficacy in real-world use, providing valuable data for healthcare professionals, regulatory agencies, and patients. Adequate mechanisms must be in place for postmarket safety monitoring, as per the FDA document[26].

1. **Good Pharmacovigilance Practices and Pharmacoepidemiologic Assessment-**This document by the FDA guides the industry on the identification of safety signals, assessment of pharmaco epidemiology and development of a pharmacovigilance plan. The investigation of a safety signal is done through a nonrandomized observational study following 3 different methods, viz.

a) Pharmaco epidemiologic studies, b) Registries, c) Surveys [29].

2. **Postmarketing Adverse Experience Reporting for Human Drugs and Licensed Biological Products: Clarification of What to Report**- In this document, the FDA clarifies the complete information that is necessary for the submission of an adverse event along with the management of the safety data on patient contacts. The complete information consists of an identifiable patient, an identifiable reporter, a suspected drug or biologic and an adverse event[22]. As of January 2024, the USFDA has completed the finalization of its best practices guide for reviewing post-marketing safety surveillance of drugs and biologics. This manual underscores the heightened safety scrutiny applied to biosimilar supplements and Periodic Safety Update Reports (PSURs), necessitating vigilant monitoring of post-marketing safety data specifically pertaining to biosimilars. Among various changes, the finalized document no longer mandates FDA reviewers to examine data regarding the reference product when assessing an adverse event associated with a biosimilar[30].

ACTS APPLICABLE FOR IBPs

- ✓ **Public Health Service Act, 1944 [PHS]:** Section 351(k) (7) of the PHS act apprises about the reference biologic exclusivity, which specifies that the sponsor shall not submit and that the FDA shall not license an application for a biosimilar.
- ✓ **Biologics Price Competition and Innovation Act, 2009 [BPCIA]:** This was passed to establish a shortened licensure process for a biosimilar or interchangeable biologic[21].
- ✓ **Patient Protection and Affordable Care Act, 2010:** Now referred to as the Affordable Care Act (ACA), this is a comprehensive healthcare reform law that has the following primary goals: i) availability of economical healthcare insurance to more people, ii) to expand the Medicaid program iii) to support methods for lowering the cost of healthcare [31].
- ✓ **Advancing Education on Biosimilars Act of 2021:** This is a bill that was passed by the United States Congress that states that the FDA must develop and improve education programs addressing healthcare providers about the prescription of biologics and biosimilars[32].

RECENT REGULATORY PROPOSITION FOR IBP

In March 2024, the "FDA's FY 2025 Legislative Proposals" included a budget request titled: "Eliminate the Statutory Distinction Between the Approval Standard for Biosimilar and Interchangeable Biosimilar Products and Deem that Approved Biosimilars are Interchangeable" This request aims to remove the regulatory differentiation between the approval standards for interchangeable biologic and biosimilar, thereby automatically designating approved biosimilars as interchangeable upon initial approval. In this proposal, it was articulated that, a lot of confusion and misinterpretation has been caused by the existing statutory differentiation between a biosimilar and its respective interchangeable biosimilars and interchangeable biological product, particularly among patients and healthcare providers, regarding the safety and efficacy of biosimilars and whether these interchangeable biosimilars have better safety and efficacy as compared to their counterparts. The FDA aims to modify section 351 of the Public Health Service (PHS) Act to eliminate the separate regulatory standard interchangeability. Thereby ensuring that any new biologic approved henceforth can be used as an interchangeable biologic immediately after the approval from FDA. This proposed change realigns the U.S. biosimilar program to the scientific and regulatory approach followed by other leading regulatory bodies such as the European Union, where biosimilars are deemed interchangeable with their reference products upon approval. Moreover, this proposal is anticipated to enhance the adoption of biosimilars, potentially leading to increased competition, improved access, and enhanced affordability of these products[33].

CONCLUSION

Interchangeable biological products have been the cause of major development in the pharmaceutical industry. They have contributed to increased access to biological therapies while upholding highly regulated safety standards. The USFDA regulatory framework defines the interchangeability criteria and enforces the regulatory requirements of IBPs before the substitution at the pharmacy level can be performed without physician intervention. The state-level variations in substituting IBPs and stringent monitoring of post-market safety are some of the major challenges in adopting IBPs. The currently available and followed guidelines help streamline the approval process for biosimilars and serve to align the US regulatory approach with international standards, accelerating the uptake of biosimilars and IBPs. However, The FDA's recent proposal eliminates the regulatory differences between interchangeable biologics and biosimilars to reduce confusion among healthcare providers and patients and provide clear information regarding their safety and efficacy. This helps fast-track the approval process for biosimilars and serves to align the US regulatory approach with international standards, accelerating the uptake of biosimilars and IBPs. Thus with the paradigm shift in the biological sector, it is necessary to collaborate with the regulatory authorities, healthcare providers and also industry stakeholders to overcome the existing barriers and provide the promise of

enhanced patient care with the IBP. The prospects for biological therapies lie in the ability to deliver its two goals innovation and accessibility. Thus paving the way for an equitable and sustainable healthcare system.

ACKNOWLEDGMENT

We would like to thank Acharya & BM Reddy College of Pharmacy for providing us with this opportunity.

REFERENCES

1. FDA. Biological Product Definitions What is a biological product? Available on https://www.fda.gov/files/drugs/published/Biological-Product-Definitions.pdf [Assessed 23 Dec 2023].
2. Center for Biologics Evaluation and Research. What Are "Biologics" Questions and Answers. FDA.2019 Feb 28; Available on https://www.fda.gov/about-fda/center-biologics-evaluation-and-research-cber/what-are-biologics-questions-and-answers [Assessed 23 Dec 2023].
3. Makurvet FD. Biologics versus small molecules: Drug costs and patient access. Medicine in Drug Discovery. 2020 Nov;9(9):100075. doi: 10.1016/j.medidd.2020.100075
4. Zhao L, Ren T, Wang DD. Clinical pharmacology considerations in biologics development. ActaPharmacologicaSinica. 2012 Nov 1;33(11):1339–47. doi: 10.1038/aps.2012.51
5. Paul J Declerck. Biologicals and biosimilars: science and implications - GaBI Journal. gabi-journal.net. 2012. doi: 10.5639/gabij.2012.0101.005 available on http://gabi-journal.net/biologicals-and-biosimilars-a-review-of-the-science-and-its-implications.html
6. Ghosh S. Biologics Market. Future Market Insights; Aon https://www.futuremarketinsights.com/reports/biologics-market [Assessed 24 Dec 2023].
7. Chandani Patel. US Biosimilars Market Analysis Report 2022 to 2030. www.insights10.com. 2023 Oct. Available on https://www.insights10.com/report/us-biosimilars-market-analysis/ [Assessed 24 Dec 2023].
8. Darrow JJ, Chong JE, Kesselheim AS. Reconsidering the scope of US state laws allowing pharmacist substitution of generic drugs. BMJ. 2020;369. doi: https://doi.org/10.1136/bmj.m2236 available on https://www.bmj.com/content/369/bmj.m2236
9. FDA. Interchangeable Biological Products. Available on https://www.fda.gov/media/151094/download [Assessed 24 Dec 2023].
10. Koyfman BH. Biosimilarity and Interchangeability in the Biologics Price Competition and Innovation Act of 2009 and FDA's 2012 Draft Guidance for Industry. Biotechnology Law Report. 2013 Aug;32(4):238–51.
11. Amgen. Substitution & Interchangeability | BioEngage from Amgen Biosimilars [Internet]. www.amgenbiosimilars.com. Available from: https://www.amgenbiosimilars.com/bioengage/prescribing-biosimilars/substitution-and-interchangeability 10.1002/sim.5569 [Assessed 24 Apr2024].
12. biopharma-reporter.com. Biosimilar interchangeability: Do you know your switching from your substitution? [Internet]. biopharma-reporter.com. 2017. Available from: https://www.biopharma-reporter.com/Article/2017/03/21/Biosimilr-switching-interchangeability-and-substitution-the-EU-view 10.1002/sim.5569 [Assessed 24 May 2024].
13. GaBI. The evolution of switching and substitution of biosimilars in Europe [Internet]. gabionline.net. 2017. Available from: https://gabionline.net/reports/The-evolution-of-switching-and-substitution-of-biosimilars-in-EuropeLászló Endrényi, Chiann C, Shein Chung Chow, LászlóTóthfalusi. On the interchangeability of biologic drug products. Statistics in Medicine. 2012 Aug 22;32(3):434–41. doi: 10.1002/sim.5569 [Assessed 24 May 2024].
14. LászlóEndrényi, Chiann C, Shein Chung Chow, LászlóTóthfalusi. On the interchangeability of biologic drug products. Statistics in Medicine. 2012 Aug 22;32(3):434–41. doi: 10.1002/sim.5569
15. Li E, Ramanan S, Green L. Pharmacist Substitution of Biological Products: Issues and Considerations. Journal of Managed Care & Specialty Pharmacy. 2015 Jul;21(7):532–9. doi: 10.18553/jmcp.2015.21.7.532.
16. Humphreys S. Understanding interchangeable biosimilars at the federal and state levels. The American Journal of Managed Care. 2023 Aug 1;29(Spec. No. 7):SP545–8. doi: 10.37765/ajmc.2023.89419
17. Drugs.com. How many biosimilars have been approved in the United States?. Drugs.com. 2019 available on

https://www.drugs.com/medical-answers/many-biosimilars-approved-united-states-3463281/ [Assessed 24 Dec 2023].

18. FDA. Purplebook. 2022. Available on https://purplebooksearch.fda.gov/ [Assessed 25 Dec 2023].
19. Office of the Commissioner. FDA Approves First Interchangeable Biosimilar for Two Rare Diseases [Internet]. FDA. 2024. Available from: https://www.fda.gov/news-events/press-announcements/fda-approves-first-interchangeable-biosimilar-two-rare-diseases [Assessed 30 May 2024].
20. Peterson J, Budlong H, Affeldt T, Skiermont K, Kyllo G, Heaton A. Biosimilar Products in the Modern U.S. Health Care and Regulatory Landscape. Journal of Managed Care & Specialty Pharmacy. 2017 Dec;23(12):1255–9. doi: 10.18553/jmcp.2017.23.12.1255
21. FDA. Biosimilar Product Regulatory Review and Approval. Available on https://www.fda.gov/files/drugs/published/Biosimilar-Product-Regulatory-Review-and-Approval.pdf [Assessed 26 Dec 2023]
22. FDA. Guidance for Industry Reference Product Exclusivity for Biological Products Filed Under section 351(a) of the PHS Act draft guidance. Available on https://www.fda.gov/media/89049/download [Assessed 28 Dec 2023]
23. Goode R, Chao B. Biological patent thickets and delayed access to biosimilars, an American problem. Journal of Law and the Biosciences. 2022 Jul 1;9(2).
24. Van de Wiele VL, Beall RF, Kesselheim AS, Sarpatwari A. The characteristics of patents impacting availability of biosimilars. Nature Biotechnology. 2022 Jan;40(1):22–5.
25. Knox R, Curfman G. The Humira patent thicket, the Noerr–Pennington doctrine and antitrust's patent problem. Nature Biotechnology. 2022 Dec;40(12):1761–3.
26. FDA. Considerations in Demonstrating Interchangeability With a Reference Product Guidance for Industry. 2019. Available on https://www.fda.gov/media/124907/download [Assessed 27 Dec 2023]
27. Alvarez DF, Wolbink G, Cronenberger C, Orazem J, Kay J. Interchangeability of Biosimilars: What Level of Clinical Evidence is Needed to Support the Interchangeability Designation in the United States? BioDrugs. 2020 Sep 29;34(6):723–32. doi: 10.1007/s40259-020-00446-7
28. FDA. Guidance for Industry Good Pharmacovigilance Practices and Pharmacoepidemiologic Assessment Clinical Medical. 2005. Available on https://www.fda.gov/files/drugs/published/Good-Pharmacovigilance-Practices-and-Pharmacoepidemiologic-Assessment-March-2005.pdf [Assessed 28 Dec 2023].
29. FDA. Guidance for Industry Postmarketing Adverse Experience Reporting for Human Drug and Licensed Biological Products: Clarification of What to Report. 1997 Available on https://www.fda.gov/media/71635/download [Assessed 28 Dec 2023].
30. FDA. Best Practices in Drug and Biological Product Postmarket Safety Surveillance for FDA Staff DRAFT [Internet]. 2024 Jan. Available from: https://www.fda.gov/media/130216/download [Assessed 28 Dec 2023].
31. U.S. Department of Health & Human Services. About the Affordable Care Act. 2022 available on https://www.hhs.gov/healthcare/about-the-aca/index.html [Assessed 28 Dec 2023].
32. Sen. Hassan MW [D N. S.164 - 117th Congress (2021-2022): Advancing Education on Biosimilars Act of 2021. available on https://www.congress.gov/bill/117th-congress/senate-bill/164 [Assessed on 9 Jan 2024].
33. FDA. FY25 LEGISLATIVE PROPOSALS [Internet]. 2024 Mar. Available from: https://www.fda.gov/media/176924/download?attachment [Assessed on 6 May 2024].

Table 1: List of approved interchangeable biological products[17, 18, 19]

Biologic proper name & use category	Reference product – company	Biosimilar – Company	Interchangeable biological product - company

Adalimumab -Rheumatoid arthritis, IBD, psoriasis, psoriatic arthritis, ankylosing arthritis	**"Humira"** by *AbbVieInc*	**"Amjevita"** (adalimumab-atto) by Amgen Inc **"Hadlima"**(adalimumab-bwwd) by Samsung Bioepis Co Ltd **"Hulio"** (adalimumab-fkjp) by Mylan Pharms Inc. **"Hyrimoz"** (adalimumab-adaz) by Sandoz Inc **"Idacio"** (adalimumab-aacf) by Fresenius Kabi USA **"Yuflyma"** (adalimumab-aaty) by Celltrion **"Yusimry"** (adalimumab-aqvh) by Coherus Biosciences Inc.	**"Abrilada"** (adalimumab-afzb) by Pfizer Inc **"Cyltezo"**(adalimumab-adbm) by BoehringerIngelheim **"Simlandi"** (adalimumab-ryvk) by Alvotech and Teva Pharmaceutical Industries Ltd. **"Hyrimoz"** (adalimumab-adaz) by Sandoz Inc. (Certain strengths only)
Aflibercept-neovascular age-related macular degeneration, diabetic macular edema, myopic choroidal neovascularization, macularedema associated with retinal vein occlusion, and diabetic retinopathy.	**"Eylea"** by Regeneron	-	**"Opuviz"** (aflibercept-yszy) by Samsung Bioepis Co., Ltd. **"Yesafili"** (aflibercept-jbvf) by Biocon Biologics Inc.
Denosumab - prevents bone-related complications of cancer	**"Prolia"** by Amgen Inc. **"Xgeva"** by Amgen Inc.	-	**"Jubbonti"** (denosumab-bbdz) by Sandoz Inc. **"Wyost"**(denosumab-bbdz)
Eculizumab - paroxysmal nocturnal hemoglobinuria (PNH), atypical hemolytic uremic syndrome (aHUS)	**"Soliris"** by Alexion Pharmaceuticals, Inc.	-	**"Bkemv"** (eculizumab-aeeb) by Amgen Inc.
Insulin glargine - Diabetes	**"Basaglar"** by Eli Lilly and Co **"Lantus"** by Sanofi Aventis US **"Semglee"**byViatris Inc. **"Toujeo"** by Sanofi US Services	-	**"Rezvoglar"** (insulin glargine-aglr) by Eli Lilly Co **"Semglee"** (insulin glargine-yfgn) by Mylan Pharms Inc

Ranibizumab -Age-related macular degeneration	**"Lucentis"** by Genentech **"Susvimo"** by Genentech Inc	-	**"Byooviz"** (ranibizumab-nuna) by Samsung Bioepis Co Ltd **"Cimerli"** (ranibizumab-eqrn) by Coherus Biosciences Inc
Ustekinumab - Plaque psoriasis, psoriatic arthritis, Crohn disease, ulcerative colitis	**"Stelara"** by Janssen Biotech	-	**"Wezlana"** (ustekinumab-auub) by Amgen Inc

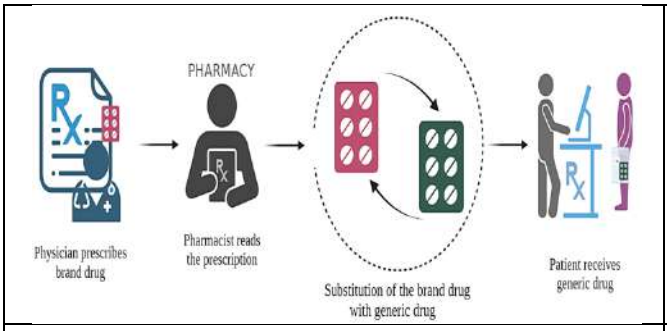

Figure 1: Substitution of drug products at the pharmacy level

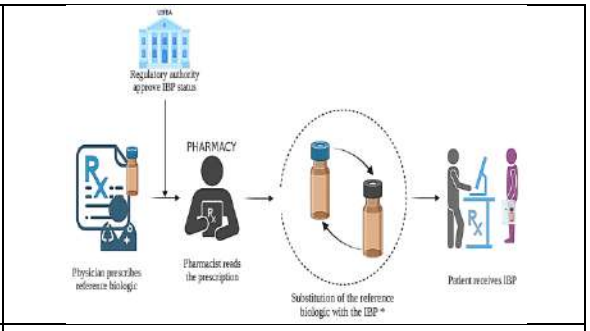

Figure 2: Substitution of biological products at the pharmacy level

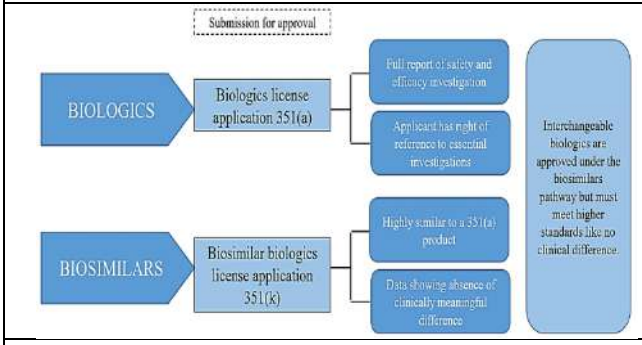

Figure 3: Connections between biologics, biosimilars and interchangeable biological products[15]

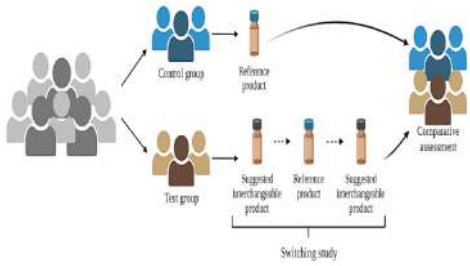

Figure 4: The concept of switching study

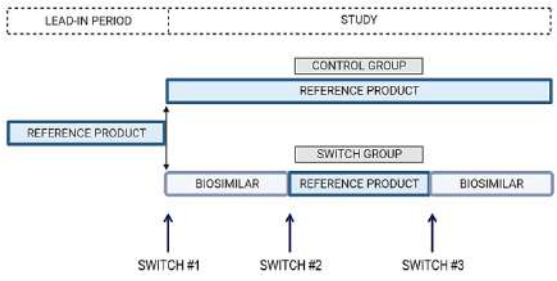

Figure 5: Dedicated switching study design

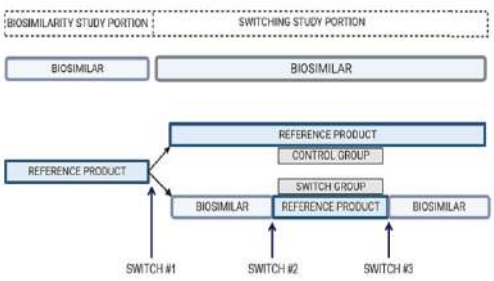

Figure 6: Integrated study design

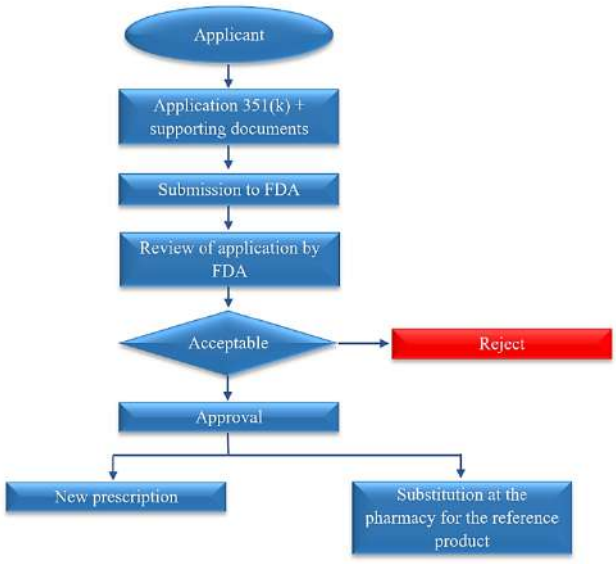

Figure 7: General process flow for interchangeable biological products

Indian Journal of Natural Sciences www.tnsroindia.org.in ©IJONS

Vol.15 / Issue 88 / Feb / 2025 *International Bimonthly (Print) – Open Access* *ISSN: 0976 – 0997*

RESEARCH ARTICLE

New Technique for Improving Assignment Problem Using Phythagorean Fuzzy Sets: A New Similarity Measure and Score Function

Sharmila Banu S[1] and Prasanna A[2]

[1]Assistant Professor, PG and Research Department of Mathematics, Jamal Mohamed College (Autonomous), Affiliated to Bharathidasan University, Tiruchirappalli-620024, Tamil Nadu, India.
[2]Assistant Professor, PG and Research Department of Mathematics, Jamal Mohamed College (Autonomous), Affiliated to Bharathidasan University, Tiruchirappalli-620024, Tamil Nadu, India.

Received: 21 Jun 2024 Revised: 03 Jul 2024 Accepted: 13 Aug 2024

***Address for Correspondence**
Sharmila Banu S
Assistant Professor,
PG and Research Department of Mathematics,
Jamal Mohamed College (Autonomous),
Affiliated to Bharathidasan University,
Tiruchirappalli-620024,
Tamil Nadu, India.
E. Mail: sharmilasheik0408@gmail.com

ABSTRACT

Real-world situations are imprecise due to imprecision and/or accuracy, making it impossible to pinpoint the exact value of the measured values. Sometimes a lack of information or time makes it difficult for decision-makers to express their ideas. In order to enable decision-makers to freely voice their input, information regarding imprecision is presented in a fuzzy manner. Fuzzy sets (FS) and intuitionistic fuzzy sets (IFS) are useful tools for describing uncertainty in ambiguous circumstances. Numerous models for The Pythagorean fuzzy set (PFS) has a larger domain space than the intuitionistic fuzzy set to describe the membership grade. This algorithm requires a lower number of iterations to reach optimal. We have proposed a method to solve the Pythagorean fuzzy assignment problem (PFAP) using the proposed similarity measure and a score function. To validate this algorithm, numerical examples are given to explain the methodology.

Keywords: Pythagorean Fuzzy Set; Similarity Measure; Score Function; Assignment Problem.

INTRODUCTION

A linear programming problem (LPP) that addresses scheduling and allocation is called an assignment issue. Because the resources that are available are not all equally efficient in carrying out diverse tasks, assignment problems arise.

While it is expected in traditional assignment problems that the decision-maker is certain of the exact cost of the assignment problem, in reality, these parameters are inaccurate. The fuzzy set (FS) was developed by Zadeh (1965) to address ambiguity in practical applications. The centroid approach was employed by Gurukumaresan *et al*. (2020) to solve the fuzzy assignment problem. Tsai and colleagues (1999) conducted research on multi-objective fuzzy manpower deployment. Chanas *et al*. (1984) utilized parametric programming to solve the transportation problem by treating supply and demand as fuzzy integers. Generalized similarity measures for Pythagorean fuzzy sets and their applications to multiple attribute decision-making were the focus of Verma & Merigó's 2019 research. Fuzzy assignment difficulties and fuzzy traveling salesman problems were resolved by Kumar and Gupta (2011) using various membership functions. Using the fuzzy PROMETHEE II approach, Yuen and Ting (2012) chose the textbooks. The work of Thakre *et al*. (2018) employees at LIC who use fuzzy assignment problems. In order to account for the imprecise and hazy information found in the practical problem, various writers have proposed expansions of the fuzzy set. An expansion of the fuzzy set is the intuitionistic fuzzy set (IFS), as forth by Atanassov (1984). He took into account the element's membership and non-membership. 2015 saw the resolution of the intuitionistic fuzzy assignment by Roseline and Amirtharaj. assignment problem using the intuitionistic fuzzy number (IFN) ranking method. The intuitionistic fuzzy set method of TOPSIS was applied by Boran *et al*. (2012) to solve the challenge of renewable energy. Mukherjee and Basu (2012) used the scoring function and similarity measure to solve the assignment problem under IFS. In 2014, Kumar and Bajaj presented the issue of an interval-valued A Pythagorean fuzzy set (PFS) was first presented by Yager (2013). When non-membership degree (λ) + membership degree (λ), Yager triumphs. (φ) >1 within IFS. The square sum of the membership degree and the non-membership degree must be less than or equal to for PFS to be an extension of IFS.1 ($\lambda_{\mathcal{A}}(u)$^2 + $\varphi_{\mathcal{A}}(u)$^2 ≤ 1) For decision makers (DM), the broader preference domain is provided by the concept of Pythagorean fuzzy sets (PFS). DMs are able to specify what they support and oppose in terms of membership level as $\lambda(x)$ = 4/5, ϕ (x)= 2/5. In this case, 4/5+2/5>1 is not valid in IFS but squaring (4/5) ^2 + (2/5) ^2 <1 suggests that the intuitionistic fuzzy set is less appropriate than the Pythagorean fuzzy set. Paul Augustine Ejegwa (2019) studied the Pythagorean fuzzy set and how to use max-min composition to apply it to career placement. The Pythagorean fuzzy multi-criteria problem was resolved by Fei and Deng [18]. The decision-making approach under the Pythagorean fuzzy Yager weighted operators was proposed by Shahzadi *et al*. (2018). Some findings for Pythagorean fuzzy sets were defined by Peng and Yang (2015). Numerous writers throughout the era presented the Pythagorean similarity measure and scoring function. The novel similarity metric for Pythagorean fuzzy sets was created by Agheli *et al*. (2022) and applied to multiple-criteria decision-making. In order to use PFS for multi-criteria decision-making, Zhang and Xu (2014) worked on TOPSIS. In order to analyze the issue, Peng & Yang (2016) established the interval-valued Pythagorean fuzzy number (IVPFN) score function and distance measure. Following that, in order to get over some of the drawbacks of the scoring function established by Peng & Yang (2016), Garg [25] suggested the score function for PFN and IVPFN. We have devised a strategy in this work to use Pythagorean fuzzy values to solve the assignment problem. The score function that Garg (2017) defined has a few restrictions. We have suggested a new score function in order to get around these restrictions. To support our findings, we have also created the new similarity metric. There is currently no literature on Pythagorean fuzzy assignment problems with score function and similarity measure. The structure of the paper is as follows: In Section 2, certain fundamental concepts related to FS, IFS, PFS, and arithmetic operations on Pythagorean fuzzy numbers are covered. We have presented a new similarity metric and score function in Section 3. Furthermore, the drawbacks of previously established score functions have been highlighted. Section 4 provides the methods for solving PFAP utilizing the similarity measure and scoring function. This section also includes examples that serve as illustrations. The comparative analysis and concluding remarks are presented in Section 5.

Preliminaries

In this section, we have discussed some basic definitions and arithmetic operations that are required for our work.

Definition 2.1 (1965):

A fuzzy set (FS) $\tilde{\mathcal{A}}$ is defined on universal set U as $\tilde{\mathcal{A}}$ = {⟨u, $\lambda_{\mathcal{A}}$(u)|u ∈ U⟩},
characterized by the membership function $\lambda_{\mathcal{A}}(u)$: U→ [0,1]. Here $\lambda_{\mathcal{A}}$(u) is the membership degree of the element u to the set A.

Definition 2.2 (1984):
An intuitionistic fuzzy set A on U is defined as a set of ordered pair given by $\tilde{\mathcal{A}} = \{\langle u, \lambda_{\tilde{\mathcal{A}}}(u), \phi_{\tilde{\mathcal{A}}}(u)\rangle | u \in U\}$,where $\lambda_{\tilde{\mathcal{A}}}(u), \phi_{\tilde{\mathcal{A}}}(u): U \rightarrow [0,1]$are the degree of membership and degree of non-membership of the element $u \in U$, with the condition $(\lambda_{\tilde{\mathcal{A}}}(u)) + (\phi_{\tilde{\mathcal{A}}}(u)) \leq 1$, the degree of indeterminacy is given by $\phi_{\tilde{\mathcal{A}}}(u) = 1 - \lambda_{\tilde{\mathcal{A}}}(u) - \phi_{\tilde{\mathcal{A}}}(u)$

Definition 2.3 (2013):
A Pythagorean fuzzy set $\tilde{A}$ on U is defined as given by $\tilde{\mathcal{A}} = \{< u, \lambda_{\mathcal{A}}(u), \varphi_{\mathcal{A}}(u) > | u \in U\}$, where$\lambda_{\mathcal{A}}(u)$, $\varphi_{\mathcal{A}}(u): U \rightarrow [0,1]$ are the degree of membership and degree of non-membership of the element $u \in U$, with the condition $(\lambda_{\mathcal{A}}(u))^2 + (\varphi_{\mathcal{A}}(u))^2 \leq 1$, the degree of indeterminacy is given by $\varphi_{\mathcal{A}}(u) = \sqrt{1 - (\lambda_{\mathcal{A}}{}^2 + \varphi_{\mathcal{A}}{}^2)}$. The domain of a Pythagorean fuzzy set is larger than intuitionistic fuzzy sets. While working in the space of PFS, one may have much more choice of assigning value to member and non membership from [0, 1].

Definition 2.4 (2015):
The addition, multiplication, and scalar multiplication on two PFNs $\tilde{\mathcal{A}}_1 = < \lambda_{\mathcal{A}_1}(u), \varphi_{\mathcal{A}_1}(u) >$ and $\tilde{\mathcal{A}}_2 = < \lambda_{\mathcal{A}_2}(u), \varphi_{\mathcal{A}_2}(u) >$ are defined as follows:

i. $\tilde{\mathcal{A}}_1 \oplus \tilde{\mathcal{A}}_2 = \langle \sqrt{\lambda^2_{\mathcal{A}_1} + \lambda^2_{\mathcal{A}_2} - \lambda^2_{\mathcal{A}_1}\lambda^2_{\mathcal{A}_2}}, \varphi^2_{\mathcal{A}_1}\varphi^2_{\mathcal{A}_2} \rangle$,

ii. $\tilde{\mathcal{A}}_1 \otimes \tilde{\mathcal{A}}_2 = \langle \lambda^2_{\mathcal{A}_1}\lambda^2_{\mathcal{A}_2}, \sqrt{\varphi^2_{\mathcal{A}_1} + \varphi^2_{\mathcal{A}_2} - \varphi^2_{\mathcal{A}_1}\varphi^2_{\mathcal{A}_2}} \rangle$,

iii. $k\tilde{\mathcal{A}}_1 = \langle \sqrt{1 - (1 - \lambda^2_{\mathcal{A}_1})^k}, \varphi^k_{\mathcal{A}_1} \rangle$, k>0

3. Similarity Measure and Score Function of Pythagorean Fuzzy Set :
The new similarity metric and Pythagorean fuzzy set score function have been defined in this section.
Definition 3.1:
Suppose$\tilde{\mathcal{A}}$ and $\tilde{\mathcal{B}}$ be two PFSs. The similarity measure $\tilde{\mathcal{A}} \times \tilde{\mathcal{B}}$be two PFSs SM:$\tilde{\mathcal{A}} \times \tilde{\mathcal{B}} \rightarrow [0, 1]$ is defined as follows

$$S(\tilde{\mathcal{A}}, \tilde{\mathcal{B}}) = \frac{\sum_{j=1}^{m} \lambda^2_{\tilde{\mathcal{A}}}(u_j).\lambda^2_{\tilde{\mathcal{B}}}(u_j) + \varphi^2_{\tilde{\mathcal{A}}}(u_j).\varphi^2_{\tilde{\mathcal{B}}}(u_j)}{\sum_{j=1}^{m}\left[\left(\varphi^2_{\tilde{\mathcal{A}}}(u_j).\varphi^2_{\tilde{\mathcal{B}}}(u_j)\right) + \left(\varphi^4_{\tilde{\mathcal{A}}}(u_j).\varphi^4_{\tilde{\mathcal{B}}}(u_j)\right)\right]}$$

Theorem 3.1: Similarity measure (SM) between two PFS $\tilde{\mathcal{A}}$ and$\tilde{\mathcal{B}}$, then the following are true.
1. $0 \leq S(\tilde{\mathcal{A}}, \tilde{\mathcal{B}}) < 1$
2. $S(\tilde{\mathcal{A}}, \tilde{\mathcal{B}}) = 1 \; iff \; \mathcal{A} = B$
3. $S(\tilde{\mathcal{A}}, \tilde{\mathcal{B}}) = S(\tilde{\mathcal{B}}, \tilde{\mathcal{A}})$
4. $S(\tilde{\mathcal{A}}, \tilde{\mathcal{C}}) \leq S(\tilde{\mathcal{A}}, \tilde{\mathcal{B}})$ and $S(\tilde{\mathcal{A}}, \tilde{\mathcal{C}}) \leq S(\tilde{\mathcal{A}}, \tilde{\mathcal{B}})$ for all $\tilde{\mathcal{A}}, \tilde{\mathcal{B}}, \tilde{\mathcal{C}}$ such that $\tilde{\mathcal{A}} \subseteq \tilde{\mathcal{B}} \subseteq \tilde{\mathcal{C}}$.

Proof:
1. Since for all $u_j, 1 \leq j \leq m$,
we have
$\lambda^2_{\tilde{\mathcal{A}}}(u_j).\lambda^2_{\tilde{\mathcal{B}}}(u_j) \leq \lambda^4_{\tilde{\mathcal{A}}}(u_j) \vee \lambda^4_{\tilde{\mathcal{B}}}(u_j)$ and
$\varphi^2_{\tilde{\mathcal{A}}}(u_j).\varphi^2_{\tilde{\mathcal{B}}}(u_j) \leq \varphi^4_{\tilde{\mathcal{A}}}(u_j).\varphi^4_{\tilde{\mathcal{B}}}(u_j)$.
Therefore, for each u_j, we have
$[\lambda^2_{\tilde{\mathcal{A}}}(u_j).\lambda^2_{\tilde{\mathcal{B}}}(u_j) + \varphi^2_{\tilde{\mathcal{A}}}(u_j).\varphi^2_{\tilde{\mathcal{B}}}(u_j)] \leq [\{\varphi^2_{\tilde{\mathcal{A}}}(u_j).\varphi^2_{\tilde{\mathcal{B}}}(u_j)\} + \{\varphi^4_{\tilde{\mathcal{A}}}(u_j) \vee \varphi^4_{\tilde{\mathcal{B}}}(u_j)\}]$
Therefore, for all $u_j, 1 \leq j \leq m$,
we have

$$\sum_{j=1}^{m}[\lambda^2_{\tilde{\mathcal{A}}}(u_j).\lambda^2_{\tilde{\mathcal{B}}}(u_j) + \varphi^2_{\tilde{\mathcal{A}}}(u_j).\varphi^2_{\tilde{\mathcal{B}}}(u_j)] \leq \sum_{j=1}^{m}[\{\lambda^4_{\tilde{\mathcal{A}}}(u_j) \vee \lambda^4_{\tilde{\mathcal{B}}}(u_j)\} + \{\varphi^4_{\tilde{\mathcal{A}}}(u_j) \vee \varphi^4_{\tilde{\mathcal{B}}}(u_j)\}] \leq S^S(\tilde{\mathcal{A}}, \tilde{\mathcal{B}}) \leq 1$$

2. Suppose $S(\tilde{\mathcal{A}}, \tilde{\mathcal{B}}) = 1, \frac{\sum_{j=1}^{m}[\lambda_{\tilde{\mathcal{A}}}^2(u_j).\lambda_{\tilde{\mathcal{B}}}^2(u_j) + \varphi_{\tilde{\mathcal{A}}}^2(u_j).\varphi_{\tilde{\mathcal{B}}}^2(u_j)]}{\sum_{j=1}^{m}[\{\lambda_{\tilde{\mathcal{A}}}^4(u_j).\lambda_{\tilde{\mathcal{B}}}^4(u_j)\}+\{\varphi_{\tilde{\mathcal{A}}}^4(u_j).\varphi_{\tilde{\mathcal{B}}}^4(u_j)\}]} = 1$

$$\sum_{j=1}^{m}[\lambda_{\tilde{\mathcal{A}}}^2(u_j).\lambda_{\tilde{\mathcal{B}}}^2(u_j) + \varphi_{\tilde{\mathcal{A}}}^2(u_j).\varphi_{\tilde{\mathcal{B}}}^2(u_j)] = \sum_{j=1}^{m}[\{\lambda_{\tilde{\mathcal{A}}}^4(u_j).\lambda_{\tilde{\mathcal{B}}}^4(u_j)\} + \{\varphi_{\tilde{\mathcal{A}}}^4(u_j).\varphi_{\tilde{\mathcal{B}}}^4(u_j)\}]$$

Now, we claim that

$$\lambda_{\tilde{\mathcal{A}}}^2(u_j).\lambda_{\tilde{\mathcal{B}}}^2(u_j) = \lambda_{\tilde{\mathcal{A}}}^4(u_j).\lambda_{\tilde{\mathcal{B}}}^4(u_j) \text{ and}$$

$$\varphi_{\tilde{\mathcal{A}}}^2(u_j).\varphi_{\tilde{\mathcal{B}}}^2(u_j) = \varphi_{\tilde{\mathcal{A}}}^4(u_j).\varphi_{\tilde{\mathcal{B}}}^4(u_j).$$

suppose $\lambda_{\tilde{\mathcal{A}}}^2(u_j).\lambda_{\tilde{\mathcal{B}}}^2(u_j) \neq \lambda_{\tilde{\mathcal{A}}}^4(u_j).\lambda_{\tilde{\mathcal{B}}}^4(u_j)$,

since

$\lambda_{\tilde{\mathcal{A}}}^2(u_j).\lambda_{\tilde{\mathcal{B}}}^2(u_j) \leq \lambda_{\tilde{\mathcal{A}}}^4(u_j).\lambda_{\tilde{\mathcal{B}}}^4(u_j)$, there exist $k_1 > 0$ such that

$\lambda_{\tilde{\mathcal{A}}}^2(u_j).\lambda_{\tilde{\mathcal{B}}}^2(u_j) + k_1 = \lambda_{\tilde{\mathcal{A}}}^4(u_j).\lambda_{\tilde{\mathcal{B}}}^4(u_j)$.

Similarly, there exists $k_2 > 0$ Such that

$\varphi_{\tilde{\mathcal{A}}}^2(u_j).\varphi_{\tilde{\mathcal{B}}}^2(u_j) + k_2 = \varphi_{\tilde{\mathcal{A}}}^4(u_j).\varphi_{\tilde{\mathcal{B}}}^4(u_j)$

By hypothesis it follows that $k_1 + k_2 = 0$.

$\Rightarrow k_1 = -(k_2)$, which is not possible.

$\Rightarrow \lambda_{\tilde{\mathcal{A}}}^2(u_j).\lambda_{\tilde{\mathcal{B}}}^2(u_j) = \lambda_{\tilde{\mathcal{A}}}^4(u_j).\lambda_{\tilde{\mathcal{B}}}^4(u_j)$ and $\varphi_{\tilde{\mathcal{A}}}^2(u_j).\varphi_{\tilde{\mathcal{B}}}^2(u_j) = \lambda_{\tilde{\mathcal{A}}}^4(u_j).\lambda_{\tilde{\mathcal{B}}}^4(u_j)$

$$\lambda_{\tilde{\mathcal{A}}}^2(u_j) = \lambda_{\tilde{\mathcal{B}}}^2(u_j)$$

$$\varphi_{\tilde{\mathcal{A}}}^2(u_j).\varphi_{\tilde{\mathcal{B}}}^2(u_j)$$

Hence $\tilde{\mathcal{A}} = \tilde{\mathcal{B}}$.

3. $S(\tilde{\mathcal{A}}, \tilde{\mathcal{B}}) = S(\tilde{\mathcal{B}}, \tilde{\mathcal{A}})$ is trivial.

4. For three PFs $\tilde{\mathcal{A}}, \tilde{\mathcal{B}}$ and $\tilde{\mathcal{C}}$ in U. The similarity measures between $\tilde{\mathcal{A}}, \tilde{\mathcal{B}}$ and $\tilde{\mathcal{C}}$ in U are given as

$$S(\tilde{\mathcal{A}}, \tilde{\mathcal{B}}) = \frac{\sum_{j=1}^{m}\lambda_{\tilde{\mathcal{A}}}^2(u_j).\lambda_{\tilde{\mathcal{B}}}^2(u_j) + \varphi_{\tilde{\mathcal{A}}}^2(u_j).\varphi_{\tilde{\mathcal{B}}}^2(u_j)}{\sum_{j=1}^{m}[\{\lambda_{\tilde{\mathcal{A}}}^4(u_j) \vee \lambda_{\tilde{\mathcal{B}}}^4(u_j)\} + \{\varphi_{\tilde{\mathcal{A}}}^4(u_j) \vee \varphi_{\tilde{\mathcal{B}}}^4(u_j)\}]}$$

$$S(\tilde{\mathcal{A}}, \tilde{\mathcal{C}}) = \frac{\sum_{j=1}^{m}\lambda_{\tilde{\mathcal{A}}}^2(u_j).\lambda_{\tilde{\mathcal{C}}}^2(u_j) + \varphi_{\tilde{\mathcal{A}}}^2(u_j).\varphi_{\tilde{\mathcal{C}}}^2(u_j)}{\sum_{j=1}^{m}[\{\lambda_{\tilde{\mathcal{A}}}^4(u_j) \vee \lambda_{\tilde{\mathcal{C}}}^4(u_j)\} + \{\varphi_{\tilde{\mathcal{A}}}^4(u_j) \vee \varphi_{\tilde{\mathcal{C}}}^4(u_j)\}]}$$

Let $\tilde{\mathcal{A}} \subseteq \tilde{\mathcal{B}} \subseteq \tilde{\mathcal{C}}$ for all $u_j \in \tilde{U}$, we have $\lambda_{\tilde{\mathcal{A}}}^2(u_j) \leq \lambda_{\tilde{\mathcal{B}}}^2(u_j) \leq \lambda_{\tilde{\mathcal{C}}}^2(u_j)$,

$$\varphi_{\tilde{\mathcal{A}}}^2(u_j) \geq \varphi_{\tilde{\mathcal{B}}}^2(u_j) \geq \varphi_{\tilde{\mathcal{C}}}^2(u_j).$$

$\Rightarrow \lambda_{\tilde{\mathcal{A}}}^4(u_j) \leq \lambda_{\tilde{\mathcal{B}}}^4(u_j) \leq \lambda_{\tilde{\mathcal{C}}}^4(u_j), \varphi_{\tilde{\mathcal{A}}}^2(u_j) \geq \varphi_{\tilde{\mathcal{B}}}^2(u_j) \geq \varphi_{\tilde{\mathcal{C}}}^4(u_j)$

We claim that for all $u_j \in \tilde{U}$, we have

$$\frac{\lambda_{\tilde{\mathcal{A}}}^2(u_j).\lambda_{\tilde{\mathcal{B}}}^2(u_j)}{\lambda_{\tilde{\mathcal{B}}}^4(u_j) \vee \varphi_{\tilde{\mathcal{A}}}^4(u_j)} \leq \frac{\lambda_{\tilde{\mathcal{A}}}^2(u_j).\lambda_{\tilde{\mathcal{C}}}^2(u_j)}{\lambda_{\tilde{\mathcal{C}}}^4(u_j) \vee \varphi_{\tilde{\mathcal{A}}}^4(u_j)}$$

Similarly, we have

$$\frac{\varphi_{\tilde{\mathcal{A}}}^2(u_j).\varphi_{\tilde{\mathcal{B}}}^2(u_j)}{\lambda_{\tilde{\mathcal{B}}}^4(u_j) \vee \varphi_{\tilde{\mathcal{A}}}^4(u_j)} \leq \frac{\varphi_{\tilde{\mathcal{A}}}^2(u_j).\varphi_{\tilde{\mathcal{C}}}^2(u_j)}{\lambda_{\tilde{\mathcal{C}}}^4(u_j) \vee \varphi_{\tilde{\mathcal{A}}}^4(u_j)}$$

By adding all above equations, we have

$$\frac{\sum_{j=1}^{m}\lambda_{\tilde{\mathcal{A}}}^2(u_j).\lambda_{\tilde{\mathcal{C}}}^2(u_j) + \varphi_{\tilde{\mathcal{A}}}^2(u_j).\varphi_{\tilde{\mathcal{C}}}^2(u_j)}{\sum_{j=1}^{m}[\{\lambda_{\tilde{\mathcal{A}}}^4(u_j) \vee \lambda_{\tilde{\mathcal{C}}}^4(u_j)\} + \{\varphi_{\tilde{\mathcal{A}}}^4(u_j) \vee \varphi_{\tilde{\mathcal{C}}}^4(u_j)\}]} \leq$$

$$\frac{\sum_{j=1}^{m}\lambda_{\tilde{\mathcal{A}}}^2(u_j).\lambda_{\tilde{\mathcal{B}}}^2(u_j) + \varphi_{\tilde{\mathcal{A}}}^2(u_j).\varphi_{\tilde{\mathcal{B}}}^2(u_j)}{\sum_{j=1}^{m}[\{\lambda_{\tilde{\mathcal{A}}}^4(u_j) \vee \lambda_{\tilde{\mathcal{B}}}^4(u_j)\} + \{\varphi_{\tilde{\mathcal{A}}}^4(u_j) \vee \varphi_{\tilde{\mathcal{B}}}^4(u_j)\}]}$$

Therefore, $S(\tilde{\mathcal{A}}, \tilde{\mathcal{C}}) \leq S^s(\tilde{\mathcal{A}}, \tilde{\mathcal{B}})$. Similarly $S^s(\tilde{\mathcal{A}}, \tilde{\mathcal{C}}) \leq S(\tilde{\mathcal{B}}, \tilde{\mathcal{C}})$.

Methodology for Pythagorean fuzzy assignment problem using the score function

Step 1 First, have a look at the decision matrix for the Pythagorean fuzzy assignment problem $G = \{(L_{ij})\}_{m \times n}$

$(L_{ij}) = \langle \lambda_{ij}(x), \varphi_{ij}(x) \rangle, i = 1,2,\ldots..m, j = 1,2\ldots..n$ are Pythagorean fuzzy numbers

Step 2 Check to see if the issue is balanced. Add dummy variables to the problem if it isn't balanced in order to make it a balanced assignment problem

Step 3 Determine each cost value's similarity measure using the Pythagorean positive ideal solution (PPIS) $L^+ = \langle 1,0 \rangle$

$$S(L, L^+) = \frac{\sum_{j=1}^{m} \lambda_L^2(x_j).\lambda_{L^+}^2(x_j) + \varphi_L^2(x_j).\varphi_{L^+}^2(x_j)}{\sum_{j=1}^{m}\left[\left(\lambda_L^4(x_j) \vee \lambda_{L^+}^4(x_j)\right) + \left(\varphi_L^4(x_j) \vee \varphi_{L^+}^4(x_j)\right)\right]}$$

New Algorithmic Approach For Solving Fuzzy Assignment Problem

Step1: Create the cost matrix. Think of the job as a column and the individuals as rows.

Step2: Locate and label the highest element in each assignment matrix column.

Step3: From the maximum column, choose the smallest value. Next, divide each row and column of the matrix's FAP by its lowest value.

Step4: Select and assign the lowest value in the same column after dividing by the minimum value in the column. Next, eliminate the entire column and row.

Step5: After completing step4, Move on to Step2.

Step6: For the FAP, repeat steps 3–5, allocating a row and a column.

Step7: Assess the optimal course of action.

Example;1

Table 1

	1	**2**	**3**	**4**
A	(0.8,0.9)	(0.7,0.7)	(0.6,0,8)	(0.5,0.6)
B	(0.46,0.75)	(0.36,0.7)	(0.56,0.8)	(0.5,0.9)
C	(0.83,0.5)	(0.8,0.53)	(0.2,0.9)	(0.74,0.5)
D	(0.63,0.55)	(0.67,0.36)	(0.20,0.82)	(0.6,0.9)

Solution:

Step1: convert fuzzy number into crip number by using this formula

$$S(\ ,^+) = \frac{\sum_{=1}.^2().^2_+()+^2().^2_+()}{\sum_{=1}\left[\left(^4() \vee^4_+()\right)+\left(^4() \vee^4_+()\right)\right]} = \frac{(0.8)^2(1)^2+(0.9)^2(0)^2}{(0.8)^4\vee(1)^4+(0.9)^4\vee(0)^4}$$

= 0.29

	1	**2**	**3**	**4**
A1	0.29	0.39	0.25	0.22
A2	0.16	0.10	0.22	0.15
A3	0.64	0.59	0.02	0.51
A4	0.36	0.44	0.02	0.21

Step2: Verify the balance of the provided problem. Find the lowest cost in each column, then deduct that cost from each cost in the matching column

PERSONS		**JOB**			**PENALTY**
	A	**B**	**C**	**D**	
1	0.13	0.29	0.23	0.7	(0.06)
2	0	0	0.2	0	(0)
3	0.98	0.49	0	0.36	(0.36)
4	0.2	0.34	0	0.06	(0.06)
PENALTY	(0.13)	(0.29)	(0)	(0.06)	

Select the row with the lowest assignment charges in the column (which is 0); the maximum penalty is 0.36. Complete the assignment and mark the expenses in the appropriate row and column.

Step3: again find the penalty

PERSONS		JOBS		PENALTY
	A	B	D	
1	0.13	0.29	0.07	(0.06)
2	0	0	0	(0)
4	0.2	0.34	0.06	(0.14)
PENALTY	(0.13)	(0.29)	(0.06)	

Step4: repeat the same process

PERSONS	JOBS		PENALTY
	A	D	
1	0.13	0.07	(0.06)
4	0.2	0.06	(0.14)
PENALTY	(0.7)	(0.01)	

The optimum assignment is

PERSONS	JOBS	ASSIGMENT COST
A	1	0.29
B	2	0.10
C	3	0.02
D	4	0.29

CONCLUSIONS

The aforementioned examples have effectively illustrated the proposed similarity measure and score function as a possible instrument for resolving the Pythagorean fuzzy sets assignment problem. It is clear from the analysis that using the similarity measure and score function produced more accurate and dependable findings. The innovative score function presented in this paper has the following advantages over the current approaches found in the literature:

(i) A new approach for solving assignments has a straightforward presentation that allows it to greatly reduce the possibility of information loss, as described by Peng & Yang (2016) and Garg's (2017). It is anticipated that there will be some values for which the Peng & Yang (2016) and Garg (2017) scoring functions will not produce meaningful findings.

(ii) We have also noticed that the score values of the cell (2,2) representing (iii) the diversity and fuzziness of the decision maker's assessment information can be well reflected and modeled using the suggested similarity measure, which cannot be solved using the score function provided by Garg (2017).

REFERENCES

1. Agheli, B., Adabitabar Firozja, M., Garg, H. (2022), *Similarity measure for Pythagorean fuzzy sets and application on multiple criteria decision making. Journal of Statistics and Management Systems*, 25(4), 749-769; https://e-tarjome.com/storage/panel/fileuploads/2022-08-28/1661661062_e17146.pdf
2. Gurukumaresan, D., Duraisamy, C., Srinivasan, R., Vijayan, V. (2020), *Optimal solution of fuzzy assignment problem with centroid methods. Materials Today: Proceedings*, 37, 553-555;https://www.dl.begellhouse.com/journals/52034eb04b657aea,468587191a97aaba,6532277240021d5f.html

3. Kumar, G., & Bajaj, R. K. (2014). *On solution of interval valued intuitionistic fuzzy assignment problem using similarity measure and score function*. *International Journal of Mathematical and Computational Sciences*, *8*(4), 715-720 https://core.ac.uk/download/pdf/211918891.pdf
4. Peng, X., Yang, Y. (2016), *Fundamental properties of interval-valued Pythagorean fuzzy aggregation operators. International Journal of Intelligent Systems,* 31(5), 444-487;https://www.deepdyve.com/lp/wiley/fundamental-properties-of-interval-valued- pythagorean-fuzzy-FEX4KBdA3b
5. Zadeh, L. A. (1965), *Fuzzy sets. Information and Control,* 8(3), 338-353https://www.sciencedirect.com/science/article/pii/S001999586590241X
6. Dernoncourt, F. (2013). Introduction to fuzzy logic. Massachusetts Institute of Technology, 21https://www.researchgate.net/publication/267041266_Introduction_to_fuzzy_logic
7. Rao, S. S., &Srinivas, M. (2016). An Effective Algorithm to Solve Assignment Problems: Opportunity Cost Approach. International Journal of Mathematics and Scientific Computing, 6,https://demovtu.veltech.edu.in/wp-content/uploads/2016/04/Paper-10-2016.pdf
8. Srinivasan, A., & Geetharamani, G. (2013). Method for solving fuzzy assignment problem. Applied Mathematical Sciences, 7(113), 5607-5619 https://iaeme.com/MasterAdmin/Journal_uploads/IJARET/ VOLUME_11_ISSUE_2/IJARET_11_02_034.pdf
9. Srinivasan, R., Nakkeeran, T., & S aveetha, G. Evaluation of fuzzy non-preemptive priority queues in intuitionistic pentagonal fuzzy numbers using centroidal approach. https://iaeme.com/Home/article_id/IJARET_10_01_041
10. Taha, H. A. (2013). Operations research: an introduction. Pearson Education India http://zalamsyah.staff.unja.ac.id/wp-content/uploads/sites/286/2019/11/9-Operations-Research- An Introduction-10th-Ed.-Hamdy-A-Taha.pdf
11. Thakre, T. A., Chaudhari, O. K., & Dhawade, N. R. (2018). Placement of staff in LIC using fuzzy assignment problem. International Journal of Mathematics Trends and Technology (IJMTT), 53(4), 259-266.[11] Thiruppathi, A., & Iranian, Dhttps://ijmttjournal.org/archive/ijmtt-v53p532

Indian Journal of Natural Sciences *www.tnsroindia.org.in ©IJONS*

Vol.15 / Issue 88 / Feb / 2025 *International Bimonthly (Print) – Open Access* *ISSN: 0976 – 0997*

RESEARCH ARTICLE

Assessing Seed Germination of Kalanamak Rice Varieties under Saline Conditions: A Comparative Study

Omisha Kannaojiya [1] and Kumari Sunita[2]*

[1]Research Scholar, Department of Botany, Deen Dayal Upadhyaya Gorakhpur University, Gorakhpur, Uttar Pradesh, India.
[2]Assistant Professor, Department of Botany, Deen Dayal Upadhyaya Gorakhpur University, Gorakhpur, Uttar Pradesh, India

Received: 21 Nov 2024 Revised: 03 Dec 2024 Accepted: 03 Jan 2025

***Address for Correspondence**
Kumari Sunita
Assistant Professor,
Department of Botany,
Deen Dayal Upadhyaya Gorakhpur University,
Gorakhpur, Uttar Pradesh, India
E.Mail: ksunita78@gmail.com

ABSTRACT

Salinity is one of the socio-economic issues that affects the plant most. It is a global concern as it decreases crop productivity. Kalanamak rice is the prestigious heritage of Uttar Pradesh, known for its unique aroma. This study investigates the impact of salinity stress on the germination parameters of four varieties of Kalanamak rice:Bauna Kalanamak 102, Bauna Kalanamak 101, Kalanamak KN3,and Kalanamak Kiran. There were five treatments with four different concentrations of NaCl (100,200,300, and 400 mM), including a control one. The outcomes showed that Kalanamak Kiran has performed better than the other varieties at every NaCl concentration. After 200 mM NaCl, all varieties showed a significant decline in seed vigour index, germination rate index, and germination percentage. Additionally, the mean germination time rose as salinity levels rises. These results underline the potential of Kalanamak Kiran for cultivation in saline-prone areas and highlights the differences in salt tolerance between Kalanamak rice varieties.

Keywords: Kalanamak Rice, NaCl, Mean germination time, Germination Percentage , Seed Vigour Index

INTRODUCTION

Rice is among the most crucial staple food crops globally, according to World Economic Forum report indicates that 85% of the world's rice production is concentrated in only 10 countries. India is second most largest producer in the world after China. As a staple food, rice is a key part of the diet for more than half of the world's population.

Kalanamak rice is one of the ancient aromatic rice of India. It is grown near the terai region of UP like Siddharth nagar, Basti, Gonda, Gorakhpur. It is popularly known as lord Buddha's gift to the people. Previously there were four varieties of kalanamak rice but now two new variety has been published by the Indian agriculture research institute (IARI) which are Pusa Narendra Kalanamak 1638 and Pusa Narendra Kalanamak 1652. Abiotic stress are the environmental factors which affects the plant most. One of the abiotic factors impacting rice production and growth globally is salinity. In the rice germination, vegetative and reproductive stages are the most crucial one that significantly affect salinity. After droughts salinity is one of the abiotic stresses that lowers rice productivity (Mohammed *et.al* 2007) Salinity affects 20% of the total farmed land and about 50% of the irrigated areas (Devkota et al., 2015). Even with salinity levels of 3 dS/m, which can result in a 10% yield loss, a noticeable reduction in yield is evident. Under moderate saline conditions, this reduction can escalate to as much as 50% (Umali, 1993). Soil salinity has a direct impact on the biochemical, physiological, anatomical, and morphological characteristics of plants. Plants can be classified as either halophyte or glycophyte in terms of their responses to salinity stress. are Plants like halophytes capable of tolerating relatively high levels of salt, such as 400 mM NaCl, while glycophytes are adapted to withstand only lower salt concentrations (Maas & Nieman, 1978).In plants, salt stress has both ionic and osmotic effects, resulting in membrane disorganization, metabolic toxicity, and the production ofhydrogen peroxide (H2O2) as a reactive oxygen species (ROS), can cause oxidative damage (Halliwell, 1987; Chaparzadeh *et al*., 2004).Rice is primarily affected by salt injury during the germination, vegetative, and reproductive stages (Pradheeban *et al.,* 2014;

Anshori *et al*., 2018).The seed germination stage is seen more tolerant of saline stress than the vegetative and reproductive stages are (Singh and Flowers,2010).The initial stage of seed germination involves water absorption through imbibition, a process that can be affected by high salt concentrations in the water, leading to ion toxicity within the seed (Levitt, 1980). Recent research has shown that, in saline conditions, the imbibition rate has a negative correlation with seed germination. Imbibition may be reduced to increase seed germination. Germination is a crucial phase in the lifecycle of many plants, and tolerance to salt during this period is essential for successful establishment (Maranon *et al.,* 1989).Germination is an important stage in the life of many plants, and salt tolerance during this stage is critical for establishment (Maranon *et al*., 1989).The capacity for germination under saline conditions varies between different crops and among various varieties of the same crop. Additionally, salt stress is a significant impediment to seed germination in many plants, often more so than at other growth stages.Heenan *et al*.(1988) found that rice is highly susceptible to the negative effects of salinity during its early growth stages, including germination, immature seedling development, and early development. Salinity can negatively affect seed germination through two primary mechanisms. The first is osmotic stress, where high salt concentrations outside the seed make it difficult for the seed to absorb water. The second is ion toxicity, where excessive ions are absorbed by the seed, disrupting essential embryonic processes.

MATERIALS AND METHODS

The present investigation was conducted at the Plant physiology and PGPR laboratory of DDU Gorakhpur University, Gorakhpur. For this experiment four varieties of kalanamak rice has been taken i.e Kalanamak KN3, Bauna Kalanamak 101, Bauna Kalanamak 102, Kalanamak KIRAN.Seeds of kalanamak rice were obtained from Participatory rural development foundation (PRDF) Gorakhpur. The seeds were germinated in sterile Petri dishes with a 120 mm diameter. Every Petri dish was cleaned with tap water, rinsed with distilled water, and then heated to 120°C for 15 minutes in a hot air oven to sterilise it.Three replications of a completely randomised block design were used to assemble the Petri dishes. Each Petri dish with double-layer Whatman paper held 20 seeds in total. In order to manage fungal infection during germination, seedlings of kalanamak rice were surface sterilised for one minute using 0.1% $HgCl_2$ (Ramakrishna *et al.,* 1991). After draining and thrice rinsing with distilled water, the seeds were left to continue germination in the dark on moist double-layer new Whatman paper. Ten millilitres of the suitable solution or NaCl (100, 200, 300, and 400 mM) was then poured to each Petri dish (Asgharipour and Rafici, 2011). As a control, distilled water was utilised. For fifteen days, the Petri dishes were stored. Every day during this time, the Petri dishes were monitored. Five millilitres of distilled water were added to the Petri dishes every day. The

following formula is used to calculate the mean germination time, germination percentage(%), germination index, and seed vigour index.

Mean germination time

Abnormal germination was characterized by seedlings exhibiting stunted main root development. Following the criterion established by Goertz and Coons(1989), a seed was considered germinated when its radicle reached a length of 10 mm. Germination rate was assessed using the mean germination time. MGT was calculated using the formula outlined by Ellis and Roberts (1981): MGT = (Dn)/n, where 'D' represents the day of counting and 'n' represents the number of seeds germinating on that day. It's important to note that cotyledon weights were excluded from both fresh and dry weight comparisons.

Germination index

As stated by the Association of Official Seed Analysts (AOSA, 1983), the following formula was used to determine the Germination Index (GI):

$$GI = \frac{[\text{Number of Germinated seeds in first count}]}{\text{Days of first count}} + \ldots\ldots + \frac{\text{seeds in finalcount}]}{\text{Days of first count}}$$

Germination percentage

Seed germination was monitored daily in accordance with the Association of Official Seed Analysts Handbook(AOSA, 1990) for seedling evaluation. Germination counts were taken at 24-hour intervals. Germination percentage was determined 20 days after the start of the germination period. Following the methods of Cokkizgin and Cokkizgin and Tanveer *et al.*(2010), GP was calculated by dividing the number of germinated seeds in each Petri dish by the total number of seeds initially placed in the dish and multiplying the result by 100.

Seed vigour index

In accordance with Baki and Anderson (1973), the seed vigour index (SVI) was computed as follows:
SVI = [GP (%) x Seedling length (cm)]

Statistical analysis

The study employed a complete randomised block (CRD) design with three replicates. The data were analysed using the Statistical Analysis System software SPSS 16.0 for analysis of variance. Treatment means were deemed significantly different at $p < 0.05$. The Least Significant Difference (LSD) test was used to evaluate mean separation (Duzgunes*et al.,* 1983).

RESULTS AND DISCUSSION

Effect of NaCl on mean germination time

The complicated process of germination involves a variety of biochemical and physiological modifications that activate the embryo. Salinity during seed germination results in a number of issues.First, it reduces water imbibition due to the medium's lower osmotic potential (Munns & Tester, 2008) and second, it causes nutrient imbalances and toxicity (Rajendran et al., 2009). Salinity induced by NaCl significantly impacts the germination percentage of Kalanamak rice seeds. Analysis of the data presented in Figure 1 indicates that the Kalanamak Kiran variety demonstrates superior germination rates compared to the other three varieties studied. While all varieties exhibit satisfactory germination up to a 200 mM concentration of NaCl, their germination percentages decline sharply at 300 mM and 400 mM concentrations. Notably, Kalanamak Kiran maintains a relatively higher germination percentage under these elevated salinity conditions compared to the other varieties. The highest germination percentage observed under control conditions was 98.33% for the Kalanamak 101 variety. For a 100 mM NaCl concentration, the

highest germination rate was 98.33%, achieved by the Kalanamak KIRAN variety. At 200 mM NaCl, both Kalanamak 101 and Kalanamak KIRAN varieties exhibited a germination percentage of 98.33%. Under a 400 mM NaCl concentration, the Kalanamak KIRAN variety maintained the highest germination rate at 81.66%. Conversely, the lowest germination percentage under control conditions was 93.33% for the Kalanamak 102 variety. At a 100 mM NaCl concentration, Kalanamak KN3 had the lowest germination rate of 91%. For 200 mM NaCl, Kalanamak KN3 exhibited a germination rate of 91.66%. At 300 mM NaCl, both Kalanamak 101 and Kalanamak KN3 has showed the lowest germination percentage of 80%. Finally, at 400 mM NaCl, the lowest germination rate was 36.66%, observed in the Kalanamak KN3 variety. Kaymakanova (2009) investigated the impact of salinity on bean germination, concluding that increased salinity levels impede germination primarily through osmotic stress, which inhibits water uptake, and ion toxicity. Similarly, Wu et al. (2015) examined the effects of salinity on sunflower seeds and found that exposure to 200 mmol NaCl (approximately 12 dS/m) resulted in a 23% reduction in the germination rate index compared to the control group.

Effect of NaCl on germination rate index (GI)

Salinity stress can significantly inhibit seed germination and reduce the germination index, a measure of the speed and uniformity of seed germination. The results indicate that the germination rate index decreases as the concentration of NaCl increases. Figure 2 demonstrates that the Kalanamak Kiran variety exhibits superior germination rates compared to the other three varieties studied. Specifically, the germination rate index at 400 mM NaCl is 3.72, compared to 6.061 in the control for the Kalanamak Kiran variety.Similar studies corroborates these findings. Dehnavi et al. (2020) reported that in sorghum, increasing salinity from 100 mM NaCl to 200 mM NaCl reduced the germination index by over 50%. Siddig et al. (2014) found that in chickpea, 100 mM NaCl reduced the germination index by 30% compared to the control, while 200 mM NaCl reduced it by over 80%. Tarchoun et al. (2022) observed that in squash landraces, the germination index decreased by 60-90% under 100-300 mM NaCl stress compared to non-saline conditions.

Effect of NaCl on mean germination time

Salinity reduces the germination rate and increases the mean germination time (MGT) of rice seeds, as elevated NaCl levels consistently lead to increased MGT. The results indicate that the Kalanamak Kiran variety exhibits the best mean germination time among the four varieties studied. Specifically, the MGT for the Kalanamak Kiran variety increased by 71.8% at 400 mM NaCl compared to the control. In the Bauna Kalanamak 101 and Bauna Kalanamak 102 varieties, MGT increased by 79.58% and 76.73%, respectively. The highest increase in MGT was observed in the Kalanamak KN3 variety, which showed a 105.15% increase compared to the control.Numerous studies have shown similar results, indicating that increasing NaCl (salt) levels can significantly delays the MGT of various crop seeds without necessarily affecting the final germination percentage. For instance, Atak *et al*. (2006) found that in triticale, increasing NaCl levels from 5.9 dS/m to 13.2 dS/m progressively increased the MGT by over 15% without altering the final germination percentage. Kaya *et al*. (2008) reported that in chickpea, 100 mM NaCl increased the MGT by 30% compared to the control one, while 200 mM NaCl increased it by over 80%. Muhammad et al. (2005) observed that in squash landraces, the MGT increased by 60-90% under 100-300 mM NaCl stress compared to non-saline conditions.

Effect of NaCl on Seed Vigour Index

Salinity has a significant negative impact on the seed vigour index (SVI) in various crops during seed germination. In the Bauna Kalanamak 102 variety, the SVI decreases from 1542 (control) to 274 (400 mM). Similarly, in the Bauna Kalanamak 101 variety, the SVI decreases from 1195 to 164. The most substantial decrease was observed in the Kalanamak KN3 variety, where the SVI dropped from 2084 to 57.33. Among all the varieties, Kalanamak KIRAN showed relatively better results, with the SVI decreasing from 1757.5 to 349.3. Irik et al. (2024) studied the effects of salinity on pumpkin cultivars and found that SVI decreased in all cultivars with increasing salinity levels. The highest SVI value was observed in the control treatment (1130.12) and the lowest (599.78) at 10 EC salinity.The Develi cultivar exhibited SVI values ranging from 1425.7 to 620, while the Urgupcultivar showed a range of 1099.6 to 656.8. The Hybrid cultivar had the lowest range, spanning from 865 to 522.5. These findings align with previous research on salinity's impact on seed vigour. Irik*et al*. (2024) observed a similar trend in pepper, where increasing salinity levels

corresponded to a decrease in SVI. Specifically, their study found the highest SVI in the control group (0 mM NaCl) and the lowest SVI in the highest salinity treatment (200 mM NaCl). Rajabi *et al*. (2020)further confirmed this relationship in their work on sorghum genotypes, noting a significant reduction in SVI across all genotypes exposed to salinity. This reduction in seed vigour can be attributed to the osmotic and pseudo-drought stress induced by high concentrations of Na+ and Cl- ions in the growth medium. These ions hinder water uptake by plant tissues, ultimately impairing seed viability."

CONCLUSION

Salinity is a significant abiotic stressor that negatively impacts seed germination across many crop species. Rice, in particular, exhibits relatively high tolerance to salinity during germination compared to other crops, though different varieties display varying levels of tolerance. As the result suggests NaCl levels exceeding 200 mM can significantly reduce the germination percentage in all the four varieties of Kalanamak rice. High salinity decreases the osmotic potential of the soil, leading to reduced water uptake by seeds during imbibition, which inhibits or delays germination. The results indicate that Kalanamak KIRAN is more tolerant to salinity than other Kalanamak rice varieties. As NaCl concentration increases, the mean germination time of seeds increases and the germination index decreases. Understanding the effects of salinity on rice is crucial for developing strategies to enhance crop productivity in saline environments. High concentrations of NaCl in the germination medium create an osmotic potentialthat hinders the ability of rice seeds to imbibe water (Li et al., 2022; Kumar et al., 2021). Excess sodium (Na+) and chloride (Cl-) ions from NaCl can be toxic to the rice embryo and endosperm tissues. Salinity induces the generation of reactive oxygen species (ROS), which can damage cellular components and biomolecules in the rice embryo and endosperm (Li et al., 2022; Sohn et al., 2021). ROS can cause lipid peroxidation, protein denaturation, and DNA damage, leading to reduced germination and seedling vigour. In conclusion, salinity stress significantly affects the germination index of rice seeds by inhibiting seed germination, reducing seedling growth, and influencing genetic traits. Addressing these impacts through targeted strategies is essential for improving the resilience and productivity of rice crops in saline conditions.

Statement and declarations

Funding

This research received no specific grant from any funding agency in the public, commercial, or not-for-profit sectors.

Authors Contribution

OK conducted the literature review and data analysis. KS conceptualized the study and contributed to manuscript drafting.

Conflicts of interest

The authors affirm that their work is free from any influence due to conflicts of interest.

REFERENCES

1. Mohammed, A. R., Mathews, R. B., & Van Oosterom, E. J. (2007). Modelling the impact of salinity and drought stresses on rice growth and yield. Agricultural Water Management, 88(1-3), 57-66.
2. Devkota, K. P., McDonald, A. J., Khadka, L., Khadka, A., Paudel, G., Devkota, M., & Siddiqui, S. (2015). Fertilizers, hybrids, and the sustainable intensification of maize systems in the rainfed mid-hills of Nepal Agricultural Systems, 138, 29-37.
3. Umali, D. L. (1993). Irrigation-induced salinity: A growing problem for development and the environment. World Bank Technical Paper No. 215. The World Bank.

4. Maas, E. V., & Nieman, R. H. (1978). Physiology of plant tolerance to salinity. In G. A. Jung (Ed.), Crop tolerance to suboptimal land conditions(pp. 277-299). American Society of Agronomy.
5. Halliwell, B. (1987). Oxidative damage, lipid peroxidation and antioxidant protection in chloroplasts. Chemistry and Physics of Lipids, 44(2-4), 327-340.
6. Chaparzadeh, N., D'Amico, M. L., Khavari-Nejad, R. A., Izzo, R., & Navari-Izzo, F. (2004). Antioxidative responses of Calendula officinalis under salinity conditions. Plant Physiology and Biochemistry, 42(9), 695-701.
7. Pradheeban, L., Thavaprakash, N., &Tharshiny, V. (2014). Salinity tolerance in rice: Focus on high yield characteristics at seedling stage. Journal of Agricultural Sciences, 9(1), 29-41.
8. Anshori, M. F., Safitri, H., & Hadiati, S. (2018). Evaluation of salinity stress response at seedling stage in rice. Indonesian Journal of Agricultural Research, 21(1), 10-20.
9. Singh, A. K., & Flowers, T. J. (2010). The physiology and molecular biology of the effects of salinity on rice. Critical Reviews in Plant Sciences*, 29(6), 381-409.
10. Chakraborty, K., Bhaduri, D., Meena, H. N., &Kalariya, K. (2016). External potassium (K+) application improves salinity tolerance by promoting ion homeostasis, osmotic adjustment and antioxidant defense system in contrasting peanut genotypes. *Plant Physiology and Biochemistry, 103, 143-153.
11. Levitt, J. (1980). Responses of Plants to Environmental Stresses: Water, Radiation, Salt, and Other Stresses. Academic Press.
12. Maranon, T. Garc, A.L. and Troncoso, A. (1989). Salinity and germination of annual Melilotus from the Guadalquivir delta (SW Spain). Plant and Soil, 119, 223-228.
13. Heenan, D.P., Lewin, L.G., & McCaffery, D.W. (1988). Salinity tolerance in rice varieties at different growth stages. Australian Journal of Experimental Agriculture, 28(3), 343-349.
14. Ramakrishna, A., Rao, P.S., & Reddy, A.R. (1991). Effect of seed treatments on the germination and seedling growth of sorghum under salinity stress. Seed Science and Technology, 19(1), 107-117.
15. Asgharipour, M.R., & Rafici, M. (2011). Effect of salinity on germination and seedling growth of lentil (Lens culinaris Medik). Journal of Applied Sciences Research, 7(11), 1330-1333.
16. Goertz, S., & Coons, J.M. (1989). Germination and early seedling growth of several tree species in relation to moisture stress. Canadian Journal of Forest Research, 19(7), 1013-1017.
17. Association of Official Seed Analysts. (1990). Rules for Testing Seeds. Journal of Seed Technology, 12, 1-112.
18. Cokkizgin, A., &Cokkizgin, H. (2010). Effects of salt stress on germination and seedling growth of some lentil (Lens culinaris Medik.) varieties. World Applied Sciences Journal, 11(4), 540-544.
19. Tanveer, A., Tasneem, M., Khaliq, A., Javaid, M.M., & Chaudhry, M.N. (2010). Influence of seed size and ecological factors on the germination and emergence of field bindweed (Convolvulus arvensis). Weed Biology and Management, 10(1), 18-24.
20. Abdul-Baki AA, Anderson JO. Vigour determination of soybean seed by multiplecriteria.*Crop Science*.1973; 13: 630 – 633. doi: 10.2135/cropsci1973.0011183X00130006013x
21. Düzgüneş, O., Kesici, T., Kavuncu, O., & Gürbüz, F. (1983). Statistical Methods in Research. Ankara University Faculty of Agriculture Press.
22. Munns, R., & Tester, M. (2008). Mechanisms of salinity tolerance. Annual Review of Plant Biology, 59, 651-681.
23. Rajendran, K., Tester, M., & Roy, S.J. (2009). Quantifying the three main components of salinity tolerance in cereals. Plant, Cell & Environment, 32(3), 237-249.
24. Kaymakanova, M. (2009). Impact of salinity on bean (Phaseolus vulgaris L.) seed germination. Bulgarian Journal of Agricultural Science, 15(6), 536-541.
25. Wu, G., Liu, S., Zhao, Y., Wang, W., Kong, Z., & Tang, D. (2015). Effects of salinity on sunflower (Helianthus annuus L.) seed germination and seedling growth. Agricultural Water Management, 159, 335-344.
26. Dehnavi, M.M., Malakouti, M.J., &Afyuni, M. (2020). Effects of salinity stress on germination indices of sorghum (Sorghum bicolor L.). Journal of Plant Nutrition, 43(11), 1714-1724.
27. Siddig, K., Hameed, K.M., Ibrahim, A.M.H., & Quick, J.S. (2014). Response of chickpea (Cicer arietinum L.) genotypes to salinity stress. Agricultural Water Management, 146, 166-172.

28. Tarchoun, N., Serret, M.D., Bouzid, S., Araus, J.L., &Lachaal, M. (2022). Germination responses of squash landraces under saline conditions. Journal of Agronomy and Crop Science, 208(1), 100-110.
29. Atak, M., Çikili, Y., Korkmaz, H., & Turgut, K. (2006). Effect of salinity on seed germination of triticale (×TriticosecaleWittmack). Journal of Agronomy and Crop Science, 192(6), 444-450.
30. Kaya, M.D., Okçu, G., Atak, M., Çikili, Y., &Kolsarıcı, Ö. (2008). Seed treatments to overcome salt and drought stress during germination in sunflower (Helianthus annuus L.). European Journal of Agronomy, 28(1), 62-69.
31. Muhammad, A., Ibrahim, Y., Ibrahim, S., & Khaliq, A. (2005). Influence of salinity on seed germination and early seedling growth of squash landraces. Pakistan Journal of Botany, 37(2), 341-349.
32. Irik, E., Öztürk, L., & Türkan, İ. (2024). Effects of salinity stress on seed vigour index in wheat (Triticum aestivum L.) cultivars. Plant Physiology and Biochemistry, 174, 114-122.
33. Rajabi, A., Amiri, R., Mohammadi, M., & Shafiei, S. (2020). Effects of salinity stress on seed vigour index in sorghum (Sorghum bicolor L.) genotypes. Journal of Plant Nutrition, 43(7), 969-978.
34. Li, H., Wang, Y., Liu, X., & Zhang, H. (2022). Impact of NaCl stress on water imbibition and seedling development in rice (Oryza sativa L.). Journal of Plant Physiology, 273, 153275.
35. Kumar, A., Khan, M.M.A., Jahan, M.S., & Khatun, S. (2021). Effects of salt stress on rice (Oryza sativa L.) seed germination and seedling growth parameters. Journal of Crop Science and Biotechnology, 24(3), 187-196.
36. Sohn, E.J., Kang, K., Huh, Y.S., & Lee, S.C. (2021). Salinity-induced oxidative stress and antioxidant defence mechanisms in rice embryos. Plant Growth Regulation, 93(2), 245-257.

Table 1: Summary of analysis of variance for all the analyzed parameter.(p < 0.05)

	Source of variations	Df	Mean of Square			
			Varitеis of Kalanamak rice			
			V1	**V2**	**V3**	**V4**
GP	NaCl	4	426.667	237.500	1819.167	165.000
	Error	10	76.667	8.333	51.667	23.333
	LSD value		15.929	5.251	13.076	439.889
GRI	NaCl	4	1.678	1.977	4.996	2.213
	Error	10	.177	.040	.169	.073
	LSD value		0.765	0.363	0747	139.97
MGT	NaCl	4	.842	.572	.436	.777
	Error	10	.067	.020	.057	.068
	LSD value		0.470	0.257	0.434	0.474.06
SVI	NaCl	4	844431.983	593201.817	1927415.567	1099042.233
	Error	10	58464.617	5920.167	68764.867	11061.067
	LSD value		439.889	139.979	477.067	191.335

Table 2: Showing Germination percentage in four varieties of Kalanamak rice. V1- Bauna Kalanamak 102, V2- Bauna Kalanamak 101, V3- Kalanamak KN3, V4- Kalanamak KIRAN (Mean ±Standard deviation).(RSD -Relative Standard Deviation)

		GP						
	V1		V2		V3		V4	
	AVG	RSD	AVG	RSD	AVG	RSD	AVG	RSD
CONTROL	93.33333 ±7.637626	0.000818	98.33333 ±2.88675	0.000294	96.66667 ±	0.00029 9	96.66667±2.886751	0.00029 9

			1		2.886751			
100mM	93.33333± 7.637626	0.000818	96.66667 ±2.886751	0.000299	91.66667 ± 10.40833	0.001135	98.33333±2.886751	0.000294
200 mM	93.33333± 2.886751	0.000309	98.33333 ±2.886751	0.000294	91.66667 ±7.637626	0.000833	98.33333±2.886751	0.000294
300 mM	80±5	0.000625	86.66667 ±2.886751	0.000333	80± 5	0.000625	88.33333±7.637626	0.000865
400 mM	66.66667± 15.27525	0.002291	78.33333 ±2.886751	0.000369	36.66667 ± 7.637626	0.002083	81.66667±5.773503	0.000707

Table 3: Showing Germination Rate Index in four varieties of Kalanamak rice. V1- Bauna Kalanamak 102, V2- Bauna Kalanamak 101, V3- Kalanamak KN3, V4- Kalanamak KIRAN (Mean ±Standard deviation)(RSD -Relative Standard Deviation)

		Gri						
	V1		V2		V3		V4	
	AVG	RSD	AVG	RSD	AVG	RSD	AVG	RSD
CONTROL	5.033333± 0.594652	0.001181	6.066667± 0.169148	0.000279	5.6 ±0.231541	0.231541	6.061111± 0.26684	0.00044
100mM	4.361508± 0.485761	0.001114	5.25119± 0.071696	0.000137	4.786243 ±0.471476	0.471476	5.306349± 0.139023	0.000262
200 mM	4.637037± 0.093198	0.000201	4.950529± 0.315951	0.000638	4.835317 ±0.408528	0.408528	5.099735± 0.255158	0.0005
300 mM	4.146825± 0.055855	0.000135	4.501984± 0.144442	0.000321	4.171429 ±0.338102	0.338102	4.700794± 0.353219	0.000751
400 mM	3.045238± 0.531048	0.001744	3.901984± 0.216462	0.000555	2.194444 ±0.536536	0.536536	3.721958±	0.000791

Table 4: Showing Mean Germination Time in four varieties of Kalanamak rice. V1- Bauna Kalanamak 102, V2- Bauna Kalanamak 101, V3- Kalanamak KN3, V4- Kalanamak KIRAN (RSD -Relative Standard Deviation) (Mean ±Standard deviation).

		MGT						
	V1		V2		V3		V4	
	AVG	RSD	AVG	RSD	AVG	RSD	AVG	RSD
CONTROL	4.240764± 0.158067	0.000373	3.726316± 0.162136	0.000435	3.930702± 0.132636	0.000337	3.62193± 0.100564	0.000278
100mM	5.155831± 0.322195	0.000625	4.25614± 0.181204	0.000426	4.527632± 0.465226	0.001028	4.249123± 0.329077	0.000774
200 mM	5.263158± 0.455803	0.000866	4.814912 ±0.102	0.000212	4.486928± 0.186618	0.000416	4.483333 ±0.419325	0.000935
300 mM	5.526316±	1.97E-18	4.594771	0.00015	4.540359±	0.000176	4.293494	0.00047

	1.09E-15		±0.06886		0.079732		±0.201898	
400 mM	5.526316± 5.526316	1.97E-18	4.681944 ±0.162464	0.000347	3.738095± 0.085846	0.00023	5.039216 ±0.067924	0.000135

Table 5 : Showing Seed Vigour Index in four varieties of Kalanamak rice. V1- Bauna Kalanamak 102, V2- Bauna Kalanamak 101, V3- Kalanamak KN3, V4- Kalanamak KIRAN (Mean ±Standard deviation). (RSD -Relative Standard Deviation)

		SVI						
	V1		V2		V3		V4	
	AVG	RSD	AVG	RSD	AVG	RSD	AVG	RSD
CONTROL	1542.667± 113.1838	0.000734	1195.5± 41.11873	0.000344	2084± 214.2714	0.001028	1757.5± 152.888	0.00087
100mM	1278.833± 163.6813	0.00128	1170.5± 88.51695	0.000756	1790± 168.0357	0.000939	1427.333± 119.7553	0.000839
200 mM	891.6667± 487.2428	0.005464	1111± 28.51315	0.000257	1366.5± 295.5956	0.002163	722.6667 ±79.25486	0.001097
300 mM	478± 77.32399	0.001618	672.1667± 137.7283	0.002049	865± 426.8384	0.004935	533.6667 ±60.25225	0.001129
400 mM	274.3333± 96.6247	0.003522	164.5± 17.10994	0.00104	57.33333± 10.40833	0.001815	349.3333 ±87.62182	0.002508

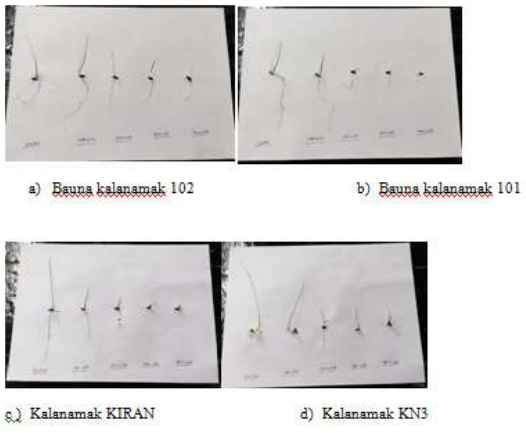

Figure 1. Figure showing seeds of all four varieties of Kalanamak rice under five treatments (Control, 100mM, 200mM, 300mM and 400mM)

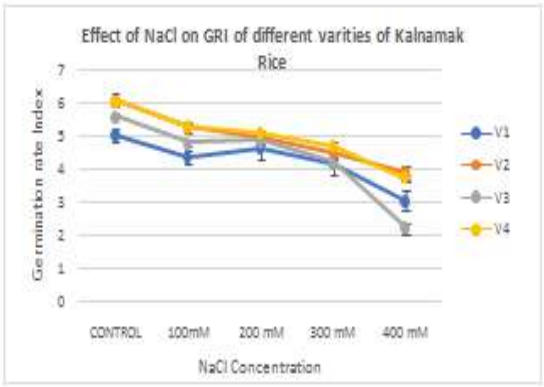

Graph 1 :Showing Germination rate index in four varieties of Kalanamak rice. (.V1- Bauna Kalanamak 102, V2- Bauna Kalanamak 101, V3- Kalanamak KN3, V4- Kalanamak KIRAN

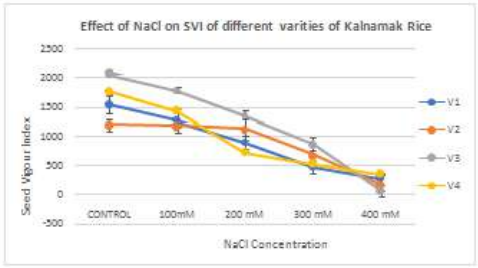

Graph 2 :Showing Seed Vigour Index in four varieties of Kalanamak rice. (.V1- Bauna Kalanamak 102, V2- Bauna Kalanamak 101, V3- Kalanamak KN3, V4- Kalanamak KIRAN

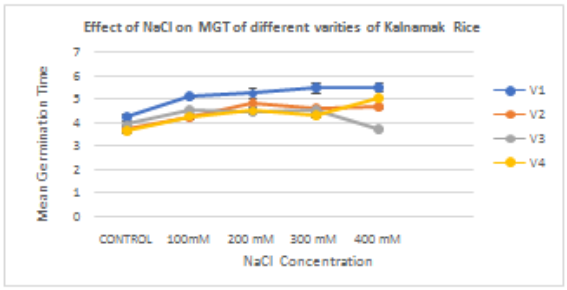

Graph 3 :Showing Mean Germination Time in four varieties of Kalanamak rice. (.V1- Bauna Kalanamak 102, V2- Bauna Kalanamak 101, V3- Kalanamak KN3, V4- Kalanamak KIRAN

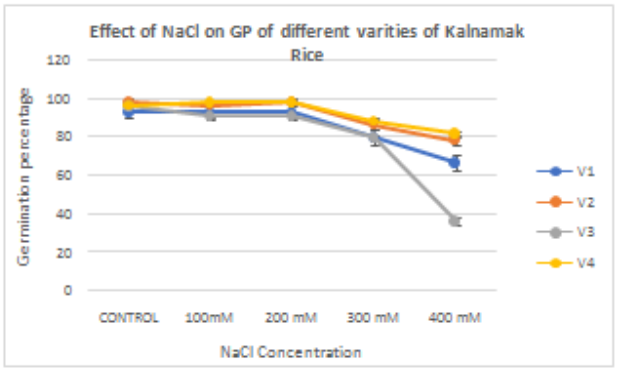

Graph 4 :Showing Germination percentage in four varieties of Kalanamak rice. (.V1- Bauna Kalanamak 102, V2- Bauna Kalanamak 101, V3- Kalanamak KN3, V4- Kalanamak KIRAN

Indian Journal of Natural Sciences www.tnsroindia.org.in ©IJONS

Vol.15 / Issue 88 / Feb / 2025 *International Bimonthly (Print) – Open Access* *ISSN: 0976 – 0997*

RESEARCH ARTICLE

A Study on Barriers of Using Library Resources by the Arts & Science Self Finance Colleges in Kanyakumari District

V. Jeyakala[1] and P.L Beryl[2]

[1]Librarian, Holy Cross College (Autonomous), Nagercoil -4
[2]Counsellor, Holy Cross College (Autonomous), Nagercoil -4

Received: 21 Jun 2024 Revised: 03 Jul 2024 Accepted: 13 Aug 2024

***Address for Correspondence**
V. Jeyakala
Librarian,
Holy Cross College (Autonomous),
Nagercoil -4
E. Mail: jaisteiv@gmail.com

ABSTRACT

Most of the studies analyse only the users and their usage whereas this study attempts to analyse their barriers in library usage. Resources are for use / Documents are for use is the first laws of library science. Without usage library and resources are waste. Therefore the authors tried to find out the reasons for the non usage. First identified the non-users and found out their barriers in using the library print and electronic resources. This study is an appeal to the academic authorities to remodify the curriculum. So that all could avail the library resources.

Keywords: Barriers, non-user, non-usage, resources etc.

INTRODUCTION

"An information system may be used, then, but not be useful; It may be useful, but not used. It may even be neither useful nor used. It is ideal if it is both used and useful: (Kochen, 1976). A non-user of a library is one who has a right to use the library but he does not so over a specific period and/or for a specific sample of collection or transactions. Here we are not concerned with involuntary non-users who unfortunately do not have a library to use, but interested in involuntary or wilful non-users of a given library (Slater, 1984). There are different types of non-users. They are absolute non-users, marginal users, unusual user, etc. Apart from information seekers, non-users are more in colleges.

Origin of the Research Problem

The 47thAslib annual Conference deliberation is that the need for "exploration of the un-served who they are, what they need, how to reach them, and who is to reach them". Gross (1974) emphasized the deprived users and their

information malnutrition especially among practitioners like doctors, dentists, teachers etc., and the negligence of library system.

Interdisciplinary Relevance

Barriers of usage of library resources are not only a library science but education oriented. The educational curriculum does it motivate the students to make use of the library or it is a barrier. Marketing of information, cost benefits etc. are related to this topic. Hence it is a multidisciplinary approach.

Review of Research and Development:

There are a number of related and relevant studies conducted by various experts only more relevant studies' reviews are listed hereunder.

Lawrence Mary (2014) conducted a study on Barriers in using library Resource in Arts and Science Colleges and found out that the university syllabus is the reason for not using the library.

Atherson (1977) had pointed out as a small segment of rightful users of a library really use their library. The numbers of users who have need for information far exceed those actually use information.

Wilson (1977) stated that the ratio of actual users of a library serves as a rough measure of the impact of the library and its market penetration capability. At the same time one should be aware of limitations of user studies, including spillover effect of use, indirect use of a library and various interactions of users with a library.

Grose (1974) suggested that non-users are the groups of people in an affluent society who are never given the means to satisfy their needs, or are geographically cut off from center of provision which are theoretically open to them or are so occupied that even while surrounded by all they need never shop to enjoy it an suffer a form of information malnutrition.

International Status

The process of a user coming in contact with a source of information depends on many factors. In the developed countries usage of information resources may be high but there are huge numbers of non-users. Depending upon their need and the source (library) the users' ratio is determined. Irrespective of caste, creed and colour, the non-usage students are high in number. Mostly they depend upon their PCs and Internet.

National Status

The developing country like India the non-users are high in number. They are not bothered about their need and source (library). The students only depend upon their curriculum and the related books alone. The vast readers, knowledge seekers and researchers need library resources. They are very few whether national or international level.

Significance of the Study

Non-usage of library resources is a common problem faced by all librarians. The library resources have been wasted without proper usage. There may be various reasons for the non-usage. Ignorance of the sources about the sources, dependent on the alternatives available and the degree of interpretedness of the source are some of the reasons for non-usage. The barriers should be identified,testedand rectified through proper recommendations to the concern. Therefore the researcher has stated the problem to undergo this study.

Objectives

The objectives framed for the study are:

1. To identify the non-users among the library members in Arts and Science Colleges.
2. To trace out the barriers for the non-usage and
3. To recommend and suggest the ways to reduce the non-usage of library resources.

Hypothesis

There is no significant difference between the barriers among the students based on discipline, locality, area and economic status.

Methodology

The researcher visited all the Self finance Arts and Science Colleges in Kannyakumari District to collect the basic data about the users and the non-users. Then the researcher designs a questionnaire on the basis of the objectives. Systematic random sampling will be followed to collect data. The researcher visited in person to collect data from the non-users. Separate questionnaire for the users and faculty, will also be prepared to identify the barriers. The collected data is coded, edited, tabulated and calculated accordingly.

Data Analysis and Interpretation

There are 11 self finance Arts& Science Colleges in Kanyakumari District. The total population of the study is 13208 excluding scholars. The period of study is 2010-2020. From each college randomly selected 120 students among the non users of the library resources. Only 5% of the students are the library users. 10% of the non library users were selected for the study. The well framed questionnaire was circulated and collected the data. Table 2 depicts the clear picture of the non users visiting the library. Table 3 explains the actual barriers in using the library resources available in the college libraries. Due to the technological explosion most of the students depend upon Internet facility in their cell phones itself. The hypothesis also tested and found out that all the barriers are equally important, hence the null hypothesis is rejected. Table 4 states that they need compulsory Library hour. Even though it is in the time table no one follows in the undergraduate level. Mostly it is applicable to the post graduate and research scholars alone. The authorities should take necessary steps to implement the suggestion so that the non users ratio will be reduced. Non-users ratio will be reduced. The Librarians should follow the ethics of librarianship. The faculty members also teach them the value of books, journals and current affairs so that they could withstand in life. Proper motivation and orientation to the freshers are more important than any one. To encourage them by giving prizes for the maximum users of the library resources either print or electronic sources.

CONCLUSION

The researchers should pay more attention in finding out the gap between users and non users. It is very dangerous in the education system so that our future generation will not enter into the library building. Internet provides all data, information in their hand through computer or cell phone. Lakhs and lakshs of money is spent to the library sources but the result is very poor. The librarians prepare a budget but what is the status of available sources should be studied and analysed systematically. Proper immediate steps should be taken with the support of authorities and co operation of teachers.

REFERENCES

1. Flowers, L (1995). Non-user of the upper Goldbum library service. *The Australian Library Journal, (67-85)*.
2. Harris, C. (1984) . Studying the non-user. In: the use of information in aChanging world: Proceedings of the forty-second FID Congress hels at the Hauge, the Netherlands, 24-27 September, 1984. Ed. By A. Van Derbaan and A.A. Winters Amsterdam: North-Holland, 1984, p. 69-75.
3. Lange, J.M. (1988). Public library users, non- users , and type of library use. *Public Library Quarterly,* 8(1/2), 49-67.
4. Lubans, J. (1971). Non-use of an academic library. College and Research Libraries. 32(5), 362-67.
5. Sridar, M. S. (1994). Non-use and non-users of libraries. *Library Science With a Slant documentation and information Studies, 31(3), 115-128.*
6. Strategic Planning and Marketing Cultural Development (2000). Non-user.survey September – October 2000. Coventry Libraries
7. Zweizig, D. &Drevin, B. (1977). Public library use, users, uses: Advances in knowledge of characteristics and needs of the adults clientele of American public libraries. *Advance in Librarianship, 7,* 232-255.

Table 1 Basic data – Sampling

Gender		Arts	Science	Total
Male	Female			
640	680	920	400	1320

Source : Primary data

Table 2 Frequency of visit to the Library

S.No	Frequency of visit	Reason	No. of respondents
1	Twice in a year	Membership	845
2	Once in a year	No dues	1320
3	Once in 3 years	No dues	280

Source: Primary data

Table 3 Distribution of barriers

S.No	Barriers	Responses	Percent
1	Locality	58	4.39
2	Lack of time	76	5.75
3	Laziness	45	3.40
4	No need Reference	94	7.12
5	Personal own books	46	3.48
6	Don't know the importance	22	1.66
7	No one motivated	47	3.56
8	Do not know how to use	34	2.57
9	No need for Exam	142	10.75
10	Only for Clever	62	4.69
11	Not in the curriculum	230	17.42
12	Waste of time	18	1.36
13	Gender problem	34	2.57
14	Required books not available	76	5.75
15	Library staff very strict	36	2.72
16	Available in Internet	300	22.72
	Total	1320	100

Source: Primary data

Table 4 Suggestions to rectify the problems

S.No	Suggestions	Responses	Percentage
1	Proper motivation	208	15.75
2	Change in curriculum	72	5.45
3	Classroom Seminars	68	5.15
4	Assignments in general topic	110	8.33
5	Compulsory Competitions	70	5.30
6	Teachers bring themduring library period	210	15.90
7	Library staff cooperation	110	8.33
8	Compulsory library hour	472	35.75
	Total	1320	100

Source: Primary data

Indian Journal of Natural Sciences *www.tnsroindia.org.in ©IJONS*

Vol.15 / Issue 88 / Feb / 2025 *International Bimonthly (Print) – Open Access* *ISSN: 0976 – 0997*

RESEARCH ARTICLE

Biomedical Application and Characterization of Extended Pratibha Distribution

Ravikumar K[1], Thomas Mathew[2] and Prasanth C B[3]*

[1]Associate Professor, Department of Statistics, Government Victoria College, Palakkad, (Affiliated to University of Calicut), Kerala, India.
[2]Principal, Associate Professor and Research Guide, Department of Statistics, M.D. College, Pazhanji, Thrissur, (Affiliated to University of Calicut), Kerala, India.
[3]Assistant Professor, Department of Statistics, Sree Kerala Varma College, Thrissur, (Affiliated to University of Calicut), Kerala. India.

Received: 21 Nov 2024 Revised: 03 Dec 2024 Accepted: 13 Jan 2025

***Address for Correspondence**
Prasanth C B
Assistant Professor,
Department of Statistics,
Sree Kerala Varma College, Thrissur,
(Affiliated to University of Calicut),
Kerala. India.
E.Mail: prasanthwarriercb@keralavarma.ac.in

ABSTRACT

The main objectives of this work are to introduce a new version of Pratibha distribution known as Extended Pratibha Distribution (EPD) and to establish its biomedical significance. Asymmetrical distributions can be derived by using method of weighted distribution modelling. Here a weight function is added with the parent distribution. The characteristics of the distribution are detailed. The formulated distribution has been presented with distinct structural properties like moments, hazard rate function, reliability function and moment generating function. The maximum likelihood estimation approach has also been utilized to find out its parameters. When an investigator records observations in nature using a particular stochastic model, the recorded observations distribution would vary from the original distribution unless each observation has been provided an equal chance of being recorded. Here, the newly implemented concept of distribution known as weighted distributions comes into play, and it is crucial for modelling statistical data arising from various branches of knowledge. As results from classical distributions are insufficient for many datasets, the application of the developed distribution has been demonstrated by fitting a real data set to assess its superiority. The biomedical application is mentioned, by taking birth weight of 130 randomly selected newborn babies from a Hospital in Chennai is noted from January 2023 – June 2024 for the same.

Keywords: Pratibha distribution, hazard rate, weighted distribution, reliability measures, maximum likelihood estimation.

INTRODUCTION

The weight at birth of a normal baby should be anywhere between 2.5 kilograms (kg) and 4.5kg. According to the WHO, the average birth weight of a full-term male baby is 3.3kg and the average birth weight of a full-term female is 3.2 kg. Afterwards a baby will gain from 140 grams to 200 grams per week up till the 6-month mark. Usually boys are a little heavier than girls. In general, first babies are lighter than their siblings. The distribution of birth weight is studied and its characterisation is derived with respect to many probability distributions. The statistical theoretical aspects should be synchronised with reality if they are to be accepted. There are some innovative methods to derive new probability distributions which shows better fit than many conventional distributions. Weighted distributions are incredibly helpful in distribution theory due to the fact that they add a new parameter to the existing distribution.(It is a mere coincidence, that there is no connectivity for the name of the method 'weighed distribution' and the applied variable 'weight') This additional parameter gives more flexibility and superiority to the current distribution's behaviour. We can address the conceptualization of the model stipulation and data representation issues by using the weighted distributions. Weighted distributions are commonly encountered in various fields like clustered sampling modelling, biomedicine, reliability, family data analysis, meta-analysis, ecology, and other domains pertaining to appropriate statistical model development. Numerous scholars have made outstanding contributions and investigated significant weighted probability models and their applications in managing diverse lifetime data sets from multiple applied domains. The new weighted inverse Rayleigh distribution and its application were proposed by Aydin [1]. The weighted inverse Ailamujia distribution has been introduced by Ahmad et al.[2] and applied to real-world data. The Poisson-weighted exponential distribution and a new count data model is introduced by Dar *et al* [3] and applied in the analysis of vaccine adverse events and insurance claims. A new extended Gumbel distribution is derived by Fayomi *et al* [4] and the weighted Ishita distribution was introduced by Hassan et al.[5], along with its properties and uses. The statistical characteristics of the weighted Shanker distribution were introduced by Helal et al[6]. Prabavathi and Elangovan[7] introduced the weighted Shambhu distribution, along with its characteristics and uses. Weighted Pratibha distribution with properties and application in flood dataset detailed by Prodhanii and Shanker[8]. It is an extension of the Pratibha distribution, a newly proposed distribution with only one parameter by Shanker[9]. An extended Suja distribution with statistical properties and applications is derived by Shanker *et al* [10] with weighted distribution method. Numerous statistical characteristics of the suggested distribution have been examined, including the hazard function, moments, etc. The moment and maximum likelihood estimation methods are utilized to find out the proposed distribution parameters.

MATERIALS AND METHODS

Extended Pratibha Distribution (EPD)

The Probability Density Function (PDF) of Pratibha distribution is,

$$f(x;\theta) = \frac{\theta^3}{\theta^3+\theta+2}\left(\theta + x + x^2\right) e^{-\theta x};\ x > 0,\ \theta > 0 \tag{1}$$

and the Cumulative Distribution Function(CDF) of Pratibha distribution is,

$$F(x;\theta) = 1 - \left(1 + \frac{\theta x(\theta x + \theta + 2)}{\theta^3+\theta+2}\right) e^{-\theta x};\quad x > 0,\ \theta > 0 \tag{2}$$

Consider *X* to be a non-negative random variable having PDF $f(x)$. Suppose its non-negative weight function is $w(x)$, then the PDF of the weighted random variable X_w has been provided by

$$f_w(x) = \frac{w(x)\,f(x)}{E(w(x))},\ x > 0.,\ \text{where}\, E(w(x)) = \int w(x)\,f(x)dx < \infty.$$

If the weight function *w(x) = xc, the* following distribution is called weighted distribution. To attain the Pratibha distribution's weighted version- known as EPD, its PDF has been written as

$$f_w(x) = \frac{x^c f(x)}{E(x^c)} \tag{3}$$

Where $E(x^c) = \int_0^\infty x^c f(x)dx$

$$E(x^c) = \frac{\theta^3\Gamma(c+1) + \theta\Gamma(c+2) + \Gamma(c+3)}{\theta^c(\theta^3 + \theta + 2)} \tag{4}$$

Now substituting eqns (1) and (4) in eqn (3), we would get the required PDF of EPD as

$$f_w(x) = \frac{x^c\theta^{c+3}}{\left(\theta^3\Gamma(c+1) + \theta\Gamma(c+2) + \Gamma(c+3)\right)}\left(\theta + x + x^2\right)e^{-\theta x} \tag{5}$$

and the CDF of EPD could be determined as

$$F_w(x) = \int_0^x f_w(x)dx$$

$$= \int_0^x \frac{x^c\theta^{c+3}}{\left(\theta^3\Gamma(c+1) + \theta\Gamma(c+2) + \Gamma(c+3)\right)}\left(\theta + x + x^2\right)e^{-\theta x}dx$$

$$F_w(x) = \frac{1}{\left(\theta^3\Gamma(c+1) + \theta\Gamma(c+2) + \Gamma(c+3)\right)}\left(\theta^{c+4}\int_0^x x^c e^{-\theta x}dx + \theta^{c+3}\int_0^x x^{c+1}e^{-\theta x}dx + \theta^{c+3}\int_0^x x^{c+2}e^{-\theta x}dx\right)$$

Put $\theta x = t \Rightarrow \theta dx = dt \Rightarrow dx = \frac{dt}{\theta}$, Also $x = \frac{t}{\theta}$, As $x \to x,\ t \to \theta x$ and as $x \to 0,\ t \to 0$

Following the above equation's simplification, the CDF of the EPD will be found as

$$F_w(x) = \frac{1}{\left(\theta^3\Gamma(c+1) + \theta\Gamma(c+2) + \Gamma(c+3)\right)}\left(\theta^3\gamma(c+1,\ \theta x) + \theta\gamma(c+2,\ \theta x) + \gamma(c+3,\ \theta x)\right) \tag{6}$$

The asymmetric nature of PDF and the nature of CDF is clear from the Figure 1 and Figure 2 respectively.

RESULTS AND DISCUSSION

The reliability function, reverse hazard rate function and hazard rate function of the weighted Pratibha distribution were acquired in this given section.

Reliability Function

This is also known as the survival function and the reliability function of EPD will be determined as,

$$R(x) = 1 - F_w(x)$$

$$= 1 - \frac{1}{\left(\theta^3\Gamma(c+1) + \theta\Gamma(c+2) + \Gamma(c+3)\right)}\left(\theta^3\gamma(c+1,\ \theta x) + \theta\,\gamma(c+2,\ \theta x) + \gamma(c+3,\theta x)\right)$$

Hazard Function

The force of mortality or hazard rate is another name for the hazard function, which is determined by

$$h(x) = \frac{f_w(x)}{1 - F_w(x)} = \frac{x^c\theta^{c+3}(\theta + x + x^2)\ e^{-\theta x}}{(\theta^3\Gamma(c+1) + \theta\Gamma(c+2) + \Gamma(c+3)) - (\theta^3\gamma(c+1,\ \theta x) + \theta\,\gamma(c+2,\ \theta x) + \gamma(c+3,\ \theta x))}$$

The following figures show the nature of Reliability (Figure 3) and Hazard Rate (Figure 4).

The nature of reliability and the nature of hazard rate is clear from the Figure 3 and Figure 4 respectively.

Likelihood Ratio Test

Suppose the random sample *X1, X2,…., Xn* of size *n* from the Pratibha or weighted Pratibha distribution. To determine its superiority, the hypothesis is to be analyzed.

$H_o : f(x) = f(x;\theta)$ V/s $H_1 : f(x) = f_w(x;\theta,c)$

The given below statistic rule is applied to describe whether the random sample of 'n' size comes from the weighted Pratibha distribution or the Pratibha distribution.

$$\Delta = \frac{L_1}{L_o} = \prod_{i=1}^{n}\frac{f_w(x;\theta,c)}{f(x;\theta)} = \prod_{i=1}^{n}\left(\frac{x_i^{\,c}\theta^c(\theta^3 + \theta + 2)}{\left(\theta^3\Gamma(c+1) + \theta\Gamma(c+2) + \Gamma(c+3)\right)}\right)$$

$$\Delta = \frac{L_1}{L_o} = \left(\frac{\theta^c(\theta^3 + \theta + 2)}{\left(\theta^3\Gamma(c+1) + \theta\Gamma(c+2) + \Gamma(c+3)\right)}\right)^n \prod_{i=1}^{n} x_i^{\,c}$$

We must not retain the null hypothesis, if

$$\Delta = \left(\frac{\theta^c(\theta^3 + \theta + 2)}{\left(\theta^3\Gamma(c+1) + \theta\Gamma(c+2) + \Gamma(c+3)\right)}\right)^n \prod_{i=1}^{n} x_i^{\,c} > k$$

Alternatively, we ought to decline to uphold the null hypothesis, where

$$\Delta^* = \prod_{i=1}^{n} x_i^{\,c} > k\left(\frac{\left(\theta^3\Gamma(c+1) + \theta\Gamma(c+2) + \Gamma(c+3)\right)}{\theta^c(\theta^3 + \theta + 2)}\right)^n, \qquad \Delta^* = \prod_{i=1}^{n} x_i^{\,c} > k^*, \text{Where} k^* = k\left(\frac{\left(\theta^3\Gamma(c+1) + \theta\Gamma(c+2) + \Gamma(c+3)\right)}{\theta^c(\theta^3 + \theta + 2)}\right)^n$$

Whether the $2log\ \Delta$ is distributed as a chi-square distribution with 1 degree of freedom if the sample is large of size *n*

and also chi-square distribution is applied and considers the *p*-value. Therefore, if the probability value is provided, it should be corrected such that the null hypothesis is to be rejected.

$p\left(\Delta^* > \gamma^*\right)$, Where $\gamma^* = \prod_{i=1}^{n} x_i^{\,c}$ is minimum than a particular level of significance and $\prod_{i=1}^{n} x_i^{\,c}$ is the observed value of the statistic Δ^*.

Structural Properties

The EPD's various statistical characteristics, like moments, moment generating function, and characteristic function, will be derived and examined in this section.

Moments

Consider the random variable *X* following EPD with the parameters θ &*c*, then the *rth* order moment *E*(*X r*) of random variable *X* will be determined as

$$E(X^r) = \mu_r' = \int_0^\infty x^r f_w(x)dx = \int_0^\infty x^r \frac{x^c \theta^{c+3}}{\left(\theta^3\Gamma(c+1) + \theta\Gamma(c+2) + \Gamma(c+3)\right)}\left(\theta + x + x^2\right)e^{-\theta x}dx$$

$$E(X^r) = \mu_r' = \frac{\theta^{c+3}}{\left(\theta^3\Gamma(c+1) + \theta\Gamma(c+2) + \Gamma(c+3)\right)}\left(\begin{array}{l}\theta\int_0^\infty x^{(c+r+1)-1}e^{-\theta x}dx + \int_0^\infty x^{(c+r+2)-1}e^{-\theta x}dx \\ \\ +\int_0^\infty x^{(c+r+3)-1}e^{-\theta x}dx\end{array}\right) \quad (7)$$

After the simplification, we obtain from equation (7)

$$E(X^r) = \mu_r' = \frac{\theta^3\Gamma(c+r+1) + \theta\Gamma(c+r+2) + \Gamma(c+r+3)}{\theta^r\left(\theta^3\Gamma(c+1) + \theta\Gamma(c+2) + \Gamma(c+3)\right)} \quad (8)$$

Now by substituting *r* = 1, 2, 3, and 4 in equation (8), attain the required first 4 moments of EPD as,

$$E(X) = \mu_1' = \frac{\theta^3\Gamma(c+2) + \theta\Gamma(c+3) + \Gamma(c+4)}{\theta\left(\theta^3\Gamma(c+1) + \theta\Gamma(c+2) + \Gamma(c+3)\right)},$$

$$E(X^2) = \mu_2' = \frac{\theta^3\Gamma(c+3) + \theta\Gamma(c+4) + \Gamma(c+5)}{\theta^2\left(\theta^3\Gamma(c+1) + \theta\Gamma(c+2) + \Gamma(c+3)\right)}$$

$$E(X^3) = \mu_3' = \frac{\theta^3\Gamma(c+4) + \theta\Gamma(c+5) + \Gamma(c+6)}{\theta^3\left(\theta^3\Gamma(c+1) + \theta\Gamma(c+2) + \Gamma(c+3)\right)},$$

$$E(X^4) = \mu_4' = \frac{\theta^3\Gamma(c+5) + \theta\Gamma(c+6) + \Gamma(c+7)}{\theta^4(\theta^3\Gamma(c+1) + \theta\Gamma(c+2) + \Gamma(c+3))},$$

$$\text{Variance} = \frac{\theta^3\Gamma(c+3) + \theta\Gamma(c+4) + \Gamma(c+5)}{\theta^2(\theta^3\Gamma(c+1) + \theta\Gamma(c+2) + \Gamma(c+3))} - \left(\frac{\theta^3\Gamma(c+2) + \theta\Gamma(c+3) + \Gamma(c+4)}{\theta(\theta^3\Gamma(c+1) + \theta\Gamma(c+2) + \Gamma(c+3))}\right)^2$$

$$S.D(\sigma) = \sqrt{\left(\frac{\theta^3\Gamma(c+3) + \theta\Gamma(c+4) + \Gamma(c+5)}{\theta^2(\theta^3\Gamma(c+1) + \theta\Gamma(c+2) + \Gamma(c+3))} - \left(\frac{\theta^3\Gamma(c+2) + \theta\Gamma(c+3) + \Gamma(c+4)}{\theta(\theta^3\Gamma(c+1) + \theta\Gamma(c+2) + \Gamma(c+3))}\right)^2\right)}$$

Harmonic Mean

The H.M of the introduced EPD will be determined as

$$H.M = E\left(\frac{1}{x}\right) = \int_0^\infty \frac{1}{x} f_w(x)dx = \int_0^\infty \frac{1}{x} \frac{x^c\,\theta^{c+3}}{\left(\theta^3\Gamma(c+1) + \theta\Gamma(c+2) + \Gamma(c+3)\right)} \left(\theta + x + x^2\right) e^{-\theta x} dx$$

$$H.M = \frac{\theta^{c+3}}{\left(\theta^3\Gamma(c+1) + \theta\Gamma(c+2) + \Gamma(c+3)\right)} \left(\theta \int_0^\infty x^{(c+1)-2} e^{-\theta x} dx + \int_0^\infty x^{(c+1)-1} e^{-\theta x} dx + \int_0^\infty x^{(c+2)-1} e^{-\theta x} dx\right) \quad (9)$$

After the simplification of equation (9), we attain

$$H.M = \frac{\theta(\theta^2\Gamma(c+1) + \theta\Gamma(c+1) + \Gamma(c+2))}{\left(\theta^3\Gamma(c+1) + \theta\Gamma(c+2) + \Gamma(c+3)\right)}$$

Moment Generating function and Characteristic Function

If we take the random variable X, from the EPD with the parameters θ & c, the moment-generating function of the suggested model is,

$$M_X(t) = E\left(e^{tx}\right) = \int_0^\infty e^{tx} f_w(x)dx$$

Taylor's series allows us to obtain

$$M_X(t) = \int_0^\infty \left(1 + tx + \frac{(tx)^2}{2!} + \ldots\right) f_w(x)dx = \int_0^\infty \sum_{j=0}^\infty \frac{t^j}{j!} x^j f_w(x)dx = \sum_{j=0}^\infty \frac{t^j}{j!} \mu_j'$$

$$M_X(t) = \sum_{j=0}^\infty \frac{t^j}{j!} \left(\frac{\theta^3\Gamma(c+j+1) + \theta\Gamma(c+j+2) + \Gamma(c+j+3)}{\theta^j(\theta^3\Gamma(c+1) + \theta\Gamma(c+2) + \Gamma(c+3))}\right)$$

$$M_X(t) = \frac{1}{\left(\theta^3\Gamma(c+1) + \theta\Gamma(c+2) + \Gamma(c+3)\right)} \sum_{j=0}^\infty \frac{t^j}{j!\theta^j} \left(\theta^3\Gamma(c+j+1) + \theta\Gamma(c+j+2) + \Gamma(c+j+3)\right)$$

Similarly, the characteristic function of EPD will be determined as

$$\varphi_X(t) = M_X(it)$$

$$M_X(it) = \frac{1}{\left(\theta^3\Gamma(c+1)+\theta\Gamma(c+2)+\Gamma(c+3)\right)} \sum_{j=0}^{\infty} \frac{it^j}{j!\theta^j}\left(\theta^3\Gamma(c+j+1)+\theta\Gamma(c+j+2)+\Gamma(c+j+3)\right) \quad (10)$$

Parameter estimation and Fisher's Information Matrix

The maximum likelihood estimation approach is applied to find out the parameters of the EPD. If we take the weighted Pratibha distribution and consider a random sample of size n (X1, X2,...Xn), the likelihood function could be expressed as

$$L(x) = \prod_{i=1}^{n} f_w(x) = \frac{\theta^{n(c+3)}}{\left(\theta^3\Gamma(c+1)+\theta\Gamma(c+2)+\Gamma(c+3)\right)^n} \prod_{i=1}^{n}\left(x_i^{\,c}\left(\theta + x_i + x_i^{\,2}\right) e^{-\theta x_i}\right)$$

The log-likelihood function could be defined as,

$$\log L = n(c+3)\log\theta - n\log\left(\theta^3\Gamma(c+1)+\theta\Gamma(c+2)+\Gamma(c+3)\right) + c\sum_{i=1}^{n}\log x_i$$

$$+ \sum_{i=1}^{n}\log\left(\theta + x_i + x_i^{\,2}\right) - \theta\sum_{i=1}^{n} x_i \quad (11)$$

The following normal equations are now established by differentiating the log-likelihood equation (11) with respect

to parameters θ & c.

$$\frac{\partial \log L}{\partial\theta} = \frac{n(c+3)}{\theta} - n\left(\frac{3\theta^2\Gamma(c+1)+\Gamma(c+2)}{\left(\theta^3\Gamma(c+1)+\theta\Gamma(c+2)+\Gamma(c+3)\right)}\right) + \sum_{i=1}^{n}\left(\frac{1}{\left(\theta + x_i + x_i^{\,2}\right)}\right) - \sum_{i=1}^{n} x_i = 0$$

$$\frac{\partial \log L}{\partial c} = n\log\theta - n\psi\left(\theta^3\Gamma(c+1)+\theta\Gamma(c+2)+\Gamma(c+3)\right) + \sum_{i=1}^{n}\log x_i = 0$$

Where ψ (.) is the digamma function (a special function which is given by the logarithmic derivative of the gamma function).

The nonlinear equations above the system are extremely difficult to solve algebraically due to their complex form, which is derived from the above system of likelihood equations. For this reason, we estimate the required parameters of the suggested distribution utilizing numerical techniques such as the Newton-Raphson method.In order to determine the CI, we consider the asymptotic normality outcomes. We have that if $\hat{\alpha} = (\hat{\theta}, \hat{c})$ denotes the MLE *of* $\alpha = (\theta, c)$. We can obtain the results as $\sqrt{n}(\hat{\alpha} - \alpha) \to N_2(0, I^{-1}(\alpha))$ Where $I^{-1}(\alpha)$ is Fisher's information matrix.i.e.,

$$I(\alpha) = -\frac{1}{n}\begin{pmatrix} E\left(\frac{\partial^2 \log L}{\partial \theta^2}\right) & E\left(\frac{\partial^2 \log L}{\partial \theta\, \partial c}\right) \\ E\left(\frac{\partial^2 \log L}{\partial c\, \partial \theta}\right) & E\left(\frac{\partial^2 \log L}{\partial c^2}\right) \end{pmatrix}$$ where,

$$E\left(\frac{\partial^2 \log L}{\partial \theta^2}\right) = -\frac{n(c+3)}{\theta^2} - n\left(\frac{(\theta^3\Gamma(c+1)+\theta\Gamma(c+2)+\Gamma(c+3))\,(6\theta\Gamma(c+1)) - (3\theta^2\Gamma(c+1)+\Gamma(c+2))^2}{(\theta^3\Gamma(c+1)+\theta\Gamma(c+2)+\Gamma(c+3))^2}\right)$$

$$-\sum_{i=1}^{n}\left(\frac{1}{(\theta + x_i + x_i^2)^2}\right)$$

$$E\left(\frac{\partial^2 \log L}{\partial c^2}\right) = -n\psi'\left(\theta^3\Gamma(c+1)+\theta\Gamma(c+2)+\Gamma(c+3)\right)$$

,

$$E\left(\frac{\partial^2 \log L}{\partial \theta\, \partial c}\right) = \frac{n}{\theta} - n\psi\left(\frac{3\theta^2\Gamma(c+1)+\Gamma(c+2)}{\left(\theta^3\Gamma(c+1)+\theta\Gamma(c+2)+\Gamma(c+3)\right)}\right)$$

Since α being unknown, we estimate $I^{-1}(\alpha)$ by $I^{-1}(\hat{\alpha})$ and this can be used to determine asymptotic confidenci nterval for θ and c.

Simulation Analysis

From the simulated data, we get the descriptive statistics as Table 1. The MLE of the parameters applied here as **θ^=** 1.6191and **c^=** 1.912 ≈ 2, Mean ≥Median ≥Mode. Implies a clear asymmetricity and indicates the positive skewness nature. Our modified distributions are meant to such asymmetrical distributed real data.

Application

This section shows that the EPD fits better than the Pratibha, Pranav, Uma, and Shanker distributions while examining a real-world data set. The data set is: The birth weight of 130 randomly selected newborn babies from a Hospital in Chennai is noted from January 2023 – June 2024 (Table 2). The R software has been applied to find out the unknown parameters and determine the model comparison criteria such as BIC (Bayesian Information Criterion), AIC (Akaike Information Criterion), AICC (Akaike Information Criterion Corrected), and -2logL (where L is the likelihood function) to calculate the performance of EPD over the Pratibha, Pranav, Uma, and Shanker distributions. . Formulas are used to get the criteria values listed below.

$$AIC = 2k - 2\log L, \qquad BIC = k\log n - 2\log L \qquad \text{and} \qquad AICC = AIC + \frac{2k(k+1)}{n-k-1}$$

Where –2logL is the maximized value of the log-likelihood function under the considered model, n is the sample size, and k is the number of parameters in the statistical model. The distribution is better, while displaying lower BIC, AIC, AICC, and -2logL criteria values. Here, S.E Standard Error, KS Kolmogorov–Smirnov statistic, CI confidence interval. It is quite evident from the Table 3 that the EPD has the lesser *BIC*, *AIC*,*AICC,* and *-2logL* values than the Pratibha, Pranav, Uma, and Shanker distributions, which reveals that EPD gives a better fit. Hence, it could be concluded that EPD gives quite satisfactory results over Pratibha, Pranav, Uma, and Shanker distributions.

CONCLUSION

The establishment and development of the Extended Pratibha distribution (EPD) is detailed. The weighted distribution technique was applied to the classical distribution to create the novel one that is being presented. Numerous statistical properties have been investigated, including moment generating function, hazard rate function, moments, reverse hazard function, and reliability function. Additionally, the maximum likelihood estimation approach had been utilized to find out its parameters. The importance of such distribution for asymmetrical dataset is established. In order to show the proposed distribution's goodness of fit, an application has finally been fitted by using a real biomedical data set - the birth weight of 130 randomly selected newborn babies from a Hospital in Chennai, and the results indicate that the EPD fits the data better than the Pratibha, Pranav, Uma, and Shanker distributions. There is a scope of fitting many such real data sets to the newly derived asymmetric distribution and thereby can analyse the characteristics of the same.

REFERENCES

1. Aydın D. The new weighted inverse Rayleigh distribution and its application. Facta *Universitatis, Series: Mathematics and Informatics* [Internet]. 2019 Oct 4;34(3):511. https://doi.org/10.22190/fumi1903511a
2. Ahmad A, Ain S, Tripathi R. The weighted inverse Ailamujia distribution with applications to real life data. *PJS – Pakistan Journal of Statistics* [Internet]. 2022;38(4):451–71. https://www.pakjs.com/wp-content/uploads/2022/10/38403.pdf
3. Dar SA, Hassan A, Bilal AP, Wani SA. A new count data model applied in the analysis of vaccine adverse events and insurance claims. *Statistics in Transition New Series* [Internet]. 2021 [cited 2021 Nov 12];22(3):157–74. https://doi.org/10.21307/stattrans-2021-032
4. Fayomi A, Khan S, Tahir MH, Algarni A, Jamal F, Reman Abu-Shanab. A new extended gumbel distribution: Properties and application. *PLOS ONE* [Internet]. 2022 May 27;17(5):e0267142–2. https://doi.org/10.1371/journal.pone.0267142
5. Hassan A, Dar A, Para B. A new generalization of Ishita distribution:properties and applications. *Journal of Applied Probability and Statistics* [Internet]. 2019;14(2):53–67. https://japs.isoss.net/14(2)4%2012038.pdf
6. Helal TS, Elsehetry AM, Elshaarawy RS. Statistical Properties of Weighted Shanker Distribution. *The Journal of Business and Environmental Sciences* [Internet]. 2022 Oct 12;1(1):141–53. https://jcese.journals.ekb.eg/article_269495.html
7. Prabavathi G, Elangovan R. Shambhu distribution: Properties and application to model real life data. *Journal of Information and Computational Science* [Internet]. 2023 [cited 2023];13(2). https://joics.org/vol-13-issue-2-2023
8. Prodhanii HR, Shanker R. Weighted Pratibha distribution with properties and application in flood dataset. *Biometrics & Biostatistics International Journal* [Internet]. 2024 May 21;13(2):52–7. https://medcraveonline.com/BBIJ/BBIJ-13-00414.pdf
9. Shanker R. Pratibha distribution with properties and application. *Biometrics & Biostatistics International Journal* [Internet]. 2023 Sep 28;13(5):136–42. https://medcraveonline.com/BBIJ/BBIJ-12-00397.pdf
10. Shanker R, Das R, Kamlesh Kumar Shukla. An extended Suja distribution with statistical properties and applications. *Biometrics & Biostatistics International Journal* [Internet]. 2024 Mar 5 [cited 2024 Aug 12];13(1):16–21. https://doi.org/10.15406/bbij.2024.13.00409

Table 1. Descriptive Statistics of simulated data with respect to EPD

Mean	2.7075	Skewness	0.595954
Standard Error	0.077565	Range	3.725
Median	2.5625	Minimum	0.94
Mode	1.91	Maximum	4.665
Standard Deviation	0.884372	Sum	351.975

Sample Variance	0.782114	Count	5000
Kurtosis	-0.56299	Confidence Level(95.0%)	0.153463

Table 2: The birth weight of 130 randomly selected newborn babies.

3.480	1.560	1.910	2.625	3.580	1.940	1.910	2.630	3.595	2.610
2.195	1.910	2.630	3.595	2.610	3.480	2.555	1.910	2.625	3.580
3.115	4.450	2.160	2.225	3.120	4.485	1.965	2.230	3.165	2.225
1.870	2.400	3.450	2.300	1.900	2.500	3.500	2.300	1.900	1.700
1.910	2.650	3.700	1.250	1.980	2.660	3.780	1.250	2.010	1.700
3.925	1.800	2.040	2.825	4.035	1.280	2.085	2.890	4.120	2.690
2.090	2.900	4.170	1.940	2.090	2.935	4.240	1.800	2.135	1.930
4.255	1.505	2.155	2.965	4.280	1.950	2.190	3.000	4.305	2.960
2.195	3.100	4.370	1.615	2.220	3.150	4.450	1.960	2.225	1.750
4.485	1.965	2.230	3.165	4.570	1.965	2.300	3.345	4.605	3.115
2.325	3.375	4.665	1.940	2.095	2.935	4.240	1.850	2.135	1.770
3.480	2.555	1.910	2.625	3.580	0.940	1.910	2.630	3.595	2.610
3.480	2.550	2.190	2.625	2.570	2.195	3.105	4.375	2.065	2.610

Table 3: Distribution fitting -MLE, S.E, criteria (AIC, BIC, AICC, -2logL, CI, KS, P

Distri-bution	MLE	S.E	-2logL	AIC	BIC	AICC	95%CI	KS	P-value
EPD	$\hat{\theta} = 1.6230$ $\hat{c} = 1.8350$	$\hat{\theta} = 0.2220$ $\hat{c} = 0.5411$	268.93	272.89	277.75	273.04	(1.54, 1.71) (1.74, 1.93)	0.0290	0.7977
Pratibha	$\hat{\theta} = 0.9101$	$\hat{\theta} = 0.0531$	288.54	290.50	292.88	290.50	(0.86, 0.96)	0.0385	0.7709
Pranav	$\hat{\theta} = 1.2121$	$\hat{\theta} = 0.0541$	285.61	287.56	289.99	287.61	(1.07, 1.18)	0.1446	0.6301
Uma	$\hat{\theta} = 1.2140$	$\hat{\theta} = 0.0613$	283.71	285.69	288.12	285.75	(1.09, 1.19)	0.1450	0.6205
Shanker	$\hat{\theta} = 0.6501$	$\hat{\theta} = 0.0463$	299.37	301.37	303.80	301.42	(0.62, 0.68)	0.1115	0.6409

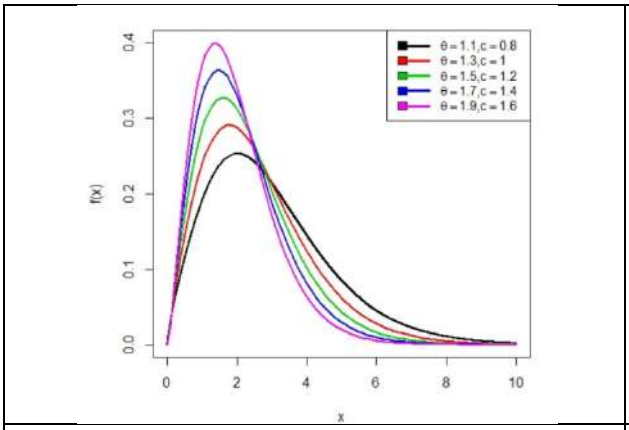

Figure 1. PDF of EPD

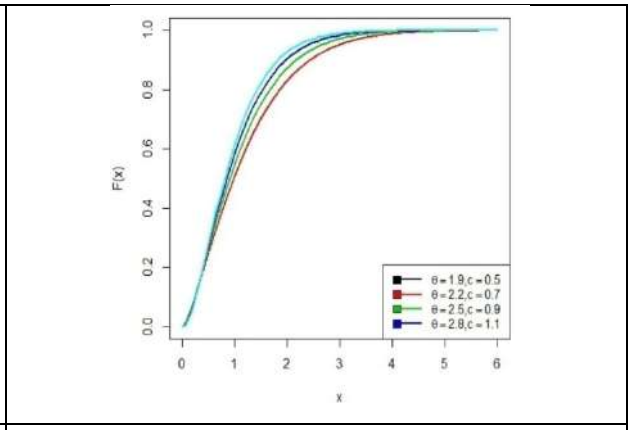

Figure 2. CDF of EPD

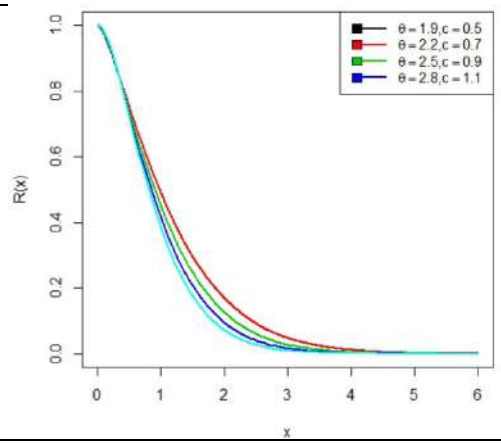

Figure 3. Reliability of EPD

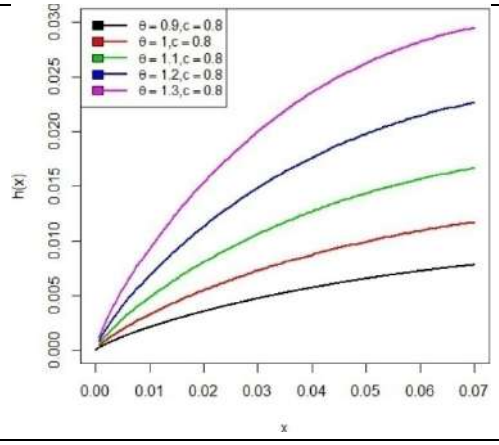

Figure 4. Hazard Rate of EPD

RESEARCH ARTICLE

Investigating the Perception and Knowledge of Medical Students on the Role of Metaverse in Healthcare

Sunil Kumar D[1]*, G Hari Prakash[2], Deepika Yadav[2] and Arun Gopi[3]

[1]Professor and Head, Department of Community Medicine, JSS Medical College, JSS Academy of Higher Education and Research (Deemed to be University), Mysuru, Karnataka, India.
[2]Ph.D Scholar, Department of Community Medicine, JSS Medical College, JSS Academy of Higher Education and Research (Deemed to be University), Mysuru, Karnataka, India.
[3]Assistant Professor, Department of Community Medicine, JSS Medical College, JSS Academy of Higher Education and Research (Deemed to be University), Mysuru, Karnataka, India.

Received: 21 Nov 2024 Revised: 03 Dec 2024 Accepted: 02 Jan 2025

***Address for Correspondence**
Sunil Kumar D
Professor and Head,
Department of Community Medicine,
JSS Medical College, JSS Academy of Higher Education and Research (Deemed to be University),
Mysuru, Karnataka, India.

ABSTRACT

Metaverse is an emerging paradigm for enhancing healthcare delivery, medical education, and patient care through immersive virtual environments and interactions. However, little is known about the preparedness of future healthcare providers such as medical students for integrating metaverse-enabled care approaches. This cross-sectional study surveyed 312 medical students from multiple Indian institutions to assess their awareness, perceptions, attitudes, and knowledge levels regarding metaverse in healthcare. Through multiple-choice questions, participants completed a validated questionnaire capturing demographics, technology exposure, metaverse perceptions on a 5-point Likert scale, and knowledge levels. Students expressed cautiously optimistic opinions, recognizing potential benefits and voicing concerns about costs, ethics, and human-technology balance. Approximately 40% reported a fair or good understanding of the metaverse, indicating knowledge gap. Students favored applications in education, clinical practice, care coordination, and overcoming barriers to access. Knowledge levels were poorer among females, younger students, and those in their initial years of study, highlighting target groups for educational efforts. This study provides timely insights into Indian medical students' preparedness for metaverse integration into healthcare. The findings revealed knowledge gaps and mixed perceptions, especially among younger female cohorts. Targeted training and curricular integration can enhance competencies related to metaverse-enabled care. Our work contributes much-needed evidence to inform guidelines for effectively leveraging technologies such as the metaverse to advance medicine.

Keywords: Metaverse; Medical Education; Healthcare; Medical Students; Perceptions; Knowledge; Attitudes

INTRODUCTION

The digital transformation of healthcare continues to unlock new possibilities for enhancing care quality, improving access, reducing costs, and enabling better experiences for patients and providers. Emerging technologies such as artificial intelligence, augmented reality, virtual reality, and telehealth have begun reshaping healthcare delivery and medical education.[1] One nascent technology garnering significant interest for its potential healthcare applications is metaverse.[2] metaverse refers to immersive, shared virtual 3D environments inwhich users interact through digital avatars.[3] By converging physical and virtual worlds, the metaverse blurs the boundaries between real and digital, offering unprecedented opportunities for collaboration, communication, and interaction [6]. While gaining traction in the entertainment and social domains, the metaverse's prospects in healthcare have captivated professionals and researchers. The metaverse can profoundly impact healthcare processes and outcomes across education, practice, research, and administration.[4] It may enable experiential medical education at scale through virtual patients, realistic procedural simulations, and collaborative cross-geography training [5]. Clinically, metaverse-enabled interfaces can enhance telehealth consultation, remote monitoring, and multidisciplinary case evaluations.[6] Social virtual environments can facilitate care coordination, conferences, and patient engagement initiatives.[7] Metaverse-based approaches can augment clinical research, public health surveillance, and health system administration. [8–10] Despite the growing discourse on the metaverse's potential for healthcare transformation, empirical insights into the preparedness of current and future healthcare providers remain limited. Assessing medical trainees' perceptions, attitudes, and knowledge levels is key to successful integration with education and practice.[11] As future healthcare leaders, medical students are pivotal in shaping emerging technology adoption, including the metaverse ones. Their viewpoints can significantly influence their eventual utilization in clinical practice and medical education. This study addresses this critical knowledge gap by investigating medical students' perspectives on the metaverse in transforming healthcare delivery, education, patient care, and public health. The objectives were to assess students' perceptions of and attitudes towards metaverse-enabled healthcare. Evaluation of knowledge regarding metaverse applications in medicine The findings will provide insights into students' readiness to adopt immersive technologies such as the metaverse, shaping guidelines for successful medical curriculum and practice integration. This timely study surveyed a representative sample of 312 medical students using validated instruments to meet the objectives. It will contribute much-needed evidence on trainee perspectives to inform and optimize metaverse deployment in healthcare transformation.

METHODOLOGY

In this cross-sectional study, 312 participants were recruited through convenience sampling, adhering to the following inclusion criteria: current enrolment in a graduate medical education program (MBBS) and voluntary informed consent. Data were collected using a pre-validated, multi-part electronic questionnaire, which included inquiries into sociodemographic factors, patterns of internet usage, perceptions of the metaverse in healthcare (assessed via a 5-point Likert scale), levels of knowledge (assessed through multiple-choice and short-answer questions), and opinions regarding potential applications of the metaverse in medical education, clinical practice, and public health. Before the full-scale administration, the questionnaire underwent a pilot testing phase to ensure clarity and comprehensibility. Participation in the study was anonymous and voluntary, with stringent safeguards to maintain confidentiality. The collected data were analyzed using SPSS version 26. Descriptive statistics were computed for all variables, and associations between socio demographic factors and knowledge levels were explored using appropriate statistical tests, such as the chi-square test and correlation analysis, based on the type and distribution of the variables. Qualitative responses were meticulously coded and categorized through content analysis. The initiation of the study followed the acquisition of clearance from the Institutional Ethics Review Board. Before participation, informed consent was obtained from all participants, and throughout the study, strict measures were upheld to maintain the confidentiality of participants' responses. The study's outcome involved categorizing knowledge and perceptions, employing the median method to determine corresponding cutoff points for both scores.

RESULTS

Most participants were aged between 18 to 22 years (83.4%) and belonged to the female gender (50.9%). Most participants were in the second year of study (47.2%), residing in urban areas (95.7%), and identified as Hindu (89.0%). Regarding the family type, 74.8% were from nuclear families. The largest group of participants had one sibling (70.6%) (Table 1). Table 2 presents the internet usage practices of the participants, along with their technological awareness and experiences. The data shows that most respondents (99.4%) use the internet multiple times per day, with a preference for mobile devices, particularly tablets (90.8%). Social media use is the most common activity (37.04%), followed by online research or studying (31.65%) and streaming video or music (25.40%). Only a smaller proportion of participants engage in activities such as online shopping (13.97%), online news reading (11.08%), and online gaming (7.91%).Regarding technological awareness, 57.7% of the participants are familiar with the metaverse concept, while 42.3% are unaware. Additionally, almost half of the respondents (49.1%) have prior experience with virtual reality or augmented reality technology. Regarding healthcare-related technology, 22.7% of the participants have received training or education on technology use in healthcare, and 35.6% have received healthcare services remotely(Table 2). Most participants expressed a "Neutral" stance towards using the metaverse to improve patient care (36.2%), indicating a lack of strong opinions.

However, a substantial proportion had positive perceptions, with 31.9% "Somewhat Agreeing" and 23.3% "Strongly Agreeing" that the metaverse can improve patient care. Similarly, participants held mixed views regarding the benefits of virtual and augmented reality in healthcare, with 35.6% "Somewhat Agreeing" and 23.9% "Strongly Agreeing," while 33.7% remained "Neutral."Regarding using the metaverse to improve patient outcomes, participants were more inclined towards a "Neutral" stance (40.5%). However, a considerable percentage of "Somewhat Agreed" (34.4%) and "Strongly Agreed" (18.4%) with its potential impact. Participants were generally open to the idea that learning more about the metaverse could be beneficial in healthcare, with 38.7% "Somewhat Agreeing" and 23.9% "Strongly Agreeing," although 30.1% remained "Neutral." Opinions regarding the future prevalence of metaverse adoption in healthcare were more evenly distributed, with 34.4% "Somewhat Agreeing" and 30.1% "Strongly Agreeing," while 28.2% remained "Neutral." However, participants were relatively unsure about the metaverse's potential to solve healthcare professional shortages in remote areas, as 36.2% remained "Neutral" and 31.3% "Somewhat Agreed."Regarding potential concerns, participants expressed a range of views on the impact of the metaverse on healthcare costs and patient privacy. While 39.3% remained "Neutral" regarding cost increase, 25.8% "Strongly Agreed" with the notion, and 24.5% "Somewhat Agreed." Similarly, opinions on increased patient privacy were varied, with 38.7% "Neutral," 27.0% "Somewhat Agreed," and 18.4% "Strongly Agreed."For COVID-19 education and prevention, most participants (55.2%) suggested using "Virtual reality simulations" as an engaging method. Additionally, "Interactive educational games" (19.0%) and "Online webinars" (25.8%) were also considered effective tools for disseminating information and raising awareness.

Regarding air pollution awareness, participants recommended "Virtual reality simulations" (39.9%) and "Interactive educational games" (31.9%) as immersive ways to raise awareness. "Online campaigns" (28.2%) were also valuable in promoting behavioural change to reduce air pollution levels.For educating people about proper nutrition and healthy eating habits, "Online nutrition workshops" (37.4%) were the most preferred option, followed closely by "Virtual cooking classes" (33.1%) and "Interactive educational games" (29.4%).To promote healthy lifestyle choices and prevent NCDs, participants highlighted the significance of "Virtual fitness classes" (50.9%) as an interactive and accessible means. "Interactive educational games" (23.3%) and "Online health coaching" (25.8%) were also considered effective methods.Participants endorsed "Teletherapy sessions" (41.1%) as a viable option for providing mental healthcare services, particularly in areas with limited access. "Virtual support groups" (33.7%) and "Online mental health coaching" (25.2%) were also suggested to facilitate mental healthcare delivery.Finally, to improve maternal and child healthcare in India, participants suggested "Online prenatal and postnatal care" (49.7%) as an effective approach. "Virtual childbirth education classes" (28.8%) and "Telemedicine consultations" (21.5%) were also identified as valuable means to enhance healthcare services. Regarding the current level of knowledge, the majority

of participants reported having a "Fair" level of knowledge about the metaverse (37.4%), while 40.5% considered their knowledge to be "Poor." In terms of experience, a similar pattern emerged, with 46.0% reporting a "Fair" experience and 35.6% stating their experience was "Poor." Participants recognized various potential benefits of the metaverse in healthcare. Most prominently, 30.45% believed it could lead to "Improved medical education and training," followed by "Enhanced research capabilities" (12.42%) and "Improved communication and collaboration among healthcare professionals" (15.82%). However, they also expressed concerns, with "Technical difficulties or malfunctions" being the most prominent potential drawback (36.30%), followed by "Lack of personal interaction between providers and patients" (28.77%).Regarding challenges, "Technical challenges such as cost and infrastructure" were perceived as the most significant (53.69%), followed by "Ethical challenges such as privacy concerns and data security" (35.57%).

Participants identified "Enhanced medical education and training" as a critical area for improvement (41.98%), along with "Improved communication and collaboration among healthcare professionals" (28.14%).Ethical concerns related to privacy and data security were prevalent (48.15%), followed by "The potential for biased algorithms or decision-making processes" (34.57%). Additionally, participants acknowledged the ethical implications of using technology to replace or augment human interactions in healthcare (18.52%).Regarding predictions, most believed that the metaverse would become more common and widely used across the industry (47.85%). However, 36.20% thought it would remain niche and only be adopted by certain institutions, while 15.95% believed the healthcare industry would not adopt it as a whole.As for potential opportunities, "Enhanced medical education and training" was highlighted as the most significant (62.37%), followed by "Improved patient care and outcomes" (37.11%) and "Increased accessibility to healthcare services" (19.07%). Conversely, potential threats were perceived as "Technical difficulties or malfunctions" (40.40%) and "Ethical concerns around privacy and data security" (40.85%).
57.1% of participants expressed a "Negative Perception," while 42.9% had a "Positive Perception" towards the metaverse.Regarding knowledge, 52.1% were categorized as having "Poor Knowledge," and 47.9% were classified as having "Good Knowledge."(Table 3).

Table 4 shows the factors associated with knowledge levels regarding the metaverse among the 312 medical student participants. Several sociodemographic factors were analyzed to determine their relationship with knowledge levels categorized as "Poor Knowledge" and "Good Knowledge." The data indicates statistically significant associations between knowledge levels and the variables age, gender, year of study, and religion.For age, a greater proportion of younger students aged 18-22 had poor knowledge (89.4%) compared to students in older age groups. The chi-square test showed a significant p-value of 0.022, indicating age is a related factor.Regarding gender, females had poorer knowledge (57.6%) than males (42.4%). This difference was statistically significant based on the chi-square test (p=0.006).The year of study also showed a significant association with knowledge levels (p=0.028), with higher percentages of 2nd-year students in the poor knowledge category (28.9%) versus good knowledge (19.4%). Later years showed a reversal in percentages between the two knowledge levels.Finally, Hindu students constituted a significantly higher proportion of the poor knowledge group (92.9%) versus good knowledge (84.6%), with a p-value of 0.003.Other sociodemographic factors like residence, family type, and siblings did not have statistically significant associations with knowledge levels.(Table 4).

Age has a positive correlation coefficient of 0.192 with a statistically significant p-value of 0.014, indicating a positive association between age and perception score. However, "Year of Study" has a correlation coefficient of 0.133 with a p-value of 0.091, suggesting a weak positive association that is not statistically significant (Figure-1). Similarly, the factor "Residence" has a correlation coefficient of -0.089 with a p-value of 0.256, indicating a weak negative association that is not statistically significant.On the other hand, for the "Knowledge Score, Age has a positive correlation coefficient of 0.208 with a statistically significant p-value of 0.008, suggesting a positive association between age and knowledge score. The "Year of Study" factor shows a correlation coefficient of 0.252 with a highly significant p-value of 0.001, indicating a moderate positive association between the year of study and knowledge score(Figure-2). However, the factor "Residence" has a correlation coefficient of 0.010 with a p-value of 0.902, suggesting a negligible association that is not statistically significant (Table 5).

DISCUSSION

This study provides timely insights into Indian medical students' awareness, perceptions, and knowledge regarding integrating metaverse in healthcare transformation. Our findings revealed moderate awareness but limited in-depth knowledge about the metaverse among students. Just ~40% expressed fair or good understanding, suggesting metaverse concepts have not permeated medical curricula substantially yet. This corroborates conclusions from preliminary surveys indicating inadequate exposure to emerging technologies like virtual reality and blockchain in medical education.[12]Targeted training on metaverse-based care approaches is warranted at the undergraduate level. Students had mixed perceptions regarding metaverse in healthcare, with cautious optimism. Most recognized potential benefits in enhancing education, care delivery, outcomes, and future adoption, align with assertions made in conceptual frameworks.[6,13] However, concerns exist around costs, privacy, human-technology balance, and over-reliance, reiterating issues raised in earlier discourses.[8,14] Interestingly, prior technology exposure did not predict more favourable attitudes, contrasting assumptions in previous opinion pieces.[15] These nuanced insights can shape integration acceptable to future providers. This study identified knowledge gaps among younger, female, junior, and Hindu students. The findings indicate target demographics for prioritized education on metaverse-based care. Additionally, the present curricula seem inadequate in imparting applied knowledge regarding emerging technologies, as suggested previously.[16] Updates incorporating advances like the metaverse could make medical education more holistic and aligned with practice.[9]

Students identified promising usecases in education, clinical practice, public health promotion, and overcoming access barriers. The suggested applications align with those proposed in earlier publications.[3] Our findings provide empirical evidence of end-user perceptions of metaverse utility across healthcare domains.This study helps address the lack of empirical insights on stakeholder perceptions regarding the metaverse, noted in previous expert commentaries.[2,10,17] Our work provides novel data on students' viewpoints and situates the findings within the context of earlier theoretical frameworks. Moreover, we substantiate the presence of knowledge gaps highlighted across preliminary surveys and reiterate curricular improvements recommended previously.[5,17] The associations between sociodemographic factors and knowledge levels offer new data compared to preceding research. Furthermore, the suggested applications align with the earlier use cases but provide empirical user perspectives.[3,6,15] The study by Dwivedi et al. provides further evidence of the transformational potential of metaverse technologies like virtual and augmented reality in enhancing medical education, surgical training, patient care, and research. Their emphasis on the metaverse fostering seamless,immersive interactions and collaboration aligns with our findings, where students highlighted these as key advantages.[18]Suh et al.'s review also reiterates the nascent but growing metaverse applications in health education, promotion, and delivery.[19]The research gaps highlighted in these studies about the development and assessment of health promotion programs in the metaverse mirror the aims of our study. Our work helps advance knowledge in this area by eliciting medical students' perspectives. This study makes important contributions by elucidating medical students' preparedness for transformative technologies like the metaverse in healthcare. The findings have implications for education, policy, and practice. The limitations of convenience sampling, self-reported assessments, and single-country setting constrain generalizability. Factors like teaching methods, resources, and policies can also mediate knowledge acquisition. Future studies should consider multi-centre random sampling, objective knowledge assessments via metaverse simulations, and comparative analyses across diverse contexts. Exploring provider perspectives alongside students will also offer holistic insights.A s the metaverse gains momentum as a transformative technological concept, its potential applications in healthcare hold great promise. This study contributes to the evolving discourse by shedding light on medical students' perceptions and knowledge of the metaverse's role in healthcare. By investigating their awareness, attitudes, and expectations, this research provides insights into the readiness of the future healthcare workforce to embrace the metaverse.

Acknowledgements
The authors express gratitude to the medical students who participated in this study, generously contributing their time and insights.

Disclosure statement: The authors report there are no competing interests to declare.
Funding: Nil

REFERENCES

1. Smith AC, Thomas E, Snoswell CL, et al. Telehealth for global emergencies: Implications for coronavirus disease 2019 (COVID-19). J Telemed Telecare. 2020;26:309–313.
2. Virtual reality and the transformation of medical education - PMC [Internet]. [cited 2023 Aug 10]. Available from: https://www.ncbi.nlm.nih.gov/pmc/articles/PMC6798020/.
3. Shao L, Tang W, Zhang Z, et al. Medical metaverse: technologies, applications, challenges and future. J Mech Med Biol. 2023;23:2350028.
4. Ahuja AS, Polascik BW, Doddapaneni D, et al. The Digital Metaverse: Applications in Artificial Intelligence, Medical Education, and Integrative Health. Integr Med Res. 2023;12:100917.
5. Chengoden R, Victor N, Huynh-The T, et al. Metaverse for Healthcare: A Survey on Potential Applications, Challenges and Future Directions. 2022.
6. Ahmadi Marzaleh M, Peyravi M, Shaygani F. A revolution in health: Opportunities and challenges of the Metaverse. EXCLI J. 2022;21:791–792.
7. Massetti M, Chiariello GA. The metaverse in medicine. Eur Heart J Suppl J Eur Soc Cardiol. 2023;25:B104–B107.
8. Ali S, Abdullah, Armand TPT, et al. Metaverse in Healthcare Integrated with Explainable AI and Blockchain: Enabling Immersiveness, Ensuring Trust, and Providing Patient Data Security. Sensors. 2023;23:565.
9. Khay-Guan AY. The future of medical education. Singapore Med J. 2019;60:3–8.
10. Sun M, Xie L, Liu Y, et al. The metaverse in current digital medicine. Clin EHealth. 2022;5:52–57.
11. Aungst TD, Patel R. Integrating Digital Health into the Curriculum—Considerations on the Current Landscape and Future Developments. J Med Educ Curric Dev. 2020;7:2382120519901275.
12. Bhugaonkar K, Bhugaonkar R, Masne N. The Trend of Metaverse and Augmented & Virtual Reality Extending to the Healthcare System. Cureus. 2022;14:e29071.
13. Kim EJ, Kim JY. The Metaverse for Healthcare: Trends, Applications, and Future Directions of Digital Therapeutics for Urology. Int Neurourol J. 2023;27:S3-12.
14. Frontiers | From Big Data to Precision Medicine [Internet]. [cited 2023 Aug 10]. Available from: https://www.frontiersin.org/articles/10.3389/fmed.2019.00034/full.
15. Khan ZF, Alotaibi SR. Applications of Artificial Intelligence and Big Data Analytics in m-Health: A Healthcare System Perspective. J Healthc Eng. 2020;2020:e8894694.
16. Kassutto SM, Baston C, Clancy C. Virtual, Augmented, and Alternate Reality in Medical Education: Socially Distanced but Fully Immersed. Sch. 2:651–664.
17. Jha N, Shankar PR, Al-Betar MA, et al. Undergraduate Medical Students' and Interns' Knowledge and Perception of Artificial Intelligence in Medicine. Adv Med Educ Pract. 2022;13:927–937.
18. Dwivedi YK, Hughes L, Baabdullah AM, et al. Metaverse beyond the hype: Multidisciplinary perspectives on emerging challenges, opportunities, and agenda for research, practice and policy. Int J Inf Manag. 2022;66:102542.
19. Suh I, McKinney T, Siu K-C. Current Perspective of Metaverse Application in Medical Education, Research and Patient Care. Virtual Worlds. 2023;2:115–128.

Table 1: Sociodemographic characteristics of the study participants

Sociodemographic characteristics	N	%
Age (in years)		
18-22	136	83.4
22-26	22	13.5
26-30	3	1.8
30 and above	2	1.2
Gender		
Male	80	49.1
Female	83	50.9
Year of study		
Second year	77	47.2
Third year	70	42.9
Fourth year	1	0.6
Fifth year	11	6.7
PG	4	2.5
Residence		
Urban	156	95.7
Rural	7	4.3
Religion		
Hindu	145	89.0
Muslim	8	4.9
Christian	6	3.7
Sikh	2	1.2
Other	2	1.2
Type of family		
Nuclear Family	122	74.8
Joint Family	41	25.2
Siblings		
None	22	13.5
1	115	70.6
2	20	12.3
3	3	1.8
4 or more	3	1.8

Values are expressed as frequency and percentage.

Table 2: Internet Usage Practice among the study participants

Internet Usage Practice		Count	Column N %
How often do you use the internet?	Multiple times per day	310	99.40%
	Once per day	2	0.60%
	A few times per week	0	0.00%
	Once a week or less	0	0.00%
What type of device do you use	Desktop computer	2	0.60%
	Laptop computer	2	0.60%
	Smartphone	284	90.80%
	Tablet	25	8.00%
	Other	0	0.00%
Which of the following activities do you regularly engage in on the internet?	Social media use (e.g., Facebook, Twitter, Instagram)	224	37.04%
	Online shopping	84	13.97%
	Streaming video or music	152	25.40%
	Online research or studying	190	31.65%
	Online news reading	66	11.08%
	Online gaming	48	7.91%
	Reading novels	2	0.32%
	Watching lectures	2	0.32%
	eBooks	2	0.32%
Do you know the concept of the metaverse?	Yes	180	57.70%
	No	132	42.30%
Have you ever used virtual reality or augmented reality technology before	Yes	153	49.10%
	No	159	50.90%
Have you ever received any training or education on the use of technology in healthcare	Yes	71	22.70%
	No	241	77.30%
Have you ever received healthcare services remotely	Yes	111	35.60%
	No	201	64.40%
Values are expressed as frequency and percentage.			

Table 3: Perception and knowledge regarding metaverse among study participants

Perception	N	%
Negative Perception	178	57.1
Positive Perception	134	42.9
Knowledge Levels		
Poor Knowledge	162	52.1
Good Knowledge	150	47.9
Values are expressed as frequency and percentage.		

Table 4:Factors associated with the Knowledge level of the study participants

Sociodemographic variables		Knowledge Levels					
		Poor Knowledge		Good Knowledge			
		N	%	N	%	chi-square	p-value
Age in Years	18-22	152	89.40%	108	76.90%	9.609	.022*,b
	22-26	14	8.20%	28	19.20%		
	26-30	2	1.20%	4	2.60%		
	30 and above	2	1.20%	2	1.30%		
Gender	Male	69	42.40%	85	56.40%	7.542	.006*
	Female	93	57.60%	65	43.60%		
Year of Study	Second year	50	28.90%	27	19.40%	10.836	.028*
	Third year	30	17.30%	40	28.80%		
	Fourth-year	50	28.90%	30	21.60%		
	Fifth year	43	24.90%	42	30.20%		
Residence	Urban	155	95.30%	143	96.20%	0.636	0.425
	Rural	8	4.70%	6	3.80%		
Religion	Hindu	151	92.90%	127	84.60%	15.808	.003*,b,c
	Muslim	6	3.50%	10	6.40%		
	Christian	2	1.20%	10	6.40%		
	Sikh	4	2.40%	0	0.00%		
	Other	0	0.00%	4	2.60%		
Type of family	Nuclear Family	115	70.60%	118	79.50%	2.254	0.133
	Joint Family	48	29.40%	31	20.50%		
Siblings	None	15	9.40%	27	17.90%	9.063	.060b
	1	118	72.90%	102	67.90%		

	2	23	14.10%	15	10.30%		
	3	4	2.40%	2	1.30%		
	4 or more	2	1.20%	4	2.60%		
Values are expressed as frequency and percentage. The P-value is a chi-square test, and a p-value less than 0.05 is considered statistically significant.							

Table 5: Correlation of knowledge scores and perceptions scores with sociodemographic variables

Demographic variables		**Perception Score**	**Knowledge Score**
Age in Years	Correlation Coefficient	.192*	.208**
	Sig. (2-tailed)	0.014	0.008
Year of study	Correlation Coefficient	0.133	.252**
	Sig. (2-tailed)	0.091	0.001
Residence	Correlation Coefficient	-0.089	0.010
	Sig. (2-tailed)	0.256	0.902
Correlation is significant at the 0.05 level (2-tailed)			

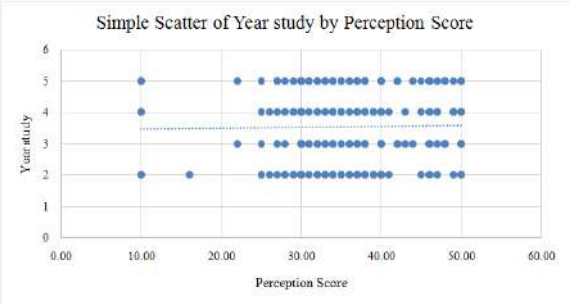

Figure 1: Scatter plot of Year of study Vs Perception Score among the study participants

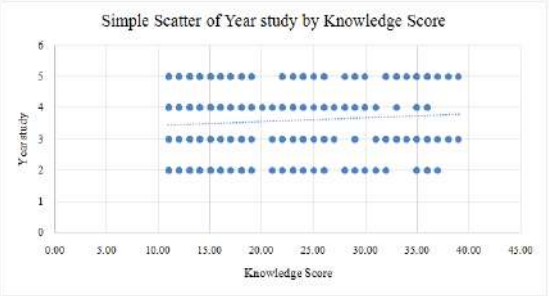

Figure 2: Scatter plot of Year of study Vs knowledge Score among the study participants

RESEARCH ARTICLE

Validity of an Aneroid Manometer with Rubber Tube to Measure Respiratory Muscle Strength

Tvisha Patel[1]*, Arvind Kumar[2], Zarana Khamar[1], Neelam Rathod[3] and Kartik Patel[4]

[1]Ph.D Scholar, Venus Institute of physiotherapy, At Bhoyan Rathod, Opposite IFFCO, Near ONGC(WSS), Adalaj-Sertha Road, Gandhinagar, (Affiliated to Swarrnim Startup and Innovation University), Gujarat, India.
[2]Principal and Professor, Venus Institute of Physiotherapy, At Bhoyan Rathod, Opposite IFFCO, Near ONGC(WSS), Adalaj-Sertha Road, Gandhinagar, (Affiliated to Swarrnim Startup and Innovation University), Gujarat, India
[3]Ph.D Scholar, Parul Institute of Physiotherapy, Parul University, Waghodia, Vadodara, Gujarat, India
[4]Associate Professor, Department of Cardiovascular and Thoraic Surgery, U N Mehta Institute of Cardiology and Research Centre (Affiliated to B. J. Medical College), Ahmedabad, Gujarat, India.

Received: 21 Aug 2024 Revised: 20 Nov 2024 Accepted: 02 Jan 2025

***Address for Correspondence**
Tvisha Patel,
Ph.D Scholar,
Venus Institute of physiotherapy,
At Bhoyan Rathod, Opposite IFFCO,
Near ONGC(WSS),
Adalaj-Sertha Road, Gandhinagar,
(Affiliated to Swarrnim Startup and Innovation University),
Gujarat, India.
E.Mail: tvishapatel90@gmail.com

ABSTRACT

The major stabilizer and the navigator of the thoracic cage are the respiratory muscles. Thus it is essential to evaluate their strength. There are various techniques which are invasive as well as non-invasive; the present study focused on finding the validity of an aneroid manometer with rubber tube in measuring the strength of respiratory muscles. 120 healthy adults were asked to forcefully inspire and after a rest of one minute forcefully expire in the device for measuring the MIP and MEP. This was performed in sitting position. The validity of the instrument was found out with the spearmen's correlation coefficient. Equal males and females were included in the study; the mean age was 56.98 ±7.00 and 57.48 ± 6.91 years where mean height was 164.76 ± 4.92 and 158.73 ± 2.78 cms as well as the mean weight was 64.30 ± 3.49 and 60.11 ± 3.98 kgs respectively. An average BMI of the subjects was 24.1 ± 2.01 kg/m2. The p value (<0.05) shows no significant difference in the observed values. The aneroid manometer with rubber tube which is

a portable device used in the study is valid to be used for evaluation of the respiratory muscle strength in the patients known to be affected with the muscle weakness of respiratory system.

Keywords: Validity, Aneroid Manometer, Noninvasive Technique For Measurement Of Respiratory Muscle Strength, Maximum Inspiratory Pressure And Maximum Expiratory Pressure

INTRODUCTION

The major stabilizer and the navigator of the thoracic cage are the respiratory muscles. These are important for generating the negative pressure in the thorax to induce the airflow. They even have a leading role in maintaining the shape as well as the mobility of the thoracic cage. Posture and the balance of the body are the dependent factors on the muscle function surrounding the thorax. Moreover the prime respiratory muscle; the diaphragm pivots the functioning of the circulation while supporting the heart. This contributes towards the maintenance of the spinal stability. 1, 2, 3 The demand of oxygen while performing exercise or in the state of exertion lays an extra effort over the muscles of respiration, which responds in over activity followed by fatigue. As the age progresses these muscles just like another in human body depict agedness and overall weakens. The literature too is suggestive of greater oxidation in muscles as age advances.4 In a review conducted by Janssens the effect of age on the physiological alterations were seen in respiratory system and the mechanics were altered too. The study emphasized on the reduction of the compliance for the chest wall, the elastically recoiling of the alveoli in the lungs and the most important the respiratory muscle strength.5 This makes it essential to thus measure respiratory muscle strength. There are various techniques to measure them.6 muscles of respiration when contract generate force which shortens the muscle. The pressure is the reflexion of that force produced. These muscles have the property to shorten and lengthen in a rhythmic way throughout the entire life of a human, where the contractions produced can be voluntary or involuntary depend upon the technique used. There are invasive techniques for measurement of the respiratory muscle strength such as trans diaphragmatic pressure or oesophageal balloons and others. As these techniques require a certain setup and are cumbersome the non-invasive techniques are discovered which are proven to be equally reliable.

The most commonly and widely used method is measuring the maximum inspiratory and expiratory pressures through the mouth which are most commonly termed as MIP and MEP; which are non-invasive, simple, well adopted, easy to measure and convenient for the patient population too.7 this simple measurement of respiratory muscle strength is measured using an occluded mouth piece attached with a manometer which are used for diagnosing the respiratory muscle weakness caused in respiratory, cardiac or neuromuscular diseases.8 MIP is the maximal inspiratory pressure; this is for measuring the inspiratory muscle strength as it is measured when the individual actively draws in air starting from the residual volume. Likewise MEP is the maximum expiratory pressure where the phase starts from the inspiratory capacity of the patient and continues towards the total lung capacity. Here, MIP is dependent on the negative thoracic pressure generated while the MEP is comparable to the elastic recoil of the alveoli followed by the force generated by the expiratory muscles too.10 The measurements are always dependent on multiple factors such as proper positioning of the patients as well as the measuring device, the second important factor is the performance while assessing which is multifactorial such as the perception of the procedure, the motivation while performing and the most important aspect is the device used for the assessment of the respiratory muscle strength. 11 There is evidently the valid tool for assessment of these pressures available worldwide which MicroRPM pressure meter is. This is non-cost effective as well as it has two different devices to measure inspiratory and expiratory pressure.12,13,14 Other devices were constructed too which were cost effective , portable , valid as well as reliable but the focus was just on measuring the inspiratory pressure. These devices were analogue too and even digital ones,. The digital one had a multipurpose use foe assessing as well as diagnosing as it provided resistance to the flow rate.15,16 Where MEP also holds an equal importance a little is known about the instrument measuring both the respiratory muscle strength in a single unit. The aim of the present study was to

construct a device which can measure the inspiratory as well as expiratory muscle strength in a single unit. As the literature suggest the essentiality of diagnosing the weakness of these muscles also depends on age, diseases which involve neurological, surgical, cardiac, respiratory or even altered thoracic mechanics so the machine should be portable, light weight, easily available in the rural as well as the urban settings.17 The device constructed in this study was by using an aneroid manometer with a marking range of 0 to 300 mmhg with markings at every 2 mmhg. Certain devices used manometers with calibration in cmH2O and a marking of 5cmH20, the higher the difference between the readings, lesser is the accuracy. 14 this aneroid manometer was further attached to a simple flexible rubber tube omitting the rigid tube and a separate mouth piece like in other devices to prevent air leaks.18 the analogue manometers were preferred over the digital ones to avoid the battery usage as well as to avoid certain malfunctions.

MATERIALS AND METHOD

The cross sectional observational study was carried out after obtaining the ethical approval from the institute ethical committee. All the participants were enrolled after receiving an informed written consent. The study population was 120 healthy adults who were included in the study where 60 subjects were males and the rest 60 subjects were all females. The age group of the participants was 45-65 years of age. The subjects included in the study were non-smokers, without neurological or respiratory disease who were able to understand the procedure and were readily willing to participate. The subjects with cardiac or musculoskeletal disease related to thorax or diagnosed with acute respiratory infections and were doing routine respiratory physiotherapy was excluded from the study. 19 A trained physiotherapist collected the data using the device. All the participants were given a descriptive followed with a practical demonstration of the procedure. The personal details were meanwhile assessed for like age, weight and height for BMI calculation. The weight was measured wearing light clothes on the weighing scale and the height was evaluated barefoot with a wall fixed stadiometer. The BMI was then calculated in kg/m2 to consider the subjects who were with normal BMI. Maximum respiratory pressures were assessed in the sitting position. The patient was asked to take a deep breath starting from the FRC from the rubber tube and letting it hold for one second for evaluation of MIP. After a rest of one minute the subjects were asked to blow as much as possible in the rubber tube while trying to hold it for one second for measuring MEP. The readings were recorded in mmHG. A nose clip was used to ensure entire breathing through mouth. A constant command was provided to each participant for accuracy of results.
Data analysis was performed using SPSS software 20 for finding the inter class correlation coefficient between the data for knowing the validity of the aneroid manometer. The data was compared with the published data as well as with the data obtained using the reference equation for knowing the respiratory muscle strength of all the study participants.

RESULTS

A total of 120 adults (60 M, 60F) were included in the study, the mean age of the males included was 56.98 ±7.00 and 57.48 ± 6.91 years where mean height was 164.76 ± 4.92 and 158.73 ± 2.78 cms as well as the mean weight was 64.30 ± 3.49 and 60.11±3.98 kgs respectively. An average BMI of the subjects was 24.1 ± 2.01 kg/m2. The observed values using the device were expressed as mean ± standard deviation and were compared with the reference equation (Table 1, Graph 1) and even with the published data (Table 2, Graph 2). The p value (<0.05) shows no significant difference in the observed values which is suggestive of the values observed by the aneroid manometer to be comparable with that obtained with using the equation as well as with the published data.

DISCUSSION

The present study focused on finding the validity for using an aneroid manometer with rubber tube to assess the respiratory muscle strength. The correlation coefficient was found to be 0.9, which in turn is considered highly

reliable (as more than 0.8). The device can be used to measure both inspiratory as well as expiratory muscle strength which was a limitation of many devices available or tested. 11,15,16,18 The value of MIP obtained in our study was 93.69 ± 5.18 in males and 70.47 ± 2.96 in females. These values were similar to those found in a study conducted in Indian population by veenakirannambiar *et al.* in 2015. Similarly the values of MEP were found relatable too where the present study had MEP in males as 85.57 ± 5.20 and females were 64.04 ± 4.77. There are several techniques for assessing the respiratory muscle strength where the use of tube mouth piece versus the flanged ones are evaluated and the studies recommend the use of tube mouth piece over the flanged ones as the tube ones were yielding to better results. This was according to the ATS authors guidelines. But the authors even commented for the easy use of flanged mouth piece.21 The other important factor while evaluating the strength of respiratory muscle comes is the technique learning. Some studies suggest more number of trials for greater reliability which were countered by the studies where fatigue of these muscles lowering the actual values. Where both the factors being equally important the present study focused on taking 3 repetitions to get an accuracy and even avoiding the fatigue of the muscles. 22
A very little is known about the devices available for measuring of respiratory muscle strength both, which is easy to use, portable as well as conveniently available in India. The outcomes of the device used in the present study were compared with the study conducted by Dimitriadis *et al* (14) in 2011 where the reliability of MicroRPM machine was studied. The validity found in their study was 0.86 to 0.90 in sitting position which was comparable with the correlation coefficient of our study of 0.9 to 0.99. Aldrich and Spiro *et al* 23 in their study measured the MIP for eighteen times each in 10 healthy subjects to determine the number to repetitions ideal for the validity where they found no significant deviation between the coefficients of variations. Thus even a best of three readings are more than required to evaluate the readings irrespective of the type of efforts may it be maximal of submaximal. The limitation of the present study is the age group limited to just the elder population of 45 -65 years of age. There are clinical implications for the aneroid manometer with rubber tube. It can be used to measure the respiratory muscle strength i.e. both MIP and MEP in patients with respiratory or neuromuscular disorders which is evidently required for the treatment and evaluation purpose. As it is one of the only non-invasive techniques to evaluate the respiratory functions.

CONCLUSION

The aneroid manometer with rubber tube which is a portable device used in the study is valid and even reproducible that can be used to rule out the respiratory muscle strength in the patients known to be affected with the muscle weakness of respiratory system. The device can be extensively be useful in treatment of patients with neurological disorders or respiratory muscle weakness and even patients with dyspnoea or air trapping. The device can be used as a diagnostic tool to evaluate the efficacy of the treatment.

Funding Source
No funding was obtained for the present study

Conflict of Interest
None

REFERENCES

1. Hodges P.W., Eriksson A.E., Shirley D., Gandevia S.C. Intra-abdominal pressure increases stiffness of the lumbar spine. *J. Biomech.* 2005;38:1873–1880. doi: 10.1016/j.jbiomech.2004.08.016.
2. Kolar P., Sulc J., Kyncl M., Sanda J., Cakrt O., Andel R., Kumagai K., Kobesova A. Postural function of the diaphragm in persons with and without chronic low back pain. *J. Orthop. Sports Phys. Ther.* 2012;42:352–362. doi: 10.2519/jospt.2012.3830.
3. Kocjan J., Adamek M., Gzik-Zroska B., Rydel M. Network of breathing. Multifunctional role of the diaphragm: A review. *Adv. Respir. Med.* 2017;85:224–232. doi: 10.5603/ARM.2017.0037.

4. Gea J., Ausín P., Martínez-Llorens J.M., Barreiro E. Respiratory muscle senescence in ageing and chronic lung diseases. *Eur. Respir. Rev.* 2020;29:200087. doi: 10.1183/16000617.0087-2020.
5. Janssens J.P. Aging of the respiratory system: Impact on pulmonary function tests and adaptation to exertion. *Clin. Chest Med.* 2005; 26:469–484. doi: 10.1016/j.ccm.2005.05.004.
6. Caruso P, Albuquerque AL, Santana PV, Cardenas LZ, Ferreira JG, Prina E, Trevizan PF, Pereira MC, Iamonti V, Pletsch R, Macchione MC, Carvalho CR. Diagnostic methods to assess inspiratory and expiratory muscle strength. J Bras Pneumol. 2015 Mar-Apr;41(2):110-23. doi: 10.1590/S1806-37132015000004474. PMID: 25972965; PMCID: PMC4428848.
7. Mętel S, Kostrzon M, Adamiak J, Janus P. Respiratory Muscle Function in Older Adults with Chronic Respiratory Diseases after Pulmonary Rehabilitation in Subterranean Salt Chambers. J Clin Med. 2023 Aug 4;12(15):5120. doi: 10.3390/jcm12155120. PMID: 37568522; PMCID: PMC10419711.
8. Laveneziana P, Albuquerque A, Aliverti A, *et al*. ERS statement on respiratory muscle testing at rest and during exercise. *EurRespir J*. 2019; 53(6) doi: 10.1183/13993003.01214-2018.
9. ATS/ERS Statement on respiratory muscle testing. *Am J RespirCrit Care Med.* 2002;166(4):518–624. doi: 10.1164/rccm.166.4.518.
10. Silveira BMF, Pereira MCB, Cardoso DR, Ribeiro-Samora GA, Martins HR, Parreira VF. New method for evaluating maximal respiratory pressures: Concurrent validity, test-retest, and inter-rater reliability. Braz J Phys Ther. 2021 Nov-Dec;25(6):741-748. doi: 10.1016/j.bjpt.2021.04.012. Epub 2021 May 14. PMID: 34119441; PMCID: PMC8721068.
11. Measurement of respiratory muscle strength; Thorax 50, 1131-1135:1995.
12. Medical Device Depot inc. [homepage on the Internet]. c2020 [updated 2020 Jul 29; cited 2020 Jul 29]. Available from: https:// www.medicaldevicedepot.com/MicroDirectMicroRPM-Pressure-Meter-p/rpm01.html
13. Dimitriadis Z, Kapreli E, Konstantinidou I, Oldham J, Strimpakos N. Test/retest reliability of maximum mouth pressure measurement with the MicroRPM in healthy volunteers. Respir Care 2011; 56:776-82.
14. Jalan NS, Daftari SS, Retharekar SS, Rairikar SA, Shyam AM, Sancheti PK. Intra- and inter-rater reliability of maximum inspiratory pressure measured using a portable capsule-sensing pressure gauge device in healthy adults. Can J RespirTher. 2015 spring; 51(2):39-42. Erratum in: Can J RespirTher. 2015 summer; 51(3):72. PMID: 26089737; PMCID: PMC4467477.
15. Stavrou VT, Tourlakopoulos KN, Daniil Z, Gourgoulianis KI. Respiratory Muscle Strength: New Technology for Easy Assessment. Cureus. 2021 May 2;13(5):e14803. doi: 10.7759/cureus.14803. PMID: 34094759; PMCID: PMC8168762.
16. Vikram V. Holla, Shweta Prasad, Pramod Kumar Pal, Chapter 16 - Neurological effects of respiratory dysfunction,Editor(s): Robert Chen, Patrice G. Guyenet,Handbook of Clinical Neurology,Elsevier,Volume 189,2022,Pages 309-329,ISSN 0072-9752
17. Sarvesh *et al*., Inter and Intra-rater Reliability & Validity of Dhiraj Maximum Inspiratory Pressure Device. Int. j. clin. biomed. res. 2020;6(3):13-17.
18. Volianitis S, McConnell AK, Jones DA. Assessment of maximum inspiratory pressure prior submaximal respiratory muscle activity ('warm-up') enhances maximum inspiratory activity and attenuates the learning effect of repeated measurement. Respiration 2001;68:22-7.
19. Richman J, Makrides L, Prince B. Research methodology and applied statistics; part 3: Measurement procedures in research. Physiother Can 1980;32:253-7.
20. American Thoracic Society/European Respiratory Society. ATS/ ERS statement on respiratory muscle testing. Am J RespirCrit Care Med 2002; 166:518-624.
21. Clanton TL, Diaz PT. Clinical assessment of the respiratory muscles. Physical Ther 1995; 75:983-95.
22. Aldrich TK, Spiro PS. Maximal inspiratory pressure: Does reproducibility indicate full effort? Thorax 1995; 50:40-3.

Table.1: Comparison of the Observed Value with Values Obtained Using Equation

Outcomes	ANEROID MANOMETER	EQUATION	P value
MIP MALES	93.69 ± 5.18	93.91 ± 5.09	0.719
MEP MALES	85.57 ± 5.20	85.93 ± 5.28	0.543
MIP FEMALES	70.47 ± 2.96	70.33 ± 3.00	0.776
MEP FEMALES	64.04 ± 4.77	64.51 ± 4.82	0.522

Table.2: Comparison of the Observed Value with the Published Data (Device)

Outcomes	ANEROID MANOMETER	PUBLISHEDDATA	P value
MIP MALES	93.69 ± 5.18	96.16 ± 14.63	0.278
MEP MALES	85.57 ± 5.20	88.90 ± 14.33	0.08
MIP FEMALES	70.47 ± 2.96	73.28 ± 11.93	0.06
MEP FEMALES	64.04 ± 4.77	66.67 ± 10.83	0.07

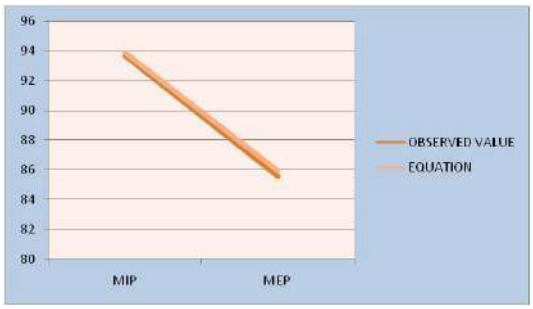

Graph.1: Comparison of Means of Observed Value With Equation

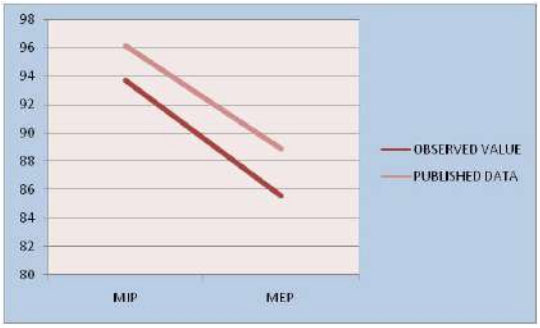

Graph.2: Comparison of Means of Observed Value With Published Data

RESEARCH ARTICLE

Harnessing the Power of Bioactive Peptides in Cancer Therapy

Tanjima Tarique Laskar*

Assistant Professor, Department of Pharmaceutical Science, University of Science and Technology, Meghalaya, India.

Received: 21 Nov 2024 Revised: 03 Dec 2024 Accepted: 21 Jan 2025

***Address for Correspondence**
Tanjima Tarique Laskar
Assistant Professor,
Department of Pharmaceutical Science,
University of Science and Technology,
Meghalaya, India.
E.Mail: tanjimatarique.12@gmail.com

ABSTRACT

Peptide-based therapies propose the potential opportunity for the management of serious illnesses like cancer which is prevalent world-wide. Despite advancements in anticancer medications, the use of different approaches to treat cancer is frequently linked to unfavourable side effects and multidrug resistance which has spurred the development of innovative therapeutic approaches. Due to the numerous advantages of naturally occurring and modified anticancer peptides over the available treatment modalities it has drawn a lot of attention recently and are emerging as potential therapeutic and diagnostic approach for cancer therapy. In the past few years, cancer patients have been showing eagerness for adherence to supplementary medicines to enhance the effectiveness of prevailing cancer treatments. There are numerous conventional perspectives for cancer treatment but as the century advances, prominence have been put forth to more efficacious and less pernicious natural sources. The current study deals with an apprise contemplation of naturally derived bioactive peptides possessing cardinal cytotoxic effects and also highlights multitudinous proffer mechanisms by which the natural bioactive peptides exert cytotoxic effects against cancerous cells.

Keywords: Bioactive peptides, Membrane-active & non-active, Natural sources, Mechanism, Types

INTRODUCTION

Cancer menaces a significant threat to global human health and well-being and it is considered as a one of the prime roots of morbidity. As per World Health Organization (WHO), approximately 20 million fatalities were attributed to cancer and among which lungs, prostate, colorectal and stomach cancer are being most prevalent in males whereas breast, colorectal, lung, cervical and thyroid cancer being more ubiquitous in females[1-3].The present gold standard cancer treatment consists of a three-pronged approach including surgical intervention, radiation therapy and

chemotherapeutic drugs[4].Nevertheless, traditional method possesses various limitations including lack of examination tests for cancer detection at early stage and absence of tailored medicament delivery approaches for specific tumours. Furthermore, the majority of conventional anticancer drugs are unable to differentiate among healthy cells and malignant cells which results in undesirable side effects as well as systemic toxicity in the body [5,6].Over the past decades, individuals diagnosed with cancer have shown a growing interest in incorporating complementary medicine (CM) into their treatment regimen. The aim is to enhance their overall well-being, augment the effectiveness of conventional cancer therapies, improve survival rates and alleviate the adverse effects associated with both the treatments and the disease itself.[7].One classification of complementary medicine involves the utilization of organic substances specifically naturally derived biopeptides which are short sequences of amino acids (3-20 AAs) found within a protein that have advantageous impacts on the adjustment and control of processes of metabolism and have promising effects in curing ailments[8].

Biopeptides which have the ability for management and avoiding diseases lie dormant within a parent protein and it must be liberated via food processing, enzymatic hydrolysis, microbial fermentations or using various novel approaches to manifest their favourable effects[9]. These peptides possess the ability to inhibit the growth and proliferation of malignant cancerous cells and induce programmed cell death or apoptosis in cancer cells. Natural compounds particularly peptides have garnered significant interest as a promising substitute for treatment of cancer owing to its advantageous features including the high specificity and affinity for target molecules as well as their lower toxicity compared to traditional chemical drugs which have made them promising and encouraging alternatives for treatment[10,11].Approaches for the generation and purification of peptides primarily consists of various approaches such as membrane separation, ultra filtration, chromatography and ion exchange procedures. Naturally occurring biologically active peptides are typically made up of of 2-50 amino acid residues possessing a molecular weight of about 102-103 Dalton. Consequently, they can effortlessly penetrate into the membrane of cells and cause death of malignant cells[12].With the progress in the field of biomedical research, a significant number of naturally derived biologically active peptides have been identified which were extracted and isolated from animals, plants as well as venoms of organisms which display potent biological activities[13-15].

NATURALLY OCCURING BIOACTIVE PEPTIDES

(a)Antimicrobial peptides: Antimicrobial Peptides (AMPs) are amphiphilic peptides that can be obtained from a broad spectrum of microbes which are encoded with genes obtained from inherent cells of immune system and serves as first line of defence against invasion of pathogenic organisms. Therapeutic use of amphiphilic peptides has garnered considerable interest recently due to their extensive actions and less probability of inciting resistance. Various membrane inactive peptides with non-damaging-to-membrane mechanisms such as prevention of angiogenesis and stimulation of pathways of apoptosis have been noted for substances such as Pentostatin and Properdistatin[16,17].Antimicrobials according to their structural characteristics are classified into various categories such as cysteine-rich AMPs, β-sheet AMPs (α-defensins and β-defensins), AMPs possessing α-helices (LL-37 Cathelicidin, Cecropins and Magainins), AMPs with elongated confirmation (rich in glycine, proline, tryptophan, arginine, and/or histidine) and peptide loop with a solitary disulfide bond(Bactenecin). A large number of AMPs have positive charges with amphipathic configurations in non-polar solvents. They attach to bacterium cell membranes (negatively charges) through electrostatic connections and thereby disturb their operation leading to demise of these single-celled organisms or these pore-forming peptides can induce either necrosis or apoptosis leading to cellular demise[18,19]. In case of necrotic cell death, the AMPs attacks on the cancerous cell surfaces possessing negatively-charges and cause breakdown of cells whereas in case of programmed cell death (apoptosis) they lead to disturbance of the mitochondrial membranes. Apart from AMPs, some other Peptides with venomous nature such as Melittin and Masteroplans are also reported which causes rupture of both prokaryotic and eukaryotic cell membranes[20-23].

(b)Peptides from plant sources: Various natural peptides derived from plant sources including rice, soy protein, wheat germ protein, chickpeas, mung-bean protein, black soy bean and azuki bean are reported to exert potent carcinogenic actions on a wide range of cancerous cell lines. A research finding has demonstrated the introduction of

five natural biologically active peptides extracted from beans (GEGSGA, GLTSK, MPACGSS, LSGNK and MTEEY) which was found to exert antiproliferative activity on cell lines of human colon cancer (HCT-116, RKO, and KM12L4) via regulation of proliferation of cells, promoting cell cycle arrest and apoptotic cell-death[24]. A biopeptide extracted from chick peashas been found to exhibit anti-proliferative activity in the cell lines of breast cancer (MDA-MB231 and MCF-7) by upregulation of P53 protein expression, regulating the progression of cell cycle and intracellular apoptosis pathways [25]. Peptides namely SSDEEVREEKELDLSSNE and KELPPSDADW obtained from wheat germ protein were evaluated on lung cancer cells(A549). The findings revealed that peptides had promoted the anti-proliferative activity by inducing cytotoxicity to the cancer cells [26]. Papain-hydrolysed mung bean protein yielded some bioactive peptides (Glu-Gly-Ala, Val-Glu-Gly, Leu-Ala-Phe and Pro-Gln-Gly) which were investigated against hepatocellular carcinoma (HepG2) and it was found that the peptides had exerted anticancer activity by induction of apoptosis in hepatocellular carcinoma (HepG2) cells[27]. Another bioactive peptide called Lunasin obtained from soybean and wheat had displayed promising anticancer potential owing to its unique amino acid sequence Arg-Gly-Asp which helps in cellular adherence. It has been widely used as adjuvant therapy for cancer as it can alleviate the occurrence of colorectal, breast and various other cancers. Lunasin has been incorporated into the genome of rice which functions as supplementary food for cancer patients and it is globally recognized as a propitious approach for development of convenient supplement for people affected by cancer[28-30].

(c) Bioactive peptides from animal sources: Two short chain bioactive peptides were derived from the hydrolysate protein of *Tegillarca granosa* which was reported to counteract the surplus production of free radicals within cells in oxidative stress and attenuate the risk of cancer development. Moreover, the peptides also possess noteworthy antiproliferative properties against human prostate (PC-3, DU-145), lung (H-1299) and cervical(HeLa) cancer cell lines[31]. Another source of bioactive peptides namely KT2 and RT2 derived from crocodile were evaluated for anticancer effect on cell lines for cervical cancer(HeLa and CaSki) and it was found that the peptides had caused significant death of the cancer cells[32]. Roe protein obtained from *Epinephelus lanceolatus* also yields some bioactive peptide hydrolysates when broken down using the enzyme protease. The peptides had displayed antiproliferative effects on cell lines of oral cancer (Ca9-22 and CAL 27) via apoptosis and stopping cell cycle progression in sub-G1 phase [33]. Dolastatin 10, a marine derived peptide isolated from molluscs exhibits antineoplastic properties. In a cancer investigation study, it was found that the peptide had displayed antimitotic properties by preventing tubulin polymerization and microtubule growth[34-36]. Another anticancer peptide extracted from the goat liver and spleen (ACPB-3) had demonstrated carcinogenic activity against human gastric cancer cell lines (BGC-823 and GCSCs) by limiting the proliferation of cells [37].One more anticancer peptide(molecular weight 8 kDa) was isolated from spleen of goats which had suppressed the human colon cancer(HCT116) cells proliferation by increasing cancer cell apoptosis viaup regulating poly (ADP-ribose) polymerase (PARP) and p53 expression and down regulation Mcl-1 expression[38].

(d) Bioactive peptides from venoms: Snake, scorpion, spider, honeybee and cone snail venoms possesses peptides which are enriched with chemotherapeutic agents and are used for treatment of variety of human cancers. TsAP-1 and TsAP-2 are peptides found in the venom of *Tityus serrulatus* that have growth-inhibiting properties on adenocarcinoma (NCI-H838) and squamous carcinoma (NCI-H157). Furthermore, TsAP-2 demonstrated three times greater activity than TsAP-1 in prostate cancer (PC-3), breast cancer (MCF-7) and a human glioblastoma (U251) cell line[39].A library of scorpion venom revealed the presence of Gonear restide extracted from *Androctonus mauritanicus*. This peptide had demonstrated potential as an anticancer agent in *in vitro* tests and had proved as an effective approach for various cancers with minimal damage towards erythrocytes and epithelial cells. It had successfully inhibited the growth of cancer cells of colon by targeting the G1 phase of cell cycle [40].In another research study, it was found that Human erythroleukemia K562 cells are cytotoxically affected by the peptide latarcin 2a (Ltc2a) which is extracted from spider venom. The peptide causes cell death by enabling blebbing, swelling and instability of the plasma membrane. Another anticancer bioactive peptide lycosin-1 derived from spider venom interferes with cell signalling pathways and reduces essential protein activities and thus effectively inhibits the growth of cancer cells[41]. Another peptide named as Mastoparan is a class of amphiphilic cationic polypeptides obtained from venom of *Vespula lewisii* possesses anticancer properties. When Mastoparan was delivered specifically

to tumour cells, it had selectively induced mitochondrial permeability transition and destroyed cancer cells while leaving healthy cells unharmed [42]. Mechanisms underlying the activity of naturally derived peptides on cancer cell lines .

Active peptides have acquired considerable significance owing to its positive impact on health of humans. The benefits of active peptides as an alternative medicine include their ability to deeply penetrate tissues because of their small size, lower toxicity, increased permeability and ability to diffuse through cells. Bioactive peptides from various sources with anticancer activity are enlisted below in table no. 1:

PRODUCTION OF BIOACTIVE PEPTIDES

Peptides with biological activity are typically derived from protein sources of either plant, animal, microbes or venoms of organisms and their advantageous effects have been taken into account in a multidimensional research study. A bioactive peptide is obtained through the extraction process from the original protein which can be accomplished via several methods such as enzymatic breakdown, microbial fermentation or digestion in the gastrointestinal tract. The primary approach for obtaining bioactive peptide is through enzymatic hydrolysis as it doesn't yield harmful metabolites and it can mimic digestion of gastrointestinal tract resulting in shorter reaction time. Among the commercially available enzymes, those employed for extracting peptides with antitumor properties include pepsin, flavorzyme, pancreatin, chymotrypsin, trypsin, alcalase and papain[103].Hydrolysis of peptides via enzymes is the most widely adopted method for producing peptides owing to its high specificity, mild reaction conditions, lack of residual organic solvents and toxic chemicals in the end product of peptides. However, the industry is searching for alternatives due to the expensiveness of enzymes, lesser yields and less availability of food-grade enzymes. Novel methods such as higher hydrostatic pressure, ultrasound techniques, ohmic heating, pulsed electric fields, microwave-assisted extractions and subcritical water hydrolysis are being used frequently now a days to prepare bioactive peptides. These technologies are mostly used in conjunction with the enzymatic approach because of their more effectivity than conventional procedures. Due to their environmental friendliness and sustainable properties the inclination towards the production of bioactive peptides using innovative technology is growing significantly[104].

CONCLUSION

Historically organic products have made a tremendous contribution in the field of drug development and pharmacotherapy specifically for treatment of cancer activity. Currently there is a heightened focus on identification of anticancer drugs that are highly effective with minimal toxicity. Biologically active peptides derived from natural sources are believed to exhibit diverse activities including anticancer properties. Increasing evidence suggests that natural bioactive peptides possessing carcinogenic property can induce death of cells by targeting multiple proteins of cells and triggers apoptosis both intracellularly and extracellularly. The review aims to highlight the various naturally isolated peptides obtained from multiple sources and highlights the property, classification and mechanism of action on various cancer cell lines. Therefore, peptides being safer, highly selective, efficacious and well tolerated has garnered interest of patients as a better alternative for cancer therapy and it will help broaden the applicability of bioactive peptides as potent therapeutics for the treatment of unmet medical needs of cancer.

ACKNOWLEDGEMENT

The author is thankful to University of Science and Technology Meghalaya

REFERENCES

1. Poston, G. J. Global cancer surgery: the Lancet Oncology review. Eur J Surg Oncol. 2015, 41,1559-1561.
2. Norouzi, P.; Mirmohammadi, M.; Houshdar Tehrani, M. H. Anticancer peptides mechanisms, simple and complex. Chem Biol Interact. 2022, 368, 110194

3. Sung, H.; Ferlay, J.; Siegel, R. L.; Laversanne, M.; Soerjomataram, I.; Jemal, A.; Bray, F. Global Cancer Statistics 2020: GLOBOCAN estimates of incidence and mortality worldwide for 36 cancers in 185 countries. CA Cancer J Clin. 2021, 71, 209-249
4. Peer D, Karp JM, Hong S, Farokhzad OC, Margalit R and Langer R: Nanocarriers as an emerging platform for cancer therapy. Nat Nanotechnol 2: 751-760, 2007
5. Amit D and Hochberg A: Development of targeted therapy for bladder cancer mediated by a double promoter plasmid expressing diphtheria toxin under the control of H19 and IGF2-P4 regulatory sequences. J Transl Med 8: 134, 2010
6. Kang TH, Mao CP, He L, Tsai YC, Liu K, La V, Wu TC and Hung CF: Tumor-targeted delivery of IL-2 by NKG2D leads to accumulation of antigen-specific CD8+ T cells in the tumor loci and enhanced anti-tumor effects. PLoS One 7: e35141, 2012
7. Witt CM, Balneaves LG, Cardoso MJ, Cohen L, Greenlee H, Johnstone P, Kuc€ uk O, Mailman J, Mao € JJ. A comprehensive definition for integrative oncology. JNCI Monogr. 2017; 2017(52). doi:10.1093/jncimonographs/lgx012
8. Singh BP, Vij S, Hati S. Functional significance of bioactive peptides derived from soybean. Peptides. 2014; 54:171–9.
9. Fields F, Falla TJ, Rodan K, Bush L. Bioactive peptides: signaling the future. J Cosmet Dermatol. 2009; 8(1):8–13. doi:10.1111/j.1473-2165.2009.00416.x
10. Segura-Campos, M., Chel-Guerrero, L., Betancur-Ancona, D., Hernandez-Escalante, V.M., 2011. Bioavailability of bioactive peptides. Food Rev. Int. 27, 213–226.
11. Wang, X., Yu, H., Xing, R., Li, P., 2017b. Characterization, preparation, and purification of marine bioactive Peptides. Biomed Res. Int. 2017
12. Tyagi, A., Tuknait, A., Anand, P., Gupta, S., Sharma, M., Mathur, D., Joshi, A., Singh, S., Gautam, A., Raghava, G.P., 2014. CancerPPD: a database of anticancer Peptides and proteins. Nucleic Acids Res. 43, D837–D843.
13. Wang, L.; Qu, L.; Lin, S.; Yang, Q.; Zhang, X.; Jin, L.; Dong, H.; Sun, D. Biological functions and applications of antimicrobial peptides. Curr Protein Pept Sci. 2022, 23, 226-24 Weinberg, R., Hanahan, D., 2000. The hallmarks of cancer. Cell 100, 57–70.
14. Reddy, P.A., Jones, S.T., Lewin, A.H., Carroll, F., 2012. Synthesis of hemopressin Peptides by classical solution phase fragment condensation. Int. J. Pept. 2012.
15. Koskimaki, J.E., Karagiannis, E.D., Rosca, E.V., Vesuna, F., Winnard Jr., P.T., Raman, V., Bhujwalla, Z.M., Popel, A.S., 2009. Peptides derived from type IV collagen, CXC chemokines, and thrombospondin-1 domain-containing proteins inhibit neovascularization and suppress tumor growth in MDA-MB-231 breast cancer xenografts. Neoplasia (NY) 11, 1285.
16. Li, Y., Xiang, Q., Zhang, Q., Huang, Y., Su, Z., 2012. Overview on the recent study of antimicrobial Peptides. origins, functions, relative mechanisms and application. Peptides 37, 207–215.
17. Lien, S., Lowman, H.B., 2003. Therapeutic peptides. Trends Biotechnol. 21, 556–562.
18. Marr, A.K., Gooderham, W.J., Hancock, R.E., 2006. Antibacterial Peptides for therapeutic use: obstacles and realistic outlook. COPHAR 6, 468–472.
19. Bohmov ¨ a, ´ E., Pola, R., Pechar, M., Parnica, J., Machova, ´ D., Janouˇskov´ a, O., Etrych, T., 2020. Polymer cancer ostatics containing cell-penetrating peptides: internalization efficacy depends on peptide type and spacer length. Pharmaceutics 12, 59. https:// doi.org/10.3390/pharmaceutics12010059
20. He, W., Yan, J., Jiang, W., Li, S., Qu, Y., Niu, F., Yan, Y., Sui, F., Wang, S., Zhou, Y., 2018. Peptide-induced self-assembly of therapeutics into a well-defined nanoshell with tumor-triggered shape and charge switch. Chem. Mater. 30, 7034–7046. https://doi. org/10.1021/acs.chemmater.8b02572.
21. J Boohaker, R., W Lee, M., Vishnubhotla, P., LM Perez, J., R Khaled, A., 2012. The use of therapeutic Peptides to target and to kill cancer cells. Curr. Med. Chem. 19, 3794–3804.
22. Liu, F.-H., Hou, C.-Y., Zhang, D., Zhao, W.-J., Cong, Y., Duan, Z.-Y., Qiao, Z.-Y., Wang, H., 2018. Enzyme-sensitive cytotoxic peptide–dendrimer conjugates enhance cell apoptosis and deep tumor penetration. Biomater. Sci. 6, 604–613.

23. Mirza, A.Z., 2019. Advancement in the development of heterocyclic nucleosides for the treatment of cancer-A review. Nucleosides Nucleotides Nucleic Acids 38, 836–857.
24. Vital DAL, De Mejıa EG, Dia VP, Loarca-Piña G. Peptides in common bean´fractions inhibit human colorectal cancer cells. Food Chem (2014) 157:347–55. doi: 10.1016/j.foodchem.2014.02.050
25. Xue Z, Wen H, Zhai L, Yu Y, Li Y, Yu W, et al. Antioxidant activity and anti-proliferative effect of a bioactive peptide from chickpea (Cicer arietinum L.). Food Res Int (2015) 77:75–81. doi: 10.1016/j.foodres.2015.09.027
26. Karami Z, Peighambardoust SH, Hesari J, Akbari-Adergani B, Andreu D. Antioxidant, anticancer and ACE-inhibitory activities of bioactive peptides from wheat germ protein hydrolysates. Food Bioscience (2019) 32:100450. doi: 10.1016/ j.fbio.2019.100450
27. Li M, Zhang Y, Xia S, Ding X. Finding and isolation of novel peptides with antiproliferation ability of hepatocellular carcinoma cells from mung bean protein hydrolysates. J Funct Foods (2019) 62:103557. doi: 10.1016/j.jff.2019.103557
28. Fernández-Tomé S , Xu F , Han Y , Hernández-Ledesma B, Xiao H. Inhibitory effects of peptide lunasin in colorectal cancer HCT-116 cells and their tumorspherederived subpopulation. Int J Mol Sci (2020) 21:537. doi: 10.3390/ijms21020537
29. Hsieh C-C, Wang C-H, Huang Y-S. Lunasin attenuates obesity-associated metastasis of 4T1 breast cancer cell through anti-inflammatory property. Int J Mol Sci (2016) 17:2109. doi: 10.3390/ijms17122109
30. Ren G, Hao Y, Zhu Y, Shi Z, Zhao G. Expression of bioactive lunasin peptide in transgenic rice grains for the application in functional food. Molecules (2018) 23:2373. doi: 10.3390/molecules23092373
31. Chi CF, Hu FY, Wang B, Li T, Ding GF. Antioxidant and anticancer peptides from the protein hydrolysate of blood clam (Tegillarca granosa) muscle. J Funct Foods (2015) 15:301–13. doi: 10.1016/j.jff.2015.03.045
32. Theansungnoen T, Maijaroen S, Jangpromma N, Yaraksa N, Daduang S, Temsiripong T, et al. Cationic antimicrobial peptides derived from crocodylus siamensis leukocyte extract, revealing anticancer activity and apoptotic induction on human cervical cancer cells. Protein J (2016) 35:202–11. doi: 10.1007/s10930-016-9662-1
33. Yang JI, Tang JY, Liu YS, Wang HR, Lee SY, Yen CY, et al. Roe protein hydrolysates of giant grouper (Epinephelus lanceolatus) inhibit cell proliferation of oral cancer cells involving apoptosis and oxidative stress. BioMed Res Int (2016) 2016:8305073. doi: 10.1155/2016/8305073
34. Gentilucci L, Tolomelli A, Squassabia F. Peptides and peptidomimetics in medicine, surgery and biotechnology. Curr Med Chem (2006) 13:2449–66. doi: 10.2174/092986706777935041
35. Simmons TL, Andrianasolo E, McPhail K, Flatt P, Gerwick WH. Marine natural products as anticancer drugs. Mol Cancer Ther (2005) 4:333–42. doi: 10.1158/1535- 7163.333.4.2
36. Donia M, Hamann MT. Marine natural products and their potential applications as anti-infective agents. Lancet Infect Dis (2003) 3:338–48. doi: 10.1016/S1473-3099(03) 00655-8
37. Yu L, Yang L, An W, Su X. Anticancer bioactive peptide-3 inhibits human gastric cancer growth by suppressing gastric cancer stem cells. J Cell Biochem (2014) 115:697– 711. doi: 10.1002/jcb.24711
38. Su L-Y, Shi Y-X, Yan M-R, Xi Y, Su X-L. Anticancer bioactive peptides suppress human colorectal tumor cell growth and induce apoptosis via modulating the PARP-p53-Mcl-1 signaling pathway. Acta Pharmacologica Sin (2015) 36:1514–9. doi: 10.1038/ aps.2015.80
39. Guo X, Ma C, Du Q, Wei R, Wang L, Zhou M, et al. Two peptides, TsAP-1 and TsAP-2, from the venom of the Brazilian yellow scorpion, Tityus serrulatus: evaluation of their antimicrobial and anticancer activities. Biochimie (2013) 95:1784–94. doi: 10.1016/j.biochi.2013.06.003
40. Li B, Lyu P, Xi X, Ge L, Mahadevappa R, Shaw C, et al. Triggering of cancer cell cycle arrest by a novel scorpion venom-derived peptide-Gonearrestide. J Cell Mol Med (2018) 22:4460–73. doi: 10.1111/jcmm.13745
41. Liu Z, Deng M, Xiang J, Ma H, Hu W, Zhao Y, et al. A novel spider peptide toxin suppresses tumor growth through dual signaling pathways. Curr Mol Med (2012) 12:1350–60. doi: 10.2174/156652412803833643
42. Yoon KA, Kim K, Nguyen P, Seo JB, Park YH, Kim K-G, et al. Comparative bioactivities of mastoparans from social hornets Vespa crabro and Vespa analis. J AsiaPacific Entomology (2015) 18:825–9. doi: 10.1016/j.aspen.2015.10.006
43. Yu, L., Yang, L., An, W., Su, X., 2014. Anticancer bioactive peptide-3 inhibits human gastric cancer growth by suppressing gastric cancer stem cells. J. Cell. Biochem. 115, 697–711.

44. Luesch, H., Yoshida, W.Y., Moore, R.E., Paul, V.J., Corbett, T.H., 2001. Total structure determination of apratoxin a, a potent novel cytotoxin from the marine cyanobacterium Lyngbya m ajuscula. J. Am. Chem. Soc. 123, 5418–5423.
45. Dennison, S.R., Harris, F., Phoenix, D.A., 2007. The interactions of aurein 1.2 with cancer cell membranes. Biophys. Chem. 127, 78–83.
46. Marcotte, I., Wegener, K.L., Lam, Y.-H., Chia, B.C., de Planque, M.R., Bowie, J.H., Auger, M., Separovic, F., 2003. Interaction of antimicrobial Peptides from Australian amphibians with lipid membranes. Chem. Phys. Lipids 122, 107–120.
47. Rozek, T., Wegener, K.L., Bowie, J.H., Olver, I.N., Carver, J.A., Wallace, J.C., Tyler, M.J., 2000. The antibiotic and anticancer active aurein Peptides from the Australian bell frogs Litoria aurea and Litoria raniformis: the solution structure of aurein 1.2. Eur. J. Biochem. 267, 5330–5341.
48. Han, B., Gross, H., Goeger, D.E., Mooberry, S.L., Gerwick, W.H., 2006. Aurilides B and C, cancer cell toxins from a Papua New Guinea collection of the marine cyanobacterium Lyngbya m ajuscula. J. Nat. Prod. 69, 572–575.
49. Tao, Y.-w., Lin, Y.-c., She, Z.-g., Lin, M.-t., Chen, P.-x., Zhang, J.-y., 2015. Anticancer activity and mechanism investigation of beauvericin isolated from secondary metabolites of the mangrove endophytic fungi. Curr. Med. Chem.-Anti-Cancer Agents 15, 258–266.
50. Hemscheidt, T., Puglisi, M.P., Larsen, L.K., Patterson, G.M., Moore, R.E., Rios, J.L., Clardy, J., 1994. Structure and biosynthesis of borophycin, a new boeseken complex of boric acid from a marine strain of the blue-green alga Nostoc linckia. J. Org. Chem. 59, 3467–3471.
51. Nowruzi, B., Blanco, S., Nejadsattari, T., 2018a. Chemical and molecular evidences for the poisoning of a duck by Anatoxin-a, Nodularin and Cryptophycin at the coast of Lake Shoormast (Mazandaran Province, Iran). Int. J. Algae 20. https://doi.org/ 10.1615/InterJAlgae.v20.i4.30.
52. Eliassen, L.T., Berge, G., Leknessund, A., Wikman, M., Lindin, I., Løkke, C., Ponthan, F., Johnsen, J.I., Sveinbjørnsson, B., Kogner, P., 2006. The antimicrobial peptide, lactoferricin B, is cytotoxic to neuroblastoma cells in vitro and inhibits xenograft growth in vivo. Int. J. Cancer 119, 493–500.
53. Liu, Y.; Tavana, O.; Gu, W. p53 modifications: exquisite decorations of the powerful guardian. J Mol Cell Biol. 2019, 11, 564-577.
54. Li, B.; Lyu, P.; Xie, S.; Qin, H.; Pu, W.; Xu, H.; Chen, T.; Shaw, C.; Ge, L.; Kwok, H. F. LFB: A Novel Antimicrobial Brevinin-Like Peptide from the Skin Secretion of the Fujian Large Headed Frog, Limnonectes fujianensi. Biomolecules. 2019, 9, 242.
55. Zahedifard, F.; Lee, H.; No, J. H.; Salimi, M.; Seyed, N.; Asoodeh, A.; Rafati, S. Anti-leishmanial activity of Brevinin 2R and its Lauric acid conjugate type against L. major: In vitro mechanism of actions and in vivo treatment potentials. PLoS Negl Trop Dis. 2019, 13, e0007217.
56. Emelianova, A.A., Kuzmin, D.V., Panteleev, P.V., Sorokin, M., Buzdin, A.A., Ovchinnikova, T.V., 2018. Anticancer activity of the goat antimicrobial peptide ChMAP-28. Front. Pharmacol. 9, 1501.
57. Xia, L., Wu, Y., Ma, J., Yang, J., Zhang, F., 2016. The antibacterial peptide from Bombyx mori cecropinXJ induced growth arrest and apoptosis in human hepatocellular carcinoma cells. Oncol. Lett. 12, 57–62.
58. Chen, Z., Song, Y., Chen, Y., Huang, H., Zhang, W., Ju, J., 2012. Cyclic heptapeptides, cordyheptapeptides C–E, from the marine-derived fungus Acremonium persicinum SCSIO 115 and their cytotoxic activities. J. Nat. Prod. 75, 1215–1219.
59. Isaka, M., Srisanoh, U., Lartpornmatulee, N., Boonruangprapa, T., 2007. ES-242 derivatives and cycloheptaPeptides from Cordyceps sp. Strains BCC 16173 and BCC 16176. J. Nat. Prod. 70, 1601–1604.
60. Li, B., Gao, M.H., Zhang, X.C., Chu, X.M., 2006a. Molecular immune mechanism of Cphycocyanin from Spirulina platensis induces apoptosis in HeLa cells in vitro. Biotechnol. Appl. Biochem. 43, 155–164.
61. Nowruzi, B., Blanco, S., Nejadsattari, T., 2018a. Chemical and molecular evidences for the poisoning of a duck by Anatoxin-a, Nodularin and Cryptophycin at the coast of Lake Shoormast (Mazandaran Province, Iran). Int. J. Algae 20.
62. Lai, J.-Y., Yu, J., Mekonnen, B., Falck, J., 1996. Synthesis of curacin A, an antimitotic cyclopropane-thiazoline from the marine cyanobacterium Lyngbya majuscula. Tetrahedron Lett. 37, 7167–7170.

63. Torres, M.D., Andrade, G.P., Sato, R.H., Pedron, C.N., Manieri, T.M., Cerchiaro, G., Ribeiro, A.O., de la Fuente-Nunez, C., Oliveira Jr., V.X., 2018. Natural and redesigned wasp venom Peptides with selective antitumoral activity. Beilstein J. Org. Chem. 14, 1693–1703.
64. Fruitwala, S.; El-Naccache, D. W.; Chang, T. L. Multifaceted immune functions of human defensins and underlying mechanisms. Semin Cell Dev Biol. 2019, 88, 163-172.
65. Liu, S.; Zhou, L.; Li, J.; Suresh, A.; Verma, C.; Foo, Y. H.; Yap, E. P.; Tan, D. T.; Beuerman, R. W. Linear analogues of human betadefensin 3: concepts for design of antimicrobial peptides with reduced cytotoxicity to mammalian cells. ChemBioChem. 2008, 9, 964-973.
66. Huang, L., Chen, D., Wang, L., Lin, C., Ma, C., Xi, X., Chen, T., Shaw, C., Zhou, M., 2017. Dermaseptin-ph: a novel peptide with antimicrobial and anticancer activities from the skin secretion of the south american orange-legged leaf frog, pithecopus (phyllomedusa) hypochondrialis. Molecules 22, 1805. https://doi.org/10.3390/ molecules22101805.
67. Simmons, T.L., Nogle, L.M., Media, J., Valeriote, F.A., Mooberry, S.L., Gerwick, W.H., 2009. Desmethoxymajusculamide C, a cyanobacterial depsipeptide with potent cytotoxicity in both cyclic and ring-opened forms. J. Nat. Prod. 72, 1011–1016.
68. Lachia, M., Moody, C.J., 2008. The synthetic challenge of diazonamide A, a macrocyclic indole bis-oxazole marine natural product. Nat. Prod. Rep. 25, 227–253.
69. Tokuda, H., Nishino, H., Shirahashi, H., Murakami, N., Nagatsu, A., Sakakibara, J., 1996. Inhibition of 12-O-tetradecanoylphorbol-13-acetate promoted mouse skin papilloma by digalactosyl diacylglycerols from the fresh water cyanobacterium Phormidium tenue. Cancer Lett. 104, 91–95.
70. Zahedifard, F.; Lee, H.; No, J. H.; Salimi, M.; Seyed, N.; Asoodeh, A.; Rafati, S. Anti-leishmanial activity of Brevinin 2R and its Lauric acid conjugate type against L. major: In vitro mechanism of actions and in vivo treatment potentials. PLoS Negl Trop Dis. 2019, 13, e0007217.
71. Zhu, Y., Cheng, J., Min, Z., Yin, T., Zhang, R., Zhang, W., Hu, L., Cui, Z., Gao, C., Xu, S., 2018. Effects of fucoxanthin on Autophagy, and apoptosis in SGC-7901cells and the mechanism. J. Cell. Biochem. 119, 7274–7284.
72. Jeyamogan, S.; Khan, N. A.; Sagathevan, K.; Siddiqui, R. Sera/organ lysates of selected animals living in polluted environments exhibit cytotoxicity against cancer cell lines. Anticancer Agents Med Chem. 2019, 19, 2251-2268.
73. Stratmann, K., Burgoyne, D.L., Moore, R.E., Patterson, G.M., Smith, C.D., 1994. Hapalosin, a cyanobacterial cyclic depsipeptide with multidrug-resistance reversing activity. J. Org. Chem. 59, 7219–7226.
74. Lai, W.-T., Cheng, K.-L., Baruchello, R., Rondanin, R., Marchetti, P., Simoni, D., Lee, R. M., Guh, J.-H., Hsu, L.-C., 2016. Hemiasterlin derivative (R)(S)(S)-BF65 and Akt inhibitor MK-2206 synergistically inhibit SKOV3 ovarian cancer cell growth. Biochem. Pharmacol. 113, 12–23
75. Hassana, M.A.-k., Azeminb, W.-A., Dharmaraja, S., Mohdb, K.S., 2016. Hepcidin TH1-5 induces apoptosis and activate Caspase-9 in MCF-7 cells. J. Appl. Pharm. Sci. 6, 081–086.
76. Chang, W.-T., Pan, C.-Y., Rajanbabu, V., Cheng, C.-W., Chen, J.-Y., 2011. Tilapia (Oreochromis mossambicus) antimicrobial peptide, hepcidin 1–5, shows antitumor activity in cancer cells. Peptides 32, 342–352. https://doi.org/10.1016/j. peptides.2010.11.003.
77. Chen, J.-Y., Lin, W.-J., Lin, T.-L., 2009. A fish antimicrobial peptide, tilapia hepcidin TH2-3, shows potent antitumor activity against human fibrosarcoma cells. Peptides 30, 1636–1642.
78. Cioca, D., Kitano, K., 2002. Induction of apoptosis and CD10/neutral endopeptidase expression by jaspamide in HL-60 line cells. Cell Mol. Life Sci. CMLS 59, 1377–1387.
79. Patathananone, S., Thammasirirak, S., Daduang, J., Chung, J.G., Temsiripong, Y., Daduang, S., 2016. Bioactive compounds from crocodile (Crocodylus siamensis) white blood cells induced apoptotic cell death in hela cells. Environ. Toxic 31, 986–997.
80. Theansungnoen, T., Maijaroen, S., Jangpromma, N., Yaraksa, N., Daduang, S., Temsiripong, T., Daduang, J., Klaynongsruang, S., 2016. Cationic antimicrobial Peptides derived from Crocodylus siamensis leukocyte extract, revealing anticancer activity and apoptotic induction on human cervical cancer cells. Protein J. 35, 202–211.

81. Theansungnoen, T., Maijaroen, S., Jangpromma, N., Yaraksa, N., Daduang, S., Temsiripong, T., Daduang, J., Klaynongsruang, S., 2016. Cationic antimicrobial Peptides derived from Crocodylus siamensis leukocyte extract, revealing anticancer activity and apoptotic induction on human cervical cancer cells. Protein J. 35, 202–211.
82. Li, J., Xue, Y., Yuan, J., Lu, Y., Zhu, X., Lin, Y., Liu, L., 2016a. Lasiodiplodins from mangrove endophytic fungus Lasiodiplodia sp. 318#. Nat. Prod. Res. 30, 755–760.
83. Aghazadeh, H.; Memariani, H.; Ranjbar, R.; Pooshang Bagheri, K. The activity and action mechanism of novel short selective LL-37-derived anticancer peptides against clinical isolates of Escherichia coli. Chem Biol Drug Des. 2019, 93, 75-83
84. Abedin, M., Wang, D., McDonnell, M., Lehmann, U., Kelekar, A., 2007. Autophagy delays apoptotic death in breast cancer cells following DNA damage. Cell Death Differ. 14, 500–510.
85. Gu, W., Cueto, M., Jensen, P.R., Fenical, W., Silverman, R.B., 2007. Microsporins A and B: new histone deacetylase inhibitors from the marine-derived fungus Microsporum cf. Gypseum and the solid-phase synthesis of microsporin A. Tetrahedron 63, 6535–6541.
86. Sun, H.-X., Chen, L.-Q., Zhang, J., Chen, F.-Y., 2014. Anti-tumor and immunomodulatory activity of peptide fraction from the larvae of Musca domestica. J. Ethnopharmacol. 153, 831–839.
87. Wijesekara, I., Li, Y.-X., Vo, T.-S., Van Ta, Q., Ngo, D.-H., Kim, S.-K., 2013. Induction of apoptosis in human cervical carcinoma HeLa cells by neoechinulin A from marinederived fungus Microsporum sp. Process Biochem. 48, 68–72.
88. Chen, X.; Zhang, L.; Ma, C.; Zhang, Y.; Xi, X.; Wang, L.; Zhou, M.; Burrows, J. F.; Chen, T. A novel antimicrobial peptide, Ranatuerin2PLx, showing therapeutic potential in inhibiting proliferation of cancer cells. Biosci Rep. 2018, 38, BSR20180710.
89. Leisch, M., Egle, A., Greil, R., 2019. Plitidepsin: a potential new treatment for relapsed/ refractory multiple myeloma. Future Oncol. 15, 109–120. https://doi.org/10.2217/ fon-2018-0492.
90. Zhou, S.-l., Wang, M., Zhao, H.-g., Huang, Y.-h., Lin, Y.-y., Tan, G.-h., Chen, S.-l., 2016. Penicilazaphilone C, a new antineoplastic and antibacterial azaphilone from the Marine Fungus Penicillium sclerotiorum. Arch. Pharm. Res. 39, 1621–1627.
91. Tornesello, A. L.; Borrelli, A.; Buonaguro, L.; Buonaguro, F. M.; Tornesello, M. L. Antimicrobial peptides as anticancer agents: functional properties and biological activities. Molecules. 2020, 25, 2850.
92. Yu, Z., Lang, G., Kajahn, I., Schmaljohann, R., Imhoff, J.F., 2008. Scopularides A and B, cyclodepsiPeptides from a marine sponge-derived fungus, Scopulariopsis brevicaulis. J. Nat. Prod. 71, 1052–1054.
93. Liang, X., Zhang, X.-Y., Nong, X.-H., Wang, J., Huang, Z.-H., Qi, S.-H., 2016. Eight linear Peptides from the deep-sea-derived fungus Simplicillium obclavatum EIODSF 020. Tetrahedron 72, 3092–3097.
94. Chen, Y., Xu, X., Hong, S., Chen, J., Liu, N., Underhill, C.B., Creswell, K., Zhang, L., 2001. RGD-Tachyplesin inhibits tumor growth. Cancer Res. 61, 2434–2438.
95. Erba, E., Bergamaschi, D., Ronzoni, S., Faretta, M., Taverna, S., Bonfanti, M., Catapano, C., Faircloth, G., Jimeno, J., D'incalci, M., 1999. Mode of action of thiocoraline, a natural marine compound with anti-tumour activity. Br. J. Cancer 80, 971–980.
96. Lam, Y., Ng, T., Wang, H., 2001. Antiproliferative and antimitogenic activities in a peptide from puffball mushroom Calvatia caelata. Biochem. Biophys. Res. Commun. 289, 744–749.
97. Zhang, P., Xiao-Ming, L., Xin-Xin, M., Attila, M., Tibor, K., Bin-Gui, W., 2018. Correction: varioloid A, a new indolyl-6, 10b-dihydro-5aH-[1] benzofuro [2, 3-b] indole derivative from the marine alga-derived endophytic fungus Paecilomyces variotii EN-291. Beilstein J. Org. Chem. 14, 2394–2395.
98. Zhou, L.N., Gao, H.Q., Cai, S.X., Zhu, T.J., Gu, Q.Q., Li, D.H., 2011. Two new cyclic PentaPeptides from the marine-derived fungus Aspergillus versicolor. Helv. Chim. Acta 94, 1065–1070.
99. Carroll, A.R., Feng, Y., Bowden, B.F., Coll, J.C., 1996. Studies of Australian ascidians. 5. Virenamides A− C, new cytotoxic linear peptides from the colonial didemnid ascidian Diplosoma virens. J. Org. Chem. 61, 4059–4061.
100. Edler, M.C., Fernandez, A.M., Lassota, P., Ireland, C.M., Barrows, L.R., 2002. Inhibition of tubulin polymerization by vitilevuamide, a bicyclic marine peptide, at a site distinct from colchicine, the vinca alkaloids, and dolastatin 10. Biochem. Pharmacol. 63, 707–715.

101. Oh, D.-C., Jensen, P.R., Fenical, W., 2006. Zygosporamide, a cytotoxic cyclic depsipeptide from the marine-derived fungus Zygosporium masonii. Tetrahedron Lett. 47, 8625–8628.
102. Chalamaiah M, Yu W, Wu J. Immunomodulatory and anticancer protein hydrolysates (peptides) from food proteins: A review. Food Chem. 2018; 245: 205–22.
103. Lee, H. T.; Lee, C. C.; Yang, J. R.; Lai, J. Z.; Chang, K. Y. A large-scale structural classification of antimicrobial peptides. Biomed Res Int. 2015, 2015, 475062.
104. Ulug SK, Jahandideh F, Wu J. Novel technologies for the production of bioactive peptides. Trends in Food Science & Technology. 2021 Feb 1;108:27-39.3(19):2221-32.

Table 1: Naturally occurring peptides with their mechanism of action for various cancer types on cell lines.

Source	Peptides	Mechanism	Cancer type	Cancer cell line	References
Goat livers or spleens	ACPB	Inhibits the growth of HCT116 cell lines, promotes UV-induced apoptosis, enhances the expression levels of PARP and p53 and downregulates the expression of Mcl-1.	Human colorectal tumour cell line	GCSCs, BGC-823, CD44+, HCT116	[43,44]
Lyngbyaboulloni	Apratoxin A	Arrests cells cycle	Cervical cancer	HeLa	[45]
Litoria aureaand Litoriaraniformis	Aurein 1.2	Interactswith T98G cells membrane lipid	Glioblastoma multiforme	T98G	[46-48]
Japanesesea hare,Dollabellaauricularia, marine cyanobacterium,Lyngbyam ajuscula	Aurilide	Apoptosis and cytotoxicity	NA	NCI-H460	[49]
Fusarium sp.	Beauvericin	Inhibits growth and induces apoptosis	Human epidermoid carcinoma	KB	[50]
Nostoc linckia and Streptomyces griseus	Borophycin	Cytotoxicity	Epidermoid carcinoma, colorectal adenocarcinoma	KB&LoVo	[51,52]
Bovine/Bos Taurus	Bovin Lactoferricin	Induce apoptosis	Leukemic and neuroblastoma	Meth A	[53]
Limnonectesfujianensis	Brevinin	Penetrating into the lipidic bilayer	Lungcancer, glioblastoma, colon cancer, melanoma	U251MG,MDA-MB-231, HCT116, A549,SW480, H460, B16-F10, SMMC7721	[54]
Rana ridibunda	Brevinin 2R	Lysosomal pathway and autophagy-like	Breast adenocarcino	HeLa, MCF-7,	[55]

		cell damage	ma and lung carcinoma	A549	
Bufobufogargarizans	Buforin IIb	Mitochondrial apoptosis	Leukaemia, breast, prostate, and colon cancer	hepG2, DU145, MDA-MB-231, PC-3, MCF-7.	[56]
Caprahircus	ChMAP-28	Cytotoxicity	NA	A431, HL-60, HEK 293 T, HEF, SKBR-3, NHA	[57]
Bombyx mori	CecropinXJ	Growth Inhibition	Urinary bladder cancer, fibrosarcoma, gastric carcinoma, HCC, leukaemia	Huh-7	[58]
Acremonium persicinum	Cordyheptapeptide	Cytotoxic activity	Small cell lung cancer, Oral human epidermoid carcinoma, breast cancer	SF-268, NCI-H460, MCF-7	[59,60]
Spirulina platensis	C-phycocyanin(C-PC)	Apoptosis induction	NA	HeLa cells	[61]
Nostoc sp. ATCC 53789, Nostoc sp. GSV 224	Cryptophycin-52	Disruption of function and integrity of tubulin	Human solid tumours	Human tumour cell lines	[62]
Lyngbyamajuscule	Curacin A	Tubulin polymerization inhibition by attachment at colchicine site	NA	L1210	[63]
Oreumenesdecoratus	Decoralin (Dec-NH2)	Necrotic death of MCF-7 cells	Breast cancer	MCF-7	[64]
Homo sapiens	α-Defensins	Cytolytic activity	Human myeloid leukaemia cell line	U937, HCT-116, MCF-7, A549, PC-3, HeLa	[65]
Homo sapiens	β-Defensin-3	Binding to cell membrane to cause cytolysis	Several cancers	HCT-116, MCF-7, A549, PC-3, HeLa, U937	[66]
Pithecopus	Dermaseptin- PH	Disruption of	Several cancers	H157, MCF-	[67]

(Phyllomedusa) hypochondrialis		permeability function of cell membrane		7, MDA-MB-435S, U251MG, PC-3	
Cyanobacteria/ Lyngbyamajuscula	Desmethoxymajuscu lamide C (DMMC)	Actin depolymerization	Human colon cancer	HCT-116	[68]
AscidianDiazona chinensis	Diazonamide A	Inhibition polymerization of tubulin,blocks cell division	Human cervical carcinoma, osteosarcoma	HeLa cell	[69]
Phormidium tenue	Digalactosyl diacylglycerols (DGDGs)	Inhibition of TPA induced cancer growth	Breast cancer	NA	[70,71]
Brown seaweeds	Fucoxanthin	Apoptosis via up-regulation of beclin-1, LC3, down regulation of Bcl-2	Gastric cancer	SGC7901	[72]
Acanthoscurriagomesiana	Gomesin	Carpet model induced membrane destruction	Melanoma and leukaemia	PC-3, MDA-MB-231	[73]
Hapalosiphonwelwitschii	Hapalosin	Increases the activity ofTaxol and Vinblastine in P-glycoproteinoverexp ressing cells	Ovarian cancer	SKVLB1	[74]
Marine sponges	Hemiasterlins	Inhibition of microtubule assembly, cell cycle arrest, Apoptosis	Ovarian cancer	SKOV3	[75]
Mozambique Tilapia (Oreochromis mossambicus)	Hepcidin	Apoptosis induction	Cervical,liver, breast cancer	HeLa, HepG2, MCF-7	[76-78]
Jaspis stellifera	Jaspamide (Jasplakinolide) KT2 and RT2	Activation of Caspase-3, downregulation of Bcl-2, polymerization of Actin, Apoptosis.	Prostate cancer, human promyelocytic leukaemia	HL-60, U937, THP-1	[79]
Crocodylussiamensis	KT2 and RT2	Upregulates TRAIL R2, Fas, TNF RI.	NA	HeLa	[80,81]
Marine mollusk/ Elysia rufescens	Kahalalide F (KF)	Infringement of mitochondrial and lysosomal membrane	Ovarian, prostate, breast, colon,liver tumour	NSCLC	[82]
Mangroveendophytic fungus / Lasiodiplodia species	Lasiodiplodin	Cytotoxicity	Human cancer	THP1, A549, HCT-116, MDa-MB-435,	[83]

				HepG2, THP1	
Humans/ Homo sapiens	LL-37	Toroidal pore mechanism	Oral squamous carcinoma	PC-3, MCF-7, HT-29	[84]
Xenopus laevis	Magainin	Apoptosis	Human cervical carcinoma	HeLa	[85]
Microsporum cf. gypseum	Microsporins A& B	Histone deacetylase degradation	Human colon adenocarcinoma	HCT-116	[86]
Musca domestica	MDPF	Inhibition of cell by damaging Th1-based protective cell-mediated immunity.	Sarcoma cancer	S180	[87]
Microsporum sp., Aspergillus sp., Eurotium rubrum	Neoechinulin A	Apoptosis via down-regulation of Bcl-2, up-regulation of expression ofBax and activation of the caspase-3 pathway	Cervical cancer	HeLa	[88]
Phyllomedussabicolor	Phylloseptin-PH	Penetrating into the lipidic bilayer	Breast cancer	HeLa, MCF-7, A549	[89]
Tunicate / Applidium albicans	Plitidepsin	Cell-cycle arrest, Apoptosis	breast, thyroid, lung cancer	PC12, HeLa cell, MDA-MB-231	[90]
Penicillium sclerotiorum M-22	Penicilazaphilones B& C	Cytotoxicity	Skin cancer, gastric cancer	B-16, SGC-7901, M-10.	[91]
Hoplobatrachustigerinus	Ranatuerin-2PLx	Cell apoptosis	Prostate cancer cell	PC-3	[92]
Scopulariopsisbrevicauli	Scopularide A& B	Growth inhibition	Pancreas, colon tumour	Colo357, Panc89, HT29	[93]
Simplicilliumobclavatum EIODSF 020	Simplicilliumtides A, G, E& H	Cytotoxicity	Human leukaemia	HL-60, K562	[94]
Tachypleustridentatus	Tachyplesin	Plasma membrane disruption via lipid interaction	Melanoma,Prostate, endothelial cancer	TSU (prostate), B16 (melanoma)	[95]
Micromonospora marina	Thiocoraline	Arresting cell cycles G1 phase, decreasing rate of progression of S phase towards G2/M phases	LoVo, SW620	NA	[96]
Calvatia caelata	Ubiquitin-like peptide	Inhibition of ribonuclease and translation process	Breast cancer	Splenocytes	[97]
Paecilomycesvariotii EN-291	Varioloid A, B	Cytotoxicity	Lung, colon, hepatoma	A549, HCT116,	[98]

			cancer	HepG2	
Aspergillus versicolor (ZLN-60)	Versicotides A, B	Cytotoxicity	NA	P388	[99]
Diplosoma virens, Didemnumcuculiferum, Polysyncrantonlithostrotum	Virenamides A–C	Degradation of the activity of topoisomerase II enzyme	NA	P388, HT29, CV1, A549	[100]
Diplosoma virens, /Didemnumcuculiferum, Polysyncrantonlithostrotum	Vitilevuamide	Arresting the polymerization of tubulin	Lymphocytic leukaemia	P388	[101]
Fungi / Zygosporiummasonii	Zygosporamide	Cytotoxicity	CNS, renal cancer	NCI60, SF-268 RXF 393	[102]

RESEARCH ARTICLE

On The Diophantine Equation $\eta^{\alpha}+11^{\beta}=\gamma^{2}$, Where $\eta \equiv 2(\mathrm{mod}\ 33)$ and $\eta+1$ is a Square Free Number

Janaki G[1] and Gowri Shankari A[2]*

[1]Associate Professor, PG and Research Department of Mathematics, Cauvery College for Women (Autonomous), (Affiliated to Bharathidasan University), Tiruchirappalli, Tamil Nadu, India.
[2]Assistant Professor, PG and Research Department of Mathematics, Cauvery College for Women (Autonomous), (Affiliated to Bharathidasan University), Tiruchirappalli, Tamil Nadu, India.

Received: 23 Aug 2024 Revised: 12 Oct 2024 Accepted: 31 Dec 2024

***Address for Correspondence**
Gowri Shankari A
Assistant Professor,
PG and Research Department of Mathematics,
Cauvery College for Women (Autonomous),
(Affiliated to Bharathidasan University),
Tiruchirappalli, Tamil Nadu, India.
E.Mail: gowrirajinikanth@gmail.com

ABSTRACT

In this research paper, Diophantine equation has been explored $\eta^{\alpha}+11^{\beta}=\gamma^{2}$ has only one solution $(\eta,\alpha,\beta,\gamma)=(2,3,0,3)$, where η is a positive integer with $\eta \equiv 2(\mathrm{mod}33)$ and $\eta+1$ is not square free number. Also α,β,γ are the defined non-negative integers.

Keywords: Catalan conjecture, Congruence, Diophantine equation, Exponential Diophantine equation.
2010 Mathematics Subject Classification: 11D61

INTRODUCTION

Non-negative solutions has been addressed by many arithmeticians (x, y, and z) for Diophantine equations in the frame $a^x+ b^y = z^2$, Here, the values for a and b are fixed [1-3]. The Catalan conjecture solves multitudinously exponential Diophantine equations [4 & 5]. In 2011, A few non-negative solutions to the diophantine equation $2^x+ p^y = z^2$, were given by Suvarnamani [6], here in this equation p defines an odd prime. In the year of 2013, Sroysang [7] demonstrated that $(x, y, z) = (3, 0, 3)$ is the non-negative solution of the diophantine equation $2^x+ 19^y= z^2$. In 2020, Burshtein [8] identified all positive integer solutions to the diophantine equations $13^x - 5^y = z^2$ and $19^x -5^y = z^2$. In 2023, Tadee [9] researched the diophantine equations $9^x- 3^y = z^2$ and $13^x - 7^y = z^2$. T he diophantine equation $5^x - 3^y = z^2$

has all non-negative integer solutions, according to Thongnak and colleagues [10]. Tangjai and another author [11] demonstrated in 2021 that *(p, x, y, z) = (2, 0, 3, 3)* is a not a negative integer solution to the diophantine equation represented as $3^x+p^y=z^2$, where *p* is the prime, $p \equiv 2 \pmod 3$, and y cannot be divided by 4. Borah and Dutta [12] explored the exponential Diophantine equations, specifically those of the type $n^x + 24^y = z^2$, for $n \equiv 5 \text{ or } 7 \pmod 8$. It is of special interest to note that the equation $5^x + 24^y = z^2$ possesses a distinct positive integral solution, (2,1,7). Riemel T [13] proved that there exists a unique solution for exponential diophantine equations of the type $x^m - 1 = 2^n + 24^{k+2}$, as an odd positive integer, x, and $x-1 = 2^{2k+1}$, *k* is a non-negative integer, where, *m* and *n* are exponents looking as unknowns in the equation. The solution provided has the form *(m, n) = (2, 2k + 2)*. According to Janaki G. and Gowri Shankari A [14], the exponential diophantine equation $2^a+n^{2b} =c^2$, with *n = 1, 2, 3,...,* and *a, b, and c* all not a negative integers, has a unique solution in the form of (a, b, c) = (3, 0, 3). As per [15], the exponential equation of the following form $(n^2-1)^u+n^{2v}=w^2$, with n=2,3,4,5 has only one solution (1,0,n). This article highlights all non-negative solutions to the Diophantine equation $\eta^\alpha +11^\beta = \gamma^2$, where η is a not a negative integer and $\eta \equiv 2(\text{mod}33)$ and $\eta + 1$ is a square free number.

MATERIALS AND METHODS

PRELIMINARIES

Preposition 2.1(Catalan's conjecture): Diophantine equation $a^x-b^y=1$ *has a unique solution (a, b, x, y) = (3, 2, 2, 3),* Here *a, b, x* and *y* represents the integers with $min\{a,b,x,y\}>1$.
Further, let's look at three lemmas derived from the above-mentioned theorem by the Catalan.

Lemma 2.1: If η is an integer in such a way that $\eta \equiv 2(\text{mod}33)$ then $\eta \equiv 2(\text{mod}3)$ or $\eta \equiv 2(\text{mod}11)$.

Proof: Let η be an integer in such a way that $\eta \equiv 2(\text{mod}33)$ then $\eta - 2 = 33\tau$ for some integer τ. Thus $\eta - 2 = 3(11\tau)$ or $\eta - 2 = 11(3\tau)$. Hence $\eta \equiv 2(\text{mod}3)$ or $\eta \equiv 2(\text{mod}11)$.

Lemma 2.2: [2] The Diophantine equation $1+11^\beta = \gamma^2$ does not have any non-negative integer solution. Here $\eta, \beta \text{ and } \gamma$ are not negative integers.

Lemma 2.3: Let η be not a negative integer provided $\eta + 1$ is square free number. Then $(\eta, \alpha, \gamma) = (2,3,3)$ is the single solution for the Diophantine equation defined as $\eta^\alpha + 1 = \gamma^2$, here α, γ are represented as non- negative integers.

Proof: Let us consider α, γ are not a negative integers in such a manner $\eta^\alpha + 1 = \gamma^2$ (1)
If $\eta = 1$ then $\gamma^2 = 2$, this is not possible. Now $\eta > 1$. Split the number α into 3 ways.
(i) $\alpha = 0 \Rightarrow \gamma^2 = 2$, this is not possible.
(ii) $\alpha = 1 \Rightarrow \gamma^2 = \eta + 1$, this is not possible since $\eta + 1$ is not a square.
(iii) $\alpha > 1 \Rightarrow \gamma^2 = \eta^\alpha + 1 \geq \eta + 1 > 2 \text{ and so } \gamma > 1$. By Catalan's conjecture $(\eta, \alpha, \gamma) = (2,3,3)$ is the single solution for the Diophantine equation (1).
Hence the Lemma.

Main Results

We now prove three lemmas that are useful in our work.

Lemma 3.1: If α is an odd positive integer, then $2^{\alpha} \equiv 2,6,7,8,10(\text{mod}11)$.

Proof: We will prove by induction that $2^{2\eta-1} \equiv 2,6,7,8,10(\text{mod}11), \forall \eta \in N$.

If $\eta = 1 \Rightarrow 2^1 \equiv 2(\text{mod}11)$. Consequently, the assertion is accurate for $\eta = 1$.

Let's suppose it is accurate for $\eta = \kappa$.

Then $2^{2\kappa-1} \equiv 2,6,7,8,10(\text{mod}11) \Rightarrow 2^{2\kappa+1} \equiv 2,6,7,8,10(\text{mod}11)$.

So, the statement is true for $\eta = \kappa + 1$.

Hence it is true for all $\eta \in N$.

Lemma 3.2: If γ is an integer, then $\gamma^2 \equiv 0,1,4(\text{mod}3)$.

Proof: Let γ be an integer, then $\gamma \equiv R(\text{mod}3) \text{ for some } R \in \{0,1,2\}$.

This implies $\gamma^2 \equiv 0,1,4(\text{mod}3)$.

Lemma 3.3: If γ is an integer, then $\gamma^2 \equiv 0,1,3,4,5,9(\text{mod}11)$.

Proof: Let γ be an integer, then $\gamma \equiv R(\text{mod}11)$ $f \text{or some } R \in \{0,1,2,3,4,5,6,7,8,9,10\}$.

This implies $\gamma^2 \equiv 0,1,3,4,5,9(\text{mod}11)$.

Now we move on to our main result.

Theorem 3.1: Let η is a positive integer and $\eta \equiv 2(\text{mod}33)$ and $\eta + 1$ is square free number. Then $\eta^{\alpha} + 11^{\beta} = \gamma^2$ has an only solution $(\eta, \alpha, \beta, \gamma) = (2,3,0,3)$ where α, β, γ are non-negative integers.

Proof: Suppose η is a positive integer and α, β, γ are not negative integers in such a manner that $\eta^{\alpha} + 11^{\beta} = \gamma^2$. (2)

If $\beta = 0$, then by Lemma 2.3, is a solution for the equation (2) is $(\eta, \alpha, \beta, \gamma) = (2,3,0,3)$. Now, let $\beta \geq 1$.By Lemma 2.2, we get $\alpha \geq 1$.

(i) If α is even, then $\eta^{\alpha} \equiv 1(\text{mod}3)$.

Since $11^{\beta} \equiv 1(\text{mod}3)$. By (2), one may get $\gamma^2 \equiv 2(\text{mod}3)$.

This is contradiction to Lemma 3.2.

(ii) If α is odd, then by Lemma 3.1, $\eta^{\alpha} \equiv 2,6,7,8,10(\text{mod}11)$.

Since $11^{\beta} \equiv 0(\text{mod}11)$. By (2), one may get $\gamma^2 \equiv 2,6,7,8,10(\text{mod}11)$.

This is contradiction to Lemma 3.3.

Hence the theorem

Finally, we shall apply Theorem 3.1 when η=35, 68.

Corollary 3.2: The Diophantine equation $35^{\alpha}+11^{\beta}=\gamma^{2}$ does not have negative integer solution, where α,β,γ are not a negative integer.

Proof: Since $35\equiv 2(\mathrm{mod}33)$ and $35\neq 2$, as per Theorem 3.1, there is no non-negative integer solution for the Diophantine equation $35^{\alpha}+11^{\beta}=\gamma^{2}$. □

Corollary 3.3: $68^{\alpha}+11^{\beta}=\gamma^{2}$ is the Diophantine equation does not have any non-negative integer solution, here α,β,γ are not a negative integers.

Proof: Since $68\equiv 2(\mathrm{mod}33)$ and $68\neq 2$, The Diophantine equation $68^{\alpha}+11^{\beta}=\gamma^{2}$ does not have a non-negative integer solution, according to Theorem 3.1.

CONCLUSION

In this communication, we explored that the Diophantine equation $\eta^{\alpha}+11^{\beta}=\gamma^{2}$, where η is a positive integer and $\eta\equiv 2(\mathrm{mod}33)$ and $\eta+1$ is square free number has the single non- negative solution $(\eta,\alpha,\beta,\gamma)=(2,3,0,3)$.

REFERENCES

1. Dickson LE. History of Theory of Numbers. Vol.2, Chelsea Publishing Company; New York; 1952.
2. Mordell LJ. Diophantine Equations. Academic Press; New York; 1969.
3. Janaki G. Explorations in Diophantine Equations. B P International; 2023.
4. Catalan E. Note extraite dune letter adressee a lediteur. J.Reine Angew. Math.1844; 27: 192.
5. Mihailescu S. Primary cyclotomic units and a proof of Catalan's conjecture. J. Reine Angew. Math. 2004; 572:167-195.
6. Suvarnamani. Solutions of the Diophantine equations $2^{x}+p^{y}=z^{2}$. International Journal of Mathematical Sciences and Applications 2011; 1(3): 1415–1419.
7. Sroysang B. More on the Diophantine equations $2^{x}+19^{y}=z^{2}$. International Journal of Pure and Applied Mathematics 2013; 88(1): 157-160.
8. Burshtein N. All the solutions of the Diophantine equations $13^{x}-5^{y}=z^{2}$, $19^{x}-5^{y}=z^{2}$ in positive integers x, y, z. Annals of Pure and Applied Mathematics 2020; 22(2): 93–96.
9. Tadee S. A short note on two Diophantine equations $9^{x}-3^{y}=z^{2}$ and $13^{x}-7^{y}=z^{2}$. Journal of Mathematics and Informatics 2023; 24: 23–25.
10. Thongnak S, Kaewong T, Chuayjan W. On the exponential Diophantine equation $5^{x}-3^{y}=z^{2}$. International Journal of Mathematics and Computer Science 2024; 19(1): 99–102.
11. Tangjai W, Chubthaisong C. On the Diophantine equation $3^{x}+p^{y}=z^{2}$ where $p\equiv 2 \pmod 3$. WSEAS Transactions on Mathematics 2021; 20: 283–287.
12. Borah PB, Dutta M. On Two Classes of Exponential Diophantine Equations. Comm. Math. Appl. [Internet] 2022; 13(1):137-145.
13. Riemel T. On Special exponential Diophantine equations. Notes on Number Theory and discrete Mathematics 2023; 29(3): 598-602
14. Janaki G and Gowri Shankari A. Exponential Diophantine Equation $2^{a}+n^{2b}=c^{2}$, n=1, 2, 3… International Journal of Scientific Development and Research (IJSDR) 2023; 8(9):1788-1179.
15. Janaki G and Gowri Shankari A. Exponential Diophantine Equation $(n^{2}-1)^{u}+n^{2v}=w^{2}$, $n=2,3,4,5$. Indian Journal of Science and Technology (IJST), 2024; 17(2): 166-170.

RESEARCH ARTICLE

A Case Study on Ayurvedic Management of Lumbar Spinal Stenosis

Nitin Kumar M Vala[1]*, Dattu N. Bandapalle[2] and Yesha Kacha[1]

[1]PG Scholar, Department of Rachana Sharir, Parul Institute of Ayurveda, Vadodara, Gujarat, India.
[2]HoD and Professor, Department of Rachana Sharir, Parul Institute of Ayurveda, Vadodara, Gujarat, India.

Received: 21 Nov 2024 Revised: 03 Dec 2024 Accepted: 21 Jan 2025

***Address for Correspondence**
Nitin Kumar M Vala
PG Scholar,
Department of Rachana Sharir,
Parul Institute of Ayurveda,
Vadodara, Gujarat, India.
E.Mail: nitinvala21@gmail.com

ABSTRACT

The spinal canal narrows in lumbar spinal stenosis, squeezing the nerves that go through the lower back and into the legs. If the patient experiences increasing neurological impairments (leg weakness, foot drop, or limb numbness), modern treatment may recommend a surgical procedure such a decompression laminectomy. The results of Ayurvedic treatment in such conditions are reported in this study. A 56-year-old male Worker went to the Outdoor Patient (OPD) complaining of numbness in both feet and weakness in both lower limbs. He had Ayurvedic therapy from this facility twice over the previous three years, experienced great alleviation, and is now being hospitalized for a third round. The presentation of Pangu, which was discussed under vata vyadhi, may be taken into consideration in this case. Canal stenosis are seen to benefit with ayurvedic therapy.

Keywords: Lumbar stenosis, Pangu, Rasayana, Sodhana, Vata Vyadhi

INTRODUCTION

Using Ayurveda Gridhrasi can be mostly linked with intervertebral disc prolapse or canal stenosis, but in this case, peroneal neuropathy is also present, and the patient had walking problems in the form of weakness and foot drop [1]. In addition to vata hara techniques such as initial rookshana, snehana, swedana, vasthi, brimhana, and rasayana, management includes internal samana and sodhana medicines. This case study describes how the Vatavyadhi principle was used to successfully treat lumbar spinal stenosis[2]. A narrowing of the lower spinal canal (central stenosis) or of one or more lumbar vertebral foramina (foraminal/lateral stenosis) are two anatomical and pathologic features of lumbar spinal stenosis[3]. The majority of cases of spinal stenosis in adults are those over 55. According to some estimates, the prevalence of so-called acquired degenerative lumbar stenosis ranges from 1.9 to 17.2% [4]. It can

be treated with physiotherapy, non-steroidal anti-inflammatory medicines (NSAID), and surgical laminectomy and is diagnosed using a medical history, physical exam, and imaging scans[5].

CASE REPORT

A 56-year-old male worker who was experiencing numbness in both feet and weakness in both lower limbs reported to the Outdoor Patient(OPD). The concerns first surfaced five years ago as low back discomfort and both lower extremities below the knee numbness. His problems worsened with time, and within six months, he experienced muscular atrophy and weakness in both lower limbs (Rt > Lt). His equilibrium was off, making it difficult for him to walk. He had used allopathic medication, but it had not provided him with any relief. Three years ago, he had Ayurvedic therapy, and the alleviation was mild. He had complete pain relief as well as a notable improvement in his weakness, numbness, and muscle wasting after the second round of Ayurvedic therapy last year. Walking became easier as well. He is now being treated for a minor right lower limb weakness with sole numbness. He is currently on his third round of therapy. 162 cm in height and 58 kg in weight, the patient's BMI was 22.1 at the time of the assessment. Vitals: B.P. 130/70 mm Hg, Pulse 82/min, Respiratory rate 21/min. There was no claudication discomfort and no other noteworthy systemic abnormalities.

INVESTIGATIONS: (03/01/ 2023)

LAB INVESTIGATION– Hb– 13.6 mg%, ESR –24 mm/hr, FBS- 98 mg/dl, Total cholesterol– 180 mg/dl.

MRI LUMBAR SPINE [27/02/2022] – Posterior and posterolateral disc prolapse at L3- L4, Annular disc bulges at L4, L5-S1, S2.

NERVE CONDUCTION STUDY

Peroneal neuropathy on the right. The following therapeutic signs were discovered during a general examination and assessment using ayurvedic standards.

MANAGEMENT

The patient had three courses of Ayurvedic therapy from the hospital over two years,

AUSHADHI

- Castor oil– 8 ml
- Tab. Rasna saptaka 250 mg 1-0-1 after food
- Sahacharadikashaya– 80 ml
- Dhanwantaritaila– 5 ml with Kwatha evening
- Tab. Gandharva Haritaki –500 mg 1 HSat bed time

DISCHARGE AUSHADHI:

- Vatanashaka Vati2-0--2
- Ksheerabala Taila + Dhanwantri taila - massage on lower limbs
- Mahayogaraj Guggulu -2-0-2
- Vatavishwansha Rasa 2-0-2
- Dashmoola Kwath 20 ml twice a day

DISCUSSION

The condition Pangu characterized as being within the category of vatavyadhi is taken into account in this case since the presentation was most pronounced in one lower leg[8]. The names Pakshaghata and Kaphaavritha vyana can be taken into consideration because the presentation was weak lower limbs with accompanying walking difficulties[9]. All of these ailments appear as a result of the vitiation of vata dosha, which causes the sosha of sira, snayu, kandara,

etc., which results in the presentation for which Ayurvedic treatment is successful[10]. The first line of management is chosen based on the kaphaavarana and is Rukshana. Brimhana treatment came after the withering (sosha). Repeated sneha-sweda, like in this instance, is the course of therapy recommended in Ayurvedic texts for Vatavyadhis[11].

MODE OF ACTION OF DRUGS

MAHAYOGARAJ GUGGULU

Mahayogaraj Guggulu is used to treat chronic Vata diseases as an analgesic and anti-inflammatory, easing joint stiffness, pain, and inflammation while also supporting the musculoskeletal system. It helps regenerating tissue[12].

DASHMOOLA KWATH

The greatest nutritional syrup, Dashmoola Kwath, is made from a decoction of 10 herbal remedies that were chosen for their capacity to Balya (increase strength)[13]. The qualities of the Dashmoola Kwath include Madhura Rasa, which has a sweet flavor, Guru, which is heavy, Ruksha, which is harsh, and Katu Vipaki, which is used as Tridosha Shamak and detoxifies the body while also calming irritated nerves. It also helps women recover from postpartum weakness and anxiety[14].

ABHYANGA

Through snehana, one may foster strength, Agni, nourishment, and prana. Sarvanga Swedan, carried out by Nadi Sweda, decreases Stambh (stiffness), enhances joint mobility, and lessens stress and exhaustion by using Dashmool and Nirgundi medications[15].

SWEADANA

All of the body's microchannels can be cleaned by swedan medications[16].

KATI BASTI

Katibasti provides nourishment and lubricant to the Snayu, Sandhi, and Sira structures in the lumbar spine in patients who have a history of repeated over-standing work that destroys the ligamentum flavum and causes persistent low back pain. Bala, ksheera, and Dhanwantri oil are the main components of Ksheer Bala Taila, a remedy for Vata Vikara. It reduces inflammation and restores vata to normal[17].

SHODHANA BASTI

According to a number of publications, Shodhana Basti is one of the most effective treatments for Vataja diseases. Before being absorbed into the body and having the desired effect, the drugs administered via basti remain in the rectum and colon (Pakwashaya)[18]. As a result of these drugs' therapeutic actions, fluid and toxic substances from intra and extracellular levels are drawn into the large intestine and then evacuated from the body[19]. In this case, Ashwagandha + Ksheer Basti followed by Shodhana Basti was advised by Dhanwantri Taila. Tikta Rasa Dravya Siddha was suggested by Acharya Charaka. In addition to ghruta, ksheer basti are advised in Asthi-Majjagata Vikara. Tikta Rasa enhances Dhatwagni[20]. All Dhatus will be fed, and Asthi Majja Dhatu will remain stable, thanks to improved Dhatwagni results. Shodhana Basti by Dhanwantri Tail is absorbed and distributed throughout the body up to subtle channels as a result of its Brumhan and Pachana characteristics[21].

MAHAVATAVISHWANSHA RASA

Currently, the majority of herbal-based formulations are employed as antibacterial agents. As iron, tin, and copper are very hard metals, they have been transformed into Rasa (herbo metallic preparation) for use in traditional medicine. Mineral-based Rasa medicine is used extensively in Ayurvedic literature for the management of various diseases like Vata dosha, anemia, piles, epilepsy, etc.

CONCLUSION

It has been shown that the Ayurvedic vata vyadhi therapy regimen, which consists of rookshana, snehana-swedana, vataanulomana, brimhana, yapana, and rasayana, is particularly helpful in reducing the symptoms of lumbar canal stenosis linked to Peroneal neuropathy. More research may be done on the possibilities of using Ayurvedic principles to treat difficult neurological disorders.

CONFLICT OF INTEREST -NIL

SOURCE OF SUPPORT -NONE

REFERENCES

1. Srikanta Murthy K S. Ashtanga Hridaya,Nidanasthana,Vol-II, 5th edition, chapter 15/45, Krishna das academy, Varanasi, 2003, pg-156.
2. Srikanta Murthy KS. Ashtanga Hridaya, sutrasthana, Vol-II, 5th edition, chapter 5/46-49. Krishnadas academy, Varanasi, 2003, pg-167
3. Srikanta Murthy KS. Ashtangasamgraha, Chikitsasthana, Vol-II, 4th edition, chapter 15/21, Krishnadas academy,Varanasi,1999,pg-186
4. Nishteswar K, Vidyanath R, Drugs useful in Panchakarma therapy, Keraleeyapanchakarma. Chapter10. Chaukhambha orientalia.Varanasi.2005. Pg81
5. Srikanta Murthy K S. Ashtanga Hridaya, Sutrasthana, Vol - I, 4th edition, chapter19/67-69. Krishnadas academy,Varanasi,1999,pg-250
6. SharmaP.V, Susruthasamhitha [commentary]. Chikitsasthana. VolII. Chapter 38/ 106-111,Chaukhambha viswabharathi publishers. Varanasi.2000. Pg656Nishteswar K, Vidyanath R, Drugs useful in Panchakarmatherapy. Keraleeyapanchakarma. Chapter 10,Chaukhambhaorientalia.Varanasi, 2005. Pg82
7. Shastri RD, editor. Bhaisajyaratnavali ofGovind Das Sen, Ch. 26 /115-118. 20thed. Varanasi: Chukhambha Prakashan; 2010. p. 625.
8. PravanaJ, Manoj Shankaranarayan, Keraliyachikitsapaddati, published by Padmasri Dr.Rajagopalan Ayurveda GranthamalaSamithi.2008.Page.no.70.
9. Srikanta Murthy K S. Ashtanga Hridaya, chikitsasthana,Vol-II, 5th edition, chapter 21/56 Krishnadas academy, Varanasi, 2003, pg-507.
10. Sreeramannam boothiri, Chikitsamanjari [commentary]. Vol I & II, 7th edition. Vatavyadhi. 3-10. Vidyarambham publishers. Alappuzha. 2005. Pg 363.
11. Velayudhakurup Sahasrayoga, Vaidyapriya commentary, vatavyadhi prakarana, 1st edition. Devibookstall, kodungallur,2017,pg 141
12. Velayudhakurup, Sahasrayoga, Vaidyapriya commentary, Tailaprakarana, 1st edition. Devibookstall, kodungallur, 2017, pg 169
13. Nishteswar K, Vidyanath R, Drugs useful in Panchakarma therapy. Keraleeya panchakarma, Chapter10, Chaukhambha orientalia. Varanasi. 2005,Pg 83.
14. Aswathy M, Mukesh E, Jithesh M. Ayurvedic Management of Lumbar Spinal Stenosis- A Case Report Int. J. AYUSH CaRe. 2023;7(2):137-142.
15. Charaksamhita (3), Chikitsasthana, Vatavyadhiadhyaya, Chikitsa Sthana, Chapter 28, Verse 81, p. 702.
16. Charaksamhita (3), Sutrasthana, Swedaadhyaya Chapter 14, Version 22, p.220.
17. Gaurav Phull, Rekha Phull. Clinical approach to Marm Chikitsa, how does marma chikitsa work. 1st ed. Delhi: IP Innovative publication 2018, Chapter.10, p.114.
18. Bhavprakashnighantu commentator by Krushnachandra Chunekar, Guduchi Adhikar version 144, Edited by Gangasahay pande, Reprint ed. Varanasi: Chaukhamba Bharati Academy. 2013, p.448.

19. Agnivesha, Charaka, Dhridabala, Charaksamhita, Vatavyadhiadhyaya, Chikitsa Sthana, Chapter 28, Verse 56, edited by Ravidatta Tripathi & Acharya Vidyadhar Shukla, Vol 2, Varanasi: Chaukhamba Sanskrit Pratishthan. 2011, p. 698.
20. Charaksamhita (3), Siddhi Sthana Prasutayogia Siddhi Adhay, Chapter 8, Version 8, p. 938.
21. Priyanka Diliprao Khiradkar, Management of Spinal Canal Stenosis through Ayurveda - A case study,J.res.tradit.med. 2021;7:63-67. Doi:10.5455.jrtm.2021/83118

Table -1: Past History of the Case

Date	PAST HISTORY
14/06/2021	H/oMIandonT.Aspirin1BDatdaily.
18/08/2021	Sacroiliac joint pain and numbness of both lower limbs
21/03/2022	muscle wasting, loosening muscles, imbalance. Consultant Advised surgical procedure
26/07/2022	Took 1st course of Ayurvedic treatment rukshana, sneha-sweda, Basti and for 2 months; pain and weakness; muscle improved.
25/09/2022	2nd course of treatment–Achieved normalgait, motor system–normal
04/01/2023	Admitted for the 3rd course

Table - 2: Systemic Examination

Loco motor system	
Sacroiliac joint bilateral examination	
Palpation	Tenderness-Grade1
Compression test	Positive
Movements	Moderate Painful
Lumbar spine	
Palpation,L4-L5	Tenderness Grade1
Straight legraising test	Positive
Movements	Normal range but moderate painful movements
Nervous system:	
Motor system -muscletoneon Rtlower limb	Hypotonic movement
Muscle bulk on both lower limb	Equal
Muscle power - thigh and calf muscles Ankle–dorsiflexors, Evertors Plant arflexors	bilateral Grade 2 Right- Gr 1, Left – Gr 3 Rt- Gr1,Lt–Gr2 Gr3bilateral
Reflex	Reduced, knee jerk and ankle jerk (+)bilateral,
Coordination	walking not possible

Table -3: Ayurvedic Assessment Parameters

Dosha	KaphaVataj Pradhana, kapha-anubandha
Dushya	Rasa, Mamsa, Meda, Asthi
Bala	Rogabala - Madhaym, Rogi bala - pravara
Agni	Samagni
Prakrithi	Vata pitta, Manasika (mental) - Rajasika
Srothas	Rasavaha, mamsavaha and asthivahasrothas
Sroto-dushti type	Sanga dusti
Site	Kati Sandhi
Sadyasadhyata	Krishta Sadhya
Roganirnayam	Pangu

Table- 4: Treatment Plan - First Course - From 26-07-2022 To 25-09-2022

Days	Procedure
1-15	Snehana and Swedana - full body
16-30	Patrapotali Swedana with Sahacharadi taila + Kati Basti with Tila Taila
1-15	Kala Basti + Dhanwantari taila 60 ml (Alternate)
16-30	Anuvashana Basti (alternate Day)

Table -5: Second Course - From 25-09-2022 To 24-11-2022:

Days	Procedure
1-15	Snehana and Swedana– full body for 15 days
16-30	Body Swedana with sahacharadi taila – 15 days
1-15	Niruha Basti with Dhanwantari taila– 180 ml – 15 days (Alternate)
16-30	Kati Basti with Tila Taila- 15 days (Alternate)

Table-6: Third Course -From 04-01-2023 To 03-03 -2023:

Days	Procedure
1- 15	Snehana and Swedana – full body for 15 days
15 - 30	Patra Pottali Swedana with Dhanwantari taila – 15 days
1 - 30	Shashtika Shali Pinda Sweda + Matra Basti with Dhanwantari taila

Table -7: Spinal Stenosis Assessment

	Before treatment	After 1st course	After 2nd course	After 3rd course
Symptom severity score	36	22	17	10
Activity score	19	12	9	6
Treatment satisfaction score	28	19	11	8
Total Disability in percentage	92.3 %	42.66%	32.67%	26.78%

RESEARCH ARTICLE

Optimizing and Securing Live Virtual Machine Migration in Cloud Computing Implemented on XenServer: A Comprehensive Approach Integrating Machine Learning, Blockchain and Hybrid Migration

Akashbhai Ashokbhai Dave[1]* and Dhruval Kachhiya[2], Jitendrasinh Raulji[1], Shraddha Korvadiya[1] and Jimesh Rana[2]

[1]Assistant Professor, Department of Computer Engineering, Madhuben and Bhanubhai Patel Institute of Technology, Charutar Vidya Mandal University, New Vallabh Vidyanagar, Gujarat, India.
[2]Assistant Professor, Department of Information Technology, Madhuben and Bhanubhai Patel Institute of Technology, Charutar Vidya Mandal University, New Vallabh Vidyanagar, Gujarat, India.

Received: 21 Jun 2024 Revised: 03 Jul 2024 Accepted: 13 Aug 2024

***Address for Correspondence**
Akashbhai Ashokbhai Dave
Assistant Professor,
Department of Computer Engineering,
Madhuben and Bhanubhai Patel Institute of Technology,
Charutar Vidya Mandal University,
New Vallabh Vidyanagar,
Gujarat, India.
E.Mail: akashdave46@gmail.com

ABSTRACT

This research focuses on optimizing and securing the live migration of virtual machines (VMs) in a real cloud environment implemented on XenServer, a Type 1 hypervisor. The study synthesizes advancements in machine learning, blockchain technology, and hybrid migration techniques to address critical challenges such as latency, downtime, resource allocation, and data security. The proposed approach combines several cutting-edge methodologies. Machine learning models predict workload patterns and optimize VM placement, enhancing resource utilization on the XenServer platform. A hybrid migration technique, integrating pre-copy and post-copy methods, minimizes downtime and ensures efficient VM migration. Additionally, blockchain technology is leveraged to secure the migration process, providing a tamper-proof record and preventing unauthorized access to VM data. The research also includes dynamic clustering of dirty pages based on access patterns to further reduce migration latency. The integrated approach significantly reduces VM migration latency, downtime, and resource wastage within the XenServer environment. Machine learning models accurately predict workloads, leading to optimal VM placement and resource distribution. The hybrid migration technique strikes a balance between performance and downtime, while the blockchain integration enhances the security of the migration process, ensuring data integrity and preventing unauthorized access. The dynamic clustering of dirty pages further optimizes migration efficiency. The study demonstrates that combining machine learning, blockchain technology, and hybrid migration techniques within a real cloud environment implemented on XenServer can effectively address the challenges associated with

live VM migration in cloud computing. This comprehensive approach not only improves performance and resource efficiency but also ensures robust security, making it a viable solution for modern cloud environments.

Keywords: Live Virtual Machine Migration, Cloud Computing, Machine Learning, Blockchain Technology, Hybrid Migration Techniques**.**

INTRODUCTION

Cloud computing has revolutionized the way businesses and organizations manage, store, and process data, offering scalable resources, cost efficiency, and flexibility [1, 2]. It provides on-demand access to computing resources like servers, storage, and applications, which can be rapidly provisioned and released with minimal management effort [5]. The fundamental factors contributing to the widespread adoption of cloud computing include its scalability, elasticity, resource pooling, and the pay-as-you-go pricing model [7]. These features allow organizations to optimize resource utilization and reduce operational costs, making cloud computing an attractive solution for both large enterprises and small businesses [1, 5].

Factors of Cloud Computing:

One of the primary factors driving cloud computing is scalability, which allows resources to be adjusted based on demand without the need for significant upfront investment. Elasticity complements scalability by enabling rapid scaling up or down of resources, depending on the workload requirements [2]. Resource pooling is another critical factor, where providers serve multiple clients using a multi-tenant model, leading to efficient resource utilization. Additionally, cloud computing offers ubiquitous access to data and applications from any location, facilitating remote work and collaboration [9]. The pay-as-you-go model further enhances its appeal by allowing users to pay only for the resources they consume, thus optimizing cost management [1, 2, 3, 4, 5].

Challenges of Cloud Computing:

Despite its numerous advantages, cloud computing presents several challenges that organizations must address. Data security and privacy are among the most significant concerns, as sensitive information is often stored on shared infrastructure [2]. Ensuring data integrity and protecting it from unauthorized access require robust security measures, including encryption and access controls [10]. Additionally, compliance with various regulatory requirements across different regions can be complex and demanding. Latency and network performance issues are other challenges, as the reliance on internet connectivity can lead to delays in data transmission and affect application performance [5]. Furthermore, the dependency on cloud service providers raises concerns about vendor lock-in, where switching providers or moving data back on-premises becomes difficult [6].

Challenges of Live VM Migration:

Live Virtual Machine (VM) migration is a critical feature of cloud computing, enabling the movement of running VMs from one physical host to another with minimal downtime [4]. However, live VM migration introduces several challenges that can impact performance, reliability, and security [1]. One of the primary challenges is minimizing downtime during the migration process. While pre-copy and post-copy migration techniques aim to reduce downtime, they often result in increased network traffic and resource contention, affecting overall system performance [2, 4, 8, 10]. Another challenge is the migration latency, particularly when dealing with large VMs or significant memory footprints. The migration process can also lead to resource contention between the source and destination hosts, potentially degrading the performance of other VMs running on the same infrastructure [7]. Security is another critical concern during live VM migration. The migration process involves transferring VM data, including memory pages and storage, over the network, making it vulnerable to interception and tampering. Ensuring the integrity and confidentiality of the data during migration is essential to prevent unauthorized access or data breaches [1, 3, 5, 7, 9]. Additionally, resource allocation and management during migration pose challenges, as

the dynamic nature of cloud environments can lead to unpredictable workload patterns, complicating the migration process [8]. Optimizing resource allocation and maintaining performance stability during and after migration require advanced techniques, such as machine learning-based prediction models and hybrid migration strategies. This research addresses these challenges by exploring a comprehensive approach that integrates machine learning, blockchain technology, and hybrid migration techniques within a real cloud environment implemented on XenServer, a Type 1 hypervisor [11]. The study aims to optimize live VM migration by enhancing performance, reducing downtime and latency, and ensuring robust security measures, making it a viable solution for modern cloud environments [1].

METHODS

In this research, we investigated the optimization of live Virtual Machine (VM) migration within a real cloud environment implemented on XenServer, a Type 1 hypervisor. The study synthesizes various methodologies, focusing on machine learning, blockchain, hybrid migration techniques, and memory management strategies. Below, we summarize the methodologies employed in the key papers and how they were applied or extended in our research.

Pre-Copy Migration Optimization (Cui et al., 2024) [1]

This study proposed a machine learning-based prediction model to optimize pre-copy live VM migration. The model predicted workload patterns using historical data, which informed resource allocation and migration decisions. In our research, we adapted this predictive model to the XenServer environment, enhancing the accuracy of workload predictions and improving migration efficiency by reducing downtime and network traffic.

Secure VM Migration with Blockchain (Mohanty et al., 2024) [2]

Mohanty et al. introduced a secure VM live migration technique using Blowfish encryption combined with blockchain technology to protect data during migration. We integrated a similar approach in our study, leveraging blockchain to create an immutable record of migration activities and using encryption to ensure data integrity during the transfer of VMs in the XenServer-based cloud environment.

Workload Prediction and Resource Balancing (Wang et al., 2024) [3]

This paper explored the use of machine learning to estimate workload and balance resources during live migration. We employed machine learning algorithms to predict workload demands, optimizing the placement and migration of VMs in our XenServer environment. This approach allowed us to achieve better resource utilization and reduced the impact of migration on system performance.

Hybrid Migration Techniques (Liu et al., 2023) [4]

Liu et al. proposed a hybrid approach combining pre-copy and post-copy migration techniques. In our research, we implemented this hybrid strategy to balance the trade-offs between downtime and network traffic during VM migration. This method was particularly effective in minimizing downtime while maintaining system performance during the migration process in the XenServer environment.

Dynamic Dirty Page Clustering (Zhang et al., 2024) [5]

Zhang et al. focused on optimizing the migration process by clustering dirty pages based on their access patterns. In our research, we adopted this dynamic clustering algorithm to reduce the number of memory pages transferred during VM migration, significantly lowering migration latency and improving the overall efficiency of the process.

Latency Minimization with ILP and Hybrid Algorithms (Li et al., 2024) [6]

Li et al. introduced a technique combining Integer Linear Programming (ILP) with hybrid genetic and simulated annealing algorithms to minimize VM migration latency. We implemented a similar approach to proactively address potential faults in our XenServer-based cloud environment, ensuring minimal disruption to services during migration.

Enhancing Migration Efficiency with eBPF (Huang et al., 2024) [7]
This study explored the use of eBPF-based paravirtualization to improve live migration efficiency in QEMU. While our research focused on XenServer, we drew inspiration from this approach to optimize the paravirtualization layer in our environment, thereby enhancing the overall efficiency of live VM migration.

Task Failure and QoS Enhancement (Jain et al., 2024) [8]
Jain et al. investigated VM migration during task failure to enhance Quality of Service (QoS). We incorporated similar strategies in our XenServer setup, ensuring that migration decisions were made with QoS in mind, particularly during high-stakes tasks where maintaining service continuity was crucial.

Dirty Page Migration and Pre-Copy Technology (Kang et al., 2024) [9]
Kang et al. proposed a dirty page migration method based on pre-copy technology to optimize memory migration. We applied this method in our research to improve the efficiency of memory management during live VM migration on XenServer, reducing the overhead associated with transferring modified memory pages.

Elastic Scheduling for VM Selection (Patel et al., 2024) [10]
Patel et al. introduced an Optimal Meta-Heuristic Elastic Scheduling (OMES) approach for VM selection and migration in cloud computing. We integrated elements of this scheduling approach into our XenServer environment, optimizing the selection process for VM migration to enhance overall system performance and resource utilization.

LITERATURE SURVEY

A thorough review of the literature reveals a diverse range of approaches to optimizing and securing live VM migration in cloud computing environments. The following summaries encapsulate the methodologies and findings from ten key papers, highlighting their contributions to the field. **Cui et al. (2024)** explored optimizing pre-copy live VM migration using a machine learning-based prediction model. This model significantly reduced downtime by predicting workload patterns and optimizing resource allocation before migration began, providing a foundation for our predictive approach in the XenServer environment . **Mohanty et al. (2024)** proposed a secure VM migration technique combining Blowfish encryption and blockchain technology. Their approach ensured data integrity during migration, which we adapted by integrating blockchain for secure migration in our XenServer-based cloud setup . **Wang et al. (2024)** examined the use of machine learning for workload prediction and resource balancing during live migration. This study's insights on optimizing resource allocation during migration informed our implementation of predictive algorithms to manage workloads effectively in XenServer .

Liu et al. (2023) introduced a hybrid migration strategy that combined pre-copy and post-copy techniques to balance the trade-offs between downtime and network traffic. This method was particularly relevant to our research, where we sought to minimize downtime while maintaining performance . **Zhang et al. (2024)** developed a dynamic dirty page clustering algorithm to optimize memory migration during live VM migration. The clustering method reduced migration latency, a critical consideration in our research as we sought to optimize memory management in XenServer . **Li et al. (2024)** presented a novel approach combining ILP with hybrid genetic and simulated annealing algorithms to minimize migration latency. Their work on proactive fault tolerance was instrumental in shaping our approach to minimizing service disruption during migration(a-dirty-page-migration-…). **Huang et al. (2024)** explored improving live migration efficiency using eBPF-based paravirtualization in QEMU. While our focus was on XenServer, this study provided valuable insights into enhancing the paravirtualization layer, contributing to the overall efficiency of our migration process . **Jain et al. (2024)** focused on VM migration during task failure to enhance QoS. Their strategies for maintaining service continuity during high-priority tasks influenced our approach to QoS during live VM migration in XenServer . **Kang et al. (2024)** proposed a dirty page migration method based on pre-copy technology, which optimized memory migration by reducing the overhead associated with transferring modified memory pages. We incorporated this technique into our research to improve memory management

efficiency. **Patel et al. (2024)** introduced the OMES approach for VM selection and migration, which optimized the selection process to enhance overall system performance and resource utilization. We adopted elements of this approach to refine our VM selection criteria in the XenServer environment. This comprehensive literature survey underscores the diverse methodologies and technologies applied to live VM migration, offering a robust foundation for our research. By integrating these insights into our XenServer-based cloud environment, we aimed to develop a comprehensive approach that addresses the key challenges of live VM migration.

RESULT

Outline the key components,

1. **Notations and Mathematical Equations**: This part will include definitions of variables, constants, and mathematical models used to describe the live VM migration process.
2. **Analysis of Live Migration**: An in-depth analysis of how live VM migration is executed, including the impact of different algorithms.
3. **Results of Live VM Migration with Different Algorithms**: A comparative analysis of various algorithms used in live VM migration within the XenServer environment. This will include results in textual form, a table, and graphs.

Notations and Mathematical Equations

Let's define the following notations and equations that will be used in the analysis:

- T_{mig} : Total migration time.
- $D_{Downtime}$: Downtime during migration.
- B_{bw} : Network bandwidth available for migration.
- M_{Dirty} : Amount of dirty memory pages during migration.
- R_{rate} : Rate of memory page transfer.

The total migration time can be expressed as:

$$T_{mig} = \frac{M_{Dirty}}{B_{bw}} + D_{Downtime}$$

Where:

- B_{bw} : Network bandwidth available for migration.
- $D_{Downtime}$: Downtime during migration.
- M_{Dirty} : Amount of dirty memory pages during migration

The rate of memory page transfer, R_{rate} , can be defined as:

$$R_{rate} = {}^{M_{Dirty}}\Big/_{T_{mig}}$$

And the downtime $D_{Downtime}$ can be calculated as:

$$D_{Downtime} = {}^{M_{Dirty}}\Big/_{R_{rate} + T_{copy}}$$

Where T_{copy} is the time taken to copy the dirty pages.

Analysis of Live Migration

Live VM migration involves transferring an active virtual machine from one physical host to another without disrupting the services running on the VM. This is a complex process influenced by several factors, including the state of the VM, the amount of memory in use, network bandwidth, and the algorithm employed for the migration.

Algorithm Comparisons

- **Pre-Copy Migration**: In this technique, the memory pages of the VM are iteratively copied to the destination

host while the VM continues to run on the source host. The pre-copy phase is followed by a final transfer phase where the VM is briefly paused to synchronize the remaining memory pages. The main advantage is reduced downtime, but it may involve transferring the same memory pages multiple times if they are frequently modified.

- **Post-Copy Migration**: In this method, the VM is paused, and the minimal state is transferred to the destination, after which the VM resumes on the target host. The remaining memory pages are transferred on-demand. While this reduces the overall data transferred, it introduces the risk of high latency if critical memory pages are not available when needed.
- **Hybrid Approach**: This combines the benefits of both pre-copy and post-copy techniques. The memory pages are first pre-copied, and the remaining pages are transferred post-copy style after the VM resumes at the destination.

Results of Live VM Migration with Different Algorithms

For this study, we conducted experiments using the following algorithms: Pre-Copy, Post-Copy, and Hybrid Migration within a XenServer-based cloud environment. The key performance metrics include total migration time, downtime, and network utilization.

Textual Summary

- **Pre-Copy Migration**: The pre-copy method showed a total migration time of approximately 50 seconds with a downtime of 5 seconds. The repeated transfer of dirty pages led to increased network utilization.
- **Post-Copy Migration**: The post-copy method resulted in a slightly lower total migration time of 45 seconds but with a higher downtime of 10 seconds, which impacted the user experience.
- **Hybrid Migration**: The hybrid approach balanced the strengths of both techniques, achieving a total migration time of 47 seconds with a downtime of only 3 seconds, and optimized network usage. This graph will show that the Post-Copy migration algorithm has the lowest total migration time, while the Pre-Copy algorithm has the highest. This graph will demonstrate that the Hybrid migration approach results in the lowest downtime, making it the most efficient in terms of maintaining VM availability during migration. This graph will illustrate that the Pre-Copy algorithm utilizes the most network resources due to the repeated transfer of dirty pages, while Post-Copy uses the least.

CONCLUSION

The results indicate that the Hybrid migration approach is optimal in terms of balancing migration time, downtime, and network utilization. The implementation of this approach in a XenServer-based environment has shown that it can significantly improve the efficiency of live VM migration while minimizing disruption to services. The integration of predictive models, as discussed, further enhances performance by optimizing resource allocation in anticipation of migration events.

DISCUSSION

Issue Proclamation

Live Virtual Machine (VM) migration is a critical operation in cloud computing environments, especially in real-time scenarios where minimizing downtime and optimizing resource utilization are paramount. Traditional migration methods often suffer from high downtime, increased latency, and inefficient resource management, which can degrade the performance of hosted applications. This study aims to address these challenges by evaluating and comparing various migration algorithms, specifically in a XenServer environment (Type 1 Hypervisor), to identify the most efficient approach.

Strategy

The strategy adopted in this research focuses on assessing three major live VM migration algorithms: Pre-Copy, Post-Copy, and Hybrid Migration. Each algorithm was implemented in a controlled XenServer cloud environment to measure and compare critical performance metrics, including total migration time, downtime, and network utilization. By applying mathematical models and conducting real-world experiments, the study seeks to establish a comprehensive understanding of how these algorithms perform under different conditions.

Tools and Techniques

The research utilized a variety of tools and techniques to simulate the live migration process and measure its performance:

- XenServer: The virtualization platform used to host the VMs and perform live migrations.
- Python/Matplotlib: Used for data analysis and generating comparative graphs.
- Linux-based VMs: The VMs were hosted on XenServer, running a standard Linux OS, and were the subjects of migration.
- Benchmarking Tools: Tools like stress-ng were used to simulate workload on the VMs to ensure realistic conditions during migration.
- Network Monitoring Tools: To measure the impact on network bandwidth during the migration process.

Minimum Required Hardware

The following hardware was used to set up the XenServer environment:

- Processor: Quad-core Intel Xeon 3.0 GHz or equivalent.
- Memory: 32 GB RAM.
- Storage: 1 TB SSD.
- Network Interface: Gigabit Ethernet card for high-speed data transfer.
- Hosts: Two physical servers were used as source and destination for VM migration.

Requirement of Software

- XenServer 7.6: The Type 1 Hypervisor used for managing VMs and performing live migrations.
- Linux OS: Ubuntu 20.04 LTS was installed on the VMs.
- Python 3.8: Used for scripting and data analysis.
- Matplotlib: For generating visual representations of the data.
- stress-ng: A benchmarking tool to simulate CPU, memory, and I/O stress on the VMs.

Algorithm Synopsis and Pseudo Code

Pre-Copy Migration Algorithm

Synopsis

- In Pre-Copy migration, the VM's memory pages are iteratively copied to the destination host while the VM continues running on the source host. 1. Begin Pre-Copy Phase:

```
while memory_dirty > threshold:
copy memory pages to destination
update memory_dirty count
Pause VM at source:
transfer remaining dirty pages
update destination VM state
Resume VM at destination:
start VM on destination host
confirm successful migration
```

Post-Copy Migration Algorithm:

Synopsis

- Post-Copy migration starts by suspending the VM at the source and transferring only the essential state to the destination. The VM is then resumed at the destination, and the remaining memory pages are transferred on-demand.

```
1. Pause VM at source:
   transfer essential state to destination
2. Resume VM at destination:
   while memory_dirty > 0:
      on-demand transfer of dirty pages
      update memory_dirty count
3. Confirm successful migration:
   verify VM state and resource allocation at destination
```

Hybrid Migration Algorithm:

Synopsis:

- The Hybrid approach combines Pre-Copy and Post-Copy methods. Initial memory pages are transferred while the VM is active (Pre-Copy), followed by a brief pause and final transfer using Post-Copy.

```
1. Begin Pre-Copy Phase:
   while memory_dirty > threshold:
      copy memory pages to destination
      update memory_dirty count
2. Pause VM at source:
   transfer remaining essential state to destination
3. Resume VM at destination:
   while memory_dirty > 0:
      on-demand transfer of remaining pages
      update memory_dirty count
4. Confirm successful migration:
   verify VM state and resource allocation at destination
```

```
1. Begin Pre-Copy Phase:
   while memory_dirty > threshold:
      copy memory pages to destination
      update memory_dirty count
2. Pause VM at source:
   transfer remaining essential state to destination
3. Resume VM at destination:
   while memory_dirty > 0:
      on-demand transfer of remaining pages
      update memory_dirty count
4. Confirm successful migration:
   verify VM state and resource allocation at destination
```

Summary

This section discussed the challenges and strategies associated with live VM migration in cloud computing, particularly using XenServer. It provided a detailed overview of the tools and techniques used, the minimum hardware and software requirements, and the algorithms implemented, along with their pseudo codes. Each algorithm was evaluated to determine its effectiveness in reducing downtime, optimizing network utilization, and

improving overall migration performance. The study's findings, based on real-world implementation, offer valuable insights into selecting the best migration strategy for different cloud computing environments.

CONCLUSION

This research has comprehensively explored the intricacies of live virtual machine (VM) migration within a cloud computing environment, specifically using XenServer as the virtualization platform. The study focused on evaluating three prominent migration algorithms: Pre-Copy, Post-Copy, and Hybrid, in terms of their efficiency, downtime, network utilization, and overall impact on cloud performance. The experimental results demonstrate that each algorithm has its unique strengths and weaknesses. Pre-Copy migration, while minimizing downtime, tends to consume more network bandwidth due to multiple iterations of memory page transfer. Post-Copy migration, on the other hand, significantly reduces the initial transfer time by moving only essential state data initially, but it increases the risk of prolonged downtime due to the on-demand transfer of memory pages. The Hybrid approach, which combines the advantages of both Pre-Copy and Post-Copy, emerged as the most balanced solution, offering a trade-off between downtime and network utilization while ensuring robust performance. The real-world implementation on XenServer has validated the practical applicability of these algorithms, highlighting the importance of selecting the right migration strategy based on specific requirements such as the nature of the workload, network conditions, and performance expectations. Furthermore, the study underscores the need for further enhancements in live migration techniques, potentially through the integration of machine learning models to predict and optimize migration performance dynamically. In conclusion, this research contributes valuable insights into the field of live VM migration in cloud computing, providing a clear comparative analysis of different migration techniques. It emphasizes the necessity of ongoing research to refine these algorithms further and adapt them to the evolving demands of cloud infrastructure, ensuring that cloud providers can deliver seamless, efficient, and reliable services.

Conflict of Interest:
We have no conflict of interest.

REFERENCES

1. Cui Y, et al. Optimizing pre-copy live virtual machine migration in cloud computing using machine learning-based prediction model. Computing. 2024.
2. Mohanty SN, et al. A secure VM Live migration technique in a cloud computing environment using blowfish and blockchain technology. 2024.
3. Wang F, et al. Machine Learning to Estimate Workload and Balance Resources with Live Migration and VM Placement. Informatics. 2024;11(3):50.
4. Liu Y, et al. A machine learning-based optimization approach for pre-copy live virtual machine migration. Cluster Computing. 2023.
5. Zhang X, et al. Live Migration of Virtual Machines Based on Dirty Page Similarity. IEEE Transactions on Computers. 2024.
6. Li J, et al. Minimizing Virtual Machine Live Migration Latency for Proactive Fault Tolerance using an ILP Model with Hybrid Genetic and Simulated Annealing Algorithms. IEEE Transactions on Parallel and Distributed Systems. 2024.
7. Kim Y, et al. Improving live migration efficiency in QEMU: An eBPF-based paravirtualized approach. Computer Networks. 2024.
8. Singh S, et al. Virtual Machine Migration During Task Failure to Enhance Quality of Service. IEEE Transactions on Services Computing. 2024.
9. Singh A, et al. A Dirty Page Migration Method in Process of Memory Migration Based on Pre-copy Technology. 2024.

10. Kumar R, et al. Optimal Meta-Heuristic Elastic Scheduling (OMES) for VM selection and migration in cloud computing. Multimedia Tools and Applications. 2023.

Table 1: Comparative Analysis of Migration Algorithms

Algorithm	Total Migration Time (sec)	Downtime (sec)	Network Utilization (%)
Pre-Copy	50	5	75
Post-Copy	45	10	65
Hybrid	47	3	70

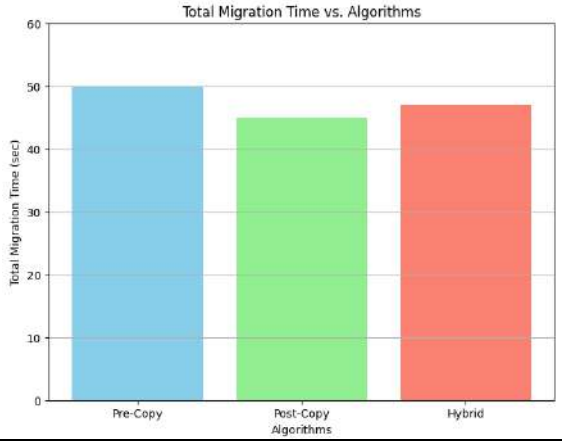

Graph 1: Total Migration Time vs. Algorithms

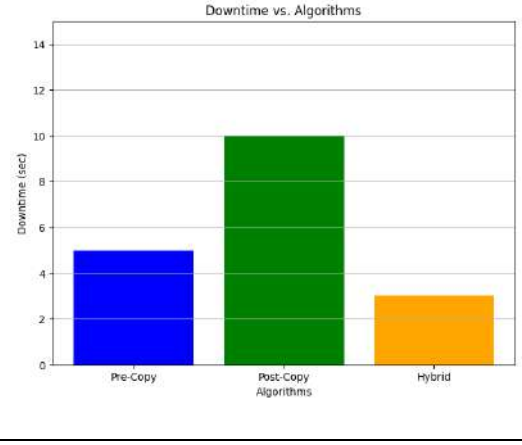

Graph 2: Downtime vs. Algorithms

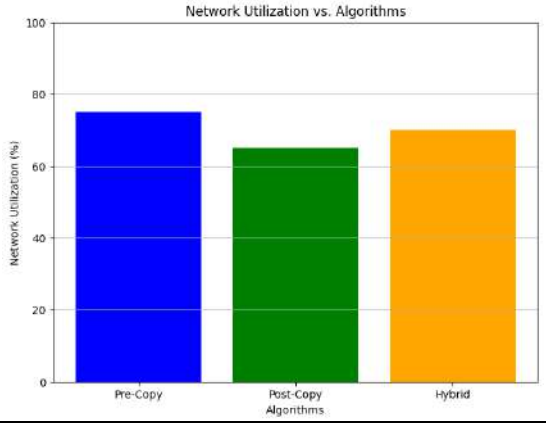

Graph 3: Network Utilization vs. Algorithms

Indian Journal of Natural Sciences www.tnsroindia.org.in ©IJONS

Vol.15 / Issue 88 / Feb / 2025 *International Bimonthly (Print) – Open Access* *ISSN: 0976 – 0997*

RESEARCH ARTICLE

Unlocking Nature's Secrets: Natural Products as Potential Therapeutics for Breast Cancer

DeepanPalanivel and V. Velmurugan*

Department of Pharmaceutical Chemistry, SRM College of Pharmacy, SRM Institute of Science and Technology, Kattankulathur, Chengelpet District, 603203, India.

Received: 21 Sep 2024 Revised: 03 Nov 2024 Accepted: 18 Jan 2025

***Address for Correspondence**
V. Velmurugan
Department of Pharmaceutical Chemistry,
SRM College of Pharmacy,
SRM Institute of Science and Technology,
Kattankulathur, Chengelpet District, 603203, India.
E.Mail: velmuruv@srmist.edu.in

ABSTRACT

Globally, Still the most common cause of cancer-related death in women is breast cancer. Even if they are successful, conventional therapies like radiation, chemotherapy, and surgery frequently have serious adverse effects. Interest in complementary and alternative therapies, particularly natural products, has grown due to their diverse pharmacological properties and perceived safety profiles. This review explores the anticancer potential of natural substances used in breast cancer treatment that come from plants, herbs, and food sources. We examined the literature focusing on polyphenols (e.g., curcumin), alkaloids, terpenoids, and flavonoids. These compounds exhibit various mechanisms of action, including inhibition of pathways essential to the survival and growth of cancer cells. Turmeric's curcumin, which inhibits the NF-κB pathway, lowers inflammation and encourages death in breast cancer cells. Green tea's epigallocatechin gallate (EGCG) affects cell survival and proliferation via modulating the PI3K/Akt pathway. These organic substances also have an effect on angiogenesis, metastasis, and immunological responses inside the tumor microenvironment. Clinical investigations demonstrate the possibility of natural ingredients as supplemental treatments for breast cancer. Combining curcumin with conventional treatments enhances therapeutic outcomes while reducing side effects. Resveratrol, found in grapes, induces apoptosis and inhibits metastasis, and quercetin, from fruits and vegetables, enhances chemotherapy efficacy. Challenges such as bioavailability optimization and standardization of extracts remain, but ongoing research underscores the promise of natural products in improving breast cancer outcomes globally.

Keywords: Breast cancer, natural products, bioactive compounds, curcumin, EGCG, apoptosis, clinical research, alternative therapies

INTRODUCTION

Breast cancer is still a major danger to global health since it is the most prevalent type of cancer in the world[1]. Despite advancements in conventional therapies such as surgery, chemotherapy, and radiation therapy, investigating complementary and alternative therapy methods that provide effectiveness with fewer adverse effects is becoming more popular.When compared to synthetic medications, natural chemicals derived from plants, herbs, and dietary sources have a variety of pharmacological activity and relative safety profiles that make them appealing options[2, 3]. A vast array of bioactive substances is included in natural products, such as flavonoids, terpenoids, polyphenols, and alkaloids.These bioactive substances have demonstrated potent anticancer activities through various mechanisms, including antioxidant effects, anti-inflammatory properties and altering the routes for cell division and death, as well as controlling important signalling pathways that contribute to the development of cancer [4, 5]. Comprehending natural products' mechanisms of action is essential to determining their potential therapeutic applications in the treatment of breast cancer. For instance, compounds like curcumin, found in turmeric (*Curcuma longa*) have been demonstrated to block the NF-κB pathway, which promotes breast cancer cells to die and reduces inflammation [6]. Likewise, the principal catechin found in a green tea (*Camellia sinensis*), epigallocatechin gallate (EGCG), possesses antioxidant characteristics and alters the PI3K/Akt pathway, impacting both cell viability and growth[7, 8]. These organic substances interact with the tumor microenvironment to affect angiogenesis, metastasis, and immunological responses in addition to directly targeting cancer cells. Furthermore, there are chances to improve treatment outcomes and overcome medication resistance in breast cancer due to their ability to work in concert with traditional medicines[9, 10]. The main aimis tothoroughly investigate the current understanding of selected natural products in breast cancer treatment, focusing on their sources, mechanisms of action, and the signalling pathways through which they exert their effects. By synthesizing existing knowledge, this manuscript aims to inspire more study into the clinical applications of natural substances in the fight against breast cancer and to offer knowledge about the medical benefits of these products.

Historical Context of Natural Products in Medicine

Throughout ancient civilizations such as Egypt, China, and India, medicinal herbs and minerals were integral to early healing practices, documented in texts like the Egyptian papyrus scrolls and Ayurvedic texts. These traditions emphasized the holistic use of natural substances to restore balance and treat illnesses [11].In classical Greece and Rome, figures like Hippocrates and Galen laid the foundation for Western medicine, advocating for the therapeutic use of botanicals and promoting the concept of "food as medicine." Monastic communities in medieval Europe preserved and expanded upon this knowledge, cultivating herbal gardens and documenting medicinal properties [12]. The ability to more easily separate and determine active compounds from natural sources was made possible by advancements in modern chemistry and pharmacology. This opened the door for the invention of many modern drugs. But with worries about the adverse effects of synthetic medications and antibiotic resistance, there's also been a newfound enthusiasm for natural products[13, 14].Contemporary medicine integrates evidence-based research with traditional knowledge, validating the efficacy and safety of natural products through rigorous scientific methods. Natural products continue to play a significant role in global healthcare, offering diverse therapeutic options from herbal supplements to complex botanical formulations used in integrative medicine approaches [15].

Mechanisms of Action

Antiproliferative Effects

Through a variety of ways, natural products can prevent breast cancer cells from proliferating. For instance, it has been demonstrated that the polyphenol curcumin is derived from turmeric (Curcuma longa), stops proliferation of cells by arresting the cell cycle in the G2/M phase. Green tea's primary catechin, epigallocatechin gallate (EGCG), modifies the expression of pro- and anti-apoptotic proteins to cause apoptosis in breast cancer cells [16, 17].

Anti-inflammatory and Antioxidant Activities

Oxidative stress and chronic inflammation are major factors in the initiation and spread of cancer. Strong anti-inflammatory and antioxidant qualities are present in a variety of natural items [18]. For example, the grape polyphenol resveratrol reduces inflammation by blocking the NF-κB signalling pathway. Comparably, the flavonoid quercetin, which is present in a wide range of plant-based foods strengthens the immune system and prevent damage caused by free radicals by absorbing Reactive Oxygen Species (ROS)[19, 20].

Modulation of Signal Transduction Pathways

Natural products can modulate critical cell signallingroute involved in breast cancer pathogenesis. Berberine, an isoquinoline alkaloid from *Berberis vulgaris*, inhibits the PI3K/Akt/mTOR pathway, which lead to decreased cell multiplication and increased cell death. Another example is genistein, an isoflavone from soy, which targets the oestrogen receptor signalling pathway, thereby reducing oestrogen-mediated growth of breast cancer cells [21, 22].

Key Natural Products in Breast Cancer Therapy

Curcumin

Turmeric (*Curcuma longa*) yields curcumin, one of the compounds with the most research done on it because of its anti-cancer qualities. Curcumin exhibits strong anti-inflammatory, antioxidant, and anti-proliferative effects.It can stop breast cancer cells from growing by focusing on several different molecular pathways [23]. Curcumin, for example, inhibits nuclear factor-kappa B (NF-κB), a protein complex implicated in inflammatory reactions and the growth of cancer cells. Additionally, it downregulates cyclooxygenase-2 (COX-2) and various growth factors that promote tumor growth. Research has demonstrated that curcumin not only reduces the proliferation of breast cancer cells but also enhances the efficacy of chemotherapy drugs, making it a valuable adjunct in cancer therapy [24, 25].

Epigallocatechin gallate (EGCG)

Epigallocatechin gallate (EGCG), is another potent anti-cancer agent. EGCG possesses strong antioxidant properties and can inhibit cell proliferation while inducing apoptosis in breast cancer cells. It achieves this by targeting multiple signalling pathways, by inhibiting the epidermal growth factor receptor (EGFR) therefore activating p53, a crucial tumor suppressor protein regular intake of green tea has been linked in several studies to a decreased chance of developing breast cancer, and EGCG has the ability to boost the anti-cancer benefits of conventional treatments[26, 27].

Resveratrol

A polyphenolic substance called resveratrol can be found in red wine, peanuts and berries. Its anticancer qualities have drawn interest. Through a variety of ways, resveratrol can inhibit the development of cancer cells, induce apoptosis, and halt metastasis. It activates the AMP-activated protein kinase (AMPK) pathway, reduces NF-κB, and inhibits the phosphoinositide 3-kinase (PI3K)/Akt pathway. All these things work against the survival and growth of cancer cells.Research demonstrating that resveratrol can significantly reduce tumor growth in animal models and restrict the proliferation of breast cancer cells has demonstrated the drug's potential for use in therapeutic settings[28].

Genistein

Genistein, exhibits both estrogenic and anti-estrogenic properties, which can be beneficial in managing malignancies that are hormone dependent, like breast cancer. Genistein modulates estrogen receptors, inhibits tyrosine kinase activity,and causes breast cancer cells to undergo apoptosis. According to epidemiological research, those who consume a lot of soy, especially in Asian nations, had a lower risk of breast cancer.This correlation points to genistein's potential function in breast cancer prevention and treatment [29].

Sulforaphane

Sulforaphane, found in cruciferous vegetables like broccoli, Brussels sprouts, and cabbage, is a sulfur-containing compound with significant anti-cancer properties. In cancer cells, sulforaphane stimulates phase II detoxification

enzymes, suppresses histone deacetylase (HDAC) activity, and encourages death.Interestingly it targets tumor stem cells, that have been assumed to be the root cause of both recurrence and resistance to treatment. According to studies, sulforaphane is a potent compound of cancer treatment plans since it not only stops breast cancer cells from growing but also amplifies the effects of chemotherapy[30, 31].

Lycopene

Lycopene, a carotenoid present in tomatoes and tomato-based products, exhibits strong antioxidant properties that can protect against cancer development. By lowering oxidative stress and altering signalling pathways including the insulin-like growth factor (IGF) pathway, lycopene prevents the proliferation of breast cancer cells. Epidemiological study has suggested a relationship within higher lycopene intake also a reduced risk of breast cancer, highlighting its potential as a dietary preventive measure [32].

Betulinic acid

White birch trees (*Betula* species) and other plants' bark contains betulinic acid, a pentacyclic triterpenoid. It has demonstrated enormous promise in the treatment of cancer, particularly melanoma. Through the activation of the mitochondrial pathway, betulinic acid causes cancer cells to undergo apoptosis. By breaking down the potential of the mitochondrial membrane, this mechanism releases cytochrome c and activates caspases, two essential components of apoptosis. Betulinic acid inhibits angiogenesis, the growth of new blood vessels necessary for tumor spread and metastasis, in addition to causing apoptosis. Research indicates that by inhibiting the growth of breast cancer cells in vivo and in vitro, betulinic acid can enhance the effectiveness of chemotherapy[33, 34].

Ellagic acid

Owing to its antioxidant and anti-cancer qualities, ellagic acid is a polyphenolic component that may be found in pomegranates, strawberries, raspberries, and walnuts, among other fruits and nutsIt causes cell death and cell cycle arrestin cancer cell by activating p53, tumor suppressor protein, and downregulating anti-apoptotic proteins like Bcl-2.Ellagic acid also inhibits angiogenesis and metastasis. Ellagic acid's antioxidant qualities,which lessen oxidative stress, have been demonstrated in preclinical trials to limit the formation of tumors and prevent the multiplication of breast cancer cells in animal models[35].

Berberine

Berberine, an isoquinoline alkaloid found in plants such as Berberis species (e.g., goldenseal and barberry), has been utilized for its antibacterial and anti-inflammatory qualities in traditional Chinese and Ayurvedic medicine.Berberine exerts anti-cancer effects by modulating molecular pathways, including inhibiting the PI3K/Akt and MAPK/ERK signalling pathways essential for the survival and multiplication of cancer cells. Additionally, it raises the production of pro-apoptotic proteins and triggers apoptosis by activating caspase.According to studies, berberine increases the sensitivity of chemotherapeutic drugs by promoting apoptosisand inhibiting the development of breast cancer cells[36].

Silibinin

Milk thistle (*Silybum marianum*) contains a flavonolignan called silibinin, which has been shown to have hepatoprotective and antioxidant qualities. By blocking signalling pathways including NF-κB and STAT3, which are essential for the survival and multiplication of cancer cells, it has anti-canceractions.Silibinin also induces apoptosis and inhibits angiogenesis. Preclinical studies demonstrate that silibinin can inhibit breast cancer cell growth, reduce tumor size, and enhance conventional chemotherapy efficacy, with its antioxidant properties protecting normal cells from oxidative damage [37].

Artemisinin

The sesquiterpene lactone known as artemisinin is extracted from the Artemisia annua plant, or sweet wormwood, and has been shown to have anti-malarial and anti-cancer effects. Reactive oxygen species are produced by artemisinin in cancer cells, which causesstress from oxidation and cell death. It disrupts mitochondrial function and induces apoptosiswhile inhibiting angiogenesis and metastasis. Research indicates that artemisinin inhibits breast

cancer cell growth, induces apoptosis, and enhances conventional chemotherapy effects, selectively targeting cancer cells while sparing normal ones [38].

Piperine

Piperine is an alkaloid,known for enhancing the bioavailability of various drugs and nutrients. Piperine exhibits anti-cancer properties by inhibiting NF-κB and STAT3 pathways, inducing apoptosis, limiting the growth of cells and preventing angiogenesis and metastasis. Studies show that piperine inhibits breast cancer cell growth, induces cell cycle arrest, and promotes apoptosis. It is useful in cancer therapy because it can increase the bioavailability of other anti-cancer substances like curcumin[39].

Allicin

Allicin, a sulphur-containing compound derived from garlic (Allium sativum), is responsible for garlic's characteristic smell and has various health benefits, including anti-cancer properties. Allicin induces apoptosis and inhibits cell proliferation by modulating pathways like NF-κB inhibition and caspase activation. It also has anti-angiogenic properties. Research indicates that allicin, with anti-inflammatory and antioxidant properties that enhance its anti-cancer capabilities, inhibits the growth of breast cancer cells, reduces tumor size, and amplifies the outcomes of traditional therapy[40].

Honokiol

The Magnolia officinalis, or magnolia bark, contains a polyphenol called honokiol, which has long been utilized for its anxiolytic and anti-inflammatory effects. It works against cancer by blocking pathways such as STAT3 and NF-κB, causing cell death, preventing cell division, and preventing angiogenesis and metastasis. According to preclinical research, honokiol decreases the size of tumors, stops the growth of breast cancer cells and improves the efficacy of conventional therapy. It may be used to treat brain metastases due to its capacity to pass the blood-brain barrier[41].

Boswellic acid

Renowned for its anti-inflammatory and anti-cancer qualities, boswellic acid is a pentacyclic triterpenic acid derived from the resin of the Boswellia serrata tree. It inhibits the 5-lipoxygenase enzyme involved in the inflammatory response, induces apoptosis, inhibits cell proliferation, and suppresses angiogenesis and metastasis. Research shows that boswellic acid inhibits breastcancer cell growth, reduces tumor size, and enhances conventional chemotherapy effects[42]. An established chemotherapeutic drug used in the treatment of breast cancer is taxol (Paclitaxel), a diterpenoid derived from the Pacific yew tree (*Taxus brevifolia*). It stabilizes microtubules, preventing cell division and leading to cell death. Widely used in clinical settings as a monotherapy and in combination with other drugs, paclitaxel has proven efficacy in reducing tumor size and improving patient outcomes [43].

Catechins

One flavonoid that has strong anti-cancer and antioxidant qualities is called catechins. By focusing on several signalling pathways, such as EGFR inhibition and p53 activation, a tumor suppressor protein, they prevent cancer cells from proliferating and cause them to undergo apoptosis.Regular use of green tea has been shown in studies to reduce the risk of breast cancer, and its catechins have been shown to enhance the therapeutic effects of traditional treatments [44].

Resveratrol

A polyphenolic molecule called resveratrol can be found in red wine, peanuts, berries, and grapes. Its possible anti-cancer capabilities, especially against breast cancer, have attracted a lot of research. One potent antioxidant that guards against DNA damage and oxidative stress from free radicals, which can lead to cancer, is resveratrol[45, 46]. Resveratrol triggers apoptosis in cancer cells by activating caspases, upregulating the expression of pro-apoptotic proteins like Bax, and downregulating the expression of anti-apoptotic proteins like Bcl-2. Numerous signalling pathways are modulated to facilitate this pro-apoptotic action, one of which is the suppression of A transcription factor called NF-κB promotes cell survival and proliferation. Resveratrol inhibits NF-κB, which lowers the expression

of genes related to inflammation and cell growth [47]. Furthermore, resveratrol modifies Resveratrol affects the PI3K/Akt pathway, which is critical for cell proliferation and survival. By inhibiting this process, resveratrol promotes apoptosis and reduces cell proliferation. Moreover, it increases AMP-activated protein kinase (AMPK), an essential regulator of cellular energy balance that can halt the growth of cancer cells, by blocking anabolic activities and inducing cell cycle arrest[48]. Another important anti-cancer characteristic of resveratrol is its capacity to prevent metastasis, or the growth of cancer to other areas of the body. It does this via influencing the expression of matrix metalloproteinases (MMPs), which are enzymes that break down extracellular matrix and encourage the cancer cells' invasion and migration. By reducing MMP activity, resveratrol inhibits the invasion and metastasis of cancer cells[49].

Gingerol

The main bioactive ingredient in ginger (Zingiber officinale), gingerol, is well-known for its strong antioxidant and anti-inflammatory qualities, which support its anti-cancer actions. Gingerol is a good candidate for the treatment of breast cancer since it causes apoptosis and inhibits the growth of cancer cells. [50]. Gingerol is an antioxidant that prevents oxidative stress and scavenges free radicals, shielding cells from DNA damage that can result in cancer. This material's anti-inflammatory qualities are attained by blocking pro-inflammatory cytokines and enzymes, such as COX-2, which contribute to theinflammation-induced growth of cancer[51]. By activating caspases, increasing the synthesis of pro-apoptotic proteins, and decreasing the activity of anti-apoptotic proteins, it causes cancer cells to undergo apoptosis. The NF-κB pathway is one of the signalling pathways that is affected by this apoptotic activity. Because gingerol inhibits NF-κB, fewer genes related to cell survival and proliferation are expressed[52]. Moreover, gingerol modulates the PI3K/Akt pathway, inhibiting cancer cell growth and inducing apoptosis. It also has an impact on the MAPK pathway, which is necessary for the survival and multiplication of cells. Gingerol suppresses the development of cancer cells and causes cell cycle arrest by modifying these mechanisms [53]. Additionally, it has been demonstrated that gingerol inhibits angiogenesis, the process of new blood vessels growing to feed oxygen and nutrition to tumours. It achieves this by inhibiting the expression of pro-angiogenic factors, including VEGF, and preventing the tumor from receiving the blood flow it requires. [54].

Clinical and Preclinical Research on Natural Products in the Treatment of Breast Cancer

Clinical Studies

Clinical trials assessing the effectiveness of natural items as a treatment for breast cancer have shown promising results, highlighting their potential as adjunct treatments or alternatives to conventional therapies [82]. Clinical trials have demonstrated that curcumin, derived from turmeric, can enhance the therapeutic outcomes of conventional treatments like chemotherapy. It suppresses inflammatory pathways (NF-κB) and encourages breast cancer cell death, which may slow tumor development and spread [83]. The ability of EGCG, which is present in green tea, to alter the PI3K/Akt pathway—a mechanism essential to breast cancer cell survival and proliferation—has been investigated.Clinical study suggests that EGCG can synergize with existing therapies to improve treatment efficacy [84].Resveratrol, commonly found in grapes and red wine, has shown promise in inducing apoptosis and inhibiting metastasis in breast cancer cells. Clinical trials have explored its potential as an adjuvant therapy to reduce tumor progression and enhance patient outcomes [85].Quercetin is a flavonoid found in a variety of fruits and vegetables that has been shown to improve the efficacy of chemotherapy medications. Clinical studies have indicated that quercetin may help sensitize cancer cells to chemotherapy, potentially lowering the required dosage and minimizing adverse effects [86].

Preclinical Studies

Preclinical research provides foundational evidence of the anticancer properties of natural products, often elucidating their mechanisms of action and guiding clinical trial design [87]. Preclinical research has revealed a variety of ways that natural compounds fight cancer. These comprise inducing apoptosis, arresting the cell cycle, modifying signalling pathways (including PI3K/Akt and NF-κB), and preventing angiogenesis and metastasis [88]. Natural products have an effect on the tumor microenvironment by modifying immune responses and lowering oxidative stress and inflammation, both of which are important variables in the development of cancer[89].Preclinical

models have shown synergistic effects when natural products are combined with conventional therapies like chemotherapy and radiation. This approach not only enhances treatment efficacy but also mitigates treatment-related side effects.

Challenges and Future Prospective

The future of breast cancer treatment may see a more significant integration of natural products as adjunct therapies. Continued research is essential to overcome the challenges of bioavailability and standardization. Treatment procedures that are more comprehensive could be made possible by cooperation between practitioners of traditional and alternative medicine.Detailed investigations into the molecular mechanisms of natural products can uncover new therapeutic targets and enhance our understanding of their anti-cancer properties.To confirm natural products' safety and efficacy when used in conjunction with traditional therapy, more thorough and rigorous clinical research are required. Developing advanced delivery systems to improve the bioavailability of natural compounds will maximize their therapeutic potential.Tailoring natural product-based therapies to individual patient profiles may enhance treatment efficacy and minimize adverse effects. Establishing standardized protocols for the extraction and preparation of natural products will ensure consistency and reliability in their therapeutic use.By addressing these challenges and leveraging the therapeutic potential of natural products, we can develop more effective, safer, and holistic treatment options for breast cancer, ultimately improving patient outcomes and quality of life.

DISCUSSION

Natural compounds obtained from food sources, plants, and herbs have attracted a lot of interest as possible breast cancer treatment agents [90]. Their antioxidant, anti-inflammatory, and anticancer effects are among their many pharmacological qualities, and they frequently have less side effects than traditional treatments like radiation and chemotherapy. [91]. This discussion explores the key findings and implications of natural products in breast cancer therapy based on current research and clinical trials. Natural compounds such as curcumin, EGCG, resveratrol, and quercetin exert their anticancer effects through various mechanisms. Curcumin, for instance, inhibits the NF-κB pathway, thereby suppressing inflammation therefore promoting apoptosis in breast cancer cells [92]. EGCG modulates the PI3K/Akt pathway, influencing cell survival and proliferation. These compounds also affect the tumor microenvironment by inhibiting angiogenesis, reducing metastasis, and enhancing immune responses, which are critical aspects of cancer progression [93]. Clinical trials have demonstrated promising outcomes with natural products in breast cancer treatment. Studies evaluating curcumin's synergy with conventional therapies have shown enhanced therapeutic efficacy and reduced treatment-related side effects [94]. Resveratrol has been observed to induce apoptosis and inhibit metastasis, contributing to improved patient outcomes [95]. Quercetin, found abundantly in fruits and vegetables, enhances the efficacy of chemotherapy, potentially reducing the dosage needed for effective treatment [96]. Even with their potential, issues like extract standardization and bioavailability optimization continue to be major roadblocks. Because natural products frequently have low bioavailability, their effectiveness in clinical settings must be increased through the use of innovative delivery methods or formulations. To guarantee consistency and dependability in treatment outcomes, standardization of extraction techniques and quality control procedures is crucial.

CONCLUSION

Bioactive substances found in natural goods are numerous and show great potential in the treatment of breast cancer.Their diverse mechanisms of action, which include apoptosis induction, modulation of signalling pathways, and influence on the tumor microenvironment, highlight their multifaceted role in cancer therapy. Clinical research supports their efficacy as adjunct therapies, offering safer alternatives or synergistic enhancements to conventional treatments. Moving forward, continued research efforts are crucial to overcome existing challenges and maximize the therapeutic benefits of natural products. Mechanistic studies should delve deeper into understanding their interactions within biological systems, however more clinical research is required to confirm their safety and

efficacyacross diverse patient populations. Collaboration between traditional and modern medicine practitioners will be instrumental in integrating these natural compounds into comprehensive treatment protocols. In conclusion natural products could be beneficial additions to the breast cancer arsenal, with the potential to improve patient outcomes as well as quality of life. These substances may open the door to innovative treatment approaches that enhance current standards of care by tackling scientific and clinical issues.

REFERENCES

1. Wilkinson L, Gathani T. Understanding breast cancer as a global health concern. The British journal of radiology. 2022;95(1130):20211033
2. Shrihastini V, Muthuramalingam P, Adarshan S, Sujitha M, Chen JT, Shin H, Ramesh M. Plant derived bioactive compounds, their anti-cancer effects and in silico approaches as an alternative target treatment strategy for breast cancer: An updated overview. Cancers. 2021;13(24):6222.
3. Karia P, Patel KV, Rathod SS. Breast cancer amelioration by Butea monosperma in-vitro and in-vivo. Journal of ethnopharmacology. 2018;217:54-62.
4. Sorrenti V, Burò I, Consoli V, Vanella L. Recent advances in health benefits of bioactive compounds from food wastes and by-products: Biochemical aspects. International Journal of Molecular Sciences. 2023;24(3):2019.
5. Roy A, Khan A, Ahmad I, Alghamdi S, Rajab BS, Babalghith AO, Alshahrani MY, Islam S, Islam MR. Flavonoids a bioactive compound from medicinal plants and its therapeutic applications. BioMed Research International. 2022;2022(1):5445291.
6. Sharifi-Rad J, Rayess YE, Rizk AA, Sadaka C, Zgheib R, Zam W, Sestito S, Rapposelli S, Neffe-Skocińska K, Zielińska D, Salehi B. Turmeric and its major compound curcumin on health: bioactive effects and safety profiles for food, pharmaceutical, biotechnological and medicinal applications. Frontiers in pharmacology. 2020;11:550909.
7. Singh BN, Shankar S, Srivastava RK. Green tea catechin, epigallocatechin-3-gallate (EGCG): mechanisms, perspectives and clinical applications. Biochemical pharmacology. 2011;82(12):1807-21.
8. Ferrari E, Bettuzzi S, Naponelli V. The potential of epigallocatechin gallate (EGCG) in targeting autophagy for cancer treatment: A narrative review. International journal of molecular sciences. 2022;23(11):6075.
9. Dias AS, Helguero L, Almeida CR, Duarte IF. Natural compounds as metabolic modulators of the tumor microenvironment. Molecules. 2021 ;26(12):3494.
10. Talib WH, Alsayed AR, Barakat M, Abu-Taha MI, Mahmod AI. Targeting drug chemo-resistance in cancer using natural products. Biomedicines. 2021 ;9(10):1353.
11. Metwaly AM, Ghoneim MM, Eissa IH, Elsehemy IA, Mostafa AE, Hegazy MM, Afifi WM, Dou D. Traditional ancient Egyptian medicine: A review. Saudi journal of biological sciences. 2021;28(10):5823-32.
12. Petrovska BB. Historical review of medicinal plants' usage. Pharmacognosy reviews. 2012;6(11):1.
13. Atanasov AG, Zotchev SB, Dirsch VM, Supuran CT. Natural products in drug discovery: advances and opportunities. Nature reviews Drug discovery. 2021;20(3):200-16.
14. Chaachouay N, Zidane L. Plant-derived natural products: a source for drug discovery and development. Drugs and Drug Candidates. 2024 19;3(1):184-207.
15. Naeem, A.; Hu, P.; Yang, M.; Zhang, J.; Liu, Y.; Zhu, W.; Zheng, Q. Natural Products as Anticancer Agents: Current Status and Future Perspectives. *Molecules* 2022;27,8367.
16. Farghadani R, Naidu R. Curcumin: modulator of key molecular signaling pathways in hormone-independent breast cancer. Cancers. 2021;13(14):3427.
17. Sohn SI, Priya A, Balasubramaniam B, Muthuramalingam P, Sivasankar C, Selvaraj A, Valliammai A, Jothi R, Pandian S. Biomedical applications and bioavailability of curcumin—An updated overview. Pharmaceutics. 2021;13(12):2102.
18. Farhan M, Rizvi A. The pharmacological properties of red grape polyphenol resveratrol: Clinical trials and obstacles in drug development. Nutrients. 2023;15(20):4486.

19. Koushki M, Amiri-Dashatan N, Ahmadi N, Abbaszadeh HA, Rezaei-Tavirani M. Resveratrol: A miraculous natural compound for diseases treatment. Food Science & Nutrition. 2018;6(8):2473-90.
20. Meng T, Xiao D, Muhammed A, Deng J, Chen L, He J. Anti-inflammatory action and mechanisms of resveratrol. Molecules. 2021;26(1):229.
21. Farooqi AA, Qureshi MZ, Khalid S, Attar R, Martinelli C, Sabitaliyevich UY, Nurmurzayevich SB, Taverna S, Poltronieri P, Xu B. Regulation of cell signaling pathways by berberine in different cancers: searching for missing pieces of an incomplete jig-saw puzzle for an effective cancer therapy. Cancers. 2019;11(4):478.
22. Dewi C, Fristiohady A, Amalia R, Khairul Ikram NK, Ibrahim S, Muchtaridi M. Signaling pathways and natural compounds in triple-negative breast cancer cell line. Molecules. 2022;27(12):3661.
23. Giordano A, Tommonaro G. Curcumin and cancer. Nutrients. 2019;11(10):2376.
24. Peng Y, Ao M, Dong B, Jiang Y, Yu L, Chen Z, Hu C, Xu R. Anti-inflammatory effects of curcumin in the inflammatory diseases: status, limitations and countermeasures. Drug design, development and therapy. 2021;4503-25.
25. Moon DO. Curcumin in cancer and inflammation: an in-depth exploration of molecular interactions, therapeutic potentials, and the role in disease management. International Journal of Molecular Sciences. 2024;25(5):2911.
26. Musial C, Kuban-Jankowska A, Gorska-Ponikowska M. Beneficial properties of green tea catechins. International journal of molecular sciences. 2020 ;21(5):1744.
27. Farhan M. Green tea catechins: nature's way of preventing and treating cancer. International journal of molecular sciences. 2022;23(18):10713.
28. Khattar S, Khan SA, Zaidi SA, Darvishikolour M, Farooq U, Naseef PP, Kurunian MS, Khan MZ, Shamim A, Khan MM, Iqbal Z. Resveratrol from dietary supplement to a drug candidate: An assessment of potential. Pharmaceuticals. 2022;15(8):957.
29. Bhat SS, Prasad SK, Shivamallu C, Prasad KS, Syed A, Reddy P, Cull CA, Amachawadi RG. Genistein: a potent anti-breast cancer agent. Current Issues in Molecular Biology. 2021;43(3):1502-17.
30. Kaiser AE, Baniasadi M, Giansiracusa D, Giansiracusa M, Garcia M, Fryda Z, Wong TL, Bishayee A. Sulforaphane: A broccoli bioactive phytocompound with cancer preventive potential. Cancers. 2021;13(19):4796.
31. Asif Ali M, Khan N, Kaleem N, Ahmad W, Alharethi SH, Alharbi B, Alhassan HH, Al-Enazi MM, Razis AF, Modu B, Calina D. Anticancer properties of sulforaphane: current insights at the molecular level. Frontiers in oncology 2023;13:1168321.
32. Imran M, Ghorat F, Ul-Haq I, Ur-Rehman H, Aslam F, Heydari M, Shariati MA, Okuskhanova E, Yessimbekov Z, Thiruvengadam M, Hashempur MH. Lycopene as a natural antioxidant used to prevent human health disorders. Antioxidants2020;9(8):706.
33. Tuli HS, Sak K, Gupta DS, Kaur G, Aggarwal D, Chaturvedi Parashar N, Choudhary R, Yerer MB, Kaur J, Kumar M, Garg VK. Anti-inflammatory and anticancer properties of birch bark-derived betulin: recent developments. Plants 2021;10(12):2663.
34. Lou H, Li H, Zhang S, Lu H, Chen Q. A review on preparation of betulinic acid and its biological activities. Molecules 2021;14;26(18):5583.
35. Golmohammadi M, Zamanian MY, Jalal SM, Noraldeen SA, RamírezCoronel AA, Oudaha KH, Obaid RF, Almulla AF, Bazmandegan G, Kamiab Z. A comprehensive review on Ellagic acid in breast cancer treatment: From cellular effects to molecular mechanisms of action. Food Science & Nutrition 2023;11(12):7458-68.
36. Neag MA, Mocan A, Echeverría J, Pop RM, Bocsan CI, Crişan G, Buzoianu AD. Berberine: Botanical occurrence, traditional uses, extraction methods, and relevance in cardiovascular, metabolic, hepatic, and renal disorders. Frontiers in pharmacology2018;9:557.
37. Ramasamy K, Agarwal R. Multitargeted therapy of cancer by silymarin. Cancer letters 2008;269(2):352-62.
38. Zhou X, Suo F, Haslinger K, Quax WJ. Artemisinin-type drugs in tumor cell death: mechanisms, combination treatment with biologics and nanoparticle delivery. Pharmaceutics 2022;14(2):395.

39. Tripathi AK, Ray AK, Mishra SK. Molecular and pharmacological aspects of piperine as a potential molecule for disease prevention and management: evidence from clinical trials. Beni-Suef university journal of basic and applied sciences2022;11(1):16.
40. Shang A, Cao SY, Xu XY, Gan RY, Tang GY, Corke H, Mavumengwana V, Li HB. Bioactive compounds and biological functions of garlic (Allium sativum L.). Foods2019;8(7):246.
41. Ong CP, Lee WL, Tang YQ, Yap WH. Honokiol: a review of its anticancer potential and mechanisms. Cancers 2019;12(1):48.
42. Trivedi VL, Soni R, Dhyani P, Sati P, Tejada S, Sureda A, Setzer WN, Faizal Abdull Razis A, Modu B, Butnariu M, Sharifi-Rad J. Anti-cancer properties of boswellic acids: mechanism of action as anti-cancerous agent. Frontiers in pharmacology2023;14:1187181.
43. Weaver BA. How Taxol/paclitaxel kills cancer cells. Molecular biology of the cell2014;25(18):2677-81.
44. Musial C, Kuban-Jankowska A, Gorska-Ponikowska M. Beneficial properties of green tea catechins. International journal of molecular sciences 2020;21(5):1744.
45. Farhan M. Cytotoxic Activity of the Red Grape Polyphenol Resveratrol against Human Prostate Cancer Cells: A Molecular Mechanism Mediated by Mobilization of Nuclear Copper and Generation of Reactive Oxygen Species. Life 2024;14(5):611.
46. Farhan M. Cytotoxic Activity of the Red Grape Polyphenol Resveratrol against Human Prostate Cancer Cells: A Molecular Mechanism Mediated by Mobilization of Nuclear Copper and Generation of Reactive Oxygen Species. Life 2024;14(5):611.
47. Farhan M, Rizvi A. The pharmacological properties of red grape polyphenol resveratrol: Clinical trials and obstacles in drug development. Nutrients 2023;15(20):4486.
48. Jang JY, Im E, Kim ND. Mechanism of resveratrol-induced programmed cell death and new drug discovery against cancer: a review. International journal of molecular sciences. 2022;23(22):13689.
49. Song B, Wang W, Tang X, Goh RM, Thuya WL, Ho PC, Chen L, Wang L. Inhibitory potential of resveratrol in cancer metastasis: From biology to therapy. Cancers 2023;15(10):2758.
50. Mao QQ, Xu XY, Cao SY, Gan RY, Corke H, Beta T, Li HB. Bioactive compounds and bioactivities of ginger (Zingiber officinale Roscoe). Foods 2019;8(6):185.
51. Alharbi KS, Nadeem MS, Afzal O, Alzarea SI, Altamimi AS, Almalki WH, Mubeen B, Iftikhar S, Shah L, Kazmi I. Gingerol, a natural antioxidant, attenuates hyperglycemia and downstream complications. Metabolites 2022;12(12):1274.
52. Choi NR, Choi WG, Kwon MJ, Woo JH, Kim BJ. [6]-Gingerol induces caspase-dependent apoptosis in bladder cancer cells via MAPK and ROS signaling. International Journal of Medical Sciences 2022;19(7):1093.
53. Sp N, Kang DY, Lee JM, Bae SW, Jang KJ. Potential antitumor effects of 6-gingerol in p53-dependent mitochondrial apoptosis and inhibition of tumor sphere formation in breast cancer cells. International journal of molecular sciences 2021;22(9):4660.
54. Kim EC, Min JK, Kim TY, Lee SJ, Yang HO, Han S, Kim YM, Kwon YG. [6]-Gingerol, a pungent ingredient of ginger, inhibits angiogenesis in vitro and in vivo. Biochemical and biophysical research communications 2005;335(2):300-8.
55. Adepoju FO, Duru KC, Li E, Kovaleva EG, Tsurkan MV. Pharmacological potential of betulin as a multitarget compound. Biomolecules 2023;13(7):1105.
56. Sharifi-Rad J, Quispe C, Castillo CM, Caroca R, Lazo-Vélez MA, Antonyak H, Polishchuk A, Lysiuk R, Oliinyk P, De Masi L, Bontempo P. Ellagic Acid: A Review on Its Natural Sources, Chemical Stability, and Therapeutic Potential. Oxidative medicine and cellular longevity 2022;2022(1):3848084.
57. Zhu Y, Xie N, Chai Y, Nie Y, Liu K, Liu Y, Yang Y, Su J, Zhang C. Apoptosis induction, a sharp edge of berberine to exert anti-cancer effects, focus on breast, lung, and liver cancer. Frontiers in Pharmacology 2022;13:803717.
58. Kim SH, Choo GS, Yoo ES, Woo JS, Lee JH, Han SH, Jung SH, Kim HJ, Jung JY. Silymarin inhibits proliferation of human breast cancer cells via regulation of the MAPK signaling pathway and induction of apoptosis. Oncology Letters 2021;21(6):1-10.

59. Lu BW, Baum L, So KF, Chiu K, Xie LK. More than anti-malarial agents: therapeutic potential of artemisinins in neurodegeneration. Neural regeneration research 2019;14(9):1494-8.
60. Benayad S, Wahnou H, El Kebbaj R, Liagre B, Sol V, Oudghiri M, Saad EM, Duval RE, Limami Y. The promise of Piperine in cancer chemoprevention. Cancers2023;15(22):5488.
61. Zugaro S, Benedetti E, Caioni G. Garlic (*Allium sativum L.*) as an ally in the treatment of inflammatory bowel diseases. Current Issues in Molecular Biology2023;45(1):685-98.
62. Fried LE, Arbiser JL. Honokiol, a multifunctional antiangiogenic and antitumor agent. Antioxidants & redox signaling 2009;11(5):1139-48.
63. Roy NK, Parama D, Banik K, Bordoloi D, Devi AK, Thakur KK, Padmavathi G, Shakibaei M, Fan L, Sethi G, Kunnumakkara AB. An update on pharmacological potential of boswellic acids against chronic diseases. International journal of molecular sciences 2019;20(17):4101.
64. Kampan NC, Madondo MT, McNally OM, Quinn M, Plebanski M. Paclitaxel and its evolving role in the management of ovarian cancer. BioMed research international 2015;2015(1):413076.
65. Singh BN, Shankar S, Srivastava RK. Green tea catechin, epigallocatechin-3-gallate (EGCG): mechanisms, perspectives and clinical applications. Biochemical pharmacology 2011;82(12):1807-21.
66. Sharifi-Rad J, Rayess YE, Rizk AA, Sadaka C, Zgheib R, Zam W, Sestito S, Rapposelli S, Neffe-Skocińska K, Zielińska D, Salehi B. Turmeric and its major compound curcumin on health: bioactive effects and safety profiles for food, pharmaceutical, biotechnological and medicinal applications. Frontiers in pharmacology 2020;11:550909.
67. Ko JH, Sethi G, Um JY, Shanmugam MK, Arfuso F, Kumar AP, Bishayee A, Ahn KS. The role of resveratrol in cancer therapy. International journal of molecular sciences 2017;18(12):2589.
68. Trejo-Solís C, Pedraza-Chaverrí J, Torres-Ramos M, Jiménez-Farfán D, Cruz Salgado A, Serrano-García N, Osorio-Rico L, Sotelo J. Multiple molecular and cellular mechanisms of action of lycopene in cancer inhibition. Evidence-Based Complementary and Alternative Medicine 2013;2013(1):705121.
69. Sharifi-Rad J, Quispe C, Imran M, Rauf A, Nadeem M, Gondal TA, Ahmad B, Atif M, Mubarak MS, Sytar O, Zhilina OM. Genistein: an integrative overview of its mode of action, pharmacological properties, and health benefits. Oxidative medicine and cellular longevity 2021;2021(1):3268136.
70. Ho E, Clarke JD, Dashwood RH. Dietary sulforaphane, a histone deacetylase inhibitor for cancer prevention. The Journal of nutrition 2009;139(12):2393-6.
71. Kciuk M, Alam M, Ali N, Rashid S, Głowacka P, Sundaraj R, Celik I, Yahya EB, Dubey A, Zerroug E, Kontek R. Epigallocatechin-3-gallate therapeutic potential in cancer: mechanism of action and clinical implications. Molecules 2023;28(13):5246.
72. Jang WY, Hwang JY, Cho JY. Ginsenosides from Panax ginseng as key modulators of NF-κB signaling are powerful anti-inflammatory and anticancer agents. International Journal of Molecular Sciences 2023;24(7):6119.
73. Rather RA, Bhagat M. Quercetin as an innovative therapeutic tool for cancer chemoprevention: Molecular mechanisms and implications in human health. Cancer medicine 2020;9(24):9181-92.
74. Dhyani P, Quispe C, Sharma E, Bahukhandi A, Sati P, Attri DC, Szopa A, Sharifi-Rad J, Docea AO, Mardare I, Calina D. Anticancer potential of alkaloids: a key emphasis to colchicine, vinblastine, vincristine, vindesine, vinorelbine and vincamine. Cancer cell international 2022;22(1):206.
75. Thorn CF, Oshiro C, Marsh S, Hernandez-Boussard T, McLeod H, Klein TE, Altman RB. Doxorubicin pathways: pharmacodynamics and adverse effects. Pharmacogenetics and genomics 2011;21(7):440-6.
76. Maximov PY, Abderrahman B, Fanning SW, Sengupta S, Fan P, Curpan RF, Rincon DM, Greenland JA, Rajan SS, Greene GL, Jordan VC. Endoxifen, 4-hydroxytamoxifen and an estrogenic derivative modulate estrogen receptor complex mediated apoptosis in breast cancer. Molecular pharmacology 2018;94(2):812-22.
77. Sharma S, Shukla MK, Sharma KC, Tirath, Kumar L, Anal JM, Upadhyay SK, Bhattacharyya S, Kumar D. Revisiting the therapeutic potential of gingerols against different pharmacological activities. Naunyn-Schmiedeberg's Archives of Pharmacology 2023;396(4):633-47.
78. Tong X, C Pelling J. Targeting the PI3K/Akt/mTOR axis by apigenin for cancer prevention. Anti-Cancer Agents in Medicinal Chemistry (Formerly Current Medicinal Chemistry-Anti-Cancer Agents) 2013;13(7):971-8.

79. Ren JI, Lu Y, Qian Y, Chen B, Wu TA, Ji G. Recent progress regarding kaempferol for the treatment of various diseases. Experimental and therapeutic medicine2019;18(4):2759-76.
80. Khan N, Syed DN, Ahmad N, Mukhtar H. Fisetin: a dietary antioxidant for health promotion. Antioxidants & redox signaling 2013;19(2):151-62.
81. Ahmadi A, Mortazavi Z, Mehri S, Hosseinzadeh H. Protective and therapeutic effects of Scutellariabaicalensis and its main active ingredients baicalin and baicalein against natural toxicities and physical hazards: a review of mechanisms. DARU Journal of Pharmaceutical Sciences 2022;30(2):351-66.
82. Kan LL, Chan BC, Leung PC, Wong CK. Natural-product-derived adjunctive treatments to conventional therapy and their immunoregulatory activities in triple-negative breast cancer. Molecules 2023;28(15):5804.
83. Cacciola NA, Cuciniello R, Petillo GD, Piccioni M, Filosa S, Crispi S. An overview of the enhanced effects of curcumin and chemotherapeutic agents in combined cancer treatments. International Journal of Molecular Sciences 2023;24(16):12587.
84. Almatroodi SA, Almatroudi A, Khan AA, Alhumaydhi FA, Alsahli MA, Rahmani AH. Potential therapeutic targets of epigallocatechin gallate (EGCG), the most abundant catechin in green tea, and its role in the therapy of various types of cancer. Molecules 2020;25(14):3146.
85. Kursvietiene L, Kopustinskiene DM, Staneviciene I, Mongirdiene A, Kubová K, Masteikova R, Bernatoniene J. Anti-cancer properties of resveratrol: a focus on its impact on mitochondrial functions. Antioxidants 2023;12(12):2056.
86. Sharma S, Cwiklinski K, Mahajan SD, Schwartz SA, Aalinkeel R. Combination modality using quercetin to enhance the efficacy of docetaxel in prostate cancer cells. Cancers 2023;15(3):902.
87. Chunarkar-Patil P, Kaleem M, Mishra R, Ray S, Ahmad A, Verma D, Bhayye S, Dubey R, Singh HN, Kumar S. Anticancer Drug Discovery based on Natural products: from computational approaches to Clinical studies. Biomedicines 2024;12(1):201.
88. Choudhari AS, Mandave PC, Deshpande M, Ranjekar P, Prakash O. Phytochemicals in cancer treatment: From preclinical studies to clinical practice. Frontiers in pharmacology 2020;10:1614.
89. Zhang W, Li S, Li C, Li T, Huang Y. Remodeling tumor microenvironment with natural products to overcome drug resistance. Frontiers in Immunology 2022;13:1051998.
90. Olayiwola Y, Gollahon L. Natural Compounds and Breast Cancer: Chemo-Preventive and Therapeutic Capabilities of Chlorogenic Acid and Cinnamaldehyde. Pharmaceuticals 2024;17(3):361.
91. Zari AT, Zari TA, Hakeem KR. Anticancer properties of eugenol: A review. Molecules 2021;26(23):7407.
92. Nan Y, Su H, Zhou B, Liu S. The function of natural compounds in important anticancer mechanisms. Frontiers in Oncology 2023;12:1049888.
93. Marín V, Burgos V, Pérez R, Maria DA, Pardi P, Paz C. The potential role of Epigallocatechin-3-Gallate (EGCG) in breast cancer treatment. International Journal of Molecular Sciences 2023;24(13):10737.
94. Farghadani R, Naidu R. Curcumin as an enhancer of therapeutic efficiency of chemotherapy drugs in breast cancer. International Journal of Molecular Sciences2022;23(4):2144.
95. Ko JH, Sethi G, Um JY, Shanmugam MK, Arfuso F, Kumar AP, Bishayee A, Ahn KS. The role of resveratrol in cancer therapy. International journal of molecular sciences 2017;18(12):2589.
96. Aghababaei F, Hadidi M. Recent advances in potential health benefits of quercetin. Pharmaceuticals 2023;16(7):1020.

Table 1. A concise overview of various natural products, their sources, modes of action, and the signalling pathways

Natural Product	Source	Mode of Action	Signalling Pathways Involved	Ref.
Betulinic Acid	Birch bark	Induces apoptosis, inhibits Bcl-2, modulates NF-κB, MAPK	NF-κB, MAPK	55
Ellagic Acid	Berries (e.g., strawberries)	Antioxidant, anti-inflammatory, induces apoptosis, modulates PI3K/Akt, NF-κB	PI3K/Akt, NF-κB	56

Berberine	Berberis species	prevents the growth of cells,triggersapoptosis,modulates AMPK, NF-κB	AMPK, NF-κB	57
Silibinin	Milk thistle	Antioxidant, anti-inflammatory, stops cell division and triggers apoptosis, modulates STAT3, MAPK	STAT3, MAPK	58
Artemisinin	Sweet wormwood	Induces apoptosis, modulates NF-κB, MAPK	NF-κB, MAPK	59
Piperine	Black pepper	Enhances bioavailability, stops cell division and triggers apoptosis modulates PI3K/Akt, NF-κB	PI3K/Akt, NF-κB	60
Allicin	Garlic	Antioxidant, anti-inflammatory, induces apoptosis, modulates NF-κB, MAPK	NF-κB and MAPK	61
Honokiol	Magnolia bark	Antioxidant, anti-inflammatory, induces apoptosis, modulates PI3K/Akt, NF-κB	PI3K/Akt, NF-κB	62
Boswellic Acid	Boswellia serrata	Anti-inflammatory, induces apoptosis, modulates NF-κB, MAPK	NF-κB, MAPK	63
Taxol (Paclitaxel)	Pacific yew tree	Stabilizes microtubules, induces apoptosis, modulates MAPK, PI3K/Akt	MAPK, PI3K/Akt	64
Catechins	Green tea	Antioxidant, stops cell division and triggers apoptosis,modulates MAPK, PI3K/Akt	MAPK, PI3K/Akt	65
Curcumin	Turmeric	Antioxidant, anti-inflammatory, induces apoptosis, modulates PI3K/Akt, NF-κB	PI3K/Akt, NF-κB	66
Resveratrol	Grapes, berries, peanuts, red wine	Antioxidant, induces apoptosis, inhibits metastasis, modulates NF-κB, PI3K/Akt, AMPK	NF-κB, PI3K/Akt, AMPK	67
Lycopene	Tomatoes	Antioxidant, inhibits cell proliferation, modulates IGF pathway	IGF pathway	68
Genistein	Soybeans	Modulates estrogen receptors, induces apoptosis, inhibits tyrosine kinase	Estrogen receptors, tyrosine kinase	69
Sulforaphane	Cruciferous vegetables	Induces detoxification enzymes, inhibits HDAC, promotes apoptosis	HDAC	70
EGCG (Epigallocatechin gallate)	Green tea (*Camellia sinensis*)	Antioxidant, anti-cancer	EGFR, PI3K/Akt, MAPK pathways	71
Ginsenosides	Ginseng (*Panax ginseng*)	Anti-inflammatory, immune modulation	EGFR, MAPK, NF-κB pathways	72
Quercetin	Fruits, vegetables	Antioxidant, anti-inflammatory	PI3K/Akt, NF-κB, MAPK pathways	73
Docetaxel (Taxotere)	Pacific yew tree (*Taxus brevifolia*)	Cytotoxic	Microtubule stabilization, apoptosis induction	
Vincristine	Periwinkle plant (*Catharanthus roseus*)	Cytotoxic	Microtubule depolymerization, cell cycle arrest	74
Doxorubicin	*Streptomyces peucetius*	Cytotoxic	DNA damage response, apoptosis	75

			induction	
Tamoxifen	Synthetic derivative of tamoxifen	Hormonal	Estrogen receptor (ER) signaling inhibition	76
Gingerol	Ginger	Antioxidant, anti-inflammatory, induces apoptosis, inhibits angiogenesis	NF-κB, PI3K/Akt, MAPK	77
Apigenin	Parsley, celery	Antioxidant, induces apoptosis, inhibits cell proliferation	NF-κB, PI3K/Akt	78
Kaempferol	Tea, broccoli, grapefruit	Antioxidant, anti-inflammatory, induces apoptosis	NF-κB, PI3K/Akt	79
Fisetin	Strawberries, apples, persimmons	Antioxidant, induces apoptosis, inhibits cell proliferation	NF-κB, PI3K/Akt	80
Baicalein	*Scutellariabaicalensis* (Chinese skullcap)	Antioxidant, anti-inflammatory, induces apoptosis	NF-κB, PI3K/Akt	81

Vol.15 / Issue 88 / Feb / 2025 *International Bimonthly (Print) – Open Access* *ISSN: 0976 – 0997*

RESEARCH ARTICLE

Transformations in Yetthinahole Catchment Area, Hassan District, Karnataka: A Machine Learning and Geo Informatics Study of Land Cover Over Time

Mahesha D B[1]* and Shivanna

[1]Assistant Professor, Division of Geoinformatics, School of Life Sciences, JSS Academy of Higher Education and Research (Deemed to be University), Mysuru, Karnataka, India.
[2]Professor (Rtd.), Department of Marine Geology, Mangalore University, Konaje, Dakshina Kannada, Karnataka, India

Received: 21 Oct 2024 Revised: 03 Dec 2024 Accepted: 18 Jan 2025

***Address for Correspondence**
Mahesha D B
Assistant Professor,
Division of Geoinformatics,
School of Life Sciences,
JSS Academy of Higher Education and Research (Deemed to be University),
Mysuru, Karnataka, India.
E.Mail: maheshmaruguli@jssuni.edu.in

ABSTRACT

In the present study, we explore the dynamics of land cover transitions within the Yetthinahole catchment area, situated in the Hassan district of Karnataka state over a period extending from 1973 to 2023, leveraging advanced methodologies in Geoinformatics and machine learning. The catchment has undergone extensive changes, influenced by agricultural expansion, urbanization, deforestation, and climate change, leading to significant alterations in the landscape. These changes call for a thorough examination of its growing land surface patterns to informed decision-making and sustainable development. This analysis incorporates integration of survey of India toposheets and satellite imageries. The methodology developed combines remote sensing data with the sophisticated machine learning technique, Support Vector Machines (SVM), to precisely classify and measure the extent of land cover alterations. The use of Geoinformatics tools, including Geographic Information System (GIS), was crucial in processing, analysing and visualizing the data, revealing the study areas temporal changes. Through the application of Geoinformatics and machine learning techniques, the study provides support for a well-versed evaluation system for the sustainable use of natural resources.

Keywords: Machine learning, Geoinformatics, Support Vector Machines, Yetthinahole, land cover.

INTRODUCTION

In this study, we explore land cover changes over time in Yetthinahole catchment area, Hassan District, Karnataka, employing machine learning and geoinformatics techniques. Research on land cover changes in Yetthinahole catchment aids sustainable planning and conservation efforts crucial for ecosystem health and resource management. Land cover mapping has become one of the essential studies in environmental and geoscience. Since the introduction of remote sensing, land cover mapping has gained popularity among scientists and researchers (Alberti, 2008). Land cover mapping is a technique of mapping the features on the earth's surface using remote sensing imageries and deploying different tools and algorithms (Alberti, 2008). Over the years, various pattern recognition techniques have been developed to automate this process from remote sensor imagery. Support vector machines (SVM) is one of them (Bazi & Melgani, 2006). Support Vector Machine (SVM) stands as a supervised learning paradigm pivotal in discerning optimal hyperplanes for partitioning data across distinct categories (Bazi & Melgani, 2006). In the realm of land cover delineation from remote sensing imagery, SVM emerges as a potent tool for classifying diverse land cover categories, leveraging complex mathematical formulations and feature extraction methodologies to accomplish precise categorization tasks (Foody & Mathur, 2004). Land cover mapping, a critical component of environmental monitoring and land management, has significantly benefited from advancements in machine learning and geoinformatics. This review aims to elucidate recent research findings and methodologies concerning land cover mapping, the technological innovations facilitating it, the integration of machine learning techniques, and the advantages attributed to employing machine learning in this domain.

Land Cover Mapping: Land cover mapping involves the classification and characterization of different surface types, including forests, water bodies, urban areas, and agricultural lands (Friedl & Brodley, 1997). Traditional methods relied on manual interpretation of aerial imagery, but recent advances in remote sensing technology have revolutionized the field (Friedl & Brodley, 1997). Satellite sensors like Landsat, Sentinel, and MODIS provide multispectral data, enabling comprehensive land cover assessments at various spatial and temporal scales (Friedl & Brodley, 1997). Technology in Landcover Mapping: Geoinformatics, the integration of geographic information systems (GIS), remote sensing, and spatial analysis, plays a pivotal role in land cover mapping (Lillesand et al., 2014). GIS platforms offer powerful tools for processing and analyzing spatial data, facilitating the creation of accurate land cover maps (Lillesand et al., 2014). Additionally, the development of high-resolution satellite imagery and LiDAR technology has enhanced the precision and detail of land cover mapping (Khatami et al., 2016). Machine Learning for Land Cover Mapping: Machine learning algorithms have emerged as effective tools for automating land cover classification tasks (Pal & Mather, 2005). Supervised learning methods, including support vector machines (SVM), random forests, and neural networks, have been widely utilized for their ability to learn complex patterns from training data and classify land cover types with high accuracy (Belgiu & Dragut, 2016).

Furthermore, unsupervised learning techniques, such as clustering algorithms, enable exploratory analysis of unlabeled datasets, aiding in land cover classification (K-means, Gaussian Mixture Models) (Jain et al., 1999). Chakraborty et al. (2020), the authors delve into the significance of employing machine learning and geoinformatics in studying land cover changes. They emphasize the importance of understanding transformations in specific regions, such as the Yetthinahole catchment area in Hassan District, Karnataka, for effective environmental management (Chakraborty et al., 2020). By integrating advanced techniques, such as remote sensing and spatial analysis, researchers can elucidate temporal variations in land cover patterns, facilitating informed decision-making processes for sustainable development (Chakraborty et al., 2020). A study by Kumar et al. (2019) investigates land cover changes using machine learning and geoinformatics in the Yetthinahole catchment area, Hassan District, Karnataka. They emphasize the importance of such research in informing sustainable land management strategies (Kumar et al., 2019). Advantages of Machine Learning in Landcover Mapping: The adoption of machine learning in land cover mapping offers several advantages over traditional methods (Foody & Mathur, 2004). Firstly, machine learning algorithms can process large volumes of remote sensing data quickly and efficiently, enabling timely land cover assessments (Foody & Mathur, 2004). Secondly, these algorithms can handle complex datasets with multiple

spectral bands, temporal layers, and spatial attributes, enhancing the accuracy and detail of land cover maps (Platt, 1999). Additionally, machine learning models are adaptable and scalable, allowing for the integration of diverse data sources and the customization of classification criteria to suit specific study areas and objectives (Liu et al., 2020). In summary, the integration of machine learning and geoinformatics holds tremendous potential for advancing our understanding of land cover dynamics over time. By leveraging sophisticated algorithms and cutting-edge technology, researchers can generate comprehensive land cover maps that inform sustainable land management practices and support environmental conservation efforts (Foody & Mathur, 2004; Lillesand et al., 2014).

RESEARCH GAP

Despite the improvement in the technological aspects, there's a research gap in comprehensive integration of satellite data, SVM classification, and GIS visualization for analyzing multi-decadal land cover changes in Yetthinahole catchment (Khatami et al., 2016; Bazi & Melgani, 2006; Lillesand et al., 2014). Such a study would bridge understanding gaps and enhance decision-making for sustainable land management in the region (Chakraborty et al., 2020; Kumar et al., 2019).

Objectives of the study

- To generate a land cover cartographic representation of catchment are from 1973-2023 utilizing Support Vector Machine (SVM) algorithmic methodology.
- To quantitate land cover dynamics in Yetthinahole catchment area spanning from 1973 to 2023.
- To utilize geoinformatics methodologies for scrutinizing land cover patterns and comprehending spatiotemporal land surface alterations.

STUDY AREA

In Karnataka state, the catchment area of Yetthinahole is located in the western ghat but in South West part of Sakleshpur taluk of Hasan district (Figure 1). It extends for a length between 76°36′E and 76°45′E longitude and for a width between 12°44′N and 12°58′N latitude. The area has an overall surface measurement of 292 sq. km.The elevation varies from 171m to 1130m above mean sea level resulting in dense network of streams while the landforms are undulating. The study area consists mainly of loamy soils that include sandy loam to clay loam types (Ramachandra T.V., 2015).

MATERIALS AND METHODS

DATA AND SOFTWARE USED

The study utilized SOI toposheets (1:50,000 scale, 1968-69), Landsat imageries (1973-2023) from USGS Earth Explorer, and LISS III imageries (2011) from Bhuvan Portal for land use/land cover mapping. Vector layers were sourced from SoI and KGIS for location maps. ArcMap 10.8.2 was used for training sites and SVM classification, MS Excel for data analysis, and a Garmin GPS device for field data collection (Table 1).

METHODOLOGY

In the present study two sections are made mainly involves the preparation of land use land cover mapping and its accuracy assessment.

LAND USE/ LAND COVER MAPPING

A training set with 30p pixels, as per the spectral reflectance level of remote sensing image, adequately captures the spectral characteristics of the target class(Foody & Mathur, 2004). Additionally, edge spectral responses from the target land-cover spectral space serve as potent support vectors, surpassing those located at the center of the spectral cluster(Mountrakis, Im, & Ogole, 2011). The edge training set, comprising mixed and corner pixels, contributes to creating an optimal hypersphere(Pal & Mather, 2005).Our approach leverages the phenomenon where mixed pixels,

straddling class boundaries, exhibit dual spectral responseseach dominated by adjacent classes separated by that boundary(Schneider, 2012). These mixed spectral responses, proximate in the feature space, yield informative outliers that effectively constrain the hypersphere(Melgani & Bruzzone, 2004).After generating training sites, followed by training the Support Vector Machine (SVM) algorithm using these selected sites(Vapnik, 1995). Subsequently, the image undergoes classification into optimized classes(Mountrakis et al., 2011).

ACCURACY ASSESSMENT

To evaluate the accuracy of this classification, we conducted rigorous accuracy assessments. An equalized stratified random sampling method was employed in this study to evaluate the accuracy of each land use classification (Congalton & Green, 2009). Random point tools were utilized to perform the classification accuracy assessment (Stehman, 1997). Kappa analysis, a discrete multivariate technique (Jensen, 2007), was used for accuracy evaluation (Jensen, 2007). Sixty points from each class were randomly chosen and verified against the LULC classified map. The map's accuracy was determined by comparing the thematic map with ground observation points (Congalton & Green, 2009).

RESULTS AND DISCUSSIONS

As seen in the Table 2 and Figure (2(a), (b), (c), (d), (e) and (f)) dense forest declines steadily from 156.06 sq km (1973) to 96.06 sq km (2023) due to deforestation and land conversion. Plantation *(tea, coffee, forest species)* increase consistently from 62.04 sq km (1973) to 90.04 sq km (2023), reflecting increase in economic crop cultivation. Grasslands fluctuate but remain relatively stable, resilient to changes. Cropland expands significantly from 7.27 sq km (1973) to 39.43 sq km (2023), indicating agricultural intensification. Built-up areas grow steadily from 1.23 sq km (1973) to 6.70 sq km (2023), reflecting urbanization. Water body coverage remains relatively stable, while roads and railways expand notably, indicating infrastructure development (Figure 3). In Table 3Grassland's PA and UA values range from 0.78 to 1.00, indicating variability and high KC values. Water body accuracy fluctuates significantly, with KC reflecting this variability. Dense forest maintains high PA, UA, and KC values, indicating stable classification. Plantation accuracy varies from 0.72 to 1.00, with corresponding KC values. Cropland shows considerable variability in accuracy, with KC reflecting this. Infrastructure accuracy ranges from 0.62 to 1.00, with KC mirroring accuracy metrics.

CONCLUSIONS

The use of advanced Geoinformatics and machine learning techniques, notably Support Vector Machines (SVM), enabled precise analysis of land cover changes in the Yetthinahole catchment area. The study reveals significant impacts of agricultural expansion, urbanization, and deforestation on land cover. Integrating ground data and satellite imagery enhanced accuracy, providing valuable insights for decision-making and sustainable land management strategies.

REFERENCES

1. Alberti, M. (2008). Advances in urban ecology: Integrating humans and ecological processes in urban ecosystems. Springer Science & Business Media.
2. Bazi, Y., & Melgani, F. (2006). Toward an optimal SVM classification system for hyperspectral remote sensing images. IEEE Transactions on Geoscience and Remote Sensing, 44(11), 3374-3385.
3. Alberti, M. (2008). Advances in Urban Ecology: Integrating Humans and Ecological Processes in Urban Ecosystems. Springer.
4. Bazi, Y., & Melgani, F. (2006). Toward an optimal SVM classification system for hyperspectral remote sensing images. IEEE Transactions on Geoscience and Remote Sensing, 44(11), 3374-3385.

5. Foody, G. M., & Mathur, A. (2004). A relative evaluation of multiclass image classification by support vector machines. IEEE Transactions on Geoscience and Remote Sensing, 42(6), 1335-1343.
6. Friedl, M. A., & Brodley, C. E. (1997). Decision tree classification of land cover from remotely sensed data. Remote Sensing of Environment, 61(3), 399-409.
7. Lillesand, T., Kiefer, R. W., & Chipman, J. (2014). Remote Sensing and Image Interpretation. John Wiley & Sons.
8. Khatami, R., Mountrakis, G., & Stehman, S. V. (2016). A meta-analysis of remote sensing research on supervised pixel-based land-cover image classification processes. ISPRS Journal of Photogrammetry and Remote Sensing, 114, 127-137.
9. Pal, M., & Mather, P. M. (2005). Support vector machines for classification in remote sensing. International Journal of Remote Sensing, 26(5), 1007-1011.
10. Belgiu, M., & Dragut, L. (2016). Random forest in remote sensing: A review of applications and future directions. ISPRS Journal of Photogrammetry and Remote Sensing, 114, 24-31.
11. Jain, A. K., Murty, M. N., & Flynn, P. J. (1999). Data clustering: A review. ACM Computing Surveys (CSUR), 31(3), 264-323.
12. Chakraborty, S., et al. (2020). Application of machine learning techniques for land cover mapping using remote sensing data. Journal of Environmental Management, 258, 110058.
13. Kumar, S., et al. (2019). Monitoring land cover changes in the Yetthinahole catchment area using machine learning techniques. Journal of Environmental Informatics, 34(2), 123-133.
14. Platt, J. (1999). Probabilistic outputs for support vector machines and comparisons to regularized likelihood methods. Advances in Large Margin Classifiers, 10(3), 61-74.
15. Liu, Y., et al. (2020). Machine learning approaches for land cover classification: A review. ISPRS Journal of Photogrammetry and Remote Sensing, 164, 283-295.
16. Khatami, R., Mountrakis, G., & Stehman, S. V. (2016). A meta-analysis of remote sensing research on supervised pixel-based land-cover image classification processes. ISPRS Journal of Photogrammetry and Remote Sensing, 114, 127-137.
17. Bazi, Y., & Melgani, F. (2006). Toward an optimal SVM classification system for hyperspectral remote sensing images. IEEE Transactions on Geoscience and Remote Sensing, 44(11), 3374-3385.
18. Lillesand, T., Kiefer, R. W., & Chipman, J. (2014). Remote Sensing and Image Interpretation. John Wiley & Sons.
19. Chakraborty, S., et al. (2020). Application of machine learning techniques for land cover mapping using remote sensing data. Journal of Environmental Management, 258, 110058.
20. Kumar, R., Singh, A., & Pandey, A. (2019). Land cover change detection using machine learning and geoinformatics in Yetthinahole catchment, Hassan District, Karnataka. Journal of the Indian Society of Remote Sensing, 47(2), 245-256.
21. Foody, G. M., & Mathur, A. (2004). A relative evaluation of multiclass image classification by support vector machines. IEEE Transactions on Geoscience and Remote Sensing, 42(6), 1335-1343.
22. Mountrakis, G., Im, J., & Ogole, C. (2011). Support vector machines in remote sensing: A review. ISPRS Journal of Photogrammetry and Remote Sensing, 66(3), 247-259.
23. Pal, M., & Mather, P. M. (2005). Support vector machines for classification in remote sensing. International Journal of Remote Sensing, 26(5), 1007-1011.
24. Schneider, A. (2012). Monitoring land cover and land use dynamics with multi-temporal remote sensing data: An approach towards an operational monitoring system. Remote Sensing of Environment, 124, 147-160.
25. Melgani, F., & Bruzzone, L. (2004). Classification of hyperspectral remote sensing images with support vector machines. IEEE Transactions on Geoscience and Remote Sensing, 42(8), 1778-1790.
26. Vapnik, V. N. (1995). The nature of statistical learning theory. Springer-Verlag.
27. Congalton, R. G., & Green, K. (2009). Assessing the Accuracy of Remotely Sensed Data: Principles and Practices. CRC Press.
28. Stehman, S. V. (1997). Selecting and interpreting measures of classification accuracy. Remote Sensing of Environment, 62(1), 77-89.
29. Jensen, J. R. (2007). Remote Sensing of the Environment: An Earth Resource Perspective. Pearson Education.

Table 1: Data and software used for the study.

Sl.No.	Data	Source	Description
1.	SOI toposheet	SOI, GoI.	Toposheet od 1: 50000 scale, having No. 48P9, 48P10 and No.48P13, 48P14 of first edition surveyed during 1968-69 used for the collection of training sites.
2.	Landsat Imageries	USGS Earth Explorer Portal.	Landsat imageries of different spatial resolution, used to derive the land use land cover map of 1973, 1981, 1991, 2001 and 2023.
3.	LISS III	Bhuvan Portal	LISS III imageries of 23.5m spatial resolution, used to derive the land use land cover map of 2011.
4.	Study area vector layers	SoI, GOI and KGIS	To prepare location maps
Software			
1.	ArcMap 10.8	ESRI	Preparation of training sites and SVM classification
2.	MS Excel	Microsoft	Data Analysis
3.	GPS Device	Garmin	Field Data collection

Table 2: Land Use/Land Cover Changes Over Five Decades

Class	1973	1981	1991	2001	2011	2023
Dense Forest	156.06	143.25	116.72	110.56	107.26	96.06
Plantation	62.04	73.07	82.56	84.23	88.27	90.04
Grassland	63.59	60.55	62.55	53.90	52.78	50.46
Cropland	7.27	12.37	24.95	35.53	34.26	39.43
Built-up	1.23	1.18	2.57	3.21	4.70	6.70
Waterbody	0.80	0.80	0.79	0.80	0.80	0.78
Other (Road/Railway)	1.18	1.05	1.36	3.69	3.93	8.53
Area (km²)	**292**	**292**	**292**	**292**	**292**	**292**

Table 3: Classification accuracy assessment results.

	1973				1981				1991				2001				2011				2023			
Class	**PA**	**UA**	**OA**	**KC**	**PA**	**UA**	**OA**	**KC**	**PA**	**UA**	**OA**	**KC**	**PA**	**UA**	**OA**	**KC**	**PA**	**UA**	**OA**	**KC**	**PA**	**UA**	**OA**	**KC**
Grassland	0.93	0.88	0.83	0.78	0.82	0.82	0.85	0.78	1.00	1.00	0.92	0.90	1.00	0.95	0.92	0.90	0.95	1.00	0.90	0.86	0.93	1.00	0.98	0.96
Waterbody	0.90	0.90			0.73	0.80			0.79	1.00			0.67	1.00			0.13	1.00			1.00	0.10		
Dense Forest	0.87	1.00			0.92	0.89			0.92	0.85			0.98	0.93			0.95	0.87			1.00	1.00		
Plantation	0.82	0.90			0.72	0.76			1.00	0.88			1.00	0.95			1.00	0.82			1.00	1.00		
Cropland	0.43	0.90			0.90	0.90			1.00	1.00			1.00	0.71			1.00	1.00			1.00	1.00		
Other(Road/Railway)	1.00	0.62			0.80	0.80			1.00	1.00			0.77	1.00			0.79	1.00			1.00	1.00		

Note -PA- Producer Accuracy, UA- User Accuracy, OA- Overall Accuracy, KC – Kappa Coefficient

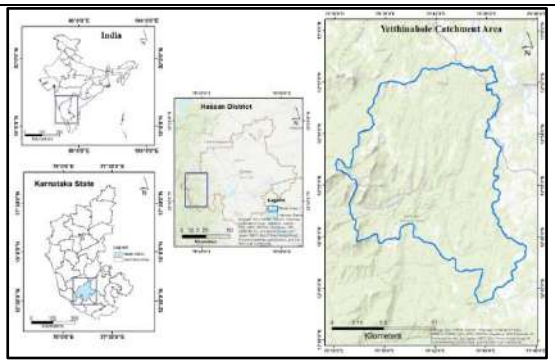

Figure 1: Location map of the Yetthinahole Catchment area, showing the topography of the terrain. The coordinates are in degree minute seconds in the maps.

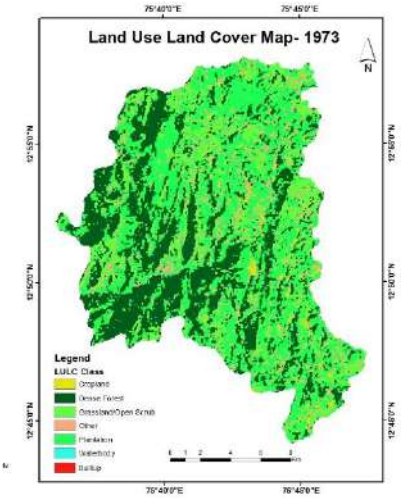

Figure 2(a) - In 1973, the specified area featured 156.06 sq km of dense forest, 62.04 sq km of plantations, 63.59 sq km of grassland, 7.27 sq km of cropland, 1.23 sq km of built-up areas, 0.80 sq km of water bodies, and 1.18 sq km of roads/railways.

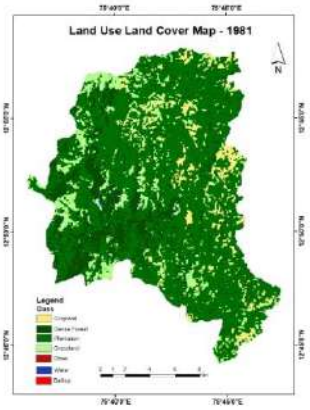

Figure 2(b) - In 1981, the landscape comprised 143.25 sq km of dense forest, 73.07 sq km of plantations, 60.55 sq km of grassland, 12.37 sq km of cropland, 1.18 sq km of built-up areas, 0.80 sq km of waterbodies, and 1.05 sq km of roads/railways.

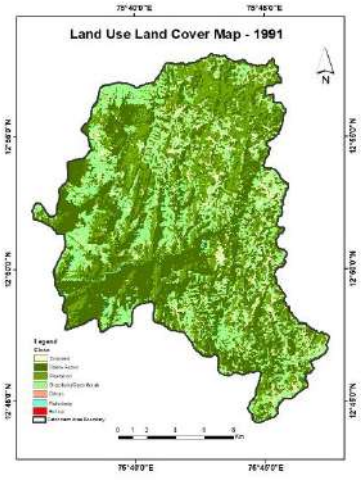

Figure 2(c) - In 1991, the landscape exhibited 116.72 sq km of dense forest, 82.56 sq km of plantations, 62.55 sq km of grassland, 24.95 sq km of cropland, 2.57 sq km of built-up areas, 0.79 sq km of waterbodies, and 1.36 sq km of roads/railways

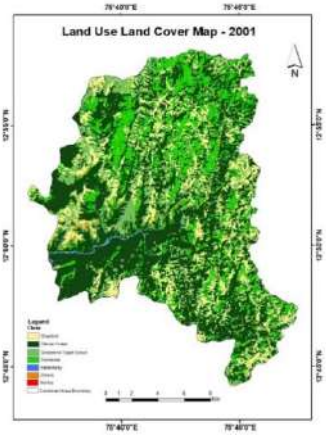

Figure 2(d) - In 2001, the landscape comprised 110.56 sq km of dense forest, 84.23 sq km of plantations, 53.90 sq km of grassland, 35.53 sq km of cropland, 3.21 sq km of built-up areas, 0.80 sq km of waterbodies, and 3.69 sq km of roads/railways.

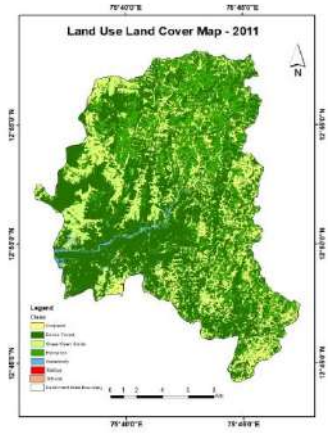

Figure 2(e) - In 2011, the landscape featured 107.26 sq km of dense forest, 88.27 sq km of plantations, 52.78 sq km of grassland, 34.26 sq km of cropland, 4.70 sq km of built-up areas, 1.94 sq km of waterbodies, and 3.93 sq km of roads/railways.

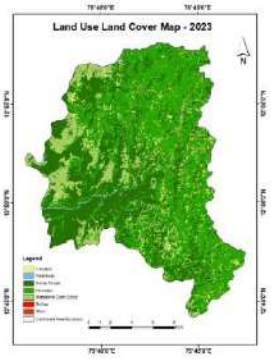

Figure 2(f)- In 2023, the landscape exhibited 96.06 sq km of dense forest, 90.04 sq km of plantations, 50.46 sq km of grassland, 39.43 sq km of cropland, 6.70 sq km of built-up areas, 0.78 sq km of waterbodies, and 8.53 sq km of roads/railways.

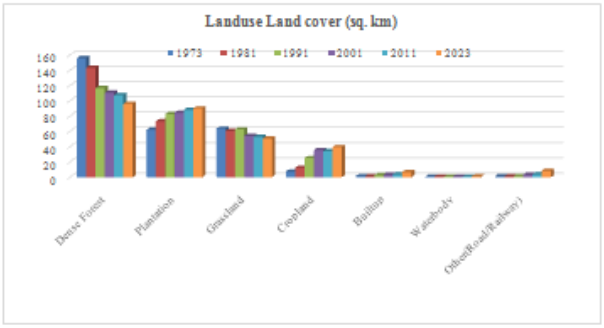

Figure 3 - Changes in Land Use/Land Cover Over Five Decades.

Vol.15 / Issue 88 / Feb / 2025 *International Bimonthly (Print) – Open Access* *ISSN: 0976 – 0997*

RESEARCH ARTICLE

Investigating the Effectiveness of Treadmill vs Non Incremental Exercise with Breathing on Pulmonary Function and VO2 Max in Obese Children

AR Roxy[1]*, Nagaraj Srinivasan[2],Balchandar.V[3], Senthil Kumar.B[4] and Jeyakumar.S[5]

[1]Associate Professor, Department of Physiotherapy, UCA College of Paramedical Science, (Affiliated to Dr. M.G.R. Medical University), Chennai, Tamil Nadu, India.
[2]Professor, Department of Physiotherapy, Jaya College of Paramedical Science, (Affiliated to Dr. M.G.R. Medical University), Chennai, Tamil Nadu, India.
[3]Principal and Professor, Department of Physiotherapy, Jaya College of Paramedical Science, (Affiliated to Dr. M.G.R. Medical University), Chennai, Tamil Nadu, India.
[4]Principal and Professor, Department of Physiotherapy, UCA college of Paramedical Science, (Affiliated to Dr. M.G.R. Medical University), Chennai, Tamil Nadu, India.
[5]Professor and Research Supervisor, Department of Physiotherapy, School of Health Science, University of Bangalore, Karnataka, India.

Received: 21 Nov 2024 Revised: 03 Dec 2024 Accepted: 31 Jan 2025

***Address for Correspondence**
AR Roxy
Associate Professor,
Department of Physiotherapy,
UCA College of Paramedical Science,
(Affiliated to Dr. M.G.R. Medical University),
Chennai, Tamil Nadu, India.

ABSTRACT

Childhood obesity poses significant health risks, including impaired pulmonary function and reduced cardiorespiratory fitness. This study aims to compare the effectiveness of treadmill training with diaphragmatic breathing exercises (Group A) versus non-treadmill exercise with diaphragmatic breathing exercises (Group B) in improving pulmonary function and VO2 max in obese children. Forty obese children aged 12 to 18 years were randomly assigned to Group A or Group B. Pre-test assessments included spirometry tests and the Cooper test to measure pulmonary function and VO2 max, respectively. Both groups underwent six weeks of supervised exercise sessions five days a week. Group A engaged in treadmill training, while Group B participated in non-treadmill exercises. Post-intervention assessments were conducted, and data were analyzed using descriptive and inferential statistics. Both Group A and Group B showed significant improvements in VO2 max post-intervention. No significant differences were observed in pulmonary function between the two groups. Both interventions proved effective in enhancing cardio respiratory fitness among obese children. Treadmill training and non-treadmill exercises, coupled with diaphragmatic breathing exercises, demonstrate effectiveness in improving cardio respiratory fitness in obese children. Promoting regular physical activity and proper breathing techniques is crucial in managing childhood obesity and optimizing health outcomes.

Keywords: Childhood obesity, treadmill training, non-treadmill exercise, pulmonary function, VO2 max, cardiorespiratory fitness.

INTRODUCTION

The escalating prevalence of childhood obesity represents a formidable challenge to public health worldwide. Characterized by excessive fat accumulation, childhood obesity not only poses immediate health risks but also augments the likelihood of encountering various maladies in adulthood. Apart from heightened future health hazards, obese children often grapple with respiratory difficulties, cardiovascular ailments, insulin resistance, and psychological distress.(1) This study endeavors to address the urgent imperative for effective interventions to alleviate the adverse effects of obesity, with a specific focus on enhancing pulmonary function and cardiorespiratory fitness. A plethora of research studies have elucidated the deleterious impacts of obesity on pulmonary function, encompassing reductions in vital capacity (VC), forced vital capacity (FVC), and forced expiratory volume in one second (FEV1). The altered respiratory mechanics attributable to obesity, such as increased chest wall fat and diminished respiratory compliance, contribute significantly to compromised lung function.(2,3) Furthermore, obesity exacerbates small airway occlusion and diaphragmatic displacement, culminating in decreased respiratory reserve volume and heightened dead space ventilation during exercise. Aerobic exercise training emerges as a promising avenue for enhancing pulmonary function and cardiorespiratory fitness in obese individuals, with treadmill training and incremental exercise emerging as predominant modalities.(4)

METHODOLOGY

This study employed a randomized controlled trial design to investigate the effectiveness of two exercise interventions—treadmill training with diaphragmatic breathing exercises (Group A) and non-treadmill exercise with diaphragmatic breathing exercises (Group B)—in improving pulmonary function and VO2 max in obese children. Forty obese children aged 12 to 18 years, with a BMI exceeding 25 kg/m² and no history of regular exercise, were recruited for the study. Random sampling techniques were utilized to ensure the formation of comparable groups, and randomization was achieved using computer-generated random numbers.(5) Pre-test assessments included spirometry tests to measure forced vital capacity (FVC), forced expiratory volume in one second (FEV1), and the FEV1/FVC ratio, providing baseline data on lung function. Additionally, cardiorespiratory fitness was assessed using the Cooper test, where participants were instructed to perform aerobic exercise within a set timeframe to estimate VO2 max. The intervention period spanned six weeks, during which Group A engaged in treadmill training sessions five days a week, incorporating aerobic exercise and diaphragmatic breathing exercises. In contrast, Group B participated in non-treadmill exercise sessions five days a week, also including aerobic exercise and diaphragmatic breathing exercises, but without the use of treadmills. Ethical considerations were meticulously observed, with informed consent obtained from participants and guardians, and approval from the relevant ethics committee.

RESULTS AND DISCUSSION

Data collection involved recording demographic information, pre-test assessments, intervention adherence, and post-intervention outcomes. Descriptive statistics, including mean and standard deviation, were computed for continuous variables, while inferential statistics utilized paired samples t-tests for intra-group comparisons and independent samples t-tests for inter-group comparisons to assess intervention effectiveness.(6,7,8) The findings of this study revealed significant improvements in VO2 max for both Group A and Group B, indicating the efficacy of both treadmill and non-treadmill exercise interventions in enhancing cardiorespiratory fitness among obese children. No significant differences were observed in pulmonary function between the two groups, suggesting that both interventions were equally effective in improving lung function.(9) These results underscore the importance of incorporating regular aerobic exercise and diaphragmatic breathing exercises into the routine of obese children to

promote overall health and fitness. While treadmill training may offer certain advantages, such as convenience and controlled intensity, non-treadmill exercises can be equally beneficial and accessible for improving cardiorespiratory fitness.(10,11,12)

Result
Test Statistic : t=0.82
P-Value = 0.416>0.05

Result
Test Statistic: t = -2.43
p-value = 0.020 < 0.05

CONCLUSION

In conclusion, this study demonstrates the effectiveness of both treadmill training and non-treadmill exercise interventions in improving cardiorespiratory fitness among obese children.(13,14) Both interventions yielded significant improvements in VO2 max, with no significant differences in pulmonary function observed between the groups. These findings emphasize the importance of promoting regular physical activity, regardless of the specific exercise modality, to address the health challenges associated with childhood obesity comprehensively. (15)Further research is warranted to explore additional factors influencing the effectiveness of exercise interventions and develop tailored strategies for managing childhood obesity effectively.

Recommendations
1. Encourage kids to do different exercises regularly to get fitter and healthier.
2. Teach them how to breathe properly while exercising to make their lungs and heart stronger.
3. Help them make changes to their lifestyle for the long term, like eating healthier and exercising regularly.(16,17,18)

Limitations
1. Not many kids were part of the study, so we can't be sure if the results apply to all obese kids.
2. The study only lasted six weeks, so we don't know if the benefits will last a long time.
3. The study was only done in one place, so it might not be the same everywhere.
4. We didn't look at what the kids were eating, which could also affect how healthy they are.
5. Even though we tried to be fair, some kids might have done better or worse because of other reasons like how much they wanted to exercise.

REFERENCES

1. Carey, I. M., Cook, D. G., & Strachan, D. P. (1999). The effect of adiposity and weight change on forced expiratory volume decline in a longitudinal study of adults. International Journal of Obesity and Related Metabolic Disorders, 23(9), 979-985.
2. Cooper, K. H. (1968). A means of assessing maximal oxygen intake. Journal of the American Medical Association, 203, 135-138.
3. Cooper, V. O. (2015). Validity of Cooper's 12 min run test for estimation of maximum oxygen uptake in male university students. Biology of Sport, 32(1), 159-163.
4. Dreher, M., &Kabitz, H. J. (2012). Impact of obesity on exercise performance and pulmonary rehabilitation. Respirology, 17(3), 578-584.

5. Golfield, G. S., Cloutier, P., Maltory, R., &Prud'home, D. (2006). Validity of foot to foot bioelectrical impedance analysis in overweight and obese children and parents. Journal of Sport Medicine and Physical Fitness, 46(3), 447-453.
6. International Journal of Therapies and Rehabilitation Research. (2016). Effect of treadmill training on ventilator functional and physical performance in obese children.
7. Lazaus, R., Colditz, G., Berkey, C. S., &Spieler, F. E. (1997). Effort of body fat on ventilatory function in children and adolescents: Cross-sectional findings from a random population sample of school children. Pediatric Pulmonology, 24(3), 187-194.
8. Meyers, P. V., Faustinelli, S. P., & Cowan, P. A. (2005). Identifying children at risk for obesity, type 2 diabetes, and cardiovascular disease. Diabetic Spectrum, 18(4), 213-220.
9. Thyagarajan, B., Jacobs, D. R. Jr., Apostal, G. G., Smith, L. J., Jensen, R. L., & Crapo, R. (2008). Longitudinal association of body mass index with lung function: The CARDIA study. Respiratory Research, 9(1), 31.
10. World Health Organization. (2000). Obesity: Preventing and managing the global epidemic (Report No. 894; ISBN: 05123054).
11. West, J. B. (2008). Respiratory physiology: Principles and basic aspects. São Paulo: Artmed.
12. Zavorsky, G. S., & Hoffman, S. L. (2005). Pulmonary gas exchange in the morbidly obese. Obesity Reviews, 9, 326-339.
13. Koenig, S. M. (2001). Pulmonary complications of obesity. American Journal of Medical Sciences, 321, 249-279.
14. Sabahebjami, H., &Gartside, P. S. (1996). [Chest]. Chest, 110, 1425-1429.
15. Steele, R. M., Finucane, F. M., Griffin, S. J., & Wareham, N. (2009). Obesity is associated with altered lung function independently of physical activity and fitness. Obesity (Silver Spring), 17(3), 578-584.
16. Cooper, V. O. (2017). Effect of diaphragm breathing exercise applied on the basis of overload principle. Journal of Physical Therapy Science, 29(6), 1054-1056.
17. Koening, S. M. (2012). Ventilatory response to aerobic exercise in obese children. BioScience Research, 9(1), 35-40.
18. Iradoust, K. (2015). The effect of selected aerobic exercise on pulmonary function of high school obese girls. International Journal of School Health, 2(4), 32-36.

Table:1 t-Test: Two-Sample Assuming Equal Variances

	A_FEV1/FVC%_Diff	B_FEV1/FVC%_ Diff
Mean	-0.004	-0.035
SD	0.088	0.143
Variance	0.008	0.020
Observations	20	20
Pooled Variance	0.014	
Hypothesized Mean Difference	0	
df	38	
t Stat	0.82	
P(T<=t) one-tail	0.208	
t Critical one-tail	1.69	
P(T<=t) two-tail	0.416	
t Critical two-tail	2.02	

Table:2 t-Test: Two-Sample Assuming Equal Variances

	A_VO2MAX_Diff	B_VO2MAX_Diff
Mean	18.530	20.610
SD	2.238	3.115
Variance	5.006	9.706

Observations	20	20
Pooled Variance	7.356	
Hypothesized Mean Difference	0	
Df	38	
t Stat	-2.43	
P(T<=t) one-tail	0.010	
t Critical one-tail	1.69	
P(T<=t) two-tail	0.020	
t Critical two-tail	2.02	

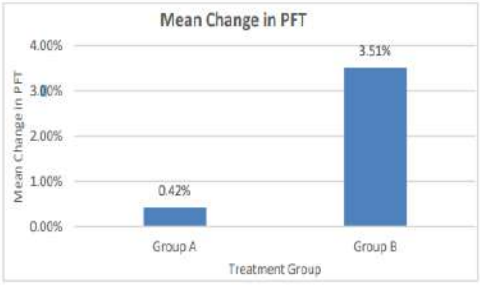

Fig:1

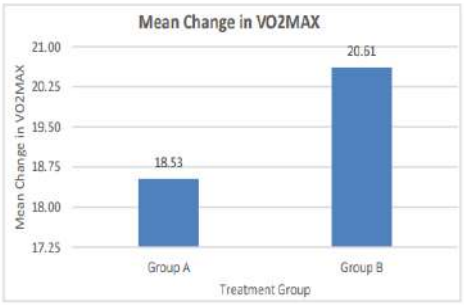

Fig:2

Vol.15 / Issue 88 / Feb / 2025 *International Bimonthly (Print) – Open Access* *ISSN: 0976 – 0997*

RESEARCH ARTICLE

Formulation and Preliminary Pharmaceutical Evaluation of a Polyherbal Ointment used in Scabies

Dhayagude Kiran Tukaram[1]*, Jyothy .K .B[2], Gurupadayya .B .M[3] and Srihari Sheshagiri[4]

[1]PG Scholar, Department of Pediatrics (Kaumarabhritya), JSS Ayurveda Medical College, Mysuru, (Affiliated to Rajiv Gandhi University of Health Sciences, Bangalore), Karnataka, India.
[2]Professor, Department of Pediatrics (Kaumarabhritya), JSS Ayurveda Medical College, Mysuru, (Affiliated to Rajiv Gandhi University of Health Sciences, Bangalore), Karnataka, India.
[3]Professor, Department of Pharmaceutical Chemistry, JSS College of Pharmacy, JSS Academy of Higher Education and Research, (Deemed to be University), Mysuru, Karnataka, India.
[4]Professor, and Head, Department of Pediatrics (Kaumarabhritya), JSS Ayurveda Medical College, Mysuru, (Affiliated to Rajiv Gandhi University of Health Sciences, Bangalore), Karnataka, India.

Received: 21 Nov 2024 Revised: 03 Dec 2024 Accepted: 27 Jan 2025

***Address for Correspondence**
Dhayagude Kiran Tukaram
PG Scholar,
Department of Pediatrics (Kaumarabhritya),
JSS Ayurveda Medical College, Mysuru,
(Affiliated to Rajiv Gandhi University of Health Sciences, Bangalore),
Karnataka, India.

ABSTRACT

Ointments serve various purposes when applied topically, but synthetic antimicrobials often lead to adverse effects. Ayurveda literature suggests topical application (*Lepa*) of herbs and minerals as a remedy forPruritis, Scabies, Tinea, Urticarial rashes, and microbial infections. Ayurveda pharmaceutical techniques support the preparation of ointment using various ingredients for better acceptability and convenience.The polyherbal ointmentwas prepared at a GMP-certified pharmacy as per the standard protocol which contained authentically sourced. ***Acorus calamus*** Linn. (*Vacha*), *Berberis aristata* (*Daruharidra*), and*Brassica Juncea (Sarshapa)*along with coconut oil and beeswax as the base. The trituration method was employed for the preparation of the ointment. As per the standard determination, thin-layer chromatography of the raw drugs was performed. The organoleptic characteristics, preliminary phytochemical analysis,a nd physico-chemical analysis were performed on the prepared ointment. Thin-layer chromatography of the raw drugs revealed the presence of qualitative organic compounds like Alpha Aserone, Alpha Pinene, Berberine, Palmatine, Sinapine, Gallic acid, and Ellagic acid. The ointment exhibited a pale-yellow hue and was non-gritty, smooth, and soft. It demonstrated excellent spreadability, with a measured value of 19.16 g/cm/s, extrudability percentage of 87.43%, indicating favorable ease of application and viscosity of332.9 cP which supported the less shear rate of the product. Based on these properties, the herbal ointment emerged as the most suitable form for classical *Lepa* when prepared andanalyzed. The present study demonstrates the preliminary standards of the polyherbal ointment which was abundant in the proven phytochemicals that are majorly antifungal, antibacterial, and anti-inflammatory in action.

Keywords: Ayurveda; *Lepa*; Herbal Ointment; Scabies

INTRODUCTION

Multiple drug resistance has become a significant concern in contemporary times, primarily due to the widespread and indiscriminate use of commercial antimicrobial drugs in treating various infectious diseases.[1,2] Ayurvedic pharmacology offers diverse internal and external formulations tailored for specific conditions of different diseases. The inclusion of primary and secondary formulations in Ayurved a stands unique in the traditional knowledge of pharmacy. The five primary formulations include *Swarasa* (fresh herbal juice), *Kalka*(herbal paste), *Kwatha*(Decoction), *Hima*(cold infusion), and,*Phanta*(hot infusion). *Lepa* (ointment),[3]which involves applying medicinal paste externally over the body parts, aims to leverage its topical therapeutic effects. This method prescribes the duration of application/contact with the affected part of the body and the quantity of the application in terms of thickness over the applied area of the body.[3] This is said to differ based on the characteristics of the affected skin/type of lesion. Notably, the polyherbalointment selected for the present study is identified as a potent herbal formulation in classical Ayurveda literature. This is recommended for topical application in clinical conditions like Eczema, Scabies**,** and, inflammatory conditions.[4] This formulation consists of equal parts of ***Acorus calamus*** *Linn*. (*Vacha*), *Berberis aristata* (*Daruharidra*),and*Brassica Juncea (Sarshapa)* along with the base as coconut oil and bee wax.

Despite the pharmaceutical industry's production of numerous new antimicrobial drugs over the past three decades, microorganisms' resistance to these drugs has been on the rise. Synthetic drugs, generally known for their ability to develop resistance, are also linked to adverse effects on the host, such as hypersensitivity, immune suppression, and allergic reactions.[5] In contrast to synthetic drugs, plant-based materials have historically played a crucial role in human health maintenance.[6] These natural products serve as a primary source for drug development in the pharmaceutical industry. In rural areas worldwide, residents often rely on locally available plant materials for the management of the complaints rather than OTC products containing chemical constituents. Consequently, there is a global shift towards embracing traditional herbal medicines, which are not only easily obtainable but also compatible with human living without many adverse reactions. However, availability in ready-to-use forms for topical application is still a research area due to less shelf life and unclear data about the bioavailability of herbal constituents in newer drug forms like ointment/spray/liniment. ***Acorus calamus*** *Linn.* (*Vacha*)is traditionally applied externally on inflamed skin conditions and wounds[7] and is used extensively in therapeutics. It also has a strong aroma, which is useful in the different sterilization methods.[8] Recent research has demonstrated its potential antifungal,[9,10,11]anti-inflammatory,[12] Insecticidal,[13] antibacterial,[14,15,16] anthelmintic,[15] and, Analgesic[17] activities. *Berberis aristata(Daruharidra)* contains Berberine[18,19], which is one of its important alkaloids. Scientific studies have confirmed itsanti-inflammatory[20] action with wound healing properties.[21] *Brassica Juncea (Sarshapa)commonly known as* Brown mustard, is a type of mustard that has been used as food and medicine for many years worldwide and it showed antibacterial,[22] antifungal [23,24,25] and,anti-inflammatory [26,27,28,29,30] activities. The herbal ointment in the present study is a topical formulation prepared freshly as per the classical literature of Ayurveda. Astraditional preparations face challenges such as stability and patient acceptance, modern pharmaceutical analytical tests were employed to check the characteristics of the herbalointment using appropriate tests.

MATERIALS AND METHODS

Acorus calamus *Linn.(Vacha), Berberis aristate (Daruharidra),Brassica Juncea (Sarshapa)* each 150 gms, Coconut oil 4.5 liters and Bee vax 200 gms, were sourced from an Ayurveda raw drug vendor of Mysuru, Karnataka, India.Authentication was conducted at the Pharmacognosy laboratory of Ayurveda Medical College, Mysuru, Karnataka. Table 1 shows raw materials. **The herbal drugs** each of 150 gm were washed first by tap water flow, and manual cleaning was done. A total of 430g of drugs was obtained after cleaning.Thin layer chromatography of all three raw drugs was performed as per the following steps.[31]For *Berberis aristata*, the standard solution was prepared

by dissolving Berberine and Palmatine samples with methanol in separate volumetric flasks. The sample solution was prepared by dissolving *Daruharidra*in Methanol. Aluminum sheets coated with silica gel 60 served as the TLC plate and the mobile phase was Chloroform: Methanol in a ratio of 8 volumes: 2 volumes. 10 µl of standard and sample solution were spotted in a silica-coated TLC plate and the mobile phase was allowed to run up to 80% of the plate. The plate was dried by air and then observed in a UV chamber at 254nm. The standard and sample solutions of *Acorus calamus* Linn. were prepared by dissolving the alpha-pinene standard with the mobile phase and it was 8 volumes of n-Hexane: 2 volumes of Ethyl acetate over the Aluminium sheets coated with silica gel 60 as the TLC plate. To detect *Alpha-asarone*, the standard solution was prepared by dissolving it with the mobile phase, and the sample solution was prepared by crushed *Vacha* extracted in Chloroform. The mobile phase was Toluene: Ethyl acetate (8 volumes: 2 volumes).The standard solution of *Brassica juncea* was prepared by dissolving theSinapin with the mobile phase and it was 1 volume of Methyl ethyl ketone: 8 volumes of Ethyl acetate :1 volume of Formic acid over the Aluminium sheets coated with silica gel 60 as the TLC plate. The sample solution was prepared by a crushed mustard sample extracted in Chloroform. The rest of the steps were followed as in the case of *Berberis aristata*. The sample solution to detect gallic and ellagic acid was prepared by dissolving crushed sarshap a and extracting it in methanol. Aluminum sheets coated with silica gel 60 served as the TLC plate and the mobile phase was 3 volumes Toluene:3 volumes ethylacetate:1 volume formic acid:0.5 volume methanol. 10 µl of standard and sample solution were spotted in a silica-coated TLC plate and the mobile phase was allowed to run up to 80% of the plate. The plate was dried by air and then observed in a UV chamber at 280nm.Phytochemical analysis of raw drugs was carried out as per the standard procedures.[32,33]

Preparation of the ointment[34,35]

The ointment was prepared as per the classical literature and the SOP of Ayurveda pharmacopeia, The individual ingredients are specified in Table 1. The purified coarse powder of all the herbal drugs was sieved through a 100-mesh sieve to ensure thorough blending and then combined in equal parts. Sixteen parts of water were added to these ingredients [Fig. 1], and the mixture was heated over a low flame until it reduced to one-fourth of its original quantity, forming the decoction [Fig. 2]. The decoction was then filtered through a standard sieve to collect in a steel container. Coconut oil, in one-eighth of the quantity of the decoction, was added and heated again over a low flame until it achieved the desired physical properties of the oil, indicating readiness for external application. The oil was then filtered and stored in an airtight container [Fig. 3]. Bee wax was added after melting in a water bath later to this processed oil at a ratio of 1:5 and triturated continuously until the ointment-like consistency was achieved. [Fig. 4]. The ointment was then stored in airtight containers of 20 grams each [Fig. 5,6]. After the ointment preparation; organoleptic, and physicochemical analytical tests were conducted according to the established standards. The above ointment was prepared in a GMP-certified unit, in Mysuru, Karnataka, India.

Organoleptic Analysis and Physico-chemical Analysis of ointment[36]

The ointment was evaluated for its color, texture, odor, skin irritation test, and, taste. Physicochemical analysis included pH, solubility, spreadability, extrudability, viscosity, and loss on drying. The pH of the sample is measured in the Systronics digital pH meter.Solubility was tested in chloroform (5 parts of solvent required for 1 part of solute), alcohol (80 parts of solvent required for 1 part of solute), and in water. For the determination of spread ability, an excess sample was applied between two glass slides, then it was compressed to a uniform thickness. A weight of 50g was added to the pan. It was calculated by using the following formula, S = M * L / T= Value in g/cm/sec[37] where S=Spreadability, M = weight tied to upper slide, L = length moved on the glass slides, and T = time taken to separate the slides. To test extrudability, the herbal formulation was filled in standard-capped collapsible aluminum tubes and sealed by crimping to the end. The weight of the tube was 15g and the sample weight was 9.87g. The tubes were placed between two glass slides and were clamped. 1 kg was placed over the slides, and the cap was removed. The extruded gel was collected and weighed. For standards, the percentage was considered as >90%-excellent, >80% -good, and >70% -fair. Viscosity was determined by using a Brookfield DV-II+Pro viscometer. The spindle was inserted into the test medium before the fluid level reached the immersion groove on the spindle's draft, at which point the viscosity was measured. Viscosity measurements were carried out at room temperature (24-26^{o}C).Loss on drying was measured at the drying temperature of 80^{o}C.(Table 2).

Observations

During the herbal drug immersion in water, the water in the jar remained unchanged and the sediments settled at the bottom upon standing. The initial procurement weight of the raw drugs was 450g, and after cleaning it was 430g which was used for preparation of decoction before ointment preparation. Approximately 5% loss occurred during the physical cleaning process. The melting and mixing of 2kg of the base i.e. bee wax typically took around 10 minutes on average, during the ointment preparation. Additionally, the trituration of the base, herbal drugs, and 1litre coconut oil lasted approximately 20 minutes on average. The total quantity of the procured ointment was 2kg.

RESULTS

The results of the study are depicted in Table3 and Figures 7,8,9 and 10.

DISCUSSION

Ointments serve various purposes when applied topically, including protection, disinfection, moisturization, itch relief, and tightening of the skin.[38] Typically, these formulations lack water and usually contain one or more active ingredients either in suspension, solution, or dispersion. Ointment bases can be categorized as hydrocarbon-based (oleaginous), absorbent, or water-soluble types.[39] The idea of administering medications through the skin has always been appealing because the skin is easily accessible, covers a large surface area, interacts with circulatory and lymphatic systems, and allows for non-invasive delivery methods.[40] In the case of skin diseases like scabies, especially in children, ointment serves the purpose of healing very effectively. When it contains only herbal and natural ingredients, the safety of children can also be assured to a greater level in contrast to chemical-based ointments. This also assures safety against accidental contact/ oral ingestion of ointments which is a usual incident in the case of smaller children. The polyherbal ointment in the present study was prepared based on the classical literature of Ayurveda due to which the authenticity of the formulation is unquestionable. There was no variation in the ingredients or the method of preparation. All the ingredients used were authenticated as per the available standards. Its organoleptic, phytochemical, and physicochemical properties were analyzed by suitable parameters to ensure the preliminary qualitative and quantitative standards. It contained three common and easily available herbal drugs, bee wax, and coconut oil as the base. In skincare, bee wax serves as an occlusive to form a semi-occlusive barrier that reduces water loss from the skin, functioning as a humectant to retain moisture, and acting as an emollient to soften and soothe the skin.[41] Coconut oil contains the active compounds lauric acid and monolaurin, both of which have proven activity against *Staphylococcus epidermidis, E coli*s, and *Candida albicans.*[42]

All three herbs i.e. ***Acoruscalamus*** *Linn., Berberis aristata*, and *Brassica Juncea (Sarshapa)*, have been scientifically recognized for their antimicrobial andanti-inflammatory effects. Phytochemical analysis of ***Acorus calamus*** *Linn.* (*Vacha*), *Berberis aristata* (*Daruharidra*),*Brassica Juncea (Sarshapa)* revealed the presence of Alpha and Beta Asaron, Berberiene and Palmatineand Sinapine and Gallic and Ellagic acid respectively. Thus, the phytochemical analysis proved the presence of active alkaloids in the raw drugs. Building upon this foundation, the classical herbal *lepa* was prepared into an ointment to enhance efficacy in skin conditions along with its usability, and stability. During the preparation process, a portion of the ointment is often lost due to adherence to beakers, ointment tiles, or pads. To compensate for this loss, an excess quantity was prepared. When heat was necessary to melt the bee wax, a water bath with controlled low temperatures was employed, as ointment bases typically liquefy around 70°C. These heating devices ensured precise temperature control, preventing overheating of the ingredients. The cooling phase was crucial and was not hastened by submerging the melt in water or ice, as this could alter the consistency of the final product, resulting in a firmer texture than desired. Trituration, for approximately 20 minutes, was performed in a uniform pattern to ensure proper homogenization, especially since powder of drugs was used to prepare decoction and then the ointment. The final ointment was smooth and non-irritant when applied to the skin, owing to the fat/wax base and the homogenization procedure. If the ointment becomes irritant, it will cause redness, itching, and burning sensations over the area where the ointment is applied. By the human skin contact test, the prepared ointment was proven non-irritant which ensures that it is user-friendly. This characteristic is highly useful when the

ointment is indicated in children and the elderly population. Coconut oil and bee wax as the base in the ointment might be the contributors to this benefit as they have proven skin-soothing actions. The fragrance of an ointment also matters when applied externally. Many patients tend to avoid herbal ointments due to their specific smell causing social embarrassment. In turn, a chemical fragrant when used in ointments acts as an allergen too.[43]In this preparation, a mild-moderate fragrance of coconut oil was detected which is natural, insensitive over the skin, and pleasing in herbal ointment. The normal pH of human skin ranges from 4.5 to 6.5, indicating it is naturally slightly acidic. This acidic environment, known as the 'acid mantle,' is maintained by factors such as sebaceous glands, sweat glands, and normal skin flora. The pH of the polyherbal ointment was found to be within the acceptable range for human skin, specifically at 6.22, which is mildly acidic proving its compatibility for human usage. The product was insoluble in water which allows it to remain over the applied area of skin even after in contact with water. This stands useful, especially in children for better clinical efficacy. The base of the ointment contains non-polarmedium and long-chain fatty acids i.e. in coconut oil and non-polar long-chainfatty acids in bee wax. A new approach in topical skin delivery is lipid nanosystems.[44]The trituration in the lipid base might have helped to some extent in this drug delivery approach which needs further analysis. The spreadability of the formulation was measured at 19.16 g/cm/s, indicating how effectively the formulation spreads across the application surface when a small amount of shear force is applied. The value is suggestive that applying this polyherbal ointment over the affected skin would be easier. The loss on drying was found to be 1.1% at the drying temperature of 80^{o}C, which showed less water content in the ointment. This would enhance the stability and shelf life of the ointment when stored in air-tight containers. Extrudability of the prepared ointment was 87.43% which is in 'good' category which assures the user convenience of the product. Good extrudability refers to the quality that the ointment can be squeezed out of the container easily. 332.9cp was the noted viscosity of the prepared ointment which is suggestive of more shear rate. This allows the user to spread the ointment easily over the skin and allows uniform distribution.

CONCLUSION

The prepared poly herbal ointment contained ***Acorus calamus*** Linn. *(Vacha), Berberis aristata (Daruharidra),Brassica Juncea (Sarshapa*) along with coconut oil and bee wax as the base. Upon phytochemical analysis of the herbal drugs, revealed the presence of major active antifungal, anti-bacterial, and anti-inflammatory contents. The organoleptic characteristics of the ointment were indicative of a user-friendly product. According to the results of the physicochemical analysis also, the values supported better qualities like pH, spreadability, extrudability, viscosity, and loss on drying of the ointment. These findings endorse the efficacy of herbal ointment as a potent skin and user-friendly topical application for variousskin conditions. It also revealed the preliminary standards of the polyherbal ointment which can be used for clinical and research purposes.

Financial support and sponsorship
Nil.

Conflicts of interest
There are no conflicts of interest.

REFERENCES

1. Davies J. Inactivation of the antibiotics and the dissemination of resistance genes. Science. April, 1994; 264(5157):375-82.
2. Service R.F. Antibiotics that resist resistance. Science. November 1995; 270(5237):724-727.
3. Srivastava S. Sharangdharasamhita of Acharya Sharangadhara. Purvakhanda, 4th edition. Varanasi; Choukhamba Orientalia; 2005. 4 and 424p.

4. *Sushrutha, Sushrutha Samhita* edited with Ayurveda-tattva-*sandipika*Hindi commentary by KavirajaAmbikadutta Shastri, Edition: Reprint 2015, *Chikitsasthana*, 9/43, published by Chaukambha Sanskrit Sansthan. Varanasi., p.68.
5. Ahamad I., Mehmood Z. and Mohammad F. Screening of some Indian medicinal plants for their antimicrobial properties. J. Ethnopharmacol. September, 1998. 62(2):183-193.
6. Rao A. S, Nayanatara A. K, Kaup R. S, Sharma A, Kumar A. B, Bhavesh D, Kishan V.K and Pai R.S. Potential Antibacterial and Antifungal Activity of Aqueous Extract of CynodonDactylon. Int. Journal of Pharma. Sci. Research. November, 2011; Vol. 2(11): 2889-2893.
7. Kingston, C.; Jeeva, S.; Jeeva, G.M.; Kiruba, S.; Mishra, B.P.; Kannan, D. Indigenous knowledge of using medicinal plants in treating skin diseases in Kanyakumari district, Southern India. Indian J. Tradit. Knowl. 2009, 8, 196–200.
8. Shalini, Kumari &Chandel, Shikha &Atri, Shikha &Guleria, Shikha &Bhardwaj, Indu &Rolta, Rajan. (2022). The therapeutic properties and applications of Acorus calamus (Sweet Flag): a review. Asian Journal of Microbiology, Biotechnology and Environmental Sciences. 122-136. 10.53550/ajmbes.2022.v24i01.022.
9. Rawal, P., Adhikari, R. S., Danu, K. and Tiwari, A. 2015. Antifungal activity of Acorus calamus against Fusarium oxysporumf. sp. Lycopersii. International Journal of Current Microbiology and Applied Sciences. 4(11): 710-715.
10. Lee, J. Y., Lee, J. Y., Yun, B. S. and Hwang, B.K. 2004. Antifungal activity of β-asarone from rhizomes of Acorus gramineus. Journal of Agriculture and Food Chemistry. 52(4) : 776-780
11. Rita, W. S., Kawuri, R. and Swantara, I. M. D. 2017. The essential oil contents of Jeringau (Acorus calamus L.) Rhizomes and their antifungal activity against Candida albicans. Journal of Health Science and Medicine. 1(1): 33-38.
12. Kim, H., Han, T. H. and Lee, S. G., 2009. Anti-inflammatory activity of a water extract of Acorus calamus L. leaves on keratinocyte HaCaT cells. Journal of Ethnopharmacology. 122(1): 149-156.
13. Liu, X. C., Zhou, L.G., Liu, Z. L. and Du, S.S. 2013. Identification of insecticidal constituents of the essential oil of Acorus calamus rhizomes against Liposcelis bostrychophilaBadonnel. Molecules 18(5): 5684-5696.
14. Muchtaromah, B., Hayati, A. and Agustina, E. 2019. Phytochemical Screening and Antibacterial Activity of Acorus calamus L. Extracts. JurnalBiodjati. 4(2): 68- 78
15. McGaw, L. J., Jäger, A. K., Van Staden, J. and Eloff, J. N. 2002. Isolation of β-asarone, an antibacterial and antihelmintic compound, from Acorus calamus in South Africa. South African Journal of Botany. 68(1): 31-35.
16. Pawar, R., Barve, S. and Zambare, V. 2020. In vitro antibacterial activity of Acorus calamus extract on methicillin-resistant Staphylococcus aureus wound isolates and reduced invasion into mucosal fibroblasts. Vegetos. 33(4): 712-721.
17. Jayaraman, R., Anitha, T. and Joshi, V. D. 2010.Analgesic and anticonvulsant effects of Acorus calamus roots in mice. International Journal of Pharmatechnology Research. 2(1): 552-555.
18. Blasko, G., Murugesan, N., Freyer, A. J., Shamma, M., & Ansari, A. A. Karachine: an unusual protoberberine alkaloid. Journal of the American Chemical Society. 1982; 104(7), 2039-2041.
19. Rahman, A., & Ansari, A. A. Alkaloids of Berberis aristata-isolation of aromoline and oxyberberine. Journal of the Chemical Society of Pakistan. 2011; 5(4), 283.
20. Shahid M, Rahim T, Shahzad A., Tajuddin, Latif A, Fatma T, Rashid M, Raza Adil and Mustafa S. Ethnobotanical studies on Berberis aristata DC. Root extracts. African J of Biotechnology 2009 February 18; 8 (4): 556-63.
21. Biswas Tuhin Kant, Mukherjee Biswapati. Plant Medicines of Indian Origin for Wound Healing Activity: A Review. Int J of Lower Extremity Wounds 2003 Mar; 2(1): 25-39.
22. Engels C, Schieber A, Gänzle MG. Sinapic acid derivatives in defatted oriental mustard (Brassica juncea L.) seed meal extracts using UHPLC-DAD-ESI-MSn and identifcation of compounds with antibacterial activity. Eur Food Res Technol. 2012;234(3):535-42.
23. Khan SA, Shahid S, Jameel M, Ahmad A. In vitro antibacterial, antifungal and GC-MS analysis of seeds of Mustard Brown. Int J Pharm Chem. 2016;6(4):107-15.

24. Kang CA, Shin SW. Studies on compositions and antifungal activities of essential oils from cultivars of Brassica juncea L. Korean. Int J Pharmacol. 2001;32(2):140-4.
25. Ogidi OI, George DG, Enenebeaku UE, Esie NG, Akpan UM. Efficacy evaluation of extracts of Brassica juncea (Brown mustard) seeds as potential antimicrobial agent against pathogenic microbes. J Med Plants Res. 2019;7(4):263-5.
26. Khandayataray P, Murthy MK. Qualitative and quantitative phytochemical screening, antioxidant and anti-inflammatory activities of acetone extract of Brassica juncea L. Leaf. Asian J Biochem Res Int. 2019;5(1):1-15. doi: 10.9734/ajrb/2019/v5i130078.
27. Xian YF, Hu Z, Ip SP, Chen JN, Su ZR, Lai XP, et al. Comparison of the anti-inflammatory effects of Sinapis alba and Brassica juncea in mouse models of inflammation. Phytomedicine. 2018; 50:196-204. doi: 10.1016/j.phymed.2018.05.010, PMID 30466979.
28. Sharma A, Rai PK. Assessment of bioactive compounds in Brassica juncea using chromatographic techniques. J PharmacognPhytochem. 2018;7(3):1274-7.
29. Mayank K, Manjul PS. Pharmacognostic Standardization and HPTLC Fingerprinting of Prosopis cineraria; An Ayurveda Mentioned Plant. PharmacognCommn. 2019;9(1):21-6.
30. Lowry OH, Rosebrough NJ, Farr AL, Randall RJ. Protein measurement with the folin phenol reagent. J Biol Chem. 1951;193(1):265-75. doi: 10.1016/S0021-9258(19) 52451-6, PMID 14907713.
31. Moulishankar, Anguraj & Ganesan, Prasanna & Elumalai, Madhivanan & Lakshmanan, Karthikeyan. (2021). Significance of TLC and HPTLC in Phytochemical Screening of Herbal Drugs. Journal of Global Pharma Technology. 13. 30-45.
32. The Ayurvedic Pharmacopoeia of India, 1st Edition, Reprint, New Delhi Govt. of India, Ministry of Health and Family welfare, Department of Indian Systems of Medicine 2001, Part I, Appendix Vol.IV, 206-218p.
33. Khandelwala KR, and Sethi VK, Practical Pharmacognosy. 24ed., Nirali Prakashan, 2014:25.1-25.9p.
34. Soumya KR, Krishnamurthy MS. Pharmaceutical study of Tiladi Lepa and its modification to ointment form. Ayurpharm Int J Ayur Alli Sci 2016; 5:114-20.
35. Reddy KRC. Bhaisajya Kalpana Vijananam. 4th ed. Varanasi: Chaukhambha Sanskrit Bhawan; 2014. p. 413-4.
36. The Ayurvedic Pharmacopoeia of India. Part I, Vol. VI. Appendix 2.2. New Delhi: Government of India, Ministry of Health and Family Welfare, Department of AYUSH; 2008. p. 242-51.
37. Chen MX. Formulation and evaluation of antibacterial creams and gels containing metal ions for topical application. J Pharm 2016;2016:10
38. Awad El-Gied AA, Abdelkareem AM, Hamedelniel EI. Investigation of cream and ointment on antimicrobial activity of Mangifera indica extract. J Adv Pharm Technol Res 2015; 6:53-7.
39. Rajveer B, Monica O, Patil PH, Nawandar KS. A review on ointment and ointment bases. World J Pharm Res 2017; 5:335-45.
40. Alalor CA. Evaluation of the antibacterial activity of herbal ointments formulated with methanolic extract of Cassia alata. Asian J Biomed Pharm Sci 2012;2:15-9.
41. Nong Y, Maloh J, Natarelli N, Gunt HB, Tristani E, Sivamani RK. A review of the use of beeswax in skincare. *J Cosmet Dermatol*. 2023; 22: 2166-2173. doi:10.1111/jocd.15718
42. de Oliveira SF, Lôbo IP, da Cruz RS, Andrioli JL, da Mata CPSM, Soares GA, Santos EDC, Aguiar-Oliveira E, Franco M, da Conceição AO. Antimicrobial activity of coconut oil-in-water emulsion on *Staphylococcus epidermidis* and *Escherichia coli* EPEC associated to *Candida kefyr*. Heliyon. 2018 Nov 13;4(11): e00924. doi: 10.1016/j.heliyon. 2018.e00924. PMID: 30761360; PMCID: PMC6286180.
43. van Amerongen CCA, Ofenloch RF, Cazzaniga S, Elsner P, Gonçalo M, Naldi L, Svensson Å, Bruze M, Schuttelaar MLA. Skin exposure to scented products used in daily life and fragrance contact allergy in the European general population - The EDEN Fragrance Study. Contact Dermatitis. 2021 Jun;84(6):385-394. doi: 10.1111/cod.13807. Epub 2021 Mar 2. PMID: 33576005; PMCID: PMC8247875.
44. Akombaetwa N, Ilangala AB, Thom L, Memvanga PB, Witika BA, Buya AB. Current Advances in Lipid Nanosystems Intended for Topical and Transdermal Drug Delivery Applications. Pharmaceutics. 2023 Feb 15;15(2):656. doi: 10.3390/pharmaceutics15020656. PMID: 36839978; PMCID: PMC9967415.

Table 1. Raw materials for ointment preparation

Sl. No.	Ingredients	Botanical Name	Part used	Quantity in 1gm of ointment
1	*Vacha*	*Acorus calamus* Linn.	Rhizome	0.033gm
2	*Daruharidra*	*Berberis aristata* DC.	Rhizome	0.033gm
3	*Sarshapa*	*Brassica Juncea*.	Seeds	0.033gm
4	Coconut oil	*Cocos nucifera*	Oil	0.875 gm
5	Bee- wax	-----	----	0.117gm

Table 2 Chromatographic conditions for TLC

Raw drugs	Mobile phase	TLC plate	Standard solution	Sample solution	Inj. volume	Detection frequency
Berberis aristata(Daruharidra)	8 volumes Chloroform: 2 volumes Methanol	Aluminum sheets coated with silica gel 60	Dissolving Berberine and Palmatine samples with methanol	Methanolic extract	10 µl	UV at 254nm.
Acorus calamus Linn. *(Vacha)*	8 volumes n-Hexane: 2 volumes Ethyl acetate		Dissolving alpha-pinene with n-hexane: ethyl acetate	Dissolving with n-Hexane: Ethyl acetate		
	8 volumes n-Hexane: 2 volumes Ethyl acetate		Dissolving Alpha-asaronewith n-hexane: ethyl acetate.	Crushed and extracted in Chloroform		
Brassica Juncea. *(Sarshapa)*	1 volume Methyl ethyl ketone: 8 volumes Ethyl acetate :1 volume Formic acid		Dissolving sinapinewith Methyl ethyl ketone: Ethyl acetate: volume Formic acid.	Crushed and extracted in Chloroform		
	3 volumes Toluene:3 volumes ethylacetate:1 volume formic acid:0.5 volume methanol.		Dissolving Ellagic and Gallic acid with methanol	Crushed and extracted in methanol		UV at 280 nm

Table 3. Organoleptic and Physicochemical characteristics of the polyherbal ointment

Sl. No.	Parameters / Particular	Findings
1	Color	Pale Yellow
2	Consistency	Smooth, Semisolid
3	Odour	Of coconut oil
4	Taste	Tasteless
5	Skin irritation test	Non irritant
6	pH	6.22
7	Solubility	Insoluble in water
8	Spreadability	19.16gcm/sec
9	Extrudability	87.43%
10	Viscosity	332.9 cp
11	Loss on Drying	1.1%

Fig 1. Powder of all drugs

Fig 2.Preparation of decoction

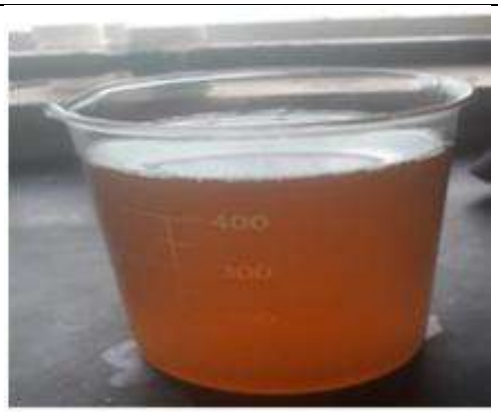

Fig. 3. Processed coconut oil

Fig.4 Prepared Ointment

Fig. 5 & 6 Polyherbal Ointment stored in an air-tight container

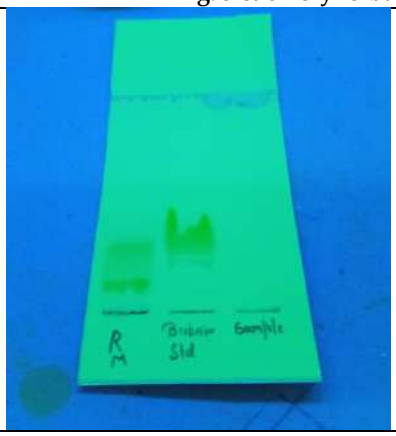

Fig. 7. Under UV 254 nm

Fig. 8. Under UV 366nm

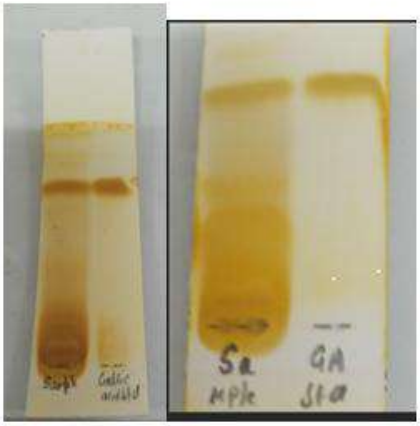

Fig. 9 & 10 Under UV 280 nm

RESEARCH ARTICLE

BiAlexNet: A Novel Approach for Fruit Disease Identification

G. Sathya Priya[1]* and M. Safish Mary[2]

[1]Research Scholar (Reg.21211282282010), Department of Computer Science, St. Xavier's College (Autonomous), Palayamkottai, (Affiliated to Manonmaniam Sundaranar University, Abishekapatti, Tirunelveli), Tamil Nadu, India.
[2]Assistant Professor, Department of Computer Science, St. Xavier's College (Autonomous), Palayamkottai, (Affiliated to Manonmaniam Sundaranar University, Abishekapatti, Tirunelveli), Tamil Nadu, India.

Received: 09 July 2024 Revised: 10 Oct 2024 Accepted: 20 Nov 2024

***Address for Correspondence**
G. Sathya Priya
Research Scholar (Reg.21211282282010),
Department of Computer Science,
St. Xavier's College (Autonomous), Palayamkottai,
(Affiliated to Manonmaniam Sundaranar University, Abishekapatti, Tirunelveli),
Tamil Nadu, India.
E.Mail: sathya.gsp2020@gmail.com

ABSTRACT

Fruits serve as a vital source of nutrients, yet the detrimental impact of various diseases on fruits poses a significant challenge. This challenge is a leading cause of financial losses globally. Therefore, the crucial task of identifying and categorizing various fruit diseases demands utmost attention. In particular, Citrus fruit diseases contribute to substantial decline in fruit yield. To address this issue, the development of an automated identification system for citrus fruit diseases becomes imperative. Recent advancements in deep learning methods have shown promise in solving various computer vision problems, prompting their application to the complex task of recognizing citrus fruit diseases. The application of an efficient deep learning technique facilitates not only the identification but also the accurate classification of various citrus fruit diseases. The core emphasis of this research lies in the identification of citrus fruit diseases utilizing the BiAlexNet method. The primary objective of the proposed model is to differentiate between healthy citrus fruits and those affected by common diseases like black spot, canker, scab, greening, and Melanose. Through the integration of multiple layers and tuned preprocessing methods the model effectively extracts complementary discriminative features. Rigorous evaluations against various state-of-the-art deep learning models on citrus datasets showcase the BiAlexNet Model's superior performance across a spectrum of evaluation metrics. Boasting an impressive accuracy of 95.33%, the proposed model emerges as a valuable decision support tool for farmers in their quest to classify citrus fruit diseases.

Keywords: Citrus fruit disease, BiAlexNet, Fruit disease Identification, Non Local Means.

INTRODUCTION

In the realm of agriculture, researchers are persistently working towards enhancing food production, improving taste, reducing costs, and ultimately increasing profitability. The cultivation of fruit trees holds significant importance in the economic development of various regions. Fruit diseases can cause significant damage to crop yields, resulting in financial losses for farmers and food shortages for communities. It is approximated that global crop losses attributed to plant diseases can vary from 10% to 25% [1]. Citrus fruits such as lemon, orange, lime etc are the major fruits produced in India. India is the third largest citrus fruit yielding country. Among the well-recognized fruit-bearing plant species, citrus plants stand out for their rich reserves of antioxidants and widespread cultivation in the Indian subcontinent, the Middle East, and Africa. Citrus plants offer numerous health benefits and serve as a fundamental raw material in the food industry, contributing to the production of a wide array of food-products such as jam, sweets, ice cream, confectionery, and more [2]. Citrus fruit production in India faces significant challenges, with citrus plants being susceptible to various infections, such as black spots, cankers, scabs, greening, and melanose, leading to substantial crop losses. The proposed approach utilizes a comprehensive deep learning model BiAlexNet, to automatically detect citrus fruit diseases. This research seeks to mitigate losses, reduce costs, and enhance product quality, contributing to the overall development of the agricultural industry.

RELATED WORKS

In recent times, deep learning has become a formidable tool in advancing profitable agriculture, particularly in the realms of fruit disease diagnosis and yield prediction. Numerous investigations have showcased the effectiveness of deep learning in detecting diseases. Existing literature extensively discusses various techniques proposed for fruit disease identification and classification, including image processing techniques. When fruits are lost due to diseases, farmers face financial loss and communities may get affected from food shortages. Therefore, the intervention of deep learning is crucial for promoting sustainable agricultural practices. In this context, the literature suggests diverse methodologies for interpreting images of fruit which has diseases. Several previous studies are summarized and evaluated below.

Rozario et al. (2016) presented an innovative approach for identifying infected regions in fruits, employing a two-step method. The initial stage involved enhancing the contrast of the input image through a combination of the median filter and histogram equalization. Subsequently, a modified color-based segmentation technique using K-means clustering was implemented in the second step, facilitating the extraction of infected regions. The use of K-means clustering proven to be a efficacious approach for extracting diseases in apples and bananas, exhibiting superior performance [3]. Amara et al. (2017) proposed an implementation of a method grounded in deep learning was employed for the automated classification of banana diseases. This work showed increased performance in disease identification by using the LeNet architecture for classification, which handled complicated backgrounds and high spite effectively [4]. Rehman et al. (2019) conducted an extensive survey focusing on diverse statistical machine learning techniques across various agricultural domains. This research give information about the suitability of specific statistical machine learning techniques for particular agricultural purposes, as well as the limitations associated with each method. The research also explores the potential applications of statistical machine learning technologies in the future and is shedding light on potential advancements and developments in the field [5].

Section – 3

METHODOLOGY

This figure shows the general diagram of the proposed BiAlexNet model for citrus fruit disease identification. The main process for citrus fruit disease identification involves image acquisition, preprocessing and finally identification using the proposed architecture. The details of every block in Figure 1 are examined.

Data Acquisition

The images were taken from online sources [6]. This article introduces a dataset comprising 3117 images of both healthy and diseased citrus fruits, which helps researchers to apply various deep learning and image processing algorithms in the identification of citrus fruit diseases. The dataset categorizes the infected images into five classes out of which one class is healthy and the other four have distinct diseases affecting citrus fruits, namely Black Spot, Canker, Scab, Greening. Each class is described in table 1. For instance, the black spot, also known as CBS, appears when the plant has disease, and the weather conditions are favorable for the disease. Symptoms include small, curved lesions with dark squares on the citrus leaves and fruits, with a spectral range for spot diameter of 0.12 to 0.4. Rainfall blown by the wind causes canker spots. On citrus fruits, tiny, circular lesions that are between two and ten millimeters in size arise. Similarly, fungal and plant tissue combine to cause scab outbreaks in citrus fruit species, presenting as flat lesions with pink to light brown colorations. As a saprophyte, melanose is characterized by its severity, which is determined by the total number of inoculum units that damage dead wood inside the tree canopy. A little dark spot filled with reddish-brown gum is one of the symptoms; the size of the spot depends on how old the fruit was when it got infected. This article's Figures 1 through 5 show self-annotated images of citrus fruits that are both healthy and diseased.

Benefits of the dataset:

This dataset offers a visual record of citrus plant. Using this dataset, researchers can evaluate a variety of different computer vision and image processing methods for the visual feature-based diagnosis of various diseases. It supports a large number of feature selectors and feature extractors through textural descriptors and color schemes of different types of citrus diseases. It is difficult for researchers to identify disease symptoms with the naked eye because this data is collected in a natural environment with varying weather conditions and light intensities[7, 8].

Preprocessing:

Preprocessing involves image enhancement, image denoising and data augmentation.

Image Enhancement: For fruit disease identification Contrast Limited Adaptive Histogram Equalization (CLAHE) technique is used CLAHE is used to enhance the contrast of images, making the details more visible by improving the overall quality of the image. It is especially useful for improving the visibility of features in images that have non-uniform illumination or varying light conditions. CLAHE limits the amplification of noise during the contrast enhancement process, helping to maintain the overall image quality and prevent the introduction of unwanted artifacts. The adaptive nature of CLAHE allows it to adjust the contrast enhancement locally in different regions of an image. This helps in preserving the natural appearance of the image while enhancing the details in specific areas. It is especially valuable in applications where visibility and contrast are crucial for accurate analysis and interpretation.

Image Denoising: For image denoisinng NLM (Non-Local Means) technique is used. It is primarily used for reducing noise from images. One of the main advantages of the NLM algorithm is its ability to preserve edges and fine details in images, even while reducing noise. Several parameters define the behavior of the tuned NLM technique. These parameters include:

h: 20, which controls the strength of the denoising. hForColor: 20, similar to h, but it specifically controls the strength of filtering for color images. templateWindowSize: 13, which represents the size of the patch used for searching for similar patches. A larger value allows for a wider search, resulting in smoother images, while a smaller value preserves more fine details but might not remove all the noise. searchWindowSize: 15, which represents the size of the neighborhood used for searching. Similar to templateWindowSize, a larger value leads to smoother images, and a smaller value preserves more details. After applying the denoising algorithm to the images, it will look smooth and clean, with reduced or eliminated noise. The denoising process works by identifying and removing unwanted noise elements while preserving the essential structures and details of the original image. As a result, the denoised images will exhibit improved clarity, enhanced sharpness, and more distinct edges, thereby leading to a clear and more visually appealing appearance. The removal of noise often results in a more refined look, making the images more

suitable for citrus fruit disease identification. Data Augmentation: Data augmentation serves as a potent technique employed to artificially enlarge a dataset by implementing diverse transformations on the existing data. While it does not introduce new, unseen data points, it can help in improving the performance and generalization of deep learning models and it helps generate augmented versions of input data by applying various transformations. These transformations include random rotations within a specified degree range, horizontal and vertical shifting, flipping, shearing, and zooming. The fill_mode parameter determines the method for completing recently generated pixels, with the 'nearest' mode using the nearest pixel value from the original image. Other options such as centering, normalization, and ZCA(Zero component analysis) whitening can also be applied to the data. By implementing these changes to the pre-existing images, data augmentation gives the model access to a larger collection of examples for learning. This in turn lowers the chance of overfitting and improves the model's ability to generalize to new data. Data augmentation additionally makes the model more resilient to changes in the input data, such as adjustments to direction, scale, or viewpoint. This is especially helpful when working with real-world data that may show unpredictability. Moreover, by virtually expanding the dataset, data augmentation provides the model with a larger amount of training data, which is especially beneficial when the original dataset is limited in size. Although data augmentation cannot provide entirely new information to the model but its ability to enhance the learning process and improve the model's robustness makes it a crucial technique in the training of deep learning models, particularly when the dataset is constrained.

PROPOSED MODEL

Convolutional Neural Networks (CNN), a specific type of deep learning approach, have become the top choice in various fields for recognizing objects in images. The ability to pick up on subtle details that might go unnoticed by people makes CNN so effective. CNN is a super observant detective for images. CNN can directly understand visual patterns straight from the tiny dots that make up images, and they do it with very little preparation needed. Hence, CNN isa smart image classification algorithm that help us see and comprehend things we might overlook on our own. A CNN architecture known as AlexNet made notable progress in the 2012 ImageNet Large Scale Visual Recognition Challenge (ILSVRC). It marked a breakthrough by demonstrating remarkable performance in image classification tasks, outperforming traditional computer vision methods. Bidirectional Long Short-Term Memory, or BiLSTM, is an architecture with two LSTM layers that can process sequences of inputs both forwards and backwards. In the proposed BiAlexNet model, a tuned Alexnet architecture is utilized. It consists of five convolutional layers and maxpooling layers strategically integrated into the initial blocks of the network. After the batch normalization, the selected features are flattened and reshaped. Following this the two Bidirectional LSTM layers were added. Then the fully connected layers were utilized. To prevent overfitting dropout layer is used.

Convolutional Maxpooling Layers

Five convolutional and maxpooling layers are used in this model followed by batch normalization layer. The first layer is a two dimensional convolutional layer which initiates the neural network architecture by applying 16 filters of size 3x3 to the inputs. This convolutional operation extracts various features from the image through a rectified linear activation function (ReLU). The 'same' padding ensures that the spatial dimensions of the output match those of the input. Additionally, L2 regularization is applied to the convolutional kernel to prevent overfitting. The following equation depicts the operations carried out within a convolution layer.

$$Z = \sigma(W * X + b) \quad (1)$$

Where,

- X is the input to the layer,
- W is the set of convolutional filters,
- b is the bias term,
- σ is the ReLU activation function.

The ReLU activation functions introduce non-linearity, allowing the network to capture intricate patterns in the feature space. Graphically, the ReLU function looks like a linear function for positive values of x and is flat (zero) for negative values.

$$ReLU(x) = max(0, x) \quad (2)$$

Where,

- x is the input to the function.
- max(0,)max(0,x) returns the maximum of 0 and x.

If the input x is positive, the ReLU function returns x; if x is negative, it returns 0.

For the next four convolutional layers, filter size only changes in the order 32,64,122,184 respectively. Following every convolutional layer, there is a Maxpooling layer which reduces the spatial dimensions by taking the maximum value within a 2x2 window. This down-sampling operation helps in capturing the most relevant features while reducing computational complexity.

The max-pooling operation can be expressed as:

$$MaxPooled(Y) = max(2 \times 2\ window\ in\ Y) \quad (3)$$

Where, Y is the output of the previous layer.

Batch Normalization

Batch Normalization layer normalizes the activations passed by the previous layer, contributing to the stability and efficiency of the training process. It mitigates issues related to internal covariate shift and contributes to faster convergence during training, promoting the overall robustness of the model.

The batch normalization operation can be expressed as:

$$BatchNorm(X) = \gamma\sigma 2 + \varepsilon(X - \mu) + \beta \quad (4)$$

Where

- μ is the mean and 2σ2 is the variance of X over the mini-batch.
- γ is the scale parameter,
- $\beta$is the shift parameter,
- ϵ is a small constant to prevent division by zero.

After that, the features were flattened and reshaped. Flatten layer transforms the multi-dimensional output from the convolutional layers into a one-dimensional vector. Reshape layer further adjusts the shape to (1, -1). These layers collectively create a feature hierarchy, capturing intricate patterns and details in the input image. The flattened and reshaped output serves as input for subsequent layers, enabling the neural network to learn complex representations for image recognition tasks.

Bidirectional LSTM Layers

Bidirectional LSTM layers are added to the network architecture. These layers contribute to the model's ability to effectively capture temporal dependencies and patterns in data.With the help of bidirectional LSTMs, which process input sequences both forward and backward, the model is able to extract data from contexts that are both past and future. This bidirectionality is particularly beneficial in understanding the temporal dynamics of sequential data, allowing the network to distinguish patterns that may span across multiple time steps. The first BiLSTM layer, with 125 LSTM units, is configured with the activation functions 'tanh' and 'sigmoid' for the cell state updates and gate operations, respectively. The 'tanh' activation function facilitates the modeling of complex temporal relationships, while the 'sigmoid' recurrent activation governs the flow of information through the memory cells. Return_sequences=True, the argument, indicates that this layer returns the entire output sequence instead of simply the end output. The second Bidirectional LSTM layer follows a similar configuration, with 225 LSTM units and default settings for return_sequences, implying that it produces the final sequence output. Additionally, a Batch Normalization layer is incorporated after the Bidirectional LSTM layers. Collectively, these components create a neural network architecture capable of effectively capturing and leveraging temporal dependencies within the data.

The forward and backward LSTM operations can be expressed as:

$h_t^f, c_t^f = LSTM\_Cell\_Forward(X_t, h_{t-1}^f, c_{t-1}^f)$ (5)

This equation computes the new hidden state h_t^f and cell state c_t^f in the forward pass of a single LSTM cell, given the input X_t and the previous hidden state h_{t-1}^f and cell state c_{t-1}^f.

$h_t^f c_t^b = LSTM\_Cell\_Backward(X_t, h_{t+1}^b, c_{t-1}^b)$ (6)

This equation computes the new hidden state h_t^f and cell state c_t^b in the backward pass of a single LSTM cell, given the input X_t and the previous hidden state h_{t+1}^b and cell state c_{t-1}^b

Fully Connected Layers:

Following the batch normalization layer this architecture utilizes the two Fully Connected layers with 465 units followed by a Dropout layer and Batch Normalization layer. The rectified linear unit (ReLU) activation function is used in the first Dense layer. The second Dense layer consists of 365 units and also utilizes the ReLU activation function. Similar to the first Dense layer, it further refines the representation learned by the network, capturing intricate patterns and details. The fully connected layer connects each of its input units to every output unit. The fully connected operation can be expressed as:

$Z = \sigma(W.X + b)$ (7)

Where,

- W as the weight matrix,
- b as the bias term,
- σ as the ReLU activation function.

Dropout Layer:

After the fully connected layera dropout layer is utilized with dropout rate of 0.5. It removes a predetermined percentage of connections at random from training. This helps prevent overfitting by promoting the robustness and generalization capability of the model. Batch Normalization is applied following the Dropout layer. It contributes to the overall efficiency and convergence of the model by maintaining consistent activations across mini-batches. These fully connected layers, along with the dropout and batch normalization form a crucial part of the network's capacity to learn complex representations and generalize well to unseen data.

The dropout operation can be expressed as:

$Droput(X) = X \odot M$ (8)

Where,

- p as the dropout probability,
- $\odot$ as the element-wise multiplication.
- M is a binary mask with elements sampled from a Bernoulli distribution with probability p.

The final layer of the neural network is the output layer, often referred to as the classification layer. It takes the high-level features learned by the preceding layers and transforms them into probabilities for each class. In this specific architecture, it is a fully connected layer with 5 units, indicating the number of classes or categories in the classification task. The activation function used is 'softmax.' In multi-class classification problems, the'softmax' activation function is frequently employed. It creates probability distributions across the various classes from the raw output scores (logits). The values that SoftMax generates add up to 1, signifying the probability of the input falling into each class. The formula for the softmax function for a vector z with K elements is given by:

$$Softmax(Z) = \frac{e^Z}{\sum_j e^{Z_j}} \quad (9)$$

Where

- softmax(z)i is the i-th element of the softmax output vector.
- e is the base of the natural logarithm (Euler's number).

- *zi* is the *i*-th element of the input vector *z*.
- The denominator is the sum of the exponentials of all elements in the input vector *z*.

In essence, the output layer offers the neural network's last series of predictions. Using an appropriate loss function, such as categorical crossentropy for multi-class classification, the model modifies its weights during training in order to minimize the difference between predicted probability and actual class labels. In inference or testing, the class with the highest probability is selected as the predicted class. This architecture is designed for a classification task with five distinct classes, and the 'softmax' activation ensures a normalized and interpretable output for effective probability-based decision-making

RESULTS AND DISCUSSION

The experimental assessment of the BiAlexnet model relies on the specified architectural and training parameters. The algorithm's performance is evaluated using test data on a laptop PC featuring an Intel(R) Core(TM) i3-6100U CPU @ 2.30GHz, with 4.00 GB of RAM. The deep learning model and result calculations are executed within the Jupyter Notebook environment. The training and test loss graph of the BiAlexnet architecture are illustrated in Figure 7 & 8. Notably, both training and test losses gradually converge towards a minimum, signifying effective learning and model generalization by the conclusion of the graph. The training time for the BiAlexNet model is 14 seconds per epoch. The model is trained with batch size of 64 and 300 epochs. The suggested approach is simple to use and easy, considering its excellent results. The resulting confusion matrix, which is shown in Figure 9, gives a graphic depiction of the classification accuracy for each category. Moreover, a number of performance indicators are calculated, such as F1-score, accuracy, recall, and precision. These metrics provide a thorough evaluation of the model's performance in classification tasks and shed light on how well it can recognize and differentiate between various classes.

Comparison of the proposed model with previous studies

In the area of fruit disease identification, various studies have employed distinct methods, each showcasing its own level of accuracy. The primary objective of this study is to demonstrate the efficiency of the BiAlexNet model in accurately identifying fruit diseases. Unlike previous research based on deep learning, our study stands out due to its methodological contributions. In Below, we compare our study with previous works that employed different deep learning methods, focusing on accuracy as a key metric. The results indicate that our proposed method achieves comparable accuracy to previous studies and it shows effectiveness in fruit disease identification.Notable studies and their respective methods, along with the achieved accuracies, are outlined below:

CONCLUSION

In conclusion, this research endeavors to leverage advanced image processing techniques, specifically adaptive filtering and Kalman filter methods, for noise reduction and enhancement of essential image features. The incorporation of the tuned non-local means algorithm further ensures efficient image restoration, preserving the original quality and clarity of the images. Additionally, our focus extends to the development of a customized hybrid model, amalgamating a modified AlexNet and a BiLSTM network, with the primary goal of achieving the identification of fruit diseases. Through a thorough benchmarking process, we have demonstrated the superior functionality of our indicated hybrid BiAlexNet model when compared to other state-of-the-art models in the field. The model's simplicity and efficiency contribute to its effectiveness in autonomously and comprehensively detecting fruit diseases, offering a streamlined disease identification process for farmers and agricultural experts. Overall, this research significantly advances the application of image processing and deep learning techniques in agriculture, providing valuable tools for enhancing image quality and automating disease identification, ultimately contributing to improved crop management and agricultural sustainability.

FUTURE WORK

In future, this research could explore incorporating advanced sensor technologies like IoT devices and drones, enhancing data collection for more accurate disease identification. It might delve into refining model architectures, considering deep neural networks with attention mechanisms or transformer architectures for improved performance. Expanding disease identification to cover a broader range, incorporating climate and environmental factors, and developing user-friendly interfaces for farmers are potential areas of growth.

REFERENCES

1. Nitaigour Premchand Mahalik, "Intelligent Computing for Sustainable Energy and Environment" Springer, 2021.
2. A. Khattak et al., "Automatic Detection of Citrus Fruit and Leaves Diseases Using Deep Neural Network Model," in IEEE Access, vol. 9, pp. 112942-112954, 2021, doi:10.1109/ACCESS.2021.3096895.
3. Rozario, L. J., Rahman, T., & Uddin, M. S. (2016). Segmentation of the region of defects in fruits and vegetables. International Journal of Computer Science and Information Security, 14(5), 399.10.
4. Dubey, Shiv Ram, and Anand Singh Jalal. "Apple Disease Classification Using Color, Texture and
5. Rehman, T.U., Mahmud, M.S., Chang, Y.K., Jin, J., & Shin, J. (2019). Current and future applications of statistical machine learning algorithms for agricultural machine vision systems. Comput. Electron.
6. Agric., 156, 585-605.Research Data - Mendeley Data. https://data.mendeley.com/research-data/? Accessed 27 Jan. 2024.
7. Bahtiar, A. R., Santoso, A. J. & Juhariah, J. Deep learning detected nutrient deficiency in chili plant. In 2020 8th International Conference on Information and Communication Technology (ICoICT), 1–4 (2020).
8. Jana, A. R. S. S. S. Design and analysis of pepper leaf disease detection using deep belief network. Eur.J. Mol. Clin. Med. 7(9), 1724–1731 (2020).

Table 1: Number of samples belonging to each class in the citrus fruit disease dataset

Class	Number of Samples
Blackspot	1246
Canker	1054
Greening	160
Scab	241
Healthy	416
Total Images	3117

Table 2. Layers and parameters of the proposed BiAlexnet model

Layer Name	Size	Filter Size	Stride	Padding	Output channel
Conv	2*2	3*3	1	Same	16
Maxpooling		2*2	-	-	-
Conv	1*1	3*3	1	Same	32
Maxpool	-	2*2	-	-	-
Conv	1*1	3*3	1	Same	64
Maxpooling	-	2*2	1	-	-
Conv	1*1	3*3	-	Same	122
Maxpooling	-	2*2	1	-	-
Conv	1*1	3*3	-	Same	184
Maxpoolng	-	2*2	-	-	-
Flatten	-	-	-		-

Bidirectional	-	-	-	-	-
Bidirectional	-	-	-	-	-
Dense	-	-	-	-	465
Dense	-	-	-	-	365
Dropout	-	-	-	-	-
BatchNormalizatiion	-	-	-	-	-
Dense	-	-	-	-	5

Table 3: Training Parameters

Optimizer	Epoch	Batch Size	Learning Rate	Decay	Beta_1	Beta-2
Adam	300	64	0.00001	0.0001	0.9	0.999

Table 4: Callback: Reduce Learning Rate on Plateau

Parameter	monitor	patience	factor	min_lr
Value	val_accuracy	1	0.2	0.0001

Table 5 Comparison of the proposed model with previous studies

Accuracy	Precision	F1-Score	Specificity	Sensitivity	False Positive Rate
$\frac{TP+TN}{TP+TN+FP+FN}$	$\frac{TP}{TP+FP}$	$\frac{2*Precision*Recall}{Precision+Recall}$	$\frac{TN}{TN+FP}$	$\frac{TP}{TP+FN}$	$\frac{FP}{FP+TN}$
95.33	95.42	95.33	95.34	97.63	99.50

Table 5

Study	Method	Accuracy
Ahmad Elarby et.al,. [42]	AlexNet and VGG19	94%
Cheng Dong et.al,. [43]	Improved AlexNet	94.70%
Alkan A et.al,. [44]	AlexNet + TL	92.5%
Hason, Antor mahamudul et al,.[45]	Improved CNN(AlexNet)	93%
Shradha Verma et al,. [46]	Alexnet	93.4%

Table 6

AlexNet	BiAlexNet model With orginal data	BiAlexNet model with data preprocessed using adaptive filtering and NLP data	BiAlexNet model with data preprocessed using adaptive filtering and Tuned NLP data
92.12%	92.26%	93.89%	95.33%

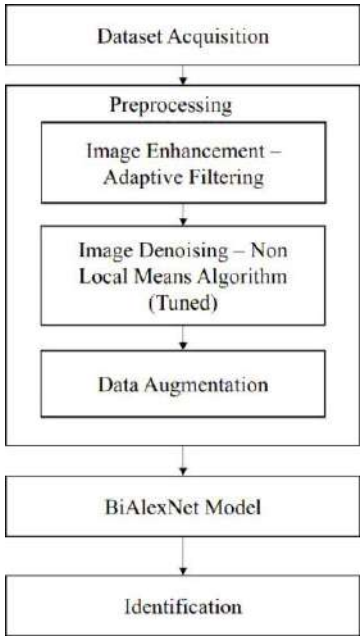

Fig.1. Data Acquisition

Fig 2. Black Spot

Fig 3. Canker

Fig 4. Greening

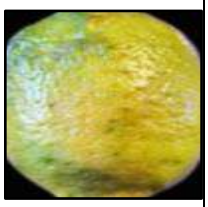

Fig 5. Healthy

Fig 6.Scab

Fig.2-6. Sample images of citrus fruit disease dataset

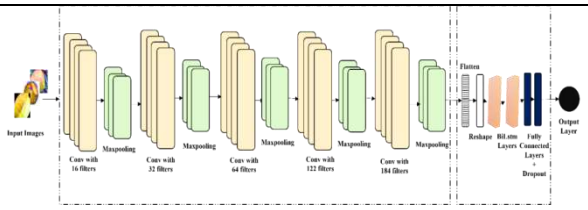

Fig 7. Proposed BiAlexNet Architecture

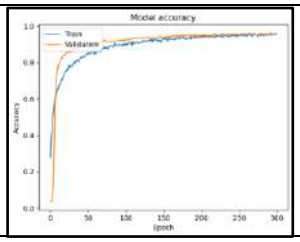

Fig:8

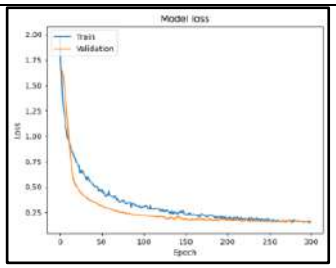

Fig: 9

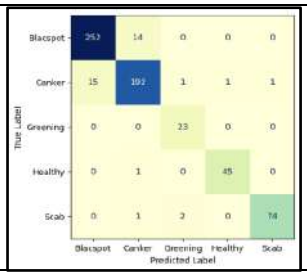

Fig: 10

RESEARCH ARTICLE

Promoting Mental Well-Being: The Importance of Multidisciplinary Strategies In Mental Health Care

Kanchan Joshi

Assistant Professor, Jigyasa University, Dehradun, Uttarakhand, India.

Received: 21 Sep 2024 Revised: 10 Nov 2024 Accepted: 31 Dec 2024

***Address for Correspondence**
Kanchan Joshi
Assistant Professor,
Jigyasa University,
Dehradun, Uttarakhand, India.
E.Mail:

ABSTRACT

Mental well-being, encompassing emotional, psychological, and social health, is vital for overall health, influencing physical health, cognitive function, and social relationships. It extends beyond the absence of mental illness, involving positive states such as happiness, resilience, and the ability to cope with life's challenges. Poor mental well-being is linked to chronic physical conditions, while good mental health promotes healthy behaviors and strengthens social connections. Public health initiatives that focus on mental well-being can prevent mental health disorders, save healthcare costs, and maximize productivity in society. In the treatment of mental illnesses, a multidisciplinary approach involving psychologists, psychiatrists, social workers, medical practitioners, educators, and community organizations ensures that all factors influencing a person's mental health-the emotional, social, and biological-are treated as a whole. This results in better treatment outcomes, such as individualized care, stronger patient adherence, and responsiveness to changing needs. Successful examples of this strategy are collaborative care models and school-based mental health programs that have demonstrated effectiveness in enhancing both individual and community health outcomes.

Keywords: Mental well-being, encompassing emotional, psychological, and social health, is vital for overall health, influencing physical health, cognitive function, and social relationships.

INTRODUCTION

Mental well-being is defined as an integral component of health in general because it determines physical health, cognitive functioning, and social relationships (World Health Organization, 2005). Mental well-being is understood to be the emotional, psychological, and social soundness of people. By thought processes, feelings, actions, and how individuals react towards stress, relate with others, and the ability of making choices, it falls under the definition

(Keyes, 2002). In addition to having no mental illness, mental wellbeing further means positive mental states that are happiness, life satisfaction, or resilience. It also includes the ability to respond to the challenges of life and survive in different conditions (Ruggeri, K., *et al.* (2020). Increasingly, mental wellbeing is being recognized in both the clinical and public health world as important to total health. There is evidence demonstrating that poor mental wellbeing goes with an increased risk for chronic physical conditions, like heart disease, diabetes, and obesity (Steptoe *et al.,* 2013). On the contrary, excellent mental well-being promotes good habits such as physical activities, good nutrition, and following doctor's prescriptions. It therefore lowers the susceptibility to a range of illnesses. Second, mental wellbeing enables a close social life which is key to both personal and collective resilience (Tamminen, N., *et al.* (2020).). Therefore, mental well-being benefits not only the individual quality of life but also leads to overall health outcomes and societal productivity. The key issue that connects directly with public health in regards to individual and collective health outcomes is mental well-being. A population having good levels of mental well-being would have low incidences of mental disorders, healthier physical conditions, and overall well-being (Dodge *et al.,* 2012). Public health measures with mental well-being in the foreground prevent mental health disorder emergence, save on health expenditure, and increase productivity among various societies. Mental well-being is critical for building resilience and strengthening social cohesion, especially at such trying times as a pandemic or the economy disruption. Integrating mental well-being into public health policies would bring down health inequalities since early intervention and prevention through mental health promotion strategies empower everybody with resources and support towards optimal well-being. Such policy-making will be beneficial to obtain long-term inclusive health results (Parenteau, A. M. *et al.,* 2023)

Multidisciplinary Strategy in Mental Health Care

A multidisciplinary strategy in mental health refers to the coordinated and collaborative efforts of professionals from various disciplines working together to address the complex nature of mental health problems. It emphasizes the integration of expertise from different fields to provide holistic care that addresses not only the psychological aspects of mental health but also the social, biological, and environmental factors that contribute to mental well-being. A multidisciplinary approach ensures that individuals receive comprehensive, personalized treatment and support from various experts, which improves outcomes rather than relying on a single professional or approach (Katon *et al.,* 2006).In mental health care, the multidisciplinary teams usually comprise psychologists, psychiatrists, social workers, medical professionals, educators, and community organizations. The teams work together to ensure comprehensive care that addresses many aspects of mental health. In this way, the treatment is tailored to each patient's unique needs.

Key Components of a Multidisciplinary Mental Health Strategy

Psychologists and Psychiatrists

Psychologists are trained in diagnosing and treating mental health disorders through various forms of therapy, such as CBT, psychotherapy, and counseling. They try to make people understand and handle their emotions, behaviors, and thought patterns while Psychiatrists, being medical doctors who specialize in mental health, diagnose, treat, and prevent mental disorders. They frequently administer medications to mitigate psychiatric conditions such as depression, anxiety, or schizophrenia. Their contribution is crucial in controlling the biological and physiological elements of mental disorders and administering medical interventions alongside therapies (Raney, L. E. (2015). Together, these providers deliver a combination of therapy and medication, thereby providing all-inclusive treatment for psychological and medical disorders.

Social Workers

Social workers are important for the multidisciplinary approach as they assist individuals and families in navigating social, economic, and environmental issues that affect mental health. Counseling and support, especially in the context of family dynamics, housing issues, and access to community resources, are offered by them. Social workers are often involved in the practical aspects of care, helping patients' access services and advocating for them within larger social systems (Segal *et al.,* 2006). By addressing the socio-economic and environmental factors that influence mental health, they ensure that the mental health care plan is well-rounded and supportive.

Medical Practitioners

Nursing Professionals and other doctors will form a key part of the multi-disciplinary approach because often, they are the first port of call for most patients experiencing symptoms of mental illness. They form a core role in diagnosing early warning signs of mental illnesses, carrying out medical checkups, and referring the patients to specialists for further treatment. In addition to general health care, they work with mental health professionals to ensure that any physical health conditions, which could impact mental well- being, are addressed appropriately (Katon *et al.,* 2006). This approach ensures that physical illness does not worsen mental health problems and vice versa.

Educators'

Mental health care is not limited to clinical settings; educators play a crucial role in promoting mental well-being within schools and communities. Teachers and school counselors often find early warning signs of mental distress in students and collaborate with mental health professionals to develop the right interventions. School-based mental health programs seek to enhance emotional literacy, resilience, and coping skills. Educators help incorporate mental health education into curricula, reducing stigma and raising awareness about mental health among students, teachers, and families (Zabek, F *et al.,* 2023). Educators play a highly influential role in creating such environments, where mental wellness is taken care of; by encouraging a supportive, educated environment.

Alternate Therapeutic Interventions

Alternative therapists play a considerable role in supporting the mental health care system by providing complementary approaches that focus on the mind-body connection. Acupuncture, massage, yoga, and meditation are among the most common practices to reduce stress, alleviate anxiety, and improve emotional well-being. These therapies complement traditional treatments and provide an accessible alternative for individuals who may be reluctant to engage with conventional mental health services. This integration of alternative therapies makes mental health care more inclusive in terms of options that one may seek in case they require support. (Asher, G. N *et al.,* 2017)

Benefits of Multidisciplinary Collaboration in Mental Health Care

Multidisciplinary collaboration in mental health care offers a holistic approach that addresses the emotional, social, and biological aspects of mental health. Psychiatrists and psychologists focus on emotional and psychological components, while social workers manage social factors like family dynamics or housing instability, and medical doctors address biological issues, such as chronic illnesses or thyroid imbalances (Katon *et al.,* 2006). This research-based integrated care model improves the effectiveness of treatments, according to the finding that one study showed an improvement in the results among patients with depression and chronic diseases (Katon *et al.,* 2006). Also, the WHO supports the holistic approach to mental health, which includes psychological, medical, and social care toward improving patient outcomes (World Health Organization, 2005). This approach makes it easy to design an individualized treatment plan specific to the needs of a particular patient which can be combined with experience from various professionals. It differs from models that are limited to addressing only one part of care; this method includes considerations such as mental health history, family dynamics, culture, and socioeconomic status. For instance, a psychiatrist might modify medication, a therapist gives therapy, and a social worker deals with practical issues so that care is cohesive. Evidence indicates that this type of care model promotes more treatment adherence, higher patient satisfaction, and better long-term results. Further, multidisciplinary teams have flexibility to change care based on the progression of the patient's condition, which can ensure continued alignment with their needs (Alderwick, H *et al.,*2021). Multidisciplinary collaboration allows professionals from other fields to work in complete harmony, thus making sure that all the care is provided to the patient. The approach brings out an effective treatment plan with each professional being able to provide specialist insight to work towards better results. A psychiatrist may be able to adjust medications; a psychologist may be able to administer therapy, and a social worker may ensure that resources within the community are appropriate for recovery. Interagency cooperation between mental health workers may increase the participation of

the patient due to an extensive support system. The diverse set of skills and opinions provided by the team is understood to create an atmosphere that encourages patients to open up more easily, hence developing trust for better treatment. A team of professionals such as occupational therapists, nurses, and counselors are usually better at helping support a patient in their journey toward mental health. These enable consistent participation in treatment plans.

Examples of Successful Multidisciplinary Collaborations

Many examples of multidisciplinary collaboration in mental health care have shown a positive outcome. Among such is the collaborative care model adopted within primary care settings. For example, Katon *et al.'s* research, published in 2006, has shown that psychiatrists, psychologists, and case managers were effective as part of the care team in managing depression for patients who have chronic medical conditions if included in the care setting. This model greatly enhanced mental and physical health outcomes and reduced the burden of depression and improved the quality of life for the patients. Another example includes school-based mental health programs. These groups of counselors, social workers, educators, and mental health professionals together provide mental health support to the students in schools. As stated in Zabek, F *et al*., (2023) School mental health initiatives have reduced emotional and behavioral problems of students in communities that lack other means for mental health. These programs provide early intervention, preventing the escalation of mental health issues by offering students emotional, social, and academic support through coordinated efforts from various professionals. IRMs are also referred to as Individual Recovery Models, a collaborative framework that aims at increasing access to comprehensive mental health services. These models are based on the evolving needs of an individual in his or her recovery journey, with an added aim of ensuring that people have access to services addressing holistic needs for those with mental health challenges. The goals of IRMs are restoration, preservation, and promotion of individual functioning by collaborating on developing skills, competencies, and community reintegration. Healing, empowerment, and responsibility have been identified as the core elements of IRMs. Healing involves the recovery process in which individuals develop their capacity to control mental health problems within a community context, usually through better self-care and living a wellness-focused lifestyle. Empowerment is characterized by self-directedness in formulating recovery goals and building confidence in overcoming obstacles. Responsibility refers to assuming control over one's recovery by utilizing individual strengths and creating social relationships. IRMs promote personal and social processes through which dignity, respect, trust, and belonging are fostered. (Mpofu,E. 2019).

Challenges and Barriers to Implementing Multidisciplinary Approaches in Mental Healthcare system

Implementing multidisciplinary approaches in mental health care faces several challenges, primarily related to resource constraints, coordination issues, cultural and structural barriers, training gaps, and policy and regulatory obstacles (Zaman, Q. 2024). Limited funding, shortages of mental health professionals, and disparities in resources, particularly in rural or underserved areas, hinder the ability to establish comprehensive teams (Ellis, H., & Alexander, V. (2016). Coordination among providers is essential but often problematic due to poor communication, differing treatment approaches, and complex cases. Cultural differences and structural barriers, such as stigma and lack of culturally competent care, further complicate the engagement of patients from diverse backgrounds Additionally, the lack of interdisciplinary training for healthcare professionals results in inefficiencies and misunderstandings regarding roles, impacting collaboration and patient outcomes. Finally, policy and regulatory challenges, such as legal constraints against data sharing and reimbursement systems that are not favorable to collaborative care, continue to hinder effective multidisciplinary approaches (Monaghan K, Cos T. 2021). Such a challenge will require investments in resources, training, and policy reform, and a better coordination system to ensure the effective implementation of multidisciplinary care.

REFERENCES

1. Dodge, R., Daly, A., Huyton, J., & Sanders, L. (2012). The challenge of defining well- being. International Journal of Wellbeing, 2(3), 222-235.

2. Keyes, C. L. M. (2002). The mental health continuum: From languishing to flourishing in life. Journal of Health and Social Behavior, 43(2), 207-222.
3. Ruggeri, K., Garcia-Garzon, E., Maguire, Á., et al. (2020). Well-being is more than happiness and life satisfaction: A multidimensional analysis of 21 countries. *Health and Quality of Life Outcomes, 18*(1), 192. https://doi.org/10.1186/s12955-020-01423- y
4. Steptoe, A., Wardle, J., & Marmot, M. (2005). Positive affect and health-related neuroendocrine, cardiovascular, and inflammatory processes. Proceedings of the National Academy of Sciences of the United States of America, 102(18), 6508–6512. https://doi.org/10.1073/pnas.0409174102
5. Tamminen, N., Reinikainen, J., Appelqvist-Schmidlechner, K., Borodulin, K., Mäki- Opas, T., & Solin, P. (2020). Associations of physical activity with positive mental health: A population-based study. Mental Health and Physical Activity, 18, 100319. https://doi.org/10.1016/j.mhpa.2020.100319
6. World Health Organization (2005). Mental health: New understanding, new hope. World Health Report.
7. Dodge, R., Daly, A., Huyton, J., & Sanders, L. (2012). The challenge of defining wellbeing. International Journal of Wellbeing, 2(3), 222–235. https://doi.org/10.5502/ijw.v2i3.4
8. Parenteau, A. M., Boyer, C. J., Campos, L. J., Carranza, A. F., Deer, L. K., Hartman, D. T., ... & Hostinar, C. E. (2023). A review of mental health disparities during COVID-19: Evidence, mechanisms, and policy recommendations for promoting societal resilience. Development and Psychopathology, 35(4), 1821-1842.
9. Katon, W., *et al*. (2006). Collaborative care for patients with depression and chronic illnesses.
1. New England Journal of Medicine, 355(21), 2091-2099.
10. Raney, L. E. (2015). Integrating primary care and behavioral health: the role of the psychiatrist in the collaborative care model. American Journal of Psychiatry, 172(8), 721-728.
11. Segal, E. A., *et al*. (2006). Social welfare policy and advocacy: Advancing social justice. Thomson Brooks/Cole.
12. Zabek, F., Lyons, M. D., Alwani, N., Taylor, J. V., Brown-Meredith, E., Cruz, M. A., & Southall, V. H. (2023). Roles and functions of school mental health professionals within comprehensive school mental health systems. School Mental Health, 15(1), 1- 18.
13. Asher, G. N., Gerkin, J., & Gaynes, B. N. (2017). Complementary Therapies for Mental Health Disorders. The Medical clinics of North America, 101(5), 847–864. https://doi.org/10.1016/j.mcna.2017.04.004
14. Alderwick, H., Hutchings, A., Briggs, A., & Mays, N. (2021). The impacts of collaboration between local health care and non-health care organizations and factors shaping how they work: a systematic review of reviews. BMC Public Health, 21, 1-16.
15. Mpofu, E., Watts, J., & Li, Q. (2019). Community-based mental health counseling, recovery models, and multidisciplinary collaboration. Clinical Mental Health Counseling: Practicing in Integrated Systems of Care, 119.
16. Zaman, Q. (2024). Integrating Mental Health Service in Primary Care: Challenges and Opportunities. Multidisciplinary Journal of Healthcare (MJH), 1(2), 1-12.
17. Ellis, H., & Alexander, V. (2016). Eradicating barriers to mental health care through integrated service models: Contemporary perspectives for psychiatric-mental health nurses. Archives of Psychiatric Nursing, 30(3), 432-438.
18. Monaghan K, Cos T. Integrating physical and mental healthcare: Facilitators and barriers to success. Medicine Access @ Point of Care. 2021;5. doi:10.1177/23992026211050615.

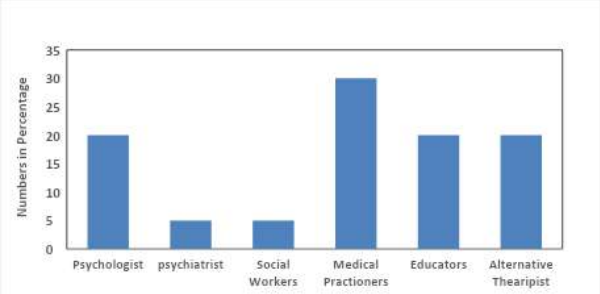

Figure.1 : Professionals involved in Mental Health Care Sector

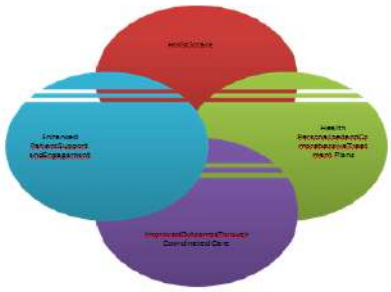

Figure.2 : Various segments of Health cares

Vol.15 / Issue 88 / Feb / 2025 *International Bimonthly (Print) – Open Access* *ISSN: 0976 – 0997*

RESEARCH ARTICLE

Some Fixed-Point Theorems in Generalized Metric Spaces

Arul Xavier A* and Maria Joseph J

Department of Mathematics, St.Joseph's College, (Affiliated to Bharathidasan University), Tiruchirappalli, Tamil Nadu, India.

Received: 21 Jun 2024 Revised: 03 Jul 2024 Accepted: 13 Aug 2024

***Address for Correspondence**
Arul Xavier A
Department of Mathematics,
St.Joseph's College,
(Affiliated to Bharathidasan University),
Tiruchirappalli, Tamil Nadu, India.
E.Mail: arulxavier3006@gmail.com

ABSTRACT

These generalizations serve as the inspiration for this study, which introduces concept of rectangle S-metric space that is extending RMS(Rectangular Metric Space) which generalizes several papers in present literature.

Keywords: Metric spaces, S-metric spaces, complex valued S_p-metric spaces,S_p-metric spaces, Rectangular metric space Common fixed point.

INTRODUCTION

Current chapter demonstrate uniqueness of fixed point theorems in rectangular metric, which generalizes certain well-known findings from recent research. Numerous mathematicians have been interested in the space's topological structure due of its application to fixed point theory. Researchers have faced a problem in recent years to offer metric spaces' different generalizations due to variety of fixed-point theorem applications. A wide variety of generalized spaces are available, including generalized quasimetric saces, quaternion valued G-metric spaces, D-metric spaces, S-metric spaces, S_b-metric spaces, S_P-metric spaces, quasi-metric spaces, complex valued S_b-metric spaces, G_b-metric spaces, A-metric spaces, G-metric spaces, b-metric spaces, complex valued G_b-metric Spspaces, along with most recent metric spaces.

Definition 1.1. Considering, S: $X^3 \rightarrow \mathbb{R}+$ be function which satisfies given criteria, and consider X be non-empty "set.

1. $\underline{S}(x,y,z)=0$ if x=y=z.
2. $\underline{S}(x,y,z)\leq\underline{S}(x,x,a)+\underline{S}(z,z,a)$ for every x,y,z ϵX & every distinct points a ϵX–x,y,z.

In" S-metric space in rectangular shape is referred to as(X,S).

Example 1.2. Considering X=N∪ {0}& specify $\underline{S}$:$X \times X \times X \to \mathbb{R}^+ \cup 0$ by
$\underline{S}(x,y,z) = \{0, \quad x = y = z\ xyz \quad otherwise$
Despite being rectangular S-metric space,(X,S) isn't considered as G-metric space or RMS.
$G(6,4,2) < G(6,6,2)$.

Example 1.3. Considering X=N∪ {0}& specify S :$X \times X \times X \to \mathbb{R}^+ \cup 0$ by
$\underline{S}(x,y,z) = \{0, \quad x = y = z\ x + y + z \quad otherwise$
Hence, rectangle S-metric space is (X, S), however it isn't RMS or G-metric space because
$G(6,4,2) < G(6,6,2)$.

Example 1.4. Considering X=N∪ {0}& specify S :$X \times X \times X \to \mathbb{R}^+ \cup 0$ by
$\underline{S}(x,y,z)=\{0, \ x = y = z\ a, \forall a \in N \quad otherwise$
However, (X, S) isn't rectangle metric space or G-metric space, while being rectangular S-metric space.
$G(x,y,z) < G(x,x,y)$.

Definition 1.5. Consider the rectangular S-metric spaces (X,G). For any $y \in X, r \geq 0$ a G-sphere having radius r & centre y is
$s_G(y,r) = \{z \in X : G(y,z,z) < r\}$

Definition 1.6. Consider the S-metric spaces (X,G) to be rectangular. A sequence $\{x_n\} \subset X$ is G-convergent "to z in rectangular S-metric topology.

Definition 1.7. Consider, 2 rectangular S-metric spaces(X,G) &,,X.,,G, a function $T : X \to \underline{X}$ Is G-Continuous at point $x \in X$ if, $T^{-1}\left(S_{\underline{G}}(f(x)), r\right) \in \tau(G), for\ all\ r \geq 0$. If ,T is G-continuous across X, then it is G-continuous.

Lemma 1.8. Considering, rectangular S-metric spaces(X, $\underline{S}$) &$\{x_n\}$. Then $\{x_n\}$ converges to x only if $\underline{S}(x_n, x, x) \to 0\ as\ n \to \infty$

Lemma 1.9. Considering, rectangular S-metric spaces(X, $\underline{S}$) &$\{x_n\}$. Then $\{x_n\}$ said to be a Cauchy" sequence only if $\underline{S}(x_n, x, x) \to 0\ as\ n, m, l \to \infty$

Main results
Banach contraction principle is an analog of subsequent theorem in partial b-metric space.

Theorem 2.1. Considering (X, ρ) be complete RMS and let $U: X \to X$ be a mapping satisfying
$\rho(Ul, Um) \leq \mu_1 \rho(l,m) + \mu_2[\rho(l, Ul) + \rho(m, Um)] + \mu_3 \frac{\rho(l,m)}{1+\rho(m,Ul)}$ (2.1)
Where $\mu_1, \mu_2, \mu_3 \geq 0\ and\ \mu_1 + 2\mu_2 + \mu_3 < 1\ \forall\ l, m \in X$. Next U having unique fixed point.

Proof: Considering, demonstrate that U is unique if it has fixed point. We will demonstrate that $\eta \in X$ fixed point of U, where Uη = η, then $\rho(\eta, \eta) = 0$ by employing (2.1), we obtain $\rho(\eta, \eta) = \rho(U\eta, U\eta)$
$\leq \mu_1 \rho(\eta, \eta) \mu_2[\rho(\eta, U\eta) + \rho(\eta, U\eta)] + \mu_3 \frac{\rho(\eta,\eta)}{1+\rho(\eta,U\eta)} \leq (\mu_1 + 2\mu_2 + \mu_3)\rho(\eta, \eta) < \rho(\eta, \eta)$, a contradiction.
Thus $\rho(\eta, \eta) = 0$.
Suppose η,η′∈ X be 2 distinct fixed points of U,i.e.,Uη=η,Uη′=η′.
Next, "there's $\rho(\eta, \eta) = \rho(\eta', \eta') = 0$.
Using (2.1), we obtain
$\rho(\eta, \eta') = \rho(U\eta, U\eta')$
$\leq \mu_1 \rho(\eta, \eta') + \mu_2[\rho(\eta, U\eta) + \rho(\eta', U\eta')] + \mu_3 \frac{\rho(\eta, \eta')}{1 + \rho(\eta', U\eta)}$
$\leq \mu_1 \rho(\eta, \eta') + \mu_2[\rho(\eta, \eta) + \rho(\eta', \eta')] + \mu_3 \frac{\rho(\eta, \eta')}{1 + \rho(\eta', \eta)}$

$\leq \mu_1\rho(\eta,\eta') + \mu_3\rho(\eta,\eta')$
$\leq (\mu_1+\mu_3)\rho(\eta,\eta')$
$(1-\mu_1-\mu_3)\rho(\eta,\eta') \leq 0$
Since", $\mu_1 + 2\mu_2 + \mu_3 < 1$,
Thus $\rho(\eta,\eta') = 0$
Therefore, $\eta = \eta'$
Hence, if U exists' fixed point, Consequently, it's distinct.
For a fixed point to exist, lt$l_0 \in X$ be an arbitrary point.
Define a sequence $\{l_n\}$ as follows: $l_n = U^n l_0, n \geq 0$
Regarding any $n \in N$, We have

$$\rho(Ul,Um) \leq \mu_1\rho(l,m) + \mu_2[\rho(l,Ul)+\rho(m,Um)] + \mu_3\frac{\rho(l,m)}{1+\rho(m,Ul)}\rho(l_n,l_{n+1}) = (Ul_{n-1},Ul_n)$$

$$\leq \mu_1\rho(l_{n-1},l_n) + \mu_2[\rho(l_{n-1},Ul_{n-1})+\rho(l_n,Ul_n)] + \mu_3\frac{\rho(l_{n-1},l_n)}{1+\rho(l_n,Ul_{n-1})}$$

$$= \mu_1\rho(l_{n-1},l_n) + \mu_2[\rho(l_{n-1},Ul_{n-1})+\rho(l_n,Ul_n)] + \mu_3\frac{\rho(l_{n-1},l_n)}{1+\rho(l_n,Ul_{n-1})}$$

$$= (\mu_1+\mu_2+\mu_3)\rho(l_{n-1},l_n) + \mu_2\rho(l_n,l_{n+1})$$

$$\rho(l_n,l_{n+1}) \leq \frac{(\mu_1+\mu_2+\mu_3)}{1-\mu_2}\rho(l_{n-1},l_n)$$

$$\rho(l_n,l_{n+1}) \leq \zeta\,\rho(l_{n-1},l_n)$$

Where $\zeta = \frac{(\mu_1+\mu_2+\mu_3)}{1-\mu_2} < 1$
Continuing this process, "having

$$\rho(l_n,l_{n+1}) \leq \zeta\,\rho(l_{n-1},l_n) \leq \zeta\zeta\,\rho(l_{n-2},l_{n-1}) = \zeta^2\rho(l_{n-2},l_{n-1}) \leq \zeta^3\rho(l_{n-3},l_{n-2}) \leq \cdots \leq \zeta^n\rho(l_0,l_1).$$

$$\rho(l_n,l_{n+1}) \leq \zeta^n\rho(l_0,l_1)\ \forall\ n \geq 0 \qquad (2.2)$$

Using" (2.1), for n,m$\in N, m > n$, having

$$\rho(l_n,l_m) \leq \rho(l_n,l_{n+1}) + \rho(l_{n+1},l_{n+2}) + \rho(l_{n+2},l_m)$$
$$\leq \rho(l_n,l_{n+1}) +, \cdots, +\rho(l_{n+4},l_m)$$
$$\leq \rho(l_n,l_{n+1}) +, \cdots, +\rho(l_{m-1},l_m)$$
$$\leq K^n\rho(l_0,l_1) + K^{n+1}\rho(l_0,l_1) +, \cdots, +K^{m-n}\rho(l_0,l_1)$$

In the above inequality, we get

$$\leq K^n(1+k+\cdots+K^n+\cdots)\rho(l_0,l_1)$$
$$= \frac{K^n}{1-K}\rho(l_0,l_1)$$

As $m,n \to \infty,\ \rho(l_n,l_m) = 0$
Hence, $\{l_n\}$"Cauchy sequence in X.
By completeness of X, there" exist $l \in X$ which contain

$$\rho(l_n,l) = \rho(l_n,l_m) = \rho(l,l) = 0 \qquad (2.3)$$

We demonstrate that l is fixed point of F.
For any, $n \in N$ we "obtain;

$$\rho(l,Ul) \leq \rho(l,l_{n+1}) + \rho(l_{n+1},l_{n+2}) + \rho(l_{n+2},Ul) = \rho(l,l_{n+1}) + \rho(l_{n+1},l_{n+2}) + \rho(l_{n+2},Ul)$$

$$\leq \rho(l,l_{n+1}) + \rho(l_{n+1},l_{n+2}) + \mu_1\rho(l_{n+1},l) + \mu_2[\rho(l_{n+1},l_{n+1}) + \rho(l,Ul)] + \mu_3\frac{\rho(l_{n+1},l)}{1+\rho(l,l_{n+1})}$$

$$= \rho(l,l_{n+1}) + \rho(l_{n+1},l_{n+2}) + \mu_1\rho(l_{n+1},l) + \mu_2\rho(l_{n+1},l_{n+2}) + \mu_{2\rho(l,Ul)} + \mu_3\frac{\rho(l_{n+1},l)}{1+\rho(l,l_{n+2})}$$

From (2.3), we have, $(1-\mu_2)\rho(l,Ul) \leq 0$
Therefore, $\rho(l,Ul) \leq 0$
$\rho(l,Ul) = 0$
Thus", $Ul = 1$
Here, ' unique fixed point of U is l'.

Theorem 2.2. Consider, (X,ρ) be a complete RMS & let $U: X \to X$ be a mapping that satisfy

$\rho(Ul, Um) \leq \mu\left\{\rho(l,m), \rho(l,Ul), \rho(m,Um), \frac{\rho(l,m)}{1+\rho(l,Ul)+\rho(m,Um)}\right\}$ (2.4)

For all $l, m \in X$ *and* $\mu \in [0,1)$. Next U contain "a unique fixed point in X.

Proof : Let's demonstrate that U is unique if a fixed point exists.

Let η,η′∈ X be two fixed points of U that is Uη = η and Uη′ = η′. From (2.4), it is evident that

$\rho(\eta, \eta') = \rho(U\eta, U\eta')$

$\leq \mu\left\{\rho(\eta,\eta'), \rho(\eta, U\eta), \rho(\eta', U\eta'), \frac{\rho(\eta,\eta')}{1+\rho(\eta,U\eta')+\rho(\eta',U\eta)}\right\}$

$= \mu\left\{\rho(\eta,\eta'), \rho(\eta,\eta), \rho(\eta',\eta'), \frac{\rho(\eta,\eta')}{1+\rho(\eta,\eta')+\rho(\eta',\eta)}\right\}$

$= \mu\rho(\eta,\eta')$

$< \rho(\eta,\eta')$, a contradiction.

Thus, $\rho(\eta,\eta') = 0$, i.e., η = η′. Therefore, U is" unique if it contain a fixed point.

Let $l_0 \in X$ be an arbitrary point.

Describe a sequences $\{l_n\}$ as "follows: $l_{n+1} = Ul_n, \forall\, n \geq 0$ Now, for any n we obtain from (2.4) that

$\rho(l_{n+1}, l_n) = \rho(Ul_n, Ul_{n-1}) \leq \mu\left\{\rho(l_n, l_{n-1}), \rho(l_n, Ul_n), \rho(l_{n-1}, Ul_{n-1}), \frac{\rho(l_n, l_{n-1})}{1+\rho(l_n, Ul_{n-1})+\rho(l_{n-1}, Ul_n)}\right\}$

$= \mu\left\{\rho(l_n, l_{n-1}), \rho(l_n, l_{n+1}), \rho(l_{n-1}, l_n), \frac{\rho(l_n, l_{n-1})}{1+\rho(l_n, l_n)+\rho(l_{n-1}, Ul_{n+1})}\right\}$

$= \mu\{\rho(l_n, l_{n-1}), \rho(l_n, l_{n+1})\}$

Suppose $\{\rho(l_n, l_{n-1}), \rho(l_n, l_{n+1})\} = \rho(l_n, l_{n+1})$, then we obtain from the above inequality that $\rho(l_{n+1}, l_n) \leq \mu\rho(l_{n+1}, l_n) < \rho(l_{n+1}, l_n)$ a" contradiction.

Thus, $\{\rho(l_n, l_{n-1}), \rho(l_n, l_{n+1})\} = \rho(l_n, l_{n-1})$ and then from the above inequality we have,

$\rho(l_{n+1}, l_n) \leq \mu\, \rho(l_n, l_{n-1})$ on continuing this process, we have

$\rho(l_{n+1}, l_n) \leq \mu^n \rho(l_1, l_0)\ \forall\, n \geq 0.$ (2.5)

For $n, m \in N, m > n$, we "have

$\rho(l_n, l_m) \leq \rho(l_n, l_{n+1}) + \rho(l_{n+1}, l_{n+2}) + \rho(l_{n+2}, l_m)$

$\leq \rho(l_n, l_{n+1}) +, \cdots, +\rho(l_{n+4}, l_m)$

$\leq \rho(l_n, l_{n+1}) +, \cdots, +\rho(l_{m-1}, l_m)$

$\leq K^n \rho(l_0, l_1) + K^{n+1}\rho(l_0, l_1) +, \cdots, +K^{m-n}\rho(l_0, l_1)$

In the above inequality, we" get

$\leq K^n(1 + k + \cdots + K^n + \cdots)\rho(l_0, l_1)$

$= \frac{K^n}{1-K}\, \rho(l_0, l_1)$

As $K \in [0,1)$ we obtain

$\rho(l_n, l_m) = 0$

Hence, Cauchy sequence in X *is* $\{l_n\}$.

By X's completeness, there exist $l \in X$ which contain

$\rho(l_n, l) = \rho(l_n, l_m) = \rho(l, l) = 0$ (2.6)

We demonstrate that l is a fixed point of F.

For any $n \in N$, we obtain

$\rho(l, Ul) \leq \rho(l, l_{n+1}) + \rho(l_{n+1}, l_{n+2}) + \rho(l_{n+2}, Ul)$

Using (2.6) in the above inequality, we obtain $\rho(l, Ul) = 0$.

Thus, $Ul = l$.

Here, unique fixed point of U is′l'.

Corollary 2.3 Considering, X represent complete rectangular S-metric space $F : X \to X$ map for where is real number, K that satisfy $0 \leq K \leq 0.5$ that contain for every pair $x, y, z \in X$

$\underline{S(F_x, F_y, F_z) \leq KS(x, y, z)}$

Then F contain unique fixed point.

Remark 2.4. Considering be rectangular S-metric space(X, $\underline{S}$) &$d: X \times X \to [0,\infty)$ function defined by $d(x,y) = \underline{S}(x,y,y)$, Banach contradiction principle in RMS, which is an Banach contradiction principle's analogue in metric space, has been then reduced to by Corollary 2.3.

Corollary 2.5. Considering X be complete rectangular S-metric space &$F: X \to X$ map for which a real number exists, b that satisfy $0 \le b \le 0.2$ so that for every pair $x, y, z \in X$
$\underline{S}(F_x, F_y, F_z) \le b[\underline{S}(x, F_x, F_x) + \underline{S}(y, F_y, F_y) + \underline{S}(z, z, F_z)]$
F then contain a fixed point that is "unique.

Theorem 2.6. Consider X to be a complete S-metric, rectangular space &$F: X \to X$ a mapping for which there exists real number $l_i \ge 0, i = 0,1,2,3,4$ satisfying $l_1 + l_2 + l_3 + l_4 < 1$ such that for each pair $a, b, c \in X, l$
$S(F_a, F_b, F_c) \le l_1 S(a,b,c) + l_2 S(a, F_a, F_a) + l_3 S(b, F_b, b) + l_4 S(c, F_c, F_c)$
Then F contain a unique fixed point.

Proof: Considering"$a_0 \in W$"be arbitrary point.
Describe the sequence $\{a_n\}$ by $a_n = F^n a_0$.
Now, $S(a_n, a_n, a_{n+1}) = S(Fa_{n-1}, Fa_{n-1}, Fa_n)$
$\le l_1 S(a_{n-1}, a_{n-1}, a_n) + l_2 S(a_{n-1}, Fa_{n-1}, Fa_{n-1}) + l_3 S(a_{n-1}, Fa_{n-1}, Fa_{n-1}) + l_4 S(a_n, Fa_n, Fa_n)$
$= l_1 S(a_{n-1}, a_{n-1}, a_n) + l_2 S(a_{n-1}, a_n, a_n) + l_3 S(a_{n-1}, a_n, a_n) + l_4 S(a_n, a_{n+1}, a_{n+1})$
$= (l_1 + l_2 + l_3)\, S(a_{n-1}, a_{n-1}, a_n) + l_4 S(a_n, a_{n+1}, a_{n+1})$
Letting $t_n = S(a_n, a_n, a_{n+1})$
We" have,
$t_n \le (l_1 + l_2 + l_3) t_{n-1} + l_4 t_n$
$t_n \le \left(\frac{l_1 + l_2 + l_3}{1 - l_4}\right) t_{n-1}$
Then, $t_n = \lambda t_{n-1}$, where $\lambda = \frac{l_1 + l_2 + l_3}{1 - l_4} < 1$
We obtain that
$t_n = \lambda t_{n-1}$
$t_n = \lambda^2 t_{n-2}$
$\vdots \qquad \vdots$
$t_n = \lambda^n t_0$ (2.7)
A contradiction. Since $\lambda < 1, thus, \forall\, n \in N, a_0 \ne a_n$. Repeating this argument for each $n, m \in N\ with\ n \ne m, a_n \ne a_m$. Next, a sequence's terms a_n are distinct.
For each $m > n$, we "have
$S(a_n, a_m, a_m) \le S(a_n, a_n, a_{n+1}) + S(a_m, a_m, a_{n+1}) + S(a_n, a_n, a_{n+1})$
$= S(a_n, a_n, a_{n+1}) + 2S(a_m, a_m, a_{n+1})$
$S(a_n, a_m, a_m) \le t_n + 2S(a_m, a_m, a_{n+1})$
$\le t_n + 2t_{n+1} + 2^2 S(a_m, a_m, a_{n+1})$
$\le t_n + 2t_{n+1} + 2^2 t_{n+2} + 2^3 S(a_m, a_m, a_{n+1})$
$\le t_n + 2t_{n+1} + 2^2 t_{n+2} + 2^3 t_{n+3} +, \cdots, +2^{m-1} t_m$
$\le t_n + 2t_{n+1} + 2^2 t_{n+2} + 2^3 t_{n+3} + \cdots$ (2.8)
Using" (2.7) in (2.8)
$S(a_n, a_m, a_m) \le \lambda^n t_0 + 2\lambda^{n+1} t_0 + 2^2 \lambda^{n+2} t_0 +, \cdots, +2^{m-1} \lambda^{m-1} t_0$
$\le [\lambda^n + 2\lambda^{n+1} + 2^2 \lambda^{n+2} +, \cdots, +2^{m-1} \lambda^{m-1}] t_0$
$\le \lambda^n [1 + 2\lambda + (2\lambda)^2 + (2\lambda)^3 +, \cdots, +(2\lambda)^{2-m-1}] t_0$
$\le \lambda^n [1 + 2\lambda + (2\lambda)^2 + (2\lambda)^3 + \cdots] t_0$
$S(a_n, a_m, a_m) \le \lambda^n \left(1 - (2\lambda)\right)^{-1} t_0$
As $n, m \to \infty$, we obtain
$S(a_n, a_m, a_m) = \left[\lambda^n \left(1 - (2\lambda)\right)^{-1}\right] S(0, a_0, a_1) = 0$
For $n, m, j \in N$ with $n > m > j$,
We have, $S(a_n, a_m, a_m) \le S(a_n, a_n, a_{n-1}) + S(a_m, a_m, a_{n-1}) + S(a_j, a_j, a_{j-1})$

Letting $n, m, j \to \infty$ we obtain
$S(a_n, a_m, a_m) = 0$
Thus, $\{a_n\}$ is S-cauchy sequence.
If X is complete, then there is $\upsilon \in X$ that contain a_n is S-convergent to υ.
Suppose $F\upsilon \neq \upsilon$
$S(a_n, F_\upsilon, F_\upsilon) \leq \lambda S(a_{n-1}, \upsilon, \upsilon)$
Letting $n, \to \infty$, and fact that function is S-continues,
$S(\upsilon, F\upsilon, F\upsilon) \leq \lambda S(\upsilon, \upsilon, \upsilon)$
Thus $S(\upsilon, F\upsilon, F\upsilon) \leq 0$, a contradiction.
Thus, $F\upsilon = \upsilon$.

Uniqueness
Suppose $\omega \neq \upsilon$ and T$\boldsymbol{\omega}$ = $\boldsymbol{\omega}$
Then $S(F_\upsilon, F_\omega, F_\omega) \leq \lambda S(\upsilon, \upsilon, \omega)$
Since Fυ = υ and F$\boldsymbol{\omega}$ = $\boldsymbol{\omega}$
We have $S(\upsilon, \omega, \omega) = 0$
Which yields that υ = $\boldsymbol{\omega}$.
This gives unique fixed point F.

REFERENCES

1. M.Boriceanu, Strict fixed point theorem for multivalued operators in b-metric spaces,Int.J.mod.Math.,4, 285–301, 2009.
2. M.Boriceanu, Fixed point theory for multivalued generalized on a set with two b-metric,studia,univ Babes, Bolya: Math,Liv(3), 1–14, 2009.
3. Bota, M., Molnar, A. and Verga, C., On ekeland's variational principle in b-metric spaces, Fixed point theory 12(2):21–28, 2011.
4. Bota, M., Molnar, A. and Verga, C., On ekeland's variational principle in b-metric spaces,Fixed point theory 12(2):21–28, 2011.
5. Maria Joseph J and M.Marudai, Some fixed theorems in ordered and property P in G-metric spaces, International J. of Math. Sci &Engg,5,229–243, 2011.
6. A .Azam , M . Arshad and I .Beg , Banachcontraction principle on cone rectangular metricspaces , Appl . Anal . Discrete Math 32(3):243–253, 2011.

Indian Journal of Natural Sciences www.tnsroindia.org.in ©IJONS

Vol.15 / Issue 88 / Feb / 2025 *International Bimonthly (Print) – Open Access* *ISSN: 0976 – 0997*

RESEARCH ARTICLE

Robust Computational Approach for System of Singularly Perturbed Convection-Diffusion Equations with Delay Terms and Same Perturbation Parameter

S. Padmapriya[1] and Joseph Paramasivam Mathiyazhagan[2]*

[1]Assistant Professor, PG and Research Department of Mathematics, Dr Kalaignar Government Arts College, Kulithalai, Karur, (Affiliated to Bharathidasan University, Tiruchirappalli), Tamil Nadu, India.
[2]Assistant Professor, PG and Research Department of Mathematics, Bishop Heber College (Affiliated to Bharathidasan University), Tiruchirappalli Tamil Nadu, India.

Received: 21 Jun 2024 Revised: 03 Jul 2024 Accepted: 13 Aug 2024

***Address for Correspondence**
Joseph Paramasivam Mathiyazhagan
Assistant Professor,
PG and Research Department of Mathematics,
Bishop Heber College
(Affiliated to Bharathidasan University),
Tiruchirappalli Tamil Nadu, India.
E.Mail: paramasivam.ma@bhc.edu.in

ABSTRACT

This paper deals with resolving boundary layers and interior layers of a boundary value problem for the system of n- singularly perturbed second order with large spatial delay differential equations of convection diffusion type, which is considered on the interval $[0,2]$. Here, the diffusion term in each equation of the system is multiplied with the same perturbation parameter ε. We suggest a numerical method composed of a classical finite difference scheme with a piecewise uniform Shishkin mesh to resolve the layers. Later this method is shown to have first order convergence in the maximum norm uniformly in the perturbation parameter. At the end, a numerical demonstration is given to endorse the theoretical findings.

Keywords: Singularly perturbed delay differential equations, Boundary layers, Interior layers, Finite difference scheme, maximum norm, Shishkin mesh, Parameter uniform convergence.

INTRODUCTION

Singularly Perturbed Delay Differential Equations (SPDDEs) are differential equations in which the leading term is amplified with a small positive parameter ε with one or more term having shifting parameter (delay). The small parameter ε creates solutions with rapid changes (sharp gradients) near the boundary points, called boundary layers,

which are difficult to capture numerically and the presence of delays add more complexity to the solution since the solution depends on past states here, thus both complicating the numerical treatment of the problem. Recently, there has been significant focus on emerging resilient numerical schemes for solving SPDDEs. For instance, in the works [1-12], the authors have discussed various types of SPDDEs and developed different numerical schemes with uniform or non-uniform spatial discretizations and further they have proved first order, second order parameter convergence. Based on these literatures and motivated by the work of [13], we consider the special case problem " Singularly perturbed convection-diffusion system with delay term and common perturbation parameter ε", the diffusion term in every equation in this system is multiplied with the same parameter ε and each have large delay in reaction term.

The general form of such system is expressed as

$$\vec{L}\,\vec{z}\,(r) = \mathcal{E}\vec{z}^{''}(r) + \mathcal{P}(r)\vec{z}^{'}(r) - \mathcal{Q}(r)\vec{z}(r) - \mathcal{S}(r)\vec{z}(r-1) = \vec{f}(r)\ on\ (0,2) \quad (1)$$

with $\vec{z} = \vec{\varrho}$ on $[-1,0]$ and $\vec{z}(2) = \vec{\mathfrak{z}}$. (2)

For all $r\epsilon[0,2]$, $\vec{z} = (z_1, z_2, \dots., z_n)^T, \vec{f} = (f_1, f_2, \dots., f_n)^T$. $\mathcal{E}$, $\mathcal{P}$, $\mathcal{Q}$ *and* $\mathcal{S}$ are $n \times n$ matrices,

$$\mathcal{E} = \begin{pmatrix} \varepsilon & 0 \dots. & 0 \\ 0 & \varepsilon \dots. & 0 \\ \dots & \dots & \dots \\ 0 & \dots.. & \varepsilon \end{pmatrix},\ \mathcal{P} = \begin{pmatrix} p_1 & 0 & \dots & 0 \\ 0 & p_2 & \dots & 0 \\ \dots & \dots & \dots & \dots \\ 0 & \dots.. & \dots & p_n \end{pmatrix},\ \mathcal{Q} = \begin{pmatrix} q_{11} & q_{12} & \cdots & q_{1n} \\ q_{21} & q_{22} & \cdots & q_{2n} \\ \dots & \dots & \dots & \dots \\ q_{n1} & \dots.. & \dots & q_{nn} \end{pmatrix} \text{ and}$$

$$\mathcal{S} = \begin{pmatrix} s_1 & 0 & \dots & 0 \\ 0 & s_2 & \dots & 0 \\ \dots & \dots & \dots & \dots \\ 0 & \dots.. & \dots & s_n \end{pmatrix}.$$

The appearance of perturbation parameter and delay makes the solution to behave non-smoothness near boundary points and the point where the delay occurs. Thus in order to solve this type of system numerically, some special techniques are required to tackle the parameter ε and delay, and in particular the numerical scheme needs suitable mesh discretization strategy. Hence we propose a classical finite difference scheme employed with piecewise uniform Shishkin mesh to solve the above considered problem. Piecewise uniform Shishkin mesh concentrates more mesh points near the boundary layers, where the solution changes rapidly and coarsening the mesh in regions in which the solution is smooth. This helps in resolving boundary layers and to handle the delay argument, we construct the mesh in such a way that the delay argument lies on one nodal point. This suggested method ensures the first order parameter uniform convergence. Further an illustration is given to verify the theoretical results. The system (1)-(2) is considered with the following conditions that, the function $\vec{\varrho}$ is sufficiently differentiable on $[-1, 0]$, the parameter ε satisfies $0< \varepsilon <<1$. For all $r \in [0,2]$, the entries of the component of the matrices are in $\mathbb{C}^2[0,2]$ and they satisfy

$$p_l(r) \geq \alpha > 0, q_{ll}(r) + q_{lj}(r) \geq \beta > 0 \quad (3)$$

$$q_{lj}(r), s_l(r) \leq 0, \text{ for } 1 \leq l \neq j \leq n \text{ and } q_{ll}(r) > \sum_{l \neq j} \left| q_{lj}(r) + s_l(r) \right| \quad (4)$$

$$\text{and } 0 < \gamma < \min_{r \in [0,2]} \left(\sum_{j=1}^{n} q_{lj}(r) + s_l(r) \right) \text{ for } l = 1, 2, \dots, n. \quad (5)$$

From these conditions that the problem (1)-(2) has a unique solution $\vec{z}$ and $\vec{z} \in \mathbb{C}^2$, where $\mathbb{C} = \mathbb{C}^0[0,2] \cap \mathbb{C}^1(0,2) \cap \mathbb{C}^2((0,1) \cup (1,2))$. Let $\Omega = [0,2]$, $\Omega^- = (0,1)$ and $\Omega^+ = (1,2)$.

The problem (1)-(2) can be written in equivalent form as

$$\vec{L}_1\vec{z}(r) = \mathcal{E}\vec{z}^{''}(r) + \mathcal{P}(r)\vec{z}^{'}(r) - \mathcal{Q}(r)\vec{z}(r) = \vec{f}(r) + \mathcal{S}(r)\vec{\varrho}(r-1) = \vec{g}(r)\ \ on\ \Omega^- \quad (6)$$

$$\vec{L}_2\vec{z}(r) = \mathcal{E}\vec{z}^{''}(r) + \mathcal{P}(r)\vec{z}^{'}(r) - \mathcal{Q}(r)\vec{z}(r) - \mathcal{S}(r)\vec{z}(r-1) = \vec{f}(r) \quad on\ \Omega^+ \quad (7)$$

$$\vec{z}(0) = \vec{\varrho}(0),\ \vec{z}(2) = \vec{\mathfrak{z}},\ \vec{z}(1-) = \vec{z}(1+),\ \vec{z}^{'}(1-) = \vec{z}^{'}(1+) \quad (8)$$

and when ε is equal to zero, the corresponding reduced problem is given by

$$\mathcal{P}(r)\vec{z}_0^{'}(r) - \mathcal{Q}(r)\vec{z}_0(r) = \vec{g}(r) \quad on\ \Omega^-$$

$$\mathcal{P}(r)\vec{z}_0^{'}(r) - \mathcal{Q}(r)\vec{z}_0(r) - \mathcal{S}(r)\vec{z}_0(r-1) = \vec{f}(r) \quad on\ \Omega^+$$

$$\vec{z}_0(2) = \vec{\mathfrak{z}},\ \vec{z}_0(r) = \left(z_{01}(r), z_{02}(r), \dots, z_{0n}(r)\right)^T.$$

If $z_k(0) \neq z_{0k}(0)$ for any k, $1 \leq k \leq n$, then a layer of width $O(\varepsilon)$ is anticipated near $r = 0$ in every solution component $z_l, 1 \leq l \leq k$, additionally at $r = 1$, every solution component $z_l, 1 \leq l \leq k$, exhibits an interior layer of width $O(\varepsilon)$ for any k such that $1 \leq k \leq n$.

ANALYTICAL RESULTS

In this part, we provide some common analytical results of maximum principle, stability result and the estimates of derivatives related to solution of the problem (6)-(8).

Maximum Principle

Under the conditions (3)-(5), if $\vec{\mathcal{H}} = (\mathcal{H}_1, \mathcal{H}_2, \dots, \mathcal{H}_n)^T$ is any function in the domain of $\vec{\mathcal{L}}$ such that $\vec{\mathcal{H}}(0) \geq \vec{0}$, $\vec{\mathcal{H}}(2) \geq \vec{0}$, $\vec{\mathcal{L}}_1\vec{\mathcal{H}} \leq \vec{0}$ on Ω^-, $\vec{\mathcal{L}}_2\vec{\mathcal{H}} \leq \vec{0}$ on Ω^+, $[\vec{\mathcal{H}}](1) = \vec{\mathcal{H}}(1+) - \vec{\mathcal{H}}(1-) = \vec{0}$ and $[\vec{\mathcal{H}}'](1) \leq \vec{0}$ then $\vec{\mathcal{H}} \geq \vec{0}$ on Ω.

Proof. Let l^*, r^* be such that $\mathcal{H}_{l^*}(r^*) = \min_{\substack{r\in[0,2]\\ l=1,2,..,n}} \mathcal{H}_l(r)$. If $\mathcal{H}_{l^*}(r^*) \geq 0$, then there is nothing to prove. Suppose $\mathcal{H}_{l^*}(r^*) < 0$ then $r^* \notin \{0,2\}$ and $\mathcal{H}_{l^*}''(r^*) \geq 0$, $\mathcal{H}_{l^*}'(r^*) = 0$. If $r^* \epsilon\, \Omega^-$, then

$$
\begin{aligned}
(\vec{\mathcal{L}}_1\vec{\mathcal{H}})_{l^*}(r^*) &= \varepsilon\mathcal{H}_{l^*}''(r^*) + p_{l^*}(r^*)\mathcal{H}_{l^*}'(r^*) - \sum_{j=1}^{n}[\, q_{l^*j}(r^*)\mathcal{H}_j(r^*)] \\
&= \varepsilon\mathcal{H}_{l^*}''(r^*) + p_{l^*}(r^*)\mathcal{H}_{l^*}'(r^*) - q_{l^*l^*}(r^*)\mathcal{H}_{l^*}(r^*) - \sum_{j=1, j\neq l^*}^{n}[\, q_{l^*j}(r^*)\mathcal{H}_j(r^*)] \\
&\geq \varepsilon\mathcal{H}_{l^*}''(r^*) + p_{l^*}(r^*)\mathcal{H}_{l^*}'(r^*) - q_{l^*l^*}(r^*)\mathcal{H}_{l^*}(r^*) - \sum_{j=1, j\neq l^*}^{n}[\, q_{l^*j}(r^*)\mathcal{H}_{l^*}(r^*)] \\
&\geq \varepsilon\,\mathcal{H}_{l^*}''(r^*) - \sum_{j=1}^{n}\big[\, q_{l^*j}(r^*)\mathcal{H}_{l^*}(r^*)\big] > 0, \text{ this is a contradiction.}
\end{aligned}
$$

If $r^* \epsilon\, \Omega^+$, then

$$
\begin{aligned}
(\vec{\mathcal{L}}_2\vec{\mathcal{H}})_{l^*}(r^*) &= \varepsilon\mathcal{H}_{l^*}''(r^*) + p_{l^*}(r^*)\mathcal{H}_{l^*}'(r^*) - \sum_{j=1}^{n}[\, q_{l^*j}(r^*)\mathcal{H}_j(r^*)] - s_{l^*}(r^*)\mathcal{H}_{l^*}(r^*-1) \\
&= \varepsilon\mathcal{H}_{l^*}''(r^*) + p_{l^*}(r^*)\mathcal{H}_{l^*}'(r^*) - q_{l^*l^*}(r^*)\mathcal{H}_{l^*}(r^*) - \sum_{j=1, j\neq l^*}^{n}[\, q_{l^*j}(r^*)\mathcal{H}_j(r^*)] \\
&\qquad - s_{l^*}(r^*)\mathcal{H}_{l^*}(r^*-1) \\
&\geq \varepsilon\mathcal{H}_{l^*}''(r^*) + p_{l^*}(r^*)\mathcal{H}_{l^*}'(r^*) - q_{l^*l^*}(r^*)\mathcal{H}_{l^*}(r^*) - \sum_{j=1, j\neq l^*}^{n}[\, q_{l^*j}(r^*)\mathcal{H}_{l^*}(r^*)] \\
&\quad - s_{l^*}(r^*)\mathcal{H}_{l^*}(r^*) \text{ as } \mathcal{H}_{l^*}(r^*) \leq \mathcal{H}_j(r^*) \text{ and } \mathcal{H}_{l^*}(r^*) \leq \mathcal{H}_{l^*}(r^*-1) \\
&\geq \varepsilon\mathcal{H}_{l^*}''(r^*) - (\textstyle\sum_{j=1}^{n} q_{l^*j}(r^*) + s_{l^*}(r^*))\mathcal{H}_{l^*}(r^*) > 0, \text{ this is a contradiction.}
\end{aligned}
$$

Suppose $r^* = 1$, in this case we discuss about the differentiability of $\mathcal{H}_{l^*}$ at $r = 1$. If $\mathcal{H}_{l^*}'(1)$ does not exist then $[\mathcal{H}_{l^*}'](1) = \mathcal{H}_{l^*}'(1+) - \mathcal{H}_{l^*}'(1-) > 0$, which contradicts $[\mathcal{H}_{l^*}'](1) \leq 0$. If $\mathcal{H}_{l^*}$is differentiable at $r = 1$, then $p_{l^*}(1)\mathcal{H}_{l^*}'(1) - \sum_{j=1}^{n} q_{l^*j}(1)\mathcal{H}_j(1) > 0$ and all the entries of $\mathcal{P}(r), \mathcal{Q}(r)$ and $\mathcal{H}_j(r)$ are in $\mathbb{C}([0,2])$, there exists an interval $[1-h, 1)$ on which $p_{l^*}(r)\mathcal{H}_{l^*}'(r) - \sum_{j=1}^{n} q_{l^*j}(r)\mathcal{H}_j(r) > 0$. If $\mathcal{H}_{l^*}''(\hat{x}) \geq 0$ at any point $\hat{x} \in [1-h, 1)$ then $(\vec{\mathcal{L}}_1\vec{\mathcal{H}})_{l^*}(\hat{x}) \geq 0$, which is a contradiction. Thus we can assume that $\mathcal{H}_{l^*}''(r) < 0$ on $[1-h, 1)$ which implies that $\mathcal{H}_{l^*}'(r)$ is strictly decreasing on $[1-h, 1)$ and since $\mathcal{H}_{l^*}'(1) = 0$, $\mathcal{H}_{l^*}' \in \mathbb{C}((0,2))$, thus $\mathcal{H}_{l^*}'(r) > 0$ on$[1-h, 1)$, consequently the continuous function $\mathcal{H}_{l^*}(r)$ cannot have minimum at $r = 1$, which contradicts the assumption that $r^* = 1$. Hence $\vec{\mathcal{H}} \geq \vec{0}$ on Ω.

Stability Result: Under the conditions (3)-(5), if $\vec{\mathcal{H}}$ is any function in $\mathbb{C}^2$, such that $[\vec{\mathcal{H}}](1) = \vec{0}$ and $[\vec{\mathcal{H}}'](1) = \vec{0}$, then for each $l = 1,2, \dots, n$ and $r \in [0,2]$,

$$|\mathcal{H}_l(r)| \leq \max\left\{\|\vec{\mathcal{H}}(0)\|, \|\vec{\mathcal{H}}(2)\|, \frac{1}{\beta}\|\vec{\mathcal{L}}_1\vec{\mathcal{H}}\|, \frac{1}{\gamma}\|\vec{\mathcal{L}}_2\vec{\mathcal{H}}\|\right\}.$$

Proof. Let $\phi = \max\{\|\vec{\mathcal{H}}(0)\|, \|\vec{\mathcal{H}}(2)\|, \frac{1}{\beta}\|\vec{\mathcal{L}}_1\vec{\mathcal{H}}\|, \frac{1}{\gamma}\|\vec{\mathcal{L}}_2\vec{\mathcal{H}}\|\}$.

Define two functions $\vec{\mathfrak{I}}^{\pm}(r) = \phi\,\vec{e} \pm \vec{\mathcal{H}}(r)$, where $\vec{e} = (1, 1, \dots, 1)^T$.

Then $\vec{\mathfrak{I}}^{\pm}(0) \geq \vec{0}$, $\vec{\mathfrak{I}}^{\pm}(2) \geq \vec{0}$, $\vec{\mathcal{L}}_1\vec{\mathfrak{I}}^{\pm}(r) = -\mathcal{Q}(r)\phi\,\vec{e} \pm \vec{\mathcal{L}}_1\vec{\mathcal{H}}(r) \leq \vec{0}$ on Ω^- and $\vec{\mathcal{L}}_2\vec{\mathfrak{I}}^{\pm}(r) = -\mathcal{Q}(r)\phi\,\vec{e} - \mathcal{S}(r)\phi\,\vec{e} \pm \vec{\mathcal{L}}_2\vec{\mathcal{H}}(r) \leq \vec{0}$ on Ω^+. Moreover $[\vec{\mathfrak{I}}^{\pm}](1) = \pm[\vec{\mathcal{H}}](1) = \vec{0}$ and $[\vec{\mathfrak{I}}^{\pm\prime}](1) = \pm[\vec{\mathcal{H}}'](1) = \vec{0}$. From the maximum principle it follows that $\vec{\mathfrak{I}}^{\pm}(r) \geq \vec{0}$ on Ω and proves the result.

Estimates of $\vec{z}$ and its derivatives: Let the conditions (3)-(5) hold. Let $\vec{z}$ be the solution of (1)-(2). Then for all $r \in \Omega$ and $l = 1,2, \dots, n$,

$$|z_l(r)| \leq C\, max\big(\|\vec{z}(0)\|, \|\vec{z}(2)\|, \|\vec{f}\|\big),$$

$$\left|z_l^{(k)}(r)\right| \leq C\,\varepsilon^{-k}\left(\|\vec{z}(0)\| + \|\vec{z}(2)\| + \varepsilon\|\vec{f}\|\right), \text{ for } k = 1, 2 \text{ and}$$

$$\left|z_l^{(3)}(r)\right| \leq C\varepsilon^{-3}\left(\|\vec{z}(0)\| + \|\vec{z}(2)\| + \varepsilon\left\|\vec{f}\right\|\right) + \varepsilon^{-1}\left\|f_l^{'}\right\|$$

Proof. The results are proved by using the procedure adapted in [13].

Shishkin decomposition of the solution

The solution $\vec{z}$ of the problem (1)-(2) can be decomposed into $\vec{z} = \vec{x} + \vec{y}$,
where $\vec{x} = (x_1, x_2, \dots, x_n)^T$, the smooth component is the solution of

$$\vec{\mathcal{L}}_1\vec{x} = \vec{g}\ on\ \Omega^-,\ \vec{x}(0) = \vec{\hbar}\ , \vec{x}(1-) = \vec{z}_0\,(1-), \quad (9)$$

where $\vec{\hbar} = (\hbar_1, \hbar_2, \dots, \hbar_n)^T$ is to chosen.

$$\vec{\mathcal{L}}_2\vec{x} = \vec{f}\ \ on\ \ \Omega^+, \quad \vec{x}(1+) = \vec{z}_0\,(1+),\ \vec{x}(2) = \vec{z}_0\,(2), \quad (10)$$

and $\vec{y} = (y_1, y_2, \dots, y_n)^T$, the singular component is the solution of

$$\vec{\mathcal{L}}_1\vec{y} = \vec{0}\ \text{ on } \Omega^-, \qquad \vec{\mathcal{L}}_2\vec{y} = \vec{0}\ \text{ on } \Omega^+ \quad (11)$$

with $\vec{y}(0) = \vec{z}(0) - \vec{x}(0), \vec{y}(2) = \vec{z}(2) - \vec{x}(2), [\vec{y}](1) = -[\vec{x}](1), [\vec{y}'](1) = -[\vec{x}'](1)$.

Estimates of $\vec{x}$ and its derivatives

For a suitable choice of $\vec{\hbar}$, the solution of the problem $(9) - (10)$ satifies

$\left|x_l^{(k)}(r)\right| \leq C\,(1 + \varepsilon^{2-k}),$ for $1 \leq l \leq n, 1 \leq k \leq 3$ and for $r \in \Omega$.

Proof. First, the estimates of x_l's and its derivatives are proved for interval $[0,1]$ and using these bounds, the estimates of the bounds on $[1,2]$ are proved. According with the layer pattern of the solution, each component of $\vec{x}$ is decomposed with singular perturbation parameter ε as $\vec{x} = \vec{a} + \varepsilon\vec{b} + \varepsilon^2\vec{d}$, where $\vec{a} = (a_1, a_2, \dots, a_n)^T$ is the solution of

$$\mathcal{P}(r)\vec{a}^{'}(r) - \mathcal{Q}(r)\vec{a}(r) = \vec{g}(r)\ \ on\ \Omega^- \quad (12)$$

$$\mathcal{P}(r)\vec{a}^{'}(r) - \mathcal{Q}(r)\vec{a}(r) - \mathcal{S}(r)\vec{a}(r-1) = \vec{f}(r) \quad on\ \Omega^+, \quad \vec{a}(0) = \vec{\hbar}\,, \vec{a}(2) = \vec{\mathfrak{z}}, \quad (13)$$

$\vec{b} = (b_1, b_2, \dots, b_n)^T$ is the solution of

$$\mathcal{P}(r)\vec{b}^{'}(r) - \mathcal{Q}(r)\vec{b}(r) = \varepsilon^{-1}\,\mathcal{E}\vec{b}^{''}(r)\ on\ \Omega^- \quad (14)$$

$$\mathcal{P}(r)\vec{b}^{'}(r) - \mathcal{Q}(r)\vec{b}(r) - \mathcal{S}(r)\vec{b}(r-1) = \varepsilon^{-1}\,\mathcal{E}\vec{b}^{''}(r) \quad on\ \Omega^+,\ \vec{b}(2) = \vec{0}, \quad (15)$$

$\vec{d} = (d_1, d_2, \dots, d_n)^T$ is the solution of $\vec{\mathcal{L}}_1\vec{d}(r) = \varepsilon^{-1}\,\mathcal{E}\vec{d}^{''}(r)\ on\ (0,1)$ (16)

$\vec{\mathcal{L}}_2\vec{d}(r) = \varepsilon^{-1}\,\mathcal{E}\vec{d}^{''}(r)\ on\ (1,2),\ \vec{d}(2) = \vec{0}$ and $\vec{d}(0)$ remains to be chosen. (17)

Since $\varepsilon^{-1}\,\mathcal{E}$ is a matrix with bounded entries and hence using the equations (12), (14) we have for $0 \leq k \leq 3$, $\left\|\vec{a}_n^{(k)}\right\| \leq C, \left\|\vec{b}_n^{(k)}\right\| \leq C$. Proceeding in a similar way as in [13], from the equations (13), (15)-(17), by the proper choice of $\hbar_n, \hbar_{n-1}, \dots, \hbar_1$, the solution of the problem (9)-(10) satisfies the bound $\left|x_l^{(k)}(r)\right| \leq C\,(1 + \varepsilon^{2-k})$, for $1 \leq l \leq n, 1 \leq k \leq 3$ on $[0,1]$ and $[1,2]$.

Estimates of $\vec{y}$ and its derivatives

Let $\beta_1(r), \beta_2(r)$ be the layer functions defined on $[0,1]$ and $[1,2]$ as $\beta_1(r) = \exp\left(-\frac{\alpha r}{\varepsilon}\right)$ on $[0,1]$ and $\beta_2(r) = \exp\left(-\frac{\alpha(r-1)}{\varepsilon}\right)$ on $[1,2]$.

Let $\vec{y}$ be the solution of (11). Then the following estimates hold for

$1 \leq l \leq n, 1 \leq k \leq 3,\ |y_l(r)| \leq C\beta_1(r), \left|y_l^{(k)}(r)\right| \leq C\,\varepsilon^{-k}\,\beta_1(r)$ on $[0,1]$ and

$|y_l(r)| \leq C\beta_2(r), \left|y_l^{(k)}(r)\right| \leq C\,\varepsilon^{-k}\,\beta_2(r)$ on $[1,2]$.

Proof. On the interval $[0,1]$, the above results are proved by using the method adapted in [13]. And then proceeding in a similar way the results are proved for the interval $[1,2]$.

NUMERICAL METHOD

Spatial Discretization

To resolve both boundary and interior layers we discretize the solution domain using a piecewise uniform Shishkin mesh comprising M nodes. The mesh is structured as follows. Let $\Omega^{\mathrm{M}} = \Omega_1^{\mathrm{M}} \cup \Omega_2^{\mathrm{M}}$ where $\Omega_1^{\mathrm{M}} = \{r_j\}_{j=1}^{\frac{M}{2}-1}$, $\Omega_2^{\mathrm{M}} = \{r_j\}_{j=\frac{M}{2}+1}^{M-1}$ and $r_{\frac{M}{2}} = 1$. Then $\bar{\Omega}_1^{\mathrm{M}} = \{r_j\}_{j=0}^{\frac{M}{2}}$, $\bar{\Omega}_2^{\mathrm{M}} = \{r_j\}_{j=\frac{M}{2}}^{M}$, $\bar{\Omega}_1^{\mathrm{M}} \cup \bar{\Omega}_2^{\mathrm{M}} = \bar{\Omega}^{\mathrm{M}} = \{\mathrm{r_j}\}_{\mathrm{j=0}}^{\mathrm{M}}$ and $\Gamma^{\mathrm{M}} = \{0, 2\}$ and M, the number of mesh elements is taken as a multiple of 4. The interval $[0, 1]$ is divided into two subintervals $[0, \varrho], (\varrho, 1]$, where ϱ is a transition parameter defined by $\varrho = min\left\{\frac{1}{2}, \frac{2\varepsilon}{\gamma} lnM\right\}$. In each of the subintervals $[0, \varrho], (\varrho, 1]$, $\frac{M}{4}$ mesh points are placed, so that the mesh is piecewise uniform and $\varrho = \frac{1}{2}$, the mesh becomes uniform. In a similar manner the interval $[1, 2]$ is also divided into two subintervals $[1, 1 + \varrho]$, $(1 + \varrho, 2]$ by utilizing the same transition parameter. The subintervals $[0, \varrho]$, $[1, 1 + \varrho]$ are known as inner layer regions and the remaining are called outer layer regions.

The discrete problem

To solve the boundary value problem (1)-(2) numerically the following upwind classical finite difference scheme is implemented on the mesh $\bar{\Omega}^{\mathrm{M}}$.

The discrete problem is defined as

$\vec{\mathcal{L}}^N \vec{Z}(r_j) = \varepsilon\delta^2 \vec{Z}(r_j) + \mathcal{P}(r_j) D^+ \vec{Z}(r_j) - \mathcal{Q}(r_j)\vec{Z}(r_j) - \mathcal{S}(r_j)\vec{Z}(r_j - 1) = \vec{f}(r_j)$ on Ω^{M} (18)

$\vec{Z}(r_j - 1) = \vec{\varrho}(r_j - 1)$ for $r_j \in \Omega_1^{\mathrm{M}}$ and $\vec{Z} = \vec{z}$ on Γ^{M}.

This problem has an equivalent form as,

$\vec{\mathcal{L}}_1^M \vec{Z}(r_j) = \varepsilon\delta^2 \vec{Z}(r_j) + \mathcal{P}(r_j) D^+ \vec{Z}(r_j) - \mathcal{Q}(r_j)\vec{Z}(r_j) = \vec{g}(r_j)$ on Ω_1^{M} (19)

$\vec{\mathcal{L}}_2^M \vec{Z}(r_j) = \varepsilon\delta^2 \vec{Z}(r_j) + \mathcal{P}(r_j) D^+ \vec{Z}(r_j) - \mathcal{Q}(r_j)\vec{Z}(r_j) - \mathcal{S}(r_j)\vec{Z}(r_j - 1) = \vec{f}(r_j)$ on Ω_2^{M} (20)

$\vec{Z} = \vec{z}$ on Γ^M, $D^-\vec{Z}\left(r_{\frac{M}{2}}\right) = D^+\vec{Z}\left(r_{\frac{M}{2}}\right)$, where $\vec{Z}(r_j) = \left(Z_1(r_j), Z_2(r_j), \ldots, Z_n(r_j)\right)^T$.

And $0 \le j \le M - 1$, $D^+\vec{Z}(r_j) = \frac{\vec{Z}(r_{j+1}) - \vec{Z}(r_j)}{h_{j+1}}$, $D^-\vec{Z}(r_j) = \frac{\vec{Z}(r_j) - \vec{Z}(r_{j-1})}{h_j}$,

$\delta^2\vec{Z}(r_j) = \frac{1}{\bar{h}_j}\left[D^+\vec{Z}(r_j) - D^-\vec{Z}(r_j)\right]$, where $h_j = r_j - r_{j-1}, \bar{h}_j = \frac{h_j + h_{j+1}}{2}$. This is used to determine numerical approximation to the solution of (1)-(2). The discrete maximum principle and the discrete stability results are analogous to those for continuous case.

Discrete Maximum Principle

Let the conditions (3)-(5) hold. Then, for any mesh function $\vec{\psi}$, the inequalities $\vec{\psi} \ge \vec{0}$ on Γ^{M}, $\vec{\mathcal{L}}_1^M\vec{\psi} \le \vec{0}$ on Ω_1^{M}, $\vec{\mathcal{L}}_2^M\vec{\psi} \le \vec{0}$ on Ω_2^{M} and $D^+\vec{\psi}\left(r_{\frac{M}{2}}\right) - D^-\vec{\psi}\left(r_{\frac{M}{2}}\right) \le \vec{0}$ imply that $\vec{\psi} \ge \vec{0}$ on $\bar{\Omega}^{\mathrm{M}}$.

Discrete Stability Result

Let the conditions (3)-(5) hold. Then, for any mesh function $\vec{\psi}$, satisfying $D^+\psi_{l^*}\left(r_{\frac{M}{2}}\right) = D^-\psi_{l^*}\left(r_{\frac{M}{2}}\right), |\psi_l(r_j)| \le max\left\{\|\vec{\psi}(r_0)\|, \|\vec{\psi}(r_M)\|, \frac{1}{\beta}\|\vec{\mathcal{L}}_1^M\vec{\psi}\|_{\Omega_1^{\mathrm{M}}}, \frac{1}{\gamma}\|\vec{\mathcal{L}}_2^M\vec{\psi}\|_{\Omega_2^{\mathrm{M}}}\right\}$, for $l = 1, 2, \ldots, n$ and $0 \le j \le M$.

As in the continuous case the discrete solution $\vec{Z}$ can be decomposed into $\vec{X}$ and $\vec{Y}$, which are difined to be the solutions of the following discrete problems.

$\vec{\mathcal{L}}_1^N\vec{X}(r_j) = \vec{g}(r_j)$, $r_j \in \Omega_1^{\mathrm{M}}$, $\vec{X}(0) = \vec{x}(0)$, $\vec{X}\left(r_{\frac{M}{2}-1}\right) = \vec{x}(1-)$

$\vec{\mathcal{L}}_2^N\vec{X}(r_j) = \vec{f}(r_j)$, $r_j \in \Omega_2^{\mathrm{M}}$, $\vec{X}\left(r_{\frac{M}{2}+1}\right) = \vec{x}(1+)$, $\vec{X}(2) = \vec{x}(2)$ and

$\vec{\mathcal{L}}_1^M\vec{Y}(r_j) = \vec{0}$, $r_j \in \Omega_1^{\mathrm{M}}$, $\vec{Y}(0) = \vec{y}(0)$, $\vec{\mathcal{L}}_2^M\vec{Y}(r_j) = \vec{0}$, $r_j \in \Omega_2^{\mathrm{M}}$, $\vec{Y}(2) = \vec{y}(2)$,

$D^-\vec{X}\left(r_{\frac{M}{2}}\right) + D^-\vec{Y}\left(r_{\frac{M}{2}}\right) = D^+\vec{X}\left(r_{\frac{M}{2}}\right) + D^+\vec{Y}\left(r_{\frac{M}{2}}\right)$.

The error at each point $r_j \in \bar{\Omega}^{\mathrm{M}}$ is denoted by $\vec{e}(r_j) = \vec{Z}(r_j) - \vec{z}(r_j)$, then the local truncation error has the decomposition $\vec{\mathcal{L}}^M\vec{e}(r_j) = \vec{\mathcal{L}}^M(\vec{X} - \vec{x})(r_j) + \vec{\mathcal{L}}^M(\vec{Y} - \vec{y})(r_j)$.The error in the smooth and singular components is bounded in the following.

Theorem 1. Let the conditions (3)-(5) hold. If $\vec{x}$, $\vec{y}$ are the smooth and singular components of the solution of (1)-(2) and if $\vec{X}, \vec{Y}$ are the smooth and singular components of the solution of (19)-(20) then, for $i = 1, 2$, $j \neq \frac{M}{2}$.

$$\left|\vec{\mathcal{L}}_i^M(\vec{X}-\vec{x})(r_j)\right| \leq CM^{-1}, \left|\vec{\mathcal{L}}_i^M(\vec{Y}-\vec{y})(r_j)\right| \leq CM^{-1}\ln M, \qquad 0 \leq j \leq M.$$

Proof. The estimates for the derivatives of the smooth and singular components and the expression derived for the local truncation error in $\vec{X}$ and $\vec{Y}$ are found similar as in [13] and hence the required bounds hold good.

At $j = \frac{M}{2}$, for $l = 1, 2, \ldots, n$, let $h^* = \max\{h_{\frac{M}{2}}^-, h_{\frac{M}{2}}^+\}$.

Then $\left|(D^+ - D^-)e_l\left(r_{\frac{M}{2}}\right)\right| = \left|(D^+ - D^-)(z_l')\left(r_{\frac{M}{2}}\right)\right|$

$$\leq \left|\left(D^+ - \frac{d}{dr}\right)(z_l')\left(r_{\frac{M}{2}}\right)\right| + \left|\left(D^- - \frac{d}{dr}\right)(z_l')\left(r_{\frac{M}{2}}\right)\right|$$

$$\leq \frac{1}{2}h_{\frac{M}{2}}^+|z_l''(\eta_1)|_{\eta_1\in(1,2)} + \frac{1}{2}h_{\frac{M}{2}}^-|z_l''(\eta_2)|_{\eta_2\in(0,1)}$$

$$\leq Ch^* \max_{\eta\in(0,1)\cup(1,2)}|z_l''(\eta)|.$$

Using the bounds of smooth and singular components of the solution,

$$\left|(D^+ - D^-)e_l\left(r_{\frac{M}{2}}\right)\right| \leq C\frac{h^*}{\varepsilon}. \tag{21}$$

Define a set of discrete barrier functions on $\bar{\Omega}^M$, for $l = 1, 2, .., n$ by

$$\wp_l(r_j) = \begin{cases} \frac{\prod_{k=1}^{j}\left(1+\frac{\gamma h_k}{\sqrt{2\varepsilon}}\right)}{\prod_{k=1}^{\frac{M}{2}}\left(1+\frac{\gamma h_k}{\sqrt{2\varepsilon}}\right)}, & if\ 0 \leq j \leq \frac{M}{2} \\ \frac{\prod_{k=j}^{M-1}\left(1+\frac{\gamma h_{k+1}}{\sqrt{2\varepsilon}}\right)}{\prod_{k=\frac{M}{2}}^{M-1}\left(1+\frac{\gamma h_{k+1}}{\sqrt{2\varepsilon}}\right)}, & if\ \frac{M}{2} \leq j \leq M \end{cases} \tag{22}$$

From the definition of the barrier function

$$\wp_l(0) = \wp_l(2) = 0, \wp_l(1) = 1, \text{ for all } l, \ 0 \leq j \leq M. \tag{23}$$

Therefore, for all l, $0 \leq j \leq M$, $0 \leq \wp_l(r_j) \leq 1$. (24)

For $l = 1, 2, \ldots, n$ and $r_j \in \bar{\Omega}_1^M$,

$$D^+\wp_l(r_j) = \frac{\gamma}{\sqrt{2\varepsilon}}\wp_l(r_j),\ D^-\wp_l(r_j) = \frac{\gamma}{\sqrt{2\varepsilon}(1+\gamma h_j/\sqrt{2\varepsilon})}\wp_l(r_j),\ \delta^2\wp_l(r_j) \leq \frac{\gamma^2\wp_l(r_j)}{\varepsilon}, \tag{25}$$

also for $l = 1, 2, \ldots, n$ and $r_j \in \bar{\Omega}_2^M$ we have, $D^+\wp_l(r_j) = -\frac{\gamma\wp_l(r_j)}{\sqrt{2\varepsilon}(1+\gamma h_{j+1}/\sqrt{2\varepsilon})}$, $D^-\wp_l(r_j) = -\frac{\gamma\wp_l(r_j)}{\sqrt{2\varepsilon}}$, $\delta^2\wp_l(r_j) \leq \frac{\gamma^2\wp_l(r_j)}{\varepsilon}$ (26)

Therefore from (25) and (26), $\varepsilon\,\delta^2\wp_l(r_j) \leq \gamma^2\wp_l(r_j)$, for all l, j. (27)

Therefore, using the results (24) and (27)

$$\begin{aligned}\left(\vec{\mathcal{L}}_1^M\vec{\wp}\right)_l(r_j) &= \varepsilon\delta^2\wp_l(r_j) + p_l(r_j)D^+\wp_l(r_j) - \sum_{t=1}^{n} q_{lt}(r_j)\wp_t(r_j) \\ &\leq \gamma^2\wp_l(r_j) + p_l(r_j)\frac{\gamma\wp_l(r_j)}{\sqrt{2\varepsilon}} - \sum_{t=1}^{n} q_{lt}(r_j)\wp_t(r_j) \\ &\leq \gamma^2 + p_l(r_j)\frac{\gamma\wp_l(r_j)}{\sqrt{2\varepsilon}} - \sum_{t=1}^{n} q_{lt}(r_j)\wp_t(r_j) \end{aligned} \tag{28}$$

$$\begin{aligned}\left(\vec{\mathcal{L}}_2^M\vec{\wp}\right)_l(r_j) &= \varepsilon\delta^2\wp_l(r_j) + p_l(r_j)D^+\wp_l(r_j) - \sum_{t=1}^{n} q_{lt}(r_j)\wp_t(r_j) - s_l(r_j)\wp_l(r_j-1) \\ &\leq \gamma^2\wp_l(r_j) + p_l(r_j)\frac{\gamma\wp_l(r_j)}{\sqrt{2\varepsilon}(1+\gamma h_{j+1}/\sqrt{2\varepsilon})} - \sum_{t=1}^{n} q_{lt}(r_j)\wp_t(r_j) - s_l(r_j)\wp_l(r_j-1) \\ &\leq \gamma^2 + p_l(r_j)\frac{\gamma\wp_l(r_j)}{\sqrt{2\varepsilon}(1+\gamma h_{j+1}/\sqrt{2\varepsilon})} - \sum_{t=1}^{n} q_{lt}(r_j)\wp_t(r_j) - s_l(r_j)\wp_l(r_j-1) \end{aligned} \tag{29}$$

Also in particular at $j = M/2$, from (24)-(26),

$$(D^+ - D^-)\wp_l(r_j) = \left[-2\frac{\gamma\wp_l(r_j)}{\sqrt{2\varepsilon}(1+\gamma h^*/\sqrt{2\varepsilon})}\right] \leq -\frac{C}{\sqrt{\varepsilon}}. \tag{30}$$

In the following theorem, the required essentially first order parameter-uniform error estimate is given by constructing a suitable mesh function.

Theorem 2. Let $\vec{z}(r_j)$ be the solution of the continuous problem (1)-(2) and $\vec{Z}(r_j)$ be the solution of the discrete problem (18). Then, $\left\|\vec{Z}(r_j) - \vec{z}(r_j)\right\| \leq CM^{-1}\ln M$, $0 \leq j \leq M$.

Proof. Consider the mesh function $\vec{\Theta}$ given by
$\Theta_l(r_j) = C_1 M^{-1} lnM + C_2 \frac{h^*}{\sqrt{\varepsilon}} \wp_l(r_j) \pm e_l(r_j), l = 1, 2, \ldots, n,\ 0 \le j \le M$, where $C_1$and C_2 are constants such that $C_2$is suitably chosen. Then, $\Theta_l(0) = \Theta_l(2) = C_1 M^{-1} \ln M \ge 0$.
Utilizing (28) and Theorem 1

$$\left(\vec{L}_1^M \vec{\Theta}\right)_l(r_j) = -\sum_{t=1}^{n} q_{lt}(r_j)\, C_1 M^{-1} \ln M + C_2 \frac{h^*}{\sqrt{\varepsilon}} \left(\vec{L}_1^M \vec{\wp}\right)_l(r_j) \pm \left(\vec{L}_1^M \vec{e}\right)_l(r_j)$$
$$\le \sum_{t=1}^{n} q_{lt}(r_j)\, C_1 M^{-1} \ln M + C_2 \frac{h^*}{\sqrt{\varepsilon}} \left[\left(\gamma^2 + \frac{p_l(r_j)\gamma}{\sqrt{2\varepsilon}}\right) \wp_l(r_j) - \sum_{t=1}^{n} q_{lt}(r_j) \wp_t(r_j)\right] \pm CN^{-1} \ln N$$
$$\le -\sum_{t=1}^{n} q_{lt}(r_j)\, C_1 M^{-1} \ln M + C_2 R_1 + C_2 \frac{h^*}{\sqrt{\varepsilon}} \left[\gamma^2 \wp_l(r_j) - \sum_{t=1}^{n} q_{lt}(r_j) \wp_t(r_j)\right] \pm CM^{-1} \ln M,$$

where R_1 is a constant. Let $\mu_l(s_j) = \left[\gamma^2 \wp_l(r_j) - \sum_{t=1}^{n} q_{lt}(r_j) \wp_t(r_j)\right],\ l = 1, 2, .., n.$
Then choosing $C_1 \ge C_2(\|\vec{\mu}\| + R_1) + C$, we have $\left(\vec{L}_1^N \vec{\Theta}\right)_l(r_j) \le 0,$ on Ω_1^M, for $l = 1, 2, \ldots, n$. Again utilizing (29) and Theorem 1 $\left(\vec{L}_2^M \vec{\Theta}\right)_l(r_j) = -\sum_{t=1}^{n} q_{lt}(r_j)\, C_1 M^{-1} \ln M + s_l(r_j) C_1 M^{-1} \ln M + C_2 \frac{h^*}{\sqrt{\varepsilon}} \left(\vec{L}_2^M \vec{\wp}\right)_l(r_j) \pm \left(\vec{L}_2^M \vec{e}\right)_l(r_j)$

$\le$
$-C_1 \left(\sum_{t=1}^{n} q_{lt}(r_j) + s_l(r_j)\right) M^{-1} \ln M +$
$C_2 \frac{h^*}{\sqrt{\varepsilon}} \left[\left(\gamma^2 - \frac{p_l(r_j)\gamma}{\sqrt{2\varepsilon}(1+\gamma h_{j+1}/\sqrt{2\varepsilon})}\right) \wp_l(r_j) - \sum_{t=1}^{n} q_{lt}(r_j) \wp_t(r_j) - s_l(r_j) \wp_l(r_j - 1)\right] \pm CM^{-1} \ln M$

$$\le -C_1 \left(\sum_{t=1}^{n} q_{lt}(r_j) + s_l(r_j)\right) M^{-1} \ln M + C_2 R_2 + \frac{h^*}{\sqrt{\varepsilon}} \left[\gamma^2 \wp_l(r_j)\right] + C_2 \frac{h^*}{\sqrt{\varepsilon}} \left[-\sum_{t=1}^{n} q_{it}(r_j) \wp_t(r_j) - s_i(r_j) \wp_i(r_j - 1)\right] \pm CM^{-1} \ln M,$$

where R_2 is a constant. Let $\lambda_l(r_j) = \gamma^2 \wp_l(r_j) - \sum_{t=1}^{n} q_{lt}(r_j) \wp_t(r_j) - s_l(r_j) \wp_l(r_j - 1)$.
Then choosing $C_1 \ge C_2(\|\vec{\lambda}\| + |R_2|) + C$, we have $\left(\vec{L}_2^M \vec{\Theta}\right)_l(r_j) \le 0,$ on Ω_2^M, for $l = 1, 2, \ldots$,n. Also, $D^+\Theta_l(1)$-$D^-\Theta_l(1) = C_2 \frac{h^*}{\sqrt{\varepsilon}} (D^+ - D^-) \wp_l(1) \pm (D^+ - D^-) e_l\left(r_{\frac{M}{2}}\right)$

$$\le -\frac{h^*}{\sqrt{\varepsilon}} C_2 \frac{1}{\sqrt{\varepsilon}} C \pm C \frac{h^*}{\varepsilon} \le 0.$$

Hence using discrete maximum principle for $\vec{\Theta}$, it follows that $\Theta_l(r_j) \ge 0$, for $l = 1, 2, \ldots, n,\ 0 \le j \le M$. Also from (24), $\wp_l(r_j) \le 1$ therefore for sufficiently large M,

$$\left\|\vec{Z}(r_j) - \vec{z}(r_j)\right\| \le CM^{-1} \ln M, \quad \text{which completes the proof.} \qquad \bullet$$

RESULTS AND DISCUSSION

In this approach, by constructing a suitable barrier function, the stability results of the solution of the considered problem is proved for both continuous and discrete cases. Also the mesh function $\vec{\Theta}$ plays a crucial role in ensuring the first order parameter convergence of the suggested numerical method. The applicability of the scheme is investigated by the following test example. Using two mesh algorithm in [14], the maximum pointwise errors for various values of the singular perturbation parameter ε and mesh points M are calculated, the corresponding order of convergence and error constant are presented in Table1. In Two-mesh algorithm, $\vec{\varepsilon}$-uniform maximum pointwise two-mesh differences $\mathrm{T^M} = \max_{\vec{\varepsilon}} \left\|\vec{\mathrm{Z}}^{\mathrm{M}} - \hat{\vec{\mathrm{Z}}}^{2\mathrm{M}}\right\|_{\Omega^{\mathrm{M}}}$, $\vec{\varepsilon}$-uniform order of convergence $\mathrm{p^*} = \min_{\mathrm{M}} \log_2 \frac{\mathrm{T^M}}{\mathrm{T^{2M}}}$, $\vec{\varepsilon}$-uniform error constant $\mathrm{H_{p^*}} = \max_{\mathrm{M}} \frac{\mathrm{T^M M^{p^*}}}{1-2^{-\mathrm{p^*}}}$ where $\hat{\vec{\mathrm{Z}}}^{2\mathrm{M}}$ is the piecewise linear interpolants of the solution $\vec{\mathrm{Z}}^{\mathrm{M}}$.

Numerical illustration

Consider a system of SPDDE's
$\mathcal{E}\vec{z}''(r) + \mathcal{P}(r)\vec{z}'(r) - \mathcal{Q}(r)\vec{z}(r) = \vec{f_1}(r)\ on\ (0,1)$
$\mathcal{E}\vec{z}''(r) + \mathcal{P}(r)\vec{z}'(r) - \mathcal{Q}(r)\vec{z}(r) - \mathcal{S}(r)\vec{z}(r-1) = \vec{f_2}(r)\ on\ (1,2)$
with $\vec{f_1}(r) = (1 + r,\ 3r,\ 1 - 2r)^T,\ \vec{f_2}(r) = (1,\ r,\ 1)^T,\ \mathcal{E} = diag(\varepsilon, \varepsilon, \varepsilon),$

$\mathcal{P}(r) = diag(r, 1+r, 2r)$, $\mathcal{Q}(r) = \begin{pmatrix} 4 & -1 & -1 \\ -1.5 & 5 & -1.5 \\ -0.5 & -0.3 & 2.5 \end{pmatrix}$ and $\mathcal{S}(r) = diag(-1,-1,-1)$, $\vec{z}(0) = (1,\ 1,\ 1)^T$ and $\vec{z}(2) = \overrightarrow{0}$, $\varepsilon = \frac{\eta}{32}$, $\eta = \frac{1}{4}$ and $M = 512$.

CONCLUSION

In this research article, we considered a system of SPDDEs of convection-diffusion type with large spatial delay and we have developed a framework called classical finite difference scheme with piecewise uniform Shishkin mesh to find an approximate solution. With the help of given illustration, it is shown that the proposed scheme is layer resolving and is first order convergent in the maximum norm uniformly independent of the perturbation parameter. On the whole, this work provides a robust computational method in addressing complex behavior of the solution raised by both the parameter ε and delay. This approach can be extendable to higher dimensional and semi-linear SPDDEs in future.

REFERENCES

1. Miller, J, O'Riordan E, and Shishkin .G, Fitted Numerical Methods for Singular Perturbation Problems, World Scientific Publishing Co., Singapore, 1996.
2. Lins, T, Stynes, M, Numerical methods on Shishkin meshes for linear convection-diffusion problems, Computer Methods in Applied Mechanics and Engineering 190, 3527–3542, 2001.
3. Beckett, G., and Mackenzie, J. A, Convergence analysis of finite difference approximations on equidistributed grids to a singularly perturbed boundary value problem. Applied Numerical Mathematics, 35, pp. 87–109, 2000.
4. Kumar, D, and Kumari. P, Parameter-uniform numerical treatment of singularly perturbed initial-boundary value problems with large delay. Applied Numerical Mathematics, vol.153, no.412-429, 2020.
5. Daba, I.T., Duressa, G.F, Uniformly Convergent Numerical Scheme for a Singularly Perturbed Differential-Difference Equations Arising in Computational Neuroscience. Journal of Applied Mathematics and Informatics, 39, 655–676, 2021.
6. Kumar, N. S, Rao, R, N., A Second Order Stabilized Central Difference Method for Singularly Perturbed Differential Equations with a Large Negative Shift. Differential Equations and Dynamical Systems, 1-18, 2020.
7. Elango, S., Unyong, B. Numerical Scheme for Singularly Perturbed Mixed Delay Differential Equation on Shishkin Type Meshes. Fractal and Fractional, 7, 43. 2023.
8. Praveena, R. and Joseph Paramasivam, M., An Initial Value Problem for a System of 'N' singularly perturbed Delay Differential Equations with Robin Initial Conditions, Advances and Applications in Mathematical Sciences, Volume 21, Issue 8, Pages: 4661-4670, June 2022.
9. Woldaregay, M. M., Solving singularly perturbed delay differential equations via fitted mesh and exact difference method. Research in Mathematics, 9(1):2109301, 2022.
10. Tesfaye, S.K, Woldaregary, M. M., Dinka, T.G., Duressa, G.F., Fitted Numerical Scheme for Singularly Perturbed Convection-Diffusion Equation with Small Time Delay, International Journal of Mathematics and Mathematical Sciences, 3772081,15 pages, 2024.
11. Senthilkumar, L. S., and Subburayan, V, Partially Singularly Perturbed System of Delay Differential Equations and a Second Order Uniformly Convergent Method, IOP Conference Series: Materials Science and Engineering , 1130, 012011, 2021.
12. Hassen, Z. I., Duressa, G. F., and Liu, L. New approach of convergent numerical method for singularly perturbed delay parabolic convection-diffusion problems. Research in Mathematics, 10(1), 2023.
13. Saravana Sankar, K, Miller J J H, Valarmathi S. A parameter uniform fitted mesh method for a weakly coupled system of two singularly perturbed convection-diffusion equations. Mathematical Communications 24(2):193–210, 2019.

14. Kopteva, N., and O'Riordan, E., Shishkin Meshes in the Numerical Solution of Singularly Perturbed Differential Equations, International Journal of Numerical Analysis and Modeling, vol.7-3, p 93-415, 2010.

Table 1: Values of $\mathbf{T^M}$, $\mathbf{p^M}$, $\mathbf{H_p^M}$ and $\mathbf{p^*}$, $\mathbf{H_{p^*}^M}$ are shown in this table

η	**Number of mesh points M**			
	64	**128**	**256**	**512**
0.25000E+00	0. 867460E-02	0. 558775E-02	0. 414957E-02	0. 261489E-02
0.62500E-01	0. 101190E-01	0. 592004E-02	0. 431203E-02	0. 268125E-02
0.15625E-01	0. 105290E-01	0. 601233E-02	0. 436361E-02	0. 270992E-01
0.390625E-02	0. 134986E-01	0. 915321E-02	0. 436595E-02	0. 271481E-02
0.9765625E-03	0. 134986E-01	0. 915321E-02	0. 436595E-02	0. 271481E-02
T^M	0. 148851E-01	0. 117814E-01	0. 749947E-02	0. 378320E-02
p^M	0. 337354E+00	0. 651659E+00	0. 233527E+00	
C_p^M	0. 290370E+00	0. 290370E+00	0. 233527E+00	0. 148840E+00
The order of $\vec{\varepsilon}$ - uniform convergence $p^* = 0.337354$				
Computed $\vec{\varepsilon}$ - uniform error constant $C_{p^*}^M$ =0.290370				

RESEARCH ARTICLE

Perfect Edge Italian Domination of Some Product Graphs

Jyothi V* and J. Suresh Kumar

The PG and Research Department of Mathematics, NSS Hindu College, Changanacherry, Kottayam, Kerala, India.

Received: 21 Jun 2024 Revised: 03 Jul 2024 Accepted: 13 Aug 2024

***Address for Correspondence**
Jyothi V
The PG and Research Department of Mathematics,
NSS Hindu College,
Changanacherry,
Kottayam, Kerala, India.
E.Mail: jyothivnair15@gmail.com

ABSTRACT

A perfect edge Italian dominating function (PEIDF) of a graph $G = (V, E)$ is a function $f: E(G) \rightarrow \{0,1,2\}$having the property that each edge$e$ with $f(e) = 0$ is adjacent to exactly one edge e' with $f(e') = 2$ or is adjacent to exactly two edges $e_1, e_2$with $f(e_1) = 1$ and $f(e_2) = 1$. The weight of a perfect edge Italian dominating function is $\sum_{e \in E(G)} f(e)$.The minimum weight of a PEIDF of a graph G is called perfect edge Italian domination number (PEIDN) of G and the symbol $\gamma_I^{'p}(G)$is used to denote it. In this paper we determine the perfect edge Italian domination number of some graph products.

Keywords: Perfect edge Italian dominating function, Perfect edge Italian domination number.

INTRODUCTION

Let G be a simple connected graph with vertex set $V(G)$ and edge set $E(G)$. Mitchell and Hedetniemi [8] introduced edge domination in graphs as follows:"A subset F of edges of a graph Gform an edge dominating set of G if each edgeof $G$is in$F$ or is adjacent to an edge in F. The numberof edges in the smallest edge domination set is the edge domination number $\gamma'(G)$". Chellali et al. [1] introduced Roman{2}domination as a variation of Roman domination. Henning and Klostermeyer [4] renamed it as Italian domination. Haynes et al. [3] introduced the perfect Italian domination in graphs. In [5] we have introduced the edge version of Italian domination in graphs as follows: "An edge Italian dominating function(EIDF) of a graph $G = (V, E)$ is a function $f: E(G) \rightarrow \{0,1,2\}$ such that every edge x with $f(x) = 0$ is adjacent to some edge $y$with $f(y) = 2$ or at least two edges z_1 and $z_2$with $f(z_1) = f(z_2) = 1$. The weight of an edge Italian dominating function is $\sum_{x \in E(G)} f(x)$. The edge Italian domination number of G, denoted by, $\gamma_I'(G)$, is the minimum weight of all edge Italian dominating functions of G". We have initiated the study of perfect edge Italian domination in graphs in [6] and is defined as follows:"A perfect edge Italian dominating function (PEIDF) of a graph $G = (V, E)$ is a function $f: E(G) \rightarrow \{0,1.2\}$ such that every edge$e$ with $f(e) = 0$ is adjacent to

exactly one edge e' with $f(e') = 2$ or to exactly two edges e_1, e_2 with $f(e_1) = 1$ and $f(e_2) = 1$. The weight of a perfect edge Italian dominating function is $\sum_{e \in E(G)} f(e)$.The minimum weight of a PEIDF of a graph G is called perfect edge Italian domination number (PEIDN) of the graph G and is denoted $\gamma_I^{'p}(G)$". For terms and definitions not explicitly defined here, reader may refer to Harary [2] and for graph products and the related terminology, reader may refer to Richard Hammack et. al [7].

Theorem:1.1. [6]$\gamma_I^{'p}(P_n) = \left\lceil \frac{n}{2} \right\rceil$.

Theorem. 1.2.[6]$\gamma_I^{'p}(C_n) = \left\lceil \frac{n}{2} \right\rceil$.

Theorem. 1.3.[6] For a graph G, $\gamma'(G) \leq \gamma_I'(G) \leq \gamma_I^{'p}(G)$.

Theorem. 1.4. [6] For the Star $K_{1,n}$, $\gamma_I^{'p}(K_{1,n}) = 2$, $n \geq 3$.

Theorem. 1.5. [6]For the complete bipartite graph$K_{m,n}$,
$\gamma_I^{'p}(K_{m,n}) = \begin{cases} m, & if\ m = n \\ 2m, & if\ m < n \end{cases}$.

Perfect edge Italian domination number of some graph products.

Proposition 2.1.*For* $n \geq 2$, $\gamma_I^{'p}(P_2 \times P_n) = 2\left\lceil \frac{n}{2} \right\rceil$.

Proof. The graph, $P_2 \times P_n$, is a disconnected graph with exactly two components isomorphic to P_n. So, using Theorem 1.2, $\gamma_I^{'p}(P_2 \times P_n) = 2\left\lceil \frac{n}{2} \right\rceil$.

Proposition 2.2. *For* $n \geq 2$, $\gamma_I^{'p}(P_3 \times P_3) = 4$.

Proof. $P_3 \times P_3$ is a disconnected graph with two components, one is a cycle of length 4 and the other one is the star graph $K_{1,4}$. By Theorem 1.2. and Theorem 1.4, we have $\gamma_I^{'p}(C_n) = \left\lceil \frac{n}{2} \right\rceil$and $\gamma_I^{'p}(K_{1,n}) = 2$. So, $\gamma_I^{'p}(P_3 \times P_3) = \gamma_I^{'p}(C_4) + \gamma_I^{'p}(K_{1,4}) = 4$.

Proposition 2.3.*For* $n \geq 2$, $\gamma_I^{'p}(K_{1,m} \times P_n) = 4$.

Proof. Tensor product of $K_{1,m}$ and P_n is $K_{1,m} \cup K_{1,m}$. $\gamma_I^{'p}(K_{1,m}) = 2$, $\forall\, m$.
Therefore, $\gamma_I^{'p}(K_{1,m} \times P_n) = \gamma_I^{'p}(K_{1,m} \cup K_{1,m}) = \gamma_I^{'p}(K_{1,m}) + \gamma_I^{'p}(K_{1,m}) = 4$.

Proposition 2.4.*For* $n \geq 2$, $\gamma_I^{'p}(K_{1,m} \times K_{1,n}) = \begin{cases} m+2, & if\ m = n \\ 2m+2, & if\ m < n \end{cases}$.

Proof. Tensor product $K_{1,m} \times K_{1,n}$ is $K_{1,mn} \cup K_{m,n}$.
$\gamma_I^{'p}(K_{1,m} \times K_{1,n}) = \gamma_I^{'p}(K_{1,mn} \cup K_{m,n}) = \gamma_I^{'p}(K_{1,mn}) + \gamma_I^{'p}(K_{m,n})$.
Using Theorems 1.4 and 1.5, $\gamma_I'(K_{1,m} \times K_{1,n}) = 2 + \begin{cases} m, & if\ m = n \\ 2m, & if\ m < n \end{cases}$

$$= \begin{cases} m+2, & if\ m = n \\ 2m+2, & if\ m < n \end{cases}.$$

Theorem 2.5.*For the ladder graph* L_n, $\gamma_I^{'p}(L_n) = n$.

***Proof*:** We know that the ladder graph L_n is the Cartesian product of the path graph P_n and complete graph K_2. It has two copies of P_n , say P_n and $P_n{}'$ with its corresponding edges joined. Let $V(P_n) = \{u_1, u_2, u_3, \dots, u_n\}$ and $V(P_n') = \{u_1', u_2', u_3', \dots, u_n'\}$. The edges $u_i u_i'$, $i = 1\ to\ n$ connecting the two paths are called the rungs of the ladder L_n.

Give the weight 1 to each of the rungs and weight 0 to all other edges. Then, each edge with weight 0 is adjacent to exactly 2 edges with weight 1. Such an assignment of weights gives a PEIDF, f, on L_n. Then, $\sum f(e) \leq n$. For the reverse inequality, consider the two paths P_n and P_n' in L_n. From Theorem 1.1, we have $\gamma_I'^{P}(P_n) = \left\lceil \frac{n}{2} \right\rceil$ and $\gamma_I'^{P}(P_n') = \left\lceil \frac{n}{2} \right\rceil$. In a minimum PEIDF on the paths P_n and P_n' the weights 1 and 0 can be given alternatively to its edges. Consider the same PEIDF on L_n. Then, each rung of the ladder is incident to exactly two edges of weight 1 each and hence get weight 0. So, the PEIDN of L_n will be at least $2\left\lceil \frac{n}{2} \right\rceil = n$.Therefore, $\gamma_I'^{p}(L_n) = n$.

Theorem 2.6.*The Perfect edge Italian domination number Prism graph Π_n is n.*

***Proof*:** The Cartesian product of the cycle graph C_n and complete graph K_2 is the Prism graph Π_n. It can be constructed by joining corresponding vertices of two copies of the cycle graph C_n say C_n and C_n'. Let $V(C_n) = \{u_1, u_2, u_3, \dots, u_n\}$ and $V(C_n') = \{u_1', u_2', u_3', \dots, u_n'\}$. Then for $i = 1$ *to* n, the edges $e_i = u_i u_i'$ connect the two cycles.
Consider a PEIDF, f, on Π_n in which $f(e_i) = 1 \ \forall i$ and $f(e) = 0$ for all other edges. So,$\gamma_I'^{p}(\Pi_n) \leq \sum f(e) = n$. Next consider the two cycles C_n and C_n' in Π_n. From Theorem 1.2,we have $\gamma_I'^{P}(C_n) = \left\lceil \frac{n}{2} \right\rceil$ and $\gamma_I'^{P}(C_n') = \left\lceil \frac{n}{2} \right\rceil$. So, if f is a minimum PEIDF on Π_n,$\sum f(e) \geq 2\left\lceil \frac{n}{2} \right\rceil = n$. Thus, $\gamma_I'^{p}(\Pi_n) = n$.

Theorem 2.7.*For $n \geq 2$, the PEIDN of the Cartesian product of paths is given by*

$$\gamma_I'^{P}(P_n \square P_m) = \begin{cases} \dfrac{mn + 3n - 2}{2}, & if\ both\ m\ and\ n\ are\ odd \\ \dfrac{mn}{2}, & otherwise \end{cases}$$

***Proof*:** Let $V(P_n) = \{u_1, u_2, \dots, u_n\}$and $V(P_m) = \{v_1, v_2, \dots, v_m\}$.

Case.1. Both m and n are odd
Define a function $f: E(P_n \square P_m) \rightarrow \{0,1,2\}$ by

$$f(e) = \begin{cases} e = \{(u_i, v_j)(u_i, v_{j+1})\} i = 1,2, \dots, n \ and \\ \qquad j = 1,3, \dots, m-2. \\ 1, \quad e = \{(u_i, v_{m-1})(u_i, v_m)\}, \quad i = 1,2,3, \dots, n \\ e = \{(u_i, v_{m-1})(u_{i+1}, v_{m-1})\}, i = 1,2, \dots, n-1 \\ 0, \qquad otherwise \end{cases}$$

Then, $\gamma_I'^{p}(P_n \square P_m) \leq \sum f(e) = n.\left(\frac{m-1}{2}\right) + n + n - 1 = \frac{mn+3n-2}{2}$.
Let f be a minimum PEIDF on $P_n \square P_m$. For each $i = 1,2,3, \dots, n$, the subgraph induced by the vertices $(u_i v_1), (u_i v_2), (u_i v_3), \dots, (u_i v_m)$ form the path P_m. Using Theorem 1.1, we get $\gamma_I'^{p}(P_m) = \left\lceil \frac{m}{2} \right\rceil = \frac{m+1}{2}$, as m is odd.

In order to satisfy the condition for minimum PEIDF, all the edges of the path formed by the$n$ vertices $(u_1 v_{m-1}), (u_2 v_{m-1}), (u_3 v_{m-1}), \dots, (u_{n-1} v_{m-1})$ should be given the minimum positive weight 1. Then all the remaining edges of $P_n \square P_m$ can be given the weight 0 as each of them is now adjacent to exactly two edges of weight 1.Hence, $\sum f(e) \geq n\left(\frac{m+1}{2}\right) + n - 1 = \frac{mn+3n-2}{2}$. Thus, we get $\gamma_I'^{p}(P_n \square P_m) = \frac{mn+3n-2}{2}$.

Case.2: m or n is even
As Cartesian product of graphs satisfies commutative property, it is enough to consider the case when m or n is even. Let m be even.
Define a function$f: E(P_n \square P_m) \rightarrow \{0,1,2\}$ by

$$f(e) = \begin{cases} 1, \text{ if } e = \{(u_i v_j)(u_i v_{j+1})\} \text{ where } i = 1,2,3,\dots,n \\ \qquad\qquad \text{and } j = 1,3,5,\dots,m-1. \\ 0, \qquad\qquad otherwise \end{cases}$$

Then f is a PEIDF and $\gamma_I^{'p}(P_n \square P_m) \leq \sum f(e) = \left(\frac{m}{2}\right) n = \frac{mn}{2}$.

For the reverse inequality, consider any minimum PEIDF, f, on $P_n \square P_m$. For $i = 1,2,3,\dots,n$, the subgraph induced by the vertices $\{(u_i v_1), (u_i v_2), (u_i v_3), \dots, (u_i v_m)\}$ form the path P_m. Using Theorem 1.1, we have, $\gamma'_I(P_m) = \left\lceil \frac{m}{2} \right\rceil = \frac{m}{2}$, since m is even. All the other edges of $P_n \square P_m$ can be given the weight 0 as each of them is adjacent to exactly two edges of weight 1. Hence $\sum f(e) \geq n(\frac{m}{2}) = \frac{mn}{2}$. Therefore, $\gamma_I^{'p}(P_n \square P_m) = \frac{mn}{2}$.

Theorem 2.8. For $n \geq 3$,

$$\gamma_I^{'P}(P_n \square C_m) = \begin{cases} \frac{(mn+3n-2)}{2}, if\ both\ m\ and\ n\ are\ odd \\ \frac{mn}{2}, \qquad otherwise \end{cases}$$

Proof is similar to that of Theorem 2.12

Theorem 2.9. For $n \geq 3$,

$$\gamma_I^{'P}(C_n \square C_m) = \begin{cases} \frac{(m+3)n}{2}, if both m and n are odd \\ \frac{mn}{2}, \qquad otherwise \end{cases}.$$

Proof: Let $V(C_n) = \{u_1, u_2, u_3, \dots, u_n\}$ and $V(C_m) = \{v_1, v_2, v_3, \dots, v_m\}$.

Case.1. Both m and n are odd

Define a function $f: E(C_n \square C_m) \to \{0,1,2\}$ by

$$f(e) = \begin{cases} e = \{(u_i, v_j)(u_i, v_{j+1})\} \text{ where } i = 1,2,3,\dots,n \\ \qquad\qquad \text{and } j = 1,3,5,\dots,m-2. \\ 1, \quad e = \{(u_i, v_{m-1})(u_i, v_m)\}, \quad \text{where } i = 1,2,3,\dots,n. \\ \quad e = \{(u_i, v_{m-1})(u_{i+1}, v_{m-1})\} \text{where } i = 1,2,3,\dots,n-1 \\ \qquad e = \{(u_1, v_{m-1})(u_n, v_{m-1})\} \\ 0, \qquad\qquad otherwise \end{cases}$$

Then, $\gamma_I^{'P}(C_n \square C_m) \leq \sum f(e) = n.\left(\frac{m-1}{2}\right) + n + n - 1 + 1 = \frac{(m+3)n}{2}$.

For each $i = 1,2,3,\dots,n$, the subgraph induced by the vertices $(u_i v_1)$, $(u_i v_2)$, $(u_i v_3)$, $\dots$, $(u_i v_m)$ form the cycle C_m and from Theorem1.2, we have $\gamma_I^{'p}(C_m) = \left\lceil \frac{m}{2} \right\rceil = \frac{m+1}{2}$, whenm is odd. So, in a minimum PEIDF, f of $C_n \square C_m$ the weights 1 and 0 can be given alternatively to these edges. Since f is minimum, all the edges of the cycle induced by the vertices $(u_1 v_{m-1}), (u_2 v_{m-1}), (u_3 v_{m-1}), \dots, (u_{n-1} v_{m-1})$ must be given the minimum positive weight 1. Then all the remaining edges of $C_n \square C_m$ can be given the weight 0 as each of them is now adjacent to exactly two edges of weight 1. So, $\sum f(e) \geq n\left(\frac{m+1}{2}\right) + n = \frac{(m+3)n}{2}$ and the equality follows.

Case.2. m or n is even

As cartesian product of graphs satisfies commutative property, we consider only the case when $m$is even.

Define a function $f: E(C_n \square C_m) \to \{0,1,2\}$ by

$$f(e) = \begin{cases} 1, \quad \text{if } e = \{(u_i v_j)(u_i v_{j+1})\}; 1 \leq i \leq n \text{ and } j = 1,3,5,\dots,m-1. \\ 0, \qquad\qquad otherwise \end{cases}$$

Then f is a PEIDF of $C_n \square C_m$ and $\gamma_I^{'P}(C_n \square C_m) \leq \sum f(e) = \left(\frac{m}{2}\right) n = \frac{mn}{2}$.

For each $i = 1,2,3,\dots,n$, the subgraph induced by the vertices $(u_i v_1)$, $(u_i v_2)$, $(u_i v_3)$, $\dots$, $(u_i v_m)$ form the cycle C_m and from Theorem1.2, we have $\gamma_I'^{p}(C_m) = \left\lceil \frac{m}{2} \right\rceil = \frac{m}{2}$, when$m$is even. So, in a minimum PEIDF, f of $C_n \square C_m$ the weights 1 and 0 can be given alternatively to these edges. Then all the remaining edges of $C_n \square C_m$ can be given the weight 0 as each of them is now adjacent to exactly two edges of weight 1. So, $\sum f(e) \geq n\left(\frac{m}{2}\right)$ and the equality follows.

REFERENCES

1. M. T. Chellali, T. W. Haynes, S. T. Hedetniemi, and A. A. McRae, *Roman {2}-domination,* Discrete Appl. Math. 204(2016), 22–28.
2. F. Harary, *Graph Theory*, Addison Wesley, Reading Mass, 1969.
3. T.W. Haynes and M. A. Henning. "*Perfect Italian domination in trees*" *Discrete Applied Mathematics* 260 (2019): 164-177.
4. M. A. Henning and W. F. Klostermeyer, *Italian domination in trees*. Discrete Appl. Math 217(2017), 557–564.
5. V. Jyothi and J. Suresh Kumar, *Edge Italian domination in graphs*. South East Asian Journal of Mathematics and Mathematical Sciences, Volume 17, Issue 2(233-240).
6. V. Jyothi and J. Suresh Kumar,*Onperfect edge Italian domination of graphs*, communicated.
7. R. Hammack, W. Imrich and S. Klavzar, *Handbook of product graphs*, Taylor & Francis Group, LLC, 2011.
8. S. Mitchell and S.T. Hedetniemi, *Edge domination in trees*, Congr. Numer. 19 (1977), 489–509.

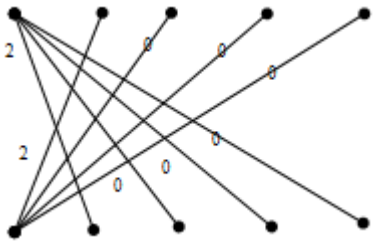

Figure 1: A minimum PEID of $K_{1,4} \times P_2$

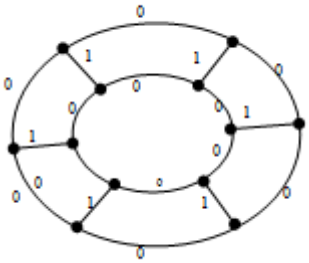

Figure1: A minimum PEIDN of Π_6

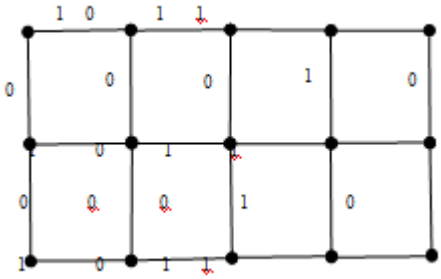

Figure 3: A minimum PEIDN of $P_3 \square P_5$

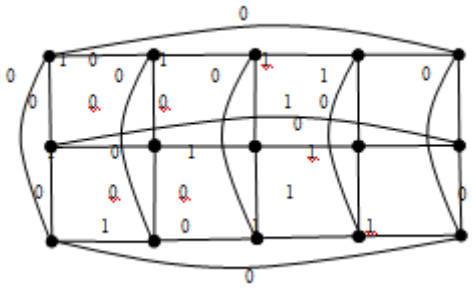

Figure 3: A minimum PEIDN $C_3 \square C_5$

RESEARCH ARTICLE

Sigma Coloring of Some Product Graphs

Preethi K Pillai* and Gowrinandana M

PG and Research Department of Mathematics, N.S.S. Hindu College, Changanacherry, Kerala, India.

Received: 21 Jun 2024 Revised: 03 Jul 2024 Accepted: 13 Aug 2024

***Address for Correspondence**
Preethi K Pillai
PG and Research Department of Mathematics,
N.S.S. Hindu College,
Changanacherry, Kerala, India.
E.Mail: preethiasokar@gmail.com

ABSTRACT

Let G be a simple connected graph and let $c: V(G) \to N$ represent the coloring of vertices in G. Let $\sigma\ (v)$ be the sum of the colors of the vertices adjacent to v for any vertex $v \in V(G)$. If, for any two adjacent vertices $u, v \in V(G), \sigma(v) \neq \sigma(u)$, then c is referred to as a Sigma coloring $(\sigma - coloring)$ of G. The Sigma chromatic number of G, represented by $\sigma(G)$, is the minimum number of colors required in a sigma coloring of G. In this paper, we investigate the sigma coloring and Sigma Chromatic number of some graph operations such as cartesian product of path with path graph, path with cycle graph path with star graphs and two star graphs. We investigate some application also

Keywords: $\sigma -$ coloring, Sigma Chromatic number, cartesian product
AMS Subject Classification Number: 05C15.

INTRODUCTION

Investigations were conducted on several graph coloring techniques [3]. As a thorough research endeavor, Gary Chartrand et al. [1] presented the Sigma coloring, a kind of vertex coloring, in 2008. Though it produces a proper vertex coloring, sigma coloring is actually an improper vertex coloring. The initial publication was presented by Gary Chartrand et al. in 2010. The Sigma chromatic number for several families of snarks, including Flower snarks, Goldberg, and Twisted Goldberg snarks problem, was found by Luis Gustavo da Soledade Gonzaga et al. [4]. We begin by recalling some basic definitions used in this paper.

Definition.1.1. The *Cartesian product* of two graphs $G_1$and $G_2$is denoted by $G_1 \square G_2$and has the vertex set, $V(G_1) \times V(G_2)$.Two vertices (u_1, v_1) *and* $(u_2, v_2)$are adjacent *in* $G_1 \square G_2$ if and only if $u_1 = u_2$ and v_1 is adjacent to v_2 in G_2 or $v_1 = v_2$ and u_1 is adjacent to u_2 in G_1 .

Definition.1.2 Let G be a simple connected graph and let $c: V(G) \to N$ represent the coloring of vertices in G. Let $\sigma\ (v)$ be the sum of the colors of the vertices adjacent to v for any vertex $v \in V(G)$. If, for any two adjacent vertices $u, v \in V(G), \sigma(v) \neq \sigma(u)$, then c is referred to as a Sigma coloring $(\sigma - coloring)$ of G. The Sigma chromatic number of G, represented by $\sigma(G)$, is the minimum number of colors required in a sigma coloring of G.

MAIN RESULTS

Proposition.2.1 [2] A nontrivial connected graph is denoted by G. If each pair of neighboring vertices in G has a different degree, then σ (G) = 1. Otherwise, it does not.

Theorem.2.2. *Cartesian product of P_m and P_n , $m > n$, is σ-colorable and its Sigma chromatic number is* $\sigma\left(P_m \square P_n\right) = \begin{cases} 1 \text{ if } m=3 \text{ and } n=3 \\ 2 \text{ for all } m \geq 4, n \geq 2. \end{cases}$

Proof. Let us take two path graphs P_m *and* P_n .
Let $G = P_m \square P_n$ and vertices are $u_i v_j$, $1 \leq i \leq m$, $1 \leq j \leq n$

Case1. Let $m = 3$ *and* $n = 3$.
Since any two adjacent vertices of the resulting graph have distinct degrees,the result follows from Proposition 2.1.

Case2. $Let m \geq 4$ $and n \geq 2$
Color the vertices using colors {1,2}as follows:
$C(u_i v_j) = 2$; $if\ i + jisodd$
$C(u_i v_j) = 1$; $if\ i + jiseven$
It is noticeable that each neighbouring vertex receives a distinct vertex sum. $C$is therefore a σ coloring with $\sigma(G) \leq 2$. Since the vertices $u_i v_j$,and $u_i v_{j+1}$, $1 \leq i \leq m$, $2 \leq j \leq n-1$ are adjacent vertices with the same degree, $\sigma(G) \neq 1$, by Proposition 2.1. Hence, $\sigma(G)$ =2.

Theorem.2.3. Cartesian product of two graphs$P_5 \square C_n$, $n \geq 3$ is σ −colorable and
$\sigma(P_5 \square C_n) = 2$.

Proof. Let $G = P_5 \square C_n$ .u_2, u_3, u_4, u_5be the vertices of P_5 , $v_1, v_2, v_3, \ldots, v_n$ be the vertices of C_n and in G vertices are taken as $u_i v_j$, $1 \leq i \leq 5$, $1 \leq j \leq n$.
Case 1. *n is even*
Color the vertices using colors {1,2}as follows:
$C(u_i v_j) = 2$; $if\ i + jisodd$
$C(u_i v_j) = 1$; $if\ i + jiseven$
It is noticeable that each neighbouring vertex receives a distinct vertex sum. C is therefore a σ coloring with $\sigma(G)$ 2.Since the vertices $u_1 v_j$,and $u_1 v_{j+1}$, $1 \leq j \leq n-1$ are adjacent vertices with the same degree, $\sigma(G) \neq 1$, by Proposition 2.1. Hence, $\sigma(G)$ =2.

Case 2. *n is odd*
Color the vertices using colors {1,2 }as follows:
$C(u_2 v_n) = 1$
$C(u_5 v_1) = 2$
$C(u_i v_j) = 2$; $if\ i + jisodd$, $1 \leq i \leq 5$,$1 \leq j \leq n$
$C(u_i v_j) = 1$; $if\ i + jiseven$, $1 \leq i \leq 5$,$1 \leq j \leq n$

It is noticeable that each neighbouring vertex receives a distinct vertex sum. $C$is therefore a σ coloring with $\sigma(G) \leq 2$. Since the vertices u_1v_j ,and u_1v_{j+1}, $1 \leq j \leq n-1$ are adjacent vertices with the same degree, $\sigma(G) \neq 1$, by Proposition 2.1. Hence, $\sigma(G)$ =2.

Theorem.2.4. Cartesian product of two graphs$P_m \square C_n$, n ≥ 3 is σ-colorable and
$\sigma(P_m \square C_n) = \begin{cases} 2 \; if \; n \; is \; even \\ 3 \; if \; n \; is \; odd \end{cases}$

Proof. Let $G = P_m \square C_n$.$u_1, u_2, u_3, \ldots, u_m$ be the vertices of P_m. $v_1, v_2, v_3, \ldots, v_n$ be the vertices of C_n and in G vertices are taken as u_iv_j , $1 \leq i \leq m$, $1 \leq j \leq n$.

Case1.*n is even*
Color the vertices using colors {1,2}as follows:
$C(u_iv_j) = 2 \; ; if \; i + j \; is \; odd$
$C(u_iv_j) = 1 \; ; if \; i + j \; is \; even$
It is noticeable that each neighbouring vertex receives a distinct vertex sum. $C$is therefore a σ coloring with $\sigma(G) \leq 2$. Since the vertices u_1v_j ,and u_1v_{j+1}, $1 \leq j \leq n-1$ are adjacent vertices with the same degree, $\sigma(G) \neq 1$, by Proposition 21. Hence, $\sigma(G)$ =2.

Case 2. *n is odd*
Color the vertices using colors {1,2,3}as follows:
$C(u_iv_j) = 2 \; ; if \; i + j \; is \; odd, \; 1 \leq i \leq m \; , 1 \leq j \leq n-1,$
$C(u_iv_j) = 1 \; ; if \; i + j \; is \; even, \; 1 \leq i \leq m \; , 1 \leq j \leq n-1,$
$C(u_iv_n) = \begin{cases} 1 \; if \; i \; is \; odd \\ 3 \; if \; i \; is \; even. \end{cases}$

It is noticeable that each neighbouring vertex receives a distinct vertex sum. C is therefore a σ coloring with $\sigma(G) \leq 3$. If possible, assume $\sigma(G)$ =1. Since the vertices u_1v_j ,and u_1v_{j+1}, $1 \leq j \leq n-1$ are adjacent vertices with the same degree, $\sigma(G) \neq 1$, by Proposition 2.1. Again, if possible, assume $\sigma(G)$ =2. Then the possibility that the vertex $u_iv_n$takes the color $1 or \; 2$ when i is even. If u_iv_n takes the color 1 if i is even then $\sigma(u_2v_n) = \sigma(u_3v_n)$ which is not possible, since$u_2v_n$and u_3v_n are adjacent. If u_iv_n takes the color 2 if i is even then $\sigma(u_iv_1) = \sigma(u_iv_n), 1 \leq i \leq m$which is not possible, since u_iv_1 and $u_iv_n, 1 \leq i \leq m$are adjacent. so $\sigma(G) \neq 2$. Clearly, c induces a $\sigma -$ coloring for the graph G so that $\sigma(G) = 3$.

Theorem.2.5. Cartesian product of two graphs$P_m \square K_{1,n}$, is σ-colorable and
$\sigma(P_m \square K_{1,n}) = \begin{cases} 1 \; if m = 3 \; , n \geq 2 \\ 2 \; if m > 3 \; , n \geq 2 \end{cases}$

Proof . Let us take two graphs $P_m \; and \; K_{1,n}$. $u_1, u_2, u_3, \ldots, u_m$ be the vertices of P_m, v_1 be the central vertex and $v_2, v_3, \ldots, v_n$ be the pendent vertices attached tov_1 in $K_{1,n}$
Let $G = P_m \square K_{1,n}$ and in G vertices are u_iv_j , $1 \leq i \leq m$, $1 \leq j \leq n+1$

Case.1. Let $m = 3 \; and n \geq 2$
Since any two adjacent vertices of the resulting graph have distinct degrees,the result follows from Proposition 2.1.

Case.2. *Let$m > 3 \; , n \geq 2$*
Color the vertices using colors {1,2}as follows:
$C(u_iv_1) = \begin{cases} 1 \; if i i s odd \\ 2 \; if i i s even. \end{cases}$, $1 \leq i \leq m.$
$C(u_iv_j) = 1 \; ; if \; i \; is odd, 2 \leq j \leq n+1$

$C(u_i v_j) = \begin{cases} 1\ if i is even, 2 \le j \le n \\ 2\ if i is even., j = n+1\ . \end{cases}$

It is noticeable that each neighbouring vertex receives a distinct vertex sum. $C$is therefore a σ coloring with $\sigma(G) \le 2$. Since the vertices $u_i v_1$, and $u_{i+1} v_1$, $2 \le i \le m-2$ are adjacent vertices with the same degree, $\sigma(G) \ne 1$, by Proposition 2.1. Hence, $\sigma(G)$ =2.

Theorem.2.6. Cartesian product of two graphs $K_{1,m} \square K_{1,n}$is σ-colorable and its Sigma chromatic number is $\sigma\left(K_{1,m} \square K_{1,n}\right) = 1$ *for all* $m, n \ge 2$.

Proof. $\{u_1, u_2, u_3, \ldots\ldots\ldots\ u_m u_{m+1},\}$ *be taken as the vertices of star* $K_{1,m}$ *and* $\{v_1, v_2, v_3, \ldots\ldots\ldots\ v_n\ , v_{n+1}\}$be *taken as the vertices* of star $K_{1,n}$.

Let $G = K_{1,m} \square K_{1,n}$.Denote the vertices of G as $u_i v_j$, $1 \le i \le m+1, 1 \le j \le n+1$.

$c(u_i v_j) = 1, 1 \le i \le m+1, 1 \le j \le n+1$.

Since any two adjacent vertices of the resulting graph have distinct degrees, the result follows from Proposition 2.1.

Application of Sigma coloring in Cartesion product of Graphs

Sigma coloring is useful in the solution of many real-world issues, such as traffic signal optimization, when it is applied to the Cartesian product of graphs.

Here is how sigma coloring can be used in the context of traffic signals

Intersection Management

In a transportation network, every crossroads can be visualized as a graph vertex. These junctions' edges are the roads that connect them. The possibility of traffic congestion can be decreased and flow can be improved by utilizing sigma coloring to make sure that nearby intersections—those that are immediately connected by a road—do not have the same signal phase.

Signal Timing

When several roads meet, complicated traffic networks can be represented by the Cartesian product of graphs. When arranging signal timings, sigma coloring makes sure that there are never two neighboring junctions with conflicting signals. This ensures smoother transitions and reduce waiting time for vehicles.

Pedestrian Safety

In urban areas, pedestrian crossings are critical. Sigma coloring can be used to coordinate pedestrian signals with vehicle signals, ensuring that pedestrians can cross without conflicting with vehicle movements.

Emergency Vehicle Routing

It is essential to have a clear road for emergency vehicles. In order to ensure that emergency vehicles face fewer red lights and can get to their destinations more quickly, sigma coloring can be used to help designs traffic signals that prioritize certain routes. By applying sigma coloring to the cartesian product of traffic networks, city planners can create more efficient and safer traffic signal systems. This approach help in minimizing conflicts, reducing congestion, and improving overall traffic flow.

REFERENCES

1. Gary Chartrand, Futaba Okamoto, Ping Zhang, *The Sigma Chromatic Number of a Graph*, Graphs and Combinatorics (2010) 26:755–773
2. G. Chartrand and P.Zhang, *Chromatic Graph Theory*, Boca Raton,Chapman&Hall Press, 2008.
3. Gallian J.A, *Dynamic Survey of Graph labelling*, The Electronic Journal of Combinatorics, 2012.

4. Luis Gustavo da SoledadeGonzaga,SheilaMorais de Almeida, *Sigma coloring on Powers of Paths and Some families of Snarks,*ElsevierScience Direct Electronic Notes in Theoretical Computer Science 346(2019)485-496.
5. F Harary, *Graph Theory*, Addison Wesley, Reading Mass(1969).

RESEARCH ARTICLE

Laplacian Spectral Properties of Probabilistic Neural Networks

S.Nithya[1]* and G. Manju[2]

[1]Assistant Professor, Department of Mathematics, St. Xavier's College (Autonomous), Palayamkottai (Affiliated to Manonmaniam Sundaranar University, Abishekapatti, Tirunelveli),Tamil Nadu, India.
[2]Reg.No:23111282092008, PG and Research Department of Mathematics, St. Xavier's College (Autonomous), Palayamkottai, (Affiliated to Manonmaniam Sundaranar University, Abishekapatti, Tirunelveli), Tamil Nadu, India.

Received: 21 Jun 2024 Revised: 03 Jul 2024 Accepted: 13 Aug 2024

***Address for Correspondence**
S.Nithya
Assistant Professor,
Department of Mathematics,
St. Xavier's College (Autonomous), Palayamkottai
(Affiliated to Manonmaniam Sundaranar University, Abishekapatti, Tirunelveli),
Tamil Nadu, India.
E.Mail: nithyasxc@gmail.com

ABSTRACT

Abstract. A neural network functions as a computational framework that emulates the organization and operations of nerve tissue and biological nervous systems, as well as artificial constructs. Serving as a fundamental component of artificial intelligence and machine learning, neural networks play a crucial role. Building upon existing research on the topological properties of neural networks, this study investigates the Laplacian spectrum of Probabilistic Neural Networks (PNNs) with both three and four layers.

Keywords: Serving as a fundamental component of artificial intelligence and machine learning, neural networks play a crucial role.

INTRODUCTION

Graph theory plays a crucial role across a broad spectrum of fields, including Molecular Chemistry, Robotics, Physics, etc. It offers a flexible framework for representing real-world scenarios through the use of vertices and edges. In [7], Specht introduced probabilistic neural network (PNN) in 1990, and then, they have emerged as a crucial class of artificial neural networks with significant applications. For further exploration of PNN applications, we suggest readers refer to [23]. In this context, we present the construction and defining structure of a 3-layered PNN, which will be utilized in the subsequent sections. As implied by its name, a 3-layered PNN consists of three layers of vertices. The first layer, known as the input layer, contains a specific number of vertices. The second layer, also

referred to as the hidden layer, is composed of a fixed number of classes, with each class comprising a certain number of vertices. The third and final layer, called the output layer, consists of vertices uniquely corresponding to the number of classes in the second layer. A key feature of a 3-layered PNN is that each vertex in the input layer is connected to all vertices in the second layer. Additionally, all vertices within a specific class in the hidden layer are connected to their corresponding unique vertex in the output layer. If the input layer contains n vertices and the hidden layer contains k classes, with each class having m vertices, the 3-layered PNN is denoted as $PNN(n,k,m)$, where $n,k,m \in Z^+$. The graphical representation of a 3-layered PNN is illustrated in Figure 1. We now present the construction and defining structure of a 4-layered PNN. Similar to its 3-layered counterpart, a 4-layered PNN consists of four layers of neurons (vertices). These layers exhibit the following characteristics: the first layer, denoted as the input layer, contains a fixed n number of vertices; the second layer, known as the pattern layer, comprises a specified k number of classes, with each class containing m vertices; the third layer, referred to as the summation layer, consists of k vertices corresponding to each class in the pattern layer; and finally, the fourth layer, identified as the output layer, comprises a single unique vertex. The architecture of a 4-layered PNN dictates that each vertex in the input layer is connected to every vertex in the pattern layer. Additionally, each group of m vertices within every class of the pattern layer is connected to its unique respective vertex in the summation layer. Furthermore, all vertices in the summation layer are connected to the unique vertex in the output layer. It is denoted as $PNN(n,k,m,1)$, $n,k,m \in Z^+$. Figure 2 illustrates the graphical representation of the 4-layered PNN, i.e., PNN(n, k, m, 1). A network graph, denoted as $\Gamma = (V(\Gamma), E(\Gamma))$, represents a generic network structure, where $V(\Gamma)$ is the set of vertices (nodes), and $E(\Gamma)$ is the set of edges. In neural networks, the layer of neurons corresponds to a set of vertices, and edges represent the connections between layers of neurons. Throughout this paper we visually represent PNN 3-layer (PNN(n,k,m)) as a graph $\Gamma_3 = (V(\Gamma_3), E(\Gamma_3))$ and PNN 4-layer (PNN(n,k,m,1)) as a graph $\Gamma_4 = (V(\Gamma_4), E(\Gamma_4))$ with cells represented as vertices and connections as edges. For more details on Laplacian spectra, see [1] and [17]. The spectrum of a graph represents the set of all eigenvalues of the adjacency matrix, taking into account their multiplicities. Let $\lambda_0, \lambda_1, \ldots, \lambda_k$ be distinct eigenvalues of a graph. G_n of order n and $m_0, m_1, \ldots, m_k$ represent their corresponding multiplicities, then the spectrum of a graph G_n is expressed as,

$$Spec(G_n) = \begin{pmatrix} \lambda_0 & \lambda_1 & \cdots & \lambda_k \\ m_0 & m_1 & \cdots & m_k \end{pmatrix}$$

or simply denoted as $Spec(G_n) = [\lambda_0]^{m_0}, [\lambda_1]^{m_1}, \ldots, [\lambda_k]^{m_k}$

LITERATURE REVIEW

In [19], the computation of degree-based topological indices for probabilistic neural networks took place. Additionally, analytical closed formulas for these novel topological indices were derived in [26]. The M-polynomial of the 3-layered PNN was established and employed as a recently developed tool for computing specific degree-based topological indices in [20]. The application of the generalized multiplicative version of Zagreb indices to probabilistic neural networks, along with the computation of other degree-based topological indices, was presented in [28]. [24] discussed thirteen irregularity indices for probabilistic neural networks (PNN), while [8] computed discrete Adriatic indices for these networks. A study on various topological structures, including maximal cliques, minimal colorings, maximal independent sets, maximal and perfect matchings, and minimum dominating sets, was conducted in [25]. Weighted-edge based topological indices were measured in [4]. In the exploration of 4-layered probabilistic neural networks, [21] computed specific degree-based topological indices and demonstrated that the indices of 4layered networks are strictly greater than those of 3-layered probabilistic neural networks. Subsequently [18] provided a comparison between the topological indices of artificial neural networks (ANN) and the Probabilistic Neural Network (PNN), assessing the impact of network structure on ANN model accuracy.

PRELIMNARIES

Theorem 3.1. [6] *If* M, N, P *and* Q *are square matrices of the same order and Q is invertible. Then*

$$\begin{vmatrix} M & N \\ P & Q \end{vmatrix} = |Q||M - NQ^{-1}P|$$

Theorem 3.2. *Let* Γ_3 *be the 3-layered probabilistic neural network PNN(n,k,m). Then the Laplacian spectrum of graph of PNN(n,k,m) is*

$$Spec(\Gamma_3) = \begin{pmatrix} n+1 & km & \mu & \nu & 0 \\ km-k & n-1 & k-1 & 1 & 1 \end{pmatrix}$$

Where

$\mu = \frac{1}{2}\left(1 + m + n \pm \sqrt{m^2 - 2mn + 2m + n^2 + 2n + 1}\right)$*and*

$$\nu = \frac{1}{2}\left(1 + m + km + n \pm \sqrt{(-1 - m - km - n)^2 - 4(km + km^2 + mn)}\right)$$

Proof

For constructing the Laplacian matrix for a 3-layer PNN(Probabilistic Neural Network), we follow a specific order of vertices for computational efficiency. The sequence begins with the input *n* neurons, followed by the output layer *m* neurons, and concludes with the hidden layer *km* neurons. The Laplacian matrix of Γ_3 is

$L(\Gamma_3) = D(\Gamma_3) - A(\Gamma_3)$

$$D = \begin{pmatrix} kmI_{(n\times n)} & 0_{(n\times k)} & \\ 0_{(k\times n)} & mI_{(k\times k)} & 0_{(n+k)\times km} \\ 0_{km\times(n+k)} & & n+1I_{km\times km} \end{pmatrix} A = \begin{pmatrix} 0_{(n+k)\times(n+k)} & P_{(n+k)\times km} \\ P^T{}_{km\times(n+k)} & O_{km\times km} \end{pmatrix}$$

Now,

$$L(\Gamma_3) = \begin{pmatrix} kmI_{(n\times n)} & 0_{(n\times k)} & \\ 0_{(k\times n)} & mI_{(k\times k)} & -P_{(n+k)\times km} \\ -P^T_{km\times(n+k)} & & n+1I_{km\times km} \end{pmatrix} P_{(n+k)\times km} = \begin{pmatrix} J_{n\times m} & J_{n\times m} & J_{n\times m} & \cdots & J_{n\times m} & J_{n\times m} \\ J_{1\times m} & O_{1\times m} & O_{1\times m} & \cdots & O_{1\times m} & O_{1\times m} \\ O_{1\times m} & J_{1\times m} & O_{1\times m} & \cdots & O_{1\times m} & O_{1\times m} \\ O_{1\times m} & 0_{1\times m} & J_{1\times m} & \cdots & O_{1\times m} & O_{1\times m} \\ \vdots & \vdots & \vdots & \ddots & \vdots & \vdots \\ O_{1\times m} & O_{1\times m} & O_{1\times m} & \cdots & J_{1\times m} & O_{1\times m} \\ O_{1\times m} & O_{1\times m} & O_{1\times m} & \cdots & O_{1\times m} & J_{1\times m} \end{pmatrix}$$

where *J* represent a matrix filled with elements equal to 1, and let *O* denote a matrix consisting entirely of zeros. Now, the characteristic polynomial of Γ_3 is given by,

$$L(\Gamma_3) - \lambda I = \begin{pmatrix} (km-\lambda)I_{(n\times n)} & 0_{(n\times k)} & \\ 0_{(k\times n)} & (m-\lambda)I_{(k\times k)} & -P_{(n+k)\times km} \\ -P^T_{km\times(n+k)} & & (n+1-\lambda)I_{km\times km} \end{pmatrix}$$

$$\mathrm{p}_{(n+k)\times km}\left((n+1-\lambda)I_{km\times km}\right)^{-1}P^T_{km\times(n+k)} = \frac{1}{n+1-\lambda}P_{(n+k)\times km}P^T_{km\times(n+k)}$$

$$= \frac{1}{n+1-\lambda}\begin{pmatrix} kmJ_n & mJ_{n\times k} \\ mJ_{k\times n} & mI_k \end{pmatrix}$$

By applying Theorem 3.1 we get that,

$$|L(\Gamma_3) - \lambda I| = (n+1-\lambda)^n \left| \begin{pmatrix} (km-\lambda)I_{(n\times n)} & 0_{(n\times k)} \\ 0_{(k\times n)} & (m-\lambda)I_{(k\times k)} \end{pmatrix} - P_{(n+k)\times km} \frac{I_{km}}{n+1-\lambda} P^T_{km\times(n+k)} \right|$$

$$= (n+1-\lambda)^{km} \left| \begin{pmatrix} (km-\lambda)I_{(n\times n)} & 0_{(n\times k)} \\ 0_{(k\times n)} & (m-\lambda)I_{(k\times k)} \end{pmatrix} - \frac{1}{n+1-\lambda} \begin{pmatrix} kmJ_n & mJ_{n\times k} \\ mJ_{k\times n} & mI_k \end{pmatrix} \right|$$

$$= (n+1-\lambda)^{km} \left(km - \lambda - \frac{nkm}{n+1-\lambda}\right)(km-\lambda)^{n-1} \Big| \left(m - \frac{m}{n+1-\lambda} - \lambda\right) I_k - \frac{m}{n+1-\lambda} J_{k\times n} \left((km-\lambda)I_n - \frac{km}{n+1-\lambda} J_n\right)^{-1} \frac{m}{n+1-\lambda I} J_{n\times k} \Big|$$

First compute the inverse of the matrix $(km-\lambda)I_n - \frac{km}{n+1-\lambda}J_n$ using the Sherman–Morrison formula given $P \in R^{n\times n}$ and $x, y \in R^n$ such that $\det(P) \neq 0$ and $\det(P + xy^T) \neq 0$, we have:

$$(P + xy^T)^{-1} = P^{-1} - \frac{P^{-1}xy^TP^{-1}}{1 + y^TP^{-1}x}$$

See [**17**] for a detailed discussion. Let $J_n = xx^T$ where $x = J_{n\times 1}$. Then,

$$\left((km-\lambda)I_n - \frac{km}{n+1-\lambda}J_n\right)^{-1} = -\frac{n+1-\lambda}{km}\left[\frac{-(km-\lambda)(n+1-\lambda)}{km} I_n + xx^T\right]^{-1} - \frac{n+1-\lambda}{km}\left[\frac{(\lambda-km)(n+1-\lambda)}{km} I_n\right]^{-1} -$$

$$= \frac{\left[\frac{(\lambda-km)(n+1-\lambda)}{km} I_n\right]^{-1} xx^T \left[\frac{(\lambda-km)(n+1-\lambda)}{km} I_n\right]^{-1}}{1 + x^T\left[\frac{(\lambda-km)(n+1-\lambda)}{km} I_n\right]^{-1} x}$$

$$= \frac{1}{(km-\lambda)}\left[I_n + \frac{km}{(\lambda-km)(\lambda-(n+1)) - nkm} J_n\right]$$

Then

$$\frac{m}{n+1-\lambda} J_{k\times n}\left((km-\lambda)I_n + \frac{km}{n+1-\lambda}J_n\right)^{-1} \frac{m}{n+1-\lambda} J_{n\times k}$$

$$= \frac{m}{n+1-\lambda} J_{k\times n}\left[\frac{1}{(km-\lambda)}\left[I_n + \frac{km}{(\lambda-km)(\lambda-(n+1)) - nkm} J_n\right]\right]\frac{m}{n+1-\lambda} J_{n\times k}$$

$$= \left[\left(\frac{m}{(n+1-\lambda)(km-\lambda)}\left(1 + \left(\frac{nkm}{(\lambda-km)(\lambda-(n+1)) - nkm}\right)\right)\right) J_{k\times n}\right]\frac{m}{n+1-\lambda} J_{n\times k}$$

$$= \left[\frac{nm^2}{(n+1-\lambda)^2(km-\lambda)}\left(1 + \left(\frac{nkm}{(\lambda-km)(\lambda-(n+1)) - nkm}\right)\right)\right] J_{k\times k} \quad (1)$$

From the above matrix, we get that:

$$\Big| \left(m - \frac{m}{n+1-\lambda} - \lambda\right) I_k - \frac{m}{n+1-\lambda} J_{k\times n}\left((km-\lambda)I_n - \frac{km}{n+1-\lambda}J_n\right)^{-1} \frac{m}{n+1-\lambda} J_{n\times k} \Big|$$

$$= \left| \left(m - \frac{m}{n+1-\lambda} - \lambda\right) I_k - \left[\frac{nm^2}{(n+1-\lambda)^2(km-\lambda)}\left(1 + \left(\frac{nkm}{(\lambda-km)(\lambda-(n+1)) - nkm}\right)\right)\right] J_k \right|$$

$$= \left(m - \frac{m}{n+1-\lambda} - \lambda\right) - \left[\frac{nkm^2}{(n+1-\lambda)^2(km-\lambda)}\left(1 + \left(\frac{nkm}{(\lambda-km)(\lambda-(n+1)) - nkm}\right)\right)\right] \times \left(m - \frac{m}{n+1-\lambda} - \lambda\right)^{k-1}$$

Now, the characteristic equation of $L(\Gamma_3)$ is given by $|L(\Gamma_3 - \lambda I)| = 0$, By substituting the above determinant ,

$$(n+1-\lambda)^{km}\left(km-\lambda-\frac{nkm}{n+1-\lambda}\right)(km-\lambda)^{n-1}$$
$$\left|\left(m-\frac{m}{n+1-\lambda}-\lambda\right)I_k-\frac{m}{n+1-\lambda}J_{k\times n}\left((km-\lambda)I_n-\frac{km}{n+1-\lambda}J_n\right)^{-1}\frac{m}{n+1-\lambda}J_{n\times k}\right|=0$$

$$(n+1-\lambda)^{km}\left(km-\lambda-\frac{nkm}{n+1-\lambda}\right)(km-\lambda)^{n-1}\left(m-\frac{m}{n+1-\lambda}-\lambda\right)^{k-1}$$
$$\left[\left(m-\frac{m}{n+1-\lambda}-\lambda\right)-\left[\frac{nkm^2}{(n+1-\lambda)^2(km-\lambda)}\left(1+\left(\frac{nkm}{(\lambda-km)\big(\lambda-(n+1)\big)-nkm}\right)\right)\right]\right]=0$$

$$(\mathrm{n}+1-\lambda)^{km-k-1}(km-\lambda)^{n-1}(\lambda^2-\lambda(n+m+1)+mn)^{k-1}(\lambda^4-(2n+m+km+2)\lambda^3$$
$$+(n^2+m+nkm+km^2+2(n+mn+km)+1)\lambda^2$$
$$-(nkm+mn+km^2+mn^2+km+km^2n)\lambda)=0$$

$$\big(\lambda-(n+1)\big)^{km-k}(km-\lambda)^{n-1}\left(\lambda-\frac{1}{2}\Big(1+m+n\pm\sqrt{m^2-2mn+2m+n^2+2n+1}\Big)\right)^{k-1}$$
$$\left[\lambda\left(\lambda-\frac{1}{2}\Big(1+m+km+n\pm\sqrt{(-1-m-km-n)^2-4(km+km^2+mn)}\Big)\right)\right]=0$$

Theorem 3.3. *Let* Γ_4 *be the* 4*-layered probabilistic neural network PNN*(*n*,*k*,*m*,1). *Then the spectrum of* Γ_4 *is given as*

$$Spec(\Gamma_4)=\begin{pmatrix} n+1 & k & km & \delta & \frac{c}{3}+\frac{\sqrt[3]{a_1+a_2}}{3\sqrt[3]{2}}-\frac{b\sqrt[3]{2}}{3\sqrt[3]{a_1+a_2}} & \frac{c}{3}-\frac{\sqrt[3]{a_1+a_2}(1\pm i\sqrt{3})}{6\sqrt[3]{2}+\frac{b(1\pm i\sqrt{3})}{3\times 2^{\frac{2}{3}}\sqrt[3]{a_1+a_2}}} & 0 \\ km-k-1 & 1 & n-1 & 1 & 1 & 1 & 1 \end{pmatrix}$$

Where

$$\delta=\frac{1}{2}(m+n+2)\pm\frac{1}{2}\sqrt{m^2-2mn+4m+n^2},c=mk+k+m+n+2$$

$a_1=-2m^3k^3+3m^2k^3+3mk^3-2k^3+3m^3k^2-6m^2k^2-3mk^2-6m^2nk^2+6mnk^2+3nk^2-3k^2+$

$3m^3k+15m^2k-6mn^2k+3n^2k-3mk+6m^2nk-9mnk+12nk+3k-2m^3-2n^3-12m^2$

$+3mn^2-3n^2-15m+3m^2n+3mn+3n$

$$a_2=\Big(4\big(-(mk+k+m+n+2)^2-3(-mk^2-m^2k-3mk-nk-k-mn-n-1)\big)^3$$
$$+(-2m^3k^3+3m^2k^3+3mk^3-2k^3+3m^3k^2-6m^2k^2-3mk^2$$
$$-6m^2nk^2+6mnk^2+3nk^2-3k^2+3m^3k+15m^2k-6mn^2k+3n^2k-3mk$$
$$+6m^2nk-9mnk+12nk+3k-2m^3-2n^3-12m^2+3mn^2-3n^2-15m+3m^2n$$
$$+3mn+3n+2)^2)^{\frac{1}{2}}+2$$

Proof. To create the Laplacian matrix for a 4-layer PNN (PNN(n,k,m,1)) efficiently, we adhere to a prescribed vertex order. This sequence initiates with the input layer's n vertices, proceeds to the summation layer's m vertices, then extends to the pattern layer's km vertices, and ultimately concludes with the output neuron. The Laplacian matrix of $L(\Gamma_4)$ is

$L(\Gamma_4)=D(\Gamma_4)-A(\Gamma_4)$

Where

$$D(\Gamma_4)=\begin{pmatrix} kmI_{n\times n} & 0_{n\times k} & \\ 0_{k\times n} & (m+1)I_{(k\times k)} & 0_{(n+k)\times(km+1)} \\ & 0_{(km+1)\times(n+k)} & (n+1)I_{km\times km} \quad 0_{km\times 1} \\ & & 0_{1\times km} \quad kI_{1\times 1} \end{pmatrix} \text{ and}$$

$$A(\Gamma_4)=\begin{pmatrix} O_{(n+k)\times(n+k)} & B_{(n+k)\times(km+1)} \\ B^T_{(km+1)\times(n+k)} & O_{(km+1)\times(km+1)} \end{pmatrix}$$

$$\text{Then the matrix is } L(\Gamma_4)=\begin{pmatrix} kmI_{n\times n} & 0_{n\times k} & \\ 0_{k\times n} & (m+1)I_{(k\times k)} & -B_{(n+k)\times(km+1)} \\ & -B^T_{(km+1)\times(n+k)} & (n+1)I_{km\times km} \quad 0_{km\times 1} \\ & & 0_{1\times km} \quad kI_{1\times 1} \end{pmatrix}$$

$$\text{where } B_{(n+k)\times(km+1)}=\begin{pmatrix} J_{n\times m} & J_{n\times m} & J_{n\times m} & \cdots & J_{n\times m} & J_{n\times m} & O_{n\times 1} \\ J_{1\times m} & O_{1\times m} & O_{1\times m} & \cdots & O_{1\times m} & O_{1\times m} & J_{1\times 1} \\ O_{1\times m} & J_{1\times m} & O_{1\times m} & \cdots & O_{1\times m} & O_{1\times m} & J_{1\times 1} \\ O_{1\times m} & 0_{1\times m} & J_{1\times m} & \cdots & O_{1\times m} & O_{1\times m} & J_{1\times 1} \\ \vdots & \vdots & \vdots & \ddots & \vdots & \vdots & \vdots \\ O_{1\times m} & O_{1\times m} & O_{1\times m} & \cdots & J_{1\times m} & O_{1\times m} & J_{1\times 1} \\ O_{1\times m} & O_{1\times m} & O_{1\times m} & \cdots & O_{1\times m} & J_{1\times m} & J_{1\times 1} \end{pmatrix}$$

here J represent a matrix filled with elements equal to 1, and let O denote a matrix consisting entirely of zeros.

$$L(\Gamma_4-\lambda I)=\begin{pmatrix} (km-\lambda)I_{n\times n} & 0_{n\times k} & \\ 0_{k\times n} & (m+1-\lambda)I_{k\times k} & -B_{(n+k)\times(km+1)} \\ & -B^T_{(km+1)\times(n+k)} & (n+1-\lambda)I_{km\times km} \quad 0_{km\times 1} \\ & & 0_{1\times km} \quad (k-\lambda)I_{1\times 1} \end{pmatrix}$$

Now,

$$B\begin{pmatrix} (n+1-\lambda)I_{km\times km} & 0_{km\times 1} \\ 0_{1\times km} & (k-\lambda)I_{1\times 1} \end{pmatrix}^{-1}B^T = B\begin{pmatrix} \frac{1}{(n+1-\lambda)}I_{km\times km} & 0_{km\times 1} \\ 0_{1\times km} & \frac{1}{(k-\lambda)}I_{1\times 1} \end{pmatrix}B^T$$

$$=\begin{pmatrix} \frac{km}{n+1-\lambda}J_n & \frac{m}{k-\lambda}J_{n\times k} \\ \frac{m}{k-\lambda}J_{k\times n} & \frac{m}{n+1-\lambda}I_{k\times k}+\frac{1}{k-\lambda}J_{k\times k} \end{pmatrix}$$

Now,

$$|L(\Gamma_4)-\lambda I| = \left|\begin{pmatrix} (n+1-\lambda)I_{km\times km} & 0_{km\times 1} \\ 0_{1\times km} & (k-\lambda)I_{1\times 1} \end{pmatrix}\right|$$

$$\left|\begin{pmatrix} (km-\lambda)I_{n\times n} & 0_{n\times k} \\ 0_{k\times n} & (m+1-\lambda)I_{k\times k} \end{pmatrix}-\begin{pmatrix} \frac{km}{n+1-\lambda}J_n & \frac{m}{n+1-\lambda}J_{n\times k} \\ \frac{m}{n+1-\lambda}J_{k\times n} & \frac{m}{n+1-\lambda}I_{k\times k}+\frac{1}{k-\lambda}J_{k\times k} \end{pmatrix}\right|$$

$$=(n+1-\lambda)^{km}(k-\lambda)\begin{vmatrix} (km-\lambda)I_{n\times n}-\frac{km}{n+1-\lambda}J_{n\times n} & -\frac{m}{n+1-\lambda}J_{n\times k} \\ -\frac{m}{n+1-\lambda}J_{k\times n} & \left(m+1-\lambda-\frac{m}{n+1-\lambda}\right)I_{k\times k}+\frac{1}{k-\lambda}J_{k\times k} \end{vmatrix}$$

Consider,

$$\begin{vmatrix} (km-\lambda)I_{n\times n}-\frac{km}{n+1-\lambda}J_{n\times n} & -\frac{m}{n+1-\lambda}J_{n\times k} \\ -\frac{m}{n+1-\lambda}J_{k\times n} & \left(m+1-\lambda-\frac{m}{n+1-\lambda}\right)I_{k\times k}+\frac{1}{k-\lambda}J_{k\times k} \end{vmatrix}$$

$$=\left(km-\lambda-\frac{nkm}{n+1-\lambda}\right)(km-\lambda)^{n-1}\left|\left(m+1-\lambda-\frac{m}{n+1-\lambda}\right)I_{k\times k}+\frac{1}{k-\lambda}J_{k\times k}-\right.$$

$$\left.\frac{m}{n+1-\lambda}J_{k\times n}((km-\lambda)I_{n\times n}-\frac{km}{n+1-\lambda}J_{n\times n})^{-1}\frac{m}{n+1-\lambda}J_{n\times k}\right|$$

Using the determinant of matrix (1), We get thaat,

$$
\begin{aligned}
|(m+1- \quad & \lambda-\frac{m}{n+1-\lambda})I_{k\times k}-\frac{1}{k-\lambda}J_{k\times k}- \\
& \frac{m}{n+1-\lambda}J_{k\times n}\left((km-\lambda)I_{n\times n}-\frac{km}{n+1-\lambda}J_{n\times n})^{-1}\frac{m}{n+1-\lambda}J_{n\times k}\right| \\
& =|\left(m+1-\lambda-\frac{m}{n+1-\lambda}\right)I_{k\times k}-\frac{1}{k-\lambda}J_{k\times k}- \\
& \left[\frac{nm^2}{(n+1-\lambda)^2(km-\lambda)}\left(1+\left(\frac{nkm}{(\lambda-km)\left(\lambda-(n+1)\right)-nkm}\right)\right)\right]J_{k\times k}| \\
& =(m+1-\lambda-\frac{m}{n+1-\lambda})^{k-1} \quad [\left(m+1-\lambda-\frac{m}{n+1-\lambda}\right)-\frac{k}{k-\lambda} \\
& \qquad -\frac{nkm^2}{\left((n+1)-\lambda\right)^2)\left((\lambda-km)\left(\lambda-(n+1)\right)-nkm\right)}]
\end{aligned}
$$

On further simplifying the above determinant, we get that,

$$
\begin{aligned}
& |L(\Gamma_4)-\lambda I|=0 \\
& (n+1-\lambda)^{km-k-2}(k-\lambda)(km-\lambda)^{n-1}(\lambda^2-\lambda(m+n+2)+mn+n+1)^{k-1} \\
& \times[-\lambda^5+(km+k+m+2n+3)\lambda^4-\lambda^3(k^2m+km^2+kmn+4km+2kn \\
& +2k+2mn+m+n^2+4n+3)+(k^2m^2+k^2mn+2k^2m+km^2n+km^2 \\
& +4kmn+4km+kn^2+2kn+k+mn^2+mn+n^2+2n+1)\lambda^2 \\
& -\lambda(k^2m^2n+k^2m^2+k^2mn+k^2m+kmn^2+2kmn+km)]=0 \\
& (n+1-\lambda)^{km-k-2}(k-\lambda)(km-\lambda)^{n-1}(\lambda^2-\lambda(m+n+2)+mn+n+1)^{k-1} \\
& \times\lambda\left(\lambda-(n+1)\right)(-\lambda^3+\lambda^2(km+k+m+n+2)-\lambda(n(k+m) \\
& +k(m(k+m+3)+1)+n+1)+km(km+k+n+1))=0
\end{aligned}
$$

$$
\begin{aligned}
\lambda \quad & ((n+1-\lambda)^{km-k-1})(k-\lambda)(km-\lambda)^{n-1} \\
& \left(\lambda-\left(\frac{1}{2}(m+n+2)\pm\frac{1}{2}\sqrt{m^2-2mn+4m+n^2}\right)\right)^{k-1} \\
& \left(\lambda-\left(\frac{c}{3}+\frac{\sqrt[3]{a_1+a_2}}{3\sqrt[3]{2}}-\frac{b\sqrt[3]{2}}{3\sqrt[3]{a_1+a_2}}\right)\right) \\
& \left(\lambda-\left(\frac{c}{3}-\frac{\sqrt[3]{a_1+a_2}\left(1\pm i\sqrt{3}\right)}{6\sqrt[3]{2}+\frac{b\left(1\pm i\sqrt{3}\right)}{3\times 2^{\frac{2}{3}}\sqrt[3]{a_1+a_2}}}\right)\right)=0
\end{aligned}
$$

CONCLUSION

In conclusion, the exploration of Laplacian spectrum of Probabilistic Neural Networks (PNNs) with three and four layers offers valuable insights into their structural characteristics. By leveraging topological indices and analyzing the spectral properties of these networks, we contribute to a deeper understanding of their behaviour and functionality. This study underscores the significance of investigating neural network architectures from a spectral perspective, providing avenues for further research and refinement in the field of artificial intelligence and machine learning.

REFERENCES

1. Ameer, F., Hanif, M. K., Talib, R., Sarwar, M. U., Khan, Z., Zulfiqa, K. Techniques, tools and applications of graph analytic, Int. J. Adv. Comput. Sci. Appl., 10, (2019).
2. Alhomaidhi, A., Al-Thukair, F., & Estrada, E. Gaussianization of the spectra of graphs and networks. Theory and applications. Journal of Mathematical Analysis and Applications, 470 (2), (2019) 876-897.
3. Alhomaidhi, A., Al-Thukair, F., & Estrada, E. Double gaussianization of graph spectra.
4. Applied Mathematical Modelling, 93, (2021) 134-147.
5. Alharbi, R., Ahmad, A., Azeem, M., & Koam, A. N. Probabilistic neural network with the concept of edge weight-based entropy. Molecular Physics, e2226773, (2023).
6. Balakrishnan, R. The energy of a graph, Linear Algebra Appl., 387, (2004) 287-295.
7. Brouwer, A. E., & Haemers, W. H. Spectra of graphs. Springer Science & Business Media,
8. (2011).
9. Donald F. Specht, Probabilistic neural networks, Neural Networks, (3), 1, (1990) 109-118.
10. Deepika, T., & Lokesha, V. Computing discrete adriatic indices of probabilistic neural network. European Journal of Pure and Applied Mathematics, 13 (5), 1149-1161 (2020).
11. Estrada, E. Characterization of 3D molecular structure. Chem. Phys. Lett. 319 (5–6), (2000) 713–718.
12. Estrada, E. Characterization of the folding degree of proteins, Bioinformatics, 18 (5), (2002) 697–704.
13. Estrada, E. Characterization of the amino acid contribution to the folding degree of proteins, Proteins, 54 (4), (2004) 727–737.
14. Estrada, E. and Rodr´ıguez-Vel´azquez, J. A. Subgraph centrality in complex networks. Physical Review E, 71(5), (2005) 056103.
15. Estrada, E., and Rodr´ıguez-Vel´azquez, J. A., Randi´c, M. Atomic branching in molecules.
16. Int.J.QuantumChem., 106 (4), (2006) 823–832.
17. Fowler, P. W., & Pisanski, T. HOMO-LUMO maps for chemical graphs. MATCH Commun. Math. Comput. Chem, 64(2), (2010) 373-390.
18. Estrada, E., Alhomaidhi, A. A., & Al-Thukair, F. Exploring the "Middle Earth" of network spectra via a Gaussian matrix function. Chaos: An Interdisciplinary Journal of Nonlinear Science, 27 (2), (2017).
19. Estrada, E. The many facets of the Estrada indices of graphs and networks, SeMA Journal., 79, (2022) 57-125.
20. Godsil, C., & Royle, G. F. Algebraic graph theory, Springer Science & Business Media, (207), (2001).
21. Gayathiri, V., & Manimaran, A. Computing Topological Indices of 3-Layered Artificial Neural Network. Contemporary Mathematics, (2023) 1135-1149.
22. Javaid, M., Cao, J. Computing topological indices of probabilistic neural network. Neural Comput & Applic 30, (2018) 3869–3876.
23. Javaid, M., Raheem, A., Abbas, M., & Cao, J. M-Polynomial Method for Topological Indices of 3-Layered Probabilistic Neural Networks. TWMS Journal of Applied and Engineering Mathematics, 9 (4), (2019) 864-875.
24. Javaid, M., Abbas, M., Liu, J. B., Teh, W. C., & Cao, J. Topological properties of fourlayered neural networks. Journal of Artificial Intelligence and Soft Computing Research, 9 (2), (2019) 111-122.
25. Jin, S., Ma R., Li, J., Eftekharnejad, S., and Zafarani, R. A spectral measure for network robustness: Assessment, design, and evolution, in IEEE International Conference on Knowledge Graph (ICKG), (2022) 97-104.
26. JJain, L. C., Vemuri, V. R., Industrial applications of neural networks, CRC Press, Boca Raton, 1988.
27. Kang, S., Chu, Y. M., Virk, A. R., Nazeer, W., and Jia, J. Computing irregularity indices for probabilistic neural network," Frontiers in Physics, 8, 359 (2020).
28. Khan, A., Hayat, S., Zhong, Y., Arif, A., Zada, L., & Fang, M. Computational and topological properties of neural networks by means of graph-theoretic parameters. Alexandria Engineering Journal, 66, (2023) 957-977.
29. Liu, J. B., Zhao, J., Wang, S., Javaid, M., & Cao, J. On the topological properties of the certain neural networks. Journal of Artificial Intelligence and Soft Computing Research, 8(4), (2018) 257-268.
30. Shang, Y. Random lifts of graphs: network robustness based on the Estrada index. Appl.

31. Math. E-Notes, 12, (2012) 53-61.
32. Sarkar, P., Mondal, S., De, N., & Pal, A. On topological properties of probabilistic neural network. Malaya J. Matematik, 7, (2019) 612-617.
33. Wu, J., Barahona, M., Tan, Y. J., & Deng, H. Z. Spectral measure of structural robustness in complex networks. IEEE Transactions on Systems, Man, and Cybernetics-Part A: Systems and Humans, 41(6), (2011) 1244-1252.
34. Zou, J., Han, Y., & So, S. S. Overview of artificial neural networks. Artificial neural networks: methods and applications, (2009) 14-22.

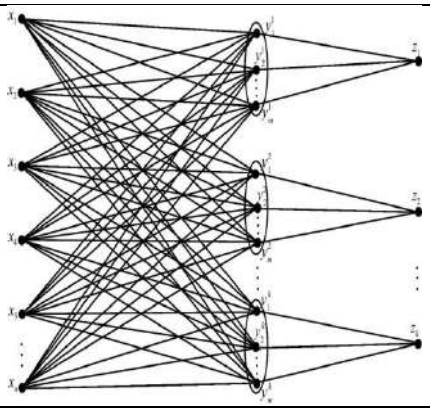

Figure 1. PNN(n,k,m)

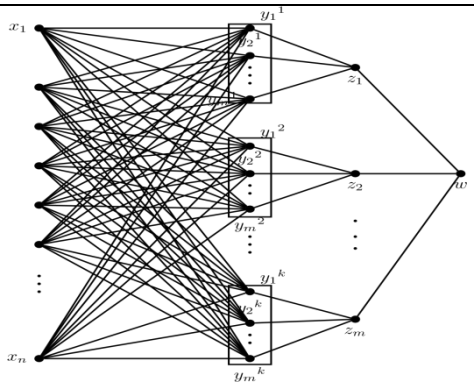

Figure 2. PNN(n,k,m,1)

RESEARCH ARTICLE

Shadow Soft Connectedness: A Recent Approach in Uncertainty Problems

P Gemsy Shirly[1]* and J Subhashini[2]

[1]Research Scholar (Reg.No:23211272092002), PG and Research Department of Mathematics, St.John's College, Palayamkottai, (Affiliated to Manonmaniam Sundaranar University, Abishekapatti, Tirunelveli), Tamil Nadu, India.

[2]Assistant Professor, PG and Research Department of Mathematics, St.John's College, Palayamkottai, (Affiliated to Manonmaniam Sundaranar University, Abishekapatti, Tirunelveli), Tamil Nadu, India.

Received: 21 Sep 2024 Revised: 03 Oct 2024 Accepted: 13 Nov 2024

***Address for Correspondence**
P Gemsy Shirly
Research Scholar (Reg.No:23211272092002),
PG and Research Department of Mathematics,
St.John's College, Palayamkottai,
(Affiliated to Manonmaniam Sundaranar University, Abishekapatti, Tirunelveli),
Tamil Nadu, India.
E.Mail: gemsyshirly12@gmail.com

ABSTRACT

Shadow soft set helps to elucidate the ambiguity associated with fuzzy soft set. This article aims to introduce the concept of shadow soft connectedness defined on shadow soft topological spaces and proved fundamental theorems of shadow soft connected spaces in detailed. Also present and develop the relation between shadow soft connected subspaces. Examples are offer to illustrate these concepts.

Keywords: Shadow soft set, Shadow soft topological space, Shadow soft connectedness, Shadow soft connected subspace.

INTRODUCTION

Uncertainty is an inherent part of life, impacting every decision we make and our perception of the world around us. It results from the unpredictable nature of events, limited knowledge, and the complexity of systems, rendering it hard to forecast outcomes with absolute confidence. Each element in a crisp set is either a member or not; there is no ambiguity. However, in certain scenarios, there are elements with uncertain or ambiguous in their categorization. To address this limitations, Pedrycz [1] introduced shadowed set theory in 1998, which incorporate a shadow region around the fuzzy set to represent elements that are ambiguous or uncertain. Studies on this concept from various perspectives and applications of shadowed sets in various fields have been studied by several researchers includes Ibrahim, A. M. et al [2], Deng and Yao [3], Cattaneo and Ciucci [4] and Zhang and Yao [5]. In 1999, Molodtsov [6]

proposed soft set for modelling uncertainties where each soft set has a suitable set of parameters associated with it. He laid down the underlying concepts of this innovative theory and effectively utilized it in various applications. Shabir and Naz [7] established soft topological spaces and investigated somebasic properties and separation axioms. The concept shadow soft setwas introduced by Alkhazaleh S [8] in 2022, which integrates the attributes of both shadowed sets and soft sets to provide unique framework for handling uncertainty in decision-making processes. The shadow soft set can be induced from fuzzy soft set by determining the shadowparameter set. In shadow soft sets, each element of soft set belongs to any of the three distinct regions namely, core region, shadow region and exclusion regions using corresponding pair of shadow threshold value (α,β) from [0,1] based on the membership grades of its elements.In the preliminary section, basic require results are presented. In the next section, shadow soft connectedness inshadow soft topological spaceSSTSwith fixed set of parameters is defined. Also, proved some important theorems related to shadow soft connected subspaces. The final section provides some concluding remarks.

PRELIMINARIES

Definition 2.1 [8]

Let U = $\{x_1, x_2, \ldots, x_n\}$ be the universal set, E= $\{e_1, e_2, \ldots, e_m\}$ be the set of parameters then (F,E) be a fuzzy soft set over U. Let *shdw*= $\{(\alpha_1, \beta_1), (\alpha_2, \beta_2) \ldots, (\alpha_m, \beta_m)\}$ be the shadow parameter set relevant to E. Let *shdw*(U)be the set of all shadowed subsets on U. A pair $(F,E)_{shdw}$ is called shadow soft set over U, where $F_{(\alpha_i,\beta_i)}$ is a mapping given by

$F_{(\alpha_i,\beta_i)}$: E→*shdw*(U)

for all i= 1,2 …mandwe can write it as $F_{(\alpha_i,\beta_i)}(e_i)=\left\{\frac{x_j}{f_i(x_j)}\right\}, \forall j= 1,2 \ldots n$ andi= 1,2 …m, where

$$f_i(x_j) = \begin{cases} 0, & \mu_i(u_j) \le \alpha_i \\ 1, & \mu_i(u_j) \ge \beta_i \\ [0,1], & \alpha_i < \mu_i(u_j) < \beta_i \end{cases}$$

Definition 2.2 [8]

A null shadow soft set$(\phi, E)_{shdw}$ over a universe U is a shadow soft set with $\phi_{(\alpha_i,\beta_i)}(e_i) = 0$, $\forall\, e_i \in E$.

Definition 2.3 [8]

An absolute shadow soft set $(\Psi,E)_{shdw}$ over a universe U is a shadow soft set with $\Psi_{(\alpha_i,\beta_i)}(e_i) = 1$, $\forall\, e_i \in E$.

SHADOW SOFT CONNECTEDNESS

Shadow soft topological space

In this subsection, we definedSSTSover initial universal setwith fixed parameter set and studied some basic results that will be used to investigate the concept of shadow soft connectedness.

Definition 3.1.1

A Shadow soft topology on (U, E) is a collection τ of shadow soft set over U if

i) $(\phi,E)_{shdw}, (\Psi,E)_{shdw} \in \tau$

ii) If$(A,E)_{shdw}, (B,E)_{shdw} \in \tau$ then $(A,E)_{shdw} \cap (B,E)_{shdw} \in \tau$

iii) If $(A_i,E)_{shdw} \in \tau$ for each $i \in I$ then $\cup_{i\in I}(A_i,E)_{shdw} \in \tau$

Then (U,τ,E) is called SSTS over U. Also, members of τ are called shadow soft open set in (U,τ, E).

Example 3.1.2

Consider U = $\{x_1, x_2, x_3\}$ and E = $\{e_1, e_2, e_3\}$

$(A,E)_{shdw}$= $\{(e_1,\left\{\frac{x_1}{0}, \frac{x_2}{1}, \frac{x_3}{1}\right\}),(e_2,\left\{\frac{x_1}{1}, \frac{x_2}{1}, \frac{x_3}{0}\right\}),(e_3,\left\{\frac{x_1}{1}, \frac{x_2}{1}, \frac{x_3}{0}\right\})\}$

$(B,E)_{shdw}$= $\{(e_1,\left\{\frac{x_1}{0}, \frac{x_2}{0}, \frac{x_3}{[0,1]}\right\}),(e_2,\left\{\frac{x_1}{[0,1]}, \frac{x_2}{1}, \frac{x_3}{0}\right\}),(e_3,\left\{\frac{x_1}{1}, \frac{x_2}{[0,1]}, \frac{x_3}{0}\right\})\}$

$(C,E)_{shdw}$= $\{(e_1,\{\frac{x_1}{0},\frac{x_2}{0},\frac{x_3}{0}\}),(e_2,\{\frac{x_1}{[0,1]},\frac{x_2}{0},\frac{x_3}{0}\}),(e_3,\{\frac{x_1}{1},\frac{x_2}{0},\frac{x_3}{0}\})\}$

Then the collection, τ ={$(\phi,E)_{shdw}$,$(\Psi,E)_{shdw}$,$(A,E)_{shdw}$,$(B,E)_{shdw}$,$(C,E)_{shdw}$}is shadow soft topology on(U, E).

Definition 3.1.3

A shadow soft set$(A,E)_{shdw}$ over U is called shadow soft closed set in (U,τ,E)if and only if its complement$(A,E)^c{}_{shdw}$is shadow soft open set in (U,τ,E).

Definition 3.1.4

An in discrete SSTS (U,τ,E) contains only $(\phi,E)_{shdw}$ and $(\Psi,E)_{shdw}$ and discrete shadow soft topologyτis the collection of all shadow soft sets over (U, E).

Theorem 3.1.5

If τ and τ′ are shadow soft topologies on (U, E) then (U,τ∩τ′,E)isSSTS .

Proof

i) Clearly $(\phi,E)_{shdw}$,$(\Psi,E)_{shdw}$∈τ∩τ′

ii) Let $(A,E)_{shdw}$,$(B,E)_{shdw}$∈τ∩τ′

Then$(A,E)_{shdw}$,$(B,E)_{shdw}$∈τ and$(A,E)_{shdw}$,$(B,E)_{shdw}$∈τ′

Which implies$(A,E)_{shdw}$∩$(B,E)_{shdw}$∈τ and $(A,E)_{shdw}$∩$(B,E)_{shdw}$∈τ′

Thus,$(A,E)_{shdw}$∩$(B,E)_{shdw}$τ∩τ′

iii) Let $(A_i,E)_{shdw}$for each i∈Ibe a family of shadow soft open sets in τ∩τ′

Then $(A_i,E)_{shdw}$∈τ and $(A_i,E)_{shdw}$∈τ′ for each i∈I

Which implies$\cup_{i\in I}(A_i,E)_{shdw}$∈τ and $\cup_{i\in I}(A_i,E)_{shdw}$∈τ′ Thus,$\cup_{i\in I}(A_i,E)_{shdw}$∈τ∩τ′

Remark 3.1.6

If(U,τ,E) and (U,τ′,E)aretwo SSTS, then (U,τ∪τ′,E)need not have to be SSTS.

Example 3.1.7

ConsiderU = $\{x_1,x_2\}$ and E = $\{e_1,e_2\}$

Let τ= {$(\phi,E)_{shdw}$,$(\Psi,E)_{shdw}$,$(A,E)_{shdw}$= $\{(e_1,\{\frac{x_1}{[0,1]},\frac{x_2}{1}\}),(e_2,\{\frac{x_1}{1},\frac{x_2}{[0,1]}\})\}$,$(B,E)_{shdw}$= $\{(e_1,\{\frac{x_1}{[0,1]},\frac{x_2}{0}\}),(e_2,\{\frac{x_1}{1},\frac{x_2}{0}\})\}$}

and τ′ ={$(\phi,E)_{shdw}$,$(\Psi,E)_{shdw}$, $(L,E)_{shdw}$= $\{(e_1,\{\frac{x_1}{1},\frac{x_2}{0}\}),(e_2,\{\frac{x_1}{1},\frac{x_2}{[0,1]}\})\}$,$(M,E)_{shdw}$= $\{(e_1,\{\frac{x_1}{0},\frac{x_2}{0}\}),(e_2,\{\frac{x_1}{1},\frac{x_2}{0}\})\}$} are shadow soft topologies

Then, τ∪τ′ = {$(\phi,E)_{shdw}$,$(\Psi,E)_{shdw}$,$(A,E)_{shdw}$,$(B,E)_{shdw}$,$(L,E)_{shdw}$,$(M,E)_{shdw}$}

Here,$(A,E)_{shdw}$,$(L,E)_{shdw}$∈τ∪τ′, but$(A,E)_{shdw}$∩$(L,E)_{shdw}$∉τ∪τ′.

Definition 3.1.8

Let(U,τ,E) and (U,τ′,E) are two SSTS, if τ⊆τ′ then τ′ is shadow soft finer than τ or τ is shadow soft coarser than τ′.

Definition 3.1.9

Let (U,τ,E) be aSSTS. Let V⊆U and$(V,E)_{shdw}$be an absolute shadow soft set on V, then

τ_V = {$(V,E)_{shdw}$∩$(A,E)_{shdw}$: $(A,E)_{shdw}$∈τ} is known as the shadow soft subspace topology over V and $(V,\tau_V,E)$is shadow soft subspace of (U,τ,E).

Shadow soft connectedness

we comprehend the notion of shadow soft connectedness of SSTS and presented fundamental theorems.

Definition 3.2.1

A shadow soft separation of a SSTS(U,τ,E)is a pair of non empty proper shadow soft open sets $(A,E)_{shdw}$ and $(B,E)_{shdw}$ in (U,τ,E)such that whose union is $(\Psi,E)_{shdw}$and $(A,E)_{shdw}\cap(B,E)_{shdw}=(\phi,E)_{shdw}$.

Definition 3.2.2

A shadow soft set$(G,E)_{shdw}$ over (U, E)is said to be the shadow soft disconnected set if there are two proper shadow soft set$(A,E)_{shdw}$and $(B,E)_{shdw}$in(U,τ,E)such that
$(G,E)_{shdw}\subseteq(A,E)_{shdw}\cup(B,E)_{shdw}$and $(A,E)_{shdw}\cap(B,E)_{shdw}=(\phi,E)_{shdw}$. If there does not exist such two proper shadow soft open sets, then$(G,E)_{shdw}$is called shadow soft connected set.

Example 3.2.3

Let U = {x_1,x_2,x_3} and E= {e_1,e_2} and τ = {$(\phi,E)_{shdw}$,$(\Psi,E)_{shdw}$,$(A,E)_{shdw}$,$(B,E)_{shdw}$,$(C,E)_{shdw}$} where
$(A,E)_{shdw}$= {$(e_1,\{\frac{x_1}{0},\frac{x_2}{0},\frac{x_3}{0}\}),(e_2,\{\frac{x_1}{0},\frac{x_2}{[0,1]},\frac{x_3}{0}\})$}
$(B,E)_{shdw}$= {$(e_1,\{\frac{x_1}{1},\frac{x_2}{0},\frac{x_3}{[0,1]}\}),(e_2,\{\frac{x_1}{[0,1]},\frac{x_2}{0},\frac{x_3}{1}\})$}
$(C,E)_{shdw}$= {$(e_1,\{\frac{x_1}{1},\frac{x_2}{0},\frac{x_3}{[0,1]}\}),(e_2,\{\frac{x_1}{[0,1]},\frac{x_2}{[0,1]},\frac{x_3}{1}\})$}
Then τis shadow soft topology on(U, E).Consider,$(L,E)_{shdw}$ and$(M,E)_{shdw}$ over U defined by
$(L,E)_{shdw}$= {$(e_1,\{\frac{x_1}{1},\frac{x_2}{[0,1]},\frac{x_3}{1}\}),(e_2,\{\frac{x_1}{1},\frac{x_2}{1},\frac{x_3}{1}\})$}
$(M,E)_{shdw}$={$(e_1,\{\frac{x_1}{0},\frac{x_2}{0},\frac{x_3}{[0,1]}\}),(e_2,\{\frac{x_1}{0},\frac{x_2}{0},\frac{x_3}{0}\})$}
Then $(M,E)_{shdw}$is shadow soft disconnected set by(A,E) $(B,E)_{shdw}$ such that
$(M,E)_{shdw}\subseteq(A,E)_{shdw}\cup(B,E)_{shdw}and(A,E)_{shdw}\cap$ $(B,E)_{shdw}=(\phi,E)_{shdw}$. Here,$(L,E)_{shdw}$ is shadow soft connected set because there does not exist such two proper shadow soft set in(U,τ,E).

Definition 3.2.4

Let(U,τ,E)be a SSTS. Then (U,τ,E)is said to be shadow soft connected space, if there does not exist a shadow soft separation. Otherwise, (U,τ,E)is shadow soft disconnected space.

Example 3.2.5

Let U = {x_1,x_2} and E= {e_1,e_2}and τ = {$(\phi,E)_{shdw}$,$(\Psi,E)_{shdw}$,$(A,E)_{shdw}$,$(B,E)_{shdw}$,
$(C,E)_{shdw}$}be shadow soft topology, where
$(A,E)_{shdw}$= {$(e_1,\{\frac{x_1}{0},\frac{x_2}{[0,1]}\}),(e_2,\{\frac{x_1}{[0,1]},\frac{x_2}{0}\})$}
$(B,E)_{shdw}$= {$(e_1,\{\frac{x_1}{0},\frac{x_2}{1}\}),(e_2,\{\frac{x_1}{[0,1]},\frac{x_2}{[0,1]}\})$}
$(C,E)_{shdw}$= {$(e_1,\{\frac{x_1}{0},\frac{x_2}{1}\}),(e_2,\{\frac{x_1}{1},\frac{x_2}{[0,1]}\})$}
Here there is no shadow soft separation exist. Hence, (U,τ,E)is shadow soft connected space.

Theorem 3.2.6

ASSTS(U,τ,E)is shadow soft connected if and only if there does not exist a non empty proper shadow soft setof (U,τ,E)which is shadow soft open and shadow soft closed.

Proof

Suppose that there exist a nonempty proper shadow soft set$(A,E)_{shdw}$ in(U,τ,E)which is shadow soft open and shadow soft closed. Then $(A,E)^{C}{}_{shd\ w}$is also both shadow soft open and shadow soft closed such that$(A,E)_{shdw}\cup(A,E)^{C}{}_{shdw}=(\Psi,E)_{shdw}$ and$(A,E)_{shdw}\cap(A,E)^{C}{}_{shdw}=(\phi,E)_{shdw}$.This gives contradiction
Conversely, suppose there does not exist a non empty proper shadow soft set of (U,τ,E)that is both shadow soft open and shadow soft closed. Suppose on the contrary(U,τ,E)is shadow soft disconnected then there exists a pair of proper non empty shadow soft open sets$(A,E)_{shdw}$and $(B,E)_{shdw}$ such that$(A,E)_{shdw}\cup(B,E)_{shdw}=$ $(\Psi,E)_{shdw}$ and$(A,E)_{shdw}\cap(B,E)_{shdw}=(\phi,E)_{shdw}$.If$(A,E)_{shdw}=(B,E)^{C}{}_{shdw}$and $(B,E)_{shdw}=(A,E)^{C}{}_{shdw}$,then$(A,E)_{shdw}$ and

$(B,E)_{shdw}$ are shadow soft closed as well, which gives contradiction.

Theorem 3.2.7
If$(U,\tau,E)$and (U,τ',E)areshadow soft connected spaces, then $(U,\tau\cap\tau',E)$is also shadow soft connected space.

Proof
Suppose $(U,\tau\cap\tau',E)$ is shadow soft disconnected space, then$(A,E)_{shdw}$and$(B,E)_{shdw}$ forms a shadow soft separation of$(U,\tau\cap\tau',E)$.It follows that,$(A,E)_{shdw}$,$(B,E)_{shdw}\in\tau$and $(A,E)_{shdw}$,$(B,E)_{shdw}\in\tau'$Therefore, we have $(A,E)_{shdw}$and $(B,E)_{shdw}$forms a shadow soft separation of $(U,\tau,E)$and (U,τ',E) which gives contradiction. Hence,$(U,\tau\cap\tau',E)$ is shadow soft connected.

Theorem 3.2.8
Let $(U,\tau',E)$is shadow soft connected space and $\tau$is shadow soft coarser than τ'then $(U,\tau,E)$is also shadow soft connected.

Proof
Suppose $(U,\tau,E)$is shadow soft disconnected, then$(A,E)_{shdw}$and $(B,E)_{shdw}$in τforms a shadow soft separation of (U,τ,E). It follows that,$(U,\tau',E)$is shadow soft disconnected space which is a contradiction.

Theorem 3.2.9
If theshadow soft set$(A,E)_{shdw}$and $(B,E)_{shdw}$forms shadow soft separation of $(U,\tau,E)$and (V,τ_V,E)be a shadow soft connected subspacewith respect to(U,τ,E). Then $(V,E)_{shdw}$is contained in either $(A,E)_{shdw}$or $(B,E)_{shdw}$.

Proof
Suppose by contrary$(V,E)_{shdw}$not contained in both $(A,E)_{shdw}$and$(B,E)_{shdw}$.Then $(V,E)_{shdw}\cap(A,E)_{shdw}$and $(V,E)_{shdw}\cap(B,E)_{shdw}$are shadow soft disjoint open sets and their union gives $(V,E)_{shdw}$
This gives a shadow soft separation of (V,τ_V,E)which is a contradiction. Therefore, one of $(V,E)_{shdw}\cap(A,E)_{shdw}$and $(V,E)_{shdw}\cap(B,E)_{shdw}$is empty Hence $(V,E)_{shdw}$is contained in either $(A,E)_{shdw}$or $(B,E)_{shdw}$.

Theorem 3.2.10
Arbitrary union of shadow soft connected subspaces of (U,τ,E)that have non empty intersection is shadow soft connected.

Proof
Let the collection of shadow soft connected subspaces of (U,τ,E) with non empty intersection be $\{(V_i,\tau_{V_i},E)\mid i\in I\}$
Suppose $(V,\tau_V,E)=\cup_{i\in I}(V_i,\tau_{V_i},E)$is shadow soft disconnected space, then two non empty proper shadow soft open sets $(A,E)_{shdw}$and $(B,E)_{shdw}$ forms a shadow soft separation of (V,τ_V,E) Since $(V_i,\tau_{V_i},E)$is shadow soft connected for each $i\in I$, one of the $(V_i,E)_{shdw}\cap(A,E)_{shdw}$and $(V_i,E)_{shdw}\cap(B,E)_{shdw}$must be empty.
Suppose $(V_i,E)_{shdw}\cap(A,E)_{shdw}=(\phi,E)_{shdw}$,which implies$(V_i,E)_{shdw}\cap(B,E)_{shdw}=(V_i,E)_{shdw}$
Therefore, $(V_i,E)_{shdw}\subset(B,E)_{shdw}$for all $i\in I$, it follows$\cup_{i\in I}(V_i,E)_{shdw}\subset(B,E)_{shdw}$
which implies $(A,E)_{shdw}$is empty which is a contradiction. Therefore, $(V,\tau_V,E)$is shadow soft connected space.

Theorem 3.2.11
Arbitrary union of a family of shadow soft connected subspaces of (U,τ,E)such that one of the members of the family has non empty intersection with every member of the family, is shadow soft connected.

Proof
Let the collection of shadow soft connected subspaces of (U,τ,E)be $\{(V_i,\tau_{V_i},E)\mid i\in I\}$and
$(V,\tau_V,E)=\cup_{i\in I}(V_i,\tau_{V_i},E)$be a union of a family of shadow soft connected subspaces of

(U,τ,E).$(V_{i0},\tau_{V_{i0}},E)$be a fixed member such that $(V_{i0},E)_{shdw} \cap (V_i,E)_{shdw} \neq (\phi,E)_{shdw}$for all$i \in I$.Then by theorem 3.2.10,$(V_{i0},E)_{shdw} \cup (V_i,E)_{shdw}$isshadow soft connectedfor all $i \in I$. Now,$\cup_{i\in I}((V_{i0},E)_{shdw} \cup (V_i,E)_{shdw}) = \cup_{i\in I}(V_i,E)_{shdw}$ and$\cap_{i\in I}((V_{i0},E)_{shdw} \cup (V_i,E)_{shdw}) = (V_{i0},E)_{shdw} \cap_{i\in I}(\cup(V_i,E)_{shdw}) \neq (\phi,E)_{shdw}$. Hence the collection $\{(V_{i0},\tau_{V_{i0}},E) \cup (V_i,\tau_{V_i},E) \mid i \in I\}$ is a shadow soft connected spaceswhich haves non empty intersection. Then by theorem 3.2.10, $(V,\tau_V,E)$is a shadow soft connected space.

CONCLUSION

In this study, we established the conceptSSTSwith fixed set of parameters. We introduced connectedness onSSTSand proved some of its important properties in detailed. We also examined how shadow soft connectedness aids in analyzing the connectivity and relationships between shadow soft topologies which can be beneficial for understanding and solving problems in different domains. These findings provide a strong foundation for further exploration on shadow soft topology and offer promising avenues for future advancement in shadow soft set theory.

REFERENCES

1. Pedrycz W. Shadowed sets: representing and processing fuzzy sets. IEEE Transactions on Systems, Man, and Cybernetics, Part B (Cybernetics). 1998 Feb;28(1):103-9.
2. Ibrahim MA, William-West TO, Kana AF, Singh D. Shadowed sets with higher approximation regions. Soft Computing. 2020 Nov;24(22):17009-33.
3. Deng X, Yao Y. Decision-theoretic three-way approximations of fuzzy sets. Information Sciences. 2014 Sep 20;279:702-15.
4. Cattaneo G, Ciucci D. Shadowed sets and related algebraic structures. FundamentaInformaticae. 2003 Jan 1;55(3-4):255-84.
5. Zhang Y, Yao J. Game theoretic approach to shadowed sets: a three-way tradeoff perspective.Information Sciences. 2020 Jan 1;507:540-52..
6. Molodtsov D. Soft set theory—first results. Computers & mathematics with applications. 1999 Feb 1;37(4-5):19-31.
7. Shabir M,Naz M. On soft topological spaces. Computers & Mathematics with Applications. 2011 Apr 1;61(7):1786-99.
8. Alkhazaleh S. Shadow Soft Set Theory. International Journal of Fuzzy Logic and Intelligent Systems. 2022 Dec 25;22(4):422-32.

RESEARCH ARTICLE

A Note on Turiyam Soft Set

Muthukamalam. M.S[1]* and J. Subhashini[2]

[1]Research Scholar (Reg. No: 22211272092007), PG and Research Department of Mathematics, St. John's College, Palayamkottai, (Affiliated to Manonmaniam Sundaranar University, Abishekapatti, Tirunelveli), Tamil Nadu, India.

[2]Assistant Professor, PG and Research Department of Mathematics, St. John's College, Palayamkottai, (Affiliated to Manonmaniam Sundaranar University, Abishekapatti, Tirunelveli), Tamil Nadu, India.

Received: 21 Jun 2024 Revised: 03 Jul 2024 Accepted: 13 Aug 2024

***Address for Correspondence**
Muthukamalam. M.S
Research Scholar (Reg. No: 22211272092007),
PG and Research Department of Mathematics,
St. John's College, Palayamkottai,
(Affiliated to Manonmaniam Sundaranar University, Abishekapatti, Tirunelveli),
Tamil Nadu, India
E.Mail: muthukamalamms@gmail.com

ABSTRACT

In this paper we study the concept of Turiyam Set which is a four-dimensional mathematical approach for dealing with issues involving Turiyam data. We introduced this concept of Turiyam Set in Soft Set and defined Turiyam Soft Set. This paper offers an essential insight for understanding Turiyam Soft Set, its set theoretical approach and the basic operations on Turiyam Soft Sets. Some properties ofTuriyam Soft Sets have been established.

Keywords: Soft Set, Turiyam Set, Turiyam Soft Set

INTRODUCTION

Lotfi A. Zadeh in 1965 [1], introduced the concept of Fuzzy Set, which involves only the membership values. Atanassov introduced the concept of Intuitionistic Fuzzy Set [2], which involves both membership and non-membership values in a set. An intriguing theoretical idea called "Soft Set Theory" was developed in 1999 by Molodtsov [3], aids in coping with life's uncertainties and directs us toward making wise decisions. Molodtsov's idea of soft set theory expresses soft set as a parameterized family of subsets under the discourse universe. In 2003, P. K. Maji, R. Biswas and A. R. Roy [4]defined the types of Soft Sets and operations on Soft Sets. Soft sets are useful for defining various functions for various parameters and the set's elements are assigned from the universal set against predetermined parameters to handle various decisions and problems in life. In 2005, Smarandache introduced the concept of NeutrosophicSet [5] as a generalisation of Intuitionistic Fuzzy Set, which deals with situations involving

indeterminacy along with membership and non-membership values. P. K. Maji studied this concept and defined Neutrosophic Soft Set in 2011 [6].In 2017, Tuhin Bera and Nirmal Kumar Mahapatra [7], introduced the Neutrosophic Soft topological spaces.Taha Yasin Ozturk, Cigdem Gunduz Aras and Sadi Bayramov in 2019 [8], re-defined the operations and introduced Neutrosophic Soft Set into topological spaces. In 2021, Prem Kumar Singh [9] proposed the theory of Turiyam Sets as an extension of Neutrosophic Set. A Turiyam Set is basically characterized by a truth membership function (t), an indeterminacy membership function (i),a falsity membership function (f) and the turiyam state or liberalization value (l). In 2023, Gamachu Adugna Ganati, V. N. Srinivasa Rao Repalle and Mamo Abebe Ashebo [10] defined Relations on Turiyam sets. In this paper, we introduce the concept of Turiyam Soft Set, which is a parameterized family of subsets of the Turiyam set.We outline some of the fundamental concepts of Turiyam Soft Sets. Some basic properties of Turiyam Soft Set have also been defined.

PRELIMINARIES

Definition 2.1 [3]
Let U be an initial universe and E be the set of parameters. Let $P(U)$ denotes the power set of U. Consider a nonempty set A, $A \subset E$. A pair (F, A) is called a Soft Set over U, where F is a mapping given by $F: A \to P(U)$.

Definition 2.2 [9]
A Turiyam set A on U has the form
$A = \{< u, t_A(u), i_A(u), f_A(u), l_A(u) >: u \in U\}$
where $t_A(u): U \to [0,1], i_A(u): U \to [0,1], f_A(u): U \to [0,1]$ and$l_A(u): U \to [0,1]$ denote the truth value, theindeterminacy value, the falsity value and the Turiyamstate (or liberal) value for each $u \in U$, correspondingly by which $t_A(u), i_A(u), f_A(u)$ and $l_A(u)$ satisfies the condition$0 \le t_A(u) + i_A(u) + f_A(u) + l_A(u) \le 4, \quad \forall u \in U$.

Turiyam Soft Set:
Set theoretic approach of Turiyam Soft Set:
The focus of this section is to define Turiyam Soft Setand its various set theoretic approach.

Definition 3.1.1:
A Turiyam Soft Set $(\mathrm{F}, \mathrm{A})_{\mathrm{L}}$ on the universe U over the fixed parameter E is defined as,
$(\mathrm{F}, \mathrm{A})_{\mathrm{L}} = \{(e, F(e)): e \in A, F(e) \in T(U)\}$
Where, T(U) denotes the set of all Turiyam Sets of U and F is a mapping from $\mathrm{F}: \mathrm{A} \to \mathrm{T}(\mathrm{U}); \ \mathrm{A} \subset \mathrm{E}$.
Note: Throughout this paper, we used U as a fixed universal set and E as a set of fixed parameters.

Example 3.1.2
Suppose there are three employees under consideration,
$\mathrm{U} = \{\mathrm{u}_1, \mathrm{u}_2, \mathrm{u}_3\}$
Consider$\mathrm{E} = \{\mathrm{e}_1, \mathrm{e}_2, \mathrm{e}_3, \mathrm{e}_4\}$, where e_1 =Honesty, e_2 = Reliability,e_3 = Punctualityande_4 = Passion.
and let,
$\mathrm{A} = \{\mathrm{e}_1, \mathrm{e}_2\} \subset E$
where e_1 stands for the parameter honesty and e_2 stands for the parameter reliability.
Suppose that,

$$\mathrm{F}(\mathrm{e}_1) = \mathrm{F}(\text{Honesty}) = \left\{\frac{\mathrm{u}_1}{0.3, 0.5, 0.4, 0.2}, \frac{\mathrm{u}_2}{0.5, 0.3, 0.4, 0.6}, \frac{\mathrm{u}_3}{0.3, 0.2, 0.4, 0.1}\right\}$$

$$\mathrm{F}(\mathrm{e}_2) = \mathrm{F}(\text{Reliability}) = \left\{\frac{\mathrm{u}_1}{0.2, 0.4, 0.3, 0.3}, \frac{\mathrm{u}_2}{0.3, 0.5, 0.4, 0.5}, \frac{\mathrm{u}_3}{0.6, 0.4, 0.3, 0.2}\right\}$$

$$(\mathrm{F}, \mathrm{A})_{\mathrm{L}} = \left\{\begin{matrix}\left(e_1, \left\{\frac{\mathrm{u}_1}{0.3, 0.5, 0.4, 0.2}, \frac{\mathrm{u}_2}{0.5, 0.3, 0.4, 0.6}, \frac{\mathrm{u}_3}{0.3, 0.2, 0.4, 0.1}\right\}\right), \\ \left(e_2, \left\{\frac{\mathrm{u}_1}{0.2, 0.4, 0.3, 0.3}, \frac{\mathrm{u}_2}{0.3, 0.5, 0.4, 0.5}, \frac{\mathrm{u}_3}{0.6, 0.4, 0.3, 0.2}\right\}\right)\end{matrix}\right\}$$

The four values of the Turiyam Soft Set represent Truth, Indeterminacy, Falseand the Liberalization values respectively.

Definition 3.1.3
Let $(\mathrm{F},\mathrm{A})_{\mathrm{L}}$ and $(\mathrm{G},\mathrm{B})_{L}$ be two Turiyam Soft Sets over U. $(\mathrm{F},\mathrm{A})_{\mathrm{L}}$ is said to be Turiyam Soft Subset of $(\mathrm{G},\mathrm{B})_{L}$ if
$\mathrm{A} \subset \mathrm{B}$
$t_{F(e)}(u) \leq t_{G(e)}(u)$, $i_{F(e)}(u) \geq i_{G(e)}(u)$, $f_{F(e)}(u) \geq f_{G(e)}(u)$, $\ell_{F(e)}(u) \leq \ell_{G(e)}(u)$, $\forall\, \mathrm{e} \in \mathrm{A}, \forall\, \mathrm{u} \in \mathrm{U}$.
It is denoted by $(\mathrm{F},\mathrm{A})_{\mathrm{L}} \subseteq (\mathrm{G},\mathrm{B})_{L}$
And obviously, $(\mathrm{G},\mathrm{B})_{L}$ is a Turiyam Soft Superset of $(\mathrm{F},\mathrm{A})_{\mathrm{L}}$.

Definition 3.1.4
Let $(\mathrm{F},\mathrm{A})_{\mathrm{L}}$and $(\mathrm{G},\mathrm{B})_{L}$ be two Turiyam Soft Sets. $(\mathrm{F},\mathrm{A})_{\mathrm{L}}$and $(\mathrm{G},\mathrm{B})_{L}$ are said to be TuriyamSoftEqualif$(\mathrm{G},\mathrm{B})_{L}$is a Turiyam Soft Subset of $(\mathrm{F},\mathrm{A})_{\mathrm{L}}and(\mathrm{F},\mathrm{A})_{\mathrm{L}}$is a Turiyam Soft Subset of$(\mathrm{G},\mathrm{B})_{L}$.

Definition 3.1.5
A Turiyam Soft Set $(\mathrm{F},\mathrm{A})_{\mathrm{L}}$ over the universe U is termed to be Empty or Null Turiyam Soft Set with respect to the parameter A if $t_{F(e)}(u) = 0, i_{F(e)}(u) = 1, f_{F(e)}(u) = 1$ and$\ell_{F(e)}(u) = 0\,;\ \forall\, u \in U;\ \forall\, e \in A$.
It is denoted by ϕ_{L}.

Definition 3.1.6
A Turiyam Soft Set $(\mathrm{F},\mathrm{A})_{\mathrm{L}}$ over the universe U is termed to be the Absolute Turiyam Soft Set with respect to the parameter A if $t_{F(e)}(u) = 1, i_{F(e)}(u) = 0, f_{F(e)}(u) = 0$ *and* $l_{F(e)}(u) = 1\,;\ \forall\, u \in U;\ \forall\, e \in A$. It is denoted by U_{L}.

Operations on Turiyam Soft Sets:
The focus of this section is to define the basic operations on Turiyam Soft Sets.

Definition 3.2.1
Let $(\mathrm{F},\mathrm{A})_{\mathrm{L}}$and $(G,B)_{L}$ be two Turiyam Soft Sets over the common universe U. Then the Union of $(\mathrm{F},\mathrm{A})_{\mathrm{L}}$ and $(G,B)_{L}$ is denoted by $(\mathrm{F},\mathrm{A})_{\mathrm{L}} \cup (G,B)_{L} = (H,C)_{L}$, where $\mathrm{C} = \mathrm{A} \cup \mathrm{B}$ and the Truth, Indeterminacy, False and Liberalization Values of $(\mathrm{H},\mathrm{C})_{\mathrm{L}}$ are as follows:

$$t_{H(e)}(u) = \begin{cases} t_{F(e)}(u), & if\ e \in A \backslash B \\ t_{G(e)}(u), & if\ e \in B \backslash A \\ \max\left(t_{F(e)}(u), t_{G(e)}(u)\right), & if\ e \in A \cap B \end{cases}$$

$$i_{H(e)}(u) = \begin{cases} i_{F(e)}(u), & if\ e \in A \backslash B \\ i_{G(e)}(u), & if\ e \in B \backslash A \\ \min\left(i_{F(e)}(u), i_{G(e)}(u)\right), & if\ e \in A \cap B \end{cases}$$

$$f_{H(e)}(u) = \begin{cases} f_{F(e)}(u), & if\ e \in A \backslash B \\ f_{G(e)}(u), & if\ e \in B \backslash A \\ \min\left(f_{F(e)}(u), f_{G(e)}(u)\right), & if\ e \in A \cap B \end{cases}$$

$$\ell_{H(e)}(u) = \begin{cases} \ell_{F(e)}(u), & if\ e \in A \backslash B \\ \ell_{G(e)}(u), & if\ e \in B \backslash A \\ \max\left(\ell_{F(e)}(u), \ell_{G(e)}(u)\right), & if\ e \in A \cap B \end{cases}$$

Example 3.2.2
Let

$$(\mathrm{F},\mathrm{A})_{\mathrm{L}} = \left\{\left(e_1, \left\{\frac{\mathrm{u}_1}{0.3, 0.4, 0.6, 0.5}, \frac{\mathrm{u}_2}{0.2, 0.4, 0.5, 0.3}, \frac{\mathrm{u}_3}{0.7, 0.8, 0.4, 0.6}\right\}\right)\right\}$$

And

$(\mathrm{G},\mathrm{B})_L = \left\{\left(e_1, \left\{\frac{u_1}{0.4,0.3,0.5,0.7}, \frac{u_2}{0.3,0.5,0.6,0.8}, \frac{u_3}{0.6,0.5,0.7,0.8}\right\}\right)\right\}$

Their union is,

$$(\mathrm{H},\mathrm{C})_L = \left\{\left(e_1, \left\{\frac{u_1}{0.4, 0.3, 0.5, 0.7}, \frac{u_2}{0.3, 0.4, 0.5, 0.8}, \frac{u_3}{0.7, 0.5, 0.4, 0.8}\right\}\right)\right\}$$

Definition 3.2.3

Let $(F,A)_L$and $(G,B)_L$ be two Turiyam Soft Sets over the common universe U. Then the Intersection of $(F,A)_L$and $(G,B)_L$ is denoted by $(F,A)_L \cap (G,B)_L = (H,C)_L$, where$\mathrm{C} = \mathrm{A} \cap \mathrm{B}$ and the Truth, Indeterminacy, False and Liberalization Values of $(\mathrm{H},\mathrm{C})_\mathrm{L}$ are as follows:

$t_{H(e)}(u) = \min\left(t_{F(e)}(u), t_{G(e)}(u)\right), \quad \forall e \in C$

$i_{H(e)}(u) = \max\left(i_{F(e)}(u), i_{G(e)}(u)\right), \quad \forall e \in C$

$f_{H(e)}(u) = \max\left(f_{F(e)}(u), f_{G(e)}(u)\right), \quad \forall e \in C$

$\ell_{H(e)}(u) = \min\left(\ell_{F(e)}(u), \ell_{G(e)}(u)\right), \quad \forall\, e \in C$

Example 3.2.4:

Let

$$(\mathrm{F},\mathrm{A})_\mathrm{L} = \left\{\left(e_1, \left\{\frac{u_1}{0.3, 0.4, 0.6, 0.5}, \frac{u_2}{0.2, 0.4, 0.5, 0.3}, \frac{u_3}{0.7, 0.8, 0.4, 0.6}\right\}\right)\right\}$$

And

$$(\mathrm{G},\mathrm{B})_L = \left\{\left(e_1, \left\{\frac{u_1}{0.4, 0.3, 0.5, 0.7}, \frac{u_2}{0.3, 0.5, 0.6, 0.8}, \frac{u_3}{0.6, 0.5, 0.7, 0.8}\right\}\right)\right\}$$

Their intersection is,

$$(\mathrm{H},\mathrm{C})_L = \left\{\left(e_1, \left\{\frac{u_1}{0.3, 0.4, 0.6, 0.5}, \frac{u_2}{0.2, 0.5, 0.6, 0.3}, \frac{u_3}{0.6, 0.8, 0.7, 0.6}\right\}\right)\right\}$$

Definition 3.2.5:

The complement of a Turiyam Soft Set $(F,A)_L$ denoted by $(\mathrm{F},\mathrm{A})_L^c$ and is defined as,

$(\mathrm{F},\mathrm{A})_L^c = (F^c, \neg A)_L$

Where, $F^c: \neg A \to T(U)$is a mapping given by,

$\mathrm{F}^c(e)$ =Turiyam Soft Complement with$t_{F_{(\mathrm{e})}^c}(u) = f_{F(\mathrm{e})}(u)$, $i_{F_{(\mathrm{e})}^c}(u) = 1 - i_{F(\mathrm{e})}(u)$,$f_{F_{(\mathrm{e})}^c}(u) = f_{F(\mathrm{e})}(u)$, $\ell_{F_{(\mathrm{e})}^c}(u) = 1 - \ell_{F(\mathrm{e})}(u)$.

Proposition 3.2.6

i) $\phi_L \cup U_L = U_L$

ii) $(F,A)_L \cup \phi_L = (F,A)_L$

iii) $(F,A)_L \cup U_L = U_L$

iv) $\phi_L \cap U_L = \phi_L$

v) $(F,A)_L \cap \phi_L = \phi_L$

vi) $(F,A)_L \cap U_L = (F,A)_L$

vii) $\phi_L^c = U_L$

viii) $U_L^c = \phi_L$

ix) $((\mathrm{F},\mathrm{A})^\mathrm{c})^\mathrm{c} = (F,A)$

CONCLUSION

This work presents the Turiyam Soft Sets by taking into account the Turiyam state. Additionally, using the parameterized family of Turiyam Soft Setssome basic operations of Turiyam Soft Sets have been defined, which aid in decision-making regarding how best to handle uncertainty and reduce the likelihood of failures.

REFERENCES

1. Zadeh, Lotfi A. "Fuzzy sets." *Information and Control* (1965).
2. Atanassov, Krassimir T., and Krassimir T. Atanassov. "Intuitionistic fuzzy sets". *Physica-Verlag HD, (1999).*
3. Molodtsov, Dmitriy. "Soft set theory—first results." *Computers & mathematics with applications* 37, no. 4-5 (1999): 19-31.
4. Maji, Pradip Kumar, Ranjit Biswas, and A. Ranjan Roy. "Soft set theory." *Computers & mathematics with applications* 45, no. 4-5 (2003): 555-562.
5. Smarandache, Florentin. "Neutrosophic set-a generalization of the intuitionistic fuzzy set." *International journal of pure and applied mathematics* 24, no. 3 (2005): 287.
6. Pabitra Kumar Maji, *Neutrosophic soft set*, Annals of Fuzzy Mathematics and Informatics Volume 5, No. 1, (January 2013), pp. 157 - 168.
7. Bera, Tuhin, and Nirmal Kumar Mahapatra. "Introduction to neutrosophic soft topological space." *Opsearch* 54, no. 4 (2017): 841-867.
8. Ozturk, Taha Yasin, Cigdem Gunduz Aras, and Sadi Bayramov. *A new approach to operations on neutrosophic soft sets and to neutrosophic soft topological spaces*. Infinite Study, 2019.
9. Singh, Prem Kumar. "Turiyam set a fourth dimension data representation." *Journal of Applied Mathematics and Physics* 9, no. 7 (2021): 1821-1828.
10. Ganati, Gamachu Adugna, V. N. Srinivasa Rao Repalle, and Mamo Abebe Ashebo. "Relations in the context of Turiyam sets." *BMC Research Notes* 16, no. 1 (2023): 49.

RESEARCH ARTICLE

A Study on 3-Regular Discrete Graphs

A. Punitha Tharani[1] and P.Saradha[2]*

[1]Associate Professor, Department of Mathematics, St. Mary's College (Autonomous), Thoothukudi, (Affiliated to Manonmaniam Sundaranar University, Abishekapatti, Tirunelveli), Tamil Nadu, India.
[2] Research Scholar(Register number: 21212212092005),Department of Mathematics, St.Mary's College (Autonomous), Thoothukudi, (Affiliated to Manonmaniam Sundaranar University, Abishekapatti, Tirunelveli), Tamil Nadu, India.

Received: 21 Oct 2024 Revised: 03 Nov 2024 Accepted: 13 Jan 2025

***Address for Correspondence**
P.Saradha
Research Scholar(Register number: 21212212092005),
Department of Mathematics,
St.Mary's College (Autonomous),
Thoothukudi, (Affiliated to Manonmaniam Sundaranar University, Abishekapatti, Tirunelveli),
Tamil Nadu, India.
E.Mail: sara1998dha@gmail.com

ABSTRACT

A cordial graph G is said to be discrete if for every vertex the number of neighbouring vertices labeled 0 and 1 differs by at most 1.Apart from keeping the distinct vertex labels and edge labels difference minimal, the cardinality of the neighbouring labels of every vertex is also taken into account. We have previously defined discrete labeling and have characterized various sorts of graphs that admit discrete labeling. In this paper we have attempted to find 3-regular discrete graphs.

Keywords: Labeling, Discrete, regular, prism, bipartite
AMS subject classification MSC (2010) No: 05C78

INTRODUCTION

Labeling of graphs is a function that maps the vertex set (edge set) to the set of labels. In our previous work, we have defined Discrete Labeling and worked on some standard and special graphs [1]. We have analysed the discrete labeling of some trees and concluded that not all trees are discrete [2]. The conditions under which some cycle related graphs admit discrete labeling were investigated [3]. In this paper, we have made an approach to find 3-regular discrete graphs. Also as an extension we have obtained conditions under which $n-$regular and $(n-1)-$regular bipartite graphs with cardinality of each partition set equal to n admit discrete labeling. The graph (V, E) discussed here are simple, connected and undirected. The terminologies and symbols used in this paper are in accordance with [4].

PRELIMINARIES

Definition 1.1: Let $G(V,E)$be a simple, connected, undirected graph.G is said to have a discrete labeling if there exist functions $d: V \to \{0,1\}$ and $e: E \to \{0,1\}$ defined by

$e(uv) = \begin{cases} 0 \ ; d(u) = d(v) \\ 1 \ ; \ d(u) \neq d(v) \end{cases} u, v \in V$for which

$|n_d(0) - n_d(1)| \leq 1$ ---(i)

$|n_e(0) - n_e(1)| \leq 1$ and ---(ii)

$|n_{N(v)}(0) - n_{N(v)}(1)| \leq 1 \ \forall \ v \in V,$ ---(iii)

where $n_d(x) and \ n_e(x)$ denote the number of vertices and edges with $d(u) = x$ and $e(uv) = x \ ; x \in \{0,1\}$ respectively and $n_{N(v)}(0) \ and \ n_{N(v)}(1)$ denote the number of neighbours of the vertex v labeled 0 and 1 respectively. A Graph G is discrete if it admits discrete labeling. Throughout the paper (i),(ii),(iii) conditions of the definition has been termed as vertex condition, edge condition and neighbouring label condition [1].

Result 1.2: The necessary condition for a graph G to satisfy discrete labeling is that $G$is cordial. Equivalently, a graph which fails to primarily admit cordial labeling is not discrete [1].

Result 1.3: Cycle graph C_n admits discrete labeling only when n is a multiple of 4[1].

Result 1.4: For $n \geq 3$, Complete graph K_n is not discrete[1].

Result 1.5: The n −sided prism is cordial if $n \not\equiv 2 \ mod \ 4$ [5].

Result 1.6: If G is a n −regular bipartite graph with partite sets A and $B$with $|A| = |B| = n$, then G is cordial [6].

Result 1.7: If G is a $(n-1)$ −regular bipartite graph with partite sets A and B with $|A| = |B| = n$, then G is cordialiff$n \equiv$0,1 mod 4 [6].

RESULTS AND DISCUSSION

Cubic Discrete graphs

Observation 2.1.1: All connected 1-regular graphs are discrete.

Observation 2.1.2: All connected 2-regular graphs are discrete if and only if $n \equiv 0 \ mod \ 4$.

(Result 1.3) In an attempt to find 3-regular discrete graphs first let us discuss under which condition n-prism graphs Y_n, a 3-regular graph admit discrete labeling.

Theorem 2.1.3: n-prism graphs $Y_n$are discrete if and only if $n \not\equiv 2 \ mod \ 4$

Proof:Y_n is the graph cartesian product $P_2 \times C_n$,where P_2 is the path graph on two vertices and C_n is the cycle graph on n vertices. An n-prism graph is isomorphic to the generalized Petersen graph $P_{n,1}$. Y_n has $2n$ vertices and $3n$ edges [7]. Let u_i $(1 \leq i \leq n)$ be the vertices of the outer cycle C_n and let v_1 be the vertex adjacent to u_n,v_2 be the vertex adjacent to u_1,v_3 be the vertex adjacent to u_2 and so on.

When $n \equiv 2 \ mod \ 4$, prism graphs are not cordial (Result 1.5) hence not discrete.(Result 1.2)

For other n, define $f: V \to \{0,1\}$ by

$f(u_{4i-3}) = f(u_{4i-2}) = 1$

$f(u_{4i-1}) = f(u_{4i}) = 0$

$f(v_{4i-3}) = f(v_{4i-2}) = 0$

$f(v_{4i-1}) = f(v_{4i}) = 1$

which gives the discrete vertex labeling. Now label the edges uv 1 if $f(u) \neq f(v)$ and 0 if $f(u) = f(v)$.The number of vertices, edges and for every vertex the neighbouring vertices labeled 0 and 1 are listed in Table 1.

For all $n, n_{N(u_{2i})}(0) = n_{N(u_{2i+1})}(0) = \begin{cases} 1 \ when \ i \ is \ odd \\ 2 \ when \ i \ is \ even \end{cases}$

$n_{N(u_{2i})}(1) = n_{N(u_{2i+1})}(1) = \begin{cases} 2 \ when \ i \ is \ odd \\ 1 \ when \ i \ is \ even \end{cases}$

$n_{N(v_1)}(0) = 2, n_{N(v_1)}(1) = 1$

$n_{N(v_{2i})}(0) = n_{N(v_{2i+1})}(0) = \begin{cases} 1 \ when \ i \ is \ odd \\ 2 \ when \ i \ is \ even \end{cases}$

$n_{N(v_{2i})}(1) = n_{N(v_{2i+1})}(1) = \begin{cases} 2 \ when \ i \ is \ odd \\ 1 \ when \ i \ is \ even \end{cases}$

In case of $n \equiv 3 \ mod \ 4$, $n_{N(u_n)}(0) = n_{N(v_n)}(1) = 1$ and $n_{N(u_n)}(1) = n_{N(v_n)}(0) = 2$.For rest of the cases the neighbours of terminal vertex stick on to the number as mentioned above. Hence from Table 1, it may be inferred that $|n_f(0) - n_f(1)| = 0$, $|n_e(0) - n_e(1)| \leq 1$ and for every vertex v,the cardinality of neighbouring vertices labeled 0 and 1 differs by at most 1. Therefore, n-prism graphs $Y_n$are discrete if and only if $n \not\equiv 2 \ mod \ 4$. An example of discretely labeled prism graph $Y_n$when $n = 7$ is depicted in Fig 1. A 3-regular graph cannot have odd number of vertices [4]. Therefore 3-regular graphs on 4, 6, 8, 10 vertices are taken and checked for discrete labeling. The following results were obtained.

2.1.4 3-regular graphs with 4 vertices is not discrete since it is isomorphic to K_4 (Result 1.4)

2.1.5 All 3-regular graphs with 6 vertices are discrete.

There are 2 cubic graphs with 6 vertices[8].

2.1.6 All 3-regular graphs with 8 vertices are discrete

There are 5 cubic graphs with 8 vertices[8].

2.1.7 All 3- regular graphs with 10 vertices are discrete

There are 19 cubic graphs with 10 vertices[8].

It is evident from the illustrations given in Fig 2 that the above mentioned results are true.

n −regular and $n-1$ regular bipartite discrete graphs

Theorem 2.2.1: If G is a n −regular bipartite graph with partite sets A and B with $|A| = |B| = n$, then G is discrete.

Proof: If G is a n −regular bipartite graph with partite sets A and B with $|A| = |B| = n$, then G is cordial (Result 1.6) Let $A = \{a_1, a_2, \dots, a_n\}$ and $B = \{b_1, b_2, \dots, b_n\}$.Now let us check whether the same labeling technique employed in [6] admits the neighbouring label condition of the definition.

Case 1: When n is even

Since every $a_i (1 \leq i \leq 2m)$ is adjacent to every $b_i (1 \leq i \leq 2m)$, by employing the labeling technique mentioned in [6] The neighbouring labels of $a_i (1 \leq i \leq 2m)$ are m 0's and m 1's.Similarly the neighbouring labels of $b_i (1 \leq i \leq 2m)$ are m 0's and m 1's. Therefore $|n_{N(v)}(0) - n_{N(v)}(1)| = 0$ for every vertex v in G when n is even.

Case 2: When n is odd

By employing the same labeling technique as in [6], where we first label $A - \{u\}$ and $B - \{v\}$ for some $u, v \in V(G)$ as in Case 1 and the label u and v with 0 and 1, we observe that each $a_i (1 \leq i \leq 2m)$and $u$is adjacent to m 0's and $m + 1$ 1's , where u is the $2m + 1^{th}$ vertex in A. Similarly each $b_i (1 \leq i \leq 2m)$and $v$is adjacent to $m + 1$ 0's and m 1's where v is the $2m + 1^{th}$ vertex in B.

Hence $|n_{N(v)}(0) - n_{N(v)}(1)| = 1$ for every vertex v in G when n is odd.

$\therefore G$ is discrete.

Corollary 2.2.2: A 3-regular bipartite graph with partite sets $|A| = |B| = 3$ is discrete.

Theorem 2.2.3: If G is $n - 1$ regular bipartite graph with partite sets A and B with $|A| = |B| = n$, then G is discrete if and only if $n \equiv 0 \ mod \ 4$.

Proof: If G is $n - 1$ regular bipartite graph with partite sets A and B with $|A| = |B| = n$, then G is cordial if and only if $n \equiv 0,1 \ mod \ 4$ (Result 1.7). Obviously, we have to only check for the cases when $n \equiv 0 \ mod \ 4$ and $n \equiv 1 \ mod \ 4$(Result 1.2).Let $A = \{a_1, a_2, \dots, a_n\}$and $B = \{b_1, b_2, \dots, b_n\}$.

When $n \equiv 0 \ mod \ 4$. Let $n = 4m, m \in N$. First we label the vertices as in [6] optimally to satisfy vertex and edge conditions of the definition.

Now, we observe that $|n_{N(a_i)}(0) - n_{N(a_i)}(1)| = |(2m - 1) - 2m| = 1, 1 \leq i \leq m$

$|n_{N(a_i)}(0) - n_{N(a_i)}(1)| = |2m - (2m - 1)| = 1, m + 1 \leq i \leq 2m$

$|n_{N(a_i)}(0) - n_{N(a_i)}(1)| = |(2m - 1) - 2m| = 1, 2m + 1 \leq i \leq 3m$

$|n_{N(a_i)}(0) - n_{N(a_i)}(1)| = |2m - (2m - 1)| = 1, 3m + 1 \leq i \leq 4m$

Also ,$|n_{N(b_i)}(0) - n_{N(b_i)}(1)| = |(2m - 1) - 2m| = 1, 1 \leq i \leq m$

$\left|n_{N(b_i)}(0) - n_{N(b_i)}(1)\right| = |(2m-1) - 2m)| = 1, m+1 \leq i \leq 2m$
$\left|n_{N(b_i)}(0) - n_{N(b_i)}(1)\right| = |2m - (2m-1)| = 1, 2m+1 \leq i \leq 3m$
$\left|n_{N(b_i)}(0) - n_{N(b_i)}(1)\right| = |2m - (2m-1)| = 1, 3m+1 \leq i \leq 4m$
Hence we can conclude that G is discrete when $n \equiv 0\ mod\ 4$.
When $n \equiv 1\ mod\ 4, n = 4m+1$
$G$is a $(n-1)$ −regular bipartite graph with the partitions A and B where $A = \{a_1, a_2, \dots, a_n\}$ and $B = \{b_1, b_2, \dots, b_n\}$. G is obtained from the complete bipartite graph by deleting the edges $a_i b_i (1 \leq i \leq 4m+1)$.When we try to label the vertices without violating the vertex label condition by equally allocating 0's and 1's to the partite set A(i.e.,) without loss of generality label the first $2m+1$ vertices of the partite set A with 0 and the next $2m$vertices with 1 which would be an optimal way of labeling the vertices without violating the vertex condition. If we do so, we find that the neighbouring label condition is violated since there exists at least one $b_i (2m+2 \leq i \leq 4m)$ for which $\left|n_{N(b_i)}(0) - n_{N(b_i)}(1)\right| = |(2m+1) - (2m-1)| = 2 \nleq 1$.Hence we find that $(n-1)-$ regular bipartite graph with partite sets A and B with $|A| = |B| = n$ is cordial when $n \equiv 1\ mod\ 4$ but not discrete. Hence by the above discussions and [6], we can infer that G is discrete if and only if $n \equiv 0\ mod\ 4$ where G is $n-1$ regular bipartite graph with partite sets A and B with $|A| = |B| = n$.

Corollary 2.2.4:A 3-regular bipartite graph with partite sets $|A| = |B| = 4$ is discrete.

CONCLUSION

In this paper we have discussed the discrete labeling of prism graphs and cubic graphs of vertices 4, 6, 8 and 10. Since larger the vertex set greater the number of cubic graphs, we have limited to 10 vertices. We have generalized the discrete labeling of n −regular and $(n-1)$ −regular bipartite graphs with partiteset $|A| = |B| = n$. Further explorations can be done on finding cubic discrete graphs with large number of vertices [8].

REFERENCES

1. A. PunithaTharani, P. Saradha, "Discrete Labeling of Some Graphs", *Indian Journal of Science and Technology,* Vol. 17(1) (2024), pp. 93-102.
2. A. PunithaTharani, P. Saradha, "Discrete Labeling of Some Trees", *Indian Journal of Natural Sciences,* Vol. 15(83) (2024), pp. 72871-72877.
3. A. PunithaTharani, P. Saradha, "Discrete Labeling of Some Cycle related Graphs", *Proceedings of National Seminar on Recent Trends in Pure and Applied Mathematics,* ISSN: 978-81-965805-3-7, pp. 76-79.
4. D.B.West, An Introduction to Graph Theory, Prentice-Hall, (2002).
5. Ibrahim Cahit, "Cordial Graphs: A Weaker Version of Graceful and Harmonious Graphs", *ArsCombinatoria*, Vol. 23(1987), pp. 201-208.
6. PranaliSapre, "Cordial Labelling Of k-Regular Bipartite Graphs for K= 1, 2, N, $N-1$ where K is the Cardinality of Each Bipartition", IOSR Journal of Mathematics (IOSR-JM), Vol. 6 (4), pp. 35-42
7. Weisstein, Eric W. Prism Graph, From *MathWorld*--A Wolfram Web Resource https://mathworld.wolfram.com/PrismGraph.html
8. M. Meringer, Fast Generation of Regular Graphs and Construction of Cages, Journal of Graph Theory, Vol. 30(1999), pp. 137-146.
9. J. A. Gallian, A dynamic survey of graph labeling, *The Electronic Journal of Combinatorics*, Vol. 24(2021).
10. A. Lourdusamy, M.Seenivasan, "Vertex equitable labeling of graphs", *Journal of Discrete Mathematical Sciences & Cryptography*, Vol. 11(2008), pp. 727-735.
11. U. M. Prajapati, K.K. Raval, "Different types of labeling of total path related graphs", *Journal of Xidian University*, Vol. 14(2020), pp. 570-576.
12. Amit.H.Rokad, Kalpesh M.Patadiya, "Cordial Labeling of Some Graphs", *Aryabhatta Journal of Mathematics and Informatics*, Vol. 9(2017), pp. 589-597.

Table 1: Cardinality of vertices, edges and neighbours of Y_n

Case	$n_f(0)$	$n_f(1)$	$n_e(0)$	$n_e(1)$	$n_{N(u_1)}(0)$	$n_{N(u_1)}(1)$
$n \equiv 0 \ mod\ 4$	n	n	$\frac{3n}{2}$	$\frac{3n}{2}$	2	1
$n \equiv 1 \ mod\ 4$	n	n	$\frac{3n+1}{2}$	$\frac{3n-1}{2}$	1	2
$n \equiv 3 \ mod\ 4$	n	n	$\frac{3n-1}{2}$	$\frac{3n+1}{2}$	2	1

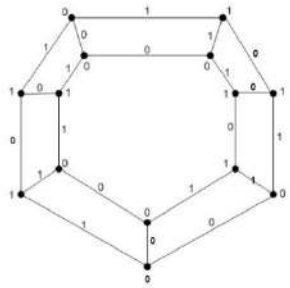

Figure1: Discrete Labeling of Y_7

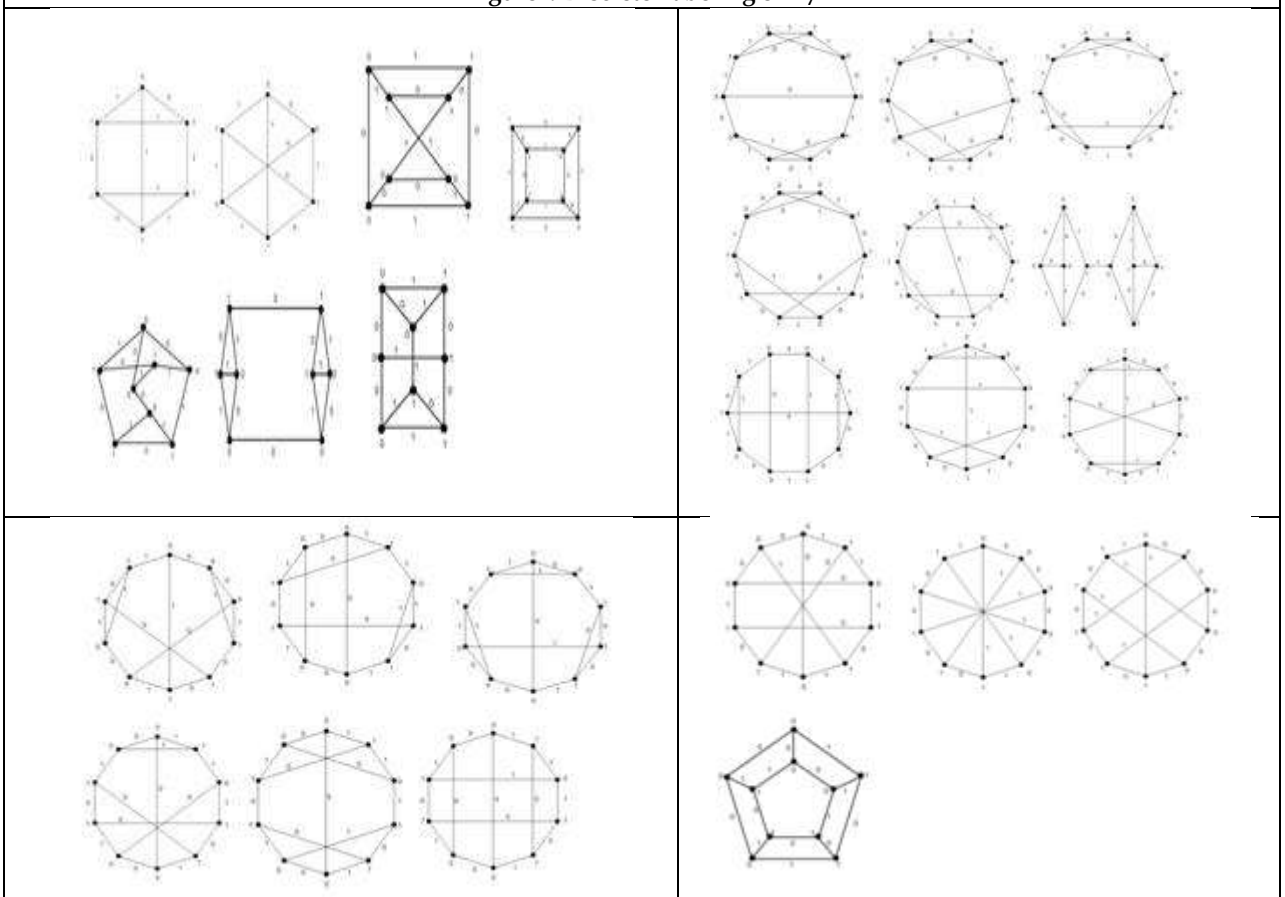

Figure 2: Discrete Labeling of Cubic graphs with vertices 6,8,10

RESEARCH ARTICLE

An Introduction to Sum-Cardinal Labeling

A. Punitha Tharani[1] and S. Pratiksha[2]*

[1]Associate Professor, Department of Mathematics, St.Mary's College (Autonomous), Thoothukudi, (Affiliated to Manonmaniam Sundaranar University, Abishekapatti, Tirunelveli), Tamil Nadu, India.
[2]Research Scholar (Register number: 21212212092004), Department of Mathematics, St.Mary's College (Autonomous), Thoothukudi, (Affiliated to Manonmaniam Sundaranar University, Abishekapatti, Tirunelveli), Tamil Nadu, India.

Received: 21 Nov 2024 Revised: 03 Dec 2024 Accepted: 13 Jan 2025

***Address for Correspondence**
S. Pratiksha
Research Scholar (Register number: 21212212092004),
Department of Mathematics, St.Mary's College (Autonomous),
Thoothukudi, (Affiliated to Manonmaniam Sundaranar University, Abishekapatti, Tirunelveli),
Tamil Nadu, India.
E.Mail: pratikshaprabhu32@gmail.com

ABSTRACT

The proposed work marks the finding of a new type of labeling where unique non-repetitive vertex and edge labels are allocated to a graph G such that the edge labels are the sum of the incident vertex labels. These labels belong to the set of natural numbers ranging up to the sum of the number of vertices and edges of G. We call this labeling as sum-cardinal labeling and represent it as s-cardinal labeling. This paper establishes s-cardinal labeling for some star and cyclic graphs. Further, some general results regarding sum-cardinal labeling have also been discussed.

Keywords: sum-cardinal, star graphs, cyclic graphs, bipartite graphs
AMS Subject Classification MSC (2010) No: 05C78

INTRODUCTION

Graph labeling was first introduced in the mid-1960s. Over the years, a number of labelings have bloomed and its necessity and inevitable role in vital areas of humankind makes it an iconic topic to be worked on. Contributions by Rosa [1], Graham and Sloane [2]in labeling graphs is vast. The Gallian survey on graph labeling contains majority of the works that deal with graph labeling [3]. The proposed work is yet another contribution to graph labeling technique. This is an extension of our previous work, so called cardinal labeling. The methodology for cardinal labeling and results for the same can be found in [4][5][6]. Now, the newly devised labeling, coined as sum-cardinal labeling,or simply s-cardinal labeling, is congruous with cardinal labeling except that the edge labels for a graph are given by the addition function of the vertex labels. For a simple connected and undirected graph G, we assign labels

to the vertices of G using the members of $\mathbb{N}$ ranging up to the sum of the order and size of G such that no vertex label is repeated and the edges of G receive elements of that range of $\mathbb{N}$ that were not previously given to the vertices under a function that sums up the label values of the incident vertices. We call this labeling as sum-cardinal labeling and any graph that admits this labeling is said to be sum-cardinal. In this paper, we have discussed s-cardinal labeling for star, bistar and cyclic graphs like globe graph, complete bipartite graphand crown graph.Further, some general considerations to be made while labeling a graph s-cardinally have also been summarized. All the notations employed here are in with reference to [7].

METHOD

Definition: Let $G(V,E)$be a simple connected undirected graph. Let $|V| = p, |E| = q$ and let $C = \{1,2,\dots,p+q\}$. G is said to admit sum-cardinal labeling if the one-to-one function F from the vertex set V into the set C generates a one-to-one edge function F^*onto the set $C\backslash F(V)$defined by $F(u) + F(v) = F^*(uv)\ \forall\ uv \in E$. A graph G is said to be sum-cardinal if it admits sum-cardinal labeling. We denote sum-cardinal labeling simply as s-cardinal labeling of G. Figure 1 serves as an example for labeling a graph s-cardinally. For this graph, $|V| = 5, |E| = 4$ and so we have $C = \{1,2,\dots,9\}$. We could see that all the members of C are uniquely assigned to the vertices and edges without repetition. Note that the edge labels are the summation of the incident vertex labels.

RESULTS AND DISCUSSION

Sum-cardinal labeling of star graphs

Theorem 1: Star $K_{1,m}$is sum-cardinal.

Proof: Let u denote the central vertex and let v_i $(i = 1,2,\dots,m)$ denote its pendant vertices. Here $|V| = m+1$, $|E| = m$ and $C = \{1,2,\dots,2m+1\}$. Define $F: V \to C$ by

$F(u) = 1,$

$F(v_i) = 2\big((m+1) - i\big), \quad i = 1,2,\dots,m$

The induced edge function F^*onto the set $C\backslash F(V)$ is given below.

$F^*(uv_i) = 2(m-i) + 3, \quad i = 1,2,\dots,m$

The resultant edge labels obtained by addition of the incident vertex labels are all distinct in C. Also vertices u and $v_i (i = 1,\dots,m)$ have distinct labels of C that are not given to $\{E\}$. The resulting labeling of the star graph is s-cardinal. Hence Star $K_{1,m}$is sum-cardinal.Figure2 serves as an example for star graph being s-cardinal.

Theorem 2: Bistar graph $(BS)_{m,n}, m \geq n$ is s-cardinal labelable.

Proof: Bistar graph is a graph obtained by joining the central vertices of two copies of the star graphs $K_{1,m}$and $K_{1,n}$respectively. The graph has $|V| = (m+n) + 2$ and $|E| = (m+n) + 1$. Let u denote the central vertex of $K_{1,m}$ and let u_i $(i = 1,2,\dots,m)$ denote its pendant vertices. Similarly, let v represent the central vertex of $K_{1,n}$with $v_j (j = 1,2,\dots n)$ as its pendant vertices. We have $C = \{1,2,\dots,2(m+n)+3\}$. Next, let us try to label the vertices of the graph using the function $F: V \to C$ that follows.

$F(u) = 1,$

$F(v) = 2(m+1) + n$

$F(u_i) = 2(m+1) + n - 2i, \quad i = 1,2,\dots,m$

$F(v_j) = j + 1, \quad j = 1,2,\dots,n$

Once we give the labels to the vertices as such, we could find that all the vertices get distinct labels of C. We proceed to label the edges by finding the sum of the incident vertex labels. Edge function $F^*$from the edge set E onto the set $C\backslash F(V)$ is defined by,

$F^*(uu_i) = 2(m+1) + (n+1) - 2i, \quad i = 1,2,\dots,m$

$F^*(vv_j) = 2(m+1) + (n+1) + j, \quad j = 1,2,\dots,n$

$F^*(uv) = 2(m+1) + (n+1)$

On doing so, it could be seen that all the edges also receive distinct labels of members of C that were not given to the vertices. Taking all this into consideration, we may draw a conclusion that the graph admits s-cardinal labeling.The example in Figure 3defends the result.

Sum-cardinal labeling of cyclic graphs

Theorem 3: Globe graph $Gl(n)$admits sum-cardinal labeling.

Proof: Globe $Gl(n)$[8] is a graph obtained from two isolated vertices joined by n paths of length 2.It is P_3 when $n = 1$ and $C_4$when $n = 2$. P_3 and C_4 is labelled s-cardinally as given in Figure 4 below.

Take $n \geq 3$. Let u, u' denote the isolated vertices and $u_1, u_2, \dots, u_n$be the remaining vertices. $Gl(n)$ has $n + 2$ vertices and $2n$ edges and hence $|C| = 3n + 2$. We define $F: V \to C$ as,

$F(u) = n + 1,$

$F(u') = 2(n + 1),$

$F(u_i) = i, \quad i = 1,2, \dots, n$

These vertex functions induce edge functions F^* from E onto $C \backslash F(V)$ given by,

$F^*(uu_i) = (n + 1) + i, \quad i = 1,2, \dots, n$

$F^*(u'u_i) = 2(n + 1) + i, \quad i = 1,2, \dots, n$

On labeling the vertices and edges of the graph under F and F^*respectively, it could be seen that distinct members of C have been assigned as distinct labels to the nodes and edges. Also, edges receive the labels that are simply the sum of incident vertex labels. Hence, we may derive a conclusion that globe is sum-cardinal.Figure 5 portrays an example for sum-cardinal labeling of globe graph $Gl(n)$when $n = 7$.

Theorem 4: Complete Bipartite graph $K_{r,s}$satisfies sum-cardinal labeling.

Proof: Let $u_i (i = 1,2, \dots, r)$ and $v_j (j = 1,2, \dots, s)$be the vertices of $K_{r,s}$. We have $|V| = r + s$, $|E| = rs$ and $C = \{1,2, \dots, r + (r + 1)s\}$. Let us define the vertex function F to C by,

$F(u_i) = i, \ \ i = 1,2, \dots, r$

$F(v_j) = (r + 1)(s + 1 - j), \ \ j = 1,2, \dots, s$

The edge labels are generated by summation of the corresponding vertex labels. Down below are the induced edge functions F^* onto $C \backslash F(V)$.

$F^*(u_i v_j) = (r + 1)(s + 1 - j) + i, \quad i = 1,2, \dots, r, \quad j = 1,2, \dots, s$

On observation, we see that all the vertices and the edges receive definite labels from the set C.From this it becomes obvious that $K_{r,s}$satisfies s-cardinal labeling. Figure 6 is an example for complete bipartite graph admitting s-cardinal labeling.

Theorem 5: Crown graph $S_n^0$is not s-cardinal for $n > 3$.

Proof: The crown graph[9] for $n \geq 3$ is the graph with vertex sets $\{u_1, u_2, \dots, u_n\}$ and $\{v_1, v_2, \dots, v_n\}$ and edge set $\{u_i v_j : 1 \leq i, j \leq n, i \neq j\}$. It has $2n$ vertices and $n(n - 1)$ edges and so C becomes $C = \{1,2, \dots, n(n + 1)\}$. It is possible to label crown graph for $n = 3$ if we assign labels to the vertices of S_3^0 as given in the illustration (Figure 7). Let us now discuss for the case when $n \geq 4$.For sum-cardinal labeling, in order to obtain the edge labels within the set C it becomes essential to prioritize allocating the smaller members of C as vertex labels. So, without loss of generality, we take the labels of the vertices $u_i, i = 1,2, \dots, n$, as $\{1,2, \dots, n\}$ respectively. Now we are left with assigning the labels to the vertices $v_1, v_2, \dots, v_n$. First we allot vertex label '$n + 1$' to the vertex v_n. We then try to obtain edge labels in decreasing label value starting from the maximum label '$n(n + 1)$'. For this, we initially allot a vertex label 'n^2' to the first vertex position of the set $\{v_1, v_2, \dots, v_n\}$; i.e., to the vertex v_1. The edges incident with $v_1$will bear the labels $\{n(n + 1), n(n + 1) - 1, \dots, n^2 + 2\}$. Next vertex label will be assigned to the vertex v_{n-1}.This vertex bears the label '$n^2 - (n - 1)$'. Successive edge labels will thereby be assigned to the edges incident with v_{n-1} in decreasing order. The third vertex label '$n(n - 2)$' will be allocated to the vertex $v_2$and edges incident with it will receive their corresponding labels. In this way, subsequent vertex labels $\{n^2 - 3n + 2, (n^2 - 3n + 2) - (n + 1), (n^2 - 3n + 2) - 2(n + 1), \dots\}$ will be given to the vertices $\{v_{n-2}, v_3, v_{n-3}, \dots\}$ respectively taken in order. In this alternating vertex labeling pattern , the vertices strictly take the label that has been allocated first and does not take the successive label coinciding with the vertex positions that follows in this alternating labeling sequence (i.e., when $n = 4$,vertexv_2 bears

the label $n^2-(n-1)=13$, and not the label that has to be given to the vertex v_{n-2}, that is, $n^2-3n+2=6$). We have labelled in such a way so as to optimally allocate the elements of C to the vertices and edges of S_n^0. On doing so, it becomes obvious that at least one member of C gets repeated as an edge label. Since crown graph S_n^0 is a $(n-1)$-regular graph, the number of labels that gets repeated increases in a sequential order as n increases. Hence, we draw a conclusion that crown graph $S_n^0$is not sum-cardinal for $n \geq 4$.

General Observationsregarding Sum-cardinal labeling

Based on the definition of sum-cardinal labeling, the following observations are made.

1) If G is sum-cardinal, then $F: V \to C \backslash F^*(E)$ is bijective.
2) Labels 1 and 2 cannot be generated by F^*. So, it has to be assigned only to the vertices.
3) The maximum label, i.e.,$|C|$, can be assigned to a vertex of G only if it is a trivial graph.
4) The second maximum label '$|C|-1$' can be assigned to a vertex of a graph only when
   i. The assigned vertex is of degree 1.
   ii. The adjacent vertex bears the label 1.
5) The '$|C|-r$' label is assigned to a vertex of G only when adjacent vertex labels belong to the set $\{1,2,\ldots,r\}$.
6) In a random attempt to label a graph G sum-cardinally, an optimal choice of labeling G would be to initially allocate the smaller members of C to the vertices of G.

Result

It is impossible to label a graph $G(V,E)s$-cardinally by assigning only odd or even labels to the vertex set V of G except trivial graph.

Proof: The proof follows from observation (2).

CONCLUSION

The newly proposed sum-cardinal labeling has been inspected for somegraphs like star, bistar, complete bipartite graph, globe graph and crown graph. By the definition of s-cardinal labeling, certain observations are evident and have been compiled. Our next work aims in proving the definition for standard graphs like path, cycle etc.

REFERENCES

1. Rosa, "On certain valuations of the vertices of a graph", Theory of Graphs,International Symposium, Rome, July 1966 (1967), pp. 349-355.
2. R. L. Graham and N. J. A. Sloane, "On additive bases and harmonious graphs", SIAM J. Alg. Discrete Methods, 1 (1980), pp. 382-404.
3. J. A. Gallian, A dynamic survey of graph labeling, The Electronic Journal of Combinatorics, 24 (2021)
4. A. Punitha Tharani, S. Pratiksha, "Cardinal Labeling of Some Standard and Special Graphs", Indian Journal of Natural Sciences, Vol.15 / Issue 83 / Apr / 2024. pp.72878-72882.
5. Punitha Tharani, S. Pratiksha, "Cardinal labeling of H-graphs", Revista Electronica De Veterinaria,Vol. 25, No. 1, pp.2251-2259(2024)
6. Punitha Tharani, S. Pratiksha, "Cardinal labeling of graphs obtained from some graph operations", Proceedings of National Conference on Advances in Discrete Mathematics, ISBN: 978-93-94510-98-2. pp. 14-19 (2024)
7. D. B. West, An Introduction to Graph Theory, Prentice-Hall, (2002).
8. L Pandiselvi, A Nellai Murugan and, S Navaneethakrishnan, "V_4 Cordial Labeling of Fan and Globe", International Journal of Applied Research; 2(4).pp. 344-350 (2016).
9. Severini, Simone and Weisstein, Eric W. "Crown Graph." From MathWorld-A Wolfram Web Resource. https://mathworld.wolfram.com/CrownGraph.html.

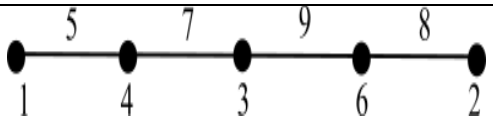

Figure 1: Sum-cardinal labeling of Path P_5

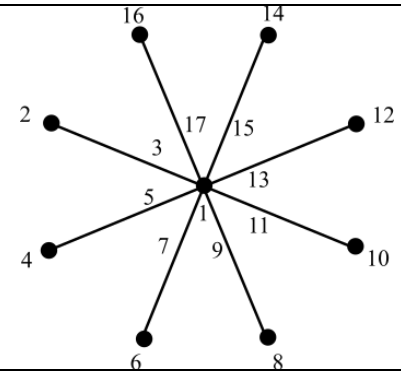

Figure 2: Sum-cardinal labeling of Star $K_{1,8}$

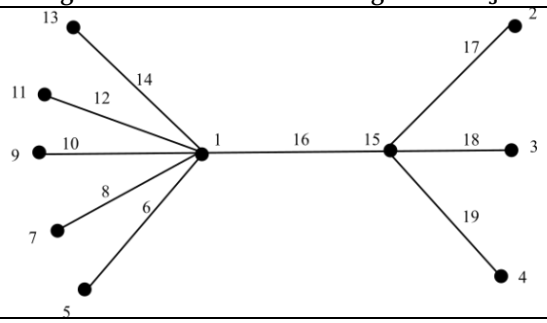

Figure 3:Sum-cardinal labeling of Bistar graph $(BS)_{5,3}$

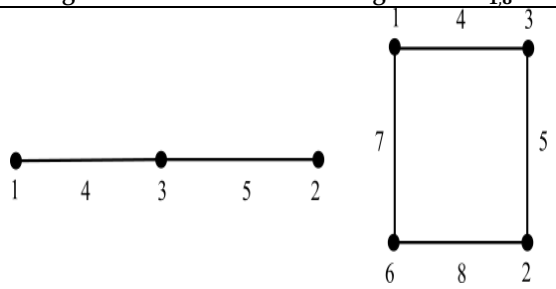

Figure 4:Sum-cardinal labeling of$P_3$and C_4

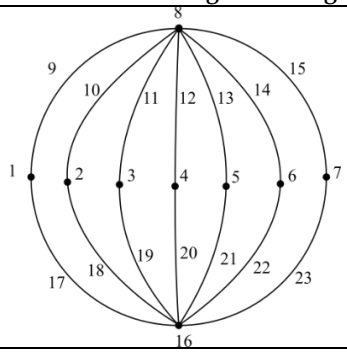

Figure 5:Sum-cardinal labeling of Globe graph Gl(7)

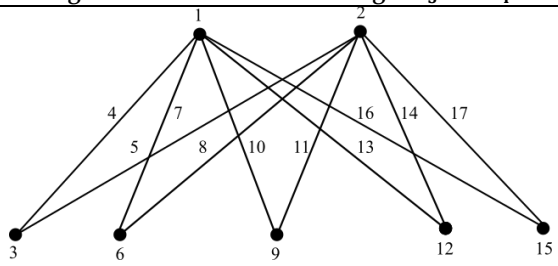

Figure 6: Sum-cardinal labeling of Complete Bipartite graph $K_{2,5}$

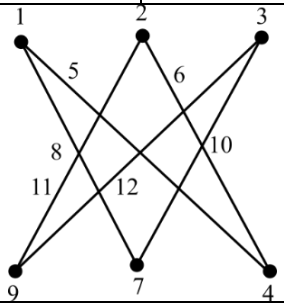

Figure 7:Sum-cardinal labeling of Crown graph S_3^0

Indian Journal of Natural Sciences *www.tnsroindia.org.in ©IJONS*

Vol.15 / Issue 88 / Feb / 2025 *International Bimonthly (Print) – Open Access* *ISSN: 0976 – 0997*

RESEARCH ARTICLE

Semitotal Edge Domination Number of Some Path and Cycle Related Graphs

A. Punitha Tharani[1] and D. Joslin Amala[2]*

[1]Associate Professor, Department of Mathematics, St. Mary's College (Autonomous), Thoothukudi, (Affiliated to Manonmaniam Sundaranar University, Abishekapatti, Tirunelveli), Tamil Nadu, India.
[2]Research Scholar, (Register No.22212212092001), Department of Mathematics, St. Mary's College (Autonomous), Thoothukudi, (Affiliated to Manonmaniam Sundaranar University, Abishekapatti, Tirunelveli), Tamil Nadu, India.

Received: 21 Nov 2024 Revised: 03 Dec 2024 Accepted: 27 Jan 2025

***Address for Correspondence**
D. Joslin Amala
Research Scholar, (Register No.22212212092001),
Department of Mathematics,
St. Mary's College (Autonomous),
Thoothukudi, (Affiliated to Manonmaniam Sundaranar University, Abishekapatti, Tirunelveli),
Tamil Nadu, India.
E.Mail: joslinamala123@gmail.com

ABSTRACT

In this paper, we introduce a new domination parameter analogous to semitotal domination number called semitotal edge domination number. A set D of edges in a graph G with no isolated edges is a semitotal edge dominating set if D is an edge dominating set of G and every edge in D is within distance 2 of another edge of D. The minimum cardinality of a semitotal edge dominating set of G is called the semitotal edge domination number and it is denoted by $\gamma_{t2e}(G)$. We determine the exact values of some standard graphs and also discuss some results on this parameter.

Keywords: graphs, semitotal domination, edge domination, semitotal edge domination.

INTRODUCTION

The graphs considered here are simple, finite, nontrivial, undirected and without isolated edges. The graph $G = (V, E)$ considered here have $n = |V|$ vertices and $m = |E|$ edges. Let G be a connected graph and$e_1 = (u_1, v_1), e_2 = (u_2, v_2)$ be two edges of G, the distance between the edges e_1 and e_2 is defined as $ed(e_1, e_2) = min\{d(u_1, u_2), d(u_1, v_2), d(v_1, u_2), d(v_1, v_2)\}$. If $ed(e_1, e_2) = 0$ then these edges are called neighbour edges[1]. The concept of semitotal domination was introduced by Wayne Goddard, Michael A. Henning and Charles A. McPillan[2]. The concept of edge domination was introduced by Mitchell and Hedetniemi[3]. A set D of edges in a graph G is called an edge dominating set if every edge in $E - D$ is adjacent to at least one edge in D. The edge

domination number $\gamma_e(G)$ is the minimum cardinality of an edge dominating set of G[4]. Any edge dominating set with $\gamma_e(G)$ edges is called a $\gamma_e(G)$ – set of G.Motivated by these domination parameters we introduce a new domination parameter called the semitotal edge domination number. In this paper we study the edge analogue of semitotal domination number.

Theorem[4]: For any connected graph$G$of order $p \geq 3$with$q$ edges and maximum degreeΔ', $\gamma_e(G) \geq \frac{q}{\Delta'+1}$.

METHODS

Definition: A set D of edges in a graph G with no isolated edges is a semitotal edge dominating set if D is an edge dominating set of G and every edge in D is within distance 2 of another edge of D. The minimum cardinality of a semitotal edge dominating set of G is called thesemitotal edge domination number and it is denoted by $\gamma_{t2e}(G)$.Any semitotal edge dominating set with $\gamma_{t2e}(G)$ edges is called a $\gamma_{t2e}(G)$ – set of G.

Example: For the graph G_1 in Figure 1, $D = \{e_2, e_5\}$ forms a $\gamma_{t2e}(G_1)$ – set. Hence $\gamma_{t2e}(G_1) = 2$.

Example: For the graph G_1 in Figure 1, $D = \{e_2, e_5\}$ forms a $\gamma_{t2e}(G_1)$ – set. Hence $\gamma_{t2e}(G_1) = 2$.

RESULTS AND DISCUSSION

Observation 1: Semitotal edge dominating set does not exist for all graphs if exists,
$\gamma_{te2}(G) \geq 2$.

Observation 2: Every semitotal edge dominating set is an edge dominating set but not conversely.

Example: For the graph G_2 in Figure 2, $D = \{e_2\}$ is an edge dominating set but not a semitotal edge dominating set.

Observation 3: If a spanning subgraph H of a graph G has a semitotaledge dominating set, then G also has a semitotaledge dominating set.

Observation 4: Let G be a connected graph and H be a spanning subgraph of G. If H has a semitotal edge dominating set then $\gamma_{t2e}(G) \leq \gamma_{t2e}(H)$.

Example: For the graph G_3 in Figure 3, $D = \{e_1, e_4\}$ is a$\gamma_{t2e}(G_3)$ – set and so $\gamma_{t2e}(G_3) = 2$. For the spanning subgraph $H_1$of G_3, $D = \{e_1, e_2, e_4, e_5\}$ is a $\gamma_{t2e}(H_1)$ – set and so $\gamma_{t2e}(H_1) = 4$. Hence $\gamma_{t2e}(G_3) < \gamma_{t2e}(H_1)$.For the spanning subgraph $H_2$of G_3, $D = \{e_1, e_5\}$is a $\gamma_{t2e}(H_2)$ – set and so $\gamma_{t2e}(H_2) = 2$. Hence$\gamma_{t2e}(G_3) = \gamma_{t2e}(H_2)$.

Exact values for some standard graphs

i) For any path P_n of order $n \geq 3$, $\gamma_{t2e}(P_n) = \begin{cases} 2, & n = 3,4 \\ \frac{n}{3}, & n \equiv 0\ (mod 3) \\ \frac{n-1}{3}, & n \equiv 1\ (mod 3) \\ \frac{n+1}{3}, & n \equiv 2\ (mod 3) \end{cases}$

ii) For any cycle C_n of order $n \geq 3$, $\gamma_{t2e}(C_n) = \begin{cases} 2, & n = 3 \\ \left\lceil \frac{n}{3} \right\rceil, & n \geq 4 \end{cases}$

iii) For any complete graph K_n of order $n \geq 3$, $\gamma_{t2e}(K_n) = \begin{cases} 2, & n = 3 \\ \left\lfloor \frac{n}{2} \right\rfloor, & n \geq 4 \end{cases}$

iv) For any complete bipartite graph $K_{m,n}$, $\gamma_{t2e}(K_{m,n}) = \begin{cases} 2, & m = 1, n \geq 2 \\ \min(m, n), & m, n \geq 2 \end{cases}$

Proof

(i) Let $G = P_n$ be a path of order $n \geq 3$. Let $E = \{e_j : 1 \leq j \leq n-1\}$ be the edge set of the path. For $n = 3,4$, it is clear from the definition that $\gamma_{t2e}(P_n) = 2$. For $n \equiv 0\ (mod 3)$, $D = \{e_2, e_5, e_8, \dots, e_{n-1}\}$ forms a $\gamma_{t2e}(G)$ – set. For $n \equiv 1\ (mod 3)$, $D = \{e_2, e_5, e_8, \dots, e_{n-2}\}$ forms a $\gamma_{t2e}(G)$ – set. For $n \equiv 2\ (mod 3)$, $D = \{e_2, e_5, e_8, \dots, e_{n-6}, e_{n-3}, e_{n-1}\}$ forms a $\gamma_{t2e}(G)$ – set. Hence the result follows.

(ii) Let $G = C_n$ be a cycle of order $n \geq 3$. Let $E = \{e_j : 1 \leq j \leq n\}$ be the edge set of the cycle. For $n = 3$, it is clear from the definition that $\gamma_{t2e}(C_n) = 2$. For $n \equiv 0\ (mod 3)$, $D = \{e_1, e_4, e_7, \dots, e_{n-2}\}$ forms a $\gamma_{t2e}(G)$ – set. For $n \equiv 1\ (mod 3)$, $D = \{e_1, e_4, e_7, \dots, e_{n-6}, e_{n-3}, e_{n-2}\}$ forms a $\gamma_{t2e}(G)$ – set. For $n \equiv 2\ (mod 3)$, $D = \{e_1, e_4, e_7, \dots, e_{n-1}\}$ forms a $\gamma_{t2e}(G)$ – set. Hence the result follows.

(iii) The proof follows from the definition of semitotal edge domination number.

(iv) Let $G = K_{m,n}$ be a complete bipartite graph.

Case (i) For $m = 1, n \geq 2$.

It represents the star graph $K_{1,n}$. Let $E = \{e_1, e_2, \dots, e_n\}$be the edge set of $K_{1,n}$. The edge e_j where $1 \leq j \leq n$ has maximum degree $n-1$. Thus an edge is enough to dominate the whole edge set of G. That is, $\gamma_e(G) - set = \{e_1\}$. Hence $D = \{e_1, e_j\}$ forms a $\gamma_{t2e}(G)$ – set, where $2 \leq j \leq n$and $e_j \in N(e_1)$. Therefore $\gamma_{t2e}(G) = 2$.

Case (ii) For $m, n \geq 2$.

Let $V = \{v_1, v_2, \dots, v_{m-1}, v_m, u_1, u_2, \dots, u_n\}$ be the vertex set and $E = \{e_{11}, e_{12}, \dots, e_{1n}, e_{21}, e_{22}, \dots e_{2n}, \dots, e_{m1}, e_{m2}, \dots, e_{mn}\}$ be the edge set of $K_{m,n}$ where $e_{11}, e_{12}, \dots, e_{1n}$ are the edges formed by connecting v_1 to the vertices $u_1, u_2, \dots, u_n$, also,$e_{21}, e_{22}, \dots e_{2n}$ are the edges formed by connectingv_2 to the vertices $u_1, u_2, \dots, u_n$ and similarly the edges $e_{31}, e_{32}, \dots e_{3n}, \dots, e_{m1}, e_{m2}, \dots, e_{mn}$ are obtained.Hence $D = \{e_{11}, e_{22}, e_{33}, \dots, e_{kk}\}$ where $k = \min(m, n)$ formsa$\gamma_{t2e}(G)$ – set. Therefore, $\gamma_{t2e}(G) = \min(m, n)$.

Theorem 1: For any connected graph G, $\gamma_e(G) \leq \gamma_{t2e}(G)$.

Proof: Every semitotal edge dominating set is an edge dominating set but not conversely, by observation 2, the result follows.

Theorem 2: For any connected graph G with $m \geq 2$ edges, $2 \leq \gamma_{t2e}(G) \leq m$.

Proof: The minimum cardinality of a semitotal edge dominating set is atleast two, by observation 1. Hence, for a connected graph G,with $m = 2$ edges, $\gamma_{t2e}(G) = m$. Thus the upper bound and the lower bound exists.

Theorem 3: For any connected graph$G$ of order $n \geq 3$ with$m$ edges and maximum degree Δ', then $\gamma_{t2e}(G) \geq \frac{m}{\Delta'+1}$.

Proof: We know that for any connected graph $G$of order $p \geq 3$with size q and maximum degree Δ',$\gamma_e(G) \geq \frac{q}{\Delta'+1}$[4]. By theorem 1, the result follows.

Theorem 4: For any connected graph G with $m \geq 2$ edgesand $\Delta'(G) = m-1$, $\gamma_{t2e}(G) = 2$.

Proof: Let G be a connected graph with an edge e of maximum degree $m-1$. Then $D = \{e, e_j\}$ is a minimum semitotal edge dominating set,where $e_j \in N(e)$. Hence $\gamma_{t2e}(G) = 2$.

Theorem 5: For any connected graph G with $m = 3$ edges, $\gamma_{t2e}(G) = m-1$ iff G is isomorphic to $P_4, C_3, K_{1,3}$.

Proof: Suppose G is isomorphic to $P_4, C_3, K_{1,3}$ then clearly $\gamma_{t2e}(G) = m-1$.

Conversely, let G be a connected graph with size 3 and $\gamma_{t2e}(G) = m - 1$. Let $D = \{e_1, e_2\}$ be the $\gamma_{t2e}(G)$ – setand $E - D = e_3$. Then obviously $\langle D \rangle = P_3$ or $K_2 \cup K_2$and $\langle E - D \rangle = K_2$. Let the degree of an edge e be denoted by $d(e)$. Since G is connected, there exists an edge e_1 *or* e_2 of P_3 is adjacent to $e_3$of K_2. Then $D = \{e_2, e_3\}$ is a minimum semitotal edge dominating set such that $\gamma_{t2e}(G) = m - 1$. If $d(e_1 \text{ or } e_2) = 2$ and $d(e_3) = 1$ then G is isomorphic to P_4. Since G is connected there exists an edge e_3 is adjacent to pendant vertices of both e_1 *and* $e_2$of P_3such that $d(e_1) = d(e_2) = d(e_3) = 2$. Then G is isomorphic to C_3. Since G is connected there exists an edge e_3 is incident to a vertex common to both e_1 and $e_2$of P_3such that $d(e_1) = d(e_2) = d(e_3) = 2$. Then G is isomorphic to $K_{1,3}$.

Theorem 6: For any connected graph G, with $m = 4$, $\gamma_{t2e}(G) = m - 2$ iff G is isomorphic to $P_5, C_4, K_{1,4}, K_{2,2}$ or any one of the graphs as shown in the Figure 4

Proof: Suppose G is isomorphic to $P_5, C_4, K_{1,4}, K_{2,2}$ or any one of the graphs as shown in the Figure 4, then clearly $\gamma_{t2e}(G) = m - 2$. Conversely, let Gbe a connected graph with size 4and $\gamma_{t2e}(G) = m - 2$. Let $D = \{e_1, e_2\}$ be the $\gamma_{t2e}(G)$ – setand $-D = \{e_3, e_4\}$. Then obviously $\langle D \rangle = P_3$(or)$K_2 \cup K_2$and $\langle E - D \rangle = P_3(or)K_2 \cup K_2$. Let the degree of an edge e be denoted by $d(e)$.

Case (i) $\langle D \rangle = P_3$and $\langle E - D \rangle = P_3$.
Since G is connected, there exists an edge e_1 *or* e_2 is adjacent to $e_3$ore_4. Then $D = \{e_2, e_3\}$ is a minimum semitotal edge dominating set such that $\gamma_{t2e}(G) = m - 2$. If $d(e_2) = d(e_3) = 2$ then G is isomorphic to P_5. Since G is connected there exists an edge e_3 is adjacent to both e_1 *and* $e_2$and e_4 is adjacent to either e_1 *or* e_2. Then $D = \{e_1, e_3\}$ is a minimum semitotal edge dominating set so that $\gamma_{t2e}(G) = m - 2$. If $d(e_1 \text{ or } e_2) = d(e_3) = 3$ and $d(e_4) = 2$ then G is isomorphic to G_4. Since G is connected there exists an edge e_3 and e_4 is adjacent toe_1 *and* e_2 respectively. Then $D = \{e_3, e_4\}$ is a minimum semitotal edge dominating set such that $\gamma_{t2e}(G) = m - 2$. If $d(e_1) = d(e_2) = d(e_3) = d(e_4) = 2$ then G is isomorphic to $K_{2,2}$. Since G is connected there exists a vertex common to both e_3 and $e_4$which is a common vertex of $e_1$and e_2. Then $D = \{e_1, e_4\}$ is a minimum semitotal edge dominating set such that $\gamma_{t2e}(G) = m - 2$. If $d(e_1) = d(e_2) = d(e_3) = d(e_4) = 3$ then G is isomorphic to $K_{1,4}$.

Case (ii) $\langle D \rangle = P_3$and $\langle E - D \rangle = K_2 \cup K_2$.
Since G is connected, there exists e_3 *and* e_4 is adjacent to e_1 ore_2 or both e_1 *and* e_2. Then $D = \{e_1, e_2\}$ is a minimum semitotal edge dominating set so that $\gamma_{t2e}(G) = m - 2$. If $d(e_1) = d(e_4) = 2$, $d(e_2) = 3$ and $d(e_3) = 1$ then G is isomorphic to G_5. If $d(e_2) = d(e_4) = 2$, $d(e_1) = 3$ and $d(e_3) = 1$ then G is isomorphic to G_6.

Theorem 7: For any connected graph G with $m \geq 4$edges and $\Delta'(G) = m - 2$, then $\gamma_{t2e}(G) = 2$.

Proof: Let G be a connected graph with size $m \geq 4$and $\Delta'(G) = m - 2$. Let e be an edge of G with maximum degree $m - 2$. Let $e_1, e_2, \ldots, e_{m-2}$ be edges adjacent to e. Since G is connected e_{m-1} is adjacent to e_j for some j, where $1 \leq j \leq m - 2$. Then $D = \{e, e_j\}$ is a minimum semitotal edge dominating set. Hence $\gamma_{t2e}(G) = 2$.

Theorem 8: For any connected graph $G$with $m \geq 5$ edgesand $\Delta'(G) = m - 3$, then $\gamma_{t2e}(G) = 2$ or 3.

Proof: Let Gbe a connected graph with size$m \geq 5$and $\Delta'(G) = m - 3$. Let $e$be an edge of maximum degree $m - 3$. Let $e_1, e_2, \ldots, e_{m-3}$ be edges adjacent to eLet e_{m-1} and e_{m-2} be the edges not adjacent to e

Case (i) Suppose e_{m-1} and e_{m-2} are not adjacent in G.Since G is connected, e_{m-1} and e_{m-2} are adjacent to e_i and e_j respectively for some$i, j \text{ and } i \neq j$where $1 \leq i, j \leq m - 3$. Then $D = \{e, e_i, e_j\}$ is a minimum semitotal edge dominating set. Hence $\gamma_{t2e}(G) = 3$

Case (ii)

Subcase (i) If e_{m-1} and e_{m-2} are adjacent in G, Since G is connected there exists e_i adjacent to both e_{m-1} and e_{m-2}, where $1 \leq i \leq m-3$. Then $D = \{e,\ e_i\}$ is a minimum semitotal edge dominating set. Hence $\gamma_{t2e}(G) = 2$.

Subcase (ii) If e_{m-1} and e_{m-2} are adjacent in G, Since G is connected there exists e_i adjacent toe_{m-1} or e_{m-2}, where $1 \leq i \leq m-3$. Then $D = \{e,\ e_{m-1}\}$ is a minimum semitotal edge dominating set. Hence $\gamma_{t2e}(G) = 2$.

CONCLUSION

In this paper we have determined the semitotal edge domination number of some standard graph and some results on this parameter are also discussed. Further, the bounds and its relationship with other graph theoretical parameters can also be investigated.

REFERENCES

1. Balci MA, Dunder P, Average Edge-Distance in Graphs, *Selcuk journal of Applied Mathematics*, Vol.11(2010), 63-70.
2. Wayne Goddard, Michael A. Henning, Charles A. McPillan, Semitotal Domination in Graphs, *Utilitas Mathematica*, Vol.94(2014), 67-81.
3. 3.Mitchell S, Hedetniemi S, Edge domination in trees, In: Proceedings of the Eigth Southern Conference on Combinatorics, Graph Theory and Computing, (1977), 489-509.
4. Kulli V.R, Sigarkanti S.C, The Connected Edge Domination Number of a Graph, Technical Report 8801, Department of Mathematics, Gulbarga University, India (1988)
5. Jayaram S.R, Line Domination in Graphs, *Graphs and Combinatorics,*Vol.3(1987), 357-363.
6. PunithaTharani A, Robina Tony A, Triple connected Line Domination Number of a Graph, *International Journal of basic and applied research,* Vol.8(2018), 494-500.
7. Teresa W. Haynes, Stephen Hedetniemi, Peter Slater, Fundamentals of Domination in Graphs, *CRC Press,* (1998).

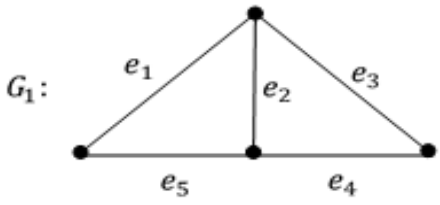

Figure 1

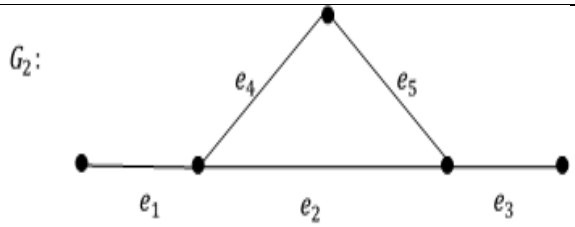

Figure 2

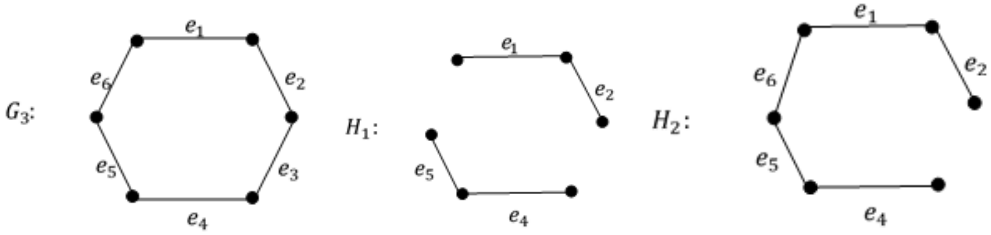

Figure 3

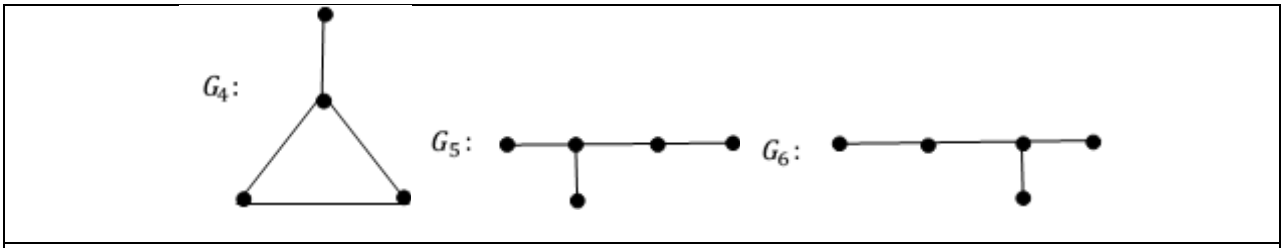

Figure 4

RESEARCH ARTICLE

Neutrosophic Interval Valued Gβ Closed Sets and its Properties

A. Divya[1] and M.Prasad[2]*

[1]Assistant Professor, PG and Research Department of Mathematics, Sri Ramakrishna College of Arts and Science (Autonomous), (Affiliated to Bharathiar University), Coimbatore, Tamil Nadu, India.
[2]Research Scholar (P/T), PG and Research Department of Mathematics, Sri Ramakrishna College of Arts and Science (Autonomous), (Affiliated to Bharathiar University), Coimbatore, Tamil Nadu, India.

Received: 21 Nov 2024 Revised: 03 Dec 2024 Accepted: 31 Jan 2025

***Address for Correspondence**
M.Prasad
Research Scholar (P/T),
PG and Research Department of Mathematics,
Sri Ramakrishna College of Arts and Science (Autonomous),
(Affiliated to Bharathiar University),
Coimbatore, Tamil Nadu, India.
E.Mail: mprasadkrishna@gmail.com

ABSTRACT

The main objective of this research article is to introduce a new kind of closed set called NIV(Gβ) closed set in Neutrosophic interval-valued topological spaces and also characterize and investigate about NIVGβ open sets with suitable examples. Fuzzy sets and intuitionistic fuzzy sets have been generalized to create neurosophic sets, which are used to represent the uncertain, imprecise, partial, and inconsistent information that can be found in the real world. Interval neutrosophic sets (INSs) have been designed to answer problems with a collection of numbers in the real unit interval instead of simply one specific integer. However, there are less reliable INS operations decision-making methods. characteristics and properties Neutrosophic interval-valued sets in the view of Neutrosophic interval-valued topological spaces. Using theorems and propositions, we conclude that the converse part of the theorems and counter examples are utilized. The operations for IVNSs are specified in this paper, The purpose of this research is to find new kind of NIV(Gβ) closed set in Neutrosophic interval valued topological spaces. And also characterise and investigate some properties of NIV Gβ closed sets and NIV Gβ open sets with suitable example,

Keywords: Neutrosophic Set , Interval valued Neutrosophic Set, Neutrosophic Interval valued topology, NIVG closed sets, NIVGβ open sets

INTRODUCTION

Zadeh[24] developed the fuzzy set in 1965, and various ideas and ways for handling imprecision and uncertainty have been put forth. Some theories, such as the intuitionistic fuzzy set put out by Atanassov[1] in the year 1986, Interval-valued fuzzy sets are another popular generalization of a regular fuzzy set. Zadeh[24] was the first to introduce the interval-valued fuzzy set. Subsequently, several authors looked into the subject and came up with

some insightful results. A subset of neutrosophy called the neutrosophic set investigates the genesis, make-up, and range of neutralities, as well as how they interact with other ideational spectra. A strong universal formal framework called the neutrosophic set has recently been developed. The neutrosophic set, albeit with technological specifications, must be made. To that end, we define the set-theoretic operations on a neutrosophic set instance, which we refer to as an interval neutrosophic set (INS). We demonstrate a number of INS attributes that are related to INS operations and relationships. Neutrosophic interval-valued soft topological spaces were introduced by Mukherjee A. in 2014. neutrosophic set where x = x(T, I, F) and T, I, and F are subintervals of [0, 1] and where x is an interval value on X. Lupianez examines the relationship between interval-value neutrosophic sets and topology. Numerous fields, including approximate reasoning, image processing, decision-making, pattern recognition, genetic algorithms, systems of categorization governed by rules, and mobile networks, utilize neutrosophic interval-valued sets. The idea of neutrosophic interval-valued topological space was put up and debated by T. Nanthini and A. Pushpalatha[17]. The purpose of this research is to find new kinds of Neutrosophic interval valued closed sets in Neutrosophic interval-valued topological spaces. And also characterize and investigate some properties of NIV Gβ closed sets and NIV Gβ open sets with suitable examples.

METHODOLOGY

Neutrosophic Set 2.1

Let X be a space of points (objects), with a generic element in X denoted by x. A Neutrosophic set ς_1 in X is characterized by a truth-membership function$T_{\varsigma_1}(x)$, a indeterminacy-membership function $I_{\varsigma_1}(x)$ and a falsity-membership function$F_{\varsigma_1}(x)$.

$T_{\varsigma_1}(x)$, $I_{\varsigma_1}(x)$ and $F_{\varsigma_1}(x)$are real standard or non-standard subsets of [0, 1].

That is $T_{\varsigma_1}(x) : X \rightarrow [0, 1]$,

$I_{\varsigma_1}(x) : X \rightarrow [0, 1]$,

$F_{\varsigma_1}(x) : X \rightarrow [0, 1]$.

There is no restriction on the sum of $T_{\varsigma_1}(x)$, $I_{\varsigma_1}(x)$ and $F_{\varsigma_1}(x)$,

so $0 - \leq \sup T_{\varsigma_1}(x) + \sup I_{\varsigma_1}(x) + \sup F_{\varsigma_1}(x) \leq 3 +$

Interval valued Neutrosophic Set 2.2

Let X be a space of points (objects), with a generic element in X denoted by x. An interval neutrosophic set (INS) ς_1 in X is characterized by truth-membership functionT_{ς_1}, indeterminacymembership function I_{ς_1} and falsity-membership function F_{ς_1}. For each point x in $T_{\varsigma_1}(x)$, $I_{\varsigma_1}(x)$ and $F_{\varsigma_1}(x) \subseteq [0, 1]$

Neutrosophic Interval valued set ς_1 is $\varsigma_1 = \{\langle [\inf T_{\varsigma_1}(x), \sup T_{\varsigma_1}(x)], [\inf I_{\varsigma_1}(x), \sup I_{\varsigma_1}(x)], [\inf F_{\varsigma_1}(x), \sup F_{\varsigma_1}(x)] \rangle\}$

Operators on Interval Neutrosophic Set 2.3

(i).$0_{NIV} = \langle [0,0], [0,0], [1,1] \rangle, 1_{NIV} = \langle [1,1], [1,1], [0,0] \rangle$,

(ii)The complement of an Neutrosophic Interval valued set ς_1 is

$$\varsigma_1^c = \begin{cases} T_{\varsigma_1^c}(x) = F_{\varsigma_1}(x) \\ \inf I_{\varsigma_1^c}(x) = 1 - \sup I_{\varsigma_1}(x) \\ \sup I_{\varsigma_1^c}(x) = 1 - \inf I_{\varsigma_1}(x) \\ F_{\varsigma_1^c}(x) = T_{\varsigma_1}(x) \end{cases}$$

(iii).The Containment relation of Neutrosophic Interval valued setς_1 and $\varsigma_2$are

$$\varsigma_1 \subseteq \varsigma_2 = \begin{cases} \left(\left(\inf T_{\varsigma_1}(x) \leq \inf T_{\varsigma_2}(x) \right), \left(\sup T_{\varsigma_1}(x) \leq \sup T_{\varsigma_2}(x) \right) \right), \\ \left(\left(\inf I_{\varsigma_1}(x) \leq \inf I_{\varsigma_2}(x) \right), \left(\sup I_{\varsigma_1}(x) \leq \sup I_{\varsigma_2}(x) \right) \right) \\ \left(\left(\inf F_{\varsigma_1}(x) \geq \inf F_{\varsigma_2}(x) \right), \left(\sup F_{\varsigma_1}(x) \geq \sup F_{\varsigma_2}(x) \right) \right) \end{cases}$$

(iv).The Union of Neutrosophic Interval valued set s ς_1 and $\varsigma_2$are

$$\varsigma_1 \cup \varsigma_2 = \begin{cases} \langle \vee(\inf T_{\varsigma_1}(x), \inf T_{\varsigma_2}(x)), \vee(\sup T_{\varsigma_1}(x), \sup T_{\varsigma_2}(x)) \rangle \\ \langle \vee(\inf I_{\varsigma_1}(x), \inf I_{\varsigma_2}(x)), \vee(\sup I_{\varsigma_1}(x), \sup I_{\varsigma_2}(x)) \rangle \\ \langle \wedge(\inf F_{\varsigma_1}(x), \inf F_{\varsigma_2}(x)), \wedge(\sup F_{\varsigma_1}(x), \sup F_{\varsigma_2}(x)) \rangle \end{cases}$$

(iv).The Intersection of interval Neutrosophic sets ς_1 and $\varsigma_2$are

$$\varsigma_1 \cap \varsigma_2 = \begin{cases} \langle \wedge(\inf T_{\varsigma_1}(x), \inf T_{\varsigma_2}(x)), \wedge(\sup T_{\varsigma_1}(x), \sup T_{\varsigma_2}(x)) \rangle \\ \langle \wedge(\inf I_{\varsigma_1}(x), \inf I_{\varsigma_2}(x)), \wedge(\sup I_{\varsigma_1}(x), \sup I_{\varsigma_2}(x)) \rangle \\ \langle \vee(\inf F_{\varsigma_1}(x), \inf F_{\varsigma_2}(x)), \vee(\sup F_{\varsigma_1}(x), \sup F_{\varsigma_2}(x)) \rangle \end{cases}$$

Definition 2.3 [10]

A Neutrosophic Interval valued topology (NIVT in short) on X is a family $N^{\tau}$of NS in N^{x} satisfying the following axioms.

1. $0_N, 1_N \in \tau_{\mathcal{N}}$
2. $J_1 \cap J_2 \in \tau_{\mathcal{N}}$ for any $J_1, J_2 \in \tau_{\mathcal{N}}$
3. $\cup J_i \in N^{\tau}$for any family $\{J_i | i \in j\} \subseteq \tau_{\mathcal{N}}$

In this case, the pair$(N^X, N^{\tau})$is called a Neutrosophic Interval valued topological space (NIVTS in short) and any NIVs in $\tau_{\mathcal{N}}$ is known as a Neutrosophic Interval valued open sets (NIVOS) in X. The complement V_1^{*c} of a NOS V_1^* in a NTS (N^X, N^{τ}). is called a Neutrosphic Interval valued closed sets (NIVCS) inX.

Definition 2.4

A NS $\varsigma_1 = \langle x, \mu_{\varsigma_1}, \sigma_{\varsigma_1}, \nu_{\varsigma_1} \rangle$ in a NIVTS $(X, \tau_{\mathcal{N}})$is called as

1. Neutrosophic Interval valued regular closed set [2] (NIV(R)CS in short) if $\varsigma_1 = N^{IVcl}(N^{IVint}(\varsigma_1))$
2. Neutrosophic Interval valued α-closed set] (NIV(α)CS in short) if $N^{IVcl}(N^{IVint}(N^{IVcl}(\varsigma_1))) \subseteq \varsigma_1$
3. Neutrosophic Interval valued semi closed set (NIV(S)CS in short) if $N^{IVint}(N^{IVcl}(\varsigma_1)) \subseteq \varsigma_1$
4. Neutrosophic Interval valued pre-closed set (NIV(P)CS in short) if $N^{IVcl}(N^{IVint}(\varsigma_1)) \subseteq \varsigma_1$
5. Neutrosophic Interval valued β-closed set(NIV(β)CS in short) if $N^{IVint}(N^{IVcl}(N^{IVint}(\varsigma_1))) \subseteq \varsigma_1$
6. Neutrosophic Interval valued generalized closed set [3] (N(G)CS in short) if $N^{IVcl}(\varsigma_1) \subseteq W$ whenever $\varsigma_1 \subseteq$ Wand W is a NIVOS in N^X.

RESULTS AND DISCUSSION

Neutrosophic interval valued Gβ closed sets

We presented the idea of the NIV(Gβ)CSs and investigated some of their fundamental traits.

Definition 3.1.1

A NIVs $\mathcal{K}_1$ in a NIVT $(\chi, \tau_{\mathcal{N}})$ is said to be a Neutrosophic interval valued generalized βclosed set (NIV(Gβ)CS for short) NIV(β)cl($\mathcal{K}_1$) $\subseteq \mathcal{W}$ whenever $\mathcal{K}_1 \subseteq \mathcal{W}$ and $\mathcal{W}$ is a NIVOS in $(\chi, \tau_{\mathcal{N}})$.

Example 3.1.2

Let $X = \{\mathcal{k}_1, \mathcal{k}_2\}$ Then $\tau_{\mathcal{N}} = \{0_{\mathcal{N}}, \upsilon_1, 1_{\mathcal{N}}\}$ is a NIVT on X where

$\upsilon_1 = \left\{\frac{\langle[0.5001,0.5002],[0.5001,0.5002],[0.5001,0.5002]\rangle}{\mathcal{k}_1}, \frac{\langle[0.4002,0.4003],[0.5001,0.5002],[0.6001,0.6002\rangle}{\mathcal{k}_2}\right\}$ and

NIVs$\varsigma_1 = \left\{\frac{\langle[0.4002,0.4003],[0.5001,0.5002],[0.6001,0.6002\rangle}{\mathcal{k}_1}, \frac{\langle[0.2001,0.2002],[0.5001,0.5002],[0.7002,0.7003]\rangle}{\mathcal{k}_2}\right\}$ is a NIV(Gβ)CS in $(X, \tau_{\mathcal{N}})$.

Theorem 3.1.3

Every NIVCS in $(X, \tau_{\mathcal{N}})$ is a NIV(Gβ)CS in $(X, \tau_{\mathcal{N}})$.

Proof

Let ς_1 be like a NIVCS in $(X, \tau_{\mathcal{N}})$. Consider that $\varsigma_1 \subseteq \mathcal{W}$ and $\mathcal{W}$ is a NIVOS in$(X, \tau_{\mathcal{N}})$. Then $(G\beta)cl(\varsigma_1) \subseteq NIVcl(\varsigma_1) = \varsigma_1 \subseteq \mathcal{W}$, by hypothesis. Hence ς_1 is a NIV(Gβ)CS in $(X, \tau_{\mathcal{N}})$.

Example 3.1.4

Let $X = \{\mathcal{k}_1, \mathcal{k}_2\}$,Then $\tau_{\mathcal{N}} = \{ 0_{\mathcal{N}}, \upsilon_1, 1_{\mathcal{N}} \}$ is a NIVT on X.

and $\upsilon_1 = \left\{\frac{\langle[0.5001,0.5002],[0.5001,0.5002],[0.5001,0.5002]\rangle}{\mathcal{k}_1}, \frac{\langle[0.4002,0.4003],[0.5001,0.5002],[0.6001,0.6002\rangle}{\mathcal{k}_2}\right\}$

Let $\varsigma_1 = \left\{\frac{\langle[0.4002,0.4003],[0.5001,0.5002],[0.6001,0.6002\rangle}{\mathcal{k}_1}, \frac{\langle[0.2001,0.2002],[0.5001,0.5002],[0.7002,0.7003]\rangle}{\mathcal{k}_2}\right\}$ be like a NIVs in X. Then ς_1 is a NIV(Gβ)CS but not a NIVCS in X.

Theorem 3.1.5

Every NIV(G)CS in $(X, \tau_{\mathcal{N}})$ is a NIV(Gβ)CS in $(X, \tau_{\mathcal{N}})$.

Proof

Let ς_1 be like a NIV(G)CS in $(X, \tau_{\mathcal{N}})$. Then if Consider that $\varsigma_1 \subseteq \mathcal{W}$ and $\mathcal{W}$ is a NIVOS in $(X, \tau_{\mathcal{N}})$. SinceNIV(Gβ)cl$(\varsigma_1) \subseteq$ NIVcl(ς_1) and NIVcl$(\varsigma_1) \subseteq \mathcal{W}$, by hypothesis, ς_1 is a NIV(Gβ)CS in X

Example 3.16

Let $X = \{\mathcal{k}_1, \mathcal{k}_2\}$,Then $\tau_{\mathcal{N}} = \{ 0_{\mathcal{N}}, \upsilon_1, 1_{\mathcal{N}} \}$is a NIVT on X.

And $\upsilon_1 = \left\{\frac{\langle[0.5001,0.5002],[0.5001,0.5002],[0.5001,0.5002]\rangle}{\mathcal{k}_1}, \frac{\langle[0.4002,0.4003],[0.5001,0.5002],[0.6001,0.6002\rangle}{\mathcal{k}_2}\right\}$

Let $\varsigma_1 = \left\{\frac{\langle[0.4002,0.4003],[0.5001,0.5002],[0.6001,0.6002\rangle}{\mathcal{k}_1}, \frac{\langle[0.2001,0.2002],[0.5001,0.5002],[0.7002,0.7003]\rangle}{\mathcal{k}_2}\right\}$

be like a NIVs in X. Then ς_1 is a NIV(Gβ)CS but not NIV(G)CS in X.

Theorem 3.1.7

Every NIV(β)CS in $(X, \tau_{\mathcal{N}})$ is a NIV(Gβ)CS in $(X, \tau_{\mathcal{N}})$.

Proof

Let ς_1 be like a NIV(β)CS in X. Consider that$\varsigma_1 \subseteq \mathcal{W}$, $\mathcal{W}$ is a NIVOS in $(X, \tau_{\mathcal{N}})$. Then since NIVβcl$(\varsigma_1) = \varsigma_1$,we have NIVβcl$(\varsigma_1) \subseteq \mathcal{W}$. Hence ς_1 is a NIV(Gβ)CS in $(X, \tau_{\mathcal{N}})$

Example 3.1.8

Let $X = \{\mathcal{k}_1, \mathcal{k}_2\}$ and

$\upsilon_1 = \left\{\frac{\langle[0.5001,0.5002],[0.5001,0.5002],[0.5001,0.5002]\rangle}{\mathcal{k}_1}, \frac{\langle[0.4002,0.4003],[0.5001,0.5002],[0.6001,0.6002\rangle}{\mathcal{k}_2}\right\}$.

Then $\tau_{\mathcal{N}} = \{ 0_{\mathcal{N}}, \upsilon_1, 1_{\mathcal{N}} \}$ is a NIVT on X.

Let $\varsigma_1 = \left\{\frac{\langle[0.4002,0.4003],[0.5001,0.5002],[0.6001,0.6002\rangle}{\mathcal{k}_1}, \frac{\langle[0.7002,0.7003],[0.5001,0.5002],[0.3002,0.3003]\rangle}{\mathcal{k}_2}\right\}$be like a NIVs in X. Then ς_1 is a NIV(Gβ)CS but not a NIV(β)CS in X.

Theorem 3.1.9

Every NIV(S)CS in $(X, \tau_{\mathcal{N}})$ is a NIV(Gβ)CS in $(X, \tau_{\mathcal{N}})$.

Proof

Let ς_1 be like a NIV(S)CS in $(X, \tau_{\mathcal{N}})$. Since every NIV(S)CS is a NIV(Gβ)CS and also we have ς_1 is a NIV(Gβ)CS in $(X, \tau_{\mathcal{N}})$.

Example 3.1.10

Let $X = \{\mathcal{k}_1, \mathcal{k}_2\}$and

$$\upsilon_1 = \left\{\frac{\langle[0.5001,0.5002],[0.5001,0.5002],[0.5001,0.5002]\rangle}{\mathcal{k}_1}, \frac{\langle[0.4002,0.4003],[0.5001,0.5002],[0.6001,0.6002\rangle}{\mathcal{k}_2}\right\}$$

Then $\tau_{\mathcal{N}} = \{ 0_{\mathcal{N}}, \upsilon_1, 1_{\mathcal{N}} \}$is a NIVT on X.
Let $\varsigma_1 = \left\{\frac{\langle[0.5001,0.5002],[0.5001,0.5002],[0.5001,0.5002]\rangle}{\hbar_1}, \frac{\langle[0.7002,0.7003],[0.5001,0.5002],[0.3002,0.3003]\rangle}{\hbar_2}\right\}$ be like a NIVs in X. Then ς_1 is a NIV(Gβ)CS but not a NIV(S)CS in X.

Theorem 3.1.11
Every NIV(P)CS in $(X, \tau_{\mathcal{N}})$ is a NIV(Gβ)CS in $(X, \tau_{\mathcal{N}})$.

Proof
The proof is obvious

Example 3.1.12
Let $X = \{\hbar_1, \hbar_2\}$ and

$$\upsilon_1 = \left\{\frac{\langle[0.5001,0.5002],[0.5001,0.5002],[0.5001,0.5002]\rangle}{\hbar_1}, \frac{\langle[0.6001,0.6002],[0.5001,0.5002],[0.4002,0.4003\rangle}{\hbar_2}\right\}$$

Then $\tau_{\mathcal{N}} = \{ 0_{\mathcal{N}}, \upsilon_1, 1_{\mathcal{N}} \}$is a NIVT on X.
Let $\varsigma_1 = \left\{\frac{\langle[0.5001,0.5002],[0.5001,0.5002],[05,0.5]\rangle}{\hbar_1}, \frac{\langle[0.7002,0.7003],[0.5001,0.5002],[0.3002,0.3003]\rangle}{\hbar_2}\right\}$
be like a NIVs in X. Then ς_1 is a NIV(Gβ)CS but not a NIV(P)CS in X.

Theorem 3.1.13
Every NIV(α)CS in $(X, \tau_{\mathcal{N}})$ is a NIV(Gβ)CS in $(X, \tau_{\mathcal{N}})$.

Proof
The proof is obvious.

Example 3.1.14
Let $X = \{\hbar_1, \hbar_2\}$ and$\upsilon_1 = \left\{\frac{\langle[0.5001,0.5002],[0.5001,0.5002],[0.5001,0.5002]\rangle}{\hbar_1}, \frac{\langle[0.6,0.6],[0.5001,0.5002],[0.4002,0.4003]\rangle}{\hbar_2}\right\}$
Then $\tau_{\mathcal{N}} = \{ 0_{\mathcal{N}}, \upsilon_1, 1_{\mathcal{N}} \}$ is a NIVT on X.
Let $\varsigma_1 = \left\{\frac{\langle[0.5001,0.5002],[0.5001,0.5002],[05,0.5]\rangle}{\hbar_1}, \frac{\langle[0.7002,0.7003],[0.5001,0.5002],[0.3002,0.3003]\rangle}{\hbar_2}\right\}$
be like a NIVs in X. Then ς_1 is a NIV(Gβ)CS but not a NIV(α)CS in $(X, \tau_{\mathcal{N}})$.

Theorem 3.1.15
Every NIV(R)CS in $(X, \tau_{\mathcal{N}})$ is a NIV(Gβ)CS in $(X, \tau_{\mathcal{N}})$.

Proof
The proof is obvious

Example 3.1.16
Let $X = \{\hbar_1, \hbar_2\}$ and

$$\upsilon_1 = \left\{\frac{\langle[0.5001,0.5002],[0.5001,0.5002],[0.5001,0.5002]\rangle}{\hbar_1}, \frac{\langle[0.4002,0.4003],[0.5001,0.5002],[0.6001,0.6002\rangle}{\hbar_2}\right\}$$

Then $\tau_{\mathcal{N}} = \{ 0_{\mathcal{N}}, \upsilon_1, 1_{\mathcal{N}} \}$ is a NIVT on X.
Let $\varsigma_1 = \left\{\frac{\langle[0.4002,0.4003],[0.5001,0.5002],[0.6001,0.6002\rangle}{\hbar_1}, \frac{\langle[0.2001,0.2002],[0.5001,0.5002],[0.7002,0.7003]\rangle}{\hbar_2}\right\}$
be like a NIVs in X. Then ς_1 is a NIV(Gβ)CS but not a NIV(R)CS in X

Diagram

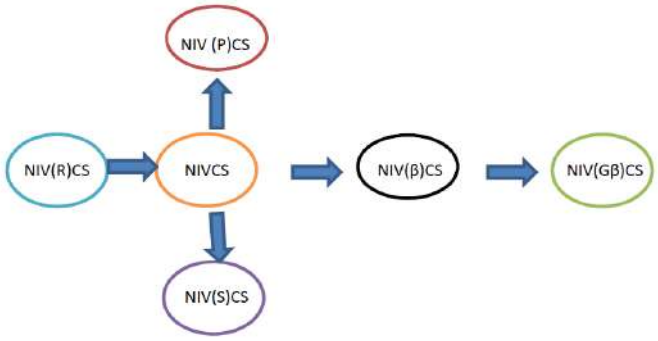

Remark 3.1.17

The union of any two NIV(Gβ)CS in $(X, \tau_{\mathcal{N}})$ is not a NIV(Gβ)CS in $(X, \tau_{\mathcal{N}})$ in general as seen from the following example

Example 3.1.18

Let $X = \{\hbar_1, \hbar_2\}$, $\upsilon_1 = \left\{\frac{\langle[0.7002,0.7003],[0.5001,0.5002],[0.3002,0.3003]\rangle}{\hbar_1}, \frac{\langle[0.8001,0.8002],[0.5001,0.5002],[0.2001,0.2002\rangle}{\hbar_2}\right\}$

$\upsilon_2 = \left\{\frac{\langle[0.6,0.6],[0.5001,0.5002],[0.4002,0.4003]\rangle}{\hbar_1}, \frac{\langle[0.7002,0.7003],[0.5001,0.5002],[0.3002,0.3003\rangle}{\hbar_2}\right\}$ and Then $\tau_{\mathcal{N}} = \{0_{\mathcal{N}}, \upsilon_1, \upsilon_2, 1_{\mathcal{N}}\}$is a NIVT on X.

Let $\varsigma_1 = \left\{\frac{\langle[0.6,0.6],[0.5001,0.5002],[04,0.4]\rangle}{\hbar_1}, \frac{\langle[0.4002,0.4003],[0.5001,0.5002],[0.3002,0.3003]\rangle}{\hbar_2}\right\}$

and $\varsigma_2 = \left\{\frac{\langle[0.4002,0.4003],[0.5001,0.5002],[0.4002,0.4003]\rangle}{\hbar_1}, \frac{\langle[0.8001,0.8002],[0.5001,0.5002],[0.2001,0.2002]\rangle}{\hbar_2}\right\}$ be two NIVS in X. Then ς_1 and ς_2 are NIV(Gβ)CS but $\varsigma_1 \cup \varsigma_2$ is not a NIV(Gβ)CS in X,

since $\varsigma_1 \cup \varsigma_2 = \left\{\frac{\langle[0.6,0.6],[0.5001,0.5002],[0.4002,0.4003]\rangle}{\hbar_1}, \frac{\langle[0.8001,0.8002],[0.5001,0.5002],[0.2001,0.2002]\rangle}{\hbar_2}\right\} \subseteq \varsigma_1$ but NIV(Gβ)cl $(\varsigma_1 \cup \varsigma_2)$ $= 1_{\mathcal{N}} \not\subset \varsigma_1$.

Remark 3.1.19

The intersection of two NIV(Gβ)CS in $(X, \tau_{\mathcal{N}})$ is not a NIV(Gβ)CS in $(X, \tau_{\mathcal{N}})$

Example 3.1.20

Let $X = \{\hbar_1, \hbar_2\}$ and $\upsilon_1 = \left\{\frac{\langle[0.5001,0.5002],[0.5001,0.5002],[0.5001,0.5002]\rangle}{\hbar_1}, \frac{\langle[0.6,0.6],[0.5001,0.5002],[0.4002,0.4003]\rangle}{\hbar_2}\right\}$.

Then $\tau_{\mathcal{N}} = \{0_{\mathcal{N}}, \upsilon_1, 1_{\mathcal{N}}\}$is a NIVT on X.

Let $\varsigma_1 = \left\{\frac{\langle[0.5001,0.5002],[0.5001,0.5002],[0.5001,0.5002]\rangle}{\hbar_1}, \frac{\langle[0.7002,0.7003],[0.5001,0.5002],[0.3002,0.3003]\rangle}{\hbar_2}\right\}$ and

$\varsigma_2 = \left\{\frac{\langle[0.6,0.6],[0.5001,0.5002],[0.4002,0.4003]\rangle}{\hbar_1}, \frac{\langle[0.6,0.6],[0.5001,0.5002],[0.4002,0.4003]\rangle}{\hbar_2}\right\}$ be like a NIVs in X.

Then ς_1 and ς_2 are NIV(Gβ)CS but $\varsigma_1 \cap \varsigma_2$ is not a NIV(Gβ)CS in X,

since $\varsigma_1 \cap \varsigma_2 = \left\{\frac{\langle[0.5001,0.5002],[0.5001,0.5002],[0.5001,0.5002]\rangle}{\hbar_1}, \frac{\langle[0.6,0.6],[0.5001,0.5002],[0.4002,0.4003]\rangle}{\hbar_2}\right\} \subseteq \upsilon_1$ but NIV(Gβ)cl$(\varsigma_1 \cap \varsigma_2) = 1_{\mathcal{N}} \not\subset \upsilon_1$.

Theorem 3.1.21

Let $(X, \tau_{\mathcal{N}})$ be like a NIVT. Then for every $\varsigma_1 \in$NIV(Gβ)C(X) and for every $\varsigma_2 \in$ NIVs(X), $\varsigma_1 \subseteq \varsigma_2 \subseteq$NIV(Gβ)cl$(\varsigma_1)$ implies $\varsigma_2 \in$NIV(Gβ)C(X)

Proof

Let $\varsigma_2 \subseteq \mathcal{W}$ and $\mathcal{W}$ be an NIVOS in $(X, \tau_{\mathcal{N}})$. Then $\varsigma_1 \subseteq \varsigma_2 \varsigma_1 \subseteq \mathcal{W}$ By hypothesis, $\varsigma_2 \subseteq$ NIV(Gβ)cl (ς_1). Therefore NIV(Gβ)cl(ς_2)⊆NIV(Gβ)cl(NIV(Gβ)cl(ς_1))=NIV(Gβ)cl(ς_1)⊆$\mathcal{W}$ since ς_1 is a NIV(Gβ)CS in $(X, \tau_{\mathcal{N}})$. Hence $\varsigma_2 \in$ NIV(Gβ)C(X).

Theorem 3.1.22

Let $(X, \tau_{\mathcal{N}})$ be like a NIVT. Then every NIVS in $(X, \tau_{\mathcal{N}})$ is a NIV(Gβ)CS in $(X, \tau_{\mathcal{N}})$ If And only If NIV(Gβ)O(X) = NIV(Gβ)C(X).

Proof

Necessity

Suppose that every NIVs in $(X, \tau_{\mathcal{N}})$ is a NIV(Gβ)CS in $(X, \tau_{\mathcal{N}})$. Let $\mathcal{W} \in$ NIVO(X). Then W ∈ NIV(Gβ)(X) and by hypothesis, NIV(Gβ)cl($\mathcal{W}$)=$\mathcal{W}$ NIV(Gβ)cl($\mathcal{W}$)

This implies NIV(Gβ)cl($\mathcal{W}$) =. Therefore $\mathcal{W} \in$NIV(Gβ)C(X). HenceNIV(Gβ)O(X)⊆ NIV(Gβ)C(X) Let $\varsigma_1 \in$NIV(Gβ)C(X). Then $\varsigma_1^c \in$NIV(Gβ)O(X) ⊆NIV(Gβ)C(X). That is $\varsigma_1^c \in$NIV(Gβ)C(X). Therefore $\varsigma_1 \in$NIV(Gβ)O(X). Hence NIV(Gβ)C(X) ⊆NIV(Gβ)O(X). Thus NIV(Gβ)O(X) =

NIV(Gβ)C(X).

Sufficiency

Suppose that NIV(Gβ)O(X) = NIV(Gβ)C(X). Let $\varsigma_1 \subseteq \mathcal{W}$ and $\mathcal{W}$ be like a NIVOS in $(X, \tau_{\mathcal{N}})$. Then $\mathcal{W} \in$NIV(Gβ)O(X) and NIV(Gβ)cl(ς_1)⊆NIV(Gβ)cl($\mathcal{W}$)=$\mathcal{W}$, since $\mathcal{W} \in$NIV(Gβ)C(X), by hypothesis. Therefore ς_1 is a NIV(Gβ)CS in X.

Theorem 3.1.23

If ς_1 is a NIVOS and a NIV(Gβ)CS in $(X, \tau_{\mathcal{N}})$, then ς_1 is a NIV(Gβ)CS in $(X, \tau_{\mathcal{N}})$.

Proof

Since $\varsigma_1 \subseteq \varsigma_1$ and ς_1 is a NIVOS in $(X, \tau_{\mathcal{N}})$, by hypothesis, NIV(Gβ)cl(ς_1)⊆ς_1. But $\varsigma_1 \subseteq$NIV(Gβ)cl(ς_1). Therefore NIV(Gβ)cl(ς_1) = ς_1. Hence ς_1 a NIV(Gβ)CS in $(X, \tau_{\mathcal{N}})$.

Theorem 3.1.24

For a NIVs ς_1 in $(X, \tau_{\mathcal{N}})$, the following conditions are equivalent:

(i) ς_1 is a NIVOS and a NIV(Gβ)CS in $(X, \tau_{\mathcal{N}})$,

(ii) ς_1 is a NIV(R)OS in $(X, \tau_{\mathcal{N}})$.

Proof

(i) ⇒ (ii) Let ς_1 be like a NIVOS and a NIV(Gβ)CS in $(X, \tau_{\mathcal{N}})$. Then NIV(Gβ)cl(ς_1)⊆ς_1.

Since NIV(Gβ)cl(ς_1) is a NIV(Gβ)CS, then there exists a NIV(P)OSς_2 such that NIVint(ς_2)⊆ NIV(Gβ)cl(ς_1)⊆ς_2 and NIVcl(NIVint(ς_2))⊆ς_2.

Now

NIVint (NIVcl (NIVint (NIV(Gβ)cl(ς_1)

))) ⊆ NIVint (NIVcl (NIVint(ς_2))) ⊆ NIVint(ς_2)⊆IV(Gβ)cl(ς_1). Now NIVint $\left(\text{NIVcl}\left(\text{NIVint}(\varsigma_1)\right)\right)$

⊆NIVint $\left(\text{NIVcl}\left(\text{NIVint}\left(\text{NIV}(G\beta)\text{cl}(\varsigma_1)\right)\right)\right)$

⊆NIV(Gβ)cl(ς_1). Therefore $\varsigma_1 \cup$NIVint(NIVcl (NIVint(ς_1)))⊆ NIV(Gβ)cl(ς_1) ⊆ς_1.

This implies that (NIVcl(NIVint(ς_1))) ⊆ς_1. Since ς_1 is a NIVOS, NIVint(ς_1)= ς_1. Therefore NIVint (NIVcl(ς_1))⊆ς_1. Since ς_1 is a NIVOS, it is a NIV(P)OS. Hence $\varsigma_1 \subseteq$ NIVint(NIVcl(ς_1)). Therefore ς_1 = NIVint (NIVcl(ς_1)). Hence ς_1 is a NIV(R)OS in $(X, \tau_{\mathcal{N}})$.

(ii) ⇒ (i) Let ς_1 be like a NIV(R)OS in $(X, \tau_{\mathcal{N}})$. Therefore ς_1 = NIVint (NIVcl(ς_1)). Since every NIV(R)OS is a NIVOS, ς_1 is a NIVOS and $\varsigma_1 \subseteq \varsigma_1$. This implies that NIVint (NIVcl(ς_1))⊆ς_1. That is NIVint (NIVcl (NIVint(ς_1))) = NIVint(NIVcl(ς_1)) ⊆ς_1. Thus ς_1 is a NIV(β)CS. Hence ς_1 is a NIV(Gβ)CS in $(X, \tau_{\mathcal{N}})$.

Theorem 3.1.25

Let $(X, \tau_{\mathcal{N}})$ be like a NIVT. Then for every $\varsigma_1 \in NIV(G\beta)C(X)$ and for every NIVsς_2 in X, $NIVint(\varsigma_1) \subseteq \varsigma_2 \subseteq \varsigma_1$ implies $\varsigma_2 \in NIV(G\beta)CS(X)$.

Proof

Let ς_1 be like a NIV(Gβ)CS in X. Then, there exists an NIV(P)OS, say $\varsigma_3$such that $NIVint(\varsigma_3) \subseteq \varsigma_1 \subseteq \varsigma_3$.By hypothesis,$\varsigma_2 \subseteq \varsigma_1$.Therefore $\varsigma_2 \subseteq \varsigma_3$.Since $(\varsigma_3) \subseteq \varsigma_1$, $NIVint(\varsigma_3) \subseteq NIVint(\varsigma_1)$ and $NIVint(\varsigma_3) \subseteq \varsigma_2$. Thus $NIVint(\varsigma_3) \subseteq \varsigma_2 \subseteq \varsigma_3$ and $\varsigma_2 \in NIV(G\beta)C(X)$. Hence, $\varsigma_2 \in NIV(G\beta)C(X)$

Properties of Neutrosophic interval Valued Gβ Open Sets

The concept has been presented in this section.NIV(Gβ)OS and investigated some of their fundamental traits.

Definition 3.2.1

The complement ς_1^c of a NIV(Gβ)CS ς_1 If A NIVT$(X, \tau_{\mathcal{N}})$ is called an Neutrosophic interval Valued generalized βopen sets (NIV(Gβ)OS for short) in X.

Theorem 3.2.2

EveryNIVOS, NIVGOS, NIVsOS, NIV(P)OS, NIV(Gβ)OS, NIVαOS, NIV(β)OS and NIV(R)OS is a NIV(Gβ)OS

Example 3.2.3

Let $X = \{\hbar_1, \hbar_2\}$ and $\upsilon_1 = \left\{\frac{\langle[0.5001,0.5002],[0.5001,0.5002],[0.5001,0.5002]\rangle}{\hbar_1}, \frac{\langle[0.4002,0.4003],[0.5001,0.5002],[0.6001,0.6002\rangle}{\hbar_2}\right\}$

Then $\tau_{\mathcal{N}} = \{0_{\mathcal{N}}, \upsilon_1, 1_{\mathcal{N}}\}$ is a NIVT on X.

Let $\varsigma_1 = \left\{\frac{\langle[0.6,0.6],[0.5001,0.5002],[0.4002,0.4003]\rangle}{\hbar_1}, \frac{\langle[0.7002,0.7003],[0.5001,0.5002],[0.2001,0.2002\rangle}{\hbar_2}\right\}$ be like a NIVS in X. Then ς_1 is a NIV(Gβ)OS but not a NIVOS, NIVGOS, NIVROS in$(X, \tau_{\mathcal{N}})$.

Example 3.2.4

Let $X = \{\hbar_1, \hbar_2\}$ and

$$\upsilon_1 = \left\{\frac{\langle[0.5001,0.5002],[0.5001,0.5002],[0.5001,0.5002]\rangle}{\hbar_1}, \frac{\langle[0.6,0.6],[0.5001,0.5002],[0.4002,0.4003]\rangle}{\hbar_2}\right\}$$

Then $\tau_{\mathcal{N}} = \{0_{\mathcal{N}}, \upsilon_1, 1_{\mathcal{N}}\}$is a NIVT on X.

Let $\varsigma_1 = \left\{\frac{\langle[0.5001,0.5002],[0.5001,0.5002],[0.5001,0.5002]\rangle}{\hbar_1}, \frac{\langle[0.3002,0.3003],[0.5001,0.5002],[0.7002,0.7003]\rangle}{\hbar_2}\right\}$

be like a NIVs in X.Then ς_1 is a NIV(Gβ)OS in X.but not a NIV(Gβ)OS, NIV(P)OS, NIV(S)OS, NIV(β)OS and NIV(α)OS in X.

Remark 3.2.5

The union of any two NIV(Gβ)OS in $(X, \tau_{\mathcal{N}})$ need not be like a NIV(Gβ)OS in $(X, \tau_{\mathcal{N}})$ in general.

Example 3.2.6

Let $X = \{\hbar_1, \hbar_2\}$ and $\upsilon_1 = \left\{\frac{\langle[0.5001,0.5002],[0.5001,0.5002],[0.5001,0.5002]\rangle}{\hbar_1}, \frac{\langle[0.6,0.6],[0.5001,0.5002],[0.4002,0.4003]\rangle}{\hbar_2}\right\}$.

Then $\tau_{\mathcal{N}} = \{0_{\mathcal{N}}, \upsilon_1, 1_{\mathcal{N}}\}$is a NIVT on X.

Let $\varsigma_1 = \left\{\frac{\langle[0.5001,0.5002],[0.5001,0.5002],[0.5001,0.5002]\rangle}{\hbar_1}, \frac{\langle[0.3002,0.3003],[0.5001,0.5002],[0.7002,0.7003]\rangle}{\hbar_2}\right\}$

And $\varsigma_2 = \left\{\frac{\langle[0.4002,0.4003],[0.5001,0.5002],[0.6001,0.6002\rangle}{\hbar_1}, \frac{\langle[0.4002,0.4003],[0.5001,0.5002],[0.6001,0.6002\rangle}{\hbar_2}\right\}$ be NIVS in X. Then ς_1 and ς_2 are NIV(Gβ)OS but $\varsigma_1 \cup \varsigma_2$ is not a NIV(Gβ)OS in X.

Remark 3.2.7

The intersection of any two NIV(Gβ)OS in $(X, \tau_{\mathcal{N}})$ need not be like a NIV(Gβ)OS in $(X, \tau_{\mathcal{N}})$ in general.

Example 3.2.8

Let $X = \{\hbar_1, \hbar_2\}$ and

$$\upsilon_1 = \left\{\frac{\langle[0.7002,0.7003],[0.5001,0.5002],[0.3002,0.3003]\rangle}{\hbar_1}, \frac{\langle[0.8001,0.8002],[0.5001,0.5002],[0.2001,0.2002]\rangle}{\hbar_2}\right\}$$

And$\upsilon_2 = \left\{\frac{\langle[0.6,0.6],[0.5001,0.5002],[0.4002,0.4003]\rangle}{\hbar_1}, \frac{\langle[0.7002,0.7003],[0.5001,0.5002],[0.3002,0.3003]\rangle}{\hbar_2}\right\}$.

Then $\tau_{\mathcal{N}} = \{0_{\mathcal{N}}, \upsilon_1, \upsilon_2, 1_{\mathcal{N}}\}$is a NIVT on X.

Let $\varsigma_1 = \left\{\frac{\langle[0.4002,0.4003],[0.5001,0.5002],[0.6001,0.6002\rangle}{\hbar_1}, \frac{\langle[0.3002,0.3003],[0.5001,0.5002],[0.4002,0.4003]\rangle}{\hbar_2}\right\}$

And $\varsigma_2 = \left\{\frac{\langle[0.4002,0.4003],[0.5001,0.5002],[0.4002,0.4003]\rangle}{\hbar_1}, \frac{\langle[0.2001,0.2002],[0.5001,0.5002],[0.8001,0.8002]\rangle}{\hbar_2}\right\}$

be two NIVs in X. Then ς_1 and ς_2 are NIV(Gβ)OS but $\varsigma_1 \cap \varsigma_2$ is not a NIV(Gβ)OS in X.

Theorem 3.2.9

Let $(X, \tau_{\mathcal{N}})$ be like a NIVT. Then for every $\varsigma_1 \in$NIV(Gβ)O(X) and for every $\varsigma_2 \in$NIVs(X), NIV(Gβ)int(ς_1) $\subseteq \varsigma_2 \subseteq \varsigma_1$ implies $\varsigma_2 \in$NIV(Gβ)O(X).

Proof

Let ς_1 be like any NIV(Gβ)OS of X and ς_2 any NIVs of X. By hypothesis NIV(Gβ)int(ς_1) $\subseteq \varsigma_2 \subseteq \varsigma_1$. Then ς_1^c is a NIV(Gβ)CS in X and $\varsigma_1^c \subseteq \varsigma_2^c \subseteq$NIV(Gβ)cl$(\varsigma_1)^C$. Then ς_2^c is a NIV(Gβ)CS in $(X, \tau_{\mathcal{N}})$.Therefore ς_2 is a NIV(Gβ)OS in $(X, \tau_{\mathcal{N}})$. Hence $\varsigma_2 \in$NIV(Gβ)O(X).

Theorem 3.2.10

Let $(X, \tau_{\mathcal{N}})$ be like a NIVT. Then for every $\varsigma_1 \in$NIVs(X) and for every $\varsigma_2 \in$NIVPO(X), $\varsigma_2 \subseteq \varsigma_1 \subseteq$NIVcl (NIVint($\varsigma_2$)) implies $\varsigma_1 \in$NIV(Gβ)O(X).

Proof

Let ς_2 be like a NIV(P)OS in $(X, \tau_{\mathcal{N}})$. Then $\varsigma_2 \subseteq$ NIVint(NIVcl(ς_2)).

By hypothesis, $\varsigma_1 \subseteq$NIVcl(NIVint(ς_2))$\subseteq$ NIVcl(NIVint(NIVin (NIVcl(ς_2))))

$\subseteq$NIVcl$\left(\text{NIVint}\left(\text{NIVcl}(\varsigma_2)\right)\right) \subseteq$NIVcl (NIVint (NIVcl($\varsigma_1$))).Therefore ς_1 is a NIV(β)OS then ς_1 is a NIV(Gβ)OS in $(X, \tau_{\mathcal{N}})$. Hence $\varsigma_1 \in$NIV(Gβ)O(X).

Theorem 3.2.11

A NIVsς_1 of a NIVT$(X, \tau_{\mathcal{N}})$ is a NIV(Gβ)OS in $(X, \tau_{\mathcal{N}})$ If And only if E $\subseteq$ NIV(Gβ)int(ς_1) whenever E is a NIVCS in $(X, \tau_{\mathcal{N}})$ and E $\subseteq \varsigma_1$

Proof

Necessity: Suppose ς_1 is a NIV(Gβ)OS in $(X, \tau_{\mathcal{N}})$. Let E be like a NIVCS in $(X, \tau_{\mathcal{N}})$ such that E $\subseteq \varsigma_1$. Then E^C is a NIVOS and $\varsigma_1^c \subseteq E^C$. By hypothesis ς_1^c is a NIV(Gβ)CS in $(X, \tau_{\mathcal{N}})$,

we have NIV(Gβ)cl(ς_1^c) $\subseteq E^C$. Therefore E $\subseteq$NIV(Gβ)int(ς_1).

Sufficiency: Let $\mathcal{W}$ be like a NIVOS in $(X, \tau_{\mathcal{N}})$ such that $\varsigma_1^c \subseteq$ W. By hypothesis, $W^C \subseteq$NIV(Gβ)int(ς_1). Therefore NIV(Gβ)cl(ς_1^c)$\subseteq$ W and ς_1^c is a NIV(Gβ)CS in $(X, \tau_{\mathcal{N}})$. Hence ς_1 is a NIV(Gβ)OS in $(X, \tau_{\mathcal{N}})$.

Theorem 3.2.12

Let $(X, \tau_{\mathcal{N}})$ be like a NIVT. Then for every $\varsigma_1 \in$NIV(Gβ)O(X) and for every NIVsς_2 in X, $\varsigma_1 \subseteq \varsigma_2 \subseteq$ NIVcl(ς_1) implies $\varsigma_2 \in$NIV(Gβ)O(X).

Proof

Let ς_1 be like a NIV(Gβ)OS in X. Then, there exists an NIV(P)OS, say ς_3 such that $\varsigma_3 \subseteq \varsigma_1 \subseteq$NIVcl($\varsigma_3$). Therefore $\varsigma_3 \subseteq \varsigma_2$ and NIVcl(ς_1) $\subseteq$ NIVcl(ς_3). Thus $\varsigma_3 \subseteq \varsigma_2 \subseteq$ NIVcl(ς_3). Hence ς_2 is a NIV(Gβ)OS in X. Then ς_2 is a NIV(Gβ)OS in X.

Applications of Neutrosophic Interval Valued Generalized β Closed Sets:
We have presented various application examples of NIV(Gβ)CS.

Definition 3.3.1
If every NIV(Gβ)CS in $(X, \tau_{\mathcal{N}})$ is a NIV(Gβ)CS in $(X, \tau_{\mathcal{N}})$, then space may be described as a Neutrosophic interval valued β $T_{\frac{1}{2}}$ (NIV(Gβ) $T_{\frac{1}{2}}$ for short) space.

Theorem 3.3.2
A NIVTS$(X, \tau_{\mathcal{N}})$ is a NIV(Gβ) $T_{\frac{1}{2}}$ space If And only if NIV(Gβ)O(X) = NIV(Gβ)O(X).

Proof
Necessity: Let ς_1 be like a NIV(Gβ)OS in $(X, \tau_{\mathcal{N}})$. Then ς_1^c is a NIV(Gβ)CS in $(X, \tau_{\mathcal{N}})$. By hypothesis, ς_1^c is a NIV(Gβ)CS in $(X, \tau_{\mathcal{N}})$ and therefore ς_1 is a NIV(Gβ)OS in $(X, \tau_{\mathcal{N}})$. Hence NIV(Gβ)O(X) = NIV(Gβ)O(X).
Sufficiency: Let ς_1 be like a NIV(Gβ)CS in $(X, \tau_{\mathcal{N}})$. Then be an is a NIV(Gβ)OS in $(X, \tau_{\mathcal{N}})$. By hypothesis, ς_1^c is a NIV(Gβ)OS in $(X, \tau_{\mathcal{N}})$ and therefore ς_1 is a NIV(Gβ)CS in $(X, \tau_{\mathcal{N}})$. Hence $(X, \tau_{\mathcal{N}})$ is a NIV(Gβ) $T_{\frac{1}{2}}$ space.

Remark 3.3.3
Not every NIV(Gβ) $T_{\frac{1}{2}}$ space is a NIV$T_{\frac{1}{2}}$ space. This can be seen easily by the following example. *Example 3.3.4*

Let $X = \{\hbar_1, \hbar_2\}$ and let $\tau_{\mathcal{N}} = \{ 0_{\mathcal{N}}, \upsilon_1, 1_{\mathcal{N}} \}$
where $\upsilon_1 = \left\{\frac{\langle[0.5001,0.5002],[0.5001,0.5002],[0.5001,0.5002]\rangle}{\hbar_1}, \frac{\langle[0.4002,0.4003],[0.5001,0.5002],[0.6001,0.6002]\rangle}{\hbar_2}\right\}$.
Then X is a NIV(Gβ) $T_{\frac{1}{2}}$ space but not a NIV$T_{\frac{1}{2}}$ –space.

Theorem 3.3.5
Let $(X, \tau_{\mathcal{N}})$ be like a NIVTS and let X be like a NIV(Gβ)$T_{\frac{1}{2}}$space. Consequently, the subsequent criteria are equivalent:

(i) $\varsigma_1 \in$NIV(Gβ)C(X),
(ii) NIVint (NIVcl (NIVint(ς_1))) $\subseteq \varsigma_1$,
(iii) NIVint(ς_1) $\in$NIVRO(X).

Proof
(i) ⇒ (ii) Let ς_1 be like a NIV(Gβ)CS in $(X, \tau_{\mathcal{N}})$. Then since X is a NIV(Gβ) $T_{\frac{1}{2}}$ space, ς_1 is a NIV(Gβ)CS in X. Since every NIV(Gβ)CS is a NIV(β)CS, we have NIVint (NIVcl (NIVint(ς_1))) $\subseteq \varsigma_1$.
(ii) ⇒ (iii) If NIVint(NIVcl(NIVint(ς_1) $\subseteq \varsigma_1$, then NIVint(ς_1) = NIVint (NIVcl (NIVint(ς_1))). Hence NIVint (ς_1) $\in$NIVRO(X).
(iii) ⇒ (i) Since NIVint(ς_1) is a NIV(R)OS in $(X, \tau_{\mathcal{N}})$.NIVint(ς_1) = NIVint(NIVcl(NIVint(ς_1))) and since NIVint(ς_1) $\subseteq \varsigma_1$, NIVint(NIVcl(NIVint(ς_1))) $\subseteq \varsigma_1$. Therefore ς_1 is a NIV(β)CS in $(X, \tau_{\mathcal{N}})$. Hence $\varsigma_1 \in$NIV(Gβ)C(X).

Definition 3.3.6
A NIVTS$(X, \tau_{\mathcal{N}})$ is said to be like a Neutrosophic interval valued β $T^*_{1/2}$ space (NIV(Gβ) $T^*_{1/2}$space for short) If every NIV(Gβ)CS is a NIVCS in $(X, \tau_{\mathcal{N}})$.

Remark: 3.3.7
Every NIV(Gβ) $T^*_{1/2}$ space is a NIV(Gβ) $T_{\frac{1}{2}}$ space.

Proof
Assume $(X, \tau_{\mathcal{N}})$ be like a NIV(Gβ)$T^*_{1/2}$ space. Let ς_1 be like a NIV(Gβ)CS in$(X, \tau_{\mathcal{N}})$. By hypothesis, ς_1 is aNIVCS. Hence ς_1 is a NIV(Gβ)CS in $(X, \tau_{\mathcal{N}})$. Thus $(X, \tau_{\mathcal{N}})$ is a NIV(Gβ) $T_{\frac{1}{2}}$ space.

Example 3.3.8
Let $X = \{\hbar_1, \hbar_2\}$ and $\tau_{\mathcal{N}} = \{ 0_{\mathcal{N}}, \upsilon_1, 1_{\mathcal{N}} \}$ be like a NIVT on X, where

$\upsilon_1 = \left\{\frac{\langle[0.5001,0.5002],[0.5001,0.5002],[0.5001,0.5002]\rangle}{\kappa_1}, \frac{\langle[0.4002,0.4003],[0.5001,0.5002],[0.6001,0.6002\rangle}{\kappa_2}\right\}$.

Then $(X, \tau_{\mathcal{N}})$ is a NIV(Gβ) $T_{\frac{1}{2}}$ space, but not a NIV(Gβ)$T^*_{1/2}$ space, since the NIVS$\upsilon_1$is a NIV(Gβ)CS in $(X, \tau_{\mathcal{N}})$ but not a NIVCS in $(X, \tau_{\mathcal{N}})$, as NIVcl$(\upsilon_1) = \upsilon_1^C \neq \upsilon_1$

CONCLUSION

The attributes of the neutrosophic interval valued set are presented in this work (INS). The concepts of union, intersection, complement, connection, and Intersection are discussed with suitable example .The definition of composition is based on the interval neutrosophic set. NIV sets Applying the theory to the logic inference system based on the interval neutrosophic set practical applications in fields like data mining, expert systems, database, bioinformatics, and question-and-answer systems, etc. A number of attributes have been demonstrated for set-theoretic operators. Neutrosophic interval valued Generalized closed sets are introduced in Neutrosophic interval valued topological spaces and also fundamental properties are discussed with suitable example. This system has a wide real life applications in Neutrosophic interval valued topological spaces

REFERENCES

1. Atanassov.K, Neutrosophic sets, Fuzzy Sets and Systems 20,87-95. (1986)
2. Arokiarani.I, Dhavaseelan.R, Jafari.S, Parimala.M: On Some New Notions and Functions in Neutrosophic topological spaces, Neutrosophic Sets and Systems, Vol. 16 (2017), pp. 16-19.DOI: doi.org/10.5281/zenodo.831915.
3. Atkinswestley.AChandrasekar.S,Neutrosophic Weakly G*-closed sets,Advances in Mathematics: Scientific Journal 9 (2020), no.5, 2853–2861.DOI: DOI:https://doi.org/10.37418/amsj.9.5.47
4. Atkinswestley.AChandrasekar.S,, Neutrosophicϱ#S closed sets in Neutrosophic topological spaces,Malaya Journal of Matematik, Vol. 8, No. 4, 1786-1791, 2020,DOI:https://doi.org/10.26637/MJM0804/0076
5. Atkinswestley.AChandrasekar.S,, Neutrosophic ϱ*-Closed Sets and its maps,Neutrosophic Sets and Systems, Vol. 36, 2020,96-107,
6. DOI:https://digitalrepository.unm.edu/nss_journal/vol36/iss1/8
7. Banupriya.V,.Chandrasekar.S: Neutrosophic αgs Continuity and Neutrosophic αgs Irresolute Maps, Neutrosophic Sets and Systems, vol. 28, 2019, pp. 162-170. DOI: 10.5281/zenodo.3382531
8. Banupriya.V,.Chandrasekar.S and Suresh.M, Neutrosophic α-generalized semi homeomorphisms,Malaya Journal of Matematik, Vol. 8, No. 4, 1824-1829, 2020.DOI :10.26637/MJM0804/0082
9. R.Dhavaseelan, S.Jafari, and Hanifpage.md.:Neutrosophic generalized α-contra-continuity, creat. math. inform. 27, no.2, 133 - 139,(2018),DOI:10.37193/CMI.2018.02.05
10. FlorentinSmarandache.:, Neutrosophic and NeutrosophicLogic, First International Conference On Neutrosophic, Neutrosophic Logic, Set, Probability, and Statistics University of New Mexico, Gallup, NM 87301, USA, smarand@unm.edu,(2002)
11. FloretinSmarandache.:, Neutrosophic Set: - A Generalization of Neutrosophic set, Journal of Defense Resources Management1,107-114,(2010).
12. Ishwarya.P, and Bageerathi..K, On Neutrosophicsemiopen sets in NTSs, International Jour. of Math. Trends and Tech. , 214-223,(2016). DOI : https://doi.org/10.14445/22315373/IJMTT-V37P529
13. Jayanthi..D αGeneralized closed Sets in NTSs, International Journal of Mathematics Trends and Technology (IJMTT)- Special Issue ICRMIT March (2018).
14. Mary Margaret.A, andTrinita Pricilla.M.,Neutrosophic Vague Generalized Pre-closed Sets in Neutrosophic Vague Topological Spaces,International Journal of Mathematics And its Applications,Volume 5, Issue 4-E, 747-759.(2017).
15. Lupianez, Interval neutrosophic sets and topology. Emerald Group publishing limited, vol 38. Nos 3/4, 2009,DOI https://doi.org/10.1108/03684920910944849

16. Mukherjee.A, Datta.M and Smarandache.F, Neutrosophic Interval valued soft topological spaces, Neutrosophic Sets and Systems, Vol 6, 2014.
17. Mondal TK and Samanta.S, Topology of interval – valued Fuzzy sets, Indian Journal Pure appl.Math.30(1):23-38(1999),DOI:10.1016/S0165-0114(98)00436-9
18. Nanthini.T and Pushpalatha.A, Interval valued Neutosophic Topological Space ,Neutrosophic Sets and Systems, Vol. 32, 2020,52-60.
19. Rajesh kannan.T , Chandrasekar.S,Neutosophic $\omega\alpha$-closed sets in Neutrosophic topological spaces, Journal Of Computer And Mathematical Sciences,vol.9(10),1400-1408 Octobe2018. DOI:10.29055/jcms/882
20. Rajesh kannan.T , Chandrasekar.S, Neutosophic α-continuous multifunction in Neutrosophic topological spaces, The International Journal of Analytical and Experimental Modal Analysis, Volume XI,IssueIX,September 2019,1360-9367
21. Rajesh kannan.T , Chandrasekar.S, Neutrosophic α-Irresolute Multifunction In Neutrosophic topological spaces, " Neutrosophic Sets and Systems 32, 1 (2020),390-400. DOI:https://digitalrepository.unm.edu/nss_journal/vol32/iss1/25
22. Rajesh kannan.T , Chandrasekar.S ,NeutrosophicPRE $-\alpha$, SEMI $-\alpha$ and PRE $-\beta$ irresolute open and closed mappings in Neutrosophic topological spaces,Malaya Journal of Matematik, Vol. 8, No. 4, 1795-1806, 2020,
23. DOI :10.26637/MJM0804/0078
24. Salama.A.A and Alblowi.S.A.., Generalized Neutrosophic Set and Generalized NTSs, Journal computer Sci. Engineering, Vol.(ii),No.(7)(2012).
25. Shanthi. V.K.,Chandrasekar.S, SafinaBegam.K, Neutrosophic Generalized Semi-closed Sets In NTSs, International Journal of Research in Advent Technology Vol.(ii),6, No.7,1739-1743, July (2018)
26. Zadeh.L.A., "Fuzzy sets", Information and control, Vol.8 (1965), 338 –353.

RESEARCH ARTICLE

Pulmonary Fibrosis Inquest: A Meticulous Examination

Ahamed Johnsha Ali. S[1]* and D. Kannan[2]

[1]Research Scholar, Department of Computer Science, Pollachi College of Arts and Science, Pollachi, (Affiliated to Bharathiyar University, Coimbatore), Tamil Nadu, India.
[2]Professor and Principal, Department of Computer Science Pollachi College of Arts and Science, Pollachi, (Affiliated to Bharathiyar University, Coimbatore), Tamil Nadu, India.

Received: 21 Nov 2024 Revised: 03 Dec 2024 Accepted:25 Jan 2025

***Address for Correspondence**
Ahamed Johnsha Ali. S
Research Scholar,
Department of Computer Science,
Pollachi College of Arts and Science, Pollachi,
(Affiliated to Bharathiyar University, Coimbatore),
Tamil Nadu, India.
E.Mail: ahamed.doit@gmail.com

ABSTRACT

Pulmonary fibrosis (PF) is the term for lung scarring, which typically results from an infection or inflammation happening on lungs. Habitually, lung tissue functions similarly to a sponge, opening and closing to exchange carbon dioxide and oxygen. The lung is less flexible and stiffer than it ought to be because of the scar tissue. The oxygen levels are consequently lower than they ought to be. Different category of damages will be happed on the lungs to the people who infected with COVID-19. Images of those infected lungs will be diagnosed to ascertain the magnitude of the infection based on tissue or airway damage. This paper briefs the review with definition, classification, and underlying symptomology of bronchioles lung disease (BLD) survey is conducted on this disease by gathering information from open dataset based on images like Computed Tomography Scan (CT) and X-RAY. This includes the details on patient's symptoms, medical history, lifestyle factors, and treatment experiences. Information is also collected from healthcare providers who have treated patients with pulmonary fibrosis. Lastly, we scrutinize the metaphors and explicit peril aspect of the serene to facilitate may contribute to PF and go over ways to subordinate the prospect of pulmonary complications and sequelae.

Keywords: PFT, CT Scans, bronchoscopy, HRCT, Spirometry, Oximetry, COPD

INTRODUCTION

Pulmonary fibrosis is a stipulation that grounds blemish and coagulate the lungs. It is a type of interstitial lung disease, which speaks about the collection issues that have effects the tissue and spaces (interstitium) around the air sacs in the lungs. Chronic lung disease called pulmonary fibrosis results in coagulating, tautness, and blemishing of lung tissue, which crafts breathing exigent. The diseases widen when lung tissue is dented and the body retorts by creating superfluous gristly tissue (fibrosis) inside the lungs, which ultimately reinstate the hale and hearty lung tissue. Although the cause of pulmonary fibrosis (idiopathic) is frequently unknown, certain drugs, autoimmune illnesses, and exposure to environmental pollutants can all be contributing factors. Chest pain, exhaustion, and a persistent dry cough are among the symptoms. Options for treatment include drugs, oxygen physiotherapy, pulmonary psychotherapy, and, in assured circumstances, lung transplantation. The aureate origination of pulmonary fibrosis is correlate with environmental subjection, such as unveiling to asbestos, silica dust, and certain chemicals, in addition to that specific medications, septicity and autoimmune disorders.The main cause of pulmonary disease can vary depending on the specific type of pulmonary disease. Smoking is the number one risk factor for the magnification of pulmonary malady, together with lung melanoma and chronic obstructive pulmonary disease (COPD) [1]. COPD is characteristically sourced by long-term revelation to exasperating gases or particulate stuff, the majority habitually commencing cigarette smoulder [2]. Pulmonary fibrosis is a process that causes lung scarring, in which fibrotic tissue blocks the movement of oxygen from inside the tiny air sacs in the lungs into the bloodstream[3][4]. Diffuse interstitial pneumonitis is a staid unceasing malady that impinges on the tissue adjoining the coelenterons, in the pleura. These stipulations enlarge whilst to facilitate pleura tissue befall chunky and taut for mysterious grounds [5].

STATEMENT OF ISSUE

Several diagnostic methodologies have been used to find out the pulmonary fibrosis which is occurred in damaged Lung. Hereditary influence will be examining by the medical experts based on the symptoms and illness happened on the lungs. To identify whether it is a genetic susceptibility this is from their family history. Next, doctors will perform a corporeal evaluation by using a stethoscope to listen to the patient's lungs for abnormal resonance, like crackles or wheezing. Your lung function may be evaluated using a variety of tests. A pulmonary function test (PFT) measures air volume, flow, and exchange to determine how well your lungs are functioning. Imaging tests that provide thorough images of your lungs and show any scarring or fibrosis include high-resolution CT scans and X-rays. A tiny camera tube may occasionally be used during a bronchoscopy to directly inspect your airways and take tissue samples. Blood testing aid in the exclusion of other illnesses including infections or autoimmune diseases that have symptoms that are similar. In the end, a biopsy is used to remove a tiny sample of tissue for microscopic inspection, which yields a conclusive diagnosis of fibrosis or scarring. This integrated method guarantees precise diagnosis of the underlying lung problem and directs the most effective itinerary of healing. It is imperative to exertion intimately in the midst of a healthcare bringer to establish the unsurpassed diagnostic approach for detecting pulmonary fibrosis-related lung damage. Untimely revealing and treatment can help dawdling the succession of the malady and perk up the outcomes.

Manifestations of Pulmonary Fibrosis

The indication of pulmonary fibrosis can enlarge unhurriedly more instant and may perhaps embrace squatness of inhalation, particularly for the period of corporeal bustle, desiccated and pushy cough, weariness and flaw, impenetrable credence trouncing, Chest discomposure or soreness, Hippocratic fingers and toes, Bluish lips or skin due to lack of oxygen, Difficulty breathing or rapid breathing, Reduced exercise tolerance, Respiratory infections. The condition can progress over time, leading to more severe symptoms and complications, such as pulmonary hypertension and respiratory failure.

Anxiety

A combination of the patient's medical history, physical examination, lung function tests, and imaging studies is usually used to diagnose pulmonary fibrosis (for instance, X-ray or CT scan), and sometimes a lung biopsy. Treatment options for pulmonary fibrosis may include medications to slow down the string of the malady, such as corticosteroids and impervious tyrannical nostrum; oxygen psychoanalysis, pulmonary psychoanalysis, and lung resettle in rigorous manifestation. To deal with their infirmity and conserve their eminence of existence, populace with cryptogenic fibrosing alveolitis must join forces narrowly with their healthcare proficient.

Age Groups

Pulmonary fibrosis can affect individuals of all ages, but it is further universally established in person of mature age around 50 years of age or elder. It is less common in brood and adolescent. While pulmonary fibrosis can transpire at any epoch, certain risk factors can increase the likelihood of developing the disease. A number of factors enhance your jeopardy of embryonic cryptogenic fibrosing alveolitis. Age does influence because older people are more likely to get the condition. In addition, men are more susceptible than women. Smoking raises the risk significantly; it is a well-known health risk. Environmental pollutants such as silica and asbestos can also cause the condition to develop. Lastly, genetics might be at play since some hereditary kinds are handed down through the generations. Understanding these risk factors is crucial for initiatives aimed at prevention and rising awareness. Pulmonary fibrosis is a serious lung condition that can affect people of various age groups. While the disease primarily impacts older adults, it can also occur in younger individuals. The management, symptoms, and support needed can vary based on age groups, so it's essential to consider these differences in care and awareness. Paediatric pulmonary fibrosis refers to cases of lung scarring or fibrosis that occur in children and adolescents. Pulmonary fibrosis can occur in young adults (18-35), impacting individuals in their late teens to mid-thirties. Cryptogenic fibrosing alveolitis is more frequently diagnosed in grown-up adults (36-64). Pulmonary fibrosis is most prevalent in the elderly population (65+). Pulmonary fibrosis can affect individuals of all age groups, and the approach to diagnosis, treatment, and support should be tailored to each specific age category. Additionally, raising awareness and conducting delve into to enhanced recognize the age-specific aspects of the disease is crucial for on the road to recovery the lives of those pretentious by pulmonary fibrosis.

Growing Global Health

Studies have suggested that pulmonary fibrosis is a growing global health concern, with an increasing number of cases being diagnosed each year. According to estimates from the American Lung Association, approximately 200,000 people in the United States are living with Idiopathic fibrosing alveolitis, the largely widespread outward appearance of pulmonary fibrosis. IPF is also estimated to affect approximately 3 million people worldwide. In Europe, the pervasiveness of Lung scarring is ballpark to be approximately 5-10 cases per 100,000 people. These estimates possibly will perchance ebb and flow contingent on the specific population being studied and the methods used to collect data. Overall, the pervasiveness of Lung scarring is likely to amplify in the imminent lifetime ascribed to features like aging populations and increased environmental exposures to toxins and pollutants. It is important for healthcare providers and policymakers to work together to improve verdict, treatment, and supervision of pulmonary fibrosis to help ebb the burden of this ailment on folks and communities.

Bereavement Pace

The Bereavement Pace of Lung scarring can fluctuate depending on an assortment of aspects such as the indispensable derivation of the malady, the relentlessness of the stipulation, and the era and general vigour of the serene. The lung malady known as pulmonary fibrosis is a long-term, progressive stipulation that grounds the lung tissue to blemish and solidify, blighting lung role. Studies have exposed that people with pulmonary fibrosis often subsist for two to five years after being detected. The survival rate can vary greatly, and some people may live for many years with the disease. It is paramount to linger cognizant that manoeuvre diagnosis and care can augment excellence of life and reduce the disease's succession. Medication, oxygen psychoanalysis, pulmonary physiotherapy, and in certain situations, lung transplants are possible forms of treatment.

These rates are based on data from the United States from 2000 to 2019. As you can see the death rate from pulmonary fibrosis increases significantly with age. It is imperative that these rates are only estimates and might show a discrepancy contingent on the population studied. If you are concerned about your menace of emerging Lung scarring, talk to your doctor.

Treatment and Management of Pulmonary Fibrosis

Although usual interstitial pneumonia does not yet have alleviate, there are a numeral healings that can be worn to direct indications and impediment the infirmity course. In relentless circumstance, lung transplantation is one of these healing, beside with linctus, oxygen psychoanalysis, and pulmonary rehabilitation. For pulmonary fibrosis unwearied to subsist longer and have a privileged prospect of endurance, untimely verdict and conduct are indispensable.

Looms To Appraise Conduct Effectiveness Or Comprehend Syndrome Succession:

To weigh up healing efficiency or realize malady headway in pulmonary fibrosis, assorted judgment technique can be engaged. Here is some frequently used loom: PFTs, or Body plethysmography, endow with a porthole hooked on the vigour of your lungs by abetting in the diagnosis and follow-up of malady like fibrosis, COPD, and asthma. Consider these an assessment of your ability to hold your breath! Spirometry records the force and velocity of your exhalations during PFTs, identifying any obstructions to airflow. Diffusion capacity, on the other hand, evaluates how well your lungs deliver oxygen to your blood. Together, these tests provide a complete picture of your lung function, which can be used to diagnose, track the course of the condition, and evaluate the efficacy of treatment. Therefore, if you're worried about your breathing, ask your doctor about PFTs—quick and painless methods to make sure your lungs are functioning at their peak. A number of additional methods provide insight into pulmonary fibrosis and its consequences outside of pulmonary function testing. Characteristic fibrotic alterations and patterns are shown by high-resolution CT scans (HRCT), which provide precise information about lung tissue features. The six-minute stride trial (6MWT) evaluates functional ability and exercise tolerance, providing information on the course of the disease and how well a treatment is working. Furthermore, the impact of the condition on day-to-day functioning is captured by quality-of-life measures such as the SF-36 or SGRQ. Blood biomarkers that show the activity and course of a disease include KL-6, SP-D, and MMPs. HRCT images are analyzed visually or quantitatively using radiographic scoring systems such as the Warrick or Ashcroft score to measure the level of fibrosis and track its evolution. A lung biopsy can sometimes offer a conclusive diagnosis, gauge the severity of the condition, and determine how well a treatment is working. It's imperative to memo that the choice of evaluation methods may diverge depending on the specific research question, available resources, and individual patient characteristics. Additionally, clinical trials and research studies often employ a combination of these methods to comprehensively evaluate treatment efficacy or disease progression in pulmonary fibrosis. Consulting with a healthcare professional or a specialized pulmonologist is crucial to conclude the largely apt evaluation strategy for an individual patient or research study.

MENACE ASPECT IN IDIOPATHIC DIFFUSE INTERSTITIAL PULMONARY FIBROSIS CASES

Chronic interstitial pneumonitis is a multifarious stipulation with an assortment of impending menace features. Whilst the literal cause of many cases relics unheard of numerous aspect have been coupled with an amplified menace of embryonic chronic interstitial pneumonitis. Pulmonary fibrosis propensity is sporadically lofty throughout numerous contributing factors. This disorder is more frequent amongst people over 50. For instance, when compared to non-smokers, smoking to a large extent amplifies peril, besides perpetrators include hitches and hazardous gist. Certain chemical, air fumes, and filth that rivet asbestos, coal, and silica may elicit respiratory mayhems. In secluded instances, heredity contributes an indispensable part; conjugal mutations of the malady have been coupled to customary gene amendment. Chronic GERD and certain autoimmune diseases valour also elevate peril medication; predominantly chemotherapy drugs, antibiotics, and some anti-inflammatory or cardiovascular medications, have been correlated to the enlargement or succession of pulmonary fibrosis in some individuals. Other health conditions like viral infections, digestive disorders, and chronic kidney disease are also potential contributing factors. Understanding these diverse risk factors can empower early detection and prevention strategies. Consult your doctor

with any concerns about your lung health. It's important to note that having one or more menace factors does not inevitably connote an individual will develop pulmonary fibrosis. The interaction between these risk factors and individual susceptibility is complex and can vary from person to person.

CRAM INVENT

The "best" study design for lung disease research depends its strengths and limitations. Irrefutable tryouts are indispensable for estimate healing helpfulness, while legion cram and case-control studies can help scrutinize peril factors and malady associations. It's often beneficial to use a combination of study designs to obtain a comprehensive understanding of the disease. The choice of study design should consider the research question, available resources, feasibility, and ethical considerations. sound out in the midst of connoisseur in the meadow can assist establishing the most appropriate study design for a specific lung disease research investigation.

Retrospective Cohort Study

In a retrospective cohort study, researchers analyze existing data from medical records or databases. Participants are classified into exposed and unexposed groups based on their previous exposures or risk factors. Data on exposure and disease outcomes are collected retrospectively. The study assesses the association between exposure and disease outcome by comparing the incidence or prevalence of the outcome in exposed and unexposed groups.

Strengths

Utilizes existing data, allows for assessment of long-term outcomes, and can evaluate multiple exposures.

Limitations

Relies on data accuracy and completeness, potential for selection bias, and difficulty in establishing temporal relationships.

Prospective Cohort Study

In a prospective cohort study, participants are identified based on their exposure status and followed over time. Revelation information is unruffled at the commencement of the swot up, and participants are then observed to assess the development of disease outcomes. The study measures the incidence of disease in exposed and unexposed groups and calculates relative risks.

Strengths

Allows for the direct assessment of temporal relationships, can collect detailed exposure data, and provides stronger evidence for causality.

Limitations

Requires long-term follow-up, can be expensive and time-consuming, and attrition or loss to follow-up may affect results.

Case-Control Study

In a case-control study, participants are selected based on disease outcome (cases) and compared to a control group without the disease. Exposure history is assessed retrospectively by evaluating the regularity of revelations in cases and controls. The swot channels probability of disclosure in cases compared to controls to assess the association between exposure and disease.

Strengths

Efficient for studying rare diseases or outcomes, allows for the assessment of multiple exposures, and relatively quick and cost-effective.

Limitations
Relies on accurate recall of past exposures, potential for recall bias, challenges in selecting appropriate controls, and difficulty establishing temporal relationships.

Clinical Trial
In a clinical trial, participants are randomly assigned to different treatment or intervention groups. The study evaluates the usefulness and wellbeing of intercessions or treatments for the disease. Controlled groups receive different interventions (e.g., drug, therapy) or placebo, and outcomes are compared between groups.

Strengths
Provides high-quality evidence for treatment effectiveness, allows for control of confounding factors, and can establish causality.

Limitations
Resource-intensive, requires ethical considerations and regulatory approvals, may have limited generalizability to real-world settings.

ORDEAL
The development process your lungs' functionality is assessed with Body plethysmography. Lung capacity, volume, flow rates, and gas exchange are all gauged early in the checkups. Your healthcare professional ought to utilize this information to recognize and deal with some lung ailments with greater efficacy. Spirometry and lung volume tests constitute some of the examinations that gauge lung capacity and airflow. The efficiency with which gases, such oxygen, circulate throughout your blood is established by further analyses. The majority of these tests are the analysis of arterial blood gases and pulse oximetry. A consideration of the respiratory system which incorporates a physical examination, Body plethysmography, and the healthcare history of the individual is commonly referred to as pulmonary function testing. Detecting out the severity of pulmonary impairment is is the paramount objective of pulmonary function testing.

RAMIFICATIONS AND CONVERSES
In the midst of the aid of chronometer machination personage can discriminate the subsistence of Covid 19 or any sort of lung malady in their cadaver as well as others cadaver. By using the proposed device, one can easily identify the existence of lung diseases and can enact accordingly. This device is portable and light weight which can be used by all the people in the world.

CONCLUSION

Lungs are the important part in a human body for respiration where a disease named pulmonary fibrosis emerges which damages the lung's tissue. Pulmonary Fibrosis affects the left part of the lungs. This leads to breathing problem and worsens the body condition. The lungs absorb oxygen from the air and move it into your blood rivulet so that it is taken by other parts of the body. This lung is useful for puffing out the waste gas when a person exhales. COVID-19 also directly affects the lungs and damages the alveoli (tiny air sacs). Lung problems through COVID-19 are pneumonia and in the furthermost critical cases it leads to acute respiratory distress syndrome (ARDS). COVID-19 will have a complication which is referred as Sepsis. It will cause enduring harm to the lungs and further organs. For such diseases, the proposed paper concentrates on finding out this disease of a person using a chronometer device. The person who uses this device will get a sign, which indicates the infection in their organ with the help of their pulse rate. This device also has an application which helps a person to detect others disease who is nearby and warns them to maintain social distancing.

REFERENCES

1. Pulmonary fibrosis and COVID-19: the potential role for antifibrotic therapy Peter M George, Athol U Wells, R Gisli Jenkins, DOI:https://doi.org/10.1016/S2213-2600 (20)30225-3.
2. Iwai, K., Mori, T., Yamada, N., Yamaguchi, M., and Hosoda, Y. (1994) Idiopathic pulmonary fibrosis. Epidemiologic approaches to occupational exposure. Am. J. Respir. Crit. Care Med. 150, 670–675.
3. Computer-Aided Diagnosis of Pulmonary Fibrosis Using Deep Learning and CT Images Christe, Andreas MD; Peters, Alan A. MD; Drakopoulos, Dionysios MD; Heverhagen, Johannes T. PhD; Geiser, Thomas MD; Stathopoulou, Thomai PhD; Christodoulidis, Stergios PhD; Anthimopoulos, Marios PhD; Mougiakakou, Stavroula G. PhD; Ebner, Lukas MD Author Information Investigative Radiology: October 2019 - Volume 54 - Issue 10 - p 627-632, doi: 10.1097/RLI.0000000000000574.
4. Interpretative strategies for lung function tests R. Pellegrino, G. Viegi, V. Brusasco, R. O. Crapo, F. Burgos, R. Casaburi, A. Coates, C. P. M. van der Grinten, P. Gustafsson, J. Hankinson, R. Jensen, D. C. Johnson, N. MacIntyre, R. McKay, M. R. Miller, D. Navajas, O. F. Pedersen, J. Wanger European Respiratory Journal 2005 26: 948-968; DOI: 10.1183/09031936.05.00035205.
5. Communication of Pulmonary Function Test Results: A Survey of Patient's Preferences Debbie Zagami, Jessica Hockenhull, Alanna Bodger, Krishna Bajee Sriram, Published: May 7, 2015, https://doi.org/10.1371/journal.pone.0126617.
6. Standardization of Spirometry 2019 Update An Official American Thoracic Society and European Respiratory Society Technical Statement Brian L. Graham, Irene Steenbruggen, Martin R. Miller, Igor Z. Barjaktarevic, Brendan G. Cooper, Graham L. Hall, Teal S. Hallstrand, David A. Kaminsky, Kevin McCarthy, Meredith C. McCormack, Cristine E. Oropez, Margaret Rosenfeld, Sanja Stanojevic, Maureen P. Swanney†, and Bruce R. Thompson; on behalf of the American Thoracic Society and the European Respiratory Society, https://doi.org/10.1164/rccm.201908-1590ST.
7. Real-world heart rate norms in the Health eHeart study, Robert Avram, Geoffrey H. Tison, Kirstin Aschbacher, Peter Kuhar, Eric Vittinghoff, Michael Butzner, Ryan Runge, Nancy Wu, Mark J. Pletcher, Gregory M. Marcus, and Jeffrey Olgin.
8. Palatini P, et al. Reproducibility of heart rate measured in the clinic and with 24-hour intermittent recorders. Am. J. Hypertens. 2000; 13:92–98. doi: 10.1016/S0895-7061(99)00170-3.
9. Schaller, M., and Park, J. H. (2011). The Behavioral Immune System (and Why It Matters). Curr. Direct. Psychol. Sci. 20, 99–103. doi: 10.1177/0963721411402596.

Table 1:Packet Delivery Ratio based on Nodes

Age Group	Age-Harmonized Transience Tempo (per 100,000 populations per year)
0-44 years	0.5
45-54 years	1.0
55-64 years	2.5
65-74 years	5.0
75-84 years	12.0
85+ years	28.0

Figure 1: Representation of Human Lungs

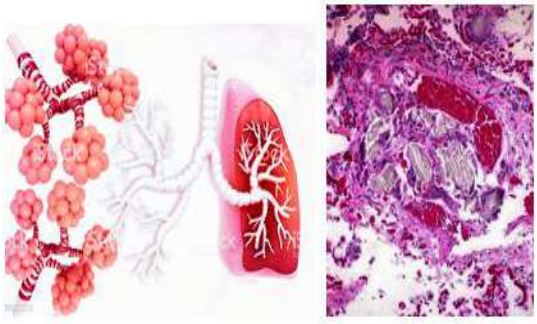

Figure 2:Pulmonary Fibrosis Case

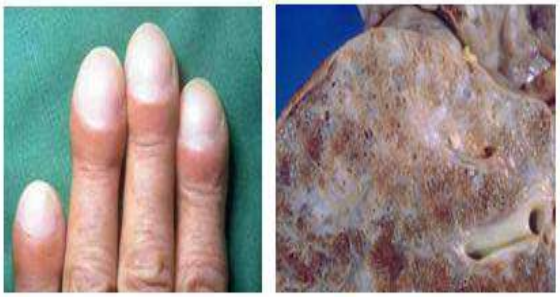

Figure 3:Clubbing of Fingers and Real-Time Image in Fibrosis

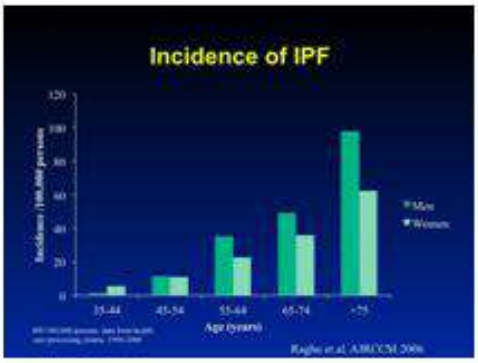

Figure 4:Incidence of IPF Age -Wise

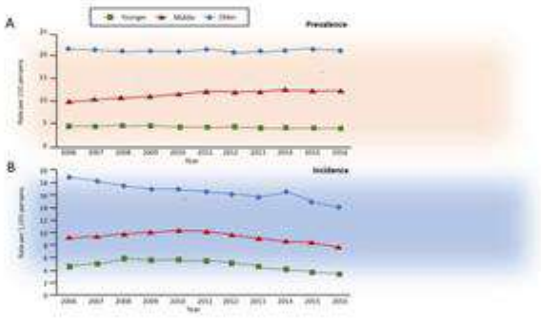

Figure 5: Rate per Person for Prevalence and Incidence

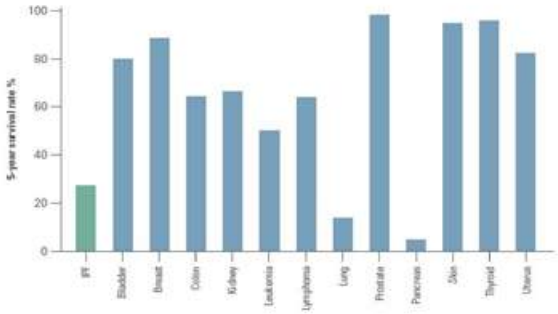

Figure 6:Comparison of the 5-Year Survival Rate for IPF

Indian Journal of Natural Sciences *www.tnsroindia.org.in ©IJONS*

Vol.15 / Issue 88 / Feb / 2025 *International Bimonthly (Print) – Open Access* *ISSN: 0976 – 0997*

RESEARCH ARTICLE

Application of Fuzzy Clustering Algorithms in Medical Diagnostics of Children

U. Abuthahir[1]* and Tamilselvi K[2]

[1]Assistant Professor, Department of Mathematics, Jamal Mohamed College (Autonomous), (Affiliated to Bharathidasan University), Tiruchirappalli, Tamil Nadu, India.
[2]Guest Lecturer, Department of Mathematics, Government Arts and Science College, Karambakudi, Pudukkottai Dist., (Affiliated to Bharathidasan University, Tiruchirappalli), Tamil Nadu, India.

Received: 21 Nov 2024 Revised: 03 Dec 2024 Accepted: 31 Jan 2025

***Address for Correspondence**
U. Abuthahir
Assistant Professor,
Department of Mathematics,
Jamal Mohamed College (Autonomous),
(Affiliated to Bharathidasan University),
Tiruchirappalli, Tamil Nadu, India.

ABSTRACT

Fuzzy clustering is a sort of bunching in which each datum point can be assigned to more than one group. The most commonly used fuzzy clustering algorithm is the fuzzy c-means algorithm (FCM). Due to significant technological advancement, old classification approaches to Childhood Blood Lead Surveillance programme are becoming increasingly complex. Because medical issues are ambiguous, fuzzy approaches are more effective than crisp ones. The goal of this study is to the classification performance of fuzzy clustering algorithms Fuzzy c-Means (FCM). The resilience of a classification method is important for achievinggoals. Among the techniques, FCM is gives the most resilient since it produces more accurate clustering results. In this work, we findings important of interventions and initiatives for reducing childhood lead exposure and developing health outcomes.

Keywords: Childhood lead exposure, membership value and fuzzy c- mean.

INTRODUCTION

Clustering is a soft computing technique that groups comparable objects in a dataset. Clustering is also known as classification. Clustering is a useful method for medical diagnostics, image segmentation, data mining, and pattern classification [1]. The thyroid gland, shaped like a butterfly, is positioned in the lower front of the neck and is one of the major endocrine glands. The thyroid gland produces hormones that regulate metabolism and balance calcium levels. It supports the brain, heart, muscles, and other organs, as well as maintaining body temperature and energy

levels. A symptom is a physical or laboratory result that suggests a condition and can help with diagnosis. A syndrome refers to a set of symptoms that describe the disease's presence and characteristics. The use of fuzzy c-means (FCM) clustering techniques in medical diagnosis has progressively expanded in recent years, owing to its usefulness in recognising patterns in medical databases that assist medical experts in detecting disorders[2]. However, its performance is heavily reliant on randomly initialised cluster centroids, which may trap the diagnosis in the problem of the local optimum. In unsupervised approaches, fuzzy c-means (FCM) clustering is the most accurate method forpicture segmentation, with smooth and pleasant results. The goal of this research is to provide a robust systematic approach for segmenting complicated medical picture cases that rely on the proposed method to participate in decision-making processes [3]. This paper discusses medical picture modalities and mathematically demonstrates the phases of the FCM clustering approach using an example. It divides magnetic resonance imaging (MRI) of the brain into four statuses to differentiate tumours within the brain. An equivalency between the notions of fuzzy clustering and soft competitive learning in clustering algorithms is offered as a unifying framework for comparing clustering systems. Furthermore, a collection of functional qualities is chosen for use as dictionary entries in the comparison of clustering techniques, which is the focus of Part II of this study [4]. Fuzzy clustering models in various circumstances. Uniquely built algorithms improve result accuracy and should be studied for future work. In certain cases, modelling procedures are data- driven, emphasising distances between locations and new cluster centres. In some other applications, such as market segmentation or patient evaluation using healthcare information, membership degree is an important factor in the method [5]. This study examines a wide spectrum of studies on well-designed mathematic models for fuzzy clustering, including evolutionary algorithms to protect children from the harmful consequences of lead exposure while also fostering healthier surroundings and communities across the country.

Background

The CDC provided the childhood blood lead surveillance programme dataset. This data we referred from kaggle.com [9]. The dataset includes children who were examined for blood lead levels in several states around the United States. The samples are divided into many classes based on their blood lead levels: age, gender, race/ethnicity, socioeconomic status, and location. The values show in table 1. The characteristics are lab tests to determine blood lead levels. These qualities are micrograms per deciliter (μg/dL), a value of total blood lead level given by a finger-prick test for children aged several years.

Mathematical Model: Fuzzy C-Means (FCM)

Fuzzy Clustering Based On Fuzzy Relation

Let c be a positive integer greater than one and let X be a subset of an s-dimensional Euclidean space $\mathbb{R}^s$ with its ordinary Euclidean norm $\|\cdot\|$. Mutually disjoint sets $B_1, \dots, B_c$ such that $B_1 \cup \cdots \cup B_c = X$ or, equivalently, the indicator function $\mu_1, \dots, \mu_c$ such that $\mu_i(x) = 1$ if $x \in B_i$ and $\mu_i(x) = 0$ if $x \notin B_i$ for all $x \in X$ and all $i = 1, \dots, c$. can be used to describe a partition of X into c clusters. Given the indicator functions $\mu = (\mu_1, \dots, \mu_c)$, X is considered to have a hard c-partition in this instance. The fuzzy set is an extension that permits $\mu(x)$ to be a function (referred to as a membership function) assuming values in the interval [0,1]. It was first presented by Zadeh [6,7] in 1965. Since he initially employed the fuzzy set in cluster analysis, Ruspini [8] created a fuzzy c-partition $\mu = (\mu_1, \dots, \mu_c)$ by the extension to allow $\mu_i(x)$ to be functions assuming values in the interval [0,1] such that $\mu_1(x) + \cdots + \mu_C(x) = 1$.

If $(x, y) = 1$, then x and y in X are said to have a relation. A (hard) relation r in X is defined as a function $r: X \times X \rightarrow$ {0,1}If and only if, for every $x, y \in X$, a (hard) relation r in X is considered an equivalence relation

(1) $R(x, x) = 1$ (reflexivity)

(2) $r(x, y) = r(y, x)$ (symmetry), and

(3) $(x, z) = r(y, z) = 1$ for some $z \in X \Longrightarrow r(x, y) = 1$ (transitivity).

By extending to include values of r in the interval [0,1], Zadeh [7] defined a fuzzy relation r in X, where $r(x, y)$ indicates the strength of the relation between x and y. According to Zadeh, a similarity relation S in X is defined as follows: for any x, y, and $z \in X$, $(x, x) = 1$ (reflexivity), $S(x, y) = S(y, x)$ (symmetry), and) $S(x, y) \geq \vee_{z \in X} (S(x, z)$ A $S(y, z))$

(transitivity), where ∨ and A stand for max and min. It is clear that the equivalency relation is basically generalized into the similarity relation S.

Let $X = \{x_1, \dots, x_n\}$ be a finite data set of $\mathbb{R}^s$. Denote $r(x_j, x_k)$ by r_{jk}, $j, k = 1, \dots, n$, and $\mu_i(x_j)$ by μ_{ij}, $i = 1, \dots, c$, $j = 1, \dots, n$, Let u_{ij} be the ij^{th} " element of $U \in V_{c\times n}$. and let V_cn be the typical vector space of real $c \times n$ matrices. we define:

$$M_c = \{U \in V_{cn} \mid \mu_{ij} \in \{0,1\} \forall i, j; \sum_{i=1}^{c} \mu_{ik} = 1 \forall k; 0 < \sum_{j=1}^{n} \mu_{ij} \forall i\}$$

Then M_c is exactly a hard c-partitions space for the finite data set X. Define $A \leq B$ if and only if $a_{ij} \leq b_{ij} \forall i, j$ where $A = [a_{ij}]$ and $B = [b_{ij}] \in V_{nn}$. Define $R \circ R = [r'_{ij}] \in V_{nn}$ with $r'_{ij} = V_{k=1}^{n}(r_{ik} \text{ A } r_{kj})$. Let

$$R_n = \{R \in V_{nn} \mid r_{ij} \in \{0,1\} \forall i, j; I \leq R; R = R^T; R = R \circ R\}$$

Then R_n is the set of all equivalence relations in X. For any $U = [\mu_{ij}] \in M_c$, let the relation matrix $R = [r_{jk}]$ in V_{nn} be defined by

$$r_{jk} = \begin{cases} 1, & \text{if } \mu_{ij} = \mu_{ik} = 1 \text{ for some } i, \\ 0, & \text{otherwise.} \end{cases}$$

Then, since R satisfies reflexivity, symmetry, and transitivity, it is evident that it is an equivalence relation corresponding to the hard c-partitions U. In other words, for any U in $U \in M_c$, there exists a relation matrix R in R, such that R corresponds to U as an equivalencerelation. For a fuzzy extension of M_c and R, let

$$M_{fc} = \{V \in V_{cn} \mid \mu_{ij} \in [0,1] \forall i, j; \sum_{i=1}^{c} \mu_{ij} = 1 \forall j; \sum_{j=1}^{n} \mu_{ij} > 0 \forall i\}$$

and

$$R_{fn} = \{R \in V_{nn} \mid r_{ij} \in [0,1] \forall i, j; I \leq R; R = R^T \text{ and } R \geq R \circ R\}$$

The set of all similarity relations in X is denoted by R_fn, and M_fc is a (nondegenerate) fuzzy c-partitions space for X. Recall that M_{fc} is the convex hull of M_c , where M_{co} is the collection of matrices obtained by weakening the last constraint of M_{fc} to M_c to $\sum^n \mu_{ij} \geq 0 \forall i$. The equivalency relation, similarity relation, and so-called hard and fuzzy c-partitions have all been discussed above. These are the primary cluster analysis representations since the basic idea behind cluster analysis is to divide a data set into c clusters, each of which has an equivalency relation that corresponds to the division. We will then concentrate on fuzzy clustering techniques that utilize fuzzy relations.

$$J_m(W, P) = \sum_{\substack{1\leq k\leq n \\ 0\leq i\leq c}} (w_{ik})^m (d_{ik})^2$$

where

$$(d_{ik}) = \|x_k - p_i\|$$

where $m \in (1, +\infty)$ is the parameter which defines the fuzziness of the resulting clusters and d_{ik} is the Euclidian distance from object x_k to the cluster center p_i.

The minimization of the objective function J_m through FCM algorithm is being performed by theiterative updation of the partition matrix using above equations

$$\mu_{i,j} = \left[\sum_{t=1}^{c} \left(\frac{\|x_j - v_i\|_A}{\|x_j - v_t\|_A} \right)^{\frac{2}{m-1}} \right]^{-1}$$

μ_i, is the membership value of j th sample and i th cluster. The number of clusters is represented by c, x_j is the j th sample and v_i cluster center of the i th cluster. ". "$_A$ represents the norm function.

The steps of FCM algorithm are as follows:

(1) Initialize the number of clusters c .
(2) Select an inner product metric Euclidean norm and the weighting metric (fuzziness).
(3) Initialize the cluster prototype $P^{(0)}$, iterative counter b = 0.
(4) Then calculate the partition matrix $W^{(b)}$.
(5) Update the fuzzy cluster centers $P^{(b+1)}$.
(6) If $\|^{(b)} - \mathbf{P}^{(b+1)}\| < \varepsilon$ then stop, otherwise repeat step 2 through 4.

MATHEMATICAL RESULTS AND DISCUSSION

Python software was used to implement the algorithms. There are several samples in the data set that are divided into three categories based on blood lead level for children. Distinct real- valued continuous lab measurements are included in each sample. The measurements include the finger-prick test ((μg/dL),), total blood level value obtained through finger-prick method, Labels ranging from three columns are used for all samples. There are three clusters produced by the algorithms FCM. In order to provide good results, these algorithms must run multiple times. With samples in each of the three clusters that FCM creates— blood lead level, age, and gender respectively. The FCM algorithm gives a flexible approach to clustering by assortment fuzzy logic, allowing for extending memberships and providing more nuanced cluster assignments compared to traditional crisp clustering methods. This mathematical method structure the basis for construction fuzzy clustering algorithms like Fuzzy C-Means for the real time practical applications, counting the analysis of childhood blood lead surveillance data as defined in the previous sections. This approach offers a sophisticated understanding of the intersections of blood lead levels, age, and gender in estimating children's lead liability by utilizing fuzzy clustering. These understandings are crucial for developing evidence-based public health policies that safeguard children's health and wellbeing. Fig 1 depicts based on the fuzzy clustering model for the Childhood Blood Lead Surveillance dataset using the three columns (blood lead level, age, and gender), Here, we shown the conclusion based on the visualized clusters. Cluster 1: This cluster essentially consists of older children, its relatively low blood lead levels. Gender distribution shows an associate but kind of skewed towards males. Cluster 2: younger children with bearable to high blood lead levels are outstanding in this cluster. It mainly includes males. Cluster 3: this cluster display a mix of ages but routinely high blood lead level across both genders.

CONCLUSION

The purpose of this study is to investigate how well fuzzy clustering techniques perform in categorization for medical diagnosis. Fuzzy c-Means (FCM), clustering method that the authors implemented. They then talked about the outcomes. The outcomes demonstrated that the FCM, can produce superior clusters. Fuzzy clustering algorithms may therefore prove to be a useful tool in the diagnosis of medical conditions. To reach maximum satisfaction, more research is required to improve categorization and accuracy performance.

REFERENCES

1. Bezdek, J. C. (2013). Pattern recognition with fuzzy objective function algorithms. Springer Science & Business Media.
2. Wu, Y., Duan, H., & Du, S. (2015). Multiple fuzzy c-means clustering algorithm in medical diagnosis. Technology and Health Care, 23(s2), S519-S527.
3. Mohammed, B. A., & Al-Ani, M. S. (2020). Digital medical image segmentation using fuzzy C-means clustering. UHD Journal of Science and Technology, 4(1), 51-58.
4. Baraldi, A., & Blonda, P. (1999). A survey of fuzzy clustering algorithms for pattern recognition. I. IEEE Transactions on Systems, Man, and Cybernetics, Part B (Cybernetics), 29(6), 778-785.
5. Li, J., & Lewis, H. W. (2016, November). Fuzzy clustering algorithms—review of the applications. In 2016 IEEE International Conference on Smart Cloud (SmartCloud) (pp. 282- 288). IEEE.
6. Zadeh, L. A. (2015). Fuzzy logic—a personal perspective. Fuzzy sets and systems, 281, 4- 20.
7. Zadeh, L. A., & Sets, F. (1971). Info. Control 8, 1965, 338-353. LA Zadeh. Similarity Relations and Fuzzy Orderings," Info. Science, 3, 177-200.
8. Ruspini, E. H. (1969). A new approach to clustering. Information and control, 15(1), 22-32. [9]. https://www.kaggle.com/datasets/cdc/childhood-blood-lead-surveillance.

Table 1

State	County	Year	Lead Level (µg/dL)	of Children Tested	Elevated Cases (%)	Population	Median Household Income ($)	Urban Classif
New York	Manhattan	2023	3.2	1500	12.5	150000	75000	Urban
California	Los Angeles	2023	2.8	2000	10.2	300000	80000	Urban
Texas	Dallas	2023	1.5	1200	8.3	250000	70000	Urban
Florida	Miami-Dade	2023	1.0	1800	6.5	200000	65000	Urban
Illinois	Cook	2023	2.5	2200	9.8	500000	90000	Urban
Ohio	Franklin	2023	1.8	1300	7.2	150000	60000	Urban
Arizona	Maricopa	2023	2.0	1700	8.1	400000	85000	Urban
Pennsylvania	Philadelphia	2023	2.3	1900	7.8	350000	72000	Urban
Texas	Harris	2023	1.2	1400	5.9	300000	68000	Urban

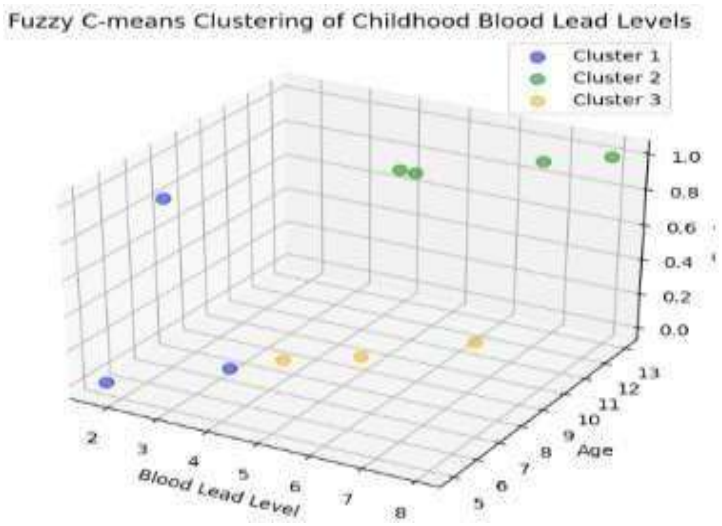
Fuzzy C-means Clustering of Childhood Blood Lead Levels
Cluster 1
Cluster 2
Cluster 3
Blood Lead Level
Age

Fig .1

RESEARCH ARTICLE

A Markovian Retrial Queueing Model with Non-Persistent Customers, Working Vacation and Vacation Interruption under a Bernoulli Schedule

S. Pazhani Bala Murugan[1]* and U.Chitra[2]

[1]Associate Professor, Department of Mathematics, Annamalai University, Annamalai Nagar, Chidambaram, Tamil Nadu, India.
[2]Assistant Professor, Department of Mathematics, Sree ManakulaVinayagar Engineering College, (Affiliated to Pondicherry University), Pondicherry, India.

Received: 21 Jun 2024 Revised: 03 Nov 2024 Accepted: 03 Jan 2025

***Address for Correspondence**
S.Pazhani Bala Murugan
Associate Professor, Department of Mathematics,
Annamalai University, Annamalai Nagar,
Chidambaram, Tamil Nadu, India.
E. Mail: spbm1966@gmail.com

ABSTRACT

In this study, we analysis of a Markovian retrial queueing model incorporating non-persistent customers, working vacation, and vacation interruption under a Bernoulli schedule. Within this model, all service times, retrial times, and vacation durations follow an exponential distribution. During the working vacation period, customers are served at a reduced speed. Upon the completion of a service when there are customers in the queue, the server either resumes regular service with probability p (i.e., the vacation is interrupted) or continues the vacation with probability 1-p. We derive the probability generating function for the number of customers in the system and compute the average number of customers and waiting time within the system. Furthermore, we examine specific cases and present numerical examples for greater clarity and understanding.

Keywords: Retrial Queue, Non - persistent, Working Vacation, Vacation Interruption, Bernoulli schedule and Steady-state equations.

INTRODUCTION

In a Retrial Queuing System, customers encountering a busy server depart the system and rejoin the queue after a random period. This queuing model frequently manifests in real-world contexts, such as web access, telecommunication networks, banking sectors, and computer systems. Notably, numerous authors have engaged in extensive discourse concerning retrial queues, with further insights available in the survey paper authored by T.

Yang and J.G.C. Templeton [19], as well as in the work of G.I. Falin [5]. Discussions within queuing systems have encompassed vacation and retrial queueing systems with working vacations. For instance, L. Servi and S. Finn [13] introduced the M/M/1 queue with working vacations (M/M/1/MV), wherein the server delivers service at a reduced pace during the normal service period without complete service interruption. Subsequently, Aissani, A., Taleb, S., Kernane, T., Saidi, G., and Hamadouche, D. (2014) extended the model to an (M/G/1) queue. Wu and Takagi [4] presented the concept of M/G/1/MWV. Kalyanaraman and Pazhani Bala Murugan [17] have developed the retrial queue with vacation, while Pazhani Bala Murugan and Santhi [18] investigated the M/G/1 retrial queue with MWV. For an in-depth examination of MV, reference can be made to [21]. In order to maximize the server's efficiency, Li and Tian (2007) introduced a working vacation interruption. During a working vacation period, the server evaluates whether there are customers in the system at a service completion instant. The vacation is either interrupted with probability p (0≤p≤1) or continues with probability q (p+q=1), as analyzed by Zhang and Shi (2009) in the M/M1 queue with Bernoulli working vacation interruption.

In their research, Krishnamorthy *et al*. [13] explore an M/G/1 retrial queue with non-persistent customers and orbital search. Upon each service completion, the server will proceed to locate customers in orbit. Upon the arrival of primary and orbital customers, they will determine whether the server is occupied. If the server is occupied, customers will either depart the system without receiving service or return to the orbit. For a comprehensive analysis of the non-persistent customer model, interested researchers can refer to the studies by Kasturi Ramanath and Kalidass [12], Pazhani Bala Murugan and Vijayashnaraj [14], and Peishu Chan, among others. In this article, the focus is on the analysis of a Markovian retrial queueing system with non-persistent customers, working vacation, and vacation interruption under a Bernoulli schedule. The structure of the article is as follows: Section 2 presents a detailed model description, section 3 explore into the analysis of the model, section 4 discusses performance measures, section 5 reveals numerical outcomes, and finally, the conclusion is presented in section 6.

Model Description

We are conducting an analysis of a Markovian retrial queue featuring working vacation and vacation interruption under Bernoulli schedule. Customer arrivals are modeled as a Poisson process with an arrival rate of λ, and the server serves customers on a first-come, first-served (FCFS) basis with exponentially distributed service times. The inter-arrival times are distributed exponentially with rate, and vacation times follow an exponential distribution with rate η respectively. During normal busy periods, the service time follows an exponential distribution with rate. During a working vacation period, if there are customers in the system at a service completion instant , the server will decide whether to interrupt the vacation with probability $p(0 \le p \le 1)$ or continues the vacation with probability q $(p + q = 1)$.Upon arrival, all customers enter the orbit with probability γ, or they leave the system without joining orbit with probability $\bar{\gamma}$ $(\gamma + \bar{\gamma} = 1)$. We assumed that inter-arrival times, service time, and working times are consider to be mutually independent.

Let us consider the Size of the system be$O(t)$attime$t$. At time t the four distinct server states are

$$Y(t) = \begin{cases} 0 \text{ if the server is not occupied in Working Vacation} \\ 1 \text{ if the server is occupied in Working Vacation} \\ 2 \text{ if the server is not occupied in Regular Service period} \\ 3 \text{ if the server is occupied in Regular Service period} \end{cases}$$

We obtain the following steady state equation is

$\lambda P_{0,0} = q\eta P_{1,0} + \mu P_{3,0};$ (1)

$(\lambda + \alpha + \theta)P_{0,n} = q\eta P_{1,n};\ n \ge 1$ (2)

$(\lambda\gamma + q\eta + \theta)P_{1,0} = \lambda P_{0,0} + \alpha P_{0,1}$ (3)

$(\lambda\gamma + \eta + \theta)P_{1,n} = \lambda P_{0,n} + \alpha P_{0,n+1} + \lambda\gamma P_{1,n-1}; n \ge 1$ (4)

$(\lambda + \alpha)P_{2,n} = \mu P_{3,n} + p\eta P_{1,n} + \theta P_{0,n};\ n \ge 1$ (5)

$(\lambda\gamma + \mu)P_{3,0} = \alpha P_{2,1} + \theta P_{1,0}$ (6)

$(\lambda\gamma + \mu)P_{3,n} = \lambda P_{2,n} + \alpha P_{2,n+1} + \theta P_{1,n} + \lambda\gamma P_{3,n-1};\ n \ge 1$ (7)

To solve the equation (1-7), We define the following probability generating functions:

$P_0(z) = \sum_{n=1}^{\infty} P_{0,n} z^n$ $P_1(z) = \sum_{n=0}^{\infty} P_{1,n} z^n$

$P_2(z) = \sum_{n=1}^{\infty} P_{2,n} z^n$ $P_3(z) = \sum_{n=0}^{\infty} P_{3,n} z^n$ (8)

The Analysis

Applying (8) into equation (1) - (7), we get

$(\lambda + \alpha + \theta)P_0(z) = q\eta P_1(z) - q\eta P_{1,0}$ (9)

$(\lambda\gamma(1-z) + \eta + \theta)P_1(z)z = \lambda z P_{0,0} + (\lambda z + \alpha)P_0(z) + p\eta z P_{1,0}$ (10)

$(\lambda + \alpha)P_2(z) = \mu P_0(z) + p\eta P_1(z) + \theta P_0(z) - [\mu P_{3.0} + p\eta P_{1,0}]$ (11)

$[\lambda\gamma(1-z) + \mu]zP_3(z) = (\lambda z + \alpha)P_2(z) + \theta z P_1(z)$ (12)

Solving the above equations (9) – (12), by using crammer's Rule we get

$(\lambda + \alpha + \theta)P_0(z) - q\eta P_1(z) + 0.P_2(z) + 0.P_3(z) = -q\eta P_{1,0}$

$-(\lambda z + \alpha)P_0(z) + (\lambda\gamma(1-z) + \eta + \theta)zP_1(z) + 0.P_2(z) + 0.P_3(z)$
$= \lambda z P_{0,0} + p\eta z P_{1,0}$

$-\theta P_0(z) - p\eta P_1(z) + (\lambda + \alpha)P_2(z) - \mu P_3(z) = -\mu P_{3.0} - p\eta P_{1,0}$

$0P_0(z) - \theta z P_1(z) - (\lambda z + \alpha)P_2(z) + (\lambda\gamma(1-z) + \mu)zP_3(z) = 0\Delta$
$= [(\lambda + \alpha + \theta)[\lambda\gamma - \lambda\gamma z + \eta + \theta]z - q\eta(\lambda z + \alpha)][(\lambda + \alpha)\lambda\gamma z - \alpha\mu](1-z)$

$\Delta_0 = \left[-q\eta P_{1,0}(\lambda\gamma - \lambda\gamma z + \eta + \theta)z + q\eta[\lambda z P_{0,0} + p\eta z P_{1,0}]\right]$
$[(\lambda + \alpha)(\lambda\gamma - \lambda\gamma z + \mu)z - \mu(\lambda z + \alpha)]$

Consider,

$P_0(z) = \frac{\Delta_0}{\Delta} = \frac{\left[-q\eta P_{1,0}(\lambda\gamma - \lambda\gamma z + \eta + \theta)z + q\eta[\lambda z P_{0,0} + p\eta z P_{1,0}]\right]}{[(\lambda+\alpha+\theta)[\lambda\gamma - \lambda\gamma z + \eta + \theta]z - q\eta(\lambda z + \alpha)]}$ (13)

Let $f(z) = [(\lambda + \alpha + \theta)[\lambda\gamma - \lambda\gamma z + \eta + \theta]z - q\eta(\lambda z + \alpha)]$ we obtain $f(0) < 0$ and $f(1) > 0$ which implies that ∃ a real root $\gamma \in (0,1)$.At$z = z_0$ in (13) is converted in to

$P_{1,0} = \frac{\lambda P_{0,0}}{(\lambda\gamma - \lambda\gamma z_0 + q\eta + \theta)} = B(z_0)\lambda P_{0,0}$ (14)

Substituting (14) in (13), we get

$P_0(z) = \frac{\lambda q\eta z\,[1 - B(z_0)(\lambda\gamma - \lambda\gamma z + q\eta + \theta)]P_{0,0}}{[(\lambda+\alpha+\theta)[\lambda\gamma - \lambda\gamma z + \eta + \theta]z - q\eta(\lambda z + \alpha)]}$ (15)

From (1)

$\mu P_{3,0} = [1 - q\eta B(z_0)]\lambda P_{0,0}$ (16)

$\Delta_1 = \lambda P_{0,0}[(\lambda + \alpha + \theta)z[1 + p\eta B(z_0)] - q\eta B(z_0)(\lambda z + \alpha)]$
$-[(\lambda + \alpha)(\lambda\gamma - \lambda\gamma z + \mu)z - \mu(\lambda z + \alpha)]$

$$\Delta_2 = \lambda z P_{0,0}(1-z)\begin{bmatrix} -[1 + p\eta B(z_0)]\begin{bmatrix} \lambda\gamma z(\lambda + \alpha + \theta)(\lambda\gamma - \lambda\gamma z + \mu + \theta) \\ -\lambda\gamma q\eta\alpha(1-z) + \mu q\eta\alpha \end{bmatrix} \\ +q\eta B(z_0)\begin{bmatrix} \lambda\gamma z(\lambda + \alpha)(\lambda\gamma - \lambda\gamma z + \mu + \theta) \\ -\lambda\gamma\alpha\eta(1-z) - \alpha\mu(\eta + \theta) \end{bmatrix} \end{bmatrix}$$

$$\Delta_3 = \lambda P_{0,0}(1-z)\begin{bmatrix} -[1 + p\eta B(z_0)]\begin{bmatrix} (\lambda + \alpha + \theta)(\lambda z + \alpha)\lambda\gamma z \\ -q\eta(\lambda z + \alpha)\alpha + (\lambda + \alpha + \theta)\theta z\alpha \end{bmatrix} \\ +q\eta B(z_0)[(\lambda z + \alpha)[(\lambda + \alpha)\lambda\gamma z - \alpha\eta]] \end{bmatrix}$$

We have

$$P_0(z) = \frac{\lambda q\eta z[1 - B(z_0)(\lambda\gamma - \lambda\gamma z + q\eta + \theta)]P_{0,0}}{(\lambda + \alpha + \theta)(\lambda\gamma - \lambda\gamma z + \eta + \theta)z - q\eta(\lambda z + \alpha)}$$

$$P_1(z) = \frac{[(\lambda + \alpha + \theta)\lambda z[1 + p\eta B(z_0)] - \lambda q\eta B(z_0)(\lambda z + \alpha)]P_{0,0}}{(\lambda + \alpha + \theta)(\lambda\gamma - \lambda\gamma z + \eta + \theta)z - q\eta(\lambda z + \alpha)}$$

$$P_2(z) = \frac{\lambda z\begin{bmatrix} -[1 + p\eta B(z_0)]\begin{bmatrix} \lambda\gamma z(\lambda + \alpha + \theta)(\lambda\gamma - \lambda\gamma z + \mu + \theta) \\ -\lambda\gamma q\eta\alpha(1-z) + \mu q\eta\alpha \end{bmatrix} \\ +q\eta B(z_0)\begin{bmatrix} \lambda\gamma z(\lambda + \alpha)(\lambda\gamma - \lambda\gamma z + \mu + \theta) \\ -\lambda\gamma\alpha\eta(1-z) - \alpha\mu(\eta + \theta) \end{bmatrix} \end{bmatrix}}{[(\lambda + \alpha + \theta)(\lambda\gamma - \lambda\gamma z + \eta + \theta)z - q\eta(\lambda z + \alpha)][(\lambda + \alpha)\lambda\gamma z - \alpha\mu]}P_{0,0}$$

$$P_3(z) = \frac{\lambda\begin{bmatrix} -[1 + p\eta B(z_0)]\begin{bmatrix} (\lambda + \alpha + \theta)(\lambda z + \alpha)\lambda\gamma z \\ -q\eta(\lambda z + \alpha)\alpha + (\lambda + \alpha + \theta)\theta z\alpha \end{bmatrix} \\ +q\eta B(z_0)[(\lambda z + \alpha)[(\lambda + \alpha)\lambda\gamma z - \alpha\eta]] \end{bmatrix}}{[(\lambda + \alpha + \theta)(\lambda\gamma - \lambda\gamma z + \eta + \theta)z - q\eta(\lambda z + \alpha)][(\lambda + \alpha)\lambda\gamma z - \alpha\mu]}P_{0,0}$$

We define

$P(z) = P_{0,0} + P_0(z) + zP_1(z) + P_2(z) + zP_3(z)$ (17)

as the probability generating function of the number of customers in the system irrespective of the server state. We find $P_{0,0}$, by using normalization condition $P(1) = 1$. Before finding $P_{0,0}$, Substituing $z = 1$, in $P_0(z), P_1(z), P_2(z)$ and $P_3(z)$

$$P_0(1) = \frac{\lambda q\eta[1 - B(z_0)(q\eta + \theta)]P_{0,0}}{(\lambda + \alpha + \theta)(\eta + \theta) - q\eta(\lambda + \alpha)}$$

$$P_1(1) = \frac{[(\lambda + \alpha + \theta)\lambda[1 + p\eta B(z_0)] - \lambda q\eta B(z_0)(\lambda + \alpha)]P_{0,0}}{(\lambda + \alpha + \theta)(\eta + \theta) - q\eta(\lambda + \alpha)}$$

$$P_2(1) = \frac{\lambda\begin{bmatrix}-[1 + p\eta B(z_0)][\lambda\gamma(\lambda + \alpha + \theta)(\mu + \theta) + \mu q\eta\alpha] \\ +q\eta B(z_0)[\lambda\gamma(\lambda + \alpha)(\mu + \theta) - \alpha\mu(\eta + \theta)]\end{bmatrix}}{[(\lambda + \alpha + \theta)(\eta + \theta) - q\eta(\lambda + \alpha)][(\lambda + \alpha)\lambda\gamma - \alpha\mu]}P_{0,0}$$

$$P_3(1) = \frac{\lambda\begin{bmatrix}-[1 + p\eta B(z_0)]\begin{bmatrix}(\lambda + \alpha + \theta)(\lambda + \alpha)\lambda\gamma \\ -q\eta(\lambda + \alpha)\alpha + (\lambda + \alpha + \theta)\theta\alpha\end{bmatrix} \\ +q\eta B(z_0)\big[(\lambda + \alpha)[(\lambda + \alpha)\lambda\gamma - \alpha\eta]\big]\end{bmatrix}}{[(\lambda + \alpha + \theta)(\eta + \theta) - q\eta(\lambda + \alpha)][(\lambda + \alpha)\lambda\gamma - \alpha\mu]}P_{0,0}$$

We have

$P(1) = 1 = P_{0,0} + P_0(1) + P_1(1) + P_2(1) + P_3(1)$

Consider, $P_0(1) = xP_{0,0}, P_1(1) = yP_{0,0}, P_2(1) = zP_{0,0}, P_3(1) = wP_{0,0}$

$\Rightarrow P_{0,0} = (1 + x + y + z + w)^{-1}$

which gives, $P_{0,0} = \frac{D(1)}{N(1)}$

Where

$D(1) = [(\lambda + \alpha + \theta)(\eta + \theta) - q\eta(\lambda + \alpha)][(\lambda + \alpha)\lambda\gamma - \alpha\mu]$

$N(1) = [(\lambda + \alpha + \theta)(\eta + \theta) - q\eta(\lambda + \alpha)][(\lambda + \alpha)\lambda\gamma - \alpha\mu]$

$+\lambda q\eta[1 - B(z_0)(q\eta + \theta)][(\lambda + \alpha)\lambda\gamma - \alpha\mu]$

$+[(\lambda + \alpha + \theta)\lambda[1 + p\eta B(z_0)] - \lambda q\eta B(z_0)(\lambda + \alpha)][(\lambda + \alpha)\lambda\gamma - \alpha\mu]$

$$+\begin{bmatrix}-[1 + p\eta B(z_0)][\lambda^2\gamma(\lambda + \alpha + \theta)(\mu + \theta) + \lambda\mu q\eta\alpha] \\ +q\eta B(z_0)[\lambda^2\gamma(\lambda + \alpha)(\mu + \theta) - \lambda\alpha\mu(\eta + \theta)]\end{bmatrix}$$

$$+\begin{bmatrix}-[1 + p\eta B(z_0)]\begin{bmatrix}(\lambda + \alpha + \theta)(\lambda + \alpha)\lambda^2\gamma \\ -\lambda q\eta(\lambda + \alpha)\alpha + (\lambda + \alpha + \theta)\lambda\theta\alpha\end{bmatrix} \\ +q\eta B(z_0)\big[(\lambda + \alpha)\lambda[(\lambda + \alpha)\lambda\gamma - \alpha\eta]\big]\end{bmatrix}$$

with the stability condition as

$$\rho = \frac{\lambda\gamma}{\mu}\left[1 + \frac{\lambda}{\alpha}\right] < 1$$

The Model's Performance Measures

Expected number of customers in the orbit when the server state is $i = 0,1,2,3$

$\backslash E(L) = P_0^{'} + P_1^{'}(1) + P_2^{'}(1) + P_3^{'}(1)$

We obtain by differentiating $P_0(z), P_1(z), P_2(z), P_3(z)$, we have

$$P_0^{'}(z) = q\eta\lambda P_{0,0}\left[\frac{N_0(z)}{D_0(z)}\right]^{'} \quad (18)$$

Where $N_0(z) = z[1 - B(z_0)(\lambda\gamma - \lambda\gamma z + q\eta + \theta)]$

$N_0^{'}(z) = [1 - B(z_0)(\lambda\gamma - \lambda\gamma z + q\eta + \theta)] + B(z_0)\lambda\gamma z$

$D_0(z) = (\lambda + \alpha + \theta)(\lambda\gamma - \lambda\gamma z + \eta + \theta)z - q\eta(\lambda z + \alpha)$

$D_0^{'}(z) = (\lambda + \alpha + \theta)(\lambda\gamma - 2\lambda\gamma z + \eta + \theta) - q\eta\lambda$

When $z = 1$ in (18) we have $P_0^{'}(1)$ the above equations becomes

$N_0(1) = 1 - B(z_0)(q\eta + \theta)$

$N_0^{'}(1) = 1 - B(z_0)(q\eta - \lambda\gamma + \theta)$

$D_0(1) = (\lambda + \alpha + \theta)(\eta + \theta) - q\eta(\lambda + \alpha)$

$D_0^{'}(1) = (\lambda + \alpha + \theta)(-\lambda\gamma + \eta + \theta) - q\eta\lambda$

Next, we have

$$P_1'(z) = \lambda P_{0,0}\left[\frac{N_1(z)}{D_1(z)}\right]' \quad (19)$$

Where

$N_1(z) = (\lambda+\alpha+\theta)\lambda z[1+p\eta B(z_0)] - \lambda q\eta B(z_0)(\lambda z+\alpha)$

$N_1'(z) = (\lambda+\alpha+\theta)[1+p\eta B(z_0)] - \lambda q\eta B(z_0)$

$D_1(z) = (\lambda+\alpha+\theta)(\lambda\gamma-\lambda\gamma z+\eta+\theta)z - q\eta(\lambda z+\alpha)$

$D_1'(z) = (\lambda+\alpha+\theta)(\lambda\gamma-2\lambda\gamma z+\eta+\theta) - q\eta\lambda$

When $z=1$ in (19) we have $P_1'(1)$ the above equations becomes

$N_1(1) = (\lambda+\alpha+\theta)[1+p\eta B(z_0)] - q\eta B(z_0)(\lambda+\alpha)$

$N_1'(1) = (\lambda+\alpha+\theta)[1+p\eta B(z_0)] - \lambda q\eta B(z_0)$

$D_1(1) = (\lambda+\alpha+\theta)(\eta+\theta) - q\eta(\lambda+\alpha)$

$D_1'(1) = (\lambda+\alpha+\theta)(-\lambda\gamma+\eta+\theta) - q\eta\lambda$

Next, we have

$$P_2'(z) = \lambda P_{0,0}\left[\frac{N_2(z)}{D_2(z)}\right]' \quad (20)$$

Where

$$N_2(z) = z\begin{bmatrix}-[1+p\eta B(z_0)]\begin{bmatrix}\lambda\gamma z(\lambda+\alpha+\theta)(\lambda\gamma-\lambda\gamma z+\mu+\theta)\\ -\lambda\gamma q\eta\alpha(1-z)+\mu q\eta\alpha\end{bmatrix}\\ +q\eta B(z_0)\begin{bmatrix}\lambda\gamma z(\lambda+\alpha)(\lambda\gamma-\lambda\gamma z+\mu+\theta)\\ -\lambda\gamma\alpha\eta(1-z)-\alpha\mu(\eta+\theta)\end{bmatrix}\end{bmatrix}$$

$$N_2'(z) = \begin{bmatrix}-[1+p\eta B(z_0)]\begin{bmatrix}\lambda\gamma z(\lambda+\alpha+\theta)(\lambda\gamma-\lambda\gamma z+\mu+\theta)\\ -\lambda\gamma q\eta\alpha(1-z)+\mu q\eta\alpha\end{bmatrix}\\ +q\eta B(z_0)\begin{bmatrix}\lambda\gamma z(\lambda+\alpha)(\lambda\gamma-\lambda\gamma z+\mu+\theta)\\ -\lambda\gamma\alpha\eta(1-z)-\alpha\mu(\eta+\theta)\end{bmatrix}\end{bmatrix}$$

$$+z\begin{bmatrix}-[1+p\eta B(z_0)][\lambda\gamma(\lambda+\alpha+\theta)(\lambda\gamma-2\lambda\gamma z+\mu+\theta)-\lambda\gamma q\eta\alpha]\\ +q\eta B(z_0)[\lambda\gamma(\lambda+\alpha)(\lambda\gamma-2\lambda\gamma z+\mu+\theta)+\lambda\gamma\alpha\eta]\end{bmatrix}$$

$D_2(z) = [(\lambda+\alpha+\theta)(\lambda\gamma-\lambda\gamma z+\eta+\theta)z - q\eta(\lambda z+\alpha)]$
$[(\lambda+\alpha)\lambda\gamma z-\alpha\mu]$

$D_2'(z) = [(\lambda+\alpha+\theta)(\lambda\gamma-\lambda\gamma z+\eta+\theta)z - q\eta(\lambda z+\alpha)][(\lambda+\alpha)\lambda\gamma z$
$+[(\lambda+\alpha+\theta)(\lambda\gamma-\lambda\gamma z+\eta+\theta)-q\eta\lambda][(\lambda+\alpha)\lambda\gamma z-\alpha\mu]$

When $z=1$ in (20) we have $P_2'(1)$ the above equations becomes

$$N_2(1) = \begin{bmatrix}-[1+p\eta B(z_0)][\lambda\gamma(\lambda+\alpha+\theta)(\mu+\theta)-\mu q\eta\alpha]\\ +q\eta B(z_0)[\lambda\gamma(\lambda+\alpha)(\mu+\theta)-\alpha\mu(\eta+\theta)]\end{bmatrix}$$

$$N_2'(1) = \begin{bmatrix}-[1+p\eta B(z_0)][\lambda\gamma(\lambda+\alpha+\theta)(\mu+\theta)+\mu q\eta\alpha]\\ +q\eta B(z_0)[\lambda\gamma(\lambda+\alpha)(\mu+\theta)-\alpha\mu(\eta+\theta)]\end{bmatrix}$$

$$+\begin{bmatrix}-[1+p\eta B(z_0)][\lambda\gamma(\lambda+\alpha+\theta)(-\lambda\gamma+\mu+\theta)-\lambda\gamma q\eta\alpha]\\ +q\eta B(z_0)[\lambda\gamma(\lambda+\alpha)(-\lambda\gamma+\mu+\theta)-\lambda\gamma\alpha\eta]\end{bmatrix}$$

$D_2(1) = [(\lambda+\alpha+\theta)(\eta+\theta) - q\eta(\lambda+\alpha)][(\lambda+\alpha)\lambda\gamma-\alpha\mu]$

$D_2'(1) = [(\lambda+\alpha+\theta)(\eta+\theta) - q\eta(\lambda+\alpha)](\lambda+\alpha)\lambda\gamma$
$+[(\lambda+\alpha+\theta)(\eta+\theta)-q\eta\lambda][(\lambda+\alpha)\lambda\gamma-\alpha\mu]$

Next, we have

$$P_3'(z) = \lambda P_{0,0}\left[\frac{N_3(z)}{D_3(z)}\right]' \quad (21)$$

Where

$$N_3(z) = \begin{bmatrix}-[1+p\eta B(z_0)]\begin{bmatrix}(\lambda+\alpha+\theta)(\lambda z+\alpha)\lambda\gamma z\\ -q\eta(\lambda z+\alpha)\alpha+(\lambda+\alpha+\theta)\theta z\alpha\end{bmatrix}\\ +q\eta B(z_0)\big[(\lambda z+\alpha)[(\lambda+\alpha)\lambda\gamma z-\alpha\eta]\big]\end{bmatrix}$$

$$N_3'(z) = \begin{bmatrix}-[1+p\eta B(z_0)]\big[(\lambda+\alpha+\theta)[(\lambda z+\alpha)\lambda\gamma+\lambda^2\gamma z+\theta\alpha-q\eta\alpha\lambda]\big]\\ +q\eta B(z_0)(\lambda+\alpha)\lambda\gamma(2\lambda z+\alpha)-\alpha\eta\lambda\end{bmatrix}D_3(z)$$
$$= [(\lambda+\alpha+\theta)(\lambda\gamma-\lambda\gamma z+\eta+\theta)z - q\eta(\lambda z+\alpha)][(\lambda+\alpha)\lambda\gamma z-\alpha\mu]$$

$D_3'(z) = [(\lambda+\alpha+\theta)(\lambda\gamma-\lambda\gamma z+\eta+\theta)z - q\eta(\lambda z+\alpha)](\lambda+\alpha)\lambda\gamma$
$+[(\lambda+\alpha+\theta)(\lambda\gamma-\lambda\gamma z+\eta+\theta)-q\eta\lambda][(\lambda+\alpha)\lambda\gamma z-\alpha\mu]$

When $z=1$ in (21) we have $P_3'(1)$ the above equations becomes

$$N_3(1) = \begin{bmatrix} -[1+p\eta B(z_0)][(\lambda+\alpha+\theta)\big((\lambda+\alpha)\lambda\gamma+\theta\alpha\big)-q\eta(\lambda+\alpha)\alpha] \\ +q\eta B(z_0)(\lambda+\alpha)[(\lambda+\alpha)\lambda\gamma-\alpha\eta] \end{bmatrix}$$

$$N_3^{'}(1) = \begin{bmatrix} -[1+p\eta B(z_0)][(\lambda+\alpha+\theta)(2\lambda^2\gamma+\alpha\lambda\gamma)+\theta\alpha-q\eta\alpha\lambda] \\ +q\eta B(z_0)(\lambda+\alpha)\lambda\gamma(2\lambda+\alpha)-\alpha\eta\lambda \end{bmatrix}$$

$$D_3(1) = [(\lambda+\alpha+\theta)(\eta+\theta)-q\eta(\lambda+\alpha)][(\lambda+\alpha)\lambda\gamma-\alpha\mu]$$

$$D_3^{'}(1) = [(\lambda+\alpha+\theta)(\eta+\theta)-q\eta(\lambda+\alpha)](\lambda+\alpha)\lambda\gamma$$
$$+[(\lambda+\alpha+\theta)(-\lambda\gamma+\eta+\theta)-q\eta\lambda][(\lambda+\alpha)\lambda\gamma-\alpha\mu]$$

NUMERICAL AND GRAPHICAL RESULTS

In this section, we are presenting numerical results to analyze the expected number of customers in the orbit . The curved graph depicted in Figure 2 and the tabulated values in the Table 1 have been derived by maintaining fixed values of $\alpha = 4, \eta = 5, \theta = 1, p = 0.6, q = 0.4, \gamma = 0.4, r = 0.2$ while varying the values of λ from 1 to 2 incremented with *0.2* , and extending the values of α from 3 to 3.4 in steps of 0.2. It has been observed that with an increase in the value of λ rises ,$E(L)$ also rises which shows the stability of the model. In this section ,we are presenting numerical results to analyze the expected number of customers in the orbit . The curved graph depicted in Figure 3 and the tabulated values in the Table 2have been derived by maintaining fixed values of $\alpha = 3, \mu = 4,\ \theta = 1, p = 0.6, q = 0.4, \gamma = 0.4, r = 0.2$ and varying the values of λ from 1 to 2 incremented with 0.2 and extending the values of η from 4.2 to 4.6 in steps of 0.2 . It has been observed that with an increase in the value of λrises ,$E(L)$ also rises which shows the stability of the model.

In this section , we are presenting numerical results to analyze the expected number of customers in the orbit . The curved graph depicted in Figure 4 and the tabulated values the Table 3 are derived by maintaining fixed values $\alpha = 3, \eta = 5,\ \theta = 1, p = 0.6, q = 0.4, \gamma = 0.4, r = 0.2$ and varying the values of λ from 1 to 2 incremented with 0.2 and extending the values of μ from 5 to 7 in steps of 1. It has been observed that with an increase in the value of λrises ,$E(L)$ also rises which shows the stability of the model. In this section, we are presenting numerical results to analyze the expected number of customers in the orbit . The curved graph depicted in Figure 4 and tabulated values the Table 4 are derived by maintaining fixed values $\alpha = 3, \mu = 4, \nu = 5, \theta = 1, p = 0.6, q = 0.4, r = 0.2$ and varying the values of λ from 1 to 2 incremented with 0.2 and extending the values of γ from 0.7 to 1.1 in steps of 0.2. . It has been observed that with an increase in the value of λrises ,$E(L)$ also rises which shows the stability of the model.

CONCLUSION

In this paper, we analyze a Markovian retrial queueing model with non-persistent customers working vacation and vacation interruption under Bernoulli schedule. We obtain the PGF for the number of customers and the mean number of customers in the orbit. We also derive the performance measures. We perform some particular cases. We illustrate some numerical results.

REFERENCES

1. A. Aissani., S. Taleb., T. Kernane., G. Saidi., and D. Hamadouche.,. "An M/G/1 retrial queue with working vacation", Advances in Intelligent Systems and Computing, 240, 443-452, (2014).
2. A.Gomez-Corral, "Stochastic analysis of a single server retrial queue with general retrial time", Naval Res. Log., 46 ,561-581, (1999).
3. B. Krishna Kumar, Pavaimadheswari and A Vijayakumar, "The M/G/1 retrial queue with feedback and starting failures", Applied Mathematical modelling, 26, pp.1057- 1075, (2002).
4. D.Wu and H.Takagi., "M/G/1 queue with multiple working vacations", Perform. Eval, 63, pp.654-681, (2006).
5. G.I.Falin., "A Survey on Retrial Queues", Queueing Systems Theory and Applications, 7, pp.127-168, (1990).

6. G.I.Falin and J.G., C.Templeton., "Retrial queues", Chapman and Hall, London, (1997).
7. Jau-chuanke., Fu-min chang., "Modified vacation Policy for M/G/1 retrial queue with balking and feedback", Computers and Industrial Engineering, 57, 433-443, (2009).
8. J.Medhi., "Stochastic Models in Queueing Theory", Second Edition (2003).
9. J.R.Artalejo., " Accessible bibliography on retrial queue", Math. Comput.Modell., 30, pp.1-6, (1999).
10. J.R.Artalejo and G.Falin., "Standard and retrial queueing systems: A Comparitive Analysis"., Rev. Math. Comput., 15, 101-129, (2002).
11. K. Kalidass and KasturiRamanath, "Time dependent analysis of M/M/1 queue with server vacations and a waiting server", QTNA, August, pp.23-26, (2011).
12. KasturiRamanath and Kalidass K: An M/G/1 retrial queue with non-persistent customers, a second optional service and different vacation policies, Applied Mathematical Sciences 2010:4(40);1967-1974.
13. Krishnamorthy A, Deepak T.G. and Joshua V.C., An M/G/1 retrial queue with nonpersistent customers and orbital search. Stochastic Analysis and Applications 2005:4;975-997.
14. PazhaniBalaMurugan S and Vijayakrishnaraj R: A bulk arrival retrial queue with nonpersistent customers and exponentially distributed multiple working vacation. AIP Conference Proceedings 2019:2177;020064.
15. K. Santhi and S. PazhaniBalaMurugan., "A Bulk input queueing system with Feedback and Single Working Vacation", Int. J. Scientific Research and Management Studies, 1(5)(2014), 168-176.
16. L.Servi and S.Finn, "M/M/1 queue with working vacations (M/M/1/WV)", Perform. Eval, 50, pp.41-52, (2002).
17. Li and Tian. N., "The M/M/1 queue with working vacation and vacation interruption"., Journal of Systems Science and System Engineering, 16, 121-127, (2007).
18. O.J.Boxma, S.Schlegel and U.Yechiali, "M/G/1 queue with waiting server timer and vacations", American Mathematical Society Translations, 2(207), pp.25-35, (2002).
19. P. Rajadurai, M. C. Saravanarajan and V.M.Chandrasekaran, "A study on M/G/1 feedback retrial queue with subject to server breakdown and repain under multiple working vacation policy", Alexandria University, Alexandria Engineering Journal, 57, 947-962, (2018).
20. R. Kalyanaraman and S.PazhaniBalaMurugan.S., "A single server retrial queue with vacation", J.Appl.Math.and Informatics, 26(3-4), pp.721-732, (2008).
21. S.PazhaniBalaMurugan and K.Santhi., "An M//G/1 retrial queue with multiple working vacation", International Journal of Mathematics and its Applications, 4(2-D), pp.35-48, (2016).
22. T.Yang and J.G.C.Templeton., "A Survey on Retrial Queues", Queue. Syst., 2, pp.201- 233, (1987).
23. T.Takine and T.Hasegawa., "A note on M/G/1 vacation system with waiting time limits", Kyoto University Adv. Appl. Prob., 22, pp.513-518, (1990).
24. V.M.Chandrasekaran, K.Indhira, M.C.Saravanarajan and P.Rajadurai, "A survey on working vacation queueing models", International Journal of Pure and Applied Mathematics, 106(6), pp.33-41, (2016).
25. Zhang and Shi., "The M/M1 queue with Bernoulli-scheduled- controlled vacation and vacation interruption", International Journal of Information and Management Sciences, 20, 579-587, (2009).

Tables

Table 1: L_s with turn over of λ

λ	$\alpha = 3$	$\alpha = 3.2$	$\alpha = 3.4$
1.0	0.0017	0.0014	0.0011
1.2	0.0038	0.0033	0.0029
1.4	0.0059	0.0053	0.0048
1.6	0.0075	0.0070	0.0065
1.8	0.0089	0.0083	0.0078
2.0	0.0100	0.0094	0.0089

Table 2: L_s with turn over of λ

λ	$\eta = 4.2$	$\eta = 4.4$	$\eta = 4.6$
1.0	0.0042	0.0034	0.0008

1.2	0.0084	0.0068	0.0018
1.4	0.0129	0.0103	0.0027
1.6	0.0166	0.0131	0.0036
1.8	0.0190	0.0151	0.0043
2.0	0.0205	0.0165	0.0049

Table 3: L_s with turn over of λ

λ	$\mu = 5$	$\mu = 6$	$\mu = 7$
1.0	0.0005	0.0002	0.0001
1.2	0.0012	0.0005	0.0003
1.4	0.0018	0.0008	0.0004
1.6	0.0024	0.0011	0.0006
1.8	0.0029	0.0014	0.0008
2.0	0.0034	0.0016	0.0009

Table 4: L_s with turn over of λ

λ	$\gamma = 0.7$	$\gamma = 0.9$	$\gamma = 1.1$
1.0	0.0047	0.0045	0.0051
1.2	0.0069	0.0064	0.0072
1.4	0.0088	0.0084	0.0102
1.6	0.0108	0.0111	0.0155
1.8	0.0131	0.0154	0.0294
2.0	0.0162	0.0244	0.1221

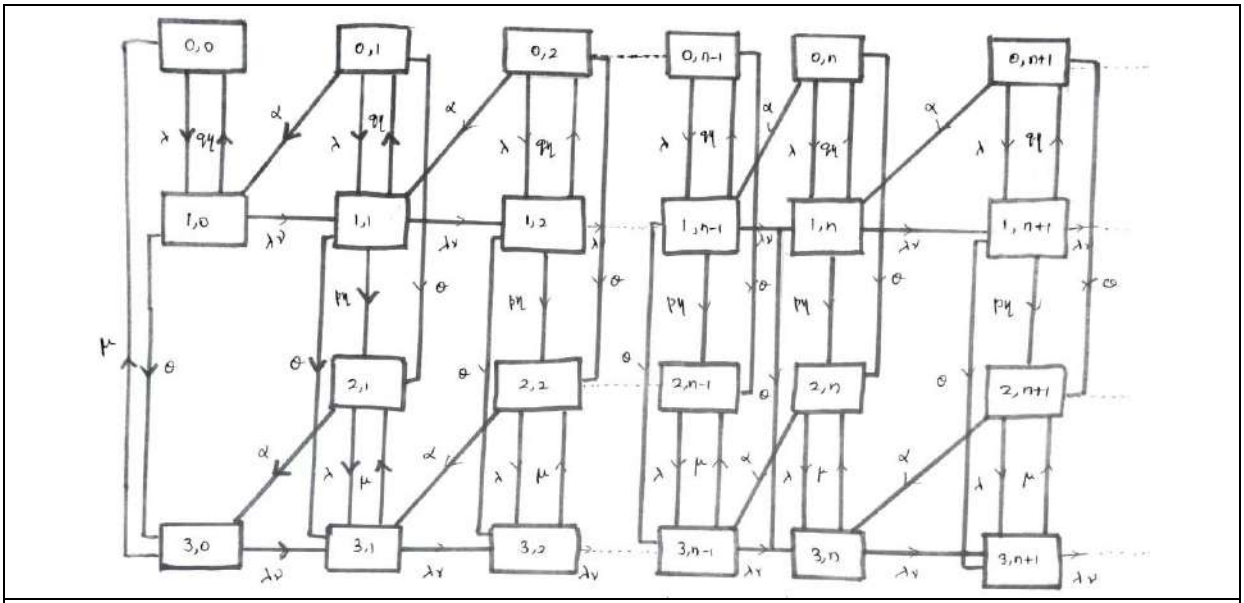

Figure 1

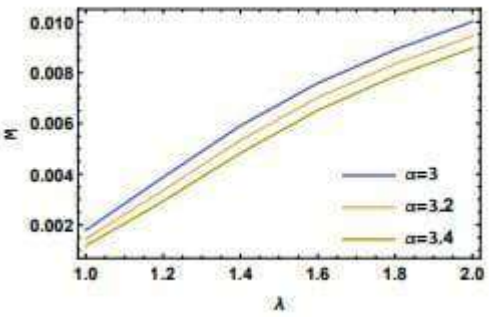

Figure 1: L_s with turn over of λ

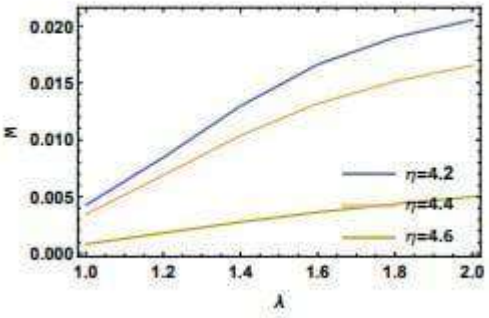

Figure 2: L_s with turn over of λ

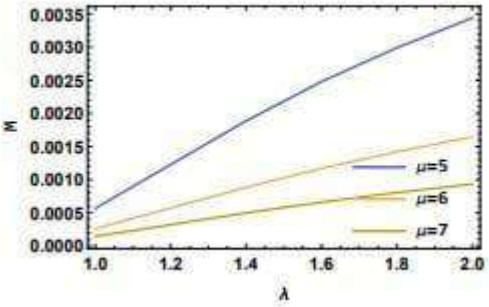

Figure 3: L_s with turn over of λ

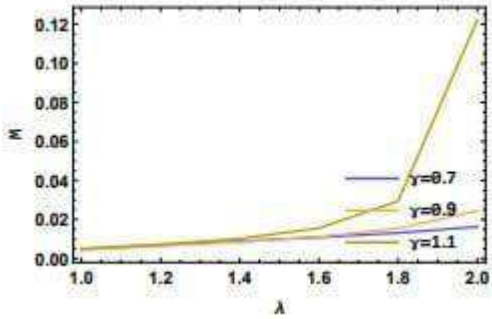

Figure 4: L_s with turn over of λ

Indian Journal of Natural Sciences www.tnsroindia.org.in ©IJONS

Vol.15 / Issue 88 / Feb / 2025 *International Bimonthly (Print) – Open Access* *ISSN: 0976 – 0997*

RESEARCH ARTICLE

A Note on Laplacian Spectrum of Fuzzy Generalized Petersen Graphs

C. Jebakiruba[1] and A. Amutha[2]*

[1]Assistant Professor, Department of Mathematics, Lady Doak College, (Affiliated to Madurai Kamaraj University), Madurai, Tamil Nadu, India.
[2]Assistant Professor, Department of Mathematics, The American College, (Affiliated to Madurai Kamaraj University), Madurai, Tamil Nadu, India.

Received: 08 Aug 2024 Revised: 03 Nov 2024 Accepted: 31 Dec 2024

***Address for Correspondence**
A. Amutha,
Assistant Professor,
Department of Mathematics,
The American College,
(Affiliated to Madurai Kamaraj University),
Madurai, Tamil Nadu, India.
E.Mail: amuthajo@gmail.com

ABSTRACT

Graphs plays a foremost role in the arena of sciences which supports in exploring and solving the factual snags. Depicting a scientific problem into a graph and finding its eigen values will overlay solutions for some problems. Petersen graph, a peculiar graph structure which opens up many different approaches in the interconnection networks toiled us to examine its Laplacian spectrum. In order to obtain its Laplacian spectrum, either from its vertex membership values or from its edge membership values, this paper analyzes the behavior of a fuzzy generalized Petersen graph with jumps two and three. This avoids the typical procedure of determining its corresponding degree matrix, adjacency matrix, Laplacian matrix, and finally its Laplacian spectrum. This is extremely time-consuming, and even with machine aid, there is a possibility of mistakes that could result in incorrect eigenvalue calculations. By labeling the generalized Petersen graph and then analyzing its structure, pattern, and behavior, some astounding findings were seen, which are covered in this study.

Keywords: Fuzzy graph, Eigen values, Degree matrix, Adjacency matrix, Laplacian matrix, Laplacian spectrum, Trace, Petersen graph

INTRODUCTION

Kaufmann in 1973 defined fuzzy graph theory on Zadeh's view on fuzzy sets [3][4]. Then Azriel Rosenfeld contributed vastly on fuzzy graph theory [2]. The Laplacian spectrum of a simple graph was discussed by Grone, Robert and Merris during 1990 [1]. Mohar, Bojan, Alavi and Chartrand focused on Laplacian spectrum of simple

graphs [6]. The spectrum of generalized Petersen graphs was dealt by Ralucca Gera and Pantelimon during 2011 where they have described spectrum through classes of graphs [5]. Fuzzy theory has vast applications which was discussed by K.H.Lee [7]. Fuzzy graph theory is an emerging concept whereas Laplacian spectrum of fuzzy graph theory, that is, eigen values of corresponding Laplacian matrix of a given fuzzy graph has not been taken up in many areas of application because of its calculation procedure which is very tedious. Even if we thought of getting machine assistance, there is no easy way for feeding the values and getting its Laplacian spectrum. When the graph becomes larger or when the number of vertices and edges increases the Laplacian matrix will be more complicated and a chance for error is high. If we make a mistake in feeding any one digit, it will affect the Laplacian spectrum in a large extent. So, we tried to find a way in which only by feeding the vertex membership values or edge membership values we can immediately get the Laplacian spectrum for the fuzzy graph. In this journey we first investigated complete fuzzy graphs and depicted an effective algorithm which only gets the values of vertex membership values and immediately gives the Laplacian spectrum [8]. Then we concentrated on fuzzy cycle. Since, the sum of eigen values of matrix is equal to the trace of that matrix, we started investigating the trace of Laplacian matrix of fuzzy graph and we got some interesting results. Then we found out a way for finding the least and greatest Laplacian spectrum of fuzzy cycle and regular fuzzy cycle. After that we obtained few results for general fuzzy graphs. Ensuing that we decided to enter into symmetric interconnection networks in particular on fuzzy generalized Petersen graphs.

1.BASIC CONCEPTS

Let G (V, E) be a simple connected graph with vertex set V and edge set E having n number of vertices and m number of edges where n, m >1. A fuzzy graph with V as the underlying set is a pair G: (σ,μ) with n vertices and m edges where σ:V→[0,1] is a fuzzy subset and μ:VxV→[0,1] is a fuzzy relation on such that μ(x,y)≤σ(x)∧σ(y) ∀x,yϵV, where stands for minimum [5][6][7]. For a fuzzy graph, adjacency matrix A(G) is a square matrix of order n and A(G) = [aij] where aij=μ(ui,uj) entry is the strength of relation between the vertices ui and uj [6][7]. The degree matrix D(G) is also a square matrix of order n and D(G) = [dij] where dij= dGvi if i=j and zero otherwise [6][7]. The Laplacian matrix L(G) is the difference between the corresponding adjacency matrix from the corresponding degree matrix [6][7]. The generalized Petersen graph, P(m, n) has vertices, respectively, edges given by V(P(m, n)) = {ai,bi, 0 ≤ i ≤ m − 1}, E(P(m, n)) = {aiai+1,aibi,bibi+n|, 0 ≤ i ≤ m − 1}, where the subscripts are expressed as integers modulo m (m ≥ 5), and n is the "skip" [9]. We fuzzified general Petersen graph by labelling it in such a way that μ(x,y)≤σ(x)∧σ(y) ∀x,yϵV, where stands for minimum and σ:V→[0,1] is a fuzzy subset and μ:VxV→[0,1] is a fuzzy relation on any graph G: (σ,μ) with n vertices and m edges. Trace of a matrix is the sum of the diagonal entries of the matrix. The Laplacian spectrum of a graph is the corresponding eigen values of Laplacian matrix of that graph.

2.MAIN RESULTS

Any mathematical concept is approachable even by a layman only when it is simple and understandable. Laplacian spectrum of fuzzy graph because of its complexity in calculation is not welcomed in many fields. If this issue can be resolved then its application can be in many fields This motivated us to start our expedition by analyzing fuzzy graphs which follows some pattern. We categorically started working on complete fuzzy graphs fuzzy cycle, vertex regular graphs and also, we enthralled in approaching eigen values of Laplacian matrix for the given graph through its trace. All through this voyage we got interesting results on general fuzzy graphs which now encouraged us to analyze fuzzy generalized Petersen graphs which gave us some interesting fall outs.

3.1 Trace of Laplacian matrix of fuzzy generalized Petersen graphs

We know that trace of a matrix is equal to the sum of its corresponding eigen values of the matrix. While examining different types of fuzzy graphs we got a formula for finding trace of the given fuzzy graph as trace = 2i. Depending on the definition of different types of fuzzy graphs, for some fuzzy graphs it is better to use its vertex membership values to find its trace whereas for certain fuzzy graphs using edge membership values will be effective. These we have already discussed in our previous paper which is in press.

We tried to approach Laplacian spectrum of the given fuzzy generalized Petersen graph through its trace. On this approach we came to know that Laplacian matrix of given fuzzy generalized Petersen graph depends only on its edge membership values. The above formula also works for fuzzy generalized Petersen graphs.
Since Laplacian spectrum for any fuzzy generalized Petersen graph depends only on its edge membership values, we started labelling it in two ways, not all edge membership values get the same value or all membership values get the same value. While we analysed it separately, we got another formula for finding trace when all membership values are same for the given fuzzy generalized Petersen graph. We can use any one formula for finding trace only when all membership values are same. If not, all edge membership values are same above formula can be used to find its trace. Here we denote fuzzy generalized Petersen graph as FP(m,2).

Theorem 3.1.1. Let P(m,2), m≥ 5 be a fuzzy generalized Petersen graph. If all membership values of P(m,2) are same and the graph is cubic graph then the trace of Laplacian matrix for the given fuzzy generalized Petersen graph is $6\mu m$.
Proof. Let FP(m,2) be the given fuzzy generalized Petersen graph. Since it is a cubic graph, the degree of each vertex will be 3μ. Also, Laplacian matrix is a 2m x 2m square matrix. Hence,
the trace of Laplacian matrix = $3\mu \times 2m$
$= 6\mu m$

3.2 Laplacian spectrum of a fuzzy P(m,2)
Here we have discussed the nature of eigen values of the corresponding Laplacian matrix for the fuzzy generalized Petersen graph with jump two. We know that the number of Laplacian spectrums for any graph depends on the number of vertices of the graph. That is, if the graph has 30 vertices, then the corresponding Laplacian matrix is a 30 x 30 matrix and there will be 30 eigen values for the corresponding Laplacian matrix. Now, let us discuss about the Laplacian spectrum when all the edges are labelled in such a way that not all edges have the same membership values. On examining the nature and behavior of the Laplacian matrix of fuzzy P(m,2) we have got the following results.

Theorem 3.2.1. For any fuzzy P(m,2) where m≥5 when not all edges have the same membership values the Laplacian spectrum are distinct or unique.
Proof. Let FP(m,2) be the given fuzzy generalized Petersen graph. Let the edges be labelled in such a way that the edge membership values are not all same. If we find the Laplacian matrix for the corresponding fuzzy generalized Petersen graph, it is a square matrix and the nilpotent part is zero. We have the property that a matrix is diagonalizable if and only if its nilpotent part is zero. Hence, the matrix is diagonalizable. We also have the property that a square matrix with distinct eigen values is only diagonalizable. Hence, the eigen values are all distinct or unique.

Note. Now, let us discuss about the Laplacian spectrum when all the edges are labelled in such a way that all edges have the same membership values. While examining the graphs after labelling we saw that FP(5,2), FP(10,2), FP(15,2),… behaves differently from FP(m,2) when m = 6,7,8,9,11,12,13,14,16,… Thus, examination of FP(m,2) we observed that depending on 'm' even or odd, the Laplacian spectrum followed a pattern. Thus, we got the following results.

Theorem 3.2.2. For any fuzzy P(m,2) where m≥6, m is even, m ≠ 5, 10, 15, ... and all edges have the same membership values then there are (m-2) distinct pairs and 4 distinct Laplacian Spectrum including the least Laplacian spectrum 0.
Proof. Let FP(m,2) be the given fuzzy generalized Petersen graph. Let the edges be labelled in such a way that the edge membership values are all same. Let us prove this theorem by induction on m. Let m = 6, then the total number of vertices in the graph is 12 and total number of edges is 18. Let 1=2=…=18= μ. Then the corresponding degree matrix D(FP(6,2)), adjacency matrix (FP(6,2)) and the Laplacian matrix L(FP(6,2)) are 12 x 12 matrix and is given by

$$L(FP(6,2))=\begin{pmatrix} 3\mu & -\mu & 0 & \dots & 0 \\ -\mu & 3\mu & -\mu & \dots & 0 \\ 0 & -\mu & 3\mu & \dots & 0 \\ 0 & 0 & -\mu & \dots & 0 \\ & \dots & \dots & \dots & \\ 0 & 0 & 0 & \dots & 3\mu \end{pmatrix}$$

Then the Laplacian spectrum is given by,

$$|L(FP(6,2)) - \lambda I| = \begin{vmatrix} 3\mu-\lambda & -\mu & 0 & \dots & 0 & 0 \\ -\mu & 3\mu-\lambda & -\mu & \dots & 0 & 0 \\ 0 & -\mu & 3\mu-\lambda & \dots & 0 & 0 \\ & & \dots & \dots & \dots & \\ 0 & 0 & 0 & \dots & 3\mu-\lambda & -\mu \\ 0 & 0 & 0 & \dots & -\mu & 3\mu-\lambda \end{vmatrix} = 0$$

$$\Rightarrow \lambda(\lambda-\lambda_1)^2(\lambda-\lambda_2)^2(\lambda-\lambda_3)^2(\lambda-\lambda_4)^2(\lambda-\lambda_5)(\lambda-\lambda_6)(\lambda-\lambda_7)=0$$

Hence, we see that four distinct eigen values are in pairs and four distinct eigen values are there.Let m = 8, then the total number of vertices in the graph is 16 and total number of edges is 24. Let $\mu_1=\mu_2=\cdots=\mu_{24}=\mu$. Then the corresponding Laplacian matrix L(FP(8,2)) are 16 x 16 matrix and is given by

$$L(FP(8,2)) = \begin{pmatrix} 3\mu & -\mu & 0 & \dots & 0 \\ -\mu & 3\mu & -\mu & \dots & 0 \\ 0 & -\mu & 3\mu & \dots & 0 \\ 0 & 0 & -\mu & \dots & 0 \\ & \dots & \dots & \dots & \\ 0 \dots & \dots & \dots & -\mu & \\ 0\,0 & 0 & \dots & 3\mu & \end{pmatrix}$$

Then the Laplacian spectrum is given by,

$$|L(FP(8,2)) - \lambda I| = \begin{vmatrix} 3\mu-\lambda & -\mu & 0 & \dots & 0 & 0 \\ -\mu & 3\mu-\lambda & -\mu & \dots & 0 & 0 \\ 0 & -\mu & 3\mu-\lambda & \dots & 0 & 0 \\ & & \dots & \dots & \dots & \\ & & \dots & \dots & \dots & \\ 0 & 0 & \dots 3\mu-\lambda & -\mu & & \\ 0 & 0 & \dots & -\mu & \mu-\lambda & \end{vmatrix} = 0$$

$$\lambda(\lambda-\lambda_1)^2(\lambda-\lambda_2)^2(\lambda-\lambda_3)^2(\lambda-\lambda_4)^2(\lambda-\lambda_5)^2(\lambda-\lambda_6)^2(\lambda-\lambda_7)(\lambda-\lambda_8)(\lambda-\lambda_9)=0$$

Hence, we see that six distinct eigen values in pairs and four distinct eigen values are there. Therefore, whenever two vertices are added we observe that we get one more distinct pair of eigen values. Hence there are 8-2=6 pairs and 4

distinct eigen values including zero. Let us assume that the result is true for m-2 number of vertices. Then we have (m-2)-2 = (m-4) pairs and 4 distinct eigen values including zero. Let us consider m = (m-2)+2, that is adding 2 vertices to (m-2), then we get (m-2) eigen values in pairs and 4 distinct eigen values including zero for its corresponding Laplacian matrix. Hence proved.

Theorem 3.2.3. For any fuzzy P(m,2) where $m \geq 7$, m is odd, $m \neq 5, 10, 15, \ldots$ and all edges have the same membership values then there are (m-1) distinct pairs and 2 distinct Laplacian spectrum including the least Laplacian spectrum 0.

Proof.Let FP(m,2) be the given fuzzy generalized Petersen graph. Let the edges be labelled in such a way that the edge membership values are all same. Let us prove this theorem by induction on m. Let m = 7, then the total number of vertices in the graph is 14 and total number of edges is 21. Let $\mu_1 = \mu_2 = \cdots = \mu_{21} = \mu$. Then the correspondingLaplacian matrix L(FP(m,2)) are 14 x 14 matrix and is given by

$$L(FP(7,2)) = \begin{pmatrix} 3\mu & -\mu & 0 & \ldots & 0 \\ -\mu & 3\mu & -\mu & \ldots & 0 \\ 0 & -\mu & 3\mu & \ldots & 0 \\ 0 & 0 & -\mu & \ldots & 0 \\ & \ldots & \ldots & \ldots & \\ 0 \ldots & \ldots & \ldots & -\mu & \\ 0\,0 & 0 & \ldots & 3\mu & \end{pmatrix}$$

Then the Laplacian spectrum is given by,

$$|L(FP(7,2)) - \lambda I| = \begin{vmatrix} 3\mu-\lambda & -\mu & 0 & \ldots & 0 & 0 \\ -\mu & 3\mu-\lambda & -\mu & \ldots & 0 & 0 \\ 0 & -\mu & 3\mu-\lambda & \ldots & 0 & 0 \\ & & \ldots & \ldots & \ldots & \\ & & \ldots & \ldots & \ldots & \\ 0 & 0 & 0 & \ldots 3\mu-\lambda- & \mu & \\ 0 & 0 & 0 & \ldots -\mu 3\mu-\lambda & & \end{vmatrix} = 0$$

$$\Rightarrow \lambda(\lambda-\lambda_1)^2(\lambda-\lambda_2)^2(\lambda-\lambda_3)^2(\lambda-\lambda_4)^2(\lambda-\lambda_5)^2(\lambda-\lambda_6)^2(\lambda-\lambda_7) = 0$$

Hence, we see that six distinct eigen values are in pairs and two distinct eigen values that includes zero are there. That is there are 7-1=6 pairs and 2 distinct eigen values including zero Let m = 9, then the total number of vertices in the graph is 18 and total number of edges is 27. Let $\mu_1 = \mu_2 = \cdots = \mu_{27} = \mu$. Then the corresponding Laplacian matrix L(FP(9,2)) is 18 x 18 matrix and is given by

$$L(FP(9,2)) = \begin{pmatrix} 3\mu & -\mu & 0 & \ldots & 0 \\ -\mu & 3\mu & -\mu & \ldots & 0 \\ 0 & -\mu & 3\mu & \ldots & 0 \\ 0 & 0 & -\mu & \ldots & 0 \\ & \ldots & \ldots & \ldots & \\ 0 \ldots & \ldots & \ldots & \ldots & -\mu \\ 0\,0 & 0 & \ldots & \ldots & 3\mu \end{pmatrix}$$

Then the Laplacian spectrum is given by,

$$|L(FP(9,2)) - \lambda I| = \begin{vmatrix} 3\mu-\lambda & -\mu & 0 & \dots & 0 & 0 & \\ -\mu & 3\mu-\lambda & -\mu & \dots & 0 & 0 & \\ 0 & -\mu & 3\mu-\lambda & \dots & 0 & 0 & \\ & \dots & \dots & \dots & & & \\ 0 & 0 & 0 & \dots & 3\mu-\lambda & -\mu & \\ 0 & 0 & 0 & \dots & -\mu & 3\mu-\lambda & \end{vmatrix} = 0$$

$$\lambda(\lambda-\lambda_1)^2(\lambda-\lambda_2)^2(\lambda-\lambda_3)^2(\lambda-\lambda_4)^2(\lambda-\lambda_5)^2(\lambda-\lambda_6)^2(\lambda-\lambda_7)^2(\lambda-\lambda_8)^2(\lambda-\lambda_9)=0$$

Hence, we see that eight distinct eigen values in pairs and two distinct eigen values including zero are there. Therefore, whenever two vertices are added we observe that we get one more distinct pair of eigen values. Hence there are 9-1=8 pairs and 2 distinct eigen values including zero. Let us assume that the result is true for m-2 number of vertices. Then we have (m-2)-1=(m-3) pairs and 2 distinct eigen values including zero. Let us consider m = (m-2)+2, that is adding 2 vertices to (m-2), then we get (m-1) eigen values in pairs and 2 distinct eigen values including zero for its corresponding Laplacian matrix. Hence proved.

Proposition 3.2.4. For fuzzy P(m,2) where m = 10, 15, 20, 25, … and all edges have the same membership values then the least Laplacian spectrum is 0 and all the other Laplacian spectrum are in distinct pairs and as distinct groups.

Theorem 3.2.5. For any FP(m,3) where $m \geq 8$, m is even, also whenm = 10, 15, ... and all edges have the same membership values then the greatest Laplacian Spectrum is $6\mu$and the least Laplacian spectrum is 0.

Proof. Let FP(m,3) be the given fuzzy generalized Petersen graph. Let the edges be labelled in such a way that the edge membership values are all same. Let us prove this theorem by induction on m. Let m = 8, then the total number of vertices in the graph is 16 and total number of edges is 24. Let $\mu_1 = \mu_2 = \cdots = \mu_{24} = \mu$. Then the corresponding Laplacian matrix L(FP(8,3)) are 16 x 16 matrix and is given by

$$L(FP(8,3)) = \begin{pmatrix} 3\mu & -\mu & 0 & \dots & 0 \\ -\mu & 3\mu & -\mu & \dots & 0 \\ 0 & -\mu & 3\mu & \dots & 0 \\ 0 & 0 & -\mu & \dots & 0 \\ & \dots & \dots & \dots & \\ 0 & 0 & 0 & \dots & 3\mu \end{pmatrix}$$

Then the Laplacian spectrum is given by,

$$|L(FP(8,3)) - \lambda I| = \begin{vmatrix} 3\mu-\lambda & -\mu & 0 & \dots & 0 & 0 \\ -\mu & 3\mu-\lambda & -\mu & \dots & 0 & 0 \\ 0 & -\mu & 3\mu-\lambda & \dots & 0 & 0 \\ & & \dots & \dots & & \\ & & \dots & \dots & & \\ 0 & 0 & 0 & \dots & 3\mu-\lambda & -\mu \\ 0 & 0 & 0 & \dots & -\mu & 3\mu-\lambda \end{vmatrix} = 0$$

$\Rightarrow \lambda(\lambda-\lambda_1)^4(\lambda-\lambda_2)^3(\lambda-\lambda_3)^3(\lambda-\lambda_4)^4(\lambda-\lambda_5)=0$

Hence, we see that the least eigen value is 0 and the greatest eigen value is $\lambda_5 = 6\mu$.
Let m = 10, then the total number of vertices in the graph is 20 and total number of edges is 30. Let $\mu_1 = \mu_2 = \cdots = \mu_{30} = \mu$. Then the corresponding Laplacian matrix L(FP(10,3)) are 20 x 20 matrix and is given by

$$L(FP(10,3))=\begin{pmatrix} 3\mu & -\mu & 0 & \dots & 0 \\ -\mu & 3\mu & -\mu & \dots & 0 \\ 0 & -\mu & 3\mu & \dots & 0 \\ 0 & 0 & -\mu & \dots & 0 \\ & \dots & \dots & \dots & \\ 0\dots & \dots & \dots & -\mu & \\ 0\,0 & 0 & \dots & 3\mu & \end{pmatrix}$$

Then the Laplacian spectrum is given by,

$$|L(FP(10,3))-\lambda I| = \begin{vmatrix} 3\mu-\lambda & -\mu & 0 & \dots & 0 & 0 & \\ -\mu & 3\mu-\lambda & -\mu & \dots & 0 & 0 & \\ 0 & -\mu & 3\mu-\lambda & \dots & 0 & 0 & \\ & & \dots & \dots & \dots & & \\ & & \dots & \dots & \dots & & \\ 0 & 0 & \dots & 3\mu-\lambda & -\mu & & \\ 0 & 0 & \dots & -\mu & \mu-\lambda & & \end{vmatrix} = 0$$

$\lambda(\lambda-\lambda_1)^4(\lambda-\lambda_2)^5(\lambda-\lambda_3)^5(\lambda-\lambda_4)^4(\lambda-\lambda_5)=0$

We see that the least eigen value is 0 and the greatest eigen value is $\lambda_5 = 6\mu$. Therefore, by induction hypothesis we see that whenever two vertices are added we observe that we get least eigen value as 0 and greatest eigen value as 6μ. Hence proved.

Note. For any FP(m,3), m = 10, 15, ... and all edges have the same membership values then also the greatest Laplacian Spectrum is 6μ and the least Laplacian spectrum is 0 which differes from the pattern that we got in analysing FP(m,2), m = 10, 15, … .

Theorem 3.2.6. For any FP(m,3) where $m \geq 7$, m is odd, m ≠ 5, 10, 15, ... and all edges have the same membership values then there are (m-1) distinct pairs and 2 distinct Laplacian spectrum including the least Laplacian spectrum 0.
Proof.Let FP(m,3) be the given fuzzy generalized Petersen graph. Let the edges be labelled in such a way that the edge membership values are all same. Let us prove this theorem by induction on m. Let m = 7, then the total number of vertices in the graph is 14 and total number of edges is 21. Let $\mu_1 = \mu_2 = \cdots = \mu_{21} = \mu$. Then the corresponding Laplacian matrix L(FP(7,3)) are 14 x 14 matrix and is given by

$$L(FP(7,3)) = \begin{pmatrix} 3\mu & -\mu & 0 & \dots & 0 \\ -\mu & 3\mu & -\mu & \dots & 0 \\ 0 & -\mu & 3\mu & \dots & 0 \\ 0 & 0 & -\mu & \dots & 0 \\ & \dots & \dots & \dots & \\ 0 \dots & \dots & \dots & -\mu & \\ 0\,0 & 0 & \dots & 3\mu & \end{pmatrix}$$

Then the Laplacian spectrum is given by,

$$|L(FP(7,3)) - \lambda I| = \begin{vmatrix} 3\mu-\lambda & -\mu & 0 & \dots & 0 & 0 \\ -\mu & 3\mu-\lambda & -\mu & \dots & 0 & 0 \\ 0 & -\mu & 3\mu-\lambda & \dots & 0 & 0 \\ & & \dots & \dots & \dots & \\ & & \dots & \dots & \dots & \\ 0 & 0 & 0 & \dots & 3\mu-\lambda & -\mu \\ 0 & 0 & 0 & \dots & -\mu & 3\mu-\lambda \end{vmatrix} = 0$$

$$\Rightarrow \lambda(\lambda-\lambda_1)^2(\lambda-\lambda_2)^2(\lambda-\lambda_3)^2(\lambda-\lambda_4)^2(\lambda-\lambda_5)^2(\lambda-\lambda_6)^2(\lambda-\lambda_7) = 0$$

Hence, we see that six distinct eigen values are in pairs and two distinct eigen values that includes zero are there. That is there are 7-1=6 pairs and 2 distinct eigen values including zero Let m = 9, then the total number of vertices in the graph is 18 and total number of edges is 27. Let $\mu_1 = \mu_2 = \cdots = \mu_{27} = \mu$. Then the corresponding Laplacian matrix L(FP(9,3)) is 18 x 18 matrix and is given by

$$L(FP(9,3)) = \begin{pmatrix} 3\mu & -\mu & 0 & \dots & 0 \\ -\mu & 3\mu & -\mu & \dots & 0 \\ 0 & -\mu & 3\mu & \dots & 0 \\ 0 & 0 & -\mu & \dots & 0 \\ & \dots & \dots & \dots & \\ 0 \dots & \dots & \dots & -\mu & \\ 0\,0 & 0 & \dots & 3\mu & \end{pmatrix}$$

Then the Laplacian spectrum is given by,

$$|L(FP(9,3)) - \lambda I| = \begin{vmatrix} 3\mu-\lambda & -\mu & 0 & \dots & 0 & 0 \\ -\mu & 3\mu-\lambda & -\mu & \dots & 0 & 0 \\ 0 & -\mu & 3\mu-\lambda & \dots & 0 & 0 \\ & & \dots & \dots & \dots & \\ 0 & 0 & 0 & \dots & 3\mu-\lambda & -\mu \\ 0 & 0 & 0 & \dots & -\mu & 3\mu-\lambda \end{vmatrix} = 0$$

$$\lambda(\lambda-\lambda_1)^2(\lambda-\lambda_2)^2(\lambda-\lambda_3)^2(\lambda-\lambda_4)^2(\lambda-\lambda_5)^2(\lambda-\lambda_6)^2(\lambda-\lambda_7)^2(\lambda-\lambda_8)^2(\lambda-\lambda_9) = 0$$

Hence, we see that eight distinct eigen values in pairs and two distinct eigen values including zero are there. Therefore, whenever two vertices are added we observe that we get one more distinct pair of eigen values. Hence there are 9-1=8 pairs and 2 distinct eigen values including zero. Let us assume that the result is true for m-2 number of vertices. Then we have (m-2)-1=(m-3) pairs and 2 distinct eigen values including zero. Let us consider m = (m-2)+2, that is adding 2 vertices to (m-2), then we get (m-1) eigen values in pairs and 2 distinct eigen values including zero for its corresponding Laplacian matrix. Hence proved.

Corollary 3.2.7. For FP(5,2) and FP(5,3) with all edges having the same membership values the exact Laplacian spectrum is 0, 5μ with algebraic multiplicity four and 2μ with algebraic multiplicity five. For example, When considering a FP(5,2) and FP(5,3), both the graphs are same. Let $\mu_1 = \mu_2 = \cdots = \mu_{15} = 0.6$ Without finding the Laplacian matrix, the Laplacian spectrum of Fig.2 is 0, 3, 3, 3, 3, 1.2, 1.2, 1.2, 1.2, 1.2.

Note: After analysing the fuzzy generalized Petersen graph of jump two and three, we could see only few similarities. Even though all are cubic graph except for FP(6,3), we cannot say that they follow the same pattern in their Laplacian spectrum.

CONCLUSION

We started this work with the goal of figuring out how to count the Laplacian spectrum directly from the fuzzy graph's vertex or edge membership values without following the standard protocol. We have now ventured into interconnection networks and explored some results regarding the spectrum of the Laplacian matrix for a fuzzy generalized Petersen graph. Our goal is to expand this as an application, so that future scholars can easily adopt the Laplacian spectrum and use it in their area of interest.

REFERENCES

1. Dutta, P., Dutta, J. & Nath, R.K. "Laplacian Spectrum of Non-Commuting Graphs of Finite Groups". *Indian J Pure Appl Math*. 49, 205-216, 2018.
2. Jahanbani, Akbar & Sheikholeslami, Seyed & Khoeilar, Rana. "On the Spectrum of Laplacian Matrix". *Mathematical Problems in Engineering*. 1-4, 2021.
3. Banerjee, Subarsha. "Laplacian spectrum of comaximal graph of the ring Z_n". *Special Matrices*. Vol.10, no.1, pp.285-298, 2022.
4. Shaowei Sun, Kinkar Chandra Das. "Normalized Laplacian spectrum of complete multipartite graphs". *Discrete Applied Mathematics*. 284: 234 – 235, 2020.
5. Wafaa Fakieh, Amal Alsaluli, Hanaa Alashwali. "Laplacian spectrum of the unit graph associated to the ring of integers modulo pq". *AIMS Mathematics*. 9(2): 4098-4108, 2024.
6. C. Dalfó, F. Duque, R. Fabila-Monroy, M.A. Fiol, C. Huemer, A.L. Trujillo Negrete, F.J. Zaragoza Martínez. "On the Laplacian spectra of token graphs". Linear Algebra and its Applications. 625: 322 – 348, 2021.
7. Al-Hawary, Talal & Al-Shalaldeh, Sumaya & Akram, Muhammad. "Certain Matrices and Energies of Fuzzy Graphs". *Turkic World Mathematical Society (TWMS) Journal of Pure and Applied Mathematics*. 14: 50 – 68, 2023.
8. Yong Peng, Xin Zhu, Feiping Nie , Wanzeng Kong, Yuan Ge. "Fuzzy graph clustering". *Information Sciences*. 571: 38 – 49, 2021.
9. Shi X, Kosari S, Talebi A.A. "Investigation of the Main Energies of Picture Fuzzy Graph and its Applications". *Int J Comput Intell Syst*.15: 31. 2022.
10. Amutha, A., Jebakiruba, C., Davamani Christober.: M. "An Effective Algorithm to Enumerate Spectrum of Laplacian Matrix for Complete Fuzzy Graphs". Data Engineering and Intelligent Computing. Advances in Intelligent Systems and Computing, vol 1407. Springer, Singapore. 2021.
11. Amutha A, Jebakiruba C. Algorithmic approach of Spur on Laplacian matrix for certain fuzzy graphs. *Advances and Applications in Mathematical Sciences*. 22(8): 1915-1924, 2023.

12. Ralucca Gera and Pantelimon Stanica,"The spectrum of generalized Petersen graphs", *Australasian Journal Of Combinatorics*, Vol.49, Pages 39 – 45, 2011.
13. Mohar, Bojan and Alavi, Y and Chartrand, G and Oellermann, O.R,"The Laplacianspectrum of graphs", *Graph theory, combinatorics, and applications*, vol.2, 871-898, 12, 1991.
14. K. H. Lee,"First Course on Fuzzy Theory and Applications", Springer Verlag, Berlin, 2005.
15. D. West, "Introduction to graph theory", 2nd Edition, Prentice Hall, Upper Saddle River, NJ.2001.

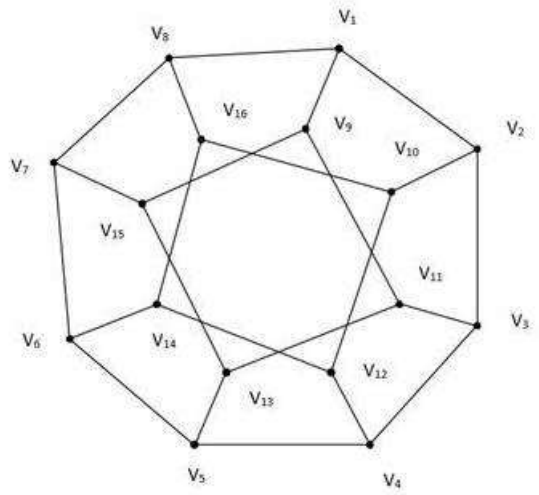

Figure.1: FP(8,2)

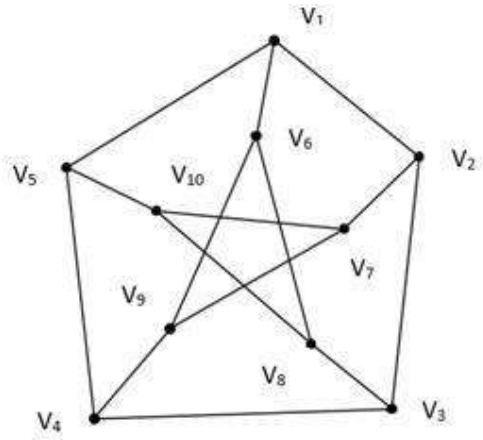

Figure.2: FP(5,2) and FP(5,3)

Indian Journal of Natural Sciences www.tnsroindia.org.in ©IJONS

Vol.15 / Issue 88 / Feb / 2025 *International Bimonthly (Print) – Open Access* *ISSN: 0976 – 0997*

RESEARCH ARTICLE

On (γ_{irkr})- – Number of Edge Added Graphs

M.Esakki Dharani[1]*, A. Nagarajan[2] and K. Palani[3]

[1]Research Scholar (Reg.No.21212232092011), Department of Mathematics, V. O. Chidambaram College, Thoothukudi (Affiliated to Manonmaniam Sundaranar University, Tirunelveli), Tamil Nadu, India.
[2]Associate Professor (Retd.), Department of Mathematics, V. O. Chidambaram College, (Affiliated to Manonmaniam Sundaranar University, Tirunelveli), Thoothukudi), Tamil Nadu, India.
[3]Associate Professor, Department of Mathematics, A.P.C. Mahalaxmi College for Women, (Affiliated to Manonmaniam Sundaranar University, Thoothukudi, Tamil Nadu, India.

Received: 21 Dec 2024 Revised: 03 Nov 2024 Accepted: 13 Jan 2025

***Address for Correspondence**
M.Esakki Dharani
Research Scholar (Reg.No.21212232092011),
Department of Mathematics, V. O. Chidambaram College,
Thoothukudi
(Affiliated to Manonmaniam Sundaranar University, Tirunelveli),
Tamil Nadu, India.
E.Mail: dhanushiya1411@gmail.com

ABSTRACT

In Graph theory, domination is one of the fundamental concepts. As a variation in domination, there are various kinds of domination in graph theory. It has many applications in various fields. One of the variations in domination is Rainbow Domination. From the Rainbow Domination concept, Independent Restrained k Rainbow Domination was introduced. The aim of this paper is to find the exact value of Independent Restrained k Rainbow domination number for path, star, cycle, complete graphs by adjoining an edge with some vertex.

Keywords: Domination, Independent, Rainbow, Restrained, Weight.
AMS Subject Classification: 05C69

INTRODUCTION

Domination plays a vital role in Graph theory. It has various applications in many fields. Rainbow domination concept was introduced by Bresar*et al.*[1]. Further it was studied by several authors. The various applications of k Rainbow domination such as location problem, network security, people allocations, signals and so on. Some new variations in Rainbow domination are Connected Rainbow domination, Independent Rainbow domination, outer Independent rainbow domination, Restrained Rainbow domination, Total Rainbow domination. Zehui shao*et al*. [8] introduces Independent Rainbow domination. Jiang H *et al*. [7] finds the total 2 rainbow domination number for k-

Regular graphs and proved the lower bounds are sharp. Gabrovsek B *et al*. [6] discussed the independent 3 rainbow dominating function for generalized Petersen graphs. The new concept Independent Restrained k Rainbow domination was introduced and discussed the minimum weight for some standard graphs[3]Also, for degree splitting graphs of path, complete, wheel, complete bipartite and helm graphs its minimum weight is determined [4].In this paper, minimum Independent Restrained k Rainbow domination number is calculated for path, star, cycle, complete graphs byadjoining an edge with some vertex.

PRELIMINARIES

Definition: 2.1

[3] Let G be a graph and $f: V(G) \rightarrow$ P[1,2, … , k] then f is said to be Independent Restrained k Rainbow Dominating Function (IRkRDF) if it satisfies the following condition (i) For every vertex u ∈ $V(G)$ such that f(u) = ∅, we have $\bigcup_{u \in N(v)} f(u) = \{1,2,..,k\}$ (ii) The vertices which are assigned with subset of k colors should be independent and the subgraph induced by the empty labeled vertices of G, contains no isolated vertices. The weight w(f) is defined as $\sum_{v \in V(G)} |f(v)|$.The minimum weight of G, is denoted by $\gamma_{irkr}(G)$ is the Independent Restrained k Rainbow Domination number.

Main Results

Theorem:3.1

If $G^*$is obtained by adding a vertex u to one of its vertices of K_n , then $\gamma_{irkr}(G^*)$ = k + 1

Proof:

Let $v_i \in V(K_n)$ where i = 1 to n and u be the new vertex added to v_n.

Define $f: V(G^*) \rightarrow$ P[1,2, … , k] by

$$f(x) = \begin{cases} \{1\} \ if \ x = u \\ \{1,2,3,\dots,k\} \ if \ x = v_1 \\ \emptyset \quad \text{otherwise} \end{cases}$$

Since, the union of open neighborhood of empty labelled vertices contains k colors, f satisfies the k- Rainbow Domination condition.

Let A = $\{v_1, u\}$ which are assigned non empty is independent. AndA' = $\{v_2, v_3, \dots, v_n\}$ which are labeled ∅ has no isolated vertices.

Hence f is IRkRDF.

Since no color is repeated, f gives a minimum weight to G'.

Further w(f) = $\sum_{i=1}^{n} |f(v_i)| + |f(u)|$

= $|f(u)| + |f(v_1)|$

∴ $\gamma_{irkr}(G^*)$ = k + 1

Remark: 3.2

i. If u be the pendant vertex to v, then assign f(u) = {1, 2, 3, …, k} or the subset of k colors and f(v) = ∅.

ii. In a path $(v_1, v_2, v_3, \dots, v_n)$ or a cycle $(v_1, v_2, v_3, \dots, v_n, v_1)$ if f(v_i) = ∅ then exactly one of the adjacent vertices gets ∅ and the other get {1,2,3,..,k}.

Corollary: 3.3

i. If $G^*$is obtained from the path P_{3m}, m ≥ 1 by adding a vertex u to one of the end vertices or to its internal vertices, then the resulting graph G^*does not admits IRkRDF. Since it fails to satisfy the condition in Remark 3.2 – (ii).

Theorem: 3.4

If G^* is obtained from the path P_{3m+1}, m ≥ 1 by adding new vertex u to v_{3m}, then $\gamma_{irkr}(G^*) = (m+1)k$

Proof:

Let $v_i \in V(P_{3m+1})$ and u be the new vertex added to some $v_{3m} \in V(P_{3m+1})$ where m ≥ 1

Define $f: V(G^*) \rightarrow$ P[1,2, … , k] by

$$f(x) = \begin{cases} \{2,3,\dots,k\} \ if\ x = v_n \\ \{1,2,\dots,k\} \ \ if\ \ x = \ v_i\ for\ i \equiv 1\ (mod\ 3)\ ;\ 1 \leq i < 3m+1 \\ \{1\} \ if\ x = u \\ \emptyset \quad \text{otherwise} \end{cases}$$

Since, the union of open neighborhood of empty labelled vertices contains k colors, f satisfies the k- Rainbow Domination condition.

Let A = $\{u, v_1, v_4, v_7 \ \dots, v_{3m+1}\}$ which are assigned non empty is independent. And A′ = $\{v_i\}$; $i \equiv 0,2(mod\ 3)$ which are labeled ∅ has no isolated vertices.Also, no color is repeated unnecessarily.

Hence f is a minimum IRkRDF.

Further w(f) = $\sum_{i=1}^{3m+1} |f(v_i)| + |f(u)|$

$= |f(v_1)| + |f(v_4)| + |f(v_7)| \ \dots + |f(v_{3m+1})| + |f(u)|$

= k+ [k +k+…+k] m times

= k + mk

∴ $\gamma_{irkr}(G^*)$ = $(m+1)k$

Theorem: 3.5

If G^* is obtained from the path P_{3m+1}, m ≥ 1 by adding new vertex u to v_2 then $\gamma_{irkr}(G^*) = (m+1)k$

Proof:

Let $v_i \in V(P_{3m+1})$ and u be the new vertex added to $v_2 \in V(P_{3m+1})$.

Define $f: V(G^*) \rightarrow$ P[1,2, … , k] by

$$f(x) = \begin{cases} \{1\} \ if\ x = u \\ \{1,2,\dots,k\} \ \ if\ \ x = \ v_i\ for\ i \equiv 1\ (mod\ 3)\ ;\ 4 \leq i \leq 3m+1 \\ \{2,3,\dots,k\} \ if\ x = v_1 \\ \emptyset \quad \text{otherwise} \end{cases}$$

Since, the union of open neighborhood of empty labelled vertices contains k colors, f satisfies the k- Rainbow Domination condition.

Let A = $\{u, v_1, v_4, v_7 \ \dots, v_{3m+1}\}$ which are assigned non empty is independent.And A′ = $\{v_i\}$; $i \equiv 0,2(mod\ 3)$ which are labeled ∅ has no isolated vertices.Also, no color is repeated unnecessarily.

Hence f is a minimum IRkRDF.

Further w(f) = $\sum_{i=1}^{3m+1} |f(v_i)| + |f(u)|$

$= |f(v_1)| + |f(v_4)| + |f(v_7)| \ \dots + |f(v_{3m+1})| + |f(u)|$

= k + [k +k+…+k] m times

= k + mk

∴ $\gamma_{irkr}(G^*)$ = $(m+1)k$

Theorem: 3.6

If G^* is obtained from the path P_{3m+1}, m ≥ 1 by adding a new vertex u to v_{3j+2} *or* v_{3j} ; 1 ≤ j ≤ m,then$\gamma_{irkr}(G^*) = (m+1)k+1$

Proof:

Let $v_i \in V(P_{3m+1})$ and u be the new vertex added to somev_{3j+2} *or* $v_{3j} \in V(P_{3m+1})$ for j = 1 to m.

Assume u is added to anyv_{3j+2}.

Define $f: V(G^*) \rightarrow$ P[1,2, … , k]by

$$f(x) = \begin{cases} \{1\} & if\ x = u \\ \{1,2,3,\dots,k\} & if\ x = v_i\ for\ i \equiv 1\ (mod\ 3)\ ;\ 1 \le i \le 3m+1 \\ \emptyset & \text{otherwise} \end{cases}$$

Since, the union of open neighborhood of empty labelled vertices contains k colors, f satisfies the k- Rainbow Domination condition.

Let A = $\{u, v_1, v_4, v_7 \dots, v_{3m+1}\}$ which are assigned non empty is Independent.And A′ = $\{v_i\}$; $i \equiv 0,2(mod)$ 3 which are labeled ∅ has no isolated vertices.

Hence f is IRkRDF.

Since no color is repeated in the neighborhood of empty labelled vertices f gives minimum weight to G'.

Further w(f) = $|f(u)| + \sum_{i=1}^{3m+1} |f(v_i)|$

w(f) = $|f(u)| + |f(v_1)| + |f(v_4)| + |f(v_7)| \dots + |f(v_{3m+1})|$

= 1 + [k +k+…+k] (m + 1) times

= (m+1) k + 1

∴ $\gamma_{irkr}(G^*) = (m+1)k + 1$

Corollary: 3.7

If G^* is obtained from the path P_{3m+1}, m ≥ 1 by adding a new vertex u to one of its end vertices or to internal vertex v_{3j+1} ; 1 ≤ j ≤ m, then the graph G' does not admits IRkRDF. Since it does not satisfy the condition in Remark 3.2 – (ii).

Theorem: 3.8

If G^* is obtained from the path P_{3m+2}, m ≥ 1 by adding new vertex u to v_{3j} ; 1 ≤ j ≤ m, then $\gamma_{irkr}(G^*) = (m+2)k$

Proof

Let $v_i \in V(P_{3m+2})$ and v be the new vertex added to some $v_{3j} \in V(P_{3m+1})$ where 1 ≤ j ≤ m

Define $f: V(G^*) \rightarrow$ P[1,2, … , k] by

If u is added to some vertex v_{3i}. Assign ∅ to f (v_{3i}) and its neighborhood f (v_{3j+1}) and f (v_{3j-1}) also. And the remaining vertices are labeled by Remark 3.2.

Assume v is added to v_3

$$f(x) = \begin{cases} \{1,2,\dots,k\} & if \begin{cases} x = u\ and\ v_5 \\ x = v_i\ for\ i \equiv 1\ mod\ 3\ ;\ 7 \le i \le 3m+2 \\ \emptyset \quad \text{otherwise} \end{cases} \end{cases}$$

Since, the union of open neighborhood of empty labelled vertices contains k colors, f satisfies the k- Rainbow Domination condition.

Let A = $\{u, v_1, v_4, v_7 \dots, v_{3m-1}\}$ which are assigned colors is independent. And A′ = $\{v_i\}$; $i \equiv 0,2(mod)$ 3 which are labeled ∅ has no isolated vertices.

Hence f is IRkRDF.

Since no color is repeated in the neighborhood of empty labelled vertices f gives minimum weight to G'.

Further w(f) = $|f(u)| + \sum_{i=1}^{3m+2} |f(v_i)|$

w(f) = $|f(v_1)| + |f(v_2)| + \dots + |f(v_{3m+2})| + |f(u)|$

= [k + k + k + k +…+k] (m + 2) times

∴ $\gamma_{irkr}(G^*) = (m+2)k$

Corollary: 3.9

i. If G^* is obtained from path P_{3m+2}, m ≥ 1 by adding new vertex u to one of its end vertices, then the graph G^* does not admits IRkRDF. Since it fails to satisfy the condition in Remark 3.2 – (ii).

ii. If G^* is obtained from the path P_{3m+2}, m ≥ 1 by adding new vertex u to v_{3j+1} or v_{3j+2}; 1 ≤ j ≤ m, then the graph G^* does not admits IRkRDF. Since it fails to satisfy the condition in Remark 3.2 – (ii).

Theorem: 3.10

If G^* is obtained from cycle graph C_{3m}, m ≥ 1 by adding a vertex u to one of its vertices, then $\gamma_{irkr}(G^*) = mk + 1$

Proof:

Let $v_i \in V(C_{3m})$ and u be the new vertex added to some v_i

Define $f: V(G^*) \rightarrow$ P[1,2, … , k]by

Case i: $i \equiv 0 \pmod 3$

$$f(x) = \begin{Bmatrix} \{1,2,\dots,k\} & if x = v_i \text{ for } i \equiv 2 \bmod 3;\ 1 \le i \le 3m \\ \{1\} & if\ x = u \\ \emptyset & \text{otherwise} \end{Bmatrix}$$

Case ii: $i \equiv 1, 2 \pmod 3$

$$f(x) = \begin{Bmatrix} \{1,2,\dots,k\} & if x = v_i \text{ for } i \equiv 0 \bmod 3;\ 1 \le i \le 3m \\ \{1\} & if\ x = u \\ \emptyset & \text{otherwise} \end{Bmatrix}$$

In all the above cases, the union of open neighborhood of empty labelled vertices contains k colors, f satisfies the k-Rainbow Domination condition.

In case 1, The vertices $\{u, v_3, v_6, v_9 \dots, v_{3m}\}$ which are assigned non empty is independent. And the empty labeled vertices v_i ; $i \equiv 1,2\ (mod\ 3)$ has no isolated vertices.

In case 2, The vertices $\{u, v_2, v_5, v_8 \dots, v_{3m-1}\}$ which are assigned non empty is independent. And thevertices v_i ; $i \equiv 0,1\ (mod\ 3)$ which are labeled ∅ has no isolated vertices.

Hence f is IRkRDF.

Since no color is repeated in the neighborhood of empty labelled vertices, f gives minimum weight to G'.

Further w(f) $= \sum_{i=1}^{3m} |f(v_i)| + |f(u)|$

Case i: $i \equiv 0 \pmod 3$

w(f) $= |f(u)| + |f(v_3)| + |f(v_6)| \dots + |f(v_{3m})|$

= 1 + [k + k +…+k] m times

∴ $\gamma_{irkr}(G') = mk + 1$

Case ii: $i \equiv 1, 2 \pmod 3$

w(f) $= |f(u)| + |f(v_2)| + |f(v_5)| + \cdots + |f(v_{3m-1})|$

= 1 + [k + k +…+k] m times

∴ $\gamma_{irkr}(G^*) = mk + 1$

Theorem: 3.11

If G^* is obtained from cycle C_{3m+1}, m ≥ 1 by adding a vertex u to one of its vertices, then $\gamma_{irkr}(G^*) = (m+1)$ k

Proof

Let $v_i \in V(C_{3m+1})$ and u be the new vertex added to some v_i

Define $f: V(G^*) \rightarrow$ P[1,2, … , k]by

Assign ∅ to f (v_i) and its neighborhood f (v_{i+1}) and f (v_{i-1}) also. And the remaining vertices are labeled by Remark 3.2 Assume new vertex v is added to v_1

$$f(x) = \begin{Bmatrix} \{1,2,\dots,k\} & if \begin{Bmatrix} x = u \\ x = v_i \text{ for } i \equiv 0 \bmod 3;\ 1 \le i \le 3m+1 \end{Bmatrix} \\ \emptyset & \text{otherwise} \end{Bmatrix}$$

Since, the union of open neighborhood of empty labelled vertices contains k colors, f satisfies the k- Rainbow Domination condition.

Let A = $\{u, v_3, v_6, v_9 \ldots, v_{3m}\}$ which are assigned non empty is independent. And the empty labeled vertices v_i ; $i \equiv 1,2\ (mod\ 3)$ has no isolated vertices.
Hence f is IRkRDF.
Since no color is repeated in the neighborhood of empty labelled vertices f gives minimum weight to G'.
Further w(f) = $|f(u)| + \sum_{i=1}^{3m+1}|f(v_i)|$
= $|f(v_3)| + |f(v_6)| \ldots + |f(v_{3m})| + |f(u)|$
= [k + k + k +…+k] (m + 1) times
$\therefore\ \gamma_{irkr}(G^*) = (m+1)k$

Corollary: 3.12
If G^* is obtained from cycle C_{3m+2}, m ≥ 1 by adding a vertex u to one of its vertices, then the resulting graph G^*does not admits IRkRDF. Since it does not satisfy the condition in Remark 3.2 – (ii)

Theorem: 3.13
If G^* is obtained from the star graph $K_{1,n}$ by adding a vertex v to some end vertex, then $\gamma_{irkr}(G^*) = \begin{cases} k+n-1 & if\ n \geq k \\ 2k & if\ n < k \end{cases}$

Proof
Let $v_i$be the end vertices where $i = 1\ to\ n$ and u be the root vertex and the new vertex v which is added to any end vertex v_i.
Define $f: V(G^*) \rightarrow P[1,2,\ldots,k]$ by
If v is added to some end vertex v_i. Then v becomes an end vertex ofG^* and the end vertex in which v is joined becomes an internal vertex of G^*.
Hence, Assign f (v) = {1,2,3..,k} and $f(v_{n-1}) = \emptyset$ by Remark 3.2-(i). Assign f(u) = ∅ and label the remaing vertices by the subset of k – colors by Remark 3.2- (i).
Assume, the new vertex v is added to the end vertex v_n

Case i: n < k

$$f(x) = \begin{cases} \{i\}\ \ if\ x = v_i\ \ where\ 1 \leq i \leq n-2 \\ \{n-1, n, n+1, \ldots, k\}\ if\ x = v_{n-1} \\ \{1,2,3,\ldots,k\}\ \ if\ x = v \\ \emptyset\ \ otherwise \end{cases}$$

Case ii: n = k

$$f(x) = \begin{cases} \{k-1, k\}\ \ if\ x = v_{n-1} \\ \{1,2,3,\ldots,k\}\ \ if\ x = v \\ \{i\}\ \ if\ x = v_i\ \ where\ 1 \leq i \leq n-2 \\ \emptyset\ \ otherwise \end{cases}$$

Case iii: n > k

$$f(x) = \begin{cases} \{i\}\ \ if\ x = v_i\ \ where\ 1 \leq i \leq k \\ \{1,2,3,\ldots,k\}\ \ if\ x = v \\ \emptyset\ \ if\ x = u \\ \{1\}\ \ otherwise \end{cases}$$

In all the above cases, the union of open neighborhood of empty labelled vertices contains k colors. Hence f satisfies the k- Rainbow Domination condition. Further, The set of vertices $\{v_1, v_2, v_3, \ldots v_{n-1}, v\}$ which are assigned non-empty labels are independent and the vertices $\{u, v_n\}$ which are assigned ∅ has no isolated vertices. Hence f is IRkRDF. By trial it is verified that f gives a minimum weight to G^*. Further w(f) =$\sum_{i=1}^{n}|f(v_i)| + |f(u)| + |f(v)|$
If n ≥ k

w(f) = $|f(v_1)| + |f(v_2)| + \ldots + |f(v_{n-1})| + |f(v)|$
= [1 + 1+ 1+ …1] (n -1) times
= n – 1 + k

If n < k

w(f) = $|f(v_1)| + |f(v_2)| + \ldots + |f(v_{n-1})| + |f(v)|$
$= [1 + 1 + \ldots + 1]$(k times) + k
= 2k

Theorem: 3.14

If $G^*$is obtained from star graph $K_{1,n-1}$, n ≥ 2 by adding a vertex v to root vertex, then
$\gamma_{irkr}(G^*)$ = max {n, k} for n ≥2.

Proof:

Let $v_i$be the end vertices where $i = 1\ to\ n-1$ and u be the root vertex and the new vertex v which is added to the root vertex. The resulting graph G' is again a star graph $k_{1,n}$.**[5]**
Define $f: V(k_{1,n}) \rightarrow$ P[1,2, … , k] by

Case i: n < k

$$f(x) = \begin{Bmatrix} \{i\}\ \ if\ \ x = v_i\ for\ 1 \le i \le n-1 \\ \{n, n+1, \ldots, k\}\ \ if\ x = v \\ \emptyset\ \ otherwise \end{Bmatrix}$$

Case ii: n = k

$$f(x) = \begin{Bmatrix} \{k\}\ \ if\ x = v \\ \{i\}\ \ if x = v_i\ for\ 1 \le i \le n-1 \\ \emptyset\ \ otherwise \end{Bmatrix}$$

Case iii:n > k

$$f(x) = \begin{Bmatrix} \{i\}\ \ if x = v_i\ for\ 1 \le i \le k \\ \{1\}\ \ if\ \begin{cases} x = v \\ x = v_{k+i}\ where\ k+1 \le k+i \le n-1 \end{cases} \\ \emptyset\ \ otherwise \end{Bmatrix}$$

In all the above cases, the union of open neighborhood of empty labelled vertices contains k colors. Hence f satisfies the k- Rainbow Domination condition. The set of end vertices $\{v_1, v_2, v_3, \ldots v_{n-1}, v\}$ which are assigned non empty labels are independent. Also, the vertex u which is assigned empty is connected.
Hence f is IRkRDF. Obviously, this f gives a minimum weight to $k_{1,n}$.
∴ w(f) = + $f(v) + f(u) + \sum_{i=1}^{n-1}|f(v_i)|$

If n ≥ k

w(f) = $|f(v_1)| + |f(v_2)| + \ldots + |f(v_{n-1})| + f(v)$
$= [1 + 1 + \ldots + 1]$ n times
= n

If n < k

w(f) = $|f(v_1)| + |f(v_2)| + \ldots + |f(v_{n-1})| + + f(v)$
= k − n + $[1 + 1 + \ldots + 1]$n times
= k – n + n = k
∴ $\gamma_{irkr}(k_{1,n})$ = max {n, k}

REFERENCES

1. Bresar.B,Henning.M, Rall.D, (2008), Rainbow domination in graphs, Taiwanese J.Math,12, pp.213-225.DOI: https://doi.org/10.11650/twjm/1500602498.
2. AbdollahzadehAhangar. H, Amjadi.J, Sheikholeslami S.M, Samodivkin .V, Volkmann .L, On the rainbow restrained domination number 2016. Ars CombinatoriaCXXV(1):pp. 209 -224.
3. Esakki Dharani. M, Nagarajan. A, andPalani. K,(2022) On Independent Restrained k- Rainbow Dominating Function, Ratio Mathematica Volume 44, pp. 349 -353.DOI:http://dx.doi.org/10.23755/rm.v44i0.924.
4. Esakki Dharani. M, Nagarajan. A, andPalani. K, On Independent Restrained k- Rainbow Domination number for Degree Splitting Graphs, Indian Journal of Natural Sciences. Issue 85 – August 2024. (Accepted)
5. Esakki Dharani. M, Nagarajan. A, andPalani. K,(2023)On Independent Restrained k- Rainbow Domination Number, National Conference on Recent Trends in Mathematical Sciences and their Applications(NCRDMSA2023) pp.129-140.
6. Gabrovsek B, Peperko A, Zerovnik J. Independent Rainbow Domination Numbers of Generalised Petersen Graphs P(n,2) and P(n,3). Mathematics. 2020; 8(6): 996. DOI: https://doi.org/10.3390/math8060996.
7. Jiang H, Rao Y. Total 2- Rainbow Domination in Graphs. Mathematics. 2022; 10(12): 2059. DOI: https://doi.org/10.3390/math10122059.
8. Zehui Shao, Zepeng Li, AljosaPeperko, Jiafu Wan. Independent rainbow domination of graphs. Bulletin of Malaysian Mathematical Society. 2019; volume 42: pp. 417- 435. DOI: https://doi.org/10.1007/s40840-017-0488-6.

RESEARCH ARTICLE

Gg β*- Closed Sets in Grill Topological Spaces

P. Gomathi Rajakumari[1*] and Jessie Theodore[2]

[1]Research scholar (Reg. No: 23121242092003), Department of Mathematics & Research Center, Sarah Tucker College, Tirunelveli - 7, Tamil Nadu, India.
[2]Assistant Professor, Department of Mathematics & Research Center, Sarah Tucker College, Tirunelveli - 7. Affiliated to Manonmaniam Sundaranar University, Abishekapatti, Tirunelveli -12, Tamil Nadu, India.

Received: 24 Aug 2024 Revised: 03 Dec 2024 Accepted: 21 Jan 2025

***Address for Correspondence**
P. Gomathi Rajakumari
Research scholar (Reg. No: 23121242092003),
Department of Mathematics & Research Center,
Sarah Tucker College,
Tirunelveli - 7, Tamil Nadu, India.
E.Mail: grkumari9495@gmail.com

ABSTRACT

In this paper, we have introduced and analyzed a Ggβ*-closed set in Grill topological spaces. Some of the basic properties of these sets are studied. Some of the generalized closed sets in topological and Grill topological spaces are compared with the Ggβ*-closed sets.

Keywords: G semi-pre local function$(\phi_{G\beta})$, Closure operator $(\Psi_{G\beta})$, $\tau_{G\beta}(X,\tau,G)$, Ggβ*-closed set.
2020 Mathematics Subject Classification: 54A05, 54A20

INTRODUCTION

The idea of grills on a topological space was first introduced by Choquet [1]. The concept of grills has shown to be a powerful supporting and useful tool in topological space. Ahmad Al-Omari and Takashi Noiri[2] introduced andanalyzed the notions of Gα-open sets, G-semi-open sets and Gβ-open sets in grilltopological spaces. Antony Rex and Jessie Theodore [3] introduced β^*- closed sets and studied its properties in topological space. The aim of this Paperis to study the β^*- closed setsas a new class of Ggβ*-closed sets in Grill topological space (X, τ, G) and some of the basic properties of these sets are studied. Also, some of the generalized closed sets in topological and grill topological spaces are compared with the Ggβ*-closed sets.

PRELIMINARIES

In a topological space (X, τ), For a subset A⊆X, Cl(A) and Int(A) denote the closure and the interior of A in (X, τ) respectively.

2.1 Definition: [1] A non-null collection G of subsets of a topological spaces X is said to be a grill on X if

1. $\phi \notin G$
2. A ∈ G and A ⊆ B implies that B ∈ G,
3. A, B ⊆ X and A ∪ B ∈ G implies that A ∈ G or B ∈ G.

2.2 Definition: [4] Let (X, τ) be a topological space and G be a grill on X. Then the triplet (X, τ, G) is called grill topological space. A mapping ϕ : P(X) → P(X) is defined by $\phi(A) = \phi_G(A,\tau) = \{x \in X: U \cap A \in G \text{ for all } U \in \tau(x)\}$ for each A ∈ P(X). The mapping ϕ is called the operator associated with the grill G and the topology τ. The map ϕ : P(X) → P(X) is a Kuratowski closure axiom defined by $\Psi(A) = A \cup \phi(A)$ for all A ∈ P(X).

2.3 Definition: A subset A of a topological space X is said to be:

1. α-open [5] if A ⊂Int(Cl(Int(A))),
2. semi-open [6] if A ⊂ Cl(Int(A)),
3. preopen [7] if A ⊂ Int(Cl(A)),
4. β-open [8] if A ⊂ Cl(Int(Cl(A))).

2.4 Definition: Let (X, τ, G) be a grill topological space. A subset A in X is said to be

1. G-open (or) ϕ -open [9] if A ⊆ Int (ϕ(A)),
2. Gα-open[2] if A ⊆ Int (Ψ(Int(A))),
3. G-preopen [9] if A ⊆ Int (Ψ(A)),
4. G-semi-open [2] if A ⊆ Ψ(Int(A)),
5. Gβ–open [2] if A ⊆ Cl(Int(Ψ(A))).

The family of all Gα-open (resp. G-preopen, G-semi-open, Gβ -open) sets in (X, τ, G) is denoted by GαO(X) (resp. GPO(X), GSO(X), GβO(X)).

2.5 Definition: A subset F in (X, τ, G) is said to be G-semi-closed(resp.G-preclosed, Gα-closed, Gβ -closed)if its complement is G-semi-open(resp. G-preopen, Gα -open, Gβ -open).

2.6 Definition: Let (X, τ, G) be a grill topological space. A subset A in X is said to be

1. Gg-closed [10] if $\phi(A) \subseteq U$ whenever $A \subseteq U$ and U is open in (X, τ),
2. Ggb-closed [11] if $\phi(A) \subseteq U$ whenever $A \subseteq U$ and U is b-open in (X, τ),
3. gG-closed [12] if $\Psi(A) \subseteq U$ whenever $A \subseteq U$ and U is open in (X, τ),
4. Grg-closed [13] if ϕ (A) ⊆U whenever A⊆U and U is regular open in (X, τ),
5. $G g^*$-closed [14] if $\phi(A) \subseteq U$ whenever $A \subseteq U$ and U is g-open in (X, τ),
6. $G(gs)^*$-closed [15] if $\phi(A) \subseteq U$ whenever $A \subseteq U$ and U is gs-open in (X, τ),
7. G(b*g)*-closed [16] if $\phi(A) \subseteq U$ whenever $A \subseteq U$ and U is b^*g -open in (X, τ),
8. Strongly Gg*-closed [14] if $\phi(int\ A) \subseteq U$ whenever $A \subseteq U$ and U is Gg-open in (X, τ, G),
9. Ggsp-closed if $\Phi_{G\beta}(A) \subseteq U$ whenever $A \subseteq U$ and U is open in (X, τ),
10. $G\hat{\eta}^*$-closed if $\Phi_{G\beta}(A) \subseteq U$ whenever $A \subseteq U$ and U is ω-open in (X, τ),
11. gsp-closed [17] if βcl(A) ⊆U whenever A⊆U and U is open in (X, τ),
12. gs-closed [18] if $scl(A) \subset U$ whenever $A \subseteq U$ and U is open in (X, τ)
13. ω closed [19] if $cl(A) \subseteq U$ whenever $A \subseteq U$ and U is semi open in (X, τ)
14. β^*-closed [3] if $\beta cl(A) \subseteq int\ U$ whenever A⊆U and U is ω-open in (X, τ),
15. b^*g -closed if $cl(A) \subseteq U$ whenever $A \subseteq U$ and U is b-open in (X, τ)
16. a pre-semiclosed[20] if βcl(A) ⊆U whenever A⊆U and U is g-open in (X, τ),

The complement of Gg-closed(resp.Ggb-closed, gG-closed, Grg-closed,$G g^*$-closed,$G(gs)^*$-closed, $G(b^*g)^*$-closed, Strongly $G g^*$-closed,Ggsp-closed,$G\hat{\eta}^*$-closed, gsp-closed, gs-closed, ω closed, β^*-closed, b^*g–closed, pre-semiclosed)

set is said to be Gg-open (resp.Ggb- open, gG- open, Grg- open, Gg^*-open, $G(gs)^*$- open, $G(b^*g)^*$- open, Strongly Gg^*- open,Ggsp-open,$G\hat{\eta}^*$-open, gsp- open, gs- open, ω-open, β^*- open, b^*g – open, pre-semi open).

2.7 Lemma:[19] A set U is ω open if and only if F ⊆ int U whenever F is semi closed and F ⊆ U.

2.8 Proposition: [3] In a topological space (X,τ), every semi-closed set(respectively α-closed,closed,*g- closed, g*-closed, $g^{\#}s$- closed, $g^{\#}$- closed) isβ^*closed set but not conversely.

2.11 Proposition:[2]For a subset A in (X,τ,G),the following properties are hold:

1. Every Gα-open sets are α-open.
2. Every G-semi-open sets are semi-open.
3. Every G-Pre open sets are Pre open.
4. Every Gβ -opensets are β -open.

G-Semi Pre Local Fuction in Grill Topological Space

3.1 Definition: Let (X, τ) be a topological space and G be a grill on X. We define a mapping $\Phi_{G\beta}: P(X) \to P(X)$ called the Gβ-operator associated with grill G and the topology τ by $\Phi_{G\beta}(A) = \{x \in X : U \cap A \in G, \text{for all } U \in G\beta O(x)\}$ where the family of semi-preopen sets $G\beta O(x) = \{U \in G\beta O(X) : x \in U\}$. Also the map$\Psi_{G\beta}: P(X) \to P(X)$ is called Gβ-closure operator defined by$\Psi_{G\beta}(A) = A \cup \Phi_{G\beta}(A)$ for all $A \in P(X)$.

For example: Let X={a, b, c}, $\tau = \{\phi, \{c\}, X\}$ and G = {{b}, {a, b}, {b, c}, X}.Then$\Phi_{G\beta}(\{a\}) = \{\phi\}$; $\Phi_{G\beta}(\{b\}) = \{b\}$;$\Phi_{G\beta}(\{c\}) = \{\phi\}$; $\Phi_{G\beta}(\{a, b\}) = \{b\}$; $\Phi_{G\beta}(\{a, c\}) = \{\phi\}$; $\Phi_{G\beta}(\{b, c\}) = \{b\}$; $\Phi_{G\beta}(\{X\}) = \{b\}$;$\Phi_{G\beta}(\{\phi\}) = \{\phi\}$;
$\Psi_{G\beta}(\{b\}) = \{b\}$; $\Psi_{G\beta}(\{a, b\}) = \{a, b\}$;$\Psi_{G\beta}(\{a, c\}) = \{a, c\}$;

3.2 Definition:

In (X, τ, G), there exists a unique topology on X given by $\tau_{G\beta} = \{U \subseteq X : \Psi_{G\beta}(X\backslash U) = X\backslash U\}$. The closure and interior of the set A in $\tau_{G\beta}$are denoted by $\tau_{G\beta} - cl(A)$ and $\tau_{G\beta} - int(A)$ respectively. For any set $A \subseteq X, \Psi_{G\beta}(A) = \tau_{G\beta} - cl(A)$.

3.3 Proposition: Let A, B be subsets of (X, τ, G). Then, for the $\Phi_{G\beta}$- local function, the following properties are hold:

1. If $A \subseteq B$, then $\Phi_{G\beta}(A) \subseteq \Phi_{G\beta}(B)$.
2. If $A \subseteq X$, then $\Phi_{G\beta}(A) = G\beta cl\left(\Phi_{G\beta}(A)\right) \subseteq \beta cl(A) \subseteq cl(A)$ and $\Phi_{G\beta}(A)$ is $G\beta$- closed.
3. If $A \subseteq X$, then $\Phi_{G\beta}\left(\Phi_{G\beta}(A)\right) \subseteq \Phi_{G\beta}(A)$.
4. If $A, B \subseteq X$, then $\Phi_{G\beta}(A \cup B) = \Phi_{G\beta}(A) \cup \Phi_{G\beta}(B)$.
5. If $A, B \subseteq X$, then $\Phi_{G\beta}(A \cap B) = \Phi_{G\beta}(A) \cap \Phi_{G\beta}(B)$.
6. If $A, B \subseteq X$, then $\Phi_{G\beta}(A) - \Phi_{G\beta}(B) = \Phi_{G\beta}(A - B) - \Phi_{G\beta}(B) \subset \Phi_{G\beta}(A - B)$.
7. If $A, B \subseteq X$, then $\Phi_{G\beta}(X - (A - B)) = \Phi_{G\beta}((X - A) \cup B)$.
8. If $U \in G\beta O(x)$, $U \cap \Phi_{G\beta}(A) = U \cap \Phi_{G\beta}(U \cap A) \subset \Phi_{G\beta}(U \cap A)$
9. If $A \subseteq X$, then $\Phi_{G\beta}(A) \subseteq cl(A)$ and $\Psi_{G\beta}(A) \subseteq cl(A)$.
10. If $A \notin G$, then $\Phi_{G\beta}(A) = \{\phi\}$.
11. If $B \notin G$, then $\Phi_{G\beta}(A \cup B) = \Phi_{G\beta}(A) = \Phi_{G\beta}(A - B)$.
12. $\Phi_{G\beta}(\phi) = \{\phi\}$.

Proof:

1. Suppose that $A \subseteq B$ and $x \notin \Phi_{G\beta}(B)$. There exists $U \in G\beta O(x)$ such that $U \cap B \notin G$. Since $A \subseteq B$, $U \cap A \notin G$ and $x \notin \Phi_{G\beta}(A)$. This proves that $\Phi_{G\beta}(A) \subseteq \Phi_{G\beta}(B)$.
2. Let $x \in G\beta cl\left(\Phi_{G\beta}(A)\right)$. Then $\Phi_{G\beta}(A) \cap U \in G$ for every $U \in G\beta O(x)$. Therefore, there exists some $y \in \Phi_{G\beta}(A) \cap U$ for every $U \in G\beta O(x)$. Since $y \in \Phi_{G\beta}(A)$, $A \cap U \in G$. Then $x \in \Phi_{G\beta}(A)$. Hence, $G\beta cl\left(\Phi_{G\beta}(A)\right) \subset \Phi_{G\beta}(A)$. Also

$\Phi_{G\beta}(A) \subset G\beta cl\left(\Phi_{G\beta}(A)\right)$.Thus $\Phi_{G\beta}(A) = G\beta cl\left(\Phi_{G\beta}(A)\right)$. Again, let $x \in G\beta cl\left(\Phi_{G\beta}(A)\right) = \Phi_{G\beta}(A)$, then $U \cap A \in G$ for every $U \in G\beta O(x)$. This implies $U \cap A \neq \phi$ for every $U \in G\beta O(x)$. Therefore, $x \in G\beta cl(A)$. This proves that $\Phi_{G\beta}(A) = G\beta cl\left(\Phi_{G\beta}(A)\right) \subseteq G\beta cl(A)$.

3. Let $x \in \Phi_{G\beta}\left(\Phi_{G\beta}(A)\right)$. Then for every $U \in G\beta O(x)$, $\Phi_{G\beta}(A) \cap U \in G$ and hence $\Phi_{G\beta}(A) \cap U \neq \phi$. Let $y \in \Phi_{G\beta}(A) \cap U$. Then $y \in \Phi_{G\beta}(A)$ for every $U \in G\beta O(y)$. Hence $A \cap U \in G$ and $x \in \Phi_{G\beta}(A)$. This shows that $\Phi_{G\beta}\left(\Phi_{G\beta}(A)\right) \subseteq \Phi_{G\beta}(A)$.
4. Since $A, B \subseteq A \cup B$ and by (i), we have $\Phi_{G\beta}(A) \subseteq \Phi_{G\beta}(A \cup B)$&$\Phi_{G\beta}(B) \subseteq \Phi_{G\beta}(A \cup B)$. Therefore $\Phi_{G\beta}(A) \cup \Phi_{G\beta}(B) \subseteq \Phi_{G\beta}(A \cup B)$. Let $x \in \Phi_{G\beta}(A \cup B)$. Then for every $U \in G\beta O(x)$, $U \cap (A \cup B) = (U \cap A) \cup (U \cap B) \in G$. Therefore, $U \cap A \in G$ or $U \cap B \in G$. This implies that $x \in \Phi_{G\beta}(A)$ or $x \in \Phi_{G\beta}(B)$ that is $x \in \Phi_{G\beta}(A) \cup \Phi_{G\beta}(B)$. Thus $\Phi_{G\beta}(A \cup B \subseteq \Phi G\beta A \cup \Phi G\beta(B)$. Hence, $\Phi G\beta A \cup B = \Phi G\beta A \cup \Phi G\beta B$.
5. Proof is similar to (iv) and the fact that $A \cap B \subseteq A$ & $A \cap B \subseteq B$.
6. Obvious from the definition.
7. Obvious with the fact that $X - (A - B) = (X - A) \cup B$.
8. Suppose that $U \in G\beta O(x)$ and $x \in U \cap \Phi_{G\beta}(A)$. Then $x \in U$ and $x \in \Phi_{G\beta}(A)$. Let V be any Gβ- open set containing x. Then $V \cap U \in G\beta O(x)$ and $V \cap (U \cap A) = (V \cap U) \cap A \in G$. This shows that$x \in \Phi_{G\beta}(U \cap A)$ and hence we obtain $U \cap \Phi_{G\beta}(A) \subseteq \Phi_{G\beta}(U \cap A)$. Moreover, $U \cap \Phi_{G\beta}(A) \subseteq U \cap \Phi_{G\beta}(U \cap A)$. Now $U \cap A \subseteq A$ and by (i), $\Phi_{G\beta}(U \cap A) \subseteq \Phi_{G\beta}(A)$ and $U \cap \Phi_{G\beta}(U \cap A) \subseteq U \cap \Phi_{G\beta}(A)$. Therefore, $U \cap \Phi_{G\beta}(A) = U \cap \Phi_{G\beta}(U \cap A) \subset \Phi_{G\beta}(U \cap A)$.
9. Let $x \notin cl(A)$, then there is an U_x such that $U_x \cap A = \phi \notin G$. This implies that $x \notin \Phi_{G\beta}(A)$. Therefore $\Phi_{G\beta}(A) \subseteq cl(A)$.Hence $A \cup \Phi_{G\beta}(A) \subseteq A \cup cl(A) = cl(A)$. Thus$\Psi_{G\beta}(A) = A \cup \Phi_{G\beta}(A) \subseteq cl(A)$.
10. Obvious from definition.
11. Proof is similar to (iv)
12. Obvious from definition.

3.4 Theorem: Let G_1 and G_2be the grills on (X,τ). Then the following properties are hold for $A \subseteq X$,

1. If $G_1 \subset G_2$, then $\Phi_{G_1\beta}(A) \subseteq \Phi_{G_2\beta}(A)$
2. If $G_1 \subset G_2$, then $\Psi_{G_1\beta}(A) \subseteq \Psi_{G_2\beta}(A)$
3. $\Phi_{(G_1 \cap G_2)\beta}(A) = \Phi_{G_1\beta}(A) \cap \Phi_{G_2\beta}(A)$

Proof:

1. Let $G_1 \subset G_2$ and $x \in \Phi_{G_1\beta}(A)$. Then $U \cap A \in G_1$ for every $U \in G\beta O(x)$. Since $G_1 \subset G_2$,$U \cap A \in G_2$ and $x \in \Phi_{G_2\beta}(A)$. Hence $\Phi_{G_1\beta}(A) \subseteq \Phi_{G_2\beta}(A)$.
2. Let $G_1 \subset G_2$. Then $\Phi_{G_1\beta}(A) \subseteq \Phi_{G_2\beta}(A)$ implies that$A \cup \Phi_{G_1\beta}(A) \subseteq A \cup \Phi_{G_2\beta}(A)$. Hence $\Psi_{G_1\beta}(A) \subseteq \Psi_{G_2\beta}(A)$.
3. By (1), we have $\Phi_{(G_1 \cap G_2)\beta}(A) \subseteq \Phi_{G_1\beta}(A)$ and $\Phi_{(G_1 \cap G_2)\beta}(A) \subseteq \Phi_{G_2\beta}(A)$. Therefore $\Phi_{(G_1 \cap G_2)\beta}(A) \subseteq \Phi_{G_1\beta}(A) \cap \Phi_{G_2\beta}(A)$. Now let $x \in \Phi_{G_1\beta}(A) \cap \Phi_{G_2\beta}(A)$. Then$x \in \Phi_{G_1\beta}(A)$ and $x \in \Phi_{G_2\beta}(A)$. Then for every $U \in G\beta O(x)$, $U \cap A \in G_1$ and $U \cap A \in G_2$and hence $U \cap A \in G_1 \cap G_2$. Therefore $x \in \Phi_{(G_1 \cap G_2)\beta}(A)$. Thus $\Phi_{G_1\beta}(A) \cap \Phi_{G_2\beta}(A) \subseteq \Phi_{(G_1 \cap G_2)\beta}(A)$. Hence $\Phi_{(G_1 \cap G_2)\beta}(A) = \Phi_{G_1\beta}(A) \cap \Phi_{G_2\beta}(A)$.

3.5 Theorem: Let A, B be subsets of (X, τ, G). Then we have the following Kuratowski closure axioms:

1. If $A \subseteq B \Rightarrow \Psi_{G\beta}(A) \subseteq \Psi_{G\beta}(B)$
2. $\Psi_{G\beta}(A) \cup \Psi_{G\beta}(B) = \Psi_{G\beta}(A \cup B)$
3. $\Psi_{G\beta}\left(\Psi_{G\beta}(A)\right) \subseteq \Psi_{G\beta}(A)$
4. $\Psi_{G\beta}(\phi) = \phi$.

Proof: All the properties are proved by using the definition of $\Psi_{G\beta}$ and Theorem 3.4

3.6 Theorem: Let G_1 and G_2be the grills on (X,τ). Then $\tau_{G_2\beta} \subseteq \tau_{G_1\beta}$ if $G_1 \subset G_2$.
Proof: Let $A \in \tau_{G_2\beta}$ be any subset of X. Therefore, by definition of $\tau_{G\beta}$, $\Psi_{G_2\beta}(X - A) = X - A$. Since $G_1 \subset G_2$, $\Psi_{G_1\beta}(X - A \subseteq \Psi G2\beta X - A$ implies that $\Psi G1\beta X - A \subseteq X - A$.
Also $X - A \subseteq \Psi_{G_1\beta}(X - A)$ because $\Psi_{G_1\beta}(X - A) = (X - A) \cup \phi_{G_1\beta}(X - A)$.
Thus $\Psi_{G_1\beta}(X - A) = X - A$ implies that $A \in \tau_{G_1\beta}$. Hence $\tau_{G_2\beta} \subseteq \tau_{G_1\beta}$.

Ggβ*- Closed Sets in Grill Topological Spaces
4.1 Definition: Let (X,τ) be a topological space and G be a grill on X. Then a subset $A \subseteq X$ is called Ggβ* closed if $\Phi_{G\beta}(A) \subseteq$ int U whenever A ⊆ U and U is ω open in (X, τ). We denote the family of all Ggβ* closed sets by Ggβ*$C(X, \tau)$.

4.2 Theorem: The union of any two Gg β*closed sets is Ggβ*closed.
Proof: Let $A \cup B \subseteq U$ and U is ω- open in (X, τ). Then $A \subseteq U$ & $B \subseteq U$. Since A and B are Ggβ*closed, $\Phi_{G\beta}(A) \subseteq$ int U and $\Phi_{G\beta}(B) \subseteq$ int U. Always $\Phi_{G\beta}(A \cup B) = \Phi_{G\beta}(A) \cup \Phi_{G\beta}(B)$. Therefore $\Phi_{G\beta}(A \cup B) \subseteq$ int U. Hence A ∪ B is Ggβ*closed.

4.3 Theorem: The intersection of any two Ggβ*closed sets is Ggβ*closed.
Proof: Let A ∩ B ⊆ U and U is ω- open in (X, τ). Since A and B are Ggβ*closed, $\Phi_{G\beta}(A) \subseteq$ int U and $\Phi_{G\beta}(B) \subseteq$ int U. Always $\Phi_{G\beta}(A \cap B) = \Phi_{G\beta}(A) \cap \Phi_{G\beta}(B)$. Therefore $\Phi_{G\beta}(A \cap B) \subseteq$ int U. Hence A ∩ B is Ggβ*closed.

4.4 Proposition:
1. Every non-member in G is Ggβ*closed set in (X, τ, G).
2. $\Phi_{G\beta}(A)$ is Ggβ*closed for every subset A of (X, τ, G).
3. If G = {{a}, {b}, {c}, {a, b}, {a, c}, {b, c}, X}, then $\Phi_{G\beta}(A) =$ spcl(A) and hence Ggβ*closed sets are β*closed.

Proof:
1. Let $A \notin G$ and $A \subseteq U$ be an ω open set in (X, τ). Then $\Phi_{G\beta}(A) = \phi$ implies that $\Phi_{G\beta}(A) \subseteq$ int U. Hence A is Ggβ*closed.
2. Let $\Phi_{G\beta}(A) \subseteq U$ and U be ω open in (X, τ). Clearly $\Phi_{G\beta}(A) \subseteq G\beta cl(A) \subseteq Gscl(A)$. Since every G- semi closed set is semi closed and scl(A) is a semi closed set, $\Phi_{G\beta}(A) \subseteq$ int U. Therefore $\Phi_{G\beta}\left(\Phi_{G\beta}(A)\right) \subseteq \Phi_{G\beta}(A) \subseteq$ int U. Hence $\Phi_{G\beta}(A)$ is Ggβ*closed.
3. Proof by corollary 2. 11(iv)

4.5 Proposition: Every member in G may or may not be Ggβ*closed set.
For example, Let X = {1, 2, 3}, τ = {ϕ, {3}, X} and G = {{3}, {1, 3}, {2, 3}, X}. Then the set {3} is not Ggβ*closed but the sets {1, 3}, {2, 3} and X are Ggβ*closed.

4.6 Theorem: Every G- semi closed set and hence Gα - closed set and G- closed set is Ggβ* closed set but not conversely.
Proof: Let $A \subseteq U$ be any G- semi closed set and U be ω open in (X, τ). Therefore, by lemma 2.7, A ⊂ int U because every G-semi closed set is semi closed. Since A is G-semi closed, $A = Gscl(A) \subseteq scl(A) \subseteq int(U)$. Therefore $\Phi_{G\beta}(A) \subseteq$ Gβcl(A) ⊆ scl(A) ⊆ int U. Hence A is Ggβ*closed.

Hence Gα - closed sets and G- closed sets are Ggβ* closed sets because every G- closed set and Gα - closed set is G- semi closed set.
4.7 Example: Let X={p, q, r, s}, τ = {ϕ, {q, r}, X} and G = {{p, r}, {q, r}, {p, q, r}, {p, r, s}, {q, r, s}, X}. Then the set {p, q} is Ggβ*closed but none of G- semi closed, Gα - closed and G- closed.

4.8 Theorem: Every $\beta^*closed$ set is $Gg\beta^*$-closed sets but not conversely.
Let $A \subset \beta^*C(\tau)$ and U be an ω open set containing A in (X,τ). Then βcl (A) ⊆ int U. Now $\Phi_{G\beta}(A) \subseteq \beta cl(A) \subseteq$ int U. Hence A is $Gg\beta^*$closed.

4.9 Example: Let X = $\{\pi_a, \pi_b, \pi_c, \pi_d\}$, $\tau = \{\phi, \{\pi_b\}, \{\pi_c, d\}, \{\pi_b, \pi_c, \pi_d\}, X\}$ and G = $\{\{\pi_b\}, \{\pi_b, \pi_c\}, \{\pi_b, \pi_d\}, \{\pi_a, \pi_b\}, \{\pi_a, \pi_b, \pi_c\}, \{\pi_a, \pi_b, \pi_d\}, \{\pi_b, \pi_c, \pi_d\}$, X}. Then the set $\{\pi_b, \pi_c\}$ is $Gg\beta^*$closed but not β^*closed.

4.10 Remark: Every semi closed set, (respectively α - closed set and closed set) is$Gg\beta^*$closed set but not conversely.
Proof: By proposition 2.8 and theorem 4.8.

4.11 Example: Let X = $\{\pi_a, \pi_b, \pi_c\}$, $\tau = \{\phi, \{\pi_a\}, X\}$ and G = $\{\{\pi_a\}, \{\pi_a, \pi_b\}, \{\pi_a, \pi_b\}$, X}. Then the set $\{\pi_a, \pi_b\}$ is $Gg\beta^*$closed but none of semi closed, α - closed and closed.

4.12 Remark: Every *g- closed set and hence g*- closed set is $Gg\beta^*$closed set but not conversely.
Proof: By proposition 2.8 and theorem 4.8.

4.13 Example: Let X = $\{\pi_a, \pi_b, \pi_c\}$, $\tau = \{\phi, \{\pi_a\}, \{\pi_b\}, \{\pi_a, \pi_b\}, X\}$ and G = $\{\{\pi_b\}, \{\pi_a, \pi_b\}, \{\pi_b, \pi_c\}$, X}. Then the set $\{\pi_b\}$ is $Gg\beta^*$closed but neither*g- closed set nor g*- closed set in X.

4.14 Remark: Every $g^{\#}s$- closed set and hence $g^{\#}$- closed set is $Gg\beta^*$closed set but not conversely.
Proof: By proposition 2.8 and theorem 4.8.

4.15 Example: Let X = $\{\pi_a, \pi_b, \pi_c, \pi_d\}$, $\tau = \{\phi, \{\pi_a, \pi_b\}, X\}$ and G = $\{\{\pi_a\}, \{\pi_a, \pi_b\}, \{\pi_a, \pi_c\}, \{\pi_a, \pi_d\}, \{\pi_a, \pi_b, \pi_c\}, \{\pi_a, \pi_b, \pi_d\}, \{\pi_a, \pi_c, \pi_d\}$, X}. Then the set $\{\pi_a, \pi_b, \pi_d\}$ is $Gg\beta^*$closed but neither $g^{\#}s$- closed set nor $g^{\#}$- closed set in X.

4.16 Theorem: Every Ggb closed set is $Gg\beta^*$closed set but not conversely.
Proof: Let $A \subseteq U$ be any Ggb closed set and U be ω open in (X,τ). Then $\phi(A) \subseteq U$. Also $\phi(A) \subseteq cl(A)$ and $cl(A)$ is closed and semi closed set. Hence by lemma 2.7, $\phi(A) \subseteq int(U)$.Therefore $\Phi_{G\beta}(A) \subseteq$ int U because $\Phi_{G\beta}(A) \subseteq \phi(A)$. Hence A is $Gg\beta^*$closed.

4.17 Example: Let X={a, b, c}, $\tau = \{\phi, \{a\}, \{a, c\}, X\}$ and G = {{a}, {a, b}, {a, c}, X}. Then the set {a, b} is $Gg\beta^*$closed but not Ggb closed.

4.18 Theorem: Every Gg* closed set is $Gg\beta^*$closed set but not conversely.
Proof: Proof is similar to theorem 4.16.
4.19 Example: Let X = {a, b, c}, $\tau = \{\phi, \{a\}, \{b\}, \{a, b\}, X\}$ and G = {{b}, {a, b}, {b, c}, X}. Then the set {a, b} is $Gg\beta^*$closed but not Gg* closed set in X.

4.20 Theorem: Every $Gg\beta^*$- closed set is Ggsp-closed set but not conversely.
Proof: Let $A \subseteq Gg\beta^*C(\tau)$ and $A \subseteq$ Uin (X,τ). Since every open set is ω open, we have $\Phi_{G\beta}(A) \subseteq$ int U = U. Therefore A is Ggsp-closed.
4.21 Theorem: Every $Gg\beta^*$- closed set is $G\hat{\eta}^*$-closed set but not conversely.
Proof: Let $A \subseteq Gg\beta^*C(\tau)$ and $A \subseteq$ U in (X,τ). Then $\Phi_{G\beta}(A) \subseteq$ int U ⊆ U. Therefore A is $G\hat{\eta}^*$-closed.

4.22 Example: Let X = $\{\pi_a, \pi_b, \pi_c, \pi_d\}$, $\tau = \{\phi, \{\pi_a, \pi_b\}, X\}$ and G = $\{\{\pi_a\}, \{\pi_a, \pi_b\}, \{\pi_a, \pi_c\}, \{\pi_a, \pi_d\}, \{\pi_a, \pi_b, \pi_c\}, \{\pi_a, \pi_b, \pi_d\}, \{\pi_a, \pi_c, \pi_d\}$, X}. Then the set $\{\pi_b\}$ is Ggsp-closed and $G\hat{\eta}^*$-closed but not $Gg\beta^*$closed set.

4.23 Proposition: Every b^*g closed set is $Gg\beta^*$closed set but not conversely.

Proof: Let $A \subset b^*gC(\tau)$ and U be an ω open set containing A in (X, τ).Then cl(A) ⊆ U.Also every closed is semi-closed, we have $cl(A)$ ⊆ int U. Therefore $\Phi_{G\beta}(A) \subseteq \phi(A) \subseteq cl(A) \subseteq$ int U. Hence A is Ggβ*closed.

4.24 Example: Let X = {a, b, c}, $\tau = \{\phi, \{b\}, \{a, b\}, \{b, c\}, X\}$ and G = {{a, c}, X}.
Then the set {a, b} is Ggβ*closed but not b^*g – closed. Thus the class of Ggβ*closed sets properly lies between the class of G semi-closed sets and the class of Ggsp- closed sets. The above discussions are shown in the following implication:

4.25 Proposition: Ggβ*closed sets are independent of Gg closed sets.

4.26 Example: Let X = {a, b, c, d}, $\tau = \{\phi, \{b\}, \{c, d\}, \{b, c, d\}, X\}$ and G = {{b}, {b, c}, {b, d}, {a, b}, {a, b, c}, {a, b, d}, {b, c, d}, X}. Then the set {b, c} is Ggβ*closed but not Gg-closed.

4.27 Example: Let X = {a, b, c}, $\tau = \{\phi, \{a\}, \{b, c\}, X\}$ and G = {{b}, {a, b}, {b, c}, X}. Then the set {b} is Gg-closed set but not Ggβ*closed.

4.28 Proposition: Ggβ*closed sets are independent of gG-closed sets.

4.29 Example: Let X = {a, b, c}, $\tau = \{\phi, \{a\}, \{b\}, \{a, b\}, X\}$ and G = {{b}, {a, b}, {b, c}, X}. Then the set {b} is Ggβ*closed but not gG closed.

4.30 Example: Let X={a, b, c, d}, $\tau = \{\phi, \{a\}, X\}$ and G = {{a}, {a, b}, {a, c}, {a, d}, {a, b, c}, {a, b, d}, {a, c, d}, X}. Then the set {a, c} is gG closedbut not Ggβ*closed.

4.31Proposition: Ggβ*closed sets are independent of G-pre closed sets, G- semi-pre closed sets and pre-semi closed sets.

4.32 Example: Let X={a, b, c}, $\tau = \{\phi, \{a\}, \{b, c\}, X\}$ and G = {{b}, {a, b}, {b, c}, X}. Then the set {a, b} is G-preclosed, G-semi-pre closed and pre-semi closed but not Ggβ*closed.

4.33 Example: Let X={a, b, c}, $\tau = \{\phi, \{b\}, \{a, b\}, \{b, c\}, X\}$ and G = {{a, c}, X}. Then the set {b, c} is Ggβ*closed but none of G-pre closed, G- semi-pre closed and pre-semi closed.

4.34 Proposition: Ggβ*closed sets are independent of Grg closed sets.

4.35 Example: Let X={a, b, c, d}, $\tau = \{\phi, \{a\}, X\}$ and G = {{a}, {a, b}, {a, c}, {a, d}, {a, b, c}, {a, b, d}, {a, c, d}, X}. Then the set {a, b} is Grg closedbut not Ggβ*closed.

4.36 Example: Let X={a, b, c, d}, $\tau = \{\phi, \{b\}, \{c, d\}, \{b, c, d\}, X\}$ and G = {{b}, {b, c}, {b, d}, {a, b}, {a, b, c}, {a, b, d}, {b, c, d}, X}. Then the set {b, c} is Ggβ*closed but not Gg-closed.

4.37 Proposition: Ggβ*closed sets are independent of $G(gs)^*$- closed sets.
4.38 Example: Let X={a, b, c}, $\tau = \{\phi, \{a\}, \{a, b\}, X\}$ and G = {{{a}, {a, b}, {a, c}, X}. Then the set {a, c} is Ggβ*closed but not $G(gs)^*$closed.

4.39 Example: Let X = {a, b, c}, $\tau = \{\phi, \{a\}, \{a, c\}, X\}$ and G = {{a}, {a, b}, {a, c}, X}. Then the set {a} is $G(gs)^*$closedbut not Ggβ*closed.

4.40 Proposition: Ggβ*closed sets are independent of $G(b^*g)^*$- closed sets.

4.41 Example: Let X={a, b, c, d}, τ = {ϕ,{b}, {c,d}, {b,c,d}, X} and G = {{b}, {b, c}, {b, d}, {a, b}, {a, b, c}, {a, b, d}, {b, c, d}, X}. Then the set {b, c} is Ggβ*closed but not $G(b^*g)^*$closed.

4.42 Example: Let X = {a, b, c}, τ = {ϕ, {a}, {a, c}, X} and G = {{a}, {a, b}, {a, c}, X}. Then the set {a, c} is $G(b^*g)^*$closedbut not Ggβ*closed.

4.43 Proposition: Ggβ*closed sets are independent of strongly Gg^*closed sets.

4.44 Example: Let X={a, b, c, d}, τ = {ϕ,{b}, {c,d}, {b,c,d}, X} and G = {{b}, {b, c}, {b, d}, {a, b}, {a, b, c}, {a, b, d}, {b, c, d}, X}. Then the set {b, c} is Ggβ*closed but not strongly $(Gg)^*$closed.

4.45 Example: Let X = {a, b, c}, τ = {ϕ, {a}, {a, c}, X} and G = {{a}, {a, b}, {a, c}, X}. Then the set {a, c} is strongly $(Gg)^*$closedbut not Ggβ*closed.

4.46 Proposition: Ggβ*closed setsare independent ofgsp- closed sets.

4.47 Example: Let X={a, b, c}, τ = {ϕ, {b}, {a,b}, {b,c}, X} and G = {{a, c}, X}. Then the set {b} is Ggβ*closed but not gsp – closed.

4.48 Example: Let X={a, b, c, d}, τ = {ϕ,{a},X} and G = {{a}, {a, b}, {a, c}, {a, d}, {a, b, c}, {a, b, d}, {a, c, d}, X}. Then the set {a, b} is gsp – closedbut not Ggβ*closed.

4.49Proposition: Ggβ*closed sets are independent of gs - closed sets.

4.50 Example: Let X={a, b, c, d}, τ = {ϕ,{a},X} and G = {{a}, {a, b}, {a, c}, {a, d}, {a, b, c}, {a, b, d}, {a, c, d}, X}. Then the set {a, c} is gs – closedbut not Ggβ*closed.

4.51 Example: Let X = {a, b, c}, τ = {ϕ, {b}, {a,b}, {b,c}, X} and G = {{a, c}, X}. Then the set {a, b} is Ggβ*closed but not gs – closed.

4.52 Proposition: Ggβ*closed sets are independent of ω- closed sets.

4.53 Example: Let X={a, b, c}, τ = {ϕ, {a}, {a,b}, X} and G = {{{a}, {a, b}, {a, c}, X}. Then the set {b} is Ggβ*closed but not ω – closed.

4.54 Example: Let X = {a, b, c, d}, τ = {ϕ, {a}, X} and G = {{a}, {a, b}, {a, c}, {a, d}, {a, b, c}, {a, b, d}, {a, c, d}, X}. Then the set {a, b} is ω – closedbut not Ggβ*closed.

The above discussions are shown in the following implication:

4.55 Theorem: Let A be a Ggβ*closed set in X. Then $\Phi_{G\beta}(A) - A$ does not contains any non-empty ω- closed set. But the converse is not true.

Proof: Suppose that A is Ggβ*closed and F is ω- closed with $F \subset \Phi_{G\beta}(A) - A$. Then $A \subset F^c$ and so $\Phi_{G\beta}(A) \subseteq \text{int}(F^c) \subset F^c$. Therefore $F \subseteq \left(\Phi_{G\beta}(A)\right)^c$ which implies $F = \phi$.

4.56 Example:

Let X = {a, b, c}, τ = {ϕ, {a,b}, X} and G = {{a}, {a, b}, {a, c}, X}. Then the set {a} is not Ggβ*closed but $\Phi_{G\beta}(A) - A = \phi$ which contains no ω- closed.

4.57 Theorem: For each $x \in X$, for each {x} is ω- closed or $\{x\}^c$ is Ggβ*closed in X.

Proof: Suppose that {x} is not ω- closed in X. Then $\{x\}^c$ is not ω open and the only ω- open set containing $\{x\}^c$ is the space itself. (i.e) $\{x\}^c \subseteq X$. Also $\Phi_{G\beta}(\{x\}^c) \subseteq X = \text{int } X$. Hence $\{x\}^c$ is Ggβ*closed.

RESULTS AND DISCUSSIONS

In this article we have defined and discussed some features of $\Phi_{G\beta}$- local function and the operator $\Psi_{G\beta}$ is a Gβ-Kuratowski closure operator. Also, we have defined and investigated the Ggβ*closed sets and compared with other generalized closed sets in topological and Grill topological spaces. Thus we have found that the class of Ggβ*closed sets properly lies between the class of G semi-closed sets and the class of Ggsp- closed sets.

REFERENCES

1. Choqet, G 1947, 'Sur les notions de filter et grill', ComptesRendus Acad. Sci. Paris, 224,171-173.
2. Al-Omari &Noiri, T (2011), 'Decomposition of continuity via grilles', Jordan J. Math. Stat., 4(1), 33-46.
3. Antony Rex Rodgio. J, Jessie Theodore & Hana SelviJansi. A, 2012, 'β^*- closed sets in topological space', International Journal of Mathematical Archive,3(3),1063-1068.
4. Roy, B & Mukherjee, M. N 2007, 'On a typical topology induced by a grill', Soochow J. Math, 33 (4), 771-786.
5. Njastad, O 1965, 'On some classes of nearly open sets', Pacific J. Math,15, 961-970.
6. Levine, N 1963, 'Semi-open sets and semi-continuity in topological spaces', Amer Math. Monthly, 70, 36-41.
7. Mashhour A. S, Abd El-Monsef M. E & El-Deeb S. N, On precontinuous and weak precontinuous mappings, Proc. Math. Phys. Soc. Egypt, 53 (1982), 47-53.
8. Andrijevic D, (1986), Semi-preopen sets, Mat. Vesnik, 38, 24-32.
9. Hatir, E &Jafari, S 2010, 'On some new classes of sets and a new decomposition of continuity via grills', J. Adv. Math. Studies, 3 (1), 33-40.
10. Dhananjoy Mandal & Mukherjee, M.N 2012, 'On a type of generalized closed sets', Bol. Soc. Paran. Mat. 301, 67-76.
11. Arockiarani I &karthika A (2012), "On A Type of Generalized B-Closed Sets in Grill Topology", International Journal of Advanced Scientific and Technical Research (ISSN: 2249-9954)
12. Indirani, K, P. Sathishmohan& V. Rajendran, (2014) 'On Generalized Grill Continuous Functions', Kong. Res. J. 1(1): 23-26, Kongunadu Arts and Science College, Coimbatore.
13. Thenmozhi1, P, Kaleeswari M &Maheswari N, 'Regular Generalized Closed Sets in Grill Topological Spaces', International Journal of Science and Research (IJSR) ISSN (Online): 2319-7064.
14. Kaleeswari, M, Maheswari, N &Thenmozhi P 2017, 'Strongly g*- Closed Sets in Grill Topological Spaces', International Journal of Mathematics Trends and Technology (IJMTT) – Volume 51 Number 1.
15. Vibin Salim Raj, S, Senthilkumaran, V &Palaniappan, Y 2021, 'Generalised Semi Closed Sets in Grill Topological Spaces', Journal of Advance Research in Mathematics and Statistics (ISSN: 2208-2409).
16. Kanchana M, SenthilKumaran V, Palaniappan Y, (2022) 'Almost Contra G(b*g) * Continuous Function In Grill Topological Spaces' ,Journal of Advance Research in Mathematics And Statistics, Volume-9 , Issue-4 , ISSN: 2208-2409
17. Dontchev, J (1995), 'On generalizing semi-preopen sets'. Mem. Fac. Sci. Kochi Uni. Ser. A Math.,35-48.
18. Arya. S.P and Nour.T,Characterization of s-normal spaces, Indian J. Pure. Appl, Math., (1990), 717-719.
19. Sheik John, 2002, 'A Study on generalizations of closed sets and continuous maps in topological and bitopological spaces', Ph.D., Thesis, Bharathiar University, Coimbatore.
20. Veera Kumar M.K.R.S, (2002),Pre-semi closed, Indian J. Math, 44(2) 165-181.

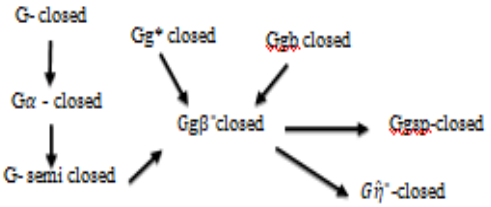

Figure: 1

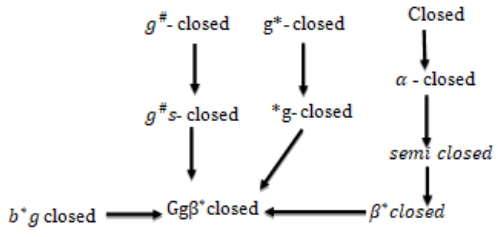

Figure:2

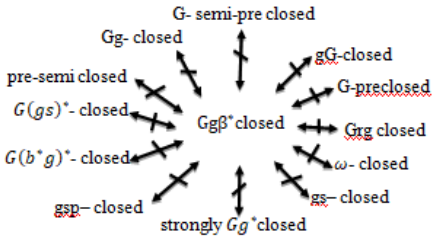

Figure: 3

Vol.15 / Issue 88 / Feb / 2025 *International Bimonthly (Print) – Open Access* *ISSN: 0976 – 0997*

RESEARCH ARTICLE

Optimization of Fuzzy Integrated Vendor–Buyer Inventory Model in Price-Dependent Demand

M. Sumathi[1], M. Sabina Begum[2]* and M. Gomathi[3]

[1]Associate Professor, Department of Mathematics, Khadhir Mohideen College, Adhirampattinam, (Affiliated to Bharathidasan University, Tiruchirappalli), Tamil Nadu, India.
[2]Research Scholar, Department of Mathematics, Khadhir Mohideen College, Adhirampattinam, (Affiliated to Bharathidasan University, Tiruchirappalli), Tamil Nadu, India.
[3]Assistant Professor, Department of Mathematics, C. Kandaswamy Naidu College for Women, Cuddalore, (Affiliated to Thiruvalluvar University, Tiruchirappalli), Tamil Nadu, India.

Received: 21 Nov 2024 Revised: 03 Dec 2024 Accepted: 13 Jan 2025

***Address for Correspondence**
M. Sabina Begum,
Research Scholar,
Department of Mathematics,
Khadhir Mohideen College, Adhirampattinam,
(Affiliated to Bharathidasan University, Tiruchirappalli),
Tamil Nadu, India.
E.Mail: sabinasharifmsc @gmail.com

ABSTRACT

This paper derives a integrated vendor–buyer inventory model in price-dependent demand in a fuzzy environment. The parameters concerned in inventory model are probably to be varied to the unsteady business environment. Therefore, it'll be a lot of realistic to apply fuzzy model instead of crisp model. In this inventory model the cost parameter are used in pentagonal fuzzy number, Removal of area method is employed to defuzzification of the total inventory cost. Here, we determine the minimize the total cost and the optimum order quantity using Lagrangian method, Finally, a valuable example will be given to extract the optimal order quantity .

Keywords: Integrated vendor–buyer inventory model, Price-dependent demand Lagrangian Method, Pentagonal Fuzzy Number, Removal of Area Method

INTRODUCTION

In the real world, every industry wants more Benefit from low manufacturing costs. Now on supply Chains, buyers aren't just worried arbitrary order quantity and when purchase is required enter inventory to provide effectively their customers. A deficiency of traditional inventory models is commonly believed to be that unmet demand is lost or delayed. In manufacturing environments, it is common for managers in a manufacturing organization to want to produce additional production units as safety stock to meet known customer demand. This phenomenon especially observed in the manufacturing process It is not possible to produce a product of right quality every time. A common definition of lead time in supply chain management is the time from the moment a customer places an order to the time they are ready to ship. If there is no finished product or working in process stock that is the time it'll take to definitely produce the order with none inventory aside from the raw materials. The topic of reducing lead time has received a lot of encouragement. Interest in recent years. Researchers with such characteristics Changed the traditional inventory model to accommodate them Implementation of the concept of lead time In the manufacturing control, controlling lead time and reducing setup costs are critical to business success and have received considerable research attention. In the present scenario many companies offer trade credit terms to attract the buyers, and the buyers would like to provide higher service to customers. And buyers want to superior serve their customers However, many industries struggle to reach their aims because they don't know how to make effective decisions under real-world problems to achieve the desired level of customer service with minimal inventory costs. Further, the following literature will be very useful Build our model. R. Uthayakumar *et al.*,[1] considered single-vendor single-buyer integrated inventory system with permissible delay in payments, controllable setup cost and lead time. Sustainable Demand is a business service that helps customers find new customers and expand into new markets. With this you can optimize your internal sales and marketing activities and sell quality. Vulnerable Demand can predict and measure changes caused by on-demand transportation conditions. It is more realistic to assume that demand depends on selling price, since higher selling prices can negatively impact customers' opportunity to purchase a product or service. A.Sutcu et al. [2] considered an EOQ model with price- and time-dependent sales price demand. The finite-stock inventory model was designed to be sensitive to changes in demand over time and sales prices. BK Dey *et al.* [3] ,developed discussed a discrete configuration inventory model, cost reduction, variable safety factor, depending on selling price, demand and investment.M.D.Roy *et al.* [4], considered supply chain model with quality control, lead-time dependent backorder and price-sensitive stochastic demand. And H.C.Chang *et al.* [5] initiated Integrated vendor–buyer cooperative inventory models with controllable lead time and ordering cost reduction.

In regular lifestyles of all people there are positive troubles like uncertain, inaccurate, incomplete and contradictory information. Fuzzy set idea is one of the maximum complete frameworks for uncertainty. In 1965, A. Zadeh [6] added this idea to investigate obscure and incomplete mathematical information, and this set is a generalization of the crisp set that takes into consideration the diploma of club of every detail of the crisp set. Render [7] produced in element of nonlinear programming methods. Taha [8] used the Lagrangian technique to cope with the troubles of uncertainty diagnosed in operations research. Roy *et al.* [9], mentioned a deteriorating multi-object stock version with fuzzy fees and assets primarily based totally on unique defuzzification techniques Sadeghal. [10],studied A Lagrangian Relaxation for a Fuzzy Random EPQ Problem with Shortages ,Chakraborty *et al.* [11,12], added The Pentagonal Fuzzy Number: Its Different Representations, Properties, Ranking, Defuzzification and its unique representation, ranking, defuzzification approach and alertness in manufacturing stock control problem. In the present paper ,we developed the inventory model of uthayakumar, *et al.* [13] to incorporate an integrated vendor–buyer supply chain model for backorder price discount and price-dependent demand using service level constraints and carbon emission cost. The objective is to determine the optimal ordering quantity for which the total cost will be minimized. An efficient Lagrangian method is developed with the Linear PFN with symmetry Number to find the optimal ordering quantity. Finally, a numerical example is presented to demonstrate the developed model and the solution procedure. The rest of this document is organized as follows. In section 2 methodology of fuzzification and defuzzification method is discussed. Section 3 describes the notations and assumptions used in this

document. We formulate this inventory model mathematically in Sec. 3. In Sect. 4, solution procedure is carried out. A numerical example is given in Sect.6 , a sensitivity analysis of the optimal solution is performed in relation to the main parameters of the system and some important managerial insights are obtained. Finally, we draw some conclusions

METHODOLOGY

Pentagonal Fuzzy Number: [11] A PFN is written as $\tilde{A} = (a_1, a_2, a_3, a_4, a_5; k)$ whose corresponding membership function is written as

$$\mu_{\tilde{A}}(x) = \begin{cases} k\dfrac{x-a_1}{a_2-a_1} \; for a_1 \le x \le a_2 \\ 1-(1-k)\dfrac{x-a_2}{a_3-a_2} \; for a_2 \le x \le a_3 \\ 1 \; for x = a_3 \\ 1-(1-k)\dfrac{a_4-x}{a_4-a_3} \; for a_3 \le x \le a_4 \\ k\dfrac{a_5-x}{a_5-a_4} \; for a_4 \le x \le a_5 \\ 0 \; for x > a_5 \end{cases} \quad \text{-----(1)}$$

α-cut or the parametric form of Pentagonal Fuzzy Number: [11] *α*-cut or parametric form of Pentagonal Fuzzy Number is written by the formulae

$$A_\alpha = \{x \in X \,/\, \mu_{\tilde{A}}(x) \ge \alpha\}$$

$$A_{1l}(\alpha) = a_1 + \frac{\alpha}{k}(a_2 - a_1) \; for \alpha \in [0, k],$$

$$A_{2l}(\alpha) = a_2 + \frac{1-\alpha}{1-k}(a_3 - a_2) \; for \alpha \in [k, 1]$$

$$A_{1r}(\alpha) = a_5 - \frac{\alpha}{k}(a_5 - a_4) \; for \alpha \in [0, k],$$

$$A_{2r}(\alpha) = a_4 - \frac{1-\alpha}{1-k}(a_4 - a_3) \; for \alpha \in [k, 1] \quad \text{-----(2)}$$

where $A_{1l}(\alpha), A_{2l}(\alpha)$ is the non decreasing function with respect to *α* and $A_{1r}(\alpha), A_{2r}(\alpha)$ is the decreasing function with respect to *α*

Defuzzification of Removal of Area Method for Pentagonal Fuzzy Number

We consider different types of areas of the corresponding Pentagonal Fuzzy Number as shown below. Then, we find the following.

$R(\tilde{A}_1, 0)$ = Area of shaded region for Figure 2 = $\dfrac{a_1 + a_2}{2}.k$

$R(\tilde{A}_2,0)$ = Area of shaded region for Figure 3 = $\frac{a_2+a_3}{2}.(1-k)$

$R(\tilde{A}_3,0)$ = Area of shaded region for Figure 4 = $a_3 . 1 = a_3$

$R(\tilde{A}_4,0)$ = Area of shaded region for Figure 5 = $\left\{a_4-\left(\frac{a_4-a_3}{2}.(1-k)\right)\right\}$

$R(\tilde{A}_5,0)$ = Area of shaded region for Figure 6 = $\frac{a_5+a_4}{2}.k$

Hence,

$$R(\tilde{D},0)=\frac{R(\tilde{A}_1,0)+R(\tilde{A}_2,0)+R(\tilde{A}_3,0)+R(\tilde{A}_4,0)+R(\tilde{A}_5,0)}{5}$$

$$= \frac{\frac{a_1+a_2}{2}.k+\frac{a_2+a_3}{2}.(1-k)+a_3+\left\{a_4-\left(\frac{a_4-a_3}{2}.(1-k)\right)\right\}+\frac{a_5+a_4}{2}.k}{5}$$

For k=1

$$= \frac{a_1+a_2+2a_3+3a_4+a_5}{10} \quad \text{---(3)}$$

Mathematical Model

Notations and Assumptions

The following notations and assumptions are accepted as used in uthayakumar, *et al.* [13], to build the proposed model. Additional notations and assumptions are used as needed. Notations and assumptions are listed in this Sections

Notations

Q	Order quantity of the buyer
K	Safety factor
V_s	Vendor's setup cost ($/setup)
L	Duration of the purchaser's lead time(days)
π_y	Backorder price discount offered by the vendor per unit
m	Number of lots delivered fromthe seller to the purchaser
S_v	Selling price
P_v	Production cost ($/unit)
R_v	Production rate (units/year)
I_v	Initial setup cost ($/setup)
T_v	Fixed transportation cost
CT_v	Variable transportation cost
H_v	Holding cost ($unit/unit time)
E_v	Variable carbon emission cost ($/unit)
F_v	Fixed carbon emission cost ($ /shipment)
β_v	backordered at the buyer's end, $0 \le \beta_v < 1$
βo_v	Upper bound of the backorder ratio, $0 \le \beta o_v < 1$
D_b	Demand
P_b	Production cost

O_b	Ordering cost ($/unit)
R_b	Reorder point ($/unit
H_b	Holding cost ($unit/unit time)
$C(L)$	Lead time crashing cost per cycle

ASSUMPTIONS

The mathematical model in this paper has been developed to support subsequent assumptions and notations.

The following assumptions are used in our model

1. This inventory system has contracts with a single seller and buyer. Sellers and buyers are from different companies and enjoy a common inventory system. The stock level has been reached up to reporting point Rb when the buyer places the order. The reorder point is $R_b = D_bL + k\sigma\sqrt{L}$ where, D_bL is the expected demand during the lead time, $k\sigma\sqrt{L}$ is safety stock.
2. Demand is taken into consideration relying at the promoting fee of the goods.
3. The lead time L consists of m components that are often free .x_i = length at minimum level, y_i = duration at normal level, and c_i = is the crashing cost per unit time. Assume

$$L_0 = \sum_{j=1}^{m} y_j$$

$c_1 \le c_2 \le \cdots \le c_m$. We assume and it is characterised by

$$L_i = L_0 - \sum_{j=1}^{i} y_j - x_j$$

i =1, 2, . . .m the lead time crashing per cycle $C(L)$ is described as

$$C(L) = c_i(L_{i-1} - L) + \sum_{j=1}^{i-1} c_j(y_j - x_j) \quad \text{--- (4)}$$

4. Here, the X pursues a normal distribution with mean D_bL and standard deviation $\sigma\sqrt{L}$. We assume that X includes a c.d.f F and the reorder point $R_b = D_bL + k\sigma\sqrt{L}$. Crashing cost of the lead time per unit time is $\frac{D_bC(L)}{Q}$.
5. Since then, the missing ones have been allowed and fully delayed. Therefore, the seller offers its customers discounts for shortages. During the inventory period, the backlog rate β0vis variable and proportional to the price discount offered by the supplier per unit π_y. That is,

$$\beta_v = \frac{\beta_{0v}\pi_y}{\pi_x}$$ where, $0 \le \beta_{0v} < 1$ and $0 \le \pi_y \le \pi_x$ --- (5)

Conventional Crisp Inventory Model

First, we assume the single setup multiple delievery (SSMD) model for all units considering transportation cost, holding cost ,setup cost and carbon emission cost for buyer and ventor. Based on the above notations and assumptions

Integrated total cost (ITC) If buyer orders lot size Q then the expected cycle length for the vendor and buyer are $\frac{mQ}{D_b}$ and $\frac{Q}{D_b}$ Here, the buyers ordering cost is $\frac{O_bD_b}{Q}$ .If the level of inventory reaches to the reorder point R_b then the order quantity Q is set by the buyer.

The average inventory of the vendor = ----(6)

The expected holding cost is derived = $\frac{H_v P_v Q}{2}\left\{m\left(1-\frac{D_b}{R_v}\right)-1+\frac{2D_b}{R_v}\right\}$ ---(7)

The expected setup cost = $\frac{S_v D_b}{mQ}+I_v\left(S_v\right)$ ---(8)

The annual transportation cost = $m\left(T_v+CT_v\right)$ ---(9)

The annual carbon emission cost = mF_v+QE_v ---(10)

The holding cost is derived from Sarkar and Majumder [14] = $H_b P_b\left\{\frac{Q}{2}+k\sigma\sqrt{L}+\left(1-\frac{\beta_{ov}\pi_y}{\pi_x}\right)\sigma\sqrt{L}\psi\left(k\right)\right\}$, ---(11)

The ordering cost is = $\frac{O_b D_b}{Q}$ ---(12)

The crashing cost is = $\frac{C(L)D_b}{Q}$ ---(13)

The total shortage is = $\frac{D_b\sigma\sqrt{L}\psi\left(k\right)}{Q}\left(\frac{\beta_{ov}\pi_y{}^2}{\pi_x}+\pi_x-\beta_{ov}\pi_y\right)$ ---(14)

Total cost function is

$$ITC(Q,m,L)=\begin{cases}\frac{S_v D_b}{mQ}+\frac{H_v P_v Q}{2}\left\{m\left(1-\frac{D_b}{R_v}\right)-1+\frac{2D_b}{R_v}\right\}+I_v\ln\left(\frac{S_{vo}}{S_v}\right)+m\left(T_v+CT_v\right)\\ +mF_v+QE_v+H_b P_b\left\{\frac{Q}{2}+k\sigma\sqrt{L}+\left(1-\frac{\beta_{ov}\pi_y}{\pi_x}\right)\sigma\sqrt{L}\psi\left(k\right)\right\}\\ +\frac{O_b D_b}{Q}+\frac{C(L)D_b}{Q}+\frac{D_b\sigma\sqrt{L}\psi\left(k\right)}{Q}\left(\frac{\beta_{ov}\pi_y{}^2}{\pi_x}+\pi_x-\beta_{ov}\pi_y\right)\end{cases}$$

$$ITC(Q,m,L)=\begin{cases}\frac{Q}{2}\left\{H_v P_v\left\{m\left(1-\frac{D_b}{R_v}\right)-1+\frac{2D_b}{R_v}\right\}+2E_v+H_b P_b\right\}\\ +\frac{D_b}{Q}\left\{\frac{S_v}{m}+O_b+C(L)+\sigma\sqrt{L}\psi\left(k\right)\left(\frac{\beta_{ov}\pi_y{}^2}{\pi_x}+\pi_x-\beta_{ov}\pi_y\right)\right\}\\ +H_b P_b\left\{k\sigma\sqrt{L}+\left(1-\frac{\beta_{ov}\pi_y}{\pi_x}\right)\sigma\sqrt{L}\psi\left(k\right)\right\}+I_v\ln\left(\frac{S_{vo}}{S_v}\right)+m\left(T_v+CT_v\right)+mF_v\end{cases}$$

--------(15)

Diff partially w.r.to Q in equ (15),we get

$$\frac{\partial ITC(Q,m,L)}{\partial Q}=\left[\begin{array}{l}\frac{1}{2}\left\{H_v P_v\left\{m\left(1-\frac{D_b}{R_v}\right)-1+\frac{2D_b}{R_v}\right\}+2E_v+H_b P_b\right\}\\ -\frac{D_b}{Q^2}\left\{\frac{S_v}{m}+O_b+C(L)+\sigma\sqrt{L}\psi(k)\left(\frac{\beta_{ov}\pi_y{}^2}{\pi_x}+\pi_x-\beta_{ov}\pi_y\right)\right\}\end{array}\right.$$

Again , Diff partially w.r.to Q in equ(15),we get

$$\frac{\partial^2 ITC(Q,m,L)}{\partial Q^2}=\left[\frac{2D_b}{Q^3}\left\{\frac{S_v}{m}+O_b+C(L)+\sigma\sqrt{L}\psi(k)\left(\frac{\beta_{ov}\pi_y{}^2}{\pi_x}+\pi_x-\beta_{ov}\pi_y\right)\right\}\right. \quad >0$$

Set $\frac{\partial ITC(Q,m,L)}{\partial Q}$ =0

we get Computation of Q at which $ITC(Q,m,L)$ is minimum Therefore, $ITC(Q,m,L)$ is convex in *Q*, for a fixed *m* and *L*. As a result, examine for the optimal derivatives, *Q* is reduce to find a local minimum. Hence, we obtain the optimal order quantity *Q* is,

$$Q=\sqrt{\frac{\left\{\left\{2\left(D_b\left\{\frac{S_v}{m}+O_b+C(L)+\sigma\sqrt{L}\psi(k)\left(\frac{\beta_{ov}\pi_y{}^2}{\pi_x}+\pi_x-\beta_{ov}\pi_y\right)\right\}\right)\right\}\right\}}{\left\{H_v P_v\left\{m\left(1-\frac{D_b}{R_v}\right)-1+\frac{2D_b}{R_v}\right\}+2E_v+H_b P_b\right\}}} \quad \text{----------(16)}$$

Fuzzy Mathematical Model

The following parameters are used in this paper to simplify the processing of fuzzy inventory models. Let's make it a fuzzy parameter.

$$ITC(Q,m,L)=\left\{\begin{array}{l}\frac{Q}{2}\left\{\tilde{H}_v\tilde{P}_v\left\{m\left(1-\frac{\tilde{D}_b}{R_v}\right)-1+\frac{2\tilde{D}_b}{R_v}\right\}+2E_v+\tilde{H}_b\tilde{P}_b\right\}\\ +\frac{\tilde{D}_b}{Q}\left\{\frac{\tilde{S}_v}{m}+\tilde{O}_b+C(L)+\sigma\sqrt{L}\psi(k)\left(\frac{\beta_{ov}\pi_y{}^2}{\pi_x}+\pi_x-\beta_{ov}\pi_y\right)\right\}\\ +\tilde{H}_b\tilde{P}_b\left\{k\sigma\sqrt{L}+\left(1-\frac{\beta_{ov}\pi_y}{\pi_x}\right)\sigma\sqrt{L}\psi(k)\right\}+I_v\ln\left(\frac{S_{vo}}{S_v}\right)+m\left(T_v+CT_v\right)+mF_v\end{array}\right. \quad \text{--(17)}$$

Computation of Q at which $ITC(Q,m,L)$ is minimum, when $\frac{\partial ITC(Q,m,L)}{\partial Q}$ =0 and where $\frac{\partial^2 ITC(Q,m,L)}{\partial Q^2} > 0$

$$Q = \sqrt{\frac{\left\{2\left(\tilde{D}_b\left\{\frac{\tilde{S}_v}{m}+\tilde{O}_b+C(L)+\sigma\sqrt{L}\psi(k)\left(\frac{\beta_{ov}\pi_y{}^2}{\pi_x}+\pi_x-\beta_{ov}\pi_y\right)\right\}\right)\right\}}{\left\{\tilde{H}_v\tilde{P}_v\left\{m\left(1-\frac{\tilde{D}_b}{R_v}\right)-1+\frac{2\tilde{D}_b}{R_v}\right\}+2E_v+\tilde{H}_b\tilde{P}_b\right\}}} \quad \text{-------(18)}$$

Mathematical Model in Fuzzy sense

let us consider the proposed inventory model of the minimum total cost is

$$I\tilde{T}C(\tilde{Q},m,L) = \begin{cases} \frac{\tilde{Q}}{2}\left\{\tilde{H}_v\tilde{P}_v\left\{m\left(1-\frac{\tilde{D}_b}{R_v}\right)-1+\frac{2\tilde{D}_b}{R_v}\right\}+2E_v+\tilde{H}_b\tilde{P}_b\right\} \\ +\frac{\tilde{D}_b}{\tilde{Q}}\left\{\frac{\tilde{S}_v}{m}+\tilde{O}_b+C(L)+\sigma\sqrt{L}\psi(k)\left(\frac{\beta_{ov}\pi_y{}^2}{\pi_x}+\pi_x-\beta_{ov}\pi_y\right)\right\} \\ +\tilde{H}_b\tilde{P}_b\left\{k\sigma\sqrt{L}+\left(1-\frac{\beta_{ov}\pi_y}{\pi_x}\right)\sigma\sqrt{L}\psi(k)\right\}+I_v\ln\left(\frac{S_{vo}}{S_v}\right)+m(T_v+CT_v)+mF_v \end{cases} \quad (19)$$

To apply Removal of Area method to de fuzzify the fuzzy total cost, and then obtain the optimal order quantity Q by using new arithmetic operation

$$IT\tilde{C}(Q,m,L)=\frac{1}{10}$$

$$\left\{\begin{array}{l}\left(\begin{array}{l}\frac{Q_1H_{v1}P_{v1}m}{2}-\frac{Q_5H_{v5}P_{v5}D_{b5}m}{2R_{v1}}-\frac{Q_5H_{v5}P_{v5}}{2}+\frac{Q_1 2\tilde{D}_{b1}H_{v1}P_{v1}}{2R_{v5}}+Q_1E_{v1}+\frac{H_{b1}P_{b1}Q_1}{2}\\+\frac{D_{b1}}{Q_5}\left\{\frac{S_v}{m}+O_{b1}+C(L)+\sigma\sqrt{L}\psi(k)\left(\frac{\beta_{ov}\pi_y{}^2}{\pi_x}+\pi_x-\beta_{ov}\pi_y\right)\right\}\\+H_{b1}P_{b1}\left\{k\sigma\sqrt{L}+\left(1-\frac{\beta_{ov}\pi_y}{\pi_x}\right)\sigma\sqrt{L}\psi(k)\right\}+I_v\ln\left(\frac{S_{vo}}{S_v}\right)+m(T_v+CT_v)+mF_v\end{array}\right)\\+\left(\begin{array}{l}\frac{Q_2H_{v2}P_{v2}m}{2}-\frac{Q_4H_{v4}P_{v4}D_{b4}m}{2R_{v2}}-\frac{Q_4H_{v4}P_{v4}}{2}+\frac{Q_2 2\tilde{D}_{b2}H_{v2}P_{v2}}{2R_{v4}}+Q_2E_{v2}+\frac{H_{b2}P_{b2}Q_2}{2}\\+\frac{D_{b2}}{Q_4}\left\{\frac{S_v}{m}+O_{b2}+C(L)+\sigma\sqrt{L}\psi(k)\left(\frac{\beta_{ov}\pi_y{}^2}{\pi_x}+\pi_x-\beta_{ov}\pi_y\right)\right\}\\+H_{b2}P_{b2}\left\{k\sigma\sqrt{L}+\left(1-\frac{\beta_{ov}\pi_y}{\pi_x}\right)\sigma\sqrt{L}\psi(k)\right\}+I_v\ln\left(\frac{S_{vo}}{S_v}\right)+m(T_v+CT_v)+mF_v\end{array}\right)\\+2\left(\begin{array}{l}\frac{Q_3H_{v3}P_{v3}m}{2}-\frac{Q_3H_{v3}P_{v3}D_{b3}m}{2R_{v3}}-\frac{Q_3H_{v3}P_{v3}}{2}+\frac{Q_3 2\tilde{D}_{b3}H_{v3}P_{v3}}{2R_{v3}}+Q_3E_{v3}+\frac{H_{b3}P_{b3}Q_3}{2}\\+\frac{D_{b3}}{Q_3}\left\{\frac{S_v}{m}+O_{b3}+C(L)+\sigma\sqrt{L}\psi(k)\left(\frac{\beta_{ov}\pi_y{}^2}{\pi_x}+\pi_x-\beta_{ov}\pi_y\right)\right\}\\+H_{b3}P_{b3}\left\{k\sigma\sqrt{L}+\left(1-\frac{\beta_{ov}\pi_y}{\pi_x}\right)\sigma\sqrt{L}\psi(k)\right\}+I_v\ln\left(\frac{S_{vo}}{S_v}\right)+m(T_v+CT_v)+mF_v\end{array}\right)\\+3\left(\begin{array}{l}\frac{Q_4H_{v4}P_{v4}m}{2}-\frac{Q_2H_{v2}P_{v2}D_{b2}m}{2R_{v4}}-\frac{Q_2H_{v2}P_{v2}}{2}+\frac{Q_4 2\tilde{D}_{b4}H_{v4}P_{v4}}{2R_{v2}}+Q_4E_{v4}+\frac{H_{b4}P_{b4}Q_4}{2}\\+\frac{D_{b4}}{Q_2}\left\{\frac{S_v}{m}+O_{b4}+C(L)+\sigma\sqrt{L}\psi(k)\left(\frac{\beta_{ov}\pi_y{}^2}{\pi_x}+\pi_x-\beta_{ov}\pi_y\right)\right\}\\+H_{b4}P_{b4}\left\{k\sigma\sqrt{L}+\left(1-\frac{\beta_{ov}\pi_y}{\pi_x}\right)\sigma\sqrt{L}\psi(k)\right\}+I_v\ln\left(\frac{S_{vo}}{S_v}\right)+m(T_v+CT_v)+mF_v\end{array}\right)\\+\left(\begin{array}{l}\frac{Q_5H_{v5}P_{v5}m}{2}-\frac{Q_1H_{v1}P_{v1}D_{b1}m}{2R_{v5}}-\frac{Q_1H_{v1}P_{v1}}{2}+\frac{Q_5 2\tilde{D}_{b5}H_{v5}P_{v5}}{2R_{v1}}+Q_5E_{v5}+\frac{H_{b5}P_{b5}Q_5}{2}\\+\frac{D_{b5}}{Q_1}\left\{\frac{S_v}{m}+O_{b5}+C(L)+\sigma\sqrt{L}\psi(k)\left(\frac{\beta_{ov}\pi_y{}^2}{\pi_x}+\pi_x-\beta_{ov}\pi_y\right)\right\}\\+H_{b5}P_{b5}\left\{k\sigma\sqrt{L}+\left(1-\frac{\beta_{ov}\pi_y}{\pi_x}\right)\sigma\sqrt{L}\psi(k)\right\}+I_v\ln\left(\frac{S_{vo}}{S_v}\right)+m(T_v+CT_v)+mF_v\end{array}\right)\end{array}\right\}$$ ----------(20)

with $0 < Q_1 \le Q_2 \le Q_3 \le Q_4 \le Q_5$ if we replace inequality conditions $0 < Q_1 \le Q_2 \le Q_3 \le Q_4 \le Q_5$. into the following inequality $Q_2 - Q_1 \ge 0$, $Q_3 - Q_2 \ge 0$, $Q_4 - Q_3 \ge 0$, $Q_5 - Q_4 \ge 0$ $Q_1 \ge 0$ In the following stages, extension of the Lagrangian method is used to find the solutions of Q_1, Q_2, Q_3, Q_4, Q_5 to minimize $IT\tilde{C}(\tilde{Q}, m, L)$

Stage 1 : To find the min $IT\tilde{C}(\tilde{Q}, m, L)$, Then

$$Q_1 = \sqrt{\frac{2D_{b5}\left\{\frac{S_v}{m} + O_{b5} + C(L) + \sigma\sqrt{L}\psi(k)\left(\frac{\beta_{ov}\pi_y^{\,2}}{\pi_x} + \pi_x - \beta_{ov}\pi_y\right)\right\}}{\left\{H_{v1}P_{v1}\left\{m\left(1 - \frac{D_{b1}}{R_{v5}}\right) - 1 + \frac{2D_{b1}}{R_{v5}}\right\} + 2E_{v1} + H_{b1}P_{b1}\right\}}} \quad (21)$$

$$Q_2 = \sqrt{\frac{2D_{b4}\left\{\frac{S_v}{m} + O_{b4} + C(L) + \sigma\sqrt{L}\psi(k)\left(\frac{\beta_{ov}\pi_y^{\,2}}{\pi_x} + \pi_x - \beta_{ov}\pi_y\right)\right\}}{\left\{H_{v2}P_{v2}\left\{m\left(1 - \frac{D_{b2}}{R_{v4}}\right) - 1 + \frac{2D_{b2}}{R_{v4}}\right\} + 2E_{v2} + H_{b2}P_{b2}\right\}}} \quad (22)$$

$$Q_3 = \sqrt{\frac{4D_{b3}\left\{\frac{S_v}{m} + O_{b3} + C(L) + \sigma\sqrt{L}\psi(k)\left(\frac{\beta_{ov}\pi_y^{\,2}}{\pi_x} + \pi_x - \beta_{ov}\pi_y\right)\right\}}{2\left\{H_{v3}P_{v3}\left\{m\left(1 - \frac{D_{b3}}{R_{v3}}\right) - 1 + \frac{2D_{b3}}{R_{v3}}\right\} + 2E_{v3} + H_{b3}P_{b3}\right\}}} \quad (23)$$

$$Q_4 = \sqrt{\frac{6D_{b2}\left\{\frac{S_v}{m} + O_{b2} + C(L) + \sigma\sqrt{L}\psi(k)\left(\frac{\beta_{ov}\pi_y^{\,2}}{\pi_x} + \pi_x - \beta_{ov}\pi_y\right)\right\}}{3\left\{H_{v4}P_{v4}\left\{m\left(1 - \frac{D_{b4}}{R_{v2}}\right) - 1 + \frac{2D_{b4}}{R_{v2}}\right\} + 2E_{v4} + H_{b4}P_{b4}\right\}}} \quad (24)$$

$$Q_5 = \sqrt{\frac{2D_{b1}\left\{\frac{S_v}{m} + O_{b1} + C(L) + \sigma\sqrt{L}\psi(k)\left(\frac{\beta_{ov}\pi_y^{\,2}}{\pi_x} + \pi_x - \beta_{ov}\pi_y\right)\right\}}{\left\{H_{v5}P_{v5}\left\{m\left(1 - \frac{D_{b5}}{R_{v1}}\right) - 1 + \frac{2D_{b5}}{R_{v1}}\right\} + 2E_{v5} + H_{b5}P_{b5}\right\}}} \quad (25)$$

Because the above show that $Q_1 > Q_2 > Q_3 > Q_4 > Q_5$, it does not satisfy the constraint $0 < Q_1 \le Q_2 \le Q_3 \le Q_4 . \le Q_5$ Therefore set K = 1 and go to Stage 2

Stage 2 : Convert the inequality constraint $Q_2 - Q_1 \geq 0$ into equality constraint $Q_2 - Q_1 = 0$. We have Lagrangian function as $L(Q_1, Q_2, Q_3, Q_4, Q_5, \lambda) = P(ITC(\tilde{Q}, m, L)) - \lambda(Q_2 - Q_1)$. we have to find the derivative of $L(Q_1, Q_2, Q_3, Q_4, Q_5, \lambda)$ with respect to Q_1, Q_2, Q_3, Q_4 Q_5, and λ equal to zero.

$$Q_1 = Q_2 = \sqrt{\frac{\begin{aligned}&2D_{b5}\left\{\frac{S_v}{m} + O_{b5} + C(L) + \sigma\sqrt{L}\psi(k)\left(\frac{\beta_{ov}\pi_y^{\,2}}{\pi_x} + \pi_x - \beta_{ov}\pi_y\right)\right\} \\ &+2D_{b4}\left\{\frac{S_v}{m} + O_{b4} + C(L) + \sigma\sqrt{L}\psi(k)\left(\frac{\beta_{ov}\pi_y^{\,2}}{\pi_x} + \pi_x - \beta_{ov}\pi_y\right)\right\}\end{aligned}}{\begin{aligned}&\left\{H_{v1}P_{v1}\left\{m\left(1 - \frac{D_{b1}}{R_{v5}}\right) - 1 + \frac{2D_{b1}}{R_{v5}}\right\} + 2E_{v1} + H_{b1}P_{b1}\right\} \\ &+\left\{H_{v2}P_{v2}\left\{m\left(1 - \frac{D_{b2}}{R_{v4}}\right) - 1 + \frac{2D_{b2}}{R_{v4}}\right\} + 2E_{v2} + H_{b2}P_{b2}\right\}\end{aligned}}} \quad (26)$$

$$Q_3 = \sqrt{\frac{4D_{b3}\left\{\frac{S_v}{m} + O_{b3} + C(L) + \sigma\sqrt{L}\psi(k)\left(\frac{\beta_{ov}\pi_y^{\,2}}{\pi_x} + \pi_x - \beta_{ov}\pi_y\right)\right\}}{2\left\{H_{v3}P_{v3}\left\{m\left(1 - \frac{D_{b3}}{R_{v3}}\right) - 1 + \frac{2D_{b3}}{R_{v3}}\right\} + 2E_{v3} + H_{b3}P_{b3}\right\}}} \quad (27)$$

$$Q_4 = \sqrt{\frac{6D_{b2}\left\{\frac{S_v}{m} + O_{b2} + C(L) + \sigma\sqrt{L}\psi(k)\left(\frac{\beta_{ov}\pi_y^{\,2}}{\pi_x} + \pi_x - \beta_{ov}\pi_y\right)\right\}}{3\left\{H_{v4}P_{v4}\left\{m\left(1 - \frac{D_{b4}}{R_{v2}}\right) - 1 + \frac{2D_{b4}}{R_{v2}}\right\} + 2E_{v4} + H_{b4}P_{b4}\right\}}} \quad (28)$$

$$Q_5 = \sqrt{\frac{2D_{b1}\left\{\frac{S_v}{m} + O_{b1} + C(L) + \sigma\sqrt{L}\psi(k)\left(\frac{\beta_{ov}\pi_y^{\,2}}{\pi_x} + \pi_x - \beta_{ov}\pi_y\right)\right\}}{\left\{H_{v5}P_{v5}\left\{m\left(1 - \frac{D_{b5}}{R_{v1}}\right) - 1 + \frac{2D_{b5}}{R_{v1}}\right\} + 2E_{v5} + H_{b5}P_{b5}\right\}}} \quad (29)$$

Because the above results show that $Q_3 > Q_4 > Q_5$, it does not satisfy the constraint $0 < Q_1 \leq Q_2 \leq Q_3 \leq Q_4 . \leq Q_5$. constraint to be equality constraint, put K = 2 and go to Stage 3.

Stage 3 : Convert the inequality constraints $Q_2 - Q_1 \geq 0$, $Q_3 - Q_2 \geq 0$, into equality constraints $Q_2 - Q_1 = 0$ and $Q_3 - Q_2 = 0$. Then the Lagrangian method is

$L(Q_1,Q_2,Q_3,Q_4,Q_5,\ \lambda_1,\lambda_2)\ = P(IT\tilde{C}(\tilde{Q},m,L)) - \lambda_1(Q_2\ -\ Q_1) - \lambda_2(Q_3\ -\ Q_2)$, we have to find the derivative of $L(Q_1,Q_2,Q_3,Q_4,Q_5,\lambda_1,\lambda_2)$ with respect to Q_1, Q_2, Q_3, Q_4,Q_5. λ_1, and λ_2 equal to zero,

$$Q_1 = Q_2 = Q_3 = \sqrt{\frac{\begin{aligned}&2D_{b5}\left\{\frac{S_v}{m}+O_{b5}+C(L)+\sigma\sqrt{L}\psi(k)\left(\frac{\beta_{ov}\pi_y{}^2}{\pi_x}+\pi_x-\beta_{ov}\pi_y\right)\right\}\\&+2D_{b4}\left\{\frac{S_v}{m}+O_{b4}+C(L)+\sigma\sqrt{L}\psi(k)\left(\frac{\beta_{ov}\pi_y{}^2}{\pi_x}+\pi_x-\beta_{ov}\pi_y\right)\right\}\\&+4D_{b3}\left\{\frac{S_v}{m}+O_{b3}+C(L)+\sigma\sqrt{L}\psi(k)\left(\frac{\beta_{ov}\pi_y{}^2}{\pi_x}+\pi_x-\beta_{ov}\pi_y\right)\right\}\end{aligned}}{\begin{aligned}&\left\{H_{v1}P_{v1}\left\{m\left(1-\frac{D_{b1}}{R_{v5}}\right)-1+\frac{2D_{b1}}{R_{v5}}\right\}+2E_{v1}+H_{b1}P_{b1}\right\}\\&+\left\{H_{v2}P_{v2}\left\{m\left(1-\frac{D_{b2}}{R_{v4}}\right)-1+\frac{2D_{b2}}{R_{v4}}\right\}+2E_{v2}+H_{b2}P_{b2}\right\}\\&+2\left\{H_{v3}P_{v3}\left\{m\left(1-\frac{D_{b3}}{R_{v3}}\right)-1+\frac{2D_{b3}}{R_{v3}}\right\}+2E_{v3}+H_{b3}P_{b3}\right\}\end{aligned}}} \tag{30}$$

$$Q_4 = \sqrt{\frac{6D_{b2}\left\{\frac{S_v}{m}+O_{b2}+C(L)+\sigma\sqrt{L}\psi(k)\left(\frac{\beta_{ov}\pi_y{}^2}{\pi_x}+\pi_x-\beta_{ov}\pi_y\right)\right\}}{3\left\{H_{v4}P_{v4}\left\{m\left(1-\frac{D_{b4}}{R_{v2}}\right)-1+\frac{2D_{b4}}{R_{v2}}\right\}+2E_{v4}+H_{b4}P_{b4}\right\}}} \tag{31}$$

$$Q_5 = \sqrt{\frac{2D_{b1}\left\{\frac{S_v}{m}+O_{b1}+C(L)+\sigma\sqrt{L}\psi(k)\left(\frac{\beta_{ov}\pi_y{}^2}{\pi_x}+\pi_x-\beta_{ov}\pi_y\right)\right\}}{\left\{H_{v5}P_{v5}\left\{m\left(1-\frac{D_{b5}}{R_{v1}}\right)-1+\frac{2D_{b5}}{R_{v1}}\right\}+2E_{v5}+H_{b5}P_{b5}\right\}}} \tag{32}$$

Because the above show that $Q_1 > Q_4$, it does not satisfy the constraint $0 < Q_1 \le Q_2 \le Q_3 \le Q_4 \le Q_5$. so K = 3 and go to Stage 4.

Stage 4 : Convert the inequality constraints $Q_2 - Q_1 \ge 0$, $Q_3 - Q_2 \ge 0$, $Q_4 - Q_3 \ge 0$,into equality constraints $Q_2 - Q_1 = 0$, $Q_3 - Q_2 = 0$ and $Q_4 - Q_3 = 0$. We optimize the Lagrangean function is given by

$$L(Q_1,Q_2,Q_3,Q_4,Q_5,\lambda_1,\lambda_2,\lambda_3)\ = P(IT\tilde{C}(\tilde{Q},m,L)) - \lambda_1(Q_2\ -\ Q_1) - \lambda_2(Q_3\ -\ Q_2) - \lambda_3(Q_4\ -\ Q_3)$$

we have to find the derivative of $L(Q_1,Q_2,Q_3,Q_4,Q_5\ \lambda_1,\lambda_2,\lambda_3)$ with respect to Q_1, Q_2, Q_3 , Q_4, Q_5,$\lambda_1,\lambda_2,$ and λ_3 equal to zero.

$$Q_1=Q_2=Q_3=Q_4=\sqrt{\frac{\begin{aligned}&2D_{b5}\left\{\frac{S_v}{m}+O_{b5}+C(L)+\sigma\sqrt{L}\psi(k)\left(\frac{\beta_{ov}\pi_y{}^2}{\pi_x}+\pi_x-\beta_{ov}\pi_y\right)\right\}\\&+2D_{b4}\left\{\frac{S_v}{m}+O_{b4}+C(L)+\sigma\sqrt{L}\psi(k)\left(\frac{\beta_{ov}\pi_y{}^2}{\pi_x}+\pi_x-\beta_{ov}\pi_y\right)\right\}\\&+4D_{b3}\left\{\frac{S_v}{m}+O_{b3}+C(L)+\sigma\sqrt{L}\psi(k)\left(\frac{\beta_{ov}\pi_y{}^2}{\pi_x}+\pi_x-\beta_{ov}\pi_y\right)\right\}\\&+6D_{b2}\left\{\frac{S_v}{m}+O_{b2}+C(L)+\sigma\sqrt{L}\psi(k)\left(\frac{\beta_{ov}\pi_y{}^2}{\pi_x}+\pi_x-\beta_{ov}\pi_y\right)\right\}\end{aligned}}{\begin{aligned}&\left\{H_{v1}P_{v1}\left\{m\left(1-\frac{D_{b1}}{R_{v5}}\right)-1+\frac{2D_{b1}}{R_{v5}}\right\}+2E_{v1}+H_{b1}P_{b1}\right\}\\&+\left\{H_{v2}P_{v2}\left\{m\left(1-\frac{D_{b2}}{R_{v4}}\right)-1+\frac{2D_{b2}}{R_{v4}}\right\}+2E_{v2}+H_{b2}P_{b2}\right\}\\&+2\left\{H_{v3}P_{v3}\left\{m\left(1-\frac{D_{b3}}{R_{v3}}\right)-1+\frac{2D_{b3}}{R_{v3}}\right\}+2E_{v3}+H_{b3}P_{b3}\right\}\\&+3\left\{H_{v4}P_{v4}\left\{m\left(1-\frac{D_{b4}}{R_{v2}}\right)-1+\frac{2D_{b4}}{R_{v2}}\right\}+2E_{v4}+H_{b4}P_{b4}\right\}\end{aligned}}} \tag{33}$$

$$Q_5=\sqrt{\frac{2D_{b1}\left\{\frac{S_v}{m}+O_{b1}+C(L)+\sigma\sqrt{L}\psi(k)\left(\frac{\beta_{ov}\pi_y{}^2}{\pi_x}+\pi_x-\beta_{ov}\pi_y\right)\right\}}{\left\{H_{v5}P_{v5}\left\{m\left(1-\frac{D_{b5}}{R_{v1}}\right)-1+\frac{2D_{b5}}{R_{v1}}\right\}+2E_{v5}+H_{b5}P_{b5}\right\}}} \tag{34}$$

Because the above show that $Q_1 > Q_5$, does not satisfy the constraint $0 < Q_1 \le Q_2 \le Q_3 \le Q_4 \le Q_5$. so K = 4 and go to Stage 5.

Stage 5 : Convert the inequality constraints $Q_2-Q_1\ge 0$, $Q_3-Q_2\ge 0$, $Q_4-Q_3\ge 0$,and $Q_5-Q_4\ge 0$ into equality constraints $Q_2 - Q_1 = 0$, $Q_3 - Q_2 = 0$,$Q_4 - Q_3 = 0$ and $Q_5-Q_4=0$. The Lagrangean function is given by

$$L(Q_1,Q_2,Q_3,Q_4,Q_5,\ \lambda_1,\lambda_2,\lambda_3,\lambda_4)=P(IT\tilde{C}(Q,m,L))-\lambda_1(Q_2-Q_1)$$
$$-\lambda_2(Q_3-Q_2)-\lambda_3(Q_4-Q_3)-\lambda_4(Q_5-Q_4)$$ we have to find the

derivative of $L\left(Q_1,Q_2,Q_3,Q_4,Q_5,\ \lambda_1,\lambda_2,\lambda_3,\lambda_4\right)$ with respect to $Q_1, Q_2, Q_3, Q_4, Q_5, \lambda_1, \lambda_2, \lambda_3, \lambda_4$ and let all the partial derivatives equal to zero

$$Q_1=Q_2=Q_3=Q_4=Q_5=\sqrt{\frac{\begin{array}{l}2D_{b5}\left\{\frac{S_v}{m}+O_{b5}+C(L)+\sigma\sqrt{L}\psi\left(k\right)\left(\frac{\beta_{ov}\pi_y^{\ 2}}{\pi_x}+\pi_x-\beta_{ov}\pi_y\right)\right\}\\+2D_{b4}\left\{\frac{S_v}{m}+O_{b4}+C(L)+\sigma\sqrt{L}\psi\left(k\right)\left(\frac{\beta_{ov}\pi_y^{\ 2}}{\pi_x}+\pi_x-\beta_{ov}\pi_y\right)\right\}\\+4D_{b3}\left\{\frac{S_v}{m}+O_{b3}+C(L)+\sigma\sqrt{L}\psi\left(k\right)\left(\frac{\beta_{ov}\pi_y^{\ 2}}{\pi_x}+\pi_x-\beta_{ov}\pi_y\right)\right\}\\+6D_{b2}\left\{\frac{S_v}{m}+O_{b2}+C(L)+\sigma\sqrt{L}\psi\left(k\right)\left(\frac{\beta_{ov}\pi_y^{\ 2}}{\pi_x}+\pi_x-\beta_{ov}\pi_y\right)\right\}\\+2D_{b1}\left\{\frac{S_v}{m}+O_{b1}+C(L)+\sigma\sqrt{L}\psi\left(k\right)\left(\frac{\beta_{ov}\pi_y^{\ 2}}{\pi_x}+\pi_x-\beta_{ov}\pi_y\right)\right\}\end{array}}{\begin{array}{l}\left\{H_{v1}P_{v1}\left\{m\left(1-\frac{D_{b1}}{R_{v5}}\right)-1+\frac{2D_{b1}}{R_{v5}}\right\}+2E_{v1}+H_{b1}P_{b1}\right\}\\+\left\{H_{v2}P_{v2}\left\{m\left(1-\frac{D_{b2}}{R_{v4}}\right)-1+\frac{2D_{b2}}{R_{v4}}\right\}+2E_{v2}+H_{b2}P_{b2}\right\}\\+2\left\{H_{v3}P_{v3}\left\{m\left(1-\frac{D_{b3}}{R_{v3}}\right)-1+\frac{2D_{b3}}{R_{v3}}\right\}+2E_{v3}+H_{b3}P_{b3}\right\}\\+3\left\{H_{v4}P_{v4}\left\{m\left(1-\frac{D_{b4}}{R_{v2}}\right)-1+\frac{2D_{b4}}{R_{v2}}\right\}+2E_{v4}+H_{b4}P_{b4}\right\}\\+\left\{H_{v5}P_{v5}\left\{m\left(1-\frac{D_{b5}}{R_{v1}}\right)-1+\frac{2D_{b5}}{R_{v1}}\right\}+2E_{v5}+H_{b5}P_{b5}\right\}\end{array}}} \tag{35}$$

The optimal order quantity is

$$\tilde{Q}=\sqrt{\begin{array}{l}2D_{b5}\left\{\frac{S_v}{m}+O_{b5}+C(L)+\sigma\sqrt{L}\psi(k)\left(\frac{\beta_{ov}\pi_y{}^2}{\pi_x}+\pi_x-\beta_{ov}\pi_y\right)\right\}\\+2D_{b4}\left\{\frac{S_v}{m}+O_{b4}+C(L)+\sigma\sqrt{L}\psi(k)\left(\frac{\beta_{ov}\pi_y{}^2}{\pi_x}+\pi_x-\beta_{ov}\pi_y\right)\right\}\\+4D_{b3}\left\{\frac{S_v}{m}+O_{b3}+C(L)+\sigma\sqrt{L}\psi(k)\left(\frac{\beta_{ov}\pi_y{}^2}{\pi_x}+\pi_x-\beta_{ov}\pi_y\right)\right\}\\+6D_{b2}\left\{\frac{S_v}{m}+O_{b2}+C(L)+\sigma\sqrt{L}\psi(k)\left(\frac{\beta_{ov}\pi_y{}^2}{\pi_x}+\pi_x-\beta_{ov}\pi_y\right)\right\}\\+2D_{b1}\left\{\frac{S_v}{m}+O_{b1}+C(L)+\sigma\sqrt{L}\psi(k)\left(\frac{\beta_{ov}\pi_y{}^2}{\pi_x}+\pi_x-\beta_{ov}\pi_y\right)\right\}\end{array}}\Big/\left\{\begin{array}{l}H_{v1}P_{v1}\left\{m\left(1-\frac{D_{b1}}{R_{v5}}\right)-1+\frac{2D_{b1}}{R_{v5}}\right\}+2E_{v1}+H_{b1}P_{b1}\\+\left\{H_{v2}P_{v2}\left\{m\left(1-\frac{D_{b2}}{R_{v4}}\right)-1+\frac{2D_{b2}}{R_{v4}}\right\}+2E_{v2}+H_{b2}P_{b2}\right\}\\+2\left\{H_{v3}P_{v3}\left\{m\left(1-\frac{D_{b3}}{R_{v3}}\right)-1+\frac{2D_{b3}}{R_{v3}}\right\}+2E_{v3}+H_{b3}P_{b3}\right\}\\+3\left\{H_{v4}P_{v4}\left\{m\left(1-\frac{D_{b4}}{R_{v2}}\right)-1+\frac{2D_{b4}}{R_{v2}}\right\}+2E_{v4}+H_{b4}P_{b4}\right\}\\+\left\{H_{v5}P_{v5}\left\{m\left(1-\frac{D_{b5}}{R_{v1}}\right)-1+\frac{2D_{b5}}{R_{v1}}\right\}+2E_{v5}+H_{b5}P_{b5}\right\}\end{array}\right.$$

----------(36)

Algorithm for finding Numerical values in Inventory Models

The algorithm below is to find the optimal order quantity and integrated total cost for both crisp sense and fuzzy sense using equations (17) to(19) respectively,. We get the optimal order quantity and the minimum integrated total cost. In addition, comparisons are given for both the l crisp model and the fuzzy model.

Algorithm

Step 1: Find the optimal order quantity and integrated total cost in the Crisp model for the specified Crisp parameter values, and then find the Crisp optimal order quantity and total integrated cost

Step 2: Determine the fuzzy integrated total cost using fuzzy arithmetic operations. fuzzy - Inventory, parameters are assumed to be Pentagonal Fuzzy Number

Step 3: For Pentagonal Fuzzy Number To apply Removal of Area method to de fuzzify integrated total cost $ITC\tilde{(}Q,m,L)$ in order to find the order quantity $\tilde{Q}$ which can be obtained by putting the first derivative of $ITC\tilde{(}Q,m,L)$ is equal to zero.

Step 4: Use extension of the Lagrangian method to find the fuzzy optimal order quantity $\tilde{Q}$ = (Q_1 =Q_2 =Q_3 = Q_4 =Q_5) which is the special method for Pentagonal Fuzzy Number. The optimal fuzzy order quantity is $\tilde{Q}$ obtained by substituting the first derivative of $ITC(\tilde{Q},m,L)$ that is equal to zero.

Step 5: To check whether or not the optimal order quantity Q obtained by Removal of Area technique is that the same as the fuzzy optimal order quantity $\tilde{Q}$

Step 6 : Compare the optimal order quantity, integrated total cost obtained from each crisp model and also the fuzzy model with their savings.

NUMERICAL EXAMPLE

Example 1:

The following numerical example shows the above solution. The solution of the numerical example is obtained using the python software. To explain the procedure for solving a crisp model, Let us consider the integrated inventory model with the following data used in in Ouyang and Chuang (2001):

D_b = 120 units / year, S_v= \$172 /order, O_b = \$200 /unit, σ = 7 units / week, H_v = 0.1 units/year , P_v = 45 units/year, R_v = 4000 units/year , T_v = 0.4 /shipment , S_{vo} = \$500 /setup I_v = 15000 units/year , F_v = 0.1 /shipment, E_v = 0.3 \$/unit , P_b =\$80 units/year , H_b =0.2 units/year , β_{ov} = 0.8 \$/unit, π_y = π_x = 150 ,k=0.845 Using equations (15) and (16) respectively, optimal order quantity Q and minimum integrated total cost $ITC(Q,m,L)$ are attained. The results are tabulated in Table 1.

Fuzzy Model

Example. 2

The data is the same as in Example 1, except that the fuzzy parameters D_b=(110,120,140,170,180)
O_b=(190,200,245,275,295)
E_v=(0.27,0.3,0.39,0.4,0.45)
R_b=(3900,4000,5225,5330,5660)
P_b=(70,80,90,115,125)
P_v =(34,45,50,64,79) H_b=(0.05,0.1,0.11,0.15,0.18) and H_v=(0.19,0.2,0.25,0.27,0.3)
The order quantity in Example. 1 is transferred as fuzzy order quantity $\tilde{Q}$ = (Q_1 =Q_2 =Q_3 = Q_4 =Q_5) with $0 < Q_1 \leq Q_2 \leq Q_3 \leq Q_4 \leq Q_5$. The proposed algorithm yields the result as shown in Table 2. Using equations (35) and (20) respectively, optimal fuzzy order quantity Pentagonal Fuzzy Number $\tilde{Q}$ and minimum fuzzy integrated total cost $ITC\tilde{(}\tilde{Q},m,L)$ are obtained. The results are tabulated in Table 1.

CONCLUSION

This document presents a fuzzy integrated buyer-supplier inventory model based on price-dependent demand. The proposed model is developed in both fuzzy and crisp environments. In the fuzzy environment, the inventory parameters are assumed to be Pentagonal Fuzzy Number. The Removal of area method is used for classified defuzzification. Evaluate the optimal total cost and optimal quantity using Lagrange. From a digital example, this fuzzy and crisp pattern was tested. The optimal order quantity and minimum integrated total cost savings with the fuzzy model are typically between 2.9% and 16.5% and between 2.9% and 11. 5%. It is also shown that the optimal order quantity and the minimum integrated total cost solution for the fuzzy case differ significantly from the solution for the crisp case. After comparing the crisp and fuzzy model, the fuzzy model is better than the crisp one. It has been found to be excellent.

REFERENCES

1. Arindam Roy ,Samarjit Kar ,Manoranjan Maiti, A deteriorating multi-item inventory model with fuzzy costs and resources based on two different defuzzification techniques, Applied Mathematical Modelling 32 (2008) 208–223
2. Avishek Chakrabort, Sankar Prasad Mondal, Shariful Alam, Ali Ahmadian,m Norazak Senu Debashis De , and Soheil Salahshour The Pentagonal Fuzzy Number:Its Different Representations, Properties, Ranking, Defuzzification and Application in Game Problems, Symmetry, 11, 2019248;
3. Avishek Chakraborty, Suman Maity, Shalini Jain, Sankar Prasad Mondal,Shariful Alam, Hexagonal fuzzy number and its distinctive representation, ranking, defuzzification technique and application in production inventory management problem , Granular Computing 2020.
4. H.C.Chang ,Liang-Yuh, Ouyang,Chia-HueiHo, Integrated vendor–buyer cooperative inventory models with controllable lead time and ordering cost reduction,European journal of operations research,170 (2006) 481-495.
5. BK Dey, B Sarkar, M Sarkar, S Pareek An integrated inventory model involving discrete setup cost reduction, variable safety factor, selling price dependent demand, and investment, RAIRO-Operations Research, 53 (2019) 39–57.
6. Javad Sadeghi , Seyed Taghi Akhavan Niaki , Mohammad Reza Malekian , Yong Wang, A Lagrangian Relaxation for a Fuzzy Random EPQ Problem with Shortages and Redundancy Allocation: Two Tuned Metaheuristics ,International Journal of Fuzzy Systems: IF: 2.198.
7. Render, B. (1994). *Quantitative analysis for management*. USA: Pearson.
8. M.D.Roy & S.S Sana, Inter-dependent lead-time and ordering cost reduction strategy: a supply chain model with quality control, lead-time dependent backorder and price-sensitive stochastic demand, Opsearch, 58 (2021) 690–710 .
9. Sarkar, B., & Majumder, A Integrated vendor-buyer supply chain model with vendor's setup cost reduction, Applied Mathematics and Computation, 224, . (2013). 362–371.
10. A.Sutcu, M. Karaoz, and A.Erclu, "An EOQ model with price and time dependent demand under the influence of complement and substitute product's selling-prices". J. Alanya Fac. Bus.Alanya Isletme Fakultesi Dergisi 3 (2011) 21–32.
11. Taha, H. A. (1997). *Operations research*. Englewood Cliffs, NJ, USA: Prentice-Hall.
12. R. Uthayakumar & B. Malleeswaran, An integrated vendor–buyer supply chain model for backorder price discount and price-dependent demand using service level constraints and carbon emission cost, International Journal of Systems Science: Operations &Logistics,2020.
13. Uthayakumar, R., & Priyan, S. Permissible delay in payments in the two-echelon inventory system with controllable setup cost and lead time under service level constraint. International Journal of Information and Management Sciences, 24(3), (2013). 193–211.
14. Zadeh, L. A,Probability measures of fuzzy events. Journal of Mathematical Analysis and Applications, 23 (1968) 421–427.

Table.1 : Summary of Optimal Solution

M	L	C(L)	Q	$ITC(Q,m,L)$	$\tilde{Q}$	$IT\tilde{C}(\tilde{Q},m,L)$	Savings (%) Optimal order quantity	Savings (%) Integrated total cost%
2	3	57.4	62.663	6659.4	60.8365	5912.4	2.9	11.2
2	4	22.4	59.4286	6591.2	58.0122	5836.6	2.4	11.4
2	6	5.6	57.8449	6557.8	56.6352	5802.4	2.1	11.5
3	3	57.4	54.6206	6728.8	47.9223	6159.4	12.3	8.5
3	4	22.4	51.5383	6650.4	45.5127	6072.5	11.7	8.7
3	6	5.6	50.0231	6213.2	44.3342	6028.9	11.3	2.9
4	3	57.4	49.3105	6809.5	40.7155	6401.3	17.4	5.9
4	4	22.4	46.3918	6722.5	38.5795	6273.4	16.8	6.7
4	6	5.6	44.9536	6679.7	37.533	6242.2	16.5	6.5

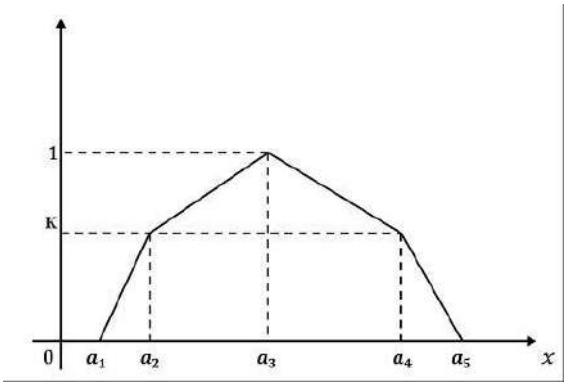

Figure.1. Linear PFN with symmetry

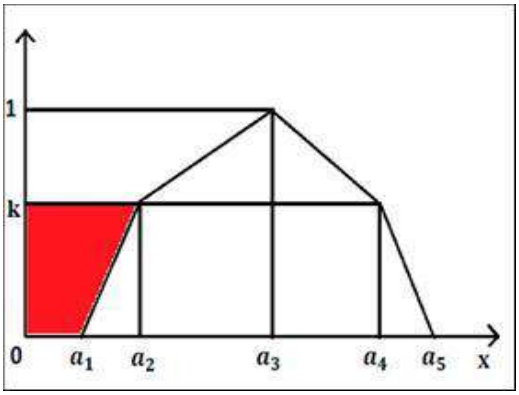

Figure.2.First step for the RA method

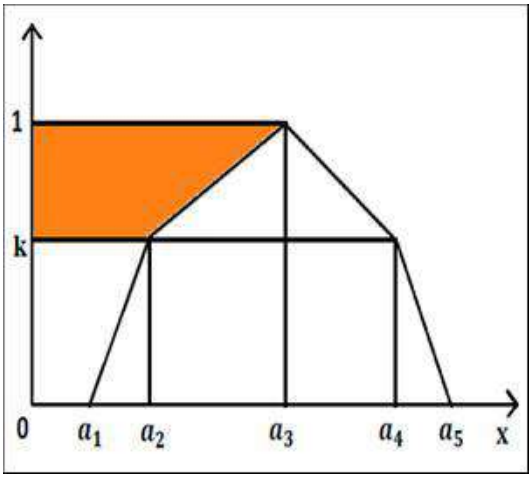

Figure 3.Second step for the RA method

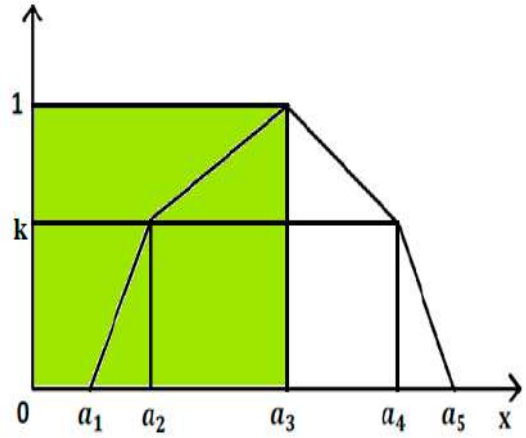

Figure 4.Third step for the RA method

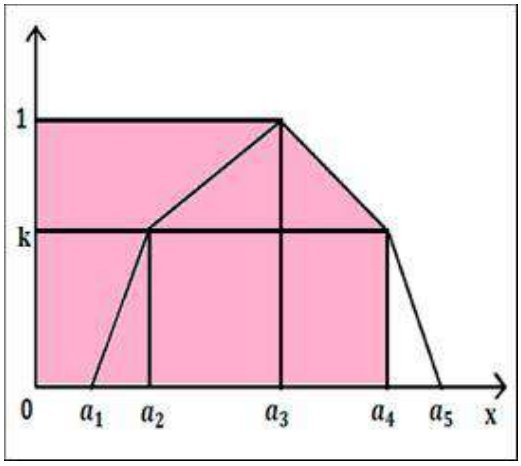

Figure 5: Fourth step for the RA method

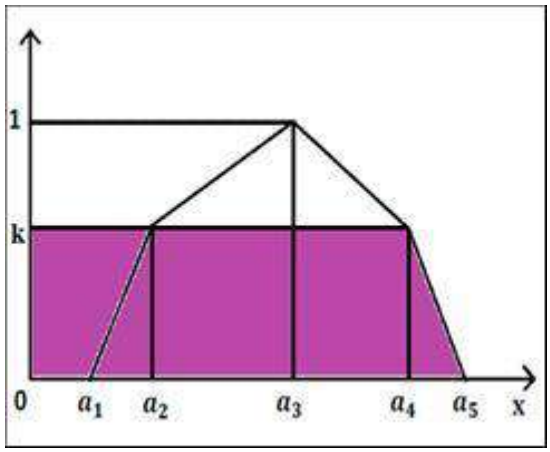

Figure 6. Fifth step for the RA method

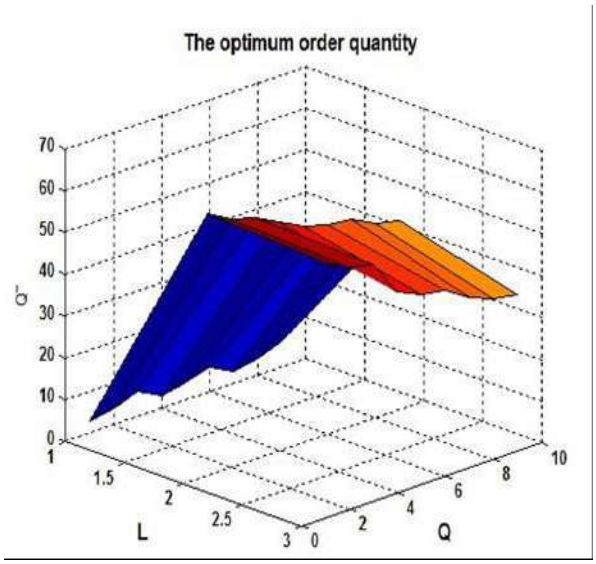

Figure 7: The Optimum order quantity

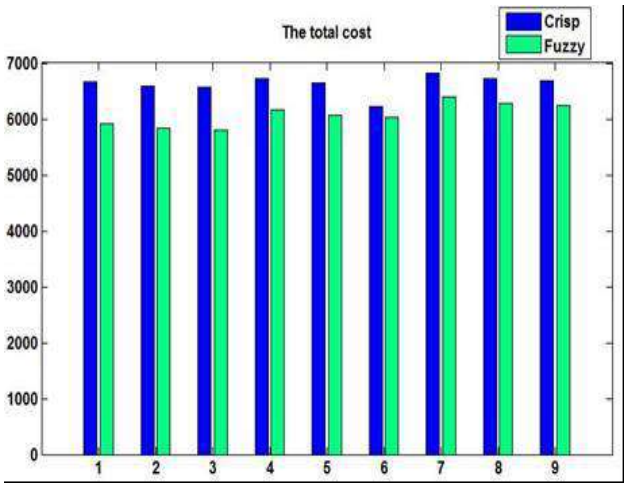

Figure.8.The total cost

RESEARCH ARTICLE

Cohesive Fuzzy Graph and its Properties

J. Jon Arockiaraj[1] and S. Sheelarani[2]*

[1]Vice Principal and HoD, Department of Mathematics, St. Joseph's College of Arts and Science (Autonomous), (Affiliated to Annamalai Unversity), Cuddalore, Tamil Nadu, India.
[2]Research Scholar, Department of Mathematics, St. Joseph's College of Arts and Science (Autonomous), (Affiliated to Annamalai Unversity), Cuddalore, Tamil Nadu, India

Received: 21 Nov 2024 Revised: 03 Dec 2024 Accepted: 02 Jan 2025

***Address for Correspondence**
Research Scholar, Department of Mathematics,
St. Joseph's College of Arts and Science (Autonomous),
(Affiliated to Annamalai Unversity),
Cuddalore, Tamil Nadu, India.
E.Mail: Mail: sheelalusy@gmail.com

ABSTRACT

A general representation of complex fuzzy graphs and hesitant fuzzy graphs is shown in a systematic manner in the current research under the new notion of cohesive fuzzy graph out of all the beneficial situations that are possible, this is the best alternating one since it has the most potential within the complex plane's expanded unit circle. A reasonable number of graphical examples are used for various concepts and some operations.

Keywords: Fuzzy graph**,** Hesitant fuzzy graph, Complex fuzzy graph, Cohesive fuzzy graph.

INTRODUCTION

A graph is simple model of relations. It shows connections between different data points, allowing people to visualize patterns and trends. They can be used in various fields like mathematics, computer science and economics to name just a few. The uses of graphs are incredibly diverse, ranging from tracking stock price movements to studying social networks. In fact, graphs are so versatile that they are essential tools in many disciplines. Whether you are student or professional, understanding graphs can greatly benefit you in analyzing data and making informed decisions. The concept behind the fuzzy graph are that can be extremely useful in various applications. The fuzzy graph is a generalization of classical graph theory, which allows for uncertainty and ambiguity to be captured in edges and vertices. Instead of precise connections between nodes, the edges in a fuzzy graph are assigned membership degrees to indicate the strength of the relationship. This enables a more flexible representation of relationships that are not strictly binary. Fuzzy graph ideas can be applied in areas like image processing, pattern recognition, and data mining. They offer a way to model complex relationships that may not have clear boundaries, making them particularly suitable for real-world problems where uncertainty is present. By incorporating fuzzy logic

into graph theory, researchers and practitioners can tackle problems that go beyond the limitations of traditional graph representations. One of the key advantages of fuzzy graphs is their ability to handle imprecise data and situations where the relationship between entities is not well-defined. This flexibility makes them a valuable tool in decision-making processes where uncertainty plays a significant role. Additionally, fuzzy graphs can be used to analyze social networks, biological systems, and other domains where traditional graph theory may fall short. Overall, fuzzy graphs provide a powerful framework for dealing with complexity and uncertainty in a wide range of applications. By embracing the idea of fuzzy relationships, researchers can gain new insights and perspectives that may not be accessible through traditional graph theory alone. Fuzzy set theory was first developed by A. Zadeh [1] in 1965. This technique is used to resolve the most effective decision-making method, offering the capacity to handle ambiguity in practical issues. The fuzzy set was expanded upon by K. Atanassov [2], who also introduced a new concept known as the "intuitionistic fuzzy set". In the recent times, many researchers proposed and extended the membership function's range to a unit disk, such as complex fuzzy set [4], After introducing the hesitant fuzzy set in 2020, Torra [3] and other researchers worked to extend the hesitant fuzzy set theory. The hesitation fuzzy graph was first presented by Pathinathan [8] in 2015.Karaaslan [9]has created a new type of hesitant fuzzy graph. Tamir et al [32] extended the fuzzy to the complex fuzzy graph (CFG). In 2019, Yagoob et al. [11] presented a complex intuitionistic fuzzy graph. Xue, M.Poonia [14], establish the theory of cohesive fuzzy set in 2023. Our main contributions are given as below: The new concept of cohesive fuzzy graph is introduced. The order, size and degree of the cohesive fuzzy graph is defined with the suitable graphical examples. The union, join, composition, complement operations of cohesive fuzzy graph with the some examples.

Advantages of our concept are given as follows:
A cohesive fuzzy graph with a phase component that specifically focuses within the group of advantageous circumstances for a specific uncertain problem with higher-dimensional that may have an extended range from the unit to the disk.
The advantage of the phase component is that it addresses periodic impreciseness.
The benefit of cohesive fuzzy graph is that it addresses more than just the circumstances in which we find it difficult to select the optimal option from a range of advantageous options. Among the many different scenarios, avoiding the unpleasant ones is also beneficial.

Cohesive fuzzy graph helps to solve both our time and energy.

Preliminary Concepts

Definition 2.1: [1] Let a non-empty set be S and a is the element in S. Then the FS $\mathbb{P}$ on S is the set of ordered pairs, $\mathbb{P} = \{< a, \lambda_{\mathbb{P}}(a) >: a \epsilon S\}$,Where $\lambda_{\mathbb{P}}(a): S \to [0,1]$ is a membership function.

Definition 2.2: [2]A fixed discourse S, let I be an IFS which is described by:
$I = \{<a, \lambda_I(a), \vartheta_I(a) > / a \in S\}$, Where $\lambda_I(a)$ is the membership degree, $\vartheta_I(a)$ is the non-membership degree of element a∈S in the [0,1]and I ⊆ S, and the condition that $0 \leq \lambda_I(a) + \vartheta_I(a) \leq 1$

Definition 2.3: [3]For a fixed set be X, an HFS function on X say h with respect to hesitant fuzzy element(shortly, HFE) which in fact returns a subset of [0,1] for X. For the easier understanding purpose, let us express the HFS in mathematically,$Z = \{<a, h_z(a) > / a \in X\}$;The term $h_z(a)$ is the membership degree of element a ∈X in [0,1].

Definition 2.4: [4] Let a universe be U, S be a CFSdescribed on Uwhich is distinguished by $\lambda_S(y)$, a membership function that assigns an element $y \in U$ to complex-valued grade of membership inS. According to the definition, $\lambda_S(y)$a complex valued function which is represented as $\gamma_S(y) exp^{i\Omega_S(y)}$ and is lies in the complex plane with the range of the circle with unit, where $i^2 = -1$, $\gamma_S(y)$ *and* $\Omega_S(y)$ are simultaneously real valued, $\gamma_S(y) \epsilon [0,1]$.The mathematical representation of CFS is:

$$S = \{(y, \lambda_S(y)) : y \in U\}$$

Definition 2.5: [5] Let Ube defined as a universe of discourse, aCIFSS added the membership function $\lambda_S(y)$ non-membership function $\Gamma_S(y)$ respectively to the CFS, which assigns any element $y \in U$. This element y is a complex-valued one which contains both the membership and non-membership values in S. According to the definition, it is defined previously that the values of $\lambda_S(y)$,$\Gamma_S(y)$and their sum always lie in the unit circle in the complex plane, and the complex membership $\lambda_S(y)$andnon-membership $\Gamma_S(y)$ are represented as $\gamma_S(y)exp^{i\Omega_{\lambda_S}(y)}$and $k_s(y)exp^{i\Omega_{\Gamma_S}(y)}$ respectively, where $i=\sqrt{-1}$, $\Omega_{\lambda_S}(y)$and $\Omega_{\Gamma_S}(y)$are simultaneously real-valued function. Further that,
Moreover,
$0 \le \gamma_S(y) \le 1, 0 \le k_s(y) \le 1, and\ \ 0 \le \gamma_S(y) + k_s(y) \le 1$
The CIFS is denoted by:

$$S = \{<y,\ \lambda_S(y) = x, \Gamma_S(y) = x^{'} >: y\ \in U\}, where$$
$$\lambda_S(y) = U \to \{x/x \in\ C, |x| \le 1\},$$
$$\Gamma_S(y) = U \to \{x^{'}/x^{'}\ \in\ C, |x^{'}| \le 1\},$$

and$|\ \lambda_S(y) + \Gamma_S(y)| \le 1$.

Definition 2.6: [12] Let a hesitant fuzzy graph be of the form $G = (V, E, \sigma, \lambda)$, where $\sigma: V \to S_f[0,1]$, and $\lambda: E \to S_f[0,1]$, is the collection of all finite subsets of [0,1], σ and λ are respectively the membership functions of the vertex set and edge set of the hesitant fuzzy graph.

Definition 2.7: [14] Let a fuzzy set be C that is defined on S, where S is fixed universal discourse;According to the function h, a cohesive fuzzy set on C, when applied on S that yields the result in a circle subset. That is,$S_1 = \{<y, h_C(a) >: a \in S\}$.Here$h_C$ is a complex valued set which is contained in the complex plane of circle with unit, meaning the membership degrees of elements $a \in\ S$ to C $\subset S$ andh_C is represented as $\gamma_C(a)exp^{i\Omega_C(a)}$, where $i=\sqrt{-1}$, $\gamma_C(a)$ and $\Omega_C(a)$ both are take real worth values and $\gamma_C(a) \in [0,1]$.

Example 2.8: [14] Thebasic representation of cohesive fuzzy set, let $P = \{y_1, y_2, y_3\}$ be the reference set. Suppose

$$h_{C_1}(a_1) = \left\{0.5\exp\pi, 0.8\exp\frac{\pi}{2}, 0.7\exp\frac{\pi}{2}\right\},$$
$$h_{C_2}(b_2) = \left\{0.6\exp\pi, 0.9\exp\pi, 0.7\exp\frac{\pi}{4}\right\},$$
$$h_{C_3}(c_3) = \left\{0.5\exp\pi, 0.7\exp\frac{\pi}{2}, 0.7\exp\pi\right\}$$

arethe membership set of $y_k (1 \le k \le 3)$ to the set C. Then, itscohesive fuzzy set can be written as

$$C = \left\{< y_1, \left\{0.5\exp\pi, 0.8\exp\frac{\pi}{2}, 0.7\exp\frac{\pi}{2}\right\} >, < y_2, \left\{0.6\exp\pi, 0.9\exp\pi, 0.7\exp\frac{\pi}{4}\right\} >, < y_3, \left\{0.5\exp\pi, 0.8\exp\frac{\pi}{2}, 0.7\exp\pi\right\}\right\}.$$

Cohesive Fuzzy Graph

Definition 3.1: Let an underlying set be U. A Cohesive fuzzy graph with U is an ordered pair $G = (\mathbb{P}, \mathbb{Q})$ where,$\mathbb{P} = (\lambda_{\mathbb{P}} e^{i\alpha_{\mathbb{P}}}, \gamma_{\mathbb{P}} e^{i\beta_{\mathbb{P}}}, \delta_{\mathbb{P}} e^{i\vartheta_{\mathbb{P}}})$ is a CHFS on a vertex set V and $\mathbb{Q} = (\lambda_{\mathbb{Q}} e^{i\alpha_{\mathbb{Q}}}, \gamma_{\mathbb{Q}} e^{i\beta_{\mathbb{Q}}}, \delta_{\mathbb{Q}} e^{i\vartheta_{\mathbb{Q}}}$

is a CHFS on edge set Ewith $\mathbb{P}: V \to D_u\{\chi \in C: |\chi| \le 1\}$ and $\mathbb{Q}: E \to D_u\{\chi \in C: |\chi| \le 1\}$, where $D_u\{\chi \in C: |\chi| \le 1\}$ is the set of all the unit disc's finite subsets, such that

$\lambda_{\mathbb{Q}}(ab)e^{i\alpha_{\mathbb{Q}}(ab)} \le \min\{\lambda_{\mathbb{P}}(a), \lambda_{\mathbb{P}}(b))\}e^{i\ min\{\alpha_{\mathbb{P}}(a), \alpha_{\mathbb{P}}(b)\}}$

$\gamma_{\mathbb{Q}}(ab)e^{i\beta_{\mathbb{Q}}(ab)} \le \min\{\gamma_{\mathbb{P}}(a), \gamma_{\mathbb{P}}(b)\}e^{i\ min\{\beta_{\mathbb{P}}(a), \beta_{\mathbb{P}}(b)\}}$

$\delta_{\mathbb{Q}}(ab)e^{i\Omega_{\mathbb{Q}}(ab)} \le \min\{\delta_{\mathbb{P}}(a), \delta_{\mathbb{P}}(b)\}e^{i\ min\{\Omega_{\mathbb{P}}(a), \Omega_{\mathbb{P}}(b)\}}$

For all a, b $\in \mathbb{P}$.

Definition 3.2: Let $\mathbb{P} = \{(a, \lambda_{\mathbb{P}}(a)e^{i\alpha_{\mathbb{P}}}, \gamma_{\mathbb{P}}(a)e^{i\beta_{\mathbb{P}}}, \delta_{\mathbb{P}}(a)e^{i\Omega_{\mathbb{P}}}) : a \in \mathbb{P}\}$ and $\mathbb{Q} = \{(ab, \lambda_{\mathbb{Q}}(ab)e^{i\alpha_{\mathbb{Q}}(ab)}, \gamma_{\mathbb{Q}}(ab)e^{i\beta_{\mathbb{Q}}(ab)}, \delta_{\mathbb{Q}}(ab)e^{i\Omega_{\mathbb{Q}}(ab)}) : ab \in \mathbb{Q}\}$ be a Cohesive fuzzy graph. Then it's order is describedby,

$O(G) = (O\lambda e^{i\alpha}, O\gamma e^{i\beta}, O\delta e^{i\Omega})$, where
$O(\lambda e^{i\alpha}) = \sum_{a_i \in V} \lambda_{\mathbb{P}}(a_i) e^{i \sum_{a_i \in V} \alpha_{\mathbb{P}}(a_i)}$
$O(\gamma e^{i\beta}) = \sum_{a_i \in V} \gamma_{\mathbb{P}}(a_i) e^{i \sum_{a_i \in V} \beta_{\mathbb{P}}(a_i)}$
$O(\delta e^{i\Omega}) = \sum_{a_i \in V} \delta_{\mathbb{P}}(a_i) e^{i \sum_{a_i \in V} \Omega_{\mathbb{P}}(a_i)}$

Definition 3.3: Let $\mathbb{P} = \{(a, \lambda_{\mathbb{P}}(a)e^{i\alpha_{\mathbb{P}}}, \gamma_{\mathbb{P}}(a)e^{i\beta_{\mathbb{P}}}, \delta_{\mathbb{P}}(a)e^{i\Omega_{\mathbb{P}}}) : a \in \mathbb{P}\}$ and $\mathbb{Q} = \{(ab, \lambda_{\mathbb{Q}}(ab)e^{i\alpha_{\mathbb{Q}}(ab)}, \gamma_{\mathbb{Q}}(ab)e^{i\beta_{\mathbb{Q}}(ab)}, \delta_{\mathbb{Q}}(ab)e^{i\Omega_{\mathbb{Q}}(ab)}) : ab \in \mathbb{Q}\}$ be a Cohesive fuzzy graph. Then its size is describedby,

$S(G) = (S\lambda e^{i\alpha}, S\gamma e^{i\beta}, S\delta e^{i\Omega})$, where
$S(\lambda e^{i\alpha}) = \sum_{a_i \neq b_i} \lambda_{\mathbb{Q}}(a_i b_i) e^{i \sum_{a_i \neq b_i} \alpha_{\mathbb{Q}}(a_i b_i)}$
$S(\gamma e^{i\beta}) = \sum_{a_i \neq b_i} \gamma_{\mathbb{Q}}(a_i b_i) e^{i \sum_{a_i \neq b_i} \beta_{\mathbb{Q}}(a_i b_i)}$
$S(\delta e^{i\Omega}) = \sum_{a_i \neq b_i} \delta_{\mathbb{Q}}(a_i b_i) e^{i \sum_{a_i \neq b_i} \Omega_{\mathbb{Q}}(a_i b_i)}$

Example 3.4: Consider a graph $G = (\mathbb{P}, \mathbb{Q})$ such that $\mathbb{P} = \{v_1, v_2, v_3\}$ and $\mathbb{Q} = \{v_1v_2, v_2v_3\}$, where $\mathbb{P}$ is a cohesive fuzzy subset of V and $\mathbb{Q}$ is a cohesive fuzzy subset of $E \subseteq V \times V$. The following can be observed that the graph shown in figure 1 as a cohesive fuzzy graph.
(i) Order of cohesive fuzzy graph $O(G) = \left(1.6e^{i3\pi}, 2.4e^{i2\pi}, 2.2e^{i1.8\pi}\right)$
(ii) Size of cohesive fuzzy graph $S(G) = \left(1.1e^{i3\pi}, 1.9e^{i\frac{3}{2}\pi}, 2.0e^{i\pi}\right)$

Definition 3.5: Let $\mathbb{P} = \{(a, \lambda_{\mathbb{P}}(a)e^{i\alpha_{\mathbb{P}}}, \gamma_{\mathbb{P}}(a)e^{i\beta_{\mathbb{P}}}, \delta_{\mathbb{P}}(a)e^{i\Omega_{\mathbb{P}}}) : a \in \mathbb{P}\}$ and $\mathbb{Q} = \{(ab, \lambda_{\mathbb{Q}}(ab)e^{i\alpha_{\mathbb{Q}}(ab)}, \gamma_{\mathbb{Q}}(ab)e^{i\beta_{\mathbb{Q}}(ab)}, \delta_{\mathbb{Q}}(ab)e^{i\Omega_{\mathbb{Q}}(ab)}) : ab \in \mathbb{Q}\}$ be a cohesive fuzzy graph. Then the degree of a vertex $a \in \mathbb{P}$ in a cohesive fuzzy graph G is defined by,
$deg_G(a) = \left(deg\ \lambda e^{i\alpha}(a), deg\ \gamma e^{i\alpha}(a), deg\ \delta e^{i\alpha}(a)\right)$, where

$$deg\ \lambda e^{i\alpha}(a) = \sum_{a \neq b} \lambda_{\mathbb{Q}}(ab) e^{i \sum_{a \neq b} \alpha_{\mathbb{Q}}(ab)}$$

$$deg\ \gamma e^{i\alpha}(a) = \sum_{a \neq b} \gamma_{\mathbb{Q}}(ab) e^{i \sum_{a \neq b} \beta_{\mathbb{Q}}(ab)}$$

$$deg\ \delta e^{i\alpha}(a) = \sum_{a \neq b} \delta_{\mathbb{Q}}(ab) e^{i \sum_{a \neq b} \Omega_{\mathbb{Q}}(ab)}$$

Definition 3.6: Let G = $(\mathbb{P}, \mathbb{Q})$ be a cohesive fuzzy graph. Then the total degree of thevertex a ∈ P in G is defined by
$td_G(a) = \left(td\ \lambda e^{i\alpha}(a), td\ \gamma e^{i\beta}(a), td\ \delta e^{i\Omega}(a)\right)$, where
$td\ \lambda e^{i\alpha}(a) = \sum_{a \neq b} \lambda_{\mathbb{Q}}(ab) e^{i \sum_{a \neq b} \alpha_{\mathbb{Q}}(ab)} + \lambda_{\mathbb{P}}(a)\ e^{i\alpha_{\mathbb{P}}(a)}$
$td\ \gamma e^{i\beta}(a) = \sum_{a \neq b} \gamma_{\mathbb{Q}}(ab) e^{i \sum_{a \neq b} \beta_{\mathbb{Q}}(ab)} + \gamma_{\mathbb{P}}(a)\ e^{i\beta_{\mathbb{P}}(a)}$
$td\ \delta e^{i\Omega}(a) = \sum_{a \neq b} \delta_{\mathbb{Q}}(ab) e^{i \sum_{a \neq b} \Omega_{\mathbb{Q}}(ab)} + \delta_{\mathbb{P}}(a)\ e^{i\Omega_{\mathbb{P}}(a)}$

Example 3.7: Consider a graph $G = (\mathbb{P}, \mathbb{Q})$ such that $\mathbb{P} = \{v_1, v_2, v_3, v_4\}$ and $\mathbb{Q} = \{v_1v_2, v_2v_3,\ v_3v_4, v_4v_1\}$. The following can be observed that the graph shown in figure 2 as a cohesive fuzzy graph.
$(i) d_G(v_1) = (0.3e^{i\frac{4}{3}\pi}, 0.5e^{i\pi}, 0.6e^{i\frac{1}{2}\pi})$,
Similarly, $d_G(v_2) = (0.5e^{i\frac{1}{2}\pi}, 0.2e^{i\pi}, 0.5e^{i\frac{1}{3}\pi})$,

$d_G(v_3)=\left(0.4e^{i\frac{1}{3}\pi}, 0.3e^{i\pi}, 0.5e^{i\frac{1}{3}\pi}\right)$,

$d_G(v_4)=\left(0.2e^{i\frac{7}{6}\pi}, 0.6e^{i\pi}, 0.6e^{i\frac{1}{2}\pi}\right)$,

(ii) $td_G(v_1)=\left(td\ \lambda e^{i\alpha}(v_1), td\ \gamma e^{i\beta}(v_1), td\ \delta e^{i\Omega}(v_1)\right)$,

$td\ \lambda e^{i\alpha}(v_1)=d_G(v_1)+\lambda_{\mathbb{P}}(a)e^{i\alpha_{\mathbb{P}}(a)}=0.3e^{i\frac{4}{3}\pi}+0.3e^{i\pi}$ in (i),$d_G(v_1)$ take the first term, $td\ \lambda e^{i\alpha}(v_1)=0.6e^{i\frac{7}{4}\pi}$,

Similarly, $td\ \gamma e^{i\beta}(v_1)=0.5e^{i\pi}+0.4e^{i\frac{1}{2}\pi}=0.9e^{i\frac{3}{2}\pi}$,

$td\ \delta e^{i\Omega}(v_1)=0.6e^{i\frac{1}{3}\pi}+0.5e^{i\frac{1}{6}\pi}=1.1e^{i\frac{1}{2}\pi}$

Therefore $td_G(v_1)=(0.6e^{i\frac{7}{4}\pi}, 0.9e^{i\frac{3}{2}\pi}, 1.1e^{i\frac{1}{2}\pi})$

Properties of Cohesive Fuzzy Graph

Definition 4.1: Union of the two cohesive fuzzy graphs

The union$G_1 \cup G_2=(\mathbb{P}_1 \cup \mathbb{P}_2, \mathbb{Q}_1 \cup \mathbb{Q}_2)$ of the two cohesive fuzzy graph is defined as follows:

$$\lambda_{\mathbb{P}_1\cup\mathbb{P}_2}(a)e^{i\alpha_{(\mathbb{P}_1\cup\mathbb{P}_2)}(a)}=\begin{cases}\lambda_{\mathbb{P}_1}(a)e^{i\alpha_{\mathbb{P}_1}(a)}, & if\ a\in\mathbb{P}_1-\mathbb{P}_2\\ \lambda_{\mathbb{P}_2}(a)e^{i\alpha_{\mathbb{P}_2}(a)}, & if\ a\in\mathbb{P}_2-\mathbb{P}_1\\ \max\{\lambda_{\mathbb{P}_1}(a),\lambda_{\mathbb{P}_2}(a)\}e^{i\max\{\alpha_{\mathbb{P}_1}(a),\alpha_{\mathbb{P}_2}(a)\}}, & if\ a\in\mathbb{P}_1\cap\mathbb{P}_2\end{cases}$$

$$\gamma_{\mathbb{P}_1\cup\mathbb{P}_2}(a)e^{i\beta_{(\mathbb{P}_1\cup\mathbb{P}_2)}(a)}=\begin{cases}\gamma_{\mathbb{P}_1}(a)e^{i\beta_{\mathbb{P}_1}(a)}, & if\ a\in\mathbb{P}_1-\mathbb{P}_2\\ \gamma_{\mathbb{P}_2}(a)e^{i\beta_{\mathbb{P}_2}(a)}, & if\ a\in\mathbb{P}_2-\mathbb{P}_1\\ \max\{\gamma_{\mathbb{P}_1}(a),\gamma_{\mathbb{P}_2}(a)\}e^{i\max\{\beta_{\mathbb{P}_1}(a),\beta_{\mathbb{P}_2}(a)\}}, & if\ a\in\mathbb{P}_1\cap\mathbb{P}_2\end{cases}$$

$$\delta_{\mathbb{P}_1\cup\mathbb{P}_2}(a)e^{i\Omega_{(\mathbb{P}_1\cup\mathbb{P}_2)}(a)}=\begin{cases}\delta_{\mathbb{P}_1}(a)e^{i\Omega_{\mathbb{P}_1}(a)}, & if\ a\in\mathbb{P}_1-\mathbb{P}_2\\ \delta_{\mathbb{P}_2}(a)e^{i\Omega_{\mathbb{P}_2}(a)}, & if\ a\in\mathbb{P}_2-\mathbb{P}_1\\ \max\{\delta_{\mathbb{P}_1}(a),\delta_{\mathbb{P}_2}(a)\}e^{i\max\{\Omega_{\mathbb{P}_1}(a),\Omega_{\mathbb{P}_2}(a)\}}, & if\ a\in\mathbb{P}_1\cap\mathbb{P}_2\end{cases}$$

$$\lambda_{\mathbb{Q}_1\cup\mathbb{Q}_2}(ab)e^{i\alpha_{(\mathbb{Q}_1\cup\mathbb{Q}_2)}(ab)}=\begin{cases}\lambda_{\mathbb{Q}_1}(ab)e^{i\alpha_{\mathbb{Q}_1}(a)}, & if\ ab\in\mathbb{Q}_1-\mathbb{Q}_2\\ \lambda_{\mathbb{Q}_2}(ab)e^{i\alpha_{\mathbb{Q}_2}(a)}, & if\ ab\in\mathbb{Q}_2-\mathbb{Q}_1\\ \max\{\lambda_{\mathbb{Q}_1}(ab),\lambda_{\mathbb{Q}_2}(ab)\}e^{i\max\{\alpha_{\mathbb{Q}_1}(ab),\alpha_{\mathbb{Q}_2}(ab)\}}, & if\ ab\in\mathbb{Q}_1\cap\mathbb{Q}_2\end{cases}$$

$$\gamma_{\mathbb{Q}_1\cup\mathbb{Q}_2}(ab)e^{i\beta_{(\mathbb{Q}_1\cup\mathbb{Q}_2)}(ab)}=\begin{cases}\gamma_{\mathbb{Q}_1}(ab)e^{i\beta_{\mathbb{Q}_1}(ab)}, & if\ ab\in\mathbb{Q}_1-\mathbb{Q}_2\\ \gamma_{\mathbb{Q}_2}(ab)e^{i\beta_{\mathbb{Q}_2}(ab)}, & if\ ab\in\mathbb{Q}_2-\mathbb{Q}_1\\ \max\{\gamma_{\mathbb{Q}_1}(ab),\gamma_{\mathbb{Q}_2}(ab)\}e^{i\max\{\beta_{\mathbb{Q}_1}(ab),\beta_{\mathbb{Q}_2}(ab)\}}, & if\ ab\in\mathbb{Q}_1\cap\mathbb{Q}_2\end{cases}$$

$$\delta_{\mathbb{Q}_1\cup\mathbb{Q}_2}(ab)e^{i\Omega_{(\mathbb{Q}_1\cup\mathbb{Q}_2)}(ab)}=\begin{cases}\delta_{\mathbb{Q}_1}(ab)e^{i\Omega_{\mathbb{Q}_1}(ab)}, & if\ ab\in\mathbb{Q}_1-\mathbb{Q}_2\\ \delta_{\mathbb{Q}_2}(ab)e^{i\Omega_{\mathbb{Q}_2}(ab)}, & if\ ab\in\mathbb{Q}_2-\mathbb{Q}_1\\ \max\{\delta_{\mathbb{Q}_1}(ab),\delta_{\mathbb{Q}_2}(ab)\}e^{i\max\{\Omega_{\mathbb{Q}_1}(ab),\Omega_{\mathbb{Q}_2}(ab)\}}, & if\ ab\in\mathbb{Q}_1\cap\mathbb{Q}_2\end{cases}$$

Example 4. Let $G_1=(\mathbb{P}_1,\mathbb{Q}_1)$ and $G_2=(\mathbb{P}_2,\mathbb{Q}_2))$ be two CHFGs where $\mathbb{P}_1=\{v_1,v_2,v_3\}$ and $\mathbb{P}_2=\{v_1,v_3,v_4,v_5\}$ as shown in figures3,4 & 5.

Proposition 4.3: Let $G_1=(\mathbb{P}_1,\mathbb{Q}_1)$ and $G_2=(\mathbb{P}_2,\mathbb{Q}_2))$ be two cohesive fuzzy graphs. Then its union resultant is again a cohesive fuzzy graph.

Definition 4.4: Join two cohesive fuzzy graphs

Let a two cohesive fuzzy graphs be $G_1 = (\mathbb{P}_1, \mathbb{Q}_1)andG_2 = (\mathbb{P}_2, \mathbb{Q}_2)$. Then its join $G_1 + G_2 = (\mathbb{P}_1 + \mathbb{P}_2, \mathbb{Q}_1 + \mathbb{Q}_2)$ is defined as follows:

$$(i)\quad \lambda_{\mathbb{P}_1+\mathbb{P}_2}(a)e^{i\alpha_{\mathbb{P}_1+\mathbb{P}_2}(a)} = \lambda_{\mathbb{P}_1\cup\mathbb{P}_2}(a)e^{i\alpha_{\mathbb{P}_1\cup\mathbb{P}_2}(a)}$$
$$\gamma_{\mathbb{P}_1+\mathbb{P}_2}(a)e^{i\beta_{\mathbb{P}_1+\mathbb{P}_2}(a)} = \gamma_{\mathbb{P}_1\cup\mathbb{P}_2}(a)e^{i\beta_{\mathbb{P}_1\cup\mathbb{P}_2}(a)}$$
$$\delta_{\mathbb{P}_1+\mathbb{P}_2}(a)e^{i\Omega_{\mathbb{P}_1+\mathbb{P}_2}(a)} = \delta_{\mathbb{P}_1\cup\mathbb{P}_2}(a)e^{i\Omega_{\mathbb{P}_1\cup\mathbb{P}_2}(a)},$$
$$if\ a \in \mathbb{P}_1 \cup \mathbb{P}_2$$

$$(ii)\quad \lambda_{\mathbb{Q}_1+\mathbb{Q}_2}(ab)e^{i\alpha_{\mathbb{Q}_1+\mathbb{Q}_2}(ab)} = \lambda_{\mathbb{Q}_1\cup\mathbb{Q}_2}(ab)e^{i\alpha_{\mathbb{Q}_1\cup\mathbb{Q}_2}(ab)}$$
$$\gamma_{\mathbb{Q}_1+\mathbb{Q}_2}(ab)e^{i\beta_{\mathbb{Q}_1+\mathbb{Q}_2}(ab)} = \gamma_{\mathbb{Q}_1\cup\mathbb{Q}_2}(ab)e^{i\beta_{\mathbb{Q}_1\cup\mathbb{Q}_2}(ab)}$$
$$\delta_{\mathbb{Q}_1+\mathbb{Q}_2}(ab)e^{i\Omega_{\mathbb{Q}_1+\mathbb{Q}_2}(ab)} = \delta_{\mathbb{Q}_1\cup\mathbb{Q}_2}(ab)e^{i\Omega_{\mathbb{Q}_1\cup\mathbb{Q}_2}(ab)},$$
$$if\ ab \in \mathbb{Q}_1 \cup \mathbb{Q}_2$$

$$(iii)\quad \lambda_{\mathbb{Q}_1+\mathbb{Q}_2}(ab)e^{i\alpha_{\mathbb{Q}_1+\mathbb{Q}_2}(ab)} = \min\{\lambda_{\mathbb{P}_1}(a), \lambda_{\mathbb{P}_2}(b)\}e^{i\min\{\alpha_{\mathbb{P}_1}(a),\, \alpha_{\mathbb{P}_2}(b)\}}$$
$$\gamma_{\mathbb{Q}_1+\mathbb{Q}_2}(ab)e^{i\beta_{\mathbb{Q}_1+\mathbb{Q}_2}(ab)} = \min\{\gamma_{\mathbb{P}_1}(a),\ \gamma_{\mathbb{P}_2}(b)\}e^{i\min\{\beta_{\mathbb{P}_1}(a),\beta_{\mathbb{P}_2}(b)\}}$$
$$\delta_{\mathbb{Q}_1+\mathbb{Q}_2}(ab)e^{i\beta_{\mathbb{Q}_1+\mathbb{Q}_2}(ab)} = \min\{\delta_{\mathbb{P}_1}(a), \delta_{\mathbb{P}_2}(b)\}e^{i\min\{\Omega_{\mathbb{P}_1}(a),\, \Omega_{\mathbb{P}_2}(b)\}}, if\ ab \in \mathbb{Q}',$$

Where$\mathbb{Q}'$ is the set of all edges joining the vertices of$\mathbb{P}_1$&$\mathbb{P}_2$, $\mathbb{P}_1 \cap \mathbb{P}_2 = \emptyset$.

Example 4.5: Let $G_1 = (\mathbb{P}_1, \mathbb{Q}_1)$ and $G_2 = (\mathbb{P}_2, \mathbb{Q}_2)$ be two cohesive fuzzy graphs where $\mathbb{P}_1 = \{v_1, v_2\}$ and $\mathbb{P}_2 = \{w_1, w_2, w_3\}$ as shown figures 6 &7.

Proposition 4.6: Let $G_1 = (\mathbb{P}_1, \mathbb{Q}_1)$ and $G_2 = (\mathbb{P}_2, \mathbb{Q}_2))$ be two cohesive fuzzy graphs. Then its join is again a cohesive fuzzy graph.

Definition 4.7:Composition of two cohesive fuzzy graphs

TheComposition $G_1 \circ G_2$ of two cohesive fuzzy graph is expressed as a pair, $G_1 \circ G_2 = (\mathbb{P}_1 \circ \mathbb{P}_2, \mathbb{Q}_1 \circ \mathbb{Q}_2)$ such that,

$$\gamma_{\mathbb{P}_1\circ\mathbb{P}_2}(a_1, a_2)e^{i\beta_{\mathbb{P}_1\circ\mathbb{P}_2}(a_1,a_2)} = \min\{\gamma_{\mathbb{P}_1}(a_1),\ \gamma_{\mathbb{P}_2}(a_2)\}e^{i\min\{\beta_{\mathbb{P}_1}(a_1),\, \beta_{\mathbb{P}_2}(a_2)\}}$$
$$\delta_{\mathbb{P}_1\circ\mathbb{P}_2}(a_1, a_2)e^{i\Omega_{\mathbb{P}_1\circ\mathbb{P}_2}(a_1,a_2)} = \min\{\delta_{\mathbb{P}_1}(a_1),\ \delta_{\mathbb{P}_2}(a_2)\}e^{i\min\{\Omega_{\mathbb{P}_1}(a_1),\, \Omega_{\mathbb{P}_2}(a_2)\}}$$
$$for\ all\ a_1, a_2 \in \mathbb{P}$$

$$(ii)\ \lambda_{\mathbb{Q}_1\circ\mathbb{Q}_2}((c, a_2)(c, b_2))e^{i\alpha_{\mathbb{Q}_1\circ\mathbb{Q}_2}((c,a_2)(c,b_2))} = \min\{\lambda_{\mathbb{P}_1}(c), \lambda_{\mathbb{Q}_2}(a_2b_2)\}e^{i\min\{\alpha_{\mathbb{P}_1}(c),\alpha_{\mathbb{Q}_2}(a_2b_2)\}}$$
$$\gamma_{\mathbb{Q}_1\circ\mathbb{Q}_2}((c, a_2)(c, b_2))e^{i\beta_{\mathbb{Q}_1\circ\mathbb{Q}_2}((c,a_2)(c,b_2))} = \min\{\gamma_{\mathbb{P}_1}(c),\ \gamma_{\mathbb{Q}_2}(a_2b_2)\}e^{i\min\{\beta_{\mathbb{P}_1}(c),\beta_{\mathbb{Q}_2}(a_2b_2)\}}$$
$$\delta_{\mathbb{Q}_1\circ\mathbb{Q}_2}((c, a_2)(c, b_2))e^{i\Omega_{\mathbb{Q}_1\circ\mathbb{Q}_2}((c,a_2)(c,b_2))} = \min\{\delta_{\mathbb{P}_1}(c), \gamma_{\mathbb{Q}_2}(a_2b_2)\}e^{i\min\{\Omega_{\mathbb{P}_1}(c),\Omega_{\mathbb{Q}_2}(a_2b_2)\}}$$
$$for\ alla \in \mathbb{P}_1, a_2b_2 \in \mathbb{Q}_2$$

$$(iii)\ \lambda_{\mathbb{Q}_1\circ\mathbb{Q}_2}((a_1, d)(b_1, d))e^{i\alpha_{\mathbb{Q}_1\circ\mathbb{Q}_2}((a_1,d)(b_1,d))} = \min\{\lambda_{\mathbb{Q}_1}(a_1b_1), \lambda_{\mathbb{P}_2}(d)\}e^{i\min\{\alpha_{\mathbb{Q}_1}(a_1b_1),\alpha_{\mathbb{P}_2}(d)\}}$$
$$\gamma_{\mathbb{Q}_1\circ\mathbb{Q}_2}((a_1, d)(b_1, d))e^{i\beta_{\mathbb{Q}_1\circ\mathbb{Q}_2}((a_1,d)(b_1,d))} = \min\{\gamma_{\mathbb{Q}_1}(a_1b_1),\ \gamma_{\mathbb{P}_2}(d)\}e^{i\min\{\beta_{\mathbb{Q}_1}(a_1b_1),\beta_{\mathbb{P}_2}(d)\}}$$
$$\delta_{\mathbb{Q}_1\circ\mathbb{Q}_2}((a_1, d)(b_1, d))e^{i\Omega_{\mathbb{Q}_1\circ\mathbb{Q}_2}((a_1,d)(b_1,d))} = \min\{\delta_{\mathbb{Q}_1}(a_1b_1), \delta_{\mathbb{P}_2}(d)\}e^{i\min\{\Omega_{\mathbb{Q}_1}(a_1b_1),\Omega_{\mathbb{P}_2}(d)\}}$$
$$for\ alld \in \mathbb{P}_2, a_1b_1 \in \mathbb{Q}_1$$

$$(iv)\ \lambda_{\mathbb{Q}_1\circ\mathbb{Q}_2}((a_1,a_2)(b_1,b_2))e^{i\alpha_{\mathbb{Q}_1\circ\mathbb{Q}_2}((a_1,a_2)(b_1,b_2))}$$
$$= min\{\lambda_{\mathbb{P}_2}(a_2), \lambda_{\mathbb{P}_2}(b_2), \lambda_{B_1}(a_1b_1)\}e^{i\min\{\alpha_{\mathbb{P}_2}(a_2),\, \alpha_{\mathbb{P}_2}(b_2),\, \alpha_{\mathbb{Q}_1}(a_1,b_1)\}}$$
$$\gamma_{\mathbb{Q}_1\circ\mathbb{Q}_2}((a_1,a_2)(b_1,b_2))e^{i\beta_{\mathbb{Q}_1\circ\mathbb{Q}_2}((a_1,a_2)(b_1,b_2))} = \min\{\gamma_{\mathbb{P}_2}(a_2),\ \gamma_{\mathbb{P}_2}(b_2),\ \gamma_{\mathbb{Q}_1}(a_1b_1)\}e^{i\min\{\beta_{\mathbb{P}_2}(a_2),\, \beta_{\mathbb{P}_2}(b_2),\, \beta_{\mathbb{Q}_1}(a_1,b_1)\}}$$
$$\delta_{\mathbb{Q}_1\circ\mathbb{Q}_2}((a_1,a_2)(b_1,b_2))e^{i\omega_{\mathbb{Q}_1\circ\mathbb{Q}_2}((a_1,a_2)(b_1,b_2))} = \min\{\delta_{\mathbb{P}_2}(a_2),\ \delta_{\mathbb{P}_2}(b_2),\ \delta_{\mathbb{Q}_1}(a_1b_1)\}e^{i\min\{\Omega_{\mathbb{P}_2}(a_2),\Omega_{\mathbb{P}_2}(b_2),\Omega_{\mathbb{Q}_1}(a_1,b_1)\}}$$
$$for\ alla_1b_1 \in \mathbb{Q}_1, a_2, b_2 \in \mathbb{P}_2, a_2 \neq b_2$$

Example 4.8: Let $G_1 = (\mathbb{P}_1, \mathbb{Q}_1)$ and $G_2 = (\mathbb{P}_2, \mathbb{Q}_2)$ be two cohesive fuzzy graphswhere $\mathbb{P}_1 = \{v_1, v_2\}$ and $\mathbb{P}_2 = \{w_1, w_2\}$ as shown in figures 8 & 9.

Proposition 4.9: Let $G_1 = (\mathbb{P}_1, \mathbb{Q}_1)$ and $G_2 = (\mathbb{P}_2, \mathbb{Q}_2))$ be two cohesive fuzzy graphs.Then its composition is again a cohesive fuzzy graph.

Definition 4.10: Complement of cohesive fuzzy graph

The Complement of cohesive fuzzy graph $G = (\mathbb{P}, \mathbb{Q})$is denoted by$\overline{G} = \left(\overline{\mathbb{P}}, \overline{\mathbb{Q}}\right)$ is defined by,

(i) $\overline{\mathbb{P}} = \mathbb{P}$,

(ii) $\lambda_{\overline{\mathbb{P}}}(a)e^{i\alpha_{\overline{\mathbb{P}}}(a)} = \lambda_{\mathbb{P}}(a)e^{i\alpha_{\mathbb{P}}(a)}$

$\gamma_{\overline{\mathbb{P}}}(a)e^{i\beta_{\overline{\mathbb{P}}}(a)} = \gamma_{\mathbb{P}}(a)e^{i\beta_{\mathbb{P}}(a)}$

$\delta_{\overline{\mathbb{P}}}(a)e^{i\Omega_{\overline{\mathbb{P}}}(a)} = \delta_{\mathbb{P}}(a)e^{i\Omega_{\mathbb{P}}(a)}$,if$a \in \mathbb{P}$,

(iii)

$$\lambda_{\overline{\mathbb{Q}}}(ab)e^{i\alpha_{\overline{\mathbb{Q}}}(ab)} = \begin{cases} 0 & if\ \lambda_B(ab)e^{i\alpha_{\mathbb{Q}}(ab)} \neq 0 \\ \min\{\lambda_{\mathbb{P}}(a), \lambda_{\mathbb{P}}(b)\}e^{i\min\{\alpha_{\mathbb{P}}(a),\, \alpha_{\mathbb{P}}(b)\}} & if\ \lambda_{\mathbb{Q}}(ab)e^{i\alpha_{\mathbb{Q}}(ab)} = 0 \end{cases}$$

$$\gamma_{\overline{\mathbb{Q}}}(ab)e^{i\beta_{\overline{\mathbb{Q}}}(ab)} = \begin{cases} 0 & if\ \gamma_B(ab)e^{i\beta_{\mathbb{Q}}(ab)} \neq 0 \\ \min\{\gamma_{\mathbb{P}}(a), \gamma_{\mathbb{P}}(b)\}e^{i\min\{\beta_{\mathbb{P}}(a),\, \beta_{\mathbb{P}}(b)\}} & if\ \gamma_{\mathbb{Q}}(ab)e^{i\beta_{\mathbb{Q}}(ab)} = 0 \end{cases}$$

$$\delta_{\overline{\mathbb{Q}}}(ab)e^{i\Omega_{\overline{\mathbb{Q}}}(ab)} = \begin{cases} 0 & if\ \delta_B(ab)e^{i\Omega_B(ab)} \neq 0 \\ \min\{\delta_{\mathbb{P}}(a), \delta_{\mathbb{P}}(b)\}e^{i\min\{\Omega_{\mathbb{P}}(a),\Omega_{\mathbb{P}}(b)\}} & if\ \delta_{\mathbb{Q}}(ab)e^{i\Omega_{\mathbb{Q}}(ab)} = 0 \end{cases}$$

Example 4.11: Consider the cohesive fuzzy graph G and its complement $\overline{G}$, as shown in figure 10 &11

CONCLUSION

This paper presents the definition of a cohesive fuzzy graph, a new type of fuzzy graph, along with graphical examples illustrating its order, size, and degree. Additionally, we talked about some properties of cohesive fuzzy graph like union, join, complement and composition. In future, we will develop the other concepts using cohesive fuzzy graph.

REFERENCES

1. L. A. Zadeh, Fuzzy sets, Inf. Control, 8 (1965), 338-353. https://doi.org/10.1016/S0019-9958(65)90241-X.
2. K. T. Atanassov, Intutionistic fuzzy sets, Fuzzy Sets Syst., 20(1986), 87-96.https://doi.org/10.1016/S0165-0114(86)80034-3.
3. D. Ramot, R.Milo, M. Friedman, A. Kandel, Complex fuzzy sets, IEEE Trans. FuzzySyst., 10 (2002), 171-186. https://doi.org/10.1109/91.995119.
4. V. Torra, Hesitant fuzzy sets, Int. J. Intell. Syst., 25(2010), 529-539. https://doi.org/10.1002/int.20418.
5. A. S. Alkouri, A. R. Salleh, Complex intuitionistic fuzzy sets, AIP Conf. Proc.,1482(2012), 464-470.
6. N. Chen, Z. Xu, M. Xia, Interval-valued hesitant preference relations and their applications to group decision making, Knowl Based Syst., 37(2013), 528-540. https://doi.org/10.1016/j.knosys.2012.09.009.
7. A.Rosenfeld, Fuzzy graphs, Academic Press, 1975, 77-95. https://doi.org/10.1016/B978-0-12-775260-0.50008-6.
8. T. Pathinathan, J. J. Arockiaraj, J.J. Roseline, Hesitancy fuzzy graphs, Indian J. Sci.Technol., 8(2015), 1-5. https://doi.org/10.17485/ijst/2015/v8i35/86672.
9. F. Karaaslan, Hesitant fuzzy graphs and their applications in decision making, J. Intell.Fuzzy Syst., 36(2019), 2729-2741.https://doi.org/10.3233/JIFS-18865.
10. M.Talafha, A.Alkouri, S. Alqaraleh, H. Zureigat, A.Aljarrah. Complexhesitant fuzzy sets and its application in multiple attributes decision-making problems, J. Intell FuzzySyst.,41(2021),7299-7327.https://doi.org/10.3233/JIFS-211156.
11. N. Yaqoob, M. Gulistan, S. Kadry, H. A. Wahab, Complex intuitionistic fuzzygraphs with appication in Cellular network provider companies, Mathematics 2019, 7, 35; https://doi.org/10.3390/math7010035.
12. M. Javaid, A. Kashif, and T. Rashid, Hesitant fuzzy graphs and their products, Fuzzy inf. Eng.,vol.12, no. 2, pp. 238-252, 2020.
13. E. AbuHijleh, Complex hesitant fuzzy graph, Fuzzy Inf. Eng., 15(2023), 149-161. https://doi.org/10.26599/FIE.2023.9270010.

14. X. Xue, M.Poonia, G. M. Abdulsahib, V. Shukla, On Cohesive Fuzzy Sets, Operations and Electromagnetic Signals and Solar Activities. Symmetry 2023, 15,595. https://doi.org/10.3390/Sym1530595.

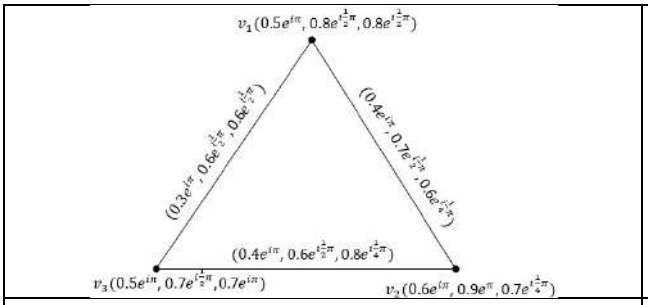

Figure 1: Cohesive fuzzy graph

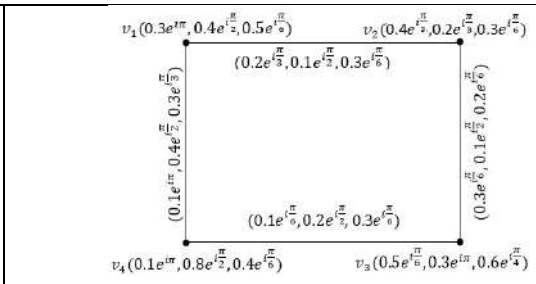

Figure 2: Cohesive fuzzy graph

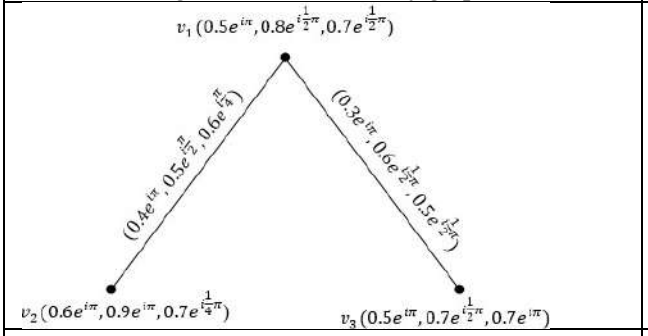

Figure 3: Cohesive fuzzy graph of G_1

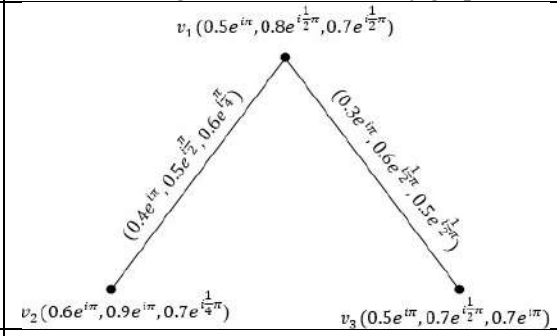

Figure 4: Cohesive fuzzy graph of G_2

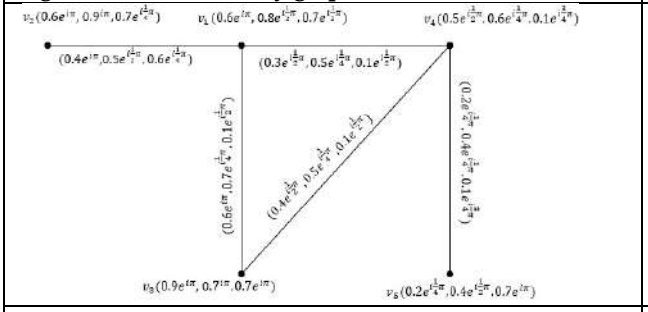

Figure 5 : Cohesive fuzzy graph of $G_1 \cup G_2$

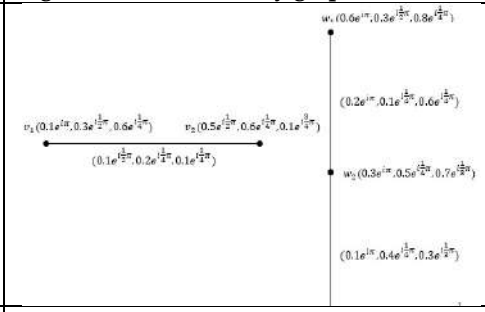

Figure 6: Cohesive fuzzy graph of G_1 and G_2

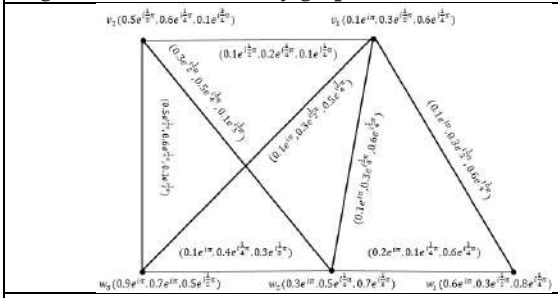

Figure7: Cohesive fuzzy graph of $G_1 + G_2$

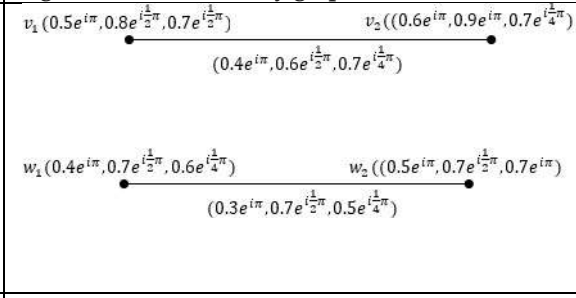

Figure 8: Cohesive fuzzy graph of G_1 and G_2

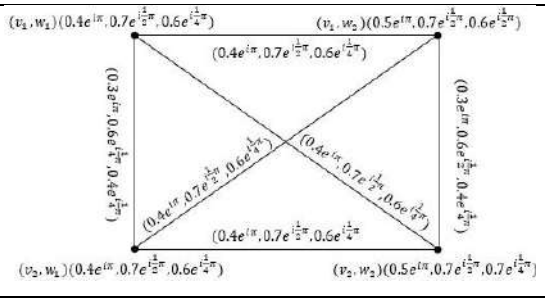

Figure 9: Cohesive fuzzy graph of G_1 and G_2

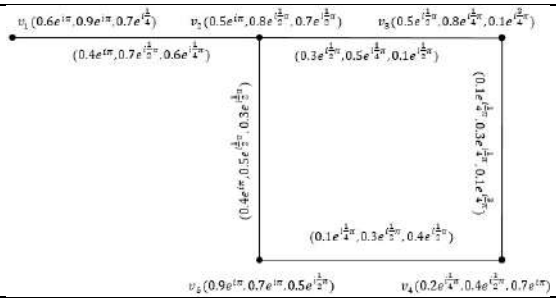

Figure 10: Cohesive fuzzy graph of G

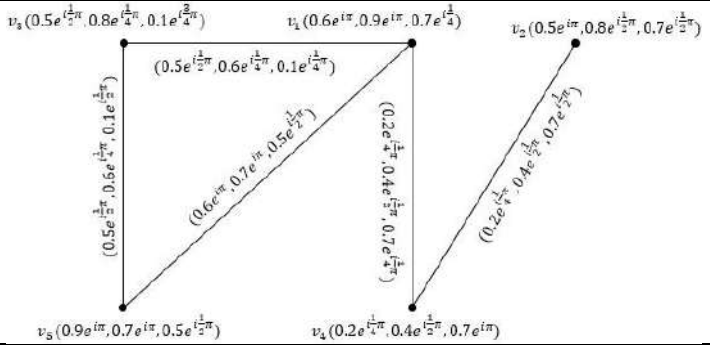

Figure 11: Cohesive fuzzy graph of $\overline{G}$

RESEARCH ARTICLE

Antibiotic Sensitivity Profile of the Waterborne Disease-Causing Bacteria, Isolated from Traditional Drinking Water Sources in Pithoragarh, Uttarakhand

Shailu Garkoti[1] and Rakesh Verma[2]*

[1]Research Scholar, Department of Zoology, L.S.M. Campus, Pithoragarh, (Affiliated to Soban Singh Jeena University, Almora), Uttarakhand, India.
[2]Assistant Professor, Department of Zoology, L.S.M. Campus, Pithoragarh, (Affiliated to Soban Singh Jeena University, Almora), Uttarakhand, India.

Received: 21 Nov 2024 Revised: 03 Dec 2024 Accepted: 03 Feb 2025

***Address for Correspondence**
Rakesh Verma
Assistant Professor, Department of Zoology,
L.S.M. Campus, Pithoragarh,
(Affiliated to Soban Singh Jeena University, Almora),
Uttarakhand, India.
E.Mail: rv.pith@gmail.com

ABSTRACT

The antibiotic sensitivity profile evaluates antibiotic efficacy against specific bacteria.The study focused on microbial contamination in water sources and associated health risks. The methodology of the study involved the monthly analysis of water samples to evaluate their quality and bacterial content. This was achieved through the use of selective culture media for bacterial isolation, antibiotic susceptibility testing to determine resistance profiles, and the Kirby-Bauer disc diffusion method for measuring zones of inhibition (ZOI).Two antibiotics were tested against each bacterium at specific concentrations. Fluctuations were observed in all water physicochemical parameters.The results of our study revealed a diverse range of physicochemical parameters, which were observed as follows, pH (6-7.9), WT (7-21 ºC), AT (10-22 ºC), TDS (232-498 mg/l), DO (5.2-7.9 mg/l),CO_2(0.4-2.6 mg/l), total alkalinity (59-287 mg/l), BOD (0.8-3.1 mg/l), and EC (308-799 µs/cm) and there was the significant value ofdifferent parameters ($p < 0.05$).The ZOI patterns varied across antibiotic concentrations for all bacterial species, with Ab1 and Ab2 exhibiting different ranges. These patterns highlight varying resistance, intermediate, and susceptibility patterns among bacteria. *E. coli* showed high resistance to amoxicillin, while chloramphenicol, ciprofloxacin, gentamicin, erythromycin, and tetracycline exhibited mixed responses, with resistance dominating most isolates.The antibiotic sensitivity profiles reveal high resistance across bacterial species. *E. coli* shows 45% resistance to amoxicillin and 50% to chloramphenicol, *Salmonella* has 50% resistance to ciprofloxacin and gentamicin, while *Shigella* exhibits 65% resistance to ciprofloxacin and 55% to gentamicin, with no ciprofloxacin susceptibility. *Campylobacter* shows severe resistance to erythromycin

(60%) and tetracycline (65%), while *Clostridium* demonstrates 70% resistance to vancomycin and metronidazole, with minimal susceptibility (5%).This study underscores the urgent need to monitor and safeguard traditional drinking water sources in Pithoragarh, emphasizing the need for effective strategies to mitigate bacterial contamination and antibiotic resistance, informing crucial public health interventions.

Keywords: Antibiotics, resistance, drinkingwater, contamination, zoneofinhibition

INTRODUCTION

In Pithoragarh city of Uttarakhand, traditional drinking water sources such as 'naula and dhara' continue to serve as vital drinking water sources for the local population. While these sources have historically been relied upon for their accessibility and convenience, concerns regarding water quality and the presence of harmful bacteria have gained prominence in recent years [1]. Water contamination brought on either directly or indirectly by sewage or other waste products of both human and animal origin is the most frequent and pervasive risk linked with drinking water [2]. Communities that rely on drinking water sources may face serious health hazards as a result of bacterial contamination. *Escherichia coli, Salmonella, Shigella,* and other bacteria can cause various waterborne illnesses, ranging in severity from moderate gastroenteritis to a serious infection that could be fatal [3]. Water contamination has been linked to the spread of disease-causing bacteria and causes various diseases such as diarrhea, dysentery, typhoid, etc. Water physio-chemical properties have a profound impact on various natural and biological processes [4].

Seasonal variation of physio-chemical parameters in different drinking water sources refers to the cyclical changes in water quality characteristics over a year. Different factors that are responsible are natural and anthropogenic, resulting in serious health threats. Various health risks like diarrhea, dysentery, typhoid, and gastrointesteris diseases can be caused due to the consumption of contaminated water [5]. Antibiotic sensitivity test, also known as antimicrobial susceptibility testing, is a laboratory procedure that assesses the effectiveness of different antibiotics against a specific bacterial infection. It helps determine which antibiotics are most effective in treating the infection, guiding healthcare professionals in selecting the most appropriate treatment [6]. Susceptibility indicates that a bacterium is readily affected by a particular antibiotic, leading to its inhibition or destruction, while resistance denotes the bacterium's ability to withstand the antibiotic's action [7]. The minimum inhibitory concentration method is a crucial technique in microbiology used to determine the lowest concentration of an antimicrobial agent, such as an antibiotic, that effectively inhibits the growth of a specific microorganism [8]. This study involves subjecting the microorganisms to varying concentrations of the antimicrobial substance. The MIC value is essential for guiding appropriate antibiotic dosages assessing the susceptibility of microorganisms to specific drugs, aiding in the development of effective treatment strategies, and the prevention of antibiotic resistance [9]. The Zone of Inhibition (ZOI) is a clear region around an antimicrobial disc where the growth of microorganisms is suppressed, serving as a key indicator of the substance's effectiveness in inhibiting bacterial growth. A Zone of Inhibition meeting or exceeding the defined breakpoints indicates bacterial susceptibility, signifying potential efficacy in treating infections. Intermediate susceptibility, represented by an intermediate zone, implies partial inhibitory effect, while a smaller zone indicates resistance, rendering the antibiotic less likely to be effective against the bacteria [10,11].

The aim of the study to conduct an antibiotic sensitivity profile on bacterial isolates from water samples of traditional drinking water sources in Pithoragarh City, Uttarakhand, was to assess the susceptibility of these bacteria to various antibiotics. The primary objective of the study analysed the water quality and then identify the most effective antibiotics for the potential treatment of waterborne infections, ensuring public health and safety in the region. This investigation holds significant importance in guiding public health interventions and policy decisions related to water quality management, helping to prevent and control waterborne diseases, and promoting safe drinking water access for the local community.

MATERIAL AND METHODS

Sample collection and Physio-chemical analysis: City Pithoragarh, which is located at 29.5829^0 N, 80.2182^0 E, in the northern part of Uttarakhand. The city has an altitude of 1,627 meters above sea level. This study was focused on the 10 different traditional drinking water sources. Monthly samples were collected according to APHA [12]. The 1000 ml sterile bottles were used to collect the water samples aseptically, and the evaluation of water quality was based on multiple critical parameters, such as pH (Hydrogen ion concentration), WT (Water temperature), AT (Air temperature), TDS (Total dissolved solids), DO (Dissolve oxygen), CO_2 (Carbon dioxide), TA (Total alkalinity), BOD (Biological oxygen demand), and EC (Electric conductivity) [12].

Preparation of general agar media and Selective media: Creating a nutrient-rich gel-like substance called agar, was used to grow a wide variety of microorganisms. This process typically includes mixing agar powder with water, heating it to dissolve it, sterilizing, and then pouring it into petri dishes to solidify for microbial culture and then isolating these bacteria [12]. Selective media are designed with specific components that favor the growth of target organisms and discourage the growth of unwanted contaminants. These media were prepared separately for the different bacteria, such as Eosin methylene blue agar media for *Escherichia coli* [13], and xylose lysin deoxycholate agar media for *Shigella* spp. [14], brilliant green agar media for *Salmonella* spp. [15], s*kirrow's Campylobacter* media for *Campylobacter* spp. [16], lactose gelatin media for *Clostridium* spp. [17].

Antibiotics disc insert: After selective media, the next step is to prepare agar media for antibiotic sensitivity testing to assess the susceptibility of the isolated bacteria to various antibiotics. This process involves spreading the bacterial culture evenly across the agar surface, followed by the placement of antibiotic discs containing different antibiotics [12]. Different antibiotics with different concentrations for the different bacteria were used (Table 1). Different antibiotic concentrations for different studies of bacteria were set according to standard procedure [18, 19, 20]. The antimicrobial agents tested included amoxicillin (10 µg) and chloramphenicol (30 µg) specifically for *E. coli* species. Ciprofloxacin (5 µg) and gentamicin (10 µg) were tested for *Salmonella* and *Shigella* species, both of which are significant causes of waterborne illnesses. For *Campylobacter* species, known for causing gastrointestinal infections, erythromycin (15 µg) and tetracycline (30 µg) were evaluated. Finally, vancomycin (30 µg) and metronidazole (5 µg) were tested for *Clostridium* species, which include *Clostridium.*

Zone of inhibition determination: For ZOI determination Kirby-bauer disc method was used. The zone of inhibition test was a simple method to assess the effectiveness of an antibiotic against bacteria. It was measured as the diameter of the clear area in millimeters. After incubating at 37 ºC for 24-48 hours, measure and record the diameter of clear zones (inhibition zones) around each disc with the help of a measuring scale (Hi-Media). The diameter of the inhibition zone surrounding each antibiotic disc, was used to categorize organisms as either sensitive, intermediate, or resistant to an antibiotic [19, 21].

Statistical analysis: The mean, standard deviation, PAST program 4.08 version [22], MS Excel data analysis software, and ANOVA, were used to analyze the summary statistical analysis of the annual data [23].

RESULTS

The analysis of the water quality of different drinking water sources was measured monthly from each source. The results of different parameters during the study, show that the value of pH varies from 6 to 7.9, WT from 7 to 21 ºC, AT from 10 to 22 ºC, TDS was 232 to 498 mg/l, DO was 5.2 to 7.9 mg/l, CO_2 from 0.4 to 2.6 mg/l, total alkalinity from 59 to 287 mg/l, BOD from 0.8 to 3.1 mg/l, and EC from 308 to 799 µs/cm, as shown in Table 2. There was a significant value of WT with other parameters ($p < 0.05$) and no significant difference in the true average values of the parameters between WT and AT, as shown in Table 3.

The antibiotic sensitivity profiles (Table 4) reveal varying resistance, intermediate, and susceptibility patterns among bacteria across different sites. *E. coli* exhibited high resistance to amoxicillin (ZOI 9-14 mm), with few isolates showing intermediate sensitivity (14-17 mm) or full susceptibility (18-20 mm). Responses to chloramphenicol ranged from resistance (ZOI 8-12 mm) to limited susceptibility (18-20 mm). *Salmonella* predominantly displayed resistance and intermediate sensitivity to ciprofloxacin, with one isolate susceptible at the minimum ZOI. Gentamicin resistance (ZOI 8-12 mm) was common, with intermediate sensitivity (14 mm) and rare susceptibility (16-25 mm). *Shigella* showed high ciprofloxacin resistance (ZOI 0-12 mm), with no full susceptibility at maximum ZOI, though intermediate responses (14-20 mm) were noted. *Campylobacter* resisted erythromycin and tetracycline (ZOI 0-10 mm) with no sensitivity recorded. *Clostridium* showed resistance and intermediate responses to vancomycin and metronidazole, with only one instance of sensitivity, which was summarized graphically in Graph 1 and Figure 1.

The antibiotic sensitivity profiles summarized in Table 5 reveal notable resistance patterns in various bacterial species. *E. coli* demonstrates resistance to Amoxicillin (45%) and Chloramphenicol (50%), with intermediate susceptibility rates of 20%, 35% and 30%, respectively. *Salmonella* shows 50% resistance to Ciprofloxacin and Gentamicin, with higher susceptibility for Gentamicin (40%) than Ciprofloxacin (5%). For *Shigella,* Ciprofloxacin resistance was 65%, with no susceptibility observed, while Gentamicin resistance was 55%, and susceptibility was 30%. *Campylobacter* exhibits severe resistance to Erythromycin (60%) and Tetracycline (65%), with no susceptible isolates. Finally, *Clostridium* displays the highest resistance rates (70%) to both Vancomycin and Metronidazole, with susceptibility rates of only 5% and no susceptibility, respectively, as shown in Graph 2. These findings highlight a critical concern regarding the emergence of antibiotic-resistant bacteria, indicating the need for stringent antibiotic stewardship and innovative treatment strategies.

DISCUSSION

In our study, we found a fluctuation in the values of various physio-chemical parameters of the water across different seasons. This finding is consistent with previous studies that examined the dynamics of the relationship between water pH and other water quality parameters in ground and surface water systems [24]. These studies also investigated groundwater characteristics, qualities, and treatments, which were similar to our findings [25]. In our study, we observed different parameter range values in different sites, similar to the findings of those who worked on the assessment of groundwater quality [26]. In the present study, we isolated different bacteria from various sources of drinking water to study antibiotic sensitivity against these isolated bacteria. This approach was similar to studies that assessed drinking water quality and examined antibiotic sensitivity of bacterial isolates [21]. We observed different antibiotic sensitivity patterns for various bacteria isolated from drinking water sources, similar to the findings on the zones of inhibition for coliform bacteria present in drinking water sources [27]. We used antibiotic disks of different concentrations according to the Kirby-Bauer method, similar to previous studies [28, 36, 37]. We also observed that different concentrations of antibiotics produced varying zones of inhibition on agar plates, consistent with studies on bacterial profiles and antibiotic susceptibility patterns found in drinking water [29]. In the present study, the 'clear zone' around the antibiotics was measured using the Kirby-Bauer disc method in different selective media, similar to studies examining the uses and limitations of disc diffusion in antibiotic sensitivity testing of bacteria [30,31]. Our study aligns with previous findings that have reported varied antibiotic zones among bacteria found in drinking water [32]. Similarities are noted regarding antibiotic sensitivity and resistance patterns among isolated microorganisms [33,34]. The identification of antibiotic-resistant bacteria in various drinking water sources aligns with observations made in a sewage treatment plant. Furthermore, our determination of minimal inhibitory concentration parallels previous findings, which utilized agar and broth dilution methods [8, 35].

CONCLUSION

The study of physicochemical parameters demonstrated notable variations in water quality across different sources. These fluctuations emphasize the need for regular monitoring to ensure safe drinking water standards. The antibiotic

sensitivity profile of bacterial isolates from the water samples of traditional drinking water sources in Pithoragarh City, Uttarakhand, provides crucial insights into the potential health risks associated with these sources. The assessment of water quality reveals its adherence to safety standards, ensuring it is suitable for consumption and public health. The results of this study reveal the susceptibility or resistance of the isolated bacteria to various antibiotics, shedding light on the effectiveness of antibiotics in combating bacterial contamination. This information is instrumental in guiding public health efforts to ensure safe and reliable drinking water access for the residents of Pithoragarh. Continued monitoring and assessment of antibiotic sensitivity profiles in water sources are essential for addressing emerging health threats and maintaining the well-being of the local population. Frequent antibiotic use has led to widespread resistance in targeted bacteria, diminishing the effectiveness of the majority of these antibiotics. This underscores the imperative for strategic approaches to address and mitigate antibiotic resistance in these cases.

ACKNOWLEDGMENT

The authors are thankful to the Department of Zoology, L.S.M Campus Pithoragarh, Uttarakhand for providing the facilities to conduct the research successfully.

REFERENCES

1. Johnston, R., Heijnen, H., & Wurzel, P., 2001. Safe water technology. United Nations Synthesis Report on Arsenic in Drinking Water, 1-98.
2. Sarwar G, Agostoni C, Carratu B, Boniglia C, Riva EJJOT., 2001. Comparative free amino acid profles of human milk and some infant formulas sold in Europe. Authors' Reply 20:92–93.
3. Qayyum S, Basharat S, Mian AH, Qayum S, Ali M, Changsheng P, Shahzad M, Sultan F., 2020. Isolation, identification, and antibacterial study of pigmented bacteria. Appl Nanosci. Doi. org/10.1007/s13204-020-01363-5.
4. Maréchal, Y., 2006. The hydrogen bond and the water molecule: The physics and chemistry of water, aqueous and bio-media. Elsevier.
5. Fazal-ur-Rehman, M., 2019. Polluted water borne diseases: Symptoms, causes, treatment and prevention. J Med Chem Sci, 2(1), 21-6.
6. Leekha, S., Terrell, C. L., & Edson, R. S., 2011. General principles of antimicrobial therapy. In Mayo Clinic proceedings (Vol. 86, No. 2, pp. 156-167). Elsevier.
7. Cloete, T. E., 2003. Resistance mechanisms of bacteria to antimicrobial compounds. International Biodeterioration & Biodegradation, 51(4), 277-282.
8. Wiegand, I., Hilpert, K., & Hancock, R. E., 2008. Agar and broth dilution methods to determine the minimal inhibitory concentration (MIC) of antimicrobial substances. Nature Protocols, 3(2), 163-175.
9. Andrews, J. M., 2001. Determination of minimum inhibitory concentrations. Journal of Antimicrobial Chemotherapy, 48 (suppl_1), 5-16.
10. Alanis, A. J., 2005. Resistance to antibiotics: are we in the post-antibiotic era. Archives of medical research, 36(6), 697-705.
11. Rahman, M., Kuhn, I., Rahman, M., Olsson-Liljequist, B., & Mollby, R., 2004. Evaluation of a scanner-assisted colorimetric MIC method for susceptibility testing of gram-negative fermentative bacteria. Applied and environmental microbiology, 70(4), 2398-2403.
12. APHA., 2012. Standard methods for the examination of water and wastewater, 22nd edn. American Public Health Association, Washington, DC.
13. Leininger, D. J., Roberson, J. R., & Elvinger, F., 2001. Use of eosin methylene blue agar to differentiate Escherichia coli from other gram-negative mastitis pathogens. Journal of Veterinary Diagnostic Investigation, 13 (3), 273-275.

14. Gaurav, A., Singh, S. P., Gill, J. P. S., Kumar, R., & Kumar, D., 2013. Isolation and identification of Shigella spp. from human fecal samples collected from Pantnagar, India. Vet World, 6(7), 376.
15. Murchie, L., Whyte, P., Xia, B., Horrigan, S., Kelly, L., & Madden, R. H., 2007. Prevalence of Salmonella in grade A whole shell eggs on the island of Ireland. Journal of Food Protection, 70(5), 1238-1240.
16. Bi, S. L., Shi, L., Yan, H., & Meng, H. C., 2013. Comparison of various culture methods (Skirrow medium, a blood-free medium, and a filtration system enriched in Bolton and Preston broths) for isolation of Campylobacter spp. from raw meat samples. Annals of Microbiology, 63, 179-185.
17. Lin, Y. T., & Labbe, R., 2003. Enterotoxigenicity and genetic relatedness of Clostridium perfringens isolates from retail foods in the United States. Applied and Environmental Microbiology, 69(3), 1642-1646.
18. National Committee for Clinical Laboratory Standards Performance standards for antimicrobial disk susceptibility tests. Approved standard M2-A6. 1997 National Committee for Clinical Laboratory Standards Wayne, Pa
19. Bauer, A. W., Kirby, W. M. M., Sherris, J. C., & Turck, M. (1966). Antibiotic susceptibility testing by a standardized single disk method. American journal of clinical pathology, 45(4_ts), 493-496.
20. Hudzicki, J. (2009). Kirby-Bauer disk diffusion susceptibility test protocol. *American society for microbiology*, *15*(1), 1-23.
21. Jayana, B. L., Prasai, T., Singh, A., & Yami, K. D., 2009. Assessment of drinking water quality of Madhapur-thimi and study of antibiotic sensitivity against bacterial isolates. Nepal Journal of Science and Technology, 10, 167- 172.
22. Hammer, Ø., & Harper, D. A., 2001. Past: paleontological statistics software package for education and data analysis. Palaeontologia electronica, 4(1), 1.
23. Heiberger, R. M., & Neuwirth, E., 2009. R through Excel: A spreadsheet interface for statistics, data analysis, and graphics (pp. 323-330). New York: Springer.
24. Saalidong, B. M., Aram, S. A., Otu, S., & Lartey, P. O., 2022. Examining the dynamics of the relationship between water pH and other water quality parameters in ground and surface water systems. PloS one, 17(1), e0262117.
25. Ojo, O. I., Otieno, F. A., & Ochieng, G. M., 2012. Groundwater: Characteristics, qualities, pollutions, and treatments: An overview. International Journal of Water Resources and Environmental Engineering, 4(6), 162-170.
26. Zidi, C., Jamrah, A., & Al-Issai, L., 2017. Assessment of groundwater quality in Al-Buraimi, Sultanate of Oman. J Mater Environ Sci, 8(4), 1266-1276.
27. Hernandez-Camarena, J. C., Graue-Hernandez, E. O., Ortiz-Casas, M., Ramirez-Miranda, A., Navas, A., Pedro-Aguilar, L., & Bautista-de Lucio, V. M., 2015. Trends in microbiological and antibiotic sensitivity patterns in infectious keratitis: 10-year experience in Mexico City. Cornea, 34(7), 778-785.
28. Yang, X., Wang, D., Zhou, Q., Nie, F., Du, H., Pang, X., & Xu, Y., 2019. Antimicrobial susceptibility testing of Enterobacteriaceae: determination of disk content and Kirby-Bauer breakpoint for ceftazidime/avibactam. BMC microbiology, 19(1), 1-7.
29. Mian, A. H., Fatima, T., Qayyum, S., Ali, K., Shah, R., Noorullah, & Ali, M., 2020. A study of bacterial profile and antibiotic susceptibility pattern found in drinking water at district Mansehra, Pakistan. Applied Nanoscience, 10, 5435-5439.
30. Dickert, H., Machka, K., & Braveny, I., 1981. The uses and limitations of disc diffusion in the antibiotic sensitivity testing of bacteria. Infection, 9(1), 18-24.
31. Biemer, J. J., 1973. Antimicrobial susceptibility testing by the Kirby-Bauer disc diffusion method. Annals of Clinical & Laboratory Science, 3(2), 135-140.
32. Nyarko, H., Arthur, S. A., & Birikorang, E., 2011. A study of antibiotic susceptibility pattern of bacteria isolates in sachet drinking water sold in the Cape Coast metropolis of Ghana.
33. Nikoonejad, A., Gharabaghi, N., Davari, M., Ayromloo, M., & Nejad Rahim, R., 2013. Sensitivity pattern and resistance against antibiotics in isolated microorganisms of hospitalized patients. Studies in Medical Sciences, 24(10), 785-790.

34. Al-Shami, H. Z., Al-Haimi, M. A., Al-dossary, O. A. E. I., Nasher, A. A. M., Al-Najhi, M. M. A., Al-Shamahy, H. A., & Al-Ankoshy, A. A. M., 2021. Patterns of antimicrobial resistance among major bacterial pathogens isolated from clinical samples in two tertiary hospitals. Sana'a, Yemen. Universal J Pharm Res, 6(5), 60-67.
35. Everage, T. J., Boopathy, R., Nathaniel, R., LaFleur, G., & Doucet, J., 2014. A survey of antibiotic-resistant bacteria in a sewage treatment plant in Thibodaux, Louisiana, USA. International Biodeterioration & Biodegradation, 95, 2-10.
36. CLSI., 2019. M100 Performance Standards for Antimicrobial Susceptibility Testing, 29th ed.; Clinical and Laboratory Standards Institute: Wayne, PA, USA.
37. Kibret, M., & Abera, B. (2011). Antimicrobial susceptibility patterns of E. coli from clinical sources in northeast Ethiopia. African Health Sciences, 11, 40-45.
38. Mehdi, L. Y., & Wannas, N. S. (2017). Isolation and Identification of Clostridium perfringens and its Enterotoxin in Food Poisoning Patients. Journal of the Faculty of Medicine Baghdad, 59(2), 145-150.

Table 1: Different types of bacterial species Zone Diameter [19, 34, 36, 37, 38]

S.no.	Bacteria	Ab	Name of antibiotics	Disc con.	Resistant	Intermediate	Susceptible
1.	*E. coli*	Ab 1	Amoxicillin	10 µg	<13mm	14-17	>17mm
		Ab 2	Choromophenicol	30 µg	<12mm	13-17	>18mm
2.	*Salmonella*	Ab 1	Ciprofloxacin	5µg	<15mm	16-20	>21mm
		Ab 2	Gentamycin	10 µg	<12mm	13-14	>15mm
3.	*Shigella*	Ab 1	Ciprofloxacin	5 µg	<15mm	16-20	>21mm
		Ab 2	Gentamycin	10 µg	<12mm	13-14	>15mm
4.	*Campylobacter*	Ab 1	Erythromycin	15 µg	<13mm	14-22	>23mm
		Ab 2	Tertracycline	30 µg	<14mm	15-18	>19mm
5.	*Clostridioum*	Ab 1	Vancomycin	30 µg	<14mm	15-16	>17mm
		Ab 2	Metronidazole	5 µg	<15mm	15-20	>21mm

Table 2: Annual data of physio-chemical parameters of different water sources

S. no.	Sites	Parameters								
		pH	WT	AT	TDS	DO	CO2	Alkalinity	BOD	EC
1.	**Site 1 (SD)**	7-7.8 7.45±0.32	10-22 16.83±4.72	7-25 18±6.01	438-524 500.41±22.94	7.2-9.5 8.7±0.60	1.5-8.2 4.99±1.90	110-148 122.5±10.81	0.7-3 1.67±0.67	334-765 588.41±155.68
2.	**Site 2 (HM)**	7.4-7.9 7.68±0.14	9-22 16.83±4.96	8-25 17.91±6.88	234-272 256.41±12.35	7.4-9.5 8.54±0.57	1.5-7.7 5.2±1.55	105-122 116.25±4.75	0.7-2.5 1.6±0.49	321-762 503.91±142.75
3.	**Site 3 (CD)**	7.1-7.8 7.52±0.25	9-23 17.58±5.14	7-27 18.33±6.86	102-208 185.25±26.98	8.4-9.3 8.84±0.33	2.1-8.1 4.86±2.02	89-122 113.75±9.09	0.8-2 1.41±0.32	340-747 577.41±148.78
4.	**Site 4 (BN)**	6.5-7.9 7.39±0.41	9-22 16.83±5.04	7-27 18.75±7.09	342-397 368.25±17.77	8.06-9.2 8.54±0.36	1.8-6.5 4.42±1.39	102-136 120.33±8.74	2.3-5 3.38±0.67	345-765 587.41±153.58
5.	**Site 5**	7.1-8 7.54±0	9-23 17.66±	7-27 18.75±	214-276	7.5-9.2	1.9-6 4.433±1.	110-145 122.50±1	1-9 2.47±2.1	344-756 516±127.

	(RD)	.32	5.10	7.08	236±17.68	8.57±0.49	45	1.27	3	00
6.	**Site 6 (LD)**	6.5-7.9 7.40±0.42	9-22 17±4.93	7-27 19.58±7.31	385-454 422.41±19.60	7.5-9.3 8.55±0.45	1.7-8.2 4.97±2.17	105-145 122.16±10.02	1.1-3.3 2.07±0.70	220-778 578.25±190.75
7.	**Site 7 (KN)**	7.1-7.9 7.53±0.29	10-22 17.83±4.34	8-27 19.83±6.61	431-521 465±25.45	6.5-9.2 8.22±0.65	1.5-9.3 5.47±2.42	112-134 121.75±6.91	2-4.4 3±0.70	344-745 586.66±152.77
8.	**Site 8 (AD)**	7-7.9 7.54±0.30	10-25 18.16±4.89	8-27 19±6.45	110-475 389.16±93.16	8-9.3 8.50±0.39	2-8.6 5.00±1.98	115-145 128.41±9.49	0.9-3.8 2.06±0.80	365-789 604.66±146.01
9.	**Site 9 (MD)**	7.1-7.9 7.55±0.28	10-23 17.41±5.19	8-27 18.75±7.04	245-287 258±15.29	7.5-9.5 8.68±0.52	2.2-7.2 4.70±1.77	115-176 134.41±20.17	1.1-2.3 1.69±0.45	343-765 597.41±146.01
10.	**Site 10 (PD)**	6.9-7.8 7.33±0.27	10-22 17.5±4.23	8-26 19.25±6.06	311-434 335.66±33.84	7.7-11.6 9.02±1.15	2.8-9.4 5.45±1.95	104-196 124.5±28.02	1.5-2.6 1.933±0.36	356-776 597.08±151.54

Table 3: Analysis of variance (ANOVA) for physicochemical parameters of different water sources

S. No.	Variation between different parameters	BGWGT	Sum of Squares (SS)	df	Mean Square (MS)	F	P value	Sig.
1	WT/AT	BG	18.20042	1	18.20042	2.034229	0.167829	NS
		WG	196.8358	22	8.947083			
		T	215.0363	23				
2	WT/pH	BG	405.1638375	1	405.1638375	91.11957308	2.79395E-09	***
		WG	97.82315833	22	4.446507197			
		T	502.9869958	23				
3	WT/TDS	BG	910339.4017	1	910339.4017	1484.771702	1.08855E-21	***
		WG	13488.58333	22	613.1174242			
		T	923827.985	23				
4	WT/CO_2	BG	1129.293204	1	1129.293204	253.329995	1.48109E-13	***
		WG	98.07149167	22	4.457795076			
		T	1227.364696	23				
5	WT/DO	BG	463.6725042	1	463.6725042	104.2979604	8.22057E-10	***
		WG	97.80435833	22	4.445652652			
		T	561.4768625	23				

6	WT/BOD	BG	1046.496	1	1046.496	236.9704	2.91E-13	***
		WG	97.15527	22	4.416148			
		T	1143.652	23				
7	WT/Alkalinity	BG	108770.2704	1	108770.2704	472.0339753	2.34516E-16	***
		WG	5069.435833	22	230.4289015			
		T	113839.7063	23				
8	WT/EC	BG	1977998.425	1	1977998.425	240.2279297	2.53724E-13	***
		WG	181144.4881	22	8233.840368			
		T	2159142.913	23				

BG=Between Group, WG=Within Group, T= Total, Non-significant value(P>0.05),*=low significant(P≤0.05),**=intermediate significant, ***=highly significant(P≤0.001)

Table 4: Annual average of the size of the zone of inhibition to different tested antibiotics in all sampling sites

Name of sites	**Name of bacteria**									
	E. coli		***Salmonella***		***Shigella***		***Campylobacter***		***Clostridium***	
	Ab1	**Ab2**	**Ab1**	**Ab2**	**Ab1**	**Ab2**	**Ab1**	**Ab2**	**Ab1**	**Ab2**
SD	13.25	12	11.75	10	11.5	9.75	13.25	10	6.5	15
HM	13.25	11	13.25	10.5	15	10.75	6.75	7.75	6.5	15
CD	15.25	13.5	14.75	12	14	11	6.75	7	8.75	6.5
BN	11.75	12	20	10.5	13.75	11	12	12.5	13.5	17
RD	15	11.25	13.5	13	16	13.25	14.5	10.75	8.5	7.76
LD	14	11.75	13	10.75	15	11.5	13.5	10.5	13	11
KN	13.25	11.5	22	14	17	11.5	13.25	14	12.5	10.5
AD	13.5	11.25	17	10.75	13.75	11	13.25	10.5	6.5	5.5
MD	14.5	13	13	11.25	13.75	11.5	14	13.5	8.5	8.5
PD	14.5	11.25	13	11.25	12	10.5	8.5	6.25	6	5.75

Table 5: Antibiotic sensitivity profile of different antibiotics

S.no.	**Name of Bacteria**	**Name of antibiotics**	**Disc concent ration**	**Different spot wise antibiotic sensitivity profile**		
				Resistant	**Intermediate**	**Susceptible**
1.	***E. coli***	Amxicillin	10 µg	50%	50%	-
		Choromophenicol	30 µg	80%	20%	-
2.	***Salmonella***	Ciprafloxin	5 µg	60%	10%	30%
		Gentamycin	10 µg	80%	20%	-
3.	***Shigella***	Ciprafloxin	5 µg	60%	20%	20%
		Gentamycin	10 µg	90%	10%	-
4.	***Campylobacter***	Erythromycin	15 µg	40%	60%	-
		Tetracyclin	30 µg	90%	10%	-
5.	***Clostridioum***	Vancomycin	30 µg	100%	0.00%	-
		Metronidazole	5 µg	70%	30%	-

Finger 1. Different size zone of inhibition surrounding the antibiotics disc

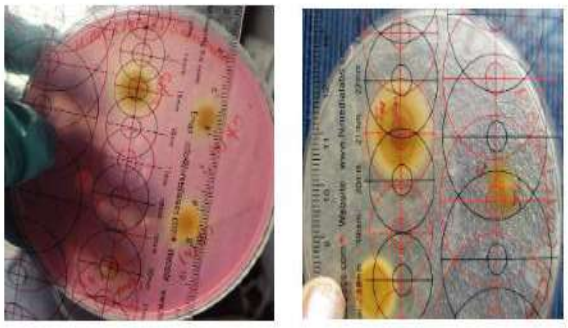

Finger 2. Measuring the zone of inhibition by using the measuring scale

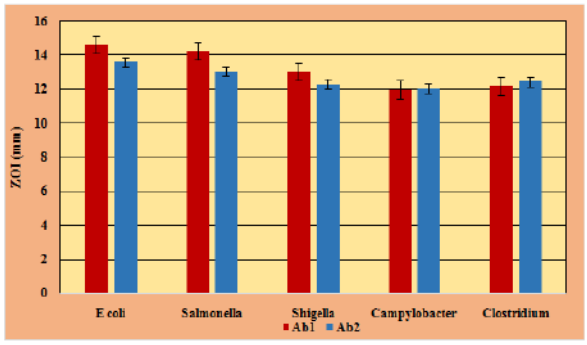

Graph 1: Annual average of the size of the zone of inhibition to different tested antibiotics

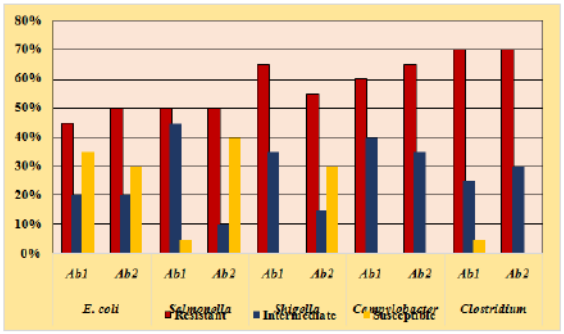

Graph 2: Antibiotic sensitivity profile of isolated bacteria

REVIEW ARTICLE

Analogy of Siddha *Varmam* Points used in the Symptomatic Management of *Cakaṉavātham* (Cervical Spondylosis) with Acupuncture and Ayurvedic *Marma Chikitsa* - A Literary Review

P.Mangaiarkarasi[1]*, T. R. Siddique Ali[2], A. Shameem Fathima[3] and M. Mohamed Musthafa[2]

[1]Senior Project Associate, CSIR-Traditional Knowledge Digital Library Unit, Point of Placing in CSIR - CLRI, Adyar, Chennai, Tamil Nadu, India.
[2]Professor, Department of Varmam Maruthuvam, Government Siddha Medical College, Arumbakkam, (Affiliated to The Tamil Nadu Dr. M.G. R. Medical University), Chennai, Tamil Nadu, India.
[3]Lecturer Grade II, Department of Udalthathuvam, Government Siddha Medical College, Arumbakkam, (Affiliated to The Tamil Nadu Dr. M.G. R. Medical University), Chennai, Tamil Nadu, India.

Received: 21 Nov 2024 Revised: 03 Dec 2024 Accepted: 27 Jan 2025

***Address for Correspondence**
P.Mangaiarkarasi,
Senior Project Associate,
CSIR-Traditional Knowledge Digital Library Unit,
Point of Placing in CSIR - CLRI, Adyar, Chennai, Tamil Nadu, India.
E.Mail: mangainarayanan@gmail.com

ABSTRACT

Many countries have their own traditional system of medicine. AYUSH (an acronym forAyurveda,Yoga,andNaturopathy,Unani,Siddha,SowgaRigpa)istraditionalsystemofmedicine which has been followed in India. The treatment methodologies of *Siddha* systeminclude *Agamarunthugal*(internal medicines), *Puramarunthugal*(external medicines) and *PuraMaruthuvam*(external therapies) [1]. Siddha and Ayurveda have its own external therapies namely *Varmam* and *Marma*. Acupunctureis one of external therapy of traditional Chines medicine. We searched the data from original classical Siddha texts that were written in Tamil language, original Ayurvedic texts translated in English, books designated as texts and referen cematerials in Siddha curriculum at Central Library of Indian System Medicine, Chennai. Additionally collected data from journals indexed in Ayush portal, Pubmed, Inflibnet, Scopus, web of science, and the search terms used are Siddha, *Varmam*, Acupuncture, Marma, Cervical Spondylosis and neck pain. Data sources explain about basic concept of these three systems of medicine. They share similar basic concepts, though similarities of the external therapies of these three systems yet not established. Comparisons between basic concepts of these external therapies are listed. Treatment for Cervical Spondylosis using external therapies like *Varmam*, Acupuncture and Marma sharesimilarities. The authors have laid the ground work for comparison of these external therapies, by taking symptomatic management of *Cakaṉavātham(*Cervical Spondylosis) as a tool and it has been found that all the three manipulating techniques are found to be remarkably similar.

Keywords: Siddha, *Varmam*, CervicalSpondylosis, Acupuncture, *Marma,* Neckpain

INTRODUCTION

Traditional system of medicine such as Siddha, Ayurveda and Chinese medicine, each has its own typical external therapies. These system share similar concepts like five element theory, vital energy circulation, three vital humors. All of them use plants, metals, minerals and animals as their source of the medicine. All of their therapeutic techniques are based on these fundamental phenomena. There siddha varma point used in the symptomatic management of *Cakaṉavātham (*Cervical spondylosis). In addition to this similarity between *Varmam*, Acupuncture, Marma is also described. Objective of this study is to evaluate the similarities of the Siddha *Varmam* points used in the symptomatic management of *Cakaṉavātham* (Cervical Spondylosis) with similar therapies in other traditional medical systems namely Chinese medicine, Ayurveda through literary review. The publications searched are Original classical Siddha texts that were written in Tamil language, Original Ayurvedic texts translated in English, Compilations done by reputed and experienced authors, Books designated as texts and reference materials in Siddha curriculum. We collected the data from journals indexed in Ayush portal, Pubmed, Inflibnet, Scopus, web of science and the search terms used are Siddha, *Varmam*, Acupuncture, *Marma* and Cervical Spondylosis, neck pain.

Cervical Spondylosis

Cervical spondylosis is defined as Arthrosis of the intervertebral joint in the cervical vertebrae [2]. Patient present with chronic pain in the neck, pain may or may not be radiating down to the arm and there is a diffuse tenderness in the cervical spine region. Cervical spondylosis is a degenerative condition of the cervical spine found almost universally in persons over 50 years of age. Around 60% of population in middle age group is affected by Cervical Spondylosis, because of lifestyle modification and inappropriate working posture. Cervical disc degeneration may lead to radiculopathy or myelopathy. Several factors should be considered in cervical disc degeneration including physical stress, biochemical abnormalities, genetic defects, Psycho physiological effects and autoimmune processes [3]. According to Siddha, Cervical spondylosis resembles *Cakaṉavātham.*

VARMAM MARUTHTHUVAM

Siddha system practiced in South India from ancient days. It is thought to have developed during the Indus civilization, which flourished between 2500 and 1700 BCE. Siddhars who were spiritual adepts and possess supernatural powers laid the foundation for this system of medicine [4]. Siddha system states that five elements exist in nature that include earth, water, fire, air, and ether [4] and they constitute the basic content of all corporeal objects. It is said there is connection between the macrocosm and microcosm [5]. *Varmam* is an inevitable treatment modality in many of the musculoskeletal and neurologic problems. *Varmam* technique is a minimal invasive procedure in which the physician uses his fingers to manipulate certain points in the body [6]. This therapy is a complete naturalistic, cost effective and less time consuming healing system to rejuvenate the body by eliminating toxic imbalance. It is safe and gives long lasting results and above all it is associated with no side effects. *Varmam* has been used in many contexts in the classical *Varmam* texts. One among them denotes that *Varmam* means energy which is the basis of whole universe. In human body this energy is called as *Vaasi* or life energy[7] and it is present in combination with Prana (*uyir aatral + pranan = vaasi*). It is considered to be the primary energy which is derived from both the parents during conception. It is entirely responsible for the intra uterine life of the fetus as multiplication of cell, organ formation etc., occurs under its influence. The life energy is constantly flowing in particular pathway in human body. It gives us immunity; it promotes faster healing process. In humans, this life energy is concentrated in certain points and they are called Varmam points. It has been said that the *Varmam* is the point of intersection of bone, muscle, tendons, nerves, blood vessels [8].

***Varmam* Manipulation Techniques**

Before manipulating the points the therapist should know the dimension of the points. Because depending on these dimensions the usage of finger and manipulation techniques are determined. *Varmam* points can be located using finger measurements. While measuring only the palmar aspect of the finger should be considered. Also fingers of the patients should be used to measure [9].

One finger measurement = breadth of index finger
Two fingers measurement = breadth of index and middle fingers
Three fingers measurement = breadth of index, middle and ring fingers
Four fingers measurement = breadth of index, middle, ring and little fingers
Five fingers measurement = breadth of index, middle, ring, little fingers and indexfinger of the other hand. Thumb should not be used.

***Varmam* and its pressure value**

During therapeutic application *Varmam* points are manipulated gently using the physician's fingers. In order to attain this some basic measures have being handled by our ancestors. This is being termed as '*Maathirai*". The magnitude of this *maathirai* varies from ¼ unit, ½ unit, ¾ unit and 1 unit [10]. Figure 1 (a, b) describe the magnitude of *mathirai.* The magnitude of the *mathirai* to be given to the patient depends on the body condition and severity of the disease. Pressure can be given continuously for a specific time or intermittently according to necessity. If given intermittently a gap of 10 seconds in between two successive manipulations is to be maintained.

Magnitude of Mathirai

Magnitude of Mathirai depends upon the pressure given from different location on our hand. For ¼ mathirai is given from wrist of the physician or tip of thumb or medial or lateral side of distal phalanx of thumb. For ½ mathirai pressure is given from elbow of the physician or distal half of distal phalanx of middle finger. For ¾ mathirai is given from the shoulder of the physician or distal ¾th of distal phalanx of middle finger. For 1 mathirai is given from neck of the physician / whole of distal phalanx of middle finger

Types of *Varmam* Applications

Ilakku murai [11]: This is the first aid measure that has to be carried out if injuries have occurred in the *Varmam* points. *Illakkuthal* means bringing down, extinguishing, loosening and softening. i.e., it is done to bring down the severity of the injury, loosen and soften the muscles and thus causes relaxation. Other applications include pressing, pacing, lifting, braiding, even and gentle clockwise or anticlockwise rotation, pinching, slipping pinch, tapping and gentle stroking. Depending on the nature of the illness, weight, age of the patient, any of these applications can be carried out.

***Varmam* points for Cakaṉavātham**

Nine points that are being manipulated for *Cakaṉavātham* are *Mudichu Varmam, Kaakattai Kaalam, Kaisulukki Varmam, Sippi Varmam, Savvu Varmam, Kaimootu Varmam, Manipanthaga Varmam, Koli Kaluthu Varmam and Kavuli Varmam.* All of the aforesaid *Varmam* points are linked with specialized energy channels called naadis [12].

Acupuncture

Acupuncture (Latin - acus - needle; puncture - to penetrate) is a technique in which practitioners stimulate accurate points on the body - most often by using thin needles through the skin. It is one of the practices used for about 5000 years [13]. Acupoints are the specific sites through which the qi is transported to the body surface. More than 400 acupoints are spread all over the body [14]. Acupoints are the loci of response to disease. Acupoints are classified either "by meridians" or "by body parts. Acupoints are classified into three categories. Acupoints are the loci of response to disease [15]. Acupoints are classified either "by meridians" or "by body parts. Acupoints are classified into three categories, Acupoints of 14 meridians (known as regular points), Extraordinary points are not attributed to 14 meridians, Ashi Points - they are also called "reflexing points", "unfixed points" or "tender spots" used for pain syndromes.

Selection of points

Points are selected from upper to lower portion of the body and from the back to the abdominal region. The number of points selected depends on the severity of the condition. The basic principle in Acupuncture treatment is to select the points along the course of meridians. This is according to the theory that diseases are related to meridians [16].

Methods for selecting Acupuncture points

Selecting points in the affected meridian to which the organs are related, selecting points from the related meridian and selecting points from several meridians. Generally, points of the exteriorly-interiorly related meridians or mother - son" related meridians are selected according to the theory of five elements.

Methods of locating Acupuncture points

'An Acupuncture point is located where it is located' – like veins, arteries or nerves. Using prominent anatomical landmarks, Using *Cun* measurement: In this method, either the finger measurement (finger *cun)* or defined landmarks of the body (body *cun)* of the patient. (1 *Cun*=2.5 cm) and the same is shown in Figure 2.

Acupuncture technique

Commonly used form is filiform needle made up of gold silver, alloy and most commonly of stainless steel. Warm needles and red hot needles are used sometimes. For the elderly and infants - shallow insertion for areas such as head, face and back is advisable. Deep insertion is preferred in obese people, young age persons, over the points on the four limbs, buttocks and abdomen
[17, 18].

Methods of puncture

Methods of needle insertion, called puncturing techniques. Three stages of puncture are Insertion, Retention and Withdrawing the needle.

Depth of the insertion

Shallow: up to 0.5 *cun*; Medium: 0.5–1 *cun*; Deep: 1 *cun*.

Direction of insertion

It may be described in terms of angle of needle make with the skin surface. There are 3 directions of insertion. Perpendicular: 90^0 to the skin, Oblique: 45^0 to the skin, Horizontal: 15^0 to the skin.

Order of inserting and removing the needles

Acupuncture is no exception to the rule that one must be orderly in one's activities. The order of the insertion and removal would, of course, vary according to the circumstances. Four possible methods are from above downwards, from proximal to distal, away from or towards the acupuncturist and less painful to the more painful points.

Retaining

"Retaining' describes the procedure of holding the needle in place after inserting it to the prescribed depth beneath the skin. Pathological conditions decide the retaining and its duration. Generally the needle is retained for15 to 20 minutes after qi is felt. Duration of needle retaining - i.e., *in situ* for about 15 minutes to 60 minutes [19]. Meanwhile, manipulations may be given at intervals until the patient feels numbness or the Acupuncture sensation known as "De Qi." in order to strengthen the therapeutic effects. If it is felt that the point is said to be correctly located and needle is inserted up to the correct depth. The manual methods of manipulation include lifting and thrusting; rotation, scrapping the handle, vibration of the needle and gentle tapping of the needle [19]. Also rotating and reinforcing maneuver; reducing maneuver are some of the maneuvers that are used. Stimulation with the needle, Depth of the puncture, retaining period, repeating the manipulations during this period, number of sessions (few to many), the gap between individual sessions (daily/ alternate days / weekly twice etc.,) and duration of entire therapeutic course

depend on the syndromic classification of Cervical spondylosis, severity of the disease, patient's age, gender and body constitution [20].

Removal of the Acupuncture needle

The needle is removed gently at the end of the treatment. Any jerky movements may cause pain. The Acupuncture point is then massaged with a dry sterile piece of cotton wool to prevent infection, or escaping of vital energy.

Marma Chikicha

Marma, the therapeutic tactile technique of Ayurveda is best described in *Sushruta Samhita* the classical Áyurvedic text. It has been said that *Marma* points lie on the vital areas of the body [21] and where muscles, blood vessels, tendons, bones and joints are in adjacent position. They have also been said as the meeting points of Váta, Pitta and Kapha, the three basic humours of life and said to influence body and mind greatly. Ayurveda stresses to apply pressure on these points during *abhyanga*or *Snehana* (oil bath) in such a way to bring back the altered life humors to normalcy and enable a healthy system. Marma Chikitsa can be compared with neuromuscular and orthopaedic science. According Ayurveda, there are 19 Marma points that, when stroked with a strong blow, can be fatal. In fact, in Ayurveda Marma Chikithsa was considered as battling technique. In olden days warriors had to have well versed knowledge of *Marmas* location, their number *(sankhya)*, size or measurement (*parimapa)* and prognostic value of afflictions over these points *(parinama bheda)*. The soldiers were even advised to use armour to protect their horses' Marma points while riding on them during battles. Practitioners used Marma-point manipulation to enhance healing the injured areas. Marma-point knowledge was mandatory for Áyurvedic surgeons. These points were supposed to be both anatomically and physiologically decisive. The strength and duration of pressure to be applied on these points depend on the age, disease and patient's pain threshold and type of *Marma point*. Manipulation techniques should be gentle in case of children, females and old people. Like that maximum pressure can be applied on *Sandhi*, *Asthi*, *Mansa* and *Snayu Marma* points can be given stronger pressure but not the *Sira Marma.* In Sanskrit Mari means death. The Sanskrit phrase, 'Maryanti Iti marmani', depicts the mortality and morbidity that is caused due to the wrong manipulation of these points. However when these Marma points are manipulated with optimal pressure and techniques smooth Prana (vital energy) flow is prompted along the nadis, which is a complex system of subtle channels. Sushruta Samhita briefly describes 107 Marma points in body. Primary Marma points correspond to seven Chakras (energy centers) of the body and from which minor points spread out laterally. These include 22 each on the lower limbs and on the arms, 12 on the front of the trunk, 14 on the back, and 37 on the head and neck. The human mind is thought be the 108th Marma.

Classification of *Marma*

In Áyurveda *Marma* points are classified in many ways and two of them are as follows.

Firstly, depending on the effects caused by the infliction [22], which is further classified as *Sadyahpranahara Marma* - causes immediate death due to sudden loss of *prana, Kalantarapranahara Marma* - death will occur in due course, Vaishalyaghna - occurs when these points injured by weapons; death will occur on removal of weapons, Vaikalyakara - when injured only deformity occurs, *Rujakara marma* - only severe pain is present without deformity. Secondly, depending on the location of *Marma* points, which are further classified as Mamsa Marma - related to muscles (there are 11 points), Shakha Marma - related legs and feet , Asthi Marma - related to bones with in the body (there are 8 points), Madhyamanga Marma is present in the trunk (it is present outside the body), Snayu Marma - related to Tendons and ligament (within the body, there are 27 Points), Jatrudhara Marma - is located in neck and head (present outside the body), Sandhi Marma - is related to joints present with in the body (there are 20 points), Shira Marma is related to nerves, veins and arteries (there are 41 points).

Significance of Marma

It removes the stumbling blocks along the intangible energy channels called *shrotas.* According to Ayurveda, vata increases as a person gets older which in turn causes degeneration. Marma therapy pacifies vatadosha; especially vyana vata and brings back it to normal. It creates physical, mental and emotional flexibility.

Comparison of External therapies

Concepts followed in *Varmam*, Acupuncture and *Marma* regarding external therapies are shown in Table 1. The comparison of energy concept in *Varmam* as *Vasi*, *qi* in Acupuncture, *Prana* in *Marma*. And the energy pathways are known as *Nadigal*, which are 12 in number in *Varmam*; Meridians / regular channels in Acupuncture, which are 14 in number and *Yogi Naadis* or *Shrothas* in *Marma*, which are 14 in number. Circulation of energy is known as flow of *Saram* in *Varmam*, flow of vital energy in Acupuncture and flow of *Prana* in *Marma*. Location of the points lie along the *Nadigal* in *Varmam*, lie along the Meridians in Acupuncture. Concept of the methods followed to locate the points in *Varmam* as *Viral Alavu* (finger measurement), In Acupuncture Cun measurement is followed and Cun measurement is based on patient's finger. In Marma, anguli measurement is followed to locate the Marma points. Confirmation of precision of Acupoints is deqi method and it is determined by monitoring patient after the completion of puncturing procedure. In Siddha *Varmam,* the strength of pressure in all the points is ¼ Mathirai and the manipulation time is 15 seconds. In Acupuncture the depth of the needle insertion ranges from 0.2 cun to 1 cun and the needle should be kept in position till *degi* is felt. In Ayurvedic *Marma*, neither the manipulation technique nor duration is specified. The locations of Varmam, Marma, and Acupoints are situated around similar areas for the management of Cervical Spondylosis and details of the same is in Table 2 and Figure 3 (a, b, c). But the manipulation methods are similar in Varmam, Marma except Acupuncture. In Acupuncture, puncturing method is followed.

DISCUSSION

From this study, sufficient evidences have been obtained that it has been demonstrated that all these external therapies for the management of cervical spondylosis in *Varma*, *Marma* and acupuncture are similar in their basic concepts, application except for a few modifications of the location and methods. In traditional Chinese system, the five elements refer to wood, fire, earth, metal and water. Human organs contain these elements. These elements can be compared to that of *Panchabootham* of *Siddha* system called ether, air, water, fire and soil. In Chinese system of medicine vital energy known as *qi* flows unobstructed throughout the body, within a closed or interconnected system consisting of seven symmetrical pairs of energy channels called meridians [23]. They can be compared to the *dhasa naadigal* of Siddha system. When *qi* circulation within the meridians is impeded, the primary universal forces namely *Yin* (associated with passivity) and yang (associated with activity) is thrown out of balance, thereby producing disease. Within this paradigm specific points along meridian acupoints, are manipulated [24]. Along with blood and body fluids *qi* maintains the normal vital activities of the human body. These can be compared with *vadha, pitha and kabha*, the three vital humors in Siddha [25] and Ayurveda. The environmental conditions, patient's age, constitution and others must be taken into account in acupuncture treatment. In Siddha system also we are following the same procedures before determining the treatment protocol. According to Chinese system of medicine, the appropriate points are selected on the basis of yin and *yang* status and the blocked meridians. Even in the Siddha literature that the author has searched for *Cakaṉavātham* [26] management (cervical spondylosis), the acupoints are selected to relieve the symptoms only and there are no particular prescription set of points for cervical spondylosis [27]. The magnitude of pressure given during Varmam manipulation in the above said points is ¼ mathirai. And that of depth of needle insertion in the corresponding acupoints is not more than 1 cun. While locating the acupoints or Varmam points, the finger measurements are to be used. The significant part is that both systems insist on using the patient's fingers for measuring. Hence it is very obvious that all the systems must have originated from a single primary system. When people migrated from place to place due to war, natural calamities etc., or for trading, there might have been sharing of the knowledge of this primary system. Also cultural exchanges among the races may also be one of the reasons. Then there might be development of other techniques and modifications in the techniques as per their need. Among all these three systems, Acupuncture of Chinese medicine is well established worldwide. In fact all the points and methodologies of acupuncture have been standardized. World health organization has accepted Acupuncture as a non pharmacologic strategy for pain management. However Varma of Siddha system has not found a place in the international field of medicine even though it has got many similarities in the basic concepts and methodologies with Acupuncture. The limitation of this study is that the author has only chosen a few points that are being utilized for cervical spondylosis. It is due to time and resources restrictions. This study can be extended to

other points mentioned for various diseases in these three traditional systems. So, the evidence for similarities and differences among these techniques can be well established.

CONCLUSION

In this study the author has proved that the *Varmam* points that are manipulated in Cervical Spondylosis are similar to those Acupuncture and Marma points. So we can use the parameters those have been utilized to standardize Acupuncture for standardizing Varmam therapy. If we do follow the appropriate research methodologies we can certainly make valid and reliable conclusions about the safety and therapeutic efficacy of *Varmam* and Marma techniques. Through them we can gain the trust and confidence of health care professionals from various specialties and apply these Indian traditional techniques for the wellbeing of mankind.

Sources of funding

None.

Conflict of Interests

The authors declare that there is no conflict of interests regarding the publication of this paper.

REFERENCES

1. Uthamarayan CS. *Siddha Maruthuvanga Churukkam.* 3rd ed. Chennai: Department of Indian Medicine and Homeopathy; 2003. p. 49, 768.
2. Mayil Vahanan Natarajan. Natarajan's Text book of Orthopedics and Traumatology. 8th ed. New Delhi: Wolters Kluwer (India) Pvt. Ltd; 2018.
3. Sturat L Weinsten, Joseph A Buckwalter. Editors. Turek's Orthopaedics Principles and their Application. 5th ed. Philadelhia: Lippincott Williams and Wilkins; 1994. p. 708.
4. Uthamarayan CS. *Thotrakirama Arachiyum Siddha Maruthuva Varalarum.* 3rd ed. Chennai: Department of Indian Medicine and Homeopathy; 2003. p. 444.
5. Venugopal PM. *Udal Thathuvam.* 3rd ed. Chennai: Department of Indian Medicine and Homeopathy; 1993.
6. Shunmugom N. *Adippadaik kalvi kai bagam - Sei bagam* with colour photos. 3rd ed.
7. Coimbatore: Thirumoolar Varmalogy Institute; 2016. p. 22, 70-71
8. Kannan Rajaram T. *Varma* points and simulation methods on the basis of Thread Measurement techniques in *Varma* Therapy. 2nd ed. Kaniyakumari: Centre for *Varma* Medicine and Research; 2015. p. 2.
9. Kannan Rajaram T. A Text book of *Varmam.* 2nd ed. Kanniyakumari: A.T.S.V.S Siddha Medical College; 2017. p.12
10. Kannan Rajaram T. *Varma* points and Relieving methods on the basis of finger measurement techniques in *Varma* therapy. 2nd ed. Kanniyakumari: Centre for *Varma* Medicine and Research; 2015. p. 2.
11. Shunmugom N. *Adippadaik kalvi kai bagam - Sei bagam* with colour photos, 3rd edition,
12. Thirumoolar varmalogy Institute, Coimbatore, 2016.70-71p
13. Thiyagarajan R , *Siddha Maruthuvam Sirrappu*, 5th ed. Chennai: Department of Indian Medicine and Homeopathy; 2017. p. 171.
14. Kannan Rajaram T. A Text book of *Varmam*, Second Edition, A.T.S.V.S, Siddha Medical College, Kanniyakumari, 2017, ISBN-978-93-80288-15-4
15. Anton Jayasuriya. Clinical Acupuncture. Reprint edition. New Delhi: B. Jain Publishers
16. (P) Ltd; 2005
17. Wang Y, Ma C, Li L, Zhang T, Gui X, Chen H. Effects on cervical spondylosis of vertebral artery type and the concentrations of plasma NPY and UII in the patients treated with the modified Acupuncture at unilateral/bilateral Renying (ST 9). Zhongguo Zhen Jiu 2018;12: 38(5):4733-7. http://dx.doi.org/10.13703/j.0255-2930.2018.05.006.

18. Irnich D, Behrens N, Gleditsch JM, Stör W, Schreiber MA, Schöps P, et al. Immediate effects of dry needling and Acupuncture at distant points in chronic neck pain: results of a randomized, double-blind, sham-controlled crossover trial. Pain 2002;99:83-89. http://dx.doi.org/10.1016/s0304-3959(02)00062-3.
19. Qin YG. Clinical observation on therapeutic effect of warming needle at spinal nerves for treatment of cervical spondylosis of nerve root type. Zhongguo Zhen Jiu 2010;30:121-3.
20. Ben-hua LUO, Jing-xian HAN. Cervical Spondylosis Treated by Acupuncture at Ligou (LR 5) Combined with Movement Therapy. Journal of Traditional Chinese Medicine 2010;30(2):113-117. https://doi.org/10.1016/S0254-6272(10)60025-8.
21. Yu S. The Therapeutic Effects of Triple Puncture and Routine Body Needling for Cervical Spondylosis. J Tradit Chin Med 2003;23(4):282-283.
22. Zhang H, Guo M, Lu X. Pulse changes in patients with cervical spondylosis before and after Acupuncture treatment. J Tradit Chin Med 2016;36(1):63-70. https://doi.org/10.1016/S0254-6272(16)30010-3
23. Claudia Focks. Atlas of Acupuncture. 1st ed. Philadelphia: Elsevier; 2008.
24. Kaviraj Kunjal Lal Bhisharatna, Editior. The Susruta Samhita. Calcutta. 1911. p. 173.
25. "https://www.nhp.gov.in/marma-theraphy_mtl "
26. Weaver MT. Acupressure: an overview of theory and application. Nurse Pract 1985;10(8):38-9,42.
27. Kreitzer MJ, Koithan M, Editors. Integrative nursing. 1st ed. New York: Oxford University Press; 2014. p. 3-16.
28. Shanmugavelu M. *Noi Nadal Noi Mudal Nadal Thirattu*. 3rd ed. Chennai: Department of Indian Medicine and Homeopathy; 2003.
29. Kuppusamy Mudaliyar KN, *Siddha Maruthuvam(Pothu)*, 6th ed. Chennai: Department of Indian Medicine and Homeopathy; 2004.
30. White P, Lewith G, Prescott P, Conway J. Acupuncture versus Placebo for the Treatment of Chronic Mechanical Neck Pain A Randomized, Controlled Trial, Ann Intern Med. 2004;141:911-919. https://doi.org/10.7326/0003-4819-141-12-200412210-00007

Table 1. Comparison of basic concepts of *Varmam*, Acupuncture and *Marma*

S.No	Concepts	*Varmam*	Acupuncture	*Marma*[21]
1	Energy	*Vaasi* [7]	*Qi* [15]	Prana
2	Energy pathway	*Naadigal* 12	14 regular Channels / Meridians [15, 16, 23]	14 *yogic naadis*/ *shrothas*
3	Circulation of energy	Occurs as flow of *Saram* (*Sara Otam*)	Occurs as flow of vital energy	Occurs as flow of *Prana*
4	Location of points	lie along the *naadigal*[12]	lie along the channels / meridians	No clear evidence; may be linked with *naadis*
5	Criteria for choosing points	No standard prescription. The points are chosen on the basis of symptoms	No standard prescription. The points are chosen on the basis of symptoms	No such concept observed
6	Methods followed to locate the points	*Viral alavu*(finger measurement) [9]	*Cun* measurement is based on patient's fingers	*Anguli*(finger) measurements of the patients
7	Specific order in the manipulation of points	Present	Present	Not specified
8	Effect of manipulation technique on therapeutic action	Depending upon pressure & manipulation, action of Varma points may	No such concept observed	No such concept observed

		change		
9	Concentration on breathing	Patient has to concentrate on breathing	Patient has to concentrate on breathing	No such concept observed
10	Confirmation of precision of points	No such concept observed	Done by deqi sensation	No such concept observed
11	Duration of manipulation	15 – 30 seconds	Up to feel of de*qi* is obtained – up to ½ hr	Not specified
12	Number of sittings	Depends on severity of the disease	Depends on severity of the disease [20]	No such concept observed
13	Days in which *Varmam* is preferred to be done	Good to be done on Thursday	No such concept observed	No such concept observed
14	Associated therapeutic technique	*Thadaval / Adangal / Pilichal* [11]	*Tuina*	*Abhyanga*
15	Contraindication	Not to be done on inflamed	Not to be done on inflamed	No such concept observed areas areas

Table 2. Comparison of Varmam [10], Acupuncture [13] and Marma [21] points for Cervical Spondylosis

S.No	System	Points	Location
4	Siddha	*Mudichu Varmam*	Over spinous process of C7
	Acupuncture	Du-14 Great Vertebra	On the midline, below the spinous process of the 7th cervical vertebra (C7)
	Ayurveda	Nil	Nil
5	Siddha	*Kaakattai Varmam*	Three finger lateral to the junction of neck with Shoulder (near Supra Clavicular fossa)
	Acupuncture	QUEPEN Empty BasinST-12	Lies in supraclavicular fossa, above clavicular midpoint, roughly 4 *cun* lateral to the anterior midline.
	Ayurveda	*Apastambha*	base- mid collarbone area
6	Siddha	*Kaisulukki Varmam*	4 inches below C7 & 3 fingers lateral to vertebral column near the medial border of scapula.
	Acupuncture	*SHENTANG* BL-44 Spirit Hall	3 *cun* lateral to the posterior midline, on the level of thelower border of the spinous process of the 5th thoracic vertebra (T5)
	Ayurveda	*Ansaphalaka*	above mid shoulder blade
4	Siddha	*Sippi Varmam*	Just below inferior angle of the scapula
	Acupuncture	*GEGUAN* BL-46 *Diaphragm's Gate*	3 *cun* lateral to the posterior midline, on the level of thelower border of the spinous process of the 7th thoracic vertebra (T7).

	Ayurveda	Brihati	between shoulder blade
10	Siddha	*Sayvu Varmam*	4 inch below the anterior axillary fold along the medial boarder of arm
	Acupuncture	P2	2 cun inferior to the axillary fold
11	Siddha	*Kavuli Varmam*	Web area between thumb & index finger
	Acupuncture	HEGU L.I.-4 Joining Valley	On the radial aspect of the hand, between 1st and 2nd metacarpal bones, closer to the 2nd metacarpal boneand approximately at its midpoint.
	Ayurveda	*Kshipra*	between thumb and index finger.
12	Siddha	Kaimootu *Varmam*	Center of the Cubital fossa
	Acupuncture	CHIZE LU-5 Cubit Marsh	In the cubital crease, on the radial aspect of the tendonof the biceps
	Ayurveda	*Kurpara*	on elbow joint
13	Siddha	Manibanthaga *Varmam*	Centre point of ventral aspect wrist joint
	Acupuncture	DALING P-7 Great Mound	Anterior wrist joint space (most distal wrist crease)
	Ayurveda	*Manibandha*	on the ventral aspect of the wrist joint
14	Siddha	*Koli Kaluthu Varmam*	Medial & lateral point of wrist
	Acupuncture	LU 9/ *TAIYUAN Supreme Abyss*	On the ventral aspect of the wrist, at the level of most distal wrist crease, on the radial aspect of the radial artery and ulnar to the tendon of the abductor pollicis longus muscle.
		Yang Valley	On the medial aspect of the wrist
		YANGGU 5.I.-5	
	Ayurveda	Nil	Nil

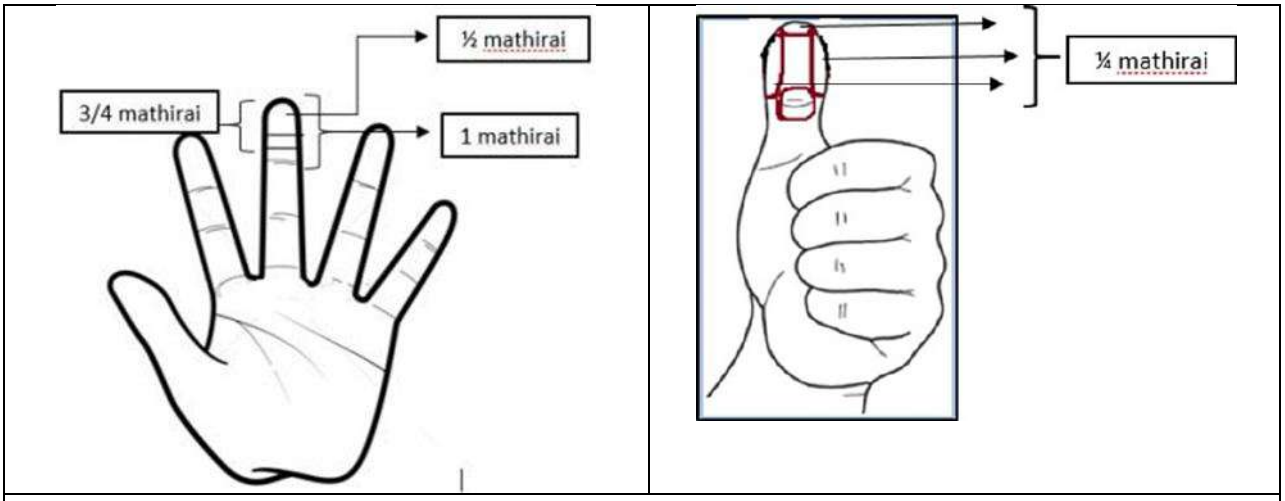

Figure 1. Pressure measurements in Varmam

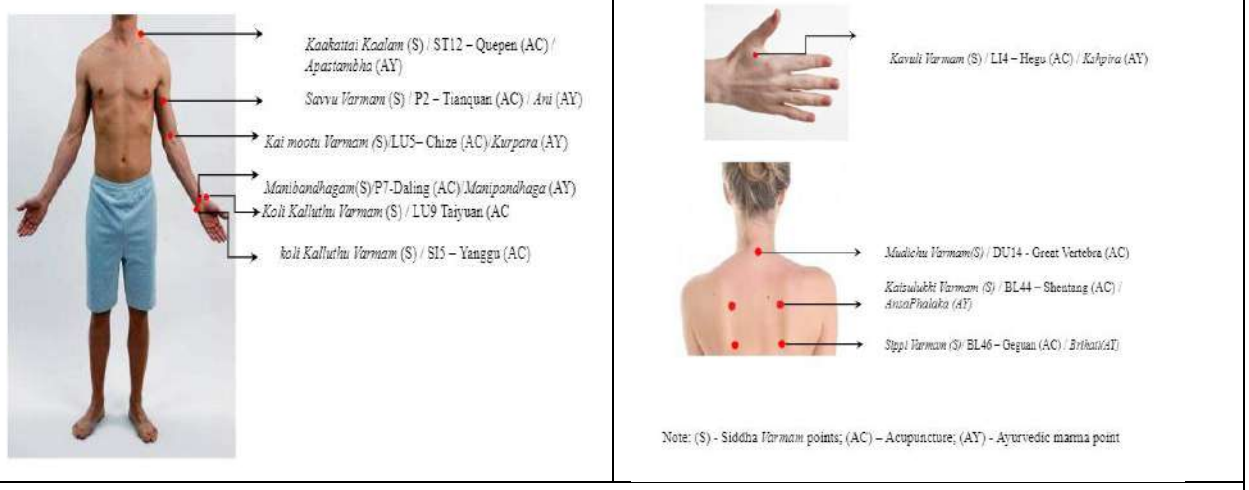

Figure 2. Comparison of location of *Varmam*, Acupuncture and *Marma* points (a)

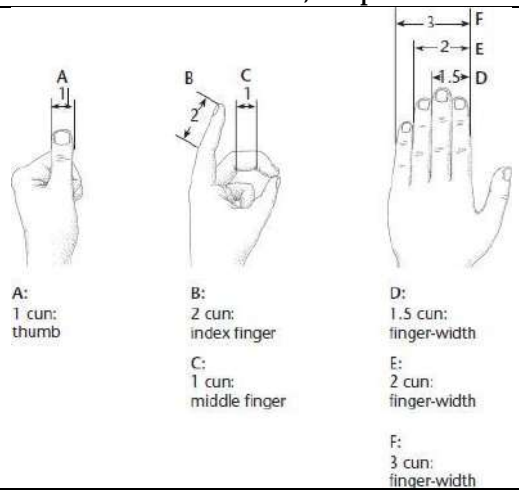

Figure 3. Finger measurements in Acupuncture

RESEARCH ARTICLE

KAP Evaluation of the Materiovigilance Program: A Comparison of Students in B Pharm and M Pharm

Ramish Khan, Arfa A Sayed, Shamita Shyam Sail, Akshata Gore, Agadi Hiremath Viswanatha Swamy and Sanatkumar Bharmu Nyamagoud*

Department of Pharmacy Practice, KLE College of Pharmacy, Vidyanagar, Hubballi -580031. A Constituent unit of KLE Academy of Higher Education and Research, Belagavi, Karnataka, India.

Received: 26 Sep 2024 Revised: 05 Dec 2024 Accepted: 21 Jan 2025

***Address for Correspondence**
Sanatkumar Bharmu Nyamagoud
Assistant Professor and Head,
Department of Pharmacy Practice,
KLE College of Pharmacy,
Vidyanagar, Hubballi.
A Constituent unit of KLE Academy of Higher Education and Research,
Belagavi, Karnataka, India.
E.Mail: dr.sanathnyamagoud@gmail.com

ABSTRACT

Materiovigilance systematically monitors adverse events related to medical devices, which require ongoing safety surveillance due to potential malfunctions. The Indian government launched the Materiovigilance Programme of India (MvPI) in 2015 to address these concerns. Medical devices are crucial in healthcare, but malfunctions can lead to serious consequences. Recognizing this, the WHO proposed a diagnostic list akin to the essential medicines list. This study examines the knowledge, attitude, and perception (KAP) of B Pharm and M Pharm students regarding materiovigilance to enhance their involvement in monitoring and reporting adverse events of medical devices. This cross-sectional study was conducted at KLE College of Pharmacy, Hubballi, involving 268 participants. A pre-test with 15 questions was followed by an educational session, then the same test was administered as a post-test. Data were analyzed using t-tests and Cronbach's alpha. There was a higher female participation (53.35%), with most students from non-medical backgrounds (87.68%). Significant knowledge and attitude improvements were observed post-education, particularly among M Pharm students. Educational interventions significantly improved knowledge, attitudes and perception towards materiovigilance amongst both the B Pharm and M Pharm students respectively with B Pharm students showing an overall significant improvement as compared to M Pharm. The study highlighted the need for continuous education to enhance student's active participation in the field of Materiovigilance.

Keywords: Materiovigilance, pharmacy, students, reporting, patients safety.

INTRODUCTION

The coordinated system for identifying, collecting, reporting, and analyzing adverse events related to medical devices is known as materiovigilance [1]. The use of medical devices in healthcare is rapidly growing as they play a crucial role in diagnosing, monitoring, and treating various diseases and conditions. Recognizing their increasing importance, the World Health Organization has recommended an essential diagnostic list, similar to the essential drug list[2]. Despite their critical role, there have been numerous instances of medical device failures, such as infants dying from incubator short circuits or hip implants causing septicaemia and malunion. These incidents underscore the necessity for continuous monitoring of medical device safety and effectiveness. Active materiovigilance can help identify and mitigate potential risks associated with medical devices to ensure patient safety[3]. In response to these concerns, the Indian government launched the Materiovigilance Program of India (MvPI) in 2015, under the IPC Ghaziabad and managed by the Ministry of Health and Family Welfare[4].This program aims to monitor adverse events related to medical devices, educate healthcare professionals on the importance of reporting these events, and generate unbiased, reliable safety data[5]. The COVID-19 pandemic has seen extensive use of medical devices such as gloves, masks, sanitizers, swab kits, and pulse oximeters, leading to some adverse events associated with these devices. To ensure accurate data collection on these adverse events, MvPI has developed a specialized Personal Protective Equipment (PPE) form[6]. Pharmacy students, particularly those pursuing B Pharm and M Pharm degrees, play a vital role in healthcare delivery and materiovigilance. However, research indicates that medical professionals, including pharmacy students, often lack knowledge about materiovigilance. This study aims to assess the Knowledge, Attitude, and Perception (KAP) of B Pharm and M Pharm students regarding materiovigilance. By identifying areas for improvement and developing targeted educational interventions, the study seeks to enhance the involvement of these students in materiovigilance activities. This, in turn, will improve patient safety and the overall quality of healthcare delivery.

MATERIALS AND METHODS

Study site

The study was conducted at KLE College of Pharmacy, Vidyanagar, Hubballi.

Study design

It was a cross-sectional, self-designed questionnaire-based study designed to evaluate the Knowledge, Attitude, and Perception of Materiovigilance among students of M Pharm and B Pharm students studying in KLE College of Pharmacy, Vidyanagar, Hubballi. A set of 15 questions were provided as a part of pre-test to the study participants and were instructed to fill the form (Google form). After the completion of pre-test, participants were exposed to an educational session which covered all the information related to the questions provided with the help of power point presentation. The same set of 15 questions were sent to the participants after the educational session for collecting the responses of post-test.

Ethical Approval

Ethical clearance was obtained from institutional ethical committee, KLE College of Pharmacy, Hubballi. IEC No. KLECOPH/IEC/2023-24/01.

Study period

The study involved planning of one month, data collection and interpretation for three months and two months respectively at KLE College of Pharmacy, Vidyanagar, Hubballi, Karnataka.

Study criteria

Inclusion criteria: Students enrolled in M Pharm and B Pharm stream in KLE College of Pharmacy, Hubballi.

Exclusion criteria: Pilot study participants were excluded from the study and students who were willing to participate in the study

Study Procedure

The faculty of the Department of Pharmacy Practice developed 15 MvPI questionnaires to evaluate three domains: Knowledge, Attitude, and Perception. The questionnaires were divided into five questions, with questions in the Knowledge domain being dichotomous and the Attitude and Perception domains using a 5.0-point Likert scale. The internal consistency of the questionnaires was evaluated using IBM SPSS 27.0 and Cronbach's alpha (α), with an α of 0.827, indicating good internal consistency. The questionnaire was distributed among 268 participants as part of a pilot survey, with 208 B Pharm participants and 60 M Pharm participants, resulting in an α of 0.827, indicating acceptable internal consistency. A pre-test was conducted, followed by a brief educational session on the topic, including definitions, aim, regulatory body, history, reporting, and types of medical devices. The same set of 15 questions was re-distributed to participants through Google forms, and responses were recorded in a post-test.

Statistical analysis

The data was entered into a Microsoft Excel spreadsheet, presented as mean ± standard deviation, and analyzed using a t-test to compare differences between groups, and descriptive and inferential statistical analyses were conducted using Excel and SPSS version 27.

Sample size

$$N = \frac{[Z_{1-\alpha/2}]2\ p\ (1-p)}{d2}$$

Where, Z is critical value,
d is allowable error,
p is sample proportion,
α is level of significance.

RESULTS

Demographic details of study participants

Table1: Demographic details of Mv participants.

The study population consisted of 268 participants, with a majority being female (53.35%) and the remainder male (46.64%). The participants ranged in age from 18 to 25 years, with the largest age group being 21 years (24.25%), followed by 22 years (16.04%) and 23 years (14.55%). The participants were predominantly from the D Pharm group (77.61%), while the rest were M Pharm students (22.38%). Most participants came from non-medical family backgrounds (87.68%), with only a small proportion from medical backgrounds (12.31%). In terms of socioeconomic status, the largest group belonged to the upper middle class (30.97%), followed by the lower class (26.11%) and lower middle class (23.50%). The majority of the participants resided in urban areas (64.14%), with the remaining 35.82% living in rural areas.

Evaluation of Knowledge among B Pharm and M Pharm students

Table2: Knowledge of Mv among B Pharm and M Pharm students.

Table 2 exhibited M Pharm students (N=60), with a higher percentage of correct responses for increased awareness and improved comprehension in areasranging from 40% to 90% for the Mv program, 48.33% to 96.67% for medical device classification, 71.67% to 96.67% the procedure for AE reporting, 43.33% to 85% for encountering AE involvingmedical devices, and 45% to 90% for medical device warnings and recalls. Pre-test knowledge of the MvPI amongB pharm students (N=208) were 31.25%, which rose to 91.35% in the post-test. In contrastof medical device classification, it improved from 32.69% to 89.90%, respectively. From 33.65% to 88.20%,there was also a significant

increase in awareness of reporting adverse events involving medical devices. From 35.10% to 86.06%reporting became more widely recognized. Lastly, knowledge about alerts or recalls of medical devices increased from 32.69% to 85.58%. Therefore, knowledge was assessed for both B Pharm and M Pharm students regarding the MvPI and its consciousness about medical device utilization, where data depicted a significant better improvement among M Pharm students in post-test compared to B Pharm. Table 3: T-test analysis of Knowledge factor between B Pharm and M Pharm The t-test analysis compared the pre- and post-test results of B. Pharm and M. Pharm students. M Pharm students (N=60) scored 2.48 (Sd.Dev 1.867), on the pre-testwith a p-value less than 0.001. In the post-test, M Pharm students scored 4.58 (Sd.Dev 1.030), again with a p-value below 0.001. The mean pre-test score for B Pharm students (N=208)was 1.65 (Sd.Dev 1.867), and the mean post-test score increased to 4.41 (Sd.Dev 1.308). The p-values for both groups were less than 0.001, indicating that the improvements in knowledge were statistically significant ($p<0.05$) and hence there was substantial improvement in both the streams and indicated that M Pharm participants showed more pronounced improvement in the post-test, respectively.

Evaluation of Attitude among B Pharm and M Pharm students

Table 4: Attitude of Mv among B Pharmand M Pharm students.

The table 4 presented M Pharm students' attitude, with the percentage of those who strongly agreed or agreed that medical devices can cause adverse events increasing from 55% in the pre-test to 68.33% in the post test. From 68.34% to 71.67%the proportion of students who strongly agreed and agreed that it was important to report adverse events caused by medical devices increased.There was a percentage increase from pre-test to post-test for the various other questions, indicating a positive shift in their attitudes. The percentage of medical devices that can cause adverse events increased from 39.90% to 70.67% among B Pharm students, those who strongly agreed and agreed respectively. In the case of B Pharm, significance in training intervention increased from 60.1% to 79.8% when agreeing on materiovigilance. Results from the post-test show that both groups have improved, with B Pharm showing higher levels of overall attitude and a significant increase in positive responses (such as "strongly agree" and "agree"). The data suggest that M. Pharm. students had more materiovigilance-related foundational knowledge, but B. Pharm. students' post-test responses showed more positive shifts, suggesting that both groups were effective. Table 5: T-test analysis of Attitude factor between B Pharm and M Pharm The t-test results that followed the intervention revealed a significant change. In the post-test, the difference was no longer significant, as M Pharm students scored mean that increased to 18.58 (Sd.Dev 6.614), with a p-value of 0.261whereas in pre-test scored a mean of 17.28 (Sd.Dev 5.428). Attitudes about the MvPI and the significance of medical device reporting significantly improved in pre-mean scores of B Pharm students (16.63), which increased to post-mean (18.82). Overall, B Pharm's intervention improvement was more evident than that of M Pharm.

Evaluation of Perception among B Pharm and M Pharm students

Table6:Perception of Mv among B Pharm and M Pharm students.

The table 6 presents the outcomes of M Pharm students (N=60).The percentage of students who strongly agreed or agreed that the Mv Program can generate evidence-based data on the safety of medical devices increased from 61.67% in the pre-test to 80% in the post-test. The percentage of those who strongly agreed or agreed that one report of an adverse event related to a medical device can make a difference in the healthcare system increased from 76% to 86.66%. There was a percentage increase from pre-test to post-test for the various other questions, indicating a positive shift in their perception.For B Pharm students' (N=208) perceptions of materiovigilance before and after the educational intervention, students demonstrated good agreement on all perception-based questions, indicating that a stronger foundational understanding of materiovigilance needs to be developed. In B Pharm, there were significant improvementsi.e., 78.83%, following the intervention. They received a score of 36.54% in the pre-testfor reporting unfavourable events leading to significant improvement. of 78.37% in the post-test. Lastly, B Pharm students made significant advancements, frequently surpassing M Pharm students or even closing the gap in some areas. Despite M Pharm students maintaining a higher baseline and consistently improving, the intervention significantly improved the perceptions of B Pharm students. This suggests that the intervention was successful in improving the students' perceptions of the importance of materiovigilance among pharmacy students. This highlights the significance of educational efforts in terms of perceptions regarding materiovigilance and its reporting of adverse events. Table 7:

T-test analysis of Perception factor between B Pharm and M Pharm Pre-test scores between B Pharm students (mean 17.16, Sd.Dev 4.785) and M Pharm students (mean 17.20, Sd.Dev 5.784) were not significantly different, according to the t-test, with a p-value of 0.19 and less than 0.01. However, M Pharm students maintained a mean score of 19.75 (Sd.Dev 5.461) on the post-test, while B Pharm students scored 19.13 (Sd.Dev 4.864). M Pharm students had improved scores by the time the assessment was over. Although B Pharm and M Pharm students scored similarly in the pre-test, by the end of the assessment, M Pharm students had improved scores.

Evaluation of Knowledge, Attitude, and Perception (KAP) domains between B Pharm and M Pharm students regarding Mv

The participants responses were categorised into three levels based on their total scores in each domain namely Poor, Moderate, and Good. The Table 8 summarizes the structure and scoring for three evaluation domains: Knowledge, Attitude, and Perception. Table 8: Scoring and categorization of KAP domains Table 9: Comparison of KAP factors between BPharm and M Pharm In terms of the Knowledge, Attitude, and Perception (KAP) factors, the data demonstrated that M Pharm students performed better than B Pharm students.B Pharm students received a score of 180 out of 208 for "Good" knowledge, while M Pharm students received 53 out of 60, and B Pharm scored higher on "Poor" 21 out of 208 compared to M Pharm students i.e.,3 out of 60. Similarly, M Pharm students scored higher on "Good" for attitude of 42 compared to B Pharm students that was 151. For perception, M Pharm students scored higher on "Good" which was 47 compared to B Pharm students155. Overall, M Pharm students portrayed better Knowledge and Perception, whereas B Pharm students portrayed better positive Attitude as compared to M Pharm.
Figure1: Post-test KAP of B Pharm Figure 2: Post-test KAP of M Pharm

DISCUSSION

Healthcare professionals in the study by MB Abhima *et al*. demonstrated a moderate level of knowledge, with 52% knowing of the ongoing initiative in India for tracking adverse events related to medical devices (MDAE). Comparably, just 40% of medical professionals in study of Selvam S *et al.* were aware of materiovigilance, demonstrating a considerable knowledge gap[7,8]. In contrast, our study showed that pharmacy students' knowledge had significantly improved; after the intervention, B Pharm students' awareness increased significantly from 31.25% to 91.35%. This indicates that educational interventions may be able to raise pharmacy students' knowledge levels above the baseline knowledge levels found in healthcare workers in previous studies. There is a discrepancy between knowledge and practice, as evidenced by the study by MB Abhima *et al.,* which revealed that although 28.2% of healthcare professionals experienced adverse events, only 10.3% reported them. Similar problems were brought to light by the Selvam S *et al* study, which found that only 56 out of 220 respondents had reported an MDAE and that 65% of healthcare workers were uninformed that their hospitals reported MDAEs[7,8].Our study, on the other hand, concentrated more on perception than practice and showed significant gains in students' views of the significance of materiovigilance and reporting. According to the perception data from our study, B Pharm students in particular had higher levels of belief in the Mv Program's efficacy and the significance of reporting adverse occurrences. Together, the studies by Samar *et al*., Rehman S *et al*., and ourselves demonstrate the value of educational interventions in enhancing healthcare workers' attitudes and understanding on materiovigilance. According to Samar *et al*.'s study, 12% of interns actively reported adverse events, indicating a practice gap despite strong initial awareness and attitudes[9]. Following a training session, nursing professionals showed a remarkable improvement in knowledge and favourable perceptions, reaching 100% awareness and significant alterations in attitudes, according to research by Rehman S *et al*[10]. Both B Pharm and M Pharm students significantly improved in knowledge and attitudes, according to our study. Even with these encouraging results, studies consistently find that it is difficult to translate better knowledge and attitudes into actual reporting habits. This underlines the need of focusing on perception in educational initiatives aimed at improving the safety culture in healthcare as a whole. Our study, in contrast to the studies of MB Abhima *et al.* and Selvam S *et al.*, concentrated on perception, revealing an important yet sometimes overlooked aspect. Because perception studies offer insight on the underlying attitudes and beliefs that influence behaviour. By addressing certain misconceptions and obstacles with customized educational interventions, it is

possible to enhance the efficacy of materiovigilance techniques through a better understanding of perceptions. In order to ensure that pharmacy students have the information and mentality necessary to actively participate in materiovigilance initiatives, it is fundamental that they focus on perception as it provides a foundation for their future professional behaviour. Despite having moderate to good knowledge and attitudes regarding materiovigilance, healthcare workers in studies MB Abhima *et al* and Selvam S *et al* revealed notable gaps in practice[7,8]. According to our research, pharmacy students were greatly benefited from focused educational interventions in terms of knowledge, attitude, and perception. The development of a thorough understanding and positive mindset toward materiovigilance, which in turn improves patient safety and healthcare outcomes, depends heavily on the priority that is placed on perception in educational programs. To provide a comprehensive approach to materiovigilance education, future research should keep examining how educational interventions affect perception.

CONCLUSION

The study confirmed noteworthy improvements in the knowledge, attitude, and perception of B Pharm and M Pharm students regarding materiovigilance following educational interventions. Both groups showed considerable gains in their understanding of materiovigilance, with B Pharm students exhibiting a prominent growth post-intervention despite M Pharm students having a higher baseline knowledge. There was a marked positive shift in attitudes towards the importance of reporting adverse events allied with medical devices, particularly among B Pharm students, indicating that targeted interventions can significantly enhance the perceived responsibility and willingness to report such events. Additionally, the intervention significantly improved the perception of the importance and effectiveness of the materiovigilance program, with B Pharm students showing a more pronounced improvement compared to M Pharm students. These findings highlight the critical role of perception-focused educational efforts in encouraging a hands-on safety culture in healthcare system. Continuous educational programs are essential to bridge the gap between knowledge and perception, ensuring that pharmacy students are well-equipped to actively participate in materiovigilance, ultimately enhancing patient safety and healthcare outcomes. This study underscores the necessity of integrating perception, alongside knowledge and attitude, into educational strategies to cultivate a comprehensive understanding and commitment to materiovigilance among future healthcare professionals.

CONFLICT OF INTEREST

The authors declare that there are no conflicts of interest.

ABBREVIATIONS

A: agree; AE: Adverse Events; B Pharm: Bachelor of Pharmacy; D: disagree; IPC: Indian Pharmacopoeia Commission; KAP: knowledge, attitude, perception; M Pharm: Master of Pharmacy; MDAE: medical device adverse event. Mv: Materiovigilance; MvPI: Materiovigilance Program of India; N: neutral; PPE: Personal Protective Equipment; SA: Strongly agree; SD: strongly disagree; Sd.Dev: Standard deviation; SPSS: Statistical Packages of Social Sciences.

REFERENCES

1. Mandanna SS, Kr S, S NR, Raju SS. A questionnaire-based study to assess the awareness of materiovigilance among health-care professionals working in a tertiary care teaching hospital in the Kurnool district. Asian Journal of Pharmaceutical and Clinical Research. 2023 Nov 7 ;177–80.
2. Panchal Y, Vyas B, Suthar K, Shah K. A study of assessing knowledge, attitude, and practice of materiovigilance among medical surgeons of Gujarat. National Journal of Physiology, Pharmacy and Pharmacology. 2022;(0):1.
3. Manna N, Mazumdar SD, Panchanan P, Das S. A study of assessing knowledge, attitude, and practice of materiovigilance among staff nurses in Medical College and Hospital, Kolkata. National Journal of Physiology, Pharmacy and Pharmacology. 2023 Jun 30 ;13(7):1584–4.

4. Date AP, Date AA, Siddiqui RA, Shende TR, Salanka HV, Quazi SH *et al*. Materiovigilance programme of India: a step towards patient safety. Int J Basic Clin Pharmacol2023;12:621-5.
5. Raju N, Deivigarajan S, Santhakumar S, Balamurugan S. Knowledge, attitude and practice of materiovigilance among nurses and healthcare technicians in a tertiary care hospital: A questionnaire-based survey. Open Access Research Journal of Biology and Pharmacy [Internet]. 2023 [cited 2024 Aug 3];9(1):038–44.
6. Samal S, Naik M, Behera S. Medical devices associated adverse events under Materiovigilance Programme of India in a Tertiary Care Hospital of Tribal District of Odisha. National Journal of Physiology, Pharmacy and Pharmacology. 2022;(0):1.
7. MB A, Philip S, Knowledge attitude and practices of materiovigilance among the medical professionals in a tertiary care centre: a cross-sectional study. 2023; 5 (4); 1100-1103.
8. Selvam S, Prassath R, Babu IJ, Raja S, Rajarathinam N. Knowledge attitude and practice of materiovigilance among healthcare professionals in tertiary care hospitals. International Journal of Basic & Clinical Pharmacology. 2024 Apr 25;13(3):358–63
9. Samar A, Sahana GN, Deepak P, Nagaral JV, Saranyaa M. Assessment of knowledge, attitude, and practice of materiovigilance among interns in a tertiary care institute: A cross-sectional study. Natl J Physiol Pharm Pharmacol 2024;14(07):1301-1303.
10. Rehman S, Ray A, Pandit S. Materiovigilance: Impact of awareness cum sensitization programme on healthcare professionals of a tertiary care teaching hospital in South Delhi. IP International Journal of Comprehensive and Advanced Pharmacology. 2022 Aug 15;7(3):146

Table.1: Demographic details of Mv participants

Demographics	**Characteristics**	**N=268 (%)**
Gender	Female	143 (53.35)
	Male	125 (46.64)
Age in years	18	27 (10.07)
	19	38 (14.17)
	20	31 (11.56)
	21	65 (24.25)
	22	43 (16.04)
	23	39 (14.55)
	24	24 (8.95)
	25	07 (2.61)
Study group	M Pharm	60 (22.38)
	D Pharm	208 (77.61)
Parents profession	Non-medical background	235 (87.68)
	Medical background	33 (12.31)
Socioeconomic status	Lower class (< 1 lakh Rupees per year)	70 (26.11)
	Lower middle class (2 to 5 lakh Rupees per year)	63 (23.50)
	Upper class (> 10 lakh Rupees per year)	18 (6.71)
	Upper lower class (1 to 2 lakh Rupees per year)	34 (12.68)
	Upper middle (5 to 15 lakh Rupees per year)	83 (30.97)
Residence	Rural	96 (35.82)
	Urban	172 (64.14)

Table 2: Knowledge of Mv among B Pharm and M Pharm students

Sl. No	Knowledge based questions	B Pharm(N=208)				M Pharm (N=60)			
		Pre test [N (%)]		Post test [N (%)]		Pre test [N (%)]		Post test [N (%)]	
		Correct	Incorrect	Correct	Incorrect	Correct	Incorrect	Correct	Incorrect
01	Are you aware of the ongoing Materiovigilance Programme of India?	65 (31.25)	143 (68.75)	190 (91.35)	18 (8.65)	24 (40)	36 (60)	54 (90)	6 (10)
02	Are you aware that the medical devices are classified into 4 categories (Category A, Category B, Category C and Category D)?	68 (32.69)	140 (67.31)	187 (89.90)	21 (10.10)	29 (48.33)	31 (51.67)	58 (96.67)	2 (3.33)
03	Are you aware of how and whom to report the adverse events caused by the medical devices?	70 (33.65)	138 (66.35)	183 (88.20)	25 (12.02)	43 (71.67)	17 (28.33)	58 (96.67)	2 (3.33)
04	Have you come across any means/forms of reporting adverse events related to medical devices?	73 (35.10)	135 (64.90)	179 (86.06)	29 (13.94)	26 (43.33)	34 (56.67)	51 (85)	9 (15)
05	Have you come across any alerts or recall about medical devices?	68 (32.69)	140 (67.31)	178 (85.58)	30 (14.42)	27 (45)	33 (55)	54 (90)	6 (10)

Table 3: T-test analysis of Knowledge factor between B Pharm and M Pharm

Sl. No.	Stream	N	Mean ± Sd. Dev		p-value
			Pre	Post	
01	B Pharm	208	1.65±1.867	4.41±1.308	<0.001*
02	M Pharm	60	2.48±1.867	4.58±1.030	<0.001*

*Significantly significant p<0.05

Table 4: Attitude of Mv among B Pharmand M Pharm students

Sl. No	Attitude based questions	B Pharm (N=208)										M Pharm (N=60)									
		Pre test [N (%)]					Post test [N (%)]					Pre test [N (%)]					Post test [N (%)]				
		SA	A	N	D	SD	SA	A	N	D	SD	SA	A	N	D	SD	SA	A	N	D	SD
01	Do you agree that medical devices can cause adverse events?	12 (5.77)	71 (34.13)	88 (42.31)	16 (7.69)	21 (10.10)	44 (21.15)	103 (49.52)	25 (12.02)	11 (5.29)	25 (12.02)	5 (8.33)	28 (46.67)	14 (23.33)	5 (8.33)	8 (13.33)	17 (28.33)	24 (40)	2 (3.33)	3 (5)	14 (23.33)
02	Do you agree that it is important to report the adverse events caused by medical devices?	37 (17.79)	78 (37.50)	56 (26.92)	19 (9.13)	18 (8.65)	52 (25.00)	103 (49.52)	17 (8.17)	12 (5.77)	24 (11.54)	13 (21.67)	28 (46.67)	6 (10)	5 (8.33)	8 (13.33)	23 (38.33)	20 (33.33)	4 (6.67)	2 (3.33)	11 (18.33)
03	Do you agree that training on materiovigil	34 (16.35)	91 (43.75)	52 (25.00)	13 (6.25)	18 (8.65)	56 (26.92)	110 (52.88)	10 (4.81)	10 (4.81)	22 (10.58)	15 (25)	22 (36.67)	8 (13.33)	4 (6.67)	11 (18.33)	22 (36.67)	23 (38.33)	4 (6.67)	1 (1.67)	10 (16.67)

	ance to the pharmacy students is essential?																			
04	Do you agree that reporting of adverse event will enhance patient safety?	33 (15.87)	94 (45.19)	46 (22.12)	13 (6.25)	22 (10.58)	52 (25.00)	114 (54.81)	18 (8.65)	07 (3.37)	17 (8.17)	16 (26.67)	27 (45)	1 (1.67)	2 (3.33)	14 (23.33)	24 (40)	24 (40)	1 (1.67)	1 (1.67)	10 (16.67)
05	Do you agree that if you come across any adverse event related to medical devices, would you report it?	31 (14.90)	92 (44.23)	51 (24.52)	16 (7.69)	18 (8.65)	53 (25.48)	113 (54.33)	15 (7.21)	07 (3.37)	20 (9.62)	8 (13.33)	35 (58.33)	3 (5)	4 (6.67)	10 (16.67)	22 (36.67)	26 (43.33)	1 (1.67)	1 (1.67)	10 (16.67)

Table 5: T-test analysis of Attitude factor between B Pharm and M Pharm

Sl. No.	Stream	N	Mean ± Sd. Dev		p-value
			Pre	Post	
01	B Pharm	208	16.63±4.152	18.82±5.457	<0.001
02	M Pharm	60	17.28±5.428	18.58±6.614	.261

*Significantly significant p<0.05

Table 6: Perception of Mv among B Pharm and M Pharm students

Sl. No	Perception based questions	B Pharm (N=208)										M Pharm (N=60)									
		Pre test [N (%)]					Post test [N (%)]					Pre test [N (%)]					Post test [N (%)]				
		SA	A	N	D	SD	SA	A	N	D	SD	SA	A	N	D	SD	SA	A	N	D	SD
01	Do you believe that India's materiovigilance programme can generate evidence-based data on medical device safety?	13 (6.25)	77 (37.02)	83 (39.90)	15 (7.21)	20 (9.62)	47 (22.60)	117 (56.23)	18 (8.65)	9 (4.33)	17 (8.17)	6 (10)	31 (51.67)	10 (16.67)	4 (6.67)	9 (15)	17 (28.33)	31 (51.67)	3 (5)	-	9 (15)
02	Do you think that one report of adverse event related	19 (9.13)	85 (40.87)	69 (33.17)	21 (10.10)	14 (6.73)	46 (22.12)	117 (56.25)	20 (9.62)	10 (4.81)	15 (7.21)	11 (18.33)	31 (51.67)	7 (11.67)	1 (1.67)	10 (16.67)	23 (38.33)	29 (48.33)	1 (1.67)	-	7 (11.67)

	to medical device will make any difference in health care system?																				
03	Are you aware of the potential consequences of not reporting adverse events related to medical devices?	14 (6.73)	62 (29.81)	104 (50.00)	13 (6.25)	15 (7.21)	48 (23.08)	106 (51.00)	33 (15.87)	09 (4.33)	12 (5.77)	6 (10)	30 (50)	15 (25)	1 (1.67)	8 (13.33)	19 (31.67)	29 (48.33)	5 (8.33)	1	6
04	Do you perceive Materiovigilance reporting as a potential area for your professional	15 (7.21)	85 (40.87)	77 (37.02)	18 (8.65)	13 (6.25)	48 (23.08)	115 (55.29)	21 (10.10)	07 (3.37)	17 (8.17)	6 (10)	30 (50)	15 (25)	-	9 (15)	23 (38.33)	26 (43.33)	6 (10)	-	5 (8.33)

	growth and development in the field of pharmacy?																			
05	Do you perceive a need for greater awareness and understanding of Materiovigilance among pharmacy students?	23 (11.06)	101 (48.56)	54 (25.96)	13 (6.25)	17 (8.17)	57 (27.40)	110 (52.88)	17 (8.17)	08 (3.85)	16 (7.69)	12 (20)	29 (48.33)	9 (15)	2 (3.33)	8 (13.33)	22 (33.67)	29 (48.33)	3 (5)	-	6 (10)

Table 7: T-test analysis of Perception factor between B Pharm and M Pharm

Sl. No.	Stream	N	Mean ± Sd. Dev		p-value
			Pre	Post	
01	B Pharm	208	17.16 ± 4.785	19.13 ±4.864	<0.001*
02	M Pharm	60	17.20 ±5.784	19.75 ±5.461	.019*

*Significantly significant p<0.05

Table 8: Scoring and categorization of KAP domains

Domain	Question format	Scoring	Poor category	Moderate category	Good category
Knowledge	Yes/No (2 options)	Yes=1, No=0	0-2 points	3 points	4-5 points
Attitude	SA,A,N,D,SD(5 options)	5,4,3,2,1	0-16 points	17-18 points	19-25 points
Perception	SA,A,N,D,SD(5 options)	5,4,3,2,1	0-16 points	17-18 points	19-25 points

Table 9: Comparison of KAP factors between B Pharm and M Pharm

Stream	**B Pharm**			**M Pharm**		
Criteria	Poor	Moderate	Good	Poor	Moderate	Good
Knowledge	21	7	180	03	04	53
Attitude	43	14	151	12	06	42
Perception	43	10	155	10	03	47

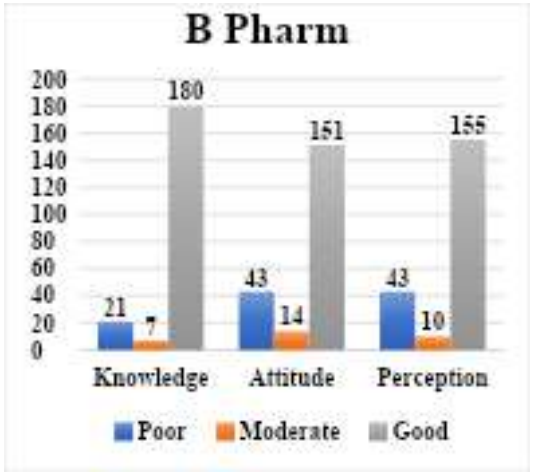

Figure 1: Post-test KAP of B Pharm

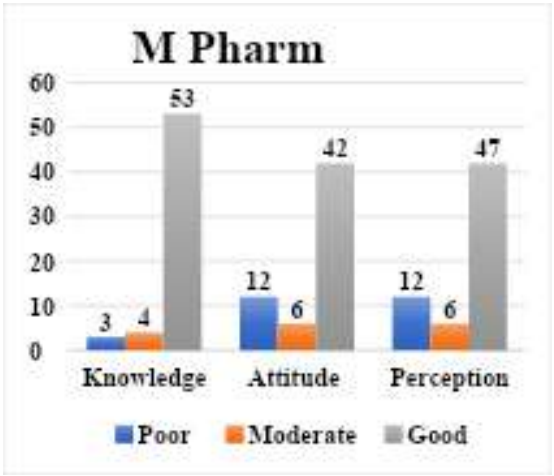

Figure 2: Post-test KAP of M Pharm